VOLUME 27 / NUMBER 18
SEPTEMBER 23, 1989
ACC. NOS. N89-24261 TO N89-25112

STAR
AN ABSTRACT JOURNAL

Scientific and Technical Aerospace Reports

PRODUCED BY THE
SCIENTIFIC AND TECHNICAL
INFORMATION
DIVISION

NASA

NATIONAL AERONAUTICS AND SPACE ADMINISTRATION

WHAT YOU CAN DO FOR *STAR*

All users of this abstract service are urged to forward reports to be considered for announcement in *STAR*. This will aid NASA in its efforts to provide the fullest possible coverage of all scientific and technical publications that might support aeronautics and space research and development. If you have prepared relevant reports (other than those that you will transmit to NASA, DoD, or DOE through the usual contract- or grant-reporting channels), please send them for consideration to the NASA Scientific and Technical Information Facility, P.O. Box 8757, BWI Airport, Maryland 21240.

Reprints of journal articles, book chapters, and conference papers are also welcome. These will be considered for announcement in *STAR's* companion journal, *International Aerospace Abstracts.*

You may specify a particular source to be included in a report announcement if you wish; otherwise the report will be placed on public sale at the National Technical Information Service. Copyrighted publications will be announced but not distributed or sold.

PURCHASE OF *STAR*

The semimonthly issues are available to registered users on annual subscription for $99.00 from the NASA Scientific and Technical Information Facility, ATTN: Registration Services, P.O. Box 8757, BWI Airport, MD 21240. *STAR* is publically available on annual subscription for $99.00 from the Superintendent of Documents, U.S. Government Printing Office, Washington, DC 20402.

PUBLISHED BY:

UNITED STATES GOVERNMENT
NATIONAL AERONAUTICS AND SPACE ADMINISTRATION
SCIENTIFIC AND TECHNICAL INFORMATION DIVISION
Scientific and Technical Aerospace Reports, Volume 27, is prepared by the NASA Scientific and Technical Information Facility operated for the National Aeronautics and Space Administration by RMS Associates.

The Administrator of the National Aeronautics and Space Administration has determined that the publication of this periodical is necessary in the transaction of the public business required by law of this Agency. Use of funds for printing this periodical has been approved by the Director of the Office of Management and Budget through March 22, 1989.

US ISSN 0036-8741

INTRODUCTION

Scientific and Technical Aerospace Reports (STAR) is a major component of a comprehensive National Aeronautics and Space Administration information system covering aeronautics, space, and supporting disciplines. *STAR* is issued on the 8th and 23rd of each month and announces current publications of the following types:

- NASA, NASA contractor, and NASA grantee reports
- Reports issued by other U.S. Government Agencies, domestic and foreign institutions, universities, and private firms
- Translations in report form
- NASA-owned patents and patent applications
- Other U.S. Government Agency and foreign patents and patent applications
- Domestic and foreign dissertations and theses

Journal, book, and conference literature, cover-to-cover journal translations, and certain foreign dissertations are announced in a companion journal, *International Aerospace Abstracts (IAA),* available on subscription from the American Institute of Aeronautics and Astronautics, Technical Information Service, 555 West 57th Street, 12th Floor, New York, New York 10019.

SUBJECT SCOPE

Subject scope of *STAR,* and *IAA* includes all aspects of aeronautics and space research and development, supporting basic and applied research, and applications. Aerospace aspects of earth resources, energy development, conservation, oceanography, environmental protection, urban transportation, and other topics of high national priority are also covered.

OTHER NASA PUBLICATIONS

Other NASA publications and information services are described in the publication, *The NASA Scientific and Technical Information System ... and How to Use It,* available without charge from the NASA Scientific and Technical Information Facility, P.O. Box 8757, BWI Airport, Maryland 21240.

HOW TO USE *STAR* SUBJECT CATEGORIES

STAR is categorized by 10 major subject divisions divided into 76 specific subject categories and one general category/division. The major subject divisions are listed in the Table of Contents, together with a note for each that defines its scope and provides any cross-references. For example:

AERONAUTICS

Includes aeronautics (general); aerodynamics; air transportation and safety; aircraft communications and navigation; aircraft design, testing and performance; aircraft instrumentation; aircraft propulsion and power; aircraft stability and control; and research and support facilities (air).

For related information see also *Astronautics.*

Each major division is further divided into as many as nine specific categories, which are identified by category numbers.

Abstracts in *STAR* are grouped by specific category, the categories appearing in sequential order. Category breaks in the abstract section are identified by the category number and title, and a scope note. Cross-references to other categories are provided as appropriate. For example:

02 AERODYNAMICS

Includes aerodynamics of bodies, combinations, wings, rotors, and control surfaces; and internal flow in ducts and turbomachinery.

For related information see also *34 Fluid Mechanics and Heat Transfer.*

CROSS-REFERENCES

Individual *STAR* abstracts are not ordinarily cross-referenced, except for certain conference reports or book translations that have had separate abstracts written for their component papers or chapters. Citations and abstracts of the components follow immediately after those of the parent document. When the subject content of a component differs sufficiently from the general content of the parent, a cross-reference citation also is printed at the end of the category to which it normally would have been assigned if it were independent.

DOCUMENTS ON MICROFICHE

Documents on microfiche[1] are designated by a pound sign (#) following the accession number. The pound sign is used without regard to the source or quality of the microfiche.

AVAILABILITIES

One or more sources from which a document announced in *STAR* is available to the public is given in each citation. The most commonly indicated sources and their acronyms or abbreviations are listed below. If the publication is available from a source other than those listed, the publisher and his address will be displayed on the availability line or in combination with the corporate source line.

Avail: NTIS. Sold by the National Technical Information Service. Prices for hard copy (HC) and microfiche (MF) are indicated by a price code following the letters HC or MF in the *STAR* citation. Current values for the price codes are given in the tables on page vii.

Initially distributed microfiche under the NTIS SRIM (Selected Research in Microfiche) is available at greatly reduced unit prices. For this service and for information concerning subscription to NASA printed reports, consult the NTIS Subscription Section, Springfield, Va. 22161.

NOTE ON ORDERING DOCUMENTS: When ordering NASA publications (those followed by the * symbol), use the N accession number. NASA patent applications (only the specifications are offered) should be ordered by the US-Patent-Appl-SN number. Non-NASA publications (no asterisk) should be ordered by the AD, PB, or other *report number* shown on the last line of the citation, not by the N accession number. It is also advisable to cite the title and other bibliographic identification.

Avail: SOD (or GPO). Sold by the Superintendent of Documents, U.S. Government Printing Office, in hard copy. The current price and order number are given following the availability line. (NTIS will fill microfiche requests, as indicated above, for those documents identified by a # symbol.)

(1) A microfiche is a transparent sheet of film, 105 by 148 mm in size, containing as many as 60 to 98 pages of information reduced to micro images (not to exceed 26:1 reduction).

Avail: BLL (formerly NLL): British Library Lending Division, Boston Spa, Wetherby, Yorkshire, England. Photocopies available from this organization at the price shown. (If none is given, inquiry should be addressed to the BLL.)

Avail: DOE Depository Libraries. Organizations in U.S. cities and abroad that maintain collections of Department of Energy reports, usually in microfiche form, are listed in *Energy Research Abstracts.* Services available from the DOE and its depositories are described in a booklet, *DOE Technical Information Center - Its Functions and Services* (TID-4660), which may be obtained without charge from the DOE Technical Information Center.

Avail: ESDU. Pricing information on specific data, computer programs, and details on ESDU topic categories can be obtained from ESDU International Ltd. Requesters in North America should use the Virginia address while all other requesters should use the London address, both of which are on page vi.

Avail: Fachinformationszentrum, Karlsruhe. Sold by the Fachinformationszentrum Energie, Physik, Mathematik GMBH, Eggenstein Leopoldshafen, Federal Republic of Germany, at the price shown in deutschmarks (DM).

Avail: HMSO. Publications of Her Majesty's Stationery Office are sold in the U.S. by Pendragon House, Inc. (PHI), Redwood City, California. The U.S. price (including a service and mailing charge) is given, or a conversion table may be obtained from PHI.

Avail: NASA Public Document Rooms. Documents so indicated may be examined at or purchased from the National Aeronautics and Space Administration, Public Documents Room (Room 126), 600 Independence Ave., S.W., Washington, D.C. 20546, or public document rooms located at each of the NASA research centers, the NASA Space Technology Laboratories, and the NASA Pasadena Office at the Jet Propulsion Laboratory.

Avail: Univ. Microfilms. Documents so indicated are dissertations selected from *Dissertation Abstracts* and are sold by University Microfilms as xerographic copy (HC) and microfilm. All requests should cite the author and the Order Number as they appear in the citation.

Avail: US Patent and Trademark Office. Sold by Commissioner of Patents and Trademarks, U.S. Patent and Trademark Office, at the standard price of $1.50 each, postage free. (See discussion of NASA patents and patent applications below.)

Avail: (US Sales Only). These foreign documents are available to users within the United States from the National Technical Information Service (NTIS). They are available to users outside the United States through the International Nuclear Information Service (INIS) representative in their country, or by applying directly to the issuing organization.

Avail: USGS. Originals of many reports from the U.S. Geological Survey, which may contain color illustrations, or otherwise may not have the quality of illustrations preserved in the microfiche or facsimile reproduction, may be examined by the public at the libraries of the USGS field offices whose addresses are listed in this Introduction. The libraries may be queried concerning the availability of specific documents and the possible utilization of local copying services, such as color reproduction.

Avail: Issuing Activity, or Corporate Author, or no indication of availability. Inquiries as to the availability of these documents should be addressed to the organization shown in the citation as the corporate author of the document.

NASA PATENTS AND PATENT APPLICATIONS

Patents and patent applications owned by NASA are announced in *STAR* under appropriate subject categories and are referenced in the *STAR* indexes. In the Report/Accession Number Index, patents are indexed by the NASA Case Number (which appears in lieu of the report number in other indexes), the U.S. Patent Number, the U.S. Patent Application Serial Number, and the U.S. Patent Class. Patent applications for which patents have not yet been issued are indexed by the NASA Case Number and the U.S. Patent Application Serial Number.

NASA *patent application specifications* are sold in paper copy by the National Technical Information Service at price code A02. Microfiche are sold at price code A01. The US-Patent-Appl-SN- number should be used in ordering either paper copy or microfiche from NTIS. Printed copies of *patents* (which are not microfiched) are available for purchase at $1.50 per copy from:

Commissioner of Patents and Trademarks
U.S. Patent and Trademark Office
Washington, D.C. 20231

When ordering patents, the U.S. Patent Number should be used, and payment must be remitted in advance, preferably by money order or check payable to the Commissioner of Patents and Trademarks. Prepaid purchase coupons for ordering are also available from the Patent and Trademark Office. The patents and patent applications announced in *STAR* are owned by NASA and are available for royalty-free licensing. Requests for licensing terms and further information should be addressed to:

Associate General Counsel for Intellectual Property/Code GP
National Aeronautics and Space Administration
Washington, D.C. 20546

ELIGIBILITY AND REGISTRATION FOR NASA INFORMATION PRODUCTS AND SERVICES

A variety of services is available to organizations of the following types that have registered with NASA to receive specific services or products:

1. NASA offices, research centers, contractors, subcontractors, grantees, and consultants;
2. Other U.S. Government agencies and their contractors;
3. Libraries in the United States that have arrangements with NASA to maintain collections of NASA documents for public reference;
4. Other organizations in the United States having a need for NASA documents in work related to aeronautics and space research;
5. Organizations abroad that have established reciprocal document exchange arrangements with NASA.

Only the central service points or central points of document acquisition and control within qualified organizations are eligible to register for NASA products and services. Domestic organizations that may be eligible to receive various classes of NASA publications and services should address their requests for registration or for further information to:

NASA Scientific and Technical Information Facility
ATTN: Registration Services
Post Office Box 8757
BWI Airport, Maryland 21240

Organizations abroad should direct requests to Manager, International STI Activities, NTT, NASA Headquarters, Washington, D.C. 20546.

AVAILABILITY OF *STAR* ABSTRACTS ON MICROFICHE

Microfiche of the abstract sections of this issue and other issues of *STAR* are available on annual subscription from NTIS as PB89-911300, Attn: Subscriptions, 5285 Port Royal Road, Springfield, Virginia 22161. Annual subscription rates are $70.00 North America; $140.00 foreign. Abstract sections for previous years retroactive to 1964 are available at the current rates. Microfiche for individual *STAR* issue abstract sections are not available.

PUBLIC COLLECTIONS OF NASA DOCUMENTS

DOMESTIC: NASA and NASA-sponsored documents and a large number of aerospace publications are available to the public for reference purposes at the library maintained by the American Institute of Aeronautics and Astronautics, Technical Information Service, 555 West 57th Street, 12th Floor, New York, New York 10019

EUROPEAN: An extensive collection of NASA and NASA-sponsored publications is maintained by the British Library Lending Division, Boston Spa, Wetherby, Yorkshire, England for public access. The British Library Lending Division also has available many of the non-NASA publications cited in *STAR*. European requesters may purchase facsimile copy or microfiche of NASA and NASA-sponsored documents, those identified by both the symbols # and * from ESA - Information Retrieval Service European Space Agency, 8-10 rue Mario-Nikis, 75738 Paris CEDEX 15, France.

FEDERAL DEPOSITORY LIBRARY PROGRAM

In order to provide the general public with greater access to U.S. Government publications, Congress established the Federal Depository Library Program under the Government Printing Office (GPO), with 50 regional depositories responsible for permanent retention of material, inter-library loan, and reference services. At least one copy of nearly every NASA and NASA-sponsored publication, either in printed or microfiche format, is received and retained by the 50 regional depositories. A list of the regional GPO libraries, arranged alphabetically by state, appears on the inside back cover. These libraries are *not* sales outlets. A local library can contact a Regional Depository to help locate specific reports, or direct contact may be made by an individual.

ADDRESSES OF ORGANIZATIONS

American Institute of Aeronautics and Astronautics
Technical Information Service
555 West 57th Street, 12th Floor
New York, New York 10019

British Library Lending Division,
Boston Spa, Wetherby, Yorkshire,
England

Commissioner of Patents and Trademarks
U.S. Patent and Trademark Office
Washington, D.C. 20231

Department of Energy
Technical Information Center
P.O. Box 62
Oak Ridge, Tennessee 37830

ESA-Information Retrieval Service
ESRIN
Via Galileo Galilei
00044 Frascati (Rome) Italy

ESDU International
P.O. Box 1633
Manassas, Virginia 22110

ESDU International, Ltd.
251-259 Regent Street
London, W1R 7AD, England

Fachinformationszentrum Energie, Physik, Mathematik GMBH
7514 Eggenstein Leopoldshafen
Federal Republic of Germany

Her Majesty's Stationery Office
P.O. Box 569, S.E. 1
London, England

NASA Scientific and Technical Information Facility
P.O. Box 8757
B.W.I. Airport, Maryland 21240

National Aeronautics and Space Administration
Scientific and Technical Information Division (NTT)
Washington, D.C. 20546

National Technical Information Service
5285 Port Royal Road
Springfield, Virginia 22161

Pendragon House, Inc.
899 Broadway Avenue
Redwood City, California 94063

Superintendent of Documents
U.S. Government Printing Office
Washington, D.C. 20402

University Microfilms
A Xerox Company
300 North Zeeb Road
Ann Arbor, Michigan 48106

University Microfilms, Ltd.
Tylers Green
London, England

U.S. Geological Survey Library
National Center - MS 950
12201 Sunrise Valley Drive
Reston, Virginia 22092

U.S. Geological Survey Library
2255 North Gemini Drive
Flagstaff, Arizona 86001

U.S. Geological Survey
345 Middlefield Road
Menlo Park, California 94025

U.S. Geological Survey Library
Box 25046
Denver Federal Center, MS914
Denver, Colorado 80225

NTIS PRICE SCHEDULES

(Effective January 1, 1989)

Schedule A
STANDARD PRICE DOCUMENTS AND MICROFICHE

PRICE CODE	NORTH AMERICAN PRICE	FOREIGN PRICE
A01	$ 6.95	$13.90
A02	10.95	21.90
A03	13.95	27.90
A04-A05	15.95	31.90
A06-A09	21.95	43.90
A10-A13	28.95	57.90
A14-A17	36.95	73.90
A18-A21	42.95	85.90
A22-A25	49.95	99.90
A99	*	*
NO1	55.00	70.00
NO2	55.00	80.00

Schedule E
EXCEPTION PRICE DOCUMENTS AND MICROFICHE

PRICE CODE	NORTH AMERICAN PRICE	FOREIGN PRICE
E01	$ 9.00	18.00
E02	11.50	23.00
E03	13.00	26.00
E04	15.50	31.00
E05	17.50	35.00
E06	20.50	41.00
E07	23.00	46.00
E08	25.50	51.00
E09	28.00	56.00
E10	31.00	62.00
E11	33.50	67.00
E12	36.50	73.00
E13	39.00	78.00
E14	42.50	85.00
E15	46.00	92.00
E16	50.50	101.00
E17	54.50	109.00
E18	59.00	118.00
E19	65.50	131.00
E20	76.00	152.00
E99	*	*

*Contact NTIS for price quote.

IMPORTANT NOTICE

NTIS Shipping and Handling Charges

U.S., Canada, Mexico — ADD $3.00 per TOTAL ORDER

All Other Countries — ADD $4.00 per TOTAL ORDER

Exceptions — Does NOT apply to:

ORDERS REQUESTING NTIS RUSH HANDLING

ORDERS FOR SUBSCRIPTION OR STANDING ORDER PRODUCTS *ONLY*

NOTE: Each additional delivery address on an order requires a separate shipping and handling charge.

VOLUME 27 NUMBER 18 / SEPTEMBER 23, 1989

TABLE OF CONTENTS

AERONAUTICS

Includes aeronautics (general); aerodynamics; air transportation and safety; aircraft communications and navigation; aircraft design, testing and performance; aircraft instrumentation; aircraft propulsion and power; aircraft stability and control; and research and support facilities (air).

For related information see also *Astronautics.*

01 AERONAUTICS (GENERAL) 2509

02 AERODYNAMICS 2509

Includes aerodynamics of bodies, combinations, wings, rotors, and control surfaces; and internal flow in ducts and turbomachinery.

For related information see also *34 Fluid Mechanics and Heat Transfer*

03 AIR TRANSPORTATION AND SAFETY 2513

Includes passenger and cargo air transport operations; and aircraft accidents.

For related information see also *16 Space Transportation* and *85 Urban Technology and Transportation.*

04 AIRCRAFT COMMUNICATIONS AND NAVIGATION 2514

Includes digital and voice communication with aircraft; air navigation systems (satellite and ground based); and air traffic control.

For related information see also *17 Space Communications, Spacecraft Communications, Command and Tracking* and *32 Communications and Radar.*

05 AIRCRAFT DESIGN, TESTING AND PERFORMANCE 2516

Includes aircraft simulation technology.

For related information see also *18 Spacecraft Design, Testing and Performance* and *39 Structural Mechanics.* For land transportation vehicles see *85 Urban Technology and Transportation.*

06 AIRCRAFT INSTRUMENTATION 2518

Includes cockpit and cabin display devices; and flight instruments.

For related information see also *19 Spacecraft Instrumentation* and *35 Instrumentation and Photography.*

07 AIRCRAFT PROPULSION AND POWER 2518

Includes prime propulsion systems and systems components, e.g., gas turbine engines and compressors; and onboard auxiliary power plants for aircraft.

For related information see also *20 Spacecraft Propulsion and Power, 28 Propellants and Fuels,* and *44 Energy Production and Conversion.*

08 AIRCRAFT STABILITY AND CONTROL 2519

Includes aircraft handling qualities; piloting; flight controls; and autopilots.

For related information see also *05 Aircraft Design, Testing and Performance.*

09 RESEARCH AND SUPPORT FACILITIES (AIR) 2520

Includes airports, hangars and runways; aircraft repair and overhaul facilities; wind tunnels; shock tubes; and aircraft engine test stands.

For related information see also *14 Ground Support Systems and Facilities (Space).*

ASTRONAUTICS

Includes astronautics (general); astrodynamics; ground support systems and facilities (space); launch vehicles and space vehicles; space transportation; space communications, spacecraft communications, command and tracking; spacecraft design, testing and performance; spacecraft instrumentation; and spacecraft propulsion and power.

For related information see also *Aeronautics*

12 ASTRONAUTICS (GENERAL) 2521

For extraterrestrial exploration see *91 Lunar and Planetary Exploration.*

13 ASTRODYNAMICS 2529

Includes powered and free-flight trajectories; and orbital and launching dynamics.

14 GROUND SUPPORT SYSTEMS AND FACILITIES (SPACE) 2529

Includes launch complexes, research and production facilities; ground support equipment, e.g., mobile transporters; and simulators.

For related information see also *09 Research and Support Facilities (Air).*

15 LAUNCH VEHICLES AND SPACE VEHICLES 2530

Includes boosters; operating problems of launch/space vehicle systems; and reusable vehicles.

For related information see also *20 Spacecraft Propulsion and Power.*

16 SPACE TRANSPORTATION 2531

Includes passenger and cargo space transportation, e.g., shuttle operations; and space rescue techniques.

For related information see also *03 Air Transportation and Safety* and *18 Spacecraft Design, Testing and Performance.* For space suits see *54 Man/System Technology and Life Support.*

17 SPACE COMMUNICATIONS, SPACECRAFT COMMUNICATIONS, COMMAND AND TRACKING 2532

Includes telemetry; space communications networks; astronavigation and guidance; and radio blackout.

For related information see also *04 Aircraft Communications and Navigation* and *32 Communications and Radar.*

18 SPACECRAFT DESIGN, TESTING AND PERFORMANCE 2532

Includes satellites; space platforms; space stations; spacecraft systems and components such as thermal and environmental controls; and attitude controls.

For life support systems see *54 Man/System Technology and Life Support.* For related information see also *05 Aircraft Design, Testing and Performance, 39 Structural Mechanics,* and *16 Space Transportation.*

19 SPACECRAFT INSTRUMENTATION 2535

For related information see also *06 Aircraft Instrumentation* and *35 Instrumentation and Photography.*

20 SPACECRAFT PROPULSION AND POWER 2535

Includes main propulsion systems and components, e.g. rocket engines; and spacecraft auxiliary power sources.

For related information see also *07 Aircraft Propulsion and Power, 28 Propellants and Fuels, 44 Energy Production and Conversion,* and *15 Launch Vehicles and Space Vehicles.*

CHEMISTRY AND MATERIALS

Includes chemistry and materials (general); composite materials; inorganic and physical chemistry; metallic materials; nonmetallic materials; propellants and fuels; and materials processing.

23 CHEMISTRY AND MATERIALS (GENERAL) 2539

24 COMPOSITE MATERIALS 2539

Includes physical, chemical, and mechanical properties of laminates and other composite materials.

For ceramic materials see *27 Nonmetallic Materials.*

25 INORGANIC AND PHYSICAL CHEMISTRY 2541

Includes chemical analysis, e.g., chromatography; combustion theory; electrochemistry; and photochemistry.

For related information see also *77 Thermodynamics and Statistical Physics.*

26 METALLIC MATERIALS 2542

Includes physical, chemical, and mechanical properties of metals, e.g., corrosion; and metallurgy.

27 NONMETALLIC MATERIALS 2544

Includes physical, chemical, and mechanical properties of plastics, elastomers, lubricants, polymers, textiles, adhesives, and ceramic materials.

For composite materials see *24 Composite Materials.*

28 PROPELLANTS AND FUELS 2548

Includes rocket propellants, igniters and oxidizers; their storage and handling procedures; and aircraft fuels.

For related information see also *07 Aircraft Propulsion and Power, 20 Spacecraft Propulsion and Power,* and *44 Energy Production and Conversion.*

29 MATERIALS PROCESSING 2548

Includes space-based development of products and processes for commercial application.

For biological materials see *55 Space Biology.*

ENGINEERING

Includes engineering (general); communications and radar; electronics and electrical engineering; fluid mechanics and heat transfer; instrumentation and photography; lasers and masers; mechanical engineering; quality assurance and reliability; and structural mechanics.

For related information see also *Physics.*

31 ENGINEERING (GENERAL) 2548

Includes vacuum technology; control engineering; display engineering; cryogenics; and fire prevention.

32 COMMUNICATIONS AND RADAR 2550

Includes radar; land and global communications; communications theory; and optical communications.

For related information see also *04 Aircraft Communications and Navigation* and *17 Space Communications, Spacecraft Communications, Command and Tracking.* For search and rescue see *03 Air Transportation and Safety,* and *16 Space Transportation.*

33 ELECTRONICS AND ELECTRICAL ENGINEERING 2553

Includes test equipment and maintainability; components, e.g., tunnel diodes and transistors; microminiaturization; and integrated circuitry.

For related information see also *60 Computer Operations and Hardware* and *76 Solid-State Physics.*

34 FLUID MECHANICS AND HEAT TRANSFER 2554

Includes boundary layers; hydrodynamics; fluidics; mass transfer and ablation cooling.

For related information see also *02 Aerodynamics* and *77 Thermodynamics and Statistical Physics.*

35 INSTRUMENTATION AND PHOTOGRAPHY 2564

Includes remote sensors; measuring instruments and gages; detectors; cameras and photographic supplies; and holography.

For aerial photography see *43 Earth Resources and Remote Sensing.* For related information see also *06 Aircraft Instrumentation* and *19 Spacecraft Instrumentation.*

36 LASERS AND MASERS 2565

Includes parametric amplifiers.

For related information see also *76 Solid-State Physics.*

37 MECHANICAL ENGINEERING 2567

Includes auxiliary systems (nonpower); machine elements and processes; and mechanical equipment.

38 QUALITY ASSURANCE AND RELIABILITY 2571

Includes product sampling procedures and techniques; and quality control.

39 STRUCTURAL MECHANICS 2572

Includes structural element design and weight analysis; fatigue; and thermal stress.

For applications see *05 Aircraft Design, Testing and Performance* and *18 Spacecraft Design, Testing and Performance.*

GEOSCIENCES

Includes geosciences (general); earth resources and remote sensing; energy production and conversion; environment pollution; geophysics; meteorology and climatology; and oceanography.

For related information see also *Space Sciences.*

42 GEOSCIENCES (GENERAL) **N.A.**

43 EARTH RESOURCES AND REMOTE SENSING **2581**

Includes remote sensing of earth resources by aircraft and spacecraft; photogrammetry; and aerial photography.

For instrumentation see *35 Instrumentation and Photography.*

44 ENERGY PRODUCTION AND CONVERSION **2583**

Includes specific energy conversion systems, e.g., fuel cells; global sources of energy; geophysical conversion; and windpower.

For related information see also *07 Aircraft Propulsion and Power, 20 Spacecraft Propulsion and Power,* and *28 Propellants and Fuels.*

45 ENVIRONMENT POLLUTION **2591**

Includes atmospheric, noise, thermal, and water pollution.

46 GEOPHYSICS **2592**

Includes aeronomy; upper and lower atmosphere studies; ionospheric and magnetospheric physics; and geomagnetism.

For space radiation see *93 Space Radiation.*

47 METEOROLOGY AND CLIMATOLOGY **2595**

Includes weather forecasting and modification.

48 OCEANOGRAPHY **2598**

Includes biological, dynamic, and physical oceanography; and marine resources.

For related information see also *43 Earth Resources and Remote Sensing.*

LIFE SCIENCES

Includes life sciences (general); aerospace medicine; behavioral sciences; man/system technology and life support; and space biology.

51 LIFE SCIENCES (GENERAL) **N.A.**

52 AEROSPACE MEDICINE **2598**

Includes physiological factors; biological effects of radiation; and effects of weightlessness on man and animals.

53 BEHAVIORAL SCIENCES **2599**

Includes psychological factors; individual and group behavior; crew training and evaluation; and psychiatric research.

54 MAN/SYSTEM TECHNOLOGY AND LIFE SUPPORT **2600**

Includes human engineering; biotechnology; and space suits and protective clothing.

For related information see also *16 Space Transportation.*

55 SPACE BIOLOGY **N.A.**

Includes exobiology; planetary biology; and extraterrestrial life.

MATHEMATICAL AND COMPUTER SCIENCES

Includes mathematical and computer sciences (general); computer operations and hardware; computer programming and software; computer systems; cybernetics; numerical analysis; statistics and probability; systems analysis; and theoretical mathematics.

59 MATHEMATICAL AND COMPUTER SCIENCES (GENERAL) **N.A.**

60 COMPUTER OPERATIONS AND HARDWARE **2601**

Includes hardware for computer graphics, firmware, and data processing.

For components see *33 Electronics and Electrical Engineering.*

61 COMPUTER PROGRAMMING AND SOFTWARE **2602**

Includes computer programs, routines, algorithms, and specific applications, e.g., CAD/CAM.

62 COMPUTER SYSTEMS **2604**

Includes computer networks and special application computer systems.

63 CYBERNETICS **2605**

Includes feedback and control theory, artificial intelligence, robotics and expert systems.

For related information see also *54 Man/System Technology and Life Support.*

64 NUMERICAL ANALYSIS **2613**

Includes iteration, difference equations, and numerical approximation.

65 STATISTICS AND PROBABILITY **2616**

Includes data sampling and smoothing; Monte Carlo method; and stochastic processes.

66 SYSTEMS ANALYSIS **2616**

Includes mathematical modeling; network analysis; and operations research.

67 THEORETICAL MATHEMATICS **2617**

Includes topology and number theory.

PHYSICS

Includes physics (general); acoustics; atomic and molecular physics; nuclear and high-energy physics; optics; plasma physics; solid-state physics; and thermodynamics and statistical physics.

For related information see also *Engineering.*

70 PHYSICS (GENERAL) **2617**

For precision time and time interval (PTTI) see *35 Instrumentation and Photography;* for geophysics, astrophysics or solar physics see *46 Geophysics, 90 Astrophysics,* or *92 Solar Physics.*

71 ACOUSTICS 2617
Includes sound generation, transmission, and attenuation.
For noise pollution see *45 Environment Pollution.*

72 ATOMIC AND MOLECULAR PHYSICS 2618
Includes atomic structure, electron properties, and molecular spectra.

73 NUCLEAR AND HIGH-ENERGY PHYSICS 2619
Includes elementary and nuclear particles; and reactor theory.
For space radiation see *93 Space Radiation.*

74 OPTICS 2620
Includes light phenomena and optical devices.
For lasers see *36 Lasers and Masers.*

75 PLASMA PHYSICS 2621
Includes magnetohydrodynamics and plasma fusion.
For ionospheric plasmas see *46 Geophysics.* For space plasmas see *90 Astrophysics.*

76 SOLID-STATE PHYSICS 2643
Includes superconductivity.
For related information see also *33 Electronics and Electrical Engineering* and *36 Lasers and Masers.*

77 THERMODYNAMICS AND STATISTICAL PHYSICS 2647
Includes quantum mechanics; theoretical physics; and Bose and Fermi statistics.
For related information see also *25 Inorganic and Physical Chemistry* and *34 Fluid Mechanics and Heat Transfer.*

SOCIAL SCIENCES

Includes social sciences (general); administration and management; documentation and information science; economics and cost analysis; law, political science, and space policy; and urban technology and transportation.

80 SOCIAL SCIENCES (GENERAL) N.A.
Includes educational matters.

81 ADMINISTRATION AND MANAGEMENT N.A.
Includes management planning and research.

82 DOCUMENTATION AND INFORMATION SCIENCE 2647
Includes information management; information storage and retrieval technology; technical writing; graphic arts; and micrography.
For computer documentation see *61 Computer Programming and Software.*

83 ECONOMICS AND COST ANALYSIS N.A.
Includes cost effectiveness studies.

84 LAW, POLITICAL SCIENCE AND SPACE POLICY N.A.
Includes NASA appropriation hearings; aviation law; space law and policy; international law; international cooperation; and patent policy.

85 URBAN TECHNOLOGY AND TRANSPORTATION 2648
Includes applications of space technology to urban problems; technology transfer; technology assessment; and surface and mass transportation.
For related information see *03 Air Transportation and Safety, 16 Space Transportation,* and *44 Energy Production and Conversion.*

SPACE SCIENCES

Includes space sciences (general); astronomy; astrophysics; lunar and planetary exploration; solar physics; and space radiation.
For related information see also *Geosciences.*

88 SPACE SCIENCES (GENERAL) N.A.

89 ASTRONOMY 2648
Includes radio, gamma-ray, and infrared astronomy; and astrometry.

90 ASTROPHYSICS 2650
Includes cosmology; celestial mechanics; space plasmas; and interstellar and interplanetary gases and dust.
For related information see also *75 Plasma Physics.*

91 LUNAR AND PLANETARY EXPLORATION 2653
Includes planetology; and manned and unmanned flights.
For spacecraft design or space stations see *18 Spacecraft Design, Testing and Performance.*

92 SOLAR PHYSICS 2653
Includes solar activity, solar flares, solar radiation and sunspots.
For related information see *93 Space Radiation.*

93 SPACE RADIATION 2656
Includes cosmic radiation; and inner and outer earth's radiation belts.
For biological effects of radiation see *52 Aerospace Medicine.* For theory see *73 Nuclear and High-Energy Physics.*

GENERAL

Includes aeronautical, astronautical, and space science related histories, biographies, and pertinent reports too broad for categorization; histories or broad overviews of NASA programs.

99 GENERAL 2657

Note: N.A. means that no abstracts were assigned to this category for this issue.

SUBJECT INDEX I-1
PERSONAL AUTHOR INDEX I-49
CORPORATE SOURCE INDEX I-57
CONTRACT NUMBER INDEX I-67
REPORT/ACCESSION NUMBER INDEX I-69

TYPICAL CITATION AND ABSTRACT

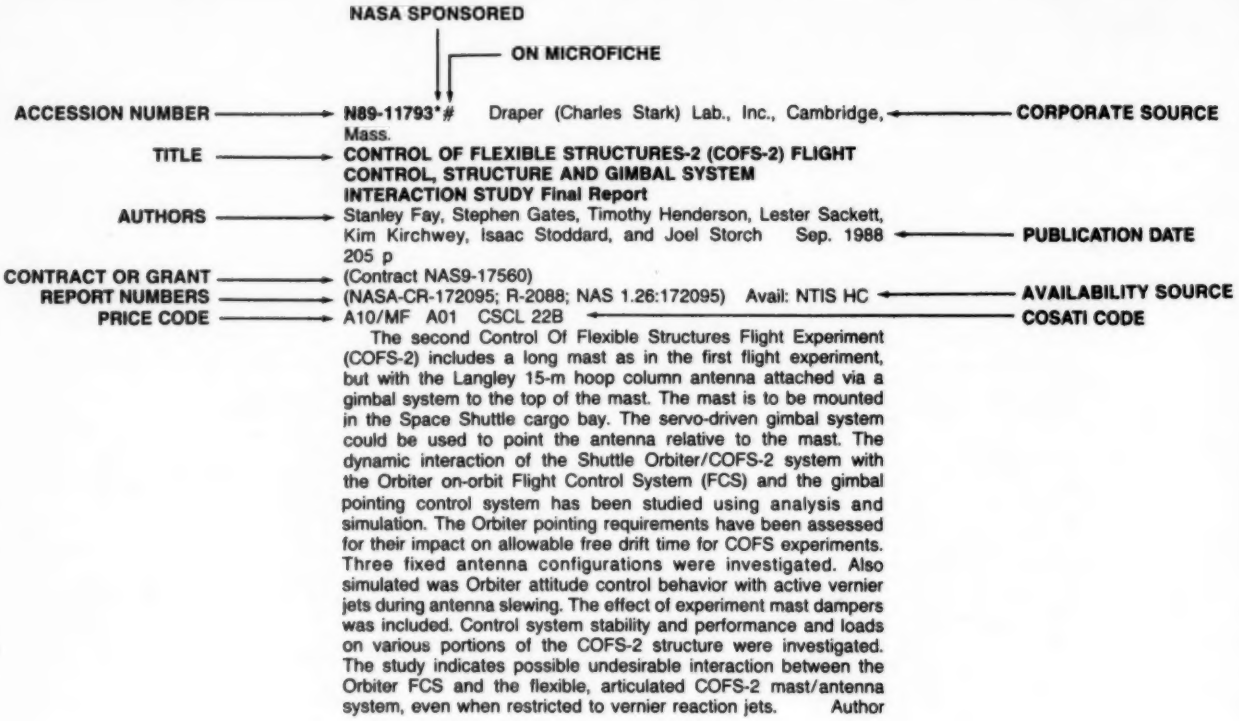
NASA SPONSORED
ON MICROFICHE
ACCESSION NUMBER
N89-11793*# Draper (Charles Stark) Lab., Inc., Cambridge, Mass.
CORPORATE SOURCE
TITLE
CONTROL OF FLEXIBLE STRUCTURES-2 (COFS-2) FLIGHT CONTROL, STRUCTURE AND GIMBAL SYSTEM INTERACTION STUDY Final Report
AUTHORS
Stanley Fay, Stephen Gates, Timothy Henderson, Lester Sackett, Kim Kirchwey, Isaac Stoddard, and Joel Storch Sep. 1988
PUBLICATION DATE
205 p
CONTRACT OR GRANT
(Contract NAS9-17560)
REPORT NUMBERS
(NASA-CR-172095; R-2088; NAS 1.26:172095) Avail: NTIS HC
AVAILABILITY SOURCE
PRICE CODE
A10/MF A01 CSCL 22B
COSATI CODE
The second Control Of Flexible Structures Flight Experiment (COFS-2) includes a long mast as in the first flight experiment, but with the Langley 15-m hoop column antenna attached via a gimbal system to the top of the mast. The mast is to be mounted in the Space Shuttle cargo bay. The servo-driven gimbal system could be used to point the antenna relative to the mast. The dynamic interaction of the Shuttle Orbiter/COFS-2 system with the Orbiter on-orbit Flight Control System (FCS) and the gimbal pointing control system has been studied using analysis and simulation. The Orbiter pointing requirements have been assessed for their impact on allowable free drift time for COFS experiments. Three fixed antenna configurations were investigated. Also simulated was Orbiter attitude control behavior with active vernier jets during antenna slewing. The effect of experiment mast dampers was included. Control system stability and performance and loads on various portions of the COFS-2 structure were investigated. The study indicates possible undesirable interaction between the Orbiter FCS and the flexible, articulated COFS-2 mast/antenna system, even when restricted to vernier reaction jets. Author

VOLUME 27 NUMBER 18 / SEPTEMBER 23, 1989

Scientific and Technical Aerospace Reports

A Semimonthly Publication of the National Aeronautics and Space Administration

01 AERONAUTICS (GENERAL)

N89-24261# Air Force Systems Command, Wright-Patterson AFB, OH. Foreign Technology Div.
TECHNOLOGY OF AIRCRAFT CONSTRUCTION (SELECTED CHAPTERS)
A. L. Abibov, N. M. Biryukov, V. V. Boytsov, V. P. Grigoryev, and S. V. Yeliseyev 13 Oct. 1988 74 p Transl. into ENGLISH from Tekhnologiya Samoletostroyeniya (USSR), Mashinostroyeniye, 1970 p 482-510
(AD-A199946; FTD-ID(RS)T-0616-88) Avail: NTIS HC A04/MF A01 CSCL 01/3

The characteristics and applications of reinforced plastics especially in regard to aircraft construction are discussed. The assembling of aircraft parts is considered. Attention is given to manufacturing practices and quality control. Examples are given.
A.D.

N89-24262* National Aeronautics and Space Administration. Ames Research Center, Moffett Field, CA.
NUMERICAL AERODYNAMIC SIMULATION
1989 33 p Original document contains color illustrations
(NASA-EP-262; NAS 1.19:262) Avail: Issuing Activity CSCL 01B

An overview of historical and current numerical aerodynamic simulation (NAS) is given. The capabilities and goals of the Numerical Aerodynamic Simulation Facility are outlined. Emphasis is given to numerical flow visualization and its applications to structural analysis of aircraft and spacecraft bodies. The uses of NAS in computational chemistry, engine design, and galactic evolution are mentioned.
A.D.

N89-24263# General Accounting Office, Washington, DC. National Security and International Affairs Div.
US MILITARY AIRCRAFT COPRODUCTION WITH JAPAN
Joseph E. Kelley 1989 12 p
(AD-A206430; GAO/T-NSIAD-89-6) Avail: NTIS HC A03/MF A01 CSCL 01/3

The United States enters into coproduction arrangements primarily for defense and foreign policy reasons. Basically, the Departments of Defense (DOD) and State have the authority and responsibility for negotiating and concluding coproduction agreements, usually Memorandums of Understanding (MOU). These government to government MOUs with Japan are commonly implemented by commercial licensed production and technical assistance agreements with the U.S. manufacturers. The F-15 program was begun at a time when Japan was targeting its aircraft industry, as well as other high technology industries, for development. Japan was steadily reducing the importance of its lower technology industries, such as shipbuilding, and favoring the development of high-technology export industries. Japan's major aircraft manufacturers expanded and upgraded their production facilities in order to handle their F-15, P-3C, and Boeing 767 work shares. Through these military and civil programs, combined, the Japanese companies expanded their production capacity, technology base, and aircraft production labor force.
GRA

02 AERODYNAMICS

Includes aerodynamics of bodies, combinations, wings, rotors, and control surfaces; and internal flow in ducts and turbomachinery.

For related information see also *34 Fluid Mechanics and Heat Transfer.*

N89-24264*# National Aeronautics and Space Administration. Langley Research Center, Hampton, VA.
EFFECT OF ADVANCED ROTORCRAFT AIRFOIL SECTIONS ON THE HOVER PERFORMANCE OF A SMALL-SCALE ROTOR MODEL
Susan L. Althoff (Army Aviation Systems Command, Hampton, VA.) Sep. 1988 35 p
(DA Proj. 1L1-61102-AH-45-A)
(NASA-TP-2832; L-16407; NAS 1.60:2832; AVSCOM-TP-88-B-001) Avail: NTIS HC A03/MF A01 CSCL 01A

A hover test was conducted on a small scale rotor model for two sets of tapered rotor blades. The baseline rotor blade set used a NACA 0012 airfoil section, whereas the second rotor blade set had advanced rotorcraft airfoils distributed along the radius. The experiment was conducted for a range of thrust coefficients and tip speeds, and the data were compared to the predictions of three analytical methods. The data show the advantage of the advanced airfoils at the higher rotor thrust levels; two of the analyses predicted the correct data trends.
Author

N89-24265*# California Polytechnic State Univ., San Luis Obispo. Dept. of Aeronautical Engineering.
THERMAL ANALYSIS OF A HYPERSONIC WING TEST STRUCTURE Final Report, Oct. 1986 - Apr. 1989
Doral R. Sandlin and Neil J. Swanson, Jr. Apr. 1989 54 p
(Contract NCC2-433)
(NASA-CR-185319; NAS 1.26:185319) Avail: NTIS HC A04/MF A01 CSCL 01A

The three-dimensional finite element modeling techniques developed for the thermal analysis of a hypersonic wing test structure (HWTS) are described. The computed results are compared to measured test data. In addition, the results of a NASA two-dimensional parameter finite difference local thermal model and the results of a contractor two-dimensional lumped parameter finite difference local thermal model will be presented.
B.G.

N89-24266*# West Virginia Univ., Morgantown. Dept. of Mechanical and Aerospace Engineering.
COMPUTATIONAL DESIGN OF LOW ASPECT RATIO WING-WINGLET CONFIGURATIONS FOR TRANSONIC WIND-TUNNEL TESTS Final Report
John M. Kuhlman and Christopher K. Brown May 1989 115 p
(Grant NAG1-625)
(NASA-CR-185016; NAS 1.26:185016) Avail: NTIS HC A06/MF A01 CSCL 01A

Computational designs were performed for three different low aspect ratio wing planforms fitted with nonplanar winglets; one of the three configurations was selected to be constructed as a wind tunnel model for testing in the NASA-Langley 7 x 10 high speed wind tunnel. A design point of M = 0.8, CL approximately equal

to 0.3 was selected, for wings of aspect ratio equal to 2.2, and leading edge sweep angles of 45 and 50 deg. Winglet length is 15 percent of the wing semispan, with a cant angle of 15 deg, and a leading edge sweep of 50 deg. Winglet total area equals 2.25 percent of the wing reference area. The design process and the predicted transonic performance for each configuration is summarized. In addition, a companion low-speed design study was conducted, using one of the transonic design wing-winglet planforms but with different camber and thickness distributions. A low-speed wind tunnel model was constructed to match this low-speed design geometry, and force coefficient data were obtained for the model at speeds of 100 to 150 ft/sec. Measured drag coefficient reductions were of the same order of magnitude as those predicted by numerical subsonic performance predictions. Author

N89-24267 Rensselaer Polytechnic Inst., Troy, NY.
AERODYNAMICS OF A LIFTING ROTOR DUE TO NEAR FIELD UNSTEADY EFFECTS Ph.D. Thesis
Robert Lowell Milliken 1988 210 p
Avail: Univ. Microfilms Order No. DA8905209

Lift deficiency functions to aid in the prediction of oscillatory loadings due to near field wake effects on a three-dimensional rotor blade in forward flight were obtained. The Pulse Transfer Function (PTF) technique was used in obtaining the lift deficiency functions. A discrete vortex model of the circulatory flow field was employed to obtain the time domain lift response to a pulse shaped transient input. The frequency domain response was then obtained by inverting the time domain response using fast Fourier transforms (FFT), from which the lift deficiency functions could be determined. To demonstrate the validity of the PTF technique, the analytical lift deficiency functions of Theodorsen and Loewy were compared with numerical representations of these functions. These lift deficiency functions and their PTF numerical counterparts agreed well in magnitude, but the error in the phase shift was large and increased with increasing reduced frequency. Lift deficiency functions for rotor blades of aspect ratios 6, 12, and 18 were plotted for advance ratios 0, 0.2, and 0.4 for each 45 degree increment about the azimuth. The results show that the effect of three dimensions is to produce a lower lift loss than calculated on the basis of two-dimensional results. The difference between the magnitude of the unsteady lift predicted by the lift deficiency functions and Theodorsen's function can be as much as 25 percent. Author

N89-24268 Lehigh Univ., Bethlehem, PA.
INTERACTION OF KARMAN VORTEX-STREET WITH AN ELLIPTICAL LEADING-EDGE Ph.D. Thesis
Ismet Gursul 1988 127 p
Avail: Univ. Microfilms Order No. DA8901868

The interaction of a Karman vortex-street with an elliptical-edge was investigated experimentally. Basic types of interaction, as a function of scale and transverse displacement of the incident vortex-street, were revealed using flow visualization. Unsteady pressure fields induced by these interactions were measured by a phase-averaging technique and correlated with the visualized flow patterns. For a generic vortex-edge interaction, measurements of the phase-averaged velocity field allowed construction of streamline and vorticity contours showing the details of the interaction, including distortion of the vortical structures near the body. The pressure field was calculated from the measured velocity field and interpreted in relation to the vortical structures. Flow visualization of free- and impinging-shear layers is simulated by prescribing the flow field and tracking the fluid markers numerically. Several aspects, including the circulation and concentration of vortices, different types of marking (timelines or streaklines), and various reference frames are considered. In the case of the vortex street edge interaction, simulation of flow visualization using the measured velocity field demonstrates possible misinterpretations. Dissert. Abstr.

N89-24269*# National Aeronautics and Space Administration. Lewis Research Center, Cleveland, OH.
CONSERVATIVE TREATMENT OF BOUNDARY INTERFACES FOR OVERLAID GRIDS AND MULTI-LEVEL GRID ADAPTATIONS
Young J. Moon (Sverdrup Technology, Inc., Cleveland, OH.) and Meng-Sing Liou 1989 18 p Presented at the 9th Computational Fluid Dynamics Conference, Buffalo, NY, 13-15 Jun. 1989; sponsored by the AIAA
(NASA-TM-102080; E-4842; NAS 1.15:102080; AIAA-89-1980)
Avail: NTIS HC A03/MF A01 CSCL 01A

Conservative algorithms for boundary interfaces of overlaid grids are presented. The basic method is zeroth order, and is extended to a higher order method using interpolation and subcell decomposition. The present method, strictly based on a conservative constraint, is tested with overlaid grids for various applications of unsteady and steady supersonic inviscid flows with strong shock waves. The algorithm is also applied to a multi-level grid adaptation in which the next level finer grid is overlaid on the coarse base grid with an arbitrary orientation. Author

N89-24270# Air Force Inst. of Tech., Wright-Patterson AFB, OH. School of Engineering.
USE OF NAVIER-STOKES METHODS TO PREDICT CIRCULATION CONTROL AIRFOIL PERFORMANCE M.S. Thesis
Steven L. Williams Mar. 1989 84 p
(AD-A206242; AFIT/GAE/AA/89M-4) Avail: NTIS HC A05/MF A01 CSCL 01/1

The predictive capability of the two-dimensional compressible mass-averaged Navier-Stokes equations was investigated for a typical circulation control air-foil. The governing equations were solved using the implicit approximate factorization algorithm of Beam-Warming with the turbulence model of Baldwin-Lomax. To account for the unique characteristics of circulation control airfoils, an empirical turbulence model correction due to Bradshaw was used. This thesis is unique in that the predictive capability of the computational method is explored by examining the importance of the empirical Bradshaw curvature correction constant on the computed results. Using a generic value of the curvature constant at various blowing coefficient levels, the computational method was able to accurately predict airfoil pitching moment and lift curve slope due to blowing. Predicted levels of airfoil lift coefficient, although reasonable, were found to be consistently low compared with experiment due to the generic curvature constant providing premature jet detachment from the Coanda surface. Computed and measured airfoil drag results followed the same trends, but lack of overall drag coefficient agreement was disappointing. Lift coefficient was found to be quite sensitive, pitching moment not sensitive, and drag coefficient moderately sensitive to the value of the curvature constant used. GRA

N89-24271# Air Force Inst. of Tech., Wright-Patterson AFB, OH. School of Engineering.
WATER TUNNEL INVESTIGATION OF THE VORTEX DYNAMICS OF PERIODICALLY PITCHED WINGS M.S. Thesis
Michael David Dec. 1988 125 p
(AD-A206359; AFIT/GAE/AA/88D-06) Avail: NTIS HC A06/MF A01 CSCL 01/1

The vortex structure above semi-span wings was investigated in the AFFDL's 24-inch water tunnel to determine the effects of periodic pitching using a saw-tooth motion. Each of the six wings was pitched about the mid-chord at nondimensional upstroke rates ranging from 0.05 to 0.30 and down-stroke rates from 0.025 to 0.600 at tunnel flow rates of 0.6 to 3.6 in/sec. Visualization of the vortices obtained through dye injection from the models was recorded using both high speed and 3/4-in. standard speed video systems. Digitized data from the high speed system provided trend data which showed the saw-tooth motion caused a hysteresis effect on the vortex breakdown location for the swept wings where during the upstroke the vortex would burst further aft than during the down-stroke. In addition, comparison of two 65-deg sweep wings with different cross sections (flat plate and NACA 0012-34)

showed a smaller hysteresis effect for the thicker wing. For the rectangular wing, increasing down-stroke rates resulted in higher dynamic stall vortex convection rates. Information was also gathered on the oscillation of static breakdown location and the effects of vortex breakdown of tunnel flow velocity. GRA

N89-24272# Flow Research, Inc., Kent, WA.
AN INVESTIGATION OF V/STOL JET INTERACTIONS IN A CROSSFLOW Final Report, 26 Sep. 1988 - 30 Mar. 1989
Suresh Menon Feb. 1989 72 p Revised Sponsored by DARPA
(Contract DAAH01-88-C-0865)
(AD-A206360; FLOW-RR-470) Avail: NTIS HC A04/MF A01 CSCL 01/1

Recently, a numerical simulation code was developed to study the interaction of the effects of a row of normal impinging jets. This model essentially simulates the hovering configuration of a V/STOL aircraft. The code solves unsteady, 3-D incompressible Navier-Stokes equations using the technique of large-eddy simulations which resolves all the length scales above the grid resolution and models the contribution of the small scales by a subgrid eddy viscosity model. The present study extends this code to include other realistic V/STOL configurations such as an obliquely impinging jet and an impinging jet in crossflow with and without a moving ground plane. These configurations model the V/STOL aircraft in pitch and in forward motion. These modifications were successfully achieved and preliminary simulations using axisymmetric forcing of the impinging jet were carried out to demonstrate the capability of the numerical code. Even with coarse mesh simulations, the results show good qualitative agreement with experimental observations. Simulation of the impinging jet in crossflow showed the formation of counterrotating streamwise vortices which has been observed in many experiments. However, it was shown that the presence of the adjacent impinging jet (which is absent in all experiments) can significantly modify the dynamics of the vortical motion in the flow field. Significant 3-dimensional vortex stretching occurs in this flow and redistribution of the total vorticity in the flow field. GRA

N89-24273# Naval Postgraduate School, Monterey, CA. Dept. of Aeronautics and Astronautics.
BOUNDARY LAYER RESPONSE TO AN UNSTEADY TURBULENT ENVIRONMENT M.S. Thesis
Robert W. Renoud Dec. 1988 123 p
(AD-A206578) Avail: NTIS HC A06/MF A01 CSCL 01/1

An experimental investigation of a wing boundary layer subjected to periodic turbulent flow at a Reynolds number of 500,000 was conducted. Non-thrusting turbulence pulses were generated at a rate of 50 pulses/s with a turbulence intensity near 10 percent. Time-varying velocity measurements were made at representative chord locations (laminar, transitional/turbulent, fully turbulent) at one angle of attack using single-element hot-wire anemometry. Characteristics of the boundary layer velocity profiles, turbulence intensity profiles, and velocity spectra and total spectral power were documented. The time-varying boundary layer response could be characterized by undisturbed flow, turbulence pulse, and recovery period. The boundary layer exhibited a cyclic transition response varying from the undisturbed flow regime to the turbulence pulse regime back to the undisturbed flow regime. The turbulence pulse penetrated into the entire boundary layer. The turbulence pulse prompted flow laminarization during the recovery period. Laminarization apparently resulted from rapid acceleration of near-surface flow within the boundary layer due to turbulence induced momentum transfer down through the boundary layer and local flow acceleration following velocity deficit of the turbulence pulse. Effects of the periodic turbulence pulse were most noticeable in the recovery period at the transitional/turbulent and fully turbulent regions of the wing. Recovery was generally characterized by lowered turbulence. GRA

N89-24274# Centre d'Etudes et de Recherches, Toulouse (France). Dept. d'Etudes et de Recherches en Aerothermodynamique.
ANALYSIS OF THE BOUNDARY LAYER OF A DELTA WING IN INCIDENCE [ANALYSE DE LA COUCHE LIMITE A L'INTRADOS D'UNE AILE EN FLECHE ET EN INCIDENCE]
G. Pailhas Apr. 1988 61 p
(Contract STPA-8595-004)
(CERT-RT-OA-26/5025-AYD; DERAT-26/5025-14; ETN-89-94522)
Avail: NTIS HC A04/MF A01

A 60 deg delta wing at 15 deg incidence is tested in a wind tunnel. The wing is an ONERA D 200 mm chord. The flow velocity is 30 m/s. The model is equipped with five arrays of pressure measuring points. A representation of the isobars shows lines parallel to the leading edge. Graphics showing the velocity profiles, transversal velocities, and turbulences are presented. ESA

N89-24275# Office National d'Etudes et de Recherches Aerospatiales, Paris (France). Direction de l'Aerodynamique.
DEVELOPMENT OF A SUPERSONIC TURBULENT BOUNDARY LAYER ON A HEATED WALL. PROPERTIES OF THE TURBULENT FIELD AND THEORETICAL APPLICATION Final Report [DEVELOPPEMENT D'UNE COUCHE LIMITE TURBULENTE SUPERSONIQUE SUR UNE PAROI CHAUFFEE. PROPRIETES DU CHAMP TURBULENT ET EXPLOITATION THEORIQUE]
L. Benkemoun and M. Salaun Jan. 1988 136 p In FRENCH
(Contract DRET-86-34-001)
(ONERA-RSF-74/7078-AY-096-A; ETN-89-94524) Avail: NTIS HC A07/MF A01

The study was carried out at external Mach numbers between 2 and 2.75 and temperature ratios to adiabatic equilibrium between 1.5 and 2. The distribution of the turbulent parameters such as Reynolds stresses are measured by laser velocimetry. The boundary limit on the heated wall is calculated using three turbulence models. The average fields are generally well predicted, while important differences between theory and experiment remain when estimating the turbulence parameters. ESA

N89-24276# Von Karman Inst. for Fluid Dynamics, Rhode-Saint-Genese (Belgium).
UNSTEADY AERODYNAMICS, VOLUME 1
1988 452 p Lecture series held in Rhode-Saint-Genese, Belgium, 18-22 Apr. 1988
(VKI-1988-07-Vol-1; ETN-89-94556) Avail: NTIS HC A20/MF A01

Flow around bluff bodies, vortex dynamics, unsteady boundary layers, and numerical and experimental techniques were discussed. For individual titles, see N89-24277 through N89-24280.

N89-24277# Virginia Polytechnic Inst. and State Univ., Blacksburg. Dept. of Engineering Science and Mechanics.
UNSTEADY AERODYNAMICS
Dean T. Mook *In* VKI, Unsteady Aerodynamics, Volume 1 1988 125 p (For primary document see N89-24276 18-02)
Avail: NTIS HC A20/MF A01

The use of vortex singularities to model subsonic aerodynamic flows is discussed. An asymptotic solution of the Navier-Stokes equation in the limiting case of infinite Reynolds number is given, as well as a definition of vorticity. The method is based on inverting the equation (Karamchetti, 1965) giving the velocity vector. The numerical solution finite element algorithm is described. Examples illustrate the application to different cases. ESA

N89-24278# Technische Hochschule, Aachen (Germany, F.R.). Lehrstuhl fuer Stahlbau.
UNSTEADY AERODYNAMIC EFFECTS ON BLUFF BODIES
H. P. Ruscheweyh *In* VKI, Unsteady Aerodynamics, Volume 1 1988 72 p (For primary document see N89-24276 18-02)
Avail: NTIS HC A20/MF A01

The physical background of aerodynamic vibration excitation phenomena is explained, including gust response, vortex resonance, galloping, interference galloping, and flutter. The

mathematical models describing vibration induction are presented. Possible measures against dangerous flow induced vibrations are discussed. ESA

N89-24279# Oxford Univ. (England). Dept. of Engineering Science.
EXPERIMENTAL TECHNIQUES IN UNSTEADY FLOWS
M. L. G. Oldfield *In* VKI, Unsteady Aerodynamics, Volume 1 1988 70 p (For primary document see N89-24276 18-02)
Avail: NTIS HC A20/MF A01

A user's guide to techniques used in making experimental measurements in unsteady aerodynamics is presented. Examples from turbomachinery flow research are described. The subjects include wind tunnel measurements, intrusive measurements, surface measurements, optical techniques, data acquisition, and data processing. ESA

N89-24280# Office National d'Etudes et de Recherches Aerospatiales, Toulouse (France). Dept. of Aerothermodynamics.
EFFECTS OF UNSTEADINESS ON TURBULENT BOUNDARY LAYERS
J. Cousteix and R. Houdeville *In* VKI, Unsteady Aerodynamics, Volume 1 1988 82 p (For primary document see N89-24276 18-02)
Avail: NTIS HC A20/MF A01

The experimental analysis of oscillating turbulent flat plate boundary layers is presented. Effects of adverse pressure gradient on oscillating turbulent boundary layers is also described. Numerical methods for the calculation of unsteady boundary layers are discussed. ESA

N89-24281# Von Karman Inst. for Fluid Dynamics, Rhode-Saint-Genese (Belgium).
UNSTEADY AERODYNAMICS, VOLUME 2
1988 352 p Lecture series held in Rhode-Saint-Genese, Belgium, 18-22 Apr. 1988
(VKI-1988-07-Vol-2; ETN-89-94557) Avail: NTIS HC A16/MF A01

Computational flow dynamics and unsteady flows were discussed. The state of the art and the available calculation procedures are reviewed. For individual titles, see N89-24282 through N89-24284.

N89-24282# Ecole Nationale Superieure de Mecanique, Nantes (France).
NUMERICAL METHODS FOR UNSTEADY FLOWS
Y. Lecointe and J. Piquet *In* VKI, Unsteady Aerodynamics, Volume 2 1988 217 p (For primary document see N89-24281 18-02)
Avail: NTIS HC A16/MF A01

Physical flow models are described in order of decreasing complexity, and typical results illustrating progress for the various flow modelling levels are discussed. Significant efforts are devoted to understanding the effects of equational level, computational grid, boundary conditions, and interactive viscous modeling. Progress in solution algorithms is detailed. Computational aeroelastic analysis shows its capability to predict complete transonic flutter boundaries for wings, including significant transonic dip features. ESA

N89-24283# Ecole Nationale Superieure de Mecanique, Nantes (France).
COMPUTATION OF THE CHARACTERISTICS OF THE WAKE PAST AN OSCILLATING CYLINDER
Y. Lecointe and J. Piquet *In* VKI, Unsteady Aerodynamics, Volume 2 1988 15 p (For primary document see N89-24281 18-02)
Avail: NTIS HC A16/MF A01

The numerical solution of the unsteady Navier-Stokes equation is used to investigate the vortex shedding characteristics behind a circular cylinder immersed in a uniform stream, and performing either superimposed in line or transverse forced oscillations of a given reduced amplitude, or transversely constrained free oscillations. Mode competition is clearly demonstrated for nonharmonic excitations. Characteristics of the lock-on phenomena are also studied. ESA

N89-24284*# National Aeronautics and Space Administration. Langley Research Center, Hampton, VA.
COMPUTATIONAL UNSTEADY AERODYNAMICS FOR LIFTING SURFACES
John W. Edwards *In* VKI, Unsteady Aerodynamics, Volume 2 1988 120 p (For primary document see N89-24281 18-02)
Avail: NTIS HC A16/MF A01 CSCL 01A

Two dimensional problems are solved using numerical techniques. Navier-Stokes equations are studied both in the vorticity-stream function formulation which appears to be the optimal choice for two dimensional problems, using a storage approach, and in the velocity pressure formulation which minimizes the number of unknowns in three dimensional problems. Analysis shows that compact centered conservative second order schemes for the vorticity equation are the most robust for high Reynolds number flows. Serious difficulties remain in the choice of turbulent models, to keep reasonable CPU efficiency. ESA

N89-24285*# National Aeronautics and Space Administration. Ames Research Center, Moffett Field, CA.
EXPERIMENTAL AERODYNAMIC CHARACTERISTICS OF A JOINED-WING RESEARCH AIRCRAFT CONFIGURATION
Stephen C. Smith and Ronald K. Stonum Apr. 1989 100 p (NASA-TM-101083; A-89074; NAS 1.15:101083) Avail: NTIS HC A05/MF A01 CSCL 01A

A wind-tunnel test was conducted at Ames Research Center to measure the aerodynamic characteristics of a joined-wing research aircraft (JWRA). This aircraft was designed to utilize the fuselage and engines of the existing NASA AD-1 aircraft. The JWRA was designed to have removable outer wing panels to represent three different configurations with the interwing joint at different fractions of the wing span. A one-sixth-scale wind-tunnel model of all three configurations of the JWRA was tested in the Ames 12-Foot Pressure Wind Tunnel to measure aerodynamic performance, stability, and control characteristics. The results of these tests are presented. Longitudinal and lateral-directional characteristics were measured over an angle of attack range of -7 to 14 deg and over an angle of sideslip range of -5 to +2.5 deg at a Mach number of 0.35 and a Reynolds number of 2.2x10(6)/ft. Various combinations of deflected control surfaces were tested to measure the effectiveness and impact on stability of several control surface arrangements. In addition, the effects on stall and post-stall aerodynamic characteristics from small leading-edge devices called vortilons were measured. The results of these tests indicate that the JWRA had very good aerodynamic performance and acceptable stability and control throughout its flight envelope. The vortilons produced a profound improvement in the stall and post-stall characteristics with no measurable effects on cruise performance. Author

N89-24286 Virginia Polytechnic Inst. and State Univ., Blacksburg.
ANALYSIS OF THE WAKE BEHIND A PROPELLER USING THE FINITE ELEMENT METHOD WITH A TWO-EQUATION TURBULENCE MODEL Ph.D. Thesis
Seung Joo Kim 1988 219 p
Avail: Univ. Microfilms Order No. DA8904992

The finite element in the form of the weak Galerkin formulation with the penalty function method was applied to several problems of axisymmetric turbulent flows including flow through a sudden pipe expansion, the stern region flow of a slender body, and flows past ducted and nonducted propellers in action. The coupled set of the Reynolds time-averaged Navier-Stokes equations and two turbulence transport equations for the turbulent kinetic energy and its rate of dissipation was solved by L/U decomposition and successive substitution with relaxation. An existing finite element code was modified with a low Reynolds number form for an appropriate treatment of wall influences on turbulence transport, which produces a better solution and provides an easier imposition

of boundary conditions by solving up to wall with no slip boundary conditions. The two-equation turbulence model with the wall modification was first successfully tested by solving the turbulent flow through a sudden pipe expansion. The numerical simulation of the stern region flow of a streamlined body resulted in an excellent agreement with the measured data in terms of the mean-flow and turbulence quantities. Turbulent shear flow past a propeller at the rear end of the same slender body, modeled by an actuator disk, were successfully solved at two rotational speeds, self-propelled and 100 percent over-thrusted, using the same two-equation model. And finally, comparisons of the wake behind a propeller were made for the self-propelled conditions of a ducted and nonducted propeller on the same streamlined body. Author

N89-24287*# Amtec Engineering, Inc., Bellevue, WA.
A ZONAL METHOD FOR MODELING POWERED-LIFT AIRCRAFT FLOW FIELDS
D. W. Roberts Mar. 1989 68 p
(Contract NAS2-12801)
(NASA-CR-177521; NAS 1.26:177521) Avail: NTIS HC A04/MF A01 CSCL 01A

A zonal method for modeling powered-lift aircraft flow fields is based on the coupling of a three-dimensional Navier-Stokes code to a potential flow code. By minimizing the extent of the viscous Navier-Stokes zones the zonal method can be a cost effective flow analysis tool. The successful coupling of the zonal solutions provides the viscous/inviscid interations that are necessary to achieve convergent and unique overall solutions. The feasibility of coupling the two vastly different codes is demonstrated. The interzone boundaries were overlapped to facilitate the passing of boundary condition information between the codes. Routines were developed to extract the normal velocity boundary conditions for the potential flow zone from the viscous zone solution. Similarly, the velocity vector direction along with the total conditions were obtained from the potential flow solution to provide boundary conditions for the Navier-Stokes solution. Studies were conducted to determine the influence of the overlap of the interzone boundaries and the convergence of the zonal solutions on the convergence of the overall solution. The zonal method was applied to a jet impingement problem to model the suckdown effect that results from the entrainment of the inviscid zone flow by the viscous zone jet. The resultant potential flow solution created a lower pressure on the base of the vehicle which produces the suckdown load. The feasibility of the zonal method was demonstrated. By enhancing the Navier-Stokes code for powered-lift flow fields and optimizing the convergence of the coupled analysis a practical flow analysis tool will result. Author

03 AIR TRANSPORTATION AND SAFETY

Includes passenger and cargo air transport operations; and aircraft accidents.

For related information see also *16 Space Transportation* and *85 Urban Technology and Transportation.*

N89-24288# Federal Aviation Administration, Atlantic City, NJ. Technical Center.
A COMPUTER SIMULATION STUDY OF LIQUID WATER CONTENT ADJUSTMENT BASED ON ICING CLOUD HORIZONTAL EXTENT
James T. Riley, James Booth, and Douglas Ferguson Dec. 1988 117 p
(DOT/FAA/CT-TN89/3) Avail: NTIS HC A06/MF A01

The analytical airfoil ice accretion prediction code LEWICE was used to determine resultant ice shapes on an airfoil when the cloud horizontal extent (CHE) - liquid water content (LWC) factor curve, as given in the Federal Aviation Regulations (FAR's), is applied for related icing conditions of LWC and CHE extent. LEWICE predicts the shape of an ice accretion that would form on an unprotected airfoil (or other 2-dimensional geometry) when exposed to icing conditions. Although LEWICE is not validated for all purposes, it can be usefully employed in a comparative study of this type to study trends in ice accretion shape as ambient conditions are systematically varied. Results must be interpreted carefully in the context of the limitations of the ice accretion model assumed by LEWICE. For the conditions included in this study, LEWICE predicts that as LWC is decreased and CHE is increased by application of the CHE-LWC factor curve of the FAR's, a larger and more severe ice shape will accrete on an unprotected airfoil. Author

N89-24289# Army Aviation Engineering Flight Activity, Edwards AFB, CA.
PRELIMINARY AIRWORTHINESS EVALUATION OF MODIFIED SECOND-GENERATION PNEUMATIC BOOT DEICING SYSTEM ON A JUH-1H Final Report, 26 Oct. 1987 - 7 Apr. 1988
James D. Brown, Charles E. Cassil, and Michael K. Herbst Oct. 1988 62 p
(AD-A206255; USAAEFA-87-08) Avail: NTIS HC A04/MF A01 CSCL 08/12

The U.S. Army Aviation Engineering Flight Activity conducted a Preliminary Airworthiness Evaluation of a modified second-generation Pneumatic Boot Deicing System (PBDS) on a JUH-1H helicopter. This consisted of a structural loads survey, level flight performance evaluation, and a qualitative handling qualities evaluation. Twelve flights were conducted for a total of 7.8 productive flight hours. Rotor system structural loads were generally lower than those reported for the unmodified second-generation PBDS. With the PBDS inflated, main rotor pitch link load reached the endurance limit at 100 knots indicated airspeed in level flight. Power required in level flight was less than or equal to power required by the unmodified second-generation PBDS. Inflating the PBDS generated moderate right yaw rates and engine torque rises as great as eight pounds per square inch. One previously identified shortcoming, the aircraft response to PBDS activation during level flight, still exists. GRA

N89-24290*# National Aeronautics and Space Administration. Ames Research Center, Moffett Field, CA.
DESIGN OF AUTOMATED SYSTEM FOR MANAGEMENT OF ARRIVAL TRAFFIC
Heinz Erzberger and William Nedell (San Jose State Univ., CA.) Jun. 1989 50 p Original contains color illustrations
(NASA-TM-102201; A-89116; NAS 1.15:102201) Avail: NTIS HC A03/MF A01 CSCL 17G

The design of an automated air traffic control system based on a hierarchy of advisory tools for controllers is described. Compatibility of the tools with the human controller, a key objective of the design, is achieved by a judicious selection of tasks to be automated and careful attention to the design of the controller system interface. The design comprises three interconnected subsystems referred to as the Traffic Management Advisor, the Descent Advisor, and the Final Approach Spacing Tool. Each of these subsystems provides a collection of tools for specific controller positions and tasks. The design of two of these tools, the Descent Advisor, which provides automation tools for managing descent traffic, and the Traffic Management Advisor, which generates optimum landing schedules is focused on. The algorithms, automation modes, and graphical interfaces incorporated in the design are described. Author

N89-24366# Aerospatiale, Cannes La Bocca (France).
HERMES ESCAPE SYSTEM
J. Colrat, H. P. Nguyen, and H. Hirsch *In* ESA, International Symposium on Europe in Space: The Manned Space System Oct. 1988 p 269-274 (For primary document see N89-24335 18-12)
Copyright Avail: NTIS HC A99/MF A01; ESA Publications Div., ESTEC, Noordwijk, Netherlands, 80 Dutch guilders

04 AIRCRAFT COMMUNICATIONS AND NAVIGATION

Includes digital and voice communication with aircraft; air navigation systems (satellite and ground based); and air traffic control.

For related information see also *17 Space Communications, Spacecraft Communications, Command and Tracking* and *Communications and Radar.*

N89-24291# Federal Aviation Administration, Washington, DC. Technical Center.

AN OPERATIONAL DEMONSTRATION AND ENGINEERING FLIGHT TEST OF THE MICROWAVE LANDING SYSTEM ON RUNWAY 22L AT CHICAGO'S MIDWAY AIRPORT Technical Note, Sep. 1988

Clifford W. Mackin, Edmund Zyzys, and Robert H. Pursel Oct. 1988 41 p

(Contract FAA-T0604-F)

(DOT/FAA/CT-TN88/42) Avail: NTIS HC A03/MF A01

At the request of the Great Lakes Region, the Federal Aviation Administration (FAA) Technical Center conducted an operational demonstration of Microwave Landing System (MLS) on runway 22L at Chicago's Midway Airport. The MLS test bed installed at the FAA Technical Center was transported to, and temporarily installed at Chicago's Midway Airport. Three engineering flighttests were conducted on August 27, 28, and 29, 1988, to verify and characterize system operation. On August 30, three demonstration flights were conducted for the aviation industry, the media, and FAA personnel. Three profiles were designed for these flights to demonstrate the operational capabilities of MLS. The operational capability of MLS was successfully demonstrated and the MLS signal in space met Category 2 instrument landing system (ILS) tolerances. Author

N89-24292# Federal Aviation Administration, Atlantic City, NJ.

CONTROLLER EVALUATION OF INITIAL DATA LINK AIR TRAFFIC CONTROL SERVICES. VOLUME 1: MINI STUDY 2 Final Report

Nicholas J. Talotta, Clark Shingledecker, Thomas Zurinskas, Karol Kerns, and Henry R. Marek Mar. 1989 37 p

(DOT/FAA/CT-89/14-Vol-1) Avail: NTIS HC A03/MF A01

The results of Mini Study 2 are detailed. This Mini Study was conducted at the Federal Aviation Administration (FAA) Technical Center utilizing the Data Link test bed. Initial Data Link air traffic control services were evaluated under part task simulation conditions in order to identify service delivery methods which optimize controller acceptance, performance, and workload. Author

N89-24293*# National Aeronautics and Space Administration. Langley Research Center, Hampton, VA.

B-737 FLIGHT TEST OF CURVED-PATH AND STEEP-ANGLE APPROACHES USING MLS GUIDANCE Technical Report, Apr. 1982 - Feb. 1986

J. R. Branstetter (Federal Aviation Administration, Hampton, VA.) and W. F. White Apr. 1989 188 p

(NASA-TM-101521; NAS 1.15:101521; FAA-PM-86/20) Avail: NTIS HC A09/MF A01 CSCL 17G

A series of flight tests were conducted to collect data for jet transport aircraft flying curved-path and steep-angle approaches using Microwave Landing System (MLS) guidance. During the test, 432 approaches comprising seven different curved-paths and four glidepath angles varying from 3 to 4 degrees were flown in NASA Langley's Boeing 737 aircraft (Transport Systems Research Vehicle) using an MLS ground station at the NASA Wallops Flight Facility. Subject pilots from Piedmont Airlines flew the approaches using conventional cockpit instrumentation (flight director and Horizontal Situation Indicator (HSI). The data collected will be used by FAA procedures specialists to develop standards and criteria for designing MLS terminal approach procedures (TERPS). The use of flight simulation techniques greatly aided the preliminary stages of approach development work and saved a significant amount of costly flight time. This report is intended to complement a data report to be issued by the FAA Office of Aviation Standards which will contain all detailed data analysis and statistics. Author

N89-24294# Federal Aviation Administration, Washington, DC. Office of Aviation Medicine.

A COMPARISON OF DETECTION EFFICIENCY ON AN AIR TRAFFIC CONTROL MONITORING TASK WITH AND WITHOUT COMPUTER AIDING

Richard I. Thackray and R. M. Touchstone Jan. 1989 12 p

(AD-A206422; DOT/FAA/AM-89/1) Avail: NTIS HC A03/MF A01 CSCL 17/7

Future levels of air traffic control automation plan to incorporate computer aiding features designed to alert the controller to upcoming problem situations by displaying information that will identify the situation and suggest possible solutions. Concerns have been expressed that reliance on such aids may lead to a reduced capacity to detect and respond to infrequent failures of the automation. The present study employed a simulated ATC monitoring task with a computer-aiding feature designed to detect possible aircraft conflict situations. The ability of subjects to detect occasional failures of the computer-aiding feature in detecting problem situations was compared with detection efficiency for these same situations when no computer aiding was provided. The hypothesis that alertness would be lower and detection less efficient with computer aiding than when no aiding was employed was not supported. Applications and limitations of the findings to the problem of complacency in automated systems are discussed. GRA

N89-24295# Deutsche Forschungs- und Versuchsanstalt fuer Luft- und Raumfahrt, Brunswick (Germany, F.R.). Inst. fuer Flugfuehrung.

IMAGE SIGNAL PROCESSING FOR FLIGHT GUIDANCE

Sep. 1988 315 p Partly in ENGLISH and GERMAN Colloquium held in Brunswick, Fed. Republic of Germany, 30-31 May 1988; sponsored by DFVLR

(DFVLR-Mitt-88-32; ISSN-0176-7739; ETN-89-94645) Avail: NTIS HC A14/MF A01; DFVLR, VB-PL-DO, Postfach 40 60 58, 5000 Cologne, Fed. Republic of Germany, DM 108

Scene reconstruction for image sequences, and aspects of image communication in air-to-ground systems are discussed. A displacement-estimation technique for aerial video scenes, and a parametric displacement estimation scheme for aerial images were studied. Terrain-aided flight navigation in near-Earth sections, and landscape-related position finding for flying systems are outlined. The determination of reference trajectories for testing navigation aids using an onboard CCD camera was investigated. The transformation of real and virtual objects into a virtual, visual environment, and the display of flight guidance information in the aircraft cockpit are discussed. Status and trends of technological image processing possibilities are outlined. A versatile flight experiment system for image processing is presented. For individual titles, see N89-24296 through N89-24307.

N89-24296# Deutsche Forschungs- und Versuchsanstalt fuer Luft- und Raumfahrt, Brunswick (Germany, F.R.). Inst. fuer Flugfuehrung.

IMAGE SIGNAL PROCESSING FOR FLIGHT GUIDANCE: OVERVIEW AND INTRODUCTION TO THE MAIN TOPICS [BILDSIGNALVERARBEITUNG FUER AUFGABEN DER FLUGFUEHRUNG. UEBERBLICK UND EINFUEHRUNG IN DIE THEMENSCHWERPUNKTE]

A. Becker *In its* Image Signal Processing for Flight Guidance Sep. 1988 p 9-24 In GERMAN; ENGLISH summary (For primary document see N89-24295 18-04)

Avail: NTIS HC A14/MF A01; DFVLR, VB-PL-DO, Postfach 40 60 58, 5000 Cologne, Fed. Republic of Germany, DM 108

The main applications of image signal processing in flight guidance are introduced, the main topics are defined, and connections between these topics are pointed out. Image signal coding for perturbation-resistant air-to-ground communication;

image aided navigation; image synthesis; and stationary and flight-fit experimental arrangements are discussed. ESA

N89-24297# Hamburg Univ. (Germany, F.R.). Fachbereich Informatik.

SCENE RECONSTRUCTION FOR IMAGE SEQUENCES c74

B. Neumann and R. Sprengel *In* DFVLR, Image Signal Processing for Flight Guidance Sep. 1988 p 25-58 In GERMAN; ENGLISH summary (For primary document see N89-24295 18-04)

Avail: NTIS HC A14/MF A01; DFVLR, VB-PL-DO, Postfach 40 60 58, 5000 Cologne, Fed. Republic of Germany, DM 108

The state of the art in the field of motion analysis of image sequences is surveyed. The basic framework of a vision system is discussed; all important subtasks of a vision system can be incorporated into this framework. Motion analysis can be considered as a two-step process encompassing motion measurement and motion interpretation. The state of the art is discussed by approching motion analysis as a scene reconstruction task. ESA

N89-24298# Deutsche Forschungs- und Versuchsanstalt fuer Luft- und Raumfahrt, Brunswick (Germany, F.R.). Inst. fuer Flugfuehrung.

ASPECTS OF IMAGE COMMUNICATION IN AIR-TO-GROUND SYSTEMS c32

R. Lippmann *In its* Image Signal Processing for Flight Guidance Sep. 1988 p 59-91 In GERMAN; ENGLISH summary (For primary document see N89-24295 18-04)

Avail: NTIS HC A14/MF A01; DFVLR, VB-PL-DO, Postfach 40 60 58, 5000 Cologne, Fed. Republic of Germany, DM 108

The fundamental methods for applying image sequence information in support of reconnaissance and navigation are introduced. For transmissions subject to jamming, the reduction of the bit rate by differential pulse code modulation in combination with reduced frame rates proves to be effective in minimizing the effects of jamming. This technique allows reconstruction of continuous scene motion by motion-adaptive frame interpolation at the receiver. Aspects of the required frame matching procedure and their relationship to the corresponding procedures required in a navigational situation are outlined. The application of the frame matching procedure for the location of moving objects and stereoscopic scene presentation is explained. ESA

N89-24299# Deutsche Forschungs- und Versuchsanstalt fuer Luft- und Raumfahrt, Brunswick (Germany, F.R.). Inst. fuer Flugfuehrung.

INVESTIGATIONS OF A DISPLACEMENT-ESTIMATION TECHNIQUE FOR AERIAL VIDEO SCENES c35

H. Doergeloh *In its* Image Signal Processing for Flight Guidance Sep. 1988 p 93-121 In GERMAN; ENGLISH summary (For primary document see N89-24295 18-04)

Avail: NTIS HC A14/MF A01; DFVLR, VB-PL-DO, Postfach 40 60 58, 5000 Cologne, Fed. Republic of Germany, DM 108

Global models for image registration were compared with regard to accuracy in several sensing situations and realization aspects, and a displacement-estimation method based on a block-matching approach was investigated and applied to typical aerial scenes. Global models for image registration and image transformation were examined for processing of aerial scenes at a ground-based receiver, especially for image interpolation, image rectification, generation of stereo image pairs or for navigation support. The parameters necessary for these models can be determined by displacement estimation methods. The results of simulations with real aerial video scenes show that for scenes with sufficient overlapping in the image content, a reliable displacement estimation is possible and that even simplified global models with realization advantages are suitable for image registration. ESA

N89-24300# Deutsche Forschungs- und Versuchsanstalt fuer Luft- und Raumfahrt, Brunswick (Germany, F.R.). Inst. for Flight Guidance.

STUDY OF A PARAMETRIC DISPLACEMENT ESTIMATION SCHEME WITH APPLICATION IN AERIAL IMAGES c35

K. Rose *In its* Image Signal Processing for Flight Guidance Sep. 1988 p 123-138 (For primary document see N89-24295 18-04)

Avail: NTIS HC A14/MF A01; DFVLR, VB-PL-DO, Postfach 40 60 58, 5000 Cologne, Fed. Republic of Germany, DM 108

An algorithm, combining a frame-differencing technique with a six-parameter affine model of motion, was applied to estimate the displacement between image frames for low frame rate aerial images. The algorithm uses points on displaced gray-level edges to estimate the local apparent horizontal and vertical displacements which are then used to determine the global motion parameters. Real video sequences were used to observe the effects of scene content, flight parameters, frame transmission rate, image coding procedures, and channel errors for simulated transmission. The algorithm produces correct displacement values if the initial estimate is within 20 pixels of the correct displacement, and is robust with respect to the image coding procedures and channel errors used for these experiments. The matching errors may be attributed to the scenes with significant edges, low contrast features or flight parameters for which the motion model is not adequate to match the actual motion. ESA

N89-24301# Deutsche Forschungs- und Versuchsanstalt fuer Luft- und Raumfahrt, Brunswick (Germany, F.R.). Inst. fuer Flugfuehrung.

BORDAUTONOMOUS TERRAIN AIDED FLIGHT NAVIGATION IN HEIGHT SECTIONS CLOSE TO TERRAIN SURFACE

F. Knabe *In its* Image Signal Processing for Flight Guidance Sep. 1988 p 139-160 In GERMAN; ENGLISH summary (For primary document see N89-24295 18-04)

Avail: NTIS HC A14/MF A01; DFVLR, VB-PL-DO, Postfach 40 60 58, 5000 Cologne, Fed. Republic of Germany, DM 108

Aspects of the board-autonomous acquisition of information are outlined using research in the field of elevation-based methods and a research project for image-supported navigation. The emphasis was in both cases on the terrain surface models. In the near-Earth regions, board-autonomous information can be obtained by comparing sensorically determined terrain features with onboard stored reference material. Elevation-oriented methods use the feature terrain elevation, while image-oriented methods use radiation emission and reflection of the terrain. ESA

N89-24302# Messerschmitt-Boelkow-Blohm G.m.b.H., Bremen (Germany, F.R.). Marine- und Sondertechnik.

LANDSCAPE-RELATED POSITION FINDING FOR FLYING SYSTEMS

W. Hornfeld *In* DFVLR, Image Signal Processing for Flight Guidance Sep. 1988 p 161-180 In GERMAN; ENGLISH summary (For primary document see N89-24295 18-04)

Avail: NTIS HC A14/MF A01; DFVLR, VB-PL-DO, Postfach 40 60 58, 5000 Cologne, Fed. Republic of Germany, DM 108

Systems/procedures for autonomous or interactive updating of onboard navigation systems using landscape characteristics are described. The Low Altitude Terrain Aided Navigation system permits the accurate finding of the flying system's own position by measuring the overflown terrain and correlation with a height model. Complete two-dimensional images are compared using the scene correlator. The contour extraction procedure and the motion vector field analysis procedure use extracted landscape information and data gained from the image, respectively. The digital card display system is a unit for interactive correlation of digital maps and sensor images of the overflown terrain. ESA

N89-24303# Deutsche Forschungs- und Versuchsanstalt fuer Luft- und Raumfahrt, Brunswick (Germany, F.R.). Inst. fuer Flugfuehrung.

DETERMINATION OF REFERENCE TRAJECTORIES FOR TESTING NAVIGATION AIDS USING AN ONBOARD CCD CAMERA

Ulrich Brokof and H.-D. Schwind (Bundesanstalt fuer Flugsicherung, Klosterlechfeld, Germany, F.R.) *In its* Image Signal Processing for Flight Guidance Sep. 1988 p 181-215 In GERMAN; ENGLISH summary (For primary document see N89-24295

18-04)
Avail: NTIS HC A14/MF A01; DFVLR, VB-PL-DO, Postfach 40 60 58, 5000 Cologne, Fed. Republic of Germany, DM 108

A flight inspection system was developed. A solid state camera onboard the test aircraft was used to make the flight inspection system independent of ground stations. In testing an instrument landing system the camera detects the field of white stripes on both ends of the runway. The flight trajectory generated by velocity data of an inertial navigation system is aided by distance data and additionally updated with the precise position information of the video system. Since this information is only available at the end of a measuring flight, the final computation is performed offline (but during the flight) by backward smoothing. The obtainable results are demonstrated by simulation calculations. ESA

N89-24304# Deutsche Forschungs- und Versuchsanstalt fuer Luft- und Raumfahrt, Brunswick (Germany, F.R.). Inst. fuer Flugfuehrung.
TRANSFORMATION OF REAL AND VIRTUAL OBJECTS INTO A VIRTUAL, VISUAL ENVIRONMENT **c35**
R. Beyer *In its* Image Signal Processing for Flight Guidance Sep. 1988 p 217-247 In GERMAN; ENGLISH summary (For primary document see N89-24295 18-04)
Avail: NTIS HC A14/MF A01; DFVLR, VB-PL-DO, Postfach 40 60 58, 5000 Cologne, Fed. Republic of Germany, DM 108

The synthesis of dynamic images for control and surveillance purposes is discussed, with emphasis on the transformation of real and virtual objects into a user-adapted representation space. The acceptance and utilization problems of complex dynamic systems can be alleviated if a pictorial presentation of the system state and the user-accessible system parameters is employed. Methods to mathematically model the objects to be displayed, to transform their pictorial representation from object space to display space, and to visualize the objects therein real time are discussed. Applications are in the field of guidance and control of aerospace vehicles, air traffic systems, teleoperations, and other dynamic processes which require an interaction with man. ESA

N89-24305# Deutsche Forschungs- und Versuchsanstalt fuer Luft- und Raumfahrt, Brunswick (Germany, F.R.). Inst. fuer Flugfuehrung.
DISPLAY OF FLIGHT GUIDANCE INFORMATION IN THE AIRCRAFT COCKPIT **c06**
H.-D. Schenk *In its* Image Signal Processing for Flight Guidance Sep. 1988 p 249-266 In GERMAN; ENGLISH summary (For primary document see N89-24295 18-04)
Avail: NTIS HC A14/MF A01; DFVLR, VB-PL-DO, Postfach 40 60 58, 5000 Cologne, Fed. Republic of Germany, DM 108

The application of computer generated electronic flight displays is discussed. It became the standard in cockpits since the introduction of the Airbus 310. The technical problems of the use of cathode ray tubes in an aircraft environment are described, and solutions for the display of cockpit information to the pilot are described. Further developments of the display technology leads to cockpit concepts using panoramic displays and the virtual presentation of cockpit control elements and the outside world. ESA

N89-24306# VTE, Brunswick (Germany, F.R.). Digital Video.
STATUS AND TRENDS OF TECHNOLOGICAL IMAGE PROCESSING POSSIBILITIES **c35**
W. Eggersluess *In* DFVLR, Image Signal Processing for Flight Guidance Sep. 1988 p 267-293 In GERMAN; ENGLISH summary (For primary document see N89-24295 18-04)
Avail: NTIS HC A14/MF A01; DFVLR, VB-PL-DO, Postfach 40 60 58, 5000 Cologne, Fed. Republic of Germany, DM 108

The state of the art and foreseeable developments in computer architecture, image memories, and devices for general signal processing are reviewed. Image processing imposes very high demands on the processing power installed in the system. Its progress therefore strongly depends on the developments in computer science and large scale integration. The development of highly integrated semiconductor elements becomes increasingly more complex and capital-intensive and hence requires larger production volumes in order to remain economical. ESA

N89-24307# Deutsche Forschungs- und Versuchsanstalt fuer Luft- und Raumfahrt, Brunswick (Germany, F.R.). Inst. fuer Flugfuehrung.
A VERSATILE FLIGHT EXPERIMENT SYSTEM FOR IMAGE PROCESSING **c32**
P. Schulz *In its* Image Signal Processing for Flight Guidance Sep. 1988 p 295-311 In GERMAN; ENGLISH summary (For primary document see N89-24295 18-04)
Avail: NTIS HC A14/MF A01; DFVLR, VB-PL-DO, Postfach 40 60 58, 5000 Cologne, Fed. Republic of Germany, DM 108

An experimental system for reconnaissance is presented, with a view to the investigation and optimization of different methods for data reduction, jamming-resistant transmission, image processing, image display, and data storage. Concerning video data reduction three methods were realized: reduction of frame rate, reduction of geometrical resolution, and differential pulse code modulation. By combining these methods the original data rate of 50 Mbit/s is reduced to values between 1024 and 64 kbit/s depending on the jamming conditions. Directional antennas, spread spectrum modulation, forward error correction, and automatic repetition upon request are used to achieve a jamming-resistant transmission. ESA

05 AIRCRAFT DESIGN, TESTING AND PERFORMANCE

Includes aircraft simulation technology.

For related information see also *18 Spacecraft Design, Testing and Performance* and *39 Structural Mechanics*.For land transportation vehicles see *85 Urban Technology and Transportation.*

N89-24308*# National Aeronautics and Space Administration. Langley Research Center, Hampton, VA.
AEROSERVOELASTIC MODELING AND APPLICATIONS USING MINIMUM-STATE APPROXIMATIONS OF THE UNSTEADY AERODYNAMICS
Sherwood H. Tiffany and Mordechay Karpel (Technion - Israel Inst. of Tech., Haifa.) Apr. 1989 13 p Presented at the AIAA 30th Structures, Structural Dynamics and Materials Conference, Mobile, AL, 3-5 Apr. 1989 Previously announced in IAA as A89-30678
(NASA-TM-101574; NAS 1.15:101574) Avail: NTIS HC A03/MF A01 CSCL 01C

Various control analysis, design, and simulation techniques for aeroelastic applications require the equations of motion to be cast in a linear time-invariant state-space form. Unsteady aerodynamics forces have to be approximated as rational functions of the Laplace variable in order to put them in this framework. For the minimum-state method, the number of denominator roots in the rational approximation. Results are shown of applying various approximation enhancements (including optimization, frequency dependent weighting of the tabular data, and constraint selection) with the minimum-state formulation to the active flexible wing wind-tunnel model. The results demonstrate that good models can be developed which have an order of magnitude fewer augmenting aerodynamic equations more than traditional approaches. This reduction facilitates the design of lower order control systems, analysis of control system performance, and near real-time simulation of aeroservoelastic phenomena. Author

N89-24309# Army Aviation Engineering Flight Activity, Edwards AFB, CA.
LOSS OF TAIL ROTOR EFFECTIVENESS EVALUATION OF THE OH-58C HELICOPTER WITH DIRECTIONAL SAS (STABILITY AUGMENTATION SYSTEM) Final Report, 23 Jun. - 25 Sep. 1987
Frederick W. Stellar, James D. Brown, Michael K. Herbst,

Christopher P. Butler, and Timothy Hathorn Aug. 1988 297 p (AD-A206181; USAAEFA-86-22) Avail: NTIS HC A13/MF A01 CSCL 01/3

The U.S. Army Aviation Engineering Flight Activity conducted a loss of tail rotor effectiveness (LTE) evaluation of the JOH-58C. The JOH-58C configuration includes a directional stability augmentation system (SAS) manufactured by the SFENA Corporation, the larger-diameter tail rotor, and the improved engine fuel control. Handling qualities were evaluated at Edwards AFB, California (elevation 2302 feet). Twenty-eight flights were conducted for a total of 26.7 productive flight test hours. Primary emphasis of the evaluation was to evaluate the handling qualities of the JOH-58C in comparison to the standard OH-58C. The limited authority SAS (7 percent of full control travel) will not significantly reduce the conditions conducive to LTE. The overall handling qualities of the JOH-58C were moderately improved compared to the standard OH-58C. The concept of a SAS which damps uncommanded yaw rates demonstrated potential for reducing conditions conducive to LTE. However, the limited authority SAS saturated at small yaw rates (deg/sec) and did not significantly reduce the characteristic high yaw rates and moderate yaw attitude excursions observed in the JOH-58C. The JOH-58C exhibited moderate pitch, roll, and yaw excursions at 15 to 25 KTAS in azimuths from 240 degrees clockwise to 280 degrees. This characteristic was a shortcoming, upgraded from a deficiency for the standard OH-58C. Five additional shortcomings, of which four were previously identified in the standard OH-58C, were noted.

GRA

N89-24310*# National Aeronautics and Space Administration. Langley Research Center, Hampton, VA.

AN INVESTIGATION OF THE OVERLAP BETWEEN THE STATISTICAL DISCRETE GUST AND THE POWER SPECTRAL DENSITY ANALYSIS METHODS

Boyd Perry, III, Anthony S. Pototzky, and Jessica A. Woods (Planning Research Corp., Hampton, VA.) Apr. 1989 15 p Presented at the AIAA 30th Structures, Structural Dynamics and Materials Conference, Mobile, AL, 3-5 Apr. 1989

(NASA-TM-101571; NAS 1.15:101571) Avail: NTIS HC A03/MF A01 CSCL 01C

The results of a NASA investigation of a claimed Overlap between two gust response analysis methods: the Statistical Discrete Gust (SDG) Method and the Power Spectral Density (PSD) Method are presented. The claim is that the ratio of an SDG response to the corresponding PSD response is 10.4. Analytical results presented for several different airplanes at several different flight conditions indicate that such an Overlap does appear to exist. However, the claim was not met precisely: a scatter of up to about 10 percent about the 10.4 factor can be expected.

Author

N89-24311# Office National d'Etudes et de Recherches Aerospatiales, Paris (France). Direction Scientifique de la Resistance des Structures.

GROUND VIBRATION TEST OF THE FOUDRE A04 TRANSALL AIRCRAFT [ESSAI DE VIBRATIONS AU SOL - PARTIEL - DE L'AVION TRANSALL FOUDRE A04. PROCES-VERBAL 20/7234-PY-382-R]

P. Lubrina Sep. 1988 68 p In FRENCH

(Contract DRET-88-34-001)

(Rept-20/7234-PY-382-R; ETN-89-94528) Avail: NTIS HC A04/MF A01

Ground test are performed to verify the aircraft dynamic behavior after structural modifications done in a study concerning inflight measurements of lightning discharges. The results show that the main vibration modes are not affected by the additions. On the other hand, the proximity of resonant frequency between the new element and some of the structure modes can reduce the fatigue life on the aircraft.

ESA

N89-24312# Swedish Defence Research Establishment, Stockholm.

THE NIGHT AND ADVERSE WEATHER CAPABILITY OF GROUND ATTACK AIRCRAFT

Erik Berglund Jan. 1989 17 p In SWEDISH; ENGLISH summary

(FOA-C-20745-2.5; ISSN-0347-3694; ETN-89-94540) Avail: NTIS HC A03/MF A01

The number of attack aircraft (including helicopters) and bombers that are operational in NATO and WP; the total load capacity of all attack aircraft; and the U.S. inventory of air to surface missiles are discussed. The aircraft are divided into different classes according to their equipment: daylight missions, IR, radar, or IR plus radar. To illustrate the short-term trends, the situation in the U.S. is shown both for 1988 and 1995. Presently there are not many aircraft that are capable of attacking small, nonstationary targets at night. The situation is, however, changing rapidly with the further procurement of FLIR detectors.

ESA

N89-24313*# National Aeronautics and Space Administration. Langley Research Center, Hampton, VA.

AEROSERVOELASTIC WIND-TUNNEL INVESTIGATIONS USING THE ACTIVE FLEXIBLE WING MODEL: STATUS AND RECENT ACCOMPLISHMENTS

Thomas E. Noll, Boyd Perry, III, Sherwood H. Tiffany, Stanley R. Cole, Carey S. Buttrill, William M. Adams, Jr., Jacob A. Houck, S. Srinathkumar, Vivek Mukhopadhyay, and Anthony S. Pototzky (Planning Research Corp., Hampton, VA.) et al Apr. 1989 14 p Presented at the AIAA 30th Structures, Structural Dynamics and Materials Conference, Mobile, AL, 3-5 Apr. 1989

(NASA-TM-101570; NAS 1.15:101570) Avail: NTIS HC A03/MF A01 CSCL 01C

The status of the joint NASA/Rockwell Active Flexible Wing Wind-Tunnel Test Program is described. The objectives are to develop and validate the analysis, design, and test methodologies required to apply multifunction active control technology for improving aircraft performance and stability. Major tasks include designing digital multi-input/multi-output flutter-suppression and rolling-maneuver-load alleviation concepts for a flexible full-span wind-tunnel model, obtaining an experimental data base for the basic model and each control concept and providing comparisons between experimental and analytical results to validate the methodologies. The opportunity is provided to improve real-time simulation techniques and to gain practical experience with digital control law implementation procedures.

Author

N89-24314*# National Aeronautics and Space Administration. Langley Research Center, Hampton, VA.

RECENT ACTIVITIES WITHIN THE AEROSERVOELASTICITY BRANCH AT THE NASA LANGLEY RESEARCH CENTER

Thomas E. Noll, Boyd Perry, III, and Michael G. Gilbert May 1989 11 p Presented at the European Forum on Aeroelasticity and Structural Dynamics, Aachen, Fed. Republic of Germany, 17-19 Apr. 1989

(NASA-TM-101582; NAS 1.15:101582) Avail: NTIS HC A03/MF A01 CSCL 01C

The objective of research in aeroservoelasticity at the NASA Langley Research Center is to enhance the modeling, analysis, and multidisciplinary design methodologies for obtaining multifunction digital control systems for application to flexible flight vehicles. Recent accomplishments are discussed, and a status report on current activities within the Aeroservoelasticity Branch is presented. In the area of modeling, improvements to the Minimum-State Method of approximating unsteady aerodynamics are shown to provide precise, low-order aeroservoelastic models for design and simulation activities. Analytical methods based on Matched Filter Theory and Random Process Theory to provide efficient and direct predictions of the critical gust profile and the time-correlated gust loads for linear structural design considerations are also discussed. Two research projects leading towards improved design methodology are summarized. The first program is developing an integrated structure/control design capability based on hierarchical problem decomposition, multilevel

optimization and analytical sensitivities. The second program provides procedures for obtaining low-order, robust digital control laws for aeroelastic applications. In terms of methodology validation and application the current activities associated with the Active Flexible Wing project are reviewed. Author

N89-24315*# Oklahoma Univ., Norman. School of Aerospace and Mechanical Engineering.
AN INTEGRATED AERODYNAMIC/PROPULSION STUDY FOR GENERIC AERO-SPACE PLANES BASED ON WAVERIDER CONCEPTS Summary Report, May - Sep. 1988
M. L. Rasmussen and George Emanuel 1989 24 p
(Grant NAG1-886)
(NASA-CR-183389; NAS 1.26:183389) Avail: NTIS HC A03/MF A01 CSCL 01C

The design of a unified aero-space plane based on waverider technology is analyzed. The overall aerodynamic design and performance of an aero-space plane are discussed in terms of the forebody, scramjet, and afterbody. Other subjects considered in the study are combustion/nozzle optimization, the idealized tip-to-tail waverider model, and the two-dimensional minimum length nozzle. Charts and graphs are provided to show the results of the preliminary investigations. Author

06 AIRCRAFT INSTRUMENTATION

Includes cockpit and cabin display devices; and flight instruments.

For related information see also *19 Spacecraft Instrumentation* and *35 Instrumentation and Photography.*

N89-24316*# Lockheed Aeronautical Systems Co., Marietta, GA. Dept. of Aeronautical Systems Development.
DIVERTER AI BASED DECISION AID, PHASES 1 AND 2 Final Report
George A. Sexton, Scott J. Bayles, Robert W. Patterson, Duane A. Schulke, and Deborah C. Williams May 1989 134 p
(Contract NAS1-18029)
(NASA-CR-181820; NAS 1.26:181820; LG88ER0116-Ph-1/2)
Avail: NTIS HC A07/MF A01 CSCL 01D

It was determined that a system to incorporate artificial intelligence (AI) into airborne flight management computers is feasible. The AI functions that would be most useful to the pilot are to perform situational assessment, evaluate outside influences on the contemplated rerouting, perform flight planning/replanning, and perform maneuver planning. A study of the software architecture and software tools capable of demonstrating Diverter was also made. A skeletal planner known as the Knowledge Acquisition Development Tool (KADET), which is a combination script-based and rule-based system, was used to implement the system. A prototype system was developed which demonstrates advanced in-flight planning/replanning capabilities. Author

N89-24305# Deutsche Forschungs- und Versuchsanstalt fuer Luft- und Raumfahrt, Brunswick (Germany, F.R.). Inst. fuer Flugfuehrung.
DISPLAY OF FLIGHT GUIDANCE INFORMATION IN THE AIRCRAFT COCKPIT
H.-D. Schenk *In its* Image Signal Processing for Flight Guidance Sep. 1988 p 249-266 In GERMAN; ENGLISH summary (For primary document see N89-24295 18-04)
Avail: NTIS HC A14/MF A01; DFVLR, VB-PL-DO, Postfach 40 60 58, 5000 Cologne, Fed. Republicof Germany, DM 108

07 AIRCRAFT PROPULSION AND POWER

Includes prime propulsion systems and systems components, e.g., gas turbine engines and compressors; and onboard auxilliary power plants for aircraft.

For related information see also *20 Spacecraft Propulsion and Power, 28 Propellants and Fuels,* and *44 Energy Production and Conversion.*

N89-24317# National Aerospace Lab., Tokyo (Japan).
CALCULATION OF SCRAMJET PERFORMANCE
Goro Masuya and Yoshio Wakamatsu Jul. 1988 33 p In JAPANESE; ENGLISH summary
(NAL-TR-987; ISSN-0389-4010) Avail: NTIS HC A03/MF A01

The performance of an airframe-integrated scramjet engine is calculated using a quasi-one-dimensional model. The forebody of the airframe is approximated as a cone. Experimental data correlations are used to estimate pressure recovery and capture area of the inlet. Assuming mixing controlled combustion, NASA's empirical relation for fuel mixing efficiency is employed to give the corresponding combustion efficiency distribution. The calculated results serve as engine data for a flight analysis of a space plane. The analysis is being extended to analyze overall engine cycles including subsystems for engine/airframe cooling and fuel supply. Author

N89-24318*# National Aeronautics and Space Administration. Lewis Research Center, Cleveland, OH.
TRANSIENT FLOW THRUST PREDICTION FOR AN EJECTOR PROPULSION CONCEPT
Colin K. Drummond 1989 10 p Presented at the 25th Joint Propulsion Conference, Monterey, CA, 10-14 Jul. 1989; sponsored by AIAA, ASME, SAE and ASEE
(NASA-TM-102078; E-4838; NAS 1.15:102078; AIAA-89-2906)
Avail: NTIS HC A02/MF A01 CSCL 21E

A method for predicting transient thrust augmenting ejector characteristics is introduced. The analysis blends classic self-similar turbulent jet descriptions with a mixing region control volume analysis to predict transient effects in a new way. Details of the theoretical foundation, the solution algorithm, and sample calculations are given. Author

N89-24319*# National Aeronautics and Space Administration. Lewis Research Center, Cleveland, OH.
A MODEL FOR PREDICTION OF STOVL EJECTOR DYNAMICS
Colin K. Drummond 1989 15 p Presented at the 20th Annual Conference on Modeling and Simulation, Pittsburgh, PA, 4-5 May 1989; cosponsored by the Univ. of Pittsburgh, IEEE and ISA
(NASA-TM-102098; E-4861; NAS 1.15:102098) Avail: NTIS HC A03/MF A01 CSCL 21E

A semi-empirical control-volume approach to ejector modeling for transient performance prediction is presented. This new approach is motivated by the need for a predictive real-time ejector sub-system simulation for Short Take-Off Verticle Landing (STOVL) integrated flight and propulsion controls design applications. Emphasis is placed on discussion of the approximate characterization of the mixing process central to thrust augmenting ejector operation. The proposed ejector model suggests transient flow predictions are possible with a model based on steady-flow data. A practical test case is presented to illustrate model calibration. Author

N89-24320*# National Aeronautics and Space Administration. Lewis Research Center, Cleveland, OH.
TURBOMACHINERY TECHNOLOGY FOR HIGH-SPEED CIVIL FLIGHT
Neal T. Saunders and Arthur J. Glassman 1989 26 p Presented at the 34th International Gas Turbine and Aeroengine Congress and Exposition, Toronto, Ontario, 4-8 Jun. 1989; sponsored by the ASME
(NASA-TM-102092; E-4746; NAS 1.15:102092) Avail: NTIS HC A03/MF A01 CSCL 21E

NASA Lewis' research and technology efforts applicable to turbomachinery for high-speed flight are discussed. The potential benefits and cycle requirements for advanced variable cycle engines and the supersonic throughflow fan engine for a high-speed civil transport application are presented. The supersonic throughflow fan technology program is discussed. Technology efforts in the basic discipline areas addressing the severe operating conditions associated with high-speed flight turbomachinery are reviewed. Included are examples of work in internal fluid mechanics, high-temperature materials, structural analysis, instrumentation and controls. Author

08 AIRCRAFT STABILITY AND CONTROL

Includes aircraft handling qualities; piloting; flight controls; and autopilots.

For related information see also *05 Aircraft Design, Testing and Performance.*

N89-24321# National Aerospace Lab., Tokyo (Japan).
WIND TUNNEL TESTS ON FLUTTER CONTROL OF A HIGH-ASPECT-RATIO CANTILEVERED WING Report No. 1
Jun. 1988 101 p In JAPANESE; ENGLISH summary
(NAL-TR-978; ISSN-0389-4010) Avail: NTIS HC A06/MF A01

Wind tunnel test results obtained on flutter control are presented. The test was conducted in the NAL 5.5 x 6.5 m low-speed wind tunnel. The wing model used in the tests assumes a future type of energy efficient transport. It has two control surfaces, one at the leading edge and the other at the trailing edge. Various control laws based on the Linear Quadratic Gaussian theory were implemented and tested with either control surface after reducing the order of the laws. The results showed a prominent effect of the leading edge control surface on flutter suppression. The maximum increase in flutter speed was 9.7 percent of the violent bending-torsion flutter. For the test, a special device was installed in the wind tunnel to prevent this highly mechanical model from being destroyed, which enabled us to execute very efficient tests. Author

N89-24322# National Aerospace Lab., Tokyo (Japan). Aircraft Aerodynamics Division.
COMPUTATIONAL AND EXPERIMENTAL RESEARCH ON BUFFET PHENOMENA OF TRANSONIC AIRFOILS
Naoki Hirose and Hitoshi Miwa Sep. 1988 22 p Presented at the IUTAM Symposium TRANSSONICUM 3, Goettingen, Fed. Republic of Germany, 24-27 May 1988
(NAL-TR-996T; ISSN-0389-4010) Avail: NTIS HC A03/MF A01

Buffet phenomena on supercritical airfoils were investigated both experimentally and numerically. The experiment was done for NACA0012 and KORN 75-06-12 airfoils using a high-speed Schlieren video tape recorder and pressure transducers. The analysis shows significant effects of the geometries and the Reynolds number. A 2-D N-S code was used to predict these phenomena. The result shows the macro-scale effects of airfoil geometry, Reynolds number and transition. A fine structure of the motion such as the periodic trailing edge pressure history was captured. The basic frequency of the buffet motion agrees well with the experiment. Author

N89-24323*# National Aeronautics and Space Administration. Ames Research Center, Moffett Field, CA.
RESULTS OF AN A109 SIMULATION VALIDATION AND HANDLING QUALITIES STUDY
Michelle M. Eshow, Diego Orlandi, Giovanni Bonaita, and Sergio Barbieri (Italian Air Force Pratica di Mare, Rome.) May 1989 31 p Presented at the 14th European Rotocraft Forum, Milan, Italy, 20-23 Sep. 1988
(NASA-TM-101062; A-88271; NAS 1.15:101062; USAAVSCOM-TR-88-A-002) Avail: NTIS HC A03/MF A01 CSCL 01C

The results for the validation of a mathematical model of the Agusta A109 helicopter, and subsequent use of the model as the baseline for a handling qualities study of cockpit centerstick requirements, are described. The technical approach included flight test, non-realtime analysis, and realtime piloted simulation. Results of the validation illustrate a time- and frequency-domain approach to the model and simulator issues. The final A109 model correlates well with the actual aircraft with the Stability Augmentation System (SAS) engaged, but is unacceptable without the SAS because of instability and response coupling at low speeds. Results of the centerstick study support the current U.S. Army handling qualities requirements for centerstick characteristics. Author

N89-24324*# National Aeronautics and Space Administration. Langley Research Center, Hampton, VA.
RESULTS OF A PARAMETRIC AEROELASTIC STABILITY ANALYSIS OF A GENERIC X-WING AIRCRAFT
Jessica A. Woods, Michael G. Gilbert, and Terrence A. Weisshaar Apr. 1989 10 p Presented at the AIAA 30th Structures, Structural Dynamics and Materials Conference, Mobile, AL, 3-5 Apr. 1989 Previously announced in IAA as A89-30858
(NASA-TM-101572; NAS 1.15:101572) Avail: NTIS HC A02/MF A01 CSCL 01C

This paper discusses the trends in longitudinal dynamic aeroelastic stability of a generic x-wing aircraft model with design parameter variations. X-wing rotor blade sweep angle, ratio of blade mass to total vehicle mass, blade structural stiffness cross-coupling and vehicle center-of-gravity location were parameters considered. The typical instability encountered is body-freedom flutter involving a low frequency interaction of the first elastic mode and the aircraft short period mode. Parametric cases with the lowest static margin consistently demonstrated the highest flutter dynamic pressures. As mass ratio was increased, the flutter boundary decreased. The decrease was emphasized as center-of-gravity location was moved forward. As sweep angle varied, it was observed that the resulting increase in forward-swept blade bending amplitude relative to aft blade bending amplitude in the first elastic mode had a stabilizing effect on the flutter boundary. Finally, small amounts of stiffness cross-coupling in the aft blades increased flutter dynamic pressure. Author

N89-24325# Air Force Inst. of Tech., Wright-Patterson AFB, OH. School of Engineering.
FLIGHT CONTROL SYSTEM FOR THE CRCA (CONTROL RECONFIGURABLE COMBAT AIRCRAFT) USING A COMMAND GENERATOR TRACKER WITH PI (PLUS INTEGRAL) FEEDBACK AND KALMAN FILTER, VOLUME 2 M.S. Thesis
Steven S. Payson Mar. 1989 315 p
(AD-A206202; AFIT/GE/ENG/89M-6-Vol-2) Avail: NTIS HC A14/MF A01 CSCL 01/4

This research develops an integrated software design package useful in the synthesis of CGT/PI/KF control systems, and uses this software package to design and evaluate a longitudinal flight control system for the Control Reconfigurable Combat Aircraft (CRCA). The software package, called CGTPIKF and built with MATRIXX commands, allows for the synthesis and evaluation of a Command Generator Tracker (CGT) which provides inputs to the system and acts as a pre-compensator, and a regulator with proportional plus integral (PI) feedback which forces the system outputs to mimic the model output. The software also allows the incorporation of a Kalman filter for estimation of the system states. Certainty equivalence can be invoked by adopting the LQC assumptions, thereby allowing the Kalman filter to be designed independently of the CGT/PI controller. The total CGT/PI/KF controller can then be evaluated and the design refined. CGTIKF is an interactive, menu driven CAD package which can be used in the development of any CGT/PI/KF control system, regardless of application. GRA

N89-24326 Virginia Polytechnic Inst. and State Univ., Blacksburg.
NUMERICAL SIMULATION OF FEEDBACK CONTROL OF AERODYNAMIC CONFIGURATIONS IN STEADY AND UNSTEADY GROUND EFFECTS Ph.D. Thesis
Abdullah Othman Nuhait 1988 188 p
Avail: Univ. Microfilms Order No. DA8904960

A general numerical simulation of closely coupled lifting surfaces in steady and unsteady ground effects was developed. This model was coupled with the equations of motion to simulate aerodynamic-dynamic interaction. The resulting model was then coupled with a feedback-control law to form a general nonlinear unsteady numerical simulation of control of an aircraft in and out of ground effect. The aerodynamic model is based on the general unsteady vortex-lattice method and the method of images. It is not restricted by plan-form, angle of attack, sink rate, dihedral angle, twist, camber, etc., as long as stall or vortex bursting does not occur. In addition, it has the versatility to model steady and unsteady aerodynamic interference. The present model can be used to simulate any prescribed flare and to model the effects of cross and/or head winds near the ground. The present results show the influences of various parameters on the aerodynamic coefficients for both steady and unsteady flows. Generally, the ground increases the aerodynamic coefficients; the greater the sink rates, the stronger the effects. Increasing the aspect ratio increases both the steady and unsteady ground effects. An exception is a large aspect-ratio wing with large camber. The present results are generally in close agreement with limited exact solutions and experimental data. In the aerodynamic-dynamic simulation, the equations of motion were solved by Hamming's predictor-corrector method. The aircraft, air stream, and control surfaces were treated as a single dynamic system. The present results demonstrate the feasibility of using the current simulation to model more complicated motions and the importance of including the unsteady ground effects when analyzing the performance of an airplane during a landing maneuver. Dissert. Abstr.

N89-24327*# National Aeronautics and Space Administration. Flight Research Center, Edwards, CA.
DEVELOPMENT AND FLIGHT TEST EXPERIENCES WITH A FLIGHT-CRUCIAL DIGITAL CONTROL SYSTEM
Dale A. Mackall Washington Nov. 1988 116 p
(NASA-TP-2857; H-1344; NAS 1.60:2857) Avail: NTIS HC A06/MF A01 CSCL 01C

Engineers and scientists in the advanced fighter technology integration (AFTI) F-16 program investigated the integration of emerging technologies into an advanced fighter aircraft. AFTI's three major technologies included: flight-crucial digital control, decoupled aircraft flight control, and integration of avionics, flight control, and pilot displays. In addition to investigating improvements in fighter performance, researchers studied the generic problems confronting the designers of highly integrated flight-crucial digital control. An overview is provided of both the advantages and problems of integration digital control systems. Also, an examination of the specification, design, qualification, and flight test life-cycle phase is provided. An overview is given of the fault-tolerant design, multimoded decoupled flight control laws, and integrated avionics design. The approach to qualifying the software and system designs is discussed, and the effects of design choices on system qualification are highlighted. Author

N89-24328*# TAU Corp., Los Gatos, CA.
OPTIMAL GUIDANCE WITH OBSTACLE AVOIDANCE FOR NAP-OF-THE-EARTH FLIGHT
Nicholas J. Pekelsma Dec. 1988 72 p
(Contract NAS2-12402)
(NASA-CR-177515; NAS 1.26:177515) Avail: NTIS HC A04/MF A01 CSCL 01C

The development of automatic guidance is discussed for helicopter Nap-of-the-Earth (NOE) and near-NOE flight. It deals with algorithm refinements relating to automated real-time flight path planning and to mission planning. With regard to path planning, it relates rotorcraft trajectory characteristics to the NOE computation scheme and addresses real-time computing issues and both ride quality issues and pilot-vehicle interfaces. The automated mission planning algorithm refinements include route optimization, automatic waypoint generation, interactive applications, and provisions for integrating the results into the real-time path planning software. A microcomputer based mission planning workstation was developed and is described. Further, the application of Defense Mapping Agency (DMA) digital terrain to both the mission planning workstation and to automatic guidance is both discussed and illustrated. Author

N89-24329*# National Aeronautics and Space Administration. Ames Research Center, Moffett Field, CA.
SURVEY OF ARMY/NASA ROTORCRAFT AEROELASTIC STABILITY RESEARCH
Robert A. Ormiston, William G. Warmbrodt, Dewey H. Hodges, and David A. Peters (Georgia Inst. of Tech., Atlanta.) Oct. 1988 183 p Prepared in cooperation with Army Aviation Systems Command, Moffett Field, CA
(NASA-TM-101026; A-88266; NAS 1.15:101026; USAAVSCOM-TR-88-A-005) Avail: NTIS HC A09/MF A01 CSCL 01C

Theoretical and experimental developments in the aeroelastic and aeromechanical stability of helicopters and tilt-rotor aircraft are addressed. Included are the underlying nonlinear structural mechanics of slender rotating beams, necessary for accurate modeling of elastic cantilever rotor blades, and the development of dynamic inflow, an unsteady aerodynamic theory for low frequency aeroelastic stability applications. Analytical treatment of isolated rotor stability in hover and forward flight, coupled rotor-fuselage stability are considered. Results of parametric investigations of system behavior are presented, and correlations between theoretical results and experimental data from small- and large-scale wind tunnel and flight testing are discussed. Author

09 RESEARCH AND SUPPORT FACILITIES (AIR)

Includes airports, hangars and runways; aircraft repair and overhaul facilities; wind tunnels; shock tubes; and aircraft engine test stands.

For related information see also *14 Ground Support Systems and Facilities (Space).*

N89-24330# Federal Aviation Administration, Atlantic City, NJ.
IMPROVED MARKING OF TAXIWAY INTERSECTIONS FOR INSTRUMENT FLIGHT RULES (IFR) OPERATIONS Interim Report
Eric S. Katz Feb. 1989 14 p
(DOT/FAA/CT-TN89/23) Avail: NTIS HC A03/MF A01 CSCL 01E

A visual aid to advice pilots that a taxiway intersection is being approached was developed at the Federal Aviation Administration (FAA) Technical Center. Subject pilots were asked to comment on the effectiveness of the taxiway intersection markings. Results of the evaluation indicate that the markings provide adequate advance warning of the approaching taxiway intersection and an indication of where to stop to ensure clearance from aircraft using the intersecting taxiway. Author

N89-24331*# National Aeronautics and Space Administration. Ames Research Center, Moffett Field, CA.
ULTRA-LIGHT DUCT FOR AN ANECHOIC WIND TUNNEL
J. Lambourion, S. Lewy, O. Papirnyk, G. Rahier, and J.-N. Remandet (Office National d'Etudes et de Recherches Aeronautiques, Paris, France) 9 Jan. 1989 11 p Transl. into ENGLISH from conference paper Presented at the 11th Colloquium on Aeronautical and Naval Acoustics, Saint-Louis, France, 15-17 Nov. 1988 Original language document was announced in IAA as A89-31819
(NASA-TM-101805; NAS 1.15:101805) Avail: NTIS HC A03/MF A01 CSCL 14B

A tunnel ultra-light (or TUL) is a duct composed of acoustically transparent cloth designed to transform an open-jet wind tunnel into a closed-jet wind tunnel. This concept is of interest (a priori) for anechoic wind tunnels because it improves the aerodynamic quality without hindering the measurement of sound in the far field. A full scale device designed for the 3 m diameter test section of CEPRA 19 was described. The apparatus installation did not develop any significant problems, and the mechanical support turned out to be excellent. Aerodynamic and acoustic tests are discussed. Certain imperfections in the installation as tested - instabilities above 25 m/s and acceptable cloth transmission up to 4kHz were revealed. The system as tested could eventually be used in certain applications, for example, in ground based transport. However, the concept of TUL must be developed further to arrive at a reliable mechanism for use in a large number of applications. Author

N89-24332# California Univ., San Diego.
ESTABLISHMENT OF AN ELECTRON BEAM LITHOGRAPHY FACILITY Final Report, 15 Aug. 1987 - 31 Jul. 1988
Sing H. Lee 13 Feb. 1989 3 p
(Grant AF-AFOSR-0060-87; AF Proj. 2305)
(AD-A206215; AFOSR-89-0343TR) Avail: NTIS HC A02/MF A01 CSCL 13/8

Enclosed is a final report on testing of an electron beam writer. This electron beam writer will be used to produce high resolution, large space bandwidth product holographic optical elements (which are versatile, passive components of opto-electronic systems), to fabricate fast, compact, active opto-electronic devices and to make masks for high speed millimeter wave devices or high frequency integrated circuits, as described in the original proposal. GRA

12 ASTRONAUTICS (GENERAL)

For extraterrestrial exploration see *91 Lunar and Planetary Exploration.*

N89-24333*# National Aeronautics and Space Administration. Ames Research Center, Moffett Field, CA.
SPACE PIONEERS AND WHERE THEY ARE NOW
Earl J. Montoya (National Aeronautics and Space Administration, Washington, DC.) and Richard O. Fimmel 1987 26 p Original contains color illustrations
(NASA-EP-264; NAS 1.19:264) Avail: NTIS HC A03/MF A01 CSCL 22A

A description of the Pioneer project, its history and achievements is given. Major discoveries concerning near and interplanetary space, the planets, and various comets are outlined. Anticipated future observations are considered. A list of Pioneer project launches, 1986 statuses, and project firsts is given. A.D.

N89-24334* National Aeronautics and Space Administration, Washington, DC.
SPACE SHUTTLE TO DEPLOY MAGELLAN PLANETARY SCIENCE MISSION
Apr. 1989 36 p
(NASA-News-Release-89-86; P89-10046) Avail: NASA Scientific and Technical Information Facility, PO Box 8757, BWI Airport, MD 21240 CSCL 22A

The objectives of Space Shuttle Mission STS-30 are described along with major flight activities, prelaunch and launch operations, trajectory sequence of events, and landing and post-landing operations. The primary objective of STS-30 is to successfully deploy the Magellan spacecraft into low earth orbit. Following deployment, Magellan will be propelled to its Venus trajectory by an Inertial Upper Stage booster. The objectives of the Magellan mission are to obtain radar images of more than 70 percent of Venus' surface, a near-global topographic map, and near-global gravity field data. Secondary STS-30 payloads include the Fluids Experiment Apparatus (FEA) and the Mesoscale Lightning Experiment (MLE). M.G.

N89-24335# European Space Agency, Paris (France).
INTERNATIONAL SYMPOSIUM ON EUROPE IN SPACE: THE MANNED SPACE SYSTEM
Valerie David, ed. and Norman Longdon, ed. Oct. 1988 646 p Partly in ENGLISH and FRENCH Symposium held in Strasbourg, France, 25-29 Apr. 1988; sponsored by BMFT, Bonn, Fed. Republic of Germany, CNES, France, ESA, France, and the Ministero per la Ricerca Scientifica e Tecnologica, Italy
(ESA-SP-277; ETN-89-94448) Copyright Avail: NTIS HC A99/MF A01; ESA Publications Div., ESTEC, Noordwijk, Netherlands, 80 Dutch guilders

European in-orbit infrastructure elements; Columbus and Hermes; vehicle technology; operation concepts; safety requirements; system operations; attached pressurized module and Man Tended Free Flyers; robotics; user support; and astronauts were discussed. For individual titles, see N89-24336 through N89-24403.

N89-24336# European Space Agency, Paris (France).
THE ARIANE 5 DEVELOPMENT PROGRAM **c15**
J. Feustel-Buechl *In its* International Symposium on Europe in Space: The Manned Space System Oct. 1988 p 41-47 (For primary document see N89-24335 18-12)
Copyright Avail: NTIS HC A99/MF A01; ESA Publications Div., ESTEC, Noordwijk, Netherlands, 80 Dutch guilders

Competition in the market for commercial launches of satellites is reviewed. The objectives of the Ariane 5 program are summarized: 6800kg payload into GTO; 18,000kg Columbus modules into LEO at 550km, and 12,000kg at 800km; Hermes into transfer orbit (21,000kg); and 98 percent reliability. The launch vehicle, launch complex, and schedule and costs are outlined. ESA

N89-24337# Bundesministerium fuer Forschung und Technologie, Bonn (Germany, F.R.). Aerospace Div.
COLUMBUS: THE EUROPEAN CONTRIBUTION TO THE INTERNATIONAL SPACE STATION **c18**
H. Strub *In* ESA, International Symposium on Europe in Space: The Manned Space System Oct. 1988 p 49-53 (For primary document see N89-24335 18-12)
Copyright Avail: NTIS HC A99/MF A01; ESA Publications Div., ESTEC, Noordwijk, Netherlands, 80 Dutch guilders

The evolution of the Columbus program from Spacelab is traced, and the technical and scientific reasons for the program are mentioned. The International Space Station scenario is outlined, including the cooperation agreements. Ground installations; logistics and transport facilities; and communication systems are described. Interfaces with Ariane 5 and Hermes are indicated. The political importance of Columbus is stressed. ESA

N89-24338# Centre National d'Etudes Spatiales, Toulouse (France).
THE HERMES PROGRAM [LE PROGRAMME HERMES] **c18**
Ph. Couillard *In* ESA, International Symposium on Europe in Space: The Manned Space System Oct. 1988 p 55-58 In FRENCH; ENGLISH summary (For primary document see N89-24335 18-12)
Copyright Avail: NTIS HC A99/MF A01; ESA Publications Div., ESTEC, Noordwijk, Netherlands, 80 Dutch guilders

The decision to initiate the Hermes program is described and the Phase 1 objectives are outlined. These include definition of mission objectives (mainly orbital servicing of Columbus MTTF's); safety analyses; and launch and reentry aspects. Critical technologies which must be developed for Hermes are indicated. ESA

N89-24339# Ministero Ricerca Scientifica e Tecnologica, Rome (Italy).
THE EUROPEAN DATA RELAY SATELLITE **c18**
F. Mazzuca *In* ESA, International Symposium on Europe in Space: The Manned Space System Oct. 1988 p 59-61 (For primary document see N89-24335 18-12)

Copyright Avail: NTIS HC A99/MF A01; ESA Publications Div., ESTEC, Noordwijk, Netherlands, 80 Dutch guilders

Communication requirements for European space programs are reviewed, and a communication system based on a data relay system is suggested. Satellites in geostationary orbit will continuously relay data between user satellites in LEO and the ground. Design drivers are reliability and flexibility, but operating requirements depend on the definition of other elements, such as Columbus and Hermes. ESA

N89-24340# European Space Agency. European Space Operations Center, Darmstadt (Germany, F.R.).
THE EUROPEAN IN-ORBIT INFRASTRUCTURE GROUND SEGMENT [LE SEGMENT SOL RELATIF AUX OPERATIONS DE L'INFRASTRUCTURE EN ORBITE EUROPEENNE]
C. Honvault *In its* International Symposium on Europe in Space: The Manned Space System Oct. 1988 p 63-70 In FRENCH (For primary document see N89-24335 18-12)
Copyright Avail: NTIS HC A99/MF A01; ESA Publications Div., ESTEC, Noordwijk, Netherlands, 80 Dutch guilders

The methodology used to define the ground segment needed for a European orbital infrastructure is described. Given the decentralized approach adopted, the need to coordinate activities is stressed. ESA

N89-24341# European Space Agency, Paris (France).
OVERALL COHERENCE OF THE EUROPEAN PROGRAMS WITHIN A LONG-TERM SPACE POLICY
G. VanReeth *In its* International Symposium on Europe in Space: The Manned Space System Oct. 1988 p 71-73 (For primary document see N89-24335 18-12)
Copyright Avail: NTIS HC A99/MF A01; ESA Publications Div., ESTEC, Noordwijk, Netherlands, 80 Dutch guilders

The need for coherence between the elements of ESA's long term space programs is stressed. Economic and technical aspects linked to the development of the in-orbit infrastructure, user programs, and ground elements are mentioned. ESA

N89-24342# Chinese Academy of Space Technology, Beijing.
CHINA'S FUTURE SPACE ACTIVITIES
Shan-Cheng Tu *In* ESA, International Symposium on Europe in Space: The Manned Space System Oct. 1988 p 79-82 (For primary document see N89-24335 18-12)
Copyright Avail: NTIS HC A99/MF A01; ESA Publications Div., ESTEC, Noordwijk, Netherlands, 80 Dutch guilders

The history and status of the Chinese space program are reviewed. Development of applications satellites, manned spacecraft, and launch vehicles are mentioned. ESA

N89-24343# Aeritalia S.p.A., Turin (Italy). Space Systems Group.
PRESSURIZED MODULE ELEMENT FOR MAN'S PRESENCE IN SPACE **c18**
Ernesto Vallerani and Elizabeth Maggio *In* ESA, International Symposium on Europe in Space: The Manned Space System Oct. 1988 p 95-100 (For primary document see N89-24335 18-12)
Copyright Avail: NTIS HC A99/MF A01; ESA Publications Div., ESTEC, Noordwijk, Netherlands, 80 Dutch guilders

The external and internal architecture of the Columbus attached pressurized module is described. The Man Tended Free Flyer derivative is presented. Laboratory operation for materials and life sciences in reduced gravity is summarized. The importance of international cooperation and Europen autonomy is stressed. ESA

N89-24344# Centre National d'Etudes Spatiales, Toulouse (France).
FRENCH NATIONAL POLICY ON THE PREPARATION OF COLUMBUS UTILIZATION
Alain Esterle and Isaac Revah *In* ESA, International Symposium on Europe in Space: The Manned Space System Oct. 1988 p 101-106 (For primary document see N89-24335 18-12)
Copyright Avail: NTIS HC A99/MF A01; ESA Publications Div., ESTEC, Noordwijk, Netherlands, 80 Dutch guilders

The qualitative and quantitative improvements to be expected from the development of Columbus, Ariane 5, and Hermes are discussed, and the way in which the French Space Agency should adapt its programs to fully exploit their possibilities is considered. Scientific, technical, and industrial implications for the user community are assessed. The need to develop user friendly interfaces is stressed. Preparatory missions for the Columbus program, involving international cooperation, are indicated. ESA

N89-24345# Messerschmitt-Boelkow-Blohm G.m.b.H., Bremen (Germany, F.R.).
MTFF USER INTERFACES **c18**
S. Gazey and K. Huse *In* ESA, International Symposium on Europe in Space: The Manned Space System Oct. 1988 p 107-110 (For primary document see N89-24335 18-12)
Copyright Avail: NTIS HC A99/MF A01; ESA Publications Div., ESTEC, Noordwijk, Netherlands, 80 Dutch guilders

The utilization interfaces of the Columbus Man Tended Free Flyers (MTFF) are described. The MTFF resources, payload accommodation, and servicing facilities are outlined. The characteristics of the manned life sciences mission involving Hermes are treated. User interfaces are compared with payload requirements as represented by MTFF reference mission and utilization studies. The rack concepts and standard and add-on features are shown. ESA

N89-24346# European Space Agency, Paris (France).
HERMES USER INTERFACES **c18**
P. Brudieu *In its* International Symposium on Europe in Space: The Manned Space System Oct. 1988 p 111-115 (For primary document see N89-24335 18-12)
Copyright Avail: NTIS HC A99/MF A01; ESA Publications Div., ESTEC, Noordwijk, Netherlands, 80 Dutch guilders

The difficulty of designing Hermes user interfaces before final mission and system decisions are made is discussed. Hermes users are identified (mainly Columbus MTFF). Interfaces with users and payloads during mission preparation is illustrated. Payload/cargo mass and volume requirements are treated. Cargo accommodation is shown. Payload related operations performed by the Hermes crew are considered. ESA

N89-24347# European Space Agency, Paris (France). Microgravity Program Management Office.
MICROGRAVITY PAYLOADS (APM AND MTFF) **c29**
Guenther Seibert and Paul Clancy *In its* International Symposium on Europe in Space: The Manned Space System Oct. 1988 p 117-121 (For primary document see N89-24335 18-12)
Copyright Avail: NTIS HC A99/MF A01; ESA Publications Div., ESTEC, Noordwijk, Netherlands, 80 Dutch guilders

The ESA microgravity program in materials sciences, physical chemistry, fluid dynamics and physics, biotechnology and biochemistry, and life sciences and radiation biology is discussed. Previous missions and the planned Columbus microgravity elements (attached pressure module, MTFF, polar platforms) are described. Payload studies for these elements are indicated. Microgravity outfitting of Columbus elements is reviewed. Critical resources are: rack space; power; toxic materials handling; crew time; and module outfitting rate and changeout. ESA

N89-24348# European Space Agency. European Space Research and Technology Center, ESTEC, Noordwijk (Netherlands).
SPACE SCIENCE USING COLUMBUS: MANNED SPACE SCIENCE
H. Olthof *In its* International Symposium on Europe in Space: The Manned Space System Oct. 1988 p 123-124 (For primary document see N89-24335 18-12)
Copyright Avail: NTIS HC A99/MF A01; ESA Publications Div., ESTEC, Noordwijk, Netherlands, 80 Dutch guilders

The scientific airlock of the Columbus attached pressurized

module is described. Potential space science experiments and areas of research with the facility are suggested: wide field cameras; cosmic gamma ray burst detectors; total radiance measurement; active plasma diagnostics; and test and calibration of new technology. ESA

N89-24349# Aerospatiale, Les Mureaux (France). Div. Systemes Strategiques et Spatiaux.
OVERVIEW OF ARIANE 5 AND HERMES PROGRAMS TECHNOLOGY [VUE GENERALE DE LA TECHNOLOGIE DANS LES PROGRAMMES ARIANE 5 ET HERMES]
F. Duret and J. Lacaze *In* ESA, International Symposium on Europe in Space: The Manned Space System Oct. 1988 p 127-131 In FRENCH; ENGLISH summary (For primary document see N89-24335 18-12)
Copyright Avail: NTIS HC A99/MF A01; ESA Publications Div., ESTEC, Noordwijk, Netherlands, 80 Dutch guilders

The design criteria for Ariane 5 and Hermes are reviewed. The Ariane design is most strongly influenced by the fact that it must be compatible with widely differing payloads: satellites, space station elements, and Hermes. Ariane is based on two solid boosters for the launch phase and a cryogenic central section which assures most of the flight into orbit, although an upper stage is used at the end of the transfer. Hermes uses little of its own power to reach orbit. Its payload is carried in a cargo bay and can be launched autonomously or with a remote manipulator. The two flight crew members plus the payload specialist are housed in an ejectable cabin. The aerodynamics problems; structural design and materials; heat shielding; electrical equipment; hydropneumatics; software; and ground and in-orbit functioning are discussed. ESA

N89-24350# European Space Agency, Paris (France). Space Transportation Systems Directorate.
THE TECHNOLOGY CONTENTS OF THE FIRST PHASE OF THE HERMES DEVELOPMENT PROGRAM **c16**
J. J. Capart and E. Slachmuylders *In its* International Symposium on Europe in Space: The Manned Space System Oct. 1988 p 133-142 (For primary document see N89-24335 18-12)
Copyright Avail: NTIS HC A99/MF A01; ESA Publications Div., ESTEC, Noordwijk, Netherlands, 80 Dutch guilders

The budget, industrial, management aspects, and schedule of the Hermes technology program are outlined. ESA

N89-24351# Avions Marcel Dassault-Breguet Aviation, Saint-Cloud (France).
HERMES AEROTHERMODYNAMIC CONCEPT **c18**
F. Cordie, M. Desloires, and J. P. Vaunois (Centre National d'Etudes Spatiales, Toulouse, France) *In* ESA, International Symposium on Europe in Space: The Manned Space System Oct. 1988 p 143-144 In FRENCH (For primary document see N89-24335 18-12)
Copyright Avail: NTIS HC A99/MF A01; ESA Publications Div., ESTEC, Noordwijk, Netherlands, 80 Dutch guilders

The problems posed for temperature control of Hermes by the wide operating range are reviewed. The design is based around a delta body and has airbrakes to assist landing. Thermal control poses special problems because of the size of the craft. The STS approach of a cold structure protected by heat shielding is not possible. The fuselage and wings are cold structures, with protection, while the nose, leading edges, winglets, and control surfaces are hot, i.e., made from heat resistant materials. The aerothermodynamic development and test program is mentioned. ESA

N89-24352# Bombrini Parodi-Delfino S.p.A., Colleferro (Italy).
ARIANE 5 SOLID BOOSTERS: OVERVIEW OF DESIGN APPROACH AND ENVISAGED TECHNOLOGIES **c15**
Roberto Fabrizi *In* ESA, International Symposium on Europe in Space: The Manned Space System Oct. 1988 p 145-151 Prepared in cooperation with Societe Europeene de Propulsion, Saint-Medard-en-Jalles, France (For primary document see N89-24335 18-12)
Copyright Avail: NTIS HC A99/MF A01; ESA Publications Div., ESTEC, Noordwijk, Netherlands, 80 Dutch guilders

Solid propellant engine (MPS) requirements for Ariane 5 are summarized, and the overall configuration is described. Component design and manufacturing are reviewed. The engine casing; thermal insulation; propellant grain; nozzle; ignition system; and program schedule are discussed. Total MPS weight is 260.7 tons, with 230 tons of propellant. The MPS develops 4907 kN average thrust, 6433 kN maximum. Total burning time is 127 sec. Average chamber pressure is 60.4 bar, 44.7 bar average. Nozzle throat diameter is 895mm. Expansion ratio is 13.2. Nozzle deflection capacity is + or - 6 deg. ESA

N89-24353# Centre National d'Etudes Spatiales, Toulouse (France).
TECHNOLOGY AND DESIGN METHOD EVOLUTION OF CRYOGENIC PROPULSION SYSTEMS: EXAMPLE OF THE MAIN ARIANE 5 STAGE **c20**
J. Borromee, D. Thevenot, H. Dederra, and A. Faure (L'Air Liquide, Sassenage, France) *In* ESA, International Symposium on Europe in Space: The Manned Space System Oct. 1988 p 153-162 (For primary document see N89-24335 18-12)
Copyright Avail: NTIS HC A99/MF A01; ESA Publications Div., ESTEC, Noordwijk, Netherlands, 80 Dutch guilders

The design criteria and methodology of the Ariane 5 main stage are reviewed. The thrust chamber, main injector, and hydrogen pump are described. Differences between the cryogenic tanks of Ariane 5 and Ariane 4 are explained. The simulation and analysis programs are indicated. ESA

N89-24354# Dornier-Werke G.m.b.H., Friedrichshafen (Germany, F.R.).
ECLS FOR COLUMBUS AND HERMES **c54**
H. Preiss, G. Kring, and R. Schaefer *In* ESA, International Symposium on Europe in Space: The Manned Space System Oct. 1988 p 163-167 (For primary document see N89-24335 18-12)
Copyright Avail: NTIS HC A99/MF A01; ESA Publications Div., ESTEC, Noordwijk, Netherlands, 80 Dutch guilders

The environment control and life support subsystems (ECLS) of Hermes and Columbus are presented. The Hermes ECLS system has to ensure adequate working conditions for three persons during a 12 day mission. It includes atmosphere, liquids, food/galley, and waste management subsystems. The Columbus ECLS supports scientific experiments in an unmanned mode for 180 days, plus 7 days servicing with 2 persons. The ECLS functions for Columbus are mainly concerned with atmosphere control and conditioning. ESA

N89-24355# Dornier-Werke G.m.b.H., Friedrichshafen (Germany, F.R.).
FUEL CELL DEVELOPMENT FOR HERMES **c44**
H. Gehrke and U. Knoebel *In* ESA, International Symposium on Europe in Space: The Manned Space System Oct. 1988 p 169-174 (For primary document see N89-24335 18-12)
Copyright Avail: NTIS HC A99/MF A01; ESA Publications Div., ESTEC, Noordwijk, Netherlands, 80 Dutch guilders

Three fuel cell system architectures for the Hermes primary power source were defined. The system has to supply 2 to 6.5 kW and 115 to 90V dc. Weight ratio must be better than 50W/kg, with volume better than 40W/liter. Accumulated operation time is over 4000hr; accumulated storage time 26,000hr. A mobile KOH system with water removal (and cooling) via the KOH loop; a mobile KOH system with water removal via the H2 loop; and an immobile KOH system with water removal via the H2 loop were chosen for further investigation. ESA

N89-24356# European Space Agency. European Space Operations Center, Darmstadt (Germany, F.R.).
FLIGHT OPERATIONS CONCEPT FOR THE EUROPEAN IN-ORBIT INFRASTRUCTURE **c66**
W. Frank and A. Sesma *In its* International Symposium on

Europe in Space: The Manned Space System Oct. 1988 p 177-183 (For primary document see N89-24335 18-12)
Copyright Avail: NTIS HC A99/MF A01; ESA Publications Div., ESTEC, Noordwijk, Netherlands, 80 Dutch guilders

The ESA in-orbit infrastructure ground segment facilities, the structure and functions of operations management, and the communications requirements between facilities and elements in orbit are described. Tactical planning to cope with, e.g., changes in mission objectives is explained. The central mission control center and operations execution management are presented. ESA

N89-24357# Centre National d'Etudes Spatiales, Toulouse (France).
HERMES-MTFF RENDEZVOUS STRATEGY AND COMPOSITE OPERATIONS **c16**
L. Marechal, F. DiMauro, D. Hoge, and W. Fehse *In* ESA, International Symposium on Europe in Space: The Manned Space System Oct. 1988 p 185-190 Prepared in cooperation with ESA, Paris, France and ESA/ESTEC, Noordwijk, Netherlands (For primary document see N89-24335 18-12)
Copyright Avail: NTIS HC A99/MF A01; ESA Publications Div., ESTEC, Noordwijk, Netherlands, 80 Dutch guilders

Hermes operations from injection into orbit to reentry are described. Parameters affecting the Hermes mission to the Columbus Man Tended Free Flyer (MTFF) are assessed. The role of the human operator in the rendezvous process is discussed. Orbital transfer and approach operations are outlined. It is concluded that the preferred approach to rendezvous and final approach should be along the V-bar. Composite configuration and composite attitude control satisfy internal servicing requirements with the present Hermes baseline. External servicing remains difficult and time consuming since the spaceplane is optimized for carrying a pressurized cargo only as requested by the servicing of the MTFF. ESA

N89-24358# Deutsche Forschungs- und Versuchsanstalt fuer Luft- und Raumfahrt, Cologne (Germany, F.R.).
TIMELINING AND OPERATIONS INTEGRATION CONCERNING APM AND MTFF **c66**
A. Davidson, K. Wedde-Muehlhausen, and K. Schmidt *In* ESA, International Symposium on Europe in Space: The Manned Space System Oct. 1988 p 191-199 (For primary document see N89-24335 18-12)
Copyright Avail: NTIS HC A99/MF A01; ESA Publications Div., ESTEC, Noordwijk, Netherlands, 80 Dutch guilders

Planning Columbus on-board operations and management of the operational interfaces of the payload ground control team are discussed. Organizational aspects which need to be considered to arrive at a feasible operations structure are assessed, based on Spacelab experience. ESA

N89-24359# Compagnia Italiana Servizi Tecnici, Rome.
INTEGRATED APPROACH FOR THE LOGISTIC SUPPORT OF THE EUROPEAN IN ORBIT INFRASTRUCTURE FROM THE NINETIES ONWARDS **c66**
A. Falciai and R. Grazi *In* ESA, International Symposium on Europe in Space: The Manned Space System Oct. 1988 p 201-205 (For primary document see N89-24335 18-12)
Copyright Avail: NTIS HC A99/MF A01; ESA Publications Div., ESTEC, Noordwijk, Netherlands, 80 Dutch guilders

An approach to ensure a cost effective logistics support to ESA's manned space program is outlined. The importance of commonality is stressed. The contribution of logistics to space commercialization is discussed. ESA

N89-24360# Aerospatiale, Les Mureaux (France). Div. Systemes Strategiques et Spatiaux.
SERVICING OF THE MTFF BY HERMES **c66**
P. Eymar and C. Cougnet (MATRA Espace, Toulouse, France) *In* ESA, International Symposium on Europe in Space: The Manned Space System Oct. 1988 p 207-214 (For primary document see N89-24335 18-12)
Copyright Avail: NTIS HC A99/MF A01; ESA Publications Div., ESTEC, Noordwijk, Netherlands, 80 Dutch guilders

Servicing tasks which Hermes performs when attached to the Columbus Man Tended Free Flyer (MTFF) are described. The first type of task involves exchange of internal racks and drawers. The most difficult part of this operation involves unloading/loading, transfer, and checkout. Exchange of external Orbital Replacement Units produces problems related to transfers from the pressurized Hermes bay to the unpressurized environment. Configurations to overcome these problems are discussed. ESA

N89-24361# Messerschmitt-Boelkow-Blohm G.m.b.H., Bremen (Germany, F.R.).
MTFF FLIGHT OPERATIONS PHASES **c66**
H. Wartenberg and H. J. Koopmann *In* ESA, International Symposium on Europe in Space: The Manned Space System Oct. 1988 p 215-232 (For primary document see N89-24335 18-12)
Copyright Avail: NTIS HC A99/MF A01; ESA Publications Div., ESTEC, Noordwijk, Netherlands, 80 Dutch guilders

Man Tended Free Flyer (MTFF) pressurized module, resource module, and servicing requirements are outlined, and flight operations are defined. The launch phase, initial activation phase, routine mission operation, and orbital servicing by Hermes are described. The MTFF ground segment infrastructure is presented. Operations planning and management are summarized. ESA

N89-24362# Elektronik-System G.m.b.H., Munich (Germany, F.R.).
MANNED INTERVENTIONS AT THE MTFF: CREW WORKLOAD ASPECTS **c54**
K. Brammer and Georg Kampfer (Panares, Munich, Germany, F.R.) *In* ESA, International Symposium on Europe in Space: The Manned Space System Oct. 1988 p 233-237 (For primary document see N89-24335 18-12)
Copyright Avail: NTIS HC A99/MF A01; ESA Publications Div., ESTEC, Noordwijk, Netherlands, 80 Dutch guilders

The scenario of a Hermes visit to a Columbus MTFF and requirements with respect to crew activities for tending the MTFF subsystems and payload were investigated. An intervention concept is derived using a medium degree of automation, with exceptions to cater for optimal workflow, and frequent and time consuming tasks. It is concluded that a 7 day servicing period is required, with most of the difficulties arising from external servicing. The need to make payloads servicing-friendly is stressed. ESA

N89-24363# Aeritalia S.p.A., Turin (Italy). Space Systems Group.
LOGISTICS ASPECTS OF COLUMBUS SERVICING AT THE SPACE STATION **c66**
Vincenzo DeFilippis and Luciano Basile *In* ESA, International Symposium on Europe in Space: The Manned Space System Oct. 1988 p 239-244 (For primary document see N89-24335 18-12)
Copyright Avail: NTIS HC A99/MF A01; ESA Publications Div., ESTEC, Noordwijk, Netherlands, 80 Dutch guilders

A common pressurized logistics module (PLM) concept derived from Spacelab/Columbus, and optimized to satisfy International Space Station needs is advocated. A long cycle PLM satisfies requirements for flexible volume to be used for dynamic storage, skipped cycle support, work space, and other applications. Shuttle and expendable transport vehicles are suggested, and the importance of commonality is stressed. ESA

N89-24364# European Space Agency. European Space Research and Technology Center, ESTEC, Noordwijk (Netherlands). Product Assurance and Safety Dept.
ESA SAFETY REQUIREMENTS **c31**
L. Tedeman *In its* International Symposium on Europe in Space: The Manned Space System Oct. 1988 p 247-251 (For primary document see N89-24335 18-12)

Copyright Avail: NTIS HC A99/MF A01; ESA Publications Div., ESTEC, Noordwijk, Netherlands, 80 Dutch guilders

The ESA safety policy, designed to protect human life, investments, and the environment is outlined. A risk assessment procedure which recognizes the lack of objective statistical data is discussed. It considers the consequences, frequency, and probability of an undesirable hazardous event. This risk assessment is applied as an iterative process during all project phases. ESA

N89-24365# European Space Agency, Paris (France).
SAFETY AND RELIABILITY OF THE ARIANE 5-HERMES COMPOSITE [SECURITE-FIABILITE COMPOSITE ARIANE 5-HERMES] **c31**
J. Marcoux, J. Charles, G. Borycki, and B. Galland (Aerospatiale, Les Mureaux, France) *In its* International Symposium on Europe in Space: The Manned Space System Oct. 1988 p 253-267 In FRENCH (For primary document see N89-24335 18-12)
Copyright Avail: NTIS HC A99/MF A01; ESA Publications Div., ESTEC, Noordwijk, Netherlands, 80 Dutch guilders

The safety/reliability approach adopted for the Hermes/Ariane 5 configuration is outlined. Risk analyses and safety measures derived from them for the launch, orbital, and return phases are summarized. The specifications tree and criticality matrix are shown. ESA

N89-24366# Aerospatiale, Cannes La Bocca (France).
HERMES ESCAPE SYSTEM **c03**
J. Colrat, H. P. Nguyen, and H. Hirsch *In* ESA, International Symposium on Europe in Space: The Manned Space System Oct. 1988 p 269-274 (For primary document see N89-24335 18-12)
Copyright Avail: NTIS HC A99/MF A01; ESA Publications Div., ESTEC, Noordwijk, Netherlands, 80 Dutch guilders

The Hermes crew escape module (CEM) is discussed. The CEM is a leakproof volume containing the cockpit and workstation in a front part designed from aerodynamic and ergonomic considerations, closed at the rear by a bulkhead. The floor is designed to sustain impact loads, leading to the choice of titanium for the cabin. Communication between the cabin and the cargo bay is assured by a tunnel closed by a hatch when insulation of the crew in the cabin is needed. The CEM can be ejected at any stage of the flight, from prelaunch to landing. The CEM can withstand a 24 hr delay in recovery, e.g., in case of ditching in the ocean. ESA

N89-24367# Deutsche Forschungs- und Versuchsanstalt fuer Luft- und Raumfahrt, Cologne (Germany, F.R.).
SYSTEM SAFETY FROM D-MISSIONS TO COLUMBUS **c31**
H. Schuermanns and W. Ziesmann *In* ESA, International Symposium on Europe in Space: The Manned Space System Oct. 1988 p 275-280 (For primary document see N89-24335 18-12)
Copyright Avail: NTIS HC A99/MF A01; ESA Publications Div., ESTEC, Noordwijk, Netherlands, 80 Dutch guilders

The Spacelab D2 mission safety concept is recalled and development of the concept to meet Columbus requirements is discussed. An example of safety participation during D1 (repairing a mirror heating facility) is described, including ground support. ESA

N89-24368# European Space Agency, Paris (France). Columbus System Engineering and Integration.
COLUMBUS SAFETY AND RELIABILITY **c31**
F. Longhurst and H. Wessels *In its* International Symposium on Europe in Space: The Manned Space System Oct. 1988 p 281-290 (For primary document see N89-24335 18-12)
Copyright Avail: NTIS HC A99/MF A01; ESA Publications Div., ESTEC, Noordwijk, Netherlands, 80 Dutch guilders

Analyses carried out to ensure Columbus reliability, availability, and maintainability, and operational and design safety are summarized. Failure modes/effects/criticality is the main qualitative tool used. The main aspects studied are fault tolerance, hazard consequence control, risk minimization, human error effects, restorability, and safe-life design. ESA

N89-24369# Deutsche Forschungs- und Versuchsanstalt fuer Luft- und Raumfahrt, Cologne (Germany, F.R.). Inst. for Aerospace Medicine.
MEDICAL AND RADIATION PROTECTION PROBLEMS IN SPACE **c52**
K. E. Klein and H. Buecker *In* ESA, International Symposium on Europe in Space: The Manned Space System Oct. 1988 p 291-302 (For primary document see N89-24335 18-12)
Copyright Avail: NTIS HC A99/MF A01; ESA Publications Div., ESTEC, Noordwijk, Netherlands, 80 Dutch guilders

Possibilities of inflight disturbances to space missions due to diseases, operation, and environment are discussed. Equipment needed for diagnosis and treatment is considered. Countermeasures are considered. Research required on the radiation hazard to space crews is suggested, including the measurement of radiation in space, the determination of its biological significance, and the establishment of radiation protection standards and of a system of dosimetric surveillance. ESA

N89-24370# Avions Marcel Dassault-Breguet Aviation, Saint-Cloud (France).
PROTECTION AGAINST IONIZING RADIATION FOR THE HERMES MISSION [PROTECTION CONTRE LES RAYONNEMENTS IONISANTS POUR LES MISSIONS HERMES] **c72**
G. Melkonian and J. Bourrieau (Centre National d'Etudes Spatiales, Toulouse, France) *In* ESA, International Symposium on Europe in Space: The Manned Space System Oct. 1988 p 303-335 In FRENCH; ENGLISH summary (For primary document see N89-24335 18-12)
(Contract ESTEC-6988/NL/PP(SC))
Copyright Avail: NTIS HC A99/MF A01; ESA Publications Div., ESTEC, Noordwijk, Netherlands, 80 Dutch guilders

Radiation sources which Hermes crews will be exposed to are described; cosmic rays; trapped particles; and solar radiation. Radiation protection measures based on mission planning; awareness of solar activity; dosimetry; shielding; and biochemical products are considered. ESA

N89-24371# European Space Agency. European Space Operations Center, Darmstadt (Germany, F.R.).
THE IMPACT OF MANNED SPACE FLIGHT OPERATIONS ON THE SAFETY AND RELIABILITY ASPECTS OF GROUND SYSTEMS REQUIREMENTS **c31**
David E. B. Wilkins *In its* International Symposium on Europe in Space: The Manned Space System Oct. 1988 p 337-347 (For primary document see N89-24335 18-12)
Copyright Avail: NTIS HC A99/MF A01; ESA Publications Div., ESTEC, Noordwijk, Netherlands, 80 Dutch guilders

Reliability and safety standards for the ESA in-orbit infrastructure ground segment are discussed. The ground segment design process is outlined. Hardware and software availability are mentioned. Human factors in operational reliability are reviewed. ESA

N89-24372# European Space Agency. European Space Operations Center, Darmstadt (Germany, F.R.).
THE ROLE OF THE HERMES FLIGHT CONTROL CENTER IN A TYPICAL HERMES/MTFF SERVICING MISSION **c14**
Christian Reinhold and Marc Francois (Centre National d'Etudes Spatiales, Toulouse, France) *In its* International Symposium on Europe in Space: The Manned Space System Oct. 1988 p 351-359 (For primary document see N89-24335 18-12)
Copyright Avail: NTIS HC A99/MF A01; ESA Publications Div., ESTEC, Noordwijk, Netherlands, 80 Dutch guilders

Nominal prime and support functions of the Hermes flight control center (HFCC) are analyzed in the context of the crew/ground sharing of responsibility for a typical Hermes mission servicing the Columbus MTFF. The support provided by the HFCC includes navigation,

medical support, spaceplane monitoring, fault diagnosis, operations replanning, and software uploading. The relationship between the HFCC and the ESA in-orbit infrastructure central mission control center is discussed. Functional requirements of the HFCC concerning real time data control, flight support, and simulation and testing are treated. ESA

N89-24373# Centre National d'Etudes Spatiales, Toulouse (France). Direction Hermes et Vols Habites.
MEANS FOR PREPARING AND RECOVERING THE HERMES SPACE PLANE [LES MOYENS DE PREPARATION ET DE RECUPERATION DE L'AVION SPATIAL HERMES] **c18**
Michel Cade and Bernard Houze *In* ESA, International Symposium on Europe in Space: The Manned Space System Oct. 1988 p 361-365 (For primary document see N89-24335 18-12)
Copyright Avail: NTIS HC A99/MF A01; ESA Publications Div., ESTEC, Noordwijk, Netherlands, 80 Dutch guilders

Installations which must be created in Europe and in French Guyana to assure the preparation, launch, and recovery of the Hermes spaceplane are outlined. Ways and means of rescuing crew in various emergency situations are summarized. ESA

N89-24374# European Space Agency, Paris (France).
THE TRAINING CONCEPT FOR ESA ASTRONAUTS AND THE ASSOCIATED FACILITIES **c53**
H. D. Hopkins *In its* International Symposium on Europe in Space: The Manned Space System Oct. 1988 p 367-369 (For primary document see N89-24335 18-12)
Copyright Avail: NTIS HC A99/MF A01; ESA Publications Div., ESTEC, Noordwijk, Netherlands, 80 Dutch guilders

The number of astronauts required for the Hermes program is estimated at 12. Training facilities needed are determined for basic training and specialized and mission training. ESA

N89-24375# Centre National d'Etudes Spatiales, Toulouse (France).
THE HERMES SYSTEM TRAINING CONCEPT [CONCEPT D'ENTRAINEMENT AU SYSTEME HERMES] **c53**
G. Gargir *In* ESA, International Symposium on Europe in Space: The Manned Space System Oct. 1988 p 371-377 In FRENCH; ENGLISH summary (For primary document see N89-24335 18-12)
Copyright Avail: NTIS HC A99/MF A01; ESA Publications Div., ESTEC, Noordwijk, Netherlands, 80 Dutch guilders

Hermes crew, crew activities, and astronaut training are discussed. Hermes astronauts will be flight crew members, mission engineers, and passengers bound for space stations. The type of training required for each type of astronaut is shown, along with the number of hours at each particular facility e.g., 1800 hr of mission training for the pilot, including 240 hr with the Hermes training airplane. ESA

N89-24376# Deutsche Forschungs- und Versuchsanstalt fuer Luft- und Raumfahrt, Oberpfaffenhofen (West Germany). Space Operation Center.
THE MANNED SPACE LABORATORIES CONTROL CENTER (MSCC) AT DFVLR, OBERPFAFFENHOFEN, GERMANY, F.R. **c14**
Joachim Kehr *In* ESA, International Symposium on Europe in Space: The Manned Space System Oct. 1988 p 379-387 (For primary document see N89-24335 18-12)
Copyright Avail: NTIS HC A99/MF A01; ESA Publications Div., ESTEC, Noordwijk, Netherlands, 80 Dutch guilders

The ESA approach for operating manned space laboratories is outlined. The ground segment and operational management structure are described. The manned space laboratories control center is presented. ESA

N89-24377# Aeritalia S.p.A., Turin (Italy). Space Systems Group.
ATTACHED PRESSURIZED MODULE (APM) CENTER FOR THE COLUMBUS ATTACHED PRESSURIZED MODULE **c18**
Giuseppe Viriglio, Luciano Battocchio, Claudio Canu, and Giovanni Rum (Piano Spaziale Nazionale, Rome, Italy) *In* ESA, International Symposium on Europe in Space: The Manned Space System Oct. 1988 p 389-393 (For primary document see N89-24335 18-12)
Copyright Avail: NTIS HC A99/MF A01; ESA Publications Div., ESTEC, Noordwijk, Netherlands, 80 Dutch guilders

A Columbus attached pressurized module center (APMC) is proposed. The APMC functions include engineering support to operation; payload user engineering support; payload integration; training; and logistics. ESA

N89-24378# European Space Agency. European Space Operations Center, Darmstadt (Germany, F.R.).
EXPERT SYSTEM FOR EUROPEAN SPACE INFRASTRUCTURE **c31**
J. Wheadon *In its* International Symposium on Europe in Space: The Manned Space System Oct. 1988 p 395-401 (For primary document see N89-24335 18-12)
Copyright Avail: NTIS HC A99/MF A01; ESA Publications Div., ESTEC, Noordwijk, Netherlands, 80 Dutch guilders

The applicability of expert systems to routine space operations is discussed. A prototype system will be developed to operate with an existing spacecraft control system to act as an operator's assistant in controlling a real time simulation model of the MARECS-B spacecraft. The contribution of expert systems to enhancing operation reliability and effectiveness will be studied. Knowledge acquisition and representation for the system will be examined. The possibility of transferring ground based operations onto autonomous spaceborne systems will be investigated. The minimum that the expert is expected to achieve is recognition of operating states and diagnosis of unit-level failures and anomalies in spacecraft subsystems. ESA

N89-24379# Telespazio, S.p.A., Rome (Italy).
THE KEY ROLE OF DATA RELAY SYSTEM (DRS) IN THE COLUMBUS COMMUNICATIONS **c32**
Victor Speziale *In* ESA, International Symposium on Europe in Space: The Manned Space System Oct. 1988 p 403-407 (For primary document see N89-24335 18-12)
Copyright Avail: NTIS HC A99/MF A01; ESA Publications Div., ESTEC, Noordwijk, Netherlands, 80 Dutch guilders

The contribution of the Data Relay System (DRS) to the Columbus program communication network is discussed. The DRS space segment and ground segment are described. User operations are outlined. The DRS is based on two geostationary satellites positioned so as to get the best compromise between the conflicting requirements of minimization of world coverage gaps and maximization of the area where data are broadcast. The DRS could also assist in orbit localization. ESA

N89-24380# Piano Spaziale Nazionale, Rome (Italy).
SCIENTIFIC UTILIZATION OF THE EUROPEAN SPACE INFRASTRUCTURE AND THE INTERNATIONAL SPACE STATION
Luciano Guerriero and Giovanni Rum *In* ESA, International Symposium on Europe in Space: The Manned Space System Oct. 1988 p 411-414 (For primary document see N89-24335 18-12)
Copyright Avail: NTIS HC A99/MF A01; ESA Publications Div., ESTEC, Noordwijk, Netherlands, 80 Dutch guilders

Missions and research programs that could benefit from a permanent space infrastructure are indicated, including space sciences, materials processing, and microgravity effects. Italian contributions to the ESA in-orbit infrastructure program are described. ESA

N89-24381# Deutsche Forschungs- und Versuchsanstalt fuer Luft- und Raumfahrt, Cologne (Germany, F.R.).
EXPERIMENTATION IN THE MAN TENDED FREE FLYER (MTFF)
H. Bauer and D. Heyland *In* ESA, International Symposium on Europe in Space: The Manned Space System Oct. 1988

p 415-427 (For primary document see N89-24335 18-12)
Copyright Avail: NTIS HC A99/MF A01; ESA Publications Div., ESTEC, Noordwijk, Netherlands, 80 Dutch guilders

Scenarios and constraints for experiments using the Columbus MTFF are outlined. Robotization and automation aspects are discussed. Experimentation on MTFF is comparable to a combination of EURECA (automated mode) and Spacelab (manned activities). Utilization of a full integrated MTFF depends on the transport capacity of Hermes. It is argued that the present Hermes design excludes an optimal use of the MTFF since the transport of consumable/samples from running experiments prevents Hermes accommodating new facilities. The baseline MTFF mission consists of payloads for metallurgy, crystallization, and biology investigations. ESA

N89-24382# Consiglio Nazionale delle Ricerche, Frascati (Italy). Istituto di Fisica dello Spazio Interplanetario.
ITALIAN SCIENTIFIC PROJECTS RELATED TO MANNED ACTIVITY IN SPACE
C. B. Cosmovici, G. Vannaroni, and R. Stalio (Trieste Univ., Italy) *In* ESA, International Symposium on Europe in Space: The Manned Space System Oct. 1988 p 429-436 (For primary document see N89-24335 18-12)
Copyright Avail: NTIS HC A99/MF A01; ESA Publications Div., ESTEC, Noordwijk, Netherlands, 80 Dutch guilders

The tethered satellite (TSS) project, and the Hitch-hiker Extreme Ultraviolet Telescope (IEH) are presented. Power generation for TSS using the plasma contactor concept; and the IEH observing program are described. A 20 km long tether could provide 18 kW of power, and would consume 64 kg of fuel per day to compensate increased drag. An energy savings of 40 percent due to the exploitation of chemical and kinetic fuel is theoretically possible. The IEH observing program consists of a few directed pointings at astronomical and solar system targets, plus random orientation determined by Shuttle attitude. ESA

N89-24383# Preussag A.G., Erdoel und Erdgas, Hannover (Germany, F.R.).
INDUSTRIAL UTILIZATION OF MICROGRAVITY: PROBLEMS IN THE REALIZATION PHASE **c29**
Karlheinz Schoenemann *In* ESA, International Symposium on Europe in Space: The Manned Space System Oct. 1988 p 437-439 (For primary document see N89-24335 18-12)
Copyright Avail: NTIS HC A99/MF A01; ESA Publications Div., ESTEC, Noordwijk, Netherlands, 80 Dutch guilders

Crystal growth of compound semiconductor material is used to illustrate the potential of space processing and to explain why industrial companies are hesitant about using spaceborne techniques. The main reasons for this hesitation are the lack of knowledge of the effects of gravity on Earth, and the lack of information on the execution of experiments in space. ESA

N89-24384# European Space Agency. European Space Research and Technology Center, ESTEC, Noordwijk (Netherlands).
THE CONCEPT OF TELESCIENCE **c31**
P. Buia *In its* International Symposium on Europe in Space: The Manned Space System Oct. 1988 p 441-445 (For primary document see N89-24335 18-12)
Copyright Avail: NTIS HC A99/MF A01; ESA Publications Div., ESTEC, Noordwijk, Netherlands, 80 Dutch guilders

The concept of telescience is defined and the ESA telescience program is introduced. Telescience is a mode of payload operation whereby ground based users can interactively control their payloads on Columbus elements. The telescience program test beds and technology support preparation; system design and simulation; and operational requirements analysis are summarized. ESA

N89-24385# LABEN Space Instrumentation and Systems, Milan (Italy). Advanced Research and Development Dept.
TELESCIENCE AND PAYLOAD CONTROL SUPPORT TECHNOLOGIES **c31**
P. Donzelli and E. Macavero *In* ESA, International Symposium on Euorpe in Space: The Manned Space System Oct. 1988 p 447-453 (For primary document see N89-24335 18-12)
Copyright Avail: NTIS HC A99/MF A01; ESA Publications Div., ESTEC, Noordwijk, Netherlands, 80 Dutch guilders

Technological options and their utilization scenarios for telescience implementation in manned space stations are outlined. On board and ground based data acquisition systems (SIMD and MIMD architecture, digital signal processing); and real time knowledge based systems to support principal investigators and payload specialists are discussed. ESA

N89-24386# MATRA Espace, Toulouse (France).
TELESCIENCE: A PROMISING OPERATIONS CENTER **c31**
Ph. LeBouar and C. Loeillet *In* ESA, International Symposium on Europe in Space: The Manned Space System Oct. 1988 p 455-463 (For primary document see N89-24335 18-12)
Copyright Avail: NTIS HC A99/MF A01; ESA Publications Div., ESTEC, Noordwijk, Netherlands, 80 Dutch guilders

The telescience operations environment and requirements are outlined, and a telescience concept is described. The concept includes a communication network and an onboard data management system. Consequences of the telesciences concept for the Columbus user support and operations centers and payload operations control center are assessed. Validation of the telescience concept is discussed. ESA

N89-24387# European Space Agency. European Space Research and Technology Center, ESTEC, Noordwijk (Netherlands).
GETTING READY FOR EVA **c54**
A. Accensi *In its* International Symposium on Europe in Space: The Manned Space System Oct. 1988 p 467-475 (For primary document see N89-24335 18-12)
Copyright Avail: NTIS HC A99/MF A01; ESA Publications Div., ESTEC, Noordwijk, Netherlands, 80 Dutch guilders

The roles of astronauts and robots in space missions are discussed. The advantages of extravehicular activity (EVA) for complex and contingency tasks is considered. The history and status of EVA programs conducted by ESA are summarized. ESA

N89-24388# Dornier-Werke G.m.b.H., Friedrichshafen (Germany, F.R.).
EVA INFORMATION SYSTEM: A MODERN WORKSTATION IN SPACE **c54**
Franz Pittermann, Pierre Larroque, and Stephane Berthier (Avions Marcel Dassault-Breguet Aviation, Saint-Cloud, France) *In* ESA, International Symposium on Europe in Space: The Manned Space System Oct. 1988 p 477-483 (For primary document see N89-24335 18-12)
Copyright Avail: NTIS HC A99/MF A01; ESA Publications Div., ESTEC, Noordwijk, Netherlands, 80 Dutch guilders

Information and communication requirements for extravehicular activity (EVA) are identified. Man-machine interfaces for EVA are discussed, and the relative merits of astronauts and robots are compared. Technologies and techniques needed in an EVA workstation are considered, and it is argued that the required technologies exist and can be adapted to space conditions. ESA

N89-24389# Tecnospazio S.p.A., Milan (Italy).
MULTIPLE ROBOT APPROACH FOR AUTOMATION OF IN-ORBIT MODULES **c18**
P. G. Magnani, G. Colombina, and C. Gerli *In* ESA, International Symposium on Europe in Space: The Manned Space System Oct. 1988 p 485-492 (For primary document see N89-24335 18-12)
Copyright Avail: NTIS HC A99/MF A01; ESA Publications Div., ESTEC, Noordwijk, Netherlands, 80 Dutch guilders

Internal automation of in-orbit modules is considered. Logistics and maintenance requirements are defined. Functional, operational, and safety requirements are listed. Mono and multiple robot solutions are compared, and it is concluded that multiple robots

are preferable, in spite of the greater simplicity of monorobot solutions. Fixed manipulators; rail-based robots; climbing robots; reconfigurable systems; and multi moving arms are described. ESA

N89-24390# Fokker B.V., Amsterdam (Netherlands).
THE HERMES ROBOT ARM (HERA) **c37**
R. Hamann, C. Blaas, and R. H. Bentall (European Space Agency. European Space Research and Technology Center, ESTEC, Noordwijk, Netherlands) *In* ESA, International Symposium on Europe in Space: The Manned Space System Oct. 1988 p 493-501 (For primary document see N89-24335 18-12)
Copyright Avail: NTIS HC A99/MF A01; ESA Publications Div., ESTEC, Noordwijk, Netherlands, 80 Dutch guilders

The orbital servicing functions provided by the Hermes robot arm (HERA) are described. The HERA desgin and verification procedures are reviewed. The HERA functions include capture of a free flying satellite; berthing, unberthing, and reberthing; payload transfer and release; ORU exchange; inspection; tool manipulation; and EVA support. ESA

N89-24391# Deutsche Forschungs- und Versuchsanstalt fuer Luft- und Raumfahrt, Cologne (Germany, F.R.).
ROBOTIC EXPERIMENTS ON SPACELAB D-2 AS TESTBED FOR FUTURE OPERATIONAL CONCEPTS **c37**
K. L. Mueller and M. Turk *In* ESA, International Symposium on Europe in Space: The Manned Space System Oct. 1988 p 503-507 (For primary document see N89-24335 18-12)
Copyright Avail: NTIS HC A99/MF A01; ESA Publications Div., ESTEC, Noordwijk, Netherlands, 80 Dutch guilders

The Spacelab D2 Robotic Technology Experiment (ROTEX), particularly the robotic arm, is described, and aspects of ROTEX relevant to Columbus are summarized. The ROTEX features relevant to Columbus payload operations include command uplink with higher data rates and less delay than in previous Spacelab missions; high quality TV pictures with predictive graphics superimposed; sole responsibility of ground teams for experiment performance; and use of expert systems for malfunction diagnostics and failure compensation. ESA

N89-24392# LABEN Space Instrumentation and Systems, Milan (Italy). Advanced Research and Development Dept.
ADVANCED MMI AND IMAGE HANDLING TO SUPPORT CREW ACTIVITIES **c54**
R. Cortinovis, B. Barni, and R. Persico *In* ESA, International Symposium on Europe in Space: The Manned Space System Oct. 1988 p 509-514 (For primary document see N89-24335 18-12)
Copyright Avail: NTIS HC A99/MF A01; ESA Publications Div., ESTEC, Noordwijk, Netherlands, 80 Dutch guilders

A concept for a crew workstation, focusing on man-machine interface (MMI) aspects related to the integrated handling of text, graphics, and visual information is presented. Window and overlay management methods, and image processing techniques for picture quality enhancement are discussed. ESA

N89-24393# Dortmund Univ. (Germany, F.R.). Inst. fuer Roboterforschung.
HIERARCHICALLY STRUCTURED CONTROL FOR INTELLIGENT ROBOTS IN SPACE **c63**
E. Freund *In* ESA, International Symposium on Europe in Space: The Manned Space System Oct. 1988 p 515-522 (For primary document see N89-24335 18-12)
Copyright Avail: NTIS HC A99/MF A01; ESA Publications Div., ESTEC, Noordwijk, Netherlands, 80 Dutch guilders

The use of robots in space is discussed and the application of multirobot systems is described. It is argued that a hierarchically structured, modular concept of automation is needed. Critical research areas are sensors and intelligent multisensor systems; teleoperation and man-machine interface; application of expert systems to space-based robots; and multiple arm and mobile robots. ESA

N89-24394# Deutsche Forschungs- und Versuchsanstalt fuer Luft- und Raumfahrt, Cologne (Germany, F.R.).
THE MICROGRAVITY USER SUPPORT CENTER (MUSC) **c29**
K. Wittmann, H. P. Schmidt, D. Padeken, B. Hildmann, E. Bennett, and B. Feuerbacher *In* ESA, International Symposium on Europe in Space: The Manned Space System Oct. 1988 p 525-530 (For primary document see N89-24335 18-12)
Copyright Avail: NTIS HC A99/MF A01; ESA Publications Div., ESTEC, Noordwijk, Netherlands, 80 Dutch guilders

Function and objectives of user support in the ESA Microgravity User Support Center (MUSC) are summarized. The MUSC functions include user information services; ground support; mission support; and scientific support. ESA

N89-24395# Naples Univ. (Italy). Inst. of Aerodynamics.
MARS MICROGRAVITY ADVANCED RESEARCH AND SUPPORT CENTER **c29**
Luigi G. Napolitano *In* ESA, International Symposium on Europe in Space: The Manned Space System Oct. 1988 p 531-540 (For primary document see N89-24335 18-12)
Copyright Avail: NTIS HC A99/MF A01; ESA Publications Div., ESTEC, Noordwijk, Netherlands, 80 Dutch guilders

The Microgravity Advanced Research and Support (MARS) center is presented. Its role in the Columbus program is described. The functions of the MARS center include basic research; microgravity experimentation; user support; technology assessment; and support to space agencies. Operational and program implementation aspects are summarized. ESA

N89-24396# Deutsche Forschungs- und Versuchsanstalt fuer Luft- und Raumfahrt, Cologne (Germany, F.R.).
CREW TRAINING ASPECTS **c53**
F. J. Demond, W. Mueller-Breitkreutz, and H. G. Neuhaeuser *In* ESA, International Symposium on Europe in Space: The Manned Space System Oct. 1988 p 541-549 (For primary document see N89-24335 18-12)
Copyright Avail: NTIS HC A99/MF A01; ESA Publications Div., ESTEC, Noordwijk, Netherlands, 80 Dutch guilders

Astronaut training for Hermes and Columbus is discussed. Experience from the German Spacelab missions is reviewed and training facilities needed for Hermes and Columbus are indicated. Two main types of facilities are proposed: an integrated system training facility with full scale mock-ups of the specific space elements; and single system training facilities, which allow training on single subsystems or payload elements. ESA

N89-24397# Selenia Spazio S.p.A., Rome (Italy).
THE COLUMBUS CREW COMMUNICATION SUBSYSTEM AND THE ON BOARD LOCAL AREA NETWORK **c32**
A. Morando, A. Francia, M. Masci, and Giu. Montalto *In* ESA, International Symposium on Europe in Space: The Manned Space System Oct. 1988 p 551-563 (For primary document see N89-24335 18-12)
Copyright Avail: NTIS HC A99/MF A01; ESA Publications Div., ESTEC, Noordwijk, Netherlands, 80 Dutch guilders

The Columbus local area network (LAN) and crew communication system is described. The architecture of the system consists of several independant network assemblies (including the onboard LAN, audio network, and video network) each dedicated to a particular type of data, and a gateway, called communication processor, supporting data exchange between onboard and ground. ESA

N89-24398# Dornier-Werke G.m.b.H., Friedrichshafen (Germany, F.R.).
SIMULATION OF WEIGHTLESSNESS WITH NEUTRAL BUOYANCY FACILITIES AND ZERO-g AIRCRAFT FOR THE PREPARATION OF EUROPEAN MANNED SPACE OPERATIONS **c14**
Dieter Isakeit *In* ESA, International Symposium on Europe in Space: The Manned Space System Oct. 1988 p 565-571 (For primary document see N89-24335 18-12)

Copyright Avail: NTIS HC A99/MF A01; ESA Publications Div., ESTEC, Noordwijk, Netherlands, 80 Dutch guilders

Weightlessness simulation using parabolic flight and large water filled tanks is described. American and Soviet experience with these techniques is reviewed, and requirements for ESA's manned space flight program are mentioned. ESA

N89-24399# Aeritalia S.p.A., Turin (Italy). Space Systems Group.

THE UTILIZATION OF THE EUROPEAN PRESSURIZED MODULE FOR NON-EUROPEAN EXPERIMENTS **c18**

G. Oelker, M. S. Lavitola, and A. Allegra *In* ESA, International Symposium on Europe in Space: The Manned Space System Oct. 1988 p 573-575 (For primary document see N89-24335 18-12)

Copyright Avail: NTIS HC A99/MF A01; ESA Publications Div., ESTEC, Noordwijk, Netherlands, 80 Dutch guilders

Physical accommodation of non European experiments in the European pressurized module on the International Space station, and ground processing of the data are considered. The need for commonality is stressed, and it is suggested that operations requiring very strict specifications and highly constraining procedures be confined to satellites. ESA

N89-24400# Aerospatiale, Toulouse (France).

LESSONS LEARNED FROM SL-1 AND D-1

P. Baudry, J.-L. Chretien, R. Furrer, U. Merbold, E. Messerschmid, Claude Nicollier, and W. Ockels (European Space Agency. European Space Research and Technology Center, ESTEC, Noordwijk, Netherlands) *In* ESA, International Symposium on Europe in Space: The Manned Space System Oct. 1988 p 579-590 (For primary document see N89-24335 18-12)

Copyright Avail: NTIS HC A99/MF A01; ESA Publications Div., ESTEC, Noordwijk, Netherlands, 80 Dutch guilders

The experience gained on the First Spacelab mission and the D1 mission is summarized. Crew tasks; crew training and preparation for flight; communication; hardware and software; experimental environment; and flight operations are covered. ESA

N89-24401# European Space Agency, Paris (France). Directorate of Space Station and Platforms.

HERMES CREW ROLE

Claude Nicollier *In its* International Symposium on Europe in Space: The Manned Space System Oct. 1988 p 591-593 (For primary document see N89-24335 18-12)

Copyright Avail: NTIS HC A99/MF A01; ESA Publications Div., ESTEC, Noordwijk, Netherlands, 80 Dutch guilders

The role of the crew on Hermes is outlined, and the optimal mix of crew and automatic systems is considered. Tasks during each flight phase, including orbial servicing of Columbus are listed. It is stressed that manual control should also be possible for each automatic phase. The small size of the crew makes extensive cross training necessary. ESA

N89-24402# Stuttgart Univ. (Germany, F.R.). Inst. for Space Systems.

SAFETY IN MANNED SPACE FLIGHT **c31**

E. Messerschmid *In* ESA, International Symposium on Europe in Space: The Manned Space System Oct. 1988 p 595-604 (For primary document see N89-24335 18-12)

Copyright Avail: NTIS HC A99/MF A01; ESA Publications Div., ESTEC, Noordwijk, Netherlands, 80 Dutch guilders

The safety policy and requirements for Hermes are reviewed. Design considerations for crew escape systems are recalled. Escape systems for spacecraft and airplanes are described. Escape systems for Hermes, including manual and powered bail-out systems; open ejection seats; encapsulated ejection seats; pressure vessel/module/cabin; nose separated capsule; and reentry capsules are compared. Problems involved in judging when to abort a mission are mentioned. ESA

N89-24403# European Space Agency, Paris (France).

THE ASTRONAUT'S FUNCTIONS ABOARD COLUMBUS **c66**

U. Merbold *In its* International Symposium on Europe in Space: The Manned Space System Oct. 1988 p 605-608 (For primary document see N89-24335 18-12)

Copyright Avail: NTIS HC A99/MF A01; ESA Publications Div., ESTEC, Noordwijk, Netherlands, 80 Dutch guilders

The role of Columbus astronauts in system operations; payload operations; and assembling is outlined. Operations on the attached pressurized module and MTFF are described. ESA

N89-24705*# National Aeronautics and Space Administration, Washington, DC.

TECHNOLOGY REQUIREMENTS FOR ADVANCED NASA MISSIONS

Henry B. Curtis *In* NASA, Lewis Research Center, Space Photovoltaic Research and Technology, 1988. High Efficiency, Space Environment, and Array Technology Apr. 1989 p 3-9 (For primary document see N89-24704 18-44)

Avail: NTIS HC A16/MF A01 CSCL 22A

13 ASTRODYNAMICS

Includes powered and free-flight trajectories; and orbital and launching dynamics.

N89-24404 Michigan Univ., Ann Arbor.

MULTIPLE-PASS AEROASSISTED PLANE CHANGE Ph.D. Thesis

Der-Ming Ma 1988 151 p

Avail: Univ. Microfilms Order No. DA8907089

In the problem of aeroassisted orbital plane change, it was found that, for a large single-pass aerodynamic plane change, an initial negative lift is used to bring the hypervelocity vehicle to a sufficiently low altitude where most aerodynamic turning is performed before exit and ascent into the final orbit. An alternative to this flight program is to leave the lifting vehicle in the initial elliptic orbit and then perform a small change in the inclination during each perigee passage through the atmosphere. The advantage of this flight program is that the heating rate and the deceleration remain low while the vehicle's lifetime is extended. Two illustrative examples were performed and it is found that for the same energy loss the multiple-pass maneuver produces the same plane change as the single-pass maneuver. The inclination of the osculating plane increases while the elliptic orbit is contracting toward circular. Of course, both the altitude and the velocity are oscillating with decreasing magnitude during the circularizing process. Due to the low aerodynamic force, the motion is nearly Keplerian. Hence, an approximate integration of the adjoint equations in the variational formulation can be performed producing an approximate law for the optimal aerodynamic control. It is proposed to use this suboptimal law in the exact equations of motion for the integration. The present numerical integration over several revolutions is long and tedious in the application of the transversality conditions. The King-Hele method of averaging as applied to the problem of orbit contraction is proposed for the integration of a reduced set of nonlinear equations using quadratic approximations of nonlinear functions. Author

14 GROUND SUPPORT SYSTEMS AND FACILITIES (SPACE)

Includes launch complexes, research and production facilities; ground support equipment, e.g., mobile transporters; and simulators.

For related information see also *09 Research and Support Facilities (Air).*

N89-24405* National Aeronautics and Space Administration. Marshall Space Flight Center, Huntsville, AL.

CONTAINERLESS GLASS FIBER PROCESSING Final Report

E. C. Ethridge and R. J. Naumann Mar. 1986 24 p
(NASA-TM-86540; NAS 1.15:86540) Avail: NTIS HC A03/MF A01 CSCL 14B

An acoustic levitation furnace system is described that was developed for testing the feasibility of containerless fiber pulling experiments. It is possible to levitate very dense materials such as platinum at room temperature. Levitation at elevated temperatures is much more difficult. Samples of dense heavy metal fluoride glass were levitated at 300 C. It is therefore possible that containerless fiber pulling experiments could be performed. Fiber pulling from the melt at 650 C is not possible at unit gravity but could be possible at reduced gravities. The Acoustic Levitation Furnace is described, including engineering parameters and processing information. It is illustrated that a shaped reflector greatly increases the levitation force aiding the levitation of more dense materials. Author

N89-24406*# National Academy of Sciences - National Research Council, Washington, DC.
REPORT OF THE COMMITTEE ON A COMMERCIALLY DEVELOPED SPACE FACILITY
Joseph F. Shea, H. Guyford Stever, W. Bowman Cutter, III, Wolfgang H. Demisch, Daniel J. Fink, Alexander H. Flax, Harry C. Gatos, Martin E. Glicksman, Louis J. Lanzerotti, and John M. Logsdon, III (George Washington Univ., Washington, DC.) et al 1989 107 p
(Contract NASw-4003)
(NASA-CR-185383; NAS 1.26:185383) Avail: NTIS HC A06/MF A01 CSCL 14B

Major facilities that could support significant microgravity research and applications activity are discussed. The ground-based facilities include drop towers, aircraft flying parabolic trajectories, and sounding rockets. Facilities that are intrinsically tied to the Space Shuttle range from Get-Away-Special canisters to Spacelab long modules. There are also orbital facilities which include recoverable capsules launched on expendable launch vehicles, free-flying spacecraft, and space stations. Some of these existing, planned, and proposed facilities are non-U.S. in origin, but potentially available to U.S. investigators. In addition, some are governmentally developed and operated whereas others are planned to be privately developed and/or operated. Tables are provided to show the facility, developer, duration, estimated gravity level, crew interaction, flight frequency, year available, power to payload, payload volume, and maximum payload mass. The potential of direct and indirect benefits of manufacturing in space are presented. Author

N89-24407 Max-Planck-Inst. fuer Physik und Astrophysik, Garching (Germany, F.R.). Inst. fuer Extraterrestrische Physik.
THE GAMMA-RAY OBSERVATORY GRO IN PERSPECTIVE
Volker Schoenfelder Dec. 1988 14 p Presented at the 27th COSPAR Plenary Meeting, Espoo, Finland, Jul. 1988 Submitted for publication
(MPE-Preprint-137; ETN-89-94582) Copyright Avail: Fachinformationszentrum Karlsruhe, 7514 Eggenstein-Leopoldshafen 2, Federal Republic of Germany

The GRO observatory is expected to make the next major steps forward in gamma ray astronomy. The instruments have complementary properties and cover more than 5 decades in energy, from 100 keV to 30 GeV. The free flying three axis stabilized observatory is planned to be launched in 1990 by the space shuttle into a low Earth orbit. ESA

N89-24408# Lawrence Livermore National Lab., CA.
CAPABILITIES AND SOME APPLICATIONS OF THE LLNL 100-kV ELECTRIC GUN
J. E. Osher, G. R. Gathers, H. H. Chau, and R. C. Weingart Jun. 1989 11 p Presented at the 3rd International Symposium on Behavior of Media Under High Dynamic Pressures, La Grande Motte, France, 5-9 Jun. 1989
(Contract W-7405-eng-48)
(DE89-006747; UCRL-98804; CONF-890661-4) Avail: NTIS HC A03/MF A01

The LLNL 100-kV electric gun is an experimental device for launching thin flyer plates at velocities as high as 20 km/s to study impact damage and shock-wave physics. The hypervelocity impact studies reported here include a damage study of spalling damage in aluminum, a study of one-dimensional shock-wave attenuation in materials, use of the well-characterized one-dimensional shock waves for equation-of-state measurements in various materials, and use of thin flyer plates at velocities up to 18 km/s to produce reverse ballistic impact on target objects such as rods to measure damage and fragmentation. Our studies include both experimental results and correlation with numerical calculations using a code such as DYNA2D. DOE

N89-24372# European Space Agency. European Space Operations Center, Darmstadt (Germany, F.R.).
THE ROLE OF THE HERMES FLIGHT CONTROL CENTER IN A TYPICAL HERMES/MTFF SERVICING MISSION
Christian Reinhold and Marc Francois (Centre National d'Etudes Spatiales, Toulouse, France) *In its* International Symposium on Europe in Space: The Manned Space System Oct. 1988 p 351-359 (For primary document see N89-24335 18-12)
Copyright Avail: NTIS HC A99/MF A01; ESA Publications Div., ESTEC, Noordwijk, Netherlands, 80 Dutch guilders

N89-24376# Deutsche Forschungs- und Versuchsanstalt fuer Luft- und Raumfahrt, Oberpfaffenhofen (West Germany). Space Operation Center.
THE MANNED SPACE LABORATORIES CONTROL CENTER (MSCC) AT DFVLR, OBERPFAFFENHOFEN, GERMANY, F.R.
Joachim Kehr *In* ESA, International Symposium on Europe in Space: The Manned Space System Oct. 1988 p 379-387 (For primary document see N89-24335 18-12)
Copyright Avail: NTIS HC A99/MF A01; ESA Publications Div., ESTEC, Noordwijk, Netherlands, 80 Dutch guilders

N89-24398# Dornier-Werke G.m.b.H., Friedrichshafen (Germany, F.R.).
SIMULATION OF WEIGHTLESSNESS WITH NEUTRAL BUOYANCY FACILITIES AND ZERO-g AIRCRAFT FOR THE PREPARATION OF EUROPEAN MANNED SPACE OPERATIONS
Dieter Isakeit *In* ESA, International Symposium on Europe in Space: The Manned Space System Oct. 1988 p 565-571 (For primary document see N89-24335 18-12)
Copyright Avail: NTIS HC A99/MF A01; ESA Publications Div., ESTEC, Noordwijk, Netherlands, 80 Dutch guilders

15 LAUNCH VEHICLES AND SPACE VEHICLES

Includes boosters; operating problems of launch/space vehicle systems; and reusable vehicles.

For related information see also *20 Spacecraft Propulsion and Power.*

N89-24409*# National Aeronautics and Space Administration. Lewis Research Center, Cleveland, OH.
THE PATHFINDER CHEMICAL TRANSFER PROPULSION PROGRAM
Ned P. Hannum, Frank D. Berkopec, and Robert L. Zurawski (National Aeronautics and Space Administration, Washington, DC.) May 1989 11 p Presented at the JANNAF Propulsion Meeting, Cleveland, OH, 23-25 May 1989
(NASA-TM-102084; E-4847; NAS 1.15:102084) Avail: NTIS HC A03/MF A01 CSCL 13B

Pathfinder is a research and technology initiative by the National Aeronautics and Space Administration (NASA) intended to strengthen the technology base of the United States civil space program in preparation for future space exploration missions. Pathfinder begins in FY-89. One of the four major thrusts of Pathfinder is Space Transfer technology. A key element of this thrust is the Chemical Transfer Propulsion program which will

provide the propulsion technology for high performance, liquid oxygen/liquid hydrogen expander cycle engines which are expected to be operated and maintained in space. These advanced engines will enhance or enable a variety of future space exploration missions. This paper describes the goals and objectives, management, technical plan, and technology transfer for the Chemical Transfer Propulsion element of Pathfinder. Author

N89-24336# European Space Agency, Paris (France).
THE ARIANE 5 DEVELOPMENT PROGRAM
J. Feustel-Buechl *In its* International Symposium on Europe in Space: The Manned Space System Oct. 1988 p 41-47 (For primary document see N89-24335 18-12)
Copyright Avail: NTIS HC A99/MF A01; ESA Publications Div., ESTEC, Noordwijk, Netherlands, 80 Dutch guilders

N89-24352# Bombrini Parodi-Delfino S.p.A., Colleferro (Italy).
ARIANE 5 SOLID BOOSTERS: OVERVIEW OF DESIGN APPROACH AND ENVISAGED TECHNOLOGIES
Roberto Fabrizi *In* ESA, International Symposium on Europe in Space: The Manned Space System Oct. 1988 p 145-151 Prepared in cooperation with Societe Europeene de Propulsion, Saint-Medard-en-Jalles, France (For primary document see N89-24335 18-12)
Copyright Avail: NTIS HC A99/MF A01; ESA Publications Div., ESTEC, Noordwijk, Netherlands, 80 Dutch guilders

16 SPACE TRANSPORTATION

Includes passenger and cargo space transportation, e.g., shuttle operations; and space rescue techniques.

For related information see also *03 Air Transportation and Safety* and *18 Spacecraft Design, Testing and Performance.* For space suits see *54 Man/System Technology and Life Support.*

N89-24410*# Martin Marietta Corp., Denver, CO.
ORBITAL TRANSFER VEHICLE: CONCEPT DEFINITION AND SYSTEM ANALYSIS STUDY Midterm Review
22 Jul. 1987 112 p
(Contract NAS8-36108)
(NASA-CR-183551; NAS 1.26:183551; MCR-87-2600) Avail: NTIS HC A06/MF A01 CSCL 22B

Findings and recommendations from the second extension of the Orbital Transfer Vehicle (OTV) concept definition and system analysis study are outlined. The extension study opens the scope of potential recommendations by introducing a variety of ambitious programs, and by making the large cargo vehicle recommended by the Space Transportation Architecture Studies available at no acquisition cost to the OTV program. It is a further objective of the extension study to evaluate the sensitivity of OTV program recommendations to scenario variations such as different mission models, different launch vehicle availability, and different space station availability. Program/mission issues are addressed including safety considerations for the Aft Cargo Carrier (ACC) OTV. Design issues related to the development of a near-term expendable OTV, engine configuration tradeoffs, lunar missions, and program evolution are discussed. Finally, aeroassist considerations for a manned Mars mission and high speed entries are presented.
A.D.

N89-24411*# Jet Propulsion Lab., California Inst. of Tech., Pasadena.
SHUTTLE PAYLOAD BAY THERMAL ENVIRONMENTS: SUMMARY AND CONCLUSION REPORT FOR STS FLIGHTS 1-5
J. H. Fu and G. R. Graves 15 Sep. 1987 435 p
(NASA-CR-185017; JPL-Publ-87-31; NAS 1.26:185017) Avail: NTIS HC A19/MF A01 CSCL 22B

The thermal data for the payload bay of the first five shuttle flights is summarized and the engineering evaluation of that data is presented. After a general discussion on mission profiles and vehicle configurations, the thermal design and flight instrumentation systems of the payload bay are described. The thermal flight data sources and a categorization of the data are then presented. A thermal flight data summarization section provides temperature data for the five phases of a typical mission profile. These are: prelaunch, ascent, on-orbit, entry and postlanding. The thermal flight data characterization section encompasses this flight data for flight to flight variations, payload effects, temperature ranges, and other variations. Discussion of the thermal environment prediction models in use by industry and various NASA Centers, and the results predicted by these models, is followed by an evaluation of the correlation between the actual flight data and the results predicted by the models. Finally, the available thermal data are evaluated from the viewpoint of the user concerned with establishing the thermal environment in the payload bay. The data deficiencies are discussed and recommendations for their elimination are presented. Author

N89-24412*# National Aeronautics and Space Administration. John F. Kennedy Space Center, Cocoa Beach, FL.
KSC ICE/FROST/DEBRIS ASSESSMENT FOR SPACE SHUTTLE MISSION STS-30R
Charles G. Stevenson, Gregory N. Katnik, and Scott A. Higginbotham 4 May 1989 214 p Original contains color illustrations
(NASA-TM-102147; NAS 1.15:102147) Avail: NTIS HC A10/MF A01 CSCL 22B

An ice/frost/debris assessment was conducted for Space Shuttle Mission STS-30R. Debris inspections of the flight elements and launch pad are performed before and after launch. Ice/frost conditions on the external tank are assessed by the use of computer programs, nomographs, and infrared scanner data during cryogenic loading of the vehicle followed by an on-pad visual inspection. High speed photography is analyzed after launch to identify ice/debris sources and evaluate potential vehicle damage. The ice/frost/debris conditions of Mission STS-30R and their overall effect on the Space Shuttle Program is documented.
Author

N89-24413*# National Aeronautics and Space Administration. Lewis Research Center, Cleveland, OH.
FIRE SAFETY APPLICATIONS FOR SPACECRAFT
Robert Friedman and Sandra L. Olson 1989 29 p Presented at the Symposium on Aircraft Fire Safety, Sintra, Portugal, 22-26 May 1989; sponsored by the AGARD/NATO Propulsion Energetics Panel
(NASA-TM-101463; E-4511; NAS 1.15:101463) Avail: NTIS HC A03/MF A01 CSCL 22B

Fire safety for spacecraft is reviewed by first describing current practices, many of which are adapted directly from aircraft. Then, current analyses and experimental knowledge in low-gravity combustion, with implications for fire safety are discussed. In orbiting spacecraft, the detection and suppression of flames are strongly affected by the large reduction in buoyant flows under low gravity. Generally, combustion intensity is reduced in low gravity. There are some notable exceptions, however, one example being the strong enhancement of flames by low-velocity ventilation flows in space. Finally, the future requirements in fire safety, particularly the needs of long-duration space stations in fire prevention, detection, extinguishment, and atmospheric control are examined. The goal of spacecraft fire-safety investigations is the establishment of trade-offs that promote maximum safety without hampering the useful human and scientific activities in space.
Author

N89-24350# European Space Agency, Paris (France). Space Transportation Systems Directorate.
THE TECHNOLOGY CONTENTS OF THE FIRST PHASE OF THE HERMES DEVELOPMENT PROGRAM
J. J. Capart and E. Slachmuylders *In its* International Symposium on Europe in Space: The Manned Space System Oct. 1988 p 133-142 (For primary document see N89-24335 18-12)

Copyright Avail: NTIS HC A99/MF A01; ESA Publications Div., ESTEC, Noordwijk, Netherlands, 80 Dutch guilders

N89-24357# Centre National d'Etudes Spatiales, Toulouse (France).
HERMES-MTFF RENDEZVOUS STRATEGY AND COMPOSITE OPERATIONS
L. Marechal, F. DiMauro, D. Hoge, and W. Fehse *In* ESA, International Symposium on Europe in Space: The Manned Space System Oct. 1988 p 185-190 Prepared in cooperation with ESA, Paris, France and ESA/ESTEC, Noordwijk, Netherlands (For primary document see N89-24335 18-12)
Copyright Avail: NTIS HC A99/MF A01; ESA Publications Div., ESTEC, Noordwijk, Netherlands, 80 Dutch guilders

17 SPACE COMM., SPACECRAFT COMM., COMMAND & TRACKING

Includes telemetry; space communications networks; astronavigation and guidance; and radio blackout.

For related information see also *04 Aircraft Communications and Navigation* and *32 Communications and Radar.*

N89-24414# National Aeronautical Lab., Bangalore (India). Systems Engineering Div.
MICROPROCESSOR BASED 32 CHANNEL PCM TELEMETRY SYSTEM
N. N. Murthy Aug. 1987 37 p
(NAL-TM-SE-8704) Avail: NTIS HC A03/MF A01

The details of a 32 channel PCM telemetry system developed to acquire data from flight experiments conducted on Pushpak aircraft and to be conducted on LCRA aircraft are presented. The system is designed using Intel 8085A central processing unit with its associated peripherals like 8255, 8251 and 8155. The system can be programmed to handle up to 32 channels of analog data. The bit rate can also be varied up to 56 Kilobits/sec. Author

18 SPACECRAFT DESIGN, TESTING AND PERFORMANCE

Includes satellites; space platforms; space stations; spacecraft systems and components such as thermal and environmental controls; and attitude controls.

For life support systems see *54 Man/System Technology and Life Support.* For related information see also *05 Aircraft Design, Testing and Performance, 39 Structural Mechanics,* and *16 Space Transportation.*

N89-24415*# Lockheed Missiles and Space Co., Sunnyvale, CA.
SUPERFLUID HELIUM TANKER STUDY (SFHT) Program Press Report
9 Aug. 1988 353 p
(Contract NAS9-17853)
(NASA-CR-172114; NAS 1.26:172114; LMSC-F223517) Avail: NTIS HC A16/MF A01 CSCL 22B

The Superfluid Helium Tanker (SFHT) design is examined for minimum up front cost, a low life cycle cost, and the maximum flexibility/adaptability consistent with the above objectives. The logic flow started with the collection and analysis of user requirements. A configuration trade-off was made to determine the baseline concept for SFHT that most nearly met all of the program objectives. The next task was to develop the baseline concept for the fluid subsystem. With this accomplished the baseline tanker was designed. The commonality task was completed and the program plan and cost estimate will be completed. Author

N89-24416*# National Aeronautics and Space Administration, Washington, DC.
THE SPACE STATION POWER SYSTEM
1989 12 p Original document contains color illustrations
(NASA-TM-101245; NAS 1.15:101245) Avail: NTIS HC A03/MF A01 CSCL 22B

The requirements for electrical power by the proposed Space Station Freedom are discussed. The options currently under consideration are examined. The three power options are photovoltaic, solar dynamic, and a hybrid system. Advantages and disadvantages of each system are tabulated. Drawings and artist concepts of the Space Station configuration are provided.
Author

N89-24417*# National Aeronautics and Space Administration, Washington, DC.
SPACE STATION: A STEP INTO THE FUTURE
Andrew J. Stofan 1989 9 p
(NASA-PAM-510/11-87) Avail: NTIS HC A02/MF A01 CSCL 22B

The Space Station is an essential element of NASA's ongoing program to recover from the loss of the Challenger and to regain for the United States its position of leadership in space. The Space Station Program has made substantial progress and some of the major efforts undertaken are discussed briefly. A few of the Space Station policies which have shaped the program are reviewed. NASA is dedicated to building a Station that, in serving science, technology, and commerce assured the United States a future in space as exciting and rewarding as the past. In cooperation with partners in the industry and abroad, the intent is to develop a Space Station that is intellectually productive, technically demanding, and genuinely useful. B.G.

N89-24418*# National Aeronautics and Space Administration. Lewis Research Center, Cleveland, OH.
REVIEW OF THE ENVIRONMENTAL EFFECTS OF THE SPACE STATION FREEDOM PHOTOVOLTAIC POWER MODULE
Henry K. Nahra 1989 8 p Proposed for presentation at the 24th Intersociety Energy Conversion Engineering Conference, Washington, DC, 6-11 Aug. 1989; sponsored by IEEE, AIAA, ANS, ASME, SAE, ACS and AIChE
(NASA-TM-102076; E-4836; NAS 1.15:102076) Avail: NTIS HC A02/MF A01 CSCL 22B

An overview is provided of the environment in the low Earth orbit (LEO), the interaction of this environment with the Photovoltaic (PV) Power system of the Space Station Freedom is reviewed, and the environmental programs are described that are designed to investigate the interactions of the LEO environment with the photovoltaic power system. Such programs will support and impact the design of the subsystems of the PV module in order to survive the design lifetime in the LEO natural and induced environment.
Author

N89-24419*# Jet Propulsion Lab., California Inst. of Tech., Pasadena.
MAGELLAN: THE UNVEILING OF VENUS
Mar. 1989 28 p Original contains color illustrations
(NASA-CR-185018; NAS 1.26:185018) Avail: NTIS HC A03/MF A01 CSCL 22B

In the late 1970s and early 1980s, the United States and the Soviet Union sent the Pioneer Venus and Venera spacecraft, respectively, to study Venus more closely and to image its surface with radar. These missions have answered many questions about Venus, but many more questions remain unanswered about the extent to which Venus' surface was shaped by volcanoes, plate tectonics, impact craters, and water and wind erosion. To help answer these remaining questions a new radar imaging spacecraft Magellan will be launched from the Space Shuttle. Magellan will spend eight months mapping most of the planet at a resolution nearly ten times better than any previous views of the surface. The mission of Magellan, the radar equipment, orbiting of Venus, planetary imaging, and surface exploration are discussed. B.G.

N89-24420*# Jet Propulsion Lab., California Inst. of Tech., Pasadena.
VOYAGER AT NEPTUNE: 1989
1989 20 p
(NASA-CR-185317; NAS 1.26:185317; JPL-Publ-400-353) Avail: NTIS HC A03/MF A01 CSCL 22B

The Voyager mission has taken advantage of a rare planetary alignment that occurs at intervals of about 175 years and affords an extraordinary opportunity: a grand tour by a single spacecraft of the outer planets Jupiter, Saturn, Uranus, and Neptune. Voyager 2 will fly past Nepture and its large moon Triton on August 24, 1989. The discovery of Neptune, along with its current history is discussed. The imaging challenges, tracking and data acquisition, and the Voyager spacecraft are explained. Data will be gathered on the ring arcs of Neptune, the atmosphere and surface of Neptune, Triton, and Nereid (the smaller moon). B.G.

N89-24421*# National Aeronautics and Space Administration. Marshall Space Flight Center, Huntsville, AL.
A METHODOLOGY FOR COMMONALITY ANALYSIS, WITH APPLICATIONS TO SELECTED SPACE STATION SYSTEMS
Lawrence Dale Thomas May 1989 99 p
(NASA-TM-100364; NAS 1.15:100364) Avail: NTIS HC A05/MF A01 CSCL 22B

The application of commonality in a system represents an attempt to reduce costs by reducing the number of unique components. A formal method for conducting commonality analysis has not been established. In this dissertation, commonality analysis is characterized as a partitioning problem. The cost impacts of commonality are quantified in an objective function, and the solution is that partition which minimizes this objective function. Clustering techniques are used to approximate a solution, and sufficient conditions are developed which can be used to verify the optimality of the solution. This method for commonality analysis is general in scope. It may be applied to the various types of commonality analysis required in the conceptual, preliminary, and detail design phases of the system development cycle. Author

N89-24422*# National Aeronautics and Space Administration. Marshall Space Flight Center, Huntsville, AL.
PRESSURE-VOLUME PROPERTIES OF METALLIC BELLOWS
Larry Kiefling May 1989 59 p
(NASA-TM-100365; NAS 1.15:100365) Avail: NTIS HC A04/MF A01 CSCL 22B

Metallic bellows are commonly used as segments of propellant feedlines for rocket-propelled vehicles to accommodate temperature-induced length variations, manufacturing tolerances, and gimbaling of the engines. These bellows sections deform radially and change volume when internal pressure varies, and the magnitude of such deformation is much higher than that for the straight, cylindrical segments of the line. The greater flexibility, or lesser stiffness, of the bellows, decreases the frequency of acoustic oscillations in the line. These acoustic oscillations are a major factor in the so-called POGO phenomena which have plagued most of the larger liquid rocket-propelled vehicles for many years. A method is developed to calculate the change in volume of a bellows due to a change in internal pressure. Results of an experiment are also presented along with a test-analysis comparison. The computer code is included. Author

N89-24423# Aerospatiale, Cannes La Bocca (France).
AUTONOMOUS GEOSTATIONARY STATIONKEEPING SYSTEM OPTIMIZATION AND VALIDATION
P. Maute, B. Blancke, J. Ph. Jahier, and F. Alby (Centre National d'Etudes Spatiales, Toulouse, France) 1988 11 p Presented at the 39th International Astronautical Federation Congress, Bangalore, India, 8-15 Oct. 1988 Previously announced in IAA as A89-17771
(Rept-882-440-117; ETN-89-94510) Avail: NTIS HC A03/MF A01

The main system features and the optimization process are presented (minimization of additional hardware and how to take advantage of additional hardware in the system architecture). The ongoing study refers to measurements of Earth, Sun, and Polaris Sensors. A validation method, based on implementation of the onboard software on a microprocessor interfaced with a computer in charge of the system environment simulation is described. ESA

N89-24424# Aerospatiale, Cannes La Bocca (France).
STATE OF THE ART OF ISO
J. Youdale 1988 32 p
(Rept-882-440-121; ETN-89-94514) Avail: NTIS HC A03/MF A01

The current status of the ISO satellite design is reviewed along with its major performance predictions. Mission critical performances and driving requirements are emphasized. The major open points remaining to be solved are the establishment of the feasibility of a straylight verification test and the selection of the best suited configuration for the instruments end to end tests. ESA

N89-24425# Aerospatiale, Cannes La Bocca (France).
FLUIDNET: A THERMAL AND HYDRAULIC SOFTWARE FOR THE PRELIMINARY SIZING OF FLUID LOOP SYSTEMS
S. Andre, J. N. Chelotti, J. F. Gory, and T. Lafon (Centre National d'Etudes Spatiales, Toulouse, France) 1988 11 p Previously announced in IAA as A89-27845
(Rept-882-440-124; ETN-89-94517) Avail: NTIS HC A03/MF A01

An interactive application computer program applicable to preliminary design of fluid loop networks in space thermal control systems is described. The main features are portability, easy implementation, speed, and flexibility. The current version is applied to thermal and hydraulic analysis of single phase fluid loops in steady state. For first application of this program is devoted to Hermes thermal control subsystem design. ESA

N89-24426 Howard Univ., Washington, DC.
ON THE DYNAMICS AND CONTROL OF THE SPACECRAFT CONTROL LABORATORY EXPERIMENT (SCOLE) CLASS OF OFFSET FLEXIBLE SYSTEMS Ph.D. Thesis
Cheick Modibo Diarra 1987 201 p
Avail: Univ. Microfilms Order No. DA8810423

A mathematical model is developed to predict the dynamics of the proposed orbiting Spacecraft Control Laboratory Experiment during the station keeping phase. The Shuttle as well as the reflector are assumed to be rigid, the mast is flexible and is assumed to undergo elastic displacements very small as compared with its length. The equations of motion are derived using a Newton-Euler formulation. The model includes the effects of gravity, flexibility, and orbital dynamics. The control is assumed to be provided to the system through the Shuttle's three torquers, and through six actuators located by pairs at two points on the mast and at the mass center of the reflector. At each of the locations, an actuator acts parallel to the roll axis while the other one acts parallel to the pitch axis. The modal shape functions are derived using the fourth order beam equation. The generic mode equations are derived to account for the effects of the control forces on the modal shapes and frequencies. The equations are linearized about a nominal equilibrium position. When the interface point between the mast and the reflector is assumed to coincide with the mass center of the reflector, it is seen that the pitch equation is decoupled from the roll and yaw motions. When the interface point is offset along the roll axis the pitch equation is still decoupled from the two other equations (roll and yaw). It is seen that the open loop system is unstable for both cases due to the (gravitationally) unfavorable moment of inertia distribution. When, in addition to the roll axis offset, a pitch axis offset is introduced into the system, the equations describing the roll, pitch, and yaw motions are seen to be all coupled together. It is further seen that, in the presence of gravity gradient torques in the system dynamics, the system assumes a new equilibrium position about which the equations will have to be linearized. Dissert. Abstr.

N89-24427*# National Aeronautics and Space Administration. Lewis Research Center, Cleveland, OH.
ENERGY STORAGE AND THERMAL CONTROL SYSTEM DESIGN STATUS
Stephen N. Simons, Bryan C. Willhoite, and Gert vanOmmering (Ford Aerospace and Communications Corp., Palo Alto, CA.) 1989 8 p Presented at the 24th Intersociety Energy Conversion Engineering Conference, Washington, DC, 6-11 Aug. 1989; cosponsored by the IEEE, AIAA, ANS, ASME, SAE, ACS and AIChE
(NASA-TM-102136; E-4933; NAS 1.15:102136) Avail: NTIS HC A02/MF A01 CSCL 22B

The Space Station Freedom electric power system (EPS) will initially rely on photovoltaics for power generation and Ni/H2 batteries for electrical energy storage. The current design for and the development status of two major subsystems in the PV Power Module is discussed. The energy storage subsystem comprised of high capacity Ni/H2 batteries and the single-phase thermal control system that rejects the excess heat generated by the batteries and other components associated with power generation and storage is described. Author

N89-24337# Bundesministerium fuer Forschung und Technologie, Bonn (Germany, F.R.). Aerospace Div.
COLUMBUS: THE EUROPEAN CONTRIBUTION TO THE INTERNATIONAL SPACE STATION
H. Strub *In* ESA, International Symposium on Europe in Space: The Manned Space System Oct. 1988 p 49-53 (For primary document see N89-24335 18-12)
Copyright Avail: NTIS HC A99/MF A01; ESA Publications Div., ESTEC, Noordwijk, Netherlands, 80 Dutch guilders

N89-24338# Centre National d'Etudes Spatiales, Toulouse (France).
THE HERMES PROGRAM [LE PROGRAMME HERMES]
Ph. Couillard *In* ESA, International Symposium on Europe in Space: The Manned Space System Oct. 1988 p 55-58 In FRENCH; ENGLISH summary (For primary document see N89-24335 18-12)
Copyright Avail: NTIS HC A99/MF A01; ESA Publications Div., ESTEC, Noordwijk, Netherlands, 80 Dutch guilders

N89-24339# Ministero Ricerca Scientifica e Tecnologica, Rome (Italy).
THE EUROPEAN DATA RELAY SATELLITE
F. Mazzuca *In* ESA, International Symposium on Europe in Space: The Manned Space System Oct. 1988 p 59-61 (For primary document see N89-24335 18-12)
Copyright Avail: NTIS HC A99/MF A01; ESA Publications Div., ESTEC, Noordwijk, Netherlands, 80 Dutch guilders

N89-24343# Aeritalia S.p.A., Turin (Italy). Space Systems Group.
PRESSURIZED MODULE ELEMENT FOR MAN'S PRESENCE IN SPACE
Ernesto Vallerani and Elizabeth Maggio *In* ESA, International Symposium on Europe in Space: The Manned Space System Oct. 1988 p 95-100 (For primary document see N89-24335 18-12)
Copyright Avail: NTIS HC A99/MF A01; ESA Publications Div., ESTEC, Noordwijk, Netherlands, 80 Dutch guilders

N89-24345# Messerschmitt-Boelkow-Blohm G.m.b.H., Bremen (Germany, F.R.).
MTFF USER INTERFACES
S. Gazey and K. Huse *In* ESA, International Symposium on Europe in Space: The Manned Space System Oct. 1988 p 107-110 (For primary document see N89-24335 18-12)
Copyright Avail: NTIS HC A99/MF A01; ESA Publications Div., ESTEC, Noordwijk, Netherlands, 80 Dutch guilders

N89-24346# European Space Agency, Paris (France).
HERMES USER INTERFACES
P. Brudieu *In its* International Symposium on Europe in Space: The Manned Space System Oct. 1988 p 111-115 (For primary document see N89-24335 18-12)
Copyright Avail: NTIS HC A99/MF A01; ESA Publications Div., ESTEC, Noordwijk, Netherlands, 80 Dutch guilders

N89-24351# Avions Marcel Dassault-Breguet Aviation, Saint-Cloud (France).
HERMES AEROTHERMODYNAMIC CONCEPT
F. Cordie, M. Desloires, and J. P. Vaunois (Centre National d'Etudes Spatiales, Toulouse, France) *In* ESA, International Symposium on Europe in Space: The Manned Space System Oct. 1988 p 143-144 In FRENCH (For primary document see N89-24335 18-12)
Copyright Avail: NTIS HC A99/MF A01; ESA Publications Div., ESTEC, Noordwijk, Netherlands, 80 Dutch guilders

N89-24373# Centre National d'Etudes Spatiales, Toulouse (France). Direction Hermes et Vols Habites.
MEANS FOR PREPARING AND RECOVERING THE HERMES SPACE PLANE [LES MOYENS DE PREPARATION ET DE RECUPERATION DE L'AVION SPATIAL HERMES]
Michel Cade and Bernard Houze *In* ESA, International Symposium on Europe in Space: The Manned Space System Oct. 1988 p 361-365 In FRENCH (For primary document see N89-24335 18-12)
Copyright Avail: NTIS HC A99/MF A01; ESA Publications Div., ESTEC, Noordwijk, Netherlands, 80 Dutch guilders

N89-24377# Aeritalia S.p.A., Turin (Italy). Space Systems Group.
ATTACHED PRESSURIZED MODULE (APM) CENTER FOR THE COLUMBUS ATTACHED PRESSURIZED MODULE
Giuseppe Viriglio, Luciano Battocchio, Claudio Canu, and Giovanni Rum (Piano Spaziale Nazionale, Rome, Italy) *In* ESA, International Symposium on Europe in Space: The Manned Space System Oct. 1988 p 389-393 (For primary document see N89-24335 18-12)
Copyright Avail: NTIS HC A99/MF A01; ESA Publications Div., ESTEC, Noordwijk, Netherlands, 80 Dutch guilders

N89-24389# Tecnospazio S.p.A., Milan (Italy).
MULTIPLE ROBOT APPROACH FOR AUTOMATION OF IN-ORBIT MODULES
P. G. Magnani, G. Colombina, and C. Gerli *In* ESA, International Symposium on Europe in Space: The Manned Space System Oct. 1988 p 485-492 (For primary document see N89-24335 18-12)
Copyright Avail: NTIS HC A99/MF A01; ESA Publications Div., ESTEC, Noordwijk, Netherlands, 80 Dutch guilders

N89-24399# Aeritalia S.p.A., Turin (Italy). Space Systems Group.
THE UTILIZATION OF THE EUROPEAN PRESSURIZED MODULE FOR NON-EUROPEAN EXPERIMENTS
G. Oelker, M. S. Lavitola, and A. Allegra *In* ESA, International Symposium on Europe in Space: The Manned Space System Oct. 1988 p 573-575 (For primary document see N89-24335 18-12)
Copyright Avail: NTIS HC A99/MF A01; ESA Publications Div., ESTEC, Noordwijk, Netherlands, 80 Dutch guilders

N89-24661*# National Aeronautics and Space Administration. Langley Research Center, Hampton, VA.
DYNAMIC ANALYSIS OF SPACE STRUCTURES INCLUDING ELASTIC, MULTIBODY, AND CONTROL BEHAVIOR
Larry Pinson and Keto Soosaar *In its* Computational Methods for Structural Mechanics and Dynamics May 1989 p 443-454 (For primary document see N89-24654 18-39)
Avail: NTIS HC A12/MF A01 CSCL 22B

N89-24832# Moog, Inc., East Aurora, NY.
DISCONNECTS FOR SPACECRAFT SERVICING APPLICATIONS Abstract Only
J. M. Cardin *In* Tactical Weapons Guidance and Control

Information Conference on Space and Military Applications of Automation and Robotics Jun. 1988 p 25 (For primary document see N89-24819 18-63)
Avail: NTIS HC A05/MF A01 CSCL 09B

N89-24838*# National Aeronautics and Space Administration. Marshall Space Flight Center, Huntsville, AL.
ORBITAL MANEUVERING VEHICLE (OMV) REMOTE SERVICING KIT Abstract Only
Norman S. Brown *In* Tactical Weapons Guidance and Control Information Conference on Space and Military Applications of Automation and Robotics Jun. 1988 p 39 (For primary document see N89-24819 18-63)
Avail: NTIS HC A05/MF A01 CSCL 22B

19 SPACECRAFT INSTRUMENTATION

For related information see also *06 Aircraft Instrumentation* and *35 Instrumentation and Photography.*

N89-24428# Bonn Univ. (Germany, F.R.). Inst. fuer Physik.
SYSTEMS FOR THE SENSITIVITY CALIBRATION OF MASS SPECTROMETERS IN SPACE FLIGHT Ph.D. Thesis [SYSTEME ZUM EICHEN DER EMPFINDLICHKEIT VON MASSENSPEKTROMETERN IM WELTRAUM]
Gerald Lehmacher Jun. 1988 56 p In GERMAN
(Bonn-IR-88-32; ISSN-0172-8741; ETN-89-93995) Avail: NTIS HC A04/MF A01

A space flight calibrating system for mass spectrometers is described. The mass spectrometer is suited for measurements of particle densities of helium, argon, krypton and nitrogen. Laboratory calibration is controled and corrected by space calibrating. For the cometary gas spectrometer, different possibilities of construction and in-space calibration are proposed. Mass spectra of organic substances are analyzed for their adaptability to in-flight calibration of mass spectrometers. ESA

N89-24429# Aerospatiale, Cannes La Bocca (France).
ISOCAM, ISO OPTICAL SUBSYSTEM CRYOGENICS, AEROSPATIALE, CANNES, FRANCE IN-HOUSE R AND D STATUS
J. F. Patin and J. L. Cecconi 1988 6 p
(Rept-882-440-123; ETN-89-94516) Avail: NTIS HC A02/MF A01

The different programs carried out to harness the complex technologies involved are reviewed. The cryogenic 4 K technological areas involved in the development of the suboptical system and camera include materials and coatings, junctions, optics attachment devices, dimensional stability, optical coatings absorptive coating, reflective coatings, thermal connections (mirror straps) and tightness of the helium circuits. ESA

20 SPACECRAFT PROPULSION AND POWER

Includes main propulsion systems and components, e.g., rocket engines; and spacecraft auxilliary power sources.

For related information see also *07 Aircraft Propulsion and Power, 28 Propellants and Fuels, 44 Energy Production and Conversion,* and *15 Launch Vehicles and Space Vehicles.*

N89-24430*# Remtech, Inc., Huntsville, AL.
SRB ASCENT AERODYNAMIC HEATING DESIGN CRITERIA REDUCTION STUDY, VOLUME 2 Final Report
W. K. Crain, C. L. Frost, and C. D. Engel 18 Jan. 1989 343 p
(Contract NAS8-35322)
(NASA-CR-183569; NAS 1.26:183569; RTR-090-01-Vol-2) Avail: NTIS HC A15/MF A01 CSCL 21H

Data are presented for the wind tunnel interference heating factor data base, the timewise tabulated ascent design environments, and the timewise plotted environments comparing the REMTECH results to the Rockwell RI-IVBC-3 results. B.G.

N89-24431# National Aerospace Lab., Tokyo (Japan).
DEVELOPMENT OF THE CRYOPANEL FOR TESTS OF XENON ION THRUSTERS
Toshio Obama, Kenichi Kajiwara, Yukio Hayakawa, Katsuhiro Miyazaki, and Shoji Kitamura Jun. 1988 32 p In JAPANESE; ENGLISH summary
(NAL-TR-981; ISSN-0389-4010) Avail: NTIS HC A03/MF A01

A cryopanel suitable for testing zenon ion thrusters was designed and tested. The target temperature of the cryopanel was below 50 K, since the vapor pressure of xenon was low enough at that temperature. This high-temperature-cryopanel has a cylindrical shape and was installed in the existing 1.5 m diameter vacuum chamber. The cryopanel-alone-tests showed the attained temperature of the cryopanel was below 50 K and the cryopanel could evacuate xenon with a pumping speed of over 600,000 L/s. But while an ion thruster was operating, the speed fell to 40,000 L/s and the continuous-operation time was restricted to about 90 minutes. It is very difficult to find other vacuum pumps that show the same performance in the same vacuum chamber at the same cost. Author

N89-24432# National Aerospace Lab., Tokyo (Japan).
THERMAL RADIATION FROM PLUMES OF SOLID PROPELLANT ROCKETS
Mamoru Takahashi, Mumeo Izumikawa, Tohru Mitani, Takashi Niioka, Hirofumi Taniguchi, and Yukio Hyodo Aug. 1988 39 p In JAPANESE; ENGLISH summary
(NAL-TR-990; ISSN-0389-4010) Avail: NTIS HC A03/MF A01

A simple method for estimating radiative heating by the plumes of solid rockets was developed. Plume shapes were approximated as bisected conical cylinders with an apex angle. Similarities in the plume shape, the size of plumes, and the distribution of radiative power are shown between subscale motors and the solid rocket boosters (SRB) of space shuttles. All radiation is assumed to be emitted from the surface of the cylinder. The effects of the interior of the plumes is confined to the emissivity of the surface. The emissivity of the plume can be related to its optical thickness, and the optical thickness can be estimated from the number density and the diameter of particles in the plume. Dependence of radiative heating on motor size and flight altitude can be explained in terms of similarities in plume radiation. Author

N89-24433*# Lockheed Missiles and Space Co., Huntsville, AL. Engineering Center.
TURBINE ROTOR/STATOR FLOWFIELD ANALYSIS
Lisa Griffin Mar. 1989 37 p
(Contract NAS8-36284)
(NASA-CR-183639; NAS 1.26:183639; LMSC-HEC-TR-F268519)
Avail: NTIS HC A03/MF A01 CSCL 21E

A numerical study of the unsteady aerodynamic and thermal environment associated with axial turbine stages is presented. Computations are performed using a modification of the ROTOR1 rotor/stator interaction code. Two different turbine states are analyzed: the first state of the United Technologies Research Center large scale rotating rig and the first state of the Space Shuttle main engine (SSME) high pressure fuel turbopump. Time-averaged blade midspan pressure and heat transfer profiles are calculated using the following different surface boundary conditions: adiabatic wall, prescribed wall temperature, and prescribed heat flux. Numerical solutions for the large scale rotating rig are compared with experimental data. Unsteady pressure envelopes are also presented for each geometry. In addition, instantaneous contours are plotted for the SSME configuration. Author

N89-24434*# Martin Marietta Aerospace, Denver, CO. Denver Astronautics Group.

SPACE STATION AUTOMATION OF COMMON MODULE POWER MANAGEMENT AND DISTRIBUTION Interim Final Report

W. Miller, E. Jones, B. Ashworth, J. Riedesel, C. Myers, K. Freeman, D. Steele, R. Palmer, R. Walsh, and J. Gohring et al Feb. 1989 572 p

(Contract NAS8-36433)

(NASA-CR-183607; NAS 1.26:183607; MCR-89-516) Avail: NTIS HC A24/MF A01 CSCL 21H

A history and description of the work performed in defining, designing, and developing the Space Station Module Power Management and Distribution System (SSM/PMAD) breadboard, complete with software is given. The hardware architecture is described along with its associated deterministic software architecture, the Artificial Intelligence (AI) systems architecture, and the methodology and process of the overall system integration. The automation system was built upon a 20 kHz ac source with redundancy of the power buses. There are two power distribution control units which furnish power to six load centers which in turn enable load circuits based upon a system generated schedule. The system possesses the capability to perform diagnosis whenever a distribution fault is encountered. The system autonomously reconfigures its operation during run-time to reschedule activities around the fault, rather than performing a system halt. A.D.

N89-24435*# National Aeronautics and Space Administration. Marshall Space Flight Center, Huntsville, AL.

SPACE SHUTTLE MAIN ENGINE HIGH PRESSURE FUEL TURBOPUMP TURBINE BLADE CRACKING

Henry Lee May 1988 57 p Original contains color illustrations

(NASA-TM-100327; NAS 1.15:100327) Avail: NTIS HC A04/MF A01 CSCL 21H

The analytical results from two-dimensional (2D) and three-dimensional (3D) finite element model investigations into the cracking of Space Shuttle Main Engine (SSME) High Pressure Fuel Turbopump (HPFTP) first- and second-stage turbine blades are presented. Specifically, the initiation causes for transverse cracks on the pressure side of the firststage blade fir tree lobes and face/corner cracks on the downstream fir tree face of the second-state blade are evaluated. Because the blade material, MAR-M-246 Hf (DS), is highly susceptible to hydrogen embrittlement in the -100 F to 400 F thermal environment, a steady-state condition (full power level = 109 percent) rather than a start-up or shut-down transient was considered to be the most likely candidate for generating a high-strain state in the fir tree areas. Results of the analyses yielded strain levels on both first- and second-stage blade fir tree regions that are of a magnitude to cause hydrogen assisted low cycle fatigue cracking. Also evident from the analysis is that a positive margin against fir tree cracking exists for the planned design modifications, which include shot peening for both first- and second-stage blade fir tree areas. Author

N89-24436*# National Aeronautics and Space Administration. Lewis Research Center, Cleveland, OH.

PERFORMANCE OF LARGE AREA XENON ION THRUSTERS FOR ORBIT TRANSFER MISSIONS

Vincent K. Rawlin 1989 12 p Presented at the 1989 JANNAF Propulsion Meeting, Cleveland, OH, 23-25 May 1989

(NASA-TM-102049; E-4801; NAS 1.15:102049) Avail: NTIS HC A03/MF A01 CSCL 21H

Studies have indicated that xenon ion propulsion systems can enable the use of smaller Earth-launch vehicles for satellite placement which results in significant cost savings. These analyses have assumed the availability of advanced, high power ion thrusters operating at about 10 kW or higher. A program was initiated to explore the viability of operating 50 cm diameter ion thrusters at this power level. Operation with several discharge chamber and ion extraction grid set combinations has been demonstrated and data were obtained at power levels to 16 kW. Fifty cm diameter thrusters using state of the art 30 cm diameter grids or advanced technology 50 cm diameter grids allow discharge power and beam current densities commensurate with long life at power levels up to 10 kW. In addition, 50 cm diameter thrusters are shown to have the potential for growth in thrust and power levels beyond 10 KW. Author

N89-24437*# Lockheed Missiles and Space Co., Huntsville, AL. Structures and Mechanics Section.

SPACE SHUTTLE MAIN ENGINE STRUCTURAL ANALYSIS AND DATA REDUCTION/EVALUATION. VOLUME 6: PRIMARY NOZZLE DIFFUSER ANALYSIS Final Report

Michael J. Foley Apr. 1989 118 p

(Contract NAS8-37282)

(NASA-CR-183669; NAS 1.26:183669; LMSC-HEC-TR-F268584-Vol-6) Avail: NTIS HC A06/MF A01 CSCL 21H

The primary nozzle diffuser routes fuel from the main fuel valve on the Space Shuttle Main Engine (SSME) to the nozzle coolant inlet mainfold, main combustion chamber coolant inlet mainfold, chamber coolant valve, and the augmented spark igniters. The diffuser also includes the fuel system purge check valve connection. A static stress analysis was performed on the diffuser because no detailed analysis was done on this part in the past. Structural concerns were in the area of the welds because approximately 10 percent are in areas inaccessible by X-ray testing devices. Flow dynamics and thermodynamics were not included in the analysis load case. Constant internal pressure at maximum SSME power was used instead. A three-dimensional, finite element method was generated using ANSYS version 4.3A on the Lockheed VAX 11/785 computer to perform the stress computations. IDEAS Supertab on a Sun 3/60 computer was used to create the finite element model. Rocketdyne drawing number RS009156 was used for the model interpretation. The flight diffuser is denoted as -101. A description of the model, boundary conditions/load case, material properties, structural analysis/results, and a summary are included for documentation. Author

N89-24438*# National Aeronautics and Space Administration. Lewis Research Center, Cleveland, OH.

CONCENTRATION OF OFF-AXIS RADIATION BY SOLAR CONCENTRATORS FOR SPACE POWER

Kent S. Jefferies 1989 10 p Proposed for presentation at the 24th Intersociety Energy Conversion Engineering Conference, Washington, DC, 6-11 Aug. 1989; sponsored by IEEE, AIAA, ANS, ASME, SAE, ACS and AIChE

(NASA-TM-102052; E-4804; NAS 1.15:102052) Avail: NTIS HC A02/MF A01 CSCL 10A

Off-axis radiation is radiation from any direction not parallel to the axis of the solar concentrator. It will be reflected to regions other than the focus of the parabolic concentrator and possibly concentrated there. Four types of off-axis radiation are discussed. These are: (1) small off-axis angles during walk-off; (2) large off-axis angles; (3) an extended off-axis source such as Earth albedo; and (4) miscellaneous off-axis sources including radio frequency sources and local point sources. A previous analytical study used a computer code named PIXEL to predict concentration of off-axis radiation and a previous experimental study used an 11-m diameter multifaceted dish concentrator to validate the PIXEL analysis. The PIXEL code was limited in that it represented concentration by an ideal parabolic reflector of light from a point source. Another code named OFFSET has been developed to represent the solar concentrator being developed for Space Station Freedom. It is a detailed, ray tracing model which represents 50 ray originating points on the Sun and reflections from 10 points on each of the 456 concentrator facets. Results of this code are generally similar to the PIXEL results although there are small differences due to the more detailed representations of the Sun and concentrator that were used in the OFFSET code. Author

N89-24439*# National Aeronautics and Space Administration. Lewis Research Center, Cleveland, OH.
SPACE STATION FREEDOM ELECTRICAL POWER SYSTEM HARDWARE COMMONALITY WITH THE UNITED STATES POLAR PLATFORM
Lorra L. Rieker and Francis M. Haraburda 1989 11 p Presented at the 24th Intersociety Energy Conversion Engineering Conference, Washington, DC, 6-11 Aug. 1989; cosponsored by the IEEE, AIAA, ANS, ASME, SAE, ACS and AIChE
(NASA-TM-102074; E-4833; NAS 1.15:102074) Avail: NTIS HC A03/MF A01 CSCL 09C

The National Aeronautics and Space Administration has adopted the policy to achieve the maximum practical level of commonality for the Space Station Freedom program in order to significantly reduce life cycle costs. Commonality means using identical or similar hardware/software for meeting common sets of functionally similar requirements. Information on how the concept of commonality is being implemented with respect to electric power system hardware for the Space Station Freedom and the U.S. Polar Platform is presented. Included is a historical account of the candidate common items which have the potential to serve the same power system functions on both Freedom and the Polar Platform. Author

N89-24440*# National Aeronautics and Space Administration. Lewis Research Center, Cleveland, OH.
FLIGHT EXPERIMENT OF THERMAL ENERGY STORAGE
David Namkoong 1989 9 p Presented at the 24th Intersociety Energy Conversion Engineering Conference, Washington, DC, 6-11 Aug. 1989; cosponsored by the IEEE, AIAA, ANS, ASME, SAE, ACS and AIChE
(NASA-TM-102081; E-4843; NAS 1.15:102081) Avail: NTIS HC A02/MF A01 CSCL 10C

Thermal energy storage (TES) enables a solar dynamic system to deliver constant electric power through periods of sun and shade. Brayton and Stirling power systems under current considerations for missions in the near future require working fluid temperatures in the 1100 to 1300+ K range. TES materials that meet these requirements fall into the fluoride family of salts. These salts store energy as a heat of fusion, thereby transferring heat to the fluid at constant temperature during shade. The principal feature of fluorides that must be taken into account is the change in volume that occurs with melting and freezing. Salts shrink as they solidify, a change reaching 30 percent for some salts. The location of voids that form as result of the shrinkage is critical when the solar dynamic system reemerges into the sun. Hot spots can develop in the TES container or the container can become distorted if the melting salt cannot expand elsewhere. Analysis of the transient, two-phase phenomenon is being incorporated into a three-dimensional computer code. The code is capable of analysis under microgravity as well as 1 g. The objective of the flight program is to verify the predictions of the code, particularly of the void location and its effect on containment temperature. The four experimental packages comprising the program will be the first tests of melting and freezing conducted under microgravity. Each test package will be installed in a Getaway Special container to be carried by the shuttle. The package will be self-contained and independent of shuttle operations other than the initial opening of the container lid and the final closing of the lid. Upon the return of the test package from flight, the TES container will be radiographed and finally partitioned to examine the exact location and shape of the void. Visual inspection of the void and the temperature data during flight will constitute the bases for code verification. Author

N89-24441# Naval Postgraduate School, Monterey, CA. Dept. of Mechanical Engineering.
MODELING TRANSIENT THERMAL BEHAVIOR IN A THRUST VECTOR CONTROL JET VANE M.S. Thesis
Margaret Mary Reno Dec. 1988 48 p
(AD-A206532) Avail: NTIS HC A03/MF A01 CSCL 21/8

An attempt was made to model the transient thermal response of jet vanes used for thrust control. A simple computer model based on lumped capacitance methods using boundary layer convection and stagnation point heating as thermal inputs appeared to adequately predict temperatures for a quarter-scale model. This report details the attempt to enlarge the model to allow comparison between thermal predictions and the results of tests on a full-scale prototype jet vane. It was determined that the model could not be considered a thermal representation of the full-scale vane assembly and several modifications were identified in order to adapt the model to full-scale applications. GRA

N89-24442# Aerospatiale, Cannes La Bocca (France).
SPACE PHOTOVOLTAIC TECHNIQUE. STATE OF THE ART, TRENDS [PHOTOVOLTAIQUE SPATIAL: ETAT DE L'ART, TENDANCES]
M. Ziliani and L. Pelenc Nov. 1986 13 p In FRENCH Presented at the Agence Francaise pour la Maitrise de l'Energie Seminaire d'Evaluation des Conventions et Contrats de Recherche Conversion Photovoltaique
(Rept-882-440-120; ETN-89-94513) Avail: NTIS HC A03/MF A01

Photovoltaic power systems currently used in satellites are reviewed. The solar panels for Meteosat, SPOT, TDF, and GSR3 are shown. The solar cells used for space application are described. The trends discussed show the expansion of the AsGa cells and an ever increasing spacecraft power demand. ESA

N89-24443*# National Aeronautics and Space Administration. Lewis Research Center, Cleveland, OH.
SUMMARY AND EVALUATION OF THE STRATEGIC DEFENSE INITIATIVE SPACE POWER ARCHITECTURE STUDY
M. Edenburn, ed. (Sandia National Labs., Albuquerque, NM.) and J. M. Smith, ed. Mar. 1989 418 p
(NASA-TM-102012; E-4724; NAS 1.15:102012) Avail: NTIS HC A18/MF A01 CSCL 10B

The Space Power Architecture Study (SPAS) identified and evaluated power subsystem options for multimegawatt electric (MMWE) space based weapons and surveillance platforms for the Strategic Defense Initiative (SDI) applications. Steady state requirements of less than 1 MMWE are adequately covered by the SP-100 nuclear space power program and hence were not addressed in the SPAS. Four steady state power systems less than 1 MMWE were investigated with little difference between them on a mass basis. The majority of the burst power systems utilized H(2) from the weapons and were either closed (no effluent), open (effluent release) or steady state with storage (no effluent). Closed systems used nuclear or combustion heat source with thermionic, Rankine, turboalternator, fuel cell and battery conversion devices. Open systems included nuclear or combustion heat sources using turboalternator, magnetohydrodynamic, fuel cell or battery power conversion devices. The steady state systems with storage used the SP-100 or Star-M reactors as energy sources and flywheels, fuel cells or batteries to store energy for burst applications. As with other studies the open systems are by far the lightest, most compact and simplist (most reliable) systems. However, unlike other studies the SPAS studied potential platform operational problems caused by effluents or vibration. Author

N89-24444*# National Aeronautics and Space Administration. Lewis Research Center, Cleveland, OH.
A NUMERICAL STUDY OF CHEMICALLY REACTING FLOW IN NOZZLES
Thomas J. VanOverbeke and Jian-Shuen Shuen (Sverdrup Technology, Inc., Cleveland, OH.) 1989 21 p Presented at the 25th Joint Propulsion Conference , Monterey, CA, 10-12 Jul. 1989; cosponsored by the AIAA, ASME, SAE and ASEE
(NASA-TM-102135; E-4932; NAS 1.15:102135; AIAA-89-2793)
Avail: NTIS HC A03/MF A01 CSCL 21H

The space station uses small rocket motors, called thrusters, for orientation control. Because of the lack of viable design tools for small rockets, the initial thruster design was basically a very small version of a large rocket motor. Thrust measurements of the initial design were lower than predicted. To improve predictions it was decided to develop a verison of the RPLUS2D reacting

flow code for thruster calculations. RPLUS2D employs an implicit finite volume, lower-upper symmetric successive overrelaxation (LU-SSOR) scheme for solving the complete two-dimensional Navier-Stokes equations and species transport equations in a coupled and very efficient manner. The combustion processes are modeled by a 9-species, 18 step finite-rate chemistry model, and the turbulence is simulated by a Baldwin-Lomax algebraic model. The code is extended to handle multiple subsonic inlet conditions where the total mass flow is governed by conditions calculated at the thruster-throat. Results are shown for a thruster design where the overall mixture ratio is hydrogen rich. A calculation of a large area ratio divergent nozzle is also presented. Author

N89-24445*# Sverdrup Technology, Inc., Cleveland, OH.
A PREMIXED HYDROGEN/OXYGEN CATALYTIC IGNITER Final Report
James M. Green Jun. 1989 9 p Presented at the 25th Joint Propulsion Conference, Monterey, CA, 10-14, Jul. 1989; cosponsored by the AIAA, ASME, SAE and ASEE
(Contract NAS3-25266)
(NASA-CR-185113; E-4787; NAS 1.26:185113; AIAA-89-2302)
Avail: NTIS HC A02/MF A01 CSCL 21H

The catalytic ignition of hydrogen and oxygen propellants was studied using a premixing hydrogen/oxygen injector. The premixed injector was designed to eliminate problems associated with catalytic ignition caused by poor propellant mixing in the catalyst bed. Mixture ratio, mass flow rate, and propellant inlet temperature were varied parametrically in testing, and a pulse mode life test of the igniter was conducted. The results of the tests showed that the premixed injector eliminated flame flashback in the reactor and increased the life of the igniter significantly. The results of the experimental program and a comparison with data collected in a previous program are given. Author

N89-24446*# National Aeronautics and Space Administration. Lewis Research Center, Cleveland, OH.
THE 5-kW ARCJET POWER ELECTRONICS
R. P. Gruber, R. W. Gott, and T. W. Haag 1989 26 p Presented at the 25th Joint Propulsion Conference, Monterey, CA, 10-12 Jul. 1989; cosponsored by the AIAA, ASME, SAE and ASEE
(NASA-TM-102108; E-4876; NAS 1.15:102108; AIAA-89-2725)
Avail: NTIS HC A03/MF A01 CSCL 10B

The initial design and evaluation of a 5 kW arcjet power electronics breadboard which as been integrated with a modified 1 kW design laboratory arcjet is presented. A single stage, 5 kW full bridge, pulse width modulated (PWM), power converter was developed which was phase shift regulated. The converter used metal oxide semiconductor field effect transistor (MOSFET) power switches and incorporated current mode control and an integral arcjet pulse ignition circuit. The unoptimized power efficiency was 93.5 and 93.9 percent at 5 kW and 50A output at input voltages of 130 and 150V, respectively. Line and load current regulation at 50A output was within one percent. The converter provided up to 6.6 kW to the arcjet with simulated ammonia used as a propellant. Author

N89-24447*# National Aeronautics and Space Administration. Lewis Research Center, Cleveland, OH.
LIQUID OXYGEN COOLING OF HYDROCARBON FUELED ROCKET THRUST CHAMBERS
Elizabeth S. Armstrong 1989 15 p Presented at the 25th Joint Propulsion Conference, Monterey, CA, 10-12 Jul. 1989; cosponsored by the AIAA, ASME, SAE and ASEE
(NASA-TM-102113; E-4886; NAS 1.15:102113; AIAA-89-2739)
Avail: NTIS HC A03/MF A01 CSCL 21H

Rocket engines using liquid oxygen (LOX) and hydrocarbon fuel as the propellants are being given serious consideration for future launch vehicle propulsion. Normally, the fuel is used to regeneratively cool the combustion chamber. However, hydrocarbons such as RP-1 are limited in their cooling capability. Another possibility for the coolant is the liquid oxygen. Combustion chambers previously tested with LOX and RP-1 as propellants and LOX as the collant demonstrated the feasibility of using liquid oxygen as a coolant up to a chamber pressure of 13.8 MPa (2000 psia). However, there was concern as to the effect on the integrity of the chamber liner if oxygen leaks into the combustion zone through fatigue cracks that may develop between the cooling passages and the hot gas side wall. In order to study this effect, chambers were fabricated with slots machined upstream of the throat between the cooling passage wall and the hot gas side wall to simulate cracks. The chambers were tested at a nominal chamber pressure of 8.6 MPa (1247 psia) over a range of mixture ratios from 1.9 to 3.1 using liquid oxygen as the coolant. The results of the testing showed that the leaking LOX did not have a deleterious effect on the chambers in the region of the slots. However, there was unexplained melting in the throat region of both chambers, but not in line with the slots. Author

N89-24448*# National Aeronautics and Space Administration. Lewis Research Center, Cleveland, OH.
SPACE STATION FREEDOM SOLAR ARRAY DESIGN DEVELOPMENT
Cindy Winslow, Kevin Bilger (Lockheed Missiles and Space Co., Sunnyvale, CA.), and Cosmo R. Baraona 1989 6 p Presented at the 24th Intersociety Energy Conversion Engineering Conference, Washington, DC, 6-11 Aug. 1989; cosponsored by the IEEE, AIAA, ANS, ASME, SAE, ACS and AIChE
(Contract NAS3-25082)
(NASA-TM-102105; E-4871; NAS 1.15:102105) Avail: NTIS HC A02/MF A01 CSCL 10B

The Space Station Freedom Solar Array Program is required to provide a 75 kW power module that uses eight solar array (SA) wings over a four-year period in low Earth orbit (LEO). Each wing will be capable of providing 23.4 kW at the 4-year design point. Lockheed Missles and Space Company, Inc. (LMSC) is providing the flexible substrate SAs that must survive exposure to the space environment, including atomic oxygen, for an operating life of fifteen years. Trade studies and development testing, important for evolving any design to maturity, are presently underway at LMSC on the flexible solar array. The trade study and development areas being investigated include solar cell module size, solar cell weld pads, panel stiffener frames, materials inherently resistant to atomic oxygen, and weight reduction design alternatives. Author

N89-24449*# Morton Thiokol, Brigham City, UT. Aerospace Group.
FIELD JOINT ENVIRONMENTAL PROTECTION SYSTEM VIBRATION/PRESSURIZATION QUALIFICATION Final Test Report
M. Cook 9 Mar. 1989 90 p
(Contract NAS8-30490)
(NASA-CR-183673; NAS 1.26:183673; TWR-17245; MTI-Publ-89343) Avail: NTIS HC A05/MF A01 CSCL 21H

The procedures used and results obtained from vibration testing the redesigned solid rocket motor (RSRM) field joint environmental protection system (FJEPS), hereafer referred to as the joint protection system (JPS) are documented. The major purposes were to certify that the flight-designed JPS will withstand the dynamic environmental conditions of the redesigned solid rocket booster, and to certify that the cartridge check valve (vent valve) will relieve pressure build-up under the JPS during the initial 120 sec of flight. Also, an evaluation of the extruded cork insulation bonding was performed after the vibration testing. Author

N89-24353# Centre National d'Etudes Spatiales, Toulouse (France).
TECHNOLOGY AND DESIGN METHOD EVOLUTION OF CRYOGENIC PROPULSION SYSTEMS: EXAMPLE OF THE MAIN ARIANE 5 STAGE
J. Borromee, D. Thevenot, H. Dederra, and A. Faure (L'Air Liquide, Sassenage, France) *In* ESA, International Symposium on Europe in Space: The Manned Space System Oct. 1988 p 153-162
(For primary document see N89-24335 18-12)
Copyright Avail: NTIS HC A99/MF A01; ESA Publications Div., ESTEC, Noordwijk, Netherlands, 80 Dutch guilders

23 CHEMISTRY AND MATERIALS (GENERAL)

N89-24450*# Clay Engineering, Alameda, CA.
ANALYSIS OF THE PLUGGING OF THE SYSTEMS AUTONOMY DEMONSTRATION PROJECT BRASSBOARD FILTERS
John C. Clay May 1989 26 p
(NASA Order A-72865-C)
(NASA-CR-177533; NAS 1.26:177533) Avail: NTIS HC A03/MF A01 CSCL 07B

A fine gray powder was clogging the brassboard filters. The powder appeared to be residue from a galvanic corrosive attack by ammonia of the aluminum and stainless steel components in the system. The corrosion was caused by water and chlorine that had entered into the system and combined with the ammonia. This combination made an electrolyte and a corrosive agent of the ammonia that attacked the metals in the system. The corroded material traveled through the system with the ammonia and clogged the filters. Key conclusions are: the debris collecting in the filters is a by-product of galvanic corrosion; the debris is principally corroded aluminum and stainless from the system; and galvanic corrosion occurred from water and chlorine that entered the system during normal and/or extreme operating and servicing conditions. Key recommendations are: use only one metal in the ammonia system-titanium, aluminum, or stainless steel; make the system as air-tight as possible (replace fittings with welded joints); and replace electron paramagnetic resonance (EPR) O-rings with neoprene O-rings, and do not use freon to clean system components.
Author

N89-24451*# National Aeronautics and Space Administration. Lewis Research Center, Cleveland, OH.
ISOTOPIC STUDY OF OXYGEN DIFFUSION IN OXIDE COATINGS
Daniel A. Gulino, Lawrence A. Kren, and Therese M. Dever (Cleveland State Univ., OH.) 1989 13 p Presented at the 16th International Conference on Metallurgical Coatings, San Diego, CA, 17-21 Apr. 1989; sponsored by the American Vacuum Society
(NASA-TM-102082; E-4764; NAS 1.15:102082) Avail: NTIS HC A03/MF A01 CSCL 11D

Diffusion of oxygen in thin films of silicon dioxide was studied using oxygen isotopically enriched in oxygen of atomic mass 18 (O-18). This subject is of interest because thin films of dielectrics such as SiO2 are proposed for use as a protective coatings for solar mirrors in low Earth orbit, which is a strongly oxidizing environment. Films of this material were prepared with a direct current magnetron using reactive sputtering techniques. To produce (O-18)- enriched SiO2, a standard 3.5-in.-diameter silicon wafer was reactively sputtered using (O-18)-enriched (95 percent) oxygen as the plasma feed gas. The films were characterized using Rutherford backscattering and Secondary Ion Mass Spectrometer (SIMS) to establish stoichiometry and purity. Subsequently, the films were exposed to an air-derived oxygen plasma in a standard laboratory plasma reactor for durations of up to 10 hr. The concentration ratio of O-16 as a function of depth was determined using SIMS profiling and compared to a baseline, nonplasma exposed sample. A value for the diffusivity of oxygen near the surface of these films was obtained and found to be about 10(-15)sq cm/sec.
Author

24 COMPOSITE MATERIALS

Includes physical, chemical, and mechanical properties of laminates and other composite materials.
For ceramic materials see *27 Nonmetallic Materials.*

N89-24452# Air Force Inst. of Tech., Wright-Patterson AFB, OH. School of Engineering.
CHARACTERIZATION OF DELAMINATION IN ADVANCED COMPOSITE MATERIALS UNDER MODE 3 LOADING CONDITIONS M.S. Thesis
Cynthia L. Lingg Dec. 1988 129 p
(AD-A206159; AFIT/GAE/AA/88D-21) Avail: NTIS HC A07/MF A01 CSCL 11/4

Delamination is the weakest and major failure mode in laminated fiber reinforced composite materials. Delamination is also a fundamental issue in the evaluation of laminated composite structures for durability and damage tolerance. This study involved the characterization of mode 3 delamination primarily using the mode 3 split cantilever beam specimen. The effects of altering four test parameters on the cantilever beam test specimen. This evaluation thickness on the mode 3 critical strain energy release value, investigation of altering crosshead rate on the mode 3 critical strain energy release rate, the effect of temperature on the mode 3 critical strain energy release rate, and the addition and subtraction of a mode 1 component on the critical strain energy release rate. For comparison, a few double split cantilever plate specimens were also tested.
GRA

N89-24453# Air Force Inst. of Tech., Wright-Patterson AFB, OH. School of Engineering.
RESPONSE OF LAYERED STRUCTURES TO THERMAL RADIATION PULSES M.S. Thesis
Vincent J. Jodoin Mar. 1989 94 p
(AD-A206355; AFIT/GNE/ENP/89M-3) Avail: NTIS HC A05/MF A01 CSCL 11/4

An approximation to the response of composite or layered structures to thermal radiation from a nuclear device was developed. The model developed uses the Extrapolated Crank-Nicolson unconditionally stable implicit finite difference scheme to approximate the nonlinear parabolic partial differential heat transfer equation. The model allows for convection at the front face and assumes the back face is insulated. The model assumes one-dimensional heat conduction in Cartesian coordinates. The program approximates Glasstone's thermal pulse shape and uses it and two different moments-matched pulses for the incident thermal radiation. The program was used to do a sensitivity analysis of pulse shape on response. The program uniquely handles the interface conditions to match the Crank-Nicolson accuracy and stability. The program was developed to be run for various thermal fluences and weapon yields. The results showed that the early transients are dependent on pulse shape. The temperature profile in the structure at the approximate time of blast arrival was not dependent on pulse shape however. It was also shown that the nonlinearity effected the peak temperature at the front face.
GRA

N89-24454# Auburn Univ., AL. Dept. of Mechanical Engineering.
IMPACT AND PENETRATION RESISTANCE OF FIBROUS COMPOSITES Progress Report, 1 Jan. - 1 Jun. 1988
L. Chen, B. Jang, L. Hwang, J. Hawkes, and R. Zee 1988 5 p
(Contract DAAL03-86-G-0211)
(AD-A206417; ARO-24804.7-MS) Avail: NTIS HC A02/MF A01 CSCL 11/4

Prevailing deformation and fracture mechanisms of fibrous composites under various loading conditions were studied. The effects of fiber hybridization on the mechanical behavior of composites was also investigated. The high strength polyethylene fibers have been shown to absorb large amount of energy prior to failure of composites. These fibers can be used in hybrids to improve the impact resistance of various composite materials. A large fiber modules or a great fiber failure strain alone does not

provide adequate fiber toughness for improving impact resistance of composites. The fibers must have both high strain and reasonably high modulus and strength. GRA

N89-24455# Kernforschungszentrum G.m.b.H., Karlsruhe (Germany, F.R.). Inst. fuer Material- und Festkoeperforschung.
THERMAL SHOCK STRENGTH OF MULTIPHASE MATERIALS Thesis - Technische Hochschule Aachen
Uwe Jauch Oct. 1988 154 p In GERMAN; ENGLISH summary
(KfK-4469; ISSN-0303-4003; ETN-89-94406) Copyright Avail: NTIS HC A08/MF A01

Theoretical and experimental prediction of multiphase porous materials behavior in cycling temperature field is studied. Thermal shock strength of two phase composite ceramic depends on the concentration of both phases and on the concentration, form, and orientation of the embedded particles of the dispersed phase. Calculated data agree with theoretical and experimental results. ESA

N89-24456# Etablissement Technique Central de l'Armement, Arcueil (France). Service Technologie des Materiaux.
BONDED ASSEMBLIES BEHAVIOR LAWS: LIGHT ALLOYS/ELASTOPLASTIC ADHESIVE Final Report [LOIS DE COMPORTEMENT D'ASSEMBLAGES COLLES ALLIAGE LEGER/ADHESIF ELASTOPLASTIQUE]
D. Bouvart, F. Schmit, R. Pauliard, and J. C. Crasson 7 Jan. 1988 44 p In FRENCH
(Contract DRET-84-1062)
(ETCA-88-R-001; ETN-89-94520) Avail: NTIS HC A03/MF A01

Mechanical tests of an epoxy adhesive presenting an elastoplastic behavior were carried out. The effects on light alloy bonded assemblies were studied under flat shearing loads. It is shown that there are good correlations between the joint adhesive behavior and the bulk measurements at low strains. At high strains the shearing curve of the joint adhesive is below that of the bulk adhesive. ESA

N89-24457# Etablissement Technique Central de l'Armement, Arcueil (France). Service Structure des Materiaux.
COMPOSITE MATERIAL BONDING: GELATION AND PROCESSING OF ADHESIVES AND PREIMPREGNATED MATERIALS [COLLAGE DES MATERIAUX COMPOSITES: GELIFICATION ET MISE EN OEUVRE DES ADHESIFS ET PREIMPREGNES]
D. Bouvart and S. Serror 19 Jan. 1988 64 p In FRENCH
(Contract DRET/ETCA/CMCM-048-201)
(ETCA-88-R-006; ETN-89-94521) Avail: NTIS HC A04/MF A01

The bonding process of composites of an epoxy nature is studied. Direct bonding of cured assemblies is compared to simultaneous polymerization of preimpregnated assemblies and adhesive. It is shown that differences in gel point and the onset of autoclave pressure have large incidence on assemblies behavior. The superiority of copolymerization is shown by the fact that breaking does not occur on joints. The choice of adhesive system must be done considering the gel points of the parts to assembly in order to optimize the pressure onset windows. ESA

N89-24458# Office National d'Etudes et de Recherches Aerospatiales, Paris (France). Direction Scientifique de la Resistance des Structures.
STUDY OF DAMAGE IN COMPOSITE MATERIALS Final Report [ETUDE DE L'ENDOMMAGEMENT DES MATERIAUX COMPOSITES]
J. Renard and F. Roudolff Aug. 1988 90 p In FRENCH
(Contract DRET-87-34-001)
(ONERA-RT-4/7256-RY-070-R; ETN-89-94525) Avail: NTIS HC A05/MF A01

The incidence of cohesion phenomena on macroscopic structures is examined. The study includes work on edge effects, transversal cracking, and damage of the fiber-matrix interface. A statistical model is used to predict the number of transversal cracks as a function of the loading. A finite element simulation computes the stress tensors at the interface in torsion tests. It is shown that the statistical predictions are accurate models, but little explanation of the material behavior is obtained. ESA

N89-24459*# National Aeronautics and Space Administration. Lewis Research Center, Cleveland, OH.
COMPOSITE BLADE STRUCTURAL ANALYZER (COBSTRAN) DEMONSTRATION MANUAL
Robert A. Aiello Apr. 1989 69 p
(NASA-TM-101957; E-4735; NAS 1.15:101957) Avail: NTIS HC A04/MF A01 CSCL 11D

The input deck setup is described for a computer code, composite blade structural analyzer (COBSTRAN) which was developed for the design and analysis of composite turbofan and turboprop blades and also for composite wind turbine blades. This manual is intended for use in conjunction with the COBSTRAN user's manual. Seven demonstration problems are described with pre- and postprocessing input decks. Modeling of blades which are solid thru-the-thickness and also aircraft wing airfoils with internal spars is shown. Corresponding NASTRAN and databank input decks are also shown. Detail descriptions of each line of the pre- and post-processing decks is provided with reference to the Card Groups defined in the user's manual. A dictionary of all program variables and terms used in this manual may be found in Section 6 of the user's manual. Author

N89-24460*# National Aeronautics and Space Administration. Lewis Research Center, Cleveland, OH.
ISOTHERMAL LIFE PREDICTION OF COMPOSITE LAMINA USING A DAMAGE MECHANICS APPROACH
Nader M. Abuelfoutouh, Michael J. Verrilli, and Gary R. Halford Jun. 1989 12 p Presented at the Symposium on High Temperature Composites, Dayton, OH, 13-15 Jun. 1989; sponsored by American Society for Composites Prepared in cooperation with Cairo Univ. (Egypt)
(NASA-TM-102032; E-4775; NAS 1.15:102032) Avail: NTIS HC A03/MF A01 CSCL 11D

A method for predicting isothermal plastic fatigue life of a composite lamina is presented in which both fibers and matrix are isotropic materials. In general, the fatigue resistances of the matrix, fibers, and interfacial material must be known in order to predict composite fatigue life. Composite fatigue life is predicted using only the matrix fatigue resistance due to inelasticity micro-mechanisms. The effect of the fiber orientation on loading direction is accounted for while predicting composite life. The application is currently limited to isothermal cases where the internal thermal stresses that might arise from thermal strain mismatch between fibers and matrix are negligible. The theory is formulated to predict the fatigue life of a composite lamina under either load or strain control. It is applied currently to predict the life of tungsten-copper composite lamina at 260 C under tension-tension load control. The calculated life of the lamina is in good agreement with available composite low cycle fatigue data. Author

N89-24461# Sandia National Labs., Albuquerque, NM. Solar Thermal Collector Technology Div.
STATUS OF THE DIRECT ABSORPTION RECEIVER PANEL RESEARCH EXPERIMENT: SALT FLOW AND SOLAR TEST REQUIREMENTS AND PLANS
Craig E. Tyner Mar. 1989 63 p
(Contract DE-AC04-76DP-00789)
(DE89-010968; SAND-88-2455) Avail: NTIS HC A04/MF A01

The Panel Research Experiment (PRE) is the first large-scale solar test of the molten nitrate salt Direct Absorption Receiver (DAR) concept. The purpose of the PRE is to demonstrate the engineering feasibility and practicality of the DAR. We will conduct the test at the Central Receiver Test Facility in Albuquerque in two phases: salt flow testing and solar testing. This is a working document to define PRE test objectives and requirements, document the test hardware design, and define test plans. DOE

25 INORGANIC AND PHYSICAL CHEMISTRY

Includes chemical analysis, e.g., chromatography; combustion theory; electrochemistry; and photochemistry.

For related information see also *77 Thermodynamics and Statistical Physics.*.

N89-24462# National Aeronautical Lab., Bangalore (India). Fluid Mechanics Div.

EXPERIMENTS ON LIQUID-VAPOUR PHASE CHANGE BETWEEN PLANE LIQUID SURFACES. PART 2: OBSERVATIONS OF LARGE TEMPERATURE JUMPS NEAR THE INTERFACES

P. N. Shankar and M. D. Deshpande May 1988 18 p
(NAL-TM-FM-8805) Avail: NTIS HC A03/MF A01

The temperature distribution in mercury vapor confined between its liquid evaporating surface and a condensing plane surface is examined. The data presented clearly exhibits the large temperature jumps at the interface boundaries which are predicted by kinetic theory; jumps as large as almost 50 percent of the applied temperature difference were observed. Author

N89-24463*# Alabama Univ., Huntsville. Dept. of Chemistry.

AUGER AND ESCA ANALYSIS Final Report

John C. Gregory [1988] 22 p
(Contract NAS8-36955)
(NASA-CR-183572; NAS 1.26:183572; Rept-727) Avail: NTIS HC A03/MF A01 CSCL 07D

X-ray photoelectron spectroscopy (XPS or ESCA) and Auger electron spectroscopy (AES) techniques are discussed. The XPS instrument is a Perkin-Elmer 5400 system which provides both elemental and chemical state information without restriction on the type of material that can be analyzed. The AES instrument is a Kratos Analytical XSAM 800 system. AES uses a beam of high energy electrons as a surface probe. Following electronic rearrangements within excited atoms by this probe, Auger electrons characteristic of each element present are emitted from the sample. Specific examples of analytic techniques and results are presented. Author

N89-24464# Princeton Univ., NJ. Dept. of Chemistry.

OXIDE-BOUND TRANSITION METAL COMPLEXES FOR METHANE ACTIVATION Annual Report, 1 Sep. 1987 - 31 Aug. 1988

Jeffrey Schwartz 1988 16 p
(Contract GRI-5086-260-1329)
(PB89-138614; GRI-88/0282) Avail: NTIS HC A03/MF A01 CSCL 07D

Methodology was developed for a model oxidation system for directly converting rhodium bis (allyl) or rhodium dihydride complexes to dioxygen or ozone adducts. Rhodium (oxygen) complexes and rhodium (ozone) complexes were prepared on either alumina or silica. Iridium analogs were prepared on silica. A series of heteropolyoxy anionic (HPA) complexes of rhodium was prepared involving both di(carbonyl) and dioxygen adducts. A crystal of TiO2 was prepared for surface studies and excellent UPS data for deposition and chemical transformations of organorhodium compounds was obtained. Angular-dependent UPS spectroscopy is being developed to enable UHV techniques to assist in structural characterization of complexes on oxide surfaces. Author

N89-24465# Oak Ridge National Lab., TN.

MULTIPLEXED ELECTRONICALLY PROGRAMMABLE MULTIMODE IONIZATION DETECTOR FOR CHROMATOGRAPHY Patent Application

M. B. Wise, inventor (to DOE) and M. V. Buchanan, inventor (to DOE) 19 May 1988 33 p
(Contract DE-AC05-84OR-21400)
(DE89-009758; PATENTS-US-A7196693;
US-Patent-Appl-SN-196693) Avail: NTIS HC A03/MF A01

The method and apparatus are presented for detecting and differentiating organic compounds based on their electron affinity. An electron capture detector cell (ECD) is operated in a plurality of multiplexed electronically programmable operating modes to alter the detector response during a single sampling cycle to acquire multiple simultaneous chromatograms corresponding to each of the different operating modes. The cell is held at a constant subatmospheric pressure while the electron collection bias voltage applied to the cell is modulated electronically to allow acquisition of multiple chromatograms for a single sample elution from a chromatograph representing three distinctly different response modes. A system is provided which automatically controls the programmed application of bias pulses at different intervals and/or amplitudes to switch the detector from an ionization mode to the electron capture mode and various degrees therebetween to provide an improved means of tuning an ECD for multimode detection and improved specificity. DOE

N89-24466*# Acurex Corp., Huntsville, AL. Aerotherm Div.

MATERIALS COMPATIBILITY WITH OXIDIZER-RICH GASES AT ELEVATED TEMPERATURES AND PRESSURE Final Report, Nov. 1987-1989

13 Apr. 1989 101 p
(Contract NAS8-36721)
(NASA-CR-183647; NAS 1.26:183647) Avail: NTIS HC A06/MF A01 CSCL 07D

An investigation of oxygen compatibility and resistance to ignition of candidate materials for use in a liquid rocket engine designed to incorporate an oxidizer rich preburner-LOX turbopump configuration was discussed. The program was divided into two basic tasks. The first task was to develop a preliminary design of an oxidizer turbopump preburner section complete with thermal and MS Parameter analyses and to develop a conceptual design of the main injector with a preliminary engine specification as the final product. The second task was directed totally at testing materials in oxygen-rich environments. Author

N89-24467# Air Force Inst. of Tech., Wright-Patterson AFB, OH. School of Engineering.

EXPERIMENTATION AND ANALYSIS OF COMPRESSION TEST METHODS FOR SINGLE FILAMENT HIGH PERFORMANCE FIBRES M.S. Thesis

Sukru Fidan Dec. 1988 149 p
(AD-A206358; AFIT/GAE/AA/88D-14) Avail: NTIS HC A07/MF A01 CSCL 07/6

The simple and reliable single filament test methods for predicting the compressive properties of fibers are a must for developing activities of fibers in laboratories because of difficulties in composite compression test methods. Therefore, in this study, two single filament compression test methods, which are elastic loop and bending beam test, are conducted for several polymeric fibers including Kevlars, PBO and PBZT and a few carbon fibers such as T-50 and P-75S, in order to obtain their compressive properties. Also the compressive failure modes of fibers, which occur as a kink band formation in polymeric fibers and as a fracture in carbon fibers are investigated. In addition, a FORTRAN program is written for numerical analysis of non-linear geometry elastica problems such as bending a single fiber with large displacements. GRA

N89-24468# Joint Inst. for Nuclear Research, Dubna (USSR). Lab. of Neutron Physics.

BACKSCATTERING SPECTRA PROCESSING FOR THE STRUCTURE OF MULTILAYER SAMPLES

R. A. Ilkhamov, D. Makhajdik, and G. M. Osetinskii 1987 7 p
In RUSSIAN; ENGLISH summary
(DE88-706325; JINR-R-10-87-926) Avail: NTIS (US Sales Only) HC A02/MF A01

The results of the structural analysis of five multilayer samples prepared from metallic and semiconductor materials are presented. The method of Rutherford backscattering spectrometry (RBS) using 1.5-3.0 MeV He-4 ion beam from a Van de Graff generator was applied. The processing of measured RBS spectrum was carried out by the computer modeling of the spectrum and comparing it with the experimental one. DOE

N89-24469# Midwest Research Inst., Golden, CO. Solar Energy Research Inst.
INCREASING THE CHEMICAL YIELD OF DESIRABLE CHEMICAL SPECIES USING SOLAR RAPID HEATING
Rosa Benito, K. Y. Wang, and Meir Carasso Mar. 1989 41 p
(Contract DE-AC02-83CH-10093)
(DE89-000881; SERI/TR-252-2953) Avail: NTIS HC A03/MF A01

This study consisted of a theoretical investigation into the possibility of increasing the chemical yield of a desired species by forcing a high heating rate of the reactants using concentrated solar flux. The particular reactants were oxygen and nitrogen in air. The study defined a sequence of thermodynamic processes beginning with atmospheric air and including the required rapid heating and quenching processes. An analytical formulation of a solar energy concentration problem was completed. This included the thermodynamic processes, resulting states, and principal chemical reactions. The resulting equations were solved and the solutions analyzed. The study demonstrated the theoretical feasibility of using concentrated solar flux to enhance the chemical yield of some desired species, and recommended identification of chemical systems in which theoretical expectations can be attained with experimental results. DOE

N89-24470# California Univ., Berkeley. Dept. of Chemistry.
QUANTUM MECHANICS OF CHEMICAL REACTIONS: RECENT DEVELOPMENTS IN REACTIVE SCATTERING AND IN REACTION PATH HAMILTONIANS
William H. Miller Dec. 1988 28 p Presented at the 6th International Congress on Quantum Chemistry, Jerusalem, Israel, 21 Aug. 1988 Prepared in cooperation with California Univ., Berkeley. Lawrence Berkeley Lab.
(Contract DE-AC03-76SF-00098)
(DE89-010438; LBL-26377; CONF-8808219-2) Avail: NTIS HC A03/MF A01

Two recent developments in the theory of chemical reaction dynamics are reviewed. First, it has recently been discovered that the S- matrix version of the Kohn variational principle is free of the Kohn anomalies that have plagued other versions and prevented its general use. This has considerably simplified quantum mechanical reactive scattering calculations, which provide the rigorous characterizations of bimolecular reactions. Second, a new kind of reaction path Hamiltonian has been developed, one based on the least motion path that interpolates linearly between the reactant and product geometry of the molecule (rather than the previously used minimum energy, or intrinsic reaction path). The form of Hamiltonian which results is much simpler than the original reaction path Hamiltonian, but more important is the fact that it provides a more physically correct description of hydrogen atom transfer reactions. DOE

N89-24471# Southern Univ., Baton Rouge, LA. Dept. of Chemistry.
MASS SPECTROMETRY
Jing-Fong Wei 1 Mar. 1989 3 p Presented at the NSF Mass Spectroscopy Workshop, Rome, GA, 28 Apr. 1989
(Contract DE-FG22-86PC-90540)
(DE89-011118; DOE/PC-90540/11; CONF-8904199-1) Avail: NTIS HC A02/MF A01

The mass spectrometer was used as an effective tool in compound identification. Recent research centered on using gas chromatography/mass spectrometry to identify the products from derivatization of aromatic amino and phenolic compounds. DOE

N89-24472# Sandia National Labs., Albuquerque, NM. Fluid and Thermal Sciences Dept.
MODELING THERMAL-MECHANICAL PROCESSES ASSOCIATED WITH THE INITIATION AND COMBUSTION OF GRANULAR ENERGETIC MATERIALS
M. R. Baer and J. W. Nunziato 1989 13 p Presented at the 3rd International Symposium on Behavior of Media Under High Dynamic Pressures, La Grande Motte, France, 5-9 Jun. 1989
(Contract DE-AC04-76DP-00789)
(DE89-007145; SAND-88-1296C; CONF-890661-5) Avail: NTIS HC A03/MF A01

In this paper, we describe a reactive multiphase flow model for the initiation and compressive combustion of dynamically compacted granular energetic materials. Numerical solutions of the reactive multiphase flow equations are obtained for various cases of dynamic compaction. Constitutive relationships of this description are determined for the granular explosive HMX and for nitrocellulose- based ball propellants. At low impact velocities, loading produces compaction without subsequent reaction. Calculations of compaction wave speed and compaction density are in good agreement with experimental observations. Compaction-induced combustion is observed for conditions of higher impact loading. A global reaction model is formulated using experimental time-to-reaction data and calculations of the initiation and combustion reveal detailed wave structures of the compaction and flame spread near the threshold to Deflagration to Detonation Transition (DDT). Predictions of the reactive one-dimensional wave fields compare favorably to experimental observations. DOE

26 METALLIC MATERIALS

Includes physical, chemical, and mechanical properties of metals, e.g., corrosion; and metallurgy.

N89-24473# Argonne National Lab., IL. Materials and Components Technology Div.
ROLE OF ALLOYING ADDITIONS IN THE OXIDATION-SULFIDATION OF Fe-BASE ALLOYS
K. Natesan and J. H. Park Mar. 1989 33 p Presented at the Symposium on Corrosion and Particle Erosion at High Temperatures, Las Vegas, NV, 27 Feb. - 3 Mar. 1989
(Contract W-31-109-eng-38)
(DE89-009825; CONF-890294-1) Avail: NTIS HC A03/MF A01

Thermogravimetric studies have been conducted on Fe-25 wt percent Cr and Fe-25 wt percent Cr-20 wt percent Ni model alloys with and without additions of refractory metals such as Nb and Zr. In addition to bulk alloying, specimens of both alloys were prepared with surface implantation of Nb. The alloys with bulk additions of Nb and Zr exhibited Cr2O3 surface scales upon exposure to air and low partial pressure O2 environments. The oxide grain size was much larger than that observed in the absence of Nb/Zr addition. In the oxygen-sulfur mixed-gas environments, the Nb- and Zr-modified alloys exhibited a barrier layer of an oxide of Nb or Zr at the Cr2O3/substrate interface; this layer minimizes the outward transport of base-metal elements, thereby extending the time for initiation of breakaway corrosion. Experiments conducted with Nb-implanted binary and ternary alloys showed no effect on the oxidation rate in air and low partial pressure O2 environments; however, the oxide grain size was substantially larger compared to that observed in the absence of implant. The Nb implant resulted in a substantial reduction in the oxidation rate of both alloys when exposed in low- and high-sulfur mixed-gas atmospheres. Information on the morphological features of the scales in these specimens as well as possible reasons for the implant benefit is presented. DOE

N89-24474# Argonne National Lab., IL. Materials Science Div.
MAGNETO-OPTICAL STUDIES OF METASTABLE 3D-TRANSITION METAL FILMS
C. Liu and S. D. Bader 1989 22 p Presented at the International Symposium on Magnetoelasticity and Electronic Structure of Transition Metals, Alloys, and Films, Duisburg, Federal Republic of Germany, 20-22 Mar. 1989
(Contract W-31-109-eng-38)
(DE89-009836; CONF-8903103-1) Avail: NTIS HC A03/MF A01

The surface magneto-optical Kerr effect is used in conjunction with structural and growth-mode characterizations to survey the surface magnetic anisotropy behavior of three metastable Fe-film systems: Fe on Cu(100), Ru(0001), and Pd(100). Each system

grows epitaxially in the ultrathin regime and exhibits the universal behavior of perpendicular ferromagnetic spin orientations below a critical thickness of 6 monolayers or less. The systems differ, however, in their monolayer-dosage magnetic properties due to interdiffusion and hybridization at the interface. Fe/Pd(100) exhibits submonolayer magnetism, while less than 2-monolayers Fe/Ru(0001) lacks a ferromagnetic signature, in accord with expectations based on moment formation in dilute Fe alloys. DOE

N89-24475# Pennsylvania State Univ., University Park. Dept. of Materials Science and Engineering.
ON SPECIMEN SHAPE EFFECTS AND THE DUCTILITY OF POROUS METALS
A. Geltmacher and D. A. Koss Feb. 1989 24 p
(Contract N00014-86-K-0381)
(AD-A206216; TR-11) Avail: NTIS HC A03/MF A01 CSCL 11/6

The influence of specimen shape on the elongation to failure has been simulated for materials containing random distributions of pores or voids. The analysis is performed utilizing a computer simulation in which distributions of pores are modeled in two dimensions as arrays of circular holes with differing hole microstructures . The simulations predict that long, narrow specimens with high aspect ratios should exhibit a loss of ductility which is most pronounced at low area fractions of voids/pores, and when the void/pore distributions exhibit a high degree of clustering. Under these conditions, the ductility data also exhibit considerable scatter. The results, which may be qualitatively understood in terms of imperfection theory, which also contains implications with regard to porosity and fracture toughness at low temperatures. GRA

N89-24476# Naval Postgraduate School, Monterey, CA.
COMPUTER SIMULATION OF COPPER IN THE LIQUID PHASE AND THE SPUTTERING OF LIQUID COPPER BY ONE KeV ARGON IONS M.S. Thesis
Raul D. Rodriguez Dec. 1988 105 p
(AD-A206264) Avail: NTIS HC A06/MF A01 CSCL 07/2

A molecular dynamics computer simulation was used to investigate several techniques of generating liquid Cu targets. The target with the best liquid characteristics was subjected to one KeV argon ion bombardment as a preliminary study of the sputtering of liquids. The techniques of warming by impulse and warming by initially displacing atoms from their equilibrium positions were compared. Both methods produced targets with good liquid properties. The energy became equally partitioned between kinetic and potential energy and all targets equilibrated within 400 fs. The range of a typical atom during the time of equilibration was found to be restricted to its initial neighborhood. The preliminary sputtering study resulted in a sputtering yield increase of 40 percent over the solid target, for a low index crystal plane. GRA

N89-24477# Naval Postgraduate School, Monterey, CA.
THE EFFECT OF HEAT INPUT AND COMPOSITION ON WELD METAL MICROSTRUCTURES IN THIN SECTION HY-130 GMAW WELDMENTS M.S. Thesis
Dean M. Pedersen Dec. 1988 94 p
(AD-A206476) Avail: NTIS HC A05/MF A01 CSCL 11/6

Thin section HY-130 is being considered by the U.S. Navy for use in decks and foundations in the SSN-21 design as a weight saving measure. Optimum welding procedures for thin section HY-130 do not currently exist, but they are being developed by David Taylor Naval Ship Research and Development Center (DTNSRDC). In this study, performed in conjunction with DTNSRDC, the effect of heat input and electrode composition on the weld metal microstructures and mechanical properties of four 12.7 mm thick HY-130 steel weldments produced by the GMAW process are reported. Microstructures were fully characterized by light and electron microscopy. Mechanical property results provided by DTNSRDC were correlated with the microstructure. The lower heat input produced microstructural refinement and a more uniform hardness. The higher carbon content electrode lowered the Ms temperature and stabilized the austenite. GRA

N89-24478# Oak Ridge National Lab., TN. Metals and Ceramics Div.
WELDABILITY AND MICROSTRUCTURAL CHARACTERIZATION OF Al-Li ALLOYS
T. Zacharia, S. A. David, J. M. Vitek, and R. P. Martukanitz 1989 10 p Presented at the 5th International Aluminum-Lithium Conference, Williamsburg, VA, 28 Mar. 1989
(Contract DE-AC05-84OR-21400)
(DE89-010183; CONF-8903109-1) Avail: NTIS HC A02

An investigation was carried out to determine the weldability, properties and microstructural characteristics of aluminum-lithium Alloys 2090 and 2091. Electron beam welds were made on 12.5-mm-thick plates to study the effect of welding conditions on the weldability and microstructure. The results indicate that these alloys are susceptible to fusion zone cracking. Following welding, a loss of hardness was observed in the fusion zone and the heat affected zone of Alloy 2090. After postweld aging the fusion zone hardness was partially restored and the heat-affected zone hardness was completely restored. Microhardness measurements did not reveal any such loss in hardness in the heat-affected zone of Alloy 2091. The result of the hot ductility tests indicate that these alloys are not susceptible to heat-affected zone cracking. DOE

N89-24479# Kernforschungszentrum G.m.b.H., Karlsruhe (Germany, F.R.). Inst. fuer Material- und Festkoerperforschung.
INVESTIGATIONS ON THE CREEP-RUPTURE BEHAVIOR OF THE AUSTENITIC STAINLESS STEEL AISI 316-NET Interim Report, Sep. 1988
M. Schirra, B. Ritter, M. delasRivas, and R. AncadeAbati Dec. 1988 47 p In GERMAN; ENGLISH summary
(KfK-4468; ISSN-0303-4003; ETN-89-94405) Copyright Avail: NTIS HC A03/MF A01

Creep-rupture tests were carried out with 17/13/2 CrNiMo austenitic steel AISI 316(L) selected as potential first-wall material for NET (Next European Torus). The test program on base material for NET shows (in the temperature range 500 to 700 C) a rupture-time-range of 20,000 hr. The results permit statements on creep and creep-rupture behavior and ductility. Metallography examinations give information about fracture behavior and demonstrate the complex precipitation. ESA

N89-24480# Office National d'Etudes et de Recherches Aerospatiales, Paris (France). Direction des Materiaux.
FUNDAMENTAL STUDIES ON ORDER EFFECTS IN METAL ALLOYS [ETUDES FONDAMENTALES SUR LES EFFETS D'ORDRE DANS LES ALLIAGES METALLIQUES]
R. Caudron, F. Ducastelle, A Finel, A. Loiseau, J. Planes, and F. Solal Mar. 1988 80 p In FRENCH and ENGLISH
(Contract DRET-87-34-001)
(ONERA-RT-14/221-M; ETN-89-94529) Avail: NTIS HC A05/MF A01

Published papers on crystalline order studies are reviewed. The methods discussed include neutron diffusion, Monte Carlo simulation, and electron microsopy. Atomic interactions are studied and applied to Pd3V and Ni3V molecules. Long period structures of various molecules are described. A complete experimental study of ordered TiAl2 structures is detailed. It confirms the existance of two structures, one of them being stable at high and low temperatures. ESA

N89-24481# Los Alamos National Lab., NM.
AMORPHOUS METAL ALLOYS PRODUCED BY MECHANICAL ALLOYING
T. J. Tiainen (Tampere Univ. of Technology, Finland) and R. B. Schwarz 1989 9 p Presented at the 5th Scandinavian Symposium on Materials Science, Copenhagen, Sweden, 22-25 May 1989
(Contract W-7405-eng-36)

(DE89-011189; LA-UR-89-1208; CONF-8905131-1) Avail: NTIS HC A02/MF A01

Mechanical alloying is a powder metallurgy method used in commercial production of high temperature superalloys. Under specific conditions, mechanical alloying allows the synthesis of amorphous metal alloys from mixtures of pure metal powders or from the powders of intermetallic compounds. Because the amorphizing transformation during mechanical alloying is a solid state reaction, most of the difficulties related to the amorphization by rapid solidification of melts can be avoided. Mechanical alloying allows the synthesis of amorphous alloys from metals with high melting temperatures and the resulting alloys have interesting properties such as high hardness and high crystallization temperatures. We used mechanical alloying for the synthesis of amorphous alloys in the binary alloy systems Ni-Sn, Nb-Si and Al-Hf. The amorphous alloy powders were characterized by X-ray diffraction, differential scanning calorimetry, scanning and transmission electron microscopy and hardness measurements. Produced alloys were compacted by hot pressing and the obtained compacts were characterized by X-ray diffraction, density and hardness measurements and by optical and scanning electron microscopy. The results of the amorphization and compaction studies are presented and discussed together with the characteristics of the mechanical alloying process. DOE

N89-24482# California Univ., Berkeley. Dept. of Materials Science and Engineering.

RESEARCH ON THE MECHANISM OF THERMAL FATIGUE IN NEAR-EUTECTIC Pb-Sn SOLDERS

J. W. Morris, Jr., D. Grivas, D. Tribula, T. Summers, and D. Frear (Sandia National Labs., Albuquerque, NM.) Jan. 1989 39 p Presented at the 13th Dept. of Navy Annual Electronics Manufacturing Seminar, China Lake, CA, 2 Mar. 1989 Prepared in cooperation with California Univ., Berkeley. Lawrence Berkeley Lab.

(Contract DE-AC03-76SF-00098)

(DE89-011430; LBL-26565; CONF-8903118-1) Avail: NTIS HC A03/MF A01

This paper discusses the microstructures of solder joints and the mechanisms of thermal fatigue, which is an important source of failure in electronic devices. The solder joints studied were near-eutectic Pb-Sn solder contacts on copper. The microstructure of the joints is described. While the fatigue life of near-eutectic solder joints is strongly dependent on the operating conditions and on the microstructure of the joint, the metallurgical mechanisms of failure are surprisingly constant. When the cyclic load is in shear at temperatures above room temperature the shear strain is inhomogeneous, and induces a rapid coarsening of the eutectic microstructure that concentrates the deformation in well-defined bands parallel to the joint interface. Fatigue cracks propagate along the Sn-Sn grain boundaries and join across the Pb-rich regions to cause ultimate failure. The failure occurs through the bulk solder unless the joint is so thin that the intermetallic layer at the interface is a significant fraction of the joint thickness, in which case failure may be accelerated by cracking through the intermetallic layer. The coarsening and subsequent failure is influenced more strongly by the number of thermal cycles than by the time of exposure to high temperature, at least for hold times up to one hour. DOE

N89-24483# Rockwell International Corp., Golden, CO.

EFFECTS OF MULTIPLE REDUCTIONS ON GRAIN REFINEMENT DURING HOT WORKING OF ALLOY 718

M. C. Mataya and D. K. Matlock (Colorado School of Mines, Golden.) 1989 24 p Presented at the International Symposium on Alloy 718 Metallurgy and Applications, Pittsburgh, PA, 12 Jun. 1989

(Contract DE-AC04-76DP-03533)

(DE89-010426; RFP-4329; CONF-890646-4) Avail: NTIS HC A03/MF A01

The simulation of microstructural evolution during primary breakdown of production sized alloy 718 ingots by radial forging was accomplished via multiple stroke axial compression testing of cylindrical specimens taken from a wrought and heat treated bar with a 254 micron grain size. Four stroke compression heat sequences were performed at a constant true strain rate of 1.0 s sup minus 1 and at temperatures of 950 C, 1050 C, and 1150 C. The applied strain per stroke for each four stroke sequence was either 0.14 to 0.23. Static, rather than dynamic, recrystallization was found to be responsible for the observed grain size refinement and its repetitive occurrence during back to back dwell periods resulted in the maintenance of a fine grain microstructure during multiple pass deformation sequences. In order of importance, the critical hot working parameters for recrystallization are temperature, dwell time between passes, and strain per pass. Microstructure was found to vary with work piece position, simulated by the applied sequence of dwell periods. DOE

N89-24484# Du Pont de Nemours (E. I.) and Co., Aiken, SC. Savannah River Lab.

HIGH TEMPERATURE MECHANICAL PROPERTIES AND MICROSCOPIC EXAMINATION OF EXTRUDED POWDER ALUMINUM

T. O. Woods, D. G. Berghaus, and H. B. Peacock 1989 14 p Presented at the Powder Metallurgy Conference, San Diego, CA, 11-14 Jun. 1989

(Contract DE-AC09-76SR-00001)

(DE89-010457; DP-MS-88-213; CONF-8906119-1) Avail: NTIS HC A03/MF A01

The purpose of this work is to examine the high temperature mechanical properties and structure of extruded powder aluminum so that its failure mechanisms can be determined. Specimens made from both extruded 101 ALCOA powder aluminum and 1100 commercial aluminum rods were mechanically tested in simple tension, simple compression, pure torsion, and combined tension-torsion and compression-torsion loadings at a test temperature of 350 C. The varied loadings are necessary to analyze material behavior because during extrusion the material is subjected to combinations of tensile, shear, and compressive deformations. Both powder aluminum and 100 aluminum specimens were tested to that stress-strain curves from the two materials could be compared to reveal differences in material properties which are due to the laminary structure of the extruded powder material. During extrusion the powder particles form a laminar structure. This structure consist of elongated particles which are separated by aluminum oxide. The brittle oxide originally coated the pre-extruded particles. DOE

27 NONMETALLIC MATERIALS

Includes physical, chemical, and mechanical properties of plastics, elastomers, lubricants, polymers, textiles, adhesives, and ceramic materials.

For composite materials see *24 Composite Materials.*

N89-24485# Idaho National Engineering Lab., Idaho Falls.

HYDROGEN ION-DRIVEN PERMEATION IN CARBONACEOUS FILMS

R. A. Anderl, D. F. Holland, and G. R. Longhurst 1988 20 p Presented at the 8th International Conference on Plasma Surface Interactions in Controlled Fusion Devices, Julich, Fed. Republic of Germany, 2 May 1988

(Contract DE-AC07-76ID-01570)

(DE89-005271; EGG-M-40087; CONF-880512-18) Avail: NTIS HC A03/MF A01

This paper presents the results of investigations into the permeation properties of amorphous carbonaceous, a-C:H, films produced by plasmachemical deposition techniques. Carbonaceous films on iron substrates with thickness ranging from 60 nm to 110 nm were subjected to high fluence implantations with mass analyzed D3+ ions with energies ranging from 600 eV to 3000 eV and fluxes ranging from 5 times 10(14) D/sq cm-s to 5 times 10(15) D/sq cm-s, respectively. Deuterium re-emission upstream, deuterium permeation downstream and secondary ions sputtered from the implantation surface were measured as a function of implantation fluence for specimens at 420 K. The present studies

indicate that the a-C:H film permeability is directly related to the time, hence the fluence, required to achieve isotopic replacement and saturation of the deuterium ion beam atoms stopped in the implant region. Once the deuterium saturation level is achieved in the layer, a significant fraction of the implanting ions can result in permeation. For the present experiment, this permeation factor was much higher than that for uncoated iron specimens subjected to similar beam conditions. Carbon sputter yields of 0.008 to 0.01 C/D were determined in this work for 1000-eV to 400-eV deuterium ions incident on a-C:H films. DOE

N89-24486*# Woven Structures, Inc., Compton, CA.
DEVELOPMENT OF TAILORABLE ADVANCED BLANKET INSULATION FOR ADVANCED SPACE TRANSPORTATION SYSTEMS Contractor Report, Aug. 1985 - Dec. 1986
Dominic P. Calamito 15 Apr. 1987 182 p
(Contract NAS2-12253)
(NASA-CR-177444; NAS 1.26:177444) Avail: NTIS HC A09/MF A01 CSCL 11B

Two items of Tailorable Advanced Blanket Insulation (TABI) for Advanced Space Transportation Systems were produced. The first consisted of flat panels made from integrally woven, 3-D fluted core having parallel fabric faces and connecting ribs of Nicalon silicon carbide yarns. The triangular cross section of the flutes were filled with mandrels of processed Q-Fiber Felt. Forty panels were prepared with only minimal problems, mostly resulting from the unavailability of insulation with the proper density. Rigidizing the fluted fabric prior to inserting the insulation reduced the production time. The procedures for producing the fabric, insulation mandrels, and TABI panels are described. The second item was an effort to determine the feasibility of producing contoured TABI shapes from gores cut from flat, insulated fluted core panels. Two gores of integrally woven fluted core and single ply fabric (ICAS) were insulated and joined into a large spherical shape employing a tadpole insulator at the mating edges. The fluted core segment of each ICAS consisted of an Astroquartz face fabric and Nicalon face and rib fabrics, while the single ply fabric segment was Nicalon. Further development will be required. The success of fabricating this assembly indicates that this concept may be feasible for certain types of space insulation requirements. The procedures developed for weaving the ICAS, joining the gores, and coating certain areas of the fabrics are presented. Author

N89-24487*# National Aeronautics and Space Administration. Lewis Research Center, Cleveland, OH.
TIME DEPENDENT RELIABILITY MODEL INCORPORATING CONTINUUM DAMAGE MECHANICS FOR HIGH-TEMPERATURE CERAMICS
Stephen F. Duffy (Cleveland State Univ., OH.) and John P. Gyekenyesi May 1989 20 p
(Contract NCC3-99)
(NASA-TM-102046; E-4794; NAS 1.15:102046) Avail: NTIS HC A03/MF A01 CSCL 11C

Presently there are many opportunities for the application of ceramic materials at elevated temperatures. In the near future ceramic materials are expected to supplant high temperature metal alloys in a number of applications. It thus becomes essential to develop a capability to predict the time-dependent response of these materials. The creep rupture phenomenon is discussed, and a time-dependent reliability model is outlined that integrates continuum damage mechanics principles and Weibull analysis. Several features of the model are presented in a qualitative fashion, including predictions of both reliability and hazard rate. In addition, a comparison of the continuum and the microstructural kinetic equations highlights a strong resemblance in the two approaches. Author

N89-24488*# Clemson Univ., SC. Center for Advanced Engineering Fibers.
THERMOPLASTIC COATING OF CARBON FIBERS Annual Report, 1988 - 1989
D. D. Edie, G. C. Lickfield, L. E. Allen, and J. R. McCollum 1989 136 p
(Grant NAG1-680)
(NASA-CR-185047; NAS 1.26:185047) Avail: NTIS HC A07/MF A01 CSCL 11C

A continuous powder coating system was developed for coating carbon fiber with LaRC-TPI (Langley Research Center-Thermoplastic Polyimide), a high-temperature thermoplastic polymide invented by NASA-Langley. The coating line developed used a pneumatic fiber spreader to separate the individual fibers. The polymer was applied within a recirculating powder coating chamber then melted using a combination of direct electrical resistance and convective heating to make it adhere to the fiber tow. The tension and speed of the line were controlled with a dancer arm and an electrically driven fiber wind-up and wind-off. The effects of heating during the coating process on the flexibility of the prepreg produced were investigated. The uniformity with which the fiber tow could be coated with polymer also was examined. Composite specimens were fabricated from the prepreg and tested to determine optimum process conditions. The study showed that a very uniform and flexible prepeg with up to 50 percent by volume polymer could be produced with this powder coating system. The coating line minimized powder loss and produced prepeg in lengths of up to 300 m. The fiber spreading was found to have a major effect on the coating uniformity and flexibility. Though test results showed low composite tensile strengths, analysis of fracture surfaces under scanning electron microscope indicated that fiber/matrix adhesion was adequate. Author

N89-24489# Pacific Northwest Labs., Richland, WA.
ANALYSIS OF PACKED-PARTICLE REARRANGEMENT DURING COLLOIDAL CERAMIC PROCESSING: GAMMA-RAY DENSITOMETRY AND A REVIEW OF ALTERNATIVE METHODS
C. H. Schilling, W. D. Samuels, and I. A. Aksay Mar. 1989 17 p Presented at the Symposium on Advanced Techniques for Characterizing Ceramics, San Francisco, CA, 25 Oct. 1988
(Contract DE-AC06-76RL-01830)
(DE89-009066; PNL-SA-15944; CONF-8810346-1) Avail: NTIS HC A03/MF A01

Electrostatic and steric repulsion forces that arise during colloidal processing of ceramics affect packed-particle arrangements in the powder consolidation stage and may influence microstructure development during sintering. A gamma-ray attenuation apparatus is used for nondestructive in situ measurement of porosity and composition during drying, sintering, and a wide range of consolidation processes. A study is presented which utilizes the apparatus to analyze solution chemistry effects on packed-particle rearrangement during sedimentation of colloidal alpha Al sub 2 O sub 3. Advantages of gamma-ray densitometry for the analysis of ceramic particle rearrangement are compared with those of alternative methods, such as rheology studies, consolidation kinetic modeling, permeability measurements, and various techniques for analyzing porous media. Gamma-ray densitometers may be used to augment these alternative techniques and assist in the development of more advanced rearrangement models. DOE

N89-24490# California Univ., Berkeley. Lawrence Berkeley Lab. Materials and Chemical Sciences Div.
BONDING AND CHEMISTRY OF HYDROCARBON MONOLAYERS ON METAL SURFACES
B. E. Bent and G. A. Somorjai Jul. 1988 72 p Presented at the Catalysts in Petroleum Refining Conference, Kuwait, 4-8 Mar. 1989
(Contract DE-AC03-76SF-00098)
(DE89-009311; LBL-25627; CONF-8903101-1) Avail: NTIS HC A04/MF A01

Results from ultra-high vacuum surface analysis techniques over the last ten years have dramatically increased our understanding of how unsaturated hydrocarbons react with metal surfaces. We review what has been learned, utilizing results from our laboratory on the bonding and chemistry of ethylene and benzene to illustrate general principles. DOE

N89-24491# University Coll., Cardiff (Wales). Dept. of Physics Electronics and Electrical Engineering.
OPTIMISATION OF THE FIGURE OF MERIT OF MODIFIED SILICON-GERMANIUM ALLOYS Final Technical Report, 1987 - 1989
D. M. Rowe Feb. 1989 23 p
(Contract DAJA45-87-C-0048; DA Proj. 1L1-61103-BH-57)
(AD-A206420; R/D-5857-PH-01) Avail: NTIS HC A03/MF A01 CSCL 07/2

Silicon germanium alloys are established thermoelectric materials for high temperature applications and have been successfully used in the fabrication of the thermocouples of radioisotope thermoelectric generators which provided the onboard electrical power to several U.S. space vehicles. Recently, material development scientists have focused attention on possible improvements in the figure of merit of alloys based on silicon-germanium through an increase in alpha 2o (the so-called electrical figure of merit, or power factor). In the final report is embodied the results of a program of work to develop a realistic working theoretical model of the silicon germanium alloy systems and its use in identifying and investigating the parameters which determine the value of the electrical figure of merit. GRA

N89-24492# Southwest Research Inst., San Antonio, TX. Laser Applications Group.
LASER-INDUCED-FLUORESCENCE INSPECTION OF POLYURETHANE AND RELATED MATERIALS, PHASE 1 Final Report, 28 Mar. 1986 - 15 Nov. 1988
R. H. Hill, Jr. 15 Nov. 1988 81 p
(Contract DLA900-84-C-0910)
(AD-A206423; Rept-17-7958-828) Avail: NTIS HC A05/MF A01 CSCL 07/3

Laser induced fluorescence has been used as the basis for a new nondestructive inspection technique. A strong correlation between laser-induced-fluorescence intensity and tensile strength of several polyurethane-based systems has been demonstrated. Various parameters, such as excitation and detection wavelengths, have been experimentally investigated. Successful laboratory experiments employing fiber-optic bundles indicate that practical implementation of this method is possible. A portable instrument to determine the physical condition of fabric-reinforced polyurethane fuel tanks used by the U.S. Army is one immediate application, but the method may also be applicable for use on other elastomeric materials. GRA

N89-24493# California Univ., San Diego, La Jolla. Dept. of Chemistry.
REACTIONS OF (ETA 5-C5H5) (ETA 5-C5Me5) Zr(Si(SiMe3)3)X (X = Cl, Me) COMPLEXES WITH CARBON MONOXIDE AND THE ISOCYANIDE 2,6 Me2C6H3NC. CRYSTAL STRUCTURE OF (ETA 5-C5H5) (ETA 5-C5Me5)Zr(ETA 2-C(N-2,6 Me2C6H3) Si(SiMe3)3)Cl
Frederick H. Elsner, T. D. Tilley, Arnold L. Rheingold, and Steven J. Geib 1988 16 p
(Grant AF-AFOSR-0228-85; AF Proj. 2303)
(AD-A206494; AFOSR-89-0346TR) Avail: NTIS HC A03/MF A01 CSCL 07/3

Early transition metal silyl compounds are proving to have a rich reaction chemistry that is distinct from that of late transition metal silyl derivatives. For example, early transition metal (do) silyl complexes are reactive toward insertions of unsaturated substrates into their M-Si bonds, whereas late metal silyls typically are not. We are interested in the factors that influence this insertion chemistry, and have observed that the reactivity of early metal-silicon bonds varies considerably as the metal, and substituents at both the metal and silicon, are changed. Here we describe some insertion chemistry that has been observed for the mixed-ring zirconium silyls. GRA

N89-24494# Army Natick Research and Development Command, MA.
THE EFFECTS OF SUPERCRITICAL FLUIDS ON HIGH PERFORMANCE POLYMERS Final Report, Oct. 1985 - Sep. 1987
David Remy and Leonard A. Levasseur Feb. 1989 39 p
(AD-A206515; NATICK/TR-89/022) Avail: NTIS HC A03/MF A01 CSCL 07/6

High performance polymers in current use have achieved a remarkable degree of ballistic protection. In spite of this characteristic the performance characteristic of many of these polymers falls considerably below theoretically predicted levels. There is considerable room for improvement in the properties of ballistic polymers in terms of chemical design, morphology, and fabrication changes for existing and new polymer structures. The project objective is to investigate the process of using supercritical fluids (SCF) to expand the parameters available for fiber fabrication or polymer modification with the aim of improving the performance properties of existing polymeric materials. Specifically, the research is intended to explore various aspects of SCF technology in order to form a basis from which further research on enhancement of ballistic properties can be accomplished. This preliminary study, therefore, is not comprehensive but it identifies areas of high potential for further work. GRA

N89-24495# North Carolina Univ., Chapel Hill. Dept. of Chemistry.
IN-SITU STRESS MEASUREMENTS DURING THERMAL OXIDATION OF SILICON Interim Technical Report
E. A. Irene and E. Kobeda 14 Mar. 1989 21 p
(Contract N00014-89-J-1178)
(AD-A206546; TR-22) Avail: NTIS HC A02/MF A01 CSCL 07/4

A two beam laser reflection technique was used to measure SiO2 film stress during Si oxidation, i.e., in-situ at the growth temperature. Results show a higher compressive intrinsic film stress near the Si-SiO2 interface and a lower stress in the bulk of the SiO2 film. Thermal stress is also measured by monitoring the SiO2 film covered Si substrate curvature changes during temperature excursions. Our new results are in general agreement with previous ex-situ stress measurements and may indicate that film stress, being highest at the interface, influences the interface reaction in Si oxidation. GRA

N89-24496# Midwest Research Inst., Golden, CO. Solar Energy Research Inst.
INVESTIGATIONS OF THE ORIGINS OF METASTABLE, LIGHT-INDUCED CHANGES IN HYDROGENATED AMORPHOUS SILICON Final Subcontract Report, 1 Feb. 1986 - 30 Mar. 1988
J. D. Cohen (Oregon Univ., Eugene.) Mar. 1989 37 p
(Contracts DE-AC02-83CH-10093; EG-77-C-01-4042)
(DE89-000890; SERI/STR-211-3448) Avail: NTIS HC A03/MF A01

This report contains results of Phase 2 of research to investigate metastable defect creation processes in hydrogenated amorphous silicon. The study relied primarily on junction capacitance methods to monitor the changes in deep defect distribution. Results obtained applying capacitance profiling methods to the study of undoped samples are summarized and indicate a significant role of extrinsic impurities in the degree of light-induced degradation that occurred. Photocapacitance transient measurements were taken to investigate changes in undoped a-Si:H. Studies were also begun of metastable changes in n-type doped a-Si:H samples by using both the drive-level capacitance profiling technique and transient photocapacitance methods, and results are described. DOE

N89-24497# IIT Research Inst., Bartlesville, OK.
DEVELOPMENT OF AN ENGINEERING METHODOLOGY FOR APPLYING FOAM TECHNOLOGY
Frank T. H. Chung and David A. Hudgins May 1989 58 p
(Contract DE-FC22-83FE-60149)
(DE89-000740; NIPER-374) Avail: NTIS HC A04/MF A01

This research project investigated foam generation and propagation in porous media over greater distances than most previous investigations had studied. The effects of surfactant concentration, oil saturation, and injection modes on foam generation and propagation in porous media were studied. A 30 ft long slim tube packed with sand was used for foam flow experiments. Accompanying the foam flow tests, experiments were conducted to study foam behavior in micromodels. The micromodels were designed to simulate the structure of porous media. Theoretical studies were also performed in parallel with the laboratory studies to develop a method to predict the propagation of surfactant in porous media and to investigate the effects of dispersion, dead-end pore capacitance, and adsorption and desorption on surfactant transport in porous media. DOE

N89-24498# Argonne National Lab., IL. Materials Science Div.
HIGH-RESOLUTION ELECTRON MICROSCOPY OF METAL/CERAMIC INTERFACES
K. L. Merkle Mar. 1989 9 p Presented at the Acta-Scripta Conference on Metal-ceramic Interfaces, Santa Barbara, CA, 16-18 Jan. 1989
(Contract W-31-109-eng-38)
(DE89-012396; CONF-890165-3) Avail: NTIS HC A02/MF A01

In the present work we chose simple fcc metal/metal-oxide systems which have large misfits and which are not expected to form reaction layers at the interface. The interfaces are generated as matrix-precipitate boundaries. The precipitates appear as reaction products of internal reduction or internal oxidation. Several useful features are associated with these preparation methods: (1) Since the geometry of the interface can within the constraints due to the lattice mismatch freely develop, information on low energy faces may be obtained. (2) Impurity effects are minimized due to the very large total surface area of the precipitates. (3) A common low index zone axis between precipitate and matrix is often present, and, therefore, studies by high resolution electron microscopy are possible. DOE

N89-24499# Oak Ridge National Lab., TN.
CERAMIC TECHNOLOGY FOR ADVANCED HEAT ENGINES PROJECT DATA BASE Summary Report, Sep. 1988
B. L. P. Booker Mar. 1989 100 p
(Contract DE-AC05-84OR-21400)
(DE89-012888; ORNL/M-755) Avail: NTIS HC A05/MF A01

A large volume and wide variety of data on the behavior of advanced ceramic materials are currently being generated within the Ceramic Technology for Advanced Heat Engines project (CTAHE). This is the second in a series of reports summarizing the data stored in the microcomputer-based CTAHE data base. Each report features a different class of ceramics, with as much information on materials in that class as has then been processed. This report concentrates on zirconia-based ceramics. DOE

N89-24500# Oak Ridge National Lab., TN.
CERAMIC TECHNOLOGY FOR ADVANCED HEAT ENGINES PROJECT Semiannual Progress Report, Apr. - Sep. 1988
Mar. 1989 502 p
(Contract DE-AC05-84OR-21400)
(DE89-012890; ORNL/TM-11116) Avail: NTIS HC A22

The Ceramic Technology For Advanced Heat Engines Project was developed by the Department of Energy's Office of Transportation Systems (OTS) in Conservation and Renewable Energy. This project, part of the OTS's Advanced Materials Development Program, was developed to meet the ceramic technology requirements of the OTS's automotive technology programs. Significant accomplishments in fabricating ceramic components for the Department of Energy (DOE), National Aeronautics and Space Administration (NASA), and Department of Defense (DoD) advanced heat engine programs have provided evidence that the operation of ceramic parts in high-temperature engine environments is feasible. However, these programs have also demonstrated that additional research is needed in materials and processing development, design methodology, and data base and life prediction before industry will have a sufficient technology base from which to produce reliable cost-effective ceramic engine components commercially. DOE

N89-24501# Sandia National Labs., Albuquerque, NM.
SOL-GEL PROCESSING OF CONTROLLED PORE FILMS
C. J. Brinker, G. C. Frye, A. J. Hurd, K. J. Ward, and C. S. Ashley 1989 22 p Presented at the 4th International Conference on Ultrastructure Processing of Ceramics, Glasses and Composites, Tucson, AZ, 19 Feb. 1989
(Contract DE-AC04-76DP-00789)
(DE89-013584; SAND-88-2392C; CONF-890275-4) Avail: NTIS HC A03/MF A01

During sol-gel film formation via dipping, polymeric precursors are aggregated on the substrate surface by a process involving gravitational flow, drying, and continued condensation reactions. To understand film formation in situ, we use ellipsometric imaging and infrared spectroscopy. The structure and porosity of the deposited film are determined by SAXS, ellipsometry, and surface acoustic wave (SAW) methods. We find that weakly-branched silicate precursors deposited near the isoelectric point of silica result in dense films (volume percent porosity, V(sub p) is less than 5 percent) in which any pores present have radii is less than 0.2 nm, regardless of precursor size. More compact precursors result in films in which the porosity and refractive index are controlled by the size of the precursor species prior to deposition and the relative rates of condensation and evaporation during deposition. The porosity and refractive index of these films may be varied as follows: volume percent porosity (0 less than or equal to V(sub p) less than or equal to 56 percent); pore radius (0 less than or equal to r less than or equal to 3.1 nm); surface area (1.2 less than or equal to S less than or equal to 263 sq m/g); refractive index (1.18 less than or equal to n less than or equal to 1.45). For repulsive, monosized particulate precursors, higher coating rates promote ordering providing an additional means of pore size control. DOE

N89-24502# Southwest Research Inst., San Antonio, TX.
CHARACTERIZATION OF PORE EVOLUTION IN CERAMICS DURING CREEP FAILURE AND DENSIFICATION
1989 39 p
(Contract DE-FG05-84ER-45063)
(DE89-013599; DOE/ER-45063/4) Avail: NTIS HC A03/MF A01

The processes involved in pore formation/removal can control the failure of ceramics at both high and low temperatures. Failure during creep at elevated temperatures, under all states of stress, is very sensitive to average porosity; such failure involves the nucleation, growth, and eventual coalescence of multiple pores. On the other hand, the failure of ceramics at lower temperatures is a weakest link process, with the number, distribution, size(s), and shapes of inherent pores within a ceramic body frequently constituting its principal weak links. Thus, a thorough understanding of the mechanisms of pore formation/removal is required such that pore formation can be minimized during creep and the opposite process, pore removal, can be maximized during densification. A three-year research program designed to substantially extend the previous work on pore revolution during both creep and densification is proposed herein. DOE

N89-24649*# Goodrich (B. F.) Co., Akron, OH.
FEATURES AND CHARACTERIZATION NEEDS OF RUBBER COMPOSITE STRUCTURES
Farhad Tabaddor *In* NASA, Langley Research Center, Computational Methods for Structural Mechanics and Dynamics, Part 1 May 1989 p 211-247 (For primary document see N89-24638 18-39)
Avail: NTIS HC A15/MF A01 CSCL 11C

28 PROPELLANTS AND FUELS

Includes rocket propellants, igniters, and oxidizers; their storage and handling procedures; and aircraft fuels.

For related information see also *07 Aircraft Propulsion and Power, 20 Spacecraft Propulsion and Power,* and *44 Energy Production and Conversion.*

N89-24503# Joint Inst. for Nuclear Research, Dubna (USSR). Scientifical-Methodical Div.
EXPLOSIVE-EMITTER CATHODE PRODUCED USING THE HEAVY ION TRACK TECHNIQUE
G. N. Akapev and S. A. Korenev 1988 8 p In RUSSIAN; ENGLISH summary Submitted for publication
(DE88-706304; JINR-13-88-347) Avail: NTIS (US Sales Only) HC A02/MF A01

A cathode based on thin metallic foils with a homogeneous needle surface is described. The cathode was manufactured using the heavy ion track technique which permits the production of cathodes with an unlimited area and a needle density ranging from about 10(3) to 10(9) needles per sq cm. An electron gun using this type of cathode has a current of 200 to 900 A and an energy of 100 to 300 keV. The cross section of the electron beam is fairly uniform. It is shown that needle emitters of similar shape and size play the principal role in forming a homogeneous cathode plasma. DOE

N89-24504# Los Alamos National Lab., NM.
METHANE TO METHANOL CONVERSION
Wayne C. Danen, John L. Lyman, Cheryl K. Rofer, Richard C. Oldenborg, Gerald E. Streit, and Monte J. Ferris 1989 9 p Presented at the Natural Gas Research and Development, Morgantown, WV, 18-19 Apr. 1989
(Contract W-7405-eng-36)
(DE89-011194; LA-UR-89-1171; CONF-890492-2) Avail: NTIS HC A02/MF A01

The objective of this research effort is to understand the fundamental chemistry necessary to develop a process to effect the partial oxidation of methane to methanol using air or oxygen. The goal is to develop and economically viable process to convert natural gas or methane from coal gasification products to a liquid fuel that is readily transported. DOE

29 MATERIALS PROCESSING

Includes space-based development of products and processes for commercial applications.

For biological materials see *55 Space Biology.*

N89-24505*# National Aeronautics and Space Administration. Goddard Space Flight Center, Greenbelt, MD.
PROCEEDINGS OF THE GODDARD SPACE FLIGHT CENTER WORKSHOP ON ROBOTICS FOR COMMERCIAL MICROELECTRONIC PROCESSES IN SPACE
3 Dec. 1987 210 p Workshop held in Greenbelt, MD, 2-3 Dec. 1987
(NASA-TM-101233; NAS 1.15:101233) Avail: NTIS HC A10/MF A01 CSCL 22A

Potential applications of robots for cost effective commercial microelectronic processes in space were studied and the associated robotic requirements were defined. Potential space application areas include advanced materials processing, bulk crystal growth, and epitaxial thin film growth and related processes. All possible automation of these processes was considered, along with energy and environmental requirements. Aspects of robot capabilities considered include system intelligence, ROM requirements, kinematic and dynamic specifications, sensor design and configuration, flexibility and maintainability. Support elements discussed included facilities, logistics, ground support, launch and recovery, and management systems. A.D.

N89-24347# European Space Agency, Paris (France). Microgravity Program Management Office.
MICROGRAVITY PAYLOADS (APM AND MTFF)
Guenther Seibert and Paul Clancy *In its* International Symposium on Europe in Space: The Manned Space System Oct. 1988 p 117-121 (For primary document see N89-24335 18-12)
Copyright Avail: NTIS HC A99/MF A01; ESA Publications Div., ESTEC, Noordwijk, Netherlands, 80 Dutch guilders

N89-24383# Preussag A.G., Erdoel und Erdgas, Hannover (Germany, F.R.).
INDUSTRIAL UTILIZATION OF MICROGRAVITY: PROBLEMS IN THE REALIZATION PHASE
Karlheinz Schoenemann *In* ESA, International Symposium on Europe in Space: The Manned Space System Oct. 1988 p 437-439 (For primary document see N89-24335 18-12)
Copyright Avail: NTIS HC A99/MF A01; ESA Publications Div., ESTEC, Noordwijk, Netherlands, 80 Dutch guilders

N89-24394# Deutsche Forschungs- und Versuchsanstalt fuer Luft- und Raumfahrt, Cologne (Germany, F.R.).
THE MICROGRAVITY USER SUPPORT CENTER (MUSC)
K. Wittmann, H. P. Schmidt, D. Padeken, B. Hildmann, E. Bennett, and B. Feuerbacher *In* ESA, International Symposium on Europe in Space: The Manned Space System Oct. 1988 p 525-530 (For primary document see N89-24335 18-12)
Copyright Avail: NTIS HC A99/MF A01; ESA Publications Div., ESTEC, Noordwijk, Netherlands, 80 Dutch guilders

N89-24395# Naples Univ. (Italy). Inst. of Aerodynamics.
MARS MICROGRAVITY ADVANCED RESEARCH AND SUPPORT CENTER
Luigi G. Napolitano *In* ESA, International Symposium on Europe in Space: The Manned Space System Oct. 1988 p 531-540 (For primary document see N89-24335 18-12)
Copyright Avail: NTIS HC A99/MF A01; ESA Publications Div., ESTEC, Noordwijk, Netherlands, 80 Dutch guilders

N89-24820*# National Aeronautics and Space Administration. Marshall Space Flight Center, Huntsville, AL.
AN AUTOMATED PROTEIN CRYSTAL GROWTH FACILITY ON THE SPACE STATION Abstract Only
Melody Herrmann *In* Tactical Weapons Guidance and Control Information Conference on Space and Military Applications of Automation and Robotics Jun. 1988 p 3 (For primary document see N89-24819 18-63)
Avail: NTIS HC A05/MF A01 CSCL 22A

N89-24821# Teledyne Brown Engineering, Huntsville, AL.
THE IMPACT OF AN IVA ROBOT ON THE SPACE STATION MICROGRAVITY ENVIRONMENT Abstract Only
Phillip E. Harman *In* Tactical Weapons Guidance and Control Information Conference on Space and Military Applications of Automation and Robotics Jun. 1988 p 4 (For primary document see N89-24819 18-63)
Avail: NTIS HC A05/MF A01 CSCL 09B

31 ENGINEERING (GENERAL)

Includes vacuum technology; control engineering; display engineering; cryogenics; and fire prevention.

N89-24506# National Aerospace Lab., Tokyo (Japan).
AN ATOMIC OXYGEN GENERATION FACILITY FOR SPACE ENVIRONMENTAL TESTINGS
Yasuo Watanabe, Yoshinori Fujimori, and Michio Nishida Aug. 1988 16 p In JAPANESE; ENGLISH summary
(NAL-TR-989; ISSN-0389-4010) Avail: NTIS HC A03/MF A01

Preliminary experiments in producing atomic oxygen for space environmental testings were conducted. O-atoms were generated by injecting molecular oxygen into a preionized argon plasma. A mixture of argon plasma and oxygen was expanded through a sonic orifice into a low pressure chamber as a free jet. To confirm

the generation of O-atoms and to examine the possibility of forming a molecular beam from the supersonic free jet, population densities of the electronic excitation levels 3p(3)P and 3p(5)P of atomic oxygen were measured along the free jet centerline. The population densities satisfied the flux condition of low earth orbit. Author

N89-24507*# National Aeronautics and Space Administration. Marshall Space Flight Center, Huntsville, AL.
FURTHER DEVELOPMENTS IN MODELING DIGITAL CONTROL SYSTEMS WITH MA-PREFILTERED MEASUREMENTS
Michael E. Polites Washington Mar. 1989 20 p
(NASA-TP-2909; M-612; NAS 1.60:2909) Avail: NTIS HC A03/MF A01 CSCL 13B

State variable representations are presented for a continuous-time plant driven by a zero-order-hold with multirate-sampled measurements prefiltered by multi-input/multi-output moving average (MA) processes. These representations have broad application, but are known to be useful in the aerospace field for modeling systems with star trackers and some state-of-the-art rate-gyroscopes and accelerometers. Author

N89-24508*# National Aeronautics and Space Administration. Langley Research Center, Hampton, VA.
MULTIDISCIPLINARY OPTIMIZATION FOR ENGINEERING SYSTEMS: ACHIEVEMENTS AND POTENTIAL
Jaroslaw Sobieszczanski-Sobieski Mar. 1989 23 p Presented at the DFVLR Seminar on Optimization, Bonn, Fed. Republic of Germany, 7-8 Jun. 1989
(NASA-TM-101566; NAS 1.15:101566) Avail: NTIS HC A03/MF A01 CSCL 13B

The currently common sequential design process for engineering systems is likely to lead to suboptimal designs. Recently developed decomposition methods offer an alternative for coming closer to optimum by breaking the large task of system optimization into smaller, concurrently executed and, yet, coupled tasks, identified with engineering disciplines or subsystems. The hierarchic and non-hierarchic decompositions are discussed and illustrated by examples. An organization of a design process centered on the non-hierarchic decomposition is proposed. Author

N89-24509*# Texas A&M Univ., College Station. Dept. of Computer Science
TELE-AUTONOMOUS CONTROL INVOLVING CONTACTS: THE APPLICATIONS OF A HIGH PRECISION LASER LINE RANGE SENSOR Interim Report
R. A. Volz, L. Shao, M. W. Walker, and L. A. Conway (Michigan Univ., Ann Arbor.) 22 May 1989 17 p
(Grant NAG5-1024)
(NASA-CR-184995; NAS 1.26:184995) Avail: NTIS HC A03/MF A01 CSCL 13B

The object localization algorithm based on line-segment matching is presented. The method is very simple and computationally fast. In most cases, closed-form formulas are used to derive the solution. The method is also quite flexible, because only few surfaces (one or two) need to be accessed (sensed) to gather necessary range data. For example, if the line-segments are extracted from boundaries of a planar surface, only parameters of one surface and two of its boundaries need to be extracted, as compared with traditional point-surface matching or line-surface matching algorithms which need to access at least three surfaces in order to locate a planar object. Therefore, this method is especially suitable for applications when an object is surrounded by many other work pieces and most of the object is very difficult, is not impossible, to be measured; or when not all parts of the object can be reached. The theoretical ground on how to use line range sensor to located an object was laid. Much work has to be done in order to be really useful. Author

N89-24510# Lawrence Livermore National Lab., CA.
VISCOSITY OF SOLIDS DETERMINED BY SHOCK WAVE ACTION ON HEMISPHERICAL INDENTATIONS
Dennis Maiden, Art Mitchell, and Mark Wilkins 31 Jan. 1989 17 p Presented at the 3rd International Symposium on Behavior of Media Under High Dynamic Pressures, La Grande Motte, France, 5-9 Jun. 1989
(Contract W-7405-eng-48)
(DE89-008035; UCRL-100064; CONF-890661-7) Avail: NTIS HC A03/MF A01

An experimental technique for determining the viscosity of solids is investigated. The technique was developed by Mali from the Institute of Hydrodynamics at Novosibirsk. It involves determining the jet-no-jet condition from a shock wave impacting a plate with hemispherical indentations. The indentation radius when a jet does not form identifies a critical Reynolds number. Numerical simulations of the experiment are performed using a viscoplastic constitutive model. The viscosity is determined by adjusting it until the speed of the jet and the critical Reynolds number match experiment. Results show that the viscosity of copper is two orders of magnitude lower than Mali's, but are in agreement with data derived from shock wave profiles by USA authors. DOE

N89-24364# European Space Agency. European Space Research and Technology Center, ESTEC, Noordwijk (Netherlands). Product Assurance and Safety Dept.
ESA SAFETY REQUIREMENTS
L. Tedeman *In its* International Symposium on Europe in Space: The Manned Space System Oct. 1988 p 247-251 (For primary document see N89-24335 18-12)
Copyright Avail: NTIS HC A99/MF A01; ESA Publications Div., ESTEC, Noordwijk, Netherlands, 80 Dutch guilders

N89-24365# European Space Agency, Paris (France).
SAFETY AND RELIABILITY OF THE ARIANE 5-HERMES COMPOSITE [SECURITE-FIABILITE COMPOSITE ARIANE 5 - HERMES]
J. Marcoux, J. Charles, G. Borycki, and B. Galland (Aerospatiale, Les Mureaux, France) *In its* International Symposium on Europe in Space: The Manned Space System Oct. 1988 p 253-267 In FRENCH (For primary document see N89-24335 18-12)
Copyright Avail: NTIS HC A99/MF A01; ESA Publications Div., ESTEC, Noordwijk, Netherlands, 80 Dutch guilders

N89-24367# Deutsche Forschungs- und Versuchsanstalt fuer Luft- und Raumfahrt, Cologne (Germany, F.R.).
SYSTEM SAFETY FROM D-MISSIONS TO COLUMBUS
H. Schuermanns and W. Ziesmann *In* ESA, International Symposium on Europe in Space: The Manned Space System Oct. 1988 p 275-280 (For primary document see N89-24335 18-12)
Copyright Avail: NTIS HC A99/MF A01; ESA Publications Div., ESTEC, Noordwijk, Netherlands, 80 Dutch guilders

N89-24368# European Space Agency, Paris (France). Columbus System Engineering and Integration.
COLUMBUS SAFETY AND RELIABILITY
F. Longhurst and H. Wessels *In its* International Symposium on Europe in Space: The Manned Space System Oct. 1988 p 281-290 (For primary document see N89-24335 18-12)
Copyright Avail: NTIS HC A99/MF A01; ESA Publications Div., ESTEC, Noordwijk, Netherlands, 80 Dutch guilders

N89-24371# European Space Agency. European Space Operations Center, Darmstadt (Germany, F.R.).
THE IMPACT OF MANNED SPACE FLIGHT OPERATIONS ON THE SAFETY AND RELIABILITY ASPECTS OF GROUND SYSTEMS REQUIREMENTS
David E. B. Wilkins *In its* International Symposium on Europe in Space: The Manned Space System Oct. 1988 p 337-347 (For primary document see N89-24335 18-12)
Copyright Avail: NTIS HC A99/MF A01; ESA Publications Div., ESTEC, Noordwijk, Netherlands, 80 Dutch guilders

N89-24378# European Space Agency. European Space Operations Center, Darmstadt (Germany, F.R.).
EXPERT SYSTEM FOR EUROPEAN SPACE INFRASTRUCTURE
J. Wheadon *In its* International Symposium on Europe in Space: The Manned Space System Oct. 1988 p 395-401 (For primary document see N89-24335 18-12)
Copyright Avail: NTIS HC A99/MF A01; ESA Publications Div., ESTEC, Noordwijk, Netherlands, 80 Dutch guilders

N89-24384# European Space Agency. European Space Research and Technology Center, ESTEC, Noordwijk (Netherlands).
THE CONCEPT OF TELESCIENCE
P. Buia *In its* International Symposium on Europe in Space: The Manned Space System Oct. 1988 p 441-445 (For primary document see N89-24335 18-12)
Copyright Avail: NTIS HC A99/MF A01; ESA Publications Div., ESTEC, Noordwijk, Netherlands, 80 Dutch guilders

N89-24385# LABEN Space Instrumentation and Systems, Milan (Italy). Advanced Research and Development Dept.
TELESCIENCE AND PAYLOAD CONTROL SUPPORT TECHNOLOGIES
P. Donzelli and E. Macavero *In* ESA, International Symposium on Europe in Space: The Manned Space System Oct. 1988 p 447-453 (For primary document see N89-24335 18-12)
Copyright Avail: NTIS HC A99/MF A01; ESA Publications Div., ESTEC, Noordwijk, Netherlands, 80 Dutch guilders

N89-24386# MATRA Espace, Toulouse (France).
TELESCIENCE: A PROMISING OPERATIONS CENTER
Ph. LeBouar and C. Loeillet *In* ESA, International Symposium on Europe in Space: The Manned Space System Oct. 1988 p 455-463 (For primary document see N89-24335 18-12)
Copyright Avail: NTIS HC A99/MF A01; ESA Publications Div., ESTEC, Noordwijk, Netherlands, 80 Dutch guilders

N89-24402# Stuttgart Univ. (Germany, F.R.). Inst. for Space Systems.
SAFETY IN MANNED SPACE FLIGHT
E. Messerschmid *In* ESA, International Symposium on Europe in Space: The Manned Space System Oct. 1988 p 595-604 (For primary document see N89-24335 18-12)
Copyright Avail: NTIS HC A99/MF A01; ESA Publications Div., ESTEC, Noordwijk, Netherlands, 80 Dutch guilders

32 COMMUNICATIONS AND RADAR

Includes radar; land and global communications; communications theory; and optical communications.

For related information see also *04 Aircraft Communications and Navigation* and *17 Space Communications, Spacecraft Communications, Command and Tracking.* For search and rescue see *03 Air Transportation and Safety,* and *16 Space Transportation.*

N89-24511*# Virginia Polytechnic Inst. and State Univ., Blacksburg. Dept. of Electrical Engineering.
FEASIBILITY STUDY OF A SYNTHESIS PROCEDURE FOR ARRAY FEEDS TO IMPROVE RADIATION PERFORMANCE OF LARGE DISTORTED REFLECTOR ANTENNAS Final Report, 25 Feb. 1988 - 24 Feb. 1989
W. L. Stutzman and W. T. Smith 1989 21 p
(Grant NAG1-859)
(NASA-CR-184974; NAS 1.26:184974) Avail: NTIS HC A03/MF A01 CSCL 20N

Surface errors on parabolic reflector antennas degrade the overall performance of the antenna. The errors are in the form of roughness on the surface, distortions in the shape, or structural design details. They cause amplitude and phase errors in the aperture field which lower the gain, raise the sidelobes, and fill in the nulls. These are major problems in large space reflector antennas. Planned mobile satellite communications systems having limited signal margin need high gain from the space reflectors. Future multiple beam antenna systems requiring spatial isolation to allow frequency reuse could be rendered useless if high sidelobes are present. High sidelobes are also responsible for noise. Ways of compensating for surface errors by pattern synthesis using an array of feed antennas are examined. Pattern corrections are directed specifically toward portions of the pattern requiring improvements. The pattern synthesis does not require knowledge of the surface errors. Both the amplitude and phase of the high side lobes caused by the distortion are required. Author

N89-24512 British Broadcasting Corp., Kingswood (England). Engineering Div.
PROTECTION OF VHF INTERNATIONAL DISTRESS FREQUENCIES FROM HARMONIC RADIATION DUE TO DIGITAL TELEVISION EQUIPMENT
J. Middleton 1989 16 p
(BBC-RD-1989/1) Avail: Issuing Activity

Digital television picture processing equipment uses a luminance sampling frequency of 13.5 MHz, which can give rise to harmonics at 121.5 and 243 MHz. If such equipment becomes sufficiently widespread as will probably be the case with MAC/packet receivers, it is possible that the cumulative radiation could become significantly high. Since these frequencies are used by the international distress services there is a potential for interference if this unwanted radiation is not controlled at the point of manufacture. Over the last two years this problem was studied by the BBC in conjunction with the EBU. The conclusion is that the distress services will be protected provided that digital television picture processing equipment meets existing electromagnetic compatibility (EMC) standards for information technology equipment. In the case of domestic television this should not present a problem, but for studio equipment, because of its size and complexity, EMC compliance may not be so easy. Author

N89-24513# Naval Postgraduate School, Monterey, CA.
AR (AUTOREGRESSIVE) MODELING OF COHERENCE IN TIME DELAY AND DOPPLER ESTIMATION M.S. Thesis
Jun Lee Dec. 1988 89 p
(AD-A205239) Avail: NTIS HC A05/MF A01 CSCL 17/8

The estimation of time delay and Doppler difference of a signal arriving at two physically separated sensors is investigated in this thesis. Usually, modified cross power spectrum coupled with Doppler compensation is used to detect a common, passive signal received at two separated sensors. Another successful approach uses the cross coherence to achieve this goal. This thesis modifies these two techniques to model the Doppler difference via an autoregressive (AR) technique. Analytical results are derived and experimentally verified via a computer simulation. Performance at high and low signal to noise ratios (SNRs) is examined. GRA

N89-24514*# National Aeronautics and Space Administration. Langley Research Center, Hampton, VA.
ON THE CAUSALITY OF PLASMA PERMITTIVITY
C. R. Cockrell Apr. 1989 14 p
(NASA-TM-101551; NAS 1.15:101551) Avail: NTIS HC A03/MF A01 CSCL 20N

Causal solutions for effective relative complex permittivities of plasmas are derived. Both lossless and lossy plasmas are considered. Author

N89-24515# National Severe Storms Lab., Norman, OK.
GROUND CLUSTER FILTERS FOR STAGGERED PULSE TRAINS Final Report
Dusan S. Zrnic and Zoran Banjanin (Oklahoma Univ., Norman.) Mar. 1989 70 p
(Contract DTFA01-80-Y-10524)
(DOT/FAA/SA-89/2) Avail: NTIS HC A04/MF A01

Several methods for cancelling ground clutter on Doppler weather radars that operate with staggered pulse repetition times (PRT's) are investigated. A scheme is developed that consists of two filters that operate sequentially, so that the overall filter is

time-varying, with periodically changing coefficients. This filter is analyzed theoretically and through simulations for a stagger ratio of 3/2, which extends the unambiguous velocity interval (at a wavelength of 5 cm) to 50 m/s. The amplitude characteristic of the filter over this interval is very good, but the phase characteristic, which is nonlinear in about 40 percent of the interval, requires that a special decision logic be used for velocity estimation. At high signal-to-noise ratio (greater than 20 dB), mean velocities obtained from the output meet terminal Doppler weather radar specifications. Author

N89-24516# Los Alamos National Lab., NM.
AUDITORY SPEECH PREPROCESSORS
George Zweig 1989 7 p Presented at the DARPA Speech and Natural Language Workshop, Philadelphia, PA, 21 Feb. 1989
(Contract W-7405-eng-36)
(DE89-009280; LA-UR-89-939; CONF-890291-1) Avail: NTIS HC A02/MF A01

A nonlinear transmission line model of the cochlea (Zweig 1988) is proposed as the basis for a novel speech preprocessor. Sounds of different intensities, such as voiced and unvoiced speech, are preprocessed in radically different ways. The Q's of the preprocessor's nonlinear filters vary with input amplitude, higher Q's (longer integration times) corresponding to quieter sounds. Like the cochlea, the preprocessor acts as a subthreshold laser that traps and amplifies low level signals, thereby aiding in their detection and analysis. DOE

N89-24517# Sandia National Labs., Albuquerque, NM. Antenna Development Div.
THE FREQUENCY RESPONSE OF PHASED-ARRAY ANTENNAS
B. C. Brock Feb. 1989 55 p
(Contract DE-AC04-76DP-00789)
(DE89-009710; SAND-88-2667) Avail: NTIS HC A04/MF A01

The phased-array antenna will be examined from the point of view of effects caused by changes in frequency. Both simple linear arrays and the more complex conformal array are examined. For the conformal array, a comparison between a corporate-feed structure and a row series-feed structure is included. There are two primary effects which will be discussed: beam-pointing errors and distortion of large bandwidth signals. A formula for estimating the operating or tunable array bandwidth for narrow-bandwidth signals is derived. An expression for the wide-bandwidth-signal transfer function is also obtained and examined. It will be shown that the transfer function depends both on the array scan angle and the position within the mainbeam. DOE

N89-24518*# Ohio State Univ., Columbus. ElectroScience Lab.
ANALYSIS OF THE EM SCATTERING FROM ARBITRARY OPEN-ENDED WAVEGUIDE CAVITIES USING AXIAL GAUSSIAN BEAM TRACKING Final Report
R. J. Burkholder and P. H. Pathak Dec. 1988 80 p
(Grant NAG3-476)
(NASA-CR-185054; NAS 1.26:185054; Rept-719630-1) Avail: NTIS HC A05/MF A01 CSCL 20N

The electromagnetic (EM) scattering from a planar termination located inside relatively arbitrarily shaped open-ended waveguide cavities with smoothly curved interior walls is analyzed using a Gaussian Beam (GB) expansion of the incident plane wave fields in the open end. The cavities under consideration may contain perfectly-conducting interior walls with or without a thin layer of material coating, or the walls may be characterized by an impedance boundary condition. In the present approach, the GB's are tracked only to the termination of the waveguide cavity via beam reflections from interior waveguide cavity walls. The Gaussian beams are tracked approximately only along their beam axes; this approximation which remains valid for relatively well focussed beams assumes that an incident GB gives rise to a reflected GB with parameters related to the incident beam and the radius of curvature of the wall. It is found that this approximation breaks down for GB's which come close to grazing a convex surface and when the width of the incident beam is comparable to the radius of curvature of the surface. The expansion of the fields at the open end depend on the incidence angle only through the expansion coefficients, so the GB's need to be tracked through the waveguide cavity only once for a wide range of incidence angles. At the termination, the sum of all the GB's are integrated using a result developed from a generalized reciprocity principle, to give the fields scattered from the interior of the cavity. The rim edge at the open end of the cavity is assumed to be sharp and the external scattering from the rim is added separately using Geometrical Theory of Diffraction. The results based on the present approach are compared with solutions based on the hybrid asymptotic modal method. The agreement is found to be very good for cavities made up of planar surfaces, and also for cavities with curved surfaces which are not too long with respect to their width. Author

N89-24519*# Ohio State Univ., Columbus. ElectroScience Lab.
A HYBRID ASYMPTOTIC-MODAL ANALYSIS OF THE EM SCATTERING BY AN OPEN-ENDED S-SHAPED RECTANGULAR WAVEGUIDE CAVITY
P. H. Law, R. J. Burkholder, and P. H. Pathak Dec. 1988 53 p
(Grant NAG3-476)
(NASA-CR-185053; NAS 1.26:185053; Rept-719630-2) Avail: NTIS HC A04/MF A01 CSCL 20N

The electromagnetic fields (EM) backscatter from a 3-dimensional perfectly conducting S-shaped open-ended cavity with a planar interior termination is analyzed when it is illuminated by an external plane wave. The analysis is based on a self-consistent multiple scattering method which accounts for the multiple wave interactions between the open end and the interior termination. The scattering matrices which described the reflection and transmission coefficients of the waveguide modes reflected and transmitted at each junction between the different waveguide sections, as well at the scattering from the edges at the open end are found via asymptotic high frequency methods such as the geometrical and physical theories of diffraction used in conjunction with the equivalent current method. The numerical results for an S-shaped inlet cavity are compared with the backscatter from a straight inlet cavity; the backscattered patterns are different because the curvature of an S-shaped inlet cavity redistributes the energy reflected from the interior termination in a way that is different from a straight inlet cavity. Author

N89-24520*# National Aeronautics and Space Administration. Lewis Research Center, Cleveland, OH.
MICROWAVE CHARACTERISTICS OF GaAs MMIC INTEGRATABLE OPTICAL DETECTORS
Paul C. Claspy, Scott M. Hill (Case Western Reserve Univ., Cleveland, OH.), and Kul B. Bhasin Jun. 1989 6 p Presented at the IEEE MTT-S International Microwave Symposium, Long Beach, CA, 13-15 Jun. 1989
(NASA-TM-101485; E-4621; NAS 1.15:101485) Avail: NTIS HC A02/MF A01 CSCL 20N

Interdigitated photoconductive detectors were fabricated on microwave device structures, making them easily integratable with Monolithic Microwave Integrated Circuits (MMIC). Detector responsivity as high as 2.5 A/W and an external quantum efficiency of 3.81 were measured. Response speed was nearly independent of electrode geometry, and all detectors had usable response at frequencies to 6 GHz. A small signal model of the detectors based on microwave measurements was also developed. Author

N89-24521# Oak Ridge National Lab., TN.
ICRF ANTENNA DESIGNS FOR CIT AND ALCATOR C-MOD
R. H. Goulding, F. W. Baity, P. L. Goranson, D. J. Hoffman, P. M. Ryan, D. J. Traylor, and J. J. Yugo 1989 4 p Presented at the 8th Topical Conference on Radio Frequency Power in Plasmas, Irvine, CA, 1 May 1989
(Contract DE-AC05-84OR-21400)
(DE89-011579; CONF-8905120-4) Avail: NTIS HC A02/MF A01

An ion cyclotron range of frequencies (ICRF) launcher for the Compact Ignition Tokamak (CIT) has been designed. This launcher

incorporates four current straps in a 2 x 2 configuration. The current straps consist of end-fed loops that are grounded in the middle. An antenna similar in geometry, size, and feed configuration to a single strap of the CIT launcher will be built for use on Alcator C-Mod. The design must provide maximum power levels of 4 MW/port for CIT and 2 MW/port for C-Mod, pulse lengths of 5 to 10 s for CIT and 1 s for C-Mod, and power densities up to 2 kW/sq cm. The design uses a Faraday shield consisting of Inconel rods with mechanically attached graphite tiles; the shield and the current strap are cooled by radiating to a gas-cooled backplane. A feed configuration compatible with the end-fed antenna design has been developed and features tunability in three bands in the range 65 to 130 MHz. It uses an external resonant loop with integral tuning elements. It has been designed to maximize power handling capabilities, minimize space requirements, and facilitate remote handling. DOE

N89-24522# Lawrence Livermore National Lab., CA.
CHARACTERIZATION OF RADIATION BOUNDARY CONDITIONS USED IN THE FINITE-DIFFERENCE TIME-DOMAIN METHOD
Scott L. Ray 29 Dec. 1988 6 p Presented at the Institute of Electrical and Electronics Engineers (IEEE) Antennas Propagation Society (AP-S) International Symposium, San Jose, CA, 26-30 Jun. 1989
(Contract W-7405-eng-48)
(DE89-005662; UCRL-100192; CONF-890660-1) Avail: NTIS HC A02/MF A01

When the Finite-Difference Time-Domain (FDTD) method is applied to open region scattering and coupling problems, some artificial mechanism must be employed to simulate the infinite region on the necessarily finite spatial grid. The current method of choice is to use a Radiation Boundary Condition (RBC) based on an approximate one-way wave equation. This popularity is due to several factors; these RBC's are local in space, (usually) explicit in time, and can be quite accurate. Typically, these RBC's are tested numerically. A pulse is launched from a local region on the interior of an FDTD grid and allowed to propagate out of the problem space. The reflected field is measure after an appropriate clear-time, providing a measure of the RBC's effectiveness. Unfortunately, it is difficult to extract precise information relating the RBC error to the frequency and angle of incidence of the outgoing wave and to the cell and time step sizes from this type of measurement. An alternate, analytic, approach to testing RBC's is presented in this paper. This approach provides a more effective means of characterizing various RBC's and comparing their accuracy in different parameter regimes. DOE

N89-24523# Sandia National Labs., Albuquerque, NM. Antenna Development.
ANALYSIS OF A PROBE-METALLIC SLEEVE FEED SYSTEM FOR A RECTANGULAR WAVEGUIDE
John M. Jarem (Alabama Univ., Huntsville.) 1989 4 p Presented at the Institute of Electrical and Electronics Engineers (IEEE) Antennas Propagation Society (AP-S) International Symposium, San Jose, CA, 26 Jun. 1989
(Contract DE-AC04-76DP-00789)
(DE89-006769; SAND-89-7052C; CONF-890660-6) Avail: NTIS HC A02/MF A01

An important set of antenna and microwave problems are the problems of determining the electromagnetic currents and fields which occur when a metallic probe is used to excite a rectangular waveguide and the associated problem of how best to tune the above probe in order that the input impedance of the probe is matched to the coaxial cable feed of the system. The above problems are of interest in the areas of phased arrays, excitation of slotted antennas or any area where rectangular waveguides are to be excited. The present paper will be concerned with the second problem mentioned above, namely the problem of how to tune a probe in a rectangular waveguide. The tuning will be accomplished by surrounding the rectangular waveguide probe with a metallic sleeve. A metallic sleeve is used to tune the feed system because the dimensions and position of the sleeve provide three convenient parameters h(1), h(2) and r(s) which may be used to vary the input impedance of the overall system. DOE

N89-24524# Sandia National Labs., Albuquerque, NM.
TWO-DIMENSIONAL PHASE CORRECTION OF SYNTHETIC APERTURE RADAR IMAGERY
Dennis C. Ghiglia and Gary A. Mastin 1989 5 p Presented at the Optical Society of America Signal Recovery Synthesis 3, Cape Cod, MA, 14 Jun. 1989
(Contract DE-AC04-76DP-00789)
(DE89-007086; SAND-89-0411C; CONF-890679-1) Avail: NTIS HC A02/MF A01

A two-dimensional Synthetic Aperture Radar (SAR) phase correction algorithm is described as a natural extension of a one-dimensional technique developed previously. It embodies many similarities to phase gradient speckle imaging and incorporates improvements in phase estimation. Diffraction limited performance has been obtained on actual SAR imagery regardless of scene content or phase error structure. The algorithm is computationally efficient, robust, and easily implemented on a general purpose computer or special purpose hardware. DOE

N89-24298# Deutsche Forschungs- und Versuchsanstalt fuer Luft- und Raumfahrt, Brunswick (Germany, F.R.). Inst. fuer Flugfuehrung.
ASPECTS OF IMAGE COMMUNICATION IN AIR-TO-GROUND SYSTEMS
R. Lippmann *In its* Image Signal Processing for Flight Guidance Sep. 1988 p 59-91 In GERMAN; ENGLISH summary (For primary document see N89-24295 18-04)
Avail: NTIS HC A14/MF A01; DFVLR, VB-PL-DO, Postfach 40 60 58, 5000 Cologne, Fed. Republic of Germany, DM 108

N89-24307# Deutsche Forschungs- und Versuchsanstalt fuer Luft- und Raumfahrt, Brunswick (Germany, F.R.). Inst. fuer Flugfuehrung.
A VERSATILE FLIGHT EXPERIMENT SYSTEM FOR IMAGE PROCESSING
P. Schulz *In its* Image Signal Processing for Flight Guidance Sep. 1988 p 295-311 In GERMAN; ENGLISH summary (For primary document see N89-24295 18-04)
Avail: NTIS HC A14/MF A01; DFVLR, VB-PL-DO, Postfach 40 60 58, 5000 Cologne, Fed. Republic of Germany, DM 108

N89-24379# Telespazio, S.p.A., Rome (Italy).
THE KEY ROLE OF DATA RELAY SYSTEM (DRS) IN THE COLUMBUS COMMUNICATIONS
Victor Speziale *In* ESA, International Symposium on Europe in Space: The Manned Space System Oct. 1988 p 403-407 (For primary document see N89-24335 18-12)
Copyright Avail: NTIS HC A99/MF A01; ESA Publications Div., ESTEC, Noordwijk, Netherlands, 80 Dutch guilders

N89-24397# Selenia Spazio S.p.A., Rome (Italy).
THE COLUMBUS CREW COMMUNICATION SUBSYSTEM AND THE ON BOARD LOCAL AREA NETWORK
A. Morando, A. Francia, M. Masci, and Giu. Montalto *In* ESA, International Symposium on Europe in Space: The Manned Space System Oct. 1988 p 551-563 (For primary document see N89-24335 18-12)
Copyright Avail: NTIS HC A99/MF A01; ESA Publications Div., ESTEC, Noordwijk, Netherlands, 80 Dutch guilders

N89-24952# Abastumani Astrophysical Observatory, Georgia (USSR).
ON THE NATURE OF A TYPICAL PULSARS RADIO EMISSION
A. Z. Kazbegi, G. Z. Machabeli, G. I. Melikidze, and V. V. Usov (Academy of Sciences, USSR, Moscow) *In* ESA, Proceedings of an International School and Workshop on Plasma Astrophysics, Volume 1 Jan. 1989 p 271-276 (For primary document see N89-24910 18-75)
Avail: NTIS HC A18/MF A01; ESA Publications Div., ESTEC, Noordwijk, Netherlands, 45 US dollars or 80 Dutch guilders

33 ELECTRONICS AND ELECTRICAL ENGINEERING

Includes test equipment and maintainability; components, e.g., tunnel diodes and transistors; microminiaturization; and integrated circuitry.

For related information see also *60 Computer Operations and Hardware* and *76 Solid-State Physics.*

N89-24525# Sandia National Labs., Albuquerque, NM.
ELECTROPHORETICALLY APPLIED DIELECTRICS FOR AMORPHOUS METAL FOILS USED IN PULSED POWER SATURABLE REACTORS
D. J. Sharp, H. C. Harjes, and G. A. Mann 1989 7 p Presented at the Spring Meeting of the Materials Research Society, San Diego, CA, 24 Apr. 1989
(Contract DE-AC04-76DP-00789)
(DE89-009322; SAND-89-0649C; CONF-890426-2) Avail: NTIS HC A02/MF A01

Amorphous metal foil-wound inductors have been tested as ferromagnetic saturable inductive elements for pulsed-power (multi-terawatt) switching modules in the inertial confinement fusion program at Sandia National Laboratories. In simulated capacitor testing premature dielectric breakdown of thin polyethylene terephthalate film insulation in the inductor windings occurs at considerably below 2500 V. This appears to be due to inadvertant dielectric damage from micro-spikes on the amorphous foil surface. Electron micrographs and dielectric breakdown data illustrate that electrophoretically-applied dielectric coatings, deposited from organic aqueous colloid dispersions, can be used to provide insulating coatings on the foil which provide a 240 percent improvement (6000 V) in the breakdown strength of wound amorphous foil inductors. The theory and operation of a dedicated electrophoretic continuous coating system is described. The machine was constructed and successfully applied for dielectric coating of amorphous metal foil. Additional possible applications exist for practical dielectric coating of metallic films or foils used in various commercial wound-type capacitor structures. DOE

N89-24526# Argonne National Lab., IL. Energy and Environmental Systems Div.
ANALYSIS OF LIFE CYCLE COSTS FOR ELECTRIC VANS WITH ADVANCED BATTERY SYSTEMS
W. W. Marr, W. J. Walsh, and J. F. Miller Nov. 1988 8 p Presented at the Society of Automotive Engineers International Congress and Exposition, Detroit, MI, 27 Feb. - 3 Mar. 1989
(Contract W-31-109-eng-38)
(DE89-009807; CONF-890240-3) Avail: NTIS HC A02/MF A01

The performance of advanced Zn/Br2, LiAl/FeS, Na/S, Ni/Fe, and Fe/Air batteries in electric vans was compared to that of tubular lead-acid technology. The MARVEL computer analysis system evaluated these batteries for the G-Van and IDSEP vehicles over two driving schedules. Each of the advanced batteries exhibited the potential for major improvements in both range and life cycle cost compared with tubular lead-acid. A sensitivity analysis revealed specific energy, battery initial cost, and cycle life to be the dominant factors in reducing life cycle cost for the case of vans powered by tubular lead-acid batteries. DOE

N89-24527# Power Spectra, Inc., Fremont, CA.
A LONGLIFE, HIGHVOLTAGE, SHORTPULSE GENERATOR BASED ON OPTICALLY ACTIVATED BULK AVALANCHE SEMICONDUCTOR SWITCH, PHASE 2 Final Report
27 Jan. 1989 14 p
(Contract N00014-88-C-0024)
(AD-A206078) Avail: NTIS HC A02/MF A01 CSCL 09/1

Power Spectra, Inc. under private funding, has developed a unique high power, efficient microwave frequency semiconductor switch. This Bulk Avalanche Semiconductor Switch (BASS) utilizes optically-triggered avalanche in bulk semi-insulating gallium arsenide to provide the on-state conductivity. The very high avalanche gain makes this switch ideal for high power, high frequency applications requiring high optical efficiency. The switch is triggered with a semiconductor laser which eliminates the requirement for large, delicate and inefficient lasers required by other light-activated switches. Power Spectra has developed proprietary techniques to eliminate filamentary avalanche and to ensure long switch life. The elimination of large lasers also ensures that the switch is capable of operation at high PRF. GRA

N89-24528# Naval Postgraduate School, Monterey, CA.
CHANNEL AND SWITCHBOX ROUTING USING A GREEDY BASED CHANNEL ALGORITHM WITH OUTWARD SCANNING TECHNIQUE M.S. Thesis
Michael J. Roderick Dec. 1988 149 p
(AD-A206545) Avail: NTIS HC A07/MF A01 CSCL 20/3

The problem of channel routing and for that matter routing in general has been attacked in a heuristic manner vice analytical. This is not necessarily wrong, however it means that there is not always a solution to the problem. Channel routing is one of the most important phases in VLSI CAD (Very Large Scale Integration Computer Aided Design). It performs the detailed routing of a given channel. The switchbox is a four sided channel area, rectangular in shape, with nets entering from all four sides. There has been much work done in the channel and switchbox routing areas. The Greedy router, a proven heuristic, is one of the important building blocks for most of today's detailed routers and is used as basis for this thesis. Most routers scan the routing area using a left to right scanning method. This thesis attempts a different variation in routing, using an outward scanning technique. The thesis demonstrates how this new algorithm can be applied to various channel routing problems, by performing tests and making comparisons. The thesis also demonstrates how this new router can be used as a CAD tool. The new router assumes that all pins and wiring lie on a common grid, and that vertical wires are on one layer horizontal on another. The thesis also shows how this new channel router can be modified to allow for a switchbox router implementation. GRA

N89-24529*# National Aeronautics and Space Administration. Lewis Research Center, Cleveland, OH.
PHOTOVOLTAIC POWER SYSTEM OPERATION IN THE MARS ENVIRONMENT
Joseph Appelbaum (Tel-Aviv Univ., Israel) and Dennis J. Flood 1989 13 p Presented at the 24th Intersociety Energy Conversion Engineering Conference, Washington, DC, 6-11 Aug. 1989; cosponsored by the IEEE, AIAA, ANS, ASME, SAE, ACS and AIChE
(NASA-TM-102075; E-4740; NAS 1.15:102075) Avail: NTIS HC A03/MF A01 CSCL 10A

Detailed information on the environmental conditions on Mars are very desirable for the design of photovoltaic systems for establishing outposts on the Martian surface. The variation of solar insolation (global, direct, and diffuse) at the Viking lander's locations is addressed. It can be used, to a first approximation, for other latitudes. The radiation data is based on measured optical depth of the Martian atmosphere derived from images taken of the sun with a special diode on the Viking cameras; and computation based on multiple wavelength and multiple scattering of the solar radiation. The data are used to make estimates of photovoltaic system power, area and mass for a surface power system using regenerative fuel cells for storage and nighttime operation. Author

N89-24530*# Hughes Aircraft Co., Torrance, CA. Electron Dynamics Div.
DEVELOPMENT OF A 75-WATT 60-GHz TRAVELING-WAVE TUBE FOR INTERSATELLITE COMMUNICATIONS
A. L. Rousseau, I. Tammaru, and J. P. Vaszari Sep. 1988 129 p
(Contract NAS3-23351)
(NASA-CR-182135; W-10301; NAS 1.26:182135) Avail: NTIS HC A07/MF A01 CSCL 09A

This program covers the initial design and development of a 75 watt, 60 GHz traveling-wave tube for intersatellite communications. The objective frequency band was 59 to 64 GHz, with a minimum tube gain of 35 dB. The objective overall efficiency

at saturation was 40 percent. The tube, designated the 961H, used a coupled-cavity interaction circuit with periodic permanent magnet beam focusing to minimize the weight. For efficiency enhancement, it incorporated a four-stage depressed collector capable of radiation cooling in space. The electron gun had a low-temperature (type-M) cathode and an isolated anode. Two tubes were built and tested; one feasibility model with a single-stage collector and one experimental model that incorporated the multistage collector. Author

N89-24531# Swedish Defence Research Establishment, Linkoeping. Dept. of Information Technology.
ELECTROOPTICAL FEED AND CONTROL IN MICROWAVE APPLICATIONS
Boerje Carlegrim and Marie Johansson Dec. 1988 40 p In SWEDISH; ENGLISH summary
(FOA-C-30514-3.2; ISSN-0347-3708; ETN-89-94542) Avail: NTIS HC A03/MF A01; Swedish Defence Research Establishment, Linkoeping, Sweden, 50 Swedish crowns

In complex microwave systems, such as active phased array antennas, many conditions are required for the distribution of the signals to and from the different subassemblies and it is necessary that the representative functions and the control interconnection networks are adapted to the use of small microwave chips of low mass and volume. Advances in the field of high speed modulation and demodulation of optical signals and the use of very rapid lasers make it possible to realize these demands. It is today possible to transmit microwave signals with the use of optical technology. ESA

N89-24532*# Analex Corp., Cleveland, OH.
COMPUTED PERFORMANCE OF THE HALF-SCALE ACCURATE ANTENNA REFLECTOR Final Report
Kevin M. Lambert May 1989 33 p
(Contract NAS3-24564)
(NASA-CR-182284; E-4748; NAS 1.26:182284) Avail: NTIS HC A03/MF A01 CSCL 09C

The performance of the half-scale, accurate antenna reflector was studied. The antenna is evaluated for use as a compact range reflector. The reflector is studied for use with three separate feed antennas. Author

N89-24533# Sandia National Labs., Albuquerque, NM.
RADIATION HARDENED, OPTICALLY-TRIGGERED THYRISTOR SWITCHES: PRELIMINARY DATA ON THREE DEVICE DESIGNS
R. C. Hughes, T. E. Zipperian, H. T. Weaver, T. M. Brennen, B. E. Hammons, and R. B. Caldwell Mar. 1989 25 p
(Contract DE-AC04-76DP-00789)
(DE89-011469; SAND-88-2645) Avail: NTIS HC A03/MF A01

In this report we discuss the design, fabrication and testing of three different thyristor switches. The goal of the program is to create thyristors that are more radiation hard than existing silicon based devices, by using 3 to 5 compound semiconductor fabrication technology. The thyristors were tested for dark switching, optical switching with a solid state laser, and radiation induced switching with a 3 nanosecond X-ray pulse. Two of three designs showed great promise for a radiation hardened switch; they could be easily triggered with a low power laser at voltages well below those required for switching at 3 times 10(9) rads/sec dose rate. DOE

N89-24534# Lawrence Livermore National Lab., CA.
EMBEDDED CONDUCTORS BY ELECTROCHEMICAL PLANARIZATION
Robert J. Contolini, Anthony F. Bernhardt, and Davis B. Tuckerman Apr. 1989 11 p Presented at the 175th Meeting of the Electrochemical Society, Los Angeles, CA, 7 May 1989
(Contract W-7405-eng-48)
(DE89-011632; UCRL-100692; CONF-890518-2) Avail: NTIS HC A03/MF A01

An electrochemical process is described for planarization of metal interconnect layers on integrated circuits and multichip modules. Electroplating is used to deposit metal over a patterned SiO2 dielectric, followed by electropolishing to remove excess metal. Electropolishing simultaneously smooths and further flattens the surface. The process yields a planar surface with conductors embedded in the etched regions of the dielectric. It is shown that pulsed plating is superior to galvanostatic plating in this application. DOE

N89-24535# Edgerton, Germeshausen and Grier, Inc., Idaho Falls, ID.
ERC NICKEL CADIUM BATTERY PERFORMANCE TESTS AND COMPARISONS WITH LEAD-ACID BATTERIES
Robert L. Crumley, Jasper E. Hardin, Randy D. MacDowall, and Andrew F. Burke 1988 90 p
(Contract DE-AC07-76ID-01570)
(DE89-009753; DOE/ID-10184) Avail: NTIS HC A05

A battery pack consisting of eighteen 6-V, roll-bonded nickel-cadmium (NiCd) batteries, manufactured by Energy Research Corporation (ERC), was evaluated by the Idaho National Engineering Laboratory, Electric and Hybrid Vehicle Program for electric vehicle applications. The purpose of the testing was to determine the capacity and performance characteristics of the battery pack and to obtain data which would permit direct comparison with other selected EV application batteries. Laboratory charge/discharge characterization and vehicle dynamometer tests were performed with the NiCd battery pack in the Battery and Dynamometer Laboratories of the Idaho National Engineering Laboratory (INEL) Research Center. Testing was done in accordance with the Electric Vehicle Test Procedures of the Society of Automotive Engineers (SAE J227). DOE

N89-24841# Honeywell, Inc., Minnetonka, MN. Defense Systems Group.
AUTOMATED MILLIMETER WAVE (AMW) TRANSDUCER TESTING IN A ROBOTIC/VISION TEST CELL Abstract Only
Mark Francis *In* Tactical Weapons Guidance and Control Information Conference on Space and Military Applications of Automation and Robotics Jun. 1988 p 44 (For primary document see N89-24819 18-63)
Avail: NTIS HC A05/MF A01 CSCL 09B

34 FLUID MECHANICS AND HEAT TRANSFER

Includes boundary layers; hydrodynamics; fluidics; mass transfer; and ablation cooling.

For related information see also *02 Aerodynamics* and *77 Thermodynamics and Statistical Physics.*

N89-24536# National Aerospace Lab., Tokyo (Japan). Aeroengine Div.
INTERACTION MECHANISMS BETWEEN TIP LEAKAGE FLOW AND THE PASSAGE VORTEX IN A LINEAR TURBINE ROTOR CASCADE
Atsumasa Yamamoto and Fujio Mimura Jun. 1988 22 p
(NAL-TR-983T; ISSN-0389-4010) Avail: NTIS HC A03/MF A01

In order to study the loss generation mechanisms due to the tip-leakage flow in turbine rotor passages, extensive traverse measurements were made of the three-dimensional flows in a low-speed linear cascade for various tip-clearance sizes and for various cascade inlet flow angles (or incidences). Effects of the leakage flow on the cascade downstream flow fields and interactions between the leakage flow and the passage vortices were discussed in detail based on the traverse measurements and flow-visualization tests in terms of secondary flows and the associated losses. Other traverses of the tip-casing endwall flows were also performed, both inside and outside the tip-clearance gap, using a micro five-hole pitot tube to reveal the axial development of the interaction throughout the cascade passage. Overall loss characteristics of the present high-turning cascade

with blunt leading- and trailing-edges were obtained and compared with those predicted by the Ainley-Mathieson method. Author

N89-24537# National Aerospace Lab., Tokyo (Japan). Aeroengine Div.
THREE-DIMENSIONAL FLOWS AND LOSS GENERATION MECHANISMS IN A LINEAR TURBINE ROTOR CASCADE AT VARIOUS INCIDENCE CONDITIONS
Atsumasa Yamamoto and Hiroyuki Nouse Jun. 1988 26 p (NAL-TR-984T; ISSN-0389-4010) Avail: NTIS HC A03/MF A01

Effects of the incidence on cascade three-dimensional flows and on the associated loss mechanism occurring in a low-speed linear turbine rotor cascade are described. For five different incidences from 7.2 to -53.3 degrees, the cascade flow was surveyed in detail at fifteen or sixteen planes located axially throughout the cascade. Blade-to-blade flows at the cascade midspan and near the endwalls, meridional flows along the blade surfaces, and static and total pressures within the cascade were analyzed and the results were represented in three-dimensional forms using vectors, scalar contours and streaklines. New insight into the incidence effects and many quantitative experimental facts of turbine cascade flows are found. Author

N89-24538*# Stanford Univ., CA. Center for Turbulence Research.
STUDYING TURBULENCE USING NUMERICAL SIMULATION DATABASES, 2. PROCEEDINGS OF THE 1988 SUMMER PROGRAM
Dec. 1988 291 p Summer Program held in Stanford, CA, 27 Jun. - 22 Jul. 1988 Sponsored by NASA, Ames Research Center, Moffett Field, CA Original contains color illustrations
(Contract NCC2-460)
(NASA-CR-184905; NAS 1.26:184905; SU-CTR-S88) Avail: NTIS HC A13/MF A01 CSCL 20D

The focus of the program was on the use of direct numerical simulations of turbulent flow for study of turbulence physics and modeling. A special interest was placed on turbulent mixing layers. The required data for these investigations were generated from four newly developed codes for simulation of time and spatially developing incompressible and compressible mixing layers. Also of interest were the structure of wall bounded turbulent and transitional flows, evaluation of diagnostic techniques for detection of organized motions, energy transfer in isotropic turbulence, optical propagation through turbulent media, and detailed analysis of the interaction of vortical structures. For individual titles, see N89-24539 through N89-24561.

N89-24539*# National Aeronautics and Space Administration. Ames Research Center, Moffett Field, CA.
CHAOS IN A SPATIALLY-DEVELOPING PLANE MIXING LAYER
J. G. Broze, Fazle Hussain (Houston Univ., TX.), and J. C. Buell *In* Stanford Univ., Studying Turbulence Using Numerical Simulation Databases, 2. Proceedings of the 1988 Summer Program Dec. 1988 p 3-18 (For primary document see N89-24538 18-34)
Avail: NTIS HC A13/MF A01 CSCL 20D

A spatially-developing plane mixing layer was analyzed for chaotic behavior. A direct numerical simulation of the Navier-Stokes equations in a 2-D domain infinite in y and having inflow-outflow boundary conditions in x was used for data. Spectra, correlation dimension and the largest Lyapunov exponent were computed as functions of downstream distance x. When forced at a single (fundamental) frequency with maximum amplitude, the flow is periodic at the inflow but becomes aperiodic with increasing x. The aperiodic behavior is caused by the presence of a noisy subharmonic caused by the feedback between the necessarily nonphysical inflow and outflow boundary conditions. In order to overshadow this noise the flow was also studied with the same fundamental forcing and added random forcing of amplitude upsilon prime sub R/delta U = 0.01 at the inlet. Results were qualitatively the same in both cases: for small x, spectral peaks were sharp and dimension was nearly 1, but as x increased a narrowband spectral peak grew, spectra decayed exponentially at high frequencies and dimension increased to greater than 3. Based on these results, the flow appears to exhibit deterministic chaos. However, at no location was the largest Lyapunov exponent found to be significantly greater than zero. Author

N89-24540*# National Aeronautics and Space Administration. Ames Research Center, Moffett Field, CA.
INFLOW/OUTFLOW BOUNDARY CONDITIONS AND GLOBAL DYNAMICS OF SPATIAL MIXING LAYERS
J. C. Buell and P. Huerre (University of Southern California, Los Angeles.) *In* Stanford Univ., Studying Turbulence Using Numerical Simulation Databases, 2. Proceedings of the 1988 Summer Program Dec. 1988 p 19-27 (For primary document see N89-24538 18-34)
Avail: NTIS HC A13/MF A01 CSCL 20D

The numerical simulation of incompressible spatially-developing shear flows poses a special challenge to computational fluid dynamicists. The Navier-Stokes equations are elliptic and boundary equations need to be specified at the inflow and outflow boundaries in order to compute the fluid properties within the region of interest. It is, however, difficult to choose inflow and outflow conditions corresponding to a given experimental situation. Furthermore the effects that changes in the boundary conditions or in the size of the computational domain may induce on the global dynamics of the flow are presently unknown. These issues are examined in light of recent developments in hydrodynamic stability theory. The particular flow considered is the spatial mixing layer but it was expected that similar phenomena were bound to occur in other cases such as channel flow, the boundary layer, etc. A short summary of local/global and absolute/convective instability concepts is given. The results of numerical simulations are presented which strongly suggest that global resonances may be triggered in domains of finite streamwise extent although the evolution of the perturbation vorticity field is everywhere locally convective. A relationship between finite domains and pressure sources which might help in devising a scheme to eliminate these difficulties is discussed. Author

N89-24541*# Stanford Univ., CA.
PHASE DECORRELATION, STREAMWISE VORTICES AND ACOUSTIC RADIATION IN MIXING LAYERS
C. M. Ho, Y. Zohar, R. D. Moser, M. M. Rogers, S. K. Lele, and J. C. Buell (National Aeronautics and Space Administration. Ames Research Center, Moffett Field, CA.) *In its* Studying Turbulence Using Numerical Simulation Databases, 2. Proceedings of the 1988 Summer Program Dec. 1988 p 29-39 Sponsored in part by Navy (For primary document see N89-24538 18-34)
Avail: NTIS HC A13/MF A01 CSCL 20D

Several direct numerical simulations were performed and analyzed to study various aspects of the early development of mixing layers. Included are the phase jitter of the large-scale eddies, which was studied using a 2-D spatially-evolving mixing layer simulation; the response of a time developing mixing layer to various spanwise disturbances; and the sound radiation from a 2-D compressible time developing mixing layer. Author

N89-24542*# Stanford Univ., CA.
A NUMERICAL STUDY OF BIFURCATIONS IN A BAROTROPIC SHEAR FLOW
P. Huerre, L. R. Keefe, G. Meunier, L. G. Redekopp, P. R. Spalart, and M. M. Rogers (National Aeronautics and Space Administration. Ames Research Center, Moffett Field, CA.) *In its* Studying Turbulence Using Numerical Simulation Databases, 2. Proceedings of the 1988 Summer Program Dec. 1988 p 41-47 (For primary document see N89-24538 18-34)
Avail: NTIS HC A13/MF A01 CSCL 20D

In the last few years, more and more evidence has emerged suggesting that transition to turbulence may be viewed as a succession of bifurcations to deterministic chaos. Most experimental and numerical observations have been restricted to Rayleigh-Benard convection and Taylor-Couette flow between concentric cylinders. An attempt is made to accurately describe

the bifurcation sequence leading to chaos in a 2-D temporal free shear layer on the beta-plane. The beta-plane is a locally Cartesian reduction of the equations describing the dynamicss of a shallow layer of fluid on a rotating spherical planet. It is a valid model for large scale flows of interest in meteorology and oceanography.
Author

N89-24543*# Stanford Univ., CA.
DYNAMICS OF COHERENT STRUCTURES IN A PLANE MIXING LAYER
Fazle Hussain, R. D. Moser, T. Colonius, P. Moin, and M. M. Rogers (National Aeronautics and Space Administration. Ames Research Center, Moffett Field, CA.) *In its* Studying Turbulence Using Numerical Simulation Databases, 2. Proceedings of the 1988 Summer Program Dec. 1988 p 49-55 (For primary document see N89-24538 18-34)
Avail: NTIS HC A13/MF A01 CSCL 20D

An incompressible, time developing 3-D mixing layer with idealized initial conditions was simulated numerically. Consistent with the suggestions from experimental measurements, the braid region between the dominant spanwise vortices or rolls develops longitudinal vortices or ribs, which are aligned upstream and downstream of a roll and produce spanwise distortion of the rolls. The process by which this distortion occurs is explained by studying a variety of quantities of dynamic importance (e.g., production of enstrophy, vortex stretching). Other quantities of interest (dissipation, helicity density) are also computed and discussed. The currently available simulation only allows the study of the early evolution (before pairing) of the mixing layer. New simulations in progress will relieve this restriction. Author

N89-24544*# National Aeronautics and Space Administration. Ames Research Center, Moffett Field, CA.
SUBHARMONIC RESONANCE IN A MIXING LAYER
N. N. Mansour, Fazle Hussain (Houston Univ., TX.), and J. C. Buell *In* Stanford Univ., Studying Turbulence Using Numerical Simulation Databases, 2. Proceedings of the 1988 Summer Program Dec. 1988 p 57-68 (For primary document see N89-24538 18-34)
Avail: NTIS HC A13/MF A01 CSCL 20D

The subharmonic resonance phenomenon in a spatially evolving mixing layer is studied using direct simulations of the 2-D Navier-Stokes equations. The computational domain extends to + or - infinity in the cross-stream direction with U(1) = 1.25 and U(2) = 0.25 imposed at + infinity and - infinity respectively. The domain is finite in the streamwise direction with inflow and outflow boundary conditions imposed at x/delta sub omega = 0 and 100, respectively. A hyperbolic-tangent mean velocity profile is assumed at the inlet and the Reynolds number based on the inlet vorticity thickness and velocity difference is Re = 600. It is observed that the phase angle between the fundamental and its subharmonic plays a key role in the spatial development of these modes. Contour plots of vorticity show that varying the phase will have a dramatic effect on the dynamics of the vortices. Pairing or shredding is observed depending on the phase. Fourier decomposition of the time traces show that the fundamental grows, saturates and decays with the downstream distance. The subharmonic has a similar behavior. However, the level at which the modes will saturate is affected by the phase. At 0 deg phase, it was found that as the fundamental saturates, the growth rate of the subharmonic is enhanced. At 90 deg phase, it was found that as the fundamental saturates, the growth rate of the subharmonic is inhibited. In the later case, the growth rate of the subharmonic recovers after saturation of the fundamental. These results are in qualitative agreement with experimental data. Author

N89-24545*# Stanford Univ., CA.
SCALAR ENTRAINMENT IN THE MIXING LAYER
N. D. Sandham, M. G. Mungal, J. E. Broadwell (California Inst. of Tech., Pasadena.), and W. C. Reynolds *In its* Studying Turbulence Using Numerical Simulation Databases, 2. Proceedings of the 1988 Summer Program Dec. 1988 p 69-76 (For primary document see N89-24538 18-34)
Avail: NTIS HC A13/MF A01 CSCL 20D

New definitions of entrainment and mixing based on the passive scalar field in the plane mixing layer are proposed. The definitions distinguish clearly between three fluid states: (1) unmixed fluid, (2) fluid engulfed in the mixing layer, trapped between two scalar contours, and (3) mixed fluid. The difference betwen (2) and (3) is the amount of fluid which has been engulfed during the pairing process, but has not yet mixed. Trends are identified from direct numerical simulations and extensions to high Reynolds number mixing layers are made in terms of the Broadwell-Breidenthal mixing model. In the limit of high Peclet number (Pe = ReSc) it is speculated that engulfed fluid rises in steps associated with pairings, introducing unmixed fluid into the large scale structures, where it is eventually mixed at the Kolmogorov scale. From this viewpoint, pairing is a prerequisite for mixing in the turbulent plane mixing layer. Author

N89-24546*# Stanford Univ., CA.
USE OF PASSIVE SCALAR TAGGING FOR THE STUDY OF COHERENT STRUCTURES IN THE PLANE MIXING LAYER
B. R. Ramaprian (Washington State Univ., Pullman.), N. D. Sandham, M. G. Mungal, and W. C. Reynolds *In its* Studying Turbulence Using Numerical Simulation Databases, 2. Proceedings of the 1988 Summer Program Dec. 1988 p 77-89 (For primary document see N89-24538 18-34)
Avail: NTIS HC A13/MF A01 CSCL 20D

Data obtained from the numerical simulation of a 2-D mixing layer were used to study the feasibility of using the instantaneous concentration of a passive scalar for detecting the typical coherent structures in the flow. The study showed that this technique works quite satisfactorily and yields results similar to those that can be obtained by using the instantaneous vorticity for structure detection. Using the coherent events educed by the scalar conditioning technique, the contribution of the coherent events to the total turbulent momentum and scalar transport was estimated. It is found that the contribution from the typical coherent events is of the same order as that of the time-mean value. However, the individual contributions become very large during the pairing of these structures. The increase is particularly spectacular in the case of the Reynolds shear stress. Author

N89-24547*# National Aeronautics and Space Administration. Ames Research Center, Moffett Field, CA.
SENSITIVITY OF MIXING LAYERS TO THREE-DIMENSIONAL FORCING
J. J. Riley, P. D. Mourad (Washington Univ., Seattle.), R. D. Moser, and M. M. Rogers *In* Stanford Univ., Studying Turbulence Using Numerical Simulation Databases, 2. Proceedings of the 1988 Summer Program Dec. 1988 p 91-116 (For primary document see N89-24538 18-34)
Avail: NTIS HC A13/MF A01 CSCL 20D

It is well known that turbulent mixing layers are dominated by large scale, fairly coherent structures, and that these structures are related to the stability characteristics of the flow. These facts have led researchers to attempt controlling such flows by selectively forcing certain unstable modes, which can in addition have the effect of suppressing other modes. Much of the work on controlling the mixing layer has relied on forcing 2-D instabilities. The results of forcing 3-D instabilities are addressed. The objectives of the work are twofold: to understand how a mixing layer responds to 3-D perturbations, and to test the validity of an amplitude expansion in predicting the mixing layer development. The amplitude expansion could be very useful in understanding and predicting the 3-D response of the flow to a variety of initial conditions.
Author

N89-24548*# Stanford Univ., CA.
SAMPLING INHOMOGENEOUS TURBULENT FIELDS
R. J. Adrian, P. Moin, and R. D. Moser (National Aeronautics and Space Administration. Ames Research Center, Moffett Field, CA.) *In its* Studying Turbulence Using Numerical Simulation Databases, 2. Proceedings of the 1988 Summer Program Dec. 1988

p 117-121 (For primary document see N89-24538 18-34)
(Grant NSF ATM-86-00509)
Avail: NTIS HC A13/MF A01 CSCL 20D

The reconstruction of an inhomogeneous random process from a finite number of discrete samples can be performed in terms of the Karhunen-Loeve (KL) expansion for that process. The n(th) eigenfunction has n - 1 zero crossings which are the sampling points for the inhomogeneous process. The rapid variation of the KL eigenfunctions makes it unnecessary to have a high density of sampling (or grid points) near the wall. However, this result should not be construed to indicate that with spectral simulations significantly fewer grid points are required with the KL expansion as compared to other orthogonal expansions. Moin and Moser (1989) have shown that the advantage of the KL expansion over Chebychev expansion rapidly diminishes when high percentage (say 90 percent) energy recovery is demanded. Author

N89-24549*# Stanford Univ., CA.
DYNAMICAL INTERPRETATION OF CONDITIONAL PATTERNS
R. J. Adrian, R. D. Moser, and P. Moin (National Aeronautics and Space Administration. Ames Research Center, Moffett Field, CA.) *In its* Studying Turbulence Using Numerical Simulation Databases, 2. Proceedings of the 1988 Summer Program Dec. 1988 p 123-129 (For primary document see N89-24538 18-34)
(Grant NSF ATM-86-00509)
Avail: NTIS HC A13/MF A01 CSCL 20D

While great progress is being made in characterizing the 3-D structure of organized turbulent motions using conditional averaging analysis, there is a lack of theoretical guidance regarding the interpretation and utilization of such information. Questions concerning the significance of the structures, their contributions to various transport properties, and their dynamics cannot be answered without recourse to appropriate dynamical governing equations. One approach which addresses some of these questions uses the conditional fields as initial conditions and calculates their evolution from the Navier-Stokes equations, yielding valuable information about stability, growth, and longevity of the mean structure. To interpret statistical aspects of the structures, a different type of theory which deals with the structures in the context of their contributions to the statistics of the flow is needed. As a first step toward this end, an effort was made to integrate the structural information from the study of organized structures with a suitable statistical theory. This is done by stochastically estimating the two-point conditional averages that appear in the equation for the one-point probability density function, and relating the structures to the conditional stresses. Salient features of the estimates are identified, and the structure of the one-point estimates in channel flow is defined. Author

N89-24550*# National Aeronautics and Space Administration. Ames Research Center, Moffett Field, CA.
TURBULENCE PRODUCTION NEAR WALLS: THE ROLE OF FLOW STRUCTURES WITH SPANWISE ASYMMETRY
P. Henrik Alfredsson, Arne V. Johansson (Royal Inst. of Tech., Lund, Sweden), and John Kim *In* Stanford Univ., Studying Turbulence Using Numerical Simulation Databases, 2. Proceedings of the 1988 Summer Program Dec. 1988 p 131-141 (For primary document see N89-24538 18-34)
Avail: NTIS HC A13/MF A01 CSCL 20D

Space-time evolution of near wall flow structures is described by conditional sampling methods, in which conditional averages are formed at various stages of development of shear layer structures. The development of spanwise asymmetry of the structures was found to be important in the creation of the structures and for the process of turbulence production. Author

N89-24551*# Stanford Univ., CA.
PRESSURE-STRAIN-RATE EVENTS IN HOMOGENEOUS TURBULENT SHEAR FLOW
James G. Brasseur (Pennsylvania State Univ., University Park.) and Moon J. Lee *In its* Studying Turbulence Using Numerical Simulation Databases, 2. Proceedings of the 1988 Summer Program Dec. 1988 p 143-156 (For primary document see N89-24538 18-34)
Avail: NTIS HC A13/MF A01 CSCL 20D

A detailed study of the intercomponent energy transfer processes by the pressure-strain-rate in homogeneous turbulent shear flow is presented. Probability density functions (pdf's) and contour plots of the rapid and slow pressure-strain-rate show that the energy transfer processes are extremely peaky, with high-magnitude events dominating low-magnitude fluctuations, as reflected by very high flatness factors of the pressure-strain-rate. A concept of the energy transfer class was applied to investigate details of the direction as well as magnitude of the energy transfer processes. In incompressible flow, six disjoint energy transfer classes exist. Examination of contours in instantaneous fields, pdf's and weighted pdf's of the pressure-strain-rate indicates that in the low magnitude regions all six classes play an important role, but in the high magnitude regions four classes of transfer processes, dominate. The contribution to the average slow pressure-strain-rate from the high magnitude fluctuations is only 50 percent or less. The relative significance of high and low magnitude transfer events is discussed. Author

N89-24552*# Stanford Univ., CA.
MULTIFRACTAL SPECTRA IN HOMOGENEOUS SHEAR FLOW
A. E. Deane (Brown Univ., Providence, RI.) and L. R. Keefe *In its* Studying Turbulence Using Numerical Simulation Databases, 2. Proceedings of the 1988 Summer Program Dec. 1988 p 157-167 (For primary document see N89-24538 18-34)
Avail: NTIS HC A13/MF A01 CSCL 20D

Employing numerical simulations of 3-D homogeneous shear flow, the associated multifractal spectra of the energy dissipation, scalar dissipation and vorticity fields were calculated. The results for (128) cubed simulations of this flow, and those obtained in recent experiments that analyzed 1- and 2-D intersections of atmospheric and laboratory flows, are in some agreement. A two-scale Cantor set model of the energy cascade process which describes the experimental results from 1-D intersections quite well, describes the 3-D results only marginally. Author

N89-24553*# National Aeronautics and Space Administration. Ames Research Center, Moffett Field, CA.
ENERGY TRANSFER IN ISOTROPIC TURBULENCE AT LOW REYNOLDS NUMBERS
J. A. Domaradzki (University of Southern California, Los Angeles.) and R. S. Rogallo *In* Stanford Univ., Studying Turbulence Using Numerical Simulation Databases, 2. Proceedings of the 1988 Summer Program Dec. 1988 p 169-177 (For primary document see N89-24538 18-34)
Avail: NTIS HC A13/MF A01 CSCL 20D

Detailed measurements were made of energy transfer among the scales of motion in incompressible turbulent fields at low Reynolds numbers generated by direct numerical simulation. It was observed that although the transfer resulted from triad interactions that were non-local in k space, the energy always transferred locally. The results are consistent with the notion of non-uniform advection of small weak eddies by larger and stronger ones, similar to transfer processes in the far dissipation range at high Reynolds numbers. Author

N89-24554*# National Aeronautics and Space Administration. Ames Research Center, Moffett Field, CA.
TURBULENCE CHARACTERISTICS INSIDE A TURBULENT SPOT IN PLANE POISEUILLE FLOW
D. S. Henningson, John Kim, and P. Henrik Alfredsson (Royal Inst. of Tech., Lund, Sweden) *In* Stanford Univ., Studying Turbulence Using Numerical Simulation Databases, 2. Proceedings of the 1988 Summer Program Dec. 1988 p 179-192 (For primary document see N89-24538 18-34)
Avail: NTIS HC A13/MF A01 CSCL 20D

In wall-bounded shear flows the transition to turbulence through localized disturbances goes through a pattern starting with a development of shear layers. The localized normal velocity fluctuations induce normal vorticity through the lift-up effect. These

shear layers become unstable to secondary disturbances, and if the amplitudes of the disturbances are large enough, a turbulent spot develops. Investigations of the spot in boundary layers has shown that the turbulent part of the spot is very similar to a fully developed boundary layer. Wygnanski et al. (1976) showed that the mean profile at the center-symmetry plane has a logarithmic region and Johansson et al. (1987) showed that both the higher-order statistics and flow structures in the spot were the same as in the corresponding fully developed flow. In what respects the turbulence inside the Poiseuille spot is similar to fully developed turbulent channel flow is studied. The numerically simulated spot is used, where the characteristics inside the spot are compared to those of the wave packet in the wingtip area. A recent experimental investigation of the velocity field associated with the Poiseuille spot by Klingmann et al. is used for comparison. E.R.

N89-24555*# Stanford Univ., CA.
EDDIES, STREAMS, AND CONVERGENCE ZONES IN TURBULENT FLOWS
J. C. R. Hunt, A. A. Wray (National Aeronautics and Space Administration. Ames Research Center, Moffett Field, CA.), and P. Moin *In its* Studying Turbulence Using Numerical Simulation Databases, 2. Proceedings of the 1988 Summer Program Dec. 1988 p 193-208 Original contains color illustrations (For primary document see N89-24538 18-34)
Avail: NTIS HC A13/MF A01 CSCL 20D

Recent studies of turbulent shear flows have shown that many of their important kinematical and dynamical properties can be more clearly understood by describing the flows in terms of individual events or streamline patterns. These events or flow regions are studied because they are associated with relatively large contributions to certain average properties of the flow, for example kinetic energy, Reynolds stress, or to particular processes in the flow, such as mixing and chemical reactions, which may be concentrated at locations where streamlines converge for fast chemical reactions (referred to as convergence or C regions), or in recirculating eddying regions for slow chemical reactions. The aim of this project was to use the numerical simulations to develop suitable criteria for defining these eddying or vortical zones. The C and streaming (S) zones were defined in order to define the whole flow field. It is concluded that homogeneous and sheared turbulent flow fields are made up of characteristic flow zones: eddy, C, and S zones. A set of objective criteria were found which describe regions in which the streamlines circulate, converge or diverge, and form high streams of high velocity flow. E.R.

N89-24556*# Massachusetts Inst. of Tech., Cambridge.
THEORETICAL MODEL FOR VITA-EDUCED COHERENT STRUCTURES IN THE WALL REGION OF A TURBULENT BOUNDARY LAYER
Marten T. Landahl *In* Stanford Univ., Studying Turbulence Using Numerical Simulation Databases, 2. Proceedings of the 1988 Summer Program Dec. 1988 p 209-220 (For primary document see N89-24538 18-34)
Avail: NTIS HC A13/MF A01 CSCL 20D

Experiments on wall-bounded shear flows (channel flows and boundary layers) have indicated that the turbulence in the region close to the wall exhibits a characteristic intermittently formed pattern of coherent structures. For a quantitative study of coherent structures it is necessary to make use of conditional sampling. One particularly successful sampling technique is the Variable Integration Time Averaging technique (VITA) first explored by Blackwelder and Kaplan (1976). In this, an event is assumed to occur when the short time variance exceeds a certain threshold multiple of the mean square signal. The analysis presented removes some assumptions in the earlier models in that the effects of pressure and viscosity are taken into account in an approximation based on the assumption that the near-wall structures are highly elongated in the streamwise direction. The appropriateness of this is suggested by the observations but is also self consistent with the results of the model which show that the streamwise dimension of the structure grows with time, so that the approximation should improve with the age of the structure. E.R.

N89-24557*# Stanford Univ., CA.
THE STRUCTURE OF SHEARED TURBULENCE NEAR A PLANE BOUNDARY
Moon J. Lee and J. C. R. Hunt (Cambridge Univ., England) *In its* Studying Turbulence Using Numerical Simulation Databases, 2. Proceedings of the 1988 Summer Program Dec. 1988 p 221-241 (For primary document see N89-24538 18-34)
Avail: NTIS HC A13/MF A01 CSCL 20D

An analysis is presented of how a plane boundary affects the structure of turbulence in a sheared free stream. A uniform-shear boundary layer (USBL) is formulated with slip velocity condition at the surface, and inhomogeneous rapid distortion theory is applied. The effects of blocking by the surface on the turbulence structure in USBL is compared with those in the shear-free boundary layer (SFBL). Shear produces highly anisotropic eddies elongated in the flow direction. The vertical velocity variance is reduced with shear at all heights, roughly in proportion to the reduction in the homogeneous value, but the shape of the profile remains unchanged only near the surface. The streamwise integral scales increase with shear, indicating elongation of the streamwise extent of eddies. E.R.

N89-24558*# Stanford Univ., CA.
ANALYSIS OF HOMOGENEOUS TURBULENT REACTING FLOWS
A. D. Leonard, J. C. Hill (Iowa Univ., Iowa City.), S. Mahalingam, and J. H. Ferziger *In its* Studying Turbulence Using Numerical Simulation Databases, 2. Proceedings of the 1988 Summer Program Dec. 1988 p 243-255 (For primary document see N89-24538 18-34)
Avail: NTIS HC A13/MF A01 CSCL 20D

Full turbulence simulations at low Reynolds numbers were made for the single-step, irreversible, bimolecular reaction between non-premixed reactants in isochoric, decaying homogeneous turbulence. Various initial conditions for the scalar field were used in the simulations to control the initial scalar dissipation length scale, and simulations were also made for temperature-dependent reaction rates and for non-stoichiometric and unequal diffusivity conditions. Joint probability density functions (pdf's), conditional pdf's, and various statistical quantities appearing in the moment equations were computed. Preliminary analysis of the results indicates that compressive strain-rate correlates better than other dynamical quantities with local reaction rate, and the locations of peak reaction rates seem to be insensitive to the scalar field initial conditions. Author

N89-24559*# Southern Methodist Univ., Dallas, TX.
CUT-AND-CONNECT OF TWO ANTIPARALLEL VORTEX TUBES
Mogens V. Melander and Fazle Hussain (Houston Univ., TX.) *In* Stanford Univ., Studying Turbulence Using Numerical Simulation Databases, 2. Proceedings of the 1988 Summer Program Dec. 1988 p 257-286 (For primary document see N89-24538 18-34)
(Contract N00014-87-K-0126)
Avail: NTIS HC A13/MF A01 CSCL 20D

Motivated by an early conjecture that vortex cut-and-connect plays a key role in mixing and production of turbulence, helicity and aerodynamic noise, the cross-linking of two antiparallel viscous vortex tubes via direct numerical simulation is studied. The Navier-Stokes equations are solved by a dealiased pseudo-spectral method with 64 cubed grid points in a periodic domain for initial Reynolds numbers Re up to 1000. The vortex tubes are given an initial sinusoidal perturbation to induce a collision and keep the two tubes pressed against each other as annihilation continues. Cross-sectional and wire plots of various properties depict three stages of evolution: (1) Inviscid induction causing vortex cores to first approach and form a contact zone with a dipole cross-section, and then to flatten and stretch; (2) Vorticity annihilation in the contact zone accompanied by bridging between the two vortices at both ends of the contact zone due to a collection of cross-linked vortex lines, now orthogonal to the initial vortex tubes. The direction of dipole advection in the contact zone reverses; and (3) Threading

of the remnants of the original vortices in between the bridges as they pull apart. The crucial stage 2 is shown to be a simple consequence of vorticity annihilation in the contact zone, link-up of the un-annihilated parts of vortex lines, and stretching and advection by the vortex tube swirl of the cross-linked lines, which accumulate at stagnation points in front of the annihilating vortex dipole. It is claimed that bridging is the essence of any vorticity cross-linking and that annihilation is sustained by stretching of the dipole by the bridges. Vortex reconnection details are found to be insensitive to asymmetry. Modeling of the reconnection process is briefly examined. The 3D spatial details of scalar transport (at unity Schmidt number), enstrophy production, dissipation and helicity are also examined. E.R.

N89-24560*# Stanford Univ., CA.
HEAD-ON COLLISION OF VISCOUS VORTEX RINGS
S. Stanaway, K. Shariff, and Fazle Hussain (Houston Univ., TX.) *In its* Studying Turbulence Using Numerical Simulation Databases, 2. Proceedings of the 1988 Summer Program Dec. 1988 p 287-309 (For primary document see N89-24538 18-34)
(Contract N00014-87-K-0670)
Avail: NTIS HC A13/MF A01 CSCL 20D

The head-on collision of two identical axisymmetric viscous vortex rings is studied through direct simulations of the incompressible Navier-Stokes equations. The initial vorticity distributions considered are those of Hill's spherical vortex and of rings with circular Gaussian cores, each at Reynolds numbers of about 350 and 1000. The Reynolds number is defined by Gamma/Nu, the ratio of circulation to viscosity. As the vortices approach each other by self-induction, the radii increase by mutual induction, and vortic cancels through viscous cross-diffusion across the collision plane. Following contact, the vorticity distribution in the core forms a head-tail structure (for the cases considered). The characteristic time of vorticity annihilation is compared with that of a 3D collision experiment and 3D numerical simulations. It is found that the annihilation time is somewhat longer in the axisymmetric case than it is in the symmetry plane of the experiment and 3D numerical simulation. By comparing the annihilatiom time with a viscous timescale and a circulation timescale, it is deduced that both the strain rate due to local effects and to 3D vorticity realignment are important. E.R.

N89-24561*# Stanford Univ., CA.
OPTICAL PROPAGATION THROUGH A HOMOGENEOUS TURBULENT SHEAR FLOW
C. Randall Truman (New Mexico Univ., Albuquerque.) and Moon J. Lee *In its* Studying Turbulence Using Numerical Simulation Databases, 2. Proceedings of the 1988 Summer Program Dec. 1988 p 311-320 Previously announced in IAA as A89-25313 Sponsored in part by AF (For primary document see N89-24538 18-34)
Avail: NTIS HC A13/MF A01 CSCL 20D

Effects of organized turbulent structures on the propagation of an optical beam in a homogeneous shear flow were studied. A passive-scalar field in a computed turbulent shear flow is used to represent index-of-refraction fluctuations, and phase errors induced in a coherent optical beam by turbulent fluctuations are computed. The organized vortical structures produce a scalar distribution with elongated regions of intense fluctuations which have an inclination with respect to the mean flow similar to that of the characteristic hairpin eddies. It is found that r.m.s. phase error is minimized by propagating approximately normal to the inclined vortical structures. Two-point correlations of vorticity and scalar fluctuation suggest that the regions of intense scalar fluctuation are produced primarily by the hairpin eddies. Author

N89-24562*# Old Dominion Univ., Norfolk, VA. Dept. of Mechanical Engineering and Mechanics.
NAVIER-STOKES ANALYSIS OF COLD SCRAMJET-AFTERBODY FLOWS Progress Report , 1 Dec. 1988 - 1 Apr. 1989
Oktay Baysal, Walter C. Engelund, and Mohamed E. Eleshaky Apr. 1989 13 p
(Grant NAG1-811)
(NASA-CR-184949; NAS 1.26:184949) Avail: NTIS HC A03/MF A01 CSCL 20D

The progress of two efforts in coding solutions of Navier-Stokes equations is summarized. The first effort concerns a 3-D space marching parabolized Navier-Stokes (PNS) code being modified to compute the supersonic mixing flow through an internal/external expansion nozzle with multicomponent gases. The 3-D PNS equations, coupled with a set of species continuity equations, are solved using an implicit finite difference scheme. The completed work is summarized and includes code modifications for four chemical species, computing the flow upstream of the upper cowl for a theoretical air mixture, developing an initial plane solution for the inner nozzle region, and computing the flow inside the nozzle for both a N2/O2 mixture and a Freon-12/Ar mixture, and plotting density-pressure contours for the inner nozzle region. The second effort concerns a full Navier-Stokes code. The species continuity equations account for the diffusion of multiple gases. This 3-D explicit afterbody code has the ability to use high order numerical integration schemes such as the 4th order MacCormack, and the Gottlieb-MacCormack schemes. Changes to the work are listed and include, but are not limited to: (1) internal/external flow capability; (2) new treatments of the cowl wall boundary conditions and relaxed computations around the cowl region and cowl tip; (3) the entering of the thermodynamic and transport properties of Freon-12, Ar, O, and N; (4) modification to the Baldwin-Lomax turbulence model to account for turbulent eddies generated by cowl walls inside and external to the nozzle; and (5) adopting a relaxation formula to account for the turbulence in the mixing shear layer. A.D.

N89-24563*# National Aeronautics and Space Administration. Ames Research Center, Moffett Field, CA.
AERODYNAMIC INTERACTION BETWEEN VORTICAL WAKES AND LIFTING TWO-DIMENSIONAL BODIES
Paul M. Stremel Mar. 1989 34 p Previously announced in IAA as A88-22785
(NASA-TM-101074; A-89047; NAS 1.15:101074) Avail: NTIS HC A03/MF A01 CSCL 20D

Unsteady rotor wake interactions with the empennage, tail boom, and other aerodynamic surfaces of a helicopter have a significant influence on its aerodynamic performance, the ride quality, and vibration. A numerical method for computing the aerodynamic interaction between an interacting vortex wake and the viscous flow about arbitrary two-dimensional bodies was developed to address this helicopter problem. The method solves for the flow field velocities on a body-fitted computational mesh using finite-difference techniques. The interacting vortex wake is represented by an array of discrete vortices which, in turn, are represented by a finite-core model. The evolution of the interacting vortex wake is calculated by Lagrangian techniques. The viscous flow field of the two-dimensional body is calculated on an Eulerian grid. The flow around circular and elliptic cylinders in the absence of an interacting vortex wake was calculated. These results compare very well with other numerical results and with results obtained from experiment and thereby demonstrate the accuracy of the viscous solution. The interaction of a rotor wake with the flow about a 4 to 1 elliptic cylinder at 45 degree incidence was calculated for a Reynolds number of 3000. The results demonstrate the significant variations in the lift and drag on the elliptic cylinder in the presence of the interacting rotor wake. Author

N89-24564 Texas A&M Univ., College Station.
BASIC FLOW FIELD AND HEAT TRANSFER STUDIES ABOUT THREE CYLINDERS OF DIFFERENT DIAMETER IN TRANSVERSE FLOW Ph.D. Thesis
Leonard Scott Miller 1988 185 p
Avail: Univ. Microfilms Order No. DA8903380

The flow field and heat transfer characteristics of a model composed of three cylinders of different diameter was studied, at a Reynolds number of 100,000. A wide range of experimental techniques were employed to identify the fluid dynamic behavior of the model including flow visualization, laser Doppler anemometry

(LDA), and static pressure measurements. The model included provisions for cooling and direct measurement of the heat flux about the circumference of the model elements. The flow features on and surrounding the model were identified in detail. The front cylinder of the model had a dominant effect on the overall fluid dynamic character of the model. The aft cylinder was totally immersed within the separated and reversed flow region of the wake. Heat transfer was observed to have only a small effect on the basic flow field character of the model. The local Nusselt number variation about the center and aft cylinders of the model was identified. The front cylinder contributed significantly to the heat transfer between the other model elements and the flow. The center cylinder cooled the flow about the aft cylinder of the model. Author

N89-24565# Japan Atomic Energy Research Inst., Tokyo. Dept. of High-Temperature Engineering.
NUMERICAL STUDY ON LAMINAR CIRCULAR JET OF CARBONIC ACID GAS DISCHARGING INTO STAGNANT AIR
Motoo Fumizawa, Makoto Hishida, and Tomoaki Kunugi Oct. 1988 32 p In JAPANESE; ENGLISH summary
(DE88-757249; JAERI-M-88-208) Avail: NTIS (US Sales Only) HC A03/MF A01

The flow behavior of the circular jet of two component gases is the most fundamental study in that of multi-component gases. The objective of present study is to investigate numerically the fluid flow and diffusion behavior of laminar circular jet of carbonic acid gas (CO2) discharging into stagnant air along gravity force. The flow and CO2 mass fraction distribution analysis was carried out by modified TEAM (Turbulent Elliptic Algorithm Manchester) code which solved elliptic equations using staggered grid system. As the result, the followings were obtained in the range of Froude number Fr = 0.007 to 0.7: (1) Axial velocity increased along down stream because the jet accelerated by gravity force. (2) It was necessary to obtain accurate radial velocity to evaluate CO2 mass fraction distribution. (3) In the case of low Froude number, half radii of axial velocity and CO2 mass fraction distribution increased along the flow direction as well as the conventional buoyant jet. In the case of relatively high Froude number, however, half radius of axial velocity distribution was constant and half radius of CO2 mass fraction decreased along the flow direction. DOE

N89-24566# California Univ., Davis.
VELOCITY AND SCALAR FIELDS OF TURBULENT PREMIXED FLAME IN STAGNATION FLOW
P. Cho, C. K. Law, R. K. Cheng, and I. G. Shepherd (California Univ., Berkeley. Lawrence Radiation Lab.) Aug. 1988 21 p Presented at the 22nd International Symposium on Combustion, Seattle, WA, 14-18 Aug. 1988
(Contract DE-AC03-76SF-00098)
(DE89-009336; LBL-26747; CONF-880802-10) Avail: NTIS HC A03/MF A01

Detailed experimental measurements of the scalar and velocity statistics of premixed methane/air flames stabilized by a stagnation plant are reported. Conditioned and unconditioned velocity of two components and the reaction progress variables are measured by using a two-component laser Doppler velocimetry techniques and Mie scattering techniques, respectively. Experimental conditions cover equivalence ratios of 0.9 and 1.0, incident turbulence intensities of 0.3 to 0.45 m/s, and global stretch rates of 100 to 150 sec sup minus 1. The experimental results are analyzed in the context of the Bray-Moss-Libby flamelet model of these flames. The results indicate that there is no turbulence production within the turbulent flame brush and the second and third order turbulent transport terms are reduced to functions of the difference between the conditioned mean velocity. The result of normalization of these relative velocities by the respective velocity increase across laminar flames suggest that the mean unconditioned velocity profiles are self-similar. DOE

N89-24567# Lawrence Livermore National Lab., CA.
CHALLENGES IN COMPUTATIONAL STATISTICAL MECHANICS
Berni J. Alder 1 Mar. 1989 12 p Presented at the Conference on Grand Challenges To Computational Science, Molokai, HI, 3-6 Jan. 1989
(Contract W-7405-eng-48)
(DE89-009922; UCRL-100753; CONF-8901101-1) Avail: NTIS HC A03/MF A01

Three challenges in statistical physics shall be discussed. The first is, how accurately does one have to solve the classical equations of motion of how many particles to make reliable hydrodynamic predictions. The second is, how to calculate the energy of a molecule to chemical accuracy. The third is, what model captures the essence of the high temperature superconductors. DOE

N89-24568*# Institute for Computer Applications in Science and Engineering, Hampton, VA.
NUMERICAL STUDY OF TURBULENT SECONDARY FLOWS IN CURVED DUCTS Final Report
N. Hur, S. Thangam, and C. G. Speziale (Stevens Inst. of Tech., Hoboken, NJ.) Apr. 1989 27 p
(Contract NAS1-18605)
(NASA-CR-181830; NAS 1.26:181830; ICASE-89-25) Avail: NTIS HC A03/MF A01 CSCL 20D

The pressure driven, fully-developed turbulent flow of an incompressible viscous fluid in curved ducts of square cross-section is studied numerically by making use of a finite volume method. A nonlinear Kappa - Iota model is used to represent the turbulence. The results for both straight and curved ducts are presented. For the case of fully-developed turbulent flow in straight ducts, the secondary flow is characterized by an eight-vortex structure for which the computed flowfield is shown to be in good agreement with available experimental data. The introduction of moderate curvature is shown to cause a substantial increase in the strength of the secondary flow and to change the secondary flow pattern to either a double-vortex or a four-vortex configuration. Author

N89-24569*# California Polytechnic State Univ., San Luis Obispo.
AN EXPERIMENTAL STUDY OF A THREE-DIMENSIONAL THRUST AUGMENTING EJECTOR USING LASER DOPPLER VELOCIMETRY
Bruce Lowell Storms May 1989 132 p
(Contract NCC2-484)
(NASA-CR-177531; NAS 1.26:177531) Avail: NTIS HC A07/MF A01 CSCL 20D

Flow field measurements were obtained in a three-dimensional thrust augmenting ejector using laser Doppler velocimetry and hot wire anemometry. The primary nozzle, segmented into twelve slots of aspect ratio 3.0, was tested at a pressure ratio of 1.15. Results are presented on the mean velocity, turbulence intensity, and Reynolds stress progressions in the mixing chamber of the constant area ejector. The segmented nozzle was found to produce streamwise vortices that may increase the mixing efficiency of the ejector flow field. Compared to free jet results, the jet development is reduced by the presence of the ejector walls. The resulting thrust augmentation ratio of this ejector was also calculated to be 1.34. Author

N89-24570# Massachusetts Univ., Amherst. Dept. of Mathematics and Statistics.
VORTEX DYNAMICS AND VORTEX BREAKDOWN Annual Report, 1 Mar. 1987 - 28 Feb. 1988
Melvyn S. Berger 16 Aug. 1988 5 p
(Grant AF-AFOSR-0170-87; AF Proj. 2304)
(AD-A206470; AFOSR-89-0351TR) Avail: NTIS HC A02/MF A01 CSCL 20/4

Topics studied include: (1) being able to determine analytically vortex rings and bubbles with swirl via the Stokes stream-function from an isoperimetric variational viewpoint extending previous work, and (2) in the case of thin vortex rings being able to establish analytically the Hamiltonian formulation and the calculus of variations. GRA

N89-24571# Naval Postgraduate School, Monterey, CA.
NATURAL CONVECTION COOLING OF A 3 BY 3 ARRAY OF RECTANGULAR PROTRUSIONS IN AN ENCLOSURE FILLED WITH DIELECTRIC LIQUID: EFFECTS OF BOUNDARY CONDITIONS AND COMPONENT ORIENTATION M.S. Thesis
Edgardo I. Torres Dec. 1988 138 p
(AD-A206474) Avail: NTIS HC A07/MF A01 CSCL 20/4

An experimental investigation of natural convection immersion cooling of two configurations of discrete heat sources in an enclosure filled with Fluorinert FC-75 has been conducted. A three by three array of rectangular protrusions was employed. In the first study, using the same equipment set-up of Benedict, the influence of changing the enclosure bottom surface boundary condition of flow patterns and heat transfer characteristics was examined. Both insulated and uniform temperature boundary conditions were considered. In the second set of experiments, a new chamber with the protrusions oriented vertically was assembled and effects of component orientation on the heat transfer characteristics were examined. In addition, timewise variations of temperature in several locations were measured and interpreted at different power levels. GRA

N89-24572# California Inst. of Tech., Pasadena. Graduate Aeronautical Labs.
UNSTEADY AND SEPARATED FLOWS Annual Technical Report, 1 Oct. 1987 - 30 Sep. 1988
P. E. Dimotakis, A. Leonard, and A. Roshko 30 Nov. 1988 22 p
(Contract F49620-86-C-0134)
(AD-A206539; AFOSR-89-0386TR) Avail: NTIS HC A03/MF A01 CSCL 20/4

A computer controlled system for the X-carriage on the Tow Tank has been installed. A force balance for measuring dynamic forces on models carried by the carriage has been built and installed. Initial measurements of such forces have been obtained on a flat-plate airfoil at various angles of attack. Optical and computer components have been assembled and integrated into a system for acquiring and processing streakline images of fluorescent particles in flow fields in water. Water-tunnel experiments on a Liebeck airfoil showed that a large cavity on the upper surface (to establish a free shear layer along the pressure plateau) promotes reattachment into the adverse pressure gradient and delays stall. GRA

N89-24573# Institut de Mecanique des Fluides de Lille (France). Groupe Mecanique du Vol.
PREDICTION METHODS FOR DYNAMIC STABILITY PARAMETERS: EFFECTS OF ANGULAR STABILITY [METHODES DE PREVISION DES PARAMETRES DE STABILITE DYNAMIQUE. EFFET DES VITESSES DE ROTATION]
N. Tsihlas and J. B. Paquet 1 Jul. 1988 74 p In FRENCH
(Contract DRET-84-003-04)
(IMFL-88/18; ETN-89-94523) Avail: NTIS HC A04/MF A01

Fast and low cost methods to estimate the effects of angular velocities on immersed bodies are presented. The semi-empirical analysis is based on ESDU and USAF DATCOM methods. The predictions are compared to experimental results. Sideforces and dynamic parameters are estimated. A theoretical approach allows one to compute the virtual mass and inertia and to model turbulence. Results from an aircraft and a submarine are discussed. ESA

N89-24574# Office National d'Etudes et de Recherches Aerospatiales, Paris (France). Direction de l'Aerodynamique.
INTERACTION BETWEEN AN OBLIQUE SHOCK WAVE AND A TURBULENT BOUNDARY LAYER [INTERACTION ENTRE UNE ONDE DE CHOC OBLIQUE ET UNE COUCHE LIMITE TURBULENTE SE DEVELOPPANT SUR UNE PAROI CHAUFFEE EN ECOULEMENT SUPERSONIQUE]
L. Benkemoun and M. Salaun Apr. 1988 42 p In FRENCH
(Contract DRET-86-34-001)
(ONERA-RT-76/7078-AY-096-A; ETN-89-94526) Avail: NTIS HC A03/MF A01

The interaction is developed on a heated wall at external Mach numbers of 2.4 and temperature ratio to adiabatic equilibrium between 1 and 2. The deflection angle of the shock generator was 8.75 deg. The effect of the shock wave intensity was visualized by shadowscopy and explored with laser velocimeter. The results are intended to be used to design a large experimental campaign. ESA

N89-24575*# National Aeronautics and Space Administration. Lewis Research Center, Cleveland, OH.
NONLINEAR EVOLUTION OF INTERACTING OBLIQUE WAVES ON TWO-DIMENSIONAL SHEAR LAYERS
M. E. Goldstein and S.-W. Choi Jun. 1989 33 p
(NASA Order C-99066-G)
(NASA-TM-102030; E-4404-1; NAS 1.15:102030; ICOMP-89-10)
Avail: NTIS HC A03/MF A01 CSCL 20D

The effects of critical layer nonlinearity are considered on spatially growing oblique instability waves on nominally two-dimensional shear layers between parallel streams. The analysis shows that three-dimensional effects cause nonlinearity to occur at much smaller amplitudes than it does in two-dimensional flows. The nonlinear instability wave amplitude is determined by an integro-differential equation with cubic type nonlinearity. The numerical solutions to this equation are worked out and discussed in some detail. The numerical solutions always end in a singularity at a finite downstream distance. Author

N89-24576*# Universities Space Research Association, Huntsville, AL.
INLET TURBULENCE INTENSITY LEVEL AND CROSS-STREAM DISTRIBUTION EFFECTS ON THE HEAT TRANSFER IN PLANE WALL JETS Final Report
A. A. Adeniji-Fashola May 1989 18 p
(Contract NAS8-37130)
(NASA-CR-183652; NAS 1.26:183652) Avail: NTIS HC A03/MF A01 CSCL 20D

The effect of the turbulence intensity level and its cross-stream distribution at the inlet on the numerical prediction of the heat transfer in a two-dimensional turbulent-wall jet was investigated. The investigation was carried out within the framework of the standard kappa-epsilon turbulence model. The predicted Nusselt number showed the influence of the turbulence intensity level and its cross-stream distribution at the inlet to be significant but restricted to the first 15 slot widths from the inlet slot. Beyond this location, all the predictions were observed to collapse onto a single curve which exhibited a maximum over-prediction of about 30 percent when compared with the available experimental data. Author

N89-24577*# National Aeronautics and Space Administration. Lewis Research Center, Cleveland, OH.
SOME CHARACTERISTICS OF BYPASS TRANSITION IN A HEATED BOUNDARY LAYER
K. H. Sohn, J. E. OBrien, and E. Reshotko (Case Western Reserve Univ., Cleveland, OH.) 1989 8 p Presented at the 7th Symposium on Turbulent Shear Flows, Stanford, CA, 21-23 Aug. 1989; sponsored by the Turbulent Shear Flow Committee
(NASA-TM-102126; E-4912; NAS 1.15:102126) Avail: NTIS HC A02/MF A01 CSCL 20D

Experimental measurements of both mean and conditionally sampled characteristics of laminar, transitional and low Reynolds number turbulent boundary layers on a heated flat plate are presented. Measurements were obtained in air over a range of freestream turbulence intensities from 0.3 percent to 6 percent with a freestream velocity of 30.5 m/s and zero pressure gradient. Conditional sampling performed in the transitional boundary layers indicate the existence of a near-wall drop in intermittency, especially pronounced at low intermittencies. Nonturbulent intervals were observed to possess large levels of low-frequency unsteadiness, and turbulent intervals had peak intensities as much as 50 percent higher than were measured at fully turbulent stations. Heat transfer

results were consistent with results of previous researchers and Reynolds analogy factors were found to be well predicted by laminar and turbulent correlations which accounted for unheated starting length. A small dependence of the turbulent Reynolds analogy factors on freestream turbulence level was observed. Laminar boundary layer spectra indicated selective amplification of unstable frequencies. These instabilities appear to play a dominant role in the transition process only for the lowest freestream turbulence level studied, however. Author

N89-24578*# Research Inst. for Advanced Computer Science, Moffett Field, CA.
DOMAIN DECOMPOSITION ALGORITHMS AND COMPUTATION FLUID DYNAMICS
Tony F. Chan (California Univ., Los Angeles.) Aug. 1988 19 p Presented at the 2nd International Conference on Parallel and Vector Processing, Tromso, Norway, Jun. 1988 Submitted for publication
(Contracts NCC2-387; DE-FG03-87ER-25037; DAAL03-88-K-0085; NSF DMS-87-14612)
(NASA-CR-185405; NAS 1.26:185405; RIACS-TR-88.21) Avail: NTIS HC A03/MF A01 CSCL 20D

In the past several years, domain decomposition was a very popular topic, partly motivated by the potential of parallelization. While a large body of theory and algorithms were developed for model elliptic problems, they are only recently starting to be tested on realistic applications. The application of some of these methods to two model problems in computational fluid dynamics are investigated. Some examples are two dimensional convection-diffusion problems and the incompressible driven cavity flow problem. The contruction and analysis of efficient pre-conditioners for the interface operator to be used in the iterative solution of the interface solution is described. For the convection-diffusion problems, the effect of the convection term and its discretization on the performance of some of the preconditioners is discussed. For the driven cavity problem, the effectiveness of a class of boundary probe preconditioners is discussed. Author

N89-24579*# Sterling Federal Systems, Inc., Palo Alto, CA.
TURBULENT FLOW IN A 180 DEG BEND: MODELING AND COMPUTATIONS Final Report
Upender K. Kaul Feb. 1989 51 p
(Contract NAS2-11555)
(NASA-CR-4141; NAS 1.26:4141) Avail: NTIS HC A04/MF A01 CSCL 20D

A low Reynolds number k-epsilon turbulence model was presented which yields accurate predictions of the kinetic energy near the wall. The model is validated with the experimental channel flow data of Kreplin and Eckelmann. The predictions are also compared with earlier results from direct simulation of turbulent channel flow. The model is especially useful for internal flows where the inflow boundary condition of epsilon is not easily prescribed. The model partly derives from some observations based on earlier direct simulation results of near-wall turbulence. The low Reynolds number turbulence model together with an existing curvature correction appropriate to spinning cylinder flows was used to simulate the flow in a U-bend with the same radius of curvature as the Space Shuttle Main Engine (SSME) Turn-Around Duct (TAD). The present computations indicate a space varying curvature correction parameter as opposed to a constant parameter as used in the spinning cylinder flows. Comparison with limited available experimental data is made. The comparison is favorable, but detailed experimental data is needed to further improve the curvature model. Author

N89-24580*# Sterling Federal Systems, Inc., Palo Alto, CA.
TRANSPIRATION COOLING OF HYPERSONIC BLUNT BODIES WITH FINITE RATE SURFACE REACTIONS
William D. Henline Feb. 1989 35 p
(Contract NAS2-11555)
(NASA-CR-177516; A-89018; NAS 1.26:177516) Avail: NTIS HC A03/MF A01 CSCL 20D

The convective heat flux blockage to blunt body and hypersonic vehicles by transpiration cooling are presented. The general problem of mass addition to laminar boundary layers is reviewed. Results of similarity analysis of the boundary layer problem are provided for surface heat flux with transpiration cooling. Detailed non-similar results are presented from the numerical program, BLIMPK. Comparisons are made with the similarity theory. The effects of surface catalysis are investigated. Author

N89-24581*# High Technology Corp., Hampton, VA.
AN ALGEBRAIC HOMOTOPY METHOD FOR GENERATING QUASI-THREE-DIMENSIONAL GRIDS FOR HIGH-SPEED CONFIGURATIONS
Anutosh Moitra Washington NASA Jul. 1989 80 p
(Contract NAS1-18240)
(NASA-CR-4242; NAS 1.26:4242) Avail: NTIS HC A05/MF A01 CSCL 20D

A fast and versatile procedure for algebraically generating boundary conforming computational grids for use with finite-volume Euler flow solvers is presented. A semi-analytic homotopic procedure is used to generate the grids. Grids generated in two-dimensional planes are stacked to produce quasi-three-dimensional grid systems. The body surface and outer boundary are described in terms of surface parameters. An interpolation scheme is used to blend between the body surface and the outer boundary in order to determine the field points. The method, albeit developed for analytically generated body geometries is equally applicable to other classes of geometries. The method can be used for both internal and external flow configurations, the only constraint being that the body geometries be specified in two-dimensional cross-sections stationed along the longitudinal axis of the configuration. Techniques for controlling various grid parameters, e.g., clustering and orthogonality are described. Techniques for treating problems arising in algebraic grid generation for geometries with sharp corners are addressed. A set of representative grid systems generated by this method is included. Results of flow computations using these grids are presented for validation of the effectiveness of the method.
Author

N89-24582# California Inst. of Tech., Pasadena.
CALTECH-DOE PROGRAM ON NUMERICAL ANALYSIS, SCIENTIFIC COMPUTING AND FUNDAMENTAL STUDIES OF FLUID MECHANICS Final Report, 1 Apr. 1986 - 31 Mar. 1989
1989 10 p
(Contracts DE-AS03-76ER-72012; DE-AA03-76SF-00767)
(DE89-010828; DOE/ER-72012/T7) Avail: NTIS HC A02/MF A01

Topics briefly discussed in this paper are: vortex dynamics, vertical flow and separated flow; free surface flows at low Reynolds number; concurrent linear algebra routines; concurrent continuation and invariant manifolds; concurrent multigrid continuation methods; auto-software; Taylor-vortex flows; boundary conditions for infinite domains; numerical and analytical studies of evolutionary systems; numerical methods for stiff differential equations; vortex reconnection; and a study of finite amplitude bifurcations in plane Poiseville flow. DOE

N89-24583# Cornell Univ., Ithaca, NY.
DEVELOPMENT AND UTILIZATION OF NEW DIAGNOSTICS FOR DENSE-PHASE PNEUMATIC TRANSPORT Quarterly Progress Report, 1 Jan. - 31 Mar. 1989
M. Y. Louge and J. T. Jenkins 1989 8 p
(Contract DE-AC22-88PC-88947)
(DE89-011381; DOE/PC-88947/T2) Avail: NTIS HC A02/MF A01

The main objective of this work is to develop probes for local measurements of solid velocity and holdup in dense gas-solid flows. In this context, capacitance probes are designed to measure local, time-dependent particle concentrations. In addition, a new optical fiber probe based on laser-induced-phosphorescence is developed to measure particle velocities. The principles for the capacitance and optical diagnostics were given in our first quarterly

report. In this period, we have extended our experimental study of the effective dielectric constant of particle-fluid mixtures to consider porous particles. For these particles, we have found that the effective dielectric constant follows a model due to Boettcher with good accuracy. In the development of the fiber-optic probe, we have focused on the preparation of copper-doped zinc sulfide, which we have impregnated into silica gel particles. DOE

N89-24584# University of Southern California, Los Angeles. Dept. of Mechanical Engineering.
MECHANICS/HEAT-TRANSFER RELATION FOR PARTICLE FLOWS Quarterly Report
Charles S. Campbell Jan. 1989 9 p
(Contract DE-FG22-88PC-88913)
(DE89-011382; DOE/PC-88913/T1) Avail: NTIS HC A02/MF A01

This investigation attempts to explore the effect of the mechanical behavior of particle-fluid systems on their apparent thermal behavior. Three cases will be studied. The first two will examine the relationship between the particle-pressure and the heat transfer in gas and liquid fluidized beds. (Both gas and liquid fluidized beds will be studied to try and ascertain the effects of bubbling (which appears in gas-fluidized beds but is generally absent if the continuous phase is a liquid) on the particle pressure and its effects on the heat transfer.) The last will study the effective thermal conductivity of suspensions as they are sheared in a coaxial cylinder rheometer. This first quarter has been spent largely in design and construction. Of the three apparatuses to be used in this project, only the gas fluidized bed existed at this site prior to this investigation, but even it is being modified to aid the proposed studies. The other two are being built from scratch. In addition, the displacement sensor in the particle pressure transducer for the gas fluidized bed, has been changed from a fiber optic to a capacitance type. Furthermore an analysis has shown that the present design of the particle pressure transducer will not work in the liquid fluidized bed, but the analysis also indicates that a modified design with a porous membrane will solve the problem. DOE

N89-24585# Lawrence Livermore National Lab., CA.
A SECOND-ORDER PROJECTION METHOD FOR THE INCOMPRESSIBLE NAVIER STOKES EQUATIONS ON QUADRILATERAL GRIDS
John B. Bell, Jay M. Solomon, and William G. Szymczak (Naval Surface Warfare Center, Silver Spring, MD.) Apr. 1989 13 p Presented at the 9th American Institute of Aeronatuics and Astronautics (AIAA) Computational Fluid Dynamics Conference, Buffalo, NY, 14-16 Jun. 1989
(Contract W-7405-eng-48)
(DE89-010242; UCRL-100879; CONF-8906111-1) Avail: NTIS HC A03/MF A01

This paper describes a second-order projection method for the incompressible Navier-Stokes equations on a logically-rectangular quadrilateral grid. The method uses a second-order fractional step scheme in which one first solves diffusion-convection equations to predict intermediate velocities which are then projected onto the space of divergence-free vector fields. The spatial discretization of the diffusion-convection equations is accomplished by formally transforming the equations to a uniform computational space. The diffusion terms are then discretized using standard finite-difference approximations. The convection terms are discretized using a second-order Godunov method that provides a robust discretization of these terms at high Reynolds number. The projection is approximated using a Galerkin procedure that uses a local basis for discretely divergence-free vector fields. Numerical results are presented illustrating the performance of the method. DOE

N89-24586# Sandia National Labs., Albuquerque, NM.
TWO-PHASE FLOW MEASUREMENTS BY NUCLEAR MAGNETIC RESONANCE IMAGING
R. C. Givler, P. D. Majors, S. A. Altobelli, and E. Fukushima 1989 6 p Presented at the International Conference on Mechanics of Two-phase Flows, Taipei, Taiwan, 12 Jun. 1989 Prepared in cooperation with Lovelace Foundation for Medical Education and Research, Albuquerque, NM
(Contract DE-AC04-76DP-00789)
(DE89-011850; SAND-88-2741C; CONF-8906126-1) Avail: NTIS HC A02/MF A01

Nonuniform velocity and concentration profiles have been measured for suspensions of heavy particles flowing in horizontal tubes. All measurements were performed during steady flow conditions; mean particle concentrations were chosen between 1-10 percent and mean flow Reynolds numbers (based upon the fluid properties and the tube diameter) did not exceed 30. The time-averaged measurements were recorded noninvasively by using a flow-compensating, three-dimensional, pulse Fourier transform, nuclear magnetic resonance (NMR) technique. This method records both the fluid velocity and particle concentration information from a single experiment. Techniques have been implemented to resolve spatially the axial fluid velocity and particle concentration on a plane normal to the flow direction. This NMR scheme permits detailed analysis of the flow-induced structure of two-phase systems that will help to construct and verify the mathematical models used to predict multiphase flow behavior. DOE

N89-24587# Argonne National Lab., IL. Intense Pulsed Neutron Source and Materials Science Div.
INELASTIC SCATTERING FROM LIQUID He4 IN AEROGEL GLASS
W. M. Snow and P. E. Sokol 1988 5 p Presented at the Workshop on Momentum Distributions, Argonne, IL, 24 Oct. 1988
(Contract W-31-109-eng-38; NSF DMR-87-04288)
(DE89-012381; CONF-8810118-6) Avail: NTIS HC A02/MF A01

The physics of liquid and solid ^{4}He in restricted geometries has motivated a number of interesting experiments. Recent experiments include detailed measurements of the phase diagram for bulk liquid in vycor, showing a suppression of the superfluid transition and elevation of the melting pressure, and measurements of the superfluid fraction in vycor, aerogel, and zerogel glasses near the lambda point, in which critical exponents differ from the pure ^{4}He values have been observed. Many striking features in several of the experiments on helium in restricted geometries are poorly understood. We have performed inelastic neutron scattering measurements of liquid helium in aerogel glass above and below the superfluid transition for two samples of different porosities. The kinetic energy (KE) of the confined liquid is the same as that of the bulk liquid in the normal phase, but is clearly higher than the bulk values in the superfluid phase. The observed scattering in the superfluid phase is more peaked than in the normal phase: consistent with the presence of a Bose condensate. An estimate of the condensate fraction using a modification of a method due to Sears yields values consistent with those estimated for the bulk liquid. DOE

N89-24588# Lawrence Livermore National Lab., CA.
ON THE REFRACTION OF LONGITUDINAL WAVES IN COMPRESSIBLE MEDIA
Leroy F. Henderson (Sydney Univ., Australia) Jul. 1988 53 p
(Contract W-7405-eng-48)
(DE89-012922; UCRL-53853) Avail: NTIS HC A04/MF A01

The refraction of plane shock waves in media with arbitrary equations of state is discussed. Previous work is reviewed briefly, and a rigorous definition of wave impedance is formulated. Earlier definitions are shown to be unsatisfactory. The impedance is combined with the boundary conditions at the media interface in order to study both head-on and oblique shock incidence. The impedance determines the nature of the reflected and transmitted waves, their intensities, and the fractions of energy and power that are reflected and transmitted. The refractive index is also defined; it determines whether or not a wave will be refracted and also helps to determine whether the wave system will be regular or irregular. The fundamental law of refraction is derived and shown to be a consequence of the fact that an arbitrary point on a shock or an expansion wave follows a ray path of

minimum time between any points on the path. This is a generalization of Fermat's principle to media that are deformed and convected by the waves propagating through them. There is also a detailed discussion of a wide variety of refractions at head-on and at glancing incidence. DOE

N89-24969# Academy of Sciences (USSR), Moscow. Inst. of Space Research.
GENERATION OF LARGE-SCALE VORTICES IN COMPRESSIBLE HELICAL TURBULENCE
O. G. Chkhetiani and V. V. Gvaramadze (Abastumani Astrophysical Observatory, Georgia, USSR) *In* ESA, Proceedings of an International School and Workshop on Plasma Astrophysics, Volume 1 Jan. 1989 p 363-369 (For primary document see N89-24910 18-75)
Avail: NTIS HC A18/MF A01; ESA Publications Div., ESTEC, Noordwijk, Netherlands, 45 US dollars or 80 Dutch guilders

35 INSTRUMENTATION AND PHOTOGRAPHY

Includes remote sensors; measuring instruments and gages; detectors; cameras and photographic supplies; and holography.

For aerial photography see *43 Earth Resources and Remote Sensing.* For related information see also *06 Aircraft Instrumentation,* and *19 Spacecraft Instrumentation.*

N89-24589# Interior Dept., Washington, DC.
GEOLOGICAL GYROCOMPASS Patent Application
M. H. McKeown and S. C. Beason 11 Aug. 1988 9 p Filed 11 Aug. 1988
(PB89-133086; Pat-Appl-7-231-017) Avail: NTIS HC A02/MF A01 CSCL 14B

The geological gyrocompass is an accurate, portable instrument useful for geologic mapping and surveying which employs an aircraft gyrocompass, strike reference bars, a pair of sights and levelling devices for horizontally levelling the instrument. A clinometer graduated in degrees indicates the dip of the surface being measured. GRA

N89-24590*# Lockheed Missiles and Space Co., Palo Alto, CA.
SMM X-RAY POLYCHROMATOR Final Report
Keith T. Strong, Bernhard M. Haisch, comp., James R. Lemen, comp., L. W. Acton, H. S. Bawa, E. S. Claflin, S. L. Freeland, G. L. Slater, D. L. Kemp, and G. A. Linford et al May 1988 127 p
(Contract NAS5-28713)
(NASA-CR-180791; NAS 1.26:180791) Avail: NTIS HC A07/MF A01 CSCL 14B

The range of observing and analysis programs accomplished with the X-Ray Polychromator (XRP) instruments during the decline of solar cycle 21 and the rise of the solar cycle 22 is summarized. Section 2 describes XRP operations and current status. This is meant as a guide on how the instrument is used to obtain data and what its capabilities are for potential users. The science section contains a series of representative abstracts from recently published papers on major XRP science topics. It is not meant to be a complete list but illustrates the type of science that can come from the analysis of the XRP data. There then follows a series of appendixes that summarize the major data bases that are available. Appendix A is a complete bibliography of papers and presentations produced using XRP data. Appendix B lists all the spectroscopic data accumulated by the Flat Crystal Spectrometer (FCS). Appendix C is a compilation of the XRP flare catalogue for events equivalent to a GOES C-level flare or greater. It lists the start, peak and end times as well as the peak Ca XIX flux. A.D.

N89-24591*# National Aeronautics and Space Administration. Lewis Research Center, Cleveland, OH.
HOLOGRAPHIC INTERFEROMETRY WITH AN INJECTION SEEDED Nd:YAG LASER AND TWO REFERENCE BEAMS
Arthur J. Decker May 1989 23 p
(NASA-TM-102056; E-4809; NAS 1.15:102056) Avail: NTIS HC A03/MF A01 CSCL 20F

The performance of twin injection seeded Nd:YAG lasers is compared with the performance of an argon-ion laser for recording dual-reference-beam holograms in AGFA 8E56 emulsion. Optical heterodyning is used to measure interference, and the results are expressed in terms of heterodyning signal level and intensity signal-to-noise. The Nd:YAG laser system is to be used for optical inspections of structures for cracks, defects, gas leaks, and structural changes. Author

N89-24592# Allied-Signal Aerospace Co., Kansas City, MO.
PIEZOELECTRIC FILM LOAD CELL ROBOT COLLISION DETECTOR Patent Application
John R. Lembke, inventor (to DOE) 15 Mar. 1988 14 p
(Contract DE-AC04-76DP-00613)
(DE89-010117; PATENTS-US-A7168367;
US-Patent-Appl-SN-168367) Avail: NTIS HC A03/MF A01

A piezoelectric load cell which can be utilized for detecting collisions and obstruction of a robot arm end effector includes a force sensing element of metallized polyvinylidene fluoride (PVDF) film. The piezoelectric film sensing element and a resilient support pad are clamped in compression between upper and lower plates. The lower plate has a central recess in its upper face for supporting the support pad and sensing element, while the upper plate has a corresponding central projection formed on its lower face for bearing on the sensing element and support pad. The upper and lower plates are dowelled together for concentric alignment and screwed together. The upper and lower plates are also adapted for mounting between the robot arm wrist and end effector. DOE

N89-24593*# National Aeronautics and Space Administration. Lewis Research Center, Cleveland, OH.
ON THE DYNAMIC RESPONSE OF PRESSURE TRANSMISSION LINES IN THE RESEARCH OF HELIUM-CHARGED FREE PISTON STIRLING ENGINES
Eric L. Miller (Sverdrup Technology, Inc., Cleveland, OH.) and James E. Dudenhoefer 1989 8 p Prepared for presentation at the 24th Intersociety Energy Conversion Engineering Conference, Washington, DC, 6-11 Aug. 1989; sponsored in part by IEEE, AIAA, ANS, ASME, SAE, ACS, and AIChE
(NASA-TM-102121; E-4902; NAS 1.15:102121) Avail: NTIS HC A02/MF A01 CSCL 14B

In free piston Stirling engine research the integrity of both amplitude and phase of the dynamic pressure measurements is critical to the characterization of cycle dynamics and thermodynamics. It is therefore necessary to appreciate all possible sources of signal distortion when designing pressure measurement systems for this type of research. The signal distortion inherent to pressure transmission lines is discussed. Based on results from classical analysis, guidelines are formulated to describe the dynamic response properties of a volume-terminated transmission tube for applications invoiving helium-charged free piston Stirling engines. The scope and limitations of the dynamic response analysis are considered. Author

N89-24594*# Morton Thiokol, Brigham City, UT. Aerospace Group.
TELEDYNE TABER 206-1000 AND 2210-3000 PRESSURE TRANSDUCER PROOF TEST AND BURST TEST Final Test Report
G. A. Ricks May 1989 51 p
(Contract NAS8-30490)
(NASA-CR-183672; NAS 1.26:183672; TWR-19248;
WBS-HQ302-10-10; ECS-SS-2801; MTI-Publ-89734) Avail: NTIS HC A04/MF A01 CSCL 14B

The range accuracy and structural integrity of the Teledyne Taber 206-1000 and 2210-3000 pressure transducers are verified and multiple uses are studied to determine is they have a significant effect on the transducers. Burst pressure for these transducers was also established. The Teledyne Taber 206-1000 pressure

transducer is used to measure chamber pressure on full-scale space shuttle rocket motors. The Teledyne Taber 2210-3000 pressure transducer is used to measure igniter pressure. The Teledyne Taber transducer has very good temperature stability and was used on all full-scale solid rocket motors, so there is a large data base established using this transducer. Author

N89-24595# Varian Associates, Palo Alto, CA. Microwave Tube Div.
THE 280 GHz GYRO-BWO DESIGN STUDY Final Report
Jul. 1988 44 p Sponsored by Lawrence Livermore National Lab., CA
(Contract W-7405-eng-48)
(DE89-011644; UCRL-21168) Avail: NTIS HC A03/MF A01

This report summarizes the results of a design study of a 280 GHz Gyro-BWO tunable source. The purpose of this study is to identify and propose viable design alternatives for any significant technological risk associated with building an operational BWO system. The tunable Gyro-BWO system will have three major components: a Gyro-BWO microwave tube, a superconducting magnet, and a power supply/modulator. The design tasks for this study in order of decreasing importance are: design and specification of the superconducting magnet; preliminary design and layout of a Gyro-BWO microwave tube; and specification for the power supply/modulator. DOE

N89-24596# Sandia National Labs., Albuquerque, NM.
DEMONSTRATION OF A TIME PROJECTION COMPTON SPECTROMETER
G. T. Baldwin, C. O. Landron, J. R. Lee, R. J. Leeper, and L. J. Lorence, Jr. 1989 20 p Presented at the Instrumentation for Nuclear Weapons Effects Testing Conference, Monterey, CA, 5 Jun. 1989
(Contract DE-AC04-76DP-00789)
(DE89-010743; SAND-89-0267C; CONF-890694-5) Avail: NTIS HC A03/MF A01

The Time Projection Compton Spectrometer (TPCS) is a device that we have developed to determine the energy spectrum of X rays from short-pulse, high-intensity sources. We use the TPCS to measure X-ray energies above 100 keV, for sources with endpoint energies no higher than about 2 MeV. In this paper, I will first describe the device and how it works, then present the results and analysis of our tests on SPEED. I will discuss sources of error and conclude by summarizing the advantages and suitability of the TPCS approach. DOE

N89-24597# Notre Dame Univ., IN. Dept. of Materials Science and Engineering.
OPTOELECTRONIC VELOCIMETER DEVELOPMENT
T. H. Kosel and K. Anand 20 Apr. 1989 36 p Prepared in cooperation with Oak Ridge National Lab., TN
(Contract DE-AC05-84OR-21400)
(DE89-012283; ORNL/Sub-86-91346/01) Avail: NTIS HC A03/MF A01

Development of an optoelectronic velocimeter technique for rapid, accurate measurement of erodent particle velocities is discussed. The technique, based on measurement of electronic pulses from particles passing through and blocking light beams, has been developed for the purpose of measuring the velocities of erodent particles rebounding from surfaces. It is also well suited for measurement of incident particle velocities in erosion rate measurements, in which a need exists due to the power law dependence of erosion rate on particle velocity. Two methods, based on time of flight through a single light beam and between the leading edges of a pair of light beams have been examined. Experimental results obtained from both with computer-interfaced electronics are presented. DOE

N89-24299# Deutsche Forschungs- und Versuchsanstalt fuer Luft- und Raumfahrt, Brunswick (Germany, F.R.). Inst. fuer Flugfuehrung.
INVESTIGATIONS OF A DISPLACEMENT-ESTIMATION TECHNIQUE FOR AERIAL VIDEO SCENES
H. Doergeloh *In its* Image Signal Processing for Flight Guidance Sep. 1988 p 93-121 In GERMAN; ENGLISH summary (For primary document see N89-24295 18-04)
Avail: NTIS HC A14/MF A01; DFVLR, VB-PL-DO, Postfach 40 60 58, 5000 Cologne, Fed. Republic of Germany, DM 108

N89-24300# Deutsche Forschungs- und Versuchsanstalt fuer Luft- und Raumfahrt, Brunswick (Germany, F.R.). Inst. for Flight Guidance.
STUDY OF A PARAMETRIC DISPLACEMENT ESTIMATION SCHEME WITH APPLICATION IN AERIAL IMAGES
K. Rose *In its* Image Signal Processing for Flight Guidance Sep. 1988 p 123-138 (For primary document see N89-24295 18-04)
Avail: NTIS HC A14/MF A01; DFVLR, VB-PL-DO, Postfach 40 60 58, 5000 Cologne, Fed. Republic of Germany, DM 108

N89-24304# Deutsche Forschungs- und Versuchsanstalt fuer Luft- und Raumfahrt, Brunswick (Germany, F.R.). Inst. fuer Flugfuehrung.
TRANSFORMATION OF REAL AND VIRTUAL OBJECTS INTO A VIRTUAL, VISUAL ENVIRONMENT
R. Beyer *In its* Image Signal Processing for Flight Guidance Sep. 1988 p 217-247 In GERMAN; ENGLISH summary (For primary document see N89-24295 18-04)
Avail: NTIS HC A14/MF A01; DFVLR, VB-PL-DO, Postfach 40 60 58, 5000 Cologne, Fed. Republic of Germany, DM 108

N89-24306# VTE, Brunswick (Germany, F.R.). Digital Video.
STATUS AND TRENDS OF TECHNOLOGICAL IMAGE PROCESSING POSSIBILITIES
W. Eggersluess *In* DFVLR, Image Signal Processing for Flight Guidance Sep. 1988 p 267-293 In GERMAN; ENGLISH summary (For primary document see N89-24295 18-04)
Avail: NTIS HC A14/MF A01; DFVLR, VB-PL-DO, Postfach 40 60 58, 5000 Cologne, Fed. Republic of Germany, DM 108

36 LASERS AND MASERS

Includes parametric amplifiers.
For related information see also *76 Solid-State Physics.*

N89-24598# National Aerospace Lab., Tokyo (Japan).
A REMOTE LASER-PROBING SYSTEM FOR COMBUSTION MEASUREMENTS
Mitsuo Gomi, Kunihisa Eguchi, and Yasuo Watanabe Jun. 1988 20 p In JAPANESE; ENGLISH summary
(NAL-TR-979; ISSN-0389-4010) Avail: NTIS HC A03/MF A01

The simultaneous measurement of velocity and temperature in combustion flows by the combined use of a laser Doppler velocimeter (LDV) and coherent anti-Stokes Raman spectroscopy (CARS) was studied. In order to avoid hostile surroundings in the combustion area, high power laser beams for CARS were sent to the test section over a distance of 44 meters by a pipe with corner mirrors. The LDV and CARS signals were sent back to the measurement room by fiber optics. Using a specific mirror, four beams for both the LDV and the CARS were focused onto the measuring point by a lens. The signals thus generated were passed through dichroic mirrors and interfero-filters. The coincidence of the LDV and the CARS signals was checked by the lag time between the two signals. Velocity-temperature correlations were given for turbulent flames behind a bluff-body flame stabilizer. Author

N89-24599*# Hampton Inst., VA. Dept. of Physics.
DEVELOPMENT OF MID-INFRARED SOLID STATE LASERS FOR SPACEBORNE LIDAR Progress Report, 13 Oct. 1988 - 13 Apr. 1989
Donald A. Whitney and Kyong H. Kim Apr. 1989 39 p
(Grant NAG1-877)
(NASA-CR-185012; NAS 1.26:185012) Avail: NTIS HC A03/MF A01 CSCL 20E

The laser performance of a Ho(3+):Tm(3+):Cr(3+):YAG

crystal was measured under flashlamp pumping at various operating temperatures. The normal mode laser thresholds of a Ho(3+)(0.45 at. percent):Tm(3+)(2.5 at. percent):Cr(3+)(1.5 at. percent):YAG crystal were found to range from 26 to 50 J between 120 and 200 K with slope efficiencies up to 0.36 percent with a 60 percent reflective output mirror. From the Q-switched operations a slope efficiency corresponding to 90 percent of the normal mode operation was observed. Laser wavelengths were measured for various operating conditions and fluorescence spectra were obtained at various temperatures in order to help understand the dynamic energy processes among the Ho(3+), Tm(3+), and Cr(3+) ions. A pulse forming network for a flashlamp pumped Cr:GSAG laser, which is to be used as a high power laser diode simulator in rare earth laser pumping, was completed and tested. The network provided critically damped, 1 ms FWHM, square pulses with a rise time of about 160 micrometers at an input electrical energy of 300 J. Author

N89-24600# Lawrence Livermore National Lab., CA.
TWO DIMENSIONAL ANALYSIS OF A NOVETTE LASER GENERATED STRESS-IMPULSE EXPERIMENT
Glen Dahlbacka (Plasma Research Corp., Alameda, CA.) 13 Oct. 1988 17 p
(Contract W-7405-eng-48)
(DE89-009909; UCRL-21167) Avail: NTIS HC A03

The NOVETTE Laser was used to irradiate aluminum disks at fluences of 100 to 20,000 J/sq cm. Besides the intrinsic interest in the coupling coefficient for .53 micron light in highly 1D (Ins) interactions, the shots were used to qualify diagnostics to be used in other tests. The coupling coefficient data has been analyzed with respect to 1D calculations by Bookless. The results indicate that the experiments generate twice the impulse calculated by a 1D model at least at 12,000 J/sq cm. 2D calculations predict an impulse of 16. 3 ktaps vs a measured 12.5 ktaps at 12,000 J/sq cm. 1D calculations predict 6.3 ktap. 46 percent of the 2D impulse is from plume reradiation to target surface outside the spot at times much later than the initial interaction time of 1 ns. The 2D calculation predicted a peak stress of 90 kbars at a depth of 1.5 mm into the target. Observations using a Manganin gage were 68 kbars. The ratio of calculated to observed stress is about the same as the ratio of calculated to observed impulse. The difference in stresses may be due to a lack of material strength in the EOS for LASNEX. Alternatively, an error in the estimate of the gauge depth by as little as .2 mm can also explain the stress discrepancy as could an absorption of 75 percent of the incident light from that calculated. At this time, however, there is a 50 percent apparent uncertainty in the calculation of impulse at 10 terawatts/sq cm on aluminum when 2D effects are accounted for. DOE

N89-24601*# Lightwave Electronics Corp., Mountain View, CA.
PROTOTYPE LASER-DIODE-PUMPED SOLID STATE LASER TRANSMITTERS Final Report, Apr. 1987 - Jun. 1989
Thomas J. Kane, Emily A. P. Cheng, and Richard W. Wallace Jun. 1989 65 p
(Contract NAS7-999)
(NASA-CR-185056; NAS 1.26:185056) Avail: NTIS HC A04/MF A01 CSCL 20E

Monolithic, diode-pumped Nd:YAG ring lasers can provide diffraction-limited, single-frequency, narrow-linewidth, tunable output which is adequate for use as a local oscillator in a coherent communication system. A laser was built which had a linewidth of about 2 kHz, a power of 5 milliwatts, and which was tunable over a range of 30 MHz in a few microseconds. This laser was phase-locked to a second, similar laser. This demonstrates that the powerful technique of heterodyne detection is possible with a diode-pumped laser used as the local oscillator. Laser diode pumping of monolithic Nd:YAG rings can lead to output powers of hundreds of milliwatts from a single laser. A laser was built with a single-mode output of 310 mW. Several lasers can be chained together to sum their power, while maintaining diffraction-limited, single frequency operation. This technique was demonstrated with two lasers, with a total output of 340 mW, and is expected to be practical for up to about ten lasers. Thus with lasers of 310 mW, output of up to 3 W is possible. The chaining technique, if properly engineered, results in redundancy. The technique of resonant external modulation and doubling is designed to efficiently convert the continuous wave, infrared output of our lasers into low duty-cycle pulsed green output. This technique was verified through both computer modeling and experimentation. Further work would be necessary to develop a deliverable system using this technique. Author

N89-24602# Hughes Research Labs., Malibu, CA.
COOPERATIVE PHENOMENA FOR NEW COHERENT RADIATION SOURCES Final Report, 14 May 1987 - 14 Jun. 1988
R. A. McFarlane Oct. 1988 48 p
(Contract F49620-85-C-0058)
(AD-A206368; AFOSR-89-0321TR) Avail: NTIS HC A03/MF A01 CSCL 07/2

The principal objective of this research is to investigate, both theoretically and experimentally, cooperative optical transitions in solids, with the goal of finding efficient systems for the generation of upconverted stimulated emission. Of interest also are new optical pair effects and studies of the resonance fluorescence and coherence on cooperative transitions. In the third year of the program, significant advances were made in the experimental aspects. Measurements of upconversion dynamics were made in erbium-doped crystals and in a fluorozirconate glass. Upconversion laser operation was observed at two visible wavelengths in YLiF4:Er 5 percent and pumping pathways identified. Spectral and lifetime studies are reported for promising new laser host materials. GRA

N89-24603# Ortel Corp., Alhambra, CA.
VERTICAL EMITTING, RING GEOMETRY, ULTRA-LOW THRESHOLD AND ULTRA-HIGH SPEED QUANTUM WELL LASERS FOR OPTICAL INTERCONNECT Status Report, Jul. 1988 - Jan. 1989
Nadav Bar-Chaim 18 Feb. 1989 5 p
(Contract N00014-88-C-0483)
(AD-A206427) Avail: NTIS HC A02/MF A01 CSCL 09/3

The main emphasis during this period has been placed on the following efforts: (1) establishing a system and a method to fabricate gratings; (2) growing and qualifying quantum well GaAs/GaAlAs material generated in our low pressure MOCVD reactor; (3) fabrication of ultra-low threshold buried heterostructure lasers using liquid phase epitaxy regrowth; and (4) processing of standard double heterostructure ring lasers in order to determine the losses associated with curved structures. A system was designed and set up for fabrication of submicron gratings in order to be able to generate gratings required for vertically emitting lasers. The system consists of a He-Cd laser which emits light in the 325 nm UV line. The light is spatially filtered and expanded and then split into a couple of beams that create an interference pattern. Using this system we have exposed GaAs wafers that were coated with positive photoresist to create gratings with periods in the range of 0.2 to 1.0 micron. (A typical second order grating for GaAlAs laser is 0.24 micron). GRA

N89-24604# Los Alamos National Lab., NM.
APPLICATIONS OF INFRARED LASER SPECTROSCOPY TO LASER CHEMISTRY AND LASER DEVELOPMENT
Robin S. McDowell and A. K. Viswanath, ed. 1989 21 p
Presented at the Conference of Laser Applications in Spectroscopy and Optics, Madras, India, 1 Jan. 1989
(Contract W-7405-eng-36)
(DE89-011196; LA-UR-89-1161; CONF-8901123-1) Avail: NTIS HC A03/MF A01

The impact on infrared molecular spectroscopy of high-resolution tunable laser sources and laser-controlled Fourier-transform spectrometers is discussed, with special reference to rovibrational spectra of spherical-top molecules such as CH4, OsO4, SiF4, SF6, and UF6. The role of tunable laser spectroscopy in analyzing the CF4 laser, resulting in the precise prediction of lasing frequencies between 605 and 655/cm, is

described. Studies of overtone and combination bands of SF6 enable the vibrational anharmonicity to be determined, resulting in a more detailed description of the pump transitions involved in laser photochemistry, and of higher vibrational levels and pathways to excitation and dissociation. This permits more accurate calculations of vibrational state densities for spherical-top molecules. Implications for the photochemistry of species, such as SiF4, SF6, UF6, and Ni(Co)4, are discussed. DOE

N89-24605# Lawrence Livermore National Lab., CA. Beam Research Program.
ENGINEERING DESIGN OF THE INTERACTION WAVEGUIDE FOR HIGH-POWER ACCELERATOR-DRIVEN MICROWAVE FREE-ELECTRON LASERS
D. B. Hopkins, H. W. Clay, B. W. Stallard, A. L. Throop, G. Listvinsky, and M. A. Makowski (TRW, Inc., Redondo Beach, CA.) 16 Mar. 1989 15 p Presented at the 13th Particle Accelerator Conference, Chicago, IL, 20-23 Mar. 1989
(Contract W-7405-eng-48)
(DE89-011896; UCRL-99635; CONF-890335-135) Avail: NTIS HC A03/MF A01

Linear Induction Accelerators (LIAs) operating at beam energies of a few million electron volts and currents of a few thousand amperes are suitable drivers for Free-Electron Lasers (FELs). Such lasers are capable of producing gigawatts of peak power and megawatts of average power at microwave frequencies. Such devices are being studied as possible power sources for future high-gradient accelerators and are being constructed for plasma heating applications. At high power levels, the engineering design of the interaction waveguide presents a challenge. This paper discusses several concerns, including electrical breakdown and metal fatigue limits, choice of material, and choice of operating propagation mode. DOE

N89-24606# Lawrence Livermore National Lab., CA.
ATMOSPHERIC EFFECTS ON LASER PROPAGATION
Thomas J. Karr 16 Mar. 1989 12 p Presented at the SPIE Conference on Optics, Electro-optics and Laser Applications in Science and Engineering, Los Angeles, CA, 15-20 Jan. 1989
(Contract W-7405-eng-48)
(DE89-012287; UCRL-100789; CONF-890145-25) Avail: NTIS HC A03/MF A01

The linearized theory of thermal blooming instabilities is reviewed. The dispersion relation is derived for unstable modes with and without correction. Perfect phase-only correction is unstable at all spatial scales, while perfect field conjugation is stable at all scales. Various atmospheric phenomena such as turbulence, diffusion and wind shear may mitigate or dampen the instabilities. Full nonlinear time-dependent computer simulations of laser atmospheric propagation agree with the dispersion relation for small perturbations, and show saturation and nonlinear mode beating at long times. DOE

N89-24827# Robotic Vision Systems, Inc., Melville, NY.
A SYSTEM FOR HIGH RESOLUTION 3D MAPPING USING LASER RADAR AND REQUIRING NO BEAM SCANNING MECHANISMS
Paul Rademacher *In* Tactical Weapons Guidance and Control Information Conference on Space and Military Applications of Automation and Robotics Jun. 1988 p 18 (For primary document see N89-24819 18-63)
Avail: NTIS HC A05/MF A01 CSCL 09B

37 MECHANICAL ENGINEERING

Includes auxiliary systems (nonpower); machine elements and processes; and mechanical equipment.

N89-24607*# National Aeronautics and Space Administration. Lewis Research Center, Cleveland, OH.
COMPARISON OF PREDICTED AND MEASURED TEMPERATURES OF UH-60A HELICOPTER TRANSMISSION
Harold H. Coe Washington Apr. 1989 15 p
(NASA-TP-2911; NAS 1.60:2911; E-4588; AVSCOM-TR-89-C-010)
Avail: NTIS HC A03/MF A01 CSCL 13I

The 2109-kW (2828-hp) UH-60A Black Hawk helicopter transmission was one of the transmissions used to obtain an experimental data base. Component improvements or new transmission concepts can thus be evaluated by comparison with the established data. Results of efficiency and vibration tests of the UH-60A have been reported previously. In this investigation the transmission was instrumented internally and tested over a range of operating conditions. The speed was varied from 50 to 100 percent of the full rated value, and the torque was varied from 10 to 100 percent of the full rated value. Temperatures of internal bearings and gears were measured. The computer program Planetsys was used to simulate the thermal performance of this transmission. The calculated temperatures were then compared with the corresponding measured values. The highest measured temperature was 405 K (270 F) on the outer race of the high-speed input shaft roller bearing, at the 100-percent power condition. In general, the predicted temperatures compared very well with the measured values, most of them being within 5 kelvin (9 F). Specifically, the temperatures predicted for the single-row spherical roller planetary bearing averaged only about 4 kelvin (8 F) lower than the highest measured value. Author

N89-24608*# Maryland Univ., College Park. Electrical Engineering Dept.
REAL TIME CONTROL FOR NASA ROBOTIC GRIPPER Semiannual Progress Report
Carole A. Salter and John S. Baras 15 Feb. 1989 16 p
(Grant NAG5-1047)
(NASA-CR-184978; NAS 1.26:184978) Avail: NTIS HC A03/MF A01 CSCL 13I

Control laws (in some optimal sense) are being developed for the gripper/nut runner end effector. Control laws for the gripper and nut runner portions of the end effector may be developed independently since these two systems are decoupled. A hybrid force/position controller will be used for both the gripper and nut runner. The development of the gripper controller is explained. Sensory data available to the controller is obtained from an array of strain gages as well as a linear potentiometer. Applying well known optimal control theoretic principles, the control which minimizes the transition time between positions is obtained. In addition, a robust force control scheme is developed to contend with the strain gage drift caused by extreme temperature variations encountered in space. Author

N89-24609 Wisconsin Univ., Madison.
GENERALIZED SOLUTION FOR THE OPTIMAL PREHENSION STATE USING END EFFECTORS WITH MULTI-ARTICULATED FINGERS Ph.D. Thesis
Ashraf Mahmoud Badreldin 1988 230 p
Avail: Univ. Microfilms Order No. DA8826036

A general formulation for the mechanics of the grasp with elastic multi-articulated fingers is presented. A procedure utilizing linear programming is given for computing a unique solution for the gripping forces and moments at the contact areas which insures stability of the grasp at the considered configuration. It takes into consideration all the frictional forces and moments. It is computationally efficient and could be used in real time. This procedure is particularly useful when the deformation or the precision motion of the grasped object is to be monitored along a task. It is also useful in designing end effectors for handling delicate objects. An optimization algorithm is given to determine the best gripping configuration for any shape object undergoing any task using end effectors with any number of fingers. Author

N89-24610# Sandia National Labs., Albuquerque, NM.
VISION SYSTEM TESTING FOR TELEOPERATED VEHICLES
Douglas E. McGovern and Dwight P. Miller Mar. 1989 96 p
(Contract DE-AC04-76DP-00789)
(DE89-009713; SAND-88-3123) Avail: NTIS HC A05/MF A01

This study compared three forward-looking vision systems

consisting of a fixed mount, black and white video camera system, a fixed mount, color video camera system and a steering-slaved color video camera system. Subjects were exposed to a variety of objects and obstacles over a marked, off-road, course while either viewing videotape or performing actual teleoperation of the vehicle. The subjects were required to detect and identify those objects which might require action while driving such as slowing down or maneuvering around the object. Subjects also estimated the same video systems as in the driving task. Two modes of driver interaction were tested: actual remote driving, and noninteractive video simulation. Remote driving has the advantage of realism, but is subject to variability in driving strategies and can be hazardous to equipment. Video simulation provides a more controlled environment in which to compare vision-system parameters, but at the expense of some realism. Results demonstrated that relative differences in performance among the visual systems are generally consistent in the two test modes of remote driving and simulation. A detection-range metric was found to be sensitive enough to demonstrate performance differences viewing large objects. It was also found that subjects typically overestimated distances, and when in error judging clearance, tended to overestimate the gap between the objects. DOE

N89-24611# Argonne National Lab., IL.
CONTINUOUS CRYOPUMP WITH A METHOD FOR REMOVAL OF SOLIDIFIED GASES Patent Application
L. W. Carlson, inventor (to DOE) and H. Herman, inventor (to DOE) May 1988 15 p
(Contract W-31-109-eng-38)
(DE89-009760; PATENTS-US-A7190567; US-Patent-Appl-SN-190567) Avail: NTIS HC A03/MF A01

An improved cryopump is presented for the removal of gases from a high vacuum, comprising a cryopanel incorporating honeycomb structure, refrigerant means thermally connected to the cryopanel, and a rotatable channel moving azimuthally around an axis located near the center of the cryopanel, removing gases adsorbed within the honeycomb structure by subliming them and conducting them outside the vacuum vessel. DOE

N89-24612# Los Alamos National Lab., NM.
SHAFT ADJUSTER Patent Application
Herbert H. Harry, inventor (to DOE) 11 Mar. 1988 12 p
(Contract W-7405-eng-36)
(DE89-010119; PATENTS-US-A7167206; US-Patent-Appl-SN-167206) Avail: NTIS HC A03/MF A01

A method for the adjustment and alignment of shafts in high power devices is presented. A plurality of adjacent rotatable angled cylinders are positioned between a base and the shaft to be aligned which when rotated introduce an axial offset. The apparatus is electrically conductive and constructed of a structurally rigid material. The angled cylinders allow the shaft such as the center conductor in a pulse line machine to be offset in any desired alignment position within the range of the apparatus. DOE

N89-24613# Southwest Research Inst., San Antonio, TX. Fuels and Lubricants Research Facility.
ROLE OF SULFUR OXIDES IN WEAR AND DEPOSIT FORMATION IN ARMY DIESEL ENGINES Interim Report, Oct. 1985 - Sep. 1987
David W. Naegeli and Howard W. Marbach, Jr. Dec. 1988 71 p
(Contracts DAAK70-87-C-0043; DAAK70-85-C-0007; DA Proj. 1T1-61102-AH-51)
(AD-A206054; BFLRF-248) Avail: NTIS HC A04/MF A01 CSCL 21/7

In some locations outside the continental United States, U.S. Military ground mobility equipment uses fuel with an increased sulfur content. Fuel sulfur has been identified as a primary contributor to diesel engine wear indicates that sulfuric acid mist formed within the combustion chamber is responsible for corrosive attack of the cylinder bore and piston ring areas. Deposit formation has been more of a mystery in that the literature tends to support the theory that reaction of organically bound sulfur with the fuel and lubricant is the principal cause. Studies presented here suggest that sulfur dioxide (SO2) formed in the combustion of fuel-bound sulfur is the primary cause of higher cylinder bore/ring wear and deposit formation in diesel engines. GRA

N89-24614# Oak Ridge National Lab., TN. Fuel Recycle Div.
ADVANCED SERVOMANIPULATOR REMOTE MAINTENANCE DEMONSTRATION
T. L. Ray and E. C. Bradley Mar. 1989 50 p
(Contract DE-AC05-84OR-21400)
(DE89-010188; ORNL/TM-10847) Avail: NTIS HC A03/MF A01

The advanced servomanipulator (ASM) is a dual-arm, force-reflecting, master/slave servomanipulator that was designed for remote maintenance applications and is digitally controlled. The ASM is installed in the Maintenance Systems Test Area (MSTA) of the Fuel Recycle Division at the Oak Ridge National Laboratory. The unique aspect of ASM is that the slave arms were designed to be remotely maintainable, using a similar remote manipulator system, to maximize availability and minimize downtime. This test report describes the results of the maintenance testing conducted on ASM. Demonstration of the ability to maintain ASM remotely is an important precursor to the ultimate application of ASM in a totally remote facility. The approach taken in the design of ASM was for the manipulator slave arms to be composed of modules capable of being removed and replaced by another manipulator system of similar capabilities. The ASM incorporates gear and torque tube drives with drive couplings that facilitate remote maintenance. Although the use of special fixtures is normally discouraged for remote maintenance, special fixtures were required for this demonstration due to the complex nature of the slave arms. This test was performed to demonstrate that the ASM slave arms could be completely disassembled and reassembled remotely. DOE

N89-24615 California Univ., Los Angeles.
OBJECTIVE AND CONSTRAINT FUNCTIONS FOR THE ANALYSIS AND DESIGN OF ROBUST CONTROL SYSTEMS Ph.D. Thesis
Michael Allen Leal 1988 110 p
Avail: Univ. Microfilms Order No. DA8906146

Three aspects of control system design and analysis are studied; energy dissipation rate, actuator constraints, and stability robustness. Design methods for linear-quadratic optimal control do not treat these issues effectively and simulations must be used to examine these issues. The development of functions and concepts is emphasized to allow the aforementioned issues to be addressed in the design process by using numerical optimization codes to select key system parameters. Author

N89-24616# Sandia National Labs., Albuquerque, NM. Applied Mechanics Div. 1.
INCORPORATION OF SURFACE TENSION INTO THE STRUCTURAL FINITE ELEMENT CODE SANCHO
J. R. Weatherby, R. D. Krieg, and C. M. Stone Mar. 1989 36 p
(Contract DE-AC04-76DP-00789)
(DE89-011354; SAND-89-0509) Avail: NTIS HC A03/MF A01

To analytically model soldering and welding processes it is necessary to track the deformation of a material as it changes from a solid to a liquid and then back again to a solid. Because it is the residual stress state in the solid that is of primary interest, the most suitable tools for studying this class of problems appear to be Lagrangian finite element codes that are typically used in the analysis of solids. It is possible to obtain solutions to hydrostatic fluids problems using a Lagrangian finite element code by allowing the fluid phase of the material to sustain a deviatoric stress component that is very small in magnitude relative to the hydrostatic pressure that exists in the material. The capability to model surface tension phenomena was added to the finite element code SANCHO. SANCHO is a Lagrangian finite element code that uses a dynamic relaxation scheme to solve nonlinear problems involving quasistatic loading of two-dimensional solids. SANCHO is formulated so that it properly accounts for large deformations. This report details the

theory and implementation of the method used to model surface tension. With this new capability, SANCHO can be used to solve surface tension problems that are more complex than the problems that can be treated with other more tradition methods of surface tension analysis. DOE

N89-24617# Sandia National Labs., Albuquerque, NM. Computational Physics and Mechanics Div.
CAVITY DIMENSIONS FOR HIGH VELOCITY PENETRATION EVENTS: A COMPARISON OF CALCULATIONAL RESULTS WITH DATA
Lubomyra N. Kmetyk and Paul Yarrington May 1989 43 p
(Contract DE-AC04-76DP-00789)
(DE89-011351; SAND-88-2693) Avail: NTIS HC A03/MF A01

Calculations were performed with the CTH and HULL finite difference wavecodes to evaluate computational capabilities for predicting depth and diameter of target cavities produced in high velocity penetration events. The calculations simulated selected tests in a set of armor penetration experiments conducted by the US Army Ballistic Research Laboratory and reported earlier in the literature. The tests and simulations involved penetration of semi-infinite targets by long rod projectiles over a range of impact velocities from 1.3 to 4.5 km/sec. Comparisons are made between the calculated and measured dimensions of the target cavities, and the sensitivity of the predicted results to target property variations is investigated. DOE

N89-24618# Purdue Univ., West Lafayette, IN. Dept. of Mechanical Engineering.
EFFICIENCY STUDY OF OIL COOLING OF A SCREW COMPRESSOR
David R. Tree and M. G. McKellar Apr. 1989 35 p
(Contract DE-FG01-87CE-15245)
(DE89-011417; DOE/CE-15245/T1; PU-0561-1; HL89-7) Avail: NTIS HC A03/MF A01

One of the major goals of all compressor manufacturers is to build as efficient a compressor as possible. Over the last several years improvements to the design of screw compressors has made them efficiently competitive with other types of compressors, especially at large loads. The primary purpose of this research is to investigate four different methods of cooling a 250 horsepower compressor and determine their effects on the efficiency of the compressor. Two conventional methods, liquid injection and thermosyphon cooling, and two new methods, V-PLUS and Fresco oil injection, are investigated. The screw compressor used in the tests was a VRS-500 screw compressor made by the Vilter Manufacturing Corporation. DOE

N89-24619# Argonne National Lab., IL. Energy and Environmental Systems Div.
MAGLEV VEHICLES AND SUPERCONDUCTOR TECHNOLOGY: INTEGRATION OF HIGH-SPEED GROUND TRANSPORTATION INTO THE AIR TRAVEL SYSTEM
Larry R. Johnson, Donald M. Rote, John R. Hull, Howard T. Coffey, James G. Daley, and Robert F. Giese Apr. 1989 130 p
(Contract W-31-109-eng-38)
(DE89-012241; ANL/CNSV-67) Avail: NTIS HC A07/MF A01

This study was undertaken to (1) evaluate the potential contribution of high-temperature superconductors (HTSCs) to the technical and economic feasibility of magnetically levitated (maglev) vehicles, (2) determine the status of maglev transportation research in the United States and abroad, (3) identify the likelihood of a significant transportation market for high-speed maglev vehicles, and (4) provide a preliminary assessment of the potential energy and economic benefits of maglev systems. HTSCs should be considered as an enhancing, rather than an enabling, development for maglev transportation because they should improve reliability and reduce energy and maintenance costs. Superconducting maglev transportation technologies were developed in the United States in the late 1960s and early 1970s. Federal support was withdrawn in 1975, but major maglev transportation programs were continued in Japan and West Germany, where full-scale prototypes now carry passengers at speeds of 250 mi/h in demonstration runs. Maglev systems are generally viewed as very-high-speed train systems, but this study shows that the potential market for maglev technology as a train system, e.g., from one downtown to another, is limited. Rather, aircraft and maglev vehicles should be seen as complementing rather than competing transportation systems. If maglev systems were integrated into major hub airport operations, they could become economical in many relatively high-density US corridors. Air traffic congestion and associated noise and pollutant emissions around airports would also be reduced. DOE

N89-24620# Sandia National Labs., Albuquerque, NM.
DIFFUSION WELDING OF ELECTRICAL INTERCONNECTS TO SILICON SOLAR CELLS
Charles E. Albright and Donald O. Holte (Ohio State Univ., Columbus.) May 1989 151 p Prepared in cooperation with Ohio State Univ., Columbus.
(Contract DE-AC04-76DP-00789)
(DE89-012250; SAND-88-7041) Avail: NTIS HC A08/MF A01

The purpose of this study was to develop diffusion welding variables for the joining of silicon solar cells to metal electrical interconnects by laboratory experimentation. Diffusion welding electrical interconnects to silicon solar cells can be accomplished at pressures above 2000 psi and temperatures above 250 C without the aid of an inert or protective atmosphere. The high residual stress associated with the mismatch in coefficients of thermal expansion between the solar cell and the interconnect is the cause for cell cracking upon cooling from the welding temperature and weld damage due to thermal cycling. When Kovar interconnects, or copper interconnects inserted between Kovar interconnects, are used, the residual stress in the cell is reduced and cells survive the welding and cooling cycle. Accelerated thermal cycling does not cause major damage to the diffusion welds on solar cell-interconnect assemblies that use Kovar as an interconnect material. DOE

N89-24621# Ohio State Univ., Columbus. Dept. of Welding Engineering.
Nd:YAG LASER WELDABILITY OF RS/PM Al-BFe-2Mo SHEET
S. Krishnaswamy, W. A. Baeslack, III, and T. Lienert (Sandia National Labs., Albuquerque, NM.) 1989 6 p Presented at the 2nd International Conference on Trends in Welding Research, Gatlinburg, TN, 15 May 1989
(Contract DE-AC04-76DP-00789)
(DE89-013588; SAND-89-1317C; CONF-8905118-7) Avail: NTIS HC A02/MF A01

The microstructure, mechanical properties and fracture characteristics of a pulsed Nd:YAG laser weld in a Rapid Solidification/Powder Metallurgy (RS/PM) Al-8 wt percent Fe-2.3 wt percent Mo alloy have been investigated. Results showed the high power density but low total energy input associated with pulsed Nd:YAG laser welding to promote extremely rapid Fusion Zone (FZ) cooling rates in the vicinity of 10(5) C/s. The weld FZ microstructure consisted primarily of submicron-sized spherical dispersoids in a matrix of fine dendritic-alpha aluminum. A dispersoid-coarsened Heat-Affected Zone (HAZ) was also observed in the boundary between successive, overlapping melt zones. Transverse-weld tensile testing found fracture to occur in the unaffected base metal indicating 100 percent weld joint efficiency. Longitudinal-weld bend ductility testing revealed fracture initiation and propagation to be associated with the HAZ between successive melt zones at a bend ductility level only marginally below that of the base metal. DOE

N89-24390# Fokker B.V., Amsterdam (Netherlands).
THE HERMES ROBOT ARM (HERA)
R. Hamann, C. Blaas, and R. H. Bentall (European Space Agency. European Space Research and Technology Center, ESTEC, Noordwijk, Netherlands) *In* ESA, International Symposium on Europe in Space: The Manned Space System Oct. 1988 p 493-501 (For primary document see N89-24335 18-12)
Copyright Avail: NTIS HC A99/MF A01; ESA Publications Div., ESTEC, Noordwijk, Netherlands, 80 Dutch guilders

N89-24391# Deutsche Forschungs- und Versuchsanstalt fuer Luft- und Raumfahrt, Cologne (Germany, F.R.).
ROBOTIC EXPERIMENTS ON SPACELAB D-2 AS TESTBED FOR FUTURE OPERATIONAL CONCEPTS
K. L. Mueller and M. Turk *In* ESA, International Symposium on Europe in Space: The Manned Space System Oct. 1988 p 503-507 (For primary document see N89-24335 18-12)
Copyright Avail: NTIS HC A99/MF A01; ESA Publications Div., ESTEC, Noordwijk, Netherlands, 80 Dutch guilders

N89-24651*# Texas Univ., Austin.
ADAPTIVE METHODS, ROLLING CONTACT, AND NONCLASSICAL FRICTION LAWS
J. T. Oden *In* NASA, Langley Research Center, Computational Methods for Structural Mechanics and Dynamics, Part 1 May 1989 p 269-289 (For primary document see N89-24638 18-39)
Avail: NTIS HC A15/MF A01 CSCL 13I

N89-24653*# National Aeronautics and Space Administration. Langley Research Center, Hampton, VA.
EXPLOITING SYMMETRIES IN THE MODELING AND ANALYSIS OF TIRES
Ahmed K. Noor, C. M. Andersen, and John A. Tanner *In its* Computational Methods for Structural Mechanics and Dynamics, Part 1 May 1989 p 317-329 (For primary document see N89-24638 18-39)
Avail: NTIS HC A15/MF A01 CSCL 13I

N89-24662*# Massachusetts Inst. of Tech., Cambridge. Dept. of Mechanical Engineering.
DYNAMICS OF FLEXIBLE MULTI-BODY MECHANISMS AND MANIPULATORS. PART 1: AN OVERVIEW
Steven Dubowsky *In* NASA, Langley Research Center, Computational Methods for Structural Mechanics and Dynamics May 1989 p 455-458 (For primary document see N89-24654 18-39)
Avail: NTIS HC A12/MF A01 CSCL 13I

N89-24663*# Massachusetts Inst. of Tech., Cambridge.
APPLICATION OF FINITE-ELEMENT METHODS TO DYNAMIC ANALYSIS OF FLEXIBLE SPATIAL AND CO-PLANAR LINKAGE SYSTEMS, PART 2
Steven Dubowsky *In* NASA, Langley Research Center, Computational Methods for Structural Mechanics and Dynamics May 1989 p 459-489 (For primary document see N89-24654 18-39)
Avail: NTIS HC A12/MF A01 CSCL 13I

N89-24664*# Iowa Univ., Iowa City. Coll. of Engineering.
DYNAMICS OF ARTICULATED STRUCTURES
Edward J. Haug *In* NASA, Langley Research Center, Computational Methods for Structural Mechanics and Dynamics May 1989 p 491-515 (For primary document see N89-24654 18-39)
Avail: NTIS HC A12/MF A01 CSCL 13I

N89-24668*# Massachusetts Inst. of Tech., Cambridge. Space Systems Lab.
NONLINEAR CHARACTERISTICS OF JOINTS AS ELEMENTS OF MULTI-BODY DYNAMIC SYSTEMS
Edward F. Crawley *In* NASA, Langley Research Center, Computational Methods for Structural Mechanics and Dynamics May 1989 p 543-569 (For primary document see N89-24654 18-39)
Avail: NTIS HC A12/MF A01 CSCL 13I

N89-24822# Kader Robotics, Inc., Huntsville, AL.
DUAL-ARM ROBOTS FOR TELEROBOTIC IVA OPERATIONS ON THE SPACE STATION Abstract Only
M. Carl Ziemke, Jac Kader, and Larry Yawn *In* Tactical Weapons Guidance and Control Information Conference on Space and Military Applications of Automation and Robotics Jun. 1988 p 5 (For primary document see N89-24819 18-63)
Avail: NTIS HC A05/MF A01 CSCL 09B

N89-24829# Rexham Aerospace and Defense Group, Huntsville, AL.
STABILIZED IMAGE SYSTEM FOR MOBILE ROBOTS Abstract Only
David Samuel Stauffer and Edward Watts *In* Tactical Weapons Guidance and Control Information Conference on Space and Military Applications of Automation and Robotics Jun. 1988 p 20 (For primary document see N89-24819 18-63)
Avail: NTIS HC A05/MF A01 CSCL 09B

N89-24831# Air Force Inst. of Tech., Wright-Patterson AFB, OH.
DEVELOPMENT OF A HYBRID SIMULATOR FOR ROBOTIC MANIPULATORS Abstract Only
Peter M. VanWirt and Michael B. Leahy, Jr. *In* Tactical Weapons Guidance and Control Information Conference on Space and Military Applications of Automation and Robotics Jun. 1988 p 23 (For primary document see N89-24819 18-63)
Avail: NTIS HC A05/MF A01 CSCL 09B

N89-24834# Martin Marietta Corp., Denver, CO.
THE DARPA AUTONOMOUS LAND VEHICLE: A PHASE 1 RETROSPECTIVE AND A PROSPECTIVE FOR THE FUTURE Abstract Only
Robert J. Douglass *In* Tactical Weapons Guidance and Control Information Conference on Space and Military Applications of Automation and Robotics Jun. 1988 p 29 (For primary document see N89-24819 18-63)
Avail: NTIS HC A05/MF A01 CSCL 09B

N89-24835# Sandia National Labs., Albuquerque, NM.
DEVELOPMENT OF A MAN-PORTABLE CONTROL UNIT FOR A TELEOPERATED LAND VEHICLE Abstract Only
Douglas E. McGovern and Shannon V. Spires *In* Tactical Weapons Guidance and Control Information Conference on Space and Military Applications of Automation and Robotics Jun. 1988 p 30 (For primary document see N89-24819 18-63)
Avail: NTIS HC A05/MF A01 CSCL 09B

N89-24836# Air Force Inst. of Tech., Wright-Patterson AFB, OH.
ROBOTIC VISUAL SERVO CONTROL FOR AIRCRAFT GROUND REFUELING Abstract Only
Mikel M. Miller, Michael B. Leahy, Jr., and Matthew Habrisky *In* Tactical Weapons Guidance and Control Information Conference on Space and Military Applications of Automation and Robotics Jun. 1988 p 31 (For primary document see N89-24819 18-63)
Avail: NTIS HC A05/MF A01 CSCL 09B

N89-24837# Stevens Inst. of Tech., Hoboken, NJ. Dept. of Mechanical Engineering.
INSERTION WITH TWO COORDINATED ARMS Abstract Only
Frederic L. Swern and Stephen J. Tricamo *In* Tactical Weapons Guidance and Control Information Conference on Space and Military Applications of Automation and Robotics Jun. 1988 p 38 (For primary document see N89-24819 18-63)
Avail: NTIS HC A05/MF A01 CSCL 09B

N89-24839# Olis Engineering, Sedalia, CO.
INFLATABLE END EFFECTOR TOOLS Abstract Only
Carter K. Lord *In* Tactical Weapons Guidance and Control Information Conference on Space and Military Applications of Automation and Robotics Jun. 1988 p 40 (For primary document see N89-24819 18-63)
Avail: NTIS HC A05/MF A01 CSCL 09B

N89-24840# Honeywell, Inc., New Brighton, MN.
ROBOT ASSEMBLY OF MICROSCOPIC COMPONENT IN MILLIMETER WAVE DEVICES Abstract Only
Steven R. Prokosch *In* Tactical Weapons Guidance and Control

Information Conference on Space and Military Applications of Automation and Robotics Jun. 1988 p 43 (For primary document see N89-24819 18-63)
Avail: NTIS HC A05/MF A01 CSCL 09B

N89-24843# Tech-U-Fit Corp., Alexandria, VA.
TESTING THE FEASIBILITY OF USING A TELEOPERATED ROBOT FOR REMOTE, DEXTEROUS OPERATIONS Abstract Only
John A. Molino and Linda J. Langley *In* Tactical Weapons Guidance and Control Information Conference on Space and Military Applications of Automation and Robotics Jun. 1988 p 48 (For primary document see N89-24819 18-63)
Avail: NTIS HC A05/MF A01 CSCL 09B

N89-24844# Rockwell International Corp., Downey, CA.
ORU GUIDELINES FOR TELEROBOTIC COMPATIBILITY Abstract Only
Margaret M. Clarke and Davoud Manouchehri *In* Tactical Weapons Guidance and Control Information Conference on Space and Military Applications of Automation and Robotics Jun. 1988 p 49 (For primary document see N89-24819 18-63)
Avail: NTIS HC A05/MF A01 CSCL 09B

N89-24845# Teledyne Brown Engineering, Huntsville, AL.
GROUND CONTROL OF SPACE BASED ROBOTIC SYSTEMS Abstract Only
K. E. Farnell and S. F. Spearing *In* Tactical Weapons Guidance and Control Information Conference on Space and Military Applications of Automation and Robotics Jun. 1988 p 50 (For primary document see N89-24819 18-63)
Avail: NTIS HC A05/MF A01 CSCL 09B

N89-24846# Vanderbilt Univ., Nashville, TN.
A GENERALIZED METHOD FOR AUTOMATIC DOWNHAND AND WIREFEED CONTROL OF A WELDING ROBOT AND POSITIONER Abstract Only
Ken Fernandez and George E. Cook *In* Tactical Weapons Guidance and Control Information Conference on Space and Military Applications of Automation and Robotics Jun. 1988 p 54 (For primary document see N89-24819 18-63)
Avail: NTIS HC A05/MF A01 CSCL 09B

N89-24849*# Alabama Univ., Huntsville.
USING A SIMULATION ASSISTANT IN MODELING MANUFACTURING SYSTEMS Abstract Only
Bernard J. Schroer, Fan T. Tseng, S. X. Zhang, and John W. Wolfsberger *In* Tactical Weapons Guidance and Control Information Conference on Space and Military Applications of Automation and Robotics Jun. 1988 p 62 Prepared in cooperation with NASA. Marshall Space Flight Center, Huntsville, AL (For primary document see N89-24819 18-63)
Avail: NTIS HC A05/MF A01 CSCL 13I

N89-24850# Alabama Univ., Huntsville. Applied Optics Center.
ALGORITHM FOR DISPLAY OF AUTOMATED NONDESTRUCTIVE THICKNESS MEASUREMENTS Abstract Only
Jeroen vanderZijp *In* Tactical Weapons Guidance and Control Information Conference on Space and Military Applications of Automation and Robotics Jun. 1988 p 63 (For primary document see N89-24819 18-63)
Avail: NTIS HC A05/MF A01 CSCL 09B

N89-24852# Sandia National Labs., Albuquerque, NM.
A DEMONSTRATION OF RETRO-TRAVERSE USING A SEMI-AUTONOMOUS LAND VEHICLE Abstract Only
Douglas E. McGovern, Paul R. Klarer, and David P. Jons *In* Tactical Weapons Guidance and Control Information Conference on Space and Military Applications of Automation and Robotics Jun. 1988 p 66 (For primary document see N89-24819 18-63)
Avail: NTIS HC A05/MF A01 CSCL 09B

N89-24853# KMS Fusion, Inc., Ann Arbor, MI.
A KNOWLEDGE REPRESENTATION SCHEME FOR A ROBOTIC LAND VEHICLE ROUTE PLANNER Abstract Only
Patrick J. McNally *In* Tactical Weapons Guidance and Control Information Conference on Space and Military Applications of Automation and Robotics Jun. 1988 p 68 (For primary document see N89-24819 18-63)
Avail: NTIS HC A05/MF A01 CSCL 09B

N89-24854# Sparta, Inc., Huntsville, AL.
IRIS: AN INTELLIGENT ROBOT INSERTION EXPERT SYSTEM Abstract Only
William Teoh *In* Tactical Weapons Guidance and Control Information Conference on Space and Military Applications of Automation and Robotics Jun. 1988 p 69 (For primary document see N89-24819 18-63)
Avail: NTIS HC A05/MF A01 CSCL 09B

38 QUALITY ASSURANCE AND RELIABILITY

Includes product sampling procedures and techniques; and quality control.

N89-24622# Aerospatiale, Cannes La Bocca (France).
STUDY ON COST EFFICIENCY OF PRODUCT ASSURANCE IN SPACE PROGRAMS [ETUDE DES RAPPORTS COUT-EFFICACITE DE L'ASSURANCE PRODUIT DANS LES PROGRAMMES SPATIAUX]
Ph. Giudicelli 1988 7 p In FRENCH; ENGLISH summary (Rept-882-440-122; ETN-89-94515) Avail: NTIS HC A02/MF A01

Starting from survey of the European space industry the role played by product assurance methods was investigated. The subjects discussed include product assurance management, quality assurance, software quality, reliability/availability, safety aspects, high reliability procuring, and qualification procedures. It is concluded that a large effort to qualify personnel is necessary.
ESA

N89-24623*# National Aeronautics and Space Administration. Marshall Space Flight Center, Huntsville, AL.
A NONCONTACTING SCANNING PHOTOELECTRON EMISSION TECHNIQUE FOR BONDING SURFACE CLEANLINESS INSPECTION
Raymond L. Gause Feb. 1989 61 p
(NASA-TM-100361; NAS 1.15:100361) Avail: NTIS HC A04/MF A01 CSCL 14D

Molecular contamination of bonding surfaces can drastically affect the bond strength that can be achieved and therefore the structural integrity and reliability of the bonded part. The presence of thin contaminant films on bonding surfaces can result from inadequate or incomplete cleaning methods, from oxide growth during the time between cleaning (such as grit blasting) and bonding, or from failure to properly protect cleaned surfaces from oils, greases, fingerprints, release agents, or deposition of facility airborne molecules generated by adjacent manufacturing or processing operations. Required cleanliness levels for desired bond performance can be determined by testing to correlate bond strength with contaminant type and quantity, thereby establishing the degree of contamination that can be tolerated based on the strength that is needed. Once the maximum acceptable contaminant level is defined, a method is needed to quantitatively measure the contaminant level on the bonding surface prior to bonding to verify that the surface meets the established cleanliness requirement. A photoelectron emission technique for the nondestructive inspection of various bonding surfaces, both metallic and nonmetallic, to provide quantitative data on residual contaminant levels is described. The technique can be used to scan surfaces at speeds of at least 30 ft/min using a servo system to maintain required sensor to surface spacing. The fundamental

operation of the photoelectron emission sensor system is explained and the automated scanning system and computer data acquisition hardware and software are described. Author

39 STRUCTURAL MECHANICS

Includes structural element design and weight analysis; fatigue; and thermal stress.

For applications see *05 Aircraft Design, Testing and Performance* and *18 Spacecraft Design, Testing and Performance.*

N89-24624*# National Aeronautics and Space Administration. Langley Research Center, Hampton, VA.
CSM TESTBED DEVELOPMENT AND LARGE-SCALE STRUCTURAL APPLICATIONS
Norman F. Knight, Jr., R. E. Gillian, Susan L. McCleary, C. G. Lotts, E. L. Poole, A. L. Overman, and S. C. Macy (Planning Research Corp., Washington, DC.) Washington Apr. 1989 25 p Original contains color illustrations
(NASA-TM-4072; L-16499; NAS 1.15:4072) Avail: NTIS HC A03/MF A01 CSCL 20K

A research activity called Computational Structural Mechanics (CSM) conducted at the NASA Langley Research Center is described. This activity is developing advanced structural analysis and computational methods that exploit high-performance computers. Methods are developed in the framework of the CSM Testbed software system and applied to representative complex structural analysis problems from the aerospace industry. An overview of the CSM Testbed methods development environment is presented and some new numerical methods developed on a CRAY-2 are described. Selected application studies performed on the NAS CRAY-2 are also summarized. Author

N89-24625# National Aerospace Lab., Tokyo (Japan).
ANALYSIS OF ADAPTIVE PLANAR TRUSS STRUCTURES
Aug. 1988 26 p In JAPANESE; ENGLISH summary
(NAL-TR-988; ISSN-0389-4010) Avail: NTIS HC A03/MF A01

The structural concept of adaptive planar truss structures is evaluated from the viewpoints of both geometrical adaptivity and dynamic characteristics, and an attempt is made to clarify the basic idea concerning what kind of adaptive planar truss structures are desirable to realize the concept in real structure hardware. The basic octet elements for planar truss structures and their various modified configurations, including cube elements, are arranged for the idea of adaptive elements. Two ways of obtaining an appropriate curved surface from a flat truss structure, that is, the bending concept and the shear concept, are related to the adaptive elements. Two ways of obtaining an appropriate curved surface from a flat truss structure, that is, the bending concept and the shear concept, are related to the adaptive elements. Stiffness properties of some basic adaptive planar truss structures, which consist of cube elements, in a comparatively moderate or small scale are investigated through vibration analysis using the Finite Element Method (FEM). Vibration characteristics for various configurations, such as flat, parabolic cylinder, elliptic paraboloid and hyperbolic paraboloid are shown. Author

N89-24626*# National Aeronautics and Space Administration. Langley Research Center, Hampton, VA.
RESEARCH IN STRUCTURES, STRUCTURAL DYNAMICS AND MATERIALS, 1989
William F. Hunter, comp. and Ahmed K. Noor, comp. (George Washington Univ., Hampton, VA.) Apr. 1989 88 p Proceedings of the AIAA/ASME/ASCE/AHS/ASC 30th Structures, Structural Dynamics and Materials Conference, Mobile, AL, 3-5 Apr. 1989
(NASA-CP-10024; NAS 1.55:10024) Avail: NTIS HC A05/MF A01 CSCL 20K

Topics addressed include: composite plates; buckling predictions; missile launch tube modeling; structural/control systems design; optimization of nonlinear R/C frames; error analysis for semi-analytic displacement; crack acoustic emission; and structural dynamics. For individual titles, see N89-24627 through N89-24633.

N89-24627*# Texas A&M Univ., College Station. Dept. of Mechanical Engineering.
A STUDY OF COMPOSITE PLATES WITH HOLES/INCLUSIONS
Ronald Bense and Ozden Ochoa *In* NASA, Langley Research Center, Research in Structures, Structural Dynamics and Materials, 1989 Apr. 1989 p 3-12 (For primary document see N89-24626 18-39)
Avail: NTIS HC A05/MF A01 CSCL 20K

Delamination characterization of a plate with a hole/inclusion is presented. A closed form solution is developed to obtain stresses on the boundary of hole/inclusion in the plate. Once the location with the highest tangential stress is identified, a Finite Element Method analysis of a laminate under tensile loading is considered. The models are presented for the closed form and Finite Element Method. The examples are for (+ or - 35/0/90)s laminate of AS4/3501-6. Tensile, biaxial, and shear loads are considered. Author

N89-24628*# Rockwell International Corp., Downey, CA. Space Transportation Systems Div.
LOCAL STIFFENER AND SKIN POCKET BUCKLING PREDICTION BY SPECIAL PASCO MODELING TECHNIQUE: CORRELATION TO TEST DATA
Dah N. Yin, Vu M. Tran, and Patrick M. Swift *In* NASA, Langley Research Center, Research in Structures, Structural Dynamics and Materials, 1989 Apr. 1989 p 13-21 (For primary document see N89-24626 18-39)
Avail: NTIS HC A05/MF A01 CSCL 20K

Waffle panels are often used on fuselage structures such as that of the Space Shuttle. The waffle panel design is an efficient design for carrying biaxial, in-plane, and shear loads. The WAFFLE program was designed for application on waffle panels. The Panel Analysis and Sizing Code (PASCO) program was designed for analyzing and sizing uniaxially stiffened panels. The application of the PASCO program in conjunction with the WAFFLE program is discussed to account for both the fillet radius and the presence of stiffness in both directions. The results of the tests are used to verify that these adjustments are valid and necessary if accurate analysis of the waffle panel is to be achieved. B.G.

N89-24629*# Kaman Aerospace Corp., Bloomfield, CT.
MODELING THE MISSILE-LAUNCH TUBE PROBLEM IN DYSCO
Alex Berman and Bruce A. Gustavson *In* NASA, Langley Research Center, Research in Structures, Structural Dynamics and Materials, 1989 Apr. 1989 p 23-33 (For primary document see N89-24626 18-39)
Avail: NTIS HC A05/MF A01 CSCL 20K

DYSCO is a versatile, general purpose dynamic analysis program which assembles equations and solves dynamics problems. The executive manages a library of technology modules which contain routines that compute the matrix coefficients of the second order ordinary differential equations of the components. The executive performs the coupling of the equations of the components and manages the solution of the coupled equations. Any new component representation may be added to the library if, given the state vector, a FORTRAN program can be written to compute M, C, K, and F. The problem described demonstrates the generality of this statement. Author

N89-24630*# TRW Space Technology Labs., Los Angeles, CA.
INFLUENCE OF TIME LAG AND NONCOLOCATION ON INTEGRATED STRUCTURAL/CONTROL SYSTEM DESIGNS
R. A. Manning and L. A. Schmit (California Univ., Los Angeles.) *In* NASA, Langley Research Center, Research in Structures, Structural Dynamics and Materials, 1989 Apr. 1989 p 35-45 (For primary document see N89-24626 18-39)

(Grant NsG-1490)
Avail: NTIS HC A05/MF A01 CSCL 20K

Recent research efforts have led to the development of simultaneous structural/control system design procedures. Absent in any of the work is the time delay present in the control system sensors and actuators and the computational time delay for synthesizing actuator commands from sensor measurements. Madden has shown that the time delay present in the control system can have profound effects on the resulting system performance and stability regardless of its source. In addition, many of the simultaneous structural/control system design procedures have used colocated sensors and actuators for implementation of the control system. In actual practice, colocation in not always possible. The issue of stability degradation when using noncolocated sensor and actuators was raised. The integrated structural/control system design procedure is extended to include the effects of time lag and noncolocation of sensors and actuators on the resulting optimum designs. Author

N89-24631*# Florida Univ., Gainesville. Dept. of Civil Engineering.

INTEGRATED OPTIMIZATION OF NONLINEAR R/C FRAMES WITH RELIABILITY CONSTRAINTS

Alfredo Soeiro and Marc Hoit *In* NASA, Langley Research Center, Research in Structures, Structural Dynamics and Materials, 1989 Apr. 1989 p 47-54 (For primary document see N89-24626 18-39)
Avail: NTIS HC A05/MF A01 CSCL 20K

A structural optimization algorithm was researched including global displacements as decision variables. The algorithm was applied to planar reinforced concrete frames with nonlinear material behavior submitted to static loading. The flexural performance of the elements was evaluated as a function of the actual stress-strain diagrams of the materials. Formation of rotational hinges with strain hardening were allowed and the equilibrium constraints were updated accordingly. The adequacy of the frames was guaranteed by imposing as constraints required reliability indices for the members, maximum global displacements for the structure and a maximum system probability of failure. Author

N89-24632*# General Motors Research Labs., Warren, MI. Dept. of Engineering Mechanics.

ERROR ANALYSIS FOR SEMI-ANALYTIC DISPLACEMENT DERIVATIVES WITH RESPECT TO SHAPE AND SIZING VARIABLES

Peter A. Fenyes and Robert V. Lust *In* NASA, Langley Research Center, Research in Structures, Structural Dynamics and Materials, 1989 Apr. 1989 p 55-66 (For primary document see N89-24626 18-39)
Avail: NTIS HC A05/MF A01 CSCL 20K

Sensitivity analysis is fundamental to the solution of structural optimization problems. Consequently, much research has focused on the efficient computation of static displacement derivatives. As originally developed, these methods relied on analytical representations for the derivatives of the structural stiffness matrix (K) with respect to the design variables (b sub i). To extend these methods for use with complex finite element formulations and facilitate their implementation into structural optimization programs using the general finite element method analysis codes, the semi-analytic method was developed. In this method the matrix the derivative of K/the derivative b sub i is approximated by finite difference. Although it is well known that the accuracy of the semi-analytic method is dependent on the finite difference parameter, recent work has suggested that more fundamental inaccuracies exist in the method when used for shape optimization. Another study has argued qualitatively that these errors are related to nonuniform errors in the stiffness matrix derivatives. The accuracy of the semi-analytic method is investigated. A general framework was developed for the error analysis and then it is shown analytically that the errors in the method are entirely accounted for by errors in delta K/delta b sub i. Furthermore, it is demonstrated that acceptable accuracy in the derivatives can be obtained through careful selection of the finite difference parameter. Author

N89-24633*# Georgia Inst. of Tech., Atlanta. Engineering Science and Mechanics Program.

ACOUSTIC EMISSION FROM A GROWING CRACK

Laurence J. Jacobs *In* NASA, Langley Research Center, Research in Structures, Structural Dynamics and Materials, 1989 Apr. 1989 p 67-76 (For primary document see N89-24626 18-39)
Avail: NTIS HC A05/MF A01 CSCL 20K

An analytical method is being developed to determine the signature of an acoustic emission waveform from a growing crack and the results of this analysis are compared to experimentally obtained values. Within the assumptions of linear elastic fracture mechanics, a two dimensional model is developed to examine a semi-infinite crack that, after propagating with a constant velocity, suddenly stops. The analytical model employs an integral equation method for the analysis of problems of dynamic fracture mechanics. The experimental procedure uses an interferometric apparatus that makes very localized absolute measurements with very high fidelity and without acoustically loading the specimen. Author

N89-24634*# Texas A&M Univ., College Station. Dept. of Aerospace Engineering.

A STUDY OF MATERIAL DAMPING IN LARGE SPACE STRUCTURES Final Technical Report

A. L. Highsmith and D. H. Allen Apr. 1989 78 p
(Grant NAG9-192)
(NASA-CR-180076; NAS 1.26:180076; MM-5679-89-9) Avail: NTIS HC A05/MF A01 CSCL 20K

A constitutive model was developed for predicting damping as a function of damage in continuous fiber reinforced laminated composites. The damage model is a continuum formulation, and uses internal state variables to quantify damage and its subsequent effect on material response. The model is sensitive to the stacking sequence of the laminate. Given appropriate baseline data from unidirectional material, and damping as a function of damage in one crossply laminate, damage can be predicted as a function of damage in other crossply laminates. Agreement between theory and experiment was quite good. A micromechanics model was also developed for examining the influence of damage on damping. This model explicitly includes crack surfaces. The model provides reasonable predictions of bending stiffness as a function of damage. Damping predictions are not in agreement with the experiment. This is thought to be a result of dissipation mechanisms such as friction, which are not presently included in the analysis. Author

N89-24635*# National Aeronautics and Space Administration. Lewis Research Center, Cleveland, OH.

TRIBOLOGY: THE STORY OF LUBRICATION AND WEAR

Donald H. Buckley, William R. Jones, Jr., Harold E. Sliney, Erwin V. Zaretsky, Dennis P. Townsend, and Stuart H. Loewenthal 1985 145 p Seminar F-107 held in Cleveland, OH, 18 Oct. 1985
(NASA-TM-101430; E-4535; NAS 1.15:101430) Avail: NTIS HC A07/MF A01 CSCL 20K

Topics addressed include: lubrication and design of high speed rolling element bearings, high speed gears, and traction drives. For individual titles, see N89-24636 through N89-24636.

N89-24636*# National Aeronautics and Space Administration. Lewis Research Center, Cleveland, OH.

SOLID LUBRICANT MATERIALS FOR HIGH TEMPERATURES: A REVIEW

Harold E. Sliney *In its* Tribology: The Story of Lubrication and Wear 1985 p 55-81 Submitted for publication (For primary document see N89-24635 18-39)
Avail: NTIS HC A07/MF A01 CSCL 20K

Solid lubricants that can be used above 300 C in air are discussed, including coatings and self-lubricating composite bearing materials. The lubricants considered are representative dichalcogenides, graphite, graphite fluoride, polyimides, soft oxides,

oxidatively stable fluorides, and hard coating materials. A few general design considerations revelant to solid lubrication are interspersed. Author

N89-24637*# Lockheed Missiles and Space Co., Palo Alto, CA. Research and Development Div.
THE COMPUTATIONAL STRUCTURAL MECHANICS TESTBED ARCHITECTURE. VOLUME 5: THE INPUT-OUTPUT MANAGER DMGASP
Carlos A. Felippa (Colorado Univ., Boulder.) Mar. 1989 158 p (Contract NAS1-18444)
(NASA-CR-178388; NAS 1.26:178388; LMSC-D878511-Vol-5)
Avail: NTIS HC A08/MF A01 CSCL 20K

This is the fifth of a set of five volumes which describe the software architecture for the Computational Structural Mechanics Testbed. Derived from NICE, an integrated software system developed at Lockheed Palo Alto Research Laboratory, the architecture is composed of the command language (CLAMP), the command language interpreter (CLIP), and the data manager (GAL). Volumes 1, 2, and 3 (NASA CR's 178384, 178385, and 178386, respectively) describe CLAMP and CLIP and the CLIP-processor interface. Volumes 4 and 5 (NASA CR's 178387 and 178388, respectively) describe GAL and its low-level I/O. CLAMP, an acronym for Command Language for Applied Mechanics Processors, is designed to control the flow of execution of processors written for NICE. Volume 5 describes the low-level data management component of the NICE software. It is intended only for advanced programmers involved in maintenance of the software. Author

N89-24638*# National Aeronautics and Space Administration. Langley Research Center, Hampton, VA.
COMPUTATIONAL METHODS FOR STRUCTURAL MECHANICS AND DYNAMICS, PART 1
W. Jefferson Stroud, ed., Jerrold M. Housner, ed., John A. Tanner, ed., and Robert J. Hayduk, ed. Washington May 1989 329 p Workshop held in Hampton, VA, 19-21 Jun. 1985
(NASA-CP-3034-Pt-1; L-16560-Pt-1; NAS 1.55:3034-Pt-1) Avail: NTIS HC A15/MF A01 CSCL 20K

The structural analysis methods research has several goals. One goal is to develop analysis methods that are general. This goal of generality leads naturally to finite-element methods, but the research will also include other structural analysis methods. Another goal is that the methods be amenable to error analysis; that is, given a physical problem and a mathematical model of that problem, an analyst would like to know the probable error in predicting a given response quantity. The ultimate objective is to specify the error tolerances and to use automated logic to adjust the mathematical model or solution strategy to obtain that accuracy. A third goal is to develop structural analysis methods that can exploit parallel processing computers. The structural analysis methods research will focus initially on three types of problems: local/global nonlinear stress analysis, nonlinear transient dynamics, and tire modeling. For individual titles, see N89-24639 through N89-24653.

N89-24639*# Hibbitt, Karlsson and Sorensen, Providence, RI.
SOME ISSUES IN NUMERICAL SIMULATION OF NONLINEAR STRUCTURAL RESPONSE
H. D. Hibbitt *In* NASA, Langley Research Center, Computational Methods for Structural Mechanics and Dynamics, Part 1 May 1989 p 7-23 (For primary document see N89-24638 18-39)
Avail: NTIS HC A15/MF A01 CSCL 20K

The development of commercial finite element software is addressed. This software provides practical tools that are used in an astonishingly wide range of engineering applications that include critical aspects of the safety evaluation of nuclear power plants or of heavily loaded offshore structures in the hostile environments of the North Sea or the Arctic, major design activities associated with the development of airframes for high strength and minimum weight, thermal analysis of electronic components, and the design of sports equipment. In the more advanced application areas, the effectiveness of the product depends critically on the quality of the mechanics and mechanics related algorithms that are implemented. Algorithmic robustness is of primary concern. Those methods that should be chosen will maximize reliability with minimal understanding on the part of the user. Computational efficiency is also important because there are always limited resources, and hence problems that are too time consuming or costly. Finally, some areas where research work will provide new methods and improvements is discussed. Author

N89-24640*# Boeing Military Airplane Development, Seattle, WA.
COMPUTERIZED STRUCTURAL MECHANICS FOR 1990'S: ADVANCED AIRCRAFT NEEDS
A. V. Viswanathan and B. F. Backman *In* NASA, Langley Research Center, Computational Methods for Structural Mechanics and Dynamics, Part 1 May 1989 p 25-49 (For primary document see N89-24638 18-39)
Avail: NTIS HC A15/MF A01 CSCL 20K

The needs for computerized structural mechanics (CSM) as seen from the standpoint of the aircraft industry are discussed. These needs are projected into the 1990's with special focus on the new advanced materials. Preliminary design/analysis, research, and detail design/analysis are identified as major areas. The role of local/global analyses in these different areas is discussed. The lessons learned in the past are used as a basis for the design of a CSM framework that could modify and consolidate existing technology and include future developments in a rational and useful way. A philosophy is stated, and a set of analyses needs driven by the emerging advanced composites is enumerated. The roles of NASA, the universities, and the industry are identified. Finally, a set of rational research targets is recommended based on both the new types of computers and the increased complexity the industry faces. Computerized structural mechanics should be more than new methods in structural mechanics and numerical analyses. It should be a set of engineering applications software products that combines innovations in structural mechanics, numerical analysis, data processing, search and display features, and recent hardware advances and is organized in a framework that directly supports the design process. Author

N89-24641*# National Aeronautics and Space Administration. Langley Research Center, Hampton, VA.
NONLINEAR RESPONSE OF A BLADE-STIFFENED GRAPHITE-EPOXY PANEL WITH A DISCONTINUOUS STIFFENER: WORK IN PROGRESS
Norman F. Knight, Jr., William H. Greene, and W. Jefferson Stroud *In its* Computational Methods for Structural Mechanics and Dynamics, Part 1 May 1989 p 51-65 (For primary document see N89-24638 18-39)
Avail: NTIS HC A15/MF A01 CSCL 20K

The problem of calculating detailed stress distributions around discontinuities in buckled, composite structural components for use with the various analytical failure prediction techniques has not been thoroughly explored. The purpose here is the application of computational methods to the detailed stress analysis problem which is the focus of this session of the workshop. One approach to uncovering the difficulties of this type of analysis and to providing specific directions for future research in this area is a direct attack on the problem using currently available analysis tools. A candidate problem has been selected and experiences from calculating its structural response are described. Author

N89-24642*# Lockheed Missiles and Space Co., Palo Alto, CA.
COMPUTATIONAL PROCEDURES FOR POSTBUCKLING OF COMPOSITE SHELLS
G. M. Stanley and Carlos A. Felippa *In* NASA, Langley Research Center, Computational Methods for Structural Mechanics and Dynamics, Part 1 May 1989 p 67-87 (For primary document see N89-24638 18-39)
Avail: NTIS HC A15/MF A01 CSCL 20K

A recently developed finite-element capability for general nonlinear shell analysis, featuring the use of three-dimensional constitutive equations within an efficient resultant-oriented

framework, is employed to simulate the postbuckling response of an axially compressed composite cylindrical panel with a circular cutout. The problem is a generic example of modern composite aircraft components for which postbuckling strength (i.e., fail-safety) is desired in the presence of local discontinuities such as holes and cracked stiffeners. While the computational software does a reasonable job of predicting both the buckling load and the qualitative aspects of postbuckling (compared both with experiment and another code) there are some discrepancies due to: (1) uncertainties in the nominal layer material properties, (2) structural sensitivity to initial imperfections, and (3) the neglect of dynamic and local material delamination effects in the numerical model. Corresponding refinements are suggested for the realistic continuation of this type of analysis. Author

N89-24643*# California Univ., Los Angeles.
A REVIEW OF SOME PROBLEMS IN GLOBAL-LOCAL STRESS ANALYSIS
Richard B. Nelson *In* NASA, Langley Research Center, Computational Methods for Structural Mechanics and Dynamics, Part 1 May 1989 p 89-101 (For primary document see N89-24638 18-39)
Avail: NTIS HC A15/MF A01 CSCL 20K

The various types of local-global finite-element problems point out the need to develop a new generation of software. First, this new software needs to have a complete analysis capability, encompassing linear and nonlinear analysis of 1-, 2-, and 3-dimensional finite-element models, as well as mixed dimensional models. The software must be capable of treating static and dynamic (vibration and transient response) problems, including the stability effects of initial stress, and the software should be able to treat both elastic and elasto-plastic materials. The software should carry a set of optional diagnostics to assist the program user during model generation in order to help avoid obvious structural modeling errors. In addition, the program software should be well documented so the user has a complete technical reference for each type of element contained in the program library, including information on such topics as the type of numerical integration, use of underintegration, and inclusion of incompatible modes, etc. Some packaged information should also be available to assist the user in building mixed-dimensional models. An important advancement in finite-element software should be in the development of program modularity, so that the user can select from a menu various basic operations in matrix structural analysis. Author

N89-24644*# Georgia Inst. of Tech., Atlanta.
SOME COMMENTS ON GLOBAL-LOCAL ANALYSES
Satya N. Atluri *In* NASA, Langley Research Center, Computational Methods for Structural Mechanics and Dynamics, Part 1 May 1989 p 103-121 (For primary document see N89-24638 18-39)
Avail: NTIS HC A15/MF A01 CSCL 20K

The main theme concerns methods that may be classified as global (approximate) and local (exact). Some specific applications of these methods are found in: fracture and fatigue analysis of structures with 3-D surface flaws; large-deformation, post-buckling analysis of large space trusses and space frames, and their control; and stresses around holes in composite laminates. Author

N89-24645*# Virginia Polytechnic Inst. and State Univ., Blacksburg.
ON COMPUTATIONAL SCHEMES FOR GLOBAL-LOCAL STRESS ANALYSIS
J. N. Reddy *In* NASA, Langley Research Center, Computational Methods for Structural Mechanics and Dynamics, Part 1 May 1989 p 123-134 (For primary document see N89-24638 18-39)
Avail: NTIS HC A15/MF A01 CSCL 20K

An overview is given of global-local stress analysis methods and associated difficulties and recommendations for future research. The phrase global-local analysis is understood to be an analysis in which some parts of the domain or structure are identified, for reasons of accurate determination of stresses and displacements or for more refined analysis than in the remaining parts. The parts of refined analysis are termed local and the remaining parts are called global. Typically local regions are small in size compared to global regions, while the computational effort can be larger in local regions than in global regions. Author

N89-24646*# California Univ., Los Angeles.
GLOBAL FUNCTIONS IN GLOBAL-LOCAL FINITE-ELEMENT ANALYSIS OF LOCALIZED STRESSES IN PRISMATIC STRUCTURES
Stanley B. Dong *In* NASA, Langley Research Center, Computational Methods for Structural Mechanics and Dynamics, Part 1 May 1989 p 135-149 (For primary document see N89-24638 18-39)
Avail: NTIS HC A15/MF A01 CSCL 20K

An important consideration in the global local finite-element method (GLFEM) is the availability of global functions for the given problem. The role and mathematical requirements of these global functions in a GLFEM analysis of localized stress states in prismatic structures are discussed. A method is described for determining these global functions. Underlying this method are theorems due to Toupin and Knowles on strain energy decay rates, which are related to a quantitative expression of Saint-Venant's principle. It is mentioned that a mathematically complete set of global functions can be generated, so that any arbitrary interface condition between the finite element and global subregions can be represented. Convergence to the true behavior can be achieved with increasing global functions and finite-element degrees of freedom. Specific attention is devoted to mathematically two-dimensional and three-dimensional prismatic structures. Comments are offered on the GLFEM analysis of NASA flat panel with a discontinuous stiffener. Methods for determining global functions for other effects are also indicated, such as steady-state dynamics and bodies under initial stress. Author

N89-24647*# George Washington Univ., Hampton, VA.
GLOBAL-LOCAL METHODOLOGIES AND THEIR APPLICATION TO NONLINEAR ANALYSIS
Ahmed K. Noor *In* NASA, Langley Research Center, Computational Methods for Structural Mechanics and Dynamics, Part 1 May 1989 p 151-167 (For primary document see N89-24638 18-39)
Avail: NTIS HC A15/MF A01 CSCL 20K

An assessment is made of the potential of different global-local analysis strategies for predicting the nonlinear and postbuckling responses of structures. Two postbuckling problems of composite panels are used as benchmarks and the application of different global-local methodologies to these benchmarks is outlined. The key elements of each of the global-local strategies are discussed and future research areas needed to realize the full potential of global-local methodologies are identified. Author

N89-24648*# Washington Univ., Saint Louis, MO.
APPLICATION OF THE p-VERSION OF THE FINITE-ELEMENT METHOD TO GLOBAL-LOCAL PROBLEMS
Barna A. Szabo *In* NASA, Langley Research Center, Computational Methods for Structural Mechanics and Dynamics, Part 1 May 1989 p 169-178 (For primary document see N89-24638 18-39)
Avail: NTIS HC A15/MF A01 CSCL 20K

A brief survey is given of some recent developments in finite-element analysis technology which bear upon the three main research areas under consideration in this workshop: (1) analysis methods; (2) software testing and quality assurance; and (3) parallel processing. The variational principle incorporated in a finite-element computer program, together with a particular set of input data, determines the exact solution corresponding to that input data. Most finite-element analysis computer programs are based on the principle of virtual work. In the following, researchers consider only programs based on the principle of virtual work and denote the exact displacement vector field corresponding to some specific set of input data by vector u(EX). The exact solution vector u(EX)

is independent of the design of the mesh or the choice of elements. Except for very simple problems, or specially constructed test problems, vector u(EX) is not known. Researchers perform a finite-element analysis (or any other numerical analysis) because they wish to make conclusions concerning the response of a physical system to certain imposed conditions, as if vector u(EX) were known. Author

N89-24649*# Goodrich (B. F.) Co., Akron, OH.
FEATURES AND CHARACTERIZATION NEEDS OF RUBBER COMPOSITE STRUCTURES **c27**
Farhad Tabaddor *In* NASA, Langley Research Center, Computational Methods for Structural Mechanics and Dynamics, Part 1 May 1989 p 211-247 (For primary document see N89-24638 18-39)
Avail: NTIS HC A15/MF A01 CSCL 11C

Some of the major unique features of rubber composite structures are outlined. The features covered are those related to the material properties, but the analytical features are also briefly discussed. It is essential to recognize these features at the planning stage of any long-range analytical, experimental, or application program. The development of a general and comprehensive program which fully accounts for all the important characteristics of tires, under all the relevant modes of operation, may present a prohibitively expensive and impractical task at the near future. There is therefore a need to develop application methodologies which can utilize the less general models, beyond their theoretical limitations and yet with reasonable reliability, by proper mix of analytical, experimental, and testing activities. Author

N89-24650*# Akron Univ., OH.
NONLINEAR HIERARCHICAL SUBSTRUCTURAL PARALLELISM AND COMPUTER ARCHITECTURE **c62**
Joe Padovan *In* NASA, Langley Research Center, Computational Methods for Structural Mechanics and Dynamics, Part 1 May 1989 p 249-267 (For primary document see N89-24638 18-39)
Avail: NTIS HC A15/MF A01 CSCL 09B

Computer architecture is investigated in conjunction with the algorithmic structures of nonlinear finite-element analysis. To help set the stage for this goal, the development is undertaken by considering the wide-ranging needs associated with the analysis of rolling tires which possess the full range of kinematic, material and boundary condition induced nonlinearity in addition to gross and local cord-matrix material properties. Author

N89-24651*# Texas Univ., Austin.
ADAPTIVE METHODS, ROLLING CONTACT, AND NONCLASSICAL FRICTION LAWS **c37**
J. T. Oden *In* NASA, Langley Research Center, Computational Methods for Structural Mechanics and Dynamics, Part 1 May 1989 p 269-289 (For primary document see N89-24638 18-39)
Avail: NTIS HC A15/MF A01 CSCL 13I

Results and methods on three different areas of contemporary research are outlined. These include adaptive methods, the rolling contact problem for finite deformation of a hyperelastic or viscoelastic cylinder, and non-classical friction laws for modeling dynamic friction phenomena. Author

N89-24652*# Texas A&M Univ., College Station.
CONTACT SOLUTION ALGORITHMS **c61**
John T. Tielking *In* NASA, Langley Research Center, Computational Methods for Structural Mechanics and Dynamics, Part 1 May 1989 p 291-316 (For primary document see N89-24638 18-39)
Avail: NTIS HC A15/MF A01 CSCL 09B

Two algorithms for obtaining static contact solutions are described in this presentation. Although they were derived for contact problems involving specific structures (a tire and a solid rubber cylinder), they are sufficiently general to be applied to other shell-of-revolution and solid-body contact problems. The shell-of-revolution contact algorithm is a method of obtaining a point load influence coefficient matrix for the portion of shell surface that is expected to carry a contact load. If the shell is sufficiently linear with respect to contact loading, a single influence coefficient matrix can be used to obtain a good approximation of the contact pressure distribution. Otherwise, the matrix will be updated to reflect nonlinear load-deflection behavior. The solid-body contact algorithm utilizes a Lagrange multiplier to include the contact constraint in a potential energy functional. The solution is found by applying the principle of minimum potential energy. The Lagrange multiplier is identified as the contact load resultant for a specific deflection. At present, only frictionless contact solutions have been obtained with these algorithms. A sliding tread element has been developed to calculate friction shear force in the contact region of the rolling shell-of-revolution tire model. Author

N89-24653*# National Aeronautics and Space Administration. Langley Research Center, Hampton, VA.
EXPLOITING SYMMETRIES IN THE MODELING AND ANALYSIS OF TIRES **c37**
Ahmed K. Noor, C. M. Andersen, and John A. Tanner *In its* Computational Methods for Structural Mechanics and Dynamics, Part 1 May 1989 p 317-329 (For primary document see N89-24638 18-39)
Avail: NTIS HC A15/MF A01 CSCL 13I

A computational procedure is presented for reducing the size of the analysis models of tires having unsymmetric material, geometry and/or loading. The two key elements of the procedure when applied to anisotropic tires are: (1) decomposition of the stiffness matrix into the sum of an orthotropic and nonorthotropic parts; and (2) successive application of the finite-element method and the classical Rayleigh-Ritz technique. The finite-element method is first used to generate few global approximation vectors (or modes). Then the amplitudes of these modes are computed by using the Rayleigh-Ritz technique. The proposed technique has high potential for handling practical tire problems with anisotropic materials, unsymmetric imperfections and asymmetric loading. It is also particularly useful for use with three-dimensional finite-element models of tires. Author

N89-24654*# National Aeronautics and Space Administration. Langley Research Center, Hampton, VA.
COMPUTATIONAL METHODS FOR STRUCTURAL MECHANICS AND DYNAMICS
W. Jefferson Stroud, ed., Jerrold M. Housner, ed., John A. Tanner, ed., and Robert J. Hayduk, ed. Washington May 1989 256 p Workshop held in Hampton, VA, 19-21 Jun. 1985
(NASA-CP-3034-Pt-2; L-16560-Pt-2; NAS 1.55:3034-Pt-2) Avail: NTIS HC A12/MF A01 CSCL 20K

Topics addressed include: transient dynamics; transient finite element method; transient analysis in impact and crash dynamic studies; multibody computer codes; dynamic analysis of space structures; multibody mechanics and manipulators; spatial and coplanar linkage systems; flexible body simulation; multibody dynamics; dynamical systems; and nonlinear characteristics of joints. For individual titles, see N89-24655 through N89-24668.

N89-24655*# National Aeronautics and Space Administration. Ames Research Center, Moffett Field, CA.
IMPROVING TRANSIENT ANALYSIS TECHNOLOGY FOR AIRCRAFT STRUCTURES
R. J. Melosh (Duke Univ., Durham, NC.) and Mladen Chargin *In* NASA, Langley Research Center, Computational Methods for Structural Mechanics and Dynamics May 1989 p 343-353 (For primary document see N89-24654 18-39)
Avail: NTIS HC A12/MF A01 CSCL 20K

Aircraft dynamic analyses are demanding of computer simulation capabilities. The modeling complexities of semi-monocoque construction, irregular geometry, high-performance materials, and high-accuracy analysis are present. At issue are the safety of the passengers and the integrity of the structure for a wide variety of flight-operating and emergency conditions. The technology which supports engineering of aircraft structures using computer simulation is examined. Available computer support is briefly

described and improvement of accuracy and efficiency are recommended. Improved accuracy of simulation will lead to a more economical structure. Improved efficiency will result in lowering development time and expense. Author

N89-24656*# Northwestern Univ., Evanston, IL.
EXPLICIT, IMPLICIT, AND HYBRID METHODS
T. Belytschko *In* NASA, Langley Research Center, Computational Methods for Structural Mechanics and Dynamics May 1989 p 355-368 (For primary document see N89-24654 18-39)
Avail: NTIS HC A12/MF A01 CSCL 20K

Time integration methods can be separated into two groups: explicit and implicit. Methods which do not involve the solution of any algebraic equations are called explicit, while those that require the solution of equations are called implicit. The relative advantages and disadvantages of explicit and implicit methods are summarized. The major trend in the past decade of research was to use hybrization methods to take advantage of the complementary nature of the positive attributes of explicit and implicit integration. These trends are briefly discussed. B.G.

N89-24657*# Brown Univ., Providence, RI. Div. of Engineering.
UNCONDITIONALLY STABLE CONCURRENT PROCEDURES FOR TRANSIENT FINITE-ELEMENT ANALYSIS
Michael Ortiz and Bahram Nour-Omid (California Univ., Berkeley.) *In* NASA, Langley Research Center, Computational Methods for Structural Mechanics and Dynamics May 1989 p 369-381 (For primary document see N89-24654 18-39)
Avail: NTIS HC A12/MF A01 CSCL 20K

A family of algorithms was outlined which would appear to be particularly well-suited for implementation in a parallel environment. This is due to the fact that for any partition of the mesh each subdomain in the partition can be processed over a time step simultaneously and independently of the rest. The method eliminates the need for assembling and factorizing large global arrays while retaining the unconditional stability properties of the algorithms used at the local level. To critically appraise the proposed methodology, two limiting cases were considered: element-by-element mesh partitions, and coarse mesh partitions. It was concluded that while the proposed methodology can be useful in sequential machines, it would appear to be promising as it bears on computation. It should also be emphasized that extensions of the method to nonlinear problems are possible.
Author

N89-24658*# Grumman Aerospace Corp., Bethpage, NY.
TRANSIENT ANALYSIS TECHNIQUES IN PERFORMING IMPACT AND CRASH DYNAMIC STUDIES
A. B. Pifko and R. Winter *In* NASA, Langley Research Center, Computational Methods for Structural Mechanics and Dynamics May 1989 p 383-406 (For primary document see N89-24654 18-39)
Avail: NTIS HC A12/MF A01 CSCL 20K

Because of the emphasis being placed on crashworthiness as a design requirement, increasing demands are being made by various organizations to analyze a wide range of complex structures that must perform safely when subjected to severe impact loads, such as those generated in a crash event. The ultimate goal of crashworthiness design and analysis is to produce vehicles with the ability to reduce the dynamic forces experienced by the occupants to specified levels, while maintaining a survivable envelope around them during a specified crash event. DYCAST is a nonlinear structural dynamic finite element computer code that started from the plans systems of a finite element program for static nonlinear structural analysis. The essential features of DYCAST are outlined. B.G.

N89-24659*# Lawrence Livermore National Lab., CA.
APPLICATION AND IMPLEMENTATION OF TRANSIENT ALGORITHMS IN COMPUTER PROGRAMS **c61**
David J. Benson *In* NASA, Langley Research Center, Computational Methods for Structural Mechanics and Dynamics May 1989 p 407-418 Previously announced as N86-15968 (For primary document see N89-24654 18-39)
(Contract W-7405-eng-48)
Avail: NTIS HC A12/MF A01 CSCL 09B

A brief introduction is given to the nonlinear finite element programs developed at Lawrence Livermore National Laboratory. The four programs are DYNA3D and DYNA2D, which are explicit hydrocodes, and NIKE3D and NIKE2D, which are implicit programs. The main emphasis is on DYNA3D with asides about the other programs. During the past year several new features were added to DYNA3D, and major improvements were made in the computational efficiency of the shell and beam elements. Most of these new features and improvements will eventually make their way into the other programs. The emphasis in the computational mechanics effort was always, and continues to be, efficiency. To get the most out of the supercomputers, all Crays, the programs were vectorized where possible. Several of the more interesting capabilities of DYNA3D will be described and the impact on efficiency will be discussed. Some of the recent work on NIKE3D and NIKE2D will also be presented. In the belief that a single example is worth a thousand equations, the theory is skipped entirely and the examples presented. DOE

N89-24660*# National Aeronautics and Space Administration. Langley Research Center, Hampton, VA.
RECENT DEVELOPMENTS IN DEPLOYMENT ANALYSIS SIMULATION USING A MULTI-BODY COMPUTER CODE **c61**
Jerrold M. Housner *In its* Computational Methods for Structural Mechanics and Dynamics May 1989 p 435-441 (For primary document see N89-24654 18-39)
Avail: NTIS HC A12/MF A01 CSCL 09B

Deployment is a candidate mode for construction of structural space systems components. By its very nature, deployment is a dynamic event, often involving large angle unfolding of flexible beam members. Validation of proposed designs and conceptual deployment mechanisms is enhanced through analysis. Analysis may be used to determine member loads thus helping to establish deployment rates and deployment control requirements for a given concept. Futhermore, member flexibility, joint free-play, manufacturing tolerances, and imperfections can affect the reliability of deployment. Analyses which include these effects can aid in reducing risks associated with a particular concept. Ground tests which can play a similar role to that of analyses are difficult and expensive to perform. Suspension systems just for vibration ground tests of large space structures in a 1 g environment present many challenges. Suspension of a structure which spatially expands is even more challenging. Analysis validation through experimental confirmation on relatively small simple models would permit analytical extrapolation to larger more complex space structures.
Author

N89-24661*# National Aeronautics and Space Administration. Langley Research Center, Hampton, VA.
DYNAMIC ANALYSIS OF SPACE STRUCTURES INCLUDING ELASTIC, MULTIBODY, AND CONTROL BEHAVIOR **c18**
Larry Pinson and Keto Soosaar *In its* Computational Methods for Structural Mechanics and Dynamics May 1989 p 443-454 (For primary document see N89-24654 18-39)
Avail: NTIS HC A12/MF A01 CSCL 22B

The problem is to develop analysis methods, modeling stategies, and simulation tools to predict with assurance the on-orbit performance and integrity of large complex space structures that cannot be verified on the ground. The problem must incorporate large reliable structural models, multi-body flexible dynamics, multi-tier controller interaction, environmental models including 1g and atmosphere, various on-board disturbances, and linkage to mission-level performance codes. All areas are in serious need of work, but the weakest link is multi-body flexible dynamics.
Author

N89-24662*# Massachusetts Inst. of Tech., Cambridge. Dept. of Mechanical Engineering.
DYNAMICS OF FLEXIBLE MULTI-BODY MECHANISMS AND MANIPULATORS. PART 1: AN OVERVIEW **c37**

Steven Dubowsky *In* NASA, Langley Research Center, Computational Methods for Structural Mechanics and Dynamics May 1989 p 455-458 (For primary document see N89-24654 18-39)
Avail: NTIS HC A12/MF A01 CSCL 13I

Flexibility can be a major limitation to the performance of high performance conventional machine systems. The current status of robotic manipulators is limited by the effects of system flexibility. The status of current commercial robots, anticipated development in 5 and 10 years is outlined. B.G.

N89-24663*# Massachusetts Inst. of Tech., Cambridge.
APPLICATION OF FINITE-ELEMENT METHODS TO DYNAMIC ANALYSIS OF FLEXIBLE SPATIAL AND CO-PLANAR LINKAGE SYSTEMS, PART 2 **c37**
Steven Dubowsky *In* NASA, Langley Research Center, Computational Methods for Structural Mechanics and Dynamics May 1989 p 459-489 (For primary document see N89-24654 18-39)
Avail: NTIS HC A12/MF A01 CSCL 13I

An approach is described to modeling the flexibility effects in spatial mechanisms and manipulator systems. The method is based on finite element representations of the individual links in the system. However, it should be noted that conventional finite element methods and software packages will not handle the highly nonlinear dynamic behavior of these systems which results form their changing geometry. In order to design high-performance lightweight systems and their control systems, good models of their dynamic behavior which include the effects of flexibility are required. Author

N89-24664*# Iowa Univ., Iowa City. Coll. of Engineering.
DYNAMICS OF ARTICULATED STRUCTURES **c37**
Edward J. Haug *In* NASA, Langley Research Center, Computational Methods for Structural Mechanics and Dynamics May 1989 p 491-515 (For primary document see N89-24654 18-39)
Avail: NTIS HC A12/MF A01 CSCL 13I

An articulated structure is defined as an assembly of flexible bodies that may be coupled by kinematic connections and force elements that permit large relative displacement and rotation. Kinematics of such systems is defined using one reference frame for each body in the system and deformation modal coordinates that define displacement fields within flexible bodies. Deformation kinematics are defined by both elastic vibration and static correction deformation modes. Linear elastic deformation is presumed; i.e., a linear stress-strain relation is valid and relative displacements within each elastic component are small enough so that the theory of linear elasticity applies. Coupling of reference and modal coordinates leads to a system of nonlinear equations of motion. Methods of automatically generating and solving these equations of motion are outlined. Author

N89-24665*# Jet Propulsion Lab., California Inst. of Tech., Pasadena.
MODAL REDUCTION STRATEGIES FOR INTERCONNECTED FLEXIBLE BODIES SIMULATION
F. O. Eke and G. K. Man *In* NASA, Langley Research Center, Computational Methods for Structural Mechanics and Dynamics May 1989 p 517-526 (For primary document see N89-24654 18-39)
Avail: NTIS HC A12/MF A01 CSCL 09B

Multi-body dynamics programs require characterization of each body. The Galileo spacecraft system modes to be retained were determined using available criteria, modal influence coefficients, and bode. The descent to component level was achieved via a two-phase diagonalization process starting with submatrices of truncated augmented system modal matrix. Author

N89-24666*# Lockheed Missiles and Space Co., Palo Alto, CA.
COMPUTATIONAL ASPECTS OF MULTIBODY DYNAMICS **c61**
K. C. Park *In* NASA, Langley Research Center, Computational Methods for Structural Mechanics and Dynamics May 1989 p 527-536 (For primary document see N89-24654 18-39)
Avail: NTIS HC A12/MF A01 CSCL 20K

Computational aspects are addressed which impact the requirements for developing a next generation software system for flexible multibody dynamics simulation which include: criteria for selecting candidate formulation, pairing of formulations with appropriate solution procedures, need for concurrent algorithms to utilize computer hardware advances, and provisions for allowing open-ended yet modular analysis modules. Author

N89-24667*# DYNACS Engineering Co., Inc., Clearwater, FL.
CONSTRAINT ELIMINATION IN DYNAMICAL SYSTEMS
R. P. Singh and P. W. Likins (Lehigh Univ., Bethlehem, PA.) *In* NASA, Langley Research Center, Computational Methods for Structural Mechanics and Dynamics May 1989 p 537-541 (For primary document see N89-24654 18-39)
Avail: NTIS HC A12/MF A01 CSCL 13I

Large space structures (LSSs) and other dynamical systems of current interest are often extremely complex assemblies of rigid and flexible bodies subjected to kinematical constraints. A formulation is presented for the governing equations of constrained multibody systems via the application of singular value decomposition (SVD). The resulting equations of motion are shown to be of minimum dimension. Author

N89-24668*# Massachusetts Inst. of Tech., Cambridge. Space Systems Lab.
NONLINEAR CHARACTERISTICS OF JOINTS AS ELEMENTS OF MULTI-BODY DYNAMIC SYSTEMS **c37**
Edward F. Crawley *In* NASA, Langley Research Center, Computational Methods for Structural Mechanics and Dynamics May 1989 p 543-569 (For primary document see N89-24654 18-39)
Avail: NTIS HC A12/MF A01 CSCL 13I

As the connecting elements in multi-body structures, joints play a pivotal role in the overall dynamic response of these systems. Obviously, the linear stiffness of the joint strongly influences the system frequencies, but the joints are also likely to be the dominant sources of damping and nonlinearities, especially in aircraft and space structures. The general characteristics of such joints will be discussed. Then the state of the art in nonlinear joint characterization techniques will be surveyed. Finally, the impact that joints have on the overall response of structures will be evaluated. Author

N89-24669*# Georgia Inst. of Tech., Atlanta. School of Aerospace Engineering.
ANALYSIS OF SHELL-TYPE STRUCTURES SUBJECTED TO TIME-DEPENDENT MECHANICAL AND THERMAL LOADING Semiannual Status Report
G. J. Simitses May 1989 9 p
(Grant NAG3-534)
(NASA-CR-184989; NAS 1.26:184989) Avail: NTIS HC A02/MF A01 CSCL 20K

The objective is to develop a general mathematical model and solution methodologies for analyzing structural response of thin, metallic shell-type structures under large transient, cyclic, or static thermomechanical loads. Among the system responses, which are associated with these load conditions, are thermal buckling, creep buckling, and racheting. Thus, geometric as well as material-type nonlinearities (of high order) can be anticipated and must be considered in the development of the mathematical model. Furthermore, this must also be accommodated in the solution procedures. Author

N89-24670 Bath Univ. (England).
EQUATIONS OF MOTION FOR VISCOELASTIC MOVING CRACK PROBLEMS Ph.D. Thesis
G. Goleniewski 1988 124 p
Avail: Univ. Microfilms Order No. BRDX84322

The problem of steady-state crack propagation under antiplane strain in a Maxwell liquid is considered, using the critical crack

opening displacement fracture criterion and incorporating a finite craze zone over which cohesive forces act. Stress and displacement fields are obtained by use of the Wiener-Hopf technique, and from these plots of nominal stress intensity factor and work-rate of applied tractions are generated, demonstrating variation with respect to the craze zone length (the energy absorbed by the zone being held constant) and relaxation time (relative to a characteristic timescale). The curves for a finite craze zone size deviate considerably from those near the sharp crack limit. Quasi-static crack propagation in a standard linear solid is investigated for two different crack geometries, one semi-infinite, the other finite. Viscoelastic displacements are obtained from their elastic counterparts by use of a correspondence principle. The fracture initiation time is evaluated in each case, and from this it is possible to deduce quasi-static crack motion. The method of matched asymptotic expansions is used to investigate accelerating crack growth in a standard linear solid (in the subsonic velocity range). The outer problem is found to reduce to the elastic accelerating crack problem in Mode 3, while the inner problem is one of steady-state motion. Stress intensity factor matching is performed for various choices of crack face loading. Finally, the steady-state work on the Maxwell liquid is extended to the standard linear solid, and the inner matched expansions problem is treated for the supersonic range of the latter material and for the subsonic range of the power law material. Dissert. Abstr.

N89-24671 Texas A&M Univ., College Station.
MICROSCOPIC DELAMINATION PROCESSES AND THE RESULTING CRACK TIP STRAIN FIELDS OF GRAPHITE/EPOXY COMPOSITES Ph.D. Thesis
Michael Frank Hibbs 1988 238 p
Avail: Univ. Microfilms Order No. DA8903353

The microscopic failure mechanisms for five graphite/epoxy composites with different degrees of resin toughness were examined. Correlations between these failure mechanisms and the resulting delamination toughness were made for mode 1, mode 2, and mixed mode loadings. A combination of scanning electron microscope (SEM) real time fracture observations and post-failure fractography was used to identify the microscopic fracture mechanisms. The mode 1, mode 2 and mixed mode energy release rates were determined using unidirectional double cantilever beam specimens. The mode 1 delamination energy release rate, G(I sub c), was calculated using linear beam theory, an area method, and a compliance calibration analysis. Two techniques for measuring the microscopic crack tip strain fields were developed and tested. Both stereoimaging and direct measurement of crack tip displacements from SEM electron beam induced reference marks were shown to be effective in measuring crack tip displacements and strains. Also, careful observations of the neat resin and composite fractured surfaces were made to evaluate the use of fracture morphology in failure analysis of composite materials. Dissert. Abstr.

N89-24672 Texas A&M Univ., College Station.
IMPROVED ANALYSIS OF LAMINATED HETEROGENEOUS BEAMS AND ASSOCIATED FORMULATION OF A NEW FINITE ELEMENT METHOD Ph.D. Thesis
Shafiqul Islam Khandoker 1988 129 p
Avail: Univ. Microfilms Order No. DA8903362

By discretizing a beam through the thickness into hypothetical layers, the explicit relations between transverse strains and inter-layer transverse stresses are determined. An expression for the displacement field is then obtained using Kozik's equation. This kinematics based equation provides an exact displacement within the limitation of linear theory of elasticity. The resulting displacement and strain fields are functions of the reference surface displacements and transverse inter-layer stresses. The constitutive relations and the equations of equilibrium for each layer are utilized in an analytical solution employed to determine the inter-layer stresses. As an alternative approach, a finite element method based on a modified form of the Hu-Washizu variational principle is formulated. Also included are several case studies of homogeneous and heterogeneous beams. The results for displacement and stress fields closely approximate exact solutions for both homogeneous and heterogeneous beams. The bending stresses in heterogeneous beams are especially accurate as compared to values obtained by either classical or ad-hoc beam theories. Author

N89-24673*# National Aeronautics and Space Administration. Langley Research Center, Hampton, VA.
LARGE-SCALE STRUCTURAL ANALYSIS: THE STRUCTURAL ANALYST, THE CSM TESTBED AND THE NAS SYSTEM
Norman F. Knight, Jr., Susan L. McCleary, Steven C. Macy, and Mohammad A. Aminpour (Analytical Services and Materials, Inc., Hampton, VA.) Mar. 1989 106 p Original contains color illustrations
(NASA-TM-100643; NAS 1.15:100643) Avail: NTIS HC A06/MF A01 CSCL 20K

The Computational Structural Mechanics (CSM) activity is developing advanced structural analysis and computational methods that exploit high-performance computers. Methods are developed in the framework of the CSM testbed software system and applied to representative complex structural analysis problems from the aerospace industry. An overview of the CSM testbed methods development environment is presented and some numerical methods developed on a CRAY-2 are described. Selected application studies performed on the NAS CRAY-2 are also summarized. Author

N89-24674*# Georgia Inst. of Tech., Atlanta.
ANALYSIS OF INTERLAMINAR FRACTURE IN COMPOSITES UNDER COMBINED LOADING Semiannual Report, 12 Aug. 1988 - 11 Feb. 1989
Erian A. Armanios 1989 31 p Presented at the 30th Structures, Structural Dynamics and Materials Conference, Mobile, AL, Apr. 1989
(Grant NAG1-637)
(NASA-CR-185055; NAS 1.26:185055; E-16-654) Avail: NTIS HC A03/MF A01 CSCL 20K

Delamination is a predominant failure mode in continuous fiber reinforced laminated composite structures. One type of delamination is the transverse crack tip delamination which originates at the tip of transverse matrix cracks. An analytical model based on the sublaminate approach and fracture mechanics is developed to study the growth of such delaminations. Plane strain conditions are assumed and estimates are provided for the total strain energy release rate as well as the mode 1 and mode 2 contribution. The energy release rate estimates are used in combination with a simple failure law to predict critical delamination growth strains and stresses. These predictions are compared with experimental data on T300/934 Graphite Epoxy (+ or - 25/90 nano seconds) laminates in the range n=.5 to 8. A good agreement is demonstrated for the range of n where the experimental observations indicate transverse crack tip delamination to be the predominant failure mode. Author

N89-24675# Florida Univ., Gainesville. Dept. of Civil Engineering.
CENTRIFUGAL MODELING OF UNDERGROUND STRUCTURES SUBJECTED TO BLAST LOADING Final Report, Sep. 1985 - May 1987
Habibollah Tabatabai, David Bloomquist, M. C. McVay, John J. Gill, and F. C. Townsend Mar. 1988 319 p
(Contract F08635-83-C-0136)
(AD-A206424; ESL-TR-87-62) Avail: NTIS HC A14/MF A01 CSCL 14/2

Reliable and economical design of survivable underground military structures requires better understanding of the complex parameters involved. Small-scale model testing of such systems offers major cost savings compared to full-scale tests. The laws of similitude and scaling relationships require some form of dead-load compensation to account properly for the effect of gravity stresses in scaled models. This can be accomplished by subjecting the scaled model to an increased acceleration field by use of a centrifuge. The objectives of this research were to determine the significance of gravity stresses on the response of underground

structures subjected to blast loading. Discussion of the scaling relationships and procedures for model construction are presented. A complete instrumentation set-up for the measurements of shock pressures, strains and acceleration on the structure was designed, built and tested. This includes development of polyvinylidene fluoride piezoelectric shock pressure transducers and associated electronics. A series of tests at high-gravity and low-gravity environments were performed on 1/60 and 1/82-scale models of an underground protective structure subjected to a scaled blast loading. Based on the test results, it is concluded that the structural responses in the two gravity fields are different and that such parameters as wave speed, pressure magnitudes and structural strains are higher in the high-gravity tests. GRA

N89-24676*# National Aeronautics and Space Administration. Langley Research Center, Hampton, VA.
CHARACTERIZATION OF THE BENDING STIFFNESS OF LARGE SPACE STRUCTURE JOINTS
K. Chauncey Wu May 1989 18 p
(NASA-TM-101565; NAS 1.15:101565) Avail: NTIS HC A03/MF A01 CSCL 20K

A technique for estimating the bending stiffness of large space structure joints is developed and demonstrated for an erectable joint concept. Experimental load-deflection data from a three-point bending test was used as input to solve a closed-form expression for the joint bending stiffness which was derived from linear beam theory. Potential error sources in both the experimental and analytical procedures are identified and discussed. The bending stiffness of a mechanically preloaded erectable joint is studied at three applied moments and seven joint orientations. Using this technique, the joint bending stiffness was bounded between 6 and 17 percent of the bending stiffness of the graphite/epoxy strut member. Author

N89-24677*# National Aeronautics and Space Administration. Langley Research Center, Hampton, VA.
DEVELOPMENT OF HIGHER-ORDER MODAL METHODS FOR TRANSIENT THERMAL AND STRUCTURAL ANALYSIS
Charles J. Camarda and Raphael T. Haftka (Virginia Polytechnic Inst. and State Univ., Blacksburg.) Feb. 1989 39 p
(NASA-TM-101548; NAS 1.15:101548) Avail: NTIS HC A03/MF A01 CSCL 20K

A force-derivative method which produces higher-order modal solutions to transient problems is evaluated. These higher-order solutions converge to an accurate response using fewer degrees-of-freedom (eigenmodes) than lower-order methods such as the mode-displacement or mode-acceleration methods. Results are presented for non-proportionally damped structural problems as well as thermal problems modeled by finite elements. Author

N89-24678*# Astro Aerospace Corp., Carpinteria, CA.
INVESTIGATION OF STRUCTURAL BEHAVIOR OF CANDIDATE SPACE STATION STRUCTURE
John M. Hedgepeth and Richard K. Miller Jun. 1989 128 p
(Contract NAS1-17536)
(NASA-CR-181746; NAS 1.26:181746; AAC-TN-1152) Avail: NTIS HC A07/MF A01 CSCL 20K

Quantitative evaluations of the structural loads, stiffness and deflections of an example Space Station truss due to a variety of influences, including manufacturing tolerances, assembly operations, and operational loading are reported. The example truss is a dual-keel design composed of 5-meter-cube modules. The truss is 21 modules high and 9 modules wide, with a transverse beam 15 modules long. One problem of concern is the amount of mismatch which will be expected when the truss is being erected on orbit. Worst-case thermal loading results in less than 0.5 inch of mismatch. The stiffness of the interface is shown to be less than 100 pounds per inch. Thus, only moderate loads will be required to overcome the mismatch. The problem of manufacturing imperfections is analyzed by the Monte Carlo approach. Deformations and internal loads are obtained for ensembles of 100 example trusses. All analyses are performed on a personal computer. The necessary routines required to supplement commercially available programs are described. Author

N89-24679*# National Aeronautics and Space Administration. Langley Research Center, Hampton, VA.
RESULTS OF THE ROUND ROBIN ON OPENING-LOAD MEASUREMENT CONDUCTED BY ASTM TASK GROUP E24.04.04 ON CRACK CLOSURE MEASUREMENT AND ANALYSIS
Edward P. Phillips May 1989 39 p
(NASA-TM-101601; NAS 1.15:101601) Avail: NTIS HC A03/MF A01 CSCL 20K

An experimental Round Robin on the measurement of the opening load in fatigue crack growth tests was conducted on Crack Closure Measurement and Analysis. The Round Robin evaluated the current level of consistency of opening load measurements among laboratories and to identify causes for observed inconsistency. Eleven laboratories participated in the testing of compact and middle-crack specimens. Opening-load measurements were made for crack growth at two stress-intensity factor levels, three crack lengths, and following an overload. All opening-load measurements were based on the analysis of specimen compliance data. When all of the results reported (from all participants, all measurement methods, and all data analysis methods) for a given test condition were pooled, the range of opening loads was very large--typically spanning the lower half of the fatigue loading cycle. Part of the large scatter in the reported opening-load results was ascribed to consistent differences in results produced by the various methods used to measure specimen compliance and to evaluate the opening load from the compliance data. Another significant portion of the scatter was ascribed to lab-to-lab differences in producing the compliance data when using nominally the same method of measurement. Author

N89-24680 California Univ., Los Angeles.
ADVANCES IN DUAL METHODS AND CONVEX APPROXIMATIONS FOR STRUCTURAL OPTIMIZATION Ph.D. Thesis
Hichem Smaoui 1988 149 p
Avail: Univ. Microfilms Order No. DA8906126

A methodology for structural optimization based on dual methods and convex separable approximations is discussed. A perturbation technique is introduced in order to remove the nondifferentiability of the dual function which arises when linear constraints are present in the approximate problem. This perturbation technique extends the generality of the dual method to problems involving linear inequality constraints and nonlinear equality constraints. A variable metric method used in conjunction with an active set strategy is proposed to solve the duals of separable convex optimization problems. This first order method is more reliable than the Newton's method used in DUAL-2, because it does not break down when the Hessian matrix becomes singular or nearly singular. An approximation is proposed which uses diagonal second derivatives as a basis for a general and systematic rule which locates the asymptotes in the method of moving asymptotes. These features are integrated in a research computer program developed to computationally demonstrate their effectiveness by solving several test problems. Moreover, a detailed description is given for a parallel algorithm which was implemented on an Intel Hypercube to assess the speed-up factor and the efficiency of parallel processing when applied to the dual algorithm. Dissert. Abstr.

N89-24681*# National Aeronautics and Space Administration. Langley Research Center, Hampton, VA.
GLOBAL/LOCAL STRESS ANALYSIS OF COMPOSITE PANELS
Jonathan B. Ransom and Norman F. Knight, Jr. Jun. 1989 54 p Presented at the 3rd Joint ASCE/ASME Mechanics Conference, Santa Barbara, CA, 9-12 Jul. 1989
(NASA-TM-101622; NAS 1.15:101622) Avail: NTIS HC A04/MF A01 CSCL 20K

A method for performing a global/local stress analysis is

described, and its capabilities are demonstrated. The method employs spline interpolation functions which satisfy the linear plate bending equation to determine displacements and rotations from a global model which are used as boundary conditions for the local model. Then, the local model is analyzed independent of the global model of the structure. This approach can be used to determine local, detailed stress states for specific structural regions using independent, refined local models which exploit information from less-refined global models. The method presented is not restricted to having a priori knowledge of the location of the regions requiring local detailed stress analysis. This approach also reduces the computational effort necessary to obtain the detailed stress state. Criteria for applying the method are developed. The effectiveness of the method is demonstrated using a classical stress concentration problem and a graphite-epoxy blade-stiffened panel with a discontinuous stiffener. Author

N89-24682# Lawrence Livermore National Lab., CA.
MEASUREMENT OF BOND STRENGTH AT METAL/CERAMIC INTERFACES
Gerald L. Nutt, William Lai, Kenneth E. Froeschner, and Wayne E. King Apr. 1989 9 p Presented at the Spring Meeting of the Materials Research Society, San Diego, CA, 24-29 Apr. 1989
(Contract W-7405-eng-48)
(DE89-011638; UCRL-100915; CONF-890426-7) Avail: NTIS HC A02/MF A01

We report on a method for measuring the bond strength of metal ceramic interfaces. Test specimens are created by vapor depositing a metal film on a ceramic substrate. The specimen is impacted with a thin metallic flyer sending a short planar shock pulse into the ceramic. If the shape and amplitude of the wave is properly controlled the interface will spontaneously disbond creating new free surfaces. Measurements indicate the disbonding process occurs in less than 1.0 ns, which we believe is too short for crack propagation along existing flaws. Therefore, we conclude that simultaneous breaking of atomic bonds rather than propagation and coalescence of cracks is the means by which the film and substrate are separated. The free surface velocity of the metal overlayer is monitored during spall by laser interferometry. The data constitute a direct measurement of the bond strength. The measured bond strengths are reproducible and do not show a dependence on shock amplitude for identically prepared specimens. DOE

N89-24683# Sandia National Labs., Albuquerque, NM.
DYNAMICS AND STATIC BEHAVIOR OF METAL GUSSETS IN CASK IMPACT LIMITERS
S. W. Attaway and H. R. Yoshimura 1989 9 p Presented at the International Symposium on Packaging and Transporting of Radioactive Materials, Washington, DC, 11 Jun. 1989
(Contract DE-AC04-76DP-00789)
(DE89-011879; SAND-89-1222C; CONF-890631-4) Avail: NTIS HC A02/MF A01

Static and dynamic analyses of an impact limiter for a spent fuel cask have been performed using the finite element analysis code PRONTO2D (Taylor and Flanagan, 1987). The impact limiter contained wood as the energy absorbing material, with the wood confined by a cylindrical metal outer skin and sixteen metal stiffeners (gussets). The object of these analyses was to determine how the wood interacts with the metal stiffeners and to determine if the impact limiter would behave differently under static versus dynamic loading conditions. Originally, the metal gusset strength was assumed to be limited by the elastic buckling load. Further analysis showed that the gusset strength was not limited to the elastic buckling load and that each gusset contributed significantly to the impact limiter's strength. The current analyses investigated the strength of a flat plate or gusset used in impact limiter systems. DOE

N89-24684# Lawrence Livermore National Lab., CA. Dept. of Civil Engineering.
A DISCUSSION ON USING LANCZOS VECTORS AND RITZ VECTORS FOR COMPUTING DYNAMIC RESPONSES Final Report
Harn C. Chen and Robert L. Taylor 1988 69 p Prepared in cooperation with California Univ., Berkeley
(Contract W-7405-eng-48)
(DE89-012322; UCRL-21192; UCB/SEMM-88/15; UCB/SEMM-88/16; UCB/SEMM-88/17) Avail: NTIS HC A04/MF A01

This report on structural engineering, mechanics and materials is divided into three parts: a discussion on using Lanczos vectors and Ritz vectors for computing dynamic responses; solution of viscously damped linear systems using a finite element displacement formulation; and vibration analysis of fluid-solid systems using a finite element displacement formulation. DOE

42 GEOSCIENCES (GENERAL)

No abstracts in this category.

43 EARTH RESOURCES AND REMOTE SENSING

Includes remote sensing of earth resources by aircraft and spacecraft; photogrammetry; and aerial photography.

For instrumentation see *35 Instrumentation and Photography.*

N89-24685# Instituto de Pesquisas Espaciais, Sao Jose dos Campos (Brazil). Ministerio da Ciencia e Technologia.
MICROWAVE X-BAND RADIOMETRIC CHARACTERIZATION OF BRAZILIAN SOILS BY MEASUREMENT OF THE COMPLEX PERMITTIVITY
Ulf Walter Palme Jun. 1988 7 p Presented at IGARSS '88, Edinburgh, Scotland, 15 Sep. 1988
(INPE-4588-PRE/1319) Avail: NTIS HC A02/MF A01

The main activities and strategies in microwave radiometry are described for applications in agriculture in Brazil. Some relevant results regarding measurements of the complex permittivity (epsilon*) and estimates of emissivity for soils from tropical areas in function of soil moisture, at 10.62 GHz, are presented. Difficulties related to the measurement of epsilon* and mu* of important Brazilian soils (dielectric/ferromagnetic mixture) are highlighted. Author

N89-24686*# California Univ., Santa Barbara. Dept. of Geography.
IMPROVEMENT AND EXTENSION OF A RADAR FOREST BACKSCATTERING MODEL Semiannual Report
David S. Simonett and Yong Wang 10 May 1989 18 p
(Grant NAG5-1010)
(NASA-CR-184975; NAS 1.26:184975) Avail: NTIS HC A03/MF A01 CSCL 02F

Radar modeling of mangal forest stands, in the Sundarbans area of Southern Bangladesh, was developed. The modeling employs radar system parameters with forest data on tree height, spacing, biomass, species combinations, and water (including slightly conductive water), content both in leaves and trunks of the mangal. For Sundri and Gewa tropical mangal forests, six model components are proposed, which are required to explain the contributions of various forest species combinations in the attenuation and scattering of mangal vegetated nonflooded or flooded surfaces. Statistical data of simulated images were compared with those of SIR-B images both to refine the modeling

procedures and to appropriately characterize the model output. The possibility of delineation of flooded or nonflooded boundaries is discussed. Author

N89-24687*# Michigan Univ., Ann Arbor. School of Natural Resources.
ESTIMATING POPULATION SIZE OF PYGOSCELID PENGUINS FROM TM DATA Final Report
Charles E. Olson, Jr., Mathew R. Schwaller, and Paul A. Dahmer (Environmental Research Inst. of Michigan, Ann Arbor.) Aug. 1987 45 p
(Contract NAS5-28755)
(NASA-CR-180081; NAS 1.26:180081) Avail: NTIS HC A03/MF A01 CSCL 06C

An estimate was made toward a continent wide population of penguins. The results indicate that Thematic Mapper data can be used to identify penguin rookeries due to the unique reflectance properties of guano. Strong correlations exist between nesting populations and rookery area occupied by the birds. These correlations allow estimation of the number of nesting pairs in colonies. The success of remote sensing and biometric analyses leads one to believe that a continent wide estimate of penguin populations is possible based on a timely sample employing ground based and remote sensing techniques. Satellite remote sensing along the coastline may well locate previously undiscovered penguin nesting sites, or locate rookeries which have been assumed to exist for over a half century, but never located. Observations which found that penguins are one of the most sensitive elements in the complex of Southern Ocean ecosystems motivated this study. Author

N89-24688# Deutsche Forschungs- und Versuchsanstalt fuer Luft- und Raumfahrt, Oberpfaffenhofen (West Germany).
NECESSITY AND BENEFIT OF THE X-SAR SPACE SHUTTLE EXPERIMENT
Wolfgang Keydel and Herwig Oettl Oct. 1988 41 p In GERMAN; ENGLISH summary Original contains color illustrations
(DFVLR-Mitt-88-29; ISSN-0176-7736; ETN-89-94375) Avail: NTIS HC A03/MF A01; DFVLR, VB-PL-DO, Postfach 90 60 58, 5000 Cologne, Federal Republic of Germany, 26.50 deutsche marks

The X, L, and C-band synthetic aperture radars (SAR) planned to fly in 1992 on space shuttle missions are investigated for their effectiveness in Earth surface vegetation classification and recognition. The scattering of electromagnetic waves by twigs, leaves, branches, and trunks permits vegetation growth length estimation. Earth surface roughness is analyzed by Rayleigh criterion. The SAR sensors are well adapted to Earth surface observation independently of daylight and atmospheric conditions. ESA

N89-24689# Aerospatiale, Cannes La Bocca (France).
THE ADVANCED OCEAN CHLOROPHYLL METER (OCM). A SPECTRAL IMAGING DEVICE FOR THE OBSERVATION OF THE OCEANS [L'ADVANCED OCM: UN SPECTRO-IMAGEUR POUR L'OBSERVATION DES OECANS]
G. Cerutti-Maori 1988 4 p In FRENCH
(Rept-882-440-118; ETN-89-94511) Avail: NTIS HC A02/MF A01

The main results of a feasibility study are presented. The ESA project concerns an optical multispectral radiometer of the pushbroom type for the study of the oceans in the solar spectrum (0.4 to 1.1 microns). The goal is to establish the space-time distribution of chlorophyll. The instrument choice includes the use of charge coupled devices in mosaic layout. The payload is 62 kg with 90 watts power requirements and a 0.8 reliability. ESA

N89-24690# Laboratoire de Meteorologie Dynamique du CNRS, Palaiseau (France).
ON THE FUTURE DEVELOPMENT AND MANAGEMENT OF SPECTROSCOPIC DATABASE FOR RADIATIVE TRANSFER FROM THE ISSUES OF RECENT RELATED WORKSHOPS
N. Husson and A. Chedin 1988 3 p Presented at the International Radiation Symposium, Lille, France, 18-24 Aug. 1988
(ETN-89-94530) Avail: NTIS HC A02/MF A01

Computer accessible compilations of spectroscopic line parameters, in the infrared to microwave spectral region, are made available in data bases, for molecules of interest in remote sensing or climatic studies. The necessity to create these data bases is summarized as an introduction to future development and management of spectroscopic data bases. ESA

N89-24691# Laboratoire de Meteorologie Dynamique du CNRS, Palaiseau (France).
REFINEMENTS IN THE CLOUD DETECTION SCHEME OF THE 3I SYSTEM. COMPARISON WITH AVHRR PRODUCTS
Chantal Claud, Noelle A. Scott, Claude Kergomard, and Jean-Claude Gascard 1988 3 p Presented at the International Radiation Symposium, Lille, France, 18-24 Aug. 1988
(ETN-89-94531) Avail: NTIS HC A02/MF A01

The improved initialization inversion is designed for retrieving meteorological parameters from operational satellites of the Tiros-N series. Refinements in the cloud detection scheme are presented, and particularly the detection of low clouds over sea ice covered areas. The method is based on the discrimination between open water and sea ice from microwave observation and the detection of clouds by comparing two infrared channels. The results are validated using AVHRR observations. ESA

N89-24692# European Space Agency, Paris (France).
IMAGING SPECTROMETRY FOR LAND APPLICATIONS
T. D. Guyenne, ed. Nov. 1988 56 p Workshop held in Frascati, Italy, 19-21 Apr. 1988 Original contains color illustrations
(ESA-SP-1101; ISSN-0379-6566; ETN-89-94447) Copyright Avail: NTIS HC A04/MF A01; ESA Publications Div., ESTEC, Noordwijk, Netherlands, 10 dollars or 25 Dutch guilders

Airborne fluorescence land imagers, high resolution spectrometers for the Earth Observation System, imaging spectrometers, and ESA programs were discussed. For individual titles, see N89-24693 through N89-24701.

N89-24693# European Space Agency. European Space Research and Technology Center, ESTEC, Noordwijk (Netherlands). Earth Observation Preparatory Program.
ESA'S PLANNED ACTIVITIES IN THE FIELD OF IMAGING SPECTROMETRY FOR EARTH OBSERVATION
M. Rast *In its* Imaging Spectrometry for Land Applications Nov. 1988 p 7-10 (For primary document see N89-24692 18-43)
Copyright Avail: NTIS HC A04/MF A01; ESA Publications Div., ESTEC, Noordwijk, Netherlands, 10 dollars or 25 Dutch guilders

Imaging requirements oriented towards a high resolution imaging spectrometer dedicated to land applications are assessed. A set of recommendations for future action is included. ESA

N89-24694# Moniteq Ltd., Concord (Ontario).
THE FLI AIRBORNE IMAGING SPECTROMETER: A HIGHLY VERSATILE SENSOR FOR MANY APPLICATIONS
R. A. H. Buxton *In* ESA, Imaging Spectrometry for Land Applications Nov. 1988 p 11-16 Original contains color illustrations (For primary document see N89-24692 18-43)
Copyright Avail: NTIS HC A04/MF A01; ESA Publications Div., ESTEC, Noordwijk, Netherlands, 10 dollars or 25 Dutch guilders

The characteristics and applications of the Fluorescence Line Imager (FLI) are described. The FLI was used to acquire imagery over vegetated land targets during 4.5 yr. The first design was based on sensing the solar-stimulated fluorescence of chlorophyll in plankton in water from space. Images of the chlorophyll red edge in stressed vegetation are applied to evaluate forest decline, mineral and hydrocarbon exploration, and landfill. ESA

N89-24695*# Jet Propulsion Lab., California Inst. of Tech., Pasadena.
HIRIS: NASA'S HIGH-RESOLUTION IMAGING SPECTROMETER FOR THE EARTH OBSERVING SYSTEM (EOS)
J. Dozier and M. Herring *In* ESA, Imaging Spectrometry for Land Applications Nov. 1988 p 17-25 Original contains color illustrations (For primary document see N89-24692 18-43)
Copyright Avail: NTIS HC A04/MF A01; ESA Publications Div., ESTEC, Noordwijk, Netherlands, 10 dollars or 25 Dutch guilders CSCL 14B

The HIRIS design includes 10 nm spectral bands from 0.4 to 2.5 micron at 30 m spatial resolution over a 24 or 30 km swath. This resolution allows identification of many minerals in rocks and soils, important algal pigments in oceans and inland water and spectral changes in land canopy. In the 824 km orbit altitude proposed, the cross track pointing capability allows 4 to 5 views during a 16 day revisit cycle. ESA

N89-24696# Natural Environmental Research Council, London (England). British National Space Centre.
THE ACTIVITIES OF THE BRITISH NATIONAL SPACE CENTRE (BNSC) IN THE FIELD OF IMAGING SPECTROMETRY
S. A. Briggs, S. J. Mackin, T. J. Munday, N. J. Drake, E. J. Milton (Southampton Univ., England), and E. M. Rollin *In* ESA, Imaging Spectrometry for Land Applications Nov. 1988 p 27-33 Original contains color illustrations (For primary document see N89-24692 18-43)
Copyright Avail: NTIS HC A04/MF A01; ESA Publications Div., ESTEC, Noordwijk, Netherlands, 10 dollars or 25 Dutch guilders

Results obtained with the Airborne Imaging Spectrometer and the GER II scanner in geological applications are discussed. Ground segment activities in terms of data processing and information extraction methods are described and the key role of field spectrometry in the understanding of remotely sensed data is discussed. ESA

N89-24697# Deutsche Forschungs- und Versuchsanstalt fuer Luft- und Raumfahrt, Oberpfaffenhofen (West Germany). Inst. fuer Optoelektronik.
DFVLR ACTIVITIES RELATED TO IMAGING SPECTROMETRY
G. Kritikos, H. vanderPiepen, and M. Schroeder *In* ESA, Imaging Spectrometry for Land Applications Nov. 1988 p 35-41 Original contains color illustrations (For primary document see N89-24692 18-43)
Copyright Avail: NTIS HC A04/MF A01; ESA Publications Div., ESTEC, Noordwijk, Netherlands, 10 dollars or 25 Dutch guilders

The institute's research, technologies, and application activities related to imaging spectroscopy are discussed. Special emphasis is given to the development of an airborne programmable imaging spectrometer. The main application is the monitoring of water color and fluorescence for research in marine biology, ecology, water pollution, sediment transport, and climatology. ESA

N89-24698# Institute of Ocean Sciences, Sidney (British Columbia).
DEVELOPMENT OF AN IMAGING SPECTROMETER FOR REMOTE SENSING: THE FLI PROGRAM
J. F. R. Gower *In* ESA, Imaging Spectrometry for Land Applications Nov. 1988 p 43-45 (For primary document see N89-24692 18-43)
Copyright Avail: NTIS HC A04/MF A01; ESA Publications Div., ESTEC, Noordwijk, Netherlands, 10 dollars or 25 Dutch guilders

The Fluorescence Line Imager (FLI) spectrometer development is described. The original design intends to detect the near surface distribution of phytoplankton in sea water by imaging the naturally stimulated fluorescence emission from chlorophyll-a. The use of CCD detectors results in flexibility in the positioning of spectral bands in the sensor. The design requirements for sea and land application are outlined. Examples of FLI applications are given. ESA

N89-24699# Centre National d'Etudes Spatiales, Toulouse (France).
ACTIVITIES OF CNES IN THE FIELD OF IMAGING SPECTROMETRY
P. Vermande, D. Alcayde, and M. Combes-Despa (Observatoire de Paris-Meudon, France) *In* ESA, Imaging Spectrometry for Land Applications Nov. 1988 p 47-49 (For primary document see N89-24692 18-43)
Copyright Avail: NTIS HC A04/MF A01; ESA Publications Div., ESTEC, Noordwijk, Netherlands, 10 dollars or 25 Dutch guilders

The CNES Institute's research activities in the field of imaging spectrometry are summarized. The developments include operational field spectroradiometers, transportable imaging spectrometer (TIS), velocity sensors to control image drift in the focal plane (VS), signal compression, balloon flight tests of TIS and VS, and airborne imagery. ESA

N89-24700# Deutsche Forschungs- und Versuchsanstalt fuer Luft- und Raumfahrt, Oberpfaffenhofen (West Germany).
THE EARSEL IMAGING SPECTROMETRY WORKING GROUP
F. Lehmann *In* ESA, Imaging Spectrometry for Land Applications Nov. 1988 p 51-54 Original contains color illustrations (For primary document see N89-24692 18-43)
Copyright Avail: NTIS HC A04/MF A01; ESA Publications Div., ESTEC, Noordwijk, Netherlands, 10 dollars or 25 Dutch guilders

The activities of an interdisciplinary working group for Earth sciences spectrometry are discussed. The main topic is the development of an infrastructure for the intercommunication of different European laboratories, working in laboratory and field spectroscopy, development, testing and application of airborne high spectral resolution optical sensors, and the definition of future space remote sensing instruments. ESA

N89-24701# Canada Centre for Remote Sensing, Ottawa (Ontario).
IMAGING SPECTROMETRY AT THE CANADA CENTRE FOR REMOTE SENSING
R. A. Neville *In* ESA, Imaging Spectrometry for Land Applications Nov. 1988 p 55-56 (For primary document see N89-24692 18-43)
Copyright Avail: NTIS HC A04/MF A01; ESA Publications Div., ESTEC, Noordwijk, Netherlands, 10 dollars or 25 Dutch guilders

The institute's activities in the field are discussed. The supportive role in the development of the Fluorescence Line Imager, providing calibration facilities and assistance in installations in aircraft is described. ESA

44 ENERGY PRODUCTION AND CONVERSION

Includes specific energy conversion systems, e.g., fuel cells; global sources of energy; geophysical conversion; and windpower.

For related information see also *07 Aircraft Propulsion and Power, 20 Spacecraft Propulsion and Power,* and *28 Propellants and Fuels.*

N89-24702# National Aerospace Lab., Tokyo (Japan).
EXPERIMENTAL COMPONENT MODE SYNTHESIS APPLIED TO THE SOLAR ARRAY TYPE STRUCTURE
Keiji Komatsu, Masaaki Sano, Shigeo Sanbongi, Takashi Kai, and Susumu Toda Aug. 1988 23 p In JAPANESE; ENGLISH summary
(NAL-TR-994; ISSN-0389-4010) Avail: NTIS HC A03/MF A01

A component mode synthesis technique based on experimentally determined modal parameters is presented. The

test structure is a solar array type plate, which is divided into three parts and four flexible connective parts. In the synthesis, the measured modes are approximated in polynomials to produce rotational degrees of freedom. The results synthesized are in good agreement with the test results obtained from a combined structure. Author

N89-24703# Solarex Corp., Newtown, PA.
RESEARCH ON HIGH-EFFICIENCY, SINGLE-JUNCTION, MONOLITHIC, THIN-FILM AMORPHOUS SILICON SOLAR CELLS, PHASE 2 Annual Subcontract Report, 1 Jan. 1985 - 31 Jan. 1986
D. E. Carlson, R. R. Ayra, M. S. Bennett, A. Catalano, R. V. DAiello, C. R. Dickson, J. McVeigh, J. Newton, J. ODowd, and R. S. Oswald et al Sep. 1988 137 p Prepared for Midwest Research Inst., Golden, CO
(Contract DE-AC02-83CH-10093)
(DE89-000849; SERI/STR-211-3408) Avail: NTIS HC A08/MF A01

Results of the second phase of research on high-efficiency, single-junction, monolithic, thin-film a-Si solar cells are presented. Five glow-discharge deposition systems, including a in-line, multichamber system, were used to grow both doped and undoped a-Si:H. A large number of silane and disilane gas cylinders were analyzed with a gas chromatography/mass spectroscopy system. Strong correlations were found between the breakdown voltage, the deposition rate, the diffusion length, and the conversion efficiency for varying cathode-anode separations in a DC glow-discharge deposition mode. Tin oxide films were grown by chemical vapor deposition with either tetramethyl tin (TMT) or tin tetrachloride (TTC). The best were grown with TMT, but TTC films had a more controlled texture for light trapping and provided a better contact to the p-layer. The best results were obtained with 7059 glass substrates. Efficiencies as high as 10.86 percent were obtained in p-i-n cells with superlattice p-layers and as high as 10.74 percent in cells with both superlattice p- and n-layers. Measurements showed that the boron-doping level in the p-layer can strongly affect transport in the i-layer, which can be minimized by reactive flushing before i-layer deposition. Stability of a-Si:H cells is improved by light doping. Author

N89-24704*# National Aeronautics and Space Administration. Lewis Research Center, Cleveland, OH.
SPACE PHOTOVOLTAIC RESEARCH AND TECHNOLOGY, 1988. HIGH EFFICIENCY, SPACE ENVIRONMENT, AND ARRAY TECHNOLOGY
Washington Apr. 1989 362 p Conference held in Cleveland, OH, 19-21 Apr. 1988
(NASA-CP-3030; E-4587; NAS 1.55:3030) Avail: NTIS HC A16/MF A01 CSCL 10A

The 9th Space Photovoltaic Research and Technology conference was held at the NASA Lewis Research Center from April 19 to 21, 1988. The papers and workshop summaries report remarkable progress on a wide variety of approaches in space photovoltaics, for both near and far term applications. Among the former is the recently developed high efficiency GaAs/Ge cell, which formed the focus of a workshop discussion on heteroepitaxial cells. Still aimed at the long term, but with a significant payoff in a new mission capability, are InP cells, with their potentially dramatic improvement in radiation resistance. Approaches to near term, array specific powers exceeding 130 W/kg are also reported, and advanced concentrator panel technology with the potential to achieve over 250 W/sq m is beginning to take shape. For individual titles, see N89-24705 through N89-24738.

N89-24705*# National Aeronautics and Space Administration, Washington, DC.
TECHNOLOGY REQUIREMENTS FOR ADVANCED NASA MISSIONS **c12**
Henry B. Curtis *In* NASA, Lewis Research Center, Space Photovoltaic Research and Technology, 1988. High Efficiency, Space Environment, and Array Technology Apr. 1989 p 3-9
(For primary document see N89-24704 18-44)
Avail: NTIS HC A16/MF A01 CSCL 22A

Two recent reports, one by the National Commission on Space and the second by the Ride committee, have urged NASA to look at a variety of future missions. Among these are manned missions to Mars and permanent bases on the moon and Mars. Addressed here is a wide variety of technologies needed for such missions as well as areas where power is required. An estimate of power ranges and photovoltaic opportunities is also presented. Author

N89-24706*# Air Force Aero Propulsion Lab., Wright-Patterson AFB, OH.
SPACE POWER TECHNOLOGY 21: PHOTOVOLTAICS
Joseph Wise *In* NASA, Lewis Research Center, Space Photovoltaic Research and Technology, 1988. High Efficiency, Space Environment, and Array Technology Apr. 1989 p 10-15
(For primary document see N89-24704 18-44)
Avail: NTIS HC A16/MF A01 CSCL 10A

The Space Power needs for the 21st Century and the program in photovoltaics needed to achieve it are discussed. Workshops were conducted in eight different power disciplines involving industry and other government agencies. The Photovoltaics Workshop was conducted at Aerospace Corporation in June 1987. The major findings and recommended program from this workshop are discussed. The major finding is that a survivable solar power capability is needed in photovoltaics for critical Department of Defense missions including Air Force and Strategic Defense Initiative. The tasks needed to realize this capability are described in technical, not financial, terms. The second finding is the need for lightweight, moderately survivable planar solar arrays. High efficiency thin III-V solar cells can meet some of these requirements. Higher efficiency, longer life solar cells are needed for application to both future planar and concentrator arrays with usable life up to 10 years. Increasing threats are also anticipated and means for avoiding prolonged exposure, retraction, maneuvering and autonomous operation are discussed. Author

N89-24707*# National Aeronautics and Space Administration. Lewis Research Center, Cleveland, OH.
PROGRESS IN INDIUM PHOSPHIDE SOLAR CELL RESEARCH
Irving Weinberg, Clifford K. Swartz, and R. E. Hart, Jr. *In its* Space Photovoltaic Research and Technology, 1988. High Efficiency, Space Environment, and Array Technology Apr. 1989 p 19-27 (For primary document see N89-24704 18-44)
Avail: NTIS HC A16/MF A01 CSCL 10A

Progress, dating from the start of the Lewis program, is reviewed emphasizing processing techniques which have achieved the highest efficiencies in a given year. To date, the most significant achievement has been attainment of AM0 total area efficiencies approaching 19 percent. Although closed tube diffusion is not considered to be an optimum process, reasonably efficient 2cm x 2cm and 1cm x 2cm InP cells have been produced in quantity by this method with a satellite to be launched in 1990 using these cells. Proton irradiation of these relatively large area cells indicates radiation resistance comparable to that previously reported for smaller InP cells. A similar result is found for the initial proton irradiations of ITO/InP cells processed by D. C. sputtering. With respect to computer modelling, a comparison of n/p homojunction InP and GaAs cells of identical geometries and dopant concentrations has confirmed the superior radiation resistance of InP cells under 1 MeV electron irradiations. Author

N89-24708*# Spire Corp., Bedford, MA.
InP SHALLOW-HOMOJUNCTION SOLAR CELLS
Christopher Keavney, Mark B. Spitzer, Stanley M. Vernon, Victor E. Haven, and Godfrey Augustine (Georgia Inst. of Tech., Atlanta.) *In* NASA, Lewis Research Center, Space Photovoltaic Research and Technology, 1988. High Efficiency, Space Environment, and Array Technology Apr. 1989 p 28-40 (For primary document see N89-24704 18-44)
Avail: NTIS HC A16/MF A01 CSCL 10A

Indium phosphide solar cells with very thin n-type emitters have been made by both ion implantation and metalorganic

chemical vapor deposition. Air mass zero efficiencies as high as 18.8 percent (NASA measurement) have been achieved. Although calculations show that, as is the case with GaAs, a heterostructure is expected to be required for the highest efficiencies attainable, the material properties of InP give the shallow-homojunction structure a greater potential than in the case of GaAs. The best cells, which were those made by ion implantation, show open-circuit voltage (V sub oc) of 873 mV, short-circuit current of 357 A/sq m (35.7 mA/sq cm), and fill factor of 0.829. Improvements are anticipated in all three of these parameters. Internal quantum efficiency peaks at over 90 percent in the red end of the spectrum, but drops to 54 percent in the blue end. Other cells have achieved 74 percent in the blue end. Detailed modeling of the data indicates that a high front surface recombination velocity is responsible for the low blue response, that the carrier lifetime is high enough to allow good carrier collection from both the base and the emitter, and that the voltage is base-limited. Author

N89-24709*# Midwest Research Inst., Golden, CO. Solar Energy Research Inst.

AN EMPIRICAL STUDY OF THE PERFORMANCE OF APMOVPE AM0 InP HOMOJUNCTION SOLAR CELLS AS A FUNCTION OF EMITTER THICKNESS AND DOPING, AND BASE DOPING

M. W. Wanlass, T. A. Gessert, K. A. Emery, and T. J. Coutts *In* NASA, Lewis Research Center, Space Photovoltaic Research and Technology, 1988. High Efficiency, Space Environment, and Array Technology Apr. 1989 p 41-57 (For primary document see N89-24704 18-44)

Avail: NTIS HC A16/MF A01 CSCL 10A

Their excellent radiation resistance and conversion efficiencies greater than 20 percent, measured under global conditions, make InP shallow-homojunction solar cells very attractive for space or terrestrial application. In addition, modeling studies show that, for optimized design, efficiencies of these devices should exceed 20 percent even under AM0 conditions. However, a systematic experimental investigation of the influence of the various cell design parameters on cell performance has not as yet been made. For the n+/p/p+ structures investigated in the previous modeling study, the design parameters include the impurity concentrations and thicknesses of the emitter and base layers. In the work reported here, researchers discuss an experimental investigation of the effects on cell performance of varying the impurity concentrations of the emitter and base and thickness of the emitter. Author

N89-24710*# Arizona State Univ., Tempe. Center for Solid State Electronics Research.

N/P InP HOMOJUNCTION SOLAR CELLS WITH AN In0.53Ga0.47As CONTACTING LAYER GROWN BY LIQUID PHASE EPITAXY

C. C. Shen and K. Y. Choi *In* NASA, Lewis Research Center, Space Photovoltaic Research and Technology, 1988. High Efficiency, Space Environment, and Array Technology Apr. 1989 p 58-65 (For primary document see N89-24704 18-44)

Avail: NTIS HC A16/MF A01 CSCL 10A

N/P InP homojunction solar cells with an In sub 0.53 Ga sub 0.47 As contacting layer were fabricated by liquid phase epitaxy (LPE). Electron-Beam-Induced-Current (EBIC) measurements were performed on several selected samples. It was found that the background doping level in the base region sometimes results in a deep junction, which greatly affects the cell performance. Author

N89-24711*# National Aeronautics and Space Administration. Lewis Research Center, Cleveland, OH.

PREDICTED PERFORMANCE OF InP SOLAR CELLS IN CASSEGRAINIAN AND SLATS SPACE CONCENTRATOR ARRAYS AT 20 TO 100 AM0, 80 TO 100 C

Chandra Goradia, William Thesling, Manju Ghalla Goradia (Cleveland State Univ., OH.), Irving Weinberg, and Clifford K. Swartz *In its* Space Photovoltaic Research and Technology, 1988. High Efficiency, Space Environment, and Array Technology Apr. 1989 p 66-78 (For primary document see N89-24704 18-44)

Avail: NTIS HC A16/MF A01 CSCL 10A

Researchers have calculated the expected performance dependence of near-optimally designed shallow homojunction n+pp+InP solar cells on incident intensities up 200 AM0 and temperatures up to 100 C (373K). Both circular and rectangular cells have been considered, the former for use in a Cassegrainian concentrator array at 100 AM0, 80 to 100 C and the latter for use in a Slats type concentrator array at 20 AM0 80 to 100 C. Calculation of the temperature dependence of the performance parameters I sub sc, V sub oc, FF and eta was done by first verifying that the use of the measured temperature variation of I sub sc, of the best published value of the temperature dependence of the bandgap of InP, and of the temperature dependences of the lifetimes and mobilities of electrons and holes the same as in equivalently doped GaAs, gave calculated results that closely matched measured data on the temperature variation of I sub sc, V sub oc, and FF of four existing InP cells at 1 AM0. It was then assumed that the same temperature dependences of I sub sc, the bandgap and lifetimes and mobilities would hold in the near-optimally designed cells at the higher concentrations. Author

N89-24712*# Astrosystems International, Inc., Newark, DE. AstroPower Div.

MODELLING AND DESIGN OF HIGH PERFORMANCE INDIUM PHOSPHIDE SOLAR CELLS

Sandra L. Rhoads and Allen M. Barnett (Delaware Univ., Newark.) *In* NASA, Lewis Research Center, Space Photovoltaic Research and Technology, 1988. High Efficiency, Space Environment, and Array Technology Apr. 1989 p 79-89 (For primary document see N89-24704 18-44)

Avail: NTIS HC A16/MF A01 CSCL 10A

A first principles pn junction device model has predicted new designs for high voltage, high efficiency InP solar cells. Measured InP material properties were applied and device parameters (thicknesses and doping) were adjusted to obtain optimal performance designs. Results indicate that p/n InP designs will provide higher voltages and higher energy conversion efficiencies than n/p structures. Improvements to n/p structures for increased efficiency are predicted. These new designs exploit the high absorption capabilities, relatively long diffusion lengths, and modest surface recombination velocities characteristic of InP. Predictions of performance indicate achievable open-circuit voltage values as high as 943 mV for InP and a practical maximum AM0 efficiency of 22.5 percent at 1 sun and 27 C. The details of the model, the optimal InP structure and the effect of individual parameter variations on device performance are presented. Author

N89-24713*# State Univ. of New York, Buffalo. Dept. of Electrical and Computer Engineering.

DEEP LEVELS AND RADIATION EFFECTS IN p-InP

W. A. Anderson, A. Singh, K. Jiao, and B. Lee *In* NASA, Lewis Research Center, Space Photovoltaic Research and Technology, 1988. High Efficiency, Space Environment, and Array Technology Apr. 1989 p 90-98 (For primary document see N89-24704 18-44)

Avail: NTIS HC A16/MF A01 CSCL 10A

A survey was conducted on past studies of hole traps in InP. An experiment was designed to evaluate hole traps in Zn-doped InP after fabrication, after electron irradiation and after annealing using deep level transient spectroscopy. Data similar to that of Yamaguchi was seen with observation of both radiation-induced hole and electron traps at E sub A=0.45 eV and 0.03 eV, respectively. Both traps are altered by annealing. It is also shown that trap parameters for surface-barrier devices are influenced by many factors such as bias voltage, which probes traps at different depths below the surface. These devices require great care in data evaluation. Author

N89-24714*# Rensselaer Polytechnic Inst., Troy, NY. Dept. of Electrical, Computer and Systems Engineering.
ENCAPSULATED DIFFUSION OF SULPHUR INTO InP
K. K. Parat, J. M. Borrego, and S. K. Ghandhi *In* NASA, Lewis Research Center, Space Photovoltaic Research and Technology, 1988. High Efficiency, Space Environment, and Array Technology Apr. 1989 p 99-107 (For primary document see N89-24704 18-44)
Avail: NTIS HC A16/MF A01 CSCL 10A

This talk outlines a simple process for the fabrication of n(+)-p solar cells in indium phosphide. Large area cells (greater than 0.25 sq cm) have been made by this process, with a photovoltaic conversion efficiency of 15.21 percent under AM0 conditions of illumination. An ideality factor of 1.1 and a saturation current density of 8 x 10 to the minus 15th power A/sq cm have been observed for these cells. The technique for cell fabrication involves the diffusion of sulfur into InP by an open tube process, and gives highly reproducible results from run to run. A vacuum-deposited layer of gallium sulphide (Ga2S3) was used as the source for sulfur diffusion, with a chemically vapor deposited SiO2 cap layer to prevent decomposition of the InP surface during heat treatment. Diffusions were carried out in a flowing nitrogen ambient at 585 to 708 C, and characterized by their surface carrier concentration and the diffusion constant. The diffusion profile for sulfur in InP is estimated to be of the complementary error function type. The activation energy of the diffusion was estimated to be 1.94 eV. The technique described here is ideally suited for the fabrication of shallow n(+)-p junctions in InP, and has been used for space-borne solar cells. Author

N89-24715*# TRW Space Technology Labs., Redondo Beach, CA.
THE IMPACT OF SOLAR CELL TECHNOLOGY ON PLANAR SOLAR ARRAY PERFORMANCE
Michael W. Mills and Richard M. Kurland *In* NASA, Lewis Research Center, Space Photovoltaic Research and Technology, 1988. High Efficiency, Space Environment, and Array Technology Apr. 1989 p 111-121 (For primary document see N89-24704 18-44)
Avail: NTIS HC A16/MF A01 CSCL 10A

The results of a study into the potential impact of advanced solar cell technologies on the characteristics (weight, cost, area) of typical planar solar arrays designed for low, medium and geosynchronous altitude earth orbits are discussed. The study considered planar solar array substrate designs of lightweight, rigid-panel graphite epoxy and ultra-lightweight Kapton. The study proposed to answer the following questions: Do improved cell characteristics translate into array-level weight, size and cost improvements; What is the relative importance of cell efficiency, weight and cost with respect to array-level performance; How does mission orbital environment affect array-level performance. Comparisons were made at the array level including all mechanisms, hinges, booms, and harnesses. Array designs were sized to provide 5kW of array power (not spacecraft bus power, which is system dependent but can be scaled from given values). The study used important grass roots issues such as use of the GaAs radiation damage coefficients as determined by Anspaugh. Detailed costing was prepared, including cell and cover costs, and manufacturing attrition rates for the various cell types.
Author

N89-24716*# Jet Propulsion Lab., California Inst. of Tech., Pasadena.
ADVANCED PHOTOVOLTAIC SOLAR ARRAY DEVELOPMENT
Richard M. Kurland (TRW Space Technology Labs., Redondo Beach, CA.) and Paul Stella *In* NASA, Lewis Research Center, Space Photovoltaic Research and Technology, 1988. High Efficiency, Space Environment, and Array Technology Apr. 1989 p 122-137 (For primary document see N89-24704 18-44)
Avail: NTIS HC A16/MF A01 CSCL 10A

Phase 2 of the Advanced Photovoltaic Solar Array (APSA) program, started in mid-1987, is currently in progress to fabricate prototype wing hardware that will lead to wing integration and testing in 1989. The design configuration and key details are reviewed. A status of prototype hardware fabricated to date is provided. Results from key component-level tests are discussed. Revised estimates of array-level performance as a function of solar cell device technology for geosynchronous missions are given. Author

N89-24717*# Boeing Co., Seattle, WA. Dept. of Electronics.
DEVELOPMENT OF TANDEM CELLS CONSISTING OF GaAs SINGLE CRYSTAL AND CuInSe2/CdZnS POLYCRYSTALLINE THIN FILMS
Namsoo P. Kim, Billy J. Stanbery, Ronald P. Gale, and Robert W. McClelland (Kopin Corp., Taunton, MA.) *In* NASA, Lewis Research Center, Space Photovoltaic Research and Technology, 1988. High Efficiency, Space Environment, and Array Technology Apr. 1989 p 138-145 (For primary document see N89-24704 18-44)
Avail: NTIS HC A16/MF A01 CSCL 10A

The tandem cells consisting of GaAs single crystal and CuInSe2 polycrystalline thin films are being developed under the joint program of the Boeing Co. and Kopin Corp. to meet the increasing power needs for future spacecraft. The updated status of this program is presented along with experimental results such as cell performance, and radiation resistance. Other cell characteristics including the specific power of and the interconnect options for this tandem cell approach are also discussed. Author

N89-24718*# Boeing Co., Seattle, WA. Dept. of Electronics.
DIRECTIONS FOR FURTHER DEVELOPMENT OF GaAs/CuInSe2 THIN FILM TANDEM CELLS
Billy J. Stanbery *In* NASA, Lewis Research Center, Space Photovoltaic Research and Technology, 1988. High Efficiency, Space Environment, and Array Technology Apr. 1989 p 146-150 (For primary document see N89-24704 18-44)
Avail: NTIS HC A16/MF A01 CSCL 10A

Multijunction thin film solar cells utilizing GaAs and CuInSe2 as semiconductor absorbers are rapidly developing, becoming a viable technology for space power systems with an unparalleled combination of high efficiency, low mass, and high radiation tolerance. The prospect for evolutionary improvement of this type of cell towards efficiency of approximately equals 30 percent and specific power greater than 1 kW/kg while retaining the attribute of high radiation tolerance are good. Limitations of the present configuration and possible avenues for circumventing these problems are presented. Author

N89-24719*# National Aeronautics and Space Administration. Lewis Research Center, Cleveland, OH.
ULTRA-THIN, LIGHT-TRAPPING SILICON SOLAR CELLS
Geoffrey A. Landis *In its* Space Photovoltaic Research and Technology, 1988. High Efficiency, Space Environment, and Array Technology Apr. 1989 p 151-161 (For primary document see N89-24704 18-44)
Avail: NTIS HC A16/MF A01 CSCL 10A

Design concepts for ultra-thin (2 to 10 microns) high efficiency single-crystal silicon cells are discussed. Light trapping allows more light to be absorbed at a given thickness, or allows thinner cells of a given Jsc. Extremely thin cells require low surface recombination velocity at both surfaces, including the ohmic contacts. Reduction of surface recombination by growth of heterojunctions of ZnS and GaP on Si has been demonstrated. The effects of these improvements on AM0 efficiency is shown. The peak efficiency increases, and the optimum thickness decreases. Cells under 10 microns thickness can retain almost optimum power. The increase of absorptance due to light trapping is considered. This is not a problem if the light-trapping cells are sufficiently thin. Ultra-thin cells have high radiation tolerance. A 2 microns thick light-trapping cell remains over 18 percent efficient after the equivalent of 20 years in geosynchronous orbit. Including a 50 microns thick coverglass, the thin cells had specific power after irradiation over ten times higher than the baseline design.
Author

N89-24720*# Energy Conversion Devices, Inc., Troy, MI. Sovonics Solar Systems, Inc.

DEPLOYABLE AEROSPACE PV ARRAY BASED ON AMORPHOUS SILICON ALLOYS

Joseph J. Hanak, Lee Walter, David Dobias, and Harvey Flaisher *In its* Space Photovoltaic Research and Technology, 1988. High Efficiency, Space Environment, and Array Technology Apr. 1989 p 162-163 Sponsored in part by Defense Nuclear Agency (For primary document see N89-24704 18-44)

Avail: NTIS HC A16/MF A01 CSCL 10A

The development of the first commercial, ultralight, flexible, deployable, PV array for aerospace applications is discussed. It is based on thin-film, amorphous silicon alloy, multijunction, solar cells deposited on a thin metal or polymer by a proprietary, roll-to-roll process. The array generates over 200 W at AM0 and is made of 20 giant cells, each 54 cm x 29 cm (1566 sq cm in area). Each cell is protected with bypass diodes. Fully encapsulated array blanket and the deployment mechanism weigh about 800 and 500 g, respectively. These data yield power per area ratio of over 60 W/sq m specific power of over 250 W/kg (4 kg/kW) for the blanket and 154 W/kg (6.5 kg/kW) for the power system. When stowed, the array is rolled up to a diameter of 7 cm and a length of 1.11 m. It is deployed quickly to its full area of 2.92 m x 1.11 m, for instant power. Potential applications include power for lightweight space vehicles, high altitude balloons, remotely piloted and tethered vehicles. These developments signal the dawning of a new age of lightweight, deployable, low-cost space arrays in the range from tens to tens of thousands of watts for near-term applications and the feasibility of multi-100 kW to MW arrays for future needs. Author

N89-24721*# National Aeronautics and Space Administration. Lewis Research Center, Cleveland, OH.

HIGH EFFICIENCY GaAs-Ge TANDEM SOLAR CELLS GROWN BY MOCVD

S. M. Vernon, S. P. Tobin, C. Bajgar, Victor E. Haven, L. M. Geoffroy, D. R. Lillington (Spectrolab, Inc., Sylmar, CA.), and R. E. Hart, Jr. *In its* Space Photovoltaic Research and Technology, 1988. High Efficiency, Space Environment, and Array Technology Apr. 1989 p 167-176 (For primary document see N89-24704 18-44)

Avail: NTIS HC A16/MF A01 CSCL 10A

High conversion efficiency and low weight are obviously desirable for solar cells intended for space applications. One promising structure is GaAs on Ge. The advantages of using Ge wafers as substrates include the following: they offer high efficiency by forming a two-junction tandem cell; low weight combined with superior strength allows usage of thin (3 mil) wafers; and they are a good substrate for GaAs, being lattice matched, thermal expansion matched, and available as large-area wafers. Author

N89-24722*# Westinghouse Research and Development Center, Pittsburgh, PA.

RESPONSE OF SINGLE JUNCTION GaAs/GaAs AND GaAs/Ge SOLAR CELLS TO MULTIPLE DOSES OF 1 MeV ELECTRONS

D. L. Meier, J. R. Szedon, J. Bartko, and M. A. Chung (Air Force Wright-Patterson Aeronautical Labs., Wright-Patterson AFB, OH.) *In* NASA, Lewis Research Center, Space Photovoltaic Research and Technology, 1988. High Efficiency, Space Environment, and Array Technology Apr. 1989 p 177-189 (For primary document see N89-24704 18-44)

Avail: NTIS HC A16/MF A01 CSCL 10A

A comparison of the radiation tolerance of MOCVD-grown GaAs cells and GaAs/Ge cells was undertaken using 1 MeV electrons. The GaAs/Ge cells are somewhat more tolerant of 1 MeV electron irradiation and more responsive to annealing than are the GaAs/GaAs cells examined in this study. However, both types of cells suffer a greater degradation in efficiency than has been observed in other recent studies. The reason for this is not certain, but it may be associated with an emitter thickness which appears to be greater than desired. The deep level transient spectroscopy (DLTS) spectra following irradiation are not significantly different for the GaAs/Ge and the GaAs/GaAs cells, with each having just two peaks. The annealing behavior of these peaks is also similar in the two samples examined. It appears that no penalty in radiation tolerance, and perhaps some benefit, is associated with fabricating MOCVD GaAs cells on Ge substrates rather than GaAs substrates. Author

N89-24723*# Astrosystems International, Inc., Newark, DE. AstroPower Div.

A THREE SOLAR CELL SYSTEM BASED ON A SELF-SUPPORTING, TRANSPARENT AlGaAs TOP SOLAR CELL

Gerald H. Negley, Sandra L. Rhoads, Nancy E. Terranova, James B. McNeely, and Allen M. Barnett (Delaware Univ., Newark.) *In* NASA, Lewis Research Center, Space Photovoltaic Research and Technology, 1988. High Efficiency, Space Environment, and Array Technology Apr. 1989 p 190-200 (For primary document see N89-24704 18-44)

(Contract F33615-88-C-2807)

Avail: NTIS HC A16/MF A01 CSCL 10A

Development of a three solar cell stack can lead to practical efficiencies greater than 30 percent (1x,AM0). A theoretical efficiency limitation of 43.7 percent at AM0 and one sun is predicted by this model. Including expected losses, a practical system efficiency of 36.8 percent is anticipated. These calculations are based on a 1.93eV/1.43eV/0.89eV energy band gap combination. AlGaAs/GaAs/GaInAsP materials can be used with a six-terminal wiring configuration. The key issues for multijunction solar cells are the top and middle solar cell performance and the sub-bandgap transparency. AstroPower has developed a technique to fabricate AlGaAs solar cells on rugged, self-supporting, transparent AlGaAs substrates. Top solar cell efficiencies greater than 11 percent AM0 have been achieved. State-of-the-art GaAs or InP devices will be used for the middle solar cell. GaInAsP will be used to fabricate the bottom solar cell. This material is lattice-matched to InP and offers a wide range of bandgaps for optimization of the three solar cell stack. Liquid phase epitaxy is being used to grow the quaternary material. Initial solar cells have shown open-circuit voltages of 462 mV for a bandgap of 0.92eV. Design rules for the multijunction three solar cell stack are discussed. The progress in the development of the self-supporting AlGaAs top solar cell and the GaInAsP bottom solar cell is presented. Author

N89-24724*# Joint Center for Graduate Study, Richland, WA. Tri-Cities University Center.

INVESTIGATION OF HIGH EFFICIENCY GaAs SOLAR CELLS

Larry C. Olsen, Glen Dunham, F. W. Addis, Dan Huber, and Kurt Linden (Spire Corp., Bedford, MA.) *In* NASA, Lewis Research Center, Space Photovoltaic Research and Technology, 1988. High Efficiency, Space Environment, and Array Technology Apr. 1989 p 203-220 (For primary document see N89-24704 18-44)

Avail: NTIS HC A16/MF A01 CSCL 10A

Investigations of basic mechanisms which limit the performance of high efficiency GaAs solar cells are discussed. P/N heteroface structures have been fabricated from MOCVD epiwafers. Typical AM1 efficiencies are in the 21 to 22 percent range, with a SERI measurement for one cell being 21.5 percent. The cells are nominally 1.5 x 1.5 cm in size. Studies have involved photoresponse, T-I-V analyses, and interpretation of data in terms of appropriate models to determine key cell parameters. Results of these studies are utilized to determine future approaches for increasing GaAs solar cell efficiencies. Author

N89-24725*# Delaware Univ., Newark. Dept. of Electrical Engineering.

A NEW STRUCTURE FOR COMPARING SURFACE PASSIVATION MATERIALS OF GaAs SOLAR CELLS

Gregory C. DeSalvo and Allen M. Barnett *In* NASA, Lewis Research Center, Space Photovoltaic Research and Technology, 1988. High Efficiency, Space Environment, and Array Technology Apr. 1989 p 221-228 (For primary document see N89-24704 18-44)

(Grant NAG3-422)

Avail: NTIS HC A16/MF A01 CSCL 10A

The surface recombination velocity (S sub rec) for bare GaAs is typically as high as 10 to the 6th power to 10 to the 7th power cm/sec, which dramatically lowers the efficiency of GaAs solar cells. Early attempts to circumvent this problem by making an ultra thin junction (xj less than .1 micron) proved unsuccessful when compared to lowering S sub rec by surface passivation. Present day GaAs solar cells use an GaAlAs window layer to passivate the top surface. The advantages of GaAlAs in surface passivation are its high bandgap energy and lattice matching to GaAs. Although GaAlAs is successful in reducing the surface recombination velocity, it has other inherent problems of chemical instability (Al readily oxidizes) and ohmic contact formation. The search for new, more stable window layer materials requires a means to compare their surface passivation ability. Therefore, a device structure is needed to easily test the performance of different passivating candidates. Such a test device is described. Author

N89-24726*# Delaware Univ., Newark. Dept. of Electrical Engineering.

IMPROVED DEFECT ANALYSIS OF GALLIUM ARSENIDE SOLAR CELLS USING IMAGE ENHANCEMENT

Louis C. Kilmer, Christiana Honsberg, Allen M. Barnett, and James E. Phillips *In* NASA, Lewis Research Center, Space Photovoltaic Research and Technology, 1988. High Efficiency, Space Environment, and Array Technology Apr. 1989 p 229-237 (For primary document see N89-24704 18-44)

(Contract F33615-86-C-2723)

Avail: NTIS HC A16/MF A01 CSCL 10A

A new technique has been developed to capture, digitize, and enhance the image of light emission from a forward biased direct bandgap solar cell. Since the forward biased light emission from a direct bandgap solar cell has been shown to display both qualitative and quantitative information about the solar cell's performance and its defects, signal processing techniques can be applied to the light emission images to identify and analyze shunt diodes. Shunt diodes are of particular importance because they have been found to be the type of defect which is likely to cause failure in a GaAs solar cell. The presence of a shunt diode can be detected from the light emission by using a photodetector to measure the quantity of light emitted at various current densities. However, to analyze how the shunt diodes affect the quality of the solar cell the pattern of the light emission must be studied. With the use of image enhancement routines, the light emission can be studied at low light emission levels where shunt diode effects are dominant. Author

N89-24727*# Sverdrup Technology, Inc., Cleveland, OH.

AGING BEHAVIOR OF Au-BASED OHMIC CONTACTS TO GaAs

Navid S. Fatemi *In* NASA, Lewis Research Center, Space Photovoltaic Research and Technology, 1988. High Efficiency, Space Environment, and Array Technology Apr. 1989 p 238-249 Previously announced as N88-25831 (For primary document see N89-24704 18-44)

Avail: NTIS HC A16/MF A01 CSCL 10A

Gold based alloys, commonly used as ohmic contacts for solar cells, are known to react readily with GaAs. It is shown that the contact interaction with the underlying GaAs can continue even at room temperature upon aging, altering both the electrical characteristics of the contacts and the nearby pn junction. Au-Ge-Ni as-deposited (no heat-treatment) contacts made to thin emitter (0.15 microns) GaAs diodes have shown severe shunting of the pn junction upon aging for several months at room temperature. The heat-treated contacts, despite showing degradation in contact resistance, did not affect the underlying pn junction. Au-Zn-Au contacts to p-GaAs emitter (0.2 microns) diodes, however, showed slight improvement in contact resistance upon 200 C isothermal annealing for several months, without degrading the pn junction. The effect of aging on electrical characteristics of the as-deposited and heat-treated contacts and the nearby pn junction, as well as on the surface morphology of the contacts are presented.

Author

N89-24728*# National Aeronautics and Space Administration. Lewis Research Center, Cleveland, OH.

CHEMICAL ETCHING AND ORGANOMETALLIC CHEMICAL VAPOR DEPOSITION ON VARIED GEOMETRIES OF GaAs

Sheila G. Bailey, Geoffrey A. Landis, and David M. Wilt *In its* Space Photovoltaic Research and Technology, 1988. High Efficiency, Space Environment, and Array Technology Apr. 1989 p 250-263 (For primary document see N89-24704 18-44)

Avail: NTIS HC A16/MF A01 CSCL 10A

Results of micron-spaced geometries produced by wet chemical etching and subsequent OMCVD growth on various GaAs surfaces are presented. The polar lattice increases the complexity of the process. The slow-etch planes defined by anisotropic etching are not always the same as the growth facets produced during MOCVD deposition, especially for deposition on higher-order planes produced by the hex groove etching. Author

N89-24729*# Applied Solar Energy Corp., City of Industry, CA.

STATUS OF GaAs SOLAR CELL PRODUCTION

Milton Yeh, Frank Ho, and Peter A. Iles *In* NASA, Lewis Research Center, Space Photovoltaic Research and Technology, 1988. High Efficiency, Space Environment, and Array Technology Apr. 1989 p 267-271 (For primary document see N89-24704 18-44)

Avail: NTIS HC A16/MF A01 CSCL 10A

Recent experience in producing GaAs solar cells, to meet the full requirements of space-array manufacturers is reviewed. The main problems have been in extending MOCVD technology to provide high throughput of high quality epitaxial layers, and to integrate the other important factors needed to meet the full range of user requirements. Some discussion of evolutionary changes is also given. Author

N89-24730*# Applied Solar Energy Corp., City of Industry, CA.

FLEXIBILITY IN SPACE SOLAR CELL PRODUCTION

Scott Khemthong and Peter A. Iles *In* NASA, Lewis Research Center, Space Photovoltaic Research and Technology, 1988. High Efficiency, Space Environment, and Array Technology Apr. 1989 p 272-276 (For primary document see N89-24704 18-44)

Avail: NTIS HC A16/MF A01 CSCL 10A

The wide range of cells that must be available from present-day production lines for space solar cells are described. After over thirty years of space-cell use, there is very little standardization in solar cell design. It is not generally recognized what a wide range of designs must remain available on cell production lines. This range of designs is surveyed. Author

N89-24731*# Spectrolab, Inc., Sylmar, CA.

GALLIUM ARSENIDE WELDED PANEL TECHNOLOGY FOR ADVANCED SPACEFLIGHT APPLICATIONS

D. R. Lillington, M. S. Gillanders, G. F. J. Garlick, B. T. Cavicchi, G. S. Glenn, and S. P. Tobin (Spire Corp., Bedford, MA.) *In* NASA, Lewis Research Center, Space Photovoltaic Research and Technology, 1988. High Efficiency, Space Environment, and Array Technology Apr. 1989 p 277-285 (For primary document see N89-24704 18-44)

Avail: NTIS HC A16/MF A01 CSCL 10A

A significant impediment to the widespread use of GaAs solar cells in space is the cost and weight of the GaAs substrate. In order to overcome these problems, Spectrolab is pursuing thin cell technologies encompassing both liquid phase epitaxy (LPE) GaAs on GaAs and MOCVD GaAs on Ge cells. Spectrolab's experience in the manufacture of 4 to 6 mil 2 cm x 4 cm GaAs cells on a LPE production line is discussed. By thinning the cells at a late state of processing, production yields comparable to 12 mil cells have been achieved. Data are presented showing that GaAs cells can be welded without degradation and have achieved minimum average efficiencies of 18 percent AM0, 28 C with efficiencies up to 20 percent. Spectrolab, in conjunction with Spire Corporation has also been pursuing GaAs on Ge cell technology in support of larger area lighter weight power systems. Data are presented showing that individual 2 cm x 2 cm, 8 mil cell efficiencies up to 21.7 percent have been achieved. Efficiencies up to 24 percent AM0 will be possible by optimizing the GaAs/Ge interface.

Cells have been welded without degradation using silver interconnects and have been laid down on an aluminum honeycomb/graphite facesheet substrate to produce a small coupon. The efficiency was 18.1 percent at AM0, 28 C. Author

N89-24732*# National Aeronautics and Space Administration. Lewis Research Center, Cleveland, OH.
DOMED FRESNEL LENS CONCENTRATOR TECHNOLOGY FOR SPACE APPLICATION
Michael F. Piszczor, Jr. and Mark J. ONeill (ENTECH Corp., Dallas-Fort Worth Airport, TX.) *In its* Space Photovoltaic Research and Technology, 1988. High Efficiency, Space Environment, and Array Technology Apr. 1989 p 286-291 (For primary document see N89-24704 18-44)
Avail: NTIS HC A16/MF A01 CSCL 10A

Over the past three years, NASA Lewis and Entech, Inc. have been investigating the use of high efficiency refractive photovoltaic concentrators for use in space. The design currently under investigation uses a square domed Fresnel lens to focus light on a GaAs concentrator cell. A prismatic cell cover, which directs light away from the front contacts and thus eliminates metalization losses, is applied to the top of the GaAs cell to further enhance array efficiency. The latest experimental results based on testing the GaAs cell/prism cover assembly at standard and operating conditions are presented. Author

N89-24733*# Varian Associates, Palo Alto, CA.
THE 25 PERCENT-EFFICIENT GaAs CASSEGRAINIAN CONCENTRATOR CELL
H. C. Hamaker, M. Grounner, N. R. Kaminar, M. S. Kuryla, M. J. Ladle, D. D. Liu, H. F. MacMillan, L. D. Partain, G. F. Virshup, and J. G. Werthen et al *In* NASA, Lewis Research Center, Space Photovoltaic Research and Technology, 1988. High Efficiency. Space Environment, and Array Technology Apr. 1989 p 292-297 Prepared in cooperation with Sandia National Labs., Albuquerque, NM (For primary document see N89-24704 18-44)
Avail: NTIS HC A16/MF A01 CSCL 10A

Very high-efficiency GaAs Cassegrainian solar cells have been fabricated in both the n-p and p-n configurations. The n-p configuration exhibits the highest efficiency at concentration, the best cells having an efficiency eta of 24.5 percent (100X, AM0, temperature T = 28 C). Although the cells are designed for operation at this concentration, peak efficiency is observed near 300 suns (eta = 25.1 percent). To our knowledge, this is the highest reported solar cell efficiency for space applications. The improvement in efficiency over that reported at the previous SPRAT conference is attributed primarily to lower series resistance and improved grid-line plating procedures. Using previously measured temperature coefficients, researchers estimate that the n-p GaAs cells should deliver approximately 22.5 percent efficiency at the operating conditions of 100 suns and T = 80 C. This performance exceeds the NASA program goal of 22 percent for the Cassegrainian cell. One hundred Cassegrainian cells have been sent to NASA as deliverables, sixty-eight in the n-p configuration and thirty-two in the p-n configuration. Author

N89-24734*# Aerospace Corp., Los Angeles, CA.
CONTAMINATION EFFECTS OF GPS NAVSTAR SOLAR ARRAY PERFORMANCE
Dean C. Marvin and Warren C. Hwang *In* NASA, Lewis Research Center, Space Photovoltaic Research and Technology, 1988. High Efficiency, Space Environment, and Array Technology Apr. 1989 p 301-305 (For primary document see N89-24704 18-44)
Avail: NTIS HC A16/MF A01 CSCL 10A

The solar arrays on Navstars 1 to 6 have been limiting the electrical power capabilities in the extended life (beyond the 5 year design life). The departure from predicted performance consists of an extra 2.5 percent per year degradation beyond the radiation model estimates. This degradation is unusual in showing a linear rather than exponential decay with time. The performance of the arrays on these satellites has been examined in order to predict future behavior and to make refined projections on the Navstar 7 to 11 solar arrays. Evidence obtained from flight experiments on Navstar 5 and 6, and from laboratory experiments, suggests that contamination of the solar arrays while on orbit may be responsible. The evidence for photo-induced contamination of spacecraft surfaces is presented, and the effect on solar array output in the case of the GPS satellites is shown to be consistent with the observed anomalies. Author

N89-24735*# Naval Research Lab., Washington, DC.
THE EXPERIMENTS OF LIPS 3
J. G. Severns, R. M. Hobbs, N. P. Elliott, R. H. Towsley, and G. F. Virshup (Varian Associates, Palo Alto, CA.) *In* NASA, Lewis Research Center, Space Photovoltaic Research and Technology, 1988. High Efficiency, Space Environment, and Array Technology Apr. 1989 p 306-322 (For primary document see N89-24704 18-44)
Avail: NTIS HC A16/MF A01 CSCL 10A

LIPS 3 is a member of the Living Plume Shield series of spacecraft. In each LIPS project, the plume shield, a simple sheet metal cone, was structurally stiffened, and an active satellite was then built around it. The original purpose of the plume shield was to prevent the plume from solid propellent engines, which are fired outside the atmosphere after the aerodynamic shroud is jettisoned, from reaching the primary payload. The surface of LIPS 3 facing the plume also functioned in this manner, but the anterior surfaces were unaffected, and it was there that all solar arrays, sensors, and experiments were mounted. The purpose of LIPS 3 was to provide a test bed for new space power sources. With the long delays projected for schedules of the STS and other major launch systems, it appeared that a decade might pass before long term flight data could be obtained on many new and innovative power sources. The fact that a launch scheduled for early in 1987 required a plume shield was seen as a unique opportunity to obtain some of this data in a timely manner. The LIPS 3 system, the experiments placed aboard, and the experiment data acquisition subsystem are described. Various problems were encountered during integration and after launch; those which appear to effect the accuracy of experimental results are discussed. A preliminary description is given of the accuracy of the flight experiment data. Author

N89-24736*# Midwest Research Inst., Golden, CO. Solar Energy Research Inst.
AM0 EFFICIENCY MEASUREMENTS
Keith Emery and Carl Osterwald *In* NASA, Lewis Research Center, Space Photovoltaic Research and Technology, 1988. High Efficiency, Space Environment, and Array Technology Apr. 1989 p 323-331 (For primary document see N89-24704 18-44)
Avail: NTIS HC A16/MF A01 CSCL 10A

Procedures for measuring the air mass zero (AM0) current versus voltage characteristics and calculating the efficiency are discussed. The various factors influencing the determination of the efficiency include the I-V measurement system, reference cell calibration, standard reporting conditions, area measurement, light source characteristics, temperature measurement and control, and the measurement procedures. Each of these sources contributes to the precision index and bias limit which is combined to obtain the total uncertainty in the efficiency. These factors are discussed as well as how to minimize differences in the reported AM0 efficiency of a given PV cell between various laboratories. Author

N89-24737*# National Aeronautics and Space Administration. Lewis Research Center, Cleveland, OH.
A COMPARISON OF THE RADIATION TOLERANCE CHARACTERISTICS OF MULTIJUNCTION SOLAR CELLS WITH SERIES AND VOLTAGE-MATCHED CONFIGURATIONS
James M. Gee (Sandia National Labs., Albuquerque, NM.) and Henry B. Curtis *In its* Space Photovoltaic Research and Technology, 1988. High Efficiency, Space Environment, and Array Technology Apr. 1989 p 332-338 Previously announced as N86-24017 (For primary document see N89-24704 18-44)

(Contract DE-AC04-76DP-00789)
Avail: NTIS HC A16/MF A01 CSCL 10A

The effect of series and voltage-matched configurations on the performance of multijunction solar cells in a radiation environment was investigated. It was found that the configuration of the multijunction solar cell can have a significant impact on its radiation tolerance characteristics. Author

N89-24738*# Wayne State Univ., Detroit, MI.
RADIATION RESISTANCE STUDIES OF AMORPHOUS SILICON FILMS
James R. Woodyard and J. Scott Payson *In* NASA, Lewis Research Center, Space Photovoltaic Research and Technology, 1988. High Efficiency, Space Environment, and Array Technology Apr. 1989 p 339-347 (For primary document see N89-24704 18-44)
(Grant NAG3-833)
Avail: NTIS HC A16/MF A01 CSCL 10A

Hydrogenated amorphous silicon thin films were irradiated with 2.00 MeV helium ions using fluences ranging from 1E11 to 1E15 cm(-2). The films were characterized using photothermal deflection spectroscopy and photoconductivity measurements. The investigations show that the radiation introduces sub-band-gap states 1.35 eV below the conduction band and the states increase supralinearly with fluence. Photoconductivity measurements suggest the density of states above the Fermi energy is not changing drastically with fluence. Author

N89-24739# Midwest Research Inst., Golden, CO. Solar Energy Research Inst.
RESEARCH ON HIGH-EFFICIENCY, SINGLE-JUNCTION, MONOLITHIC, THIN-FILM AMORPHOUS SILICON SOLAR CELLS Final Report, 1 Oct. 1983 - 31 Jan. 1987
A. E. Delahoy, E. Eser, F. Kampas, and R. Lenskold Mar. 1989 114 p Prepared in cooperation with Chronar Corp., Princeton, NJ
(Contract DE-AC02-83CH-10093)
(DE89-000893; SERI/STR-211-3447) Avail: NTIS HC A06/MF A01

This report contains results of research designed to fabricate single-junction p-i-n solar cells with 12 percent efficiency at air-mass 1 with an area of about 1 sq cm and submodules of interconnected single-junction cells with 8 percent efficiency and areas of about 1000 sq cm. An objective was to control light-induced degradation to less than 2 percent over 720 hours of AMI illumination. A secondary objective was to design, construct, and operate a multichamber deposition system that would deposit p-i-n cells over an area of 1000 sq cm. The best efficiency obtained was 10.8 percent with a small-area cell (0.08 cm^2). The best stabilities and efficiencies were obtained with conventional p-i-n a-SiC:H/a-Si:H heterostructures, p-i-n/p-i-n tandem cells, and structures containing transitional affinity-graded i-layers. Small- and large-area efficiencies stayed below performance goals by about 1 percent , however. The multichamber deposition system was designed and operated, but a problem remained with boron contamination of the i-layer that should be investigated further. DOE

N89-24740# Swedish Defence Research Establishment, Stockholm.
CONTROL RESEARCH IN WINDPOWER PROJECT 506259 UTILIZATION Final Report, Part 4
Eskil Ulen Jan. 1989 34 p In SWEDISH; ENGLISH summary
(Contract NEA-506259-4)
(FOA-C-20746-2.7; ISSN-0347-3694; ETN-89-94541) Avail: NTIS HC A03/MF A01

Control systems design is analyzed for a windpowered generator with variable velocity. A project for a simplified wind-diesel construction, without a separate bearing was investigated. Yaw motion influence on the lateral motion of the tower was studied. This effect can be attenuated with a better design of the yaw servomotors. The rotor speed was used as out-signal, instead of the acceleration which is proportional to the aerodynamic moment, but the method of computing the acceleration is difficult. Feedback control and mean square errors are outlined. ESA

N89-24741*# Sverdrup Technology, Inc., Cleveland, OH.
NASA LEWIS STIRLING ENGINE COMPUTER CODE EVALUATION Final Report
Timothy J. Sullivan Jan. 1989 43 p
(Contracts NAS3-24105; DE-AI01-85CE-50112)
(NASA-CR-182248; DOE/NASA/4105-4; E-4580; NAS 1.26:182248) Avail: NTIS HC A03/MF A01

In support of the U.S. Department of Energy's Stirling Engine Highway Vehicle Systems program, the NASA Lewis Stirling engine performance code was evaluated by comparing code predictions without engine-specific calibration factors to GPU-3, P-40, and RE-1000 Stirling engine test data. The error in predicting power output was -11 percent for the P-40 and 12 percent for the Re-1000 at design conditions and 16 percent for the GPU-3 at near-design conditions (2000 rpm engine speed versus 3000 rpm at design). The efficiency and heat input predictions showed better agreement with engine test data than did the power predictions. Concerning all data points, the error in predicting the GPU-3 brake power was significantly larger than for the other engines and was mainly a result of inaccuracy in predicting the pressure phase angle. Analysis into this pressure phase angle prediction error suggested that improvements to the cylinder hysteresis loss model could have a significant effect on overall Stirling engine performance predictions. Author

N89-24742# Clarkson Univ., Potsdam, NY. Dept. of Mechanical Engineering.
RADIOMETRIC MEASUREMENT OF TEMPERATURE DISTRIBUTIONS IN SOLAR CAVITY RECEIVERS
E. F. Thacher and P. S. Giannola Mar. 1989 191 p Prepared in cooperation with United Technologies Research Center, East Hartford,
(Contract DE-AC04-76DP-00789)
(DE89-011467; SAND-89-7026) Avail: NTIS HC A09/MF A01

An engineering tool incorporating a scanning infrared radiometer, an image digitizer, a microcomputer, and the software to drive the system was developed to allow remote mapping of the temperature distribution in solar cavity receivers. Using enclosure analysis, the infrared image processing program extracts the irradiance map from the radiosity map of the cavity to yield an emissive power map. Using the calibration curve of the radiometer and the emissivity of the surface of the cavity, the emissive power map is transformed into a temperature map. The system was tested by comparing its calculated temperatures to temperatures measured by thermocouples at several locations on the surfaces of heated model cavity receivers. The average relative error for the cavities ranged from 4.6 percent to 34.9 percent, with the relative error on the base usually less than half that on the wall. Some work was also carried out to compensate the detected radiosity field for the system transfer function error of the scanner system. DOE

N89-24743# Midwest Research Inst., Golden, CO. Solar Energy Research Inst.
PHOTOVOLTAIC ADVANCED RESEARCH AND DEVELOPMENT PROJECT: SOLAR RADIATION RESEARCH Annual Report, 1 Oct. 1987 - 30 Sep. 1988
C. J. Riordan, R. L. Hulstrom, T. W. Cannon, T. L. Stoffel, and D. R. Myers Feb. 1989 26 p
(Contract DE-AC02-83CH-10093)
(DE89-000884; SERI/PR-215-3445) Avail: NTIS HC A03/MF A01

This report summarizes work performed in FY 1988 by the Solar Energy Research Institute's Resource Assessment and Instrumentation Branch, Solar Electric Research Division, under the Solar Radiation Research Task of the SERI Photovoltaic Advanced Research and Development Project. The objectives of this task are to implement improved solar radiation models and data bases and to develop specialized instrumentation and

measurement techniques needed to help develop a technical understanding of the relationships between photovoltaic device performance and variations in outdoor solar radiation. DOE

N89-24744# Colorado State Univ., Fort Collins. Solar Energy Applications Lab.
DEVELOPING, TESTING, EVALUATING AND OPTIMIZING SOLAR HEATING AND COOLING SYSTEMS
S. Karaki May 1989 19 p
(Contract DE-FG03-86SF-16306)
(DE89-011831; DOE/SF-16306/14) Avail: NTIS HC A03/MF A01

The objective is to develop and test various integrated solar heating, cooling and domestic hot water systems, and to evaluate their performance. Systems composed of new, as well as previously tested, components are carefully integrated so that effects of new components on system performance can be clearly delineated. The program for 1989-90 is separated into seven tasks. There are asks for each of the three solar houses, a project to build and test several generic solar water heaters, a task involving development of an improved evacuated tube collector, a management task, and a task under which an international workshop will test IEA Task 4 models. The objectives and progress in each task are described in this report. DOE

N89-24745# Pacific Northwest Labs., Richland, WA.
US FUEL CELL RESEARCH AND APPLICATIONS, 1960--1989
B. R. Kinzey and R. K. Sen Apr. 1989 44 p
(Contract DE-AC06-76RL-01830)
(DE89-012244; PNL-6892) Avail: NTIS HC A03/MF A01

This paper provides an overview of the major fuel cell Research and Development (R and D) programs funded by the US government and the private sector, with a particular focus on terrestrial applications. Included in this overview is information on funding levels, project descriptions and goals, and selected accomplishments. Brief assessments as to the proximity of commercialization for each of the primary types of fuel cells are also furnished. DOE

N89-24355# Dornier-Werke G.m.b.H., Friedrichshafen (Germany, F.R.).
FUEL CELL DEVELOPMENT FOR HERMES
H. Gehrke and U. Knoebel *In* ESA, International Symposium on Europe in Space: The Manned Space System Oct. 1988 p 169-174 (For primary document see N89-24335 18-12)
Copyright Avail: NTIS HC A99/MF A01; ESA Publications Div., ESTEC, Noordwijk, Netherlands, 80 Dutch guilders

45 ENVIRONMENT POLLUTION

Includes atmospheric, noise, thermal, and water pollution.

N89-24746*# Alabama Univ., Huntsville. Center for Applied Optics.
CONTAMINATION EFFECTS STUDY Final Report
Dec. 1988 28 p
(Contract NAS8-36955)
(NASA-CR-183613; NAS 1.26:183613) Avail: NTIS HC A03/MF A01 CSCL 13B

The in-situ optical surface measurement system is a facility designed to study the deleterious effects of particulate materials on the surface reflectivities of optical materials in the vacuum ultraviolet (VUV). This arrangement is designed to simulate the on-orbit effects of contamination and degradation of optical surfaces. This simulation is accomplished through the use of non-coherent VUV sources illuminating optical surfaces located in a high vacuum chamber. Several sources of contamination are employed. The reflectivity is measured both at the specular reflection as well as at two scattered positions, forward and reverse. The system components are described and an operating procedure is given. A.D.

N89-24747# Tennessee Valley Authority, Norris.
THE IMPORTANCE OF CLIMATOLOGICAL VARIABILITY AND THE RATE AT WHICH WASTE IS ADDED TO MODELING WATER BUDGET OF LANDFILLS
Steven C. Young and Roger B. Clapp (Oak Ridge National Lab., TN.) 1989 20 p Presented at the 4th International Conference on Solving Ground Water Problems with Models, Indianapolis, IN, 7 Feb. 1989
(Contract DE-AC05-84OR-21400)
(DE89-008917; CONF-890262-2) Avail: NTIS HC A03/MF A01

A transient one-dimensional wetting front model was developed to predict water budgets for landfills. The model simulates the moisture profile by a series of blocks, each of which has a uniform soil moisture content. The model can simulate the continual stacking of waste by adding blocks, which represent new waste layers. The model can be programmed to build up a landfill at a given rate and to cap the landfill with a liner once a specific height has been reached. The wetting front model has been compared with models that solve the Richards Equation directly. In past studies the results between the two types of models compared well, but the wetting front model solved problems with a fraction of the computer time. Because of its efficient algorithms, the wetting front model is well suited for Monte Carlo simulation of different meteorological conditions in order to produce probability density functions for runoff, evapotranspiration, and leachate generation. In order to simulate different meteorological conditions, the TVA developed RGEN, which generates hourly rainfall, and EGEN which generates daily potential evaporation rates. The results of the numerous runs with the wetting front model were used to determine the potential importance of climatological variability and the effects of the rate at which new waste is added on the water budget of dry-stack fly ash landfills. DOE

N89-24748# Oak Ridge National Lab., TN. Environmental Science Div.
BIBLIOGRAPHY ON TROPICAL RAIN FORESTS AND THE GLOBAL CARBON CYCLE. VOLUME 2: SOUTH ASIA
Elizabeth P. Flint, John F. Richards, and F. M. OHara Feb. 1989 352 p
(Contract DE-AC05-84OR-21400)
(DE89-008971; ORNL/CDIAC-24/V2) Avail: NTIS HC A16/MF A01

This bibliography covers the literature on tropical rain forests, tropical deforestation, land-use change, tropical forest conversion, and shifting cultivation in South Asia (predominantly India, Pakistan, and Bangladesh but also including contributions in Burma, Ceylon, Malaysia, and Sri Lanka). It covers not only rain-forest ecosystems but also other ecosystems that border, derive from, or influence rain forests. The literature included was selected because of its contribution to understanding the global carbon cycle, changes in that cycle, and rain forests' role in that cycle. Journal articles, books, and reports from 1880 to 1988 are included. The more than 4200 entries of this bibliography are ordered alphabetically by author and are indexed by subject and author. DOE

N89-24749# Argonne National Lab., IL. Biological, Environmental and Medical Research Div.
THE RELATIONSHIP BETWEEN IN-LAKE SULFATE CONCENTRATION AND ESTIMATES OF ATMOSPHERIC SULFUR DEPOSITION FOR SUBREGIONS OF THE EASTERN LAKE SURVEY
Barry M. Lesht and Jack D. Shannon Mar. 1989 14 p
(Contract W-31-109-eng-38)
(DE89-009868; ANL-9009868) Avail: NTIS HC A03/MF A01

Estimated amounts of the total sulfur deposition at each of the 1798 lakes in the U.S. Environmental Protection Agency's Eastern Lake Survey, obtained by using the ASTRAP model, were compared with the survey measurements of in-lake sulfate concentration on a subregional basis. In general, the sample median in-lake sulfate concentration was qualitatively correlated with the sample median estimated total sulfur deposition, with in-lake concentration increasing with increased estimated deposition. Two subregions, 3A (southern Blue Ridge) and 3B

(Florida), however, did not fit this relationship. In-lake sulfate concentrations were higher than expected in Florida and lower than expected in the southern Blue Ridge. Comparison of our modeled total sulfur deposition with estimated amounts of wet-only sulfate deposition were in good agreement in terms of subregional rank order. More detailed comparison of the magnitudes of the estimates was not done because others reported deposition in terms of the estimated population medians, obtained by using a weighting procedure based on alkalinity map class, instead of as sample medians and also used the weighting procedure to estimate the subregional median in-lake sulfate concentration. DOE

N89-24750# Lawrence Livermore National Lab., CA.
BEYOND CO2: THE OTHER GREENHOUSE GASES
Donald J. Wuebbles May 1989 18 p Presented at the 82nd Air and Waste Management Association Annual Meeting and Exhibition, Anaheim, CA, 25-30 Jun. 1989
(Contract W-7405-eng-48)
(DE89-011893; UCRL-99883; CONF-890692-8) Avail: NTIS HC A03/MF A01

Most of the concern about potential effects of greenhouse gases on the future state of climate has been related to the growing atmospheric concentrations of carbon dioxide. Concentrations of a number of other radiatively important atmospheric trace constituents are also changing, many at rates much larger than the current rate of change in CO2 concentrations. For example, the methane concentration is increasing one percent per year, while the concentrations of several chlorofluorocarbons are increasing by 4 to 5 percent per year. In each case, the increasing concentrations of these gases, which are emitted at the earth's surface, is thought to be related primarily to human activities. The combined effects of these other greenhouse gases on climate could be cumulatively as large as those estimated for CO2. Besides the direct radiative effects that these gases can have on climate, there are also potential indirect effects on climate through their chemical interactions with other greenhouse gases, such as ozone and water vapor. Evidence is mounting that such indirect effects are occurring. This paper describes what is known regarding these changing greenhouse gas concentrations and their budgets, and examines the uncertainties affecting their influence on climate. It also attempts to establish criteria for determining their potential effects on climate in relation to CO2. DOE

N89-24751# Lawrence Livermore National Lab., CA.
FIELD STUDIES FOR DETERMINING THE CHARACTERISTICS AND DYNAMICS OF LOCAL CIRCULATIONS
Paul H. Gudiksen, William E. Clements, Rayford P. Hosker, Jr., C. David Whiteman, William D. Neff, Richard L. Coulter, and G. Eugene Start (National Oceanic and Atmospheric Administration, Idaho Falls, ID.) Apr. 1989 35 p Presented at the 2nd International Workshop on Real-time Computing of the Environmental Consequences of an Accidental Release to the Atmosphere from a Nuclear Installation, Luxembourg, Luxembourg, 15-19 May 1989
(Contract W-7405-eng-48)
(DE89-012290; UCRL-100924; CONF-8905115-2) Avail: NTIS HC A03/MF A01

This paper provides an overview of some of the most salient features of valley circulations that influence the dispersion of pollutants. The emphasis is primarily on the most important characteristics of interest to an emergency response manager who must develop emergency preparedness plans for facilities tht may be influenced by valley circulations. The discussions will be centered on the results of the Anderson Creek Valley and the Brush Creek Valley studies, to contrast the characteristics of a pooling valley with those of a draining valley. The paper also provides suggestions on the most critical measurements that are needed to define the behavior of the nocturnal valley flows that may be expected within any given valley. DOE

46 GEOPHYSICS

Includes aeronomy; upper and lower atmosphere studies; ionospheric and magnetospheric physics; and geomagnetism.

For space radiation see *93 Space Radiation.*

N89-24752*# Planetary Science Inst., Tucson, AZ.
COMPARATIVE PLANETOLOGY OF EARLY INTENSE CRATERING AND OTHER CRATERING EFFECTS Final Report, 15 May 1983 - 14 Nov. 1987
William K. Hartmann 14 Nov. 1987 94 p
(Contract NASw-3782)
(NASA-CR-182966; NAS 1.26:182966) Avail: NTIS HC A05/MF A01 CSCL 08G

Intense early cratering in the first few hundred million years of the solar system, its decline to the present rate, and the consequent effects on the evolution of planetary surfaces were studied. Author

N89-24753# National Aerospace Lab., Tokyo (Japan). Control Systems Div.
DETERMINATION OF STATION COORDINATES, EARTH ROTATION AND PLATE MOTIONS FROM LAGEOS LASER RANGING: 1983-1986
Masaaki Murata Jun. 1988 28 p
(NAL-TR-980T; ISSN-0389-4010) Avail: NTIS HC A03/MF A01

A summary of recent results of analyses of satellite laser ranging (SLR) data collected by the LAGEOS (Laser Geodynamics Satellite) for the 3.3-year period from September 1983 to December 1986 is presented. The LAGEOS data were analyzed to compute earth rotation parameters and a new global solution of the geocentric coordinates for 39 laser tracking stations. Laser station positioning was part of a simultaneous adjustment of parameters for the LAGEOS orbital elements, an along-track acceleration, a solar radiation pressure coefficient in 30-day arcs and earth rotation parameters in 5-day subarcs. The earth rotation series, computed at 5-day intervals, have an internal precision of better than 2 mas for polar motion components and 0.15 ms for the change in the length of day. For 15 selected laser stations, baseline and station coordinate changes were investigated by successive determination of station positions using annual datasets covering the 3-year period beginning in January 1984. It is shown that laser observed rates of change in baseline lengths are in general agreement with the motions predicted by the Minster-Jordan Am1-2 model. Plate motions relative to Shimosato laser station were observed for the first time using SLR data. Author

N89-24754*# Texas Univ., Austin.
LASER RANGING DATA ANALYSIS Final Report, 1988
28 Mar. 1989 25 p
(Grant NAG5-1021)
(NASA-CR-184847; NAS 1.26:184847) Avail: NTIS HC A03/MF A01 CSCL 08E

Results of the near real-time analysis of Lageos laser ranging data are reported. The data was analyzed in terms of range bias, time bias, and internal precision; and estimates for the Earth orientation parameters X sub p, Y sub p, and UT1 are obtained. The results of these analyses are reported in a variety of formats. Sample copies of the weekly summaries from the second half of 1988 are included along with an annotated distribution list of the weekly summaries. Annual summaries for 1987 and 1988 are also included. A.D.

N89-24755*# Georgia Inst. of Tech., Atlanta. School of Geophysical Sciences.
IMPROVEMENTS IN THE GLOBAL REFERENCE ATMOSPHERIC MODEL AND COMPARISONS WITH A GLOBAL 3-D NUMERICAL MODEL Semiannual Status Report, 23 Sep. 1988 - 22 Mar. 1989
C. G. Justus, F. N. Alyea, George Chimonas, and D. M. Cunnold Apr. 1989 19 p

(Grant NAG8-78; Proj. G-35-685)
(NASA-CR-184947; NAS 1.26:184947) Avail: NTIS HC A03/MF A01 CSCL 04A

The status of the Global Reference Atmospheric Model (GRAM) and the Mars Global Reference Atmospheric Model (MARS-GRAM) is reviewed. The wavelike perturbations observed in the Viking 1 and 2 surface pressure data, in the Mariner 9 IR spectroscopy data, and in the Viking 1 and 2 lander entry profiles were studied and the results interpreted. B.G.

N89-24756*# Universities Space Research Association, Boulder, CO. Program Office.
A VISITING SCIENTIST PROGRAM IN ATMOSPHERIC SCIENCES FOR THE GODDARD SPACE FLIGHT CENTER Final Report, Apr. 1984 - Sep. 1988
M. H. Davis Columbia, MD Jan. 1989 36 p
(Contract NAS5-28135)
(NASA-CR-183421; NAS 1.26:183421) Avail: NTIS HC A03/MF A01 CSCL 04A

A visiting scientist program was conducted in the atmospheric sciences and related areas at the Goddard Laboratory for Atmospheres. Research was performed in mathematical analysis as applied to computer modeling of the atmospheres; development of atmospheric modeling programs; analysis of remotely sensed atmospheric, surface, and oceanic data and its incorporation into atmospheric models; development of advanced remote sensing instrumentation; and related research areas. The specific research efforts are detailed by tasks. B.G.

N89-24757*# Massachusetts Inst. of Tech., Cambridge. Dept. of Earth, Atmospheric and Planetary Sciences.
PLATE MOTIONS AND DEFORMATIONS FROM GEOLOGIC AND GEODETIC DATA Semiannual Report, 1 Jul. - 31 Dec. 1988
Thomas H. Jordan 24 May 1989 222 p
(Grant NAG5-459)
(NASA-CR-184987; NAS 1.26:184987) Avail: NTIS HC A10/MF A01 CSCL 08G

The very long baseline interferometry (VLBI) measurements made in the western U.S. since 1979 provide discrete samples of the temporal and spatial deformation field. The interpretation of the VLBI derived rates of deformation requires an examination of geologic information and more densely sampled ground based geodetic data. Triangulation and trilateration data measured on two regional networks, one in the central Mojave Desert and one in the Coast Ranges east of the San Andreas fault, were processed. At the spatial scales spanned by these local geodetic networks, auxiliary geologic and geophysical data were utilized to examine the relation between measured incremental strain and the accommodation of strain seen in local geologic structures, strain release in earthquakes, and principal stress directions inferred from in situ measurements. VLBI data was also processed from stations distributed across the Pacific-North America plate boundary zone in the western U.S. The VLBI data were used to constrain the integrated rate of deformation across portions of the continental plate boundary in California and to provide a tectonic framework to interpret regional geodetic and geologic studies. Author

N89-24758*# National Oceanic and Atmospheric Administration, Washington, DC.
SIMULATION STUDIES OF IMPROVED SOUNDING SYSTEMS
H. Yates, D. Wark, H. Aumann, N. Evans, N. Phillips, J. Susskind, L. McMillin, A. Goldman, M. Chahine, and L. Crone (National Environmental Satellite Service Boulder, CO.) Feb. 1989 115 p Sponsored in part by NASA
(NASA-CR-185322; NAS 1.26:185322; NOAA-TR-NESDIS-42)
Avail: NTIS HC A06/MF A01 CSCL 04A

Two instrument designs for indirect satellite sounding of the atmosphere in the infrared are represented by the High Resolution Infra-Red Sounder, Model 2 (HIRS-2) and by the Advanced Meteorological Temperature Sounder (AMTS). The relative capabilities of the two instruments were tested by simulating satellite measurements from a group of temperature soundings, allowing the two participants to retrieve the temperature profiles from the simulated data, and comparing the results with the original temperature profiles. Four data sets were produced from radiosondes data extrapolated to a suitable altitude, representing continents and oceans, between 30S and 30N. From the information available, temperature profiles were retrieved by two different methods, statistical regression and inversion of the radiative transfer equation. Results show the consequence of greater spectral purity, concomitant increase in the number of spectral intervals, and the better spatial resolution in partly clouded areas. At the same time, the limitation of the HIRS-2 without its companion instrument leads to some results which should be ignored in comparing the two instruments. A clear superiority of AMTS results is shown. Author

N89-24759# Naval Postgraduate School, Monterey, CA.
CORRELATION BETWEEN SATELLITE-DERIVED AEROSOL CHARACTERISTICS AND OCEANIC DIMETHYLSULFIDE (DMS) M.S. Thesis
Richard A. Shema Dec. 1988 57 p Original contains color illustrations
(AD-A206179) Avail: NTIS HC A04/MF A01 CSCL 04/1

Since the turn of the century, the earth's climate has fluctuated between warming and cooling cycles. A warming cycle has been observed in the early 1900's. The rising global temperature has been attributed to CO2 release from the burning of fossil fuels. The absorption of IR energy emitted from the earth, or greenhouse effect, brought concern that continued warming would melt polar ice caps and permanently change global climate. However, beginning in the mid-1940's, atmospheric cooling was observed. A possible contribution to the cooling trend is an increase in the numbers of relatively small aerosol particles. These particles are efficient scatters of solar radiation. An increase in the number of scattering events causes a higher albedo, thereby creating a cooler planet. McCormick and Ludwig (1967) have presented arguments to show this relationship. Approximately forty years later, in the early 1980's, warming of the earth's climate again has been observed. GRA

N89-24760# Bonn Univ. (Germany, F.R.). Hohen Mathematisch-Naturwissenschaftlichen Fakultaet.
INVESTIGATIONS OF THE SODIUM LAYER OF THE EARTH ATMOSPHERE: PROBING WITH A TERRESTRIAL LIDAR SYSTEM AT 69 N IN WINTER Ph.D. Thesis [ZUR NATRIUM-SCHICHT IN DER ERDATMOSPHAERE: SONDIERUNG MIT EINEM BODENGEBUNDENEN LIDAR-INSTRUMENT BEI 69 DEG N IM WINTER]
Clemens Tilgner Sep. 1988 230 p In GERMAN
(Bonn-IR-88-52; ISSN-0172-8741; ETN-89-93996) Avail: NTIS HC A11/MF A01

Lidar instrument structure and operation as an optical radar is described. Lidar is evaluated for the investigation of the sodium layer in the mesosphere and mesopause region. Excitation of resonance fluorescence of sodium D2-lines and their measurements at 80 to 110 km height permit the temperature, composition, and behavior determination of the sodium layer. ESA

N89-24761# Toulon Univ. (France). Lab. de Sondages Electromagnetiques de l'Environnement Terrestre.
PLASMA AND PROPAGATION IN AURORAL AND POLAR IONOSPHERE [PLASMAS ET PROPAGATION DANS L'IONOSPHERE AURORALE ET POLAIRE]
Y. Ruin, C. Bourdier, and L. Currier Apr. 1988 69 p In FRENCH
(Contract DRET-85-168)
(ETN-89-94519) Avail: NTIS HC A04/MF A01

The automation of a decametric coherent radar was done to characterize the ion fluctuations in auroral or polar ionosphere and its influence on radioelectric transmission in those regions. Complementary theoretical studies on plasma physics and HF propagation in high latitudes are presented. It is shown that the

developed instrument is well adapted to ionospheric research in polar regions. ESA

N89-24762# Laboratoire de Meteorologie Dynamique du CNRS, Palaiseau (France).
ESTIMATING THE OUTGOING LONGWAVE RADIATION FROM THE METEOSAT INFRARED WINDOW AND WATER VAPOR BANDS
Robert S. Kandel, Frederique Cheruy, and Jean Philippe Duvel 1988 4 p Submitted for publication Sponsored in part by CNES, France
(ETN-89-94533) Avail: NTIS HC A02/MF A01

The approach is based on applying a multiple regression technique to colocated and nearly simultaneous Meteosat and Earth Radiation Budget Experiment (ERBE) data, and assuming that the ERBE scanner estimates of LW radiant existance represent the truth. Radiative transfer analysis was also used to interpret these results, in particular to estimate the sensitivitity of the signal and the broad band LW flux to temperature and humidity in the middle and upper troposphere. ESA

N89-24763# Laboratoire de Meteorologie Dynamique du CNRS, Palaiseau (France).
THREE DIMENSIONAL ANALYSIS OF THE ATMOSPHERIC STRUCTURE BY VERTICAL SATELLITE SOUNDING. INTEREST FOR WEATHER FORECASTING Ph.D. Thesis - Paris Univ. 6 [ANALYSE TRIDIMENSIONNELLE DE LA STRUCTURE DE L'ATMOSPHERE PAR SONDAGE VERTICAL SATELLITAIRE. INTERET POUR LA PREVISION DU TEMPS]
Jean-Francois Flobert 1988 158 p In FRENCH
(ETN-89-94536) Avail: NTIS HC A08/MF A01

The data transmitted by the Tiros-N operational vertical sounder onboard the polar orbit NOAA platform are analyzed. The atmospheric parameters are obtained using the Earth and the atmosphere radiation measured with the satellite radiometers by inversion of the radiation transfer equation. A fast calculation method to obtain the radiant energy from the temperature and moisture vertical profiles is described. Possible applications are discussed. ESA

N89-24764# Swedish Inst. of Space Physics, Kiruna. Inst. foer Rymdfysik.
SPECTRUM: A COMPUTER ALGORITHM TO DERIVE THE FLUX-ENERGY SPECTRUM OF PRECIPITATING PARTICLES FROM EISCAT ELECTRON DENSITY PROFILES
Sheila Kirkwood Oct. 1988 44 p
(IRF-TR-034; ISSN-0284-1738; ETN-89-94552) Avail: NTIS HC A03/MF A01

A program (SPECTRUM) that inverts electron density profiles measured by an incoherent scatter radar to obtain information on the flux-energy spectrum of precipitating electrons was developed. Improvements compared with the UNTANGLE program developed for the same purpose are described. Whereas UNTANGLE assumes that ionization has reached equilibrium, SPECTRUM includes the time rate of change of ionization. This can be measured on a time scale of a few seconds with the EISCAT radar during auroral precipitation. The fixed energies of the incident electron beams assumed in UNTANGLE are replaced by energies calculated according to the altitudes at which measurements are made. Thus the energy resolution and energy interval included in the derived spectra are determined in a physically reasonable way by the altitude resolution and the altitude interval of the electron density measurements. The equations relating the incident fluxes at each energy to the electron density at each altitude are written in matrix form which allows them to be solved using standard numerical algorithms. Proton fluxes rather than electron fluxes can be fitted. ESA

N89-24765 Montana State Univ., Bozeman.
THE GRAVITATIONAL MANY-BODY PPN LAGRANGIAN, LORENTZ INVARIANCE AND THE STRONG EQUIVALENCE PRINCIPLE TO SECOND ORDER Ph.D. Thesis
Matthew John Benacquista 1988 64 p
Avail: Univ. Microfilms Order No. DA8904744

The gravitational many-body parameterized post-Newtonian (PNN) Lagrangian for compact celestial bodies is extended to second post-Newtonian order and is constrained to exhibit the invariances observed in nature-generalized Lorentz invariance, the strong equivalence principle, and the isotropy of the gravitational potential. These invariances are imposed on the Lagrangian using an empirical approach which is based on calculated observables rather than through formal procedures involving post-Newtonian approximations of transformations. When restricted in this way, the Lagrangian possesses two free parameters which can be related to light-deflection experiments and the effect of an environment of proximate matter on such experiments. Dissert. Abstr.

N89-24766 Texas Univ., Austin.
TIME VARIATIONS IN THE EARTH'S GRAVITY FIELD FROM STARLETTE ORBIT ANALYSIS Ph.D. Thesis
Minkang Cheng 1988 209 p
Avail: Univ. Microfilms Order No. DA8901291

The time variation in the Earth's external gravitational potential, due to the solar-lunar tides, meteorological mass redistribution, and postglacial rebound of solid Earth, produce observable effects on the orbit of a near-Earth satellite. The application of the laser ranging data to the geodetic satellite Starlette, to the determination of the Earth's response to tidal and nontidal excitation was investigated. Analytical perturbation analysis and the methodology for estimating geodetic and geodynamic parameters from continuous, dynamically consistent Starlette long arc solutions spanning interval of one year and three years, are presented. Estimates for secular variations in the Earth's zonal harmonics, J sub 2, J sub 3, and J sub 4, and seasonal variations of the even degree annual and semi-annual tides, as well as 14 ocean tidal constituents (48 parameters) were obtained. The Starlette-derived values are in good agreement with other published values. The analysis of the three year Starlette orbit arc reveals that the Starlette orbit undergoes a change in its orbital inclination of (2.5 plus or minus 0.5) mas per year and a significant decrease in its orbital eccentricity due to drag model errors. Earth Rotation Parameters (ERP), were determined using Starlette laser data during the 14-month MERIT campaign. A covariance analysis showed that the accuracy of the Starlette ERP solution was limited primarily by error in the Earth's gravity field model, in particular, the first order geopotential coefficients of the PGS-1331 gravity model produced a systematic perturbation in the solution for x and y with a dominant period of 74 days and a maximum value up to 29 mas. Dissert. Abstr.

N89-24912# Royal Inst. of Tech., Stockholm (Sweden). Dept. of Plasma Physics.
ASTROPHYSICAL SIGNIFICANCE OF OBSERVATIONS AND EXPERIMENTS IN THE EARTH'S MAGNETOSPHERE
C.-G. Falthammar *In* ESA, Proceedings of an International School and Workshop on Plasma Astrophysics, Volume 1 Jan. 1989 p 9-19 (For primary document see N89-24910 18-75)
Avail: NTIS HC A18/MF A01; ESA Publications Div., ESTEC, Noordwijk, Netherlands, 45 US dollars or 80 Dutch guilders

N89-24943# Academy of Sciences (USSR), Moscow. Inst. of Space Research.
QUASI-ADIABATIC PARTICLE ACCELERATION IN MAGNETIC FIELD REVERSALS AND THE FORMATION OF THE PLASMA SHEET BOUNDARY LAYER IN THE EARTH'S MAGNETOTAIL
L. M. Zelenyi, D. V. Zogin, and J. M. Buechner (Academy of Sciences, Potsdam, German D.R.) *In* ESA, Proceedings of an International School and Workshop on Plasma Astrophysics, Volume 1 Jan. 1989 p 227-234 (For primary document see N89-24910 18-75)
Avail: NTIS HC A18/MF A01; ESA Publications Div., ESTEC, Noordwijk, Netherlands, 45 US dollars or 80 Dutch guilders

N89-24977# Imperial Coll. of Science and Technology, London (England).
NOISE-FREE NEUTRAL SHEETS
J. W. Dungey *In* ESA, Proceedings of an International School and Workshop on Reconnection in Space Plasma, Volume 2 Jan. 1989 p 15-19 (For primary document see N89-24974 18-75)
Copyright Avail: NTIS HC A15/MF A01; ESA Publications Div., ESTEC, Noordwijk, Netherlands, 45 US dollars or 80 Dutch guilders

N89-25019# Academy of Sciences, Potsdam (German D.R.). Central Inst. for Astrophysics.
ELECTROMAGNETIC ELECTRON TEMPERATURE ANISOTROPY INSTABILITY IN THE EARTH'S MAGNETOTAIL PLASMA SHEET
B. Nikutowski *In* ESA, Proceedings of an International School and Workshop on Reconnection in Space Plasma, Volume 2 Jan. 1989 p 253-258 (For primary document see N89-24974 18-75)
Copyright Avail: NTIS HC A15/MF A01; ESA Publications Div., ESTEC, Noordwijk, Netherlands, 45 US dollars or 80 Dutch guilders

47 METEOROLOGY AND CLIMATOLOGY

Includes weather forecasting and modification.

N89-24767# Finnish Meteorological Inst., Helsinki.
OROGRAPHICALLY-CAUSED MICROCLIMATE VARIATION IN THE SAARISELKA REGION
Bengt Tammelin 1988 69 p In FINNISH; ENGLISH summary
(ISBN-9-5169-7269-1; ISSN-0782-6109; MP-7) Avail: NTIS HC A04/MF A01

In the high fells of the Saariselka region of Finnish Lapland microclimatological differences attributable to orography are rather large. Over the area examined, the mean temperature and monthly degree-days do not much vary, but on any given day the differences may be considerable. For example, in the fell valleys the temperatures may be 10 to 15 degrees, even 20 C lower than on the fell tops. On the other hand, however, the chill experienced in below-zero conditions on the fell tops due to the wind is usually considerable, and may even be dangerously so. Field measurements made in the area show very clearly the relationship existing on the one hand between the temperatures at various heights and the temperature usually forecast (i.e., that at Ivalo airport), and on the other hand between these temperatures and the generally-prevailing wind and stability conditions in the area. Author

N89-24768# Finnish Meteorological Inst., Helsinki.
THE CLIMATE OF FINLAND: A BIBLIOGRAPHY WITH PARTICULAR REFERENCE TO APPLICATIONS UPDATING PART 1968-1985
Jaakko Helminen 1988 228 p In FINNISH; ENGLISH summary
(MP-10; ISBN-9-5169-7289-6; ISSN-0782-6109) Avail: NTIS HC A11/MF A01

This bibliography is the update of a bibliography by the same title. The update primary covers article references from the years 1968 to 1985. In addition to this the update consists of references to all atlases and data publications, even those published prior to 1968. Most importantly, the reference material was expanded regarding oceanographic and hydrologic references as related to climatological considerations. The references of the update were mainly arranged according to the structure of the World Climate Program (WCP). In the case of several simultaneous classes, a nested classification of the particular reference was used and the corresponding classification code numbers appear in order of the nesting in this reference. The update of the bibliography was filed as a part of a domestic database KATI, which will be updated twice annually, and through which it is possible to create an Exchange Format (ISO 2709) file for international exchange. Author

N89-24769# Finnish Meteorological Inst., Helsinki.
AN OPERATIONAL ANALYSIS AND FORECASTING METHOD OF EVAPORATION
Annakaisa Sarkanen 1988 58 p In FINNISH; ENGLISH summary
(MP-11; ISBN-9-5169-7291-8; ISSN-0782-6109) Avail: NTIS HC A04/MF A01

Daily evaporation analysis and forecasting methods are studies for May to September. The class A pan evaporation measurements were used as comparison data. Both the analysis and forecasting equations at the Jokioinen, Luonetjarvi, and Sodankyla observatories were evaluated from a large meteorological data base using the regression method. These equations were then compared with the Penman-Monteith equation. The analysis equation, computed by the regression method, is as good as the Penman-Monteith equation. Both methods describe pan evaporation records adequately. In the case of pan evaporation forecasts, the regression equation is more appropriate than the Penman-Monteith equation. The most important difference between the two equations is, perhaps, the fact, that parameters from the free atmosphere, which can be accurately predicted by numerical weather forecasting models were chosen as predictors into the regression forecast equation. The equation gives useful pan evaporation forecasts for one, two, and three days. Author

N89-24770*# Florida State Univ., Tallahassee. Dept. of Meteorology.
ANALYSIS AND USE OF VAS SATELLITE DATA Final Report, Aug. 1985 - Aug. 1988
Henry E. Fuelberg, Mark J. Andrews, John L. Beven, II, Steven R. Moore, and Bradley M. Muller Washington Mar. 1989 87 p (Grant NAG8-033)
(NASA-CR-4218; M-608; NAS 1.26:4218) Avail: NTIS HC A05/MF A01 CSCL 04B

Four interrelated investigations have examined the analysis and use of VAS satellite data. A case study of VAS-derived mesoscale stability parameters suggested that they would have been a useful supplement to conventional data in the forecasting of thunderstorms on the day of interest. A second investigation examined the roles of first guess and VAS radiometric data in producing sounding retrievals. Broad-scale patterns of the first guess, radiances, and retrievals frequently were similar, whereas small-scale retrieval features, especially in the dew points, were often of uncertain origin. Two research tasks considered 6.7 micron middle tropospheric water vapor imagery. The first utilized radiosonde data to examine causes for two areas of warm brightness temperature. Subsidence associated with a translating jet streak was important. The second task involving water vapor imagery investigated simulated imagery created from LAMPS output and a radiative transfer algorithm. Simulated image patterns were found to compare favorably with those actually observed by VAS. Furthermore, the mass/momentum fields from LAMPS were powerful tools for understanding causes for the image configurations. Author

N89-24771# National Severe Storms Lab., Norman, OK.
EFFICIENT DEALIASING OF DOPPLER VELOCITIES USING LOCAL ENVIRONMENT CONSTRAINTS Final Report
Michael D. Eilts and Steven D. Smith (UNISYS Corp., Trevose, PA.) Jan. 1989 44 p Original contains color illustrations
(Contract DTFA01-80-Y-10524)
(DOT/FAA/SA-89/1) Avail: NTIS HC A03/MF A01

A Doppler velocity dealiasing algorithm is described that processes one radial at a time by comparing that radial with a previous radial. This technique worked reliably on numerous Doppler radar data sets for clear air, thunderstorm, and severe thunderstorm situations. It was also tested on four volume scans from severe weather environments with difficult aliasing problems to determine statistically how well the algorithm performs in a worst case environment. Of some 1.2 million velocities in these

severe storms, 0.2 percent were improperly dealiased, and 93 percent of those were above 13 km height in the storm-top divergent region where shears were extreme. Every tornado, mesocyclone, gust front, microburst, and storm-top divergent signature was preserved, and could be identified by automated algorithms. This algorithm is adaptive and therefore efficient because simple checks are made initially, and progressively more sophisticated and time-consuming checks are used only if they are needed. Author

N89-24772*# Information and Control Systems, Inc., Hampton, VA.
MODELING AND CHARACTERIZATION OF THE EARTH RADIATION BUDGET EXPERIMENT (ERBE) NONSCANNER AND SCANNER SENSORS Final Report
Nesim Halyo, Dhirendra K. Pandey, and Deborah B. Taylor Mar. 1989 182 p
(Contract NAS1-18018)
(NASA-CR-181818; NAS 1.26:181818; FR-688104) Avail: NTIS HC A09/MF A01 CSCL 04B

The Earth Radiation Budget Experiment (ERBE) is making high-absolute-accuracy measurements of the reflected solar and Earth-emitted radiation as well as the incoming solar radiation from three satellites: ERBS, NOAA-9, and NOAA-10. Each satellite has four Earth-looking nonscanning radiometers and three scanning radiometers. A fifth nonscanner, the solar monitor, measures the incoming solar radiation. The development of the ERBE sensor characterization procedures are described using the calibration data for each of the Earth-looking nonscanners and scanners. Sensor models for the ERBE radiometers are developed including the radiative exchange, conductive heat flow, and electronics processing for transient and steady state conditions. The steady state models are used to interpret the sensor outputs, resulting in the data reduction algorithms for the ERBE instruments. Both ground calibration and flight calibration procedures are treated and analyzed. The ground and flight calibration coefficients for the data reduction algorithms are presented. Author

N89-24773# Colorado State Univ., Fort Collins. Dept. of Atmospheric Science.
FORECAST OF ATLANTIC SEASONAL HURRICANE ACTIVITY FOR 1989
William M. Gray 26 May 1989 42 p
Avail: NTIS HC A03/MF A01

A forecast of tropical cyclone activity for the Atlantic Ocean region (including the Caribbean Sea and the Gulf of Mexico) during 1989 is presented. This forecast is based on ongoing research (Gray, 1984a, 1984b, 1988a, 1988b, 1988c, 1988d; Gray et al., 1987) which relates the amount of seasonal Atlantic tropical cyclone activity to four factors: (1) the El Nino (EN); (2) the Quasi-Biennial Oscillation of equatorial stratospheric wind (QBO); (3) Gulf of Mexico and Caribbean Basin Sea-Level Pressure Anomalies (SLPA); and (4) lower latitude Caribbean Basin 200 mb Zonal Wind Anomalies (ZWA). Information received up to 26 May 1989 indicates that the 1989 hurricane season can be expected to have about 4 hurricanes, 7 total named storms of both hurricane and tropical storm intensity, and about 15 hurricane days. This means that the 1989 Atlantic hurrican season will likely be a below average hurricane season. This suppression is due to the expected unfavorable influences of an easterly phase QBO and higher than normal SLPA. This forecast will be updated on 1 August, before the start of the most active part of the hurricane season. Background information on hurricane activity over the last 40 years is also presented. Author

N89-24774 Hawaii Univ., Honolulu.
THE RELATIONSHIP BETWEEN INTRASEASONAL DISTURBANCE ACTIVITY AND INTERANNUAL VARIATION OF THE TROPICAL ATMOSPHERE Ph.D. Thesis
Xueliang Wang 1988 174 p
Avail: Univ. Microfilms Order No. DA8902860

The relationship between intraseasonal activity (cluster of disturbances) and interannual variation of tropical atmosphere is investigated using outgoing longwave radiation (OLR) and wind data. The space and time scale of the disturbance cluster are much larger than those of individual disturbances. Two constructed period bands (2 to 15 and 30 to 60 day) of disturbance activity exhibit different spatial and temporal variations on interannual time scale. The 2 to 15 day activity is primarily associated with interannual variations, while the 30 to 60 day activity is strongest over the equatorial Indian Ocean and western Pacific prior to ENSO onset. The 30 to 60 day oscillation is one of the triggering mechanisms for ENSO event. The results of empirical orthogonal function analysis show that ENSO, a dominant mode of interannual variations, is essentially one realization of a bimodal climate system. ENSO onset is a phase change from non-ENSO steady state to ENSO state. ENSO signal over the central-eastern Pacific is traceable to the western Pacific-Indian Ocean region (a warm pool). An interaction among intraseasonal activity, annual cycle, and interannual modes over the warm pool region may be instrumental in leading to ENSO onset. Dissert. Abstr.

N89-24775# Naval Postgraduate School, Monterey, CA.
STUDY OF EXPLOSIVE AND NONEXPLOSIVE CYCLOGENESIS DURING FGGE M.S. Thesis
Eric J. Wright Dec. 1988 87 p
(AD-A206521) Avail: NTIS HC A05/MF A01 CSCL 04/2

The purpose of this thesis is to analyze and evaluate explosive cyclogenesis during the winter of the First Global GARP Experiment (January to February 1979). Explosive cyclogenesis is defined as a decrease in the sea-level pressure at the rate of one mb per hour for a period of 12 h up to 24 h. The European Center for Medium-range Weather Forecasts (ECMWF) provided the revised analyses for evaluation and comparison of important cyclone properties in a sample of 13 explosive developing cases and eight nonexplosive cases. The specific parameters being examined include the static stability, low-level absolute vorticity, vorticity advection, eddy and mean modes of the vorticity transport, upper-level divergence, kinematic vertical velocities and the strength of the low-level baroclinity. These parameters are compared at the initial, 12 and 24 hour time periods as well as the overall 24 hour average. The statistical relationships and magnitudes of these terms indicate the most significant physical mechanisms in explosive cyclone development compared to the nonexplosive storm group. The important outcome of these results is that the kinematic vertical velocity and the upper-level forcing mechanisms are statistically separable. The large values for the upper-level process suggest that the upper tropospheric wave influence is most likely producing the stronger vertical motions. GRA

N89-24776# National Climatic Center, Asheville, NC.
CLIMATIC ATLAS OF THE OUTER CONTINENTAL SHELF WATERS AND COASTAL REGIONS OF ALASKA. VOLUME 3: CHUKCHI-BEAUFORT SEA
William A. Brower, Jr., Ronald G. Baldwin, Claude N. Williams, Jr., James L. Wise, and Lynn D. Leslie (Alaska Univ., Anchorage.) 1988 515 p Prepared in cooperation with Interior Dept., Washington, DC and Naval Oceanography Command Detachment, Asheville, NC
(AD-A206525; NAVAIR-50-1C-553-Vol-3; MMS-87-0013-Vol-3)
Avail: NTIS HC A22/MF A01 CSCL 04/2

This climatic study consists of monthly charts and tables of: (1) clouds, (2) precipitation, (3) visibility-tables, (4) ceiling-visibility (mid-range/low range), (5) wind-visibility cloudiness, (6) scalar mean wind speed, (7) wind speed less than 11 and greater or equal to 34 knots, (8) wind speed 11 to 21 and 22 to 33 knots, (9) surface wind roses, (10) air and sea temperature, (11) wave height-isopleths, (12) wave height-tables, and (13) surface current (seasonal). GRA

N89-24777# Office National d'Etudes et de Recherches Aerospatiales, Paris (France). Direction de la Physique Generale.
LIGHTNING INFLIGHT STUDY ONBOARD A TRANSALL AIRCRAFT. DEFINITION OF THE ONBOARD INSTRUMENTS Final Report [ETUDE DE FOUDROIEMENT EN VOL SUR AVION TRANSALL PREPARATION DE LA CAMPAGNE D'ESSAIS EN VOL. DEFINITION DE L'INSTRUMENTATION EMBARQUEE]
P. Y. Gonzales, F. Issac, J. Y. Jouan, J. P. Moreau, J. P. Aparicio, P. Gondot, and A. Delannoy Jul. 1988 103 p In FRENCH
(Contract DRET-87-001)
(ONERA-RF-19/7234-PY; ONERA-RF-19/7154-PY; ETN-89-94527) Avail: NTIS HC A06/MF A01

The description includes the developed sensors, the computer programs for data acquisition and data processing, the experimental design of the ground tests, and the optimization studies of an ionic conductivity metering cell. The 32 k on 10 bits input of the data acquisition is processed in a 386 Compaq microcomputer with a 6 MHz memory extension. Processed data are then transfered to a Cray computer via specific programs. ESA

N89-24778# Laboratoire de Meteorologie Dynamique du CNRS, Palaiseau (France).
WATER VAPOR RETRIEVALS THROUGH THE 3I (IMPROVED INITIALIZATION INVERSION) SYSTEM: APPLICATION TO TROPOSPHERIC ALTIMETRY CORRECTION
A. Chedin, Y. Tahani, N. A. Scott, and N. Husson 1988 4 p Presented at the International Radiation Symposium, Lille, France, 18-24 Aug. 1988 Sponsored in part by CNES, France
(ETN-89-94534) Avail: NTIS HC A02/MF A01

The 3I method is refined and applied to the retrieval of water vapor fields under various meteorological conditions, for various geographical areas and at global scale. Comparisons with conventional analyses or radiosondes are performed. A product based upon a mixing of 3I retrievals for clear or partly cloudy areas and the European center for medium range weather forecast analysis for overcast areas is proposed. ESA

N89-24779# Laboratoire de Meteorologie Dynamique du CNRS, Palaiseau (France).
THE RADIATION-ATMOSPHERE INTERACTION MODEL AND THE DETERMINATION OF METEOROLOGICAL AND CLIMATOLOGICAL PARAMETERS FROM SATELLITE OBSERVATIONS [LES MODELES D'INTERACTION RAYONNEMENT-ATMOSPHERE ET DETERMINATION DE PARAMETRES METEOROLOGIQUES ET CLIMATOLOGIQUES A PARTIR D'OBSERVATIONS SATELLITAIRES]
M. A. Chedin 1988 35 p In FRENCH Presented at the Ecole d'Ete Internationale de Physique Spatiale Teledetection Spatiale: Aspects Physiques et Modelisation, Toulouse, France, Aug. 1988
(ETN-89-94535) Avail: NTIS HC A03/MF A01

The equipment installed onboard the Tiros-N/NOAA satellites, the measuring principles, and the main results obtained are reviewed. The inversion of the radiative transfer equation is discussed and several solution methods are examined. The algorithm named Improved Initialization Inversion is described. Detailed results obtained with the algorithm are presented. ESA

N89-24780# Laboratoire de Meteorologie Dynamique du CNRS, Palaiseau (France).
CONTRIBUTION TO THE STUDY OF THE DIURNAL CYCLE OF CONVECTIVE CLOUDS OVER TROPICAL AFRICA FROM SATELLITE IMAGERY Ph.D. Thesis - Paris Univ. 6
Theoneste Kayiranga 1988 141 p In FRENCH; ENGLISH summary
(ETN-89-94537) Avail: NTIS HC A07/MF A01

Satellite radiometers, the methods used to characterize convection, a comparison of interannual climatic variations, an image pixel analysis including the amplitude and phase of the cycle, and the diurnal rain cycle in a particular region are described. Statistical methods were applied to monthly series available every 3 hours. It is shown that the ISCPP data allow clouding studies on a large scale. ESA

N89-24781# Laboratoire de Meteorologie Dynamique du CNRS, Palaiseau (France).
STUDY OF REPRESENTATIVITY OF THE WIND FIELDS DEDUCED FROM GEOSTATIONARY SATELLITE IMAGES. ATTRIBUTION OF HEIGHT TO WIND VECTORS AND LARGE SCALE AVERAGE FIELDS DEDUCED FROM WATER VAPOR IMAGERY Ph.D. Thesis - Paris Univ. 7 [ETUDE DE LA REPRESENTATIVITE DES CHAMPS DE VENT DEDUITS DE L'IMAGERIE DES SATELLITES GEOSTATIONAIRES: ATTRIBUTION D'UNE ALTITUDE AUX VECTEURS VENTS ET CHAMPS MOYENS GRANDE ECHELLE DEDUITS DE L'IMAGERIE VAPEUR D'EAU]
Mohammed Saad Guessous 1988 179 p In FRENCH
(ETN-89-94538) Avail: NTIS HC A09/MF A01

The basic algorithms used to identify the tracers and for determining the displacement vectors are presented. The contributions of the displacement computed from the Meteosat water vapor channel to climatological analysis are shown. Data from the International Satellite Cloud Climatology Project are examined. The possibility to determine by these methods the interannual variation of general circulation is demonstrated. ESA

N89-24782# Laboratoire de Meteorologie Dynamique du CNRS, Palaiseau (France).
CONTRIBUTION TO THE ESTIMATION OF PRECIPITATION IN THE SAHEL BY USING SATELLITE IMAGERY Ph.D. Thesis - Clermont-Ferrand Univ. [CONTRIBUTION A L'ESTIMATION DES PRECIPITATIONS AU SAHEL PAR L'IMAGERIE SATELLITAIRE]
Wassila Thiao 1988 182 p In FRENCH; ENGLISH summary
(Ser-DI-204; ETN-89-94539) Avail: NTIS HC A09/MF A01

A feasibility study of rainfall estimation over the Sahel for short periods with Meteosat imagery is performed. Daily rainfalls at raingages were compared to a convection index determined from Meteosat imagery cumulated over a day for a 1 deg square centered over the station during a few days of summer. For most cases there are good relationships between the convection and the rainfall indices. A linear multivariate regression of the observed precipitation on the convection index and its time variation is presented. The results show the possibility to estimate rainfall over west Africa produced by individual events from a combination of remote sensing and conventional data. ESA

N89-24783# Lawrence Livermore National Lab., CA. Atmospheric and Geophysical Sciences Div.
SIMPLIFIED CLIMATE MODELS: RATIONALE AND DESIGN
Steven J. Ghan Apr. 1989 37 p Presented at the Short Course on Development of Zonally-averaged Models of the Atmosphere, Louvain, Belgium, 17 Apr.-15 May 1989
(Contract W-7405-eng-48)
(DE89-012291; UCRL-100817; CONF-8904217-1) Avail: NTIS HC A03/MF A01

In order to address a wide range of climate issues involving climate components with a diversity of time scales and spatial scales, a hierarchy of climate models has been developed over the past two decades. This survey paper discusses the rationale for selecting relatively simple climate models over more comprehensive models for certain applications. The hierarchy of simple climate models is reviewed, beginning with the educational role played by zero-dimensional planetary energy balance models. One-dimensional radiative-convective and two-dimensional (latitude-longitude) energy balance models are recommended for many applications. Two-dimensional (latitude-altitude) dynamical models are suggested for climate issues in which the hydrological cycle plays an important role and practical considerations preclude the application of comprehensive general circulation models. DOE

48 OCEANOGRAPHY

Includes biological, dynamic, and physical oceanography; and marine resources.

For related information see also *43 Earth Resources and Remote Sensing.*

N89-24784*# Scripps Institution of Oceanography, La Jolla, CA.
BIOOPTICAL VARIABILITY IN THE GREENLAND SEA OBSERVED WITH THE MULTISPECTRAL AIRBORNE RADIOMETER SYSTEM (MARS) Final Technical Report, 21 May - 2 Jun. 1987
James L. Mueller and Charles C. Trees 31 Mar. 1989 108 p
(Grant NAG5-1022)
(NASA-CR-184856; NAS 1.26:184856; CHORS-TM-89-001)
Avail: NTIS HC A06/MF A01 CSCL 08F

A site-specific ocean color remote sensing algorithm was developed and used to convert Multispectral Airborne Radiometer System (MARS) spectral radiance measurements to chlorophyll-a concentration profiles along aircraft tracklines in the Greenland Sea. The analysis is described and the results given in graphical or tabular form. Section 2 describes the salient characteristics and history of development of the MARS instrument. Section 3 describes the analyses of MARS flight segments over consolidated sea ice, resulting in a set of altitude dependent ratios used (over water) to estimate radiance reflected by the surface and atmosphere from total radiance measured. Section 4 presents optically weighted pigment concentrations calculated from profile data, and spectral reflectances measured in situ from the top meter of the water column; this data was analyzed to develop an algorithm relating chlorophyll-a concentrations to the ratio of radiance reflectances at 441 and 550 nm (with a selection of coefficients dependent upon whether significant gelvin presence is implied by a low ratio of reflectances at 410 and 550 nm). Section 5 describes the scaling adjustments which were derived to reconcile the MARS upwelled radiance ratios at 410:550 nm and 441:550 nm to in situ reflectance ratios measured simultaneously on the surface. Section 6 graphically presents the locations of MARS data tracklines and positions of the surface monitoring R/V. Section 7 presents stick-plots of MARS tracklines selected to illustrate two-dimensional spatial variability within the box covered by each day's flight. Section 8 presents curves of chlorophyll-a concentration profiles derived from MARS data along survey tracklines. Significant results are summarized in Section 1. A.D.

51 LIFE SCIENCES (GENERAL)

No abstracts in this category.

52 AEROSPACE MEDICINE

Includes physiological factors; biological effects of radiation; and effects of weightlessness on man and animals.

N89-24785# Army Research Inst. of Environmental Medicine, Natick, MA.
SOLUTE MODEL OR CELLULAR ENERGY MODEL: PRACTICAL AND THEORETICAL ASPECTS OF THIRST DURING EXERCISE
Roger W. Hubbard, Patrick C. Szlyk, and Lawrence E. Armstrong 16 Feb. 1989 32 p
(AD-A206143; USARIEM-M22/89) Avail: NTIS HC A03/MF A01 CSCL 06/10

Most physiologists would agree that repaying the water debt incurred through evaporative cooling is part of the physiological cost of work in the heat. Pitts and coworkers emphasized that, during work in the heat, men never voluntarily drink as much water as they lose and usually replace only two-thirds of the net water loss. Rothstein et al. observed that this occurred even when water was available, and called this phenomenon voluntary dehydration. Some physiologists feel that voluntary dehydration occurs because thirst is an inadequate stimulus to drinking. On the other hand, Vokes contends one of the best examples of a perfectly functioning homeostatic system is water balance. One of our goals is to reconcile the fact that under certain conditions, both of these statements are correct. We will also try to switch the readers interest from water to salt for, although man may drink, water cannot be held until the missing osmoles are made good. This may be seen as at least one explanation of why thirst is inadequate and there are others. GRA

N89-24786# State Univ. of New York, Plattsburgh. Auditory Research Lab.
THE EFFECTS OF BLAST TRAUMA (IMPULSE NOISE) ON HEARING: A PARAMETRIC STUDY Annual Report, 1 Apr. 1986 - 31 Mar. 1987
Roger P. Hamernik, William A. Ahroon, Robert I. Davis, and George A. Turrentine 22 Jul. 1988 332 p
(Contract DAMD17-86-C-6172; DA Proj. 3M1-61102-BS-15)
(AD-A206180; ARL-88-2) Avail: NTIS HC A15/MF A01 CSCL 06/10

There are three broad goals to this project. The first and primary goal is to begin the systematic development of a data base from which one could estimate the hazards to hearing resulting from exposure to blast waves or other high level impulse noise transients. To achieve this primary objective the following two objectives must first be achieved: (1) to develop a methodology to efficiently acquire data on a large number of experimental animals that have been exposed to a variety of blast wave configurations. This includes audiometric, histological and acoustic variables; (2) to develop a set of blast wave simulation devices which can reliably generate blast waves with a variable distribution of spectral energy in a laboratory environment. This report will describe progress that was achieved on each of these objectives. Data acquisition was completed on 40 chinchillas that were exposed to one of a series of very low frequency (125 Hz) energy-content blast wave exposure paradigms. This data represents the completion of the first of four phases of a parametric study that was designed to estimate the contributions of individual blast wave exposure variables on the production hearing loss. Hearing function was measured using the auditory evoked potential (AEP) technique. The evaluation of hearing consisted of pre- and postexposure measurements of pure tone thresholds and tuning curves (masked thresholds). GRA

N89-24787# School of Aerospace Medicine, Brooks AFB, TX.
CEREBRAL LATERALITY AND HANDEDNESS IN AVIATION: PERFORMANCE AND SELECTION IMPLICATIONS Final Report, Jul. 1987 - Jun. 1988
John S. Crowley Jan. 1989 101 p
(AD-A206196; USAFSAM-TP-88-11) Avail: NTIS HC A06/MF A01 CSCL 05/8

This paper reviews the general psychology literature related to handedness and cerebral laterality, beginning with a brief discussion of the research methods employed. Aspects of laterality, including vision, audition, tactile perception, spatial ability, and language are reviewed, as well as theories of cerebral dominance patterns. The handedness literature is examined, with attention to measurement, theories of genesis, sociocultural factors, and sex differences. There are many postulated correlates of human laterality, including performance, occupation, emotions, and various diseases. References, suggest that pilots who have no strong hand preference may be at a slight disadvantage in the cockpit, whereas those who are consistently right-side dominant tend to do well. Current neuropsychological theory would suggest that the ideal aviator brain should be well lateralized, to minimize competition for hemispheric resources. There is evidence that pilots who are poorly lateralized may exhibit traits of right-left confusion. Several aircraft accidents have been attributed to pilots failing to

correctly distinguish between left and right. Performance in flight school seems to be associated with right hemispheric (visuospatial) ability, as measured by tests of cognitive function. These tests have utility in the selection of aircrew; techniques for enhancing cognitive laterality may also prove useful. GRA

N89-24788# Georgia State Univ., Atlanta.
NEUROCHEMICAL CONTROL OF CIRCADIAN RHYTHMS
Annual Report, 1 Apr. 1988 - 31 Mar. 1989
Albers H. Elliott 20 Mar. 1989 9 p
(Contract N00014-87-K-0172; RR04108)
(AD-A206213) Avail: NTIS HC A02/MF A01 CSCL 06/1

We have continued our investigation of the neurochemical systems contained in the circadian clock localized within the suprachiasmatic nucleus (SCN). Our primary focus has been to determine the circadian functions of a subpopulation of SCN interneurons in which vasoactive intestinal peptide (VIP), peptide histidine isoleucine (PHI) and gastrin releasing peptide (GRP) have been co-localized. In these studies we have demonstrated: (1) VIP/PHI neurons are found in the ventrolateral SCN where photic projections terminate, (2) a rhythm of VIP/PHI mRNA within the SCN that correlates with day-night cycle, (3) a modulation of SCN content of VIP and PHI by environmental lighting, (4) combined microinjection of VIP/PHI/GRP into the SCN mimics the phase delay of circadian rhythms produced by light, and (5) VIP/PHI/GRP alters the electrical activity of SCN single units. In other studies we have investigated the possible circadian functions of arginine vasopressin, GABA and neuropeptide Y (NPY) within the SCN, and the role of NPY within the para-ventricular nucleus on corticosterone secretion. GRA

N89-24789# Army Research Inst. of Environmental Medicine, Natick, MA.
IS SALT AT FAULT
Lawrence E. Armstrong and Robert H. Lind 28 Feb. 1989 12 p
(AD-A206518; USARIEM-M26/89) Avail: NTIS HC A03/MF A01 CSCL 06/8

This article reviews the fluid-electrolyte balance which is altered by exercise in hot environments at a variety of durations--focusing on sodium chloride losses. Recommendations are presented to assist athletes in maintaining electrolyte balance practically. Because of the journal involved, athletic situations and circumstances are highlighted. GRA

N89-24790*# National Aeronautics and Space Administration. Lyndon B. Johnson Space Center, Houston, TX.
A METHOD OF ISOLATING TREADMILL SHOCK AND VIBRATION ON SPACECRAFT
William E. Thornton Apr. 1989 18 p
(NASA-TM-100474; S-591; NAS 1.15:100474) Avail: NTIS HC A03/MF A01 CSCL 06S

A major problem is currently felt to exist in the implementation of materials processing on a spacecraft. Crystal growers place requirements of one micro-g or less on the vehicle. Simple math produces startling figures for such a restriction e.g., for each ton of vehicle mass with 10(-6) g acceleration limit; Perturbing Force limit, F = .002 lb. For each 10(5) lbs F = 0.1 lb. For each 10(6) lbs F = 1.0 lb. Forces generated by normal human movement on spacecraft of 5x10(5) pounds weight are on an order-of-magnitude greater than allowed by this specification and forces generated by locomotion on a treadmill are more than two orders-of-magnitude greater. Other exercises and normal onboard functions generate forces in between. To accommodate many essential functions it is obvious that even on a vehicle as large as Space Station, a reduction of more than two orders of magnitude in force is required. Commonly used passive shock and vibration isolation devices are complex, heavy, and also would have difficulty meeting the requirements. However, by a new arrangement, adequate isolation can be obtained. Isolation of the treadmill will be treated since it is considered the most significant disturbance at this time. Author

N89-24369# Deutsche Forschungs- und Versuchsanstalt fuer Luft- und Raumfahrt, Cologne (Germany, F.R.). Inst. for Aerospace Medicine.
MEDICAL AND RADIATION PROTECTION PROBLEMS IN SPACE
K. E. Klein and H. Buecker *In* ESA, International Symposium on Europe in Space: The Manned Space System Oct. 1988 p 291-302 (For primary document see N89-24335 18-12)
Copyright Avail: NTIS HC A99/MF A01; ESA Publications Div., ESTEC, Noordwijk, Netherlands, 80 Dutch guilders

53 BEHAVIORAL SCIENCES

Includes psychological factors; individual and group behavior; crew training and evaluation; and psychiatric research.

N89-24791# Army Research Inst. of Environmental Medicine, Natick, MA.
FIELD-DEPENDENCE AND JUDGMENT OF WEIGHT AND COLOR REVISITED: SOME IMPLICATIONS FOR THE STUDY OF SENSORY DISCRIMINATION
Bernard J. Fine Jan. 1989 20 p Submitted for publication
(DA Proj. 3M1-61102-BS-15)
(AD-A206141; USARIEM-M20/89) Avail: NTIS HC A02/MF A01 CSCL 05/8

Based on a construct termed sensitivity of the nervous system and the assumption that field-dependence is an indirect approximation of level of sensitivity, our previous research has predicted and found field-independent groups to be superior to field-dependent groups in color and weight discrimination and in contrast sensitivity. Here, we re-examine weight judgment using a more discriminating test and attempt to replicate previous color results. Seventeen females performed a weight discrimination task (15 weights, 75 to 145 grams, in 5-gram increments) on two successive days, three trials/day, and two trials on the Farnsworth-Munsell 100 Hue Test. A field-independent group (N=5) performed significantly better than a field-dependent group (N=6) on all trials of both tasks. Although N is small, this is the fifth replication (in five attempts) of the color discrimination results and a strong validation of the previous results with weights. It is suggested that in studies of sensory discrimination, some of the so-called random error now must be considered as systematic error, or bias, and that attention should be given to level of sensitivity of participants. GRA

N89-24374# European Space Agency, Paris (France).
THE TRAINING CONCEPT FOR ESA ASTRONAUTS AND THE ASSOCIATED FACILITIES
H. D. Hopkins *In its* International Symposium on Europe in Space: The Manned Space System Oct. 1988 p 367-369 (For primary document see N89-24335 18-12)
Copyright Avail: NTIS HC A99/MF A01; ESA Publications Div., ESTEC, Noordwijk, Netherlands, 80 Dutch guilders

N89-24375# Centre National d'Etudes Spatiales, Toulouse (France).
THE HERMES SYSTEM TRAINING CONCEPT [CONCEPT D'ENTRAINEMENT AU SYSTEME HERMES]
G. Gargir *In* ESA, International Symposium on Europe in Space: The Manned Space System Oct. 1988 p 371-377 In FRENCH; ENGLISH summary (For primary document see N89-24335 18-12)
Copyright Avail: NTIS HC A99/MF A01; ESA Publications Div., ESTEC, Noordwijk, Netherlands, 80 Dutch guilders

N89-24396# Deutsche Forschungs- und Versuchsanstalt fuer Luft- und Raumfahrt, Cologne (Germany, F.R.).
CREW TRAINING ASPECTS
F. J. Demond, W. Mueller-Breitkreutz, and H. G. Neuhaeuser *In* ESA, International Symposium on Europe in Space: The Manned Space System Oct. 1988 p 541-549 (For primary document

see N89-24335 18-12)
Copyright Avail: NTIS HC A99/MF A01; ESA Publications Div., ESTEC, Noordwijk, Netherlands, 80 Dutch guilders

54 MAN/SYSTEM TECHNOLOGY AND LIFE SUPPORT

Includes human engineering; biotechnology; and space suits and protective clothing.

For related information see also *16 Space Transportation.*

N89-24792*# National Academy of Sciences - National Research Council, Washington, DC. Committee on Human Factors.
HUMAN FACTORS IN AUTOMATED AND ROBOTIC SPACE SYSTEMS: PROCEEDINGS OF A SYMPOSIUM. PART 1
Thomas B. Sheridan, ed., Dana S. Kruser, ed., and Stanley Deutsch, ed. 1987 475 p Symposium held in Washington, DC, 29-30 Jan. 1987
(Contract NASw-4071)
(NASA-CR-182495; NAS 1.26:182495) Avail: NTIS HC A20/MF A01 CSCL 05H

Human factors research likely to produce results applicable to the development of a NASA space station is discussed. The particular sessions covered in Part 1 include: (1) system productivity -- people and machines; (2) expert systems and their use; (3) language and displays for human-computer communication; and (4) computer aided monitoring and decision making. Papers from each subject area are reproduced and the discussions from each area are summarized. A.D.

N89-24793*# McDonnell-Douglas Astronautics Co., Huntsville, AL.
THE HUMAN ROLE IN SPACE (THURIS) APPLICATIONS STUDY. FINAL BRIEFING
George W. Maybee Oct. 1987 73 p
(Contract NAS8-36638)
(NASA-CR-183590; NAS 1.26:183590; MDC-W5125-2) Avail: NTIS HC A04/MF A01 CSCL 05H

The THURIS (The Human Role in Space) application is an iterative process involving successive assessments of man/machine mixes in terms of performance, cost and technology to arrive at an optimum man/machine mode for the mission application. The process begins with user inputs which define the mission in terms of an event sequence and performance time requirements. The desired initial operational capability date is also an input requirement. THURIS terms and definitions (e.g., generic activities) are applied to the input data converting it into a form which can be analyzed using the THURIS cost model outputs. The cost model produces tabular and graphical outputs for determining the relative cost-effectiveness of a given man/machine mode and generic activity. A technology database is provided to enable assessment of support equipment availability for selected man/machine modes. If technology gaps exist for an application, the database contains information supportive of further investigation into the relevant technologies. The present study concentrated on testing and enhancing the THURIS cost model and subordinate data files and developing a technology database which interfaces directly with the user via technology readiness displays. This effort has resulted in a more powerful, easy-to-use applications system for optimization of man/machine roles. Volume 1 is an executive summary. A.D.

N89-24794*# National Academy of Sciences - National Research Council, Washington, DC. Committee on Human Factors.
HUMAN FACTORS IN AUTOMATED AND ROBOTIC SPACE SYSTEMS: PROCEEDINGS OF A SYMPOSIUM. PART 2
14 Aug. 1987 446 p Symposium held in Washington, DC, 29-30 Jan. 1987
(Contract NASw-4071)
(NASA-CR-182496; NAS 1.26:182496) Avail: NTIS HC A19/MF A01 CSCL 05H

Human factors research likely to produce results applicable to the development of a NASA space station is discussed. The particular sessions covered in Part 2 include: (1) computer aided monitoring and decision making; (2) telepresence and supervisory control; (3) social factors in productivity and performance; and (4) the human role in space systems. Papers from each subject area are reproduced and the discussions from each area are summarized. A.D.

N89-24795*# McDonnell-Douglas Astronautics Co., Huntsville, AL.
THE HUMAN ROLE IN SPACE (THURIS) APPLICATIONS STUDY. VOLUME 2: RESEARCH ANALYSIS AND TECHNOLOGY REPORT
George W. Maybee Oct. 1987 273 p
(Contract NAS8-36638)
(NASA-CR-183589; NAS 1.26:183589; MDC-W5141-2-Vol-2)
Avail: NTIS HC A12/MF A01 CSCL 05H

The THURIS (The Human Role in Space) application is an iterative process involving successive assessments of man/machine mixes in terms of performance, cost and technology to arrive at an optimum man/machine mode for the mission application. The process begins with user inputs which define the mission in terms of an event sequence and performance time requirements. The desired initial operational capability date is also an input requirement. THURIS terms and definitions (e.g., generic activities) are applied to the input data converting it into a form which can be analyzed using the THURIS cost model outputs. The cost model produces tabular and graphical outputs for determining the relative cost-effectiveness of a given man/machine mode and generic activity. A technology database is provided to enable assessment of support equipment availability for selected man/machine modes. If technology gaps exist for an application, the database contains information supportive of further investigation into the relevant technologies. The present study concentrated on testing and enhancing the THURIS cost model and subordinate data files and developing a technology database which interfaces directly with the user via technology readiness displays. This effort has resulted in a more powerful, easy-to-use applications system for optimization of man/machine roles. Volume 2 presents a summary of the study objectives, approach, and results and technical discussion of accomplishments in the principal study tasks of: (1) sensitivity analysis, and (2) technology readiness database development. A summary of the study conclusions and recommendations is also presented. Author

N89-24796# IBM Watson Research Center, Yorktown Heights, NY.
EVALUATION, DESCRIPTION AND INVENTION: PARADIGMS FOR HUMAN-COMPUTER INTERACTION
John M. Carroll 16 Aug. 1988 25 p
(AD-A204617) Avail: NTIS HC A03/MF A01 CSCL 23/2

Human-Computer Interaction (HCI) is an urgent and rapidly developing area of computer science research and application. As it continues to evolve and to define itself, it is possible to identify distinct paradigms, or orientations to HCI research and application. Initially, HCI work focussed on empirical laboratory evaluation of computer systems and techniques. Subsequently, empirical studies of usability were organized by and addressed to cognitive theoretical description of user behavior and experience. Currently, the focus of HCI work is shifting toward a more directive role in invention, design and development of systems and techniques. The progression of these three paradigms comprises a case study of a field discovering what it is about, and more generally, of the variety of roles available in the psychology of technology. GRA

N89-24797*# Advanced Resource Development Corp., Columbia, MD.
BRAIN-WAVE MEASURES OF WORKLOAD IN ADVANCED COCKPITS: THE TRANSITION OF TECHNOLOGY FROM LABORATORY TO COCKPIT SIMULATOR, PHASE 2 Final Report

Richard L. Horst, David L. Mahaffey, and Robert C. Munson Washington NASA 1989 187 p
(Contract NAS1-18019)
(NASA-CR-4240; NAS 1.26:4240) Avail: NTIS HC A09/MF A01 CSCL 05H

The present Phase 2 small business innovation research study was designed to address issues related to scalp-recorded event-related potential (ERP) indices of mental workload and to transition this technology from the laboratory to cockpit simulator environments for use as a systems engineering tool. The project involved five main tasks: (1) Two laboratory studies confirmed the generality of the ERP indices of workload obtained in the Phase 1 study and revealed two additional ERP components related to workload. (2) A task analysis' of flight scenarios and pilot tasks in the Advanced Concepts Flight Simulator (ACFS) defined cockpit events (i.e., displays, messages, alarms) that would be expected to elicit ERPs related to workload. (3) Software was developed to support ERP data analysis. An existing ARD-proprietary package of ERP data analysis routines was upgraded, new graphics routines were developed to enhance interactive data analysis, and routines were developed to compare alternative single-trial analysis techniques using simulated ERP data. (4) Working in conjunction with NASA Langley research scientists and simulator engineers, preparations were made for an ACFS validation study of ERP measures of workload. (5) A design specification was developed for a general purpose, computerized, workload assessment system that can function in simulators such as the ACFS. Author

N89-24798*# National Aeronautics and Space Administration. Ames Research Center, Moffett Field, CA.
DISPLAY-BASED COMMUNICATIONS FOR ADVANCED TRANSPORT AIRCRAFT
Alfred T. Lee May 1989 24 p
(NASA-TM-102187; A-89118; NAS 1.15:102187) Avail: NTIS HC A03/MF A01 CSCL 12A

The next generation of civil transport aircraft will depend increasingly upon ground-air-ground and satellite data link for information critical to safe and efficient air transportation. Previous studies which examined the concept of display-based communications in addition to, or in lieu of, conventional voice transmissions are reviewed. A full-mission flight simulation comparing voice and display-based communication modes in an advanced transport aircraft is also described. The results indicate that a display-based mode of information transfer does not result in significantly increased aircrew workload, but does result in substantially increased message acknowledgment times when compared to conventional voice transmissions. User acceptance of the display-based communication system was generally high, replicating the findings of previous studies. However, most pilots tested expressed concern over the potential loss of information available from frequency monitoring which might result from the introduction of discrete address communications. Concern was expressed by some pilots for the reduced time available to search for conflicting traffic when using the communications display system. The implications of the findings for the design of display-based communications are discussed. Author

N89-24354# Dornier-Werke G.m.b.H., Friedrichshafen (Germany, F.R.).
ECLS FOR COLUMBUS AND HERMES
H. Preiss, G. Kring, and R. Schaefer *In* ESA, International Symposium on Europe in Space: The Manned Space System Oct. 1988 p 163-167 (For primary document see N89-24335 18-12)
Copyright Avail: NTIS HC A99/MF A01; ESA Publications Div., ESTEC, Noordwijk, Netherlands, 80 Dutch guilders

N89-24362# Elektronik-System G.m.b.H., Munich (Germany, F.R.).
MANNED INTERVENTIONS AT THE MTFF: CREW WORKLOAD ASPECTS
K. Brammer and Georg Kampfer (Panares, Munich, Germany, F.R.) *In* ESA, International Symposium on Europe in Space: The Manned Space System Oct. 1988 p 233-237 (For primary document see N89-24335 18-12)
Copyright Avail: NTIS HC A99/MF A01; ESA Publications Div., ESTEC, Noordwijk, Netherlands, 80 Dutch guilders

N89-24387# European Space Agency. European Space Research and Technology Center, ESTEC, Noordwijk (Netherlands).
GETTING READY FOR EVA
A. Accensi *In its* International Symposium on Europe in Space: The Manned Space System Oct. 1988 p 467-475 (For primary document see N89-24335 18-12)
Copyright Avail: NTIS HC A99/MF A01; ESA Publications Div., ESTEC, Noordwijk, Netherlands, 80 Dutch guilders

N89-24388# Dornier-Werke G.m.b.H., Friedrichshafen (Germany, F.R.).
EVA INFORMATION SYSTEM: A MODERN WORKSTATION IN SPACE
Franz Pittermann, Pierre Larroque, and Stephane Berthier (Avions Marcel Dassault-Breguet Aviation, Saint-Cloud, France) *In* ESA, International Symposium on Europe in Space: The Manned Space System Oct. 1988 p 477-483 (For primary document see N89-24335 18-12)
Copyright Avail: NTIS HC A99/MF A01; ESA Publications Div., ESTEC, Noordwijk, Netherlands, 80 Dutch guilders

N89-24392# LABEN Space Instrumentation and Systems, Milan (Italy). Advanced Research and Development Dept.
ADVANCED MMI AND IMAGE HANDLING TO SUPPORT CREW ACTIVITIES
R. Cortinovis, B. Barni, and R. Persico *In* ESA, International Symposium on Europe in Space: The Manned Space System Oct. 1988 p 509-514 (For primary document see N89-24335 18-12)
Copyright Avail: NTIS HC A99/MF A01; ESA Publications Div., ESTEC, Noordwijk, Netherlands, 80 Dutch guilders

55 SPACE BIOLOGY

Includes exobiology; planetary biology; and extraterrestrial life.

No abstracts in this category.

59 MATHEMATICAL AND COMPUTER SCIENCES (GENERAL)

No abstracts in this category.

60 COMPUTER OPERATIONS AND HARDWARE

Includes hardware for computer graphics, firmware, and data processing.

For components see *33 Electronics and Electrical Engineering.*

N89-24799# Joint Inst. for Nuclear Research, Dubna (USSR). Lab. of High Energy.
THE 64K 16-BIT WORD BUFFER MEMORY WITH MICROPROGRAMMABLE CONTROL
A. B. Ivanov, Quoc Trung Pham, and G. A. Cheremukhina 1988

4 p In RUSSIAN; ENGLISH summary
(DE88-706303; JINR-13-88-303) Avail: NTIS (US Sales Only) HC A02/MF A01

The buffer memory unit (64K 16-bit words) with microprogrammable control is described. Wide functional possibilities permit to realize 16 modes of operation. The unit has two data inputs and is performed in CAMAC standard of 2M width. DOE

N89-24800# Argonne National Lab., IL.
ATTACHING IBM-COMPATIBLE 3380 DISKS TO CRAY X-MP
Douglas E. Engert and Joseph L. Midlock 1989 9 p Presented at the Cray User's Group Conference, Los Angeles, CA, 24 Apr. 1989
(Contract W-31-109-eng-38)
(DE89-012383; CONF-8904210-1) Avail: NTIS HC A02/MF A01

A method of attaching IBM-compatible 3380 disks directly to a Cray X-MP via the XIOP with a BMC is described. The IBM 3380 disks appear to the UNICOS operating system as DD-29 disks with UNICOS file systems. IBM 3380 disks provide cheap, reliable large capacity disk storage. Combined with a small number of high-speed Cray disks, the IBM disks provide for the bulk of the storage for small files and infrequently used files. Cray Research designed the BMC and its supporting software in the XIOP to allow IBM tapes and other devices to be attached to the X-MP. No hardware changes were necessary, and we added less than 2000 lines of code to the XIOP to accomplish this project. This system has been in operation for over eight months. Future enhancements such as the use of a cache controller and attachment to a Y-MP are also described. DOE

61 COMPUTER PROGRAMMING AND SOFTWARE

Includes computer programs, routines, alogorithms, and specific applications, e.g., CAD/CAM.

N89-24801# National Aerospace Lab., Tokyo (Japan).
HIGH SPEED IMPLEMENTATION OF NAL APPLICATION SOFTWARE PACKAGES
Kinuyo Nakamura, Masahiro Yoshida, and Masahiro Fukuda Jul. 1988 81 p In JAPANESE; ENGLISH summary
(NAL-TR-986; ISSN-0389-4010) Avail: NTIS HC A05/MF A01

The Numerical Simulator system (NS system), installed in the National Aerospace Laboratory (NAL) in February 1987, is composed of FACOM VP400, VP200, and M780 computers. The first two are vector-processor-type supercomputers and the last is a scalar computer. To extract full performance from supercomputers, it is necessary to give consideration to solution algorithms, programs and data structure, program coding, etc., to match individual supercomputers. NAL has various application software programed for a scalar computer. They are not necessarily matched for the VP400 and VP200, therefore they were tuned up to facilitate high speed processing on those supercomputers. The relative performance of the VP400, VP200, and M780 is reported by comparing computing time of the original and the tuned programs on each computer. Also, methods of effective FORTRAN programming to increase vectorization rate and high speed computation with FORTRAN programs on the machines are described. Author

N89-24802*# Illinois Univ., Urbana-Champaign. Dept. of Computer Science.
TRANSFORMATIONAL DERIVATION OF PROGRAMS USING THE FOCUS SYSTEM
Uday S. Reddy 2 Sep. 1988 22 p Submitted for publication
(Grant NAG1-613)
(NASA-CR-184875; NAS 1.26:184875) Avail: NTIS HC A03/MF A01 CSCL 09B

A program derivation support system called Focus is being constructed. It will formally derive programs using the paradigm of program transformation. The following issues are discussed: (1) the integration of validation and program derivation activities in the Focus system; (2) its tree-based user interface; (3) the control of search spaces in program derivation; and (4) the structure and organization of program derivation records. The inference procedures of the system are based on the integration of functional and logic programming principles. This brings about a synthesis of paradigms that were heretofore considered far apart, such as logical and executable specifications and constructive and transformational approaches to program derivation. A great emphasis has been placed, in the design of Focus, on achieving small search spaces during program derivation. The program manipulation operations such as expansion, simplification and rewriting were designed with this objective. The role of operations that are expensive in search spaces, such as folding, has been reduced. Program derivations are documented in Focus in a way that the high level descriptions of derivations are expressed only using program level information. All the meta-level information, together with dependencies between derivations of program components, is automatically recorded by the system at a lower level of description for its own use in replay. A.D.

N89-24803* SRI International Corp., Menlo Park, CA.
FORMAL VERIFICATION OF A FAULT TOLERANT CLOCK SYNCHRONIZATION ALGORITHM Final Report
John Rushby and Frieder vonHenke Jun. 1989 225 p
(Contract NAS1-17067)
(NASA-CR-4239; NAS 1.26:4239) Avail: NTIS HC A10/MF A01 CSCL 09B

A formal specification and mechanically assisted verification of the interactive convergence clock synchronization algorithm of Lamport and Melliar-Smith is described. Several technical flaws in the analysis given by Lamport and Melliar-Smith were discovered, even though their presentation is unusally precise and detailed. It seems that these flaws were not detected by informal peer scrutiny. The flaws are discussed and a revised presentation of the analysis is given that not only corrects the flaws but is also more precise and easier to follow. Some of the corrections to the flaws require slight modifications to the original assumptions underlying the algorithm and to the constraints on its parameters, and thus change the external specifications of the algorithm. The formal analysis of the interactive convergence clock synchronization algorithm was performed using the Enhanced Hierarchical Development Methodology (EHDM) formal specification and verification environment. This application of EHDM provides a demonstration of some of the capabilities of the system. Author

N89-24804# Office of Technology Assessment, Washington, DC.
THE ELECTRONIC SUPERVISOR: NEW TECHNOLOGY, NEW TENSIONS
Sep. 1987 148 p
(OTA-CIT-333; LC-87-619855) Avail: NTIS HC A07/MF A01; also available SOD HC $6.50 as 052-003-01082-8

The capabilities of new computer and communication technologies for monitoring employees' activities in the work-place are presented. Communication technologies such as digital private branch exchanges (PBXs), local area networks (LANs), and digital telephony in the switched network provide more capability to monitor calling patterns as well as content of telephone calls. Equipment and software for telephone calls accounting (tracking the time, destination, and cost of calls) make up the fastest growing segment of the telecommunication industry. The networking of computers, either through LANs or sometimes through the telephone system provides a broad capacity to monitor work that is performed at the computer terminal. Computer technology makes possible the continuous collection and analysis of management information about work performance and equipment use. This information is useful to managers in managing resources, planning workloads, and reducing costs. When it is applied to individual employees, however, the intensity and continuousness of

computer-based monitoring raises questions about fairness, privacy, and quality of work life. Author

N89-24805# Air Force Inst. of Tech., Wright-Patterson AFB, OH. School of Engineering.
HARDWARE MODELING WITH VHDL (VHSIC HARDWARE DESCRIPTION LANGUAGE) SIMULATION M.S. Thesis
Douglas G. Pompilio Dec. 1988 119 p
(AD-A206356; AFIT/GCS/ENG/88D-15) Avail: NTIS HC A06/MF A01 CSCL 09/1

This thesis presents a study of the VHSIC Hardware Description Language (VHDL) and its ability to accurately model digital hardware circuits. A brief background of Hardware Description Languages and VHDL is presented followed by a detailed look at VHDL's language features and semantics that support hardware modeling. This information is applied to the design and development of a VHDL simulator that supports a subset of the language. A discussion of the simulator design and implementation issues is presented. GRA

N89-24806# Naval Postgraduate School, Monterey, CA.
A SYSTOLIC ARRAY STRUCTURE FOR ON-LINE SYSTEM IDENTIFICATION M.S. Thesis
Mumtaz Tune Dec. 1988 81 p
(AD-A206412) Avail: NTIS HC A05/MF A01 CSCL 13/8

In this study, we present an algorithm for system identification for systolic array implementation. With this schema, discrete samples of input and output data of a system with uncertain characteristics are used to determine the parameters of its model. The identification algorithm is based on recursive least squares, QR decomposition, and block processing techniques with covariance resetting. The identification process is based on the use of Givens rotation. Additionally, we want to address the following problems: How the round-off error propagates in time and the implementation in closed loop adaptive control. We will compare the implementation of fixed point arithmetic with the implementation of floating point arithmetic. This is primarily a theoretical investigation to be conducted with computer simulations where numerical results will be investigated. GRA

N89-24807# Pennsylvania State Univ., University Park. Chemical Lab.
REAL-TIME SYSTEM: SPECIFICATION AND VERIFICATION Progress Report, 1 Oct. 1988 - 28 Feb. 1989
K. T. Narayana 28 Feb. 1989 13 p
(Contract N00014-89-J-1171)
(AD-A206467; AFGL-TR-89-0068) Avail: NTIS HC A03/MF A01 CSCL 12/7

Temporal Interval Logic by virtue of its abstract interval constructors offers an excellent setting for concurrent system specification. Making extensions for this logic to cater to specification of quantitative aspects of behaviors was considered useful. Extensions have been made to for specifying real-time constraints in the framework of the logic. A formal semantics has been given. A large body of realistic and nontrivial examples have been explored and specified. The examples considered suggest that real-time variants of temporal interval logic are extremely suitable for quantitative specification of behaviors. The work was published at the 9th symposium on real-time systems, held in December 1988 at Huntsville, Alabama. A revision of the paper is currently under way so as to submit it for a journal. The work needs to be explored further in the direction of decision procedures for finite state real-time controllers. In an earlier work we proved that temporal interval logic is PSpace Complete. We have obtained decision procedures and implementations. We have synthesized using our implementation a hardware arbiter. This in itself is a substantial achievement for the synthesis times in our Prolog based implementation were quite reasonable. Thus the logic was demonstrated to be useful. GRA

N89-24808# Defence Research Establishment Atlantic, Dartmouth (Nova Scotia).
WADA1: FORTRAN PROGRAM FOR WAVE DIFFRACTION ANALYSIS, VERSION 1
Samon Ando Feb. 1989 26 p
(AD-A206533; DREA-TM-89/204) Avail: NTIS HC A03/MF A01 CSCL 12/5

This Canadian document describes the FORTRAN computer program WADA1 (WAve Diffraction Analysis-version 1) developed as part of on-going research to analyze the interactions of ocean waves with marine vehicles. WADA1 calculates the hydrodynamic pressured induced by an incident sinusoidal wave and diffracted wave on arbitrary-shaped two-dimensional cylinders fixed in the free surface of deep water. WADA1 solves the linear diffraction problem by the source-distribution model. It uses the Green function that is a particular fundamental solution of the two-dimensional Laplace equation and directly satisfies the boundary conditions on the free surface, on the sea bottom, and at infinity. The amount of required input data is minimal since only the boundary condition on the body surface remains to be satisfied; however, the computation of the Green function and its gradient is complicated. Also the method fails to give a unique solution at irregular frequencies, but these usually occur outside the range of frequency of practical interest. GRA

N89-24809# National Communications System, Washington, DC.
INVESTIGATION OF VECTOR QUANTIZATION FOR THE CODING GRAY SCALE IMAGES FOR GROUP 4 FACSIMILE Final Report
Aug. 1988 99 p
(Contract DCA100-87-C-0078)
(AD-A206548; NCS-TIB-88-6) Avail: NTIS HC A05/MF A01 CSCL 25/3

Vector Quantization is a new gray scale coding technique showing the promise of large compression ratios and good picture quality. No comprehensive study analyzing Vector Quantization, as applied to Group 4 facsimile systems under carefully controlled conditions, has been performed prior to this investigation. The purpose of this study was to evaluate Vector Quantization to determine its relative effectiveness for the addition of gray scale to Group 4 facsimile. This report is comprised of six sections. Section 1.0 provides a brief synopsis of the study objectives and outlines its results and conclusions. Section 2.0 describes the initial investigation, includes a highly simplified description of the Vector Quantization concept, and concludes with a brief outline of the selected approach and the reasons for its selection. Section 3.0 gives a system overview. Section 4.0 describes the system in detail. Section 5.0 presents the simulation parameters and results. Section 6.0 closes the report with conclusions and recommendations for future investigation. GRA

N89-24810# Aerospatiale, Cannes La Bocca (France).
XCAD: A CAD OBJECT-ORIENTED VIRTUAL SOLID MODELER FOR AN EXPERT SYSTEM SHELL
B. Trousse 1988 6 p
(Rept-882-440-125; ETN-89-94518) Avail: NTIS HC A02/MF A01

Critical aspects of existing CAD systems are discussed and the approach based on a modeler implemented on an object oriented layer linked to an expert system is presented. It is shown that some of the mentioned problems are solved. This environment allows more flexible data management, more powerful and natural prototype modeling as well as automatic design reasonings. ESA

N89-24811*# SRI International Corp., Menlo Park, CA. Computer Science Lab.
FORMAL VERIFICATION OF AI SOFTWARE Final Report
John Rushby and R. Alan Whitehurst 28 Feb. 1989 156 p
(Contract NAS1-18226)
(NASA-CR-181827; NAS 1.26:181827) Avail: NTIS HC A08/MF A01 CSCL 09B

The application of formal verification techniques to Artificial Intelligence (AI) software, particularly expert systems, is investigated. Constraint satisfaction and model inversion are identified as two formal specification paradigms for different classes of expert systems. A formal definition of consistency is developed, and the notion of approximate semantics is introduced. Examples are given of how these ideas can be applied in both declarative and imperative forms. Author

N89-24812# Oak Ridge National Lab., TN. Computing and Telecommunication Div.
HOW TO (AND NOT TO) INTRODUCE COMPUTER GRAPHICS TO DESIGN PROFESSIONALS
Betsy A. Riley 1989 8 p Presented at the NCGA Conference, Philadelphia, PA, 19 Apr. 1989
(Contract DE-AC05-84OR-21400)
(DE89-010374; CONF-8904191-2) Avail: NTIS HC A02

A presentation- and publication-quality computer graphics system has been implemented at Union Carbide Corporation Nuclear Division over the past four years. Success of the implementation required close interaction between programmers and illustrators. This paper discusses the problems involved in establishing a computer graphics capability in a conventional graphic arts department. The problems dealt with fall into three areas: identifying and acquiring appropriate hardware, acquiring user-friendly software that could meet stringent quality standards, and overcoming the prejudices and misconceptions of all the people involved. DOE

N89-24813# Du Pont de Nemours (E. I.) and Co., Aiken, SC. Savannah River Lab.
APPLICATION OF LOTUS 1-2-3 TO HEAT TRANSFER ANALYSIS
F. W. Bornt 1989 9 p Presented at the Annual Meeting of the American Nuclear Society, Atlanta, GA, 4-8 Jun. 1989 Submitted for publication
(Contract DE-AC09-76SR-00001)
(DE89-010463; DP-MS-89-4; CONF-890604-3-Vugraphs) Avail: NTIS HC A02/MF A01

One often has to perform heat transfer analyses that are a bit involved for hand calculations, but are not quite large enough to justify the use of a special purpose heat transfer computer code. This paper describes the use of Lotus 1-2-3 for these in between problems. DOE

N89-24652*# Texas A&M Univ., College Station.
CONTACT SOLUTION ALGORITHMS
John T. Tielking *In* NASA, Langley Research Center, Computational Methods for Structural Mechanics and Dynamics, Part 1 May 1989 p 291-316 (For primary document see N89-24638 18-39)
Avail: NTIS HC A15/MF A01 CSCL 09B

N89-24659*# Lawrence Livermore National Lab., CA.
APPLICATION AND IMPLEMENTATION OF TRANSIENT ALGORITHMS IN COMPUTER PROGRAMS
David J. Benson *In* NASA, Langley Research Center, Computational Methods for Structural Mechanics and Dynamics May 1989 p 407-418 Previously announced as N86-15968 (For primary document see N89-24654 18-39)
(Contract W-7405-eng-48)
Avail: NTIS HC A12/MF A01 CSCL 09B

N89-24660*# National Aeronautics and Space Administration. Langley Research Center, Hampton, VA.
RECENT DEVELOPMENTS IN DEPLOYMENT ANALYSIS SIMULATION USING A MULTI-BODY COMPUTER CODE
Jerrold M. Housner *In its* Computational Methods for Structural Mechanics and Dynamics May 1989 p 435-441 (For primary document see N89-24654 18-39)
Avail: NTIS HC A12/MF A01 CSCL 09B

N89-24666*# Lockheed Missiles and Space Co., Palo Alto, CA.
COMPUTATIONAL ASPECTS OF MULTIBODY DYNAMICS
K. C. Park *In* NASA, Langley Research Center, Computational Methods for Structural Mechanics and Dynamics May 1989 p 527-536 (For primary document see N89-24654 18-39)
Avail: NTIS HC A12/MF A01 CSCL 20K

N89-24826*# Alabama Univ., Huntsville.
SPACE LANGUAGES: SOLVING THE CLASSIC SCHEDULING PROBLEM IN Ada AND LISP Abstract Only
Stephen Davis, Dan Hays, and John W. Wolfsberger (National Aeronautics and Space Administration. Marshall Space Flight Center, Huntsville, AL.) *In* Tactical Weapons Guidance and Control Information Conference on Space and Military Applications of Automation and Robotics Jun. 1988 p 16 (For primary document see N89-24819 18-63)
Avail: NTIS HC A05/MF A01 CSCL 09B

N89-24830# TREC, Inc., Huntsville, AL.
TWO DIMENSIONAL CONVOLUTE INTEGER TECHNOLOGY FOR DIGITAL IMAGE PROCESSING Abstract Only
Thomas R. Edwards *In* Tactical Weapons Guidance and Control Information Conference on Space and Military Applications of Automation and Robotics Jun. 1988 p 21 (For primary document see N89-24819 18-63)
Avail: NTIS HC A05/MF A01 CSCL 09B

N89-24842# Army Missile Command, Redstone Arsenal, AL.
DEVELOPMENT OF AN INTEGRATED CAD/CAM SYSTEM FOR WIRE HARNESS FABRICATION Abstract Only
J. M. Anderson, J. I. Locker, T. D. Morgan, L. J. Frederick, and C. D. Minor *In* Tactical Weapons Guidance and Control Information Conference on Space and Military Applications of Automation and Robotics Jun. 1988 p 46 Prepared in cooperation with Alabama Univ., Huntsville (For primary document see N89-24819 18-63)
Avail: NTIS HC A05/MF A01 CSCL 09B

N89-24848# Army Missile Command, Redstone Arsenal, AL.
A 3-D GRAPHICAL SIMULATION OF AN AUTOMATED DIRECT CHIP PROBE/TEST SYSTEM Abstract Only
D. C. Holderfield, T. D. Morgan, B. E. Martin, and J. R. Facemire *In* Tactical Weapons Guidance and Control Information Conference on Space and Military Applications of Automation and Robotics Jun. 1988 p 61 Prepared in cooperation with Alabama Univ., Huntsville (For primary document see N89-24819 18-63)
Avail: NTIS HC A05/MF A01 CSCL 09B

62 COMPUTER SYSTEMS

Includes computer networks and special application computer systems.

N89-24814# National Aerospace Lab., Tokyo (Japan).
THE DEVELOPMENT OF A JOB-JOBSTEP SCHEDULER FOR NS SYSTEM
Masako Tsuchiya Jun. 1988 48 p In JAPANESE; ENGLISH summary
(NAL-TR-977; ISSN-0389-4010) Avail: NTIS HC A03/MF A01

The concepts and the detailed functions of a Job-Jobstep scheduler which constitutes the kernal of software packages developed for the management of the NAL computer system (NS system) is presented. One of the important functions of the Job-Jobstep scheduler is to assign appropriate amounts of work load to three central processing units and several input-output processing units. As a result, the NS system retains a high CPU operating ratio and provides users with much convenience. Experiments show that the designed effectiveness of the Job-Jobstep Scheduler was achieved. Author

N89-24815*# National Aeronautics and Space Administration. Langley Research Center, Hampton, VA.
THE FAULT TREE COMPILER (FTC): PROGRAM AND MATHEMATICS
Ricky W. Butler and Anna L. Martensen (PRC Kentron, Inc.,

Hampton, VA.) Washington Jul. 1989 40 p
(NASA-TP-2915; L-16529; NAS 1.60:2915) Avail: NTIS HC A03/MF A01 CSCL 09B

The Fault Tree Compiler Program is a new reliability tool used to predict the top-event probability for a fault tree. Five different gate types are allowed in the fault tree: AND, OR, EXCLUSIVE OR, INVERT, AND m OF n gates. The high-level input language is easy to understand and use when describing the system tree. In addition, the use of the hierarchical fault tree capability can simplify the tree description and decrease program execution time. The current solution technique provides an answer precisely (within the limits of double precision floating point arithmetic) within a user specified number of digits accuracy. The user may vary one failure rate or failure probability over a range of values and plot the results for sensitivity analyses. The solution technique is implemented in FORTRAN; the remaining program code is implemented in Pascal. The program is written to run on a Digital Equipment Corporation (DEC) VAX computer with the VMS operation system. Author

N89-24816*# Institute for Computer Applications in Science and Engineering, Hampton, VA.
FILE CONCEPTS FOR PARALLEL I/O Final Report
Thomas W. Crockett May 1989 15 p
(Contracts NAS1-18107; NAS1-18605)
(NASA-CR-181843; NAS 1.26:181843; ICASE-IR-7) Avail: NTIS HC A03/MF A01 CSCL 09B

The subject of input/output (I/O) was often neglected in the design of parallel computer systems, although for many problems I/O rates will limit the speedup attainable. The I/O problem is addressed by considering the role of files in parallel systems. The notion of parallel files is introduced. Parallel files provide for concurrent access by multiple processes, and utilize parallelism in the I/O system to improve performance. Parallel files can also be used conventionally by sequential programs. A set of standard parallel file organizations is proposed, organizations are suggested, using multiple storage devices. Problem areas are also identified and discussed. Author

N89-24817* Carnegie-Mellon Univ., Pittsburgh, PA. Dept. of Electrical and Computer Engineering.
PREDEPLOYMENT VALIDATION OF FAULT-TOLERANT SYSTEMS THROUGH SOFTWARE-IMPLEMENTED FAULT INSERTION Final Report, Nov. 1987 - Nov. 1988
Edward W. Czeck, Daniel P. Siewiorek, and Zary Z. Segall Washington Jul. 1989 47 p
(Grant NAG1-190)
(NASA-CR-4244; NAS 1.26:4244) Avail: NTIS HC A03/MF A01 CSCL 09B

Fault injection-based automated testing (FIAT) environment, which can be used to experimentally characterize and evaluate distributed realtime systems under fault-free and faulted conditions is described. A survey is presented of validation methodologies. The need for fault insertion based on validation methodologies is demonstrated. The origins and models of faults, and motivation for the FIAT concept are reviewed. FIAT employs a validation methodology which builds confidence in the system through first providing a baseline of fault-free performance data and then characterizing the behavior of the system with faults present. Fault insertion is accomplished through software and allows faults or the manifestation of faults to be inserted by either seeding faults into memory or triggering error detection mechanisms. FIAT is capable of emulating a variety of fault-tolerant strategies and architectures, can monitor system activity, and can automatically orchestrate experiments involving insertion of faults. There is a common system interface which allows ease of use to decrease experiment development and run time. Fault models chosen for experiments on FIAT have generated system responses which parallel those observed in real systems under faulty conditions. These capabilities are shown by two example experiments each using a different fault-tolerance strategy. Author

N89-24818*# Research Inst. for Advanced Computer Science, Moffett Field, CA.
TOTALLY PARALLEL MULTILEVEL ALGORITHMS
Paul O. Frederickson 23 Nov. 1988 16 p
(Contract NASw-4234)
(NASA-CR-185404; NAS 1.26:185404; RIACS-TR-88.34) Avail: NTIS HC A03/MF A01 CSCL 09B

Four totally parallel algorithms for the solution of a sparse linear system have common characteristics which become quite apparent when they are implemented on a highly parallel hypercube such as the CM2. These four algorithms are Parallel Superconvergent Multigrid (PSMG) of Frederickson and McBryan, Robust Multigrid (RMG) of Hackbusch, the FFT based Spectral Algorithm, and Parallel Cyclic Reduction. In fact, all four can be formulated as particular cases of the same totally parallel multilevel algorithm, which are referred to as TPMA. In certain cases the spectral radius of TPMA is zero, and it is recognized to be a direct algorithm. In many other cases the spectral radius, although not zero, is small enough that a single iteration per timestep keeps the local error within the required tolerance. Author

N89-24650*# Akron Univ., OH.
NONLINEAR HIERARCHICAL SUBSTRUCTURAL PARALLELISM AND COMPUTER ARCHITECTURE
Joe Padovan *In* NASA, Langley Research Center, Computational Methods for Structural Mechanics and Dynamics, Part 1 May 1989 p 249-267 (For primary document see N89-24638 18-39)
Avail: NTIS HC A15/MF A01 CSCL 09B

63 CYBERNETICS

Includes feedback and control theory, artificial intelligence, robotics and expert systems.

For related information see also *54 Man/System Technology and Life Support.*

N89-24819# Tactical Weapons Guidance and Control Information Analysis Center, Chicago, IL.
CONFERENCE ON SPACE AND MILITARY APPLICATIONS OF AUTOMATION AND ROBOTICS Abstracts Only
Jun. 1988 99 p Conference held in Huntsville, AL, 21-22 Jun. 1988; sponsored by NASA, Marshall Space Flight Center, Huntsville, AL and the Army Missile Command, Huntsville, AL
(AD-A198095; GACIAC-SR-88-10) Avail: NTIS HC A05/MF A01 CSCL 09/2

Topics addressed include: robotics; deployment strategies; artificial intelligence; expert systems; sensors and image processing; robotic systems; guidance, navigation, and control; aerospace and missile system manufacturing; and telerobotics. For individual titles, see N89-24820 through N89-24855.

N89-24820*# National Aeronautics and Space Administration. Marshall Space Flight Center, Huntsville, AL.
AN AUTOMATED PROTEIN CRYSTAL GROWTH FACILITY ON THE SPACE STATION Abstract Only **c29**
Melody Herrmann *In* Tactical Weapons Guidance and Control Information Conference on Space and Military Applications of Automation and Robotics Jun. 1988 p 3 (For primary document see N89-24819 18-63)
Avail: NTIS HC A05/MF A01 CSCL 22A

The need is addressed for an automated Protein Crystal Growth experiment on the Space Station and how robotics will be integrated into the system design. This automated laboratory system will enable several hundred protein crystals to grow simultaneously in microgravity and will allow the major variables in protein crystal growth to be monitored and controlled during the experiment. Growing good quality crystals is important in determining the complete structure of the protein by X-ray diffraction. This information is useful in the research and development of medicines and other important medical and biotechnological products. Previous Protein Crystal Growth experiments indicate that the

microgravity environment of space allows larger crystals of higher quality to be grown as compared to the same crystals grown on the ground. It is therefore important to have a laboratory in space where protein crystals can be grown under carefully controlled conditions so that a crystal type can be reproduced as needed.
Author

N89-24821# Teledyne Brown Engineering, Huntsville, AL.
THE IMPACT OF AN IVA ROBOT ON THE SPACE STATION MICROGRAVITY ENVIRONMENT Abstract Only **c29**
Phillip E. Harman *In* Tactical Weapons Guidance and Control Information Conference on Space and Military Applications of Automation and Robotics Jun. 1988 p 4 (For primary document see N89-24819 18-63)
Avail: NTIS HC A05/MF A01 CSCL 09B

In order to maintain a microgravity environment during Space Station operations, it will be necessary to minimize reaction forces. These mechanical forces will typically result during reboost, docking, equipment operation, IVA robot operations, or crew activity. The impact of these accelerations on the experiments is described by focusing on those disturbances created by an IVA robot. An explanation of the robot dynamic analysis that was used to generate the forcing function as the input into a finite element model of the U.S. laboratory will be shown. These results will identify the acceleration levels at locations throughout the module in order to assess the impact a robotic system will have on space station operations and the microgravity environment. Results will also be shown for the disturbances created by other sources. The results will help quantify what g-level environment can be obtained on the station and the effect of an IVA robot. A comparison between IVA robot effects and crew motion effects on the low-g environment will be described. Author

N89-24822# Kader Robotics, Inc., Huntsville, AL.
DUAL-ARM ROBOTS FOR TELEROBOTIC IVA OPERATIONS ON THE SPACE STATION Abstract Only **c37**
M. Carl Ziemke, Jac Kader, and Larry Yawn *In* Tactical Weapons Guidance and Control Information Conference on Space and Military Applications of Automation and Robotics Jun. 1988 p 5 (For primary document see N89-24819 18-63)
Avail: NTIS HC A05/MF A01 CSCL 09B

Sometime during the middle of the next decade, the U.S. Space Station will achieve initial operating capability. The activities will be accomplished or directed by a crew of only eight to ten members. The productivity of this initial crew must be amplified by extensive use of automation and robotics. But in 1985, the astronauts expressed a strong preference for vital equipment that will be 100 percent capable of manual operation in the event of machine failure. Thus, much of the equipment in the Space Station will probably be designed for operation using controls adapted primarily for the human hand and arm. In many cases, these operations will require use of both hands. Therefore, if a machine normally operated by a robot requires direct human operation, it must be possible to maneuver the robot out of the way to permit direct manual operation. These constraints strongly emphasize the need for dexterous, dual-arm robots for Space Station IVA. One of the problems of operation of a dual-arm robot is the coordination of movement between both arms when they are simultaneously engaged in performing a task. A dual-arm robot design was produced that employs asymmetrical manipulator arms that pivot on a common radius. The advantages of this concept are described. These advantages include compactness, light weight, and reduced tendency toward interarm collisions. Author

N89-24823*# Alabama Univ., Huntsville.
HIGH LEVEL INTELLIGENT CONTROL OF TELEROBOTICS SYSTEMS Abstract Only
James McKee *In* Tactical Weapons Guidance and Control Information Conference on Space and Military Applications of Automation and Robotics Jun. 1988 p 13 Prepared in cooperation with NASA. Marshall Space Flight Center, Huntsville, AL (For primary document see N89-24819 18-63)
Avail: NTIS HC A05/MF A01 CSCL 09B

A high level robot command language is proposed for the autonomous mode of an advanced telerobotics system and a predictive display mechanism for the teleoperational model. It is believed that any such system will involve some mixture of these two modes, since, although artificial intelligence can facilitate significant autonomy, a system that can resort to teleoperation will always have the advantage. The high level command language will allow humans to give the robot instructions in a very natural manner. The robot will then analyze these instructions to infer meaning so that is can translate the task into lower level executable primitives. If, however, the robot is unable to perform the task autonomously, it will switch to the teleoperational mode. The time delay between control movement and actual robot movement has always been a problem in teleoperations. The remote operator may not actually see (via a monitor) the results of high actions for several seconds. A computer generated predictive display system is proposed whereby the operator can see a real-time model of the robot's environment and the delayed video picture on the monitor at the same time. Author

N89-24824# Alabama Univ., Huntsville.
NEUTRAL FILE DATA EXCHANGE BETWEEN SIMULATORS AND ROBOTS Abstract Only
W. D. Engelke and D. Gilliam *In* Tactical Weapons Guidance and Control Information Conference on Space and Military Applications of Automation and Robotics Jun. 1988 p 14 (For primary document see N89-24819 18-63)
Avail: NTIS HC A05/MF A01 CSCL 09B

A pair of translators was developed to study the process of translating between a robot simulation system and a robot using a neutral file language. A Deneb Robotics simulator and an IBM 7535 robot were linked using the neutral file Generic Descriptor Language (GDL). The GDL describes both the geometry and logic of a simulation or a robotic program and is designed to allow translation of logic and geometry between multiple kinematic simulators and multiple robots. The process of modeling the robot, developing the robot software on the simulator, and translating it from Deneb to GDL and finally into IBM's AML in the IBM 7535 robot are described. Author

N89-24825# Alabama Univ., Huntsville.
COOPERATING EXPERT SYSTEMS Abstract Only
Michael Brady and Donnie R. Ford *In* Tactical Weapons Guidance and Control Information Conference on Space and Military Applications of Automation and Robotics Jun. 1988 p 15 (For primary document see N89-24819 18-63)
Avail: NTIS HC A05/MF A01 CSCL 09B

The problems in applying automation to arc welding are examined for small batch size operations, and a practical adaptive control model is proposed. Two elements are identified as principal to the model: sensor fusion and expert systems. Sensor fusion provides an interpretation of the weld execution environment. The expert system accesses this interpretation, as well as a rule base, to arbitrate intelligently among competing goals, such as cost and productivity. This is accomplished using a goal reduction strategy. In order to give the model a broad base of applicability, a generic approach is taken. System development is phased in a set of steps to minimize the redundancy of effort in applying the system to welds, weld applications, or weld processes. These steps include generic engineering, weld process engineering, and application engineering. This is supported by partitioning the system into components amenable to tailoring it for the broadest possible application. These components include the process engineering laboratory, application engineering laboratory, and the field location set-up. This partitioning supports iterative development of successive weld processes and applications, and provides a functional, maintainable architecture for the system. Author

N89-24826*# Alabama Univ., Huntsville.
SPACE LANGUAGES: SOLVING THE CLASSIC SCHEDULING PROBLEM IN Ada AND LISP Abstract Only **c61**
Stephen Davis, Dan Hays, and John W. Wolfsberger (National Aeronautics and Space Administration. Marshall Space Flight

Center, Huntsville, AL.) *In* Tactical Weapons Guidance and Control Information Conference on Space and Military Applications of Automation and Robotics Jun. 1988 p 16 (For primary document see N89-24819 18-63)
Avail: NTIS HC A05/MF A01 CSCL 09B

The comparison of programming languages is best seen while evaluating similar systems. The strengths and weaknesses of both languages were investigated as the scheduler was being implemented. Some features used in both languages shall be object-oriented paradigms, parallel programming, search and production heuristics, and other classical artificial intelligence implementations. Author

N89-24827# Robotic Vision Systems, Inc., Melville, NY.
A SYSTEM FOR HIGH RESOLUTION 3D MAPPING USING LASER RADAR AND REQUIRING NO BEAM SCANNING MECHANISMS c36
Paul Rademacher *In* Tactical Weapons Guidance and Control Information Conference on Space and Military Applications of Automation and Robotics Jun. 1988 p 18 (For primary document see N89-24819 18-63)
Avail: NTIS HC A05/MF A01 CSCL 09B

The inherently high angular and range resolution capabilities associated with radar systems operating at optical frequencies are at once a blessing and a curse. Standard implementations consist of very narrow field of view optical receivers operating in conjunction with laser transmitters or even narrower illumination beamwidth. While high angular resolution is thus achieved, mechanical scanning is required to gather data over extended fields of view. The many laser pulse transmissions necessary to cover the entire field of view increase the detectability of the system by enemy sensors. A system concept is proposed which, through the use of a single laser transmitter and multiple optical receivers, largely eliminate these deficiencies. Complete 3D data over a broad angular field of view and depth of field can be gathered based upon the reflections from a single transmitted laser pulse. Covert operation is enhanced as a result of the sparse laser transmissions required. The eye safety characteristics of the system are also enhanced. Proprietary coding of optical shutters in each of the multiple optical receivers permits the number of such receivers to be reduced to a very practical few. An alternative configuration of the system reduces the number of receivers required to one, at the expense of increased data acquisition time. The multiple receiver configuration is simply a parallel processing implementation of the single receiver approach. While data rate is reduced by the single receiver configuration, it still greatly exceeds that of scanning systems, and hardware complexity is also reduced significantly. Author

N89-24828*# McDonnell-Douglas Astronautics Co., Huntington Beach, CA.
TECHNOLOGY TRANSFER: IMAGING TRACKER TO ROBOTIC CONTROLLER Abstract Only
M. S. Otaguro, L. O. Kesler, Ken Land, Harry Erwin, and Don Rhoades *In* Tactical Weapons Guidance and Control Information Conference on Space and Military Applications of Automation and Robotics Jun. 1988 p 19 Prepared in cooperation with NASA. Lyndon B. Johnson Space Center, Houston, TX (For primary document see N89-24819 18-63)
Avail: NTIS HC A05/MF A01 CSCL 09B

The transformation of an imaging tracker to a robotic controller is described. A multimode tracker was developed for fire and forget missile systems. The tracker locks on to target images within an acquisition window using multiple image tracking algorithms to provide guidance commands to missile control systems. This basic tracker technology is used with the addition of a ranging algorithm based on sizing a cooperative target to perform autonomous guidance and control of a platform for an Advanced Development Project on automation and robotics. A ranging tracker is required to provide the positioning necessary for robotic control. A simple functional demonstration of the feasibility of this approach was performed and described. More realistic demonstrations are under way at NASA-JSC. In particular, this modified tracker, or robotic controller, will be used to autonomously guide the Man Maneuvering Unit (MMU) to targets such as disabled astronauts or tools as part of the EVA Retriever efforts. It will also be used to control the orbiter's Remote Manipulator Systems (RMS) in autonomous approach and positioning demonstrations. These efforts will also be discussed. Author

N89-24829# Rexham Aerospace and Defense Group, Huntsville, AL.
STABILIZED IMAGE SYSTEM FOR MOBILE ROBOTS Abstract Only c37
David Samuel Stauffer and Edward Watts *In* Tactical Weapons Guidance and Control Information Conference on Space and Military Applications of Automation and Robotics Jun. 1988 p 20 (For primary document see N89-24819 18-63)
Avail: NTIS HC A05/MF A01 CSCL 09B

Various applications of image stabilization techniques were investigated for robotic vehicles. This technology offers a low-cost means to provide a stabilized image from a moving vehicle for steering, isolation of the gunner's targeting image from weapon recoil, and other disturbances, and possible target detection and identification while moving. It will also provide for additional flexibility in a robotic vehicle vision system by allowing for scanning without mechanical turret motion and providing capability to zoom without changing the camera lenses. An experimental system was constructed, and a preliminary evaluation of the concept was demonstrated. The results of this initial experiment system are presented and then future research activities are presented. Improvements for the system include, reducing blur while compensating for high-speed motion, eliminating gyro bias, adaptation of circuit concept to color cameras, and enhancing system interface. Concepts to eliminate inertial research effort will be a working brassboard robotic vision system that is portable and that provides flexibility to interface with standard mobile robot sensor suites. Demonstration of this technology in realistic environments and conditions is seen as a key toward its acceptance. Author

N89-24830# TREC, Inc., Huntsville, AL.
TWO DIMENSIONAL CONVOLUTE INTEGER TECHNOLOGY FOR DIGITAL IMAGE PROCESSING Abstract Only c61
Thomas R. Edwards *In* Tactical Weapons Guidance and Control Information Conference on Space and Military Applications of Automation and Robotics Jun. 1988 p 21 (For primary document see N89-24819 18-63)
Avail: NTIS HC A05/MF A01 CSCL 09B

A demonstration of results from the application of Two Dimensional Convolute Integer Operators is presented. The results for classical replacement point convolutions and magnification by interstitial point generation will be displayed on a PC microcomputer with a high resolution large screen color graphics monitor. The sensitive two dimensional frequency response of Two Dimensional Convolute Integer Operators is seen on a number of test images, ranging from a noisy German Panzer tank image to LANDSAT data. Images of a noise free tank without loss of detail, images of noise bands removed, families of edge contours from low frequency to high frequency, Laplacians, curls, magnification, and feature extraction will be presented. Two Dimensional Convolute Integer Technology represents a family of innovative image processing operators for high-speed, two dimensional frequency-sensitive, theoretically correct classical convolutions, interstitial point generation, and missing or bad value replacement. Two Dimensional Convolute Integers Operators are mathematically equivalent to partial derivatives, a correct approach towards curl, divergence, Laplacian and gradient magnitudes and directions, and high resolution magnification. This VAX-based PC-linked, high resolution, color image display convolution software is described along with TREC's Digital Image Processing Environment.
Author

N89-24831# Air Force Inst. of Tech., Wright-Patterson AFB, OH.
DEVELOPMENT OF A HYBRID SIMULATOR FOR ROBOTIC MANIPULATORS Abstract Only **c37**
Peter M. VanWirt and Michael B. Leahy, Jr. *In* Tactical Weapons Guidance and Control Information Conference on Space and Military Applications of Automation and Robotics Jun. 1988 p 23 (For primary document see N89-24819 18-63)
Avail: NTIS HC A05/MF A01 CSCL 09B

The military is pursuing the use of robot manipulators and teleoperated manipulators in hostile environments. Implementation was restricted by the rudimentary control schemes used by current manipulators. Research into improved control schemes for these manipulators is limited by the lack of simulation capability. The need for an adequate articulated robot simulation is great due to the problems of safety, money, and work space caused by operation of a robot. The PUMA 560 was chosen as a case study because it represents a class of manipulators of interest to the military and because actual PUMA 560 response data was readily available. Once the proper models were installed on a digital computer and shown to be accurate by comparison to PUMA 560 responses, the decision was made to convert the model for use on a SIMSTAR Hybrid Computer. The analog model gives the control engineer greater freedom in choices of controllers to test. It also provides the capability to run realtime man-in-the-loop simulations. This model is again verified by comparison to actual robot arm motions using the same controllers. Author

N89-24832# Moog, Inc., East Aurora, NY.
DISCONNECTS FOR SPACECRAFT SERVICING APPLICATIONS Abstract Only **c18**
J. M. Cardin *In* Tactical Weapons Guidance and Control Information Conference on Space and Military Applications of Automation and Robotics Jun. 1988 p 25 (For primary document see N89-24819 18-63)
Avail: NTIS HC A05/MF A01 CSCL 09B

The goals of U.S. space programs have created a need for large, complex, long-life spacecraft. This new generation of spacecraft has created a set of design drivers for their fluid systems. On-orbit erectability, maintainability, expandibility, and resupply are system requirements that in many cases cannot be achieved using existing component technologies. Serviceable spacecraft fluid systems require disconnects to facilitate manual, remote, or automated on-orbit maintenance and resupply. In response to this need, disconnect technology that has improved performance characteristics such as pressure drop and spillage while maintaining configurations suitable for both manual and automated/robotic operation. The state of this technology is outlined, including data generated by in-house testing, in addition to industry and government evaluation. Author

N89-24833# Advanced Control Technology, Inc., Nashville, TN.
A NEW APPROACH TO ROBOT KINEMATIC ANALYSIS Abstract Only
Mary S. Waggener, Frank Testa, and Guy O. Beale *In* Tactical Weapons Guidance and Control Information Conference on Space and Military Applications of Automation and Robotics Jun. 1988 p 25 (For primary document see N89-24819 18-63)
Avail: NTIS HC A05/MF A01 CSCL 09B

Existing methods for solving robot kinematic equations can be classified as either analytic or iterative solutions. Both classes require the derivation of the forward equations, a set of coupled transcendental equations relating end effector position and orientation to robot joint coordinates. An approach for deriving robot kinematic models is being developed which is neither iterative nor analytic. This technique requires no a priori knowledge of the robot architecture, reference coordinate frame, or gripper. The algorithm, given only empirical data, derives closed form equations for joint position as functions of desired and effector position and orientation. It can also be extended to provide models of joint derivatives. The joint models are derived from empirical data consisting of a set of end effector positions and orientations and the corresponding joint coordinates. This data may be obtained by evaluating the forward kinematic equations or from actual measurements of the end effector positions and orientations. The models are derived by fitting n dimensional hypersurfaces to the data where n is the number of independent variables. Several methods for deriving the models, including least squares polynomial approximation and spline techniques, are described. Author

N89-24834# Martin Marietta Corp., Denver, CO.
THE DARPA AUTONOMOUS LAND VEHICLE: A PHASE 1 RETROSPECTIVE AND A PROSPECTIVE FOR THE FUTURE Abstract Only **c37**
Robert J. Douglass *In* Tactical Weapons Guidance and Control Information Conference on Space and Military Applications of Automation and Robotics Jun. 1988 p 29 (For primary document see N89-24819 18-63)
Avail: NTIS HC A05/MF A01 CSCL 09B

The Autonomous Land Vehicle Program (ALV) combines advances in computer vision, automatic planning, sensors, and advanced computer architecture to create a mobile outdoor robot that can navigate autonomously on and off roads to accomplish a high level goal. During the first 2.5 year phase of the ALV program, road following demonstrations were performed. Phase 1 has demonstrated the feasibility of real-time autonomous navigation. It has seen the development of a test vehicle, laboratory and instrumented tests areas, the dissemination of data to researchers, the development of a flexible real-time hardware and software architecture, and the development of several workable approaches to real-world, real-time vision, and route and path planning. Open research issues include terrain classification and real-time segmentation techniques for images, the use of additional sensors, such as FLIR and MMW, to augment video and laser radar data, the recognition of objects, and passive ranging techniques such as motion or binocular stereo. Author

N89-24835# Sandia National Labs., Albuquerque, NM.
DEVELOPMENT OF A MAN-PORTABLE CONTROL UNIT FOR A TELEOPERATED LAND VEHICLE Abstract Only **c37**
Douglas E. McGovern and Shannon V. Spires *In* Tactical Weapons Guidance and Control Information Conference on Space and Military Applications of Automation and Robotics Jun. 1988 p 30 (For primary document see N89-24819 18-63)
Avail: NTIS HC A05/MF A01 CSCL 09B

A man-portable control unit was designed and fabricated to support teleoperation of a land vehicle. The basic control unit is configured to include the capabilities of mobile platform control, platform location and status display, sensor control and sensor output display, and weapons control, is so desired. When the platform is being driven to a new location, the operator must be able to control the platform through basic steering, braking and speed commands, obstacle recognition and avoidance, maneuvering in constricted space, and navigation with visual cues and simple dead-reckoning inputs from the vehicle. While the platform is on station, the human operator is to be able to perform the functions of surveillance, target recognition, target tracking, and weapons or designator control. A fully software-driven system was configured to meet these requirements. The man-portable control unit was developed for application to the Teleoperated Mobile Antiarmor Platform (TMAP) project. The control unit was integrated with the MICOM vehicle system and a vehicle system at Scandia National Labs. Author

N89-24836# Air Force Inst. of Tech., Wright-Patterson AFB, OH.
ROBOTIC VISUAL SERVO CONTROL FOR AIRCRAFT GROUND REFUELING Abstract Only **c37**
Mikel M. Miller, Michael B. Leahy, Jr., and Matthew Habrisky *In* Tactical Weapons Guidance and Control Information Conference on Space and Military Applications of Automation and Robotics Jun. 1988 p 31 (For primary document see N89-24819 18-63)
Avail: NTIS HC A05/MF A01 CSCL 09B

Advances in robotic and sensor technologies open opportunities for applications of robotic systems. One potential application is

the robotic refueling of aircraft. Three basic areas of research are required to accomplish robotic refueling better robotic control, visual servoing, and force control. The design and integration of visual servoing are being researched. Visual information received from a TV camera mounted to the robot refueler's boom provides the feedback data necessary for employing visual servo control techniques. The feedback data is used to visually guide the robot refueler to the refueling port. The vision-robot system (VRS), composed of a PUMA 560 robot arm and Machine Intelligence Corporation vision system, scans an area until the vision system acquires the target. Once located, the visual servo controller guides the VRS to the target. The visual servo control techniques were implemented using the PUMA 560's Val 2 programming language. Results successfully demonstrate the VSR's ability to search for a well-defined target in a noncomplex environment, and use visual servo control techniques to guide the VRS to the target. Author

N89-24837# Stevens Inst. of Tech., Hoboken, NJ. Dept. of Mechanical Engineering.
INSERTION WITH TWO COORDINATED ARMS Abstract Only **c37**
Frederic L. Swern and Stephen J. Tricamo *In* Tactical Weapons Guidance and Control Information Conference on Space and Military Applications of Automation and Robotics Jun. 1988 p 38 (For primary document see N89-24819 18-63)
Avail: NTIS HC A05/MF A01 CSCL 09B

Much work was done on the assembly of parts requiring implementation of a peg in the hole procedure using a single robotic manipulator guided by a force/torque transducer mounted near its end effector. In tasks such as the assembly of large structures, it may not be feasible for the object to be manipulated by a single robot. Two (or more) robots can more easily share the load and provide accurate end point guidance for parts mating. Force/torque sensing at each robot can support three required functions: load balancing, relief of constraint forces and insertion guidance. It is shown how information from the sensors is divided into feedback signals for the three functions in a stable manner, and gives a design example of such a system, including simulation results. Author

N89-24838*# National Aeronautics and Space Administration. Marshall Space Flight Center, Huntsville, AL.
ORBITAL MANEUVERING VEHICLE (OMV) REMOTE SERVICING KIT Abstract Only **c18**
Norman S. Brown *In* Tactical Weapons Guidance and Control Information Conference on Space and Military Applications of Automation and Robotics Jun. 1988 p 39 (For primary document see N89-24819 18-63)
Avail: NTIS HC A05/MF A01 CSCL 22B

With the design and development of the Orbital Maneuvering Vehicle (OMV) progressing toward an early 1990 initial operating capability (IOC), a new era in remote space operations will evolve. The logical progression to OMV front end kits would make available in situ satellite servicing, repair, and consummables resupply to the satellite community. Several conceptual design study efforts are defining representative kits (propellant tanks, debris recovery, module servicers); additional focus must also be placed on an efficient combination module servicer and consummables resupply kit. A remote servicer kit of this type would be designed to perform many of the early maintenance/resupply tasks in both nominal and high inclination orbits. The kit would have the capability to exchange Orbital Replacement Units (ORUs), exchange propellant tanks, and/or connect fluid transfer umbilicals. Necessary transportation system functions/support could be provided by interfaces with the OMV, Shuttle (STS), or Expendable Launch Vehicle (ELV). Specific remote servicer kit designs, as well as ground and flight demonstrations of servicer technology are necessary to prepare for the potential overwhelming need. Ground test plans should adhere to the component/system/breadboard test philosophy to assure maximum capability of one-g testing. The flight demonstration(s) would most likely be a short duration, Shuttle-bay experiment to validate servicer components requiring a micro-g environment. Author

N89-24839# Olis Engineering, Sedalia, CO.
INFLATABLE END EFFECTOR TOOLS Abstract Only **c37**
Carter K. Lord *In* Tactical Weapons Guidance and Control Information Conference on Space and Military Applications of Automation and Robotics Jun. 1988 p 40 (For primary document see N89-24819 18-63)
Avail: NTIS HC A05/MF A01 CSCL 09B

Two variations of inflatable end effector tools were developed. The primary purpose of developing this technology was to provide the capability of grasping delicate composite structural components for assembly of large structures in space. Several other benefits of this system became apparent during the course of the development effort. The inflatable end effector tools utilize controlled air pressure to inflate a bladder of two distinctive configurations to provide the grasping force. Grasping force can, therefore, be predetermined and set simply by controlling the maximum air pressure for that particular operation. Removal of the air pressure from the system deflates the bladder, releasing the item being grasped and establishing a clearance situation for repositioning of the manipulator. Advantages of the system include simplicity, compliance, variable grasping force capability, absence of point contact loads and cost. The principal disadvantage of the simpler cylindrical probe variation is the requirement for a specified diameter hole in each item to be handled. This handling point requirement is minimal, however, and many items may be handled with this configuration without modification. The telescoping probe variation does not require a specific handling point, and is therefore most versatile, although somewhat more complex. Both variations of inflatable end effector tools are currently being fabricated for testing and evaluation on the Proto-Flight Manipulator Arm.
Author

N89-24840# Honeywell, Inc., New Brighton, MN.
ROBOT ASSEMBLY OF MICROSCOPIC COMPONENT IN MILLIMETER WAVE DEVICES Abstract Only **c37**
Steven R. Prokosch *In* Tactical Weapons Guidance and Control Information Conference on Space and Military Applications of Automation and Robotics Jun. 1988 p 43 (For primary document see N89-24819 18-63)
Avail: NTIS HC A05/MF A01 CSCL 09B

A robotic system was developed to perform delicate component assembly operations which are critical to the volume production of millimeter wave transceivers. The system consists of precision robotic devices which are guided by an integrated machine vision system to acquire, orient, and assemble gallium arsenide beam leaded components to a duroid substrate. Assembly is accurate to within + or - .001 inch of a location defined by the microstrip artwork of the transceiver circuit. Component size is .008 inch wide by .025 inch long, including beam leads. A vacuum pick up tool was developed to manipulate the components. The tool does not touch the delicate gallium arsenide chip during the operation and does not apply over three grams of force to the component at any time. The components are held in position on the substrate by the tool while they are bonded to the substrate by an integrated laser soldering system. Author

N89-24841# Honeywell, Inc., Minnetonka, MN. Defense Systems Group.
AUTOMATED MILLIMETER WAVE (AMW) TRANSDUCER TESTING IN A ROBOTIC/VISION TEST CELL Abstract Only **c33**
Mark Francis *In* Tactical Weapons Guidance and Control Information Conference on Space and Military Applications of Automation and Robotics Jun. 1988 p 44 (For primary document see N89-24819 18-63)
Avail: NTIS HC A05/MF A01 CSCL 09B

Issues associated with testing millimeter wave (MMW) tranducers, Ka-band, in high volume production are addressed. The issues include tuning/testing the MMW transducer by trimming the conduction pads using a transfer mechanism tied into a laser trim and vision system, for center frequency; testing the RF parameters and matching the transceiver to a signal processor; and interfacing all elements of the test cell through the use of

robotics. The MMW transducer includes transmitter, receiver, and a MMW planar antenna. Key elements that affect testing MMW transducers in high volume production are the ability to interface the MMW transducer through the use of interconnects and testing methods because of the frequency range, Ka-band; trimming the conductor pads with the laser without damaging the substrate; and cycle time of different stations within the robotic test cell. A Manufacturing Methods and Technology (MM and T) project is defined that has addressed the issues and transitioned the testing of MMW transducers from the lab into high volume production using robotics, lasers, and state-of-the-art test techniques. The MM and T automated testing of MMW transducers allows the flexibility to test up to 75,000 MMW transceivers in high volume production. Author

N89-24842# Army Missile Command, Redstone Arsenal, AL.
DEVELOPMENT OF AN INTEGRATED CAD/CAM SYSTEM FOR WIRE HARNESS FABRICATION Abstract Only **c61**
J. M. Anderson, J. I. Locker, T. D. Morgan, L. J. Frederick, and C. D. Minor *In* Tactical Weapons Guidance and Control Information Conference on Space and Military Applications of Automation and Robotics Jun. 1988 p 46 Prepared in cooperation with Alabama Univ., Huntsville (For primary document see N89-24819 18-63)
Avail: NTIS HC A05/MF A01 CSCL 09B

The development of an integrated CAD/CAM system for wire harness fabrication is described. The Computer Integrated Manufacturing (CIM) system is based upon a desktop AutoCad Computer Aided Design workstation and MICOM's Robotized Wire Harness Assembly System (RWHAS). The CIM system extracts and processes information from a Computer Aided Wire Harness Design file to generate the input file for the RWHAS Executive Controller. The data is transferred to the RWHAS CAM system via a RS-232 interface. The RWHAS then manufactures the harness. Author

N89-24843# Tech-U-Fit Corp., Alexandria, VA.
TESTING THE FEASIBILITY OF USING A TELEOPERATED ROBOT FOR REMOTE, DEXTEROUS OPERATIONS Abstract Only **c37**
John A. Molino and Linda J. Langley *In* Tactical Weapons Guidance and Control Information Conference on Space and Military Applications of Automation and Robotics Jun. 1988 p 48 (For primary document see N89-24819 18-63)
Avail: NTIS HC A05/MF A01 CSCL 09B

The feasibility of using a teleoperated robot to perform certain procedures associated with nuclear test facilities and space station operations was assessed. Only the space station procedure is reported. The teleoperated robot being evaluated was the Central Research Laboratories' SAMSIN servomanipulator. This device is a seven degrees-of-freedom master/slave remote manipulator with bilateral reflected-force feedback. The ratio of slave/master reflected-force feedback could be varied so that either x:0 (none), 4:1 (moderate), or 1:1 (realistic) amounts of reflected force were experienced by the operator. Visual feedback was by means of 3 closed-circuit television monitors. Twenty-eight novice operators were trained to execute the following simulated space station tasks with the SAMSIN teleoperated robot: disassemble and reassemble a space station truss node. This task was accomplished along with four other nuclear-related tasks. The results proved the feasibility of using a teleoperated robot with a person in the loop to perform a simulated space station-related task. Total system performance (machines, people, training, and procedure) was demonstrated for this truss node operation. Author

N89-24844# Rockwell International Corp., Downey, CA.
ORU GUIDELINES FOR TELEROBOTIC COMPATIBILITY Abstract Only **c37**
Margaret M. Clarke and Davoud Manouchehri *In* Tactical Weapons Guidance and Control Information Conference on Space and Military Applications of Automation and Robotics Jun. 1988 p 49 (For primary document see N89-24819 18-63)
Avail: NTIS HC A05/MF A01 CSCL 09B

Design guidelines are being developed for remotely maintainable Orbital Replacement Units (ORUs) for on-orbit payloads. The quantity, complexity, and cost of on-orbit payloads will increase significantly over the next few years. These payloads will need service and maintenance as their ORUs need resupply or replacement. On-orbit maintenance can be performed by an extra vehicular activity (EVA) astronaut or by telerobotic devices. NASA and the Department of Defense are interested in concepts for ORU standardization so that payloads can be efficiently serviced by telerobotic devices. A three-step approach was followed in developing guidelines for remotely servicable ORUs: telerobotic concepts; ORU concepts and guidelines; and laboratory verification. During step one, a concept was developed for a telerobotic device capable of performing remote maintenance on a wide variety of ORUs. The concept included reach, degrees of freedom, speed and mass handling capability, and end effector description. During step two, specific guidelines were established for ORU compatibility with such a telerobotics device, including descriptions of fasteners; latches; fluid, electric, and fiber optic connectors; racks; and packaging. During step three, hard mockups were fabricated of several types of ORUs for example, standard data processor black boxes. The boxes were then successfully changed out in the Rockwell Automation and Robotics (A/R) Facility using a seven degree of freedom master/slave telerobotic device and television writing. Author

N89-24845# Teledyne Brown Engineering, Huntsville, AL.
GROUND CONTROL OF SPACE BASED ROBOTIC SYSTEMS Abstract Only **c37**
K. E. Farnell and S. F. Spearing *In* Tactical Weapons Guidance and Control Information Conference on Space and Military Applications of Automation and Robotics Jun. 1988 p 50 (For primary document see N89-24819 18-63)
Avail: NTIS HC A05/MF A01 CSCL 09B

The ability to control robotics in space is clearly an established art with the success of numerous unmanned space probes by both the U.S. and the U.S.S.R. However, these vehicles, such as the Lunakhod and Voyager, were designed to perform discrete functions, and months and years of analysis and programming were required to confidently accomplish even simple planned functions. With the advent of Space Station operations, there will be many instances where robotics will be needed to respond quickly to variable sets of environmental parameters. A system for ground control of space robotic systems is presented and the various control paradigms and operational modes are discussed. The safety aspects, operational constraints and design considerations for robotics operation in a manned environment are discussed. Author

N89-24846# Vanderbilt Univ., Nashville, TN.
A GENERALIZED METHOD FOR AUTOMATIC DOWNHAND AND WIREFEED CONTROL OF A WELDING ROBOT AND POSITIONER Abstract Only **c37**
Ken Fernandez and George E. Cook *In* Tactical Weapons Guidance and Control Information Conference on Space and Military Applications of Automation and Robotics Jun. 1988 p 54 (For primary document see N89-24819 18-63)
Avail: NTIS HC A05/MF A01 CSCL 09B

A generalized method is described for controlling a six degree-of-freedom (DOF) robot, a two DOF robot, and a two DOF positioner used for arc welding operations. The welding path is defined in the part reference frame, and robit/positioner joint angles of the equivalent eight DOF serial linkages are determined via an iterative solution. Three algorithms are presented. The first solution controls motion of the eight DOF mechanism such that proper torch motion is achieved while minimizing the sum-of-squares of joint displacements. The second algorithm adds two constraint equations to achieve torch control while maintaining part orientation so that welding occurs in the down hand position. The third algorithm adds the ability to control the proper orientation of a wire feed mechanism used in gas tungsten arc (GTA) welding operations. A verification of these algorithms is given using

ROBOSIM, a NASA-developed computer graphic simulation software package designed for robotic systems development. Author

N89-24847# Martin Marietta Labs., Baltimore, MD. Artificial Intelligence Group.
ON DESIGNING A CASE-BASED SYSTEM FOR EXPERT PROCESS DEVELOPMENT Abstract Only
Seraj Bharwani, J. T. Walls, and M. E. Jackson *In* Tactical Weapons Guidance and Control Information Conference on Space and Military Applications of Automation and Robotics Jun. 1988 p 55-57 Prepared in cooperation with Martin Marietta Corp., Huntsville, AL (For primary document see N89-24819 18-63)
Avail: NTIS HC A05/MF A01 CSCL 09B

In artificial intelligence literature, using prior experience to help solve new problem situations is termed case-based reasoning. Using case-based reasoning was proposed for learning new concepts in mathematics, for clinical problem solving, for settling legal issues based on common law, and for interpreting and resolving common sense disputes. The need for such reasoning in preforming process development tasks was discussed. In particular, the significance of compiling case histories to capture critical process knowledge and the methods of compiling and reasoning with such histories to reduce process development time and enhance its reliability were described. This approach is especially useful in situations where existing processes are modified in response to frequent product changes or when processes developed for a prototype operation have to be ported to production systems. Author

N89-24848# Army Missile Command, Redstone Arsenal, AL.
A 3-D GRAPHICAL SIMULATION OF AN AUTOMATED DIRECT CHIP PROBE/TEST SYSTEM Abstract Only **c61**
D. C. Holderfield, T. D. Morgan, B. E. Martin, and J. R. Facemire *In* Tactical Weapons Guidance and Control Information Conference on Space and Military Applications of Automation and Robotics Jun. 1988 p 61 Prepared in cooperation with Alabama Univ., Huntsville (For primary document see N89-24819 18-63)
Avail: NTIS HC A05/MF A01 CSCL 09B

The development of a 3-D graphical simulation of MICOM's Direct Chip Probe/Test (DCP/T) system is described. The DCP/T system is an automated test machine that performs full dynamic electrical testing under thermal stress on integrated circuit dies. These tests are necessary to insure that the die passes military specifications. The simulation was developed using the MCAUTO robotic simulation software package and an Evans and Sutherland graphic workstation. The simulation was used to verify DCP/T mechanical and dynamical operating parameters and to assist in the design of a second generation DCP/T system. Author

N89-24849*# Alabama Univ., Huntsville.
USING A SIMULATION ASSISTANT IN MODELING MANUFACTURING SYSTEMS Abstract Only **c37**
Bernard J. Schroer, Fan T. Tseng, S. X. Zhang, and John W. Wolfsberger *In* Tactical Weapons Guidance and Control Information Conference on Space and Military Applications of Automation and Robotics Jun. 1988 p 62 Prepared in cooperation with NASA. Marshall Space Flight Center, Huntsville, AL (For primary document see N89-24819 18-63)
Avail: NTIS HC A05/MF A01 CSCL 13I

Numerous simulation languages exist for modeling discrete event processes, and are now ported to microcomputers. Graphic and animation capabilities were added to many of these languages to assist the users build models and evaluate the simulation results. With all these languages and added features, the user is still plagued with learning the simulation language. Futhermore, the time to construct and then to validate the simulation model is always greater than originally anticipated. One approach to minimize the time requirement is to use pre-defined macros that describe various common processes or operations in a system. The development of a simulation assistant for modeling discrete event manufacturing processes is presented. A simulation assistant is defined as an interactive intelligent software tool that assists the modeler in writing a simulation program by translating the modeler's symbolic description of the problem and then automatically generating the corresponding simulation code. The simulation assistant is discussed with emphasis on an overview of the simulation assistant, the elements of the assistant, and the five manufacturing simulation generators. A typical manufacturing system will be modeled using the simulation assistant and the advantages and disadvantages discussed. Author

N89-24850# Alabama Univ., Huntsville. Applied Optics Center.
ALGORITHM FOR DISPLAY OF AUTOMATED NONDESTRUCTIVE THICKNESS MEASUREMENTS Abstract Only **c37**
Jeroen vanderZijp *In* Tactical Weapons Guidance and Control Information Conference on Space and Military Applications of Automation and Robotics Jun. 1988 p 63 (For primary document see N89-24819 18-63)
Avail: NTIS HC A05/MF A01 CSCL 09B

Automating the manufacturing processes in any environment, whether it is a complex aerospace structure or a simple mechanical part, requires defining normal human judgments such that computer-based processing can perform the same function. In automating robotics installations, there is a need for defining contours which are representative of some physical feature of the object of interest. Ordinarily these operations are considered in terms of machine vision operations. The work presented demonstrates the use of such technology for defining thickness measurements obtained through robotic ultrasonic scanning of aerospace components. Author

N89-24851# KMS Fusion, Inc., Ann Arbor, MI.
A ROBOTIC VEHICLE GLOBAL ROUTE PLANNER FOR THE 1990s Abstract Only
William J. Pollard *In* Tactical Weapons Guidance and Control Information Conference on Space and Military Applications of Automation and Robotics Jun. 1988 p 65 (For primary document see N89-24819 18-63)
Avail: NTIS HC A05/MF A01 CSCL 09B

During the 1990s, automated global route planners will take over labor intensive and hazardous tasks vehicles are asked to accomplish. The U.S. military has already designated up to 40 vehicle missions to be accomplished by automated vehicles. In addition to the military, industry is also looking for automated vehicles to perform automated movement tasks. Thus the need is clearly established, and contracts for these vehicles are continually being awarded. Vehicles designed to perform these tasks must have a global route planner that chooses the route the vehicle is to traverse. Also aboard the vehicle there must be a navigation system that confirms that the vehicle is following the desired path. While the military applications of this technology is generally off-road, the objective is to gradually move this technology to the civilian arena for the guidance of automobiles and trucks on the national highways. Also described are the data base inputs required by the global route planner, the difficulties associated with moving from off-road to on-road operation, features that should be incorporated into the driver-machine interface/display, and the requirements on the navigation system, including a summary of potential system candidates. Author

N89-24852# Sandia National Labs., Albuquerque, NM.
A DEMONSTRATION OF RETRO-TRAVERSE USING A SEMI-AUTONOMOUS LAND VEHICLE Abstract Only **c37**
Douglas E. McGovern, Paul R. Klarer, and David P. Jons *In* Tactical Weapons Guidance and Control Information Conference on Space and Military Applications of Automation and Robotics Jun. 1988 p 66 (For primary document see N89-24819 18-63)
Avail: NTIS HC A05/MF A01 CSCL 09B

A Jeep Cherokee was modified to allow remote control either by teleoperation or through computer driven commands (autonomy). This Jeep was used in the development of hardware, software, and application concepts for use of computer augmentation of remote controlled vehicles. As part of this development, a system

was configured which allows an operator to teleoperate the vehicle from one location (home base) to another (destination). At the completion of teleoperation, the operator can instruct the vehicle to return to the starting position. The vehicle then autonomously performs a retro-traverse, reversing the path by which it reached its destination. During teleoperation, operator commands are given through an operator control interface consisting of a steering wheel, brake and throttle pedals, and a video display. Commands are transmitted to the vehicle and video returned from the vehicle over RF communication links. Significant way points are identified by the operator for later use by the vehicle systems. Navigation during retro-traverse utilizes dead-reckoning inputs from steering angle encoder, odometer, and compass. Way points are linked by straight line segments. At each way point, the system determines the steering and speed commands necessary to reach the next way point in the stored path. Retro-traverse was demonstrated over open terrain. Path following accuracy and final positional control is a function of dead-reckoning system limitations. These limitations are discussed and a system utilizing improved navigation is proposed. Author

N89-24853# KMS Fusion, Inc., Ann Arbor, MI.
A KNOWLEDGE REPRESENTATION SCHEME FOR A ROBOTIC LAND VEHICLE ROUTE PLANNER Abstract Only
c37

Patrick J. McNally *In* Tactical Weapons Guidance and Control Information Conference on Space and Military Applications of Automation and Robotics Jun. 1988 p 68 (For primary document see N89-24819 18-63)
Avail: NTIS HC A05/MF A01 CSCL 09B

Knowledge representation schemes used on the Prototype Global Route Planner Project are described. The ultimate objective is to develop a military robotic vehicle route planner for missions covering several to tens of kilometers. Current efforts in vehicle mobility modeling and terrain data representation are discussed. Direct correlation between vehicle mobility characteristics and available terrain data is required for accurate mobility prediction. A combined approach using the Cross-Country Movement (CCM) model of DMA and expert derived knowledge represented in an object-based artificial intelligence model is explained. Likewise, vulnerability of a potential route is assessed during the planning activity using basic threat algorithms combined with expert-derived knowledge represented in an object-based artificial intelligence model. Trafficability and vulnerability considerations are weighted appropriately by the mission objective models, also derive through expert consultation. Finally, problems encountered with current terrain databases, mobility models, and representation schemes are discussed. Author

N89-24854# Sparta, Inc., Huntsville, AL.
IRIS: AN INTELLIGENT ROBOT INSERTION EXPERT SYSTEM Abstract Only
c37

William Teoh *In* Tactical Weapons Guidance and Control Information Conference on Space and Military Applications of Automation and Robotics Jun. 1988 p 69 (For primary document see N89-24819 18-63)
Avail: NTIS HC A05/MF A01 CSCL 09B

Teleoperated manipulators working in an unstructured environment can perform a variety of tasks. Most maneuvers are, however, similar to the classical peg-in-the-hole problem in that the manipulator must be put in the proper position and orientation prior to completing the task. Typical examples include inserting parts, connecting couplers, and opening drawers. To maneuver the manipulator to the desirable position and orientation by teleoperation is nontrivial, and requires considerable operator training. The possibility of exploiting artificial intelligence technology to tackle this problem is examined. IRIS is a prototype expert system that provides a solution to the peg-in-the-hole problem. The expert system can successfully dock the robot with a hole in the taskboard, thereby completing the insertion process. IRIS is a rule-based, data driven, forward chaining expert system. Two sensors are required to provide input to the system: a vision system that can discern the taskboard and the hole, and a ranging sensor that provides the range information. Preliminary investigation demonstrated that as long as the taskboard is placed within the work envelope in some reasonable orientation, the system can complete the mission successfully. Author

N89-24855# Army Missile Command, Redstone Arsenal, AL. Aeroballistics Analysis Branch.
PEDAGOGICAL ISSUES IN DEVELOPING A MAN-MACHINE INTERFACE FOR AN INTELLIGENT TUTORING SYSTEM Abstract Only

Willard M. Holmes *In* Tactical Weapons Guidance and Control Information Conference on Space and Military Applications of Automation and Robotics Jun. 1988 p 70 (For primary document see N89-24819 18-63)
Avail: NTIS HC A05/MF A01 CSCL 09B

The use of expert and knowledge based systems have not always met with the success in the user environment as promised or expected during the development and operation in the laboratory environment. Research has shown that several specific factors have contributed to the less than expected use and performance of expert systems when placed in the user environment. A major factor is the Man-Machine Interface (MMI) associated with the delivery systems. In many instances, the MMI function was considered only after the basic structure of the expert was established and the methodology for expert operation was demonstrated. In cases with the most reduced user acceptance are instances where the MMI function was added on after the major development effort was completed or an existing interface was expanded to meet expected user requirements. In short, the user friendliness promised or required for effective operation of the expert system in the user environment was not delivered. As knowledge based systems expand in complexity and achieve extended operation in the user environments, the MMI function becomes a major issue in developing effective and usable systems. A case in point is the MMI needs associated with an effective Intelligent Tutoring System. Reported are the results of an early research effort on major MMI issues associated with developing an Intelligent Tutoring System. The student interface or MMI is included as a major sub-element of the tutoring system and is considered an integral part of the system during development assessment of user needs. Author

N89-24856*# National Aeronautics and Space Administration. Lewis Research Center, Cleveland, OH.
NEUROMORPHIC LEARNING OF CONTINUOUS-VALUED MAPPINGS IN THE PRESENCE OF NOISE: APPLICATION TO REAL-TIME ADAPTIVE CONTROL

Terry Troudet (Sverdrup Technology, Inc., Cleveland, OH.) and Walter C. Merrill 1989 14 p Presented at the International Conference on Neural Networks, Washington, DC, 18-22 Jun. 1989; sponsored by the IEEE
(NASA-TM-101999; E-4706; NAS 1.15:101999) Avail: NTIS HC A03/MF A01 CSCL 09B

The ability of feed-forward neural net architectures to learn continuous-valued mappings in the presence of noise is demonstrated in relation to parameter identification and real-time adaptive control applications. Factors and parameters influencing the learning performance of such nets in the presence of noise are identified. Their effects are discussed through a computer simulation of the Back-Error-Propagation algorithm by taking the example of the cart-pole system controlled by a nonlinear control law. Adequate sampling of the state space is found to be essential for canceling the effect of the statistical fluctuations and allowing learning to take place. Author

N89-24857# Japan Atomic Energy Research Inst., Tokyo. Dept. of Reactor Engineering.
REPRESENTATIONS OF A LINKAGE MECHANISM BASED ON DUAL NUMBER MATRICES

Shinobu Sasaki Dec. 1988 19 p In JAPANESE; ENGLISH summary
(DE88-757273; JAERI-M-88-243) Avail: NTIS (US Sales Only) HC A03/MF A01

In this paper, the kinematics problem of robot manipulators is discussed from a viewpoint of developing a new analytical technique using a concept based on a dual number algebra. Concerning its formulation, 3 x 3 orthogonal matrices of dual number elements with a complete description of link geometry are first introduced and simple multiplication operations are sequentially performed to obtain kinematic equations. In the application process to a six-link manipulator, an expedient idea was especially effective to lighten the burden of formulation complexity involved in the last computational step. The major advantage of the present method is the capability to determine at the same time both spacial position and orientation of manipulator hand irrespective of 3 x 3 matrix operations. DOE

N89-24858# Rutgers - The State Univ., New Brunswick, NJ. Center for Expert Systems Research.
EMPIRICAL ANALYSIS AND REFINEMENT OF EXPERT SYSTEM KNOWLEDGE BASES Quarterly Report
Sholom M. Weiss and Casimir A. Kulikowski 28 Feb. 1989 23 p
(Contract N00014-87-K-0398)
(AD-A206226) Avail: NTIS HC A03/MF A01 CSCL 12/9

Classification methods from statistical pattern recognition, neural nets, and machine learning were applied to four real-world data sets. Each of these data sets has been previously analyzed and reported in the statistical, medical, or machine learning literature. The data sets are characterized by statistical uncertainty; there is no completely accurate solution to these problems. Training and testing or resampling techniques are used to estimate the true error rates of classification methods. Detailed attention is given to the analysis of performance of the neural nets using back propagation. For these problems, which have relatively few hypotheses and features, the machine learning procedures for rule induction or tree induction clearly performed best. GRA

N89-24859# Air Force Inst. of Tech., Wright-Patterson AFB, OH. School of Engineering.
FRACTIONAL-ORDER FEEDBACK IN LINEAR SYSTEMS M.S. Thesis
Kevin D. Klonoski Mar. 1989 223 p
(AD-A206241; AFIT/GA/ENY/88D-05) Avail: NTIS HC A10/MF A01 CSCL 09/1

Three methods of producing the fractional derivative or integral of an input signal are investigated. The method selected employs a circuit developed at Trent University, Ontario, Canada for use in electrochemistry research. The results presented show the circuit accurately differentiates a sinusoidal input for a frequency range spanning 0.01 Hz to 10.0 Hz. The second-order differential equation above is simulated on an analog computer. An optimal u(t) is then used for feedback modification of the original open-loop system. Improved system performance resulted. A Laplace transform method and a Mittag-Leffler expansion provide analytical predictions of the system's response. The output of the two methods is identical. Comparison of the theoretical predictions with the experimental data shows the excellent agreement with respect to the initial transient behavior and asymptotic behavior of the steady-state response for both the open- and closed-loop systems. GRA

N89-24860# SRI International Corp., Menlo Park, CA. Artificial Intelligence Center.
A DEDUCTIVE APPROACH TO AUTOMATED PLANNING Final Report
Richard J. Waldinger Feb. 1989 41 p
(Contract N00014-84-C-0706; SRI Proj. PRU-7784)
(AD-A206253) Avail: NTIS HC A03/MF A01 CSCL 12/9

The principal goal of this project is to apply techniques from automated deduction to programs in real-world and robotic planning and the synthesis of imperative programs. Expected benefits include a reduction in the human effort required to develop complex plans and programs, a reduction in the error-rate associated with planning and programming, and an increase in the ease of modifying existing plans and programs to accommodate to changes in purpose and environment. In this document problems in commonsense and robot planning are approached by methods adapted from program synthesis research; planning is regarded as an application of automated deduction. To support this approach, the authors introduce a variant of situational logic, called plan theory, in which plans are explicit objects. A machine-oriented deductive-tableau inference system is adapted to plan theory. Equations and equivalences of the theory are built into a unification algorithm for the system. Frame axioms are built into the resolution rule. Special attention is paid to the derivation of conditional and recursive plans. Inductive proofs of theorems for even the simplest planning problems, such as clearing a block, have been found to require challenging generalizations. GRA

N89-24861# Oak Ridge National Lab., TN. Instrumentation and Controls Div.
A COMPARISON OF TWO REAL-TIME CONTROL SCHEMES FOR REDUNDANT ROBOTS WITH BOUNDED JOINT VELOCITIES
J. A. Euler, R. V. Dubey (Tennessee Univ., Knoxville.), S. M. Babcock, and W. R. Hamel 1989 16 p Presented at the International Conference on Robotics and Automation, Scottsdale, AZ, 14 May 1989
(Contract DE-AC05-84OR-21400)
(DE89-002974; CONF-890522-5) Avail: NTIS HC A03/MF A01

A comparison of two real-time control schemes for redundant robots is presented. Both schemes are developed in the framework of resolved rate control, and were presented by the authors in earlier articles. The first scheme is the gradient projection scheme, which determines only the direction of the self motion for the optimization of a scalar performance criterion. The second scheme determines the direction as well as the magnitude of the self motion. However, when the magnitude of the self motion is limited by the hardware bounds on joint velocities, the results obtained using the two schemes are remarkably similar when the computational frequency is high (above 100 Hz). Therefore, the gradient projection scheme, which is computationally more efficient, is recommended. An explanation for the similarity of results is presented. Scheme 1 was implemented in real-time on a Motorola 68020 VME bus-based controller of the seven-degree-of-freedom manipulator at the Center for Engineering Systems Advanced Research (CESAR). DOE

N89-24393# Dortmund Univ. (Germany, F.R.). Inst. fuer Roboterforschung.
HIERARCHICALLY STRUCTURED CONTROL FOR INTELLIGENT ROBOTS IN SPACE
E. Freund *In* ESA, International Symposium on Europe in Space: The Manned Space System Oct. 1988 p 515-522 (For primary document see N89-24335 18-12)
Copyright Avail: NTIS HC A99/MF A01; ESA Publications Div., ESTEC, Noordwijk, Netherlands, 80 Dutch guilders

64 NUMERICAL ANALYSIS

Includes iteration, difference equations, and numerical approximation.

N89-24862# Wisconsin Univ., Madison. Center for Mathematical Sciences.
PERIODIC AND HETEROCLINIC ORBITS FOR A PERIODIC HAMILTONIAN SYSTEM Technical Summary Report
Paul H. Rabinowitz Jul. 1988 22 p
(Contract DAAL03-87-K-0043; AF-AFOSR-0202-87)
(AD-A204078; CMS-TSR-89-3) Avail: NTIS HC A03/MF A01 CSCL 12/2

The existence of multiple periodic solutions of second order Hamiltonian systems are studied which are both forced periodically in time and depend periodically on the dependent variables. Consider the Hamiltonian system: q(double dot) + V' (q) = 0 where q = (q(1),....,q(n)) and V is periodic in q sub i, 1 less than or = i less than or = n. It is known the the equation then

possesses at least n + 1 equilibrium solutions. One can: (1) can give criteria for V so that the equation has non-constant periodic solutions, and (2) prove the existence of multiple heteroclinic orbits joining maxima of V. GRA

N89-24863# Wisconsin Univ., Madison. Center for Mathematical Sciences.
THE EXACT CONDITION OF THE B-SPLINE BASIS MAY BE HARD TO DETERMINE Technical Summary Report
Carl DeBoor Jul. 1988 15 p
(Contract DAAL03-87-K-0030; NSF DMS-87-01275)
(AD-A204080; CMS-TSR-89-1) Avail: NTIS HC A03/MF A01 CSCL 12/1

The author's conjecture concerning the knot sequence whose associate B-spline sequence has maximum max-norm condition number is disproved. Related condition numbers are explored and the corresponding conjecture concerning the worst knot sequence for them is further supported by numerical results. There is numerical evidence that, in calculations devoted to bounding the p-norm condition number of the (appropriately scaled) B-spline basis, the extreme case occurs for a knot sequence without interior knots, while simple numerical examples show this not to be the case for the max-norm condition number itself. This is disappointing since it is only in the latter case that there seems to be a formula available for the condition number when there are no interior knots. Hence, even if the worst-case conjecture for the bound calculations for the p-norm condition number were proved, it would, offhand, not help in settling the problem of interest. GRA

N89-24864# Wisconsin Univ., Madison. Center for Mathematical Sciences.
LOCAL CORNER CUTTING AND THE SMOOTHNESS OF THE LIMITING CURVE Technical Summary Report
Carl deBoor Nov. 1988 11 p
(Contract DAAL03-87-K-0030; NSF DMS-87-01275)
(AD-A204092; CMS-TSR-89-18) Avail: NTIS HC A03/MF A01 CSCL 12/1

It was proved in an earlier de Boor work that corner cutting of any kind converges to a Lipschitz-continuous curve, but the question of how one might guarantee that the limiting curve be smoother than that was not considered there. Recently, Gregory and Qu (GQ) took up this question and established sufficient conditions for a certain systematic and local corner cutting scheme to give a limiting curve in C. Since GQ use the same parametrization of the successive broken lines that made the earlier de Boor argument so simple, I became intrigued and took a look at what one might say in greater generality. Specifically, I looked for conditions under which continuous differentiability of the limiting curve could be inferred from the fact that the corners of the broken lines flatten out eventually. It is the purpose of this note to prove that the limit of any local corner cutting scheme is in C provided the corners of the broken lines become increasingly flatter. A simple example is given to show that this condition is not necessary, while another simple example shows that, without localness, the condition is not sufficient, in general. Finally, as an application, Gregory and Qu's nice argument in GQ is redone. GRA

N89-24865*# National Aeronautics and Space Administration. Lewis Research Center, Cleveland, OH.
ON THE EQUIVALENCE OF A CLASS OF INVERSE DECOMPOSITION ALGORITHMS FOR SOLVING SYSTEMS OF LINEAR EQUATIONS
Nai-kuan Tsao (Wayne State Univ., Detroit, MI.) May 1989 28 p
(NASA Order C-99066-G)
(NASA-TM-102036; ICOMP-89-11; E-4785; NAS 1.15:102036)
Avail: NTIS HC A03/MF A01 CSCL 12A

A class of direct inverse decomposition algorithms for solving systems of linear equations is presented. Their behavior in the presence of round-off errors is analyzed. It is shown that under some mild restrictions on their implementation, the class of direct inverse decomposition algorithms presented are equivalent in terms of the error complexity measures. Author

N89-24866# Japan Atomic Energy Research Inst., Tokyo. Dept. of Reactor Engineering.
COMPUTATIONAL METHOD OF THE INVERSE KINEMATICS VIA SIMPLIFIED ALGEBRAIC EQUATION
Shinobu Sasaki Dec. 1988 19 p In JAPANESE; ENGLISH summary
(DE88-757269; JAERI-M-88-236) Avail: NTIS (US Sales Only) HC A03/MF A01

A transformation into an algebraic equation, proposed as a method of solving the inverse kinematics for a six-link manipulator, left a room for further improvement of the method due to invalid solutions arising from the properties of a high order polynomial. Following its initial concept, joint solutions have been determined by solving the 16th order polynomial derived from the original equation. This order, however, is still high enough from a viewpoint of practical use. On close examination returning to the original equation, an alternative idea occurred which is based on a factorization method in order to find out common factors. As a result, the kinematic relationships in question could be re-expressed in terms of a simple algebraic equation of the 8th order. This paper is concerned with detailed derivation process. DOE

N89-24867*# National Aeronautics and Space Administration. Langley Research Center, Hampton, VA.
NUMERICAL INTEGRATION OF ASYMPTOTIC SOLUTIONS OF ORDINARY DIFFERENTIAL EQUATIONS
Gaylen A. Thurston Apr. 1989 44 p
(NASA-TM-100650; NAS 1.15:100650) Avail: NTIS HC A03/MF A01 CSCL 12A

Classical asymptotic analysis of ordinary differential equations derives approximate solutions that are numerically stable. However, the analysis also leads to tedious expansions in powers of the relevant parameter for a particular problem. The expansions are replaced with integrals that can be evaluated by numerical integration. The resulting numerical solutions retain the linear independence that is the main advantage of asymptotic solutions. Examples, including the Falkner-Skan equation from laminar boundary layer theory, illustrate the method of asymptotic analysis with numerical integration. Author

N89-24868# Naval Postgraduate School, Monterey, CA.
SELF-CIRCUMFERENCE IN THE MINKOWSKI PLANE Technical Report, Oct. 1988 - Jan. 1989
Mostafa Ghandehari and Richard Pfiefer 23 Feb. 1989 26 p
(AD-A205691; NPS53-89-009) Avail: NTIS HC A03/MF A01 CSCL 12/1

Let delta(n) denote the self-circumference of a regular polygon with n sides. It will be shown that delta (n) is monotonically increasing from 6 to 2 pi if n is twice an odd number, and monotonically decreasing from 8 to 2 pi if n is twice an even number. Calculation of delta (n) for the case where n is odd as well as inequalities for self-circumference of some irregular polygons are given. Properties of the mixed area of a plane convex body and its polar dual are used to discuss the self-circumference of some convex curves. GRA

N89-24869# Air Force Inst. of Tech., Wright-Patterson AFB, OH. School of Engineering.
COMPARISON OF BASIS FUNCTION AND ITERATION SOLUTIONS TO THE FREDHOLM INTEGRAL EQUATION OF THE FIRST KIND M.S. Thesis
Michael E. Carter Mar. 1989 71 p
(AD-A206158; AFIT/GNE/ENP/89M-1) Avail: NTIS HC A04/MF A01 CSCL 12/1

The purpose of this thesis is to compare methods for solving the Fredholm integral equation of the first kind. The Fredholm equation has several practical applications including geology, superconductivity, and aerodynamics. Of specific interest is its application to determining radiation spectra using data from underground nuclear effects simulations. The two basic solution

methods studied were the basis function and the iteration methods. The basis function method is a representation of the unfolded spectrum by a series of Planckian or cubic spline functions. The iteration method scales the unfolded spectrum so that its weighted integral over a given interval matches that of the actual spectrum. Both basis function methods produced excellent results when the actual spectrum was a sum of it's basis functions. The cubic spline method produced unfolded spectra which were good approximations for discontinuous actual spectra. However, there was a significant dropoff of the spectrum for the cubic spline for higher energies. The iteration method produced accurate approximations for actual spectra that were both basis function and discontinuous spectra. There were two problems with this method: the unfolded spectra were discontinuous at the discontinuities of the weighting function and noisy data sometimes produced large discontinuities in the unfolded spectra. GRA

N89-24870# California Univ., Berkeley. Coll. of Engineering.
RESEARCH ON SELF-GENERATED STOCHASTIC MOTION Final Report, 1 Jun. 1984 - 30 Sep. 1988
A. J. Lichtenberg and M. A. Lieberman 30 Sep. 1988 6 p
(Contract N00014-84-K-0367)
(AD-A206454) Avail: NTIS HC A02/MF A01 CSCL 09/1

The purpose of the research under this contract was to study the processes by which stochastic motion is self-generated in deterministic systems, and the consequences of the resulting stochasticity. We consider representative problems, each of which incorporates one or more of the main underlying physical phenomena. Two classes of phenomena that we have studied under this contract are diffusion across overlapping resonances, and diffusion along resonances, in more than two degrees of freedom (Arnold and modulation diffusion). The former has been studied in considerable depth, and new insights involve the fine structure of the phase space or more exact calculations. The latter phenomena still may have many poorly understood aspects. GRA

N89-24871*# National Aeronautics and Space Administration. Ames Research Center, Moffett Field, CA.
SOME NOTES ON SHOCK RESOLVING FLUX FUNCTIONS. PART 1: STATIONARY CHARACTERISTICS
Timothy J. Barth May 1989 22 p
(NASA-TM-101087; A-89087; NAS 1.15:101087) Avail: NTIS HC A03/MF A01 CSCL 12A

Numerical flux functions for solving the Euler equations using exact and/or approximate solutions of the Riemann problem of gasdynamics are discussed. Under certain restrictive conditions, schemes using these flux functions produce systems of equations which can exhibit a single degree of freedom. In some instances, the solutions represented by this degree of freedom are unstable to perturbations. This local instability can seriously degrade the temporal convergence of numerical schemes. This point is demonstrated by numerical example. Author

N89-24872*# Michigan Univ., Ann Arbor.
A GENUINELY MULTI-DIMENSIONAL UPWIND CELL-VERTEX SCHEME FOR THE EULER EQUATIONS
Kenneth G. Powell and Bram vanLeer (National Aeronautics and Space Administration. Lewis Research Center, Cleveland, OH.) May 1989 22 p Presented at the 27th Aerospace Sciences Meeting, Reno, NV, 9-12 Jan. 1989; sponsored by AIAA Previously announced in IAA as A89-25084
(NASA Order C-99066-G)
(NASA-TM-102029; E-4772; NAS 1.15:102029; ICOMP-89-13; AIAA-89-0095) Avail: NTIS HC A03/MF A01 CSCL 12A

The solution of the two-dimensional Euler equations is based on the two-dimensional linear convection equation and the Euler-equation decomposition developed by Hirsch et al. The scheme is genuinely two-dimensional. At each iteration, the data are locally decomposed into four variables, allowing convection in appropriate directions. This is done via a cell-vertex scheme with a downwind-weighted distribution step. The scheme is conservative, and third-order accurate in space. The derivation and stability analysis of the scheme for the convection equation, and the derivation of the extension to the Euler equations are given. Preconditioning techniques based on local values of the convection speeds are discussed. The scheme for the Euler equations is applied to two channel-flow problems. It is shown to converge rapidly to a solution that agrees well with that of a third-order upwind solver. Author

N89-24873*# Georgia Inst. of Tech., Atlanta. School of Aerospace Engineering.
A WEAK HAMILTONIAN FINITE ELEMENT METHOD FOR OPTIMAL CONTROL PROBLEMS
Dewey H. Hodges and Robert R. Bless 1989 30 p Submitted for publication
(Grant NAG1-939)
(NASA-CR-185336; NAS 1.26:185336) Avail: NTIS HC A03/MF A01 CSCL 12A

A temporal finite element method based on a mixed form of the Hamiltonian weak principle is developed for dynamics and optimal control problems. The mixed form of Hamilton's weak principle contains both displacements and momenta as primary variables that are expanded in terms of nodal values and simple polynomial shape functions. Unlike other forms of Hamilton's principle, however, time derivatives of the momenta and displacements do not appear therein; instead, only the virtual momenta and virtual displacements are differentiated with respect to time. Based on the duality that is observed to exist between the mixed form of Hamilton's weak principle and variational principles governing classical optimal control problems, a temporal finite element formulation of the latter can be developed in a rather straightforward manner. Several well-known problems in dynamics and optimal control are illustrated. The example dynamics problem involves a time-marching problem. As optimal control examples, elementary trajectory optimization problems are treated. Author

N89-24874 Mississippi State Univ., State College.
SURFACE GRID GENERATION FOR COMPOSITE BLOCK GRIDS Ph.D. Thesis
Gerald Alan Jones 1988 186 p
Avail: Univ. Microfilms Order No. DA8905939

A system of elliptic partial differential equations is used for the generation of a grid on a general three-dimensional surface. The equations are those of Warsi as applied to surface curvilinear coordinates, and the method of solution is a point SOR iteration method with acceleration parameters to speed the convergence. First, the surface upon which the grid is to be generated is developed by generic surface methods or specified by input. Next, the boundary curves for the surface grid are produced, and the points on these curves are given in parametric coordinates as a function of the curvilinear coordinates. The grid code then takes the given surface and boundary curves and generates values of the parametric coordinates as functions of the curvilinear coordinates at points interior to the boundary curves on the surface. Finally, the code interpolates in the arrays for the Cartesian coordinates as functions of the parametric coordinates to obtain the Cartesian coordinates as functions of the curvilinear coordinates. The control functions are updated for the field points at each computational step, and specified conditions on the boundary curves (such as Neumann boundary conditions) are allowed. Computational results are presented for 0-type, C-type, and multi-block grids on both cylindrical and elliptical three-dimensional surfaces. Dissert. Abstr.

N89-24875 Mississippi State Univ., State College.
SURFACE COORDINATE GENERATION IN THREE-DIMENSIONAL ARBITRARY SHAPES BY SOLVING A SET OF SECOND ORDER ELLIPTIC PARTIAL DIFFERENTIAL EQUATIONS Ph.D. Thesis
Weihnurng Davis Tiarn 1988 76 p
Avail: Univ. Microfilms Order No. DA8905956

The problem of the numerical solution of a set of second order elliptic partial differential equations for the generation of

coordinates in arbitrary surfaces was considered. A numerical algorithm for solving the partial differential equations can be used for practically any surface provided that a companion method is available which generates the surface equation based on a given set of surface data points. The companion method was developed and it uses either the least-squares method or the Fourier-series blending method to obtain a differentiable surface equation in the form of F(x,y,z) = 0 to achieve the above noted purpose. For solving the basic partial differential equations numerically, point-SOR and a search program for the optimal acceleration parameters for each grid point are used. Also a multigrid technique was added to the grid generation algorithm for the acceleration of the numerical process. The results of coordinate generation are shown for various types of surfaces including a F-16XL aircraft. Dissert. Abstr.

N89-24876# Xerox Palo Alto Research Center, CA.
VISIBILITY WITH A MOVING POINT OF VIEW
M. W. Bern, D. P. Dobkin, and R. Grossman (Illinois Univ., Chicago.) 7 Dec. 1988 11 p
Avail: NTIS HC A03/MF A01

The 3-D visibility problems in which the viewing position moves along a straight flightpath was investigated. Two problems were focused on: determining the points along the flightpath at which the topology of the viewed scene changes, and answering ray-shooting queries for rays with origin on the flightpath. Three progressively more specialized problems are considered: general scenes, terrains, and terrains with vertical flightpaths. Author

N89-24877# Joint Inst. for Nuclear Research, Dubna (USSR). Scientifical-Methodical Div.
DYNAMIC SPECTRAL ANALYSIS IN FINITE FIELD ALGEBRAS
V. A. Kalinnikov 1988 12 p In RUSSIAN; ENGLISH summary Submitted for publication
(DE88-706333; JINR-R-11-88-320) Avail: NTIS (US Sales Only) HC A03/MF A01

A new method for recurrent calculation of dynamic spectral characteristics on the base of Fast Number-Theoretical Transforms over a Finite Field algebras is described. The estimate of its speed and accuracy is given. The questions of execution of arithmetic operations on the Galois Field elements and their hardware implementation are considered. DOE

N89-24878# Stanford Linear Accelerator Center, CA.
BEAM DYNAMICS WITH THE HAMILTON-JACOBI EQUATION
W. E. Gabella, R. D. Ruth, and R. L. Warnock Mar. 1989 4 p Presented at the 13th Particle Accelerator Conference, Chicago, IL, 20-23 Mar. 1989
(Contracts DE-AC03-76SF-00515; DE-AF02-86ER-40302)
(DE89-012269; SU-SLAC-PUB-4934; CONF-890335-145) Avail: NTIS HC A02/MF A01

We describe a non-perturbative method to solve the Hamilton-Jacobi equation for invariant surfaces in phase space. The problem is formulated in action-angle variables with a general nonlinear perturbation. The solution of the Hamilton-Jacobi equation is regarded as the fixed point of a map on the Fourier coefficients of the generating function. Periodicity of the generator in the independent variable is enforced with a shooting method. We present two methods for finding the fixed point and hence the invariant surface. A solution by plain iteration is economical but has a restricted domain of convergence. The Newton iteration is costly but yields solutions up to the dynamic aperture. Examples of lattices with sextupoles for chromatic correction are discussed. DOE

65 STATISTICS AND PROBABILITY

Includes data sampling and smoothing; Monte Carlo method; and stochastic processes.

N89-24879# Joint Inst. for Nuclear Research, Dubna (USSR). Lab. of Nuclear Problems.
EFFICIENT ESTIMATOR OF PARAMETERS AND GOODNESS-OF-FIT TEST OF MULTIVARIATE DISTRIBUTIONS FOR DATA PRESENTED BY ONE-DIMENSIONAL HISTOGRAMS
N. I. Chernov, V. S. Kurbatov, and G. A. Ososkov 1988 10 p In RUSSIAN; ENGLISH summary Submitted for publication
(DE88-706318; JINR-R-5-88-221) Avail: NTIS (US Sales Only) HC A02/MF A01

The problem of estimation of multi-dimensional distribution parameters in the case when the experimental information is presented by one-dimensional histograms is investigated. The parameter estimation method and the goodness-of-fit test generalizing the well-known chi(sup 2) one are proposed. The expression for covariance matrix is obtained. The asymptotic efficiency of the proposed method is proved. DOE

66 SYSTEMS ANALYSIS

Includes mathematical modeling; network analysis; and operations research.

N89-24880# Naval Postgraduate School, Monterey, CA.
THE USE OF SEAPLANES AS AN ADVANCED WEAPON SYSTEM M.S. Thesis
Algeu Kreniski Sep. 1988 109 p
(AD-A206243) Avail: NTIS HC A06/MF A01 CSCL 01/3

In this thesis the military potential of giant seaplanes as carriers of fighter/attack aircraft is considered. After a survey of past seaplane developments possible scenarios to demonstrate the utility of seaplane carriers are discussed. This is followed by preliminary seaplane sizing, design, and operational considerations. It is concluded that a fleet of Boeing 747-size amphibian planes carrying one or two F-5-size fighter/attack planes offers new and attractive military possibilities that merit further evaluation. GRA

N89-24356# European Space Agency. European Space Operations Center, Darmstadt (Germany, F.R.).
FLIGHT OPERATIONS CONCEPT FOR THE EUROPEAN IN-ORBIT INFRASTRUCTURE
W. Frank and A. Sesma *In its* International Symposium on Europe in Space: The Manned Space System Oct. 1988 p 177-183 (For primary document see N89-24335 18-12)
Copyright Avail: NTIS HC A99/MF A01; ESA Publications Div., ESTEC, Noordwijk, Netherlands, 80 Dutch guilders

N89-24358# Deutsche Forschungs- und Versuchsanstalt fuer Luft- und Raumfahrt, Cologne (Germany, F.R.).
TIMELINING AND OPERATIONS INTEGRATION CONCERNING APM AND MTFF
A. Davidson, K. Wedde-Muehlhausen, and K. Schmidt *In* ESA, International Symposium on Europe in Space: The Manned Space System Oct. 1988 p 191-199 (For primary document see N89-24335 18-12)
Copyright Avail: NTIS HC A99/MF A01; ESA Publications Div., ESTEC, Noordwijk, Netherlands, 80 Dutch guilders

N89-24359# Compagnia Italiana Servizi Tecnici, Rome.
INTEGRATED APPROACH FOR THE LOGISTIC SUPPORT OF THE EUROPEAN IN ORBIT INFRASTRUCTURE FROM THE NINETIES ONWARDS
A. Falciai and R. Grazi *In* ESA, International Symposium on Europe in Space: The Manned Space System Oct. 1988 p 201-205 (For primary document see N89-24335 18-12)
Copyright Avail: NTIS HC A99/MF A01; ESA Publications Div., ESTEC, Noordwijk, Netherlands, 80 Dutch guilders

N89-24360# Aerospatiale, Les Mureaux (France). Div. Systemes Strategiques et Spatiaux.
SERVICING OF THE MTFF BY HERMES
P. Eymar and C. Cougnet (MATRA Espace, Toulouse, France) *In* ESA, International Symposium on Europe in Space: The Manned Space System Oct. 1988 p 207-214 (For primary document see N89-24335 18-12)
Copyright Avail: NTIS HC A99/MF A01; ESA Publications Div., ESTEC, Noordwijk, Netherlands, 80 Dutch guilders

N89-24361# Messerschmitt-Boelkow-Blohm G.m.b.H., Bremen (Germany, F.R.).
MTFF FLIGHT OPERATIONS PHASES
H. Wartenberg and H. J. Koopmann *In* ESA, International Symposium on Europe in Space: The Manned Space System Oct. 1988 p 215-232 (For primary document see N89-24335 18-12)
Copyright Avail: NTIS HC A99/MF A01; ESA Publications Div., ESTEC, Noordwijk, Netherlands, 80 Dutch guilders

N89-24363# Aeritalia S.p.A., Turin (Italy). Space Systems Group.
LOGISTICS ASPECTS OF COLUMBUS SERVICING AT THE SPACE STATION
Vincenzo DeFilippis and Luciano Basile *In* ESA, International Symposium on Europe in Space: The Manned Space System Oct. 1988 p 239-244 (For primary document see N89-24335 18-12)
Copyright Avail: NTIS HC A99/MF A01; ESA Publications Div., ESTEC, Noordwijk, Netherlands, 80 Dutch guilders

N89-24403# European Space Agency, Paris (France).
THE ASTRONAUT'S FUNCTIONS ABOARD COLUMBUS
U. Merbold *In its* International Symposium on Europe in Space: The Manned Space System Oct. 1988 p 605-608 (For primary document see N89-24335 18-12)
Copyright Avail: NTIS HC A99/MF A01; ESA Publications Div., ESTEC, Noordwijk, Netherlands, 80 Dutch guilders

67 THEORETICAL MATHEMATICS

Includes topology and number theory.

N89-24881# Tokyo Univ., Tanashi (Japan). Inst. for Nuclear Study.
PATH INTEGRAL AND OPERATOR FORMALISM ON BORDERED RIEMANN SURFACES
Waichi Ogura Oct. 1988 17 p
(DE88-757229; INS-715) Avail: NTIS (US Sales Only) HC A03/MF A01

The operator formalism has been developed on the once punctured Riemann surfaces based on a generalized ground state condition in Refs. 6 to 9. Solving the boundary value problems on bordered Riemann surfaces, we show that the similar conditions are satisfied by a string state defined by the Polyakov path integral. The variational approach of Ohrndorf is confirmed in this context. DOE

N89-24882# Hiroshima Univ., Takehara (Japan). Research Inst. for Theoretical Physics.
STOCHASTIC QUANTIZATION OF NONLINEAR SIGMA-MODELS WITH WESS-ZUMINO TERMS
Naohito Nakazawa and Daiji Ennyu Nov. 1988 14 p
(DE88-757286; RRK-88-34) Avail: NTIS (US Sales Only) HC A03/MF A01

We investigate nonlinear sigma-models with Wess-Zumino terms in stochastic quantization based on the previously established superspace formulation of the stochastic background field method. In contrast with the ordinary quantization method, the one-loop corrections to the metric tensor in stochastic quantization are different depending on terms in which it appears. DOE

N89-24883*# Institute for Computer Applications in Science and Engineering, Hampton, VA.
ANALYTIC THEORY FOR THE DETERMINATION OF VELOCITY AND STABILITY OF BUBBLES IN A HELE-SHAW CELL. PART 2: STABILITY Final Report
Saleh Tanveer (Virginia Polytechnic Inst., Blacksburg.) Apr. 1989 25 p
(Contract NAS1-18605)
(NASA-CR-181837; NAS 1.26:181837; ICASE-89-29-Pt-2) Avail: NTIS HC A03/MF A01 CSCL 12A

The analysis is extended to determine the linear stability of a bubble in a Hele-Shaw cell analytically. Only the solution branch corresponding to largest possible bubble velocity U for given surface tension is found to be stable, while all the others are unstable, in accordance with earlier numerical results. Author

70 PHYSICS (GENERAL)

For precision time and time interval (PTTI) see *35 Instrumentation and Photography;* for geophysics, astrophysics or solar physics see *46 Geophysics, 90 Astrophysics,* or *92 Solar Physics.*

N89-24884# Sandia National Labs., Albuquerque, NM.
AN ANALYTICAL STUDY OF A VIBRATION TEST METHOD USING EXTREMAL CONTROL OF ACCELERATION AND FORCE
David O. Smallwood 1989 9 p Presented at the 35th Annual Technical Meeting of the Institute of Environmental Sciences: Building Tomorrow's Environment, Anaheim, CA, 1 May 1989
(Contract DE-AC04-76DP-00789)
(DE89-007428; SAND-89-0376C; CONF-890592-2) Avail: NTIS HC A02/MF A01

A vibration test method has been proposed where control is accomplished using extremal control of the force and acceleration at the input to a test item. This proposal is examined with several examples. The method does limit the acceleration input at frequencies where the test item responses tend to be unrealistically large. However, the method's application is not straightforward and care must be taken in the application of the method. DOE

N89-24885# Joint Inst. for Nuclear Research, Dubna (USSR). Lab. of Nuclear Reactions.
ANALYTICAL CONSIDERATION AND CALCULATION OF ELECTROSTATICAL SYSTEM BY REVERSE METHOD
N. I. Tarantin 1988 16 p In RUSSIAN; ENGLISH summary Submitted for publication
(DE88-706319; JINR-R-9-88-149) Avail: NTIS (US Sales Only) HC A03/MF A01

Analytical consideration and following calculation of electrostatical systems for the optics and the analysis of charged particles by the reverse method are described and illustrated by new results. The profiles and electrical potentials of electrodes are determined from Maxwell equations and from analytical expression of the base field instead of the traditional determination of the electrical field from the given system of the electrodes from the solution of Laplas equation as Dirichlet problem. DOE

71 ACOUSTICS

Includes sound generation, transmission and attenuation. For noise pollution see *45 Environmental Pollution.*

N89-24886*# National Aeronautics and Space Administration. Lewis Research Center, Cleveland, OH.
CRUISE NOISE OF THE SR-2 PROPELLER MODEL IN A WIND TUNNEL
James H. Dittmar Apr. 1989 29 p
(NASA-TM-101480; E-4606; NAS 1.15:101480) Avail: NTIS HC A03/MF A01 CSCL 20A

Noise data on the SR-2 model propeller were taken in the

NASA Lewis Research Center 8- by 6-Foot Wind Tunnel. The maximum blade passing tone rises with increasing helical tip Mach number to a peak level at a helical tip Mach number of about 1.05; then it remains the same or decreases at higher helical tip Mach numbers. This behavior, which has been observed with other propeller models, points to the possibility of using higher propeller tip speeds to limit airplane cabin noise while maintaining high flight speed and efficiency. Noise comparisons of the straight-blade SR-2 propeller and the swept-blade SR-7A propeller showed that the tailored sweep of the SR-7A appears to be the cause of both lower peak noise levels and a slower noise increase with increasing helical tip Mach number. Author

N89-24887# Max-Planck-Institut fuer Stroemungsforschung, Goettingen (Germany, F.R.).
CALCULATION OF AIRCRAFT NOISE IN THE VICINITY OF CIVIL AIRPORTS BY A SIMULTION PROCEDURE Thesis
Ullrich Isermann Feb. 1988 100 p In GERMAN; ENGLISH summary
(MPIS-7/1988; ISSN-0436-1199; ETN-89-94384) Avail: NTIS HC A05/MF A01; Max-Planck Institut fuer Stroemungsforschung, Boettinger Strasse 6-8, 3400 Goettingen, Federal Republic of Germany, 22 deutsche marks

Boeing 737 and Airbus A310 noise durations for takeoff, level flight, and curved flight paths are analyzed. Theoretical models are used for the analysis of the effects of flights on curved flight paths in order to calculate maximum sound levels and single event noise levels. The calculated results are confirmed by the simulation. Maximum sound levels within a turn are decreased as compared to those from flights on straight flight path and are increased outside of a turn. The single event noise levels depend on the directional characteristics of the noise source. For curved flights, the direction of maximum sound radiation forms a circular caustic with a center coinciding with the center of the curve. The area within this caustic represents an acoustic shadow zone where maximum sound levels, and single event noise levels, are decreased. ESA

N89-24888*# National Aeronautics and Space Administration. Langley Research Center, Hampton, VA.
ADVANCED TURBOPROP AIRCRAFT FLYOVER NOISE: ANNOYANCE TO COUNTER-ROTATING-PROPELLER CONFIGURATIONS WITH A DIFFERENT NUMBER OF BLADES ON EACH ROTOR: PRELIMINARY RESULTS
David A. McCurdy Jul. 1988 33 p
(NASA-TM-100638; NAS 1.15:100638) Avail: NTIS HC A03/MF A01 CSCL 20A

A laboratory experiment was conducted to quantify the annoyance of people to the flyover noise of advanced turboprop aircraft with counter-rotating propellers (CRP) having a different number of blades on each rotor (nxm, e.g., 10 x 8, 12 x 11). The objectives were: (1) compare annoyance to nxm CRP advanced turboprop aircraft with annoyance to conventional turboprop and jet aircraft; (2) determine the effects of tonal content on annoyance; and (3) determine the ability of aircraft noise measurement procedures and corrections to predict annoyance for this new class of aircraft. A computer synthesis system was used to generate 35 realistic, time-varying simulations of advanced turboprop takeoff noise in which the tonal content was systematically varied to represent combinations of 15 fundamental frequency (blade passage frequency) combinations and three tone-to-broadband noise ratios. The fundamental frequencies, which represented blade number combinations from 6 x 5 to 13 x 12 and 7 x 5 to 13 x 11, ranged from 112.5 to 292.5 Hz. The three tone-to-broadband noise ratios were 0, 15, and 30 dB. These advanced turboprop simulations along with recordings of five conventional turboprop takeoffs and five conventional jet takeoffs were presented at D-weighted sound pressure levels of 70, 80, and 90 dB to 64 subjects in an anechoic chamber. Analyses of the subjects' annoyance judgments compare the three categories of aircraft and examine the effects of the differences in tonal content among the advanced turboprop noises. The annoyance prediction ability of various noise measurement procedures and corrections is also examined. Author

72 ATOMIC AND MOLECULAR PHYSICS

Includes atomic structure, electron properties, and molecular spectra.

N89-24889*# Institute for Scientific Research, Lexington, MA.
INTRODUCTION TO DISSOCIATIVE RECOMBINATION
Steven L. Guberman and J. Brian A. Mitchell (University of Western Ontario, London.) [1989] 13 p
(Grant NAGw-1404)
(NASA-CR-184950; NAS 1.26:184950) Avail: NTIS HC A03/MF A01 CSCL 20H

Dissociative recombination (DR) of molecular ions with electrons has important consequences in many areas of physical science. Ab-initio calculations coupled with resonant scattering theory and multichannel quantum defect studies have produced detailed results illuminating the role of ion vibrational excitation, the quantum yields of the DR products, and the role of Rydberg states. The theoretical and experimental results are discussed. B.G.

N89-24890# Lawrence Livermore National Lab., CA.
SEMICLASSICAL MATRIX-ELEMENTS OF HIGH-CHARGE IONS
Richard M. More 1989 9 p Presented at the Workshop on Highly Charged Ions: New Physics and Advanced Techniques, Berkeley, CA, 13-15 Mar. 1989
(Contract W-7405-eng-48)
(DE89-009258; UCRL-100712; CONF-890387-1) Avail: NTIS HC A02/MF A01

We apply a new semiclassical method to study radiative transitions of high-charge ions. One-electron matrix-elements calculated with WKB wave-functions are compared with self-consistent field calculations for molybdenum at various stages of ionization. The WKB method is able to follow the (large) changes in the 1s yields np matrix-elements produced by ionization. DOE

N89-24891# Pennsylvania State Univ., University Park. Dept. of Physics.
ELECTRON TRANSFER, IONIZATION, AND EXCITATION IN ATOMIC COLLISIONS Progress Report
T. G. Winter 1989 6 p
(Contract DE-FG02-86ER-13549)
(DE89-010046; DOE/ER-13549/3) Avail: NTIS HC A02/MF A01

The fundamental processes of electron transfer, ionization, and excitation in ion-atom collisions are being studied at Penn State by Winter. (The related work of Alston, who recently came to Penn State, is not described here since he is not at present funded by DOE.) These collision processes are treated in the context of simple one- or two-electron systems in order to provide unambiguous results and reveal more clearly the collisional mechanisms. Three coupled-state calculations are being carried out over the present three-year period and are discussed here: a Sturmian-pseudostate study of electron transfer in collisions between protons and the hydrogenic ions He(+), Li(2+), Be(3+), ...; a triple-center, atomic-state study of ionization in collisions between alpha particles and H(1s) atoms and between protons and He(+)(1s) ions; and a coupled-state study of electron transfer and excitation in collisions between protons and neutral He atoms. DOE

N89-24892# SRI International Corp., Menlo Park, CA. Dept. of Chemical Kinetics.
FREE RADICAL-SURFACE INTERACTIONS USING MULTIPHOTON IONIZATION OF FREE RADICALS Final Technical Report, 1 Oct. 1985 - 30 Sep. 1988
Robert M. Robertson, David M. Golden, and Michael J. Rossi Jan. 1989 109 p
(Contract F49620-86-K-0001; SRI Proj. PYU-1227; AF Proj. 2303)
(AD-A206257; AFOSR-89-0302TR) Avail: NTIS HC A06/MF A01 CSCL 07/2

Free Radical and Atom Surface interactions have been studied in a low pressure reactor (Knudsen cell) where the atomic and molecular transients predominantly collide with the walls of the

reaction vessel. The approach taken involved generating the neutral transients using IR-multiphoton decomposition of an appropriate precursor and subsequently exposing the photolysis products to given surfaces at variable temperature (ambient to 450 C). The detection was performed by molecular beam sampling mass spectrometry and in situ Resonance enhanced Multiphoton Ionization using a tunable dye laser. The combination of both techniques affords the possibility to determine the kinetics of the neutral transients in quantitative terms, that is competition between first order and second-order processes, and the determination of quantitative REMPI ionization cross sections. The heterogeneous loss rate constants are cast in the form of a sticking coefficient for a specific radical on a given surface. We have investigated the interaction of CF3 radical on SiO2 and Si over a range of temperatures. SiH2 has been investigated in its interaction with solid Si- containing surfaces, and I and Br atoms have been studied as to their reaction with various surfaces. GRA

N89-24893# Pacific Northwest Labs., Richland, WA.
CHARACTERIZING THE ENERGY DEPOSITION EVENTS PRODUCED BY TRAPPED PROTONS IN LOW EARTH ORBIT
L. W. Brackenbush, L. A. Braby, and G. A. Anderson Mar. 1989 11 p Presented at the Practical Application of Microdosimetry Workshop, Munich, Federal Republic of Germany, 18-20 Oct. 1988
(Contract DE-AC06-76RL-01830)
(DE89-011218; PNL-SA-16335; CONF-8810358-1) Avail: NTIS HC A03/MF A01

Men and equipment in space vehicles in low earth orbit are exposed to a wide variety of radiations, but the majority of the dose is due to trapped protons, which have energies on the order of 100 MeV and are low LET particles. These high energy particles produce nuclear fragmentation with high LET secondaries that may be responsible for a significant fraction of dose equivalent. In order to better understand the biological effectiveness of this radiation environment, the authors have developed a portable tissue equivalent proportional counter spectrometer that automatically records the distribution of energy in a small tissue-like site as a function of time. This instrument weighs about 700 grams and will be flown on a number of future space shuttle flights. DOE

N89-24894# Toledo Univ., OH. Dept. of Physics and Astronomy.
SEMIEMPIRICAL STUDIES OF ATOMIC STRUCTURE Progress Report, 1 Jul. 1988 - 1 Apr. 1989
L. J. Curtis 1989 4 p
(Contract DE-FG05-88ER-13958)
(DE89-011419; DOE/ER-13958/1) Avail: NTIS HC A02/MF A01

The atomic structure and properties of highly-ionized many-electron systems are studied through the combined use of sensitive semiempirical data systematizations, selected precision experimental measurements, and specialized theoretical computations. Measurements are made primarily through the use of fast ion beam excitation methods, which are combined with available data from laser- and tokamak- produced plasmas, astrophysical sources, and conventional light sources. The experimental studies are strengthened through large scale ab initio calculations using the MFE Cray X-MP computer. Large blocks of data are systematized and parametrized along isoelectronic, homologous, isoionic, Rydberg, and yrast series. DOE

N89-24370# Avions Marcel Dassault-Breguet Aviation, Saint-Cloud (France).
PROTECTION AGAINST IONIZING RADIATION FOR THE HERMES MISSION [PROTECTION CONTRE LES RAYONNEMENTS IONISANTS POUR LES MISSIONS HERMES]
G. Melkonian and J. Bourrieau (Centre National d'Etudes Spatiales, Toulouse, France) *In* ESA, International Symposium on Europe in Space: The Manned Space System Oct. 1988 p 303-335 In FRENCH; ENGLISH summary (For primary document see N89-24335 18-12)
(Contract ESTEC-6988/NL/PP(SC))
Copyright Avail: NTIS HC A99/MF A01; ESA Publications Div., ESTEC, Noordwijk, Netherlands, 80 Dutch guilders

73 NUCLEAR AND HIGH-ENERGY PHYSICS

Includes elementary and nuclear particles; and reactor theory.

For space radiation see *93 Space Radiation.*

N89-24895# Continuous Electron Beam Accelerator Facility, Newport New, VA.
INDUCTIVE MEGAHERTZ BEAM POSITION MONITORS FOR CEBAF
Walter Barry 1989 29 p
(Contract DE-AC05-84ER-40150)
(CEBAF-PR-89-003) Avail: NTIS HC A03/MF A01

The Continuous Electron Beam Accelerator Facility (CEBAF) is a CW five pass recirculating linac with an energy gain of 800 MeV per pass. As a result, multiple beams of different energies are present simultaneously in the straight section beamlines. In these sections, it is required that the position of each beam be measured separately. One method of accomplishing this involves modulating the beam current for a duration of less than one revolution period. With a modulated beam, position can be measured by either a multi-gigahertz pickup operating at a harmonic of the 1.5 GHz RF, or a pickup that responds to the lower modulation frequency. The concepts of a simple inductive loop beam position monitor system based on the detection of a 1 to 10 MHz amplitude modulated beam are presented. Author

N89-24896# General Electric Co., Philadelphia, PA. Space Center.
SAFETY ANALYSIS REPORT FOR THE GALILEO MISSION. VOLUME 2, BOOK 1: ACCIDENT MODEL DOCUMENT Final Report
15 Dec. 1988 130 p
(Contract DE-AC01-79ET-32043)
(DE89-007270; DOE/ET-32043/T26-Vol-2-Bk-1) Avail: NTIS HC A07/MF A01

The Accident Model Document (AMD) is the second volume of the three volume Final Safety Analysis Report (FSAR) for the Galileo outer planetary space science mission. This mission employs Radioisotope Thermoelectric Generators (RTGs) as the prime electrical power sources for the spacecraft. Galileo will be launched into Earth orbit using the Space Shuttle and will use the Inertial Upper Stage (IUS) booster to place the spacecraft into an Earth escape trajectory. The RTG's employ silicon-germanium thermoelectric couples to produce electricity from the heat energy that results from the decay of the radioisotope fuel, Plutonium-238, used in the RTG heat source. The heat source configuration used in the RTG's is termed General Purpose Heat Source (GPHS), and the RTG's are designated GPHS-RTGs. The use of radioactive material in these missions necessitates evaluations of the radiological risks that may be encountered by launch complex personnel as well as by the Earth's general population resulting from postulated malfunctions or failures occurring in the mission operations. The FSAR presents the results of a rigorous safety assessment, including substantial analyses and testing, of the launch and deployment of the RTGs for the Galileo mission. This AMD is a summary of the potential accident and failure sequences which might result in fuel release, the analysis and testing methods employed, and the predicted source terms. Each source term consists of a quantity of fuel released, the location of release and the physical characteristics of the fuel released. Each source term has an associated probability of occurrence. DOE

N89-24897# General Electric Co., Philadelphia, PA. Space Center.
SAFETY ANALYSIS REPORT FOR THE GALILEO MISSION. VOLUME 2, BOOK 2: ACCIDENT MODEL DOCUMENT, APPENDICES Final Report
15 Dec. 1988 694 p
(Contract DE-AC01-79ET-32043)
(DE89-007271; DOE/ET-32043/T26-Vol-2-Bk-2) Avail: NTIS HC A99

This section of the Accident Model Document (AMD) presents the appendices which describe the various analyses that have been conducted for use in the Galileo Final Safety Analysis Report 2, Volume 2. Included in these appendices are the approaches, techniques, conditions and assumptions used in the development of the analytical models plus the detailed results of the analyses. Also included in these appendices are summaries of the accidents and their associated probabilities and environment models taken from the Shuttle Data Book (NSTS-08116), plus summaries of the several segments of the recent GPHS safety test program. The information presented in these appendices is used in Section 3.0 of the AMD to develop the Failure/Abort Sequence Trees (FASTs) and to determine the fuel releases (source terms) resulting from the potential Space Shuttle/IUS accidents throughout the missions. DOE

N89-24898# Nuclear Utility Services, Inc., Gaithersburg, MD.
SAFETY ANALYSIS REPORT FOR THE GALILEO MISSION. VOLUME 3, BOOK 1: NUCLEAR RISK ANALYSIS DOCUMENT, REVISION 1 Final Report
13 Jan. 1989 89 p
(Contract DE-AC01-87NE-32134)
(DE89-007272; DOE/NE-32134/T1-Vol-3-Bk-1; NUS-5126-Rev-1-Vol-3-Bk-1) Avail: NTIS HC A05/MF A01

It is the purpose of the NRAD to provide an analysis of the range of potential consequences of accidents which have been identified that are associated with the launching and deployment of the Galileo mission spacecraft. The specific consequences analyzed are those associated with the possible release of radioactive material (fuel) of the Radioisotope Thermoelectric Generators (RTGs). They are in terms of radiation doses to people and areas of deposition of radioactive material. These consequence analyses can be used in several ways. One way is to identify the potential range of consequences which might have to be dealt with if there were to be an accident with a release of fuel, so as to assure that, given such an accident, the health and safety of the public will be reasonably protected. Another use of the information, in conjunction with accident and release probabilities, is to estimate the risks associated with the mission. That is, most space launches occur without incident. Given an accident, the most probable result relative to the RTGs is complete containment of the radioactive material. Only a small fraction of accidents might result in a release of fuel and subsequent radiological consequences. The combination of probability with consequence is risk, which can be compared to other human and societal risks to assure that no undue risks are implied by undertaking the mission. DOE

N89-24899# Nuclear Utility Services, Inc., Gaithersburg, MD.
SAFETY ANALYSIS REPORT FOR THE GALILEO MISSION. VOLUME 3, BOOK 2: NUCLEAR RISK ANALYSIS DOCUMENT. APPENDICES, REVISION 1 Final Report
25 Jan. 1989 203 p
(Contract DE-AC01-87NE-32134)
(DE89-007273; DOE/NE-32134/T1-Vol-3-Bk-2; NUS-5126-Rev-1-Vol-3-Bk-2) Avail: NTIS HC A10

It is the purpose of the NRAD to provide an analysis of the range of potential consequences of accidents which have been identified that are associated with the launching and deployment of the Galileo mission spacecraft. The specific consequences analyzed are those associated with the possible release of radioactive material (fuel) of the Radioisotope Thermoelectric Generators (RTGs). They are in terms of radiation doses to people and areas of deposition of radioactive material. These consequence analyses can be used in several ways. One way is to identify the potential range of consequences which might have to be dealt with if there were to be an accident with a release of fuel, so as to assure that, given such an accident, the health and safety of the public will be reasonably protected. Another use of the information, in conjunction with accident and release probabilities, is to estimate the risks associated with the mission. That is, most space launches occur without incident. Given an accident, the most probable result relative to the RTGs is complete containment of the radioactive material. Only a small fraction of accidents might result in a release of fuel and subsequent radiological consequences. The combination of probability with consequence is risk, which can be compared to other human and societal risks to assure that no undue risks are implied by undertaking the mission. Book 2 contains eight appendices. DOE

N89-24900 Max-Planck-Inst. fuer Physik und Astrophysik, Garching (Germany, F.R.). Inst. fuer Extraterrestrische Physik.
A STUDY OF K SUP DEG SEC, LAMBDA AND LAMBDA BAR PRODUCTION IN 60 AND 200 GeV NUCLEON OAu AND pAu COLLISIONS WITH A STREAMER CHAMBER DETECTOR AT THE CERN SPS
A. Bamberger, J. Bartke, H. Bialkowska, R. Bock, R. Brockmann, S. I. Chase, C. DeMarzo, M. DePalma, I. Derado, and V. Eckardt (Max-Planck-Inst. fuer Physik und Astrophysik, Munich, Germany, F.R.) et al Jan. 1989 32 p Submitted for publication
Sponsored in cooperation with the Bundesministerium fuer Forschung und Technologie, Bonn, Germany, Federal Republic
(Contract DE-AC03-76SF-00098)
(MPE-PAE/Exp.El-198; ETN-89-94580) Copyright Avail: Fachinformationszentrum Karlsruhe, 7514 Eggenstein-Leopoldshafen 2, Federal Republic of Germany

The production of neutral strange particles is studied in 60 and 200 GeV per nucleon OAu and pAu collisions with the streamer chamber vertex spectrometer of the NA35 experiment. Ratios of neutral strange particle production to negatively charged particle production in selected regions of phase space are measured to be the same in both reactions. The rates of strange particle production in central OAu collisions are a factor of 16 higher than in pAu collisions when compared in the same regions of phase space. ESA

74 OPTICS

Includes light phenomena; and optical devices.
For lasers see *36 Lasers and Masers.*

N89-24901# National Aeronautical Lab., Bangalore (India). Systems Engineering Div.
AN INTELLIGENT FIBEROPTIC DATA BUS FOR FLY-BY-LIGHT APPLICATIONS
L. C. Manoharan and S. Muthuvel Nov. 1987 11 p
(NAL-TM-SE-8707) Avail: NTIS HC A03/MF A01

An active Fiberoptic Data Bus compatible with MIL-STD-1553B which could be used for Fly-by-light, stores management, AEW etc., on an aircraft is described. The data bus is considered intelligent because it can automatically sense which station is in the transmit mode and control the active interface accordingly, so that smooth flow of data takes place on the bus. The tests that were done on the bus to check its validity are also described. As no software is involved in the operation this could be used on any aircraft with its own software. Author

N89-24902# Japan Atomic Energy Research Inst., Tokyo. Dept. of Development.
DESIGN OF THE OPTICAL SYSTEM FOR A NEW TIME-RESOLVED X-RAY ABSORPTION SPECTROSCOPY APPARATUS
Atsumi Miyashita and Osamu Yoda Oct. 1988 54 p In JAPANESE; ENGLISH summary
(DE88-757253; JAERI-M-88-212) Avail: NTIS (US Sales Only) HC A04/MF A01

Calculations of total reflection mirror optics and analyzing crystal polychromator optics are done to design a new time-resolved soft X-ray absorption spectroscopy apparatus. This apparatus utilizes pulsed soft X-rays of pseudo-continuum energy which are generated by a pulsed laser-induced metal plasma, and covers an energy range of 90 eV similar to 3 keV. An optimal design of the optical system, i.e., optimal dimensions, setting positions and materials of the mirror and polychromator, is proposed based on the calculations of the reflectivity of the material, efficiency of the X-ray acceptance and ray-tracing. Calculations are also made on the reflectivity of several mirror materials commonly used for the X-ray diffraction and spectroscopy in the energy range up to 50 keV. Data of the reflectivity in this energy region are necessary to design an X-ray apparatus using synchrotron radiation as an X-ray source. Numerical results of the reflectivity are available. DOE

N89-24903# Los Alamos National Lab., NM. Theoretical Div.
OPTICAL CHAOS
Peter W. Milonni 1989 24 p Presented at the International School of Lasers and Applications, Krasnoyarsk, USSR, 17-23 Mar. 1989
(Contract W-7405-eng-36)
(DE89-009392; LA-UR-89-857; CONF-890392-1) Avail: NTIS HC A03/MF A01

The theoretical and experimental status of chaos in nonlinear optics and laser physics will be reviewed. Attention will then be focused on the possibility of chaotic behavior in individual atoms and molecules driven by intense radiation fields. DOE

N89-24904# Lawrence Livermore National Lab., CA.
COMBINED MICROSTRUCTURE X-RAY OPTICS
Troy W. Barbee, Jr. Feb. 1989 36 p Presented at the 3rd International Conference on Synchrotron Radiation Instrumentation, Tsukuba, Japan, 29 Aug. - 2 Sep. 1988
(Contract W-7405-eng-48)
(DE89-009902; UCRL-98732; CONF-8808141-12) Avail: NTIS HC A03/MF A01

Multilayers are man-made microstructures which vary in depth and are now of sufficient quality to be used as X-ray, soft X-ray and extreme ultraviolet optics. Gratings are man-made in plane microstructures which have been used as optic elements for most of this century. Joining of these two optical microstructures to form combined microstructure optical microstructures to form combined microstructure optical elements has the potential for greatly enhancing both the throughput and the resolution attainable in these spectral ranges. The characteristics of these new optic elements will be presented and compared to experiment with emphasis on the unique properties of these combined microstructures. These results reported are general in nature and not limited to the soft X-ray or extreme ultraviolet spectral domains and also apply to neutrons. DOE

N89-24905# Army Missile Command, Redstone Arsenal, AL.
THE CURRENT TECHNOLOGICAL STATUS OF SPATIAL LIGHT MODULATORS Final Technical Report, Oct. 1987 - Apr. 1988
Tracy D. Hudson Aug. 1988 33 p
(AD-A206328; AD-E951257; AMSMI/TR-RD-RE-88-5) Avail: NTIS HC A03/MF A01 CSCL 20/6

The major technological obstacle to optical computing and optical pattern recognition is the performance of spatial light modulators. This report is an attempt to present a realistic outlook for the future of optical computing by briefly presenting the basics of promising modulators with regard to their response times, resolution, and cost. GRA

N89-24906# Lawrence Livermore National Lab., CA.
HARD X-RAY IMAGING TELESCOPE DEVELOPMENT Final Report
Philip Lubin and Michael Seiffert (California Univ., Santa Barbara.) 1 Apr. 1989 8 p
(Contract W-7405-eng-48)
(DE89-011647; UCRL-21148) Avail: NTIS HC A02/MF A01

Progress to date has been along two major lines: computer simulations and hardware development. In order to test the desirability of various coded aperture mask designs we have performed extensive Monte Carlo computer simulations of the mask and detector arrangement. Background estimates from other balloon experiments and also other Monte Carlo simulations were included to test both detection and imaging sensitivity to point source objects as well as to extended emission regions. DOE

N89-24297# Hamburg Univ. (Germany, F.R.). Fachbereich Informatik.
SCENE RECONSTRUCTION FOR IMAGE SEQUENCES
B. Neumann and R. Sprengel *In* DFVLR, Image Signal Processing for Flight Guidance Sep. 1988 p 25-58 In GERMAN; ENGLISH summary (For primary document see N89-24295 18-04)
Avail: NTIS HC A14/MF A01; DFVLR, VB-PL-DO, Postfach 40 60 58, 5000 Cologne, Fed. Republicof Germany, DM 108

75 PLASMA PHYSICS

Includes magnetohydrodynamics and plasma fusion.

For ionospheric plasmas see *46 Geophysics.* For space plasmas see *90 Astrophysics.*

N89-24907# Lawrence Livermore National Lab., CA.
THE EFFECT OF NON-MAXWELLIAN ELECTRON DISTRIBUTIONS ON THE INTENSITY RATIO OF RESONANCE TO SATELLITE LINES
M. Lamoureux, Yim Lee, J. Dubau, and M. Cornille (Observatoire de Paris-Meudon, France) Dec. 1988 10 p Presented at the CECAM Workshop on Photoabsorption by Astrophysical and Laboratory Plasmas, Paris, France, 18 Jul. 1988
(Contract W-7405-eng-48)
(DE89-006745; UCRL-100301; CONF-8807149-2) Avail: NTIS HC A03/MF A01

Non-Maxwellian electron distributions in laser plasmas of density lower than the so-called critical density, that is where the laser beam penetrates the plasma and the inverse bremsstrahlung heating disturbs the electron distribution from its Maxwellian situation are discussed. Inverse bremsstrahlung and the competing thermalization through electron-electron collisions are the dominant processes in the plasma. The temperature diagnostic based on the ratio of the resonance to the satellite lines is considered. We are now investigating how this line intensity ratio is affected by a non-Maxwellian character of the plasma, and we will show preliminary results obtained for plasmas at low densities. We are working on other aspects of non-Maxwellian plasmas, such as ionic populations, but we present here only the issues which lead to discussions and interactions at this workshop. DOE

N89-24908# Japan Atomic Energy Research Inst., Tokyo. Fusion Experimental Reactor Team.
STEADY-STATE OPERATION REGIME OF TOKAMAK REACTOR PLASMA. CONSISTENCY ANALYSIS (I)
Kimitaka Itoh, Atsushi Fukuyama, Sanae Itoh (Hiroshima Univ., Japan), Tomonori Takizuka, Shin Yamamoto, and Shinzaburo Matsuda Sep. 1988 36 p In JAPANESE; ENGLISH summary
(DE88-756571; JAERI-M-88-171) Avail: NTIS (US Sales Only) HC A03/MF A01

Consistency of physics constraints imposed on a core plasma in a tokamak reactor is investigated. Conditions for the stationary operation of the ITER-grade plasma are listed, i.e., density limit, critical-beta, feasibilities of full current-drive and divertor functioning, and so on. The parameter regime, in which these guide lines are simultaneously satisfied, is searched for. Based on the present data base, we examine the consistency of conditions. The L-mode scaling is employed for the extrapolation. The Q-value and the size dependence are studied. The consistent working region of the stationary operation is found. If the offset-linear scaling is applied, the minimum and necessary input power is around 130 MW, which enables the full current-drive and stationary operation

with I sub p = 20 MA. When the input power is increased up to 200 MW, the Q-value of 5 can be possible. DOE

N89-24909# Japan Atomic Energy Research Inst., Tokyo. Dept. of Large Tokamak Research.
STUDY OF PARTICLE CONFINEMENT IN THE JT-60 TOKAMAK USING SKIN RADIATIVE APPROXIMATION MODEL
Sinji Koide, Katsuhiro Shimizu, Takashi Sugiyama (Toshiba Corp., Tokyo, Japan), and Takeo Nishitani Sep. 1988 51 p In JAPANESE; ENGLISH summary
(DE88-756574; JAERI-M-88-175) Avail: NTIS (US Sales Only) HC A04/MF A01

In order to analyze the particle behavior of hydrogen plasma from the observation data of H alpha line, Skin Radiative Approximation Model has been newly proposed. The characteristics of particle confinement and recycling of ohmically heated plasma in the JT-60 tokamak are investigated by this model using H alpha data of observed eight sight lines. As a result, it is inferred that recycled particles in the divertor influence the estimation of particle confinement time in comparison with that of analysis from the function fitting method using the data of three vertical sight lines. DOE

N89-24910# European Space Agency, Paris (France).
PROCEEDINGS OF AN INTERNATIONAL SCHOOL AND WORKSHOP ON PLASMA ASTROPHYSICS, VOLUME 1
T. D. Guyenne, ed. and J. J. Hunt, ed. Jan. 1989 415 p Workshop held in Varenna, Italy, 24 Aug. - 3 Sep. 1988; organized by the Varenna-Abastumani Workshop, ESA, Zentralinst. fuer Astrophysik, Germany, D.R., and the Academy of Sicences, Moscow, USSR
(ESA-SP-285-Vol-1; ISSN-0379-6566; ETN-89-94475) Avail: NTIS HC A18/MF A01; ESA Publications Div., ESTEC, Noordwijk, Netherlands, 45 US dollars or 80 Dutch guilders

Solar wind and planetary magnetospheres; the Sun and normal stars; interstellar medium and shock waves; magnetic fields in space (reconnection and dynamos); acceleration and cosmic rays; accretion disks, compact objects, and active galaxies; galactic structure dynamics and cosmology; and laboratory plasma physics were discussed. For individual titles, see N89-24911 through N89-24973.

N89-24911# Royal Inst. of Tech., Stockholm (Sweden). Dept. of Plasma Physics.
DEVELOPMENT OF ASTROPHYSICS FROM THE TELESCOPE TO THE SPUTNIK **c90**
H. Alfven *In* ESA, Proceedings of an International School and Workshop on Plasma Astrophysics, Volume 1 Jan. 1989 p 3-8 (For primary document see N89-24910 18-75)
Avail: NTIS HC A18/MF A01; ESA Publications Div., ESTEC, Noordwijk, Netherlands, 45 US dollars or 80 Dutch guilders

It is shown how progress in astrophysics is not only due to new ideas but also to the introduction of new methods of observation. The Copernican revolution was more due to the introduction of the telescope than to the heliocentric model (invented 2000 yr earlier). The decisive importance of electromagnetic effects in astrophysics originated from Langmuir's invention of the plasma probe and from Birkeland's terrella experiment and his observations of plasmas in space (aurora). A similar revolution was introduced by space research which made possible in situ measurements in cosmic plasmas and opened the X-ray and gamma ray regions to observation. The result is a drastic revision of essential parts of astrophysics (including cosmology) leading to the Plasma Universe model. ESA

N89-24912# Royal Inst. of Tech., Stockholm (Sweden). Dept. of Plasma Physics.
ASTROPHYSICAL SIGNIFICANCE OF OBSERVATIONS AND EXPERIMENTS IN THE EARTH'S MAGNETOSPHERE **c46**
C.-G. Falthammar *In* ESA, Proceedings of an International School and Workshop on Plasma Astrophysics, Volume 1 Jan. 1989 p 9-19 (For primary document see N89-24910 18-75)
Avail: NTIS HC A18/MF A01; ESA Publications Div., ESTEC, Noordwijk, Netherlands, 45 US dollars or 80 Dutch guilders

The utility of the Earth's magnetosphere as a sample of cosmical plasma, which is accessible to in situ measurements and even active experimentation is discussed. As our universe consists almost entirely of plasmas that will forever be out of reach for such scrutiny, the empirical knowledge gained in the magnetosphere should be essential to the understanding of astrophysical phenomena. The magnetosphere contains plasmas with wide ranges of density and temperature, and is also the site of a rich variety of plasma physical processes that are of fundamental astrophysical interest. In situ observation of such processes proved theories of cosmic plasma to be misleading. It provides knowledge about the behavior of real cosmic plasmas, such as conduction of electric current, support of magnetic-field aligned electric fields, filamentary and cellular structure, violation of the law of frozen-in magnetic fields, energization of charged particles, rapid release of magnetic energy, chemical separation, and critical velocity interaction between plasma and neutral gas. ESA

N89-24913# European Space Agency. European Space Research and Technology Center, ESTEC, Noordwijk (Netherlands). Space Science Dept.
ESA'S SPACE PLASMA PHYSICS MISSIONS: THE PAST AND THE FUTURE TEN YEARS
R. Schmidt *In its* Proceedings of an International School and Workshop on Plasma Astrophysics, Volume 1 Jan. 1989 p 21-27 (For primary document see N89-24910 18-75)
Avail: NTIS HC A18/MF A01; ESA Publications Div., ESTEC, Noordwijk, Netherlands, 45 US dollars or 80 Dutch guilders

Scientific results from the ISEE and GEOS missions, and the major objectives of the four-spacecraft Cluster mission are described. The GEOS 1 and 2 were launched, respectively, in Aug. 1977 and Jul. 1978; GEOS 2 replaced GEOS 1 which suffered from an orbit injection failure. The GEOS spacecraft were designed to study fields and plasmas in the geostationary orbit and to serve as reference spacecraft for the International Magnetospheric Study. The ISEE mission consisted of three spacecraft; ISEE 1 and 3 were provided by NASA and ISEE-2 was contributed by ESA. While ISEE 1 and 2 orbited in close proximity, ISEE 3 was positioned between Sun and Earth. With two closely orbiting spacecraft one is able to disentangle variations in space from variations in time in a system that constantly expands, shrinks, and changes topology. The Cluster mission will be implemented in collaboration by ESA and NASA; The Institute of Space Research (IKI) of the Soviet Academy of Science will provide at least two spacecraft. Cluster will study small scale structures in three dimensions in the Earth's plasma environment. ESA

N89-24914# Max-Planck-Inst. fuer Aeronomie, Katlenburg-Lindau (Germany, F.R.).
DIMENSIONLESS PARAMETERS FOR CLASSIFYING SOLAR WIND INTERACTIONS **c92**
V. M. Vasyliunas *In* ESA, Proceedings of an International School and Workshop on Plasma Astrophysics, Volume 1 Jan. 1989 p 31-3 (For primary document see N89-24910 18-75)
Avail: NTIS HC A18/MF A01; ESA Publications Div., ESTEC, Noordwijk, Netherlands, 45 US dollars or 80 Dutch guilders

For a systematic comparison of the various observed magnetospheres and related systems, their basic parameters are expressed in dimenionless, unit-independent form. The planetary magnetic dipole moment and the internal plasma source strength, recast as dimensionless variables, provide a unified overview of solar wind interactions with a variety of objects from strongly magnetic planets to comets. The radius of a planet has little significance for the magnetosphere in general, but a magnetosphere large compared to the planet may be needed in order to concentrate currents sufficiently to trigger auroral acceleration. A dimensionless measure of gravitational effects shows that they are important in magnetospheres of distant astrophysical objects but unimportant in magnetospheres within

the present-day solar system; magnetospheres, if any, during the formative phases of the solar system must therefore have been qualitatively different. ESA

N89-24915# Max-Planck-Inst. fuer Physik und Astrophysik, Garching (Germany, F.R.).

COSMIC LINEAR ACCELERATORS **c90**

G. Haerendel *In* ESA, Proceedings of an International School and Workshop on Plasma Astrophysics, Volume 1 Jan. 1989 p 37-4 (For primary document see N89-24910 18-75)

Avail: NTIS HC A18/MF A01; ESA Publications Div., ESTEC, Noordwijk, Netherlands, 45 US dollars or 80 Dutch guilders

The existence of field-aligned potential drops is related to unstable field-aligned currents. It is postulated that the region of instability, once set up, can propagate spontaneously into the interior of the current circuit, like a fracture in a stressed solid body, and thus achieve a fast magnetic stress relief. Most of the released magnetic energy is converted into kinetic energy of field-aligned particle beams. Parallel voltage and energy flux depend on the primary magnetic stress, the propagation properties of shear Alfven-waves, and the threshold for current instability. Numerical examples for the efficiency of such an acceleration process for three cosmic situations are given. ESA

N89-24916*# Lawrence Livermore National Lab., CA. Inst. of Geophysics and Planetary Physics.

COMPUTER SIMULATIONS OF COSMIC-RAY DIFFUSION NEAR SUPERNOVA REMNANT SHOCK WAVES

C. E. Max, A. L. Zachary, and J. Arons (California Univ., Berkeley.) *In* ESA, Proceedings of an International School and Workshop on Plasma Astrophysics, Volume 1 Jan. 1989 p 45-5 (For primary document see N89-24910 18-75)

(Contract NAGw-1301; W-7405-eng-48; NSF AST-86-15816; LLNL-89-11; NSF AST-85-03093)

Avail: NTIS HC A18/MF A01; ESA Publications Div., ESTEC, Noordwijk, Netherlands, 45 US dollars or 80 Dutch guilders

CSCL 20I

A plasma simulation model was used to study the resonant interactions between streaming cosmic-ray ions and a self-consistent spectrum of Alfven waves, such as might exist in the interstellar medium upstream of a supernova remnant shock wave. The computational model is a hybrid one, in which the background interstellar medium is an MHD fluid and the cosmic-rays are discrete kinetic particles. The particle sources for the electromagnetic fields are obtained by averaging over the fast cyclotron motions. When the perturbed magnetic field is larger than 10 percent of the background field, the macro- and microphysics are no longer correctly predicted by quasi-linear theory. The particles are trapped by the waves and show sharp jumps in their pitch-angles relative to the background magnetic field, and the effective ninety-degree scattering time for diffusion parallel to the background magnetic field is reduced to between 5 and 30 cyclotron periods. Simulation results suggest that Type 1 supernova remnants may be the principal sites of cosmic ray acceleration. ESA

N89-24917*# Iowa Univ., Iowa City. Dept. of Physics and Astronomy.

THE ELECTRON BEAM INSTABILITY REVISITED: GROWTH ABOVE AND BELOW f SUB p

I. H. Cairns *In* ESA, Proceedings of an International School and Workshop on Plasma Astrophysics, Volume 1 Jan. 1989 p 53-5 (For primary document see N89-24910 18-75)

(Grants NAGw-831; NSF ATM-87-16770)

Avail: NTIS HC A18/MF A01; ESA Publications Div., ESTEC, Noordwijk, Netherlands, 45 US dollars or 80 Dutch guilders

CSCL 20I

The growth of electrostatic waves near the plasma frequency (fp) due to an unstable electron beam is investigated by solving the unmagnetized electrostatic dispersion equation numerically. The numerical solutions are compared with analytic theories for reactive (or fluid-type) and kinetic versions of the beam instability, and for the O'Neil/Malmberg connection of the beam and Langmuir modes. Conditions for growth significantly above or below fp are given. Three general results are found: (1) The unstable waves do not grow on a mode with Langmuir dispersion except in the limit of a very dilute beam with growth on O'Neil/Malmberg's connected mode; (2) The properties of the unstable mode depend strongly on beam parameters such as beam density, speed and temperature; and (3) The frequency of maximum growth frequently lies significantly above or below fp, and differs significantly from that predicted by the Langmuir dispersion relation. Results imply important consequences for theories of strong turbulence and nonlinear wave-wave processes, and observational identification of fp from observed wave frequencies. ESA

N89-24918# Calabria Univ., Arcavacta di Rende (Italy). Dipartimento di Fisica.

MAGNETIC NEUTRAL LINES IN JUPITER'S NIGHTSIDE MAGNETOSPHERE **c91**

G. Zimbardo *In* ESA, Proceedings of an International School and Workshop on Plasma Astrophysics, Volume 1 Jan. 1989 p 57-6 (For primary document see N89-24910 18-75)

Avail: NTIS HC A18/MF A01; ESA Publications Div., ESTEC, Noordwijk, Netherlands, 45 US dollars or 80 Dutch guilders

A self-consistent axisymmetric model of Jupiter's nightside magnetosphere is presented. The plasma velocity is assumed to be purely toroidal, and the magnetic field purely poloidal. Data from the Voyager missions are used as input for the solution of the equation determining the magnetic structure. It is shown that magnetic neutral lines, i.e., X and O lines, occur with sufficiently large current disks. The X line is located between 37 and 45 Jovian radii, while the position of the O line is less well-determined. Beyond the X line an ordered radial motion develops. This may be identified either with the magnetospheric wind or with the formation of plasmoids in the Jovian magnetosphere. ESA

N89-24919*# Cornell Univ., Ithaca, NY. Lab. of Plasma Studies.

DISSIPATION OF ALFVEN WAVES IN SOLAR CORONAL ARCHES **c92**

R. N. Sudan and P. L. Similon *In* ESA, Proceedings of an International School and Workshop on Plasma Astrophysics, Volume 1 Jan. 1989 p 63-6 (For primary document see N89-24910 18-75)

(Grants NAGw-1006; NSF AST-86-00308)

Avail: NTIS HC A18/MF A01; ESA Publications Div., ESTEC, Noordwijk, Netherlands, 45 US dollars or 80 Dutch guilders

CSCL 03B

The physical mechanism by which mechanical energy is delivered to and absorbed by the solar corona is discussed. A set of MHD equations for analyzing the slow evolution of the magnetic field and the fast time of Alfven waves is presented. Alfven wave dissipation is treated. It is shown that the slow motion of the feet of coronal arches leads to irregular magnetic fields and that Alfven waves propagating in the irregular magnetic structure are dissipated through filamentation of the wave packet that generates short scales necessary for efficient dissipation. ESA

N89-24920# Toyama Univ. (Japan). Dept. of Applied Mathematics and Physics.

NON-STEADY ASTROPHYSICAL SPIRAL JETS DRIVEN BY MAGNETIC COLLAPSE AND PRESSURE **c90**

Jun-ichi Sakai *In* ESA, Proceedings of an International School and Workshop on Plasma Astrophysics, Volume 1 Jan. 1989 p 69-7 (For primary document see N89-24910 18-75)

Avail: NTIS HC A18/MF A01; ESA Publications Div., ESTEC, Noordwijk, Netherlands, 45 US dollars or 80 Dutch guilders

A theoretical model of nonsteady, astrophysical, spiral, two sided jets is investigated by means of the ideal MHD equations with the adiabatic law for both cases; gamma = 5/3 (ion dominated plasma) and gamma = 4/3 (radiation dominated plasma). It is shown that the combined effects of the radial magnetic pinch (magnetic collapse) and anisotropic plasma pressure can explosively produce super-Alfvenic two sided jets with the spiral

structure. The high energy particle acceleration during explosive jet formation is also discussed. ESA

N89-24921# Institute of Nuclear Physics, Novosibirsk (USSR).
MHD-WAVES AND THEIR NONLINEAR INTERACTION IN A PLASMA WITH MAGNETIC FLUX TUBES
M. P. Ryutova *In* ESA, Proceedings of an International School and Workshop on Plasma Astrophysics, Volume 1 Jan. 1989 p 77-8 (For primary document see N89-24910 18-75)
Avail: NTIS HC A18/MF A01; ESA Publications Div., ESTEC, Noordwijk, Netherlands, 45 US dollars or 80 Dutch guilders

Theoretical results related to the oscillations of magnetic flux tubes are reviewed, emphasizing negative energy waves. It is shown that the presence of a shear flow along the magnetic field gives rise a number of effects: the appearance of negative energy waves, reversal of the sign of radiative damping, the development of explosive instability at the nonlinear stage. The results obtained can be of interest in connection with the problem of energy accumulation and its release in the Solar atmosphere. ESA

N89-24922# European Space Agency. European Space Research and Technology Center, ESTEC, Noordwijk (Netherlands). Space Science Dept.
HELIOSEISMOLOGY AND PLASMA PHYSICS **c92**
B. N. Anderson *In its* Proceedings of an International School and Workshop on Plasma Astrophysics, Volume 1 Jan. 1989 p 83-93 (For primary document see N89-24910 18-75)
Avail: NTIS HC A18/MF A01; ESA Publications Div., ESTEC, Noordwijk, Netherlands, 45 US dollars or 80 Dutch guilders

Helioseismology, the science of using the solar global oscillations to probe the physical and dynamic structures of the solar atmosphere and the solar interior is introduced. Results show that on the global scale, understanding of the physical conditions in the solar interior are approximately correct, e.g., the depth of the convection zone, the radial dependance of the rotation curve, the temperature and the density stratifications. However, there are clear discrepancies when detailed comparisons between theories and observations are made. These discrepancies may be caused by lacking knowledge of the boundary conditions, uncertainties in the knowledge of the equation of state, or inadequate treatment of convection and magnetic fields. ESA

N89-24923# Eidgenoessische Technische Hochschule, Zurich (Switzerland). Inst. fuer Astronomie.
ALFVEN WAVE SOLITONS AND SOLAR INTERMEDIATE DRIFT BURSTS **c92**
M. Guedel, A. O. Benz, and R. A. Treumann (Max-Planck-Inst. fuer Physik und Astrophysik, Garching, Germany, F.R.) *In* ESA, Proceedings of an International School and Workshop on Plasma Astrophysics, Volume 1 Jan. 1989 p 95-9 (For primary document see N89-24910 18-75)
Avail: NTIS HC A18/MF A01; ESA Publications Div., ESTEC, Noordwijk, Netherlands, 45 US dollars or 80 Dutch guilders

Stationary solutions for Alfven solitons propagating obliquely in a homogeneous magnetic field are investigated. Due to their dispersive nature kinetic Alfven waves can evolve into soliton like structures which propagate at velocities of the order of the Alfven velocity in a direction inclined to the magnetic field. The first model keeps the plasma Beta less than me/mi. Kinetic Alfven solitons in this case can propagate at Mach numbers greater or less than 1 as dilutions or as compressions of the plasma density. In the second model the plasma contains two electron components, a hot one and a cold one. Differential equations for the plasma density are derived, and examples of numerical solutions for the plasma density profiles are presented. Both dilutive and compressional solitons are uniquely determined by Beta and the propagation velocity vector. Conditions for the existence of soliton solutions are given. Interactions between the hot and the cold electron component turn out to be significant for dilutions of the cold component. This kind of solitary density wave is applied to solar intermediate drift radio bursts. ESA

N89-24924# Saint Andrew's Univ. (Scotland). Dept. of Mathematical Sciences.
THERMAL INSTABILITY IN A STRATIFIED PLASMA
D. F. M. Hermanns and E. R. Priest *In* ESA, Proceedings of an International School and Workshop on Plasma Astrophysics, Volume 1 Jan. 1989 p 99-102 (For primary document see N89-24910 18-75)
Avail: NTIS HC A18/MF A01; ESA Publications Div., ESTEC, Noordwijk, Netherlands, 45 US dollars or 80 Dutch guilders

The thermal instability mechanism was studied in connection with observed coronal features, e.g., prominences or cool cores in loops. The thermal instability and the interaction between thermal modes and the slow magneto-acoustic subspectrum for a stratified plasma slab were considered. The relevant system of equations is formulated, and straightforward properties of the linear spectrum of a nonuniform plasma slab, i.e., the existence of continuous parts in the spectrum, are given. A numerical scheme to investigate the linear spectrum for equilibrium states with stratification is presented. The slow and thermal subspectra of a crude coronal model are given as a preliminary result. ESA

N89-24925# FOM-Inst. voor Plasmafysica, Rijnhuizen, Jutphaas (Netherlands).
KINK MODES IN CORONAL LOOPS **c92**
J. P. Goedbloed, M. Goossens, and S. Poedts (Katholieke Universiteit te Leuven, Belgium) *In* ESA, Proceedings of an International School and Workshop on Plasma Astrophysics, Volume 1 Jan. 1989 p 103-106 Sponsored by Netherlands Organization for the Advancement of Scientific Research and the Stitchting voor Fundamenteel Onderzoek de Materie, Amsterdam, Netherlands (For primary document see N89-24910 18-75)
Avail: NTIS HC A18/MF A01; ESA Publications Div., ESTEC, Noordwijk, Netherlands, 45 US dollars or 80 Dutch guilders

Insights obtained from MHD stability theory of tokamaks, in particular concerning methods of dealing with constraints and singular modes, pertaining to the dynamics of coronal loops are reviewed. In tokamaks external kink modes are stabilized by the geometric constraint that the modes should fit into the torus. In current-carrying coronal loops the opposite problem arises: the apparent absence of external kink modes, as evidenced by their long life-time, spanning many orders of magnitude of the characteristic growth-time of these instabilities. Anchoring of the foot points of the field lines in the photosphere is generally considered to be the agent responsible for stabilization. This effect is analogous to that of the stabilization of external kink modes in a tokamak by means of RF fields induced by a poloidal antenna structure. Given the overall MHD stability of a coronal magnetic loop structure, analysis of Alfven wave heating by means of the continuous spectrum may be undertaken. Here, an additional complication is encountered which turns out to be quite beneficial though from the point of view of heating efficiency: the crossing of the stable branch of the external kink mode through the continuous spectrum. This gives rise to improper modes which have both a global character and a non-integrable part which admits quasi-dissipation. ESA

N89-24926# Katholieke Universiteit te Leuven (Belgium). Inst. of Astronomy.
CORONAL HEATING BY RESONANT ABSORPTION IN RESISTIVE MHD **c92**
S. Poedts, M. Goossens, and W. Kerner (Max-Planck-Inst. fuer Physik und Astrophysik, Garching, Germany, F.R.) *In* ESA, Proceedings of an International School and Workshop on Plasma Astrophysics, Volume 1 Jan. 1989 p 107-110 (For primary document see N89-24910 18-75)
(Contract EEC-ST2J-0275-C)
Avail: NTIS HC A18/MF A01; ESA Publications Div., ESTEC, Noordwijk, Netherlands, 45 US dollars or 80 Dutch guilders

The heating of coronal loops by the process of resonant absorption of Alfven waves is studied in compressible, resistive magnetohydrodynamics. A one dimensional, cylindrical-symmetric plasma column excited periodically by means of an external driver is considered. The intrinsic dissipation spectrum which is

independent of the external driver (whose power spectrum is not known) reveals interesting features of heating by resonant absorption. Resonant absorption is very efficient for typical coronal loop parameter values. A considerable part of the energy supplied by the external driver is dissipated ohmically and converted into heat. The energy dissipation rate is almost independent of the resistivity for the relevant values of this parameter. The efficiency of the heating mechanism strongly depends on the equilibrium profiles, the wave numbers, and the frequency of the external driver. ESA

N89-24927# Academy of Sciences of the Ukrainian SSR, Kiev. Inst. of Physics and Technology.
SINGULARITIES OF THE LOCAL MHD-RESONANCES IN SOLAR CHROMOSPHERE PLASMA **c92**
V. I. Lapshin, K. N. Stepanov, and E. A. Fedutenko *In* ESA, Proceedings of an Internatinal School and Workshop on Plasma Astrophysics, Volume 1 Jan. 1989 p 111-114 (For primary document see N89-24910 18-75)
Avail: NTIS HC A18/MF A01; ESA Publications Div., ESTEC, Noordwijk, Netherlands, 45 US dollars or 80 Dutch guilders

The dissipation of the energy of the forced oscillations stipulated by convective motions at the Sun, in the local cusp-resonance regions in the high Beta chromosphere plasma is considered. If the Alfven velocity has the extremum in the resonance point the width of the resonance region and the power absorption increase. Conditions when the nonlinear effects become essential and may lead to the forming of the nonlinear (discontinuous) flows in the cusp-layer are obtained. ESA

N89-24928# California Univ., Berkeley. Dept. of Astronomy.
RELATIVISTIC SHOCKS IN ELECTRON-POSITRON PLASMAS AND POLAR CAP ACCRETION ONTO NEUTRON STARS: TWO NON-LINEAR PROBLEMS IN ASTROPHYSICAL PLASMA PHYSICS
J. Arons *In* ESA, Proceedings of an International School and Workshop on Plasma Astrophysics, Volume 1 Jan. 1989 p 117-124 Prepared in cooperation with Lawrence Livermore National Lab., CA (For primary document see N89-24910 18-75)
(Contracts W-7405-eng-48; NSF AST-86-15816; IGPP-89-11)
Avail: NTIS HC A18/MF A01; ESA Publications Div., ESTEC, Noordwijk, Netherlands, 45 US dollars or 80 Dutch guilders

Particle simulations and theory of relativistic shock waves in an e+ e- plasma simulation are outlined. Magnetic reflection of particles is an essential role in the shock structure. Instability of the reflected particles in the shock front produces intense extraordinary mode radiation. Such shocks are candidates for the particle accelerator in plerions and in extragalactic jets only if the upstream Poynting flux composes no more than 10 percent of the total. Analytical and numerical studies of radiation dominated accretion onto the magnetic poles of neutron stars are summarized. The upper limit to the photon luminosity depends upon magnetic confinement, not upon the dragging of photons into the star. Numerical solutions show the plasma forms large scale photon bubbles. The percolative loss of radiation controls the pressure and therefore the limits of magnetic confinement. Loss of magnetic confinement through resistive interchange instability is suggested as a means of generating TeV to PeV voltage drops along the magnetic field. ESA

N89-24929# Academy of Sciences (USSR), Moscow. Inst. of Space Research.
GENERATION OF X-RAY AND RADIO EMISSION BY BINARY WOLF-RAYET STARS **c93**
A. A. Galeev, N. N. Pilyugin, and V. V. Usov *In* ESA, Proceedings of an International School and Workshop on Plasma Astrophysics, Volume 1 Jan. 1989 p 125-129 (For primary document see N89-24910 18-75)
Avail: NTIS HC A18/MF A01; ESA Publications Div., ESTEC, Noordwijk, Netherlands, 45 US dollars or 80 Dutch guilders

The supersonic flow of the ionized gas in WR+OB binaries and X-ray generation are considered. X-ray emission is caused by gas heating up to temperatures of 10 million to 100 million K behind the front of shock waves which are formed in the collision of gas flowing out from the WR star with either the OB star's surface, or the gas of the OB star's wind. The distribution of hot gas temperature and concentration behind the shock front are obtained. Using these distribution, the spectral power of bremsstrahlung X-ray emission of hot gas is calculated. The probable nature of the WR star nonthermal radio emission is also discussed. ESA

N89-24930# Dublin Inst. for Advanced Studies (Ireland). School of Cosmic Physics.
PARTICLE ACCELERATION AND SHOCK WAVE STRUCTURE **c90**
L. OC. Drury *In* ESA, Proceedings of an International School and Workshop on Plasma Astrophysics, Volume 1 Jan. 1989 p 131-135 (For primary document see N89-24910 18-75)
Avail: NTIS HC A18/MF A01; ESA Publications Div., ESTEC, Noordwijk, Netherlands, 45 US dollars or 80 Dutch guilders

The role of particle acceleration in the large-scale structure and evolution of strong collisionless shocks under astrophysical conditions is considered. The reaction of these particles on the dynamical structure of the shock wave is discussed theoretically and in the light of numerical calculations. Astrophysical implications for the evolution of supernova remnants are considered. ESA

N89-24931# California Univ., Los Angeles.
RELATIVISTIC MHD FROM TWO-FLUID HYDRODYNAMICS (TFHD)
C. F. Kennel, M. E. Gedalin, and J. G. Lominadze (Abastumani Astrophysical Observatory, Georgia, USSR) *In* ESA, Proceedings of an International School and Workshop on Plasma Astrophysics, Volume 1 Jan. 1989 p 137-141 (For primary document see N89-24910 18-75)
Avail: NTIS HC A18/MF A01; ESA Publications Div., ESTEC, Noordwijk, Netherlands, 45 US dollars or 80 Dutch guilders

It is shown that the expected MHD equations may be derived from the relativistic two-fluid hydrodynamical equations, when current velocities are assumed negligible when compared to the mass flow velocity. It is found that MHD does not work in the inner part of the pulsar magnetosphere at radii smaller than that of the light cylinder. The plasma has a very anisotropic pressure and one can expect the firehose instability to develop from only the light cylinder. However, MHD works in the outer parts of the magnetosphere. ESA

N89-24932# Abastumani Astrophysical Observatory, Georgia (USSR).
THE STRUCTURE OF QUASIPERPENDICULAR COLLISIONLESS SHOCKS
M. E. Gedalin and J. G. Lominadze *In* ESA, Proceedings of an International School and Workshop on Plasma Astrophysics, Volume 1 Jan. 1989 p 143-151 (For primary document see N89-24910 18-75)
Avail: NTIS HC A18/MF A01; ESA Publications Div., ESTEC, Noordwijk, Netherlands, 45 US dollars or 80 Dutch guilders

A quasiperpendicular shock is considered as a structure evolved from a fast magnetosonic nonlinear wave. Due to the steepening and tendency towards overturning the scales become smaller and the ramp is an intermediate whistler. The noncoplanar magnetic field component in the ramp appears in a quite natural way. The ramp is characterized by a large peak of the potential electric field, its width is much smaller than the ramp width. It is shown that in such a case electrons are heated efficiently. Ions are heated also; the heating process is closely related to the shock drift acceleration. ESA

N89-24933*# Iowa Univ., Iowa City. Dept. of Physics and Astronomy.
SHOCK-ASSOCIATED PLASMA DENSITY FLUCTUATIONS IN THE INTERSTELLAR MEDIUM
S. R. Spangler *In* ESA, Proceedings of an International School and Workshop on Plasma Astrophysics, Volume 1 Jan. 1989

p 153-155 (For primary document see N89-24910 18-75)
(Grants NAGw-806; NAGw-831)
Avail: NTIS HC A18/MF A01; ESA Publications Div., ESTEC, Noordwijk, Netherlands, 45 US dollars or 80 Dutch guilders
CSCL 20I

Theories of diffuse shock acceleration of the cosmic rays that predict that there should be regions of intense Alfven waves both upstream and downstream of the shock front are considered. Observations of similar waves near solar system shock waves show that they produce substantial density fluctuations. Such density fluctuations might produce observable scattering of radio waves. Observations which searched for angular broadening or blurring of radio sources whose lines of sight pass close to or through supernova remnants are discussed. No definite cases of remnant-associated scattering are detected. However, the source CL 4, which is viewed through the Cygnus Loop supernova remnant, may be such an object and merits further observation. ESA

N89-24934# Observatoire de Paris-Meudon (France).
EXTENDED CORONAL SHOCK WAVES AND ELECTRON ACCELERATION DURING SOLAR FLARES **c92**
K.-L. Klein, G. Trottet, A. O. Benz, and S. R. Kane (California Univ., Berkeley.) *In* ESA, Proceedings of an International School and Workshop on Plasma Astrophysics, Volume 1 Jan. 1989 p 157-160 (For primary document see N89-24910 18-75)
Avail: NTIS HC A18/MF A01; ESA Publications Div., ESTEC, Noordwijk, Netherlands, 45 US dollars or 80 Dutch guilders

The radio signature of coronal shock waves and its relation to energetic electrons in the low solar atmosphere were studied, using hard X-ray and wide-band radio observations with high time resolution. The results suggest that the extended coronal shock wave plays a minor part in the acceleration of relativistic electrons observed in the low corona. ESA

N89-24935# Royal Observatory, Edinburgh (Scotland).
THE FORMATION OF INTERSTELLAR CLOUDS **c90**
M. D. Smith *In* ESA, Proceedings of an International School and Workshop on Plasma Astrophysics, Volume 1 Jan. 1989 p 161-164 (For primary document see N89-24910 18-75)
Avail: NTIS HC A18/MF A01; ESA Publications Div., ESTEC, Noordwijk, Netherlands, 45 US dollars or 80 Dutch guilders

The collapse of a cooling interstellar protocloud is investigated. Confinement is by an ambient medium rather than gravity. Large-scale thermal and magnetic pressure gradients across the cloud guide the collapse. The hot cloud is kept close to uniform by a short sound-crossing time. Prolate and oblate clouds with criteria for internal shock formation are analyzed. Cool disks and filaments are formed from the spheroidal protoclouds. The type of collapse and final sheet column density depends sensitively on the cooling function. Further collapse, if constrained to take place along field lines, then produces cold filamentary structures and striated sheets. ESA

N89-24936# Academy of Sciences (USSR), Moscow. Inst. of Space Research.
THE ROLE OF WHISTLER OSCILLATIONS IN THE FORMATION OF THE STRUCTURE OF HIGH MACH NUMBER COLLISIONLESS SHOCK **c90**
A. A. Galeev, C. F. Kennel, V. V. Krasnoselskikh, and V. V. Lobzin (Academy of Sciences, USSR, Troitsk) *In* ESA, Proceedings of an International School and Workshop on Plasma Astrophysics, Volume 1 Jan. 1989 p 165-171 (For primary document see N89-24910 18-75)
Avail: NTIS HC A18/MF A01; ESA Publications Div., ESTEC, Noordwijk, Netherlands, 45 US dollars or 80 Dutch guilders

It is shown that critical Mach number formation of the structure of the front of collisionless shock is concerned with nonlinear solitary wave packet of whistler oscillations. This critical Mach number is not the same as usually defined when ohmic dissipation alone cannot provide necessary dissipation. The consequences of this are that the gradients in the region of ramp are defined by dispersive length of the whistler oscillations; and maximum amplitude of the magnetic field is approximately of the order of value of the amplitude of the stationary points of the system of equations which describe the nonlinear waves. This provides a much larger number of the reflected ions and these ions formate foot region. Such a picture is variable because of the decay instability of the whistler waves and auto-oscillations of nonlinear whistler waves, because of the dependence of the number of reflected ions which produce the main part of dissipation from the maximum amplitude of overshoot. ESA

N89-24937# Academy of Sciences (USSR), Moscow. Inst. of Space Research.
QUASI-PERPENDICULAR COLLISIONLESS HIGH MACH NUMBER SHOCKS **c90**
A. A. Galeev, C. F. Kennel, and V. V. Krasnoselskikh (Academy of Sciences, USSR, Troitsk) *In* ESA, Proceedings of an International School and Workshop on Plasma Astrophysics, Volume 1 Jan. 1989 p 173-183 (For primary document see N89-24910 18-75)
Avail: NTIS HC A18/MF A01; ESA Publications Div., ESTEC, Noordwijk, Netherlands, 45 US dollars or 80 Dutch guilders

The problems of stationarity of high Mach number quasiperpendicular collisionless shocks are discussed. The data of particle and wave experiments of Intershock-Prognoz-10 and Prognoz-8 are used to support the hypothesis that high Mach number shocks are nonstationary and their parameters can have quasiperiodical time variations. The problems of computer simulation of dynamics of high Mach number shocks are also discussed. ESA

N89-24938# Saint Andrew's Univ. (Scotland). Dept. of Mathematical Sciences.
STRUCTURING OF PLASMAS BY A MAGNETIC FIELD
E. R. Priest *In* ESA, Proceedings of an International School and Workshop on Plasma Astrophysics, Volume 1 Jan. 1989 p 189-195 Sponsored by the United Kingdom Science and Engineering Research Council (For primary document see N89-24910 18-75)
Avail: NTIS HC A18/MF A01; ESA Publications Div., ESTEC, Noordwijk, Netherlands, 45 US dollars or 80 Dutch guilders

It is suggested that the highly structured nature of the solar corona can be understood in terms of standing MHD disturbances of several types, spread over extended regions. They can be compressions (fast or slow mode), in which the plasma pressure increases, or expansions (fast or slow mode) in which it decreases. Such interactions are also present in the inflow region of 2D steady-state magnetic reconnection models. Reconnection of 3D magnetic fields occurs when an electric field exists along a singular line (a field line with an X-type topology nearby). In general a sheared field possesses a continuum of potential singular lines and which one supports reconnection depends on the flow or electric field. Constraints on the electric field and flow are presented for reconnection at a given singular line. Such reconnection is accompanied by strong plasma jetting along the singular line. It is proposed that solar prominences are located in large curved flux tubes which are twisted up by Coriolis forces. When the twist is large enough the magnetic field near the summit has the required curvature to support plasma against gravity. As the twist increases the prominence grows in length and eventually loses equilibrium and erupts outwards into interplanetary space with a coronal mass ejection. ESA

N89-24939# Princeton Univ., NJ. Plasma Physics Lab.
THE CASE FOR A PRIMORDIAL GALACTIC FIELD **c90**
R. Kulsrud *In* ESA, Proceedings of an International School and Workshop on Plasma Astrophysics, Volume 1 Jan. 1989 p 197-201 (For primary document see N89-24910 18-75)
(Contract DE-AC02-76CH-03073)
Avail: NTIS HC A18/MF A01; ESA Publications Div., ESTEC, Noordwijk, Netherlands, 45 US dollars or 80 Dutch guilders

Two theories of the origin of the galactic magnetic field are discussed. It is shown that the first theory, of its generation by a fast magnetic dynamo, is limited by the properties of the interstellar medium which suppress the small scale motions in the turbulence,

and thus inhibit the generation of the field from a small seed field. The second theory that the galactic field is a relic of a general cosmic magnetic field existing prior to formation of our galaxy is discussed. It is pointed out that such a field would evolve to a field very similar to that which we see today. ESA

N89-24940# Dublin Inst. for Advanced Studies (Ireland). School of Cosmic Physics.

COSMIC RAYS: A SHORT SURVEY OF OPEN PROBLEMS **c93**

L. OC. Drury *In* ESA, Proceedings of an International School and Workshop on Plasma Astrophysics, Volume 1 Jan. 1989 p 205-207 (For primary document see N89-24910 18-75)
Avail: NTIS HC A18/MF A01; ESA Publications Div., ESTEC, Noordwijk, Netherlands, 45 US dollars or 80 Dutch guilders

Cosmic ray observations are summarized and compared with theory. Spectrum; anisotropy data; composition; and source power are discussed. ESA

N89-24941# Academy of Sciences (USSR), Moscow. Physical Inst.

THEORY OF RADIOEMISSION OF PULSARS **c93**

V. S. Beskin, A. V. Gurevich, and Ya. N. Istomin *In* ESA, Proceedings of an International School and Workshop on Plasma Astrophysics, Volume 1 Jan. 1989 p 209-217 (For primary document see N89-24910 18-75)
Avail: NTIS HC A18/MF A01; ESA Publications Div., ESTEC, Noordwijk, Netherlands, 45 US dollars or 80 Dutch guilders

A theory of excitation, stabilization, and propagation of electromagnetic oscillations in the relativistic plasma of pulsar magnetosphere is compared with observations. Starting point of the theory is relativistic electron-positron plasma flux flowing along open field lines in pulsar magnetosphere. This flux is unstable; curvature-plasma modes are intensily generated in it. The study of nonlinear processes shows that there proceeds a nonlinear saturation and transformation of such modes into transverse electromagnetic waves capable of leaving the magnetosphere of a neutron star. These outgoing waves are, in fact, pulsar radio emission. It is shown that using the model, it is possible to explain practically all the basic characteristics of observed pulsar radio emission. ESA

N89-24942# Academy of Sciences, Potsdam (German D.R.). Central Inst. for Astrophysics.

ADIABATIC, CHAOTIC AND QUASI-ADIABATIC CHARGED PARTICLE MOTION IN TWO-DIMENSIONAL MAGNETIC FIELD REVERSALS

J. M. Buechner and L. M. Zelenyi (Academy of Sciences, USSR, Moscow) *In* ESA, Proceedings of an International School and Workshop on Plasma Astrophysics, Volume 1 Jan. 1989 p 219-226 (For primary document see N89-24910 18-75)
Avail: NTIS HC A18/MF A01; ESA Publications Div., ESTEC, Noordwijk, Netherlands, 45 US dollars or 80 Dutch guilders

The problem of the dynamical behavior of charged particles in two-dimensional magnetic field reversals was analyzed. Discrete mappings instead of the original differential equations of motion, were used to determine the border of regularity and the transition to deterministic chaos, to provide a comprehensive investigation also of the nonadiabatic case, where the magnetic moment is not adiabatically constant. The nonlinear particle dynamics is shown to be controlled by a parameter which includes the peculiarity of the field geometry in the reversal region and the particle's energy (i.e., its total velocity). ESA

N89-24943# Academy of Sciences (USSR), Moscow. Inst. of Space Research.

QUASI-ADIABATIC PARTICLE ACCELERATION IN MAGNETIC FIELD REVERSALS AND THE FORMATION OF THE PLASMA SHEET BOUNDARY LAYER IN THE EARTH'S MAGNETOTAIL **c46**

L. M. Zelenyi, D. V. Zogin, and J. M. Buechner (Academy of Sciences, Potsdam, German D.R.) *In* ESA, Proceedings of an International School and Workshop on Plasma Astrophysics, Volume 1 Jan. 1989 p 227-234 (For primary document see N89-24910 18-75)
Avail: NTIS HC A18/MF A01; ESA Publications Div., ESTEC, Noordwijk, Netherlands, 45 US dollars or 80 Dutch guilders

The acceleration of magnetic field reversal (MFR) particles in the stationary and homogeneous electric field induced by the motion of MFR through the ambient plasma (i.e., solar wind) is considered. Assuming that the time scale of acceleration is slow in comparison with the period of orbital motion, the longitudinal invariant is introduced to describe the process of acceleration in a closed form and to obtain the laws governing the quasiadiabatic ion acceleration in the Earth's magnetotail. The similarities and differences in adiabatic and quasiadiabatic acceleration mechanisms are discussed. The results give insights to the problem of particle heating in the Earth's magnetotail and to the formation of accelerated plasma streams along the edges of the plasma sheet. ESA

N89-24944# Academy of Sciences (USSR), Moscow. Inst. of General Physics.

RADIATIVE-RESONANT MHD INTERACTIONS BETWEEN WAVES AND PARTICLES AND THE PROBLEM OF COSMIC-RAY SPECTRA **c93**

V. N. Tsytovich *In* ESA, Proceedings of an International School and Workshop on Plasma Astrophysics, Volume 1 Jan. 1989 p 235-238 (For primary document see N89-24910 18-75)
Avail: NTIS HC A18/MF A01; ESA Publications Div., ESTEC, Noordwijk, Netherlands, 45 US dollars or 80 Dutch guilders

It is shown that radiative-resonant MHD acceleration can explain the whole cosmic ray spectra for a general case of anisotropic MHD turbulence without any serious restrictions on the domain of the applicability of the results. There is the possibility not only for an explanation of jet formation but also for the generation of power-law spectrum of cosmic ray electrons in turbulence created in the interaction of jets with intergalactic medium. The estimates given show only the existence of new lines in a possible interpretation of observations. A more detailed theoretical consideration should be based on the radiative-resonant interactions together with other nonlinear and quasilinear interactions. But the given estimates take into account the most important features of radiative resonant interactions of MHD waves with cosmic rays. ESA

N89-24945*# Iowa Univ., Iowa City. Dept. of Physics and Astronomy.

EFFECTS OF UNEQUAL PARTICLE NUMBER DENSITIES ON ALFVEN WAVES

I. H. Cairns *In* ESA, Proceedings of an International School and Workshop on Plasma Astrophysics, Volume 1 Jan. 1989 p 239-242 (For primary document see N89-24910 18-75)
(Grants NAGw-831; NSF ATM-87-16770)
Avail: NTIS HC A18/MF A01; ESA Publications Div., ESTEC, Noordwijk, Netherlands, 45 US dollars or 80 Dutch guilders
CSCL 20I

Analytic plasma theory and numerical solutions of the dispersion equation are used to show that the assumption that the linear properties of the waves are determined by a charge-neutral plasma in the absence of the nonthermal particles, while the nonthermal particles cause growth or additional damping superposed onto the background, is seriously flawed even for stable plasmas. Even when the nonthermal particles do not contribute significantly to the dispersion equation, unequal thermal electron and ion number densities (due to the presence of the nonthermal particles) may cause fundamental low wave number modifications to the Alfven modes, including the creation of a new resonance and severely modified dispersion. These results are found for both cold and warm plasmas. Previous work on Alfven waves should be reevaluated in view of these results. ESA

N89-24946# Washington Univ., Saint Louis, MO. Dept of Physics.

A NEW MODEL OF PeV GAMMA-RAY SOURCES **c93**

I. A. Smith and J. I. Katz *In* ESA, Proceedings of an International

School and Workshop on Plasma Astrophysics, Volume 1 Jan. 1989 p 243-246 (For primary document see N89-24910 18-75)
Avail: NTIS HC A18/MF A01; ESA Publications Div., ESTEC, Noordwijk, Netherlands, 45 US dollars or 80 Dutch guilders

A model for the proton acceleration connected with accreting X-ray binaries is proposed. Acceleration is assumed to occur on the closed (dipole) field lines of the neutron star where the density is low and collisional losses of the energetic protons are small. Protons can be mirrored at the poles and become trapped, affording time for them to be accelerated gradually. Eventually, high energy protons escape by diffusing onto open field lines. It is postulated that potential energy of the matter accreting on the open field lines is transferred to Alfven waves that accelerate the protons on the closed field lines. Proton synchrotron radiation may be detectable from the GeV gamma-ray region to the infrared. ESA

N89-24947*# California Inst. of Tech., Pasadena. Inst. of Theoretical Physics.
NEUTRON STARQUAKES AND THE NATURE OF GAMMA-RAY BURSTS **c93**
P. Madau, O. Blaes, R. D. Blandford, and P. Goldreich *In* ESA, Proceedings of an International School and Workshop on Plasma Astrophysics, Volume 1 Jan. 1989 p 247-250 (For primary document see N89-24910 18-75)
(Grants NAGw-1303; NSF AST-86-15325; NSF AST-86-1279)
Avail: NTIS HC A18/MF A01; ESA Publications Div., ESTEC, Noordwijk, Netherlands, 45 US dollars or 80 Dutch guilders
CSCL 03B

The possibility that gamma-ray bursts originate from quakes deep in the solid crust of a neutron star is investigated. Seismic waves are radiated if shear stress is relieved by brittle fracture. However they cannot propagate directly to the surface but are temporarily trapped below a reflecting layer. The shaking of the stellar surface couples the seismic waves to Alfven waves which propagate out into the magnetosphere. The crust-magnetosphere transmission coefficient strongly increases with wave frequency and magnetic field strength. Alfven wave luminosities sufficient to power galactic gamma-ray bursts are possible if magnetic fields greater than 100 billion G cover at least part of the stellar surface. As the Alfven waves propagate out into the low density magnetosphere, they become increasingly charge starved, thereby accelerating particles to relativistic energies. ESA

N89-24948*# Iowa Univ., Iowa City. Dept. of Physics and Astronomy.
ARE SUPERNOVA REMNANTS QUASI-PARALLEL OR QUASI-PERPENDICULAR ACCELERATORS **c90**
S. R. Spangler, J. A. Leckband, and I. H. Cairns *In* ESA, Proceedings of an International School and Workshop on Plasma Astrophysics, Volume 1 Jan. 1989 p 251-254 (For primary document see N89-24910 18-75)
(Grants NAGw-806; NAGw-831)
Avail: NTIS HC A18/MF A01; ESA Publications Div., ESTEC, Noordwijk, Netherlands, 45 US dollars or 80 Dutch guilders
CSCL 03B

Observations of shock waves in the solar system which show a pronounced difference in the plasma wave and particle environment depending on whether the shock is propagating along or perpendicular to the interplanetary magnetic field are discussed. Theories for particle acceleration developed for quasi-parallel and quasi-perpendicular shocks, when extended to the interstellar medium suggest that the relativistic electrons in radio supernova remnants are accelerated by either the Q parallel or Q perpendicular mechanisms. A model for the galactic magnetic field and published maps of supernova remnants were used to search for a dependence of structure on the angle Phi. Results show no tendency for the remnants as a whole to favor the relationship expected for either mechanism, although individual sources resemble model remnants of one or the other acceleration process. ESA

N89-24949# Academy of Sciences (USSR), Moscow. Inst. of Space Inst.
TWO-STREAM INSTABILITY IN PULSAR MAGNETOSPHERES
V. V. Usov *In* ESA, Proceedings of an International School and Workshop on Plasma Astrophysics, Volume 1 Jan. 1989 p 257-260 (For primary document see N89-24910 18-75)
Avail: NTIS HC A18/MF A01; ESA Publications Div., ESTEC, Noordwijk, Netherlands, 45 US dollars or 80 Dutch guilders

Reasons that could produce two-stream instability in pulsar plasma are discussed. It is noted that if the outflow of electron-positron plasma from the pulsar vicinity is stationary, this instability either is stabilized, or its growth rate is so low that the plasma leaves the pulsar magnetosphere before the instability is developed. The electron-positron plasma creation near a pulsar may be a very nonstationary process. If this nonstationarity is accounted for, the situation radically changes allowing the two-stream instability development in the pulsar plasma. ESA

N89-24950# Abastumani Astrophysical Observatory, Georgia (USSR).
SMALL-SCALE INSTABILITIES IN ACCRETION DISKS OF COMPACT OBJECTS AND THEIR MANIFESTATIONS **c90**
G. D. Chagelishvili, R. G. Chanishvili, and J. G. Lominadze *In* ESA, Proceedings of an International School and Workshop on Plasma Astrophysics, Volume 1 Jan. 1989 p 261-264 (For primary document see N89-24910 18-75)
Avail: NTIS HC A18/MF A01; ESA Publications Div., ESTEC, Noordwijk, Netherlands, 45 US dollars or 80 Dutch guilders

Small-scale hydrodynamic instabilities (shear instability and thermal convections) which can provide turbulization of accretion disks of compact objects were analyzed. Domains of the existence of each of these instabilities are determined; it is shown that shear turbulence has no gyrotropic nature, while the thermal convection has and can generate a large-scale magnetic field. Sequences of the difference in statistic characteristics of these turbulences are described depending on the extensions of the domains of their existence. ESA

N89-24951# Abastumani Astrophysical Observatory, Georgia (USSR).
PROBLEM OF NONROTATING BLACK HOLE ACCRETION DISK MAIN ENERGY RELEASE REGION EXTENSION **c90**
G. D. Chagelishvili, J. G. Lominadze, and A. D. Rogava *In* ESA, Proceedings of an International School and Workshop on Plasma Astrophysics, Volume 1 Jan. 1989 p 265-269 (For primary document see N89-24910 18-75)
Avail: NTIS HC A18/MF A01; ESA Publications Div., ESTEC, Noordwijk, Netherlands, 45 US dollars or 80 Dutch guilders

The size of the region of the main energy release of black hole accretion disks is considered. This problem is deeply connected with accretion processes at the innermost region of accretion disk and with boundary conditions at its inner edge. It is demonstrated that the region of the main energy release is strongly localized. It is shown that for accretion onto nonrotating black holes the main portion of the liberated energy is released within a rather narrow radial range of 5 to 13 M. This property can have profound effects on spectrum and variability of the radiation of the accretion disk as a whole. In particular, the asymmetry of the main energy release region is favorable for the mechanism of the millisecond variability. ESA

N89-24952# Abastumani Astrophysical Observatory, Georgia (USSR).
ON THE NATURE OF A TYPICAL PULSARS RADIO EMISSION **c32**
A. Z. Kazbegi, G. Z. Machabeli, G. I. Melikidze, and V. V. Usov (Academy of Sciences, USSR, Moscow) *In* ESA, Proceedings of an International School and Workshop on Plasma Astrophysics, Volume 1 Jan. 1989 p 271-276 (For primary document see N89-24910 18-75)
Avail: NTIS HC A18/MF A01; ESA Publications Div., ESTEC, Noordwijk, Netherlands, 45 US dollars or 80 Dutch guilders

The possibility of the excitation of electromagnetic (t) as well

as of longitudinal-transverse (lt) waves in the magnetosphere of a typical pulsar is discussed. Two mechanisms of the t-wave excitation exist. The first is connected with the cyclotron resonance between t-waves and high-energy particles of both the tail of the distribution function and the primary beam. The second mechanism is conditioned by particle drift motion and needs to satisfy a Cherenkov resonance condition. Due to the second mechanism lt-wave excitation is also possible. The waves excited due to the cyclotron instability cause the diffusion of particles across the magnetic field. For sufficiently large pitch angles, t-wave excitation is also possible. ESA

N89-24953# Abastumani Astrophysical Observatory, Georgia (USSR).
ON THE MECHANISM OF THE FORMATION OF THE POLARIZATION CHARACTERISTICS OF PULSAR RADIATION **c93**
A. Z. Kazbegi, G. Z. Machabeli, and G. I. Melikidze *In* ESA, Proceedings of an International School and Workshop on Plasma Astrophysics, Volume 1 Jan. 1989 p 277-280 (For primary document see N89-24910 18-75)
Avail: NTIS HC A18/MF A01; ESA Publications Div., ESTEC, Noordwijk, Netherlands, 45 US dollars or 80 Dutch guilders

A model of radiation is used to explain characteristics of individual pulses of pulsars. Mode changing, existence of two orthogonal polarization modes, and rapid change of position angles from pulse to pulse are treated. ESA

N89-24954# Massachusetts Inst. of Tech., Cambridge. Center for Theoretical Geo/Cosmo Plasma Physics.
GLOBAL KINETIC THEORY OF ASTROPHYSICAL JETS
T. Chang *In* ESA, Proceedings of an International School and Workshop on Plasma Astrophysics, Volume 1 Jan. 1989 p 281-283 (For primary document see N89-24910 18-75)
Avail: NTIS HC A18/MF A01; ESA Publications Div., ESTEC, Noordwijk, Netherlands, 45 US dollars or 80 Dutch guilders

It is suggested that an astrophysical plasma stream flowing outward from a central object along an open magnetic field line with decreasing field strength generally has anisotropic velocity distributions. The electron distribution function of this type of plasma streams contains a thermally populated region and a stretched out high energy tail (or jet-like) region collimated in the outward direction of the magnetic field line. The argument is based on a global, collisional, kinetic theory. Because the kinetic jets are always pointed along the outward direction of the field lines, they are automatically collimated and assume the geometries dictated by the magnetic field. This result should be useful in the understanding of the basic structures of astrophysical objects as extragalactic radio jets, stellar winds, the solar wind, planetary polar winds, and galactic jets (e.g., SS433). ESA

N89-24955# Massachusetts Inst. of Tech., Cambridge. Center for Theoretical Geo/Cosmo Plasma Physics.
NONLINEAR OBLIQUE WHISTLERS: THEIR RELEVANCE TO NONTHERMAL COUPLING OF IONS AND ELECTRONS IN ACCRETION FLOW AND SUPERCRITICAL QUASI-PERPENDICULAR COLLISIONLESS SHOCKS
T. Chang *In* ESA, Proceedings of an International School and Workshop on Plasma Astrophysics, Volume 1 Jan. 1989 p 285-289 (For primary document see N89-24910 18-75)
Avail: NTIS HC A18/MF A01; ESA Publications Div., ESTEC, Noordwijk, Netherlands, 45 US dollars or 80 Dutch guilders

It is demonstrated that oblique whistlers may be effective in coupling and energizing plasma populations during accretion flow onto massive central objects such as black holes. These plasma collective modes could be excited by inverse ion-populations in perpendicular velocity space such as the ring-like and loss-cone type of distributions, or cross-field drifts induced by the gravitational and magnetic fields, reflection across high-Mach number collisionless shocks, density and/or magnetic field gradients. Nonlinear and turbulent states of these plasma collective modes can accelerate the electrons to large energies. It is suggested that the same nonlinear plasma modes may play a central role in the description of the structure of supercritical quasi-perpendicular collisionless shocks. ESA

N89-24956# Ecole Polytechnique, Palaiseau (France). Centre de Physique Theorique.
STRONG LANGMUIR TURBULENCE AND THE PULSAR EMISSION MECHANISM
E. Asseo, G. Pelletier, and H. Sol (Observatoire de Paris-Meudon, France) *In* ESA, Proceedings of an International School and Workshop on Plasma Astrophysics, Volume 1 Jan. 1989 p 291-294 (For primary document see N89-24910 18-75)
Avail: NTIS HC A18/MF A01; ESA Publications Div., ESTEC, Noordwijk, Netherlands, 45 US dollars or 80 Dutch guilders

The pulsar emission mechanism based on the plasma beam interaction is examined. The linear study shows that, due to obliquity of wave propagation and to magnetic field line curvature, the resulting unstable Langmuir waves have simultaneously electrostatic and electromagnetic features. The nonlinear analysis produces Langmuir solitons with associated electromagnetic features in a quite natural way. These features are compared to the characteristics of observed pulsar radio emission. ESA

N89-24957# Grenoble-1 Univ., Saint Martin d'Heres (France).
JETS AND BEAMS IN POWERFUL EXTRAGALACTIC RADIO SOURCES **c93**
G. Pelletier, J. Roland, H. Sol, and E. Asseo (Ecole Polytechnique, Palaiseau, France) *In* ESA, Proceedings of an Internatioal School and Workshop on Plasma Astrophysics, Volume 1 Jan. 1989 p 295-297 Sponsored in part by CNRS, France (For primary document see N89-24910 18-75)
Avail: NTIS HC A18/MF A01; ESA Publications Div., ESTEC, Noordwijk, Netherlands, 45 US dollars or 80 Dutch guilders

It is argued that extensions are needed for jet models of extragalactic radio sources which consider a single relativistic plasma with relativistic motion from short distances (few pc) to large distances (few 100 kpc) from the nucleus. Besides the interest in developing plasma physics motivated by these objects, there are two reasons for enriching the physics. First, the interpretation of hot spots as resulting from shocks with diffusive acceleration in a thermal classical plasma with a tenuous relativistic component is consistent with data and constrain the parameters. Second, the interpretation of relativistic motions on parsec scales as resulting from a core beam relaxing in a collimated wind is consistent with data and avoid several difficulties. ESA

N89-24958# Osservatorio Astronomico, Turin (Italy).
SYNCHROTRON THERMAL INSTABILITIES AND FILAMENTATION IN RADIO SOURCES
G. Bodo, A. Ferrari, S. Massaglia, and E. Trussoni (Consiglio Nazionale delle Ricerche, Turin, Italy) *In* ESA, Proceedings of an International School and Workshop on Plasma Astrophysics, Volume 1 Jan. 1989 p 299-302 (For primary document see N89-24910 18-75)
Avail: NTIS HC A18/MF A01; ESA Publications Div., ESTEC, Noordwijk, Netherlands, 45 US dollars or 80 Dutch guilders

The thermal instability of a magnetized plasma connected with the synchrotron emission of relativistic electrons is studied, extending analyses of Simon and Axford (1967), and Eilek and Caroff (1979). The possibility of oblique propagation of unstable perturbations with respect to the magnetic field direction; and the effect of the assumption of a power law spectrum for the relativistic electrons are considered. In addition to the classical condensation mode, it is found that also slow magnetosonic waves can be driven unstable. It is proposed that the development of this instability can lead to the formation of the filamentary structures observed in the lobes of Cygn A. ESA

N89-24959# Abastumani Astrophysical Observatory, Georgia (USSR).
PULSAR RADIO AND VISIBLE RADIATION DUE TO THE MODULATION INSTABILITY OF HIGH-FREQUENCE TRANSVERSE WAVES IN THE INHOMOGENEOUS ELECTRON-POSITRON PLASMA
A. D. Pataraya, T. A. Pataraya (Tbilisi State Univ., USSR), and B. B. Chargeishvili *In* ESA, Proceedings of an International School and Workshop on Plasma Astrophysics, Volume 1 Jan. 1989 p 303-307 (For primary document see N89-24910 18-75)
Avail: NTIS HC A18/MF A01; ESA Publications Div., ESTEC, Noordwijk, Netherlands, 45 US dollars or 80 Dutch guilders

Propagation of nonlinear transverse circularly polarized waves with characteristic frequency higher than the plasma frequency along the magnetic field in an electron-positron plasma was investigated. A modulation instability with great growth rate takes plase causing an excitation of Langmuir wave and formation of a charged bunch within the pulsar light cylinder in the region with open magnetic field lines. Propagation of a nonlinear Langmuir wave with a small angle in the magnetic field in the inhomogeneous electron-positron plasma was studied, revealing linear excitation of Alfven waves with frequency in the visible range. With the help of this transverse wave a frequency profile of intensity of the pulsar visible radiation is calculated. ESA

N89-24960# Abastumani Astrophysical Observatory, Georgia (USSR).
DECAY PROCESS AND RADIATIVE TRANSFER IN PLASMAS
R. D. Lomadze *In* ESA, Proceedings of an International School and Workshop on Plasma Astrophysics, Volume 1 Jan. 1989 p 309-311 (For primary document see N89-24910 18-75)
Avail: NTIS HC A18/MF A01; ESA Publications Div., ESTEC, Noordwijk, Netherlands, 45 US dollars or 80 Dutch guilders

Equations describing two nonlinear mechanisms of radiative transfer in plasmas: Compton scattering on electrons and decay of electromagnetic waves into electromagnetic and Langmuir waves are presented. An evolution of the emission spectral line and combined action of both effects in a plasma medium with high level of turbulence is considered. ESA

N89-24961# Academy of Sciences of the Georgian SSR, Tbilisi. Inst. of Applied Mathematics.
DRIFT TURBULENCE OF PLASMA AS A GAS OF VORTEX ENSEMBLE
G. Aburdzhaniya *In* ESA, Proceedings of an International School and Workshop on Plasma Astrophysics, Volume 1 Jan. 1989 p 313-319 (For primary document see N89-24910 18-75)
Avail: NTIS HC A18/MF A01; ESA Publications Div., ESTEC, Noordwijk, Netherlands, 45 US dollars or 80 Dutch guilders

Nonlinear properties of short wavelength drift waves in a magnetoactive plasma were analyzed. It is shown that nonlinear short wavelength drift structures can excite drift turbulence in a plasma. The turbulence is assumed to be a gas of the ensemble of weakly interacting similar vortices composing the ground state. These structures contain the trapped particles and while mixing in plasma, cause fluctuation of the density and activate the processes of the transfer. The width of the density fluctuation spectrum is much greater than the value predicted by the theory of the weak turbulence, that is in a satisfactory agreement with experimental observations. In the range of moderate pulsation amplitudes, vortex turbulence leads to the anomalous diffusion of plasma particles. It is suggested that the vortex turbulence can be responsible for the anomalous transfer of the particles and the heat, observed in plasma experiments. ESA

N89-24962# Academy of Sciences (USSR), Leningrad. Inst. of Physics and Technology.
QUANTUM RELATIVISTIC THEORY OF THE CYCLOTRON RADIATION IN A STRONGLY MAGNETIZED PLASMA WITH ANISOTROPIC TEMPERATURE
V. G. Bezchastnov and G. G. Pavlov *In* ESA, Proceedings of an International School and Workshop on Plasma Astrophysics, Volume 1 Jan. 1989 p 321-326 (For primary document see N89-24910 18-75)
Avail: NTIS HC A18/MF A01; ESA Publications Div., ESTEC, Noordwijk, Netherlands, 45 US dollars or 80 Dutch guilders

The cyclotron radiation in a tenuous, strongly magnetized plasma with anisotropic temperature is considered on the basis of the quantum relativistic theory. It is shown that the quantum effects lead to oscillations in the spectra of the absorption coefficients and emissivity if the transverse temperature sufficiently exceeds the longitudinal one. Negative absorption (maser amplification) is also possible due to quantum effects in such a plasma if the angle between the magnetic field and the wave-vector is not too close to 0 or 90 deg. ESA

N89-24963# Scuola Normale Superiore, Pisa (Italy).
SOME DYNAMICAL PROPERTIES OF ANISOTROPIC COLLISIONLESS STELLAR SYSTEMS **c90**
G. Bertin and F. Pegoraro *In* ESA, Proceedings of an International School and Workshop on Plasma Astrophysics, Volume 1 Jan. 1989 p 329-333 Sponsored in part by the CNR, Italy and the Italian Ministry of Public Education (For primary document see N89-24910 18-75)
Avail: NTIS HC A18/MF A01; ESA Publications Div., ESTEC, Noordwijk, Netherlands, 45 US dollars or 80 Dutch guilders

The linear stability analysis of collisionless anisotropic spherical stellar systems is discussed. In order to study the stability of a simple and astrophysically interesting equilibrium sequence (f inf) for such stellar systems, analytical characterizations of the f inf distribution functions are described. The linearized equations for stability are formulated, and the relevant boundary conditions are discussed. ESA

N89-24964# Commissariat a l'Energie Atomique, Saclay (France). Service d'Astrophysique.
BARS AND OPEN SPIRALS IN DENSITY WAVE THEORY **c90**
M. Tagger, J. F. Sygnet, and R. Pellat (Ecole Polytechnique, Palaiseau, France) *In* ESA, Proceedings of an International School and Workshop on Plasma Astrophysics, Volume 1 Jan. 1989 p 335-340 (For primary document see N89-24910 18-75)
Avail: NTIS HC A18/MF A01; ESA Publications Div., ESTEC, Noordwijk, Netherlands, 45 US dollars or 80 Dutch guilders

It is shown that the linear theory of density waves in flat disk galaxies can describe, together with the usual tightly wound waves of Lin and Shu, a bar-like feature which always comes with the waves and dominates in the forbidden band around corotation where they are evanescent. This result is obtained analytically and confirmed by direct numerical integration of the relevant equations. The relevance of this feature to barred galaxies and to waves driven by external forcing is reviewed. ESA

N89-24965# Observatoire de Marseille (France).
GAS FLOW IN AND AROUND BARS **c90**
E. Athanassoula *In* ESA, Proceedings of an International School and Workshop on Plasma Astrophysics, Volume 1 Jan. 1989 p 341-348 (For primary document see N89-24910 18-75)
Avail: NTIS HC A18/MF A01; ESA Publications Div., ESTEC, Noordwijk, Netherlands, 45 US dollars or 80 Dutch guilders

The flow of gas in and around barred galaxies is calculated using a second order flux splitting code. For appropriate bar models shocks form along the leading edges of the bar, at positions where dust lanes are observed in barred galaxies. The existence of an inner Lindblad resonance is a necessary, though not sufficient, condition for this. The curvature of the shock loci depends on the axial ratio of the bar. ESA

N89-24966# Abastumani Astrophysical Observatory, Georgia (USSR).
MODEL OF THE CHROMOSPHERE SPICULE FORMATION **c92**
B. B. Chargeishvili, A. D. Pataraya, and A. L. Taktakishvili *In* ESA, Proceedings of an International School and Workshop on Plasma Astrophysics, Volume 1 Jan. 1989 p 349-351 (For

primary document see N89-24910 18-75)
Avail: NTIS HC A18/MF A01; ESA Publications Div., ESTEC, Noordwijk, Netherlands, 45 US dollars or 80 Dutch guilders

By means of MHD equations and based on a proposed configuration of the magnetic field, a number of spicules per supergranule is estimated and the dependence of this number on a height of a level of the spicule formation and on latitude is obtained. The close relation of the spicule number distribution with chromospheric net (supergranular structure) is explained. The possibility of structuring of diffusive magnetic field (formation of the magnetic tubes) is shown. ESA

N89-24967# Soreq Research Establishment, Israel Atomic Energy Commission, Yavneh. Plasma Physics Dept.
HIGH-PRESSURE TWO TEMPERATURE EQUATIONS OF STATE
S. Eliezer *In* ESA, Proceedings of an International School and Workshop on Plasma Astrophysics, Volume 1 Jan. 1989 p 353-357 (For primary document see N89-24910 18-75)
Avail: NTIS HC A18/MF A01; ESA Publications Div., ESTEC, Noordwijk, Netherlands, 45 US dollars or 80 Dutch guilders

A phenomenological approach is suggested for calculating two temperature equations of state at high pressures. The Thomas-Fermi Dirac model and the SESAME equation of state are used to calculate the electron contribution while the solid gas interpolation method is used for ions. An algorithm to calculate the first and higher moments of the charge distribution within the framework of the Thomas-Fermi-Dirac model is proposed. ESA

N89-24968# Abastumani Astrophysical Observatory, Georgia (USSR).
THE FORMATION OF THE SPECTRUM OF INHOMOGENEITY OF THE DARK MATTER IN PREGALACTIC COSMIC PLASMA
T. A. Kahniashvili, V. N. Lukash, and K. A. Manukjan (Tbilisi State Univ., USSR) *In* ESA, Proceedings of an International School and Workshop on Plasma Astrophysics, Volume 1 Jan. 1989 p 359-362 (For primary document see N89-24910 18-75)
Avail: NTIS HC A18/MF A01; ESA Publications Div., ESTEC, Noordwijk, Netherlands, 45 US dollars or 80 Dutch guilders

The dynamics of large-scale cosmological perturbations of density in the Universe containing, together with ordinary interacting particles, both heavy nonbaryonic particles (which today are the dynamical dark matter) and weakly interacting relativistic particles with number density as the model free parameter. Transfer functions of the growing adiabatic and isothermal perturbation modes are obtained. The dependence of parameters of the large-scale structure of the Universe on the collisionless relativistic particle number is discussed. A cosmological test of the total number of light weakly interacting particles in the Universe is proposed. ESA

N89-24969# Academy of Sciences (USSR), Moscow. Inst. of Space Research.
GENERATION OF LARGE-SCALE VORTICES IN COMPRESSIBLE HELICAL TURBULENCE **c34**
O. G. Chkhetiani and V. V. Gvaramadze (Abastumani Astrophysical Observatory, Georgia, USSR) *In* ESA, Proceedings of an International School and Workshop on Plasma Astrophysics, Volume 1 Jan. 1989 p 363-369 (For primary document see N89-24910 18-75)
Avail: NTIS HC A18/MF A01; ESA Publications Div., ESTEC, Noordwijk, Netherlands, 45 US dollars or 80 Dutch guilders

Generation of large-scale vortices in a compressible self-gravitating turbulent medium is considered. The closed equation describing evolution of the large-scale vortices in helical turbulence with finite correlation time is obtained. This equation has a form similar to the hydromagnetic dynamo equation, which allows the vortex generation effect to be called the vortex dynamo. It is possible that principally the same mechanism is responsible both for amplification and maintenance of density waves and magnetic fields in gaseous disks of spiral galaxies. ESA

N89-24970# Soreq Research Establishment, Israel Atomic Energy Commission, Yavneh. Nuclear Research Center.
INDUCED ANNIHILATION OF PARTICLE-ANTIPARTICLE PAIRS **c77**
S. Eliezer *In* ESA, Proceedings of an International School and Workshop on Plasma Astrophysics, Volume 1 Jan. 1989 p 373-379 (For primary document see N89-24910 18-75)
Avail: NTIS HC A18/MF A01; ESA Publications Div., ESTEC, Noordwijk, Netherlands, 45 US dollars or 80 Dutch guilders

A theoretical estimation is developed for coherent amplification of gamma radiation by induced annihilation of particle-antiparticle pairs, such as electron-positron. This may lead to the development of a new class of laser systems. The induced annihilation transitions for the electron-positron plasma are compared with those of the positronium medium. ESA

N89-24971# California Inst. of Tech., Pasadena.
ON THE EXISTENCE AND STABILITY OF INTERMEDIATE SHOCKS
P. S. Coppi, R. D. Blandford, and C. F. Kennel (California Univ., Los Angeles.) *In* ESA, Proceedings of an International School and Workshop on Plasma Astrophysics, Volume 1 Jan. 1989 p 381-384 (For primary document see N89-24910 18-75)
Avail: NTIS HC A18/MF A01; ESA Publications Div., ESTEC, Noordwijk, Netherlands, 45 US dollars or 80 Dutch guilders

The question of the existence of intermediate shock waves is examined. It is pointed out that the MHD Rankine-Hugoniot conditions allow up to four types of intermediate shock discontinuity and that one of these is evolutionary. Numerical simulations, analyses of spacecraft data, and theoretical arguments suggest that intermediate shocks can form and be stable. Intermediate discontinuities are classified graphically and the preshock conditions under which they can exist are elucidated. No definitive conclusion is reached concerning the physical reality of intermediate shocks. ESA

N89-24972*# Iowa Univ., Iowa City. Dept. of Physics and Astronomy.
SIMULATION OF ELECTROSTATIC ION INSTABILITIES IN THE PRESENCE OF PARALLEL CURRENTS AND TRANSVERSE ELECTRIC FIELDS
K.-I. Nishikawa, G. Ganguli, Y. C. Lee, and P. J. Palmadesso (Naval Research Lab., Washington, DC.) *In* ESA, Proceedings of an International School and Workshop on Plasma Astrophysics, Volume 1 Jan. 1989 p 385-389 (For primary document see N89-24910 18-75)
(Contracts NAGw-1239; N00173-87-M-4338; N00014-88-K-2007; NSF ATM-85-19528)
Avail: NTIS HC A18/MF A01; ESA Publications Div., ESTEC, Noordwijk, Netherlands, 45 US dollars or 80 Dutch guilders
CSCL 20I

A spatially two-dimensional electrostatic PIC simulation code was used to study the stability of a plasma equilibrium characterized by a localized transverse dc electric field and a field-aligned drift for L is much less than Lx, where Lx is the simulation length in the x direction and L is the scale length associated with the dc electric field. It is found that the dc electric field and the field-aligned current can together play a synergistic role to enable the excitation of electrostatic waves even when the threshold values of the field aligned drift and the E x B drift are individually subcritical. The simulation results show that the growing ion waves are associated with small vortices in the linear stage, which evolve to the nonlinear stage dominated by larger vortices with lower frequencies. ESA

N89-24973# Universisad de Los Andes, Merida (Venezuela). Grupo de Astrofisica.
ON THE THERMAL STABILITY OF OPTICALLY THIN FLOWS
S. M. H. Ibanez *In* ESA, Proceedings of an International School and Workshop on Plasma Astrophysics, Volume 1 Jan. 1989 p 391-395 Prepared in cooperation with International Centre for Theoretical Physics, Trieste, Italy (For primary document see N89-24910 18-75)

(Contract C-175-81)
Avail: NTIS HC A18/MF A01; ESA Publications Div., ESTEC, Noordwijk, Netherlands, 45 US dollars or 80 Dutch guilders

The linear stability of general one-dimensional steady flows of optically thin fluids with a net heat-loss function L(rho T0) (=cooling-heating) is studied analytically. Applying the Hurwitz criteria, four modes for thermal instability are found. If L = rho sup (alpha-1) T sup Beta, a cooling flow (L greater than 0) becomes unstable when Beta is less than 1+3/gamma (1-M0 sq) M0 being the Mach number (the inequality reverses for heating flows). The remaining three instability criteria are polynomial expressions of the components of the wave number k along the flow kx and perpendicular to it k1. In the space (v0, M, kx, k1) where v0 is the steady value of the velocity and M the characteristic Mach number of the flow, they determine the regions of instability.
ESA

N89-24974# European Space Agency, Paris (France).
PROCEEDINGS OF AN INTERNATIONAL SCHOOL AND WORKSHOP ON RECONNECTION IN SPACE PLASMA, VOLUME 2
T. D. Guyenne, ed. and J. J. Hunt, ed. Jan. 1989 334 p Workshop held in Postdam, Germany, D.R., 5-9 Sep. 1988; organized by Zentralinst. fuer Astrophysik, Potsdam, Germany, D.R., ESA, the Varenna-Abastumani Workshop, and Academy of Sciences, Moscow, USSR
(ESA-SP-285-Vol-2; ISSN-0379-6566; ETN-89-94476) Copyright Avail: NTIS HC A15/MF A01; ESA Publications Div., ESTEC, Noordwijk, Netherlands, 45 US dollars or 80 Dutch guilders

The general theory of magnetic field reconnection; solar reconnection; laboratory reconnection; magnetospheric reconnection; and astrophysical reconnection were discussed. For individual titles, see N89-24975 through N89-25029.

N89-24975# Ruhr Univ., Bochum (Germany, F.R.).
ASPECTS OF THREE-DIMENSIONAL MAGNETIC RECONNECTION
K. Schindler, M. Hesse, and J. Birn (Los Alamos National Lab., NM.) *In* ESA, Proceedings of an International School and Workshop on Reconnection in Space Plasma, Volume 2 Jan. 1989 p 5-9 Sponsored by the Deutsche Forschungsgemeinschaft, Bonn, Fed. Republic of Germany (For primary document see N89-24974 18-75)
Copyright Avail: NTIS HC A15/MF A01; ESA Publications Div., ESTEC, Noordwijk, Netherlands, 45 US dollars or 80 Dutch guilders

The basic notion of magnetic reconnection is addressed. The generalization of magnetic reconnection from two to three-dimensional systems is not a straightforward procedure. It is argued that notions used to describe symmetric systems fail in genuinely three-dimensional configurations. A scheme that avoids such conceptual difficulties (general magnetic reconnection) is discussed. The formal analysis of its properties bears on important relationships between reconnection, parallel electric fields, and magnetic helicity. Actual and potential applications of general magnetic reconnection and its properties are discussed. One of the features is a stochastic mode of magnetic field connection.
ESA

N89-24976# Max-Planck-Inst. fuer Aeronomie, Katlenburg-Lindau (Germany, F.R.).
RELATION BETWEEN GLOBAL AND LOCAL ASPECTS OF RECONNECTION
V. M. Vasyliunas *In* ESA, Proceedings of an International School and Workshop on Reconnection in Space Plasma, Volume 2 Jan. 1989 p 11-14 (For primary document see N89-24974 18-75)
Copyright Avail: NTIS HC A15/MF A01; ESA Publications Div., ESTEC, Noordwijk, Netherlands, 45 US dollars or 80 Dutch guilders

The process of magnetic field line reconnection (merging) is discussed. It involves a specific class of magnetic field and plasma flow geometries where the assumed applicability of MHD on a large scale implies that non-MHD effects (no matter how small a priori) must be important in certain small-scale regions. Hence arises the controversy of to what extent the structure and the time development on various scales governed by global boundary conditions or by local plasma parameters (e.g., effective resistivity). It is argued that the answer depends on the length scale under consideration. On the smallest (microscopic) scales, local non-MHD parameters play a dominant role; on intermediate scales, they may conceivably affect some of the boundary conditions but otherwise play no role; on global scales, they are insignificant.
ESA

N89-24977# Imperial Coll. of Science and Technology, London (England).
NOISE-FREE NEUTRAL SHEETS **c46**
J. W. Dungey *In* ESA, Proceedings of an International School and Workshop on Reconnection in Space Plasma, Volume 2 Jan. 1989 p 15-19 (For primary document see N89-24974 18-75)
Copyright Avail: NTIS HC A15/MF A01; ESA Publications Div., ESTEC, Noordwijk, Netherlands, 45 US dollars or 80 Dutch guilders

The rate of reconnection in the geomagnetic tail is discussed. If this rate is to be accounted for by noise, strong turbulence is required. If noise is neglected, simple discussions of particle motion, velocity distributions, and stresses suggest an alternative solution. Electron trajectories are Speiser type and residence time is the crucial quantity. Velocity distributions are skewed, exhibiting electron viscosity. It seems appropriate to attempt two fluid modeling with anisotropic pressure. The quantitative problem of the tail needs a small spatial scale for the field and the tearing mode may be a means to this end.
ESA

N89-24978# Academy of Sciences, Potsdam (German D.R.). Central Inst. for Astrophysics.
RECONNECTION INSTABILITY IN COLLISIONLESS PLASMA
J. M. Buechner and L. M. Zelenyi (Academy of Sciences, USSR, Moscow) *In* ESA, Proceedings of an International School and Workshop on Reconnection in Space Plasma, Volume 2 Jan. 1989 p 21-28 (For primary document see N89-24974 18-75)
Copyright Avail: NTIS HC A15/MF A01; ESA Publications Div., ESTEC, Noordwijk, Netherlands, 45 US dollars or 80 Dutch guilders

It is shown that both plasma species (electrons, ions) must interact irreversibly with the tearing mode to initialize collisionless reconnection. Unfortunately, while the unmagnetized ions may dissipate energy without collisions via resonant Landau damping, magnetized electrons prevent the instability. An approach to the physics of the irreversible wave particle interaction in strongly inhomogeneous, curved magnetic fields that takes into account the appearance of deterministic chaos of the particle motion caused by the strong in inhomogeneity in magnetic field reversals is described. On the basis of these findings and of an investigation of quasiadiabatic, cucumber like orbits in extremely thin field reversals, linear stability properties of collisionless plasma in two dimensional collisionless current sheet structures is reviewed. This reconnection instability and neutral line formation can occur on sufficiently short wavelength-scales and, therefore can be treated even by a WKB approach.
ESA

N89-24979# Academy of Sciences (USSR), Moscow. Inst. of Space Research.
NONLINEAR DYNAMICS OF THE DRIFT TEARING-MODE
M. M. Kuznetsova and L. M. Zelenyi *In* ESA, Proceedings of an International School and Workshop on Reconnection in Space Plasma, Volume 2 Jan. 1989 p 29-34 (For primary document see N89-24974 18-75)
Copyright Avail: NTIS HC A15/MF A01; ESA Publications Div., ESTEC, Noordwijk, Netherlands, 45 US dollars or 80 Dutch guilders

The nonlinear evolution of the single tearing type perturbation in plasma configurations with magnetic shear is considered. The primary effect in the study of the nonlinear dynamics of magnetic perturbations is the modification of the orbits of resonant particles caused by the chain of magnetic islands, moving along the magnetic

surface due to drift effects. The structure of a parallel electric field and its influence on ion dynamics and the influence of integral effects dealing with finiteness of ion Larmor radius are incorporated in the nonlinear analysis. Nonlinear growth rates and saturation width of the magnetic islands are evaluated. The drift tearing mode is found to have metastable properties: the perturbations of finite amplitude which damp in the linear approximation appear to be nonlinearly unstable. The energetics of this hard regime of instability onset and the nonlinear stabilization mechanisms are evaluated. The influence or uniform stationary plasma background is addressed. ESA

N89-24980# Academy of Sciences, Potsdam (German D.R.). Central Inst. for Astrophysics.
RECONNECTION AND MICROTURBULENCE
J. M. Buechner, C.-V. Meister, and B. Nikutowski *In* ESA, Proceedings of an International School and Workshop on Reconnection in Space Plasma, Volume 2 Jan. 1989 p 35-40 (For primary document see N89-24974 18-75)
Copyright Avail: NTIS HC A15/MF A01; ESA Publications Div., ESTEC, Noordwijk, Netherlands, 45 US dollars or 80 Dutch guilders

Space plasma instabilities are reviewed along with the related anomalous collision frequencies, i.e., the anomalous resistivity. The most favored LHD - instability, which has a low instability threshold, is expected to saturate in the actual reconnection region with its high plasma - Beta. This coincides well with the lack of observation of enhanced electrostatic turbulence in the related regions before the onset of reconnection. Hence it seems to be necessary to study other approaches or additional mechanisms, like nonlocal processes or the coupling between the anomalous collision process and the macroscopic evolution of the configuration or to take into account the direct (resonant) irreversible interaction of reconnection modes with the (possibly chaotic) plasma particles. ESA

N89-24981# Academy of Sciences, Potsdam (German D.R.). Central Inst. for Astrophysics.
ANOMALOUS COLLISION FREQUENCY OF MAGNETOACTIVE PLASMAS WITH TWO-DIMENSIONAL ELECTROSTATIC TURBULENCE (kB=O)
C.-V. Meister *In* ESA, Proceedings of an International School and Workshop on Reconnection in Space Plasma, Volume 2 Jan. 1989 p 41-44 (For primary document see N89-24974 18-75)
Copyright Avail: NTIS HC A15/MF A01; ESA Publications Div., ESTEC, Noordwijk, Netherlands, 45 US dollars or 80 Dutch guilders

Current-driven instabilities in inhomogeneous space plasma exciting lower-hybrid-drift waves is studied. Within the nonlinear theory of electrostatic flute instabilities an expression for the anomalous collision frequency containing the energy spectrum of the waves as a parameter is obtained. In the special case of the plasma of the Earth's magnetopause a collision frequency of 0.03 to 0.3 Hz is found, which may cause substantially resistivity enhancement even in the vicinity of the neutral sheet with large plasma-beta. ESA

N89-24982# Saint Andrew's Univ. (Scotland). Dept. of Mathematical Sciences.
COMPARISON OF COMPRESSIBLE AND INCOMPRESSIBLE MODELS OF RECONNECTION
M. Jardine and E. R. Priest *In* ESA, Proceedings of an International School and Workshop on Reconnection in Space Plasma, Volume 2 Jan. 1989 p 45-49 (For primary document see N89-24974 18-75)
Copyright Avail: NTIS HC A15/MF A01; ESA Publications Div., ESTEC, Noordwijk, Netherlands, 45 US dollars or 80 Dutch guilders

Two families of reconnection models, one for a compressible and one for an incompressible plasma are compared. The effects of including compressibility are: to enhance convergence or divergence of the inflow; to increase the reconnection rate for slow-mode and hybrid compression regimes; to increase the flow speed near the diffusion region for the flux pile-up regimes; and to produce outflow jets which are faster, narrower, and have magnetic field lines with a smaller curvature. ESA

N89-24983# Academy of Sciences, Graz (Austria). Inst. fuer Weltraumforschung.
MAGNETIC RECONNECTION NEAR A STAGNATION POINT
M. F. Heyn, H. K. Biernat, R. P. Rijnbeek, and F. T. Gratton (Buenos Aires Univ., Argentina) *In* ESA, Proceedings of an International School and Workshop on Reconnection in Space Plasma, Volume 2 Jan. 1989 p 51-54 (For primary document see N89-24974 18-75)
Copyright Avail: NTIS HC A15/MF A01; ESA Publications Div., ESTEC, Noordwijk, Netherlands, 45 US dollars or 80 Dutch guilders

Starting from an exact solution of the dissipative MHD equations for a magnetic neutral layer with intrinsic stagnation point flow a normal magnetic field component is introduced as a perturbation. The resulting set of coupled ordinary differential equations is solved numerically and the behavior of the perturbed quantities with distance from the neutral layer is presented. ESA

N89-24984# Lawrence Livermore National Lab., CA.
MAGNETIC RECONNECTION SIMULATION USING THE 2.5 D ELECTROMAGNETIC DIRECT IMPLICIT CODE AVANTI
D. W. Hewett, G. E. Francis, and C. E. Max *In* ESA, Proceedings of an International School and Workshop on Reconnection in Space Plasma, Volume 2 Jan. 1989 p 55-60 (For primary document see N89-24974 18-75)
(Contract W-7405-eng-48)
Copyright Avail: NTIS HC A15/MF A01; ESA Publications Div., ESTEC, Noordwijk, Netherlands, 45 US dollars or 80 Dutch guilders

The 2.5 D electromagnetic code AVANTI is outlined. The code runs stably with arbitrarily large Delta t and is quite robust with respect to large fluctuations occurring due to small numbers of particles per cell. The code shows that the reconnection process occurs in distinct stages: (1) early spontaneous reconnection fed by the free energy of an initial anisotropy in the electron component; (2) coalescence of the resulting small-scale filaments of electron current, accompanied by electron jetting; and (3) oscillatory flow of electrons through the magnetic X-point, superposed on continuing nonlinear growth of ion-mediated reconnection. The time evolution of stage 3 is strongly dependent on Mi/Me. ESA

N89-24985# Lawrence Livermore National Lab., CA.
KINETIC SIMULATION OF MAGNETIC RECONNECTION IN THE PRESENCE OF SHEAR
G. E. Francis, D. W. Hewett, and C. E. Max *In* ESA, Proceedings of an International School and Workshop on Reconnection in Space Plasma, Volume 2 Jan. 1989 p 61-66 (For primary document see N89-24974 18-75)
(Contract W-7405-eng-48)
Copyright Avail: NTIS HC A15/MF A01; ESA Publications Div., ESTEC, Noordwijk, Netherlands, 45 US dollars or 80 Dutch guilders

The basic physical processes associated with collisionless magnetic reconnection are investigated using the implicit PIC code AVANTI. The code is based on a 2.5-D fully electromagnetic direct implicit algorithm which proved stable for arbitrary time step. This stability makes it possible to separate out the respective roles of the highly magnetized electron and the unmagnetized ions for large ion-electron mass ratios. It is found that the inclusion of a guide magnetic field (magnetic shear) severely slows the initial stages of reconnection and damps out the electrostatic ringing if local values of the guide field are above a threshold determined by questions of electron mobility. ESA

N89-24986# Ruhr Univ., Bochum (Germany, F.R.).
PARTICLE SIMULATION OF MAGNETIC RECONNECTION IN COLLISION-FREE PLASMA SHEETS
W. Zwingmann *In* ESA, Proceedings of an International School and Workshop on Reconnection in Space Plasma, Volume 2 Jan.

1989 p 67-70 Sponsored by the Deutsche Forschungsgeimschaft, Bonn, Fed. Republic of Germany and DOE, Washington, DC (For primary document see N89-24974 18-75) Copyright Avail: NTIS HC A15/MF A01; ESA Publications Div., ESTEC, Noordwijk, Netherlands, 45 US dollars or 80 Dutch guilders

The onset of geomagnetic activity initiated by a large-scale instability of the plasma sheet is studied. The ion-tearing instability is a promising candidate for the tail dynamics. The nonlinear behavior was examined using particle simulation, starting with a self-consistent static tail equilibrium including a pressure gradient along the tail axis and tail flaring. The case without electron stabilization effects is simulated by assuming a mass ratio of one. The theoretical stability criterion is confirmed. The nonlinear development for the unstable case leads to the formation and acceleration of a plasmoid, similar to observations and MHD simulations. The effect of the electron stabilization is shown by a simulation with a mass ratio of 10. For low electron temperatures, an unstable behavior is shown. ESA

N89-24987# Saint Andrew's Univ. (Scotland). Dept. of Mathematical Sciences.

MAGNETIC ENERGY CONVERSION ON THE SUN **c92**

E. R. Priest *In* ESA, Proceedings of an International School and Workshop on Reconnection in Space Plasma, Volume 2 Jan. 1989 p 73-81 (For primary document see N89-24974 18-75) Copyright Avail: NTIS HC A15/MF A01; ESA Publications Div., ESTEC, Noordwijk, Netherlands, 45 US dollars or 80 Dutch guilders

For a 3D magnetic field such as exists above sunspots or magnetic fragments of complex polarity or in prominence fields, it is suggested that reconnection may be defined to occur when there is a singular line (a field line with neighboring X-type topology and an electric field along it). In general there is a continuum of potential singular lines and which one supports reconnection depends on the flow or electric field. An example is given of how to drive reconnection all along any curved field line in a configuration with shear and it is found that strong plasma jetting occurs along the singular line. Thus in a sheared coronal configuration of potential singular lines, coronal heating may occur at small current sheets created at singular lines by the appropriate flows. ESA

N89-24988# Saint Andrew's Univ. (Scotland). Dept. of Mathematical Sciences.

THREE-DIMENSIONAL RECONNECTION FROM A GLOBAL VIEWPOINT

M. A. Berger *In* ESA, Proceedings of an International School and Workshop on Reconnection in Space Plasma, Volume 2 Jan. 1989 p 83-86 (For primary document see N89-24974 18-75) Copyright Avail: NTIS HC A15/MF A01; ESA Publications Div., ESTEC, Noordwijk, Netherlands, 45 US dollars or 80 Dutch guilders

Three-dimensional reconnection is defined in terms of changes in a magnetic field topology, even in the absence of true separatrices. Global magnetic helicity conservation at magnetopause flux transfer events is also discussed. Field topology usually means the separatrix topology. Consider for example coronal fieldlines with two end-points in the solar photosphere. Such fieldlines generate a mapping of the photosphere to itself. This mapping is often only piecewise continuous, and the separatrix surfaces separate the flux regions associated with each continuous piece. Reconnection can be defined in terms of flux across the separatrices. However, there can still be considerable structure between the separatrices, such as braiding and shearing. A fieldline topology which recognizes this structure is defined. Even in the absence of separatrices, the fieldline mapping can develop sharp gradients because of flux localization or because of stragnation points in the photospheric flow. The thin regions where these gradients occur can be employed in place of separatrices in a definition of reconnection. ESA

N89-24989# Academy of Sciences, Potsdam (German D.R.). Central Inst. for Astrophysics.

GENERATION AND NON-EQUILIBRIUM OF SOLAR ATMOSPHERIC MAGNETIC FIELDS **c92**

N. Seehafer *In* ESA, Proceedings of an International School and Workshop on Reconnection in Space Plasma, Volume 2 Jan. 1989 p 87-92 (For primary document see N89-24974 18-75) Copyright Avail: NTIS HC A15/MF A01; ESA Publications Div., ESTEC, Noordwijk, Netherlands, 45 US dollars or 80 Dutch guilders

It is suggested that the generation of dc electric currents in the solar atmosphere, needed as an energy source for flares, may be ultimately caused by the rotation of the Sun. Then, in the atmosphere, the electric current helicity, which is a pseudo-scalar quantity, should be antisymmetric with respect to the equatorial plane. An analysis of relevant observations leads to the (tentative) result that the current helicity is predominantly negative in the Northern and positive in the Southern Hemisphere, just opposite in sign to the helicity of the currents generated according to standard dynamo theory by the turbulent alpha effect in the convection zone. Current generation due to the differential rotation of the photospheric foot points of magnetic field lines, however, can explain the rule found. The explosive release of magnetic energy during flares is believed to involve magnetic reconnection. For the situation of the solar atmosphere, this reconnection concept leads to the conjecture that the surfaces consisting of magnetic field lines which touch the photosphere are preferential sites of reconnection. ESA

N89-24990# Institute of Nuclear Physics, Novosibirsk (USSR).

STABILITY OF FORCE-FREE MAGNETIC FIELDS AND THE PROBLEM OF SOLAR CORONAL HEATING **c92**

G. E. Vekstein *In* ESA, Proceedings of an International School and Workshop on Reconnection in Space Plasma, Volume 2 Jan. 1989 p 93-97 (For primary document see N89-24974 18-75) Copyright Avail: NTIS HC A15/MF A01; ESA Publications Div., ESTEC, Noordwijk, Netherlands, 45 US dollars or 80 Dutch guilders

Stability of force-free magnetic fields is considered in connection with the problem of magnetic coronal heating. The important role of line tying effect in the MHD stability condition of a linear force-free magnetic field is revealed on the basis of energy principles. The threshold of tearing mode instability in a plane sheared force-free field is analyzed. It is shown that such a field remains stable even under infinitely high values of shear localized at the edge region near a perfectly conducting boundary. ESA

N89-24991# Academy of Sciences (USSR), Gorky. Inst. of Applied Physics.

A NEUTRAL CURRENT SHEET WITH FLOWS: TEARING AND STRATIFICATION MODES AND MODELING OF CORONAL STRUCTURES **c92**

V. M. Gubchenko and V. V. Zaitsev *In* ESA, Proceedings of an International School and Workshop on Reconnection in Space Plasma, Volume 2 Jan. 1989 p 99-104 (For primary document see N89-24974 18-75)
Copyright Avail: NTIS HC A15/MF A01; ESA Publications Div., ESTEC, Noordwijk, Netherlands, 45 US dollars or 80 Dutch guilders

The nature of the solar corona fine structure is studied using a model of a neutral current sheet submerged into the solar wind plasma flow. In the vicinity of the sheet the particle distribution function is a bimaxwellian one and describes a double-velocity flow with a relative velocity less than or = 1. A relation between free parameters (sheet thickness, particle gyroradius, velocity, and pressure in a high-velocity flow) is dependent on r and determines anisotropy in the system. The system is unstable due to excitation of large-scale Weibel-type electromagnetic modes. A tearing mode and a stratification one are observed. The first and the second modes determine islands and rays respectively. Under stable conditions, sheet thickness rapidly decreases in the lower corona with an increase of r, but then in the interplanetary space its value smoothly grows. ESA

N89-24992# Saint Andrew's Univ. (Scotland). Dept. of Mathematical Sciences.
ON THE MHD STABILITY OF THE M=1 KINK MODE IN FINITE LENGTH CORONAL LOOPS **c92**
M. Velli, A. W. Hood, and G. Einaudi (Florence Univ., Italy) *In* ESA, Proceedings of an International School and Workshop on Reconnection in Space Plasma, Volume 2 Jan. 1989 p 105-109 (For primary document see N89-24974 18-75)
Copyright Avail: NTIS HC A15/MF A01; ESA Publications Div., ESTEC, Noordwijk, Netherlands, 45 US dollars or 80 Dutch guilders

A general method for studying the ideal and resistive MHD stability of plasma configurations with line-tying is presented, and applied to the case of the M=1 kink mode in coronal loops. The method consists in a truncated Fourier series approach applied to the linearized equations of motion, and is found to converge rapidly with the order of the truncation. Models of the boundary conditions at the corona-photosphere interface are discussed, and the growth rates of unstable modes are calculated for equilibrium profiles with an without a reversal in the field component connecting to the photosphere. The relevance of these modes to compact loop flares is assessed. ESA

N89-24993# Toyama Univ. (Japan). Dept. of Applied Mathematics and Physics.
PARTICLE ACCELERATION BY MAGNETIC RECONNECTION AND FAST MAGNETOSONIC SHOCK WAVES IN SOLAR FLARES **c92**
Jun-ichi Sakai and Yukiharu Ohsawa (Nagoya Univ., Japan) *In* ESA, Proceedings of an International School and Workshop on Reconnection in Space Plasma, Volume 2 Jan. 1989 p 111-116 (For primary document see N89-24974 18-75)
Copyright Avail: NTIS HC A15/MF A01; ESA Publications Div., ESTEC, Noordwijk, Netherlands, 45 US dollars or 80 Dutch guilders

Development of the theory of current loop coalescence and fast magnetosonic shock waves, particularly particle acceleration caused by these processes is reviewed. It is shown that the spiral, two sided plasma jets can be explosively driven by the plasma rotational motion induced by magnetic reconnection during the two current loop coalescence. The rebound following the plasma pinch driven by the Lorentz force can generate the fast magnetosonic shock waves. For a weak magnetic field, strong acceleration by the shocks occurs to protons only. Simultaneous acceleration of protons and electrons takes place in a rather strong magnetic field. Resonant protons gain relativistic energies within the order of the ion cyclotron period (much less than 1 s for solar plasma parameters). The electron acceleration time is shorter than the ion cyclotron period. ESA

N89-24994# Academy of Sciences, Potsdam (German D.R.). Central Inst. for Astrophysics.
DYNAMIC DEVELOPMENT OF CORONAL CURRENT SHEETS **c92**
B. Kliem *In* ESA, Proceedings of an International School and Workshop on Reconnection in Space Plasma, Volume 2 Jan. 1989 p 117-122 (For primary document see N89-24974 18-75)
Copyright Avail: NTIS HC A15/MF A01; ESA Publications Div., ESTEC, Noordwijk, Netherlands, 45 US dollars or 80 Dutch guilders

The possible interplay of tearing, coalescence, and current-driven kinetic instabilities in current sheets is considered on the basis of order of magnitude estimates of instability thresholds and scalings. Arguments are given that favor the development of internal dynamics for current sheets with stationary inflow and appropriate combination of parameters (the impulsive bursty regime of reconnection). The model relates newly emerging flux to flare energy release and provides the basis for an understanding of moving type 4 radio bursts associated with coronal mass ejections. ESA

N89-24995# Academy of Sciences, Potsdam (German D.R.). Central Inst. for Astrophysics.
POSSIBILITIES AND PROBLEMS OF THE INTERPRETATION OF SOLAR MAGNETOGRAPH MEASUREMENTS AND APPLICATIONS TO FLARE-ACTIVE REGIONS **c92**
J. Staude and A. Hofmann *In* ESA, Proceedings of an International School and Workshop on Reconnection in Space Plasma, Volume 2 Jan. 1989 p 123-128 (For primary document see N89-24974 18-75)
Copyright Avail: NTIS HC A15/MF A01; ESA Publications Div., ESTEC, Noordwijk, Netherlands, 45 US dollars or 80 Dutch guilders

The basic uncertainties encountered in the interpretation of magnetograph data, and possibilities for deriving more reliable information are reviewed. The problems are illustrated by describing the data handling of a vector magnetograph. Examples of observed flare-active regions demonstrate the state of information which can be obtained. ESA

N89-24996# Academy of Sciences, Potsdam (German D.R.). Central Inst. for Astrophysics.
ESTIMATION OF SUNSPOT MAGNETIC FIELD PARAMETERS USING THE SUPERPENUMBRAL TOPOLOGY **c92**
J. Linke and J. H. Hernandez (Pedagogical High School, Havana, Cuba) *In* ESA, Proceedings of an International School and Workshop on Reconnection in Space Plasma, Volume 2 Jan. 1989 p 129-130 (For primary document see N89-24974 18-75)
Copyright Avail: NTIS HC A15/MF A01; ESA Publications Div., ESTEC, Noordwijk, Netherlands, 45 US dollars or 80 Dutch guilders

The model of Molodensky et al. (1987) was used to investigate the fibril directions (H-alpha level) for the penumbral and supernumbral region of a sunspot, namely the main, but following spot of the small, simple active region SD 135/1984 on June 24. To reduce the number of free parameters of the model vector, magnetograms were used. Comparing structures of H-alpha filtergrams and heliograms with the theoretical field model shows that the chromospheric structure of the sunspot magnetic field is essentially a result of two subsystems. The two sources have nearly the same magnetic flux densities, a very small distance relative to the sunspot areal, and the resulting magnetic field topology has nearly a current-free configuration. These results are in good agreement with earlier investigations of this active region. ESA

N89-24997# Academy of Sciences, Potsdam (German D.R.). Central Inst. for Astrophysics.
NOTE ON AN APPARENT HIGHLY-SHEARED MAGNETIC FIELD STRUCTURE **c92**
J. Linke and G. Bachmann *In* ESA, Proceedings of an International School and Workshop on Reconnection in Space Plasma, Volume 2 Jan. 1989 p 131-132 (For primary document see N89-24974 18-75)
Copyright Avail: NTIS HC A15/MF A01; ESA Publications Div., ESTEC, Noordwijk, Netherlands, 45 US dollars or 80 Dutch guilders

Using vector magnetograms and a force-free model, the magnetic field structure of the active solar region BBR 18474 of 1982 July 15, and 1982 July 16 was investigated. Comparison of the azimuths of the current-free model of the magnetic field structure in the central part of this active region with the map of the azimuth values estimates from the observation slows good qualitative agreement. Earlier results show that the appearance of highly sheared magnetic field structure near the neutral line in the central part of this active region may be a simulated effect generated by subphotospheric current system. ESA

N89-24998# Academy of Sciences, Potsdam (German D.R.). Central Inst. for Astrophysics.
DIAGNOSTICS OF ENERGY RELEASE AND MAGNETIC FIELDS ON THE SUN BY RADIO METHODS **c92**
A. Krueger *In* ESA, Proceedings of an International School and

Workshop on Reconnection in Space Plasma, Volume 2 Jan. 1989 p 133-138 (For primary document see N89-24974 18-75)
Copyright Avail: NTIS HC A15/MF A01; ESA Publications Div., ESTEC, Noordwijk, Netherlands, 45 US dollars or 80 Dutch guilders

The impact of radio astronomy on the knowledge of energy release processes and magnetic fields in the solar atmosphere is reviewed. Solar radio astronomy takes advantage of a richness of spectral and morphological features containing information about all levels of the solar corona. The source of information, signatures of flare energy release, and radio methods of the estimation of magnetic fields are discussed. ESA

N89-24999# Academy of Sciences, Potsdam (German D.R.). Central Inst. for Astrophysics.
TREMSDORF SOLAR RADIO ASTRONOMY OBSERVATORY: THE SCIENTIFIC PROGRAM AND AN INTERESTING OBSERVATION **c89**
H. Aurass *In* ESA, Proceedings of an International School and Workshop on Reconnection in Space Plasma, Volume 2 Jan. 1989 p 139-144 Prepared in cooperation with Observatorium fuer Solare Radioastronomie, Potsdam, German Democratic Republic (For primary document see N89-24974 18-75)
Copyright Avail: NTIS HC A15/MF A01; ESA Publications Div., ESTEC, Noordwijk, Netherlands, 45 US dollars or 80 Dutch guilders

The Tremsdorf Observatory solar patrol program is presented. An example (the noise storm continuum depression and revival during a moderate type 4 burst on 5 Feb. 1986) illuminates the information content and the problems offered by relatively simple whole disk radio flux and polarization data. ESA

N89-25000# Slovak Academy of Sciences, Tatranska Lomnica (Czechoslovakia). Inst. of Astronomy.
THE RELATION BETWEEN H-ALPHA AND SXR EMISSION OF THE FLARES **c92**
A. Antalova *In* ESA, Proceedings of an International School and Workshop on Reconnection in Space Plasma, Volume 2 Jan. 1989 p 145-148 (For primary document see N89-24974 18-75)
Copyright Avail: NTIS HC A15/MF A01; ESA Publications Div., ESTEC, Noordwijk, Netherlands, 45 US dollars or 80 Dutch guilders

The evolutionary coincidence between the occurrence of the LDE flares and the formation of the evolving delta configuration, in the solar active region, was found. Fifty-one cases of LDE flares were analyzed from the viewpoint of the precise location of their flare loop arcade (located above delta configuration). The quasi-delta configurations (i.e., kinematical joining of the two stable spots of the opposite magnetic induction) are not LDE flare productive. ESA

N89-25001# Academy of Sciences (USSR), Gorky. Inst. of Applied Physics.
THE PRECURSORS OF THE 9 JULY 1982 SOLAR PROTON FLARE EVENT **c92**
V. V. Zaitsev, E. A. Averianikhina, H. Aurass, and A. Krueger (Academy of Sciences, Potsdam, German D.R.) *In* ESA, Proceedings of an International School and Workshop on Reconnection in Space Plasma, Volume 2 Jan. 1989 p 149-152 (For primary document see N89-24974 18-75)
Copyright Avail: NTIS HC A15/MF A01; ESA Publications Div., ESTEC, Noordwijk, Netherlands, 45 US dollars or 80 Dutch guilders

Observational evidence is presented that radio precursors of a big flare event cover the whole microwave-decimeter range like the following impulsive phase. The quasiperiodic preflare radio emission combined with soft and hard X-ray and H-alpha data confirms preflare energization of the active region and is compatible with a temperature dependent prominence flare loop interaction model. The preflare signatures are highly important for a preflare diagnostic of energy release site parameters. ESA

N89-25002# Observatorium fuer Solare Radioastronomie, Tremsdorf (German D.R.). Central Inst. for Astrophysics.
CORONAL MAGNETIC FIELD STRENGTHS DETERMINED FROM FIBER BURSTS **c92**
G. Mann and K. Baumgaertel (Academy of Sciences, Berlin, German D.R.) *In* ESA, Proceedings of an International School and Workshop on Reconnection in Space Plasma, Volume 2 Jan. 1989 p 153-156 (For primary document see N89-24974 18-75)
Copyright Avail: NTIS HC A15/MF A01; ESA Publications Div., ESTEC, Noordwijk, Netherlands, 45 US dollars or 80 Dutch guilders

A method of estimating coronal magnetic field strengths above active regions by means of fiber bursts appearing as a special fine structure in solar type-4 radio bursts is presented. The fiber bursts are considered as the radio signature of loss-cone instability driven whistler waves of a narrow frequency band. Numerical calculations indicate that narrow band whistlers are excited near the critical loss-cone angle. Thus, the frequency of the whistlers can be deduced. Then the magnetic field strength in the source region can be estimated by the fiber burst data adopting a coronal density model. The results are consistent with previous estimations. ESA

N89-25003# Observatorium fuer Solare Radioastronomie, Tremsdorf (German D.R.). Central Inst. for Astrophysics.
LONG-TERM EVOLUTION OF CORONAL MAGNETIC FIELDS BASED ON NOISE STORM CONTINUUM OBSERVATIONS IN THE 20TH AND 21ST CYCLE **c92**
A. Boehme *In* ESA, Proceedings of an International School and Workshop on Reconnection in Space Plasma, Volume 2 Jan. 1989 p 157-161 (For primary document see N89-24974 18-75)
Copyright Avail: NTIS HC A15/MF A01; ESA Publications Div., ESTEC, Noordwijk, Netherlands, 45 US dollars or 80 Dutch guilders

Based on the noise storms of cycles 20 and 21, the long-term variations of the radiation signatures of sunspot groups during a solar cycle were studied. The results suggest that nonpotential loops favoring the emission of a strong type 1 continuum at the low frequencies (less than 100MHz) tend to exist more frequently above the sunspot groups in the later phase of a solar cycle. ESA

N89-25004# Byurakan Observatory (USSR).
PINCH-EFFECT AND STELLAR FLARES PHYSICS **c92**
V. S. Hayrapetyan, A. G. Nikhogossian, and V. V. Vikhrev (Academy of Sciences, USSR, Moscow) *In* ESA, Proceedings of an International School and Workshop on Reconnection in Space Plasma, Volume 2 Jan. 1989 p 163-167 (For primary document see N89-24974 18-75)
Copyright Avail: NTIS HC A15/MF A01; ESA Publications Div., ESTEC, Noordwijk, Netherlands, 45 US dollars or 80 Dutch guilders

A pinch-model of primary energy release of solar and stellar flares is suggested. This model is based on the effect of transformation of floating magnetic field energy into kinetic and thermal energy in stellar plasma atmosphere. This mechanism is similar to the energy transformation process in pinch discharge. Numerical modeling of closed magnetic tube evolution in stellar plasma shows that as a result of its compression high-temperature dense plasma is formed, and becomes an impulsive source of X-ray radiation and energetic particle generation. It explains high energetic effectivity and temporal scale of magnetic energy transformation into thermal and kinetic plasma energy. ESA

N89-25005# Academy of Sciences, Potsdam (German D.R.). Central Inst. for Astrophysics.
TIME SCALES OF SOLAR MICROWAVE BURSTS AND SCENARIOS OF FLARE ENERGY RELEASE **c92**
A. Krueger, B. Kliem, and J. Hildebrandt *In* ESA, Proceedings of an International School and Workshop on Reconnection in Space Plasma, Volume 2 Jan. 1989 p 169-173 (For primary document

see N89-24974 18-75)
Copyright Avail: NTIS HC A15/MF A01; ESA Publications Div., ESTEC, Noordwijk, Netherlands, 45 US dollars or 80 Dutch guilders

Based on observational evidence that characteristic time scales of different solar microwave burst types are distributed over a wide range (0.001 to 10.000 sec), different mechanisms of energy release are considered to account for the impulsive flux increase (time scale less than 1000 sec). The coalescence instability is found to be a promising candidate to combine sufficiently short time scales with substantial energy release. ESA

N89-25006# Observatorium fuer Solare Radioastronomie, Tremsdorf (German D.R.). Central Inst. for Astrophysics.
CHAOTIC RADIOPULSATIONS AND CORONAL MAGNETIC FIELD ESTIMATES
J. Kurths and M. Karlicky (Ondrejov Observatory, Czechoslovakia) *In* ESA, Proceedings of an International School and Workshop on Reconnection in Space Plasma, Volume 2 Jan. 1989 p 175-177 (For primary document see N89-24974 18-75)
Copyright Avail: NTIS HC A15/MF A01; ESA Publications Div., ESTEC, Noordwijk, Netherlands, 45 US dollars or 80 Dutch guilders

Analyzing the time structure of a coronal pulsation event of Apr. 3 1980 provides an evolution from a regular periodic phase to an irregular behavior. The irregular stage can be described by a low-dimensional chaotic attractor. The nature of this structural change reveals that this pulsation event evolves along the Ruelle-Takens-Newhouse route to chaos. This event is discussed in terms of MHD waves in coronal loops yielding estimates of the plasma parameters in the solar corona, particularly of the magnetic field strength. ESA

N89-25007# Special Astrophysical Observatory, Nishnyi Archys (USSR).
SEARCH FOR A FINE-TIME STRUCTURE IN FLARES OF UV CET-TYPE STARS **c89**
L. A. Pustilnik, G. M. Beskin, V. F. Shvartsman, and R. E. Gershberg (Crimean Astrophysical Observatory, USSR) *In* ESA, Proceedings of an International School and Workshop on Reconnection in Space Plasma, Volume 2 Jan. 1989 p 179-181 (For primary document see N89-24974 18-75)
Copyright Avail: NTIS HC A15/MF A01; ESA Publications Div., ESTEC, Noordwijk, Netherlands, 45 US dollars or 80 Dutch guilders

The results of electrophotometrical investigations of the 65 flares with a time resolution of 0.0000005 in 8 flare stars are presented. Analysis shows no fine time structure within the scale 0.000001 to 0.1 sec. The shortest times of brightness variations are 0.3 to 0.8 s and inherent in a phase in front of flares. In four stars (UV Cet, CN Leo, Wolf 424AB, V577 Mon) very fast flare events are observed. ESA

N89-25008# Academy of Sciences (USSR), Moscow. Inst. of General Physics.
FLARE-TYPE PLASMA PROCESSES AND EXPLOSIVE DISRUPTION OF PINCH CURRENT SHEETS
A. G. Frank *In* ESA, Proceedings of an International School and Workshop on Reconnection in Space Plasma, Volume 2 Jan. 1989 p 185-192 (For primary document see N89-24974 18-75)
Copyright Avail: NTIS HC A15/MF A01; ESA Publications Div., ESTEC, Noordwijk, Netherlands, 45 US dollars or 80 Dutch guilders

The results of laboratory experiments with plane pinch current sheets (CS) are presented. Two types of CS formation regimes are discussed, linear and nonlinear. The formation of CS is shown to be the general property of magnetic configurations with neutral lines, but the magnetic structure of CS can be various. The experimental realization of the impulsive phase of magnetic reconnection indicates that ways of magnetic energy transformation depend essentially on the conditions of CS formation and its internal magnetic structure on the metastable stage. Explosive plasma heating is dominant in nonlinear regimes, while particle acceleration play an important part in linear regimes. ESA

N89-25009# Academy of Sciences (USSR), Moscow. Inst. of General Physics.
CURRENT SHEET STRUCTURE AT DIFFERENT STAGES OF MAGNETIC RECONNECTION
S. Yu Bogdanov, A. G. Frank, and V. S. Markov *In* ESA, Proceedings of an International School and Workshop on Reconnection in Space Plasma, Volume 2 Jan. 1989 p 193-198 (For primary document see N89-24974 18-75)
Copyright Avail: NTIS HC A15/MF A01; ESA Publications Div., ESTEC, Noordwijk, Netherlands, 45 US dollars or 80 Dutch guilders

The structure of the magnetic field of the plane pinch current sheet (CS) was experimentally investigated. The current distributions in different cross-sections of the CS were obtained. The structure of the current region is found to be complicated, and essentially changed in the course of the CS evolution. ESA

N89-25010# Academy of Sciences (USSR), Moscow. Inst. of General Physics.
IMPULSIVE HEATING PLASMA TURBULENCE AND MAGNETIC RECONNECTION INSIDE CURRENT SHEETS
A. G. Frank, N. P. Kyrie, and V. S. Markov *In* ESA, Proceedings of an International School and Workshop on Reconnection in Space Plasma, Volume 2 Jan. 1989 p 199-202 (For primary document see N89-24974 18-75)
Copyright Avail: NTIS HC A15/MF A01; ESA Publications Div., ESTEC, Noordwijk, Netherlands, 45 US dollars or 80 Dutch guilders

Results on the evolution of electron and ion temperatures in the current sheet (CS) are presented. Abrupt increase of both temperatures just before the impulsive phase of magnetic reconnection is discovered. The fast increase of the electron temperature is displayed in the plasma emission bursts in the spectral lines of the multiple-charged ions. Comparison of two spectral line shapes of the same multiple-charged ions determines the ion temperature in the hottest regions of the CS plasma and reveals the excitation of the nonequilibrium electric fields in the dense plasma of CS. ESA

N89-25011# Academy of Sciences (USSR), Moscow. Inst. of General Physics.
THE EVOLUTION OF MHD-PERTURBATIONS IN THE INTERSECTION REGION OF TWO SEPARATRIX PLANES
S. V. Bulanov, S. G. Shasharina, and D. Sunder (Academy of Sciences, Berlin, German D.R.) *In* ESA, Proceedings of an International School and Workshop on Reconnection in Space Plasma, Volume 2 Jan. 1989 p 203-206 (For primary document see N89-24974 18-75)
Copyright Avail: NTIS HC A15/MF A01; ESA Publications Div., ESTEC, Noordwijk, Netherlands, 45 US dollars or 80 Dutch guilders

On the basis of two simple models the problem of forced magnetic field-line reconnection in the vicinity of the intersection of two separatrix planes which corresponds to the interaction of two magnetic islands is considered. The system of MHD equations both for a hot incompressible plasma and a cold plasma is used. The characteristic time of the evolution of the perturbations and the size of their localization region are estimated. It is shown that this time is smaller than the formation time of the magnetic islands known from the literature. The space-time structure of the magnetic field and the current are displayed. ESA

N89-25012# Academy of Sciences (USSR), Irkutsk. Inst. of Terrestrial Magnetism, Ionosphere and Radiowave Propagation.
SPONTANEOUS AND FORGED RECONNECTION IN A MAGNETIC TYPE-X STRUCTURE
A. T. Altyntsev, N. V. Lebedev, and N. A. Strokin *In* ESA, Proceedings of an International School and Workshop on Reconnection in Space Plasma, Volume 2 Jan. 1989

p 207-213 (For primary document see N89-24974 18-75)
Copyright Avail: NTIS HC A15/MF A01; ESA Publications Div., ESTEC, Noordwijk, Netherlands, 45 US dollars or 80 Dutch guilders

An experimental study of the evolution of a magnetic type-X structure which is produced on a theta-pinch device is made. It is found that during the initial stage the reconnection process proceeds in a spontaneous fashion, with periodic restructurings of the current sheet and abrupt accelerations of ions. In the subsequent stage it is stationary in character, with the reconnection rate being in agreement with estimates obtained in terms of the forced reconnection Sweet-Parker model. ESA

N89-25013*# Los Alamos National Lab., NM.
MAGNETOTAIL RECONNECTION, MHD THEORY AND SIMULATIONS
J. Birn, M. Hesse, and K. Schindler (Ruhr Univ., Bochum, Germany, F.R.) *In* ESA, Proceedings of an International School and Workshop on Reconnection in Space Plasma, Volume 2 Jan. 1989 p 217-221 Sponsored by NASA, Washington, DC; DOE, Washington, DC and Deutsche Forschungsgemeinschaft, Bonn, Fed. Republic of Germany (For primary document see N89-24974 18-75)
Copyright Avail: NTIS HC A15/MF A01; ESA Publications Div., ESTEC, Noordwijk, Netherlands, 45 US dollars or 80 Dutch guilders

Magnetotail reconnection leading to plasmoid formation and ejection is discussed, emphasizing three-dimensional structures and deviations from earlier imposed symmetries, based on MHD simulations and topological considerations. In general, the separation of the plasmoid takes a finite amount of time. During this stage the plasmoid is characterized by filamentary structures of interwoven flux tubes with different topological connections. ESA

N89-25014# Ruhr Univ., Bochum (Germany, F.R.).
THE ROLE OF MAGNETIC RECONNECTION IN MAGNETOTAIL PLASMOID DYNAMICS
A. Otto *In* ESA, Proceedings of an International School and Workshop on Reconnection in Space Plasma, Volume 2 Jan. 1989 p 223-226 Sponsored by the Sonderforschungsbereich Plasmaphysik, Bochum/Juelich, Fed. Republic of Germany (For primary document see N89-24974 18-75)
Copyright Avail: NTIS HC A15/MF A01; ESA Publications Div., ESTEC, Noordwijk, Netherlands, 45 US dollars or 80 Dutch guilders

The dynamical evolution of the developing plasmoids and the influence of magnetic reconnection on the properties of plasmoids are studied. By two dimensional resistive MHD calculations it is shown that plasmoid properties depend very much on the reconnection process especially when the reconnection rate is large. Thus the early plasmoid formation is dominated by magnetic reconnection. At later times the main plasmoid acceleration is due to pressure forces while the tension of open interplanetary field lines is negligible. The comparison of different resistivity and equilibrium models reveals a definite influence of the microscopic dissipation and the initial state on magnetic reconnection and the resulting evolution of plasmoids. ESA

N89-25015# Abastumani Astrophysical Observatory, Georgia (USSR).
INDUCTIVE ACCELERATION OF PROTONS AND ELECTRONS IN PLANETARY MAGNETOTAILS **c91**
A. L. Taktakishvili and L. M. Zelenyi (Academy of Sciences, USSR, Moscow) *In* ESA, Proceedings of an International School and Workshop on Reconnection in Space Plasma, Volume 2 Jan. 1989 p 227-232 (For primary document see N89-24974 18-75)
Copyright Avail: NTIS HC A15/MF A01; ESA Publications Div., ESTEC, Noordwijk, Netherlands, 45 US dollars or 80 Dutch guilders

A unified model of particle acceleration (both electrons and ions) in planetary magnetotail due to explosive spontaneous reconnection is considered. It is shown that the inductive electric field is able to generate particle bursts with special velocity dispersion features. The proposed mechanism accelerates both species up to the MeV energies in the Earth's magnetosphere (but with the electron flux much lower than ion) and vice versa (practically only electrons) in the compact Mercury magnetosphere. The theory conforms with the experimental data obtained in terrestrial and Hermean magnetotails. ESA

N89-25016# Academy of Sciences (USSR), Irkutsk. Inst. of Terrestrial Magnetism, Ionosphere and Radiowave Propagation.
AN ANALOGY BETWEEN MAGNETOSPHERIC SUBSTORMS AND SOLAR FLARES: NEW VERSION **c92**
V. M. Mishin *In* ESA, Proceedings of an International School and Workshop on Reconnection in Space Plasma, Volume 2 Jan. 1989 p 233-240 (For primary document see N89-24974 18-75)
Copyright Avail: NTIS HC A15/MF A01; ESA Publications Div., ESTEC, Noordwijk, Netherlands, 45 US dollars or 80 Dutch guilders

The analogy between magnetospheric substorms and solar flares based on magnetic reconnection inside the active solar region as a main content of both phenomena is revised. The proposed scenario takes into account, as an additional element, the reconnection on the active region boundary which promotes the energy input to this region from outside. So, a flare, like a substorm, is not only the unloading but the driven process too. It is emphasized that efficiency of the energy input increases as L sub T sq = h sq, where L sub T is the length of the closed magnetospheric tail, and h is height of arcades. Observational tests of the model are suggested. ESA

N89-25017*# California Univ., Los Angeles. Inst. of Geophysics and Planetary Physics.
BROADBAND ELECTROSTATIC WAVES AS A CONSEQUENCE OF MAGNETOTAIL RECONNECTION
Maha Ashour-Abdalla and D. Schriver *In* ESA, Proceedings of an International School and Workshop on Reconnection in Space Plasma, Volume 2 Jan. 1989 p 241-248 (For primary document see N89-24974 18-75)
(Grants NAGw-78; NSF ATM-85-13215)
Copyright Avail: NTIS HC A15/MF A01; ESA Publications Div., ESTEC, Noordwijk, Netherlands, 45 US dollars or 80 Dutch guilders CSCL 04A

One and two-dimensional particle stimulations are used to study ion beam driven instabilities within the plasma sheet boundary layer (PSBL) and the consequences these instabilities have in terms of plasma heating. It shown that when cold lobe plasma convects into the PSBL and interacts with the ion beams, two wave modes can be driven unstable, the electron acoustic and ion-ion two stream instabilities; these waves heat the cold electrons and cold ions close to plasma sheet temperatures. ESA

N89-25018# Academy of Sciences (USSR), Moscow.
THE ROLE OF COLD ELECTRONS IN THE GENERATION OF THE HIGH-FREQUENCY PART OF BROADBAND ELECTROSTATIC NOISE
T. M. Burinskaya and C.-V. Meister (Academy of Sciences, Potsdam, German D.R.) *In* ESA, Proceedings of an International School and Workshop on Reconnection in Space Plasma, Volume 2 Jan. 1989 p 249-252 (For primary document see N89-24974 18-75)
Copyright Avail: NTIS HC A15/MF A01; ESA Publications Div., ESTEC, Noordwijk, Netherlands, 45 US dollars or 80 Dutch guilders

The change of the distribution function of the beam ions during the wave generation and the heating of the background plasma is investigated. The interaction of the warm ion beams with plasma sheet boundary layer (PSBL) plasma containing an additional cold electron component causes the generation of an electron acoustic beam resonant (EABR) instability exciting electrostatic waves over a wide frequency range. In comparison with the ion beam acoustic instability occurring when the ion beam is rather cold, the EABR

instability is better suited to explain the measured broadband electrostatic noise in the magnetotail because much warmer ion beams may be unstable, which is in better agreement with satellite experiments. Besides, the frequency range of the EABR waves is extended up closer to the local electron plasma frequency. ESA

N89-25019# Academy of Sciences, Potsdam (German D.R.). Central Inst. for Astrophysics.
ELECTROMAGNETIC ELECTRON TEMPERATURE ANISOTROPY INSTABILITY IN THE EARTH'S MAGNETOTAIL PLASMA SHEET **c46**
B. Nikutowski *In* ESA, Proceedings of an International School and Workshop on Reconnection in Space Plasma, Volume 2 Jan. 1989 p 253-258 (For primary document see N89-24974 18-75)
Copyright Avail: NTIS HC A15/MF A01; ESA Publications Div., ESTEC, Noordwijk, Netherlands, 45 US dollars or 80 Dutch guilders

The electromagnetic fire hose instability driven by an electron temperature anisotropy is considered for parallel propagating waves as a possible explanation for the observations of magnetic noise bursts in the central plasma sheet of the geomagnetic tail. The approximative condition for instability is given. The fire hose instability could generate a wave frequency spectrum up to 3Hz with a maximum growth rate at 1Hz in the central plasma sheet. ESA

N89-25020# Polish Academy of Sciences, Warsaw. Space Research Center.
ELF PLASMA TURBULENCE OBSERVED BY PROGNOZ-8 IN PLASMA JETS IN THE MAGNETOSPHERIC TAIL
J. Blecki, K. Kossacki, B. Popielawska, S. A. Romanov, and S. P. Savin (Academy of Sciences, USSR, Moscow) *In* ESA, Proceedings of an International School and Workshop on Reconnection in Space Plasma, Volume 2 Jan. 1989 p 259-262 (For primary document see N89-24974 18-75)
Copyright Avail: NTIS HC A15/MF A01; ESA Publications Div., ESTEC, Noordwijk, Netherlands, 45 US dollars or 80 Dutch guilders

Prognoz-8 observations of plasma and low-frequency (2 to 105Hz) waves in two different regions of the magnetospheric tail are presented. Dense magnetosheathlike plasma clouds apparantly detached from the magnetopause were encountered by Prognoz-8 near the high latitude nightside magnetopause. Such plasma clouds inside the magnetosphere are always associated with strong wave activity at frequencies between proton cyclotron frequency and lower hybrid frequency. Another region within the magnetospheric tail with strong plasma turbulence was observed over the plasma sheet boundary layer. ESA

N89-25021*# Los Alamos National Lab., NM.
FLUX TRANSFER EVENTS: RECONNECTION WITHOUT SEPARATORS
M. Hesse, J. Birn, and K. Schindler (Ruhr Univ., Bochum, Germany, F.R.) *In* ESA, Proceedings of an International School and Workshop on Reconnection in Space Plasma, Volume 2 Jan. 1989 p 263-268 Sponsored by NASA, Washington, DC and Deutsche Forschungsgemeinschaft, Bonn, Fed. Republic of Germany (For primary document see N89-24974 18-75)
Copyright Avail: NTIS HC A15/MF A01; ESA Publications Div., ESTEC, Noordwijk, Netherlands, 45 US dollars or 80 Dutch guilders

A topological analysis of a simple model magnetic field of a perturbation at the magnetopause modeling an apparent flux transfer event is presented. It is shown that a localized perturbation at the magnetopause can in principle open a closed magnetosphere by establishing magnetic connections across the magnetopause. Although the model field exhibits neutral points, these are not involved in the magnetic connection of the flux tubes. The topological substructure of a localized perturbation is analyzed in a simpler configuration. The presence of both signs of the magnetic field component normal to the magnetopause leads to a linkage of topologically different flux tubes, described as a flux knot, and a filamentary substructure of field lines of different topological types which becomes increasingly complicated for decreasing magnetic shear at the magnetopause. ESA

N89-25022# Alaska Univ., Fairbanks. Inst. of Geophysics.
MULTIPLE X LINE RECONNECTION AT THE DAYSIDE MAGNETOPAUSE
L. C. Lee *In* ESA, Proceedings of an International School and Workshop on Reconnection in Space Plasma, Volume 2 Jan. 1989 p 269-274 (For primary document see N89-24974 18-75)
(Contract DE-FG06-86ER-13530; NSF ATM-85-21115)
Copyright Avail: NTIS HC A15/MF A01; ESA Publications Div., ESTEC, Noordwijk, Netherlands, 45 US dollars or 80 Dutch guilders

Studies on magnetic reconnection are reviewed. The multiple X line reconnection model for the flux transfer events; the criterion for the transition from the single X line to the multiple X line reconnection; a global simulation of the dayside magnetopause reconnection; a particle simulation of single X line reconnection and multiple X line reconnection; a patchy reconnection mechanism; and a mechanism for the generation of cusp-region hydromagnetic waves are discussed. ESA

N89-25023# Academia Sinica, Beijing (China). Inst. of Space Physics.
A 2-D AND 3-D SIMULATION STUDY OF MULTIPLE X LINE RECONNECTION
Z. F. Fu *In* ESA, Proceedings of an International School and Workshop on Reconnection in Space Plasma, Volume 2 Jan. 1989 p 275-279 Sponsored in part by the Chinese National Science Foundation (For primary document see N89-24974 18-75)
(Contract DE-FG06-86ER-13530; NSF ATM-85-21115)
Copyright Avail: NTIS HC A15/MF A01; ESA Publications Div., ESTEC, Noordwijk, Netherlands, 45 US dollars or 80 Dutch guilders

An incompressible MHD simulation is used to verify the proposed multiple X line reconnectioon process at the dayside magnetosphere. The 2-D simulation results are reviewed and 3-D simulation results are reported. The condition for the occurrence and the dynamical property of the multiple X line reconnection are discussed. The 3-D topology of the reconnected flux tubes is discussed, especially the ends of the tubes. ESA

N89-25024# Leningrad State Univ. (USSR). Inst. of Physics.
THE ROLE OF THE MAGNETIC RECONNECTION IN THE SOLAR WIND/MAGNETOSPHERE INTERACTION
M. I. Pudovkin and V. S. Semenov *In* ESA, Proceedings of an International School and Workshop on Reconnection in Space Plasma, Volume 2 Jan. 1989 p 281-286 (For primary document see N89-24974 18-75)
Copyright Avail: NTIS HC A15/MF A01; ESA Publications Div., ESTEC, Noordwijk, Netherlands, 45 US dollars or 80 Dutch guilders

Processes of solar wind flow around magnetosphere and of magnetic field reconnection at the magnetopause are considered. The outside dissipative layer magnetic field is described by a frozen-in equation; at the magnetopause magnetic field lines are significantly stretched and there appears a magnetic barrier. Within the magnetic barrier solar wind flow becomes quasi-two-dimensional, and instead of a stagnation point, a stagnation line appears at the magnetopause. Existence of intensive magnetic and electric fields within the barrier results in development of magnetic reconnection. The usual boundary condition at the magnetopause has to be replaced by the Petschek condition. Having solved the system of MHD equations with boundary conditions in Petschek form, one may use that solution as boundary conditions for the reconnection problem and obtain the structure of the magnetopause. ESA

N89-25025# Leningrad State Univ. (USSR). Inst. of Physics.
IMPULSIVE RECONNECTION OF THE SKEWED MAGNETIC FIELDS AT THE MAGNETOPAUSE AS A MHD MODEL
V. S. Semenov *In* ESA, Proceedings of an International School and Workshop on Reconnection in Space Plasma, Volume 2 Jan. 1989 p 287-289 (For primary document see N89-24974 18-75)
Copyright Avail: NTIS HC A15/MF A01; ESA Publications Div., ESTEC, Noordwijk, Netherlands, 45 US dollars or 80 Dutch guilders

Unsteady reconnection in skewed fields under the finite length of X-line is considered in the frame of ideal incompressible MHD approximation. The propagation of discontinuities as well as the evolution of magnetic field, plasma flow and pressure are computed analytically for the arbitrary given function which describes the time behavior of reconnection rate. In the neighborhood of the X-line the solution looks like the Petschek solution. Plasma is strongly accelerated when crossing the moving slow shocks, which propagate along the magnetic field in different directions above and below the current sheet in skewed fields. As a consequence the process leads to the large extension of magnetic flux tubes closed across the initial current sheet. The basic features of these tubes resemble very much the behavior of dayside flux transfer events. ESA

N89-25026# Academy of Sciences, Graz (Austria). Inst. fuer Weltraumforschung.
THE STRUCTURE OF THE RECONNECTION LAYER IN THE PETSCHEK RECONNECTION MODEL: THEORY AND APPLICATION TO THE EARTH'S MAGNETOPAUSE
R. P. Rijnbeek, M. F. Heyn, H. K. Biernat, and V. S. Semenov (Leningrad State Univ., USSR) *In* ESA, Proceedings of an International School and Workshop on Reconnection in Space Plasma, Volume 2 Jan. 1989 p 291-296 Sponsored in part by the Royal Society, United Kingdom (For primary document see N89-24974 18-75)
Copyright Avail: NTIS HC A15/MF A01; ESA Publications Div., ESTEC, Noordwijk, Netherlands, 45 US dollars or 80 Dutch guilders

Reconnection is formulated in terms of a Riemann problem and the structure of the reconnection layer, which corresponds to the layer MHD wave modes in Petschek's model, is analyzed as a function of the parameters in the inflow regions. The influence of asymmetric inflow regions and the relevance to the Earth's magnetopause is discussed. ESA

N89-25027# Polish Academy of Sciences, Warsaw. Space Research Center.
A MODEL OF THE RECONNECTION PATTERN AT THE HELIOPAUSE **c92**
W. Macek and J. Bysiek *In* ESA, Proceedings of an International School and Workshop on Reconnection in Space Plasma, Volume 2 Jan. 1989 p 299-302 (For primary document see N89-24974 18-75)
(Contract CPFR-01.20)
Copyright Avail: NTIS HC A15/MF A01; ESA Publications Div., ESTEC, Noordwijk, Netherlands, 45 US dollars or 80 Dutch guilders

Plasma mixing between the solar wind and the ambient ionized component of the local interstellar medium (LISM) at the heliopause, the boundary separating both media, is discussed. By analogy with the case of planetary magnetopause it is argued that field reconnection processes may play an important role for the plasma mixing at the heliopause. The reconnection areas at the frontal heliopause as viewed from the Sun depending on the assumed direction of the external LISM magnetic field are computed. ESA

N89-25028# Academy of Sciences, Potsdam (German D.R.). Central Inst. for Astrophysics.
ON PARTICLE ENERGIZATION BY MAGNETIC FIELD LINE RECONNECTION IN EXTRAGALACTIC JETS
T. M. Kirchner *In* ESA, Proceedings of an International School and Workshop on Reconnection in Space Plasma, Volume 2 Jan. 1989 p 303-308 (For primary document see N89-24974 18-75)
Copyright Avail: NTIS HC A15/MF A01; ESA Publications Div., ESTEC, Noordwijk, Netherlands, 45 US dollars or 80 Dutch guilders

In order to investigate whether a magnetic field line reconnection process can be operative in cosmic jets for in situ reenergization of synchrotron radiating electrons, the Gold-Parker mechanism of coronal heating (originally devised for the Sun) is considered under the conditions of extragalactic jets. The power dissipated by this process, for the parameter values of two of the most powerful radio galaxies (M 87 and Cen A), amounts to 10 to the 39th to 40th power erg/s. This fits the energetic requirements of the electrons for the radio part of the synchrotron spectrum, but is possibly not enough for its optical and X-ray branch. ESA

N89-25029# European Space Agency. European Space Research and Technology Center, ESTEC, Noordwijk (Netherlands). Space Science Dept.
SPECULATION ON THE ORIGIN OF X-RAY EMISSION IN EARLY-TYPE STARS **c93**
A. M. T. Pollock *In its* Proceedings of an International School and Workshop on Reconnection in Space Plasma, Volume 2 Jan. 1989 p 309-311 (For primary document see N89-24974 18-75)
Copyright Avail: NTIS HC A15/MF A01; ESA Publications Div., ESTEC, Noordwijk, Netherlands, 45 US dollars or 80 Dutch guilders

Observations of OB and Wolf-Rayet stars showing them to be unexpectedly strong sources of X-ray and radio radiation are discussed. Nonthermal radio emission shows the presence of relativistic electrons and magnetic fields far out in the powerful stellar winds that are characteristic of these stars. This suggests an alternative interpretation of the X-ray emission to Lucy and White's shock model as a result of the rapid Compton cooling that energetic electrons would suffer against photospheric radiation. It is proposed that it is the ubiquotous presence of relativistic electrons in early-type stellar winds that is the cause of both radio and X-ray emission and that magnetic reconnection in single and colliding pairs of winds may be the agent of the electron acceleration. ESA

N89-25030# FOM-Inst. voor Plasmafysica, Rijnhuizen, Jutphaas (Netherlands).
FOM-RIJNHUIZEN CONTRIBUTIONS TO THE FIFTEENTH SYMPOSIUM ON FUSION TECHNOLOGY
Nov. 1988 61 p Symposium held in Utrecht, Netherlands, 19-23 Sep. 1988 Sponsored by the Netherlands Organization for the Advancement of Pure Research and Euratom
(Rept-88-179; ETN-89-94243) Avail: NTIS HC A04/MF A01

Experimental systems, tokamak engineering, plasma heating and equilibrium, free electron lasers, beam guiding systems, elliptical polarization, plasma control, and data acquisition were discussed. For individual titles, see N89-25031 through N89-25037.

N89-25031# FOM-Inst. voor Plasmafysica, Rijnhuizen, Jutphaas (Netherlands).
A ROLE FOR FREE ELECTRON LASERS IN FUSION
M. J. vanderWiel and P. W. vanAmersfoort *In its* FOM-Rijnhuizen Contributions to the Fifteenth Symposium on Fusion Technology Nov. 1988 p 16-29 Sponsored in part by the Netherlands Organization for the Advancement of Pure Research and Euratom (For primary document see N89-25030 18-75)
Avail: NTIS HC A04/MF A01

The principles of operation of the free electron laser (FEL) are discussed, together with the similarities and differences with classical devices like gyrotrons and ordinary lasers. The free electron laser is of potentially high efficiency and large unit size, combined with wide tunability. Projects for FEL development are overviewed. ESA

N89-25032# FOM-Inst. voor Plasmafysica, Rijnhuizen, Jutphaas (Netherlands).
ENGINEERING ASPECTS OF RTP
O. G. Kruijt, A. B. Sterk, G. vanDijk, P. Hellingman, and A. A. M. Oomens *In its* FOM-Rijnhuizen Contributions to the Fifteenth Symposium on Fusion Technology Nov. 1988 p 30-34 Sponsored by the Netherlands Organization for the Advancement of Pure Research and Euratom (For primary document see N89-25030 18-75)
Avail: NTIS HC A04/MF A01

An overview is presented for transport mechanisms in tokamak plasmas. The experimental work focuses on determining as accurately as possible the radial and poloidal structure of the plasma equilibrium and the spectra of the fluctuations of plasma density and temperature. The main technical characteristics are described, including wall conditioning, toroidal field, poloidal field, power supplies, and magnetic diagnostic procedures. ESA

N89-25033# FOM-Inst. voor Plasmafysica, Rijnhuizen, Jutphaas (Netherlands).
BEAM GUIDING SYSTEM FOR RUTHERFORD SCATTERING DIAGNOSTIC AT TEXTOR
A. Cosler, H. W. vanderVen, E. P. Barbian, G. Bertschinger, A. A. E. vanBlokland (Kernforschungsanlage, Juelich, Germany, F.R.), and E. Kemmereit *In its* FOM-Rijnhuizen Contributions to the Fifteenth Symposium on Fusion Technology Nov. 1988 p 35-38 Sponsored in part by the Netherlands Organization for the Advancement of Pure Research and Euratom (For primary document see N89-25030 18-75)
Avail: NTIS HC A04/MF A01

A beam guiding system for a neutral beam probe diagnostics is developed for implementation at the Textor experiment. Energetic helium atoms scattered on the plasma ions provided information about the local ion temperature. Time resolution is attained by sampling scattered particles measured individually by a time of flight analyzer. ESA

N89-25034# FOM-Inst. voor Plasmafysica, Rijnhuizen, Jutphaas (Netherlands).
MEQALAC: A 1 MeV MULTI-CHANNEL RF-ACCELERATOR FOR LIGHT IONS
J. G. Bannenburg, W. H. Urbanus, R. G. C. Wojke, H. Klein, A. Schempp, R. W. Thomae, T. Weis, and P. W. vanAmersfoort (Johann-Wolfgang-Goethe-Univ., Frankfurt am Main, Germany, F.R.) *In its* FOM-Rijnhuizen Contributions to the Fifteenth Symposium on Fusion Technology Nov. 1988 p 39-43 Sponsored by the Netherlands Organization for the Advancement of Pure Research; Nederlandse Ministerie von Onderwijs en Wetenschappen and Euratom (For primary document see N89-25030 18-75)
Avail: NTIS HC A04/MF A01

The installation of multiple electrostatic quadrupole array linear accelerator (MEQALAC) which is based on dividing the beam in a number of parallel beamlets, is described. An advantage of the set-up is that the total current can be increased via the number of beamlets. The space charge dominated beams are focused by arrays of miniaturized electrostatic quadrupoles. In a demonstration experiment four 2.2 mA He+ beams are accelerated from 40 to 120 keV. ESA

N89-25035# FOM-Inst. voor Plasmafysica, Rijnhuizen, Jutphaas (Netherlands).
ELLIPTICAL POLARIZATION FOR ECRH ON RTP
P. Manintveld and A. G. A. Verhoeven *In its* FOM-Rijnhuizen Contributions to the Fifteenth Symposium on Fusion Technology Nov. 1988 p 44-49 Sponsored by the Netherlands Organization for the Advancement of Pure Research and Euratom (For primary document see N89-25030 18-75)
Avail: NTIS HC A04/MF A01

The electron cyclotron resonance heating (ECRH) installation for the tokamak accelerator is described. The power is delivered by three gyrotrons. Elliptical polarization is made by a waveguide polarizer with an elliptical cross section that gradually changes with distance and has circular cross section at both ends. A second way is implemented by the reflection of a linearly polarized wave on a grooved metal plate. The measurements show that it is possible to obtain elliptical polarization using a waveguide elliptical polarizer. ESA

N89-25036# FOM-Inst. voor Plasmafysica, Rijnhuizen, Jutphaas (Netherlands).
CONTROL AND DATA ACQUISITION SYSTEM FOR THE NEUTRAL BEAM PROBE DIAGNOSTIC ON TEXTOR
A. A. E. vanBlokland, M. K. Korten (Kernforschungsanlage, Juelich, Germany, F.R.), F. D. A. deWinter, E. P. Barbian, and H. W. vanderVen *In its* FOM-Rijnhuizen Contributions to the Fifteenth Symposium on Fusion Technology Nov. 1988 p 50-53 Sponsored in part by the Netherlands Organization for the Advancement of Pure Research and Euratom (For primary document see N89-25030 18-75)
Avail: NTIS HC A04/MF A01

A neutral beam probe diagnostic using Rutherford scattering is described. The measuring method is based on elastic scattering of injected monoenergetic helium atoms by the plasma ions. The ion temperature is determined from the broadening of the energy distribution of the scattered particles. The data acquisition system, the control and monitoring system, and development status are discussed. ESA

N89-25037# FOM-Inst. voor Plasmafysica, Rijnhuizen, Jutphaas (Netherlands).
THE CONTROL AND MONITORING SYSTEM OF RTP
J. P. Nijman, W. Kooijman, A. A. M. Oomens, P. H. M. Smeets, and A. J. H. Tielemans *In its* FOM-Rijnhuizen Contributions to the Fifteenth Symposium on Fusion Technology Nov. 1988 p 54-58 Sponsored by the Netherlands Organization for the Advancement of Pure Research and Euratom (For primary document see N89-25030 18-75)
Avail: NTIS HC A04/MF A01

The control system is split into a central timing system that masters the time critical tokamak pulse sequencing and data acquisition, and a computerized system to assist the operators with the automatic configuration of timers, data recorders, and additional equipment. The software structure is discussed. A user interface is provided to coordinate control from the main console. ESA

N89-25038 Max-Planck-Inst. fuer Plasmaphysik, Garching (Germany, F.R.).
ASDEX CONTRIBUTIONS TO THE 8TH INTERNATIONAL CONFERENCE ON PLASMA SURFACE INTERACTION IN CONTROLLED FUSION DEVICES
Nov. 1988 149 p Conference held in Juelich, Fed. Republic of Germany, 2-6 May 1988, and at the International Workshop on Plasma Edge Theory, Augustusburg, Fed. Republic of Germany, 26-30 Apr. 1988
(IPP-III/139; ETN-89-94397) Copyright Avail: Fachinformationszentrum Karlsruhe, 7514 Eggenstein-Leopoldshafen 2, Fed. Republic of Germany

Work done on the ASDEX divertor tokamak is discussed. The subjects include impurities accumulation studies, scrape-off density profiles, edge and divertor simulation, recycling, neutral beam fluxes, charge exchange neutral sputtering, erosion and retention of target plate materials, material transport, and plasma induced changes of metallic diverters. For individual titles, see N89-25039 through N89-25048.

N89-25039 Max-Planck-Inst. fuer Plasmaphysik, Garching (Germany, F.R.).
IMPURITY ACCUMULATION STUDIES IN PELLET-REFUELLED ASDEX DISCHARGES
G. Fussmann, K. Krieger, R. Nolte, H. Roehr, and K.-H. Steuer *In its* ASDEX Contributions to the 8th International Conference on Plasma Surface Interaction in Controlled Fusion Devices Nov. 1988 p 1-13 (For primary document see N89-25038 18-75)
Copyright Avail: Fachinformationszentrum Karlsruhe, 7514 Eggenstein-Leopoldshafen 2, Fed. Republic of Germany

The improvements obtained in confining experiments by the repetitive injection of pellets are described. Detailed information on experimental observations made in such discharges is given. A strong accumulation of metallic impurities is observed, which leads to intolerable cooling of the plasma core region. The underlying transport changes associated with the accumulation are discussed. ESA

N89-25040 Max-Planck-Inst. fuer Plasmaphysik, Garching (Germany, F.R.).
CHARACTERIZATION OF THE ASDEX SCRAPE-OFF-LAYER DENSITY PROFILE DURING NEUTRAL BEAM HEATING
G. K. McCormick and Z. A. Pietrzyk *In its* ASDEX Contributions to the 8th International Conference on Plasma Surface Interaction in Controlled Fusion Devices Nov. 1988 p 14-33 (For primary document see N89-25038 18-75)
Copyright Avail: Fachinformationszentrum Karlsruhe, 7514 Eggenstein-Leopoldshafen 2, Fed. Republic of Germany

The scrape-off layer electron profiles in the outer midplane during phases of high neutral injection power are quantified. The diverted discharges are sustained by gas puffing. Empirical scaling conditions are introduced. The stainless steel walls of the vacuum vessel were neither carbonized nor gettered for these discharges. The importance of recycling for the scrape-off layer properties is emphasized. ESA

N89-25041 Max-Planck-Inst. fuer Plasmaphysik, Garching (Germany, F.R.).
ASDEX EDGE AND DIVERTOR SIMULATION AND THE PROBLEM OF INCOMPLETE AND INACCURATE EXPERIMENTAL DATA
W. Schneider, J. Neuhauser, G. Haas, K. McCormick, N. Tsois, and R. Wunderlich *In its* ASDEX Contributions to the 8th International Conference on Plasma Surface Interaction in Controlled Fusion Devices Nov. 1988 p 34-39 Submitted for publication (For primary document see N89-25038 18-75)
Copyright Avail: Fachinformationszentrum Karlsruhe, 7514 Eggenstein-Leopoldshafen 2, Fed. Republic of Germany

The one dimensional hydrodynamic code SOLID coupled with the two dimensional Monte Carlo neutral gas code DEGAS are used to simulate the scrape-off layer and divertor recycling region of the ASDEX tokamak. A numerical data base is created for the relevant parameter regime and compared to the limited amount of experimental data. A reasonable fit with ohmic data is obtained, assuming classical heat flow along field lines and allowing for varying divertor saturation. ESA

N89-25042 Max-Planck-Inst. fuer Plasmaphysik, Garching (Germany, F.R.).
COMPARISON OF RECYCLING IN THE ASDEX DIVERTOR BEFORE AND AFTER HARDENING
G. Haas, W. Poschenrieder, J. Neuhauser, and S. Kaesdorf *In its* ASDEX Contributions to the 8th International Conference on Plasma Surface Interaction in Controlled Fusion Devices Nov. 1988 p 40-52 (For primary document see N89-25038 18-75)
Copyright Avail: Fachinformationszentrum Karlsruhe, 7514 Eggenstein-Leopoldshafen 2, Fed. Republic of Germany

Water cooled divertor components were installed in order to be able to dissipate the heat load of long pulses of neutral beam injection. The modified geometry resulted in significant changes in gas consumption and divertor pressure. Difficulties in obtaining a good H mode are possibly connected to the modified recycling behavior. However, a regime with improved ohmic confinement and reduced recycle is found. ESA

N89-25043 Max-Planck-Inst. fuer Plasmaphysik, Garching (Germany, F.R.).
THE LOW ENERGY NEUTRAL FLUXES AND THEIR IMPURITY PRODUCTION AT THE WALLS OF ASDEX
H. Verbeek, V. Dose, O. Gehre, J. Gernhardt, G. Janeschitz, E. R. Mueller, H. Roehr, K. H. Steuer, and F. X. Soeldner *In its* ASDEX Contributions to the 8th International Conference on Plasma Surface Interaction in Controlled Fusion Devices Nov. 1988 p 53-67 (For primary document see N89-25038 18-75)
Copyright Avail: Fachinformationszentrum Karlsruhe, 7514 Eggenstein-Leopoldshafen 2, Fed. Republic of Germany

The density dependence of the neutral flux, its mean energy, and its impurity production at the walls were investigated for ohmic hydrogen and deuterium discharges using a low energy neutral particle analyzer. For hydrogen a large increase of the neutral flux with increasing density is observed, while the mean energy of the neutrals decreases. For deuterium the same behavior goes up to densities of 3.5 times 10 to the 13th power particles/cc. For higher densities the flux behaves differently for the different confinement regimes. Only in the regime of saturated ohmic confinement does the flux increase further with increasing density. ESA

N89-25044 Max-Planck-Inst. fuer Plasmaphysik, Garching (Germany, F.R.).
CHARGE EXCHANGE NEUTRAL SPUTTERING IN ASDEX
G. Staudenmaier and W. R. Wampler (Sandia National Labs., Albuquerque, NM.) *In its* ASDEX Contributions to the 8th International Conference on Plasma Surface Interaction in Controlled Fusion Devices Nov. 1988 p 68-82 (For primary document see N89-25038 18-75)
(Contract DE-AC04-76DP-00789)
Copyright Avail: Fachinformationszentrum Karlsruhe, 7514 Eggenstein-Leopoldshafen 2, Fed. Republic of Germany

Neutral fluxes to the wall of ASDEX were measured with an energy resolving carbon resistance probe, combined with a mechanical shutter providing time resolution. With two silicon overlayers of different thickness the non Maxwellian energy distribution of the charge exchange neutrals can be approximately determined. Charge exchange neutral sputtering is an important impurity source representing a lower limit for impurity generation. ESA

N89-25045 Max-Planck-Inst. fuer Plasmaphysik, Garching (Germany, F.R.).
EROSION AND RETENTION OF THE TARGET PLATE MATERIAL IN THE ASDEX DIVERTOR
G. Janeschitz, G. Fussmann, J. Hofmann, L. B. Ran, E. Taglauer, J. Roth, and H. R. Yang (Southwestern Inst. of Physics, Leshan, China) *In its* ASDEX Contributions of the 8th International Conference on Plasma Surface Interaction in Controlled Fusion Devices Nov. 1988 p 83-95 (For primary document see N89-25038 18-75)
Copyright Avail: Fachinformationszentrum Karlsruhe, 7514 Eggenstein-Leopoldshafen 2, Fed. Republic of Germany

Experiments undertaken to evaluate the retention of target produced impurities are described. A possibility existed to study the transport of the copper target plate material into the main plasma. The Cu flux emerging from the target plate and the Cu density in the main plasma were measured by spectroscopy. A poor retention is found at lower densities, but is is substantially improved at higher densities. The retention seems to be independent of the heating power. ESA

N89-25046 Max-Planck-Inst. fuer Plasmaphysik, Garching (Germany, F.R.).
MEASUREMENTS OF THE FLUX OF METALLIC IMPURITIES TO THE ASDEX DIVERTOR PLATES
E. Taglauer, A.-P. Martinelli, and G. Janeschitz *In its* ASDEX Contributions to the 8th International Conference on Plasma Surface Interaction in Controlled Fusion Devices Nov. 1988 p 96-107 (For primary document see N89-25038 18-75)
Copyright Avail: Fachinformationszentrum Karlsruhe, 7514 Eggenstein-Leopoldshafen 2, Fed. Republic of Germany

Metal impurities (Fe, Cu) fluxes to the divertor plates of ASDEX were measured using a collector probe during discharges with various plasma parameters. The Cu depositions show generally a different distribution across the scrape-off layer compared to the Fe deposition. Variations of the Cu and Fe fluxes with auxiliary heating and vessel carbonization are analyzed and discussed in view of impurity production mechanisms. ESA

N89-25047 Max-Planck-Inst. fuer Plasmaphysik, Garching (Germany, F.R.).
MATERIAL TRANSPORT AT THE VESSEL WALLS OF THE DIVERTOR TOKAMAK ASDEX
Wen-Min Wang, J. Roth, R. Behrisch, and G. Staudenmaier *In its* ASDEX Contributions to the 8th International Conference on Plasma Surface Interaction in Controlled Fusion Devices Nov. 1988 p 108-128 (For primary document see N89-25038 18-75)
Copyright Avail: Fachinformationszentrum Karlsruhe, 7514 Eggenstein-Leopoldshafen 2, Fed. Republic of Germany

Carbon tiles and probes exposed to the main flux placed at the walls of the Ti divertor plates were analyzed with respect to deposition of D and metal atoms. The lowest deposition is found where the separatrix intersects the divertor plates. The deposition is larger at the divertor entrance and the walls of the main discharge chamber. This indicates that the metal atoms deposited at the divertor plates are re-eroded. A material balance is established comparing impurity sources and sinks. ESA

N89-25048 Ruhr Univ., Bochum (Germany, F.R.). Inst. fuer Experimentalphysik.
PLASMA INDUCED CHANGES OF A METALLIC DIVERTOR NEUTRALIZER PLATE FROM ASDEX ANALYZED BY PHOTOACOUSTICS
B. K. Bein, M. Wojczak, and J. Pelzl *In* Max-Planck Institut fuer Plasmaphysik, ASDEX Contributions to the 8th International Conference on Plasma Surface Interaction in Controlled Fusion Nov. 1988 p 129-144 (For primary document see N89-25038 18-75)
Copyright Avail: Fachinformationszentrum Karlsruhe, 7514 Eggenstein-Leopoldshafen 2, Fed. Republic of Germany

A thermal wave method with acoustic detection was used to obtain space resolved thermal depth profiles and to characterize the plasma induced changes of the plate material. In the intersection region between the plasma separatrix and the neutralizer plate, the effusivity, the thermophysical parameter relevant for time dependent surface heating processes, increased 18 percent over its original value. ESA

N89-25049# Oak Ridge National Lab., TN.
THE ROLE OF THE RADIAL ELECTRIC FIELD IN ENHANCED CONFINEMENT REGIMES IN STELLARATORS
K. C. Shaing 1989 5 p Presented at the 7th International Stellarator Workshop, Oak Ridge, TN, 10 Apr. 1989
(Contract DE-AC05-84OR-21400)
(DE89-011572; CONF-890403-9) Avail: NTIS HC A02/MF A01

The confinement enhancement observed in stellarators could be attributable to the suppression of turbulent fluctuations by the radial electric field E sub r. The pressure-gradient-driven turbulence model is used to illustrate the effects of E sub r on turbulent fluctuations. A more negative value of E sub r and/or a more positive value of dE sub r/dr can reduce the fluctuation amplitudes, if dN/dr is less than 0. Here, r is the local minor radius and N is the plasma density. DOE

N89-25050# Oak Ridge National Lab., TN.
NUMERICAL METHODS FOR STELLARATOR OPTIMIZATION
R. N. Morris, C. L. Hedrick, S. P. Hirshman, J. F. Lyon, and J. A. Rome 1989 7 p Presented at the 7th International Stellarator Workshop, Oak Ridge, TN. 10 Apr. 1989
(Contract DE-AC05-84OR-21400)
(DE89-012342; CONF-890403-20) Avail: NTIS HC A02/MF A01

A numerical optimization procedure utilizing an inverse 3-D equilibrium solver, a Mercier stability assessment, a deeply-trapped-particle loss assessment, and a nonlinear optimization package has been used to produce low aspect ratio (A = 4) stellarator designs. These designs combine good stability and improved transport with a compact configuration. DOE

76 SOLID-STATE PHYSICS

Includes superconductivity.

For related information, see also *33 Electronics and Electrical Engineering* and *36 Lasers and Masers.*

N89-25051*# San Diego Semiconductors, Inc., CA.
POSITION-SENSITIVE CdTe DETECTOR USING IMPROVED CRYSTAL GROWTH METHOD Final Report
20 Sep. 1988 27 p
(Contract NAS5-30289)
(NASA-CR-183427; NAS 1.26:183427) Avail: NTIS HC A03/MF A01 CSCL 20L

The feasibility of developing a position-sensitive CdTe detector array for astronomical observations in the hard X-ray, soft gamma ray region is demonstrated. In principle, it was possible to improve the resolution capability for imaging measurements in this region by orders of magnitude over what is now possible through the use of CdTe detector arrays. The objective was to show that CdTe crystals of the quality, size and uniformity required for this application can be obtained with a new high pressure growth technique. The approach was to fabricate, characterize and analyze a 100 element square array and several single-element detectors using crystals from the new growth process. Results show that detectors fabricated from transversely sliced, 7 cm diameter wafers of CdTe exhibit efficient counting capability and a high degree of uniformity over their entire areas. A 100 element square array of 1 sq mm detectors was fabricated and operated. Author

N89-25052# Lawrence Livermore National Lab., CA.
SHOCK COMPACTION OF SUPERCONDUCTORS
W. J. Nellis, R. L. Landingham, J. B. Holt, M. B. Maple, and C. L. Seaman (California Univ., San Diego.) Sep. 1988 4 p Presented at HERAPS '88: International Seminar on High Energy Working of Rapidly Solidified Materials, Novosibirsk, USSR, 10 Oct. 1988
(Contract W-7405-eng-48)
(DE89-006744; UCRL-99694; CONF-881060-5) Avail: NTIS HC A02/MF A01

Shock compression has several features which indicate a high potential for the processing of practical superconductors and for the synthesis of new superconducting phases. By using shock waves a dynamic pressure pulse in the range 10 to 1000 kbar can be applied for a duration of order 1 micro sec. The pressures, densities, temperatures, strain rates, and quench rates are substantially larger than for conventional processing methods. High quench rates could be used to synthesize new metastable high-T sub c phases, where T sub c is the superconducting critical transition temperature. The fast nature of the process also permits the heterogeneous processing of powders. That is, by compacting powders in a micro sec, compressive energy is deposited heterogeneously on particle boundaries. This dynamic method offers the opportunity to achieve high density and to selectivity process the grain boundary region in high-T sub c superconductors. Since controlling the grain boundary region is essential to achieving high critical current density J sub c, shock compaction might produce the microstructure required for high J sub c. An example is given of shock compaction of YBa2Cu3O7 + Ag powders. DOE

N89-25053# Brookhaven National Lab., Upton, NY.
ON THE NATURE OF HIGH-TEMPERATURE SUPERCONDUCTIVITY
V. J. Emery 1988 16 p Presented at the IBM Conference on High-Temperature Superconductivity, Oberlech, Austria, 1 Aug. 1988
(Contract DE-AC02-76CH-00016)
(DE89-009525; BNL-42346; CONF-8808178-1) Avail: NTIS HC A03/MF A01

A picture of the electronic structure, magnetism and superconductivity in high T sub c oxides is obtained from a simple analysis of experiments and models of the copper oxide planes. It is shown that magnetism is associated with holes on copper and superconductivity with holes on oxygen. The pairing force is not retarded. Questions about the motion of charges in an

antiferromagnetic background and the many-body theory of high-temperature superconductivity are discussed. Differences between the cuprates and doped BaBiO3 are emphasized. DOE

N89-25054# Stanford Univ., CA. Lab. of Physics.
PHOTOTHERMAL IMAGING OF HIGH T(SUB c) SUPERCONDUCTOR
J. Fanton, G. S. Kino, and B. T. Khuri-Yakub Sep. 1988 4 p Presented at the Institute of Electrical and Electronic Engineering Ultrasonics Symposium, Chicago, IL, 2-5 Oct. 1988
(Contract DE-FG03-87ER-13797)
(DE89-009644; CONF-8810279-3) Avail: NTIS HC A02

The thermal conductivities of the new high-T sub c superconductors show marked changes with temperature, as does their electrical conductivity. As the temperature is lowered, the thermal conductivity abruptly rises near T sub c. Measurements made along the copper-oxide planes of single-crystal bismuth compounds show jumps as large as 70 percent. Since the thermal conductivity in these materials is dominated by lattice conduction, this behavior clearly demonstrates a coupling between the electrical carriers and phonons. The rise at T sub c is likely due to a reduction in phonon scattering as electrons become superconducting pairs. To date, these types of measurements have been made on amorphous samples and along the copper-oxide, or conducting, planes of single-crystal materials. Measurements are hampered by the difficulty of getting appropriately sized samples; the dimensions of single crystallites tend to be small and frequently the samples are oddly shaped. We demonstrate a simple technique for making point measurements of thermal conductivity in these materials. The technique is nondestructive, has sub-micron resolution, and can measure the conductivity in a specified direction. The goal is to make a more complete measurement of the behavior of thermal conductivity near T sub c, including measurements both along the c-axis, and along the Cu-O planes. DOE

N89-25055# Argonne National Lab., IL. Materials Science Div.
CORRELATION BETWEEN THE STRUCTURE, ENERGY, AND LOCAL ELASTIC PROPERTIES OF GRAIN BOUNDARIES IN METALS
D. Wolf, M. Kluge, and J. Lutsko 1988 8 p Presented at the MRS Symposium on Characterization of Structure and Chemistry of Defects in Materials, Boston, MA, 28 Nov. - 3 Dec. 1988
(Contract W-31-109-eng-38)
(DE89-009861; CONF-8811195-1) Avail: NTIS HC A02/MF A01

The zero-temperature energies and equilibrium volume expansions of point-defect free asymmetrical grain boundaries (GBs) involving the four densest planes in fcc bicrystals (with some higher-index plane on the other side of the interface) have been determined using an embedded-atom-method potential fitted to Au. It is found that the two asymmetrical tilt GBs at the endpoints of the related GB energy vs twist disorientation curves give rise to pronounced energy cusps. As for symmetrical GBs, a practically linear relationship between the GB energy and equilibrium volume expansion is observed. The volume expansion and the destruction of the perfect-crystal stacking at the GB are shown to cause a pronounced local decrease in the resistance toward shear parallel to the GB plane. DOE

N89-25056# Argonne National Lab., IL. Materials Science Div.
SUPERCONDUCTING PROPERTIES OF MAGNETRON SPUTTERED Bi-Sr-Ca-Cu-O AND Tl-Ba-Ca-Cu-O THIN FILMS
R. T. Kampwirth, J. H. Kang, and K. E. Gray Dec. 1988 10 p Presented at the Conference on the Science and Technology of Thin Film Superconductors, Colorado Springs, CO, 14-17 Nov. 1988
(Contract W-31-109-eng-38)
(DE89-009878; CONF-881127-5) Avail: NTIS HC A02/MF A01

Thin films of high temperature superconducting Bi-Sr-Ca-Cu-O and Tl-Ba-Ca-Cu-O have been made using multiple source magnetron sputtering. We will discuss preparation and annealing and how they affect the superconducting properties. The Bi-based films form in at least two compounds, a lower T sub c phase with a 2212 composition and T sub c0 of approximately 80 K and a higher T sub c phase with a nominal composition of 2223 and a T sub c of approximately 105 K. The higher T sub c phase is very difficult to form so that a complete superconducting path exists, requiring long annealing times at temperatures somewhat below the formation temperature. Although superconducting properties are less sensitive to stoichiometry than YBa2Cu3O(7-x), annealing temperatures must be held in a narrow range around 865 C to get the best results. Films prefer growing on (100) MgO in a highly textured polycrystalline form, with the c-axis perpendicular to the plane of the film. The Tl-based films form at least three compounds (2212, 1223, 2223) with T sub c's ranging from approximately 100 to 114 K and grow best on (100) and polycrystalline Y-ZrO2 substrates. Annealing conditions are particularly difficult because of the volatility of thallium and require samples to be annealed in sealed capsules with a controlled atmosphere of thallium and oxygen. Upper critical field measurements show a large anisotropy (approximately 15 for Bi-Sr-Ca-Cu-O and greater than or equal to 70 for Tl-Ba-Ca-Cu-O) in the parallel to perpendicular field slope ratio as might be expected from a highly textured anisotropic structure. DOE

N89-25057# Sandia National Labs., Albuquerque, NM.
A FACILITIES VIEW OF THE LOW VOLUME, HIGH PRODUCT MIX FAB
Ralph Keyser 1989 9 p Presented at the SEMI Automation Forum '89, Albuquerque, NM, 13 Apr. 1989
(Contract DE-AC04-76DP-00789)
(DE89-009970; SAND-89-0370C; CONF-8904183-1) Avail: NTIS HC A02/MF A01

Automation has been widely recognized as the next major step in semiconductor manufacturing and numerous manufacturers around the world have been spending large sums of money to develop integrated automation systems for microelectronic chip production. Automation is a manufacturing tool that can be used in many facilities both new and existing, but the power and effectiveness of any automation project can be enhanced by a facility that is designed to be automated. This paper is heavily based on experiences gained in the design, construction, and startup of Sandia's newest cleanroom known as the Microelectronics Development Laboratory (MDL). The MDL is a Class 1 facility of individual process bays organized around a central hallway. Chase areas separate the process bays, and whenever possible, equipment is mounted through the walls to allow maintenance to be done in the less clean chase areas. DOE

N89-25058# Air Force Inst. of Tech., Wright-Patterson AFB, OH. School of Engineering.
SELECTIVE PAIR LUMINESCENCE OF MAGNESIUM IN GALLIUM ARSENIDE DISSERTATION M.S. Thesis
Jeffrey R. Cavins Dec. 1988 191 p
(AD-A206160; AFIT/DS/ENP/88-2) Avail: NTIS HC A09/MF A01 CSCL 20/12

Photoluminescence (PL) and selective pair luminescence (SPL) studies were performed on vapor phase epitaxial (VPE) GaAs. The GaAs included both undoped and Mg ion implanted samples. PL from the unimplanted samples indicated Zn was the dominant impurity with slight traces of C and Si also evident. This assignment was confirmed during SPL measurements of the ion implanted samples. The effect of the Mg implant on the relative intensities of the Mg related SPL transitions was small but discernible. Photoluminescence of the ion implanted materials showed strong Mg impurity spectra; however, the Zn impurity spectra was still dominant. Additionally, a parametric study was performed on the effects of temperature and laser pump intensity on the SPL spectra. GRA

N89-25059# Chicago Univ., IL.
DYNAMICS OF GAS-SURFACE INTERACTIONS Final Technical Report, 1 Apr. 1984 - 31 May 1988
S. J. Sibener 2 Feb. 1989 49 p

(Grant AF-AFOSR-0073-84; AF Proj. 2303)
(AD-A206210; AFOSR-89-0317TR) Avail: NTIS HC A03/MF A01 CSCL 07/2

This research initiative has dealt with the interaction of atomic, molecular, electron, and optical beams with well-characterized single crystal surfaces. These studies were motivated by a desire to understand and control catalytic surface chemistry, the technological need to characterize the physical properties of thin films and surfaces, and the desire to understand how energy and momentum are exchanged at the surface of a material when it is subjected to gas-surface collisions, electron-surface collisions, optical illumination, or chemical reaction. During the past grant period, two major new scattering instruments were completed. One is a high performance neutral particle scattering apparatus, which routinely achieves an energy resolution of ca. 300 micro-eV. It has successfully performed elastic and inelastic scattering measurements on alkali halide, semiconductor, and metallic surfaces. Results are presented in this final report for Lithium Fluoride (001), Silicon (001)-(2x1), and Silver (110). The Si phonon dispersion measurements differ markedly from theoretical calculations, and strongly suggest that the dynamical properties of partially disordered surfaces merit increasing attention in this program. GRA

N89-25060# Naval Ship Research and Development Center, Bethesda, MD. Ship Materials Engineering Dept.
X-RAY PHOTOELECTRON SPECTROSCOPY STUDY OF SAMPLES IN THE Y-Ba-Cu-O SYSTEM Interim Report, Jul. 1987 - Sep. 1988
L. F. Aprigliano, B. Friedman, and R. J. Stockhausen Oct. 1988 39 p
(AD-A206260; DTRC/SME-88/74) Avail: NTIS HC A03/MF A01 CSCL 07/2

Superconducting ceramics that have critical temperatures which exceed the boiling point of liquid nitrogen (77 K) have been discovered. Preliminary studies both in the United States and Japan indicate that the superconducting properties of these ceramics can degrade with exposure to water vapor during processing. X-ray photoelectron spectroscopy (XPS) is a possible method with which to study this problem. The goal of this research was to determine if there are features in the XPS spectra of these ceramics that a spectrometer with non-monochromatic radiation can use to study this reaction. As the first step in this determination, it was necessary to ascertain the extent to which this method can discriminate between the ceramic superconductor, YBa2Cu3O7, and a poorly superconducting two phase sample, (YBa2Cu3O7 and Y2BaCuO5). This latter sample results from processing errors when attempting to make signal phase YBa2CuO7. The core-level XPS spectra for these samples were acquired in this investigation. GRA

N89-25061# Arizona Univ., Tucson. Optical Sciences Center.
LABORATORY FOR X-RAY OPTICS Final Report, 1 Sep. 1986 - 31 Aug. 1988
C. M. Falco 1 Oct. 1988 7 p
(Grant AF-AFOSR-0347-86; AF Proj. 3396)
(AD-A206468; AFOSR-89-0293TR) Avail: NTIS HC A02/MF A01 CSCL 14/2

A silicon/metals molecular beam epitaxy (MBE) apparatus was purchased with this support. The capability for producing MBE multilayer coatings for use in the 10-A to 300-A wavelength range (i.e., between soft X-rays and the extended ultraviolet, referred to here as X-UV) is unique at laboratories conducting research in the field of X-ray optics. The University of Arizona now has a complete program, with capabilities for design, fabrication, characterization, and testing of multilayer coatings for the XUV; for development of state-of-the-art instrumentation to produce and characterize these materials; and for training graduate students and visiting scientists in this important field. GRA

N89-25062# North Carolina Univ., Chapel Hill. Dept. of Chemistry.
EFFECTS OF THERMAL HISTORY ON STRESS-RELATED PROPERTIES OF VERY THIN FILMS OF THERMALLY GROWN SILICON DIOXIDE, SiO2 Interim Technical Report
J. T. Fitch, E. Kobeda, G. Lucovsky, and E. A. Irene 14 Mar. 1989 39 p
(Contract N00014-89-J-1178)
(AD-A206547; TR-25) Avail: NTIS HC A03/MF A01 CSCL 09/1

This paper presents studies of the infrared (IR) absorbance and the intrinsic stress in thermally grown very thin films (60 Augstroms to 700 Augstroms) of silicon dioxide, SiO2. These data are combined with previously obtained data for thicker thermally grown films (approximately 1200 Augstroms) to study the variation in intrinsic growth stress close to the Si/SiO2 interface. The combined data indicate that the intrinsic stress at Si/SiO2 interfaces extrapolates to the same relatively high values for oxides grown at 700 C and 1000 C, and that the distribution of Si-O-Si bond angles close to the Si/SiO2 interface, as deduced from the IR data, is quantitatively different than in the bulk of the oxide film. These two observations are explained in terms of a model based on a temperature dependent viscoelastic relaxation of the oxide stress. This model emphasizes difference in the thermal history of the SiO2 near the Si/SiO2 interface, as compared to the SiO2 that is well-removed from that interface and is in the bulk of the film and/or close to the top surface of the film. GRA

N89-25063# Max-Planck-Inst. fuer Physik und Astrophysik, Munich (Germany, F.R.). Werner-Heisenberg-Inst. fuer Physik.
INVESTIGATIONS ON FULLY DEPLETABLE CHARGE COUPLED DEVICES Thesis - Ludwig-Maximilians-Univ. [UNTERSUCHUNGEN AN VOLL DEPLETIERBAREN CHARGE COUPLED DEVICES]
Michael Sterzik Aug. 1988 66 p In GERMAN
(MPI-PAE/Exp.El-194; ETN-89-93992) Copyright Avail: NTIS HC A04/MF A01

Improvement of semiconductor drift chambers by fully depletable pn, charge coupled device is described. Two dimensional computer simulation, resolving Poisson, transport, and continuum equations confirm the foreseen electric properties and operational parameters. Laboratory measurements agree with calculated results. ESA

N89-25064# Kernforschungszentrum G.m.b.H., Karlsruhe (Germany, F.R.). Inst. fuer Technische Physik.
X-RAY INVESTIGATIONS OF CERAMIC HIGH Tc SUPERCONDUCTORS UNDER HIGH PRESSURE Thesis - Karlsruhe Univ.
W. H. Fietz Nov. 1988 79 p In GERMAN; ENGLISH summary
(KfK-4482; ISSN-0303-4003; ETN-89-94407) Copyright Avail: NTIS HC A05/MF A01

Ceramic oxide superconductors are investigated for their structural properties by X-rays under high pressure. The superconducting material La1.8Sr0.2CuO4 shows a uniform reduction of the lattice parameters up to pressures of 170 kbar. Material YBa2Cu3O7 shows an asymmetry in the reduction of the lattice parameters, explained by an excessive decrease of the lattice parameter in the direction of the b- or c- axis. The orthorhombic phase is stable in the entire temperature range of 300 K to 15 K under ambient pressure. At higher pressures a pseudo-tetragonal is reached, under the assumption of b-lattice parameter reduction. A preferential decrease of the c-lattice parameter leads to a preservation of the orthorhombic phase in the entire investigated pressure range. ESA

N89-25065# Michigan Technological Univ., Houghton. Dept. of Metallurgical Engineering.
THE EFFECTS OF GRADIENTS ON BOUNDARY STABILITY Progress Report, 31 Mar. 1988 - 15 Feb. 1989
Steve A. Hackney, M. R. Plichta, and J. K. Lee 1989 8 p

(Contract DE-FG02-87ER-45315)
(DE89-011590; DOE/ER-45315/2) Avail: NTIS HC A02

This report presents the results for the second year of a DOE funded project entitled, The Effects of Gradients on Boundary Stability, (DE-FG02-87ER-45315) in the following major areas: grain boundary and grain boundary dislocation behavior in a stress gradient; grain boundary and grain boundary dislocation behavior in a concentration gradient (DIGM); effects of unstable grain boundaries on morphological development of second phases (cellular); coherency strain and coherency loss at interfaces; thin film morphological stability under non-equilibrium conditions; and stability of interphase boundaries under non-equilibrium conditions (microscopic and macroscopic). DOE

N89-25066# Arizona Univ., Tucson.
GRAIN BOUNDARY PHASE EQUILIBRIA IN METALLIC SYSTEMS Progress Report, 1 Dec. 1986 - 30 Apr. 1989
P. A. Deymier Apr. 1989 24 p
(Contract DE-FG02-87ER-45285)
(DE89-011787; DOE/ER-45285/3) Avail: NTIS HC A03/MF A01

A method for growing high purity aluminum bicrystals with controlled misorientation and Grain Boundary (GB) plane inclination has been successfully implemented. Computer simulations of a Sigma = 5 (001) symmetric tilt GB in aluminum does not undergo premelting but exhibit a second-order transition associated with an increase in atomic mobility in the GB plane. A GB rotation transition in a Sigma = 5 bicrystal from a (210) inclination to a (38 19 1) orientation has been characterized as a first order phase transition. It takes place by differential shear of the grains across the interface. The driving force for rotation is related to the amount of torque the interface may sustain. The elastic energy contribution to segregation of point defects to planar defects is short range. This elastic contribution is long range if the GB is stresses with points of dilatation. Segregation may result in the complete filling of the interface with solute atoms or the formation of regions of high solute concentration along the interface. High resolution electron microscopy images of a near twin boundary in aluminum shows relaxation of secondary grain boundary dislocation cores when the burgers vectors are parallel to the interface plane. The relaxation leads to a local change in translation state of the GB. DOE

N89-25067# Gosudarstvennyi Komitet po Ispolzovaniyu Atomnoi Energii, Moscow (USSR). Inst. Atomnoj Ehnergii.
THEORETICAL MICROCONTACT SPECTRA OF METAL ELECTRON-PHONON COUPLING
T. N. Kulagina and A. P. Zhernov 1987 52 p In RUSSIAN; In RUSSIAN
(DE88-706280; IAE-4428/9) Avail: NTIS (US Sales Only) HC A04/MF A01

Theoretical and experimental microcontact spectra of simple and certain transition metals are discussed. The Eliashberg thermodynamic functions for the metals are considered, as well as correlations between spectra peculiarities and parameters of metals and microbridge models. DOE

N89-25068# Joint Inst. for Nuclear Research, Dubna (USSR). Lab. of High Energy.
MEASUREMENTS OF MAGNETIC FIELD OF SUPERCONDUCTING SOLENOID
Yu. V. Kulikov, V. P. Ovsyannikov, and A. Yu. Starikov 1988 4 p In RUSSIAN; ENGLISH summary
(DE88-706323; JINR-R-9-88-263) Avail: NTIS (US Sales Only) HC A02/MF A01

The method of measurements for a superconducting focusing magnetic system of the cryogenic electron-beam ion source in nonuniform regions is proposed. The experimental data show high uniformity and axial symmetry of the magnetic field. DOE

N89-25069# Academy of Sciences of the Lithuanian SSR, Vilnius. Inst. Fiziki.
MULTIPHOTON TRANSITIONS AT THE MOESSBAUER RADIATION DIFFRACTION IN CRYSTALS UNDER A WEAK ULTRASONIC FIELD
E. M. Iolin 1988 18 p In RUSSIAN; ENGLISH summary
(DE88-706341; LAFI-131) Avail: NTIS (US Sales Only) HC A03/MF A01

Results of theoretical studies on the X-ray and Moessbauer radiation diffraction in crystals under a high-frequency ultrasonic excitation (UE) are presented. It has been proved that for the perfect crystal a weak UE transforms the frequency of the gamma-quantum diffraction. A wide range of harmonics is excited in the UE frequency as well. Experiments on the Rayleigh scattering of the Moessbauer radiation (RSMR) provide the analysis of the scattered radiation in respect of energy. In a threshold situation if the sample depth holds a whole number of ultrasonic waves, the inelastic scattering grows and the elastic one decreases, while the total scattering cross section remains almost unchangeable. So the RSMR may serve as an efficient instrument for the X- and neutron acoustic resonance study, since these resonances are usually indicated by an ultrasonic quenching of anomalously passing X-rays and neutrons, and the RSMR can be also detected if there is no considerable absorption in the sample. DOE

N89-25070# California Univ., Berkeley. Lawrence Berkeley Lab. Materials and Chemical Sciences Div.
HIGH RESOLUTION ELECTRON MICROSCOPY OF INTERFACES IN TOPOTAXIAL AND EPITAXIAL REACTIONS
U. Dahmen, J. Douin, C. J. D. Hetherington, and K. H. Westmacott Dec. 1988 16 p Presented at the MRS Symposium on High Resolution Microscopy of Materials, Boston, MA, 27 Nov. - 4 Dec. 1988
(Contract DE-AC03-76SF-00098)
(DE89-010390; LBL-26545; CONF-8811196-1) Avail: NTIS HC A03

In the study of interfaces, high resolution electron microscopy (HREM) is most useful when the interface is viewed edge-on while both crystals are accurately aligned along low index zone axes. The formation of such interfaces by epitaxy or topotaxy is the natural means of obtaining structures than can be usefully analyzed by HREM. Furthermore, there is intense interest in understanding the atomic structure of such interfaces in a variety of technologically important materials. This contribution addresses such structures produced by thermal decomposition, precipitation reactions and ionized-cluster-beam deposition, and reports on the structural investigation of symmetrical and asymmetrical grain boundaries, precipitate/matrix interfaces, internal defect structure of precipitates and nanocrystalline composites. DOE

N89-25071# Ohio State Univ., Columbus. Dept. of Physics.
UNIVERSAL REDUCTION OF T(SUBc) IN STRONG COUPLING SUPERCONDUCTORS DUE TO ANDERSON/KONDO IMPURITIES
Mark Jarrell 1 Feb. 1989 19 p Presented at the Workshop on Monte Carlo Techniques for Condensed Matter, Athens, GA, 1 Feb. 1989
(Contract DE-FG02-87ER-45326)
(DE89-011225; DOE/ER-45326/10; CONF-890298-1) Avail: NTIS HC A03/MF A01

The first exact calculation of (partial derivative of T (sub c)/partial derivative of c)(sub c = 0), the initial depression of the superconducting T (sub c), due to a small concentration, c, of magnetic impurities is presented. N(0)(partial derivative of T (sub c)/ partial derivative of c)(sub c = 0) can be expressed as the product of two universal functions: f(lambda sub o), and g(T sub K/T sub co). I find that f changes rapidly as lambda(sub o) increases, and that, in contrast to previous results, the maximum absolute value of (partial derivative of T (sub c)/partial derivative of c)(sub c=0) occurs when T (sub co) = T (sub k), thus resolving a longstanding experimental puzzle. DOE

77 THERMODYNAMICS AND STATISTICAL PHYSICS

Includes quantum mechanics; theoretical physics; and Bose and Fermi statistics.

For related information see also *25 Inorganic and Physical Chemistry* and *34 Fluid Mechanics and Heat Transfer.*

N89-25072# National Aerospace Lab., Tokyo (Japan).
STUDY OF CHEMICAL REACTION MODELS FOR HIGH ENTHALPY FLOW OF AIR
Riichi Matsuzaki and Noriaki Hirabayashi Jun. 1988 20 p In JAPANESE; ENGLISH summary
(NAL-TR-982; ISSN-0389-4010) Avail: NTIS HC A03/MF A01

Three models are proposed for the study of high enthalpy, reactive flow of air. They are the dissociation model (O2, N2, O, N, NO), the seven species model (O2, N2, O, N, NO, NO(+), e(-), and the thirteen species model (O2, N2, O, N, NO, O(+), N(+), NO(+), O2(+), N2(+), A, A(+), e(-). The latter two ionization models were tested both for the equilibrium properties and for the nonequilibrium flows. For the equilibrium properties, the seven species model is inadequate in comparison with the thirteen species model, especially at low pressures. Nonequilibrium flows behind shock waves and those through a nozzle were calculated using these two models. The results show that the ionization and recombination reactions of 0 and N will affect the flow properties in the flow behind the shock wave at the Mach number of 20. On the other hand, there is insignificant difference between the two models in the nozzle flow at T(O)=7,000K and P(O) = 1MPa. The seven species model is sufficient at a Mach number smaller than about 10. Author

N89-24970# Soreq Research Establishment, Israel Atomic Energy Commission, Yavneh. Nuclear Research Center.
INDUCED ANNIHILATION OF PARTICLE-ANTIPARTICLE PAIRS
S. Eliezer *In* ESA, Proceedings of an International School and Workshop on Plasma Astrophysics, Volume 1 Jan. 1989 p 373-379 (For primary document see N89-24910 18-75)
Avail: NTIS HC A18/MF A01; ESA Publications Div., ESTEC, Noordwijk, Netherlands, 45 US dollars or 80 Dutch guilders

80 SOCIAL SCIENCES (GENERAL)

Includes educational matters.

No abstracts in this category.

81 ADMINISTRATION AND MANAGEMENT

Includes management planning and research.

No abstracts in this category.

82 DOCUMENTATION AND INFORMATION SCIENCE

Includes information management; information storage and retrieval technology; technical writing; graphic arts; and micrography.

For computer documentation see *61 Computer Programming and Software.*

N89-25073*# Jet Propulsion Lab., California Inst. of Tech., Pasadena.
UNIX-BASED DATA MANAGEMENT SYSTEM FOR THE MOBILE SATELLITE PROPAGATION EXPERIMENT (PiFEx)
Anil V. Kantak 15 Sep. 1987 76 p
(NASA-CR-185023; JPL-Publ-87-24; NAS 1.26:185023) Avail: NTIS HC A05/MF A01 CSCL 05B

A new method is presented for handling data resulting from Mobile Satellite propagation experiments such as the Pilot Field Experiment (PiFEx) conducted by JPL. This method uses the UNIX operating system and C programming language. The data management system is implemented on a VAX minicomputer. The system automatically divides the large data file housing data from various experiments under a predetermined format into various individual files containing data from each experiment. The system also has a number of programs written in C and FORTRAN languages to allow the researcher to obtain meaningful quantities from the data at hand. Author

N89-25074# Systems Research Labs., Inc., Dayton, OH.
THE AAMRL (ARMSTRONG AEROSPACE MEDICAL RESEARCH LABORATORY) BIODYNAMICS DATA BANK Summary Report, Jun. 1984 - Dec. 1988
Trudy S. Abrams, Ints Kaleps, and James W. Brinkley Dec. 1988 70 p
(Contract F33615-85-C-0530)
(AD-A206139; AAMRL-TR-88-037) Avail: NTIS HC A04/MF A01 CSCL 06/3

This report traces the development of the Harry G. Armstrong Aerospace Medical Research Laboratory (AAMRL) Biodynamics Data bank from the original concept of a National Biomechanics Data Bank proposed by Working Group 87 of the National Research Council. It describes the structure and contents of the current Biodynamics Data Bank (BDB), gives sample records of each type, describes available documentation, illustrates its potential, and suggests further development. GRA

N89-25075# Defense Technical Information Center, Alexandria, VA.
A FORECAST OF WORKLOADS AND MANPOWER REQUIREMENTS FOR THE ARCHIVING OF SCIENTIFIC AND TECHNICAL REPORTS BY THE DEFENSE TECHNICAL INFORMATION CENTER USING A SIMULATION MODEL: AN OPERATIONS RESEARCH APPROACH
Charles W. Elliott Feb. 1989 49 p
(AD-A206263) Avail: NTIS HC A03/MF A01 CSCL 05/2

At several meetings attended by the Chief of DTIC-LO, Chuck Elliott, concern was raised by several participants concerning the increasing time required to input a technical report (TR) and the growth in backlogs of TRs awaiting input. The Chief of DTIC-LO determined that this was an area that would lend itself to an operations research investigation and, through the Director of DTIC-L, requested and received the Administrator's approval to proceed with a study. Data collection was confined to DTIC-L, with no new data requirements to be imposed upon the operations directorates. There were two purposes for this: first, to refrain from imposing workload on operating units, second, (since DTIC-L is the main repository for top management information) to determine if sufficient data are already being collected by our current automated and manual information systems for management to make decisions. GRA

83 ECONOMICS AND COST ANALYSIS

Includes cost effectiveness studies.

No abstracts in this category.

84 LAW, POLITICAL SCIENCE AND SPACE POLICY

Includes NASA appropriation hearings; aviation law; space law and policy; international law; international cooperation; and patent policy.

No abstracts in this category.

85 URBAN TECHNOLOGY AND TRANSPORTATION

Includes applications of space technology to urban problems; technology transfer; technology assessment; and surface and mass transportation.

For related information see also *03 Air Transportation and Safety, 16 Space Transportation,* and *44 Energy Production and Conversion.*

N89-25076*# Research Triangle Inst., Research Triangle Park, NC. Technology Applications Team.
APPLICATIONS OF AEROSPACE TECHNOLOGY Annual Report, 1 Oct. 1986 - 30 Sep. 1987
D. J. Rouse, J. N. Brown, Jr., John Cleland, Stephen Lehrman, Lawrence Trachtman, Robert Wallace, Daniel Winfield, Nancy Court, Bernard Maggin, and Reed Barnett et al 30 Sep. 1987 190 p
(Contract NASw-3841)
(NASA-CR-181536; NAS 1.26:181536; RTI/2736/00-12F) Avail: NTIS HC A09/MF A01 CSCL 22A

Highlights are presented for the Research Triangle Institute (RTI) Applications Team activities over the past quarter. Progress in fulfilling the requirements of the contract is summarized, along with the status of the eight add-on tasks. New problem statements are presented. Transfer activities for ongoing projects with the NASA Centers are included. B.G.

N89-25077# Federal Lab. Consortium, Washington, DC.
PUTTING TECHNOLOGY TO WORK: EXAMPLES OF INDUSTRY-LABORATORY COOPERATION CONTRIBUTING TO OUR NATION'S ECONOMIC STRENGTH
Mar. 1988 155 p
(PB89-134654) Avail: NTIS HC A08/MF A01 CSCL 13B

The Nation's Federal laboratories are proving increasingly effective in contributing to the economy through technology transfer - a term that covers a wide variety of cooperative relationships. Laboratory technologies, expertise, and mission program interests form the basis for many commercial innovations, some of which are described. A collection of examples from 31 laboratories representing 7 government agencies is discussed; it should be viewed as indicative of the full potential for industry-laboratory cooperation to contribute to the nation's economic strength. Author

N89-25078*# National Aeronautics and Space Administration. Lewis Research Center, Cleveland, OH.
INITIAL CHARACTERIZATION OF A MODULAR HEAT EXCHANGER WITH AN INTEGRAL HEAT PIPE
Jeffrey G. Schreiber 1989 8 p Presented at the 24th Intersociety Energy Conversion Engineering Conference, Washington, DC, 6-11 Aug. 1989; cosponsored by the IEEE, AIAA, ANS, ASME, SAE, ACS and AIChE
(NASA-TM-102097; E-4859; NAS 1.15:102097) Avail: NTIS HC A02/MF A01 CSCL 05A

As part of the Civil Space Technology Initiative (CSTI) Advanced Technology program, a conceptual design of the Stirling space engine (SSE) was generated. The overall goal of the CSTI high capacity power element is to develop the technology base needed to meet the long duration, high capacity power requirements for future NASA space missions. The free-piston Stirling engine (FPSE) was chosen as the growth option in the CSTI program. A major goal during the conceptual design of the SSE was to reduce the number of critical joints. One area of concern was the heat exchanger assemblies that typically have the majority of critical joints. The solution proposed in the SSE conceptual design used 40 modular heat exchangers. Each module has its own integral heat pipe to transport heat from the heat source to the engine. A demonstration of the modular concept was undertaken before committing to the detailed design of the SSE heat exchangers. An existing FPSE was modified as a test bed for modular heat exchanger evaluation. The engine incorporated three heat exchanger modules, each having a sodium filled heat pipe. The thermal loading of these modules was intended to be similar to the conditions projected for the SSE modules. The engine was assembled and tests are underway. The design and fabrication of the heat exchanger modules and the engine used for these tests were described. Evaluation of the individual heat pipes before installation in the engine is described. The initial test results with the modules in operation on the engine were presented. Future tests involving the engine were outlined. Author

88 SPACE SCIENCES (GENERAL)

No abstracts in this category.

89 ASTRONOMY

Includes radio, gamma-ray, and infrared astronomy, and astrometry.

N89-25079*# Harvard Coll. Observatory, Cambridge, MA.
[IUE INVESTIGATIONS OF SN 1987A] Semiannual Status Report, Aug. 1988 - Feb. 1989
Robert P. Kirshner 4 May 1989 36 p
(Grant NAG5-841)
(NASA-CR-184973; NAS 1.26:184973) Avail: NTIS HC A03/MF A01 CSCL 03A

IUE observations of the SN 1987A began shortly after the discovery and have been frequent through 1988 and 1989, using the fine error sensor for photometry, low dispersion spectra for the supernova spectrum, and high dispersion observations for the interstellar medium when the supernova was bright and for circumstellar gas surrounding the supernova as the initial event faded. The UV data were very useful in determining which star exploded, assessing the ionizing pulse produced as the shock hit the surface of the star, and in constraining the stellar evolution that preceded the explosion through observations of a circumstellar shell. Author

N89-25080 Max-Planck-Inst. fuer Physik und Astrophysik, Garching (Germany, F.R.). Inst. fuer Extraterrestriche Physik.
SOFT X-RAY OBSERVATIONS OF THE VELA PULSAR PSR 0833-45
Hakki Oegelman and Hans-Ulrich Zimmermann Sep. 1988 25 p Submitted for publication Sponsored in part by Forschungsgemeinschaft, Bonn, Germany, F.R.

(MPE-Preprint-130; ISSN-0178-0719; ETN-89-94391) Copyright Avail: Fachinformationszentrum Karlsruhe, 7514 Eggenstein-Leopoldshafen 2, Federal Republic of Germany

Exosat images are studied for energy ranges from 0.03 to 2.4 keV. The X-ray map confirms the Einstein results which show a point like emission centered on the pulsar, a compact nebula with 1 min radius around the pulsar, and an emission region extending from the pulsar in the southwest direction out to 3 min. Filter spectroscopy allows crude spectral fits to the point like source and the compact nebula separately. Reheating by vortex creep in the crust of the neutron star can generate the observed blackbody like luminosity for reasonable values of pinning parameters. ESA

N89-25081* Max-Planck-Inst. fuer Physik und Astrophysik, Garching (Germany, F.R.). Inst. fuer Extraterrestrische Physik.

THE 158 MICRON (CII) MAPPING OF THE GALACTIC CENTER MOLECULAR CLOUDS

Reinhard Genzel, G. J. Stacey, C. H. Townes (California Univ., Berkeley.), A. Poglitsch, and N. Geis Oct. 1988 8 p Submitted for publication

(Grant NAG2-208)

(MPE-Preprint-131; ISSN-0178-0719; ETN-89-94392) Copyright Avail: Fachinformationszentrum Karlsruhe, 7514 Eggenstein-Leopoldshafen 2, Federal Republic of Germany

Maps are made with a 55 sec resolution in the region of the curved, thermal filaments and the 20 to 50 km per sec molecular clouds in Sgr A. The emission is spatially well correlated with the radio continuum in the filaments. The large intensity radiation excludes shock as the origin of the ionization. ESA

N89-25082 Max-Planck-Inst. fuer Physik und Astrophysik, Garching (Germany, F.R.). Inst. fuer Extraterrestrische Physik.

PHYSICAL CONDITIONS IN MOLECULAR CLOUDS DERIVED FROM SUB-mm AND FAR-IR SPECTROSCOPIC OBSERVATIONS

Juergen Stutzki, G. J. Stacey, Reinhard Genzel, U. U. Graf, A. I. Harris, D. T. Jaffe, J. B. Lugten (Hawaii Univ., Honolulu.), and A. Poglitsch Nov. 1988 14 p Presented at the International Symposium on Submillimeter and Millimeter Astronomy, Kona, HI, 3-6 Oct. 1988 Submitted for publication

(MPE-Preprint-135; ETN-89-94396) Copyright Avail: Fachinformationszentrum Karlsruhe, 7514 Eggenstein-Leopoldshafen 2, Federal Republic of Germany

Knowledge about the warm, dense component discovered in all reasonably high luminosity sources in the galaxy is summarized and observations in the fine structure lines of neutral and ionized atomic carbon are discussed. The best explanation for the observed extended emission in these lines is its origin in photodissociation regions on clump surfaces in a clumpy UV penetrated cloud. ESA

N89-25083# Aerospatiale, Cannes La Bocca (France).

MATERIALS FOR CRYOGENICALLY COOLED INFRARED TELESCOPES

J. F. Patin and J. L. Cecconi 1988 14 p

(Rept-882-440-119; ETN-89-94512) Avail: NTIS HC A03/MF A01

Materials with satisfactory performance between 300 and 4 K are studied in order to implement ISO satellite cryogenic equipment. The definitions of the anticorrosion treatment that meet both on ground and in orbit life requirements are also studied. The families of materials considered include optical application materials and structural/mechanical application materials with emphasis on dimensional stability and microyield strength. The test programs are described. ESA

N89-25084 Max-Planck-Inst. fuer Physik und Astrophysik, Garching (Germany, F.R.). Inst. fuer Extraterrestrische Physik.

CONSTRAINTS ON THE OPTICAL COUNTERPART OF GBS0526-66

M. Boer, K. Hurley, M. Gottardi, C. Motch, H. Pedersen, and R. L. Simonsen (Aarhus Univ., Denmark) Nov. 1988 18 p Submitted for publication

(MPE-Preprint-138; ETN-89-94583) Copyright Avail: Fachinformationszentrum Karlsruhe, 7514 Eggenstein-Leopoldshafen 2, Federal Republic of Germany

The upper limits to the magnitude of the pulsed optical emission of the object causing the L979b gamma ray burst are derived from the survey of the N49 supernova remnant carried out with a 50 cm telescope. The possibility that part of the emission is modulated, leading to a lower limit to the magnitude of a periodic component of 19.4 mV is discussed. The results are discussed in the framework of theoretical models of gamma ray bursts. ESA

N89-25085 Max-Planck-Inst. fuer Physik und Astrophysik, Garching (Germany, F.R.). Inst. fuer Extraterrestrische Physik.

HIGH SPECTRAL RESOLUTION OBSERVATIONS OF THE H2 2.12 MICRON LINE IN HERBIG-HARO OBJECTS

Hans Zinnecker, Reinhard Mundt, T. R. Geballe, and William J. Zealey (Wollongong Univ., Australia) Nov. 1988 42 p Submitted for publication

(MPE-Preprint-139; ETN-89-94584) Copyright Avail: Fachinformationszentrum Karlsruhe, 7514 Eggenstein-Leopoldshafen 2, Federal Republic of Germany

The UKIRT Fabry Perot system was used to obtain high spectral resolution line profiles (30 to 35 km/s) for Herbig Haro objects. The important mechanisms for the H2 emission include shock heating of external molecular gas in the wings of the bow shock associated with the working surface of a high velocity jet, and shock heating of external molecular gas entrained in the flow by internal shocks occurring in the jet itself and or in its boundary layer. ESA

N89-25086 Max-Planck-Inst. fuer Physik und Astrophysik, Garching (Germany, F.R.). Inst. fuer Extraterrestrische Physik.

FIRST DETECTION OF SO2 AND CH3OH EMISSION AND ONE UNIDENTIFIED LINE NEAR 800 GHz

Juergen Stutzki, Reinhard Genzel, U. U. Graf, A. I. Harris, and D. T. Jaffe (Texas Univ., Austin.) Feb. 1989 16 p Submitted for publication

(MPE-Preprint-142; ETN-89-94587) Copyright Avail: Fachinformationszentrum Karlsruhe, 7514 Eggenstein-Leopoldshafen 2, Federal Republic of Germany

Emission lines from the Orion core are analyzed. Peak main beam brightness temperatures are 7 and 9 K in a 25 sec beam. The widths and center velocities of these lines are similar to those of recently detected transitions. The SO2 emission is best modelled by an optically thick, beam diluted source. The third line, not yet identified, has its peak main beam brightness temperature at 3.5 K. ESA

N89-25087 Arizona Univ., Tucson.

INFRARED STUDIES OF ACTIVE GALAXIES Ph.D. Thesis

Walter Franklin Kailey 1988 179 p

Avail: Univ. Microfilms Order No. DA8905792

Infrared Astronomy Satellite (IRAS) observations of extragalactic objects are analyzed, supplemented by optical spectroscopy and 10 micron photometry. The relationship between various forms of activity in the nuclei of spiral galaxies and their mid- to far-infrared spectral energy distributions is explored. It is shown that more than 70 percent of galaxies with F sub 60/F sub 25 less than or equal to 3 are Seyferts, while the remainder have bright optical emission lines in their nuclear spectra. It is argued that most Seyferts are powered by their active nuclei at 25 microns, while there is some indication that Seyferts with large F sub 60/F sub 25 flux ratios are undergoing starbursts in the vicinity of their nuclei. The properties of a sample of bright, extragalactic IRAS sources are studied. A catalog containing total infrared and blue fluxes, distance estimates, recession velocities, and morphological classifications for these objects is presented. The brightest sources at mid- to far-infrared wavelengths are (in order of frequency) nearby, normal spiral galaxies; galaxies with disturbed or irregular morphology (often known as interacting galaxies); type 2 Seyferts; and dust-embedded type 1 Seyferts. All of these sources are dominated by thermal emission from dust. The distinctive spectral behavior of IR-luminous galaxies is

shown to result from the presence of compact, dust-dominated IR nuclear sources. Compact IR sources are always associated with a dust-embedded region of ionized gas in the galaxy's nucleus, which may exhibit Seyfert, LINER, or HII region characteristics. The luminosity of the compact nuclear source is well correlated with its 60/100 micron color. This relationship is a vital clue to the nature of these sources and has potential application as a standard candle. Dissert. Abstr.

N89-25088 Texas Univ., Austin.
A STUDY OF THE SOUTHERN SUPERCLUSTER Ph.D. Thesis
Shyamal Kumar Mitra 1988 432 p
Avail: Univ. Microfilms Order No. DA8901374

The Southern Supercluster is a long chain of galaxies extending from Cetus to Dorado. The densest region of the supercluster lies between supergalactic longitudes 200 to 310 degrees and supergalactic latitudes -38 to -45 degrees. From the contour maps of galaxies from the RC2 two regions A (180 degrees less than or equal to L less than or equal to 320, -30 degrees greater than or equal to B greater than or equal to -50 degrees) and B (260 degrees less than or equal to L less than or equal to 360 degrees, 0 degrees greater than or equal to B greater than or equal to -30 degrees) were delineated for detailed study. Galaxies from five categories were compiled and the basic parameters were reduced to the RC2 system. Total magnitudes were measured for 105 galaxies and the magnitudes for other galaxies were obtained from the RC3. The radial velocities of 23 galaxies were measured but most of the radial velocities were culled from the literature. A self consistent distance scale was established using tertiary distance indicators the luminosity index A(c) and the maximum rotation velocity logV(m) obtained from the HI line widths. The distance moduli were obtained using parameters logD(o) and B(T) degrees. The distance moduli from other tertiary distance indicators were obtained from published catalogues. Several maps were constructed to investigate the structure of the supercluster in 3-dimensions using the positional coordinates and a distance estimate (either from radial velocity or distance modulus). The extent, size and shape of the supercluster were determined. To investigate the variation of velocity, distance modulus and Hubble ratio numerical maps were generated and departures from the uniform Hubble flow within the supercluster were determined. Fifteen groups belonging to the supercluster were identified. The mass, luminosity, and mass-to-light ratio of the groups were computed. The total luminosity of the supercluster and its total mass were then estimated. Dissert. Abstr.

N89-25089# Smithsonian Astrophysical Observatory, Cambridge, MA.
THE APPLICATION OF TWO-DIMENSIONAL IMAGING TO VERY HIGH ENERGY GAMMA RAY ASTRONOMY Progress Report
Feb. 1989 24 p
(Contract DE-AC02-82ER-40063)
(DE89-013614; DOE/ER-40063/13) Avail: NTIS HC A03/MF A01

This report describes the following topic on gamma ray astronomy: Crab Nebula, Hercules X-1, Cygnus X-3, high resolution camera, independent trigger, Monte Carlo simulations, optical design of large reflectors, South Pole experiment, galactic plane experiment, and air shower experiment. DOE

N89-24999# Academy of Sciences, Potsdam (German D.R.). Central Inst. for Astrophysics.
TREMSDORF SOLAR RADIO ASTRONOMY OBSERVATORY: THE SCIENTIFIC PROGRAM AND AN INTERESTING OBSERVATION
H. Aurass *In* ESA, Proceedings of an International School and Workshop on Reconnection in Space Plasma, Volume 2 Jan. 1989 p 139-144 Prepared in cooperation with Observatorium fuer Solare Radioastronomie, Potsdam, German Democratic Republic (For primary document see N89-24974 18-75)
Copyright Avail: NTIS HC A15/MF A01; ESA Publications Div., ESTEC, Noordwijk, Netherlands, 45 US dollars or 80 Dutch guilders

N89-25007# Special Astrophysical Observatory, Nishnyi Archys (USSR).
SEARCH FOR A FINE-TIME STRUCTURE IN FLARES OF UV CET-TYPE STARS
L. A. Pustilnik, G. M. Beskin, V. F. Shvartsman, and R. E. Gershberg (Crimean Astrophysical Observatory, USSR) *In* ESA, Proceedings of an International School and Workshop on Reconnection in Space Plasma, Volume 2 Jan. 1989 p 179-181 (For primary document see N89-24974 18-75)
Copyright Avail: NTIS HC A15/MF A01; ESA Publications Div., ESTEC, Noordwijk, Netherlands, 45 US dollars or 80 Dutch guilders

90 ASTROPHYSICS

Includes cosmology; celestial mechanics; space plasmas; and interstellar and interplanetary gases and dust.
For related information see also *75 Plasma Physics.*

N89-25090# International Centre for Theoretical Physics, Trieste (Italy).
FACTORIZATION OF THE RELATIVISTIC PAULI EQUATION IN THE PRESENCE OF A GRAVITATIONAL FIELD
M. Melek Aug. 1988 4 p
(DE88-704749; IC-88/241) Avail: NTIS (US Sales Only) HC A02/MF A01

Attention is called to a possible solution to the problem of the ambiguity in the numerical coefficient of the correction term (h(2) R) that occurs in the Klein-Gordon and relativistic Pauli equations in the presence of a gravitational field. This solution is based on the possibility of factorizing the relativistic Pauli equation for the propagator of the spin 1/2 particle, defined by a path integral, to obtain the Dirac equation in the presence of a gravitational field. DOE

N89-25091# Los Alamos National Lab., NM.
A NEW FIELD EXPERIMENT IN THE GREENLAND ICE CAP TO TEST NEWTON'S INVERSE SQUARE LAW
Mark E. Ander, Mark A. Zumberge, Ted Lautzenhiser, Robert L. Parker, Carlos L. V. Aiken, Michael R. Gorman, Michael Martin Nieto, John R. Ferguson, and George A. McMechan 1988 21 p Presented at the 14th Texas Symposium on Relativistic Astrophysics, Dallas, TX, 11 Dec. 1988
(Contract W-7405-eng-36)
(DE89-009247; LA-UR-89-1095; CONF-881268-3) Avail: NTIS HC A03/MF A01

A geophysical experiment was conducted in a 2-km-deep hole in the Greenland ice cap at depths between 213 m and 1673 m to test for possible violations of Newton's inverse-square law. A detailed ice-sounding radar survey was carried out to 5 km from the hole and merged with regional airborne radar data to define the basement interface. Highly accurate gravity measurements were carried out to 15 km from the hole to detect lateral density changes in the bedrock. The measurements were controlled with very accurate satellite and conventional positioning techniques. The basement interface model was input into a Newtonian computation to correct the observed gravity for known earth structure resulting in an anomalous gravity gradient of +3.87 mGal. A 3 dimensional ideal body analysis of the surface and borehole gravity data provided a means of bounding all possible Newtonian solutions for lateral density variation below the ice. Solutions with regional gravity offsets greater than or equal to 10 mGal and density contrasts less than or equal to 0.30 g/cu cm are possible. We cannot unambiguously attribute the anomalous gradient to a breakdown of Newtonian gravity because there remains the possibility it is due to unexpected geological features in the rock below the ice. DOE

N89-25092# Los Alamos National Lab., NM.
RED-SHIFT EXPERIMENTS AND NON-NEWTONIAN GRAVITATIONAL FORCES
Richard J. Hughes, T. Goldman, and Michael Martin Nieto 1989 7 p Presented at the 8th Moriond Workshop on Tests of Fundamental Laws in Physics, Les Arcs, France, 1 Jan. 1989
(Contract W-7405-eng-36)
(DE89-009349; LA-UR-89-1010; CONF-890199-1) Avail: NTIS HC A02/MF A01

The contribution of scalar non-Newtonian gravitational forces to the gravitational red-shifts is derived. The constraints imposed on scalar couplings by red-shift experiments are shown to be not competitive with those imposed by geophysical inverse-square-law experiments. DOE

N89-25093 Max-Planck-Inst. fuer Physik und Astrophysik, Garching (Germany, F.R.). Inst. fuer Extraterrestrische Physik.
THE CIRCUM-NUCLEAR DISK
Reinhard Genzel Oct. 1988 17 p Submitted for publication
(MPE-Preprint-132; ISSN-0178-0719; ETN-89-94393) Copyright
Avail: Fachinformationszentrum Karlsruhe, 7514 Eggenstein-Leopoldshafen 2, Federal Republic of Germany

Knowledge about the interstellar matter between 1.7 and 10 pc from the IRS16/SGR region are summarized. The region is commonly referred to as the circum-nuclear disk. The spatial distribution of the neutral and partially ionized interstellar matter is discussed, as well as the physical parameters, excitation and dynamics. A schematic model is presented. ESA

N89-25094 Max-Planck-Inst. fuer Physik und Astrophysik, Garching (Germany, F.R.). Inst. fuer Extraterrestrische Physik.
THE ORION MOLECULAR CLOUD AND STAR FORMING REGION
Reinhard Genzel and Juergen Stutzki Dec. 1988 65 p Submitted for publication
(MPE-Preprint-140; ISSN-0178-0719; ETN-89-94585) Copyright
Avail: Fachinformationszentrum Karlsruhe, 7514 Eggenstein-Leopoldshafen 2, Federal Republic of Germany

Interstellar matter and star formation in the Orion region; the structure, origin, and kinematics of the large molecular cloud; the stellar components in and around the cloud; and the interactions of the massive stars in Orion A with their surroundings are reviewed. The BN-H-KL infrared cluster and its environment, the most recent region of massive star formation, is also discussed. ESA

N89-25095 Princeton Univ., NJ.
SELF-CONSISTENT MODELS OF SPHERICAL ACCRETION ONTO BLACK HOLES Ph.D. Thesis
Myeong-Gu Park 1988 92 p
Avail: Univ. Microfilms Order No. DA8904328

Spherically symmetric, steady-state accretion onto a black hole is considered for various dimensionless accretion rates m (=Mc(2)/L sub E, where M is the accretion rate and L sub E is the Eddington luminosity). Both one-temperature (T sub i = T sub e, where T sub i and T sub e are ion and electron temperature, respectively) and two-temperature (T sub i does not equal T sub e with energy exchange via Coulomb interactions) models are constructed by integrating relativistic hydrodynamic and radiative transfer equations. The effects of preheating, and the shocks that may result, are also considered. Self-consistent models for all m; self-consistency meaning that, at all radii, the gas is heated by the radiation it produces were found. Two sets of models (characterized by different temperatures) were found in the range 3 less than m less than 100. The dimensionless luminosity l is defined as L/L sub e is l = 5.8 x 10(-5)m(2) for m much less than 1. For low gas temperature models (T sub 3 is approximately equal to 10(4) K) and m greater than 0.1, l is approximately equal to 6 x 10(-8)m(2); high-temperature models with 3 less than m less than 100 give 3 x 10(-4) less than l less than 3 x 10(-2). Because of the effects of preheating, no steady-state high-temperature self-consistent solution exists for 0.1 less than m less than 3 or m greater than 100. Pair processes do not play an important role in these models. Also, two self-consistent models were found with a standing shock; these models have higher luminosity than the corresponding (same m) models without a shock. Another self-consistent model at the same m shows an even higher luminosity, maintained by pair creation. Dissert. Abstr.

N89-25096 California Univ., Los Angeles.
BLACK HOLE DRIVEN WINDS Ph.D. Thesis
Brian Mathew Punsly 1988 359 p
Avail: Univ. Microfilms Order No. DA8906132

The physical mechanism that allows a large scale magnetic field to torque a rapidly rotating, supermassive black hole is studied. This is an interesting problem as it was conjectured that rapidly rotating black holes are the central engines that power the observed extragalactic double radio sources. Axisymmetric solutions of the curved space-time version of Maxwell's equations in the vacuum do not torque black holes. Plasma must be introduced for the hole to mechanically couple to the field. The dynamical aspect of rotating black holes that couples the magnetic field to the hole is the following. A rotating black hole forces the external geometry of space-time to rotate. Inside of the stationary limit surface, the ergosphere, all physical particle trajectories must appear to rotate in the same direction as the black hole as viewed by the stationary observers at asymptotic infinity. It is demonstrated how plasma that is created on field lines that thread both the ergosphere and the equatorial plane will be pulled by gravity toward the equator. The steady state is an equatorial disk of plasma condensate. By the aforementioned properties of the ergosphere, the disk must rotate. Consequently, the disk acts like a unipolar generator. It drives a global current system that supports the toroidal magnetic field in an outgoing, magnetically dominated wind. This wind carries energy and angular momentum towards infinity. The spin down of the black hole is the ultimate source of this energy and angular momentum flux. Author

N89-25097 Arizona Univ., Tucson.
AN OBSERVATIONAL STUDY OF THE DYNAMICS OF MOLECULAR CLOUD CORES Ph.D. Thesis
Christopher Kidd Walker 1988 212 p
Avail: Univ. Microfilms Order No. DA8906395

One of the most fundamental questions in astronomy is how stars are formed. It is therefore ironic that to date, no object is unambiguously identified as a true protostar; an object which derives the bulk of its luminosity from accretion. While this may be ironic, it is not surprising. Stars are believed to form as a result of the gravitational collapse of a portion of a molecular cloud. Theory predicts that the cloud core in which the star is formed will be cold, dense and possess hundreds of magnitudes of extinction, rendering it opaque at visible and near-infrared wavelengths. Continuum observations at far-infrared, submillimeter, and millimeter wavelengths can be used to identify candidate protostars, but spectroscopic observations are needed to detect infall. The difficulties arise when there are systematic velocity fields present in the cloud core which are not the result of infall, such as would be produced by either a molecular outflow or rotation. Both observations and theoretical models are used to sort through these problems and develop a strategy which could be used to identify and study protostars. Dissert. Abstr.

N89-25098# Los Alamos National Lab., NM.
EFFECTS OF MAIN-SEQUENCE MASS LOSS ON STELLAR AND GALACTIC CHEMICAL EVOLUTION Ph.D. Thesis
Joyce Ann Guzik Apr. 1989 157 p
(Contract W-7405-eng-36)
(DE89-011399; LA-11554-T) Avail: NTIS HC A08/MF A01

Iowa State faculty members L.A. Willson, G.H. Bowen and C. Struck-Marcell have proposed that stars of 1 to 3 solar masses may experience mass loss of evolutionary significance during the early part of their lives on the main sequence. The suggested mass-loss mechanism is pulsation, facilitated by rapid rotation. Initial mass-loss rates may be as large as several times 10 sup minus 9 M sub o yr, diminishing during the first several times 10(8) years. The goal of this dissertation is to test the

main-sequence mass loss hypothesis via a comparison of theoretical implications to observations. Three specific areas are addressed: solar models, cluster HR diagrams, and galactic chemical evolution. DOE

N89-24911# Royal Inst. of Tech., Stockholm (Sweden). Dept. of Plasma Physics.
DEVELOPMENT OF ASTROPHYSICS FROM THE TELESCOPE TO THE SPUTNIK
H. Alfven *In* ESA, Proceedings of an International School and Workshop on Plasma Astrophysics, Volume 1 Jan. 1989 p 3-8 (For primary document see N89-24910 18-75)
Avail: NTIS HC A18/MF A01; ESA Publications Div., ESTEC, Noordwijk, Netherlands, 45 US dollars or 80 Dutch guilders

N89-24915# Max-Planck-Inst. fuer Physik und Astrophysik, Garching (Germany, F.R.).
COSMIC LINEAR ACCELERATORS
G. Haerendel *In* ESA, Proceedings of an International School and Workshop on Plasma Astrophysics, Volume 1 Jan. 1989 p 37-4 (For primary document see N89-24910 18-75)
Avail: NTIS HC A18/MF A01; ESA Publications Div., ESTEC, Noordwijk, Netherlands, 45 US dollars or 80 Dutch guilders

N89-24920# Toyama Univ. (Japan). Dept. of Applied Mathematics and Physics.
NON-STEADY ASTROPHYSICAL SPIRAL JETS DRIVEN BY MAGNETIC COLLAPSE AND PRESSURE
Jun-ichi Sakai *In* ESA, Proceedings of an International School and Workshop on Plasma Astrophysics, Volume 1 Jan. 1989 p 69-7 (For primary document see N89-24910 18-75)
Avail: NTIS HC A18/MF A01; ESA Publications Div., ESTEC, Noordwijk, Netherlands, 45 US dollars or 80 Dutch guilders

N89-24930# Dublin Inst. for Advanced Studies (Ireland). School of Cosmic Physics.
PARTICLE ACCELERATION AND SHOCK WAVE STRUCTURE
L. OC. Drury *In* ESA, Proceedings of an International School and Workshop on Plasma Astrophysics, Volume 1 Jan. 1989 p 131-135 (For primary document see N89-24910 18-75)
Avail: NTIS HC A18/MF A01; ESA Publications Div., ESTEC, Noordwijk, Netherlands, 45 US dollars or 80 Dutch guilders

N89-24935# Royal Observatory, Edinburgh (Scotland).
THE FORMATION OF INTERSTELLAR CLOUDS
M. D. Smith *In* ESA, Proceedings of an International School and Workshop on Plasma Astrophysics, Volume 1 Jan. 1989 p 161-164 (For primary document see N89-24910 18-75)
Avail: NTIS HC A18/MF A01; ESA Publications Div., ESTEC, Noordwijk, Netherlands, 45 US dollars or 80 Dutch guilders

N89-24936# Academy of Sciences (USSR), Moscow. Inst. of Space Research.
THE ROLE OF WHISTLER OSCILLATIONS IN THE FORMATION OF THE STRUCTURE OF HIGH MACH NUMBER COLLISIONLESS SHOCK
A. A. Galeev, C. F. Kennel, V. V. Krasnoselskikh, and V. V. Lobzin (Academy of Sciences, USSR, Troitsk) *In* ESA, Proceedings of an International School and Workshop on Plasma Astrophysics, Volume 1 Jan. 1989 p 165-171 (For primary document see N89-24910 18-75)
Avail: NTIS HC A18/MF A01; ESA Publications Div., ESTEC, Noordwijk, Netherlands, 45 US dollars or 80 Dutch guilders

N89-24937# Academy of Sciences (USSR), Moscow. Inst. of Space Research.
QUASI-PERPENDICULAR COLLISIONLESS HIGH MACH NUMBER SHOCKS
A. A. Galeev, C. F. Kennel, and V. V. Krasnoselskikh (Academy of Sciences, USSR, Troitsk) *In* ESA, Proceedings of an International School and Workshop on Plasma Astrophysics, Volume 1 Jan. 1989 p 173-183 (For primary document see N89-24910 18-75)
Avail: NTIS HC A18/MF A01; ESA Publications Div., ESTEC, Noordwijk, Netherlands, 45 US dollars or 80 Dutch guilders

N89-24939# Princeton Univ., NJ. Plasma Physics Lab.
THE CASE FOR A PRIMORDIAL GALACTIC FIELD
R. Kulsrud *In* ESA, Proceedings of an International School and Workshop on Plasma Astrophysics, Volume 1 Jan. 1989 p 197-201 (For primary document see N89-24910 18-75)
(Contract DE-AC02-76CH-03073)
Avail: NTIS HC A18/MF A01; ESA Publications Div., ESTEC, Noordwijk, Netherlands, 45 US dollars or 80 Dutch guilders

N89-24948*# Iowa Univ., Iowa City. Dept. of Physics and Astronomy.
ARE SUPERNOVA REMNANTS QUASI-PARALLEL OR QUASI-PERPENDICULAR ACCELERATORS
S. R. Spangler, J. A. Leckband, and I. H. Cairns *In* ESA, Proceedings of an International School and Workshop on Plasma Astrophysics, Volume 1 Jan. 1989 p 251-254 (For primary document see N89-24910 18-75)
(Grants NAGw-806; NAGw-831)
Avail: NTIS HC A18/MF A01; ESA Publications Div., ESTEC, Noordwijk, Netherlands, 45 US dollars or 80 Dutch guilders
CSCL 03B

N89-24950# Abastumani Astrophysical Observatory, Georgia (USSR).
SMALL-SCALE INSTABILITIES IN ACCRETION DISKS OF COMPACT OBJECTS AND THEIR MANIFESTATIONS
G. D. Chagelishvili, R. G. Chanishvili, and J. G. Lominadze *In* ESA, Proceedings of an International School and Workshop on Plasma Astrophysics, Volume 1 Jan. 1989 p 261-264 (For primary document see N89-24910 18-75)
Avail: NTIS HC A18/MF A01; ESA Publications Div., ESTEC, Noordwijk, Netherlands, 45 US dollars or 80 Dutch guilders

N89-24951# Abastumani Astrophysical Observatory, Georgia (USSR).
PROBLEM OF NONROTATING BLACK HOLE ACCRETION DISK MAIN ENERGY RELEASE REGION EXTENSION
G. D. Chagelishvili, J. G. Lominadze, and A. D. Rogava *In* ESA, Proceedings of an International School and Workshop on Plasma Astrophysics, Volume 1 Jan. 1989 p 265-269 (For primary document see N89-24910 18-75)
Avail: NTIS HC A18/MF A01; ESA Publications Div., ESTEC, Noordwijk, Netherlands, 45 US dollars or 80 Dutch guilders

N89-24963# Scuola Normale Superiore, Pisa (Italy).
SOME DYNAMICAL PROPERTIES OF ANISOTROPIC COLLISIONLESS STELLAR SYSTEMS
G. Bertin and F. Pegoraro *In* ESA, Proceedings of an International School and Workshop on Plasma Astrophysics, Volume 1 Jan. 1989 p 329-333 Sponsored in part by the CNR, Italy and the Italian Ministry of Public Education (For primary document see N89-24910 18-75)
Avail: NTIS HC A18/MF A01; ESA Publications Div., ESTEC, Noordwijk, Netherlands, 45 US dollars or 80 Dutch guilders

N89-24964# Commissariat a l'Energie Atomique, Saclay (France). Service d'Astrophysique.
BARS AND OPEN SPIRALS IN DENSITY WAVE THEORY
M. Tagger, J. F. Sygnet, and R. Pellat (Ecole Polytechnique, Palaiseau, France) *In* ESA, Proceedings of an International School and Workshop on Plasma Astrophysics, Volume 1 Jan. 1989 p 335-340 (For primary document see N89-24910 18-75)
Avail: NTIS HC A18/MF A01; ESA Publications Div., ESTEC, Noordwijk, Netherlands, 45 US dollars or 80 Dutch guilders

N89-24965# Observatoire de Marseille (France).
GAS FLOW IN AND AROUND BARS
E. Athanassoula *In* ESA, Proceedings of an International School and Workshop on Plasma Astrophysics, Volume 1 Jan. 1989

p 341-348 (For primary document see N89-24910 18-75)
Avail: NTIS HC A18/MF A01; ESA Publications Div., ESTEC, Noordwijk, Netherlands, 45 US dollars or 80 Dutch guilders

91 LUNAR AND PLANETARY EXPLORATION

Includes planetology; and manned and unmanned flights.
For spacecraft design or space stations see *18 Spacecraft Design, Testing and Performance.*

N89-25099*# Institute for Scientific Research, Lexington, MA.
THEORETICAL STUDIES OF IMPORTANT PROCESSES IN PLANETARY AND COMET ATMOSPHERES. RENEWEL REQUEST Progress Report, 1 Sep. 1989 - 31 Oct. 1990
Steven L. Guberman 21 Apr. 1989 30 p
(Contract NCC2-308; NAGw-1404; AF-AFOSR-0109-84)
(NASA-CR-184951; NAS 1.26:184951) Avail: NTIS HC A03/MF A01 CSCL 03B

Current efforts have focused on the dissociative recombination (DR) of O2(+), a process of great importance in planetary atmospheres. This process is difficult to study experimentally because of the need to determine the dependence of the product electronic states and kinetic energies upon the vibrational distribution of the ion and electron temperature. The knowledge of these characteristics of DR is needed to accurately model planetary ionospheres. Using a theoretical quantum chemical approach, the generation of O(1S) from DR was studied in detail.
Author

N89-25100 California Univ., San Diego.
THE VARIABLE NATURE OF THE COMET-SOLAR WIND INTERACTION Ph.D. Thesis
Karen Ruth Flammer 1988 198 p
Avail: Univ. Microfilms Order No. DA8904291

The different modes of interaction of the solar wind with a Halley-type comet as it approaches the sun are discussed. At large heliocentric distances the solar wind penetrates unimpeded onto the surface of the comet nucleus. This causes electrostatic charging and explusion of fine dust from the comet surface; a process which is modulated by the local solar wind flux. The observed irregular brightness variation of comet Halley between 11 and 8 AU (inbound) are explained in terms of this mechanism. As the comet moves closer to the sun (within 4 AU), mass loading of the solar wind by the heavy cometary ions causes the flow to slow down, thereby enhancing the convected interplanetary magnetic field significantly. This magnetic field enhancement is the earliest and most sensitive signature associated with the solar wind mass loading. Still farther in, as the mass loading approaches a critical value, a weak collisionless standing shock forms, which recedes upstream of the nucleus as the comet approaches the sun. The cometary atmosphere becomes dense enough so that a well-defined ionopause forms which separates the cometary ionospheric plasma from the contaminated solar wind plasma only when the comet is within approximately 2.2 AU from the sun. The stability of the ionopause is examined under the framework of linear magnetohydrodynamics taking into account the effects of ion-neutral drag, sources, curvature, and compressibility. Both Kelvin-Helmholtz and Rayleigh Taylor modes are excited. The growth rates of these modes are determined for various shears and density jumps at the ionopause and under different solar wind conditions. A quasi-linear theory is then used to examine the evolution of the unstable modes to finite amplitudes.
Dissert. Abstr.

N89-25101# State Univ. of New York, Plattsburgh. Dept. of Physics.
NON-DESTRUCTIVE ANALYSES OF COMETARY NUCLEUS SAMPLES USING SYNCHROTRON RADIATION
G. J. Flynn, S. R. Sutton, and M. L. Rivers (Chicago Univ., IL.) 1989 11 p Presented at the Workshop on the Analysis of Returned Comet Nucleus Samples, Milpitas, CA, 16 Jan. 1989
(Contract DE-AC02-76CH-00016)
(DE89-012536; BNL-42109; CONF-890195-2) Avail: NTIS HC A03/MF A01

Trace element abundances and abundance patterns in meteorites have proven to be diagnostic indicators of nebular and parent body fractionations, formation temperature, thermal metamorphism and, co-genesis. If comets are more primitive samples of the solar nebula than the meteorites, then trace element abundances in the returned comet nucleus samples should be better indicators of primitive solar nebula conditions than those of meteorites. Comet nucleus samples are likely to consist of a mixture of ices and mineral grains. To provide a complete picture of the elemental distributions, trace element abundance data on the bulk material, as well as separated mineral grains and ices, will be required. This paper discusses the present and future analytical capabilities.
DOE

N89-24918# Calabria Univ., Arcavacta di Rende (Italy). Dipartimento di Fisica.
MAGNETIC NEUTRAL LINES IN JUPITER'S NIGHTSIDE MAGNETOSPHERE
G. Zimbardo *In* ESA, Proceedings of an International School and Workshop on Plasma Astrophysics, Volume 1 Jan. 1989 p 57-6 (For primary document see N89-24910 18-75)
Avail: NTIS HC A18/MF A01; ESA Publications Div., ESTEC, Noordwijk, Netherlands, 45 US dollars or 80 Dutch guilders

N89-25015# Abastumani Astrophysical Observatory, Georgia (USSR).
INDUCTIVE ACCELERATION OF PROTONS AND ELECTRONS IN PLANETARY MAGNETOTAILS
A. L. Taktakishvili and L. M. Zelenyi (Academy of Sciences, USSR, Moscow) *In* ESA, Proceedings of an International School and Workshop on Reconnection in Space Plasma, Volume 2 Jan. 1989 p 227-232 (For primary document see N89-24974 18-75)
Copyright Avail: NTIS HC A15/MF A01; ESA Publications Div., ESTEC, Noordwijk, Netherlands, 45 US dollars or 80 Dutch guilders

92 SOLAR PHYSICS

Includes solar activity, solar flares, solar radiation and sunspots.
For related information see *93 Space Radiation.*

N89-25102 Council for National Academic Awards (England).
THE EQUILIBRIUM AND STABILITY OF SOLAR CORONAL MAGNETIC FIELDS Ph.D. Thesis
John P. Melville 1988 247 p
Avail: Univ. Microfilms Order No. BRDX84664

Two main areas of investigation is discussed. First, a search for solutions to the equations of magnetohydrostatics was made in an attempt to construct mathematical models of the quasi-static plasma structures embedded in a magnetic field in the solar corona. Several solutions were discovered and their behavior studied as physical parameters were varied. For example, certain non-linear solutions were found to exhibit the property that the equilibria could not exist if some mechanism were to increase the plasma pressure beyond some critical value. This kind of scenario was associated with the explosive dynamic event of the solar flare. When the equilibrium is no longer tenable, it was suggested that the stored magnetic energy is released in this violent manner. Secondly, the magnetohydrodynamic stability of two of the equilibria were studied in detail. This provides another possible mechanism for flare development. The equilibrium is subjected to a perturbation of the physical variables and the change in potential energy calculated. If a perturbation can be found for which the potential energy difference is negative, then the underlying equilibrium is linearly unstable. Specific physical criteria for the equilibria to remain stable were found. In all cases the force-balance equation takes

into account pressure magnetic and gravitational forces. In particular, the effect of the gravitational force on magnetohydrodynamic stability was investigated. Dissert. Abstr.

N89-24914# Max-Planck-Inst. fuer Aeronomie, Katlenburg-Lindau (Germany, F.R.).
DIMENSIONLESS PARAMETERS FOR CLASSIFYING SOLAR WIND INTERACTIONS
V. M. Vasyliunas *In* ESA, Proceedings of an International School and Workshop on Plasma Astrophysics, Volume 1 Jan. 1989 p 31-3 (For primary document see N89-24910 18-75)
Avail: NTIS HC A18/MF A01; ESA Publications Div., ESTEC, Noordwijk, Netherlands, 45 US dollars or 80 Dutch guilders

N89-24919*# Cornell Univ., Ithaca, NY. Lab. of Plasma Studies.
DISSIPATION OF ALFVEN WAVES IN SOLAR CORONAL ARCHES
R. N. Sudan and P. L. Similon *In* ESA, Proceedings of an International School and Workshop on Plasma Astrophysics, Volume 1 Jan. 1989 p 63-6 (For primary document see N89-24910 18-75)
(Grants NAGw-1006; NSF AST-86-00308)
Avail: NTIS HC A18/MF A01; ESA Publications Div., ESTEC, Noordwijk, Netherlands, 45 US dollars or 80 Dutch guilders
CSCL 03B

N89-24922# European Space Agency. European Space Research and Technology Center, ESTEC, Noordwijk (Netherlands). Space Science Dept.
HELIOSEISMOLOGY AND PLASMA PHYSICS
B. N. Anderson *In its* Proceedings of an International School and Workshop on Plasma Astrophysics, Volume 1 Jan. 1989 p 83-93 (For primary document see N89-24910 18-75)
Avail: NTIS HC A18/MF A01; ESA Publications Div., ESTEC, Noordwijk, Netherlands, 45 US dollars or 80 Dutch guilders

N89-24923# Eidgenoessische Technische Hochschule, Zurich (Switzerland). Inst. fuer Astronomie.
ALFVEN WAVE SOLITONS AND SOLAR INTERMEDIATE DRIFT BURSTS
M. Guedel, A. O. Benz, and R. A. Treumann (Max-Planck-Inst. fuer Physik und Astrophysik, Garching, Germany, F.R.) *In* ESA, Proceedings of an International School and Workshop on Plasma Astrophysics, Volume 1 Jan. 1989 p 95-9 (For primary document see N89-24910 18-75)
Avail: NTIS HC A18/MF A01; ESA Publications Div., ESTEC, Noordwijk, Netherlands, 45 US dollars or 80 Dutch guilders

N89-24925# FOM-Inst. voor Plasmafysica, Rijnhuizen, Jutphaas (Netherlands).
KINK MODES IN CORONAL LOOPS
J. P. Goedbloed, M. Goossens, and S. Poedts (Katholieke Universiteit te Leuven, Belgium) *In* ESA, Proceedings of an International School and Workshop on Plasma Astrophysics, Volume 1 Jan. 1989 p 103-106 Sponsored by Netherlands Organization for the Advancement of Scientific Research and the Stitchting voor Fundamenteel Onderzoek de Materie, Amsterdam, Netherlands (For primary document see N89-24910 18-75)
Avail: NTIS HC A18/MF A01; ESA Publications Div., ESTEC, Noordwijk, Netherlands, 45 US dollars or 80 Dutch guilders

N89-24926# Katholieke Universiteit te Leuven (Belgium). Inst. of Astronomy.
CORONAL HEATING BY RESONANT ABSORPTION IN RESISTIVE MHD
S. Poedts, M. Goossens, and W. Kerner (Max-Planck-Inst. fuer Physik und Astrophysik, Garching, Germany, F.R.) *In* ESA, Proceedings of an International School and Workshop on Plasma Astrophysics, Volume 1 Jan. 1989 p 107-110 (For primary document see N89-24910 18-75)
(Contract EEC-ST2J-0275-C)
Avail: NTIS HC A18/MF A01; ESA Publications Div., ESTEC, Noordwijk, Netherlands, 45 US dollars or 80 Dutch guilders

N89-24927# Academy of Sciences of the Ukrainian SSR, Kiev. Inst. of Physics and Technology.
SINGULARITIES OF THE LOCAL MHD-RESONANCES IN SOLAR CHROMOSPHERE PLASMA
V. I. Lapshin, K. N. Stepanov, and E. A. Fedutenko *In* ESA, Proceedings of an Internatinal School and Workshop on Plasma Astrophysics, Volume 1 Jan. 1989 p 111-114 (For primary document see N89-24910 18-75)
Avail: NTIS HC A18/MF A01; ESA Publications Div., ESTEC, Noordwijk, Netherlands, 45 US dollars or 80 Dutch guilders

N89-24934# Observatoire de Paris-Meudon (France).
EXTENDED CORONAL SHOCK WAVES AND ELECTRON ACCELERATION DURING SOLAR FLARES
K.-L. Klein, G. Trottet, A. O. Benz, and S. R. Kane (California Univ., Berkeley.) *In* ESA, Proceedings of an International School and Workshop on Plasma Astrophysics, Volume 1 Jan. 1989 p 157-160 (For primary document see N89-24910 18-75)
Avail: NTIS HC A18/MF A01; ESA Publications Div., ESTEC, Noordwijk, Netherlands, 45 US dollars or 80 Dutch guilders

N89-24966# Abastumani Astrophysical Observatory, Georgia (USSR).
MODEL OF THE CHROMOSPHERE SPICULE FORMATION
B. B. Chargeishvili, A. D. Pataraya, and A. L. Taktakishvili *In* ESA, Proceedings of an International School and Workshop on Plasma Astrophysics, Volume 1 Jan. 1989 p 349-351 (For primary document see N89-24910 18-75)
Avail: NTIS HC A18/MF A01; ESA Publications Div., ESTEC, Noordwijk, Netherlands, 45 US dollars or 80 Dutch guilders

N89-24987# Saint Andrew's Univ. (Scotland). Dept. of Mathematical Sciences.
MAGNETIC ENERGY CONVERSION ON THE SUN
E. R. Priest *In* ESA, Proceedings of an International School and Workshop on Reconnection in Space Plasma, Volume 2 Jan. 1989 p 73-81 (For primary document see N89-24974 18-75)
Copyright Avail: NTIS HC A15/MF A01; ESA Publications Div., ESTEC, Noordwijk, Netherlands, 45 US dollars or 80 Dutch guilders

N89-24989# Academy of Sciences, Potsdam (German D.R.). Central Inst. for Astrophysics.
GENERATION AND NON-EQUILIBRIUM OF SOLAR ATMOSPHERIC MAGNETIC FIELDS
N. Seehafer *In* ESA, Proceedings of an International School and Workshop on Reconnection in Space Plasma, Volume 2 Jan. 1989 p 87-92 (For primary document see N89-24974 18-75)
Copyright Avail: NTIS HC A15/MF A01; ESA Publications Div., ESTEC, Noordwijk, Netherlands, 45 US dollars or 80 Dutch guilders

N89-24990# Institute of Nuclear Physics, Novosibirsk (USSR).
STABILITY OF FORCE-FREE MAGNETIC FIELDS AND THE PROBLEM OF SOLAR CORONAL HEATING
G. E. Vekstein *In* ESA, Proceedings of an International School and Workshop on Reconnection in Space Plasma, Volume 2 Jan. 1989 p 93-97 (For primary document see N89-24974 18-75)
Copyright Avail: NTIS HC A15/MF A01; ESA Publications Div., ESTEC, Noordwijk, Netherlands, 45 US dollars or 80 Dutch guilders

N89-24991# Academy of Sciences (USSR), Gorky. Inst. of Applied Physics.
A NEUTRAL CURRENT SHEET WITH FLOWS: TEARING AND STRATIFICATION MODES AND MODELING OF CORONAL STRUCTURES
V. M. Gubchenko and V. V. Zaitsev *In* ESA, Proceedings of an International School and Workshop on Reconnection in Space Plasma, Volume 2 Jan. 1989 p 99-104 (For primary document see N89-24974 18-75)
Copyright Avail: NTIS HC A15/MF A01; ESA Publications Div., ESTEC, Noordwijk, Netherlands, 45 US dollars or 80 Dutch guilders

N89-24992# Saint Andrew's Univ. (Scotland). Dept. of Mathematical Sciences.
ON THE MHD STABILITY OF THE M=1 KINK MODE IN FINITE LENGTH CORONAL LOOPS
M. Velli, A. W. Hood, and G. Einaudi (Florence Univ., Italy) *In* ESA, Proceedings of an International School and Workshop on Reconnection in Space Plasma, Volume 2 Jan. 1989 p 105-109 (For primary document see N89-24974 18-75)
Copyright Avail: NTIS HC A15/MF A01; ESA Publications Div., ESTEC, Noordwijk, Netherlands, 45 US dollars or 80 Dutch guilders

N89-24993# Toyama Univ. (Japan). Dept. of Applied Mathematics and Physics.
PARTICLE ACCELERATION BY MAGNETIC RECONNECTION AND FAST MAGNETOSONIC SHOCK WAVES IN SOLAR FLARES
Jun-ichi Sakai and Yukiharu Ohsawa (Nagoya Univ., Japan) *In* ESA, Proceedings of an International School and Workshop on Reconnection in Space Plasma, Volume 2 Jan. 1989 p 111-116 (For primary document see N89-24974 18-75)
Copyright Avail: NTIS HC A15/MF A01; ESA Publications Div., ESTEC, Noordwijk, Netherlands, 45 US dollars or 80 Dutch guilders

N89-24994# Academy of Sciences, Potsdam (German D.R.). Central Inst. for Astrophysics.
DYNAMIC DEVELOPMENT OF CORONAL CURRENT SHEETS
B. Kliem *In* ESA, Proceedings of an International School and Workshop on Reconnection in Space Plasma, Volume 2 Jan. 1989 p 117-122 (For primary document see N89-24974 18-75)
Copyright Avail: NTIS HC A15/MF A01; ESA Publications Div., ESTEC, Noordwijk, Netherlands, 45 US dollars or 80 Dutch guilders

N89-24995# Academy of Sciences, Potsdam (German D.R.). Central Inst. for Astrophysics.
POSSIBILITIES AND PROBLEMS OF THE INTERPRETATION OF SOLAR MAGNETOGRAPH MEASUREMENTS AND APPLICATIONS TO FLARE-ACTIVE REGIONS
J. Staude and A. Hofmann *In* ESA, Proceedings of an International School and Workshop on Reconnection in Space Plasma, Volume 2 Jan. 1989 p 123-128 (For primary document see N89-24974 18-75)
Copyright Avail: NTIS HC A15/MF A01; ESA Publications Div., ESTEC, Noordwijk, Netherlands, 45 US dollars or 80 Dutch guilders

N89-24996# Academy of Sciences, Potsdam (German D.R.). Central Inst. for Astrophysics.
ESTIMATION OF SUNSPOT MAGNETIC FIELD PARAMETERS USING THE SUPERPENUMBRAL TOPOLOGY
J. Linke and J. H. Hernandez (Pedagogical High School, Havana, Cuba) *In* ESA, Proceedings of an International School and Workshop on Reconnection in Space Plasma, Volume 2 Jan. 1989 p 129-130 (For primary document see N89-24974 18-75)
Copyright Avail: NTIS HC A15/MF A01; ESA Publications Div., ESTEC, Noordwijk, Netherlands, 45 US dollars or 80 Dutch guilders

N89-24997# Academy of Sciences, Potsdam (German D.R.). Central Inst. for Astrophysics.
NOTE ON AN APPARENT HIGHLY-SHEARED MAGNETIC FIELD STRUCTURE
J. Linke and G. Bachmann *In* ESA, Proceedings of an International School and Workshop on Reconnection in Space Plasma, Volume 2 Jan. 1989 p 131-132 (For primary document see N89-24974 18-75)
Copyright Avail: NTIS HC A15/MF A01; ESA Publications Div., ESTEC, Noordwijk, Netherlands, 45 US dollars or 80 Dutch guilders

N89-24998# Academy of Sciences, Potsdam (German D.R.). Central Inst. for Astrophysics.
DIAGNOSTICS OF ENERGY RELEASE AND MAGNETIC FIELDS ON THE SUN BY RADIO METHODS
A. Krueger *In* ESA, Proceedings of an International School and Workshop on Reconnection in Space Plasma, Volume 2 Jan. 1989 p 133-138 (For primary document see N89-24974 18-75)
Copyright Avail: NTIS HC A15/MF A01; ESA Publications Div., ESTEC, Noordwijk, Netherlands, 45 US dollars or 80 Dutch guilders

N89-25000# Slovak Academy of Sciences, Tatranska Lomnica (Czechoslovakia). Inst. of Astronomy.
THE RELATION BETWEEN H-ALPHA AND SXR EMISSION OF THE FLARES
A. Antalova *In* ESA, Proceedings of an International School and Workshop on Reconnection in Space Plasma, Volume 2 Jan. 1989 p 145-148 (For primary document see N89-24974 18-75)
Copyright Avail: NTIS HC A15/MF A01; ESA Publications Div., ESTEC, Noordwijk, Netherlands, 45 US dollars or 80 Dutch guilders

N89-25001# Academy of Sciences (USSR), Gorky. Inst. of Applied Physics.
THE PRECURSORS OF THE 9 JULY 1982 SOLAR PROTON FLARE EVENT
V. V. Zaitsev, E. A. Averianikhina, H. Aurass, and A. Krueger (Academy of Sciences, Potsdam, German D.R.) *In* ESA, Proceedings of an International School and Workshop on Reconnection in Space Plasma, Volume 2 Jan. 1989 p 149-152 (For primary document see N89-24974 18-75)
Copyright Avail: NTIS HC A15/MF A01; ESA Publications Div., ESTEC, Noordwijk, Netherlands, 45 US dollars or 80 Dutch guilders

N89-25002# Observatorium fuer Solare Radioastronomie, Tremsdorf (German D.R.). Central Inst. for Astrophysics.
CORONAL MAGNETIC FIELD STRENGTHS DETERMINED FROM FIBER BURSTS
G. Mann and K. Baumgaertel (Academy of Sciences, Berlin, German D.R.) *In* ESA, Proceedings of an International School and Workshop on Reconnection in Space Plasma, Volume 2 Jan. 1989 p 153-156 (For primary document see N89-24974 18-75)
Copyright Avail: NTIS HC A15/MF A01; ESA Publications Div., ESTEC, Noordwijk, Netherlands, 45 US dollars or 80 Dutch guilders

N89-25003# Observatorium fuer Solare Radioastronomie, Tremsdorf (German D.R.). Central Inst. for Astrophysics.
LONG-TERM EVOLUTION OF CORONAL MAGNETIC FIELDS BASED ON NOISE STORM CONTINUUM OBSERVATIONS IN THE 20TH AND 21ST CYCLE
A. Boehme *In* ESA, Proceedings of an International School and Workshop on Reconnection in Space Plasma, Volume 2 Jan. 1989 p 157-161 (For primary document see N89-24974 18-75)
Copyright Avail: NTIS HC A15/MF A01; ESA Publications Div., ESTEC, Noordwijk, Netherlands, 45 US dollars or 80 Dutch guilders

N89-25004# Byurakan Observatory (USSR).
PINCH-EFFECT AND STELLAR FLARES PHYSICS
V. S. Hayrapetyan, A. G. Nikhogossian, and V. V. Vikhrev (Academy of Sciences, USSR, Moscow) *In* ESA, Proceedings of an International School and Workshop on Reconnection in Space Plasma, Volume 2 Jan. 1989 p 163-167 (For primary document see N89-24974 18-75)
Copyright Avail: NTIS HC A15/MF A01; ESA Publications Div., ESTEC, Noordwijk, Netherlands, 45 US dollars or 80 Dutch guilders

N89-25005# Academy of Sciences, Potsdam (German D.R.). Central Inst. for Astrophysics.
TIME SCALES OF SOLAR MICROWAVE BURSTS AND SCENARIOS OF FLARE ENERGY RELEASE
A. Krueger, B. Kliem, and J. Hildebrandt *In* ESA, Proceedings of an International School and Workshop on Reconnection in Space Plasma, Volume 2 Jan. 1989 p 169-173 (For primary document see N89-24974 18-75)
Copyright Avail: NTIS HC A15/MF A01; ESA Publications Div., ESTEC, Noordwijk, Netherlands, 45 US dollars or 80 Dutch guilders

N89-25016# Academy of Sciences (USSR), Irkutsk. Inst. of Terrestrial Magnetism, Ionosphere and Radiowave Propagation.
AN ANALOGY BETWEEN MAGNETOSPHERIC SUBSTORMS AND SOLAR FLARES: NEW VERSION
V. M. Mishin *In* ESA, Proceedings of an International School and Workshop on Reconnection in Space Plasma, Volume 2 Jan. 1989 p 233-240 (For primary document see N89-24974 18-75)
Copyright Avail: NTIS HC A15/MF A01; ESA Publications Div., ESTEC, Noordwijk, Netherlands, 45 US dollars or 80 Dutch guilders

N89-25027# Polish Academy of Sciences, Warsaw. Space Research Center.
A MODEL OF THE RECONNECTION PATTERN AT THE HELIOPAUSE
W. Macek and J. Bysiek *In* ESA, Proceedings of an International School and Workshop on Reconnection in Space Plasma, Volume 2 Jan. 1989 p 299-302 (For primary document see N89-24974 18-75)
(Contract CPFR-01.20)
Copyright Avail: NTIS HC A15/MF A01; ESA Publications Div., ESTEC, Noordwijk, Netherlands, 45 US dollars or 80 Dutch guilders

93 SPACE RADIATION

Includes cosmic radiation; and inner and outer earth's radiation belts.

For biological effects of radiation see *52 Aerospace Medicine*. For theory see *73 Nuclear and High-Energy Physics*.

N89-25103*# National Aeronautics and Space Administration. Langley Research Center, Hampton, VA.
KAON-NUCLEUS SCATTERING
Byungsik Hong, Khin Maung Maung, John W. Wilson, and Warren W. Buck (Hampton Inst., VA.) 1989 30 p
(NASA-TP-2920; L-16583; NAS 1.60:2920) Avail: NTIS HC A03/MF A01 CSCL 03A

The derivations of the Lippmann-Schwinger equation and Watson multiple scattering are given. A simple optical potential is found to be the first term of that series. The number density distribution models of the nucleus, harmonic well, and Woods-Saxon are used without t-matrix taken from the scattering experiments. The parameterized two-body inputs, which are kaon-nucleon total cross sections, elastic slope parameters, and the ratio of the real to the imaginary part of the forward elastic scattering amplitude, are presented. The eikonal approximation was chosen as our solution method to estimate the total and absorptive cross sections for the kaon-nucleus scattering. Author

N89-25104*# National Aeronautics and Space Administration. Langley Research Center, Hampton, VA.
CHARGE EXCHANGE TRANSITION PROBABILITY FOR COLLISIONS BETWEEN UNLIKE IONS AND ATOMS WITHIN THE ADIABATIC APPROXIMATION
Y. J. Xu, G. S. Khandelwal (Old Dominion Univ., Norfolk, VA.), and John W. Wilson Apr. 1989 43 p
(NASA-TM-101559; NAS 1.15:101559) Avail: NTIS HC A03/MF A01 CSCL 03B

A simple formula for the transition probability for electron exchange between unlike ions and atoms is established within the adiabatic approximation by employing the Linear Combination of Atomic Orbitals (LCAO) method. The formula also involves an adiabatic parameter, introduced by Massey, and thus the difficulties arising from the internal energy defect and the adiabatic approximation are avoided. Specific reactions Li(+++) + H to Li(++) + H(+) and Be(4+) + H to Be(3+) + H(+) are considered as examples. The calculated capture cross section results of the present work are compared with the experimental data and with the calculation of other authors over the velocity range of 10(7) cm/sec to 10(8) cm/sec. Author

N89-25105# Hiroshima Univ., Takehara (Japan). Research Inst. for Theoretical Physics.
GRAVITATIONAL ANGULAR FLUCTUATIONS OF THE COSMIC BACKGROUND RADIATION PRODUCED BY COSMOLOGICAL LINEAR PERTURBATIONS
Kenji Tomita Nov. 1988 26 p
(DE88-757287; RRK-88-37) Avail: NTIS (US Sales Only) HC A03/MF A01

The gravitational angular fluctuations of light rays produced by linear density perturbations are investigated in the Einstein-de Sitter model. It is shown that, owing to the random-walk process aroused by the perturbations, the mean square of relative angular fluctuations of two neighboring light rays increase as they propagate. If the density contrast is larger than 3 x 10(-3) for the present size 30 Mpc, the angular fluctuations for the angle difference of several minutes are so large to play a role to decrease the small-scale anisotropy of the cosmic background radiation during the propagation from the decoupling epoch to the present. They may give us also a reason to the question why few quasars can be found for z greater than 4. DOE

N89-25106 Max-Planck-Inst. fuer Physik und Astrophysik, Garching (Germany, F.R.). Inst. fuer Extraterrestrische Physik.
STRONG, SPATIALLY EXTENDED CO 7 TO 6 EMISSION FROM LUMINOUS CLOUD CORES: W51 AND DR21
D. T. Jaffe, Reinhard Genzel, A. I. Harris, J. B. Lugten, G. J. Stacey (California Univ., Berkeley.), and Juergen Stutzki Oct. 1988 38 p Submitted for publication
(Grant NSF AST-86-11784)
(MPE-Preprint-133; ISSN-0178-0719; ETN-89-94394) Copyright Avail: Fachinformationszentrum Karlsruhe, 7514 Eggenstein-Leopoldshafen 2, Federal Republic of Germany

It is concluded that three distinct molecular cloud components contribute to the CO 7 vs 6 emission, including the warm, dynamically active material which accounts for 75 percent of the velocity integrated CO emission from the two sources; a warm, quiescent material associated with the HII regions in each source; and a cool (20 to 40K) quiescent gas, which overlies some of the hot material. ESA

N89-25107 Max-Planck-Inst. fuer Physik und Astrophysik, Garching (Germany, F.R.). Inst. fuer Extraterrrestrische Physik.
COS-B GAMMA-RAY SOURCES BEYOND THE PREDICTED DIFFUSE EMISSION
H. A. Mayer-Hasselwander and G. Simpson (New Hampshire Univ., Durham.) Dec. 1988 9 p Presented at the 27th COSPAR Plenary Meeting, Espoo, Finland, Jul. 1988 Submitted for publication
(Grant NSF INT-83-14219)
(MPE-Preprint-136; ETN-89-94581) Copyright Avail: Fachinformationszentrum Karlsruhe, 7514 Eggenstein-Leopoldshafen 2, Federal Republic of Germany

A methodology to discriminate galactic source emissions from compact objects starting from COS-B gamma ray data was developed. The main features are automatic generation of source catalogs using correlation analysis, simulation of trials to derive catalog significance thresholds, and bootstrap sampling to derive

confidence intervals for source parameters. The analysis shows that half of the 2CG source are explained by concentration in the distribution of molecular hydrogen. ESA

N89-25108 Wisconsin Univ., Madison.
HIGH ENERGY PARTICLES IN SUPERNOVA REMNANTS AND THE INTERSTELLAR MEDIUM Ph.D. Thesis
Ahmed Boulares 1988 343 p
Avail: Univ. Microfilms Order No. DA8903005

The effects of high energy particles (cosmic rays) on shock structures of supernova remnants (SNRs), on the gas distribution in the interstellar medium, and on the structure of the galactic magnetic field perpendicular to the plane (along z) are studied. The observed cosmic-ray (CR) electron spectrum in light of shock acceleration in shell-like SNRs are also studied. It is found that shock acceleration of cosmic-rays with wave damping into the gas can indeed be made consistent with some astronomical observations of SNRs (e.g., Cygnus Loop), and also the observed CR electron spectrum. It is predicted that the remnant's shocks have larger velocities than inferred from pure gas shock wave models, and that the CR electrons above similar to 50 GeV must come from sources other than shell-like SNRs due to cut-offs in the shock acceleration process. The cosmic-rays are found to have an important inflating effect on the distribution of the interstellar gas, which without them would have a thinner distribution. This effect reduces the amount of dark matter required by earlier studies of the galactic gravitational potential, and consequently the Oort limit (interstellar mass density near the sun). They are also found to play a major role in the dynamics of the interstellar medium along with the magnetic field. It is found that a magnetic tension may explain the nonthermal pressure, and the radio emission distributions with z, and also provide a natural avenue for the escape of CRs from the Galaxy. Finally, wave damping near cosmic-ray shock waves is analyzed. It is found that for the wave amplitude to remain small, a very efficient damping mechanism is required. Dissert. Abstr.

N89-24929# Academy of Sciences (USSR), Moscow. Inst. of Space Research.
GENERATION OF X-RAY AND RADIO EMISSION BY BINARY WOLF-RAYET STARS
A. A. Galeev, N. N. Pilyugin, and V. V. Usov *In* ESA, Proceedings of an International School and Workshop on Plasma Astrophysics, Volume 1 Jan. 1989 p 125-129 (For primary document see N89-24910 18-75)
Avail: NTIS HC A18/MF A01; ESA Publications Div., ESTEC, Noordwijk, Netherlands, 45 US dollars or 80 Dutch guilders

N89-24940# Dublin Inst. for Advanced Studies (Ireland). School of Cosmic Physics.
COSMIC RAYS: A SHORT SURVEY OF OPEN PROBLEMS
L. OC. Drury *In* ESA, Proceedings of an International School and Workshop on Plasma Astrophysics, Volume 1 Jan. 1989 p 205-207 (For primary document see N89-24910 18-75)
Avail: NTIS HC A18/MF A01; ESA Publications Div., ESTEC, Noordwijk, Netherlands, 45 US dollars or 80 Dutch guilders

N89-24941# Academy of Sciences (USSR), Moscow. Physical Inst.
THEORY OF RADIOEMISSION OF PULSARS
V. S. Beskin, A. V. Gurevich, and Ya. N. Istomin *In* ESA, Proceedings of an International School and Workshop on Plasma Astrophysics, Volume 1 Jan. 1989 p 209-217 (For primary document see N89-24910 18-75)
Avail: NTIS HC A18/MF A01; ESA Publications Div., ESTEC, Noordwijk, Netherlands, 45 US dollars or 80 Dutch guilders

N89-24944# Academy of Sciences (USSR), Moscow. Inst. of General Physics.
RADIATIVE-RESONANT MHD INTERACTIONS BETWEEN WAVES AND PARTICLES AND THE PROBLEM OF COSMIC-RAY SPECTRA
V. N. Tsytovich *In* ESA, Proceedings of an International School and Workshop on Plasma Astrophysics, Volume 1 Jan. 1989 p 235-238 (For primary document see N89-24910 18-75)
Avail: NTIS HC A18/MF A01; ESA Publications Div., ESTEC, Noordwijk, Netherlands, 45 US dollars or 80 Dutch guilders

N89-24946# Washington Univ., Saint Louis, MO. Dept of Physics.
A NEW MODEL OF PeV GAMMA-RAY SOURCES
I. A. Smith and J. I. Katz *In* ESA, Proceedings of an International School and Workshop on Plasma Astrophysics, Volume 1 Jan. 1989 p 243-246 (For primary document see N89-24910 18-75)
Avail: NTIS HC A18/MF A01; ESA Publications Div., ESTEC, Noordwijk, Netherlands, 45 US dollars or 80 Dutch guilders

N89-24947*# California Inst. of Tech., Pasadena. Inst. of Theoretical Physics.
NEUTRON STARQUAKES AND THE NATURE OF GAMMA-RAY BURSTS
P. Madau, O. Blaes, R. D. Blandford, and P. Goldreich *In* ESA, Proceedings of an International School and Workshop on Plasma Astrophysics, Volume 1 Jan. 1989 p 247-250 (For primary document see N89-24910 18-75)
(Grants NAGw-1303; NSF AST-86-15325; NSF AST-86-1279)
Avail: NTIS HC A18/MF A01; ESA Publications Div., ESTEC, Noordwijk, Netherlands, 45 US dollars or 80 Dutch guilders
CSCL 03B

N89-24953# Abastumani Astrophysical Observatory, Georgia (USSR).
ON THE MECHANISM OF THE FORMATION OF THE POLARIZATION CHARACTERISTICS OF PULSAR RADIATION
A. Z. Kazbegi, G. Z. Machabeli, and G. I. Melikidze *In* ESA, Proceedings of an International School and Workshop on Plasma Astrophysics, Volume 1 Jan. 1989 p 277-280 (For primary document see N89-24910 18-75)
Avail: NTIS HC A18/MF A01; ESA Publications Div., ESTEC, Noordwijk, Netherlands, 45 US dollars or 80 Dutch guilders

N89-24957# Grenoble-1 Univ., Saint Martin d'Heres (France).
JETS AND BEAMS IN POWERFUL EXTRAGALACTIC RADIO SOURCES
G. Pelletier, J. Roland, H. Sol, and E. Asseo (Ecole Polytechnique, Palaiseau, France) *In* ESA, Proceedings of an Internatioal School and Workshop on Plasma Astrophysics, Volume 1 Jan. 1989 p 295-297 Sponsored in part by CNRS, France (For primary document see N89-24910 18-75)
Avail: NTIS HC A18/MF A01; ESA Publications Div., ESTEC, Noordwijk, Netherlands, 45 US dollars or 80 Dutch guilders

N89-25029# European Space Agency. European Space Research and Technology Center, ESTEC, Noordwijk (Netherlands). Space Science Dept.
SPECULATION ON THE ORIGIN OF X-RAY EMISSION IN EARLY-TYPE STARS
A. M. T. Pollock *In its* Proceedings of an International School and Workshop on Reconnection in Space Plasma, Volume 2 Jan. 1989 p 309-311 (For primary document see N89-24974 18-75)
Copyright Avail: NTIS HC A15/MF A01; ESA Publications Div., ESTEC, Noordwijk, Netherlands, 45 US dollars or 80 Dutch guilders

99 GENERAL

N89-25109*# National Aeronautics and Space Administration. Goddard Space Flight Center, Greenbelt, MD.
RESEARCH AND TECHNOLOGY, 1988 Annual Report
1988 300 p Original contains color illustrations
(NASA-TM-101246; NAS 1.15:101246) Avail: NTIS HC A13/MF A01 CSCL 05D

Flight projects and mission definition studies for 1988 are briefly described. Technology research is presented in the following areas: sensors and space technology; space communication systems; system and software engineering; user space data systems; and techniques. Studies are presented for the following space and Earth science areas: atmospheres, SN 1987A, astronomy, high energy astrophysics, land and climate, solar systems, and oceans. B.G.

N89-25110*# National Aeronautics and Space Administration. Langley Research Center, Hampton, VA.
SPACE STATION FREEDOM STRUCTURAL CHARACTERIZATION EXPERIMENT (SCE) NODE CODE
Robert L. Jensen May 1989 16 p
(NASA-TM-101594; NAS 1.15:101594) Avail: NTIS HC A03/MF A01 CSCL 22B

A method is described for naming the Space Station Freedom nodes and truss members that enhances the management, maintenance, and record keeping methods utilized by the space station. Author

N89-25111*# National Aeronautics and Space Administration, Washington, DC.
NASA INFORMATION SCIENCES AND HUMAN FACTORS PROGRAM Annual Report, 1988
Lee Holcomb, Ray Hood, Melvin Montemerlo, Martin Sokoloski, James Jenkins, Paul Smith, and John DiBattista Jul. 1989 264 p
(NASA-TM-4126; NAS 1.15:4126) Avail: NTIS HC A12/MF A01 CSCL 05D

The FY 1988 descriptions of technical accomplishments is presented in seven sections: Automation and Robotics, Communications Systems, Computer Sciences, Controls and Guidance, Data Systems, Human Factors, and Sensor Technology. Author

N89-25112*# National Aeronautics and Space Administration. Langley Research Center, Hampton, VA.
LANGLEY AEROSPACE TEST HIGHLIGHTS, 1988
May 1989 166 p
(NASA-TM-101579; NAS 1.15:101579) Avail: NTIS HC A08/MF A01 CSCL 05D

The role of the Langley Research Center is to perform basic and applied research necessary for the advancement of aeronautics and space flight, to generate new and advanced concepts for the accomplishment of related national goals, and to provide research advice, technological support, and assistance to other NASA installations, other government agencies, and industry. Some of the significant tests which were performed during calendar year 1988 in Langley test facilities, a number of which are unique in the world are highlighted. Both the broad range of the research and technology activities at the Langley Research Center and the contributions of this work toward maintaining United States leadership in aeronautics and space research are illustrated. Author

Typical Subject Index Listing

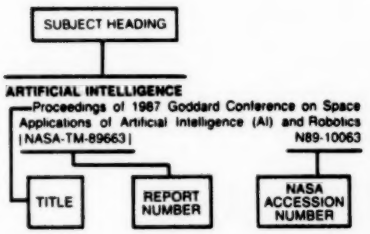

The subject heading is the key to the subject content of the document. Titles, report numbers, and accession numbers of pertinent documents are provided under each subject heading. When the title is insufficiently descriptive of the document content, a title extension has been added, separated from the title by three hyphens. The report number helps to indicate the type of document cited (e.g., NASA report, NASA translation, NASA contractor report). The NASA accession number is the number by which the document abstracts are arranged in this journal and by which the document is sold or requested. The titles, with title extensions if present, are arranged under each subject heading in ascending accession number order. The subject headings have been selected from the latest revision of the *NASA Thesaurus* (NASA SP-7064).

A

ABSORPTANCE
Contamination effects of GPS Navstar solar array performance N89-24734

ABSORPTION CROSS SECTIONS
Kaon-nucleus scattering
[NASA-TP-2920] N89-25103

ABSORPTION SPECTROSCOPY
Design of the optical system for a new time-resolved X-ray absorption spectroscopy apparatus
[DE88-757253] N89-24902

ACCELERATION (PHYSICS)
The impact of an IVA robot on the space station microgravity environment N89-24821
An analytical study of a vibration test method using extremal control of acceleration and force
[DE89-007428] N89-24884

ACCELEROMETERS
Further developments in modeling digital control systems with MA-prefiltered measurements
[NASA-TP-2909] N89-24507

ACCIDENT PRONENESS
Safety analysis report for the Galileo Mission. Volume 2, book 1: Accident model document
[DE89-007270] N89-24896
Safety analysis report for the Galileo Mission. Volume 2, book 2: Accident model document, Appendices
[DE89-007271] N89-24897
Safety analysis report for the Galileo Mission. Volume 3, book 1: Nuclear risk analysis document, revision 1
[DE89-007272] N89-24898
Safety analysis report for the Galileo Mission. Volume 3, book 2: Nuclear risk analysis document. Appendices, revision 1
[DE89-007273] N89-24899

ACCRETION DISKS
Small-scale instabilities in accretion disks of compact objects and their manifestations N89-24950
Problem of nonrotating black hole accretion disk main energy release region extension N89-24951

ACOUSTIC EMISSION
Research in structures, structural dynamics and materials, 1989
[NASA-CP-10024] N89-24626
Acoustic emission from a growing crack N89-24633
ASDEX Contributions to the 8th International Conference on Plasma Surface Interaction in Controlled Fusion Devices
[IPP-III/139] N89-25038
Plasma induced changes of a metallic divertor neutralizer plate from ASDEX analyzed by photoacoustics N89-25048

ACOUSTIC FREQUENCIES
Pressure-volume properties of metallic bellows
[NASA-TM-100365] N89-24422

ACOUSTIC LEVITATION
Containerless glass fiber processing
[NASA-TM-86540] N89-24405

ACOUSTICS
Auditory speech preprocessors
[DE89-009280] N89-24516
The effects of blast trauma (impulse noise) on hearing: A parametric study
[AD-A206180] N89-24786

ACTIVE CONTROL
Aeroservoelastic wind-tunnel investigations using the Active Flexible Wing Model: Status and recent accomplishments
[NASA-TM-101570] N89-24313

ACTIVITY CYCLES (BIOLOGY)
Neurochemical control of circadian rhythms
[AD-A206213] N89-24788

ADAPTIVE CONTROL
Cooperating expert systems N89-24825
Neuromorphic learning of continuous-valued mappings in the presence of noise: Application to real-time adaptive control
[NASA-TM-101999] N89-24856
Empirical analysis and refinement of expert system knowledge bases
[AD-A206226] N89-24858

ADDITIVES
An empirical study of the performance of APMOVPE AM0 InP homojunction solar cells as a function of emitter thickness and doping, and base doping N89-24709
N/P InP homojunction solar cells with an In0.53Ga0.47As contacting layer grown by liquid phase epitaxy N89-24710
Deep levels and radiation effects in p-InP N89-24713

ADHESIVE BONDING
Bonded assemblies behavior laws: Light alloys/elastoplastic adhesive
[ETCA-88-R-001] N89-24456
Composite material bonding: Gelation and processing of adhesives and preimpregnated materials
[ETCA-88-R-006] N89-24457

ADIABATIC CONDITIONS
Adiabatic, chaotic and quasi-adiabatic charged particle motion in two-dimensional magnetic field reversals N89-24942

ADJUSTING
Shaft adjuster
[DE89-010119] N89-24612

ADVECTION
Study of explosive and nonexplosive cyclogenesis during FGGE
[AD-A206521] N89-24775

AERIAL PHOTOGRAPHY
Investigations of a displacement-estimation technique for aerial video scenes N89-24299
Study of a parametric displacement estimation scheme with application in aerial images N89-24300

AERIAL RECONNAISSANCE
A versatile flight experiment system for image processing N89-24307

AEROASSIST
Multiple-pass aeroassisted plane change N89-24404
Orbital Transfer Vehicle: Concept definition and system analysis study
[NASA-CR-183551] N89-24410

AEROBRAKING
Development of tailorable advanced blanket insulation for advanced space transportation systems
[NASA-CR-177444] N89-24486

AERODYNAMIC CHARACTERISTICS
Aerodynamics of a lifting rotor due to near field unsteady effects N89-24267

AERODYNAMIC CONFIGURATIONS
Computational design of low aspect ratio wing-winglet configurations for transonic wind-tunnel tests
[NASA-CR-185016] N89-24266
An investigation of V/STOL jet interactions in a crossflow
[AD-A206360] N89-24272

AERODYNAMIC DRAG
Use of Navier-Stokes methods to predict circulation control airfoil performance
[AD-A206242] N89-24270

AERODYNAMIC FORCES
Unsteady aerodynamic effects on bluff bodies N89-24278
Aeroservoelastic modeling and applications using minimum-state approximations of the unsteady aerodynamics
[NASA-TM-101574] N89-24308

AERODYNAMIC HEAT TRANSFER
A computer simulation study of liquid water content adjustment based on icing cloud horizontal extent
[DOT/FAA/CT-TN89/3] N89-24288

AERODYNAMIC HEATING
Thermal analysis of a hypersonic wing test structure
[NASA-CR-185319] N89-24265
SRB ascent aerodynamic heating design criteria reduction study, volume 2
[NASA-CR-183569] N89-24430

AERODYNAMIC NOISE
Cruise noise of the SR-2 propeller model in a wind tunnel
[NASA-TM-101480] N89-24886

AERODYNAMIC STABILITY
Loss of tail rotor effectiveness evaluation of the OH-58C helicopter with directional SAS (Stability Augmentation System)
[AD-A206181] N89-24309
Multiple-pass aeroassisted plane change N89-24404

AERODYNAMICS
Langley aerospace test highlights, 1988
[NASA-TM-101579] N89-25112

AEROELASTIC RESEARCH WINGS
Aeroservoelastic wind-tunnel investigations using the Active Flexible Wing Model: Status and recent accomplishments
[NASA-TM-101570] N89-24313

AEROELASTICITY
Aeroservoelastic modeling and applications using minimum-state approximations of the unsteady aerodynamics
[NASA-TM-101574] N89-24308
Aeroservoelastic wind-tunnel investigations using the Active Flexible Wing Model: Status and recent accomplishments
[NASA-TM-101570] N89-24313
Recent activities within the Aeroservoelasticity Branch at the NASA Langley Research Center
[NASA-TM-101582] N89-24314
Results of a parametric aeroelastic stability analysis of a generic X-wing aircraft
[NASA-TM-101572] N89-24324
Survey of Army/NASA rotorcraft aeroelastic stability research
[NASA-TM-101026] N89-24329

AEROMANEUVERING
Multiple-pass aeroassisted plane change N89-24404

AERONAUTICAL ENGINEERING
The use of seaplanes as an advanced weapon system
[AD-A206243] N89-24880

AEROSOLS
Correlation between satellite-derived aerosol characteristics and oceanic dimethylsulfide (DMS)
[AD-A206179] N89-24759

AEROSPACE ENGINEERING
Numerical aerodynamic simulation
[NASA-EP-262] N89-24262
Langley aerospace test highlights, 1988
[NASA-TM-101579] N89-25112
AEROSPACE INDUSTRY
Study on cost efficiency of product assurance in space programs
[REPT-882-440-122] N89-24622
CSM testbed development and large-scale structural applications
[NASA-TM-4072] N89-24624
AEROSPACE MEDICINE
Medical and radiation protection problems in space N89-24369
Protection against ionizing radiation for the Hermes mission N89-24370
The AAMRL (Armstrong Aerospace Medical Research Laboratory) biodynamics data bank
[AD-A206139] N89-25074
AEROSPACE PLANES
An integrated aerodynamic/propulsion study for generic aero-space planes based on waverider concepts
[NASA-CR-183389] N89-24315
Hermes-MTFF rendezvous strategy and composite operations N89-24357
Timelining and operations integration concerning APM and MTFF N89-24358
Servicing of the MTFF by Hermes N89-24360
MTFF flight operations phases N89-24361
AEROSPACE SAFETY
ESA safety requirements N89-24364
Safety and reliability of the Ariane 5-Hermes composite N89-24365
System safety from D-missions to Columbus N89-24367
Columbus safety and reliability N89-24368
The impact of manned space flight operations on the safety and reliability aspects of ground systems requirements N89-24371
Safety in manned space flight N89-24402
AEROSPACE SYSTEMS
Conference on Space and Military Applications of Automation and Robotics
[AD-A198095] N89-24819
Ground control of space based robotic systems N89-24845
AFRICA
Contribution to the estimation of precipitation in the Sahel by using satellite imagery
[SER-DI-204] N89-24762
AFTERBODIES
Navier-Stokes analysis of cold scramjet-afterbody flows
[NASA-CR-184949] N89-24562
AGING (METALLURGY)
Aging behavior of Au-based ohmic contacts to GaAs N89-24727
AGRICULTURE
Microwave X-band radiometric characterization of Brazilian soils by measurement of the complex permittivity
[INPE-4586-PRE/1319] N89-24585
AILERONS
Experimental aerodynamic characteristics of a joined-wing research aircraft configuration
[NASA-TM-101083] N89-24285
AIR FLOW
Study of chemical reaction models for high enthalpy flow of air
[NAL-TR-982] N89-25072
AIR NAVIGATION
Image Signal Processing for Flight Guidance
[DFVLR-MITT-88-32] N89-24295
Bordautonomous terrain aided flight navigation in height sections close to terrain surface N89-24301
Diverter AI based decision aid, phases 1 and 2
[NASA-CR-181820] N89-24316
AIR POLLUTION
The relationship between in-lake sulfate concentration and estimates of atmospheric sulfur deposition for subregions of the eastern lake survey
[DE89-009868] N89-24749
Field studies for determining the characteristics and dynamics of local circulations
[DE89-012290] N89-24751
AIR TO SURFACE MISSILES
The night and adverse weather capability of ground attack aircraft
[FOA-C-20745-2.5] N89-24312
AIR TRAFFIC CONTROL
A comparison of detection efficiency on an air traffic control monitoring task with and without computer aiding
[AD-A206422] N89-24294
AIR TRANSPORTATION
Display-based communications for advanced transport aircraft
[NASA-TM-102187] N89-24798
AIRBORNE EQUIPMENT
Imaging Spectrometry for Land Applications
[ESA-SP-1101] N89-24692
The activities of the British National Space Centre (BNSC) in the field of imaging spectrometry N89-24696
Development of an imaging spectrometer for remote sensing: The FLI program N89-24698
Imaging spectrometry at the Canada Centre for Remote Sensing N89-24701
AIRBORNE/SPACEBORNE COMPUTERS
Lightning inflight study onboard a Transall aircraft. Definition of the onboard instruments
[ONERA-RF-19/7234-PY] N89-24777
AIRCRAFT CONFIGURATIONS
An integrated aerodynamic/propulsion study for generic aero-space planes based on waverider concepts
[NASA-CR-183389] N89-24315
AIRCRAFT CONSTRUCTION MATERIALS
Computerized structural mechanics for 1990's: Advanced aircraft needs N89-24640
Nonlinear response of a blade-stiffened graphite-epoxy panel with a discontinuous stiffener: Work in progress N89-24641
Computational procedures for postbuckling of composite shells N89-24642
AIRCRAFT CONTROL
Experimental aerodynamic characteristics of a joined-wing research aircraft configuration
[NASA-TM-101083] N89-24285
Numerical simulation of feedback control of aerodynamic configurations in steady and unsteady ground effects N89-24326
An intelligent fiberoptic data bus for fly-by-light applications
[NAL-TM-SE-8707] N89-24901
AIRCRAFT DESIGN
Results of a parametric aeroelastic stability analysis of a generic X-wing aircraft
[NASA-TM-101572] N89-24324
Multidisciplinary optimization for engineering systems: Achievements and potential
[NASA-TM-101566] N89-24508
Computerized structural mechanics for 1990's: Advanced aircraft needs N89-24640
Computational Methods for Structural Mechanics and Dynamics
[NASA-CP-3034-PT-2] N89-24654
Improving transient analysis technology for aircraft structures N89-24655
AIRCRAFT EQUIPMENT
Display of flight guidance information in the aircraft cockpit N89-24305
AIRCRAFT GUIDANCE
Image Signal Processing for Flight Guidance
[DFVLR-MITT-88-32] N89-24295
Image signal processing for flight guidance: Overview and introduction to the main topics N89-24296
Display of flight guidance information in the aircraft cockpit N89-24305
AIRCRAFT HAZARDS
A computer simulation study of liquid water content adjustment based on icing cloud horizontal extent
[DOT/FAA/CT-TN89/3] N89-24288
AIRCRAFT INDUSTRY
US military aircraft coproduction with Japan
[AD-A206430] N89-24263
Computerized structural mechanics for 1990's: Advanced aircraft needs N89-24640
AIRCRAFT LANDING
B-737 flight test of curved-path and steep-angle approaches using MLS guidance
[NASA-TM-101521] N89-24293
AIRCRAFT MODELS
Experimental aerodynamic characteristics of a joined-wing research aircraft configuration
[NASA-TM-101083] N89-24285
AIRCRAFT NOISE
Cruise noise of the SR-2 propeller model in a wind tunnel
[NASA-TM-101480] N89-24886
Advanced turboprop aircraft flyover noise: Annoyance to counter-rotating-propeller configurations with a different number of blades on each rotor: Preliminary results
[NASA-TM-100638] N89-24888
AIRCRAFT PERFORMANCE
Experimental aerodynamic characteristics of a joined-wing research aircraft configuration
[NASA-TM-101083] N89-24285
Ground vibration test of the Foudre A04 Transall aircraft
[REPT-20/7234-PY-382-R] N89-24311
Flight control system for the CRCA (Control Reconfigurable Combat Aircraft) using a command generator tracker with PI (Plus Integral) feedback and Kalman filter, volume 2
[AD-A206202] N89-24325
Development and flight test experiences with a flight-crucial digital control system
[NASA-TP-2857] N89-24327
AIRCRAFT PRODUCTION
US military aircraft coproduction with Japan
[AD-A206430] N89-24263
AIRCRAFT STABILITY
Experimental aerodynamic characteristics of a joined-wing research aircraft configuration
[NASA-TM-101083] N89-24285
AIRCRAFT STRUCTURES
Technology of aircraft construction (selected chapters)
[AD-A199946] N89-24261
Ground vibration test of the Foudre A04 Transall aircraft
[REPT-20/7234-PY-382-R] N89-24311
CSM testbed development and large-scale structural applications
[NASA-TM-4072] N89-24624
Improving transient analysis technology for aircraft structures N89-24655
AIRFOIL PROFILES
Effect of advanced rotorcraft airfoil sections on the hover performance of a small-scale rotor model
[NASA-TP-2832] N89-24264
Computational and experimental research on buffet phenomena of transonic airfoils
[NAL-TR-996T] N89-24322
AIRFOILS
A computer simulation study of liquid water content adjustment based on icing cloud horizontal extent
[DOT/FAA/CT-TN89/3] N89-24288
Unsteady and separated flows
[AD-A206539] N89-24572
AIRLOCK MODULES
Space science using Columbus: Manned space science N89-24348
AIRPORTS
Calculation of aircraft noise in the vicinity of civil airports by a simultion procedure
[MPIS-7/1988] N89-24887
ALGEBRA
Computational method of the inverse kinematics via simplified algebraic equation
[DE88-757269] N89-24866
Dynamic spectral analysis in finite field algebras
[DE88-706333] N89-24877
ALGORITHMS
Conservative treatment of boundary interfaces for overlaid grids and multi-level grid adaptations
[NASA-TM-102080] N89-24269
Unsteady aerodynamics N89-24277
Unsteady Aerodynamics, volume 2
[VKI-1988-07-VOL-2] N89-24281
Numerical methods for unsteady flows N89-24282
Tele-autonomous control involving contacts: The applications of a high precision laser line range sensor
[NASA-CR-184995] N89-24509
Two-dimensional phase correction of synthetic aperture radar imagery
[DE89-007086] N89-24524
Channel and switchbox routing using a greedy based channel algorithm with outward scanning technique
[AD-A206545] N89-24526
Domain decomposition algorithms and computation fluid dynamics
[NASA-CR-185405] N89-24578
Integrated optimization of nonlinear R/C frames with reliability constraints N89-24631
Some issues in numerical simulation of nonlinear structural response N89-24639
Contact solution algorithms N89-24652
Unconditionally stable concurrent procedures for transient finite-element analysis N89-24657
Application and implementation of transient algorithms in computer programs N89-24659
Efficient dealiasing of Doppler velocities using local environment constraints
[DOT/FAA/SA-89/1] N89-24771
Modeling and characterization of the Earth Radiation Budget Experiment (ERBE) nonscanner and scanner sensors
[NASA-CR-181818] N89-24772
The radiation-atmosphere interaction model and the determination of meteorological and climatological parameters from satellite observations
[ETN-89-94535] N89-24779
High speed implementation of NAL application software packages
[NAL-TR-986] N89-24801

Formal verification of a fault tolerant clock synchronization algorithm
[NASA-CR-4239] N89-24803
Totally parallel multilevel algorithms
[NASA-CR-185404] N89-24818
A new approach to robot kinematic analysis N89-24833
Algorithm for display of automated nondestructive thickness measurements N89-24850
On the equivalence of a class of inverse decomposition algorithms for solving systems of linear equations
[NASA-TM-102036] N89-24865
Numerical integration of asymptotic solutions of ordinary differential equations
[NASA-TM-100650] N89-24867

ALIGNMENT
Shaft adjuster
[DE89-010119] N89-24612

ALKALI HALIDES
Dynamics of gas-surface interactions
[AD-A206210] N89-25059

ALKALINE BATTERIES
US fuel cell research and applications, 1960--1989
[DE89-012244] N89-24745

ALLOYING
Role of alloying additions in the oxidation-sulfidation of Fe-base alloys
[DE89-009825] N89-24473
Amorphous metal alloys produced by mechanical alloying
[DE89-011189] N89-24481

ALLOYS
Fundamental studies on order effects in metal alloys
[ONERA-RT-14/221-M] N89-24480

ALTIMETRY
Water vapor retrievals through the 3I (Improved Initialization Inversion) system: Application to tropospheric altimetry correction
[ETN-89-94534] N89-24778

ALUMINUM
High temperature mechanical properties and microscopic examination of extruded powder aluminum
[DE89-010457] N89-24484
Two dimensional analysis of a NOVETTE laser generated stress-impulse experiment
[DE89-009909] N89-24600

ALUMINUM ALLOYS
Weldability and microstructural characterization of Al-Li alloys
[DE89-010183] N89-24478
Nd:YAG laser weldability of RS/PM Al-BFe-2Mo sheet
[DE89-013588] N89-24621

ALUMINUM GALLIUM ARSENIDES
A three solar cell system based on a self-supporting, transparent AlGaAs top solar cell N89-24723

AMIDES
Mass spectrometry
[DE89-011118] N89-24471

AMINES
Mass spectrometry
[DE89-011118] N89-24471

AMORPHOUS MATERIALS
Amorphous metal alloys produced by mechanical alloying
[DE89-011189] N89-24481
Electrophoretically applied dielectrics for amorphous metal foils used in pulsed power saturable reactors
[DE89-009322] N89-24525

AMORPHOUS SILICON
Investigations of the origins of metastable, light-induced changes in hydrogenated amorphous silicon
[DE89-000890] N89-24496
Research on high-efficiency, single-junction, monolithic, thin-film amorphous silicon solar cells, phase 2
[DE89-000849] N89-24703
Research on high-efficiency, single-junction, monolithic, thin-film amorphous silicon solar cells
[DE89-000893] N89-24739

ANALOG COMPUTERS
Fractional-order feedback in linear systems
[AD-A206241] N89-24859

ANALYTIC GEOMETRY
Self-circumference in the Minkowski plane
[AD-A205691] N89-24868

ANECHOIC CHAMBERS
Ultra-light duct for an anechoic wind tunnel
[NASA-TM-101805] N89-24331

ANISOTROPY
Quantum relativistic theory of the cyclotron radiation in a strongly magnetized plasma with anisotropic temperature --- neutron stars N89-24962
Some dynamical properties of anisotropic collisionless stellar systems N89-24963

ANNEALING
Deep levels and radiation effects in p-InP N89-24713
Response of single junction GaAs/GaAs and GaAs/Ge solar cells to multiple doses of 1 MeV electrons N89-24722
Superconducting properties of magnetron sputtered Bi-Sr-Ca-Cu-O and Tl-Ba-Ca-Cu-O thin films
[DE89-009878] N89-25056

ANNUAL VARIATIONS
Time variations in the earth's gravity field from Starlette orbit analysis N89-24766
Forecast of Atlantic seasonal hurricane activity for 1989 N89-24773
The relationship between intraseasonal disturbance activity and interannual variation of the tropical atmosphere N89-24774

ANTARCTIC REGIONS
Estimating population size of Pygoscelid Penguins from TM data
[NASA-CR-180081] N89-24687

ANTENNA ARRAYS
Feasibility study of a synthesis procedure for array feeds to improve radiation performance of large distorted reflector antennas
[NASA-CR-184974] N89-24511

ANTENNA DESIGN
ICRF antenna designs for CIT and Alcator C-Mod
[DE89-011579] N89-24521

ANTENNA FEEDS
Feasibility study of a synthesis procedure for array feeds to improve radiation performance of large distorted reflector antennas
[NASA-CR-184974] N89-24511
Analysis of a probe-metallic sleeve feed system for a rectangular waveguide
[DE89-006769] N89-24523
Computed performance of the half-scale accurate antenna reflector
[NASA-CR-182284] N89-24532

ANTENNA RADIATION PATTERNS
Feasibility study of a synthesis procedure for array feeds to improve radiation performance of large distorted reflector antennas
[NASA-CR-184974] N89-24511

ANTENNAS
The frequency response of phased-array antennas
[DE89-009710] N89-24517
ICRF antenna designs for CIT and Alcator C-Mod
[DE89-011579] N89-24521

ANTHROPOMETRY
The AAMRL (Armstrong Aerospace Medical Research Laboratory) biodynamics data bank
[AD-A206139] N89-25074

ANTIFERROMAGNETISM
On the nature of high-temperature superconductivity
[DE89-009525] N89-25053

APPLICATIONS PROGRAMS (COMPUTERS)
A methodology for commonality analysis, with applications to selected space station systems
[NASA-TM-100364] N89-24421
Flight experiment of thermal energy storage
[NASA-TM-102081] N89-24440
The computational structural mechanics testbed architecture. Volume 5: The Input-Output Manager DMGASP
[NASA-CR-178388] N89-24637
SPECTRUM: A computer algorithm to derive the flux-energy spectrum of precipitating particles from EISCAT electron density profiles
[IRF-TR-034] N89-24764
Transformational derivation of programs using the Focus system
[NASA-CR-184875] N89-24802

APPROACH CONTROL
B-737 flight test of curved-path and steep-angle approaches using MLS guidance
[NASA-TM-101521] N89-24293

APPROXIMATION
Aeroservoelastic modeling and applications using minimum-state approximations of the unsteady aerodynamics
[NASA-TM-101574] N89-24308
Local corner cutting and the smoothness of the limiting curve
[AD-A204092] N89-24864
Numerical integration of asymptotic solutions of ordinary differential equations
[NASA-TM-100650] N89-24867

ARC JET ENGINES
The 5-kW arcjet power electronics
[NASA-TM-102108] N89-24446

ARC WELDING
Cooperating expert systems N89-24825

ARCHITECTURE (COMPUTERS)
Status and trends of technological image processing possibilities N89-24306
The computational structural mechanics testbed architecture. Volume 5: The Input-Output Manager DMGASP
[NASA-CR-178388] N89-24637
Nonlinear hierarchical substructural parallelism and computer architecture N89-24650
Large-scale structural analysis: The structural analyst, the CSM Testbed and the NAS System
[NASA-TM-100643] N89-24673
Attaching IBM-compatible 3380 disks to Cray X-MP
[DE89-012383] N89-24800
How to (and not to) introduce computer graphics to design professionals
[DE89-010374] N89-24812
Application of Lotus 1-2-3 to heat transfer analysis
[DE89-010463] N89-24813
File concepts for parallel I/O
[NASA-CR-181843] N89-24816
The DARPA autonomous land vehicle: A phase 1 retrospective and a prospective for the future N89-24834

ARCTIC OCEAN
Biooptical variability in the Greenland Sea observed with the Multispectral Airborne Radiometer System (MARS)
[NASA-CR-184856] N89-24784

ARGON PLASMA
An atomic oxygen generation facility for space environmental testings
[NAL-TR-989] N89-24506

ARIANE LAUNCH VEHICLE
The Ariane 5 Development Program N89-24336
Columbus: The European contribution to the International Space Station N89-24337
Overview of Ariane 5 and Hermes programs technology N89-24349
Ariane 5 solid boosters: Overview of design approach and envisaged technologies N89-24352
Technology and design method evolution of cryogenic propulsion systems: Example of the main Ariane 5 stage N89-24353
Safety and reliability of the Ariane 5-Hermes composite N89-24365

ARMOR
Cavity dimensions for high velocity penetration events: A comparison of calculational results with data
[DE89-011351] N89-24617

ARTIFICIAL INTELLIGENCE
Diverter AI based decision aid, phases 1 and 2
[NASA-CR-181820] N89-24316
Hierarchically structured control for intelligent robots in space N89-24393
Computerized structural mechanics for 1990's: Advanced aircraft needs N89-24640
Formal verification of AI software
[NASA-CR-181827] N89-24811
Conference on Space and Military Applications of Automation and Robotics
[AD-A198095] N89-24819
High level intelligent control of telerobotics systems N89-24823
Space languages: Solving the classic scheduling problem in Ada and Lisp N89-24826
On designing a case-based system for expert process development N89-24847
Using a simulation assistant in modeling manufacturing systems N89-24849
A knowledge representation scheme for a robotic land vehicle route planner N89-24853
Pedagogical issues in developing a man-machine interface for an intelligent tutoring system N89-24855
A deductive approach to automated planning
[AD-A206253] N89-24860

ARTIFICIAL SATELLITES
Space power technology 21: Photovoltaics N89-24706
The experiments of LIPS 3 N89-24735

ASSEMBLIES
Bonded assemblies behavior laws: Light alloys/elastoplastic adhesive
[ETCA-88-R-001] N89-24456
Composite material bonding: Gelation and processing of adhesives and preimpregnated materials
[ETCA-88-R-006] N89-24457

ASSEMBLING
Robot assembly of microscopic component in millimeter wave devices N89-24840

ASTRONAUT PERFORMANCE
The human role in space (THURIS) applications study. Final briefing
[NASA-CR-183590] N89-24793
The human role in space (THURIS) applications study. Volume 2: Research analysis and technology report
[NASA-CR-183589] N89-24795

ASTRONAUT TRAINING
The training concept for ESA astronauts and the associated facilities N89-24374

The Hermes system training concept N89-24375
Crew training aspects --- Hermes, Columbus N89-24396
The astronaut's functions aboard Columbus N89-24403

ASTRONOMICAL CATALOGS
COS-B gamma-ray sources beyond the predicted diffuse emission
[MPE-PREPRINT-136] N89-25107

ASTRONOMICAL MAPS
A study of the Southern Supercluster N89-25088

ASTRONOMICAL MODELS
Non-steady astrophysical spiral jets driven by magnetic collapse and pressure N89-24920
The case for a primordial galactic field N89-24939
Cosmic rays: A short survey of open problems N89-24940
Global kinetic theory of astrophysical jets N89-24954
Jets and beams in powerful extragalactic radio sources N89-24957

ASTRONOMICAL SATELLITES
The gamma-ray observatory GRO in perspective
[MPE-PREPRINT-137] N89-24407

ASTRONOMICAL SPECTROSCOPY
SMM X-ray polychromator
[NASA-CR-180791] N89-24590
IUE investigations of SN 1987A
[NASA-CR-184973] N89-25079

ASTROPHYSICS
Proceedings of an International School and Workshop on Plasma Astrophysics, volume 1
[ESA-SP-285-VOL-1] N89-24910
Development of astrophysics from the telescope to the Sputnik N89-24911
Astrophysical significance of observations and experiments in the earth's magnetosphere N89-24912

ASYMPTOTES
Advances in dual methods and convex approximations for structural optimization N89-24680

ASYMPTOTIC METHODS
A hybrid asymptotic-modal analysis of the EM scattering by an open-ended S-shaped rectangular waveguide cavity
[NASA-CR-185053] N89-24519
Numerical integration of asymptotic solutions of ordinary differential equations
[NASA-TM-100650] N89-24867

ASYMPTOTIC SERIES
Fractional-order feedback in linear systems
[AD-A206241] N89-24859

ATLANTIS (ORBITER)
Space Shuttle to deploy Magellan planetary science mission
[NASA-NEWS-RELEASE-89-86] N89-24334

ATMOSPHERIC CHEMISTRY
Beyond CO2: The other greenhouse gases
[DE89-011893] N89-24750

ATMOSPHERIC CIRCULATION
Field studies for determining the characteristics and dynamics of local circulations
[DE89-012290] N89-24751
Study of explosive and nonexplosive cyclogenesis during FGGE
[AD-A206521] N89-24775

ATMOSPHERIC COMPOSITION
Beyond CO2: The other greenhouse gases
[DE89-011893] N89-24750
A visiting scientist program in atmospheric sciences for the Goddard Space Flight Center
[NASA-CR-183421] N89-24756

ATMOSPHERIC DIFFUSION
Field studies for determining the characteristics and dynamics of local circulations
[DE89-012290] N89-24751

ATMOSPHERIC EFFECTS
Atmospheric effects on laser propagation
[DE89-012287] N89-24606

ATMOSPHERIC ELECTRICITY
Lightning inflight study onboard a Transall aircraft. Definition of the onboard instruments
[ONERA-RF-19/7234-PY] N89-24777

ATMOSPHERIC GENERAL CIRCULATION MODELS
A visiting scientist program in atmospheric sciences for the Goddard Space Flight Center
[NASA-CR-183421] N89-24756

ATMOSPHERIC IONIZATION
SPECTRUM: A computer algorithm to derive the flux-energy spectrum of precipitating particles from EISCAT electron density profiles
[IRF-TR-034] N89-24764

ATMOSPHERIC MODELS
Improvements in the Global Reference Atmospheric Model and comparisons with a global 3-D numerical model
[NASA-CR-184947] N89-24755
Three dimensional analysis of the atmospheric structure by vertical satellite sounding. Interest for weather forecasting
[ETN-89-94536] N89-24763
Efficient dealiasing of Doppler velocities using local environment constraints
[DOT/FAA/SA-89/1] N89-24771
Simplified climate models: Rationale and design
[DE89-012291] N89-24783
Theoretical studies of important processes in planetary and comet atmospheres. Renewal request
[NASA-CR-184951] N89-25099

ATMOSPHERIC MOISTURE
A computer simulation study of liquid water content adjustment based on icing cloud horizontal extent
[DOT/FAA/CT-TN89/3] N89-24288
Estimating the outgoing longwave radiation from the Meteosat infrared window and water vapor bands
[ETN-89-94533] N89-24762
Water vapor retrievals through the 3I (Improved Initialization Inversion) system: Application to tropospheric altimetry correction
[ETN-89-94534] N89-24778

ATMOSPHERIC SOUNDING
Simulation studies of improved sounding systems
[NASA-CR-185322] N89-24758
Investigations of the sodium layer of the earth atmosphere: Probing with a terrestrial lidar system at 69 N in winter
[BONN-IR-88-52] N89-24760
Three dimensional analysis of the atmospheric structure by vertical satellite sounding. Interest for weather forecasting
[ETN-89-94536] N89-24763

ATMOSPHERIC TEMPERATURE
Correlation between satellite-derived aerosol characteristics and oceanic dimethylsulfide (DMS)
[AD-A206179] N89-24759

ATMOSPHERIC TURBULENCE
An investigation of the Overlap between the Statistical Discrete Gust and the Power Spectral Density analysis methods
[NASA-TM-101571] N89-24310

ATOMIC COLLISIONS
Electron transfer, ionization, and excitation in atomic collisions
[DE89-010046] N89-24891

ATOMIC STRUCTURE
Magneto-optical studies of metastable 3D-transition metal films
[DE89-009836] N89-24474
Semiempirical studies of atomic structure
[DE89-011419] N89-24894
On the nature of high-temperature superconductivity
[DE89-009525] N89-25053

ATTACK AIRCRAFT
The night and adverse weather capability of ground attack aircraft
[FOA-C-20745-2.5] N89-24312
Flight control system for the CRCA (Control Reconfigurable Combat Aircraft) using a command generator tracker with PI (Plus Integral) feedback and Kalman filter, volume 2
[AD-A206202] N89-24325
The use of seaplanes as an advanced weapon system
[AD-A206243] N89-24880

AUDITORY DEFECTS
The effects of blast trauma (impulse noise) on hearing: A parametric study
[AD-A206180] N89-24786

AUGER SPECTROSCOPY
Auger and ESCA analysis
[NASA-CR-183572] N89-24463

AURORAS
SPECTRUM: A computer algorithm to derive the flux-energy spectrum of precipitating particles from EISCAT electron density profiles
[IRF-TR-034] N89-24764
Cosmic linear accelerators N89-24915

AUSTENITIC STAINLESS STEELS
Investigations on the creep-rupture behavior of the austenitic stainless steel AISI 316-NET
[KFK-4468] N89-24479

AUTOMATED EN ROUTE ATC
Design of automated system for management of arrival traffic
[NASA-TM-102201] N89-24290
Controller evaluation of initial data link air traffic control services. Volume 1: Mini study 2
[DOT/FAA/CT-89/14-VOL-1] N89-24292

AUTOMATIC CONTROL
A comparison of detection efficiency on an air traffic control monitoring task with and without computer aiding
[AD-A206422] N89-24294
Space Station automation of common module power management and distribution
[NASA-CR-183607] N89-24434
Conference on Space and Military Applications of Automation and Robotics
[AD-A198095] N89-24819
An automated protein crystal growth facility on the space station N89-24820
Development of a man-portable control unit for a teleoperated land vehicle N89-24835
Automated Millimeter Wave (AMW) transducer testing in a robotic/vision test cell N89-24841
Research on self-generated stochastic motion
[AD-A206454] N89-24870

AUTOMATIC FLIGHT CONTROL
Optimal guidance with obstacle avoidance for nap-of-the-earth flight
[NASA-CR-177515] N89-24328

AUTOMATIC LANDING CONTROL
An operational demonstration and engineering flight test of the Microwave Landing System on runway 22L at Chicago's Midway Airport
[DOT/FAA/CT-TN88/42] N89-24291
B-737 flight test of curved-path and steep-angle approaches using MLS guidance
[NASA-TM-101521] N89-24293

AUTOMATION
Multiple robot approach for automation of in-orbit modules N89-24389

AUTONOMOUS NAVIGATION
Bordautonomous terrain aided flight navigation in height sections close to terrain surface N89-24301
Landscape-related position finding for flying systems N89-24302
The DARPA autonomous land vehicle: A phase 1 retrospective and a prospective for the future N89-24834
A robotic vehicle global route planner for the 1990s N89-24851
A demonstration of retro-traverse using a semi-autonomous land vehicle N89-24852

AUTONOMY
Tele-autonomous control involving contacts: The applications of a high precision laser line range sensor
[NASA-CR-184995] N89-24509

AVALANCHES
A longlife, highvoltage, shortpulse generator based on optically activated Bulk Avalanche Semiconductor Switch, phase 2
[AD-A206078] N89-24527

AXIAL FLOW TURBINES
Turbine rotor/stator flowfield analysis
[NASA-CR-183639] N89-24433

AXISYMMETRIC BODIES
Black hole driven winds N89-25096

AXISYMMETRIC FLOW
Experimental techniques in unsteady flows N89-24279
Analysis of the wake behind a propeller using the finite element method with a two-equation turbulence model N89-24286

B

B STARS
Speculation on the origin of X-ray emission in early-type stars N89-25029

BACKGROUND RADIATION
Gravitational angular fluctuations of the cosmic background radiation produced by cosmological linear perturbations
[DE88-757287] N89-25105

BACKSCATTERING
Backscattering spectra processing for the structure of multilayer samples
[DE88-706325] N89-24468
A hybrid asymptotic-modal analysis of the EM scattering by an open-ended S-shaped rectangular waveguide cavity
[NASA-CR-185053] N89-24519
Improvement and extension of a radar forest backscattering model
[NASA-CR-184975] N89-24686

BALLISTICS
The effects of supercritical fluids on high performance polymers
[AD-A206515] N89-24494

BANDWIDTH
The frequency response of phased-array antennas
[DE89-009710] N89-24517

BANGLADESH
Improvement and extension of a radar forest backscattering model
[NASA-CR-184975] N89-24686

BARIUM COMPOUNDS
Photothermal imaging of high T(sub c) superconductor [DE89-009644] N89-25054
X-ray photoelectron spectroscopy study of samples in the Y-Ba-Cu-O system [AD-A206260] N89-25060
BAROTROPIC FLOW
A numerical study of bifurcations in a barotropic shear flow N89-24542
BARRED GALAXIES
Bars and open spirals in density wave theory --- galaxies N89-24964
Gas flow in and around bars --- galaxies N89-24965
BARRELS (CONTAINERS)
Dynamics and static behavior of metal gussets in cask impact limiters [DE89-011879] N89-24683
BARYONS
A study of K sup deg sec, lambda and lambda bar production in 60 and 200 GeV nucleon OAu and pAu collisions with a streamer chamber detector at the CERN SPS [MPE-PAE/EXP.EL-198] N89-24900
BAYS (STRUCTURAL UNITS)
Shuttle payload bay thermal environments: Summary and conclusion report for STS Flights 1-5 [NASA-CR-185017] N89-24411
Space Station Freedom Structural Characterization Experiment (SCE) node code [NASA-TM-101594] N89-25110
BEAMS (RADIATION)
Analysis of the EM scattering from arbitrary open-ended waveguide cavities using axial Gaussian Beam tracking [NASA-CR-185054] N89-24518
Beam dynamics with the Hamilton-Jacobi equation [DE89-012269] N89-24878
Dynamics of gas-surface interactions [AD-A206210] N89-25059
BEAMS (SUPPORTS)
Improved analysis of laminated heterogeneous beams and associated formulation of a new finite element method N89-24672
BEARINGS
Solid lubricant materials for high temperatures: A review N89-24636
BELLOWS
Pressure-volume properties of metallic bellows [NASA-TM-100365] N89-24422
BENDING MOMENTS
Characterization of the bending stiffness of large space structure joints [NASA-TM-101565] N89-24676
BENZENE
Bonding and chemistry of hydrocarbon monolayers on metal surfaces [DE89-009311] N89-24490
BIBLIOGRAPHIES
Bibliography on tropical rain forests and the global carbon cycle. Volume 2: South Asia [DE89-008971] N89-24748
The climate of Finland: A bibliography with particular reference to applications updating part 1968-1985 [MP-10] N89-24768
BINARY ALLOYS
Amorphous metal alloys produced by mechanical alloying [DE89-011189] N89-24481
BIOLOGICAL EFFECTS
Characterizing the energy deposition events produced by trapped protons in low earth orbit [DE89-011218] N89-24893
BIRDS
Estimating population size of Pygoscelid Penguins from TM data [NASA-CR-180081] N89-24687
BLACK HOLES (ASTRONOMY)
Problem of nonrotating black hole accretion disk main energy release region extension N89-24951
Nonlinear oblique whistlers: Their relevance to nonthermal coupling of ions and electrons in accretion flow and supercritical quasi-perpendicular collisionless shocks --- black holes N89-24955
Self-consistent models of spherical accretion onto black holes N89-25095
Black hole driven winds N89-25098
BLADE TIPS
Interaction mechanisms between tip leakage flow and the passage vortex in a linear turbine rotor cascade [NAL-TR-983T] N89-24536
BLADE-VORTEX INTERACTION
Aerodynamic interaction between vortical wakes and lifting two-dimensional bodies [NASA-TM-101074] N89-24563
BLANKETS
Development of tailorable advanced blanket insulation for advanced space transportation systems [NASA-CR-177444] N89-24486
BLAST LOADS
Centrifugal modeling of underground structures subjected to blast loading [AD-A206424] N89-24675
BLUFF BODIES
Unsteady Aerodynamics, volume 1 [VKI-1988-07-VOL-1] N89-24276
Unsteady aerodynamic effects on bluff bodies N89-24278
BLUNT BODIES
Transpiration cooling of hypersonic blunt bodies with finite rate surface reactions [NASA-CR-177516] N89-24580
BOEING 737 AIRCRAFT
Calculation of aircraft noise in the vicinity of civil airports by a simultion procedure [MPIS-7/1988] N89-24887
BOLTZMANN DISTRIBUTION
The effect of non-Maxwellian electron distributions on the intensity ratio of resonance to satellite lines [DE89-006745] N89-24907
BONDING
A noncontacting scanning photoelectron emission technique for bonding surface cleanliness inspection [NASA-TM-100361] N89-24623
BOOSTER ROCKET ENGINES
Ariane 5 solid boosters: Overview of design approach and envisaged technologies N89-24352
BOUNDARY ELEMENT METHOD
On computational schemes for global-local stress analysis N89-24645
BOUNDARY LAYER CONTROL
Use of Navier-Stokes methods to predict circulation control airfoil performance [AD-A206242] N89-24270
BOUNDARY LAYER FLOW
Boundary layer response to an unsteady turbulent environment [AD-A206578] N89-24273
Inflow/outflow boundary conditions and global dynamics of spatial mixing layers N89-24540
BOUNDARY LAYER PLASMAS
Some dynamical properties of anisotropic collisionless stellar systems N89-24963
BOUNDARY LAYER SEPARATION
Unsteady and separated flows [AD-A206539] N89-24572
BOUNDARY LAYER TRANSITION
Boundary layer response to an unsteady turbulent environment [AD-A206578] N89-24273
A numerical study of bifurcations in a barotropic shear flow N89-24542
Turbulence characteristics inside a turbulent spot in plane Poiseuille flow N89-24554
Some characteristics of bypass transition in a heated boundary layer [NASA-TM-102126] N89-24577
BOUNDARY LAYERS
Analysis of the boundary layer of a delta wing in incidence [CERT-RT-OA-26/5025-AYD] N89-24274
The structure of sheared turbulence near a plane boundary N89-24557
Transpiration cooling of hypersonic blunt bodies with finite rate surface reactions [NASA-CR-177516] N89-24580
BOUNDARY LUBRICATION
Tribology: The Story of Lubrication and Wear [NASA-TM-101430] N89-24635
BOUNDARY VALUE PROBLEMS
Characterization of radiation boundary conditions used in the finite-difference time-domain method [DE89-005662] N89-24522
Global/local stress analysis of composite panels [NASA-TM-101622] N89-24681
BRANCHING (MATHEMATICS)
A numerical study of bifurcations in a barotropic shear flow N89-24542
BRAZIL
Microwave X-band radiometric characterization of Brazilian soils by measurement of the complex permittivity [INPE-4588-PRE/1319] N89-24685
BRAZING
Incorporation of surface tension into the structural finite element code SANCHO [DE89-011354] N89-24616
BREADBOARD MODELS
Space Station automation of common module power management and distribution [NASA-CR-183607] N89-24434
The 5-kW arcjet power electronics [NASA-TM-102108] N89-24446
BREMSSTRAHLUNG
The effect of non-Maxwellian electron distributions on the intensity ratio of resonance to satellite lines [DE89-006745] N89-24907
BROADBAND
Broadband electrostatic waves as a consequence of magnetotail reconnection N89-25017
BUBBLES
Analytic theory for the determination of velocity and stability of bubbles in a Hele-Shaw cell. Part 2: Stability [NASA-CR-181837] N89-24883
BUCKLING
Research in structures, structural dynamics and materials, 1989 [NASA-CP-10024] N89-24626
Nonlinear response of a blade-stiffened graphite-epoxy panel with a discontinuous stiffener: Work in progress N89-24641
Global-local methodologies and their application to nonlinear analysis N89-24647
BUFFETING
Computational and experimental research on buffet phenomena of transonic airfoils [NAL-TR-996T] N89-24322
BYPASS RATIO
Some characteristics of bypass transition in a heated boundary layer [NASA-TM-102126] N89-24577

C

CADMIUM TELLURIDES
Position-sensitive CdTe detector using improved crystal growth method [NASA-CR-183427] N89-25051
CALIBRATING
Systems for the sensitivity calibration of mass spectrometers in space flight [BONN-IR-88-32] N89-24428
Teledyne Taber 206-1000 and 2210-3000 pressure transducer proof test and burst test [NASA-CR-183672] N89-24594
Optoelectronic velocimeter development [DE89-012283] N89-24597
Modeling and characterization of the Earth Radiation Budget Experiment (ERBE) nonscanner and scanner sensors [NASA-CR-181818] N89-24772
CANTILEVER BEAMS
Characterization of delamination in advanced composite materials under mode 3 loading conditions [AD-A206159] N89-24452
Error analysis for semi-analytic displacement derivatives with respect to shape and sizing variables N89-24632
CARBON
The effect of heat input and composition on weld metal microstructures in thin section HY-130 GMAW weldments [AD-A206476] N89-24477
Physical conditions in molecular clouds derived from sub-mm and far-IR spectroscopic observations [MPE-PREPRINT-135] N89-25082
CARBON CYCLE
Bibliography on tropical rain forests and the global carbon cycle. Volume 2: South Asia [DE89-008971] N89-24748
CARBON DIOXIDE CONCENTRATION
Beyond CO2: The other greenhouse gases [DE89-011893] N89-24750
CARBON FIBERS
Thermoplastic coating of carbon fibers [NASA-CR-185047] N89-24488
CARBON MONOXIDE
Reactions of (eta 5-C5H5) (eta 5-C5Me5) Zr(Si(SiMe3)3)X (X = Cl, Me) complexes with carbon monoxide and the isocyanide 2,6 Me2C6H3NC. Crystal structure of (eta 5-C5H5) (eta 5-C5Me5)Zr(eta 2-C(N-2,6 Me2C6H3) Si(SiMe3)3)Cl [AD-A206494] N89-24493
Strong, spatially extended CO 7 to 6 emission from luminous cloud cores: W51 and DR21 [MPE-PREPRINT-133] N89-25106
CARBONACEOUS MATERIALS
Hydrogen ion-driven permeation in carbonaceous films [DE89-005271] N89-24485
CARBONIC ACID
Numerical study on laminar circular jet of carbonic acid gas discharging into stagnant air [DE88-757249] N89-24565
CARDIOVASCULAR SYSTEM
Neurochemical control of circadian rhythms [AD-A206213] N89-24788

CASCADE FLOW
Interaction mechanisms between tip leakage flow and the passage vortex in a linear turbine rotor cascade
[NAL-TR-983T] N89-24536
Three-dimensional flows and loss generation mechanisms in a linear turbine rotor cascade at various incidence conditions
[NAL-TR-984T] N89-24537
CASE HISTORIES
On designing a case-based system for expert process development N89-24847
CASSEGRAIN OPTICS
The 25 percent-efficient GaAs Cassegrainian concentrator cell N89-24733
CATALYSTS
A premixed hydrogen/oxygen catalytic igniter
[NASA-CR-185113] N89-24445
Transpiration cooling of hypersonic blunt bodies with finite rate surface reactions
[NASA-CR-177516] N89-24580
CATHODES
Explosive-emitter cathode produced using the heavy ion track technique
[DE88-706304] N89-24503
CAUCHY PROBLEM
The structure of the reconnection layer in the Petschek reconnection model: Theory and application to the earth's magnetopause N89-25026
CAUSES
On the causality of plasma permittivity
[NASA-TM-101551] N89-24514
CAVITIES
Analysis of the EM scattering from arbitrary open-ended waveguide cavities using axial Gaussian Beam tracking
[NASA-CR-185054] N89-24518
Cavity dimensions for high velocity penetration events: A comparison of calculational results with data
[DE89-011351] N89-24617
CAVITY RESONATORS
Development of a 75-watt 60-GHz traveling-wave tube for intersatellite communications
[NASA-CR-182135] N89-24530
CENTRAL ATLANTIC REGION (US)
Forecast of Atlantic seasonal hurricane activity for 1989 N89-24773
CENTRIFUGAL FORCE
Centrifugal modeling of underground structures subjected to blast loading
[AD-A206424] N89-24675
CERAMIC MATRIX COMPOSITES
Thermal shock strength of multiphase materials
[KFK-4469] N89-24455
Time dependent reliability model incorporating continuum damage mechanics for high-temperature ceramics
[NASA-TM-102046] N89-24487
CERAMICS
Thermal shock strength of multiphase materials
[KFK-4469] N89-24455
Analysis of packed-particle rearrangement during colloidal ceramic processing: Gamma-ray densitometry and a review of alternative methods
[DE89-009066] N89-24489
High-resolution electron microscopy of metal/ceramic interfaces
[DE89-012396] N89-24498
Ceramic Technology for Advanced Heat Engines Project data base
[DE89-012868] N89-24499
Ceramic technology for advanced heat engines project
[DE89-012890] N89-24500
Characterization of pore evolution in ceramics during creep failure and densification
[DE89-013599] N89-24502
Measurement of bond strength at metal/ceramic interfaces
[DE89-011638] N89-24682
X-ray investigations of ceramic high Tc superconductors under high pressure
[KFK-4482] N89-25064
CHANNEL FLOW
Dynamical interpretation of conditional patterns N89-24549
A genuinely multi-dimensional upwind cell-vertex scheme for the Euler equations
[NASA-TM-102029] N89-24872
CHANNELS (DATA TRANSMISSION)
An intelligent fiberoptic data bus for fly-by-light applications
[NAL-TM-SE-8707] N89-24901
CHAOS
Chaos in a spatially-developing plane mixing layer N89-24539
A numerical study of bifurcations in a barotropic shear flow N89-24542
Optical chaos
[DE89-009392] N89-24903
Adiabatic, chaotic and quasi-adiabatic charged particle motion in two-dimensional magnetic field reversals N89-24942
Chaotic radiopulsations and coronal magnetic field estimates N89-25006
CHARACTER RECOGNITION
The current technological status of spatial light modulators
[AD-A206328] N89-24905
CHARACTERIZATION
Modal reduction strategies for interconnected flexible bodies simulation N89-24665
CHARGE COUPLED DEVICES
Determination of reference trajectories for testing navigation aids using an onboard CCD camera N89-24303
Investigations on fully depletable charge coupled devices
[MPI-PAE/EXP.EL-194] N89-25063
CHARGE EXCHANGE
Charge exchange neutral sputtering in ASDEX N89-25044
Charge exchange transition probability for collisions between unlike ions and atoms within the adiabatic approximation
[NASA-TM-101559] N89-25104
CHARGED PARTICLES
Analytical consideration and calculation of electrostatical system by reverse method
[DE88-706319] N89-24885
Semiclassical matrix-elements of high-charge ions
[DE89-009258] N89-24890
CHEBYSHEV APPROXIMATION
The exact condition of the B-spline basis may be hard to determine
[AD-A204080] N89-24863
CHEMICAL ANALYSIS
Auger and ESCA analysis
[NASA-CR-183572] N89-24483
Mass spectrometry
[DE89-011118] N89-24471
Non-destructive analyses of cometary nucleus samples using synchrotron radiation
[DE89-012536] N89-25101
CHEMICAL ATTACK
Analysis of the plugging of the systems autonomy demonstration project brassboard filters
[NASA-CR-177533] N89-24450
CHEMICAL BONDS
Bonding and chemistry of hydrocarbon monolayers on metal surfaces
[DE89-009311] N89-24490
Measurement of bond strength at metal/ceramic interfaces
[DE89-011638] N89-24682
CHEMICAL COMPOSITION
Backscattering spectra processing for the structure of multilayer samples
[DE88-706325] N89-24468
CHEMICAL EVOLUTION
Effects of main-sequence mass loss on stellar and galactic chemical evolution
[DE89-011399] N89-25098
CHEMICAL REACTIONS
Increasing the chemical yield of desirable chemical species using solar rapid heating
[DE89-000881] N89-24469
Bonding and chemistry of hydrocarbon monolayers on metal surfaces
[DE89-009311] N89-24490
Analysis of homogeneous turbulent reacting flows N89-24558
Study of chemical reaction models for high enthalpy flow of air
[NAL-TR-982] N89-25072
CHINESE SPACE PROGRAM
China's future space activities N89-24342
CHIPS (ELECTRONICS)
A 3-D graphical simulation of an automated direct chip probe/test system N89-24848
A facilities view of the low volume, high product mix fab
[DE89-009970] N89-25057
CHLOROPHYLLS
The advanced Ocean Chlorophyll Meter (OCM). A spectral imaging device for the observation of the oceans
[REPT-882-440-118] N89-24689
The FLI airborne imaging spectrometer: A highly versatile sensor for many applications N89-24694
Development of an imaging spectrometer for remote sensing: The FLI program N89-24698
Imaging spectrometry at the Canada Centre for Remote Sensing N89-24701
Biooptical variability in the Greenland Sea observed with the Multispectral Airborne Radiometer System (MARS)
[NASA-CR-184856] N89-24784
CHROMOSPHERE
Singularities of the local MHD-resonances in solar chromosphere plasma N89-24927
Model of the chromosphere spicule formation N89-24966
CIRCADIAN RHYTHMS
Neurochemical control of circadian rhythms
[AD-A206213] N89-24788
CIRCUIT BOARDS
Natural convection cooling of a 3 by 3 array of rectangular protrusions in an enclosure filled with dielectric liquid: Effects of boundary conditions and component orientation
[AD-A206474] N89-24571
CIRCULAR CYLINDERS
Computation of the characteristics of the wake past an oscillating cylinder N89-24283
Adaptive methods, rolling contact, and nonclassical friction laws N89-24651
CIRCULATION CONTROL AIRFOILS
Use of Navier-Stokes methods to predict circulation control airfoil performance
[AD-A206242] N89-24270
CIRCUMFERENCES
Self-circumference in the Minkowski plane
[AD-A205691] N89-24868
CLASSICAL MECHANICS
CSM testbed development and large-scale structural applications
[NASA-TM-4072] N89-24624
A weak Hamiltonian finite element method for optimal control problems
[NASA-CR-185336] N89-24873
CLASSIFICATIONS
The climate of Finland: A bibliography with particular reference to applications updating part 1968-1985
[MP-10] N89-24768
CLEAN ROOMS
A facilities view of the low volume, high product mix fab
[DE89-009970] N89-25057
CLEANING
A noncontacting scanning photoelectron emission technique for bonding surface cleanliness inspection
[NASA-TM-100361] N89-24623
CLIMATE
Orographically-caused microclimate variation in the Saariselka Region
[ISBN-9-5169-7269-1] N89-24767
The climate of Finland: A bibliography with particular reference to applications updating part 1968-1985
[MP-10] N89-24768
The relationship between intraseasonal disturbance activity and interannual variation of the tropical atmosphere N89-24774
Climatic atlas of the outer continental shelf waters and coastal regions of Alaska. Volume 3: Chukchi-Beaufort Sea
[AD-A206525] N89-24776
Simplified climate models: Rationale and design
[DE89-012291] N89-24783
CLIMATOLOGY
The importance of climatological variability and the rate at which waste is added to modeling water budget of landfills
[DE89-008917] N89-24747
Climatic atlas of the outer continental shelf waters and coastal regions of Alaska. Volume 3: Chukchi-Beaufort Sea
[AD-A206525] N89-24776
The radiation-atmosphere interaction model and the determination of meteorological and climatological parameters from satellite observations
[ETN-89-94535] N89-24779
Contribution to the study of the diurnal cycle of convective clouds over tropical Africa from satellite imagery
[ETN-89-94537] N89-24780
Study of representativity of the wind fields deduced from geostationary satellite images. Attribution of height to wind vectors and large scale average fields deduced from water vapor imagery
[ETN-89-94538] N89-24781
CLOCKS
Formal verification of a fault tolerant clock synchronization algorithm
[NASA-CR-4239] N89-24803
CLOUD COVER
Refinements in the cloud detection scheme of the 3i system. Comparison with AVHRR products
[ETN-89-94531] N89-24691

CLOUD PHOTOGRAPHY
Water vapor retrievals through the 3I (improved Initialization Inversion) system: Application to tropospheric altimetry correction
[ETN-89-94534] N89-24778
CLOUD PHYSICS
The formation of interstellar clouds N89-24935
CLOUDS (METEOROLOGY)
Refinements in the cloud detection scheme of the 3I system. Comparison with AVHRR products
[ETN-89-94531] N89-24691
CLUSTER ANALYSIS
A methodology for commonality analysis, with applications to selected space station systems
[NASA-TM-100364] N89-24421
CLUTTER
Ground cluster filters for staggered pulse trains
[DOT/FAA/SA-89/2] N89-24515
COANDA EFFECT
Use of Navier-Stokes methods to predict circulation control airfoil performance
[AD-A206242] N89-24270
COASTAL WATER
Climatic atlas of the outer continental shelf waters and coastal regions of Alaska. Volume 3: Chukchi-Beaufort Sea
[AD-A206525] N89-24776
COATINGS
Combined microstructure X-ray optics
[DE89-009902] N89-24904
COCHLEA
Auditory speech preprocessors
[DE89-009280] N89-24516
COCKPITS
Display of flight guidance information in the aircraft cockpit N89-24305
Cerebral laterality and handedness in aviation: Performance and selection implications
[AD-A206196] N89-24787
CODING
Investigation of vector quantization for the coding gray scale images for Group 4 facsimile
[AD-A206548] N89-24809
COGNITION
Evaluation, description and invention: Paradigms for human-computer interaction
[AD-A204617] N89-24796
COHERENT RADIATION
Cooperative phenomena for new coherent radiation sources
[AD-A206368] N89-24602
COLLISIONAL PLASMAS
Magnetic reconnection simulation using the 2.5 D electromagnetic direct implicit code AVANTI N89-24984
COLLISIONLESS PLASMAS
The structure of quasiperpendicular collisionless shocks N89-24932
The role of whistler oscillations in the formation of the structure of high Mach number collisionless shock N89-24936
Quasi-perpendicular collisionless high Mach number shocks N89-24937
Some dynamical properties of anisotropic collisionless stellar systems N89-24963
Reconnection instability in collisionless plasma N89-24978
Kinetic simulation of magnetic reconnection in the presence of shear N89-24985
Particle simulation of magnetic reconnection in collision-free plasma sheets N89-24986
COLLISIONS
Piezoelectric film load cell robot collision detector
[DE89-010117] N89-24592
COLLOCATION
Influence of time lag and noncolocation on integrated structural/control system designs N89-24630
COLLOIDS
Analysis of packed-particle rearrangement during colloidal ceramic processing: Gamma-ray densitometry and a review of alternative methods
[DE89-009066] N89-24489
COLOR VISION
Field-dependence and judgment of weight and color revisited: Some implications for the study of sensory discrimination
[AD-A206141] N89-24791
COLUMBUS SPACE STATION
The Ariane 5 Development Program N89-24336
Columbus: The European contribution to the International Space Station N89-24337
The European in-orbit infrastructure ground segment N89-24340
Pressurized module element for man's presence in space --- Columbus N89-24343
French national policy on the preparation of Columbus utilization N89-24344
MTFF user interfaces N89-24345
Microgravity payloads (APM and MTFF) N89-24347
Space science using Columbus: Manned space science N89-24348
ECLS for Columbus and Hermes N89-24354
Flight operations concept for the European in-orbit infrastructure N89-24356
Hermes-MTFF rendezvous strategy and composite operations N89-24357
Timelining and operations integration concerning APM and MTFF N89-24358
Servicing of the MTFF by Hermes N89-24360
MTFF flight operations phases N89-24361
Manned interventions at the MTFF: Crew workload aspects N89-24362
Logistics aspects of Columbus servicing at the Space Station N89-24363
System safety from D-missions to Columbus N89-24367
Columbus safety and reliability N89-24368
Attached Pressurized Module (APM) center for the Columbus attached pressurized module N89-24377
The key role of Data Relay System (DRS) in the Columbus communications N89-24379
Scientific utilization of the European space infrastructure and the International Space Station N89-24380
Experimentation in the Man Tended Free Flyer (MTFF) N89-24381
MARS Microgravity Advanced Research and Support Center N89-24395
Crew training aspects --- Hermes, Columbus N89-24396
The Columbus crew communication subsystem and the on board local area network N89-24397
The utilization of the European pressurized module for non-European experiments --- Columbus N89-24399
The astronaut's functions aboard Columbus N89-24403
COMBUSTION CHAMBERS
Liquid oxygen cooling of hydrocarbon fueled rocket thrust chambers
[NASA-TM-102113] N89-24447
A remote laser-probing system for combustion measurements
[NAL-TR-979] N89-24598
Role of sulfur oxides in wear and deposit formation in Army diesel engines
[AD-A206054] N89-24613
COMBUSTION EFFICIENCY
Calculation of scramjet performance
[NAL-TR-987] N89-24317
COMBUSTION PRODUCTS
Role of sulfur oxides in wear and deposit formation in Army diesel engines
[AD-A206054] N89-24613
COMBUSTION TEMPERATURE
A remote laser-probing system for combustion measurements
[NAL-TR-979] N89-24598
COMET NUCLEI
The variable nature of the comet-solar wind interaction N89-25100
Non-destructive analyses of cometary nucleus samples using synchrotron radiation
[DE89-012536] N89-25101
COMETARY ATMOSPHERES
Theoretical studies of important processes in planetary and comet atmospheres. Renewel request
[NASA-CR-184951] N89-25099
COMETS
The variable nature of the comet-solar wind interaction N89-25100
COMMONALITY
A methodology for commonality analysis, with applications to selected space station systems
[NASA-TM-100364] N89-24421
Space Station Freedom electrical power system hardware commonality with the United States Polar Platform
[NASA-TM-102074] N89-24439
COMPACT GALAXIES
COS-B gamma-ray sources beyond the predicted diffuse emission
[MPE-PREPRINT-136] N89-25107
COMPACTING
Shock compaction of superconductors
[DE89-006744] N89-25052
COMPARISON
ERC nickel cadium battery performance tests and comparisons with lead-acid batteries
[DE89-009753] N89-24535
COMPOSITE MATERIALS
Technology of aircraft construction (selected chapters)
[AD-A199946] N89-24261
Response of layered structures to thermal radiation pulses
[AD-A206355] N89-24453
Impact and penetration resistance of fibrous composites
[AD-A206417] N89-24454
Study of damage in composite materials
[ONERA-RT-4/7256-RY-070-R] N89-24458
Experimentation and analysis of compression test methods for single filament high performance fibres
[AD-A206358] N89-24467
COMPOSITE STRUCTURES
Characterization of delamination in advanced composite materials under mode 3 loading conditions
[AD-A206159] N89-24452
Research in structures, structural dynamics and materials, 1989
[NASA-CP-10024] N89-24626
A study of composite plates with holes/inclusions N89-24627
Computational procedures for postbuckling of composite shells N89-24642
Some comments on global-local analyses N89-24644
Global-local methodologies and their application to nonlinear analysis N89-24647
Features and characterization needs of rubber composite structures N89-24649
Improved analysis of laminated heterogeneous beams and associated formulation of a new finite element method N89-24672
COMPRESSIBLE FLOW
Use of Navier-Stokes methods to predict circulation control airfoil performance
[AD-A206242] N89-24270
Comparison of compressible and incompressible models of reconnection N89-24982
COMPRESSION TESTS
Experimentation and analysis of compression test methods for single filament high performance fibres
[AD-A206358] N89-24467
COMPRESSOR EFFICIENCY
Efficiency study of oil cooling of a screw compressor
[DE89-011417] N89-24618
COMPUTATION
CSM testbed development and large-scale structural applications
[NASA-TM-4072] N89-24624
Computational Methods for Structural Mechanics and Dynamics, part 1
[NASA-CP-3034-PT-1] N89-24638
COMPUTATIONAL CHEMISTRY
Numerical aerodynamic simulation
[NASA-EP-262] N89-24262
COMPUTATIONAL FLUID DYNAMICS
Numerical aerodynamic simulation
[NASA-EP-262] N89-24262
Unsteady Aerodynamics, volume 1
[VKI-1988-07-VOL-1] N89-24276
Unsteady Aerodynamics, volume 2
[VKI-1988-07-VOL-2] N89-24281
Numerical methods for unsteady flows N89-24282
Computation of the characteristics of the wake past an oscillating cylinder N89-24283
Computational unsteady aerodynamics for lifting surfaces N89-24284
A zonal method for modeling powered-lift aircraft flow fields
[NASA-CR-177521] N89-24287
Computational and experimental research on buffet phenomena of transonic airfoils
[NAL-TR-996T] N89-24322
Navier-Stokes analysis of cold scramjet-afterbody flows
[NASA-CR-184949] N89-24562
Aerodynamic interaction between vortical wakes and lifting two-dimensional bodies
[NASA-TM-101074] N89-24563
Numerical study of turbulent secondary flows in curved ducts
[NASA-CR-181830] N89-24568
Nonlinear evolution of interacting oblique waves on two-dimensional shear layers
[NASA-TM-102030] N89-24575
Inlet turbulence intensity level and cross-stream distribution effects on the heat transfer in plane wall jets
[NASA-CR-183652] N89-24576
Domain decomposition algorithms and computation fluid dynamics
[NASA-CR-185405] N89-24578
On the dynamic response of pressure transmission lines in the research of helium-charged free piston Stirling engines
[NASA-TM-102121] N89-24593
Totally parallel multilevel algorithms
[NASA-CR-185404] N89-24818

A genuinely multi-dimensional upwind cell-vertex scheme for the Euler equations
[NASA-TM-102029] N89-24872

COMPUTATIONAL GRIDS
Conservative treatment of boundary interfaces for overlaid grids and multi-level grid adaptations
[NASA-TM-102060] N89-24269
Domain decomposition algorithms and computation fluid dynamics
[NASA-CR-185405] N89-24578
An algebraic homotopy method for generating quasi-three-dimensional grids for high-speed configurations
[NASA-CR-4242] N89-24581
A second-order projection method for the incompressible Navier Stokes equations on quadrilateral grids
[DE89-010242] N89-24585
Totally parallel multilevel algorithms
[NASA-CR-185404] N89-24818
Surface grid generation for composite block grids N89-24874

COMPUTER AIDED DESIGN
Fluidnet: A thermal and hydraulic software for the preliminary sizing of fluid loop systems
[REPT-882-440-124] N89-24425
Channel and switchbox routing using a greedy based channel algorithm with outward scanning technique
[AD-A206545] N89-24528
Computerized structural mechanics for 1990's: Advanced aircraft needs N89-24640
Application and implementation of transient algorithms in computer programs N89-24659
Large-scale structural analysis: The structural analyst, the CSM Testbed and the NAS System
[NASA-TM-100643] N89-24673
XCAD: A CAD object-oriented virtual solid modeler for an expert system shell
[REPT-882-440-125] N89-24810
Development of an integrated CAD/CAM system for wire harness fabrication N89-24842

COMPUTER AIDED MANUFACTURING
Computerized structural mechanics for 1990's: Advanced aircraft needs N89-24640
The 64K 16-bit word buffer memory with microprogrammable control
[DE88-706303] N89-24799
A systolic array structure for on-line system identification
[AD-A206412] N89-24806
Development of an integrated CAD/CAM system for wire harness fabrication N89-24842

COMPUTER GRAPHICS
Application and implementation of transient algorithms in computer programs N89-24659
How to (and not to) introduce computer graphics to design professionals
[DE89-010374] N89-24812

COMPUTER PROGRAMMING
Flight control system for the CRCA (Control Reconfigurable Combat Aircraft) using a command generator tracker with PI (Plus Integral) feedback and Kalman filter, volume 2
[AD-A206202] N89-24325
A review of some problems in global-local stress analysis N89-24643
Evaluation, description and invention: Paradigms for human-computer interaction
[AD-A204617] N89-24796
Transformational derivation of programs using the Focus system
[NASA-CR-184875] N89-24802

COMPUTER PROGRAMS
Flight control system for the CRCA (Control Reconfigurable Combat Aircraft) using a command generator tracker with PI (Plus Integral) feedback and Kalman filter, volume 2
[AD-A206202] N89-24325
A numerical study of chemically reacting flow in nozzles
[NASA-TM-102135] N89-24444
Cavity dimensions for high velocity penetration events: A comparison of calculational results with data
[DE89-011351] N89-24617
Local stiffener and skin pocket buckling prediction by special PASCO modeling technique: Correlation to test data N89-24628
Modeling the missile-launch tube problem in DYSCO N89-24629
Some issues in numerical simulation of nonlinear structural response N89-24639
A review of some problems in global-local stress analysis N89-24643
Transient analysis techniques in performing impact and crash dynamic studies N89-24658
Recent developments in deployment analysis simulation using a multi-body computer code N89-24660
Advances in dual methods and convex approximations for structural optimization N89-24680
WADA1: FORTRAN program for wave diffraction analysis, version 1
[AD-A206533] N89-24808
Application of Lotus 1-2-3 to heat transfer analysis
[DE89-010463] N89-24813
The Fault Tree Compiler (FTC): Program and mathematics
[NASA-TP-2915] N89-24815
Using a simulation assistant in modeling manufacturing systems N89-24849
Empirical analysis and refinement of expert system knowledge bases
[AD-A206226] N89-24858

COMPUTER STORAGE DEVICES
The 64K 16-bit word buffer memory with microprogrammable control
[DE88-706303] N89-24799

COMPUTER SYSTEMS PERFORMANCE
High speed implementation of NAL application software packages
[NAL-TR-986] N89-24801
Formal verification of AI software
[NASA-CR-181827] N89-24811
Predeployment validation of fault-tolerant systems through software-implemented fault insertion
[NASA-CR-4244] N89-24817

COMPUTER SYSTEMS PROGRAMS
Diverter AI based decision aid, phases 1 and 2
[NASA-CR-181820] N89-24316
The development of a Job-Jobstep scheduler for NS system
[NAL-TR-977] N89-24814

COMPUTER TECHNIQUES
A comparison of detection efficiency on an air traffic control monitoring task with and without computer aiding
[AD-A206422] N89-24294
The concept of telescience N89-24384
Channel and switchbox routing using a greedy based channel algorithm with outward scanning technique
[AD-A206545] N89-24528
The electronic supervisor: New technology, new tensions
[OTA-CIT-333] N89-24804
The Fault Tree Compiler (FTC): Program and mathematics
[NASA-TP-2915] N89-24815
Fractional-order feedback in linear systems
[AD-A206241] N89-24859
NASA information sciences and human factors program
[NASA-TM-4126] N89-25111

COMPUTER VISION
Stabilized image system for mobile robots N89-24829
Robotic visual servo control for aircraft ground refueling N89-24836
Robot assembly of microscopic component in millimeter wave devices N89-24840
Automated Millimeter Wave (AMW) transducer testing in a robotic/vision test cell N89-24841

COMPUTERIZED SIMULATION
Numerical aerodynamic simulation
[NASA-EP-262] N89-24262
An investigation of V/STOL jet interactions in a crossflow
[AD-A206360] N89-24272
A computer simulation study of liquid water content adjustment based on icing cloud horizontal extent
[DOT/FAA/CT-TN89/3] N89-24288
A model for prediction of STOVL ejector dynamics
[NASA-TM-102098] N89-24319
Autonomous geostationary stationkeeping system optimization and validation
[REPT-882-440-117] N89-24423
Space Shuttle Main Engine High Pressure Fuel Turbopump turbine blade cracking
[NASA-TM-100327] N89-24435
Space Shuttle Main Engine structural analysis and data reduction/evaluation. Volume 6: Primary nozzle diffuser analysis
[NASA-CR-183669] N89-24437
Modeling transient thermal behavior in a thrust vector control jet vane
[AD-A206532] N89-24441
Backscattering spectra processing for the structure of multilayer samples
[DE88-706325] N89-24468
On specimen shape effects and the ductility of porous metals
[AD-A206216] N89-24475
Computer simulation of copper in the liquid phase and the sputtering of liquid copper by one KeV argon ions
[AD-A206264] N89-24476
Methane to methanol conversion
[DE89-011194] N89-24504
AR (Autoregressive) modeling of coherence in time delay and doppler estimation
[AD-A205239] N89-24513
A second-order projection method for the incompressible Navier Stokes equations on quadrilateral grids
[DE89-010242] N89-24585
Atmospheric effects on laser propagation
[DE89-012287] N89-24606
Comparison of predicted and measured temperatures of UH-60A helicopter transmission
[NASA-TP-2911] N89-24607
Cavity dimensions for high velocity penetration events: A comparison of calculational results with data
[DE89-011351] N89-24617
Computational Methods for Structural Mechanics and Dynamics, part 1
[NASA-CP-3034-PT-1] N89-24638
Some issues in numerical simulation of nonlinear structural response N89-24639
Computational procedures for postbuckling of composite shells N89-24642
Adaptive methods, rolling contact, and nonclassical friction laws N89-24651
Exploiting symmetries in the modeling and analysis of tires N89-24653
Computational Methods for Structural Mechanics and Dynamics
[NASA-CP-3034-PT-2] N89-24654
Improving transient analysis technology for aircraft structures N89-24655
Transient analysis techniques in performing impact and crash dynamic studies N89-24658
Recent developments in deployment analysis simulation using a multi-body computer code N89-24660
Dynamic analysis of space structures including elastic, multibody, and control behavior N89-24661
Modal reduction strategies for interconnected flexible bodies simulation N89-24665
Computational aspects of multibody dynamics N89-24666
Improvement and extension of a radar forest backscattering model
[NASA-CR-184975] N89-24686
Control research in windpower project 506259 utilization
[FOA-C-20746-2.7] N89-24740
NASA Lewis Stirling engine computer code evaluation
[NASA-CR-182248] N89-24741
High speed implementation of NAL application software packages
[NAL-TR-986] N89-24801
Neutral file data exchange between simulators and robots N89-24824
Development of a hybrid simulator for robotic manipulators N89-24831
A generalized method for automatic downhand and wirefeed control of a welding robot and positioner N89-24846
A 3-D graphical simulation of an automated direct chip probe/test system N89-24848
Using a simulation assistant in modeling manufacturing systems N89-24849
Beam dynamics with the Hamilton-Jacobi equation
[DE89-012269] N89-24878
Hard X-ray imaging telescope development
[DE89-011647] N89-24906
Magnetic reconnection simulation using the 2.5 D electromagnetic direct implicit code AVANTI N89-24984
Kinetic simulation of magnetic reconnection in the presence of shear N89-24985
ASDEX edge and divertor simulation and the problem of incomplete and inaccurate experimental data N89-25041
Grain boundary phase equilibria in metallic systems
[DE89-011787] N89-25066

CONCENTRATION (COMPOSITION)
The relationship between in-lake sulfate concentration and estimates of atmospheric sulfur deposition for subregions of the eastern lake survey
[DE89-009868] N89-24749

CONCENTRATORS
Predicted performance of InP solar cells in Cassegrainian and slats space concentrator arrays at 20 to 100 AM0, 80 to 100 C N89-24711
Domed Fresnel lens concentrator technology for space application N89-24732
The 25 percent-efficient GaAs Cassegrainian concentrator cell N89-24733
The experiments of LIPS 3 N89-24735

CONCURRENT PROCESSING
Unconditionally stable concurrent procedures for transient finite-element analysis N89-24657
CONFERENCES
Unsteady Aerodynamics, volume 2 [VKI-1988-07-VOL-2] N89-24281
Image Signal Processing for Flight Guidance [DFVLR-MITT-88-32] N89-24295
International Symposium on Europe in Space: The Manned Space System [ESA-SP-277] N89-24335
Research in structures, structural dynamics and materials, 1989 [NASA-CP-10024] N89-24626
Tribology: The Story of Lubrication and Wear [NASA-TM-101430] N89-24635
Computational Methods for Structural Mechanics and Dynamics, part 1 [NASA-CP-3034-PT-1] N89-24638
Computational Methods for Structural Mechanics and Dynamics [NASA-CP-3034-PT-2] N89-24654
Imaging Spectrometry for Land Applications [ESA-SP-1101] N89-24692
Space Photovoltaic Research and Technology, 1988. High Efficiency, Space Environment, and Array Technology [NASA-CP-3030] N89-24704
Human Factors in Automated and Robotic Space Systems: Proceedings of a symposium. Part 1 [NASA-CR-182495] N89-24792
Human Factors in Automated and Robotic Space Systems: Proceedings of a symposium. Part 2 [NASA-CR-182496] N89-24794
Conference on Space and Military Applications of Automation and Robotics [AD-A198095] N89-24819
Proceedings of an International School and Workshop on Plasma Astrophysics, volume 1 [ESA-SP-285-VOL-1] N89-24910
Proceedings of an International School and Workshop on Reconnection in Space Plasma, volume 2 [ESA-SP-285-VOL-2] N89-24974
FOM-Rijnhuizen contributions to the Fifteenth Symposium on Fusion Technology [REPT-88-179] N89-25030
ASDEX Contributions to the 8th International Conference on Plasma Surface Interaction in Controlled Fusion Devices [IPP-III/139] N89-25038
CONFINEMENT
Study of particle confinement in the JT-60 tokamak using skin radiative approximation model [DE88-756574] N89-24909
CONICAL BODIES
Thermal radiation from plumes of solid propellant rockets [NAL-TR-990] N89-24432
CONNECTORS
Diffusion welding of electrical interconnects to silicon solar cells [DE89-012250] N89-24620
CONSTITUTIVE EQUATIONS
A study of material damping in large space structures [NASA-CR-180076] N89-24634
CONSTRAINTS
Constraint elimination in dynamical systems N89-24667
CONTACT LOADS
Contact solution algorithms N89-24652
CONTAINERLESS MELTS
Containerless glass fiber processing [NASA-TM-86540] N89-24405
CONTAMINATION
A noncontacting scanning photoelectron emission technique for bonding surface cleanliness inspection [NASA-TM-100361] N89-24623
Contamination effects study [NASA-CR-183613] N89-24746
CONTINUOUS RADIATION
Inductive megahertz beam position monitors for CEBAF [CEBAF-PR-89-003] N89-24895
CONTINUUM MECHANICS
Time dependent reliability model incorporating continuum damage mechanics for high-temperature ceramics [NASA-TM-102046] N89-24487
Features and characterization needs of rubber composite structures N89-24649
CONTOURS
Surface grid generation for composite block grids N89-24874
CONTRAROTATING PROPELLERS
Advanced turboprop aircraft flyover noise: Annoyance to counter-rotating-propeller configurations with a different number of blades on each rotor: Preliminary results [NASA-TM-100638] N89-24888
CONTRAST
Field-dependence and judgment of weight and color revisited: Some implications for the study of sensory discrimination [AD-A206141] N89-24791
CONTROL CONFIGURED VEHICLES
Flight control system for the CRCA (Control Reconfigurable Combat Aircraft) using a command generator tracker with PI (Plus Integral) feedback and Kalman filter, volume 2 [AD-A206202] N89-24325
CONTROL EQUIPMENT
Control research in windpower project 506259 utilization [FOA-C-20746-2.7] N89-24740
CONTROL SIMULATION
Investigation of vector quantization for the coding gray scale images for Group 4 facsimile [AD-A206548] N89-24809
CONTROL STABILITY
Results of an A109 simulation validation and handling qualities study [NASA-TM-101062] N89-24323
CONTROL SURFACES
Wind tunnel tests on flutter control of a high-aspect-ratio cantilevered wing [NAL-TR-978] N89-24321
CONTROL SYSTEMS DESIGN
Design of automated system for management of arrival traffic [NASA-TM-102201] N89-24290
Aeroservoelastic modeling and applications using minimum-state approximations of the unsteady aerodynamics [NASA-TM-101574] N89-24308
Aeroservoelastic wind-tunnel investigations using the Active Flexible Wing Model: Status and recent accomplishments [NASA-TM-101570] N89-24313
Recent activities within the Aeroservoelasticity Branch at the NASA Langley Research Center [NASA-TM-101582] N89-24314
Development and flight test experiences with a flight-crucial digital control system [NASA-TP-2857] N89-24327
Hierarchically structured control for intelligent robots in space N89-24393
Space Station automation of common module power management and distribution [NASA-CR-183607] N89-24434
Further developments in modeling digital control systems with MA-prefiltered measurements [NASA-TP-2909] N89-24507
Objective and constraint functions for the analysis and design of robust control systems N89-24615
Research in structures, structural dynamics and materials, 1989 [NASA-CP-10024] N89-24626
Influence of time lag and noncolocation on integrated structural/control system designs N89-24630
Control research in windpower project 506259 utilization [FOA-C-20746-2.7] N89-24740
Development of a hybrid simulator for robotic manipulators N89-24831
Ground control of space based robotic systems N89-24845
The control and monitoring system of RTP --- Rijnhuizen Tokamak PETULA (RTP) N89-25037
CONTROL THEORY
On the dynamics and control of the Spacecraft Control Laboratory Experiment (SCOLE) class of offset flexible systems N89-24426
Real time control for NASA robotic gripper [NASA-CR-184978] N89-24608
Dynamic analysis of space structures including elastic, multibody, and control behavior N89-24661
Application of finite-element methods to dynamic analysis of flexible spatial and co-planar linkage systems, part 2 N89-24663
NASA information sciences and human factors program [NASA-TM-4126] N89-25111
CONTROL UNITS (COMPUTERS)
Unsteady and separated flows [AD-A206539] N89-24572
CONTROLLABILITY
Results of an A109 simulation validation and handling qualities study [NASA-TM-101062] N89-24323
CONTROLLERS
Technology transfer: Imaging tracker to robotic controller N89-24828
A generalized method for automatic downhand and wirefeed control of a welding robot and positioner N89-24846
An analytical study of a vibration test method using extremal control of acceleration and force [DE89-007428] N89-24884
CONVECTION
A second-order projection method for the incompressible Navier Stokes equations on quadrilateral grids [DE89-010242] N89-24585
CONVECTION CLOUDS
Contribution to the study of the diurnal cycle of convective clouds over tropical Africa from satellite imagery [ETN-89-94537] N89-24780
CONVECTIVE FLOW
A genuinely multi-dimensional upwind cell-vertex scheme for the Euler equations [NASA-TM-102029] N89-24872
CONVECTIVE HEAT TRANSFER
Natural convection cooling of a 3 by 3 array of rectangular protrusions in an enclosure filled with dielectric liquid: Effects of boundary conditions and component orientation [AD-A206474] N89-24571
CONVERGENT-DIVERGENT NOZZLES
A numerical study of chemically reacting flow in nozzles [NASA-TM-102135] N89-24444
CONVOLUTION INTEGRALS
Two dimensional convolute integer technology for digital image processing N89-24830
COOLING
Shuttle payload bay thermal environments: Summary and conclusion report for STS Flights 1-5 [NASA-CR-185017] N89-24411
COOLING SYSTEMS
Efficiency study of oil cooling of a screw compressor [DE89-011417] N89-24618
Developing, testing, evaluating and optimizing solar heating and cooling systems [DE89-011831] N89-24744
COORDINATES
Surface coordinate generation in three-dimensional arbitrary shapes by solving a set of second order elliptic partial differential equations N89-24875
COPLANARITY
Application of finite-element methods to dynamic analysis of flexible spatial and co-planar linkage systems, part 2 N89-24663
COPPER
Computer simulation of copper in the liquid phase and the sputtering of liquid copper by one KeV argon ions [AD-A206264] N89-24476
Development of tandem cells consisting of GaAs single crystal and CuInSe2/CdZnS polycrystalline thin films N89-24717
CORDAGE
Features and characterization needs of rubber composite structures N89-24649
CORONAL LOOPS
Kink modes in coronal loops N89-24925
Coronal heating by resonant absorption in resistive MHD N89-24926
On the MHD stability of the M=1 kink mode in finite length coronal loops N89-24992
COSMIC DUST
The variable nature of the comet-solar wind interaction N89-25100
COSMIC PLASMA
Proceedings of an International School and Workshop on Plasma Astrophysics, volume 1 [ESA-SP-285-VOL-1] N89-24910
Astrophysical significance of observations and experiments in the earth's magnetosphere N89-24912
Cosmic linear accelerators N89-24915
The formation of the spectrum of inhomogeneity of the dark matter in pregalactic cosmic plasma N89-24968
COSMIC RAYS
Computer simulations of cosmic-ray diffusion near supernova remnant shock waves N89-24916
Cosmic rays: A short survey of open problems N89-24940
Radiative-resonant MHD interactions between waves and particles and the problem of cosmic-ray spectra N89-24944
Gravitational angular fluctuations of the cosmic background radiation produced by cosmological linear perturbations [DE88-757287] N89-25105
High energy particles in supernova remnants and the interstellar medium N89-25108

COSMIC X RAYS
Generation of X-ray and radio emission by binary Wolf-Rayet stars N89-24929
COSMOLOGY
Proceedings of an International School and Workshop on Plasma Astrophysics, volume 1 [ESA-SP-285-VOL-1] N89-24910
Development of astrophysics from the telescope to the Sputnik N89-24911
The formation of the spectrum of inhomogeneity of the dark matter in pregalactic cosmic plasma N89-24968
Gravitational angular fluctuations of the cosmic background radiation produced by cosmological linear perturbations [DE88-757287] N89-25105
COST ANALYSIS
A methodology for commonality analysis, with applications to selected space station systems [NASA-TM-100364] N89-24421
Study on cost efficiency of product assurance in space programs [REPT-882-440-122] N89-24622
The human role in space (THURIS) applications study. Final briefing [NASA-CR-183590] N89-24793
The human role in space (THURIS) applications study. Volume 2: Research analysis and technology report [NASA-CR-183589] N89-24795
COST EFFECTIVENESS
Improving transient analysis technology for aircraft structures N89-24655
The human role in space (THURIS) applications study. Final briefing [NASA-CR-183590] N89-24793
The human role in space (THURIS) applications study. Volume 2: Research analysis and technology report [NASA-CR-183589] N89-24795
COST REDUCTION
A methodology for commonality analysis, with applications to selected space station systems [NASA-TM-100364] N89-24421
The electronic supervisor: New technology, new tensions [OTA-CIT-333] N89-24804
COSTS
The impact of solar cell technology on planar solar array performance N89-24715
CRACK CLOSURE
Results of the Round Robin on opening-load measurement conducted by ASTM Task Group E24.04.04 on Crack Closure Measurement and Analysis [NASA-TM-101601] N89-24679
CRACK INITIATION
Space Shuttle Main Engine High Pressure Fuel Turbopump turbine blade cracking [NASA-TM-100327] N89-24435
Results of the Round Robin on opening-load measurement conducted by ASTM Task Group E24.04.04 on Crack Closure Measurement and Analysis [NASA-TM-101601] N89-24679
CRACK OPENING DISPLACEMENT
Equations of motion for viscoelastic moving crack problems N89-24670
Microscopic delamination processes and the resulting crack tip strain fields of graphite/epoxy composites N89-24671
Results of the Round Robin on opening-load measurement conducted by ASTM Task Group E24.04.04 on Crack Closure Measurement and Analysis [NASA-TM-101601] N89-24679
CRACK PROPAGATION
Study of damage in composite materials [ONERA-RT-4/7256-RY-070-R] N89-24458
Research on the mechanism of thermal fatigue in near-eutectic Pb-Sn solders [DE89-011430] N89-24482
Acoustic emission from a growing crack N89-24633
Equations of motion for viscoelastic moving crack problems N89-24670
Results of the Round Robin on opening-load measurement conducted by ASTM Task Group E24.04.04 on Crack Closure Measurement and Analysis [NASA-TM-101601] N89-24679
Measurement of bond strength at metal/ceramic interfaces [DE89-011638] N89-24682
CRACK TIPS
Microscopic delamination processes and the resulting crack tip strain fields of graphite/epoxy composites N89-24671
Analysis of interlaminar fracture in composites under combined loading [NASA-CR-185055] N89-24674
CRACKING (FRACTURING)
Space Shuttle Main Engine High Pressure Fuel Turbopump turbine blade cracking [NASA-TM-100327] N89-24435
CRACKS
Equations of motion for viscoelastic moving crack problems N89-24670
CRASH LANDING
Transient analysis techniques in performing impact and crash dynamic studies N89-24658
CRASHWORTHINESS
Transient analysis techniques in performing impact and crash dynamic studies N89-24658
CRATERING
Comparative planetology of early intense cratering and other cratering effects [NASA-CR-182966] N89-24752
CRAY COMPUTERS
Attaching IBM-compatible 3380 disks to Cray X-MP [DE89-012383] N89-24800
CREEP PROPERTIES
Characterization of pore evolution in ceramics during creep failure and densification [DE89-013599] N89-24502
CREEP RUPTURE STRENGTH
Investigations on the creep-rupture behavior of the austenitic stainless steel AISI 316-NET [KFK-4468] N89-24479
CREW PROCEDURES (INFLIGHT)
Advanced MMI and image handling to support crew activities N89-24392
Lessons learned from SL-1 and D-1 --- Spacelab N89-24400
Hermes crew role N89-24401
The astronaut's functions aboard Columbus N89-24403
CREW WORKSTATIONS
EVA Information System: A modern workstation in space N89-24388
Advanced MMI and image handling to support crew activities N89-24392
CRITICAL TEMPERATURE
X-ray photoelectron spectroscopy study of samples in the Y-Ba-Cu-O system [AD-A206260] N89-25060
CROSS FLOW
An investigation of V/STOL jet interactions in a crossflow [AD-A206360] N89-24272
CRYOGENIC EQUIPMENT
State of the art of ISO [REPT-882-440-121] N89-24424
ISOCAM, ISO optical subsystem cryogenics, Aerospatiale, Cannes, France in-house R and D status [REPT-882-440-123] N89-24429
Materials for cryogenically cooled infrared telescopes [REPT-882-440-119] N89-25083
CRYOGENIC TEMPERATURE
Development of the cryopanel for tests of xenon ion thrusters [NAL-TR-981] N89-24431
CRYOPUMPING
Development of the cryopanel for tests of xenon ion thrusters [NAL-TR-981] N89-24431
CRYSTAL GROWTH
Proceedings of the Goddard Space Flight Center Workshop on Robotics for Commercial Microelectronic Processes in Space [NASA-TM-101233] N89-24505
Position-sensitive CdTe detector using improved crystal growth method [NASA-CR-183427] N89-25051
CRYSTAL STRUCTURE
Fundamental studies on order effects in metal alloys [ONERA-RT-14/221-M] N89-24480
Reactions of (eta 5-C5H5) (eta 5-C5Me5) Zr(Si(SiMe3)3)X (X = Cl, Me) complexes with carbon monoxide and the isocyanide 2,6 Me2C6H3NC. Crystal structure of (eta 5-C5H5) (eta 5-C5Me5)Zr(eta 2-C(N-2,6 Me2C6H3) Si(SiMe3)3)Cl [AD-A206494] N89-24493
Correlation between the structure, energy, and local elastic properties of grain boundaries in metals [DE89-009861] N89-25055
The effects of gradients on boundary stability [DE89-011590] N89-25065
High resolution electron microscopy of interfaces in topotaxial and epitaxial reactions [DE89-010390] N89-25070
CRYSTALLIZATION
Amorphous metal alloys produced by mechanical alloying [DE89-011189] N89-24481
CURRENT SHEETS
A neutral current sheet with flows: Tearing and stratification modes and modeling of coronal structures N89-24991
Dynamic development of coronal current sheets N89-24994
Flare-type plasma processes and explosive disruption of pinch current sheets N89-25008
Current sheet structure at different stages of magnetic reconnection N89-25009
Impulsive heating plasma turbulence and magnetic reconnection inside current sheets N89-25010
Spontaneous and forged reconnection in a magnetic type-X structure N89-25012
Electromagnetic electron temperature anisotropy instability in the earth's magnetotail plasma sheet N89-25019
CURVE FITTING
Local corner cutting and the smoothness of the limiting curve [AD-A204092] N89-24864
CYCLOGENESIS
Forecast of Atlantic seasonal hurricane activity for 1989 N89-24773
Study of explosive and nonexplosive cyclogenesis during FGGE [AD-A206521] N89-24775
CYCLONES
Study of explosive and nonexplosive cyclogenesis during FGGE [AD-A206521] N89-24775
CYCLOTRON RADIATION
Quantum relativistic theory of the cyclotron radiation in a strongly magnetized plasma with anisotropic temperature --- neutron stars N89-24962
CYLINDRICAL BODIES
Basic flow field and heat transfer studies about three cylinders of different diameter in transverse flow N89-24564

D

DAMAGE
Study of damage in composite materials [ONERA-RT-4/7256-RY-070-R] N89-24458
A study of material damping in large space structures [NASA-CR-180076] N89-24634
DAMAGE ASSESSMENT
KSC ice/frost/debris assessment for Space Shuttle Mission STS-30R [NASA-TM-102147] N89-24412
DAMPING
A study of material damping in large space structures [NASA-CR-180076] N89-24634
Development of higher-order modal methods for transient thermal and structural analysis [NASA-TM-101548] N89-24677
DARK MATTER
The formation of the spectrum of inhomogeneity of the dark matter in pregalactic cosmic plasma N89-24968
DATA ACQUISITION
Voyager at Neptune: 1989 [NASA-CR-185317] N89-24420
Control and data acquisition system for the neutral beam probe diagnostic on TEXTOR N89-25036
Research and technology, 1988 [NASA-TM-101246] N89-25109
DATA BASE MANAGEMENT SYSTEMS
On the future development and management of spectroscopic database for radiative transfer from the issues of recent related workshops [ETN-89-94530] N89-24690
UNIX-based data management system for the Mobile Satellite Propagation Experiment (PiFEx) [NASA-CR-185023] N89-25073
DATA BASES
Ceramic Technology for Advanced Heat Engines Project data base [DE89-012888] N89-24499
On the future development and management of spectroscopic database for radiative transfer from the issues of recent related workshops [ETN-89-94530] N89-24690
Photovoltaic advanced research and development project: Solar radiation research [DE89-000884] N89-24743
Empirical analysis and refinement of expert system knowledge bases [AD-A206226] N89-24858
The AAMRL (Armstrong Aerospace Medical Research Laboratory) biodynamics data bank [AD-A206139] N89-25074

DATA LINKS
Controller evaluation of initial data link air traffic control services. Volume 1: Mini study 2
[DOT/FAA/CT-89/14-VOL-1] N89-24292
DATA MANAGEMENT
The computational structural mechanics testbed architecture. Volume 5: The Input-Output Manager DMGASP
[NASA-CR-178388] N89-24637
UNIX-based data management system for the Mobile Satellite Propagation Experiment (PiFEx)
[NASA-CR-185023] N89-25073
DATA PROCESSING
Improvements in the Global Reference Atmospheric Model and comparisons with a global 3-D numerical model
[NASA-CR-184947] N89-24755
Analysis and use of VAS satellite data
[NASA-CR-4218] N89-24770
Dynamic spectral analysis in finite field algebras
[DE88-706333] N89-24877
Efficient estimator of parameters and goodness-of-fit test of multivariate distributions for data presented by one-dimensional histograms
[DE88-706318] N89-24879
NASA information sciences and human factors program
[NASA-TM-4126] N89-25111
DATA REDUCTION
Space Shuttle Main Engine structural analysis and data reduction/evaluation. Volume 6: Primary nozzle diffuser analysis
[NASA-CR-183669] N89-24437
Modeling and characterization of the Earth Radiation Budget Experiment (ERBE) nonscanner and scanner sensors
[NASA-CR-181818] N89-24772
DATA STORAGE
The AAMRL (Armstrong Aerospace Medical Research Laboratory) biodynamics data bank
[AD-A206139] N89-25074
DATA STRUCTURES
High speed implementation of NAL application software packages
[NAL-TR-986] N89-24801
DATA TRANSMISSION
Neutral file data exchange between simulators and robots N89-24824
DAYTIME
Multiple X line reconnection at the dayside magnetopause N89-25022
DEBRIS
KSC ice/frost/debris assessment for Space Shuttle Mission STS-30R
[NASA-TM-102147] N89-24412
DECISION MAKING
Simplified climate models: Rationale and design
[DE89-012291] N89-24783
The electronic supervisor: New technology, new tensions
[OTA-CIT-333] N89-24804
Real-time system: Specification and verification
[AD-A206467] N89-24807
On designing a case-based system for expert process development N89-24847
Algorithm for display of automated nondestructive thickness measurements N89-24850
DEEP WATER
WADA1: FORTRAN program for wave diffraction analysis, version 1
[AD-A206533] N89-24808
DEFORMATION
Incorporation of surface tension into the structural finite element code SANCHO
[DE89-011354] N89-24616
Dynamics of articulated structures N89-24664
Plate motions and deformations from geologic and geodetic data
[NASA-CR-184987] N89-24757
DEGRADATION
Contamination effects of GPS Navstar solar array performance N89-24734
A comparison of the radiation tolerance characteristics of multijunction solar cells with series and voltage-matched configurations N89-24737
DEHYDRATION
Solute model or cellular energy model: Practical and theoretical aspects of thirst during exercise
[AD-A206143] N89-24785
Is salt at fault
[AD-A206518] N89-24789
DEICERS
Preliminary airworthiness evaluation of modified second-generation Pneumatic Boot Deicing System on a JUH-1H
[AD-A206255] N89-24289
DELAMINATING
Characterization of delamination in advanced composite materials under mode 3 loading conditions
[AD-A206159] N89-24452
Microscopic delamination processes and the resulting crack tip strain fields of graphite/epoxy composites N89-24671
Analysis of interlaminar fracture in composites under combined loading
[NASA-CR-185055] N89-24674
DELINEATION
A study of the Southern Supercluster N89-25088
DELTA WINGS
Analysis of the boundary layer of a delta wing in incidence
[CERT-RT-OA-26/5025-AYD] N89-24274
DEMULTIPLEXING
Microprocessor based 32 channel PCM telemetry system
[NAL-TM-SE-8704] N89-24414
DENSIFICATION
Characterization of pore evolution in ceramics during creep failure and densification
[DE89-013599] N89-24502
Shock compaction of superconductors
[DE89-006744] N89-25052
DENSITOMETERS
Analysis of packed-particle rearrangement during colloidal ceramic processing: Gamma-ray densitometry and a review of alternative methods
[DE89-009066] N89-24489
DENSITY DISTRIBUTION
Shock-associated plasma density fluctuations in the interstellar medium N89-24933
DEPLOYMENT
Recent developments in deployment analysis simulation using a multi-body computer code N89-24660
DEPOSITION
The relationship between in-lake sulfate concentration and estimates of atmospheric sulfur deposition for subregions of the eastern lake survey
[DE89-009868] N89-24749
Self-consistent models of spherical accretion onto black holes N89-25095
DEPOSITS
Role of sulfur oxides in wear and deposit formation in Army diesel engines
[AD-A206054] N89-24613
DESIGN ANALYSIS
Superfluid Helium Tanker Study (SFHT)
[NASA-CR-172114] N89-24415
Review of the environmental effects of the Space Station Freedom photovoltaic power module
[NASA-TM-102076] N89-24418
A methodology for commonality analysis, with applications to selected space station systems
[NASA-TM-100364] N89-24421
Composite Blade Structural Analyzer (COBSTRAN) demonstration manual
[NASA-TM-101957] N89-24459
Multidisciplinary optimization for engineering systems: Achievements and potential
[NASA-TM-101566] N89-24508
Modelling and design of high performance indium phosphide solar cells N89-24712
Dual-arm robots for telerobotic IVA operations on the space station N89-24822
A system for high resolution 3D mapping using laser radar and requiring no beam scanning mechanisms N89-24827
Orbital Maneuvering Vehicle (OMV) remote servicing kit N89-24838
ORU guidelines for telerobotic compatibility N89-24844
DETECTION
Free radical-surface interactions using multiphoton ionization of free radicals
[AD-A206257] N89-24892
DETERMINANTS
Research on self-generated stochastic motion
[AD-A206454] N89-24870
DEUTERIUM
Hydrogen ion-driven permeation in carbonaceous films
[DE89-005271] N89-24485
DIELECTRIC PROPERTIES
Development and utilization of new diagnostics for dense-phase pneumatic transport
[DE89-011381] N89-24583
DIELECTRICS
Explosive-emitter cathode produced using the heavy ion track technique
[DE88-706304] N89-24503
Electrophoretically applied dielectrics for amorphous metal foils used in pulsed power saturable reactors
[DE89-009322] N89-24525
Natural convection cooling of a 3 by 3 array of rectangular protrusions in an enclosure filled with dielectric liquid: Effects of boundary conditions and component orientation
[AD-A206474] N89-24571
DIESEL ENGINES
Role of sulfur oxides in wear and deposit formation in Army diesel engines
[AD-A206054] N89-24613
DIESEL FUELS
Role of sulfur oxides in wear and deposit formation in Army diesel engines
[AD-A206054] N89-24613
DIETS
Is salt at fault
[AD-A206518] N89-24789
DIFFERENTIAL EQUATIONS
Numerical integration of asymptotic solutions of ordinary differential equations
[NASA-TM-100650] N89-24867
DIFFRACTION
Combined microstructure X-ray optics
[DE89-009902] N89-24904
Multiphoton transitions at the Moessbauer radiation diffraction in crystals under a weak ultrasonic field
[DE88-706341] N89-25069
DIFFUSION
A second-order projection method for the incompressible Navier Stokes equations on quadrilateral grids
[DE89-010242] N89-24585
Encapsulated diffusion of sulphur into InP N89-24714
Research on self-generated stochastic motion
[AD-A206454] N89-24870
The effects of gradients on boundary stability
[DE89-011590] N89-25065
DIFFUSION WELDING
Diffusion welding of electrical interconnects to silicon solar cells
[DE89-012250] N89-24620
DIGITAL COMMAND SYSTEMS
Recent activities within the Aeroservoelasticity Branch at the NASA Langley Research Center
[NASA-TM-101582] N89-24314
DIGITAL FILTERS
Further developments in modeling digital control systems with MA-prefiltered measurements
[NASA-TP-2909] N89-24507
DIGITAL SIMULATION
Studying Turbulence Using Numerical Simulation Databases, 2. Proceedings of the 1988 Summer Program
[NASA-CR-184905] N89-24538
Chaos in a spatially-developing plane mixing layer N89-24539
Inflow/outflow boundary conditions and global dynamics of spatial mixing layers N89-24540
Phase decorrelation, streamwise vortices and acoustic radiation in mixing layers N89-24541
Dynamics of coherent structures in a plane mixing layer N89-24543
Subharmonic resonance in a mixing layer N89-24544
Scalar entrainment in the mixing layer N89-24545
Use of passive scalar tagging for the study of coherent structures in the plane mixing layer N89-24546
Sensitivity of mixing layers to three-dimensional forcing N89-24547
Sampling inhomogeneous turbulent fields N89-24548
Multifractal spectra in homogeneous shear flow N89-24552
Energy transfer in isotropic turbulence at low Reynolds numbers N89-24553
Eddies, streams, and convergence zones in turbulent flows N89-24555
Analysis of homogeneous turbulent reacting flows N89-24558
Cut-and-connect of two antiparallel vortex tubes N89-24559
Hardware modeling with VHDL (VHSIC Hardware Description Language) simulation
[AD-A206356] N89-24805
DIGITAL SYSTEMS
Development and flight test experiences with a flight-crucial digital control system
[NASA-TP-2857] N89-24327
Further developments in modeling digital control systems with MA-prefiltered measurements
[NASA-TP-2909] N89-24507
Hardware modeling with VHDL (VHSIC Hardware Description Language) simulation
[AD-A206356] N89-24805
DIGITAL TECHNIQUES
Two dimensional convolute integer technology for digital image processing N89-24830

DIGITAL TELEVISION
Protection of VHF international distress frequencies from harmonic radiation due to digital television equipment
[BBC-RD-1989/1] N89-24512
DIMENSIONAL ANALYSIS
Two dimensional analysis of a NOVETTE laser generated stress-impulse experiment
[DE89-009909] N89-24600
DIMENSIONLESS NUMBERS
Dimensionless parameters for classifying solar wind interactions N89-24914
DIODES
Improved defect analysis of Gallium Arsenide solar cells using image enhancement N89-24726
DIRAC EQUATION
Factorization of the relativistic Pauli equation in the presence of a gravitational field
[DE88-704749] N89-25090
DIRECT LIFT CONTROLS
Use of Navier-Stokes methods to predict circulation control airfoil performance
[AD-A206242] N89-24270
DIRECTIONAL STABILITY
Loss of tail rotor effectiveness evaluation of the OH-58C helicopter with directional SAS (Stability Augmentation System)
[AD-A206181] N89-24309
DISCONNECT DEVICES
Disconnects for spacecraft servicing applications N89-24832
DISILICIDES
Research on high-efficiency, single-junction, monolithic, thin-film amorphous silicon solar cells, phase 2
[DE89-000649] N89-24703
DISPERSING
Development of an engineering methodology for applying foam technology
[DE89-000740] N89-24497
DISPLACEMENT
Investigations of a displacement-estimation technique for aerial video scenes N89-24299
Study of a parametric displacement estimation scheme with application in aerial images N89-24300
Research in structures, structural dynamics and materials, 1989
[NASA-CP-10024] N89-24626
Integrated optimization of nonlinear R/C frames with reliability constraints N89-24631
Error analysis for semi-analytic displacement derivatives with respect to shape and sizing variables N89-24632
Dynamics of articulated structures N89-24664
Improved analysis of laminated heterogeneous beams and associated formulation of a new finite element method N89-24672
DISPLACEMENT MEASUREMENT
Results of the Round Robin on opening-load measurement conducted by ASTM Task Group E24.04.04 on Crack Closure Measurement and Analysis
[NASA-TM-101601] N89-24679
DISPLAY DEVICES
A comparison of detection efficiency on an air traffic control monitoring task with and without computer aiding
[AD-A206422] N89-24294
Display of flight guidance information in the aircraft cockpit N89-24305
Display-based communications for advanced transport aircraft
[NASA-TM-102187] N89-24798
DISSOCIATION
introduction to dissociative recombination
[NASA-CR-184950] N89-24889
DISTRIBUTED PROCESSING
Large-scale structural analysis: The structural analyst, the CSM Testbed and the NAS System
[NASA-TM-100643] N89-24673
Predeployment validation of fault-tolerant systems through software-implemented fault insertion
[NASA-CR-4244] N89-24817
DIURNAL VARIATIONS
Contribution to the study of the diurnal cycle of convective clouds over tropical Africa from satellite imagery
[ETN-89-94537] N89-24780
DIVERTERS
Comparison of recycling in the ASDEX divertor before and after hardening N89-25042
Measurements of the flux of metallic impurities to the ASDEX divertor plates N89-25046
Material transport at the vessel walls of the divertor tokamak ASDEX N89-25047
DOPPLER EFFECT
AR (Autoregressive) modeling of coherence in time delay and doppler estimation
[AD-A205239] N89-24513
DOPPLER RADAR
Efficient dealiasing of Doppler velocities using local environment constraints
[DOT/FAA/SA-89/1] N89-24771
DRAG REDUCTION
Computational design of low aspect ratio wing-winglet configurations for transonic wind-tunnel tests
[NASA-CR-185016] N89-24266
DUCT GEOMETRY
Numerical study of turbulent secondary flows in curved ducts
[NASA-CR-181830] N89-24568
DUCTILITY
On specimen shape effects and the ductility of porous metals
[AD-A206216] N89-24475
DUCTS
Turbulent flow in a 180 deg bend: Modeling and computations
[NASA-CR-4141] N89-24579
DYNAMIC CHARACTERISTICS
A discussion on using Lanczos vectors and Ritz vectors for computing dynamic responses
[DE89-012322] N89-24684
Dynamic spectral analysis in finite field algebras
[DE88-706333] N89-24877
DYNAMIC LOADS
Dynamics and static behavior of metal gussets in cask impact limiters
[DE89-011879] N89-24683
A discussion on using Lanczos vectors and Ritz vectors for computing dynamic responses
[DE89-012322] N89-24684
DYNAMIC MODELS
Recent developments in deployment analysis simulation using a multi-body computer code N89-24660
Dynamics of flexible multi-body mechanisms and manipulators. Part 1: An overview N89-24662
Application of finite-element methods to dynamic analysis of flexible spatial and co-planar linkage systems, part 2 N89-24663
Modal reduction strategies for interconnected flexible bodies simulation N89-24665
Computational aspects of multibody dynamics N89-24666
Modeling and characterization of the Earth Radiation Budget Experiment (ERBE) nonscanner and scanner sensors
[NASA-CR-181818] N89-24772
DYNAMIC RESPONSE
On the dynamic response of pressure transmission lines in the research of helium-charged free piston Stirling engines
[NASA-TM-102121] N89-24593
Nonlinear characteristics of joints as elements of multi-body dynamic systems N89-24668
DYNAMIC STABILITY
Results of a parametric aeroelastic stability analysis of a generic X-wing aircraft
[NASA-TM-101572] N89-24324
On the dynamics and control of the Spacecraft Control Laboratory Experiment (SCOLE) class of offset flexible systems N89-24426
Prediction methods for dynamic stability parameters: Effects of angular stability
[IMFL-88/18] N89-24573
DYNAMIC STRUCTURAL ANALYSIS
Survey of Army/NASA rotorcraft aeroelastic stability research
[NASA-TM-101026] N89-24329
Research in structures, structural dynamics and materials, 1989
[NASA-CP-10024] N89-24626
Modeling the missile-launch tube problem in DYSCO N89-24629
Some issues in numerical simulation of nonlinear structural response N89-24639
Nonlinear response of a blade-stiffened graphite-epoxy panel with a discontinuous stiffener: Work in progress N89-24641
Computational Methods for Structural Mechanics and Dynamics
[NASA-CP-3034-PT-2] N89-24654
Improving transient analysis technology for aircraft structures N89-24655
Dynamic analysis of space structures including elastic, multibody, and control behavior N89-24661
Application of finite-element methods to dynamic analysis of flexible spatial and co-planar linkage systems, part 2 N89-24663
Investigation of structural behavior of candidate Space Station structure
[NASA-CR-181746] N89-24678
DYNAMICAL SYSTEMS
Constraint elimination in dynamical systems N89-24667
A weak Hamiltonian finite element method for optimal control problems
[NASA-CR-185336] N89-24873
Beam dynamics with the Hamilton-Jacobi equation
[DE89-012269] N89-24878
Some dynamical properties of anisotropic collisionless stellar systems N89-24963
DYNAMO THEORY
Generation of large-scale vortices in compressible helical turbulence N89-24969

E

EARTH ALBEDO
Correlation between satellite-derived aerosol characteristics and oceanic dimethylsulfide (DMS)
[AD-A206179] N89-24759
EARTH ATMOSPHERE
A visiting scientist program in atmospheric sciences for the Goddard Space Flight Center
[NASA-CR-183421] N89-24756
EARTH CRUST
Laser ranging data analysis
[NASA-CR-184847] N89-24754
EARTH GRAVITATION
Time variations in the earth's gravity field from Starlette orbit analysis N89-24766
EARTH IONOSPHERE
Plasma and propagation in auroral and polar ionosphere
[ETN-89-94519] N89-24761
EARTH MAGNETOSPHERE
Astrophysical significance of observations and experiments in the earth's magnetosphere N89-24912
Relation between global and local aspects of reconnection --- magnetic fields N89-24976
An analogy between magnetospheric substorms and solar flares: New version N89-25016
A 2-D and 3-D simulation study of multiple X line reconnection N89-25023
EARTH OBSERVATIONS (FROM SPACE)
ESA's planned activities in the field of imaging spectrometry for Earth observation N89-24693
EARTH OBSERVING SYSTEM (EOS)
Imaging Spectrometry for Land Applications
[ESA-SP-1101] N89-24692
HIRIS: NASA's high-resolution imaging spectrometer for the Earth Observing System (EOS) N89-24695
EARTH ORBITAL ENVIRONMENTS
Review of the environmental effects of the Space Station Freedom photovoltaic power module
[NASA-TM-102076] N89-24418
An atomic oxygen generation facility for space environmental testings
[NAL-TR-989] N89-24506
EARTH ORBITS
Characterizing the energy deposition events produced by trapped protons in low earth orbit
[DE89-011218] N89-24893
EARTH ORIENTATION
Laser ranging data analysis
[NASA-CR-184847] N89-24754
EARTH RADIATION BUDGET EXPERIMENT
Estimating the outgoing longwave radiation from the Meteosat infrared window and water vapor bands
[ETN-89-94533] N89-24762
Modeling and characterization of the Earth Radiation Budget Experiment (ERBE) nonscanner and scanner sensors
[NASA-CR-181818] N89-24772
EARTH ROTATION
Determination of station coordinates, earth rotation and plate motions from LAGEOS laser ranging: 1983-1986
[NAL-TR-980T] N89-24753
EARTH TIDES
Time variations in the earth's gravity field from Starlette orbit analysis N89-24766
EARTHQUAKES
A discussion on using Lanczos vectors and Ritz vectors for computing dynamic responses
[DE89-012322] N89-24684
ECONOMIC ANALYSIS
A methodology for commonality analysis, with applications to selected space station systems
[NASA-TM-100364] N89-24421
ECONOMIC DEVELOPMENT
Putting technology to work: Examples of industry-laboratory cooperation contributing to our nation's economic strength
[PB89-134654] N89-25077
ECOSYSTEMS
Estimating population size of Pygoscelid Penguins from TM data
[NASA-CR-180081] N89-24687

EDUCATION
How to (and not to) introduce computer graphics to design professionals
[DE89-010374] N89-24812
Pedagogical issues in developing a man-machine interface for an intelligent tutoring system N89-24855
EIKONAL EQUATION
Kaon-nucleus scattering
[NASA-TP-2920] N89-25103
EJECTORS
Transient flow thrust prediction for an ejector propulsion concept
[NASA-TM-102078] N89-24318
A model for prediction of STOVL ejector dynamics
[NASA-TM-102098] N89-24319
An experimental study of a three-dimensional thrust augmenting ejector using laser Doppler velocimetry
[NASA-CR-177531] N89-24569
EL NINO
The relationship between intraseasonal disturbance activity and interannual variation of the tropical atmosphere N89-24774
ELASTIC PROPERTIES
Acoustic emission from a growing crack N89-24633
Correlation between the structure, energy, and local elastic properties of grain boundaries in metals
[DE89-009861] N89-25055
ELASTIC SCATTERING
Backscattering spectra processing for the structure of multilayer samples
[DE88-706325] N89-24468
Beam guiding system for Rutherford scattering diagnostic at TEXTOR N89-25033
ELASTOMERS
Experimentation and analysis of compression test methods for single filament high performance fibres
[AD-A206358] N89-24467
ELASTOPLASTICITY
Bonded assemblies behavior laws: Light alloys/elastoplastic adhesive
[ETCA-88-R-001] N89-24456
ELECTRIC BRIDGES
The 5-kW arcjet power electronics
[NASA-TM-102108] N89-24446
ELECTRIC CONDUCTORS
Embedded conductors by electrochemical planarization
[DE89-011632] N89-24534
ELECTRIC CONTACTS
Diffusion welding of electrical interconnects to silicon solar cells
[DE89-012250] N89-24620
Theoretical microcontact spectra of metal electron-phonon coupling
[DE88-706280] N89-25067
ELECTRIC CURRENT
AM0 efficiency measurements N89-24736
ELECTRIC EQUIPMENT TESTS
A 3-D graphical simulation of an automated direct chip probe/test system N89-24848
ELECTRIC FIELDS
MEQALAC: A 1 MeV multi-channel RF-accelerator for light ions N89-25034
The role of the radial electric field in enhanced confinement regimes in stellarators
[DE89-011572] N89-25049
ELECTRIC FURNACES
Containerless glass fiber processing
[NASA-TM-86540] N89-24405
ELECTRIC POTENTIAL
Modelling and design of high performance indium phosphide solar cells N89-24712
AM0 efficiency measurements N89-24736
Analytical consideration and calculation of electrostatical system by reverse method
[DE88-706319] N89-24885
ELECTRIC POWER PLANTS
Technology requirements for advanced NASA missions N89-24705
ELECTRIC POWER SUPPLIES
Space Station Freedom electrical power system hardware commonality with the United States Polar Platform
[NASA-TM-102074] N89-24439
ELECTRICAL FAULTS
Engineering design of the interaction waveguide for high-power accelerator-driven microwave free-electron lasers
[DE89-011896] N89-24605
ELECTRICAL IMPEDANCE
Analysis of a probe-metallic sleeve feed system for a rectangular waveguide
[DE89-006769] N89-24523
ELECTRICAL MEASUREMENT
AM0 efficiency measurements N89-24736
ELECTRICAL PROPERTIES
Optimisation of the figure of merit of modified silicon-germanium alloys
[AD-A206420] N89-24491
ELECTRICAL RESISTIVITY
Theoretical microcontact spectra of metal electron-phonon coupling
[DE88-706280] N89-25067
ELECTRO-OPTICS
Establishment of an electron beam lithography facility
[AD-A206215] N89-24332
Electrooptical feed and control in microwave applications
[FOA-C-30514-3.2] N89-24531
Optoelectronic velocimeter development
[DE89-012283] N89-24597
Investigation of high efficiency GaAs solar cells N89-24724
ELECTROCHEMISTRY
Fractional-order feedback in linear systems
[AD-A206241] N89-24859
ELECTRODES
Analytical consideration and calculation of electrostatical system by reverse method
[DE88-706319] N89-24885
ELECTROLYTES
Analysis of the plugging of the systems autonomy demonstration project brassboard filters
[NASA-CR-177533] N89-24450
Is salt at fault
[AD-A206518] N89-24789
ELECTROMAGNETIC ABSORPTION
Design of the optical system for a new time-resolved X-ray absorption spectroscopy apparatus
[DE88-757253] N89-24902
ELECTROMAGNETIC COMPATIBILITY
Protection of VHF international distress frequencies from harmonic radiation due to digital television equipment
[BBC-RD-1989/1] N89-24512
ELECTROMAGNETIC COUPLING
Nonlinear oblique whistlers: Their relevance to nonthermal coupling of ions and electrons in accretion flow and supercritical quasi-perpendicular collisionless shocks --- black holes N89-24955
ELECTROMAGNETIC FIELDS
Analysis of a probe-metallic sleeve feed system for a rectangular waveguide
[DE89-006769] N89-24523
ELECTROMAGNETIC RADIATION
The frequency response of phased-array antennas
[DE89-009710] N89-24517
Characterization of radiation boundary conditions used in the finite-difference time-domain method
[DE89-005662] N89-24522
Dynamics of gas-surface interactions
[AD-A206210] N89-25059
ELECTROMAGNETIC SCATTERING
Analysis of the EM scattering from arbitrary open-ended waveguide cavities using axial Gaussian Beam tracking
[NASA-CR-185054] N89-24518
A hybrid asymptotic-modal analysis of the EM scattering by an open-ended S-shaped rectangular waveguide cavity
[NASA-CR-185053] N89-24519
ELECTROMAGNETIC WAVE TRANSMISSION
A hybrid asymptotic-modal analysis of the EM scattering by an open-ended S-shaped rectangular waveguide cavity
[NASA-CR-185053] N89-24519
ELECTRON ACCELERATION
Extended coronal shock waves and electron acceleration during solar flares N89-24934
ELECTRON BEAMS
Establishment of an electron beam lithography facility
[AD-A206215] N89-24332
Inductive megahertz beam position monitors for CEBAF
[CEBAF-PR-89-003] N89-24895
The electron beam instability revisited: Growth above and below f sub p N89-24917
The role of cold electrons in the generation of the high-frequency part of broadband electrostatic noise --- magnetotail N89-25018
ELECTRON CAPTURE
Multiplexed electronically programmable multimode ionization detector for chromatography
[DE89-009758] N89-24465
ELECTRON CYCLOTRON HEATING
Elliptical polarization for ECRH on RTP --- Rijnhuizen Tokamak PETULA (RTP) N89-25035
ELECTRON DENSITY (CONCENTRATION)
ASDEX Contributions to the 8th International Conference on Plasma Surface Interaction in Controlled Fusion Devices
[IPP-III/139] N89-25038
Characterization of the ASDEX scrape-off-layer density profile during neutral beam heating N89-25040
Plasma induced changes of a metallic divertor neutralizer plate from ASDEX analyzed by photoacoustics N89-25048
ELECTRON DENSITY PROFILES
SPECTRUM: A computer algorithm to derive the flux-energy spectrum of precipitating particles from EISCAT electron density profiles
[IRF-TR-034] N89-24764
ELECTRON DISTRIBUTION
Global kinetic theory of astrophysical jets N89-24954
ELECTRON EMISSION
Explosive-emitter cathode produced using the heavy ion track technique
[DE88-706304] N89-24503
ELECTRON ENERGY
Electromagnetic electron temperature anisotropy instability in the earth's magnetotail plasma sheet N89-25019
ELECTRON GUNS
The 280 GHz Gyro-BWO design study
[DE89-011644] N89-24595
ELECTRON IRRADIATION
Deep levels and radiation effects in p-InP N89-24713
Response of single junction GaAs/GaAs and GaAs/Ge solar cells to multiple doses of 1 MeV electrons N89-24722
ELECTRON MICROSCOPY
High-resolution electron microscopy of metal/ceramic interfaces
[DE89-012396] N89-24498
High resolution electron microscopy of interfaces in topotaxial and epitaxial reactions
[DE89-010390] N89-25070
ELECTRON PHONON INTERACTIONS
Dynamics of gas-surface interactions
[AD-A206210] N89-25059
Theoretical microcontact spectra of metal electron-phonon coupling
[DE88-706280] N89-25067
ELECTRON PLASMA
Pulsar radio and visible radiation due to the modulation instability of high-frequence transverse waves in the inhomogeneous electron-positron plasma N89-24959
ELECTRON RADIATION
On particle energization by magnetic field line reconnection in extragalactic jets N89-25028
ELECTRON SCATTERING
The effect of non-Maxwellian electron distributions on the intensity ratio of resonance to satellite lines
[DE89-006745] N89-24907
ELECTRON STATES
The effect of non-Maxwellian electron distributions on the intensity ratio of resonance to satellite lines
[DE89-006745] N89-24907
ELECTRON TRANSFER
Electron transfer, ionization, and excitation in atomic collisions
[DE89-010046] N89-24891
Charge exchange transition probability for collisions between unlike ions and atoms within the adiabatic approximation
[NASA-TM-101559] N89-25104
ELECTRON-ION RECOMBINATION
Introduction to dissociative recombination
[NASA-CR-184950] N89-24889
ELECTRON-POSITRON PLASMAS
Induced annihilation of particle-antiparticle pairs N89-24970
ELECTRONIC EQUIPMENT
Establishment of an electron beam lithography facility
[AD-A206215] N89-24332
ELECTRONS
Inductive acceleration of protons and electrons in planetary magnetotails N89-25015
ELECTROPHORESIS
Electrophoretically applied dielectrics for amorphous metal foils used in pulsed power saturable reactors
[DE89-009322] N89-24525
ELECTROPLATING
Embedded conductors by electrochemical planarization
[DE89-011632] N89-24534
ELECTROSTATIC CHARGE
The variable nature of the comet-solar wind interaction N89-25100
ELECTROSTATIC PROBES
Analytical consideration and calculation of electrostatical system by reverse method
[DE88-706319] N89-24885
ELECTROSTATIC WAVES
The electron beam instability revisited: Growth above and below f sub p N89-24917
Broadband electrostatic waves as a consequence of magnetotail reconnection N89-25017

ELECTROSTATICS
Simulation of electrostatic ion instabilities in the presence of parallel currents and transverse electric fields N89-24972
Anomalous collision frequency of magnetoactive plasmas with two-dimensional electrostatic turbulence (kB=O) N89-24981
The role of cold electrons in the generation of the high-frequency part of broadband electrostatic noise --- magnetotail N89-25018
ELLIPTIC DIFFERENTIAL EQUATIONS
Surface grid generation for composite block grids N89-24874
Surface coordinate generation in three-dimensional arbitrary shapes by solving a set of second order elliptic partial differential equations N89-24875
ELLIPTICAL GALAXIES
Some dynamical properties of anisotropic collisionless stellar systems N89-24963
ELLIPTICAL POLARIZATION
Elliptical polarization for ECRH on RTP --- Rijnhuizen Tokamak PETULA (RTP) N89-25035
ELONGATION
On specimen shape effects and the ductility of porous metals
[AD-A206216] N89-24475
EMBEDDING
Embedded conductors by electrochemical planarization
[DE89-011632] N89-24534
EMBRITTLEMENT
Research on the mechanism of thermal fatigue in near-eutectic Pb-Sn solders
[DE89-011430] N89-24482
EMISSION SPECTRA
Vertical emitting, ring geometry, ultra-low threshold and ultra-high speed quantum well lasers for optical interconnect
[AD-A206427] N89-24603
First detection of SO2 and CH3OH emission and one unidentified line near 800 GHz
[MPE-PREPRINT-142] N89-25086
EMISSIVITY
Microwave X-band radiometric characterization of Brazilian soils by measurement of the complex permittivity
[INPE-4588-PRE/1319] N89-24685
EMITTERS
An empirical study of the performance of APMOVPE AM0 InP homojunction solar cells as a function of emitter thickness and doping, and base doping N89-24709
EMPLOYEE RELATIONS
The electronic supervisor: New technology, new tensions
[OTA-CIT-333] N89-24804
EMULSIONS
Holographic interferometry with an injection seeded Nd:YAG laser and two reference beams
[NASA-TM-102056] N89-24591
ENCAPSULATING
Encapsulated diffusion of sulphur into InP N89-24714
END EFFECTORS
Real time control for NASA robotic gripper
[NASA-CR-184978] N89-24608
Generalized solution for the optimal prehension state using end effectors with multi-articulated fingers N89-24609
Inflatable end effector tools N89-24839
END-TO-END DATA SYSTEMS
The key role of Data Relay System (DRS) in the Columbus communications N89-24379
ENERGY ABSORPTION
Coronal heating by resonant absorption in resistive MHD N89-24926
ENERGY CONVERSION
Magnetic energy conversion on the sun N89-24987
ENERGY CONVERSION EFFICIENCY
Energy storage and thermal control system design status
[NASA-TM-102136] N89-24427
Progress in indium phosphide solar cell research N89-24707
Ultra-thin, light-trapping silicon solar cells N89-24719
ENERGY DISSIPATION
Multiple-pass aeroassisted plane change N89-24404
Multifractal spectra in homogeneous shear flow N89-24552
ENERGY SPECTRA
Demonstration of a Time Projection Compton Spectrometer
[DE89-010743] N89-24596
SPECTRUM: A computer algorithm to derive the flux-energy spectrum of precipitating particles from EISCAT electron density profiles
[IRF-TR-034] N89-24764
Problem of nonrotating black hole accretion disk main energy release region extension N89-24951
ENERGY STORAGE
Photovoltaic power system operation in the Mars environment
[NASA-TM-102075] N89-24529
ENERGY TRANSFER
Pressure-strain-rate events in homogeneous turbulent shear flow N89-24551
Energy transfer in isotropic turbulence at low Reynolds numbers N89-24553
Problem of nonrotating black hole accretion disk main energy release region extension N89-24951
ENGINE CONTROL
NASA Lewis Stirling engine computer code evaluation
[NASA-CR-182248] N89-24741
ENGINE COOLANTS
Liquid oxygen cooling of hydrocarbon fueled rocket thrust chambers
[NASA-TM-102113] N89-24447
ENGINE PARTS
Space Shuttle Main Engine High Pressure Fuel Turbopump turbine blade cracking
[NASA-TM-100327] N89-24435
Ceramic technology for advanced heat engines project
[DE89-012890] N89-24500
ENGINE TESTS
Performance of large area xenon ion thrusters for orbit transfer missions
[NASA-TM-102049] N89-24436
Initial characterization of a modular heat exchanger with an integral heat pipe
[NASA-TM-102097] N89-25078
ENGINES
Ceramic Technology for Advanced Heat Engines Project data base
[DE89-012888] N89-24499
Ceramic technology for advanced heat engines project
[DE89-012890] N89-24500
ENTHALPY
Study of chemical reaction models for high enthalpy flow of air
[NAL-TR-982] N89-25072
ENTRAINMENT
Scalar entrainment in the mixing layer N89-24545
ENVIRONMENTAL CONTROL
ECLS for Columbus and Hermes N89-24354
Neurochemical control of circadian rhythms
[AD-A206213] N89-24788
ENVIRONMENTAL SURVEYS
Correlation between satellite-derived aerosol characteristics and oceanic dimethylsulfide (DMS)
[AD-A206179] N89-24759
ENVIRONMENTAL TESTS
An atomic oxygen generation facility for space environmental testings
[NAL-TR-989] N89-24506
EPITAXY
Proceedings of the Goddard Space Flight Center Workshop on Robotics for Commercial Microelectronic Processes in Space
[NASA-TM-101233] N89-24505
EPOXY MATRIX COMPOSITES
Composite material bonding: Gelation and processing of adhesives and preimpregnated materials
[ETCA-88-R-006] N89-24457
EQUATIONS OF MOTION
Challenges in computational statistical mechanics
[DE89-009922] N89-24567
Equations of motion for viscoelastic moving crack problems N89-24670
A weak Hamiltonian finite element method for optimal control problems
[NASA-CR-185336] N89-24873
EQUATIONS OF STATE
High-pressure two temperature equations of state --- plasmas N89-24967
EQUATORIAL ATMOSPHERE
The relationship between intraseasonal disturbance activity and interannual variation of the tropical atmosphere N89-24774
EROSION
Optoelectronic velocimeter development
[DE89-012283] N89-24597
Erosion and retention of the target plate material in the ASDEX divertor N89-25045
ERROR ANALYSIS
Feasibility study of a synthesis procedure for array feeds to improve radiation performance of large distorted reflector antennas
[NASA-CR-184974] N89-24511
Error analysis for semi-analytic displacement derivatives with respect to shape and sizing variables N89-24632
Formal verification of a fault tolerant clock synchronization algorithm
[NASA-CR-4239] N89-24803
On the equivalence of a class of inverse decomposition algorithms for solving systems of linear equations
[NASA-TM-102036] N89-24865
ERROR CORRECTING CODES
Efficient dealiasing of Doppler velocities using local environment constraints
[DOT/FAA/SA-89/1] N89-24771
ESA SATELLITES
The European data relay satellite N89-24339
State of the art of ISO
[REPT-882-440-121] N89-24424
The advanced Ocean Chlorophyll Meter (OCM). A spectral imaging device for the observation of the oceans
[REPT-882-440-118] N89-24689
ESCAPE SYSTEMS
Hermes escape system N89-24366
ESTIMATING
Efficient estimator of parameters and goodness-of-fit test of multivariate distributions for data presented by one-dimensional histograms
[DE88-706318] N89-24879
ETCHING
Embedded conductors by electrochemical planarization
[DE89-011632] N89-24534
Chemical etching and organometallic chemical vapor deposition on varied geometries of GaAs N89-24728
ETHYLENE
Bonding and chemistry of hydrocarbon monolayers on metal surfaces
[DE89-009311] N89-24490
EULER EQUATIONS OF MOTION
A genuinely multi-dimensional upwind cell-vertex scheme for the Euler equations
[NASA-TM-102029] N89-24872
EULER-CAUCHY EQUATIONS
Some notes on shock resolving flux functions. Part 1: Stationary characteristics
[NASA-TM-101087] N89-24871
EUROPEAN AIRBUS
Calculation of aircraft noise in the vicinity of civil airports by a simultion procedure
[MPIS-7/1988] N89-24687
EUROPEAN SPACE PROGRAMS
International Symposium on Europe in Space: The Manned Space System
[ESA-SP-277] N89-24335
The Hermes Program N89-24338
The European in-orbit infrastructure ground segment N89-24340
Overall coherence of the European programs within a long-term space policy N89-24341
Microgravity payloads (APM and MTFF) N89-24347
Flight operations concept for the European in-orbit infrastructure N89-24356
Integrated approach for the logistic support of the European in orbit infrastructure from the nineties onwards N89-24359
ESA safety requirements N89-24364
The impact of manned space flight operations on the safety and reliability aspects of ground systems requirements N89-24371
The training concept for ESA astronauts and the associated facilities N89-24374
Expert system for European space infrastructure N89-24378
Scientific utilization of the European space infrastructure and the International Space Station N89-24380
The Microgravity User Support Center (MUSC) N89-24394
MARS Microgravity Advanced Research and Support Center N89-24395
Simulation of weightlessness with neutral buoyancy facilities and zero-g aircraft for the preparation of European manned space operations N89-24398
Autonomous geostationary stationkeeping system optimization and validation
[REPT-882-440-117] N89-24423
State of the art of ISO
[REPT-882-440-121] N89-24424
ISOCAM, ISO optical subsystem cryogenics, Aerospatiale, Cannes, France in-house R and D status
[REPT-882-440-123] N89-24429
Imaging Spectrometry for Land Applications
[ESA-SP-1101] N89-24692
ESA's planned activities in the field of imaging spectrometry for Earth observation N89-24693
DFVLR activities related to imaging spectrometry N89-24697
Activities of CNES in the field of imaging spectrometry N89-24699

The EARSEL Imaging Spectrometry Working Group N89-24700
ESA's space plasma physics missions: The past and the future ten years N89-24913
Materials for cryogenically cooled infrared telescopes [REPT-882-440-119] N89-25083

EUTECTICS
Research on the mechanism of thermal fatigue in near-eutectic Pb-Sn solders [DE89-011430] N89-24482

EVAPORATION
The importance of climatological variability and the rate at which waste is added to modeling water budget of landfills [DE89-008917] N89-24747
An operational analysis and forecasting method of evaporation [MP-11] N89-24769

EVENTS
Using a simulation assistant in modeling manufacturing systems N89-24849

EVOKED RESPONSE (PSYCHOPHYSIOLOGY)
Brain-wave measures of workload in advanced cockpits: The transition of technology from laboratory to cockpit simulator, phase 2 [NASA-CR-4240] N89-24797

EXCITATION
Electron transfer, ionization, and excitation in atomic collisions [DE89-010046] N89-24891

EXERCISE PHYSIOLOGY
Is salt at fault [AD-A206518] N89-24789

EXOSAT SATELLITE
Soft X-ray observations of the Vela Pulsar PSR 0833-45 [MPE-PREPRINT-130] N89-25080

EXPERIMENT DESIGN
Space science using Columbus: Manned space science N89-24348
Experimentation in the Man Tended Free Flyer (MTFF) N89-24381
The utilization of the European pressurized module for non-European experiments --- Columbus N89-24399
Beam guiding system for Rutherford scattering diagnostic at TEXTOR N89-25033

EXPERT SYSTEMS
Expert system for European space infrastructure N89-24378
XCAD: A CAD object-oriented virtual solid modeler for an expert system shell [REPT-882-440-125] N89-24810
Formal verification of AI software [NASA-CR-181827] N89-24811
Conference on Space and Military Applications of Automation and Robotics [AD-A198095] N89-24819
Cooperating expert systems N89-24825
On designing a case-based system for expert process development N89-24847
A knowledge representation scheme for a robotic land vehicle route planner N89-24853
IRIS: An intelligent robot insertion expert system N89-24854
Pedagogical issues in developing a man-machine interface for an intelligent tutoring system N89-24855
Empirical analysis and refinement of expert system knowledge bases [AD-A206226] N89-24858

EXPLOSIONS
The effects of blast trauma (impulse noise) on hearing: A parametric study [AD-A206180] N89-24786

EXTERNAL TANKS
KSC ice/frost/debris assessment for Space Shuttle Mission STS-30R [NASA-TM-102147] N89-24412

EXTRAGALACTIC RADIO SOURCES
Black hole driven winds N89-25096

EXTRAVEHICULAR ACTIVITY
Getting ready for EVA N89-24387
EVA Information System: A modern workstation in space N89-24388
The human role in space (THURIS) applications study. Final briefing [NASA-CR-183590] N89-24793
The human role in space (THURIS) applications study. Volume 2: Research analysis and technology report [NASA-CR-183589] N89-24795

EXTREMELY HIGH FREQUENCIES
Development of a 75-watt 60-GHz traveling-wave tube for intersatellite communications [NASA-CR-182135] N89-24530

EXTRUDING
High temperature mechanical properties and microscopic examination of extruded powder aluminum [DE89-010457] N89-24484

F

F-15 AIRCRAFT
US military aircraft coproduction with Japan [AD-A206430] N89-24263

F-16 AIRCRAFT
Development and flight test experiences with a flight-crucial digital control system [NASA-TP-2857] N89-24327

FABRICATION
Technology of aircraft construction (selected chapters) [AD-A199946] N89-24261
Establishment of an electron beam lithography facility [AD-A206215] N89-24332
Encapsulated diffusion of sulphur into InP N89-24714
Advanced photovoltaic solar array development N89-24716
High efficiency GaAs-Ge tandem solar cells grown by MOCVD N89-24721
Investigation of high efficiency GaAs solar cells N89-24724
Status of GaAs solar cell production N89-24729
Flexibility in space solar cell production N89-24730
Development of an integrated CAD/CAM system for wire harness fabrication N89-24842

FABRICS
Development of tailorable advanced blanket insulation for advanced space transportation systems [NASA-CR-177444] N89-24486

FABRY-PEROT INTERFEROMETERS
High spectral resolution observations of the H2 2.12 micron line in Herbig-Haro objects [MPE-PREPRINT-139] N89-25085

FACSIMILE COMMUNICATION
Investigation of vector quantization for the coding gray scale images for Group 4 facsimile [AD-A206548] N89-24809

FACTORIZATION
Factorization of the relativistic Pauli equation in the presence of a gravitational field [DE88-704749] N89-25090

FAILURE
Characterization of pore evolution in ceramics during creep failure and densification [DE89-013599] N89-24502

FAILURE ANALYSIS
Engineering design of the interaction waveguide for high-power accelerator-driven microwave free-electron lasers [DE89-011896] N89-24605
Integrated optimization of nonlinear R/C frames with reliability constraints N89-24631

FAILURE MODES
Microscopic delamination processes and the resulting crack tip strain fields of graphite/epoxy composites N89-24671
Analysis of interlaminar fracture in composites under combined loading [NASA-CR-185055] N89-24674

FAR FIELDS
Computed performance of the half-scale accurate antenna reflector [NASA-CR-182284] N89-24532

FAR ULTRAVIOLET RADIATION
Contamination effects study [NASA-CR-183613] N89-24746
Laboratory for X-ray optics [AD-A206468] N89-25061

FATIGUE (MATERIALS)
Some comments on global-local analyses N89-24644
Results of the Round Robin on opening-load measurement conducted by ASTM Task Group E24.04.04 on Crack Closure Measurement and Analysis [NASA-TM-101601] N89-24679

FATIGUE LIFE
Space Shuttle Main Engine High Pressure Fuel Turbopump turbine blade cracking [NASA-TM-100327] N89-24435
Isothermal life prediction of composite lamina using a damage mechanics approach [NASA-TM-102032] N89-24460

FATIGUE TESTS
Results of the Round Robin on opening-load measurement conducted by ASTM Task Group E24.04.04 on Crack Closure Measurement and Analysis [NASA-TM-101601] N89-24679

FAULT TOLERANCE
Formal verification of a fault tolerant clock synchronization algorithm [NASA-CR-4239] N89-24803
The Fault Tree Compiler (FTC): Program and mathematics [NASA-TP-2915] N89-24815
Predeployment validation of fault-tolerant systems through software-implemented fault insertion [NASA-CR-4244] N89-24817

FAULT TREES
The Fault Tree Compiler (FTC): Program and mathematics [NASA-TP-2915] N89-24815

FEASIBILITY ANALYSIS
State of the art of ISO [REPT-882-440-121] N89-24424
Maglev vehicles and superconductor technology: Integration of high-speed ground transportation into the air travel system [DE89-012241] N89-24619
Testing the feasibility of using a teleoperated robot for remote, dexterous operations N89-24843

FEEDBACK CONTROL
Numerical simulation of feedback control of aerodynamic configurations in steady and unsteady ground effects N89-24326
Insertion with two coordinated arms N89-24837
Empirical analysis and refinement of expert system knowledge bases [AD-A206226] N89-24858
Fractional-order feedback in linear systems [AD-A206241] N89-24859

FEEDFORWARD CONTROL
Neuromorphic learning of continuous-valued mappings in the presence of noise: Application to real-time adaptive control [NASA-TM-101999] N89-24856

FEYNMAN DIAGRAMS
Path integral and operator formalism on bordered Riemann surfaces [DE88-757229] N89-24881

FIBER COMPOSITES
Technology of aircraft construction (selected chapters) [AD-A199946] N89-24261
Characterization of delamination in advanced composite materials under mode 3 loading conditions [AD-A206159] N89-24452
Impact and penetration resistance of fibrous composites [AD-A206417] N89-24454
Isothermal life prediction of composite lamina using a damage mechanics approach [NASA-TM-102032] N89-24460
Thermoplastic coating of carbon fibers [NASA-CR-185047] N89-24488
A study of material damping in large space structures [NASA-CR-180076] N89-24634

FIBER OPTICS
An intelligent fiberoptic data bus for fly-by-light applications [NAL-TM-SE-8707] N89-24901

FIBERS
Technology of aircraft construction (selected chapters) [AD-A199946] N89-24261
The effects of supercritical fluids on high performance polymers [AD-A206515] N89-24494

FIELD OF VIEW
Visibility with a moving point of view N89-24876

FIGHTER AIRCRAFT
The use of seaplanes as an advanced weapon system [AD-A206243] N89-24880

FIGURE OF MERIT
Optimisation of the figure of merit of modified silicon-germanium alloys [AD-A206420] N89-24491

FILAMENT WINDING
Technology of aircraft construction (selected chapters) [AD-A199946] N89-24261

FINE STRUCTURE
A neutral current sheet with flows: Tearing and stratification modes and modeling of coronal structures N89-24991
Search for a fine-time structure in flares of UV Cet-type stars N89-25007

FINITE DIFFERENCE THEORY
Characterization of radiation boundary conditions used in the finite-difference time-domain method [DE89-005662] N89-24522
Navier-Stokes analysis of cold scramjet-afterbody flows [NASA-CR-184949] N89-24562
Error analysis for semi-analytic displacement derivatives with respect to shape and sizing variables N89-24632

On computational schemes for global-local stress analysis N89-24645
FINITE ELEMENT METHOD
Analysis of the wake behind a propeller using the finite element method with a two-equation turbulence model N89-24286
Space Shuttle Main Engine High Pressure Fuel Turbopump turbine blade cracking [NASA-TM-100327] N89-24435
Incorporation of surface tension into the structural finite element code SANCHO [DE89-011354] N89-24616
Analysis of adaptive planar truss structures [NAL-TR-988] N89-24625
A study of composite plates with holes/inclusions N89-24627
Some issues in numerical simulation of nonlinear structural response N89-24639
Nonlinear response of a blade-stiffened graphite-epoxy panel with a discontinuous stiffener: Work in progress N89-24641
Computational procedures for postbuckling of composite shells N89-24642
A review of some problems in global-local stress analysis N89-24643
On computational schemes for global-local stress analysis N89-24645
Global functions in global-local finite-element analysis of localized stresses in prismatic structures N89-24646
Application of the p-version of the finite-element method to global-local problems N89-24648
Nonlinear hierarchical substructural parallelism and computer architecture N89-24650
Adaptive methods, rolling contact, and nonclassical friction laws N89-24651
Exploiting symmetries in the modeling and analysis of tires N89-24653
Unconditionally stable concurrent procedures for transient finite-element analysis N89-24657
Transient analysis techniques in performing impact and crash dynamic studies N89-24658
Application and implementation of transient algorithms in computer programs N89-24659
Application of finite-element methods to dynamic analysis of flexible spatial and co-planar linkage systems, part 2 N89-24663
Improved analysis of laminated heterogeneous beams and associated formulation of a new finite element method N89-24672
Dynamics and static behavior of metal gussets in cask impact limiters [DE89-011879] N89-24683
A weak Hamiltonian finite element method for optimal control problems [NASA-CR-185336] N89-24873
FINITE VOLUME METHOD
An algebraic homotopy method for generating quasi-three-dimensional grids for high-speed configurations [NASA-CR-4242] N89-24581
FINLAND
Orographically-caused microclimate variation in the Saariselka Region [ISBN-9-5169-7269-1] N89-24767
The climate of Finland: A bibliography with particular reference to applications updating part 1968-1985 [MP-10] N89-24768
FIRE EXTINGUISHERS
Fire safety applications for spacecraft [NASA-TM-101463] N89-24413
FIRE PREVENTION
Fire safety applications for spacecraft [NASA-TM-101463] N89-24413
FLAT PLATES
Some characteristics of bypass transition in a heated boundary layer [NASA-TM-102126] N89-24577
FLEXIBILITY
Dynamics of flexible multi-body mechanisms and manipulators. Part 1: An overview N89-24662
FLEXIBLE BODIES
Dynamics of articulated structures N89-24664
Modal reduction strategies for interconnected flexible bodies simulation N89-24665
Computational aspects of multibody dynamics N89-24666
FLEXIBLE WINGS
Aeroservoelastic modeling and applications using minimum-state approximations of the unsteady aerodynamics [NASA-TM-101574] N89-24308
Recent activities within the Aeroservoelasticity Branch at the NASA Langley Research Center [NASA-TM-101582] N89-24314
FLIGHT CONDITIONS
A computer simulation study of liquid water content adjustment based on icing cloud horizontal extent [DOT/FAA/CT-TN89/3] N89-24288
FLIGHT CONTROL
Flight control system for the CRCA (Control Reconfigurable Combat Aircraft) using a command generator tracker with PI (Plus Integral) feedback and Kalman filter, volume 2 [AD-A206202] N89-24325
Development and flight test experiences with a flight-crucial digital control system [NASA-TP-2857] N89-24327
The role of the Hermes flight control center in a typical Hermes/MTFF servicing mission N89-24372
FLIGHT CREWS
Cerebral laterality and handedness in aviation: Performance and selection implications [AD-A206196] N89-24787
FLIGHT MANAGEMENT SYSTEMS
Controller evaluation of initial data link air traffic control services. Volume 1: Mini study 2 [DOT/FAA/CT-89/14-VOL-1] N89-24292
Diverter AI based decision aid, phases 1 and 2 [NASA-CR-181820] N89-24316
FLIGHT OPTIMIZATION
Optimal guidance with obstacle avoidance for nap-of-the-earth flight [NASA-CR-177515] N89-24328
FLIGHT PATHS
Controller evaluation of initial data link air traffic control services. Volume 1: Mini study 2 [DOT/FAA/CT-89/14-VOL-1] N89-24292
B-737 flight test of curved-path and steep-angle approaches using MLS guidance [NASA-TM-101521] N89-24293
Visibility with a moving point of view N89-24876
Calculation of aircraft noise in the vicinity of civil airports by a simultion procedure [MPIS-7/1988] N89-24887
FLIGHT PLANS
Diverter AI based decision aid, phases 1 and 2 [NASA-CR-181820] N89-24316
FLIGHT SAFETY
Controller evaluation of initial data link air traffic control services. Volume 1: Mini study 2 [DOT/FAA/CT-89/14-VOL-1] N89-24292
A comparison of detection efficiency on an air traffic control monitoring task with and without computer aiding [AD-A206422] N89-24294
ESA safety requirements N89-24364
Safety in manned space flight N89-24402
FLIGHT SIMULATION
B-737 flight test of curved-path and steep-angle approaches using MLS guidance [NASA-TM-101521] N89-24293
Results of an A109 simulation validation and handling qualities study [NASA-TM-101062] N89-24323
Brain-wave measures of workload in advanced cockpits: The transition of technology from laboratory to cockpit simulator, phase 2 [NASA-CR-4240] N89-24797
Display-based communications for advanced transport aircraft [NASA-TM-102187] N89-24798
Visibility with a moving point of view N89-24876
FLIGHT TEST INSTRUMENTS
Determination of reference trajectories for testing navigation aids using an onboard CCD camera N89-24303
FLIGHT TESTS
Effect of advanced rotorcraft airfoil sections on the hover performance of a small-scale rotor model [NASA-TP-2832] N89-24264
Preliminary airworthiness evaluation of modified second-generation Pneumatic Boot Deicing System on a JUH-1H [AD-A206255] N89-24289
An operational demonstration and engineering flight test of the Microwave Landing System on runway 22L at Chicago's Midway Airport [DOT/FAA/CT-TN88/42] N89-24291
B-737 flight test of curved-path and steep-angle approaches using MLS guidance [NASA-TM-101521] N89-24293
A versatile flight experiment system for image processing N89-24307
Loss of tail rotor effectiveness evaluation of the OH-58C helicopter with directional SAS (Stability Augmentation System) [AD-A206181] N89-24309
Results of an A109 simulation validation and handling qualities study [NASA-TM-101062] N89-24323
Field joint environmental protection system vibration/pressurization qualification [NASA-CR-183673] N89-24449
The experiments of LIPS 3 N89-24735
FLOATING POINT ARITHMETIC
A systolic array structure for on-line system identification [AD-A206412] N89-24806
FLOW CHAMBERS
Natural convection cooling of a 3 by 3 array of rectangular protrusions in an enclosure filled with dielectric liquid: Effects of boundary conditions and component orientation [AD-A206474] N89-24571
FLOW DISTRIBUTION
Interaction of Karman vortex-street with an elliptical leading-edge N89-24268
Water tunnel investigation of the vortex dynamics of periodically pitched wings [AD-A206359] N89-24271
A zonal method for modeling powered-lift aircraft flow fields [NASA-CR-177521] N89-24287
A numerical study of chemically reacting flow in nozzles [NASA-TM-102135] N89-24444
Three-dimensional flows and loss generation mechanisms in a linear turbine rotor cascade at various incidence conditions [NAL-TR-984T] N89-24537
Studying Turbulence Using Numerical Simulation Databases, 2. Proceedings of the 1988 Summer Program [NASA-CR-184905] N89-24538
Use of passive scalar tagging for the study of coherent structures in the plane mixing layer N89-24546
Sensitivity of mixing layers to three-dimensional forcing N89-24547
Sampling inhomogeneous turbulent fields N89-24548
Dynamical interpretation of conditional patterns N89-24549
Turbulence production near walls: The role of flow structures with spanwise asymmetry N89-24550
Pressure-strain-rate events in homogeneous turbulent shear flow N89-24551
Multifractal spectra in homogeneous shear flow N89-24552
Energy transfer in isotropic turbulence at low Reynolds numbers N89-24553
Turbulence characteristics inside a turbulent spot in plane Poiseuille flow N89-24554
Eddies, streams, and convergence zones in turbulent flows N89-24555
Theoretical model for VITA-educed coherent structures in the wall region of a turbulent boundary layer N89-24556
The structure of sheared turbulence near a plane boundary N89-24557
Head-on collision of viscous vortex rings N89-24560
Basic flow field and heat transfer studies about three cylinders of different diameter in transverse flow N89-24564
Numerical study of turbulent secondary flows in curved ducts [NASA-CR-181830] N89-24568
Unsteady and separated flows [AD-A206539] N89-24572
FLOW MEASUREMENT
Experimental techniques in unsteady flows N89-24279
An experimental study of a three-dimensional thrust augmenting ejector using laser Doppler velocimetry [NASA-CR-177531] N89-24569
Two-phase flow measurements by nuclear magnetic resonance imaging [DE89-011850] N89-24586
FLOW STABILITY
Phase decorrelation, streamwise vortices and acoustic radiation in mixing layers N89-24541
Sensitivity of mixing layers to three-dimensional forcing N89-24547
Dynamical interpretation of conditional patterns N89-24549
Turbulence production near walls: The role of flow structures with spanwise asymmetry N89-24550
Head-on collision of viscous vortex rings N89-24560
Vortex dynamics and vortex breakdown [AD-A206470] N89-24570
Analytic theory for the determination of velocity and stability of bubbles in a Hele-Shaw cell. Part 2: Stability [NASA-CR-181837] N89-24883
FLOW VELOCITY
Development of an engineering methodology for applying foam technology [DE89-000740] N89-24497

Energy transfer in isotropic turbulence at low Reynolds numbers N89-24553
Eddies, streams, and convergence zones in turbulent flows N89-24555
Mechanics/heat-transfer relation for particle flows [DE89-011382] N89-24584
A remote laser-probing system for combustion measurements [NAL-TR-979] N89-24598
Analytic theory for the determination of velocity and stability of bubbles in a Hele-Shaw cell. Part 2: Stability [NASA-CR-181837] N89-24883

FLUENCE
Hydrogen ion-driven permeation in carbonaceous films [DE89-005271] N89-24485
Radiation resistance studies of amorphous silicon films N89-24738

FLUID FLOW
Caltech-DOE program on numerical analysis, scientific computing and fundamental studies of fluid mechanics [DE89-010828] N89-24582

FLUID MECHANICS
Caltech-DOE program on numerical analysis, scientific computing and fundamental studies of fluid mechanics [DE89-010828] N89-24582

FLUIDIZED BED PROCESSORS
Mechanics/heat-transfer relation for particle flows [DE89-011382] N89-24584

FLUORESCENCE
Cooperative phenomena for new coherent radiation sources [AD-A206368] N89-24602
The FLI airborne imaging spectrometer: A highly versatile sensor for many applications N89-24694
DFVLR activities related to imaging spectrometry N89-24697
Development of an imaging spectrometer for remote sensing: The FLI program N89-24698
Imaging spectrometry at the Canada Centre for Remote Sensing N89-24701

FLUORIDES
Flight experiment of thermal energy storage [NASA-TM-102081] N89-24440

FLUTTER
Results of a parametric aeroelastic stability analysis of a generic X-wing aircraft [NASA-TM-101572] N89-24324

FLUTTER ANALYSIS
Aeroservoelastic wind-tunnel investigations using the Active Flexible Wing Model: Status and recent accomplishments [NASA-TM-101570] N89-24313
Wind tunnel tests on flutter control of a high-aspect-ratio cantilevered wing [NAL-TR-978] N89-24321

FLY BY WIRE CONTROL
An intelligent fiberoptic data bus for fly-by-light applications [NAL-TM-SE-8707] N89-24901

FLYBY MISSIONS
Voyager at Neptune: 1989 [NASA-CR-185317] N89-24420

FOAMS
Development of an engineering methodology for applying foam technology [DE89-000740] N89-24497

FORCE-FREE MAGNETIC FIELDS
Stability of force-free magnetic fields and the problem of solar coronal heating N89-24990

FORECASTING
An operational analysis and forecasting method of evaporation [MP-11] N89-24769

FORESTS
Improvement and extension of a radar forest backscattering model [NASA-CR-184975] N89-24686

FORMALISM
Path integral and operator formalism on bordered Riemann surfaces [DE88-757229] N89-24881

FOURIER SERIES
Surface coordinate generation in three-dimensional arbitrary shapes by solving a set of second order elliptic partial differential equations N89-24875

FOURIER TRANSFORMATION
Dynamic spectral analysis in finite field algebras [DE88-706333] N89-24877

FRACTALS
Multifractal spectra in homogeneous shear flow N89-24552

FRACTURE MECHANICS
Space Shuttle Main Engine High Pressure Fuel Turbopump turbine blade cracking [NASA-TM-100327] N89-24435
On specimen shape effects and the ductility of porous metals [AD-A206216] N89-24475
Ceramic technology for advanced heat engines project [DE89-012890] N89-24500
Acoustic emission from a growing crack N89-24633
Features and characterization needs of rubber composite structures N89-24649

FRACTURE STRENGTH
Impact and penetration resistance of fibrous composites [AD-A206417] N89-24454
Microscopic delamination processes and the resulting crack tip strain fields of graphite/epoxy composites N89-24671

FRACTURES (MATERIALS)
Analysis of interlaminar fracture in composites under combined loading [NASA-CR-185055] N89-24674

FRACTURING
Some comments on global-local analyses N89-24644

FREDHOLM EQUATIONS
Comparison of basis function and iteration solutions to the Fredholm integral equation of the first kind [AD-A206158] N89-24869

FREE ELECTRON LASERS
Engineering design of the interaction waveguide for high-power accelerator-driven microwave free-electron lasers [DE89-011896] N89-24605
A role for free electron lasers in fusion N89-25031

FREE RADICALS
Free radical-surface interactions using multiphoton ionization of free radicals [AD-A206257] N89-24892

FREE-PISTON ENGINES
On the dynamic response of pressure transmission lines in the research of helium-charged free piston Stirling engines [NASA-TM-102121] N89-24593

FREEZING
Flight experiment of thermal energy storage [NASA-TM-102081] N89-24440

FRENCH SPACE PROGRAMS
French national policy on the preparation of Columbus utilization N89-24344

FREQUENCY MODULATION
Prototype laser-diode-pumped solid state laser transmitters [NASA-CR-185056] N89-24601
Inductive megahertz beam position monitors for CEBAF [CEBAF-PR-89-003] N89-24895

FRESNEL LENSES
Domed Fresnel lens concentrator technology for space application N89-24732

FRICTION
Adaptive methods, rolling contact, and nonclassical friction laws N89-24651
Contact solution algorithms N89-24652

FROST
KSC ice/frost/debris assessment for Space Shuttle Mission STS-30R [NASA-TM-102147] N89-24412

FUEL CAPSULES
Safety analysis report for the Galileo Mission. Volume 2, book 1: Accident model document [DE89-007270] N89-24896
Safety analysis report for the Galileo Mission. Volume 2, book 2: Accident model document, Appendices [DE89-007271] N89-24897
Safety analysis report for the Galileo Mission. Volume 3, book 1: Nuclear risk analysis document, revision 1 [DE89-007272] N89-24898
Safety analysis report for the Galileo Mission. Volume 3, book 2: Nuclear risk analysis document. Appendices, revision 1 [DE89-007273] N89-24899

FUEL CORROSION
Role of sulfur oxides in wear and deposit formation in Army diesel engines [AD-A206054] N89-24613

FUEL PUMPS
Space Shuttle Main Engine High Pressure Fuel Turbopump turbine blade cracking [NASA-TM-100327] N89-24435

FUEL TANKS
Laser-induced-fluorescence inspection of polyurethane and related materials, phase 1 [AD-A206423] N89-24492

FUNCTIONAL ANALYSIS
Comparison of basis function and iteration solutions to the Fredholm integral equation of the first kind [AD-A206158] N89-24869

FUSELAGES
Local stiffener and skin pocket buckling prediction by special PASCO modeling technique: Correlation to test data N89-24628
Computational procedures for postbuckling of composite shells N89-24642

G

GALACTIC CLUSTERS
A study of the Southern Supercluster N89-25088

GALACTIC EVOLUTION
The case for a primordial galactic field N89-24939
The formation of the spectrum of inhomogeneity of the dark matter in pregalactic cosmic plasma N89-24968
Effects of main-sequence mass loss on stellar and galactic chemical evolution [DE89-011399] N89-25098

GALACTIC NUCLEI
The 158 micron (CII) mapping of the galactic center molecular clouds [MPE-PREPRINT-131] N89-25081
The circum-nuclear disk [MPE-PREPRINT-132] N89-25093

GALACTIC RADIATION
The gamma-ray observatory GRO in perspective [MPE-PREPRINT-137] N89-24407
On particle energization by magnetic field line reconnection in extragalactic jets N89-25028
The 158 micron (CII) mapping of the galactic center molecular clouds [MPE-PREPRINT-131] N89-25081
Constraints on the optical counterpart of GBS0526-66 [MPE-PREPRINT-138] N89-25084
COS-B gamma-ray sources beyond the predicted diffuse emission [MPE-PREPRINT-136] N89-25107

GALACTIC STRUCTURE
Bars and open spirals in density wave theory --- galaxies N89-24964

GALERKIN METHOD
Analysis of the wake behind a propeller using the finite element method with a two-equation turbulence model N89-24286

GALILEO PROJECT
Safety analysis report for the Galileo Mission. Volume 2, book 1: Accident model document [DE89-007270] N89-24896
Safety analysis report for the Galileo Mission. Volume 2, book 2: Accident model document, Appendices [DE89-007271] N89-24897
Safety analysis report for the Galileo Mission. Volume 3, book 1: Nuclear risk analysis document, revision 1 [DE89-007272] N89-24898
Safety analysis report for the Galileo Mission. Volume 3, book 2: Nuclear risk analysis document. Appendices, revision 1 [DE89-007273] N89-24899

GALLIUM ARSENIDES
Space photovoltaic technique. State of the art, trends [REPT-882-440-120] N89-24442
Microwave characteristics of GaAs MMIC integratable optical detectors [NASA-TM-101485] N89-24520
A longlife, highvoltage, shortpulse generator based on optically activated Bulk Avalanche Semiconductor Switch, phase 2 [AD-A206078] N89-24527
N/P InP homojunction solar cells with an In0.53Ga0.47As contacting layer grown by liquid phase epitaxy N89-24710
The impact of solar cell technology on planar solar array performance N89-24715
Development of tandem cells consisting of GaAs single crystal and CuInSe2/CdZnS polycrystalline thin films N89-24717
Directions for further development of GaAs/CuInSe2 thin film tandem cells N89-24718
High efficiency GaAs-Ge tandem solar cells grown by MOCVD N89-24721
Response of single junction GaAs/GaAs and GaAs/Ge solar cells to multiple doses of 1 MeV electrons N89-24722
Investigation of high efficiency GaAs solar cells N89-24724
A new structure for comparing surface passivation materials of GaAs solar cells N89-24725
Improved defect analysis of Gallium Arsenide solar cells using image enhancement N89-24726
Aging behavior of Au-based ohmic contacts to GaAs N89-24727
Chemical etching and organometallic chemical vapor deposition on varied geometries of GaAs N89-24728
Status of GaAs solar cell production N89-24729

Gallium Arsenide welded panel technology for advanced spaceflight applications N89-24731
Domed Fresnel lens concentrator technology for space application N89-24732
The 25 percent-efficient GaAs Cassegrainian concentrator cell N89-24733
Selective pair luminescence of magnesium in gallium arsenide dissertation
[AD-A206160] N89-25058

GAMMA RAY ASTRONOMY
The gamma-ray observatory GRO in perspective
[MPE-PREPRINT-137] N89-24407
Constraints on the optical counterpart of GBS0526-66
[MPE-PREPRINT-136] N89-25084
The application of two-dimensional imaging to very high energy gamma ray astronomy
[DE89-013614] N89-25089

GAMMA RAY BURSTS
Neutron starquakes and the nature of gamma-ray bursts N89-24947
Constraints on the optical counterpart of GBS0526-66
[MPE-PREPRINT-136] N89-25084

GAMMA RAY LASERS
Induced annihilation of particle-antiparticle pairs N89-24970

GAMMA RAYS
COS-B gamma-ray sources beyond the predicted diffuse emission
[MPE-PREPRINT-136] N89-25107

GAS CHROMATOGRAPHY
Multiplexed electronically programmable multimode ionization detector for chromatography
[DE89-009758] N89-24465
Mass spectrometry
[DE89-011118] N89-24471

GAS DISSOCIATION
Theoretical studies of important processes in planetary and comet atmospheres. Renewel request
[NASA-CR-184951] N89-25099

GAS DYNAMICS
Some notes on shock resolving flux functions. Part 1: Stationary characteristics
[NASA-TM-101087] N89-24871

GAS FLOW
Numerical study on laminar circular jet of carbonic acid gas discharging into stagnant air
[DE88-757249] N89-24565
Continuous cryopump with a method for removal of solidified gases
[DE89-009760] N89-24611
Gas flow in and around bars --- galaxies N89-24965

GAS JETS
Numerical study on laminar circular jet of carbonic acid gas discharging into stagnant air
[DE88-757249] N89-24565

GAS TEMPERATURE
Self-consistent models of spherical accretion onto black holes N89-25095

GAS TUNGSTEN ARC WELDING
A generalized method for automatic downhand and wirefeed control of a welding robot and positioner N89-24846

GAS-GAS INTERACTIONS
Dynamics of gas-surface interactions
[AD-A206210] N89-25059

GAS-SOLID INTERACTIONS
Dynamics of gas-surface interactions
[AD-A206210] N89-25059

GASEOUS DIFFUSION
Isotopic study of oxygen diffusion in oxide coatings
[NASA-TM-102082] N89-24451

GAUGE THEORY
Stochastic quantization of nonlinear sigma-models with Wess-Zumino terms
[DE88-757286] N89-24882

GAUSSIAN ELIMINATION
On the equivalence of a class of inverse decomposition algorithms for solving systems of linear equations
[NASA-TM-102036] N89-24865

GEARS
Tribology: The Story of Lubrication and Wear
[NASA-TM-101430] N89-24635

GEOCENTRIC COORDINATES
Determination of station coordinates, earth rotation and plate motions from LAGEOS laser ranging: 1983-1986
[NAL-TR-980T] N89-24753

GEODETIC SATELLITES
Time variations in the earth's gravity field from Starlette orbit analysis N89-24766

GEODYNAMICS
Laser ranging data analysis
[NASA-CR-184847] N89-24754

GEOLOGY
Geological gyrocompass
[PB89-133086] N89-24589
The activities of the British National Space Centre (BNSC) in the field of imaging spectrometry N89-24696

GEOMAGNETIC TAIL
Quasi-adiabatic particle acceleration in magnetic field reversals and the formation of the plasma sheet boundary layer in the earth's magnetotail N89-24943
Noise-free neutral sheets N89-24977
Magnetotail reconnection, MHD theory and simulations N89-25013
The role of magnetic reconnection in magnetotail plasmoid dynamics N89-25014
Inductive acceleration of protons and electrons in planetary magnetotails N89-25015
Broadband electrostatic waves as a consequence of magnetotail reconnection N89-25017
The role of cold electrons in the generation of the high-frequency part of broadband electrostatic noise --- magnetotail N89-25018
Electromagnetic electron temperature anisotropy instability in the earth's magnetotail plasma sheet N89-25019
ELF plasma turbulence observed by Prognoz-8 in plasma jets in the magnetospheric tail N89-25020

GEOMAGNETISM
Particle simulation of magnetic reconnection in collision-free plasma sheets N89-24986

GEOPHYSICS
A new field experiment in the Greenland ice cap to test Newton's inverse square law
[DE89-009247] N89-25091

GERMANIUM
High efficiency GaAs-Ge tandem solar cells grown by MOCVD N89-24721
Response of single junction GaAs/GaAs and GaAs/Ge solar cells to multiple doses of 1 MeV electrons N89-24722

GET AWAY SPECIALS (STS)
Flight experiment of thermal energy storage
[NASA-TM-102081] N89-24440

GLASS
Inelastic scattering from liquid He4 in aerogel glass
[DE89-012381] N89-24587

GLASS FIBERS
Containerless glass fiber processing
[NASA-TM-86540] N89-24405

GLASS LASERS
Prototype laser-diode-pumped solid state laser transmitters
[NASA-CR-185056] N89-24601

GLIDE PATHS
B-737 flight test of curved-path and steep-angle approaches using MLS guidance
[NASA-TM-101521] N89-24293

GLOW DISCHARGES
Research on high-efficiency, single-junction, monolithic, thin-film amorphous silicon solar cells, phase 2
[DE89-000849] N89-24703

GOALS
US fuel cell research and applications, 1960--1989
[DE89-012244] N89-24745

GOLD
Correlation between the structure, energy, and local elastic properties of grain boundaries in metals
[DE89-009861] N89-25055

GOLD ALLOYS
Aging behavior of Au-based ohmic contacts to GaAs N89-24727

GOODNESS OF FIT
Efficient estimator of parameters and goodness-of-fit test of multivariate distributions for data presented by one-dimensional histograms
[DE88-706318] N89-24879

GOVERNMENT/INDUSTRY RELATIONS
Putting technology to work: Examples of industry-laboratory cooperation contributing to our nation's economic strength
[PB89-134654] N89-25077

GRAIN BOUNDARIES
Characterization of pore evolution in ceramics during creep failure and densification
[DE89-013599] N89-24502
Correlation between the structure, energy, and local elastic properties of grain boundaries in metals
[DE89-009861] N89-25055
The effects of gradients on boundary stability
[DE89-011590] N89-25065
Grain boundary phase equilibria in metallic systems
[DE89-011787] N89-25066
High resolution electron microscopy of interfaces in topotaxial and epitaxial reactions
[DE89-010390] N89-25070

GRAIN SIZE
Effects of multiple reductions on grain refinement during hot working of alloy 718
[DE89-010426] N89-24483

GRAND TOURS
Voyager at Neptune: 1989
[NASA-CR-185317] N89-24420

GRANULAR MATERIALS
Modeling thermal-mechanical processes associated with the initiation and combustion of granular energetic materials
[DE89-007145] N89-24472

GRAPHITE-EPOXY COMPOSITES
Nonlinear response of a blade-stiffened graphite-epoxy panel with a discontinuous stiffener: Work in progress N89-24641
Microscopic delamination processes and the resulting crack tip strain fields of graphite/epoxy composites N89-24671
Analysis of interlaminar fracture in composites under combined loading
[NASA-CR-185055] N89-24674
Global/local stress analysis of composite panels
[NASA-TM-101622] N89-24681

GRAVITATION
A new field experiment in the Greenland ice cap to test Newton's inverse square law
[DE89-009247] N89-25091

GRAVITATIONAL COLLAPSE
The formation of interstellar clouds N89-24935
An observational study of the dynamics of molecular cloud cores N89-25097

GRAVITATIONAL EFFECTS
Industrial utilization of microgravity: Problems in the realization phase N89-24383

GRAVITATIONAL FIELDS
Centrifugal modeling of underground structures subjected to blast loading
[AD-A206424] N89-24675
The gravitational many-body PPN Lagrangian, Lorentz invariance and the strong equivalence principle to second order N89-24765
Time variations in the earth's gravity field from Starlette orbit analysis N89-24766
Factorization of the relativistic Pauli equation in the presence of a gravitational field
[DE88-704749] N89-25090
Red-shift experiments and non-Newtonian gravitational forces
[DE89-009349] N89-25092
Gravitational angular fluctuations of the cosmic background radiation produced by cosmological linear perturbations
[DE88-757287] N89-25105

GRAY SCALE
Investigation of vector quantization for the coding gray scale images for Group 4 facsimile
[AD-A206548] N89-24809

GREEN'S FUNCTIONS
WADA1: FORTRAN program for wave diffraction analysis, version 1
[AD-A206533] N89-24808

GREENHOUSE EFFECT
Bibliography on tropical rain forests and the global carbon cycle. Volume 2: South Asia
[DE89-008971] N89-24748
Beyond CO2: The other greenhouse gases
[DE89-011893] N89-24750
Correlation between satellite-derived aerosol characteristics and oceanic dimethylsulfide (DMS)
[AD-A206179] N89-24759

GREENLAND
A new field experiment in the Greenland ice cap to test Newton's inverse square law
[DE89-009247] N89-25091

GRID GENERATION (MATHEMATICS)
An algebraic homotopy method for generating quasi-three-dimensional grids for high-speed configurations
[NASA-CR-4242] N89-24581
Surface coordinate generation in three-dimensional arbitrary shapes by solving a set of second order elliptic partial differential equations N89-24875

GROUND BASED CONTROL
The role of the Hermes flight control center in a typical Hermes/MTFF servicing mission N89-24372
The Manned Space Laboratories Control Center (MSCC) at DFVLR, Oberpfaffenhofen, Germany, F.R. N89-24376
The concept of telescience N89-24384
Telescience and payload control support technologies N89-24385
Telescience: A promising operations center N89-24386
MARS Microgravity Advanced Research and Support Center N89-24395
Display-based communications for advanced transport aircraft
[NASA-TM-102187] N89-24798

Ground control of space based robotic systems
N89-24845

GROUND EFFECT (AERODYNAMICS)
An investigation of V/STOL jet interactions in a crossflow
[AD-A206360] N89-24272
Numerical simulation of feedback control of aerodynamic configurations in steady and unsteady ground effects
N89-24326

GROUND EFFECT (COMMUNICATIONS)
Ground cluster filters for staggered pulse trains
[DOT/FAA/SA-89/2] N89-24515

GROUND STATE
Path integral and operator formalism on bordered Riemann surfaces
[DE88-757229] N89-24881

GROUND STATIONS
An operational demonstration and engineering flight test of the Microwave Landing System on runway 22L at Chicago's Midway Airport
[DOT/FAA/CT-TN88/42] N89-24291

GROUND SUPPORT SYSTEMS
The European in-orbit infrastructure ground segment
N89-24340
Flight operations concept for the European in-orbit infrastructure N89-24356
Timelining and operations integration concerning APM and MTFF N89-24358
The impact of manned space flight operations on the safety and reliability aspects of ground systems requirements N89-24371
Attached Pressurized Module (APM) center for the Columbus attached pressurized module N89-24377
The Microgravity User Support Center (MUSC)
N89-24394

GROUND-AIR-GROUND COMMUNICATION
Display-based communications for advanced transport aircraft
[NASA-TM-102187] N89-24798

GUN LAUNCHERS
Capabilities and some applications of the LLNL 100-kV electric gun
[DE89-006747] N89-24408

GUST LOADS
An investigation of the Overlap between the Statistical Discrete Gust and the Power Spectral Density analysis methods
[NASA-TM-101571] N89-24310

GUSTS
An investigation of the Overlap between the Statistical Discrete Gust and the Power Spectral Density analysis methods
[NASA-TM-101571] N89-24310

GYROCOMPASSES
Geological gyrocompass
[PB89-133086] N89-24589

GYROSCOPES
Further developments in modeling digital control systems with MA-prefiltered measurements
[NASA-TP-2909] N89-24507

H

H ALPHA LINE
The relation between H-alpha and SXR emission of the flares N89-25000

HAMILTON-JACOBI EQUATION
Beam dynamics with the Hamilton-Jacobi equation
[DE89-012269] N89-24878

HAMILTONIAN FUNCTIONS
Vortex dynamics and vortex breakdown
[AD-A206470] N89-24570
Periodic and heteroclinic orbits for a periodic Hamiltonian system
[AD-A204078] N89-24862
A weak Hamiltonian finite element method for optimal control problems
[NASA-CR-185336] N89-24873

HANDEDNESS
Cerebral laterality and handedness in aviation: Performance and selection implications
[AD-A206196] N89-24787

HARMONIC RADIATION
Protection of VHF international distress frequencies from harmonic radiation due to digital television equipment
[BBC-RD-1989/1] N89-24512

HARMONICS
Subharmonic resonance in a mixing layer N89-24544

HARNESSES
Development of an integrated CAD/CAM system for wire harness fabrication N89-24842

HAZARDS
The effects of blast trauma (impulse noise) on hearing: A parametric study
[AD-A206180] N89-24786

HEARING
The effects of blast trauma (impulse noise) on hearing: A parametric study
[AD-A206180] N89-24786

HEAT
Ceramic Technology for Advanced Heat Engines Project data base
[DE89-012888] N89-24499
Is salt at fault
[AD-A206518] N89-24789

HEAT AFFECTED ZONE
Nd:YAG laser weldability of RS/PM Al-BFe-2Mo sheet
[DE89-013588] N89-24621

HEAT FLUX
Transpiration cooling of hypersonic blunt bodies with finite rate surface reactions
[NASA-CR-177516] N89-24580

HEAT PIPES
Initial characterization of a modular heat exchanger with an integral heat pipe
[NASA-TM-102097] N89-25078

HEAT RESISTANT ALLOYS
Investigations on the creep-rupture behavior of the austenitic stainless steel AISI 316-NET
[KFK-4468] N89-24479
Time dependent reliability model incorporating continuum damage mechanics for high-temperature ceramics
[NASA-TM-102046] N89-24487
Optimisation of the figure of merit of modified silicon-germanium alloys
[AD-A206420] N89-24491

HEAT SHIELDING
Hermes aerothermodynamic concept N89-24351

HEAT SOURCES
Natural convection cooling of a 3 by 3 array of rectangular protrusions in an enclosure filled with dielectric liquid: Effects of boundary conditions and component orientation
[AD-A206474] N89-24571

HEAT STORAGE
Flight experiment of thermal energy storage
[NASA-TM-102081] N89-24440

HEAT TRANSFER
Status of the direct absorption receiver panel research experiment: Salt flow and solar test requirements and plans
[DE89-010968] N89-24461
Ceramic technology for advanced heat engines project
[DE89-012890] N89-24500
Basic flow field and heat transfer studies about three cylinders of different diameter in transverse flow
N89-24564
Inlet turbulence intensity level and cross-stream distribution effects on the heat transfer in plane wall jets
[NASA-CR-183652] N89-24576
Some characteristics of bypass transition in a heated boundary layer
[NASA-TM-102126] N89-24577
Mechanics/heat-transfer relation for particle flows
[DE89-011382] N89-24584
Application of Lotus 1-2-3 to heat transfer analysis
[DE89-010463] N89-24813

HEAT TRANSMISSION
Natural convection cooling of a 3 by 3 array of rectangular protrusions in an enclosure filled with dielectric liquid: Effects of boundary conditions and component orientation
[AD-A206474] N89-24571

HEATING EQUIPMENT
Developing, testing, evaluating and optimizing solar heating and cooling systems
[DE89-011831] N89-24744

HEAVY IONS
Explosive-emitter cathode produced using the heavy ion track technique
[DE88-706304] N89-24503

HELICOPTER CONTROL
Loss of tail rotor effectiveness evaluation of the OH-58C helicopter with directional SAS (Stability Augmentation System)
[AD-A206181] N89-24309
Optimal guidance with obstacle avoidance for nap-of-the-earth flight
[NASA-CR-177515] N89-24328

HELICOPTER PERFORMANCE
Preliminary airworthiness evaluation of modified second-generation Pneumatic Boot Deicing System on a JUH-1H
[AD-A206255] N89-24289
Results of an A109 simulation validation and handling qualities study
[NASA-TM-101062] N89-24323

HELICOPTER PROPELLER DRIVE
Comparison of predicted and measured temperatures of UH-60A helicopter transmission
[NASA-TP-2911] N89-24607

HELICOPTER WAKES
Aerodynamic interaction between vortical wakes and lifting two-dimensional bodies
[NASA-TM-101074] N89-24563

HELIOSEISMOLOGY
Helioseismology and plasma physics N89-24922

HERBIG-HARO OBJECTS
High spectral resolution observations of the H2 2.12 micron line in Herbig-Haro objects
[MPE-PREPRINT-139] N89-25085

HERMES MANNED SPACEPLANE
The Ariane 5 Development Program N89-24336
Columbus: The European contribution to the International Space Station N89-24337
The Hermes Program N89-24338
Hermes user interfaces N89-24346
Overview of Ariane 5 and Hermes programs technology N89-24349
The technology contents of the first phase of the Hermes Development Program N89-24350
Hermes aerothermodynamic concept N89-24351
ECLS for Columbus and Hermes N89-24354
Fuel cell development for Hermes N89-24355
Flight operations concept for the European in-orbit infrastructure N89-24356
Hermes-MTFF rendezvous strategy and composite operations N89-24357
Servicing of the MTFF by Hermes N89-24360
Manned interventions at the MTFF: Crew workload aspects N89-24362
Safety and reliability of the Ariane 5-Hermes composite N89-24365
Hermes escape system N89-24366
Protection against ionizing radiation for the Hermes mission N89-24370
The role of the Hermes flight control center in a typical Hermes/MTFF servicing mission N89-24372
Means for preparing and recovering the Hermes space plane N89-24373
The Hermes system training concept N89-24375
The Hermes robot arm (HERA) N89-24390
Crew training aspects --- Hermes, Columbus
N89-24396
Hermes crew role N89-24401
Safety in manned space flight N89-24402
Fluidnet: A thermal and hydraulic software for the preliminary sizing of fluid loop systems
[REPT-882-440-124] N89-24425

HETERODYNING
Prototype laser-diode-pumped solid state laser transmitters
[NASA-CR-185056] N89-24601

HETEROJUNCTIONS
Vertical emitting, ring geometry, ultra-low threshold and ultra-high speed quantum well lasers for optical interconnect
[AD-A206427] N89-24603
Ultra-thin, light-trapping silicon solar cells N89-24719

HEURISTIC METHODS
Channel and switchbox routing using a greedy based channel algorithm with outward scanning technique
[AD-A206545] N89-24528

HIERARCHIES
Multidisciplinary optimization for engineering systems: Achievements and potential
[NASA-TM-101566] N89-24508
Nonlinear hierarchical substructural parallelism and computer architecture N89-24650

HIGH ELECTRON MOBILITY TRANSISTORS
Microwave characteristics of GaAs MMIC integratable optical detectors
[NASA-TM-101485] N89-24520

HIGH ENERGY ELECTRONS
High energy particles in supernova remnants and the interstellar medium N89-25108

HIGH ENERGY OXIDIZERS
Materials compatibility with oxidizer-rich gases at elevated temperatures and pressure
[NASA-CR-183647] N89-24466

HIGH LEVEL LANGUAGES
High level intelligent control of telerobotics systems
N89-24823

HIGH PASS FILTERS
Ground cluster filters for staggered pulse trains
[DOT/FAA/SA-89/2] N89-24515

HIGH POLYMERS
The effects of supercritical fluids on high performance polymers
[AD-A206515] N89-24494

HIGH POWER LASERS
A longlife, highvoltage, shortpulse generator based on optically activated Bulk Avalanche Semiconductor Switch, phase 2
[AD-A206078] N89-24527
HIGH RESOLUTION
HIRIS: NASA's high-resolution imaging spectrometer for the Earth Observing System (EOS) N89-24695
A system for high resolution 3D mapping using laser radar and requiring no beam scanning mechanisms N89-24827
HIGH TEMPERATURE
High temperature mechanical properties and microscopic examination of extruded powder aluminum
[DE89-010457] N89-24484
Solid lubricant materials for high temperatures: A review N89-24636
HIGH TEMPERATURE SUPERCONDUCTORS
Maglev vehicles and superconductor technology: Integration of high-speed ground transportation into the air travel system
[DE89-012241] N89-24619
Shock compaction of superconductors
[DE89-006744] N89-25052
On the nature of high-temperature superconductivity
[DE89-009525] N89-25053
Superconducting properties of magnetron sputtered Bi-Sr-Ca-Cu-O and Tl-Ba-Ca-Cu-O thin films
[DE89-009878] N89-25056
HIGH VACUUM
Continuous cryopump with a method for removal of solidified gases
[DE89-009760] N89-24611
HILSCH TUBES
Cut-and-connect of two antiparallel vortex tubes N89-24559
HISTORIES
Development of astrophysics from the telescope to the Sputnik N89-24911
Effects of thermal history on stress-related properties of very thin films of thermally grown silicon dioxide, SiO2
[AD-A206547] N89-25062
HOLES (ELECTRON DEFICIENCIES)
Deep levels and radiation effects in p-InP N89-24713
HOLES (MECHANICS)
A study of composite plates with holes/inclusions N89-24627
HOLOGRAPHIC INTERFEROMETRY
Holographic interferometry with an injection seeded Nd:YAG laser and two reference beams
[NASA-TM-102056] N89-24591
HOMOGENEOUS TURBULENCE
Pressure-strain-rate events in homogeneous turbulent shear flow N89-24551
Multifractal spectra in homogeneous shear flow N89-24552
Analysis of homogeneous turbulent reacting flows N89-24558
Optical propagation through a homogeneous turbulent shear flow N89-24561
HOMOJUNCTIONS
InP shallow-homojunction solar cells N89-24708
An empirical study of the performance of APMOVPE AM0 InP homojunction solar cells as a function of emitter thickness and doping, and base doping N89-24709
N/P InP homojunction solar cells with an In0.53Ga0.47As contacting layer grown by liquid phase epitaxy N89-24710
Predicted performance of InP solar cells in Cassegrainian and slats space concentrator arrays at 20 to 100 AM0, 80 to 100 C N89-24711
HOMOTOPY THEORY
An algebraic homotopy method for generating quasi-three-dimensional grids for high-speed configurations
[NASA-CR-4242] N89-24581
HOT WORKING
Effects of multiple reductions on grain refinement during hot working of alloy 718
[DE89-010426] N89-24483
HOVERING
Effect of advanced rotorcraft airfoil sections on the hover performance of a small-scale rotor model
[NASA-TP-2832] N89-24264
An investigation of V/STOL jet interactions in a crossflow
[AD-A206360] N89-24272
HOVERING STABILITY
Survey of Army/NASA rotorcraft aeroelastic stability research
[NASA-TM-101026] N89-24329
HUMAN FACTORS ENGINEERING
Cerebral laterality and handedness in aviation: Performance and selection implications
[AD-A206196] N89-24787
Human Factors in Automated and Robotic Space Systems: Proceedings of a symposium. Part 1
[NASA-CR-182495] N89-24792
Human Factors in Automated and Robotic Space Systems: Proceedings of a symposium. Part 2
[NASA-CR-182496] N89-24794
Evaluation, description and invention: Paradigms for human-computer interaction
[AD-A204617] N89-24796
Dual-arm robots for telerobotic IVA operations on the space station N89-24822
NASA information sciences and human factors program
[NASA-TM-4126] N89-25111
HUMAN PERFORMANCE
Human Factors in Automated and Robotic Space Systems: Proceedings of a symposium. Part 1
[NASA-CR-182495] N89-24792
Human Factors in Automated and Robotic Space Systems: Proceedings of a symposium. Part 2
[NASA-CR-182496] N89-24794
Brain-wave measures of workload in advanced cockpits: The transition of technology from laboratory to cockpit simulator, phase 2
[NASA-CR-4240] N89-24797
HURRICANES
Forecast of Atlantic seasonal hurricane activity for 1989 N89-24773
HYDRAULIC EQUIPMENT
Disconnects for spacecraft servicing applications N89-24832
HYDRAULIC FLUIDS
Disconnects for spacecraft servicing applications N89-24832
HYDRAULIC TEST TUNNELS
Unsteady and separated flows
[AD-A206539] N89-24572
HYDROCARBON FUELS
Liquid oxygen cooling of hydrocarbon fueled rocket thrust chambers
[NASA-TM-102113] N89-24447
HYDRODYNAMIC EQUATIONS
Relativistic MHD from two-fluid hydrodynamics (TFHD) — space plasmas N89-24931
Generation of large-scale vortices in compressible helical turbulence N89-24969
HYDRODYNAMICS
Challenges in computational statistical mechanics
[DE89-009922] N89-24567
HYDROGEN ATOMS
High spectral resolution observations of the H2 2.12 micron line in Herbig-Haro objects
[MPE-PREPRINT-139] N89-25085
HYDROGEN EMBRITTLEMENT
Space Shuttle Main Engine High Pressure Fuel Turbopump turbine blade cracking
[NASA-TM-100327] N89-24435
HYDROGEN OXYGEN ENGINES
The Pathfinder Chemical Transfer Propulsion program
[NASA-TM-102084] N89-24409
A premixed hydrogen/oxygen catalytic igniter
[NASA-CR-185113] N89-24445
HYDROGEN OXYGEN FUEL CELLS
Summary and evaluation of the Strategic Defense Initiative Space Power Architecture Study
[NASA-TM-102012] N89-24443
HYDROGEN PLASMA
Study of particle confinement in the JT-60 tokamak using skin radiative approximation model
[DE88-756574] N89-24909
HYDROGENATION
Bonding and chemistry of hydrocarbon monolayers on metal surfaces
[DE89-009311] N89-24490
Investigations of the origins of metastable, light-induced changes in hydrogenated amorphous silicon
[DE89-000890] N89-24496
HYDROLOGICAL CYCLE
Simplified climate models: Rationale and design
[DE89-012291] N89-24783
HYPERSONIC FLOW
Navier-Stokes analysis of cold scramjet-afterbody flows
[NASA-CR-184949] N89-24562
HYPERSONIC NOZZLES
Navier-Stokes analysis of cold scramjet-afterbody flows
[NASA-CR-184949] N89-24562
HYPERSONIC SPEED
Transpiration cooling of hypersonic blunt bodies with finite rate surface reactions
[NASA-CR-177516] N89-24580
HYPERSONIC VEHICLES
Thermal analysis of a hypersonic wing test structure
[NASA-CR-185319] N89-24265
An integrated aerodynamic/propulsion study for generic aero-space planes based on waverider concepts
[NASA-CR-183389] N89-24315
HYPERVELOCITY IMPACT
Capabilities and some applications of the LLNL 100-kV electric gun
[DE89-006747] N89-24408
HYSTERESIS
Water tunnel investigation of the vortex dynamics of periodically pitched wings
[AD-A206359] N89-24271
NASA Lewis Stirling engine computer code evaluation
[NASA-CR-182248] N89-24741

I

IBM COMPUTERS
Attaching IBM-compatible 3380 disks to Cray X-MP
[DE89-012383] N89-24800
ICE
A new field experiment in the Greenland ice cap to test Newton's inverse square law
[DE89-009247] N89-25091
ICE FORMATION
A computer simulation study of liquid water content adjustment based on icing cloud horizontal extent
[DOT/FAA/CT-TN89/3] N89-24288
KSC ice/frost/debris assessment for Space Shuttle Mission STS-30R
[NASA-TM-102147] N89-24412
IDENTIFYING
Space Station Freedom Structural Characterization Experiment (SCE) node code
[NASA-TM-101594] N89-25110
IGNITERS
A premixed hydrogen/oxygen catalytic igniter
[NASA-CR-185113] N89-24445
IMAGE ANALYSIS
Contribution to the estimation of precipitation in the Sahel by using satellite imagery
[SER-DI-204] N89-24782
Biooptical variability in the Greenland Sea observed with the Multispectral Airborne Radiometer System (MARS)
[NASA-CR-184856] N89-24784
IMAGE MOTION COMPENSATION
Aspects of image communication in air-to-ground systems N89-24298
IMAGE PROCESSING
Image Signal Processing for Flight Guidance
[DFVLR-MITT-88-32] N89-24295
Image signal processing for flight guidance: Overview and introduction to the main topics N89-24296
Scene reconstruction for image sequences N89-24297
Aspects of image communication in air-to-ground systems N89-24298
Bordautonomous terrain aided flight navigation in height sections close to terrain surface N89-24301
Status and trends of technological image processing possibilities N89-24306
A versatile flight experiment system for image processing N89-24307
Optimal guidance with obstacle avoidance for nap-of-the-earth flight
[NASA-CR-177515] N89-24328
Advanced MMI and image handling to support crew activities N89-24392
Hard X-ray imaging telescope development
[DE89-011647] N89-24906
IMAGE RECONSTRUCTION
Scene reconstruction for image sequences N89-24297
Aspects of image communication in air-to-ground systems N89-24298
IMAGING SPECTROMETERS
ESA's planned activities in the field of imaging spectrometry for Earth observation N89-24693
The FLI airborne imaging spectrometer: A highly versatile sensor for many applications N89-24694
HIRIS: NASA's high-resolution imaging spectrometer for the Earth Observing System (EOS) N89-24695
The activities of the British National Space Centre (BNSC) in the field of imaging spectrometry N89-24696
DFVLR activities related to imaging spectrometry N89-24697
Development of an imaging spectrometer for remote sensing: The FLI program N89-24698
Activities of CNES in the field of imaging spectrometry N89-24699
The EARSEL Imaging Spectrometry Working Group N89-24700
Imaging spectrometry at the Canada Centre for Remote Sensing N89-24701

IMAGING TECHNIQUES
Voyager at Neptune: 1989
[NASA-CR-185317] N89-24420
Two-phase flow measurements by nuclear magnetic resonance imaging
[DE89-011850] N89-24586
Imaging Spectrometry for Land Applications
[ESA-SP-1101] N89-24692
ESA's planned activities in the field of imaging spectrometry for Earth observation N89-24693
The FLI airborne imaging spectrometer: A highly versatile sensor for many applications N89-24694
HIRIS: NASA's high-resolution imaging spectrometer for the Earth Observing System (EOS) N89-24695
The activities of the British National Space Centre (BNSC) in the field of imaging spectrometry N89-24696
DFVLR activities related to imaging spectrometry N89-24697
Development of an imaging spectrometer for remote sensing: The FLI program N89-24698
Activities of CNES in the field of imaging spectrometry N89-24699
The EARSEL Imaging Spectrometry Working Group N89-24700
Imaging spectrometry at the Canada Centre for Remote Sensing N89-24701
Stabilized image system for mobile robots N89-24829
Two dimensional convolute integer technology for digital image processing N89-24830
The DARPA autonomous land vehicle: A phase 1 retrospective and a prospective for the future N89-24834
Photothermal imaging of high T(sub c) superconductor
[DE89-009644] N89-25054
The application of two-dimensional imaging to very high energy gamma ray astronomy
[DE89-013614] N89-25089

IMPACT
The impact of an IVA robot on the space station microgravity environment N89-24821

IMPACT DAMAGE
Capabilities and some applications of the LLNL 100-kV electric gun
[DE89-006747] N89-24408

IMPACT LOADS
Transient analysis techniques in performing impact and crash dynamic studies N89-24658

IMPACT STRENGTH
Impact and penetration resistance of fibrous composites
[AD-A206417] N89-24454

IMPACT TESTS
Capabilities and some applications of the LLNL 100-kV electric gun
[DE89-006747] N89-24408
Dynamics and static behavior of metal gussets in cask impact limiters
[DE89-011879] N89-24683

IMPURITIES
An empirical study of the performance of APMOVPE AM0 InP homojunction solar cells as a function of emitter thickness and doping, and base doping N89-24709
Impurity accumulation studies in pellet-refuelled ASDEX discharges N89-25039
The low energy neutral fluxes and their impurity production at the walls of ASDEX N89-25043
Measurements of the flux of metallic impurities to the ASDEX divertor plates N89-25046
Material transport at the vessel walls of the divertor tokamak ASDEX N89-25047
Universal reduction of T(subc) in strong coupling superconductors due to Anderson/Kondo impurities
[DE89-011225] N89-25071

IN-FLIGHT MONITORING
Lightning inflight study onboard a Transall aircraft. Definition of the onboard instruments
[ONERA-RF-19/7234-PY] N89-24777

INCIDENCE
Analysis of the boundary layer of a delta wing in incidence
[CERT-RT-OA-26/5025-AYD] N89-24274

INCIDENT RADIATION
Concentration of off-axis radiation by solar concentrators for space power
[NASA-TM-102052] N89-24438

INCLUSIONS
A study of composite plates with holes/inclusions N89-24627

INCOMPRESSIBLE FLOW
Inflow/outflow boundary conditions and global dynamics of spatial mixing layers N89-24540
Dynamics of coherent structures in a plane mixing layer N89-24543
A second-order projection method for the incompressible Navier Stokes equations on quadrilateral grids
[DE89-010242] N89-24585
Comparison of compressible and incompressible models of reconnection N89-24982

INCOMPRESSIBLE FLUIDS
Numerical study of turbulent secondary flows in curved ducts
[NASA-CR-181830] N89-24568

INDENTATION
Viscosity of solids determined by shock wave action on hemispherical indentations
[DE89-008035] N89-24510

INDIUM
N/P InP homojunction solar cells with an In0.53Ga0.47As contacting layer grown by liquid phase epitaxy N89-24710
Development of tandem cells consisting of GaAs single crystal and CuInSe2/CdZnS polycrystalline thin films N89-24717
Directions for further development of GaAs/CuInSe2 thin film tandem cells N89-24718
A three solar cell system based on a self-supporting, transparent AlGaAs top solar cell N89-24723

INDIUM PHOSPHIDES
Progress in indium phosphide solar cell research N89-24707
InP shallow-homojunction solar cells N89-24708
Predicted performance of InP solar cells in Cassegrainian and slats space concentrator arrays at 20 to 100 AM0, 80 to 100 C N89-24711
Modelling and design of high performance indium phosphide solar cells N89-24712
Deep levels and radiation effects in p-InP N89-24713
Encapsulated diffusion of sulphur into InP N89-24714

INELASTIC SCATTERING
Inelastic scattering from liquid He4 in aerogel glass
[DE89-012381] N89-24587

INFLATABLE STRUCTURES
Inflatable end effector tools N89-24839

INFORMATION PROCESSING (BIOLOGY)
Brain-wave measures of workload in advanced cockpits: The transition of technology from laboratory to cockpit simulator, phase 2
[NASA-CR-4240] N89-24797

INFORMATION SYSTEMS
EVA Information System: A modern workstation in space N89-24388
NASA information sciences and human factors program
[NASA-TM-4126] N89-25111

INFORMATION TRANSFER
Display of flight guidance information in the aircraft cockpit N89-24305

INFRARED ABSORPTION
Simulation studies of improved sounding systems
[NASA-CR-185322] N89-24758

INFRARED ASTRONOMY
Physical conditions in molecular clouds derived from sub-mm and far-IR spectroscopic observations
[MPE-PREPRINT-135] N89-25082
First detection of SO2 and CH3OH emission and one unidentified line near 800 GHz
[MPE-PREPRINT-142] N89-25086

INFRARED ASTRONOMY SATELLITE
Autonomous geostationary stationkeeping system optimization and validation
[REPT-882-440-117] N89-24423
ISOCAM, ISO optical subsystem cryogenics, Aerospatiale, Cannes, France in-house R and D status
[REPT-882-440-123] N89-24429
Materials for cryogenically cooled infrared telescopes
[REPT-882-440-119] N89-25083
Infrared studies of active galaxies N89-25087

INFRARED LASERS
Development of mid-infrared solid state lasers for spaceborne lidar
[NASA-CR-185012] N89-24599
Applications of infrared laser spectroscopy to laser chemistry and laser development
[DE89-011196] N89-24604

INFRARED STARS
The Orion molecular cloud and star forming region
[MPE-PREPRINT-140] N89-25094

INFRARED TELESCOPES
Autonomous geostationary stationkeeping system optimization and validation
[REPT-882-440-117] N89-24423
State of the art of ISO
[REPT-882-440-121] N89-24424
ISOCAM, ISO optical subsystem cryogenics, Aerospatiale, Cannes, France in-house R and D status
[REPT-882-440-123] N89-24429
Materials for cryogenically cooled infrared telescopes
[REPT-882-440-119] N89-25083

INFRARED WINDOWS
Estimating the outgoing longwave radiation from the Meteosat infrared window and water vapor bands
[ETN-89-94533] N89-24762

INITIATION
Modeling thermal-mechanical processes associated with the initiation and combustion of granular energetic materials
[DE89-007145] N89-24472

INJECTORS
A premixed hydrogen/oxygen catalytic igniter
[NASA-CR-185113] N89-24445

INLET FLOW
Interaction mechanisms between tip leakage flow and the passage vortex in a linear turbine rotor cascade
[NAL-TR-983T] N89-24536

INLET NOZZLES
Space Shuttle Main Engine structural analysis and data reduction/evaluation. Volume 6: Primary nozzle diffuser analysis
[NASA-CR-183669] N89-24437

INPUT/OUTPUT ROUTINES
The computational structural mechanics testbed architecture. Volume 5: The Input-Output Manager DMGASP
[NASA-CR-178388] N89-24637
File concepts for parallel I/O
[NASA-CR-181843] N89-24816

INSPECTION
KSC ice/frost/debris assessment for Space Shuttle Mission STS-30R
[NASA-TM-102147] N89-24412
Laser-induced-fluorescence inspection of polyurethane and related materials, phase 1
[AD-A206423] N89-24492

INTEGRATED CIRCUITS
Establishment of an electron beam lithography facility
[AD-A206215] N89-24332
Microwave characteristics of GaAs MMIC integratable optical detectors
[NASA-TM-101485] N89-24520
Electrooptical feed and control in microwave applications
[FOA-C-30514-3.2] N89-24531
Embedded conductors by electrochemical planarization
[DE89-011632] N89-24534

INTERACTIONAL AERODYNAMICS
Aerodynamic interaction between vortical wakes and lifting two-dimensional bodies
[NASA-TM-101074] N89-24563

INTERACTIVE CONTROL
Landscape-related position finding for flying systems N89-24302

INTERFACES
High-resolution electron microscopy of metal/ceramic interfaces
[DE89-012396] N89-24498
Pedagogical issues in developing a man-machine interface for an intelligent tutoring system N89-24855
An intelligent fiberoptic data bus for fly-by-light applications
[NAL-TM-SE-8707] N89-24901

INTERFACIAL TENSION
Incorporation of surface tension into the structural finite element code SANCHO
[DE89-011354] N89-24616
Analytic theory for the determination of velocity and stability of bubbles in a Hele-Shaw cell. Part 2: Stability
[NASA-CR-181837] N89-24883

INTERFERENCE GRATING
Vertical emitting, ring geometry, ultra-low threshold and ultra-high speed quantum well lasers for optical interconnect
[AD-A206427] N89-24603

INTERGALACTIC MEDIA
Infrared studies of active galaxies N89-25087

INTERNATIONAL COOPERATION
US military aircraft coproduction with Japan
[AD-A206430] N89-24263
Columbus: The European contribution to the International Space Station N89-24337
Scientific utilization of the European space infrastructure and the International Space Station N89-24380
The utilization of the European pressurized module for non-European experiments --- Columbus N89-24399

INTERPLANETARY MAGNETIC FIELDS
Aspects of three-dimensional magnetic reconnection N89-24975

INTERSECTIONS
Improved marking of taxiway intersections for Instrument Flight Rules (IFR) operations
[DOT/FAA/CT-TN89/23] N89-24330

INTERSTELLAR GAS
Gas flow in and around bars --- galaxies N89-24965
The circum-nuclear disk
[MPE-PREPRINT-132] N89-25093
INTERSTELLAR MAGNETIC FIELDS
The case for a primordial galactic field N89-24939
High energy particles in supernova remnants and the interstellar medium N89-25108
INTERSTELLAR MATTER
Shock-associated plasma density fluctuations in the interstellar medium N89-24933
The circum-nuclear disk
[MPE-PREPRINT-132] N89-25093
INVISCID FLOW
Conservative treatment of boundary interfaces for overlaid grids and multi-level grid adaptations
[NASA-TM-102080] N89-24269
A zonal method for modeling powered-lift aircraft flow fields
[NASA-CR-177521] N89-24287
ION ATOM INTERACTIONS
Charge exchange transition probability for collisions between unlike ions and atoms within the adiabatic approximation
[NASA-TM-101559] N89-25104
ION BEAMS
Semiempirical studies of atomic structure
[DE89-011419] N89-24894
MEQALAC: A 1 MeV multi-channel RF-accelerator for light ions N89-25034
ION CYCLOTRON RADIATION
ICRF antenna designs for CIT and Alcator C-Mod
[DE89-011579] N89-24521
ION ENGINES
Development of the cryopanel for tests of xenon ion thrusters
[NAL-TR-981] N89-24431
Performance of large area xenon ion thrusters for orbit transfer missions
[NASA-TM-102049] N89-24436
ION EXCHANGE MEMBRANE ELECTROLYTES
US fuel cell research and applications, 1960--1989
[DE89-012244] N89-24745
ION IMPLANTATION
Role of alloying additions in the oxidation-sulfidation of Fe-base alloys
[DE89-009825] N89-24473
Hydrogen ion-driven permeation in carbonaceous films
[DE89-005271] N89-24485
InP shallow-homojunction solar cells N89-24708
ION PROPULSION
Development of the cryopanel for tests of xenon ion thrusters
[NAL-TR-981] N89-24431
Performance of large area xenon ion thrusters for orbit transfer missions
[NASA-TM-102049] N89-24436
ION PUMPS
Development of the cryopanel for tests of xenon ion thrusters
[NAL-TR-981] N89-24431
IONIZATION
Multiplexed electronically programmable multimode ionization detector for chromatography
[DE89-009758] N89-24465
Semiclassical matrix-elements of high-charge ions
[DE89-009258] N89-24890
Electron transfer, ionization, and excitation in atomic collisions
[DE89-010046] N89-24891
Study of chemical reaction models for high enthalpy flow of air
[NAL-TR-982] N89-25072
IONIZATION GAGES
Lightning inflight study onboard a Transall aircraft. Definition of the onboard instruments
[ONERA-RF-19/7234-PY] N89-24777
IONOPAUSE
The variable nature of the comet-solar wind interaction N89-25100
IONOSPHERIC PROPAGATION
Plasma and propagation in auroral and polar ionosphere
[ETN-89-94519] N89-24761
IONS
Semiclassical matrix-elements of high-charge ions
[DE89-009258] N89-24890
IRIDIUM
Oxide-bound transition metal complexes for methane activation
[PB89-138614] N89-24464
IRON ALLOYS
Role of alloying additions in the oxidation-sulfidation of Fe-base alloys
[DE89-009825] N89-24473
Effects of multiple reductions on grain refinement during hot working of alloy 718
[DE89-010426] N89-24483
Nd:YAG laser weldability of RS/PM Al-BFe-2Mo sheet
[DE89-013588] N89-24621
IRON COMPOUNDS
Magneto-optical studies of metastable 3D-transition metal films
[DE89-009836] N89-24474
IRRADIATION
Two dimensional analysis of a NOVETTE laser generated stress-impulse experiment
[DE89-009909] N89-24600
Radiation resistance studies of amorphous silicon films N89-24738
ISOTROPIC TURBULENCE
Energy transfer in isotropic turbulence at low Reynolds numbers N89-24553
ITALIAN SPACE PROGRAM
Scientific utilization of the European space infrastructure and the International Space Station N89-24380
Italian scientific projects related to manned activity in space N89-24382
ITERATIVE SOLUTION
Comparison of basis function and iteration solutions to the Fredholm integral equation of the first kind
[AD-A206156] N89-24969

J

JET AIRCRAFT NOISE
Calculation of aircraft noise in the vicinity of civil airports by a simultion procedure
[MPIS-7/1988] N89-24887
JET CONTROL
Modeling transient thermal behavior in a thrust vector control jet vane
[AD-A206532] N89-24441
JET FLOW
Numerical study on laminar circular jet of carbonic acid gas discharging into stagnant air
[DE88-757249] N89-24565
JET IMPINGEMENT
An investigation of V/STOL jet interactions in a crossflow
[AD-A206360] N89-24272
JET VANES
Modeling transient thermal behavior in a thrust vector control jet vane
[AD-A206532] N89-24441
JOINED WINGS
Experimental aerodynamic characteristics of a joined-wing research aircraft configuration
[NASA-TM-101083] N89-24285
JOINTS (JUNCTIONS)
Dynamics of articulated structures N89-24664
Nonlinear characteristics of joints as elements of multi-body dynamic systems N89-24668
Characterization of the bending stiffness of large space structure joints
[NASA-TM-101565] N89-24676
Measurement of bond strength at metal/ceramic interfaces
[DE89-011638] N89-24682
Representations of a linkage mechanism based on dual number matrices
[DE88-757273] N89-24857
A comparison of two real-time control schemes for redundant robots with bounded joint velocities
[DE89-002974] N89-24861
JUPITER ATMOSPHERE
Magnetic neutral lines in Jupiter's nightside magnetosphere N89-24918

K

K-EPSILON TURBULENCE MODEL
Inlet turbulence intensity level and cross-stream distribution effects on the heat transfer in plane wall jets
[NASA-CR-183652] N89-24576
Turbulent flow in a 180 deg bend: Modeling and computations
[NASA-CR-4141] N89-24579
KALMAN FILTERS
Flight control system for the CRCA (Control Reconfigurable Combat Aircraft) using a command generator tracker with PI (Plus Integral) feedback and Kalman filter, volume 2
[AD-A206202] N89-24325
KAONS
A study of K sup deg sec, lambda and lambda bar production in 60 and 200 GeV nucleon OAu and pAu collisions with a streamer chamber detector at the CERN SPS
[MPE-PAE/EXP.EL-198] N89-24900
Kaon-nucleus scattering
[NASA-TP-2920] N89-25103
KAPTON (TRADEMARK)
Advanced photovoltaic solar array development N89-24716
KARHUNEN-LOEVE EXPANSION
Sampling inhomogeneous turbulent fields N89-24548
KARMAN VORTEX STREET
Interaction of Karman vortex-street with an elliptical leading-edge N89-24268
KERR MAGNETOOPTICAL EFFECT
Magneto-optical studies of metastable 3D-transition metal films
[DE89-009836] N89-24474
KINEMATIC EQUATIONS
Representations of a linkage mechanism based on dual number matrices
[DE88-757273] N89-24857
Computational method of the inverse kinematics via simplified algebraic equation
[DE88-757269] N89-24866
KINEMATICS
Nonlinear hierarchical substructural parallelism and computer architecture N89-24650
Adaptive methods, rolling contact, and nonclassical friction laws N89-24651
Dynamics of articulated structures N89-24664
Constraint elimination in dynamical systems N89-24667
A new approach to robot kinematic analysis N89-24833
Computational method of the inverse kinematics via simplified algebraic equation
[DE88-757269] N89-24866
Analytic theory for the determination of velocity and stability of bubbles in a Hele-Shaw cell. Part 2: Stability
[NASA-CR-181837] N89-24883
Aspects of three-dimensional magnetic reconnection N89-24975
KINETIC ENERGY
Turbulent flow in a 180 deg bend: Modeling and computations
[NASA-CR-4141] N89-24579
KINETIC THEORY
Experiments on liquid-vapour phase change between plane liquid surfaces. Part 2: Observations of large temperature jumps near the interfaces
[NAL-TM-FM-8805] N89-24462
Global kinetic theory of astrophysical jets N89-24954
KINETICS
Kinetic simulation of magnetic reconnection in the presence of shear N89-24985
KLEIN-GORDON EQUATION
Factorization of the relativistic Pauli equation in the presence of a gravitational field
[DE88-704749] N89-25090
KNOWLEDGE REPRESENTATION
A knowledge representation scheme for a robotic land vehicle route planner N89-24853
KNUDSEN GAGES
Free radical-surface interactions using multiphoton ionization of free radicals
[AD-A206257] N89-24892

L

LAGRANGIAN EQUILIBRIUM POINTS
The gravitational many-body PPN Lagrangian, Lorentz invariance and the strong equivalence principle to second order N89-24765
LAKES
The relationship between in-lake sulfate concentration and estimates of atmospheric sulfur deposition for subregions of the eastern lake survey
[DE89-009868] N89-24749
LAMINAR BOUNDARY LAYER
Boundary layer response to an unsteady turbulent environment
[AD-A206578] N89-24273
Some characteristics of bypass transition in a heated boundary layer
[NASA-TM-102126] N89-24577
LAMINAR FLOW
Turbulence characteristics inside a turbulent spot in plane Poiseuille flow N89-24554
Numerical study on laminar circular jet of carbonic acid gas discharging into stagnant air
[DE88-757249] N89-24565

LAMINATES
Response of layered structures to thermal radiation pulses
[AD-A206355] N89-24453
Nonlinear response of a blade-stiffened graphite-epoxy panel with a discontinuous stiffener: Work in progress N89-24641
Improved analysis of laminated heterogeneous beams and associated formulation of a new finite element method N89-24672
LANDFILLS
The importance of climatological variability and the rate at which waste is added to modeling water budget of landfills
[DE89-008917] N89-24747
LANDING AIDS
Design of automated system for management of arrival traffic
[NASA-TM-102201] N89-24290
LANDING SIMULATION
Numerical simulation of feedback control of aerodynamic configurations in steady and unsteady ground effects N89-24326
LANGUAGE PROGRAMMING
Neutral file data exchange between simulators and robots N89-24824
Space languages: Solving the classic scheduling problem in Ada and Lisp N89-24826
LAPLACE TRANSFORMATION
WADA1: FORTRAN program for wave diffraction analysis, version 1
[AD-A206533] N89-24808
Fractional-order feedback in linear systems
[AD-A206241] N89-24859
LARGE SPACE STRUCTURES
Some comments on global-local analyses N89-24644
Recent developments in deployment analysis simulation using a multi-body computer code N89-24660
Dynamic analysis of space structures including elastic, multibody, and control behavior N89-24661
Characterization of the bending stiffness of large space structure joints
[NASA-TM-101565] N89-24676
LASER APPLICATIONS
Applications of infrared laser spectroscopy to laser chemistry and laser development
[DE89-011196] N89-24604
LASER BEAMS
Two dimensional analysis of a NOVETTE laser generated stress-impulse experiment
[DE89-009909] N89-24600
Optical chaos
[DE89-009392] N89-24903
LASER DOPPLER VELOCIMETERS
An experimental study of a three-dimensional thrust augmenting ejector using laser Doppler velocimetry
[NASA-CR-177531] N89-24569
A remote laser-probing system for combustion measurements
[NAL-TR-979] N89-24598
LASER INDUCED FLUORESCENCE
Laser-induced-fluorescence inspection of polyurethane and related materials, phase 1
[AD-A206423] N89-24492
LASER MATERIALS
Prototype laser-diode-pumped solid state laser transmitters
[NASA-CR-185056] N89-24601
Cooperative phenomena for new coherent radiation sources
[AD-A206368] N89-24602
Applications of infrared laser spectroscopy to laser chemistry and laser development
[DE89-011196] N89-24604
LASER OUTPUTS
Atmospheric effects on laser propagation
[DE89-012287] N89-24606
LASER PLASMA INTERACTIONS
The effect of non-Maxwellian electron distributions on the intensity ratio of resonance to satellite lines
[DE89-006745] N89-24907
LASER PLASMAS
Semiempirical studies of atomic structure
[DE89-011419] N89-24894
The effect of non-Maxwellian electron distributions on the intensity ratio of resonance to satellite lines
[DE89-006745] N89-24907
LASER PUMPING
Development of mid-infrared solid state lasers for spaceborne lidar
[NASA-CR-185012] N89-24599
Selective pair luminescence of magnesium in gallium arsenide dissertation
[AD-A206160] N89-25058
LASER RANGE FINDERS
Tele-autonomous control involving contacts: The applications of a high precision laser line range sensor
[NASA-CR-184995] N89-24509
Determination of station coordinates, earth rotation and plate motions from LAGEOS laser ranging: 1983-1986
[NAL-TR-980T] N89-24753
LASER SPECTROSCOPY
Applications of infrared laser spectroscopy to laser chemistry and laser development
[DE89-011196] N89-24604
LASER WELDING
Nd:YAG laser weldability of RS/PM Al-BFe-2Mo sheet
[DE89-013588] N89-24621
LASERS
Cooperative phenomena for new coherent radiation sources
[AD-A206368] N89-24602
LASING
Applications of infrared laser spectroscopy to laser chemistry and laser development
[DE89-011196] N89-24604
LATTICE PARAMETERS
X-ray investigations of ceramic high Tc superconductors under high pressure
[KFK-4482] N89-25064
LATTICE VIBRATIONS
Theoretical microcontact spectra of metal electron-phonon coupling
[DE88-706280] N89-25067
LAUNCH VEHICLES
Report of the committee on a commercially developed space facility
[NASA-CR-185383] N89-24406
LEAD ACID BATTERIES
Analysis of life cycle costs for electric vans with advanced battery systems
[DE89-009807] N89-24526
ERC nickel cadium battery performance tests and comparisons with lead-acid batteries
[DE89-009753] N89-24535
LEADING EDGES
Interaction of Karman vortex-street with an elliptical leading-edge N89-24268
Experimental aerodynamic characteristics of a joined-wing research aircraft configuration
[NASA-TM-101083] N89-24285
LEAKAGE
Interaction mechanisms between tip leakage flow and the passage vortex in a linear turbine rotor cascade
[NAL-TR-983T] N89-24536
LEAST SQUARES METHOD
Aeroservoelastic modeling and applications using minimum-state approximations of the unsteady aerodynamics
[NASA-TM-101574] N89-24308
Surface coordinate generation in three-dimensional arbitrary shapes by solving a set of second order elliptic partial differential equations N89-24875
LIFE (DURABILITY)
Review of the environmental effects of the Space Station Freedom photovoltaic power module
[NASA-TM-102076] N89-24418
Time dependent reliability model incorporating continuum damage mechanics for high-temperature ceramics
[NASA-TM-102046] N89-24487
Contamination effects of GPS Navstar solar array performance N89-24734
LIFE CYCLE COSTS
Superfluid Helium Tanker Study (SFHT)
[NASA-CR-172114] N89-24415
A methodology for commonality analysis, with applications to selected space station systems
[NASA-TM-100364] N89-24421
Space Station Freedom electrical power system hardware commonality with the United States Polar Platform
[NASA-TM-102074] N89-24439
Analysis of life cycle costs for electric vans with advanced battery systems
[DE89-009807] N89-24526
LIFE SUPPORT SYSTEMS
ECLS for Columbus and Hermes N89-24354
Technology requirements for advanced NASA missions N89-24705
The AAMRL (Armstrong Aerospace Medical Research Laboratory) biodynamics data bank
[AD-A206139] N89-25074
LIFT
Aerodynamics of a lifting rotor due to near field unsteady effects N89-24267
Use of Navier-Stokes methods to predict circulation control airfoil performance
[AD-A206242] N89-24270
LIFTING BODIES
Unsteady Aerodynamics, volume 2
[VKI-1988-07-VOL-2] N89-24281
Numerical methods for unsteady flows N89-24282
Numerical simulation of feedback control of aerodynamic configurations in steady and unsteady ground effects N89-24326
LIFTING ROTORS
Aerodynamics of a lifting rotor due to near field unsteady effects N89-24267
LIGHT ALLOYS
Bonded assemblies behavior laws: Light alloys/elastoplastic adhesive
[ETCA-88-R-001] N89-24456
LIGHT BEAMS
Optical propagation through a homogeneous turbulent shear flow N89-24561
LIGHT MODULATION
The current technological status of spatial light modulators
[AD-A206328] N89-24905
LIGHTNING
Ground vibration test of the Foudre A04 Transall aircraft
[REPT-20/7234-PY-382-R] N89-24311
Lightning inflight study onboard a Transall aircraft. Definition of the onboard instruments
[ONERA-RF-19/7234-PY] N89-24777
LINE SPECTRA
The FLI airborne imaging spectrometer: A highly versatile sensor for many applications N89-24694
HIRIS: NASA's high-resolution imaging spectrometer for the Earth Observing System (EOS) N89-24695
Imaging spectrometry at the Canada Centre for Remote Sensing N89-24701
First detection of SO2 and CH3OH emission and one unidentified line near 800 GHz
[MPE-PREPRINT-142] N89-25086
LINEAR ACCELERATORS
Engineering design of the interaction waveguide for high-power accelerator-driven microwave free-electron lasers
[DE89-011896] N89-24605
MEQALAC: A 1 MeV multi-channel RF-accelerator for light ions N89-25034
LINEAR ENERGY TRANSFER (LET)
Characterizing the energy deposition events produced by trapped protons in low earth orbit
[DE89-011218] N89-24893
LINEAR EQUATIONS
On the equivalence of a class of inverse decomposition algorithms for solving systems of linear equations
[NASA-TM-102036] N89-24865
LINEAR PROGRAMMING
Generalized solution for the optimal prehension state using end effectors with multi-articulated fingers N89-24609
LINEAR QUADRATIC GAUSSIAN CONTROL
Wind tunnel tests on flutter control of a high-aspect-ratio cantilevered wing
[NAL-TR-978] N89-24321
Objective and constraint functions for the analysis and design of robust control systems N89-24615
LINEAR QUADRATIC REGULATOR
On the dynamics and control of the Spacecraft Control Laboratory Experiment (SCOLE) class of offset flexible systems N89-24426
LINEAR SYSTEMS
Totally parallel multilevel algorithms
[NASA-CR-185404] N89-24818
LINES OF FORCE
Magnetic neutral lines in Jupiter's nightside magnetosphere N89-24918
A 2-D and 3-D simulation study of multiple X line reconnection N89-25023
LINKAGES
Application of finite-element methods to dynamic analysis of flexible spatial and co-planar linkage systems, part 2 N89-24663
Representations of a linkage mechanism based on dual number matrices
[DE88-757273] N89-24857
LIQUID HELIUM
Superfluid Helium Tanker Study (SFHT)
[NASA-CR-172114] N89-24415
Inelastic scattering from liquid He4 in aerogel glass
[DE89-012381] N89-24587
LIQUID METALS
Computer simulation of copper in the liquid phase and the sputtering of liquid copper by one KeV argon ions
[AD-A206264] N89-24476
LIQUID NITROGEN
X-ray photoelectron spectroscopy study of samples in the Y-Ba-Cu-O system
[AD-A206260] N89-25060

LIQUID OXYGEN
Liquid oxygen cooling of hydrocarbon fueled rocket thrust chambers
[NASA-TM-102113] N89-24447
LIQUID PHASE EPITAXY
N/P InP homojunction solar cells with an In0.53Ga0.47As contacting layer grown by liquid phase epitaxy N89-24710
A three solar cell system based on a self-supporting, transparent AlGaAs top solar cell N89-24723
Gallium Arsenide welded panel technology for advanced spaceflight applications N89-24731
LIQUID PROPELLANT ROCKET ENGINES
Technology and design method evolution of cryogenic propulsion systems: Example of the main Ariane 5 stage N89-24353
Pressure-volume properties of metallic bellows
[NASA-TM-100365] N89-24422
Liquid oxygen cooling of hydrocarbon fueled rocket thrust chambers
[NASA-TM-102113] N89-24447
LIQUID ROCKET PROPELLANTS
Materials compatibility with oxidizer-rich gases at elevated temperatures and pressure
[NASA-CR-183647] N89-24466
LIQUID SURFACES
Natural convection cooling of a 3 by 3 array of rectangular protrusions in an enclosure filled with dielectric liquid: Effects of boundary conditions and component orientation
[AD-A206474] N89-24571
LIQUID-VAPOR INTERFACES
Experiments on liquid-vapour phase change between plane liquid surfaces. Part 2: Observations of large temperature jumps near the interfaces
[NAL-TM-FM-8805] N89-24462
LIQUIDS
Incorporation of surface tension into the structural finite element code SANCHO
[DE89-011354] N89-24616
LITHIUM ALLOYS
Weldability and microstructural characterization of Al-Li alloys
[DE89-010183] N89-24478
LOADS (FORCES)
Aerodynamics of a lifting rotor due to near field unsteady effects N89-24267
Piezoelectric film load cell robot collision detector
[DE89-010117] N89-24592
Real time control for NASA robotic gripper
[NASA-CR-184978] N89-24608
Analysis of interlaminar fracture in composites under combined loading
[NASA-CR-185055] N89-24674
Investigation of structural behavior of candidate Space Station structure
[NASA-CR-181746] N89-24678
Results of the Round Robin on opening-load measurement conducted by ASTM Task Group E24.04.04 on Crack Closure Measurement and Analysis
[NASA-TM-101601] N89-24679
The impact of an IVA robot on the space station microgravity environment N89-24821
LOCAL AREA NETWORKS
The Columbus crew communication subsystem and the on board local area network N89-24397
LOGIC PROGRAMMING
Formal verification of AI software
[NASA-CR-181827] N89-24811
LOGICAL ELEMENTS
Real-time system: Specification and verification
[AD-A206467] N89-24807
LOGISTICS MANAGEMENT
Integrated approach for the logistic support of the European in orbit infrastructure from the nineties onwards N89-24359
LONGITUDINAL WAVES
On the refraction of longitudinal waves in compressible media
[DE89-012922] N89-24588
LORENTZ TRANSFORMATIONS
The gravitational many-body PPN Lagrangian, Lorentz invariance and the strong equivalence principle to second order N89-24765
LOSSES
Effects of main-sequence mass loss on stellar and galactic chemical evolution
[DE89-011399] N89-25098
LOW ASPECT RATIO WINGS
Computational design of low aspect ratio wing-winglet configurations for transonic wind-tunnel tests
[NASA-CR-185016] N89-24266
LOW PASS FILTERS
Ground cluster filters for staggered pulse trains
[DOT/FAA/SA-89/2] N89-24515
LOW REYNOLDS NUMBER
Analysis of the wake behind a propeller using the finite element method with a two-equation turbulence model N89-24286
Energy transfer in isotropic turbulence at low Reynolds numbers N89-24553
LOW TEMPERATURE
On specimen shape effects and the ductility of porous metals
[AD-A206216] N89-24475
LUMINOSITY
A study of the Southern Supercluster N89-25088
Self-consistent models of spherical accretion onto black holes N89-25095
LUNAR BASES
Technology requirements for advanced NASA missions N89-24705

M

MACH NUMBER
The role of whistler oscillations in the formation of the structure of high Mach number collisionless shock N89-24936
Quasi-perpendicular collisionless high Mach number shocks N89-24937
MACHINE LEARNING
Neuromorphic learning of continuous-valued mappings in the presence of noise: Application to real-time adaptive control
[NASA-TM-101999] N89-24856
MAGELLAN PROJECT (NASA)
Space Shuttle to deploy Magellan planetary science mission
[NASA-NEWS-RELEASE-89-86] N89-24334
Magellan: The unveiling of Venus
[NASA-CR-185018] N89-24419
MAGELLAN SPACECRAFT (NASA)
Magellan: The unveiling of Venus
[NASA-CR-185018] N89-24419
MAGNESIUM
Selective pair luminescence of magnesium in gallium arsenide dissertation
[AD-A206160] N89-25058
MAGNETIC DISKS
Attaching IBM-compatible 3380 disks to Cray X-MP
[DE89-012383] N89-24800
MAGNETIC DISTURBANCES
Thermal instability in a stratified plasma N89-24924
MAGNETIC ENERGY STORAGE
The equilibrium and stability of solar coronal magnetic fields N89-25102
MAGNETIC FIELD CONFIGURATIONS
Adiabatic, chaotic and quasi-adiabatic charged particle motion in two-dimensional magnetic field reversals N89-24942
Model of the chromosphere spicule formation N89-24966
Nonlinear dynamics of the drift tearing-mode N89-24979
Three-dimensional reconnection from a global viewpoint N89-24988
Generation and non-equilibrium of solar atmospheric magnetic fields N89-24989
Note on an apparent highly-sheared magnetic field structure --- Sun N89-24997
The evolution of MHD-perturbations in the intersection region of two separatrix planes N89-25011
Measurements of magnetic field of superconducting solenoid
[DE88-706323] N89-25068
MAGNETIC FIELD RECONNECTION
Proceedings of an International School and Workshop on Reconnection in Space Plasma, volume 2
[ESA-SP-285-VOL-2] N89-24974
Aspects of three-dimensional magnetic reconnection N89-24975
Relation between global and local aspects of reconnection --- magnetic fields N89-24976
Noise-free neutral sheets N89-24977
Reconnection instability in collisionless plasma N89-24978
Reconnection and microturbulence N89-24980
Comparison of compressible and incompressible models of reconnection N89-24982
Magnetic reconnection near a stagnation point N89-24983
Magnetic reconnection simulation using the 2.5 D electromagnetic direct implicit code AVANTI N89-24984
Kinetic simulation of magnetic reconnection in the presence of shear N89-24985
Particle simulation of magnetic reconnection in collision-free plasma sheets N89-24986
Magnetic energy conversion on the sun N89-24987
Three-dimensional reconnection from a global viewpoint N89-24988
Particle acceleration by magnetic reconnection and fast magnetosonic shock waves in solar flares N89-24993
Flare-type plasma processes and explosive disruption of pinch current sheets N89-25008
Current sheet structure at different stages of magnetic reconnection N89-25009
Impulsive heating plasma turbulence and magnetic reconnection inside current sheets N89-25010
The evolution of MHD-perturbations in the intersection region of two separatrix planes N89-25011
Spontaneous and forged reconnection in a magnetic type-X structure N89-25012
Magnetotail reconnection, MHD theory and simulations N89-25013
The role of magnetic reconnection in magnetotail plasmoid dynamics N89-25014
Broadband electrostatic waves as a consequence of magnetotail reconnection N89-25017
ELF plasma turbulence observed by Prognoz-8 in plasma jets in the magnetospheric tail N89-25020
Flux transfer events: Reconnection without separators --- magnetopause N89-25021
Multiple X line reconnection at the dayside magnetopause N89-25022
A 2-D and 3-D simulation study of multiple X line reconnection N89-25023
The role of the magnetic reconnection in the solar wind/magnetosphere interaction N89-25024
Impulsive reconnection of the skewed magnetic fields at the magnetopause as a MHD model N89-25025
The structure of the reconnection layer in the Petschek reconnection model: Theory and application to the earth's magnetopause N89-25026
A model of the reconnection pattern at the heliopause N89-25027
On particle energization by magnetic field line reconnection in extragalactic jets N89-25028
Speculation on the origin of X-ray emission in early-type stars N89-25029
MAGNETIC FIELDS
Numerical methods for stellarator optimization
[DE89-012342] N89-25050
Measurements of magnetic field of superconducting solenoid
[DE88-706323] N89-25068
Black hole driven winds N89-25096
The equilibrium and stability of solar coronal magnetic fields N89-25102
MAGNETIC FLUX
MHD-waves and their nonlinear interaction in a plasma with magnetic flux tubes N89-24921
Coronal magnetic field strengths determined from fiber bursts N89-25002
Flux transfer events: Reconnection without separators --- magnetopause N89-25021
Multiple X line reconnection at the dayside magnetopause N89-25022
MAGNETIC LEVITATION VEHICLES
Maglev vehicles and superconductor technology: Integration of high-speed ground transportation into the air travel system
[DE89-012241] N89-24619
MAGNETIC MEASUREMENT
Possibilities and problems of the interpretation of solar magnetograph measurements and applications to flare-active regions N89-24995
MAGNETIC SIGNATURES
Possibilities and problems of the interpretation of solar magnetograph measurements and applications to flare-active regions N89-24995
Estimation of sunspot magnetic field parameters using the superpenumbral topology N89-24996
Note on an apparent highly-sheared magnetic field structure --- Sun N89-24997
MAGNETIC STORMS
An analogy between magnetospheric substorms and solar flares: New version N89-25016
MAGNETO-OPTICS
Magneto-optical studies of metastable 3D-transition metal films
[DE89-009836] N89-24474
The current technological status of spatial light modulators
[AD-A206328] N89-24905
MAGNETOHYDRODYNAMIC FLOW
On the thermal stability of optically thin flows --- plasmas N89-24973
Relation between global and local aspects of reconnection --- magnetic fields N89-24976
Noise-free neutral sheets N89-24977
Comparison of compressible and incompressible models of reconnection N89-24982
Magnetic reconnection near a stagnation point N89-24983

Three-dimensional reconnection from a global viewpoint N89-24988
A neutral current sheet with flows: Tearing and stratification modes and modeling of coronal structures N89-24991
A 2-D and 3-D simulation study of multiple X line reconnection N89-25023
Impulsive reconnection of the skewed magnetic fields at the magnetopause as a MHD model N89-25025

MAGNETOHYDRODYNAMIC STABILITY
Cosmic linear accelerators N89-24915
The electron beam instability revisited: Growth above and below f sub p N89-24917
Thermal instability in a stratified plasma N89-24924
Kink modes in coronal loops N89-24925
Relativistic MHD from two-fluid hydrodynamics (TFHD) --- space plasmas N89-24931
Quasi-perpendicular collisionless high Mach number shocks N89-24937
Theory of radioemission of pulsars N89-24941
Two-stream instability in pulsar magnetospheres N89-24949
Small-scale instabilities in accretion disks of compact objects and their manifestations N89-24950
Synchrotron thermal instabilities and filamentation in radio sources N89-24958
Pulsar radio and visible radiation due to the modulation instability of high-frequence transverse waves in the inhomogeneous electron-positron plasma N89-24959
Simulation of electrostatic ion instabilities in the presence of parallel currents and transverse electric fields N89-24972
On the thermal stability of optically thin flows --- plasmas N89-24973
Stability of force-free magnetic fields and the problem of solar coronal heating N89-24990
On the MHD stability of the M=1 kink mode in finite length coronal loops N89-24992
Dynamic development of coronal current sheets N89-24994
The equilibrium and stability of solar coronal magnetic fields N89-25102

MAGNETOHYDRODYNAMIC TURBULENCE
The evolution of MHD-perturbations in the intersection region of two separatrix planes N89-25011

MAGNETOHYDRODYNAMIC WAVES
Dissipation of Alfven waves in solar coronal arches N89-24919
Non-steady astrophysical spiral jets driven by magnetic collapse and pressure N89-24920
MHD-waves and their nonlinear interaction in a plasma with magnetic flux tubes N89-24921
Alfven wave solitons and solar intermediate drift bursts N89-24923
Kink modes in coronal loops N89-24925
Coronal heating by resonant absorption in resistive MHD N89-24926
Radiative-resonant MHD interactions between waves and particles and the problem of cosmic-ray spectra N89-24944
Effects of unequal particle number densities on Alfven waves N89-24945

MAGNETOHYDRODYNAMICS
Relativistic MHD from two-fluid hydrodynamics (TFHD) --- space plasmas N89-24931
On the existence and stability of intermediate shocks --- MHD N89-24971
Magnetotail reconnection, MHD theory and simulations N89-25013
A 2-D and 3-D simulation study of multiple X line reconnection N89-25023
The structure of the reconnection layer in the Petschek reconnection model: Theory and application to the earth's magnetopause N89-25026
The variable nature of the comet-solar wind interaction N89-25100
The equilibrium and stability of solar coronal magnetic fields N89-25102

MAGNETOPAUSE
Flux transfer events: Reconnection without separators --- magnetopause N89-25021
Multiple X line reconnection at the dayside magnetopause N89-25022
The role of the magnetic reconnection in the solar wind/magnetosphere interaction N89-25024
Impulsive reconnection of the skewed magnetic fields at the magnetopause as a MHD model N89-25025
The structure of the reconnection layer in the Petschek reconnection model: Theory and application to the earth's magnetopause N89-25026

MAGNETOPLASMADYNAMICS
Structuring of plasmas by a magnetic field --- solar corona N89-24938
Nonlinear dynamics of the drift tearing-mode N89-24979

MAGNETOSONIC RESONANCE
Particle acceleration by magnetic reconnection and fast magnetosonic shock waves in solar flares N89-24993

MAGNETRON SPUTTERING
Isotopic study of oxygen diffusion in oxide coatings [NASA-TM-102082] N89-24451
Superconducting properties of magnetron sputtered Bi-Sr-Ca-Cu-O and Tl-Ba-Ca-Cu-O thin films [DE89-009878] N89-25056

MAIN SEQUENCE STARS
Effects of main-sequence mass loss on stellar and galactic chemical evolution [DE89-011399] N89-25098

MAINTENANCE
Advanced servomanipulator remote maintenance demonstration [DE89-010188] N89-24614

MAN MACHINE SYSTEMS
Hermes user interfaces N89-24346
Getting ready for EVA N89-24387
Advanced MMI and image handling to support crew activities N89-24392
Human Factors in Automated and Robotic Space Systems: Proceedings of a symposium. Part 1 [NASA-CR-182495] N89-24792
The human role in space (THURIS) applications study. Final briefing [NASA-CR-183590] N89-24793
Human Factors in Automated and Robotic Space Systems: Proceedings of a symposium. Part 2 [NASA-CR-182496] N89-24794
The human role in space (THURIS) applications study. Volume 2: Research analysis and technology report [NASA-CR-183589] N89-24795
Brain-wave measures of workload in advanced cockpits: The transition of technology from laboratory to cockpit simulator, phase 2 [NASA-CR-4240] N89-24797
Development of a hybrid simulator for robotic manipulators N89-24831
Pedagogical issues in developing a man-machine interface for an intelligent tutoring system N89-24855

MAN-COMPUTER INTERFACE
Human Factors in Automated and Robotic Space Systems: Proceedings of a symposium. Part 1 [NASA-CR-182495] N89-24792
Human Factors in Automated and Robotic Space Systems: Proceedings of a symposium. Part 2 [NASA-CR-182496] N89-24794
Evaluation, description and invention: Paradigms for human-computer interaction [AD-A204617] N89-24796

MANAGEMENT ANALYSIS
The Manned Space Laboratories Control Center (MSCC) at DFVLR, Oberpfaffenhofen, Germany, F.R. N89-24376

MANAGEMENT METHODS
The electronic supervisor: New technology, new tensions [OTA-CIT-333] N89-24804

MANAGEMENT PLANNING
A forecast of workloads and manpower requirements for the archiving of scientific and technical reports by the Defense Technical Information Center using a simulation model: An operations research approach [AD-A206263] N89-25075

MANAGEMENT SYSTEMS
The development of a Job-Jobstep scheduler for NS system [NAL-TR-977] N89-24814

MANIFOLDS (MATHEMATICS)
Periodic and heteroclinic orbits for a periodic Hamiltonian system [AD-A204078] N89-24862

MANIPULATORS
Robotic experiments on Spacelab D-2 as testbed for future operational concepts N89-24391
Piezoelectric film load cell robot collision detector [DE89-010117] N89-24592
Real time control for NASA robotic gripper [NASA-CR-184978] N89-24608
Generalized solution for the optimal prehension state using end effectors with multi-articulated fingers N89-24609
Advanced servomanipulator remote maintenance demonstration [DE89-010188] N89-24614
Dynamics of flexible multi-body mechanisms and manipulators. Part 1: An overview N89-24662
Application of finite-element methods to dynamic analysis of flexible spatial and co-planar linkage systems, part 2 N89-24663
Development of a hybrid simulator for robotic manipulators N89-24831
Insertion with two coordinated arms N89-24837
Inflatable end effector tools N89-24839
Testing the feasibility of using a teleoperated robot for remote, dexterous operations N89-24843
IRIS: An intelligent robot insertion expert system N89-24854
A comparison of two real-time control schemes for redundant robots with bounded joint velocities [DE89-002974] N89-24861
Computational method of the inverse kinematics via simplified algebraic equation [DE88-757269] N89-24866

MANNED ORBITAL LABORATORIES
Pressurized module element for man's presence in space --- Columbus N89-24343
MTFF user interfaces N89-24345
MTFF flight operations phases N89-24361
The Manned Space Laboratories Control Center (MSCC) at DFVLR, Oberpfaffenhofen, Germany, F.R. N89-24376
The concept of telescience N89-24384
Telescience and payload control support technologies N89-24385
Telescience: A promising operations center N89-24386
The space station power system [NASA-TM-101245] N89-24416
Space station: A step into the future [NASA-PAM-510/11-87] N89-24417

MANNED SPACE FLIGHT
International Symposium on Europe in Space: The Manned Space System [ESA-SP-277] N89-24335
China's future space activities N89-24342
The impact of manned space flight operations on the safety and reliability aspects of ground systems requirements N89-24371
Italian scientific projects related to manned activity in space N89-24382
Simulation of weightlessness with neutral buoyancy facilities and zero-g aircraft for the preparation of European manned space operations N89-24398
Lessons learned from SL-1 and D-1 --- Spacelab N89-24400
Safety in manned space flight N89-24402
Technology requirements for advanced NASA missions N89-24705

MANPOWER
A forecast of workloads and manpower requirements for the archiving of scientific and technical reports by the Defense Technical Information Center using a simulation model: An operations research approach [AD-A206263] N89-25075

MANUFACTURING
The impact of solar cell technology on planar solar array performance N89-24715
Flexibility in space solar cell production N89-24730
Using a simulation assistant in modeling manufacturing systems N89-24849

MANY BODY PROBLEM
Computational Methods for Structural Mechanics and Dynamics [NASA-CP-3034-PT-2] N89-24654
Recent developments in deployment analysis simulation using a multi-body computer code N89-24660
Dynamic analysis of space structures including elastic, multibody, and control behavior N89-24661
Dynamics of articulated structures N89-24664
Computational aspects of multibody dynamics N89-24666
Constraint elimination in dynamical systems N89-24667
Nonlinear characteristics of joints as elements of multi-body dynamic systems N89-24668
The gravitational many-body PPN Lagrangian, Lorentz invariance and the strong equivalence principle to second order N89-24765

MAPPING
Geological gyrocompass [PB89-133086] N89-24589
A system for high resolution 3D mapping using laser radar and requiring no beam scanning mechanisms N89-24827
The 158 micron (CII) mapping of the galactic center molecular clouds [MPE-PREPRINT-131] N89-25081
Strong, spatially extended CO 7 to 6 emission from luminous cloud cores: W51 and DR21 [MPE-PREPRINT-133] N89-25106

MARKETING
US fuel cell research and applications, 1960--1989 [DE89-012244] N89-24745

MARKING
Improved marking of taxiway intersections for Instrument Flight Rules (IFR) operations [DOT/FAA/CT-TN89/23] N89-24330

MARS (PLANET)
Technology requirements for advanced NASA missions N89-24705
MARS ATMOSPHERE
Photovoltaic power system operation in the Mars environment
[NASA-TM-102075] N89-24529
Improvements in the Global Reference Atmospheric Model and comparisons with a global 3-D numerical model
[NASA-CR-184947] N89-24755
MASS FLOW
Nonlinear oblique whistlers: Their relevance to nonthermal coupling of ions and electrons in accretion flow and supercritical quasi-perpendicular collisionless shocks --- black holes N89-24955
MASS SPECTROMETERS
Systems for the sensitivity calibration of mass spectrometers in space flight
[BONN-IR-88-32] N89-24428
Mass spectrometry
[DE89-011118] N89-24471
MASS SPECTROSCOPY
Mass spectrometry
[DE89-011118] N89-24471
MASS TRANSFER
Field studies for determining the characteristics and dynamics of local circulations
[DE89-012290] N89-24751
MATCHING
Tele-autonomous control involving contacts: The applications of a high precision laser line range sensor
[NASA-CR-184995] N89-24509
MATERIALS HANDLING
Superfluid Helium Tanker Study (SFHT)
[NASA-CR-172114] N89-24415
MATHEMATICAL LOGIC
A deductive approach to automated planning
[AD-A206253] N89-24860
MATHEMATICAL MODELS
Thermal analysis of a hypersonic wing test structure
[NASA-CR-185319] N89-24265
Recent activities within the Aeroservoelasticity Branch at the NASA Langley Research Center
[NASA-TM-101582] N89-24314
Transient flow thrust prediction for an ejector propulsion concept
[NASA-TM-102078] N89-24318
Results of an A109 simulation validation and handling qualities study
[NASA-TM-101062] N89-24323
Numerical simulation of feedback control of aerodynamic configurations in steady and unsteady ground effects N89-24326
On the dynamics and control of the Spacecraft Control Laboratory Experiment (SCOLE) class of offset flexible systems N89-24426
Time dependent reliability model incorporating continuum damage mechanics for high-temperature ceramics
[NASA-TM-102046] N89-24487
Characterization of pore evolution in ceramics during creep failure and densification
[DE89-013599] N89-24502
Viscosity of solids determined by shock wave action on hemispherical indentations
[DE89-008035] N89-24510
On the causality of plasma permittivity
[NASA-TM-101551] N89-24514
Characterization of radiation boundary conditions used in the finite-difference time-domain method
[DE89-005662] N89-24522
Development and utilization of new diagnostics for dense-phase pneumatic transport
[DE89-011381] N89-24583
Two-phase flow measurements by nuclear magnetic resonance imaging
[DE89-011850] N89-24586
Real time control for NASA robotic gripper
[NASA-CR-184978] N89-24608
Research in structures, structural dynamics and materials, 1989
[NASA-CP-10024] N89-24626
Modeling the missile-launch tube problem in DYSCO N89-24629
Acoustic emission from a growing crack N89-24633
A study of material damping in large space structures
[NASA-CR-180076] N89-24634
Constraint elimination in dynamical systems N89-24667
Analysis of shell-type structures subjected to time-dependent mechanical and thermal loading
[NASA-CR-184989] N89-24669
Dynamics and static behavior of metal gussets in cask impact limiters
[DE89-011879] N89-24683
Improvement and extension of a radar forest backscattering model
[NASA-CR-184975] N89-24686
Modelling and design of high performance indium phosphide solar cells N89-24712
XCAD: A CAD object-oriented virtual solid modeler for an expert system shell
[REPT-882-440-125] N89-24810
The impact of an IVA robot on the space station microgravity environment N89-24821
A new approach to robot kinematic analysis N89-24833
Self-circumference in the Minkowski plane
[AD-A205691] N89-24868
Analytic theory for the determination of velocity and stability of bubbles in a Hele-Shaw cell. Part 2: Stability
[NASA-CR-181837] N89-24883
Universal reduction of T(subc) in strong coupling superconductors due to Anderson/Kondo impurities
[DE89-011225] N89-25071
Study of chemical reaction models for high enthalpy flow of air
[NAL-TR-982] N89-25072
A forecast of workloads and manpower requirements for the archiving of scientific and technical reports by the Defense Technical Information Center using a simulation model: An operations research approach
[AD-A206263] N89-25075
Self-consistent models of spherical accretion onto black holes N89-25095
The equilibrium and stability of solar coronal magnetic fields N89-25102
MATRICES (MATHEMATICS)
Representations of a linkage mechanism based on dual number matrices
[DE88-757273] N89-24857
MATRIX METHODS
The exact condition of the B-spline basis may be hard to determine
[AD-A204080] N89-24863
MAXWELL FLUIDS
Equations of motion for viscoelastic moving crack problems N89-24670
MAXWELL-BOLTZMANN DENSITY FUNCTION
The effect of non-Maxwellian electron distributions on the intensity ratio of resonance to satellite lines
[DE89-006745] N89-24907
MEASURING INSTRUMENTS
Development and utilization of new diagnostics for dense-phase pneumatic transport
[DE89-011381] N89-24583
Mechanics/heat-transfer relation for particle flows
[DE89-011382] N89-24584
Research and technology, 1988
[NASA-TM-101246] N89-25109
MECHANICAL DRIVES
Tribology: The Story of Lubrication and Wear
[NASA-TM-101430] N89-24635
MECHANICAL ENGINEERING
Application and implementation of transient algorithms in computer programs N89-24659
Nonlinear characteristics of joints as elements of multi-body dynamic systems N89-24668
A discussion on using Lanczos vectors and Ritz vectors for computing dynamic responses
[DE89-012322] N89-24684
MECHANICAL PROPERTIES
Impact and penetration resistance of fibrous composites
[AD-A206417] N89-24454
High temperature mechanical properties and microscopic examination of extruded powder aluminum
[DE89-010457] N89-24484
Nd:YAG laser weldability of RS/PM Al-BFe-2Mo sheet
[DE89-013588] N89-24621
MEDICAL SCIENCE
The AAMRL (Armstrong Aerospace Medical Research Laboratory) biodynamics data bank
[AD-A206139] N89-25074
MELTING
Flight experiment of thermal energy storage
[NASA-TM-102081] N89-24440
MENTAL PERFORMANCE
Brain-wave measures of workload in advanced cockpits: The transition of technology from laboratory to cockpit simulator, phase 2
[NASA-CR-4240] N89-24797
MERCURY (PLANET)
Inductive acceleration of protons and electrons in planetary magnetotails N89-25015
MERCURY VAPOR
Experiments on liquid-vapour phase change between plane liquid surfaces. Part 2: Observations of large temperature jumps near the interfaces
[NAL-TM-FM-8805] N89-24462
MESON-NUCLEON INTERACTIONS
Kaon-nucleus scattering
[NASA-TP-2920] N89-25103
MESOSCALE PHENOMENA
Analysis and use of VAS satellite data
[NASA-CR-4218] N89-24770
MESOSPHERE
Investigations of the sodium layer of the earth atmosphere: Probing with a terrestrial lidar system at 69 N in winter
[BONN-IR-88-52] N89-24760
METAL AIR BATTERIES
Analysis of life cycle costs for electric vans with advanced battery systems
[DE89-009807] N89-24526
METAL BONDING
Bonding and chemistry of hydrocarbon monolayers on metal surfaces
[DE89-009311] N89-24490
Reactions of (eta 5-C5H5) (eta 5-C5Me5) Zr(Si(SiMe3)3)X (X = Cl, Me) complexes with carbon monoxide and the isocyanide 2,6 Me2C6H3NC. Crystal structure of (eta 5-C5H5) (eta 5-C5Me5)Zr(eta 2-C(N-2,6 Me2C6H3) Si(SiMe3)3)Cl
[AD-A206494] N89-24493
METAL FATIGUE
Engineering design of the interaction waveguide for high-power accelerator-driven microwave free-electron lasers
[DE89-011896] N89-24605
METAL FILMS
Magneto-optical studies of metastable 3D-transition metal films
[DE89-009836] N89-24474
METAL FLUORIDES
Containerless glass fiber processing
[NASA-TM-86540] N89-24405
METAL FOILS
Electrophoretically applied dielectrics for amorphous metal foils used in pulsed power saturable reactors
[DE89-009322] N89-24525
METAL IONS
Computer simulation of copper in the liquid phase and the sputtering of liquid copper by one KeV argon ions
[AD-A206264] N89-24476
METAL MATRIX COMPOSITES
Isothermal life prediction of composite lamina using a damage mechanics approach
[NASA-TM-102032] N89-24460
METAL OXIDES
High-resolution electron microscopy of metal/ceramic interfaces
[DE89-012396] N89-24498
METAL POWDER
Analysis of the plugging of the systems autonomy demonstration project brassboard filters
[NASA-CR-177533] N89-24450
METAL SURFACES
Bonding and chemistry of hydrocarbon monolayers on metal surfaces
[DE89-009311] N89-24490
METALLOGRAPHY
Fundamental studies on order effects in metal alloys
[ONERA-RT-14/221-M] N89-24480
METALS
Measurement of bond strength at metal/ceramic interfaces
[DE89-011638] N89-24682
METASTABLE STATE
Investigations of the origins of metastable, light-induced changes in hydrogenated amorphous silicon
[DE89-000890] N89-24496
METEOROLOGICAL PARAMETERS
Climatic atlas of the outer continental shelf waters and coastal regions of Alaska. Volume 3: Chukchi-Beaufort Sea
[AD-A206525] N89-24776
Water vapor retrievals through the 3I (Improved Initialization Inversion) system: Application to tropospheric altimetry correction
[ETN-89-94534] N89-24778
The radiation-atmosphere interaction model and the determination of meteorological and climatological parameters from satellite observations
[ETN-89-94535] N89-24779
Study of representativity of the wind fields deduced from geostationary satellite images. Attribution of height to wind vectors and large scale average fields deduced from water vapor imagery
[ETN-89-94538] N89-24781
Contribution to the estimation of precipitation in the Sahel by using satellite imagery
[SER-DI-204] N89-24782
METEOROLOGICAL RADAR
Ground cluster filters for staggered pulse trains
[DOT/FAA/SA-89/2] N89-24515

Efficient dealiasing of Doppler velocities using local environment constraints
[DOT/FAA/SA-89/1] N89-24771

METEOROLOGICAL SATELLITES
Analysis and use of VAS satellite data
[NASA-CR-4218] N89-24770
Contribution to the study of the diurnal cycle of convective clouds over tropical Africa from satellite imagery
[ETN-89-94537] N89-24780
Study of representativity of the wind fields deduced from geostationary satellite images. Attribution of height to wind vectors and large scale average fields deduced from water vapor imagery
[ETN-89-94538] N89-24781
Contribution to the estimation of precipitation in the Sahel by using satellite imagery
[SER-DI-204] N89-24782

METEOSAT SATELLITE
Estimating the outgoing longwave radiation from the Meteosat infrared window and water vapor bands
[ETN-89-94533] N89-24762

METHANE
Oxide-bound transition metal complexes for methane activation
[PB89-138614] N89-24464
Methane to methanol conversion
[DE89-011194] N89-24504

METHYL ALCOHOL
Methane to methanol conversion
[DE89-011194] N89-24504

MICROCOMPUTERS
Microprocessor based 32 channel PCM telemetry system
[NAL-TM-SE-8704] N89-24414
The 64K 16-bit word buffer memory with microprogrammable control
[DE88-706303] N89-24799

MICROCRACKS
Microscopic delamination processes and the resulting crack tip strain fields of graphite/epoxy composites N89-24671

MICROELECTRONICS
Proceedings of the Goddard Space Flight Center Workshop on Robotics for Commercial Microelectronic Processes in Space
[NASA-TM-101233] N89-24505
The 64K 16-bit word buffer memory with microprogrammable control
[DE88-706303] N89-24799
A facilities view of the low volume, high product mix fab
[DE89-009970] N89-25057

MICROPROCESSORS
Microprocessor based 32 channel PCM telemetry system
[NAL-TM-SE-8704] N89-24414

MICROSTRUCTURE
Role of alloying additions in the oxidation-sulfidation of Fe-base alloys
[DE89-009825] N89-24473
The effect of heat input and composition on weld metal microstructures in thin section HY-130 GMAW weldments
[AD-A206476] N89-24477
Weldability and microstructural characterization of Al-Li alloys
[DE89-010183] N89-24478
Amorphous metal alloys produced by mechanical alloying
[DE89-011189] N89-24481
Effects of multiple reductions on grain refinement during hot working of alloy 718
[DE89-010426] N89-24483
Analysis of packed-particle rearrangement during colloidal ceramic processing: Gamma-ray densitometry and a review of alternative methods
[DE89-009066] N89-24489
Nd:YAG laser weldability of RS/PM Al-BFe-2Mo sheet
[DE89-013588] N89-24621
Combined microstructure X-ray optics
[DE89-009902] N89-24904
Grain boundary phase equilibria in metallic systems
[DE89-011787] N89-25066
High resolution electron microscopy of interfaces in topotaxial and epitaxial reactions
[DE89-010390] N89-25070

MICROWAVE CIRCUITS
Microwave characteristics of GaAs MMIC integratable optical detectors
[NASA-TM-101485] N89-24520
Electrooptical feed and control in microwave applications
[FOA-C-30514-3.2] N89-24531

MICROWAVE EMISSION
Time scales of solar microwave bursts and scenarios of flare energy release N89-25005

MICROWAVE EQUIPMENT
Electrooptical feed and control in microwave applications
[FOA-C-30514-3.2] N89-24531
The 280 GHz Gyro-BWO design study
[DE89-011644] N89-24595

MICROWAVE LANDING SYSTEMS
An operational demonstration and engineering flight test of the Microwave Landing System on runway 22L at Chicago's Midway Airport
[DOT/FAA/CT-TN88/42] N89-24291
B-737 flight test of curved-path and steep-angle approaches using MLS guidance
[NASA-TM-101521] N89-24293

MICROWAVE RADIOMETERS
Microwave X-band radiometric characterization of Brazilian soils by measurement of the complex permittivity
[INPE-4588-PRE/1319] N89-24685

MICROWAVE SPECTRA
First detection of SO2 and CH3OH emission and one unidentified line near 800 GHz
[MPE-PREPRINT-142] N89-25086

MICROWAVE TUBES
The 280 GHz Gyro-BWO design study
[DE89-011644] N89-24595

MICROWAVES
Microwave characteristics of GaAs MMIC integratable optical detectors
[NASA-TM-101485] N89-24520

MIGRATION
The effects of gradients on boundary stability
[DE89-011590] N89-25065

MILITARY AIRCRAFT
Flight control system for the CRCA (Control Reconfigurable Combat Aircraft) using a command generator tracker with PI (Plus Integral) feedback and Kalman filter, volume 2
[AD-A206202] N89-24325

MILITARY TECHNOLOGY
Development of a hybrid simulator for robotic manipulators N89-24831
A robotic vehicle global route planner for the 1990s N89-24851

MILKY WAY GALAXY
The circum-nuclear disk
[MPE-PREPRINT-132] N89-25093
The Orion molecular cloud and star forming region
[MPE-PREPRINT-140] N89-25094

MILLIMETER WAVES
Development of a 75-watt 60-GHz traveling-wave tube for intersatellite communications
[NASA-CR-182135] N89-24530
Automated Millimeter Wave (AMW) transducer testing in a robotic/vision test cell N89-24841

MIMD (COMPUTERS)
Telescience and payload control support technologies N89-24385

MINKOWSKI SPACE
Self-circumference in the Minkowski plane
[AD-A205691] N89-24868

MIRRORS
Design of the optical system for a new time-resolved X-ray absorption spectroscopy apparatus
[DE88-757253] N89-24902

MISSILES
Modeling the missile-launch tube problem in DYSCO N89-24629

MISSION PLANNING
The technology contents of the first phase of the Hermes Development Program N89-24350
Timelining and operations integration concerning APM and MTFF N89-24358
Scientific utilization of the European space infrastructure and the International Space Station N89-24380
Experimentation in the Man Tended Free Flyer (MTFF) N89-24381
Getting ready for EVA N89-24387
Lessons learned from SL-1 and D-1 --- Spacelab N89-24400
Research and technology, 1988
[NASA-TM-101246] N89-25109

MIXING LAYERS (FLUIDS)
Studying Turbulence Using Numerical Simulation Databases, 2. Proceedings of the 1988 Summer Program
[NASA-CR-184905] N89-24538
Chaos in a spatially-developing plane mixing layer N89-24539
Inflow/outflow boundary conditions and global dynamics of spatial mixing layers N89-24540
Phase decorrelation, streamwise vortices and acoustic radiation in mixing layers N89-24541
Dynamics of coherent structures in a plane mixing layer N89-24543
Subharmonic resonance in a mixing layer N89-24544
Scalar entrainment in the mixing layer N89-24545
Use of passive scalar tagging for the study of coherent structures in the plane mixing layer N89-24546
Sensitivity of mixing layers to three-dimensional forcing N89-24547

MOBILE COMMUNICATION SYSTEMS
UNIX-based data management system for the Mobile Satellite Propagation Experiment (PiFEx)
[NASA-CR-185023] N89-25073

MODAL RESPONSE
Development of higher-order modal methods for transient thermal and structural analysis
[NASA-TM-101548] N89-24677

MODELS
Using a simulation assistant in modeling manufacturing systems N89-24849

MODULATORS
The current technological status of spatial light modulators
[AD-A206328] N89-24905

MOLECULAR BEAM EPITAXY
Laboratory for X-ray optics
[AD-A206468] N89-25061

MOLECULAR CLOUDS
The gamma-ray observatory GRO in perspective
[MPE-PREPRINT-137] N89-24407
The formation of interstellar clouds N89-24935
The 158 micron (CII) mapping of the galactic center molecular clouds
[MPE-PREPRINT-131] N89-25081
Physical conditions in molecular clouds derived from sub-mm and far-IR spectroscopic observations
[MPE-PREPRINT-135] N89-25082
The Orion molecular cloud and star forming region
[MPE-PREPRINT-140] N89-25094
Strong, spatially extended CO 7 to 6 emission from luminous cloud cores: W51 and DR21
[MPE-PREPRINT-133] N89-25106
COS-B gamma-ray sources beyond the predicted diffuse emission
[MPE-PREPRINT-136] N89-25107

MOLECULAR ENERGY LEVELS
Challenges in computational statistical mechanics
[DE89-009922] N89-24567

MOLECULAR SPECTRA
On the future development and management of spectroscopic database for radiative transfer from the issues of recent related workshops
[ETN-89-94530] N89-24690
First detection of SO2 and CH3OH emission and one unidentified line near 800 GHz
[MPE-PREPRINT-142] N89-25086

MOLECULAR SPECTROSCOPY
The 158 micron (CII) mapping of the galactic center molecular clouds
[MPE-PREPRINT-131] N89-25081
Physical conditions in molecular clouds derived from sub-mm and far-IR spectroscopic observations
[MPE-PREPRINT-135] N89-25082

MOLTEN SALTS
Status of the direct absorption receiver panel research experiment: Salt flow and solar test requirements and plans
[DE89-010968] N89-24461

MOLYBDENUM ALLOYS
Nd:YAG laser weldability of RS/PM Al-BFe-2Mo sheet
[DE89-013588] N89-24621

MONTE CARLO METHOD
Universal reduction of T(subc) in strong coupling superconductors due to Anderson/Kondo impurities
[DE89-011225] N89-25071
The application of two-dimensional imaging to very high energy gamma ray astronomy
[DE89-013614] N89-25089

MORPHOLOGY
The effects of gradients on boundary stability
[DE89-011590] N89-25065

MOSSBAUER EFFECT
Multiphoton transitions at the Moessbauer radiation diffraction in crystals under a weak ultrasonic field
[DE88-706341] N89-25069

MOTION STABILITY
Stabilized image system for mobile robots N89-24829

MOTOR VEHICLES
The DARPA autonomous land vehicle: A phase 1 retrospective and a prospective for the future N89-24834
Development of a man-portable control unit for a teleoperated land vehicle N89-24835
A robotic vehicle global route planner for the 1990s N89-24851

A demonstration of retro-traverse using a semi-autonomous land vehicle N89-24852
A knowledge representation scheme for a robotic land vehicle route planner N89-24853
MSAT
UNIX-based data management system for the Mobile Satellite Propagation Experiment (PiFEx) [NASA-CR-185023] N89-25073
MULTICHANNEL COMMUNICATION
Microprocessor based 32 channel PCM telemetry system [NAL-TM-SE-8704] N89-24414
MULTIPHASE FLOW
Modeling thermal-mechanical processes associated with the initiation and combustion of granular energetic materials [DE89-007145] N89-24472
Two-phase flow measurements by nuclear magnetic resonance imaging [DE89-011850] N89-24586
MULTIPHOTON ABSORPTION
Multiphoton transitions at the Moessbauer radiation diffraction in crystals under a weak ultrasonic field [DE88-706341] N89-25069
MULTIPLE ACCESS
File concepts for parallel I/O [NASA-CR-181843] N89-24816
MULTIPLEXING
Multiplexed electronically programmable multimode ionization detector for chromatography [DE89-009758] N89-24465
MULTIPROCESSING (COMPUTERS)
Nonlinear hierarchical substructural parallelism and computer architecture N89-24650
MULTIVARIATE STATISTICAL ANALYSIS
Efficient estimator of parameters and goodness-of-fit test of multivariate distributions for data presented by one-dimensional histograms [DE88-706318] N89-24879

N

NAP-OF-THE-EARTH NAVIGATION
Optimal guidance with obstacle avoidance for nap-of-the-earth flight [NASA-CR-177515] N89-24328
NASA PROGRAMS
Space station: A step into the future [NASA-PAM-510/11-87] N89-24417
Research and technology, 1988 [NASA-TM-101246] N89-25109
Langley aerospace test highlights, 1988 [NASA-TM-101579] N89-25112
NASA SPACE PROGRAMS
The Pathfinder Chemical Transfer Propulsion program [NASA-TM-102084] N89-24409
HIRIS: NASA's high-resolution imaging spectrometer for the Earth Observing System (EOS) N89-24695
Technology requirements for advanced NASA missions N89-24705
NAVIER-STOKES EQUATION
Use of Navier-Stokes methods to predict circulation control airfoil performance [AD-A206242] N89-24270
Unsteady Aerodynamics, volume 2 [VKI-1988-07-VOL-2] N89-24281
Numerical methods for unsteady flows N89-24282
Chaos in a spatially-developing plane mixing layer N89-24539
Subharmonic resonance in a mixing layer N89-24544
Dynamical interpretation of conditional patterns N89-24549
Head-on collision of viscous vortex rings N89-24560
Navier-Stokes analysis of cold scramjet-afterbody flows [NASA-CR-184949] N89-24562
A second-order projection method for the incompressible Navier Stokes equations on quadrilateral grids [DE89-010242] N89-24585
NAVIGATION AIDS
Image Signal Processing for Flight Guidance [DFVLR-MITT-88-32] N89-24295
Determination of reference trajectories for testing navigation aids using an onboard CCD camera N89-24303
Diverter AI based decision aid, phases 1 and 2 [NASA-CR-181820] N89-24316
NAVSTAR SATELLITES
Contamination effects of GPS Navstar solar array performance N89-24734
NEAR FIELDS
Computed performance of the half-scale accurate antenna reflector [NASA-CR-182264] N89-24532
NEBULAE
Soft X-ray observations of the Vela Pulsar PSR 0833-45 [MPE-PREPRINT-130] N89-25080
Strong, spatially extended CO 7 to 6 emission from luminous cloud cores: W51 and DR21 [MPE-PREPRINT-133] N89-25106
NEODYMIUM LASERS
Holographic interferometry with an injection seeded Nd:YAG laser and two reference beams [NASA-TM-102056] N89-24591
Prototype laser-diode-pumped solid state laser transmitters [NASA-CR-185056] N89-24601
NEPTUNE (PLANET)
Voyager at Neptune: 1989 [NASA-CR-185317] N89-24420
NERVOUS SYSTEM
Field-dependence and judgment of weight and color revisited: Some implications for the study of sensory discrimination [AD-A206141] N89-24791
NEURAL NETS
Neuromorphic learning of continuous-valued mappings in the presence of noise: Application to real-time adaptive control [NASA-TM-101999] N89-24856
Empirical analysis and refinement of expert system knowledge bases [AD-A206226] N89-24858
NEUROLOGY
Cerebral laterality and handedness in aviation: Performance and selection implications [AD-A206196] N89-24787
NEUTRAL BEAMS
FOM-Rijnhuizen contributions to the Fifteenth Symposium on Fusion Technology [REPT-88-179] N89-25030
Beam guiding system for Rutherford scattering diagnostic at TEXTOR N89-25033
Control and data acquisition system for the neutral beam probe diagnostic on TEXTOR N89-25036
Characterization of the ASDEX scrape-off-layer density profile during neutral beam heating N89-25040
ASDEX edge and divertor simulation and the problem of incomplete and inaccurate experimental data N89-25041
Comparison of recycling in the ASDEX divertor before and after hardening N89-25042
The low energy neutral fluxes and their impurity production at the walls of ASDEX N89-25043
Charge exchange neutral sputtering in ASDEX N89-25044
Erosion and retention of the target plate material in the ASDEX divertor N89-25045
Measurements of the flux of metallic impurities to the ASDEX divertor plates N89-25046
Material transport at the vessel walls of the divertor tokamak ASDEX N89-25047
NEUTRAL BUOYANCY SIMULATION
Simulation of weightlessness with neutral buoyancy facilities and zero-g aircraft for the preparation of European manned space operations N89-24398
NEUTRON STARS
Relativistic shocks in electron-positron plasmas and polar cap accretion onto neutron stars: Two non-linear problems in astrophysical plasma physics N89-24928
Neutron starquakes and the nature of gamma-ray bursts N89-24947
Quantum relativistic theory of the cyclotron radiation in a strongly magnetized plasma with anisotropic temperature --- neutron stars N89-24962
NEWTON METHODS
Advances in dual methods and convex approximations for structural optimization N89-24680
NICKEL CADMIUM BATTERIES
ERC nickel cadium battery performance tests and comparisons with lead-acid batteries [DE89-009753] N89-24535
NICKEL HYDROGEN BATTERIES
Energy storage and thermal control system design status [NASA-TM-102136] N89-24427
NICKEL IRON BATTERIES
Analysis of life cycle costs for electric vans with advanced battery systems [DE89-009807] N89-24526
NIGHT
Magnetic neutral lines in Jupiter's nightside magnetosphere N89-24918
NIGHT FLIGHTS (AIRCRAFT)
The night and adverse weather capability of ground attack aircraft [FOA-C-20745-2.5] N89-24312
NOISE
Neuromorphic learning of continuous-valued mappings in the presence of noise: Application to real-time adaptive control [NASA-TM-101999] N89-24856
NOISE MEASUREMENT
Ultra-light duct for an anechoic wind tunnel [NASA-TM-101805] N89-24331
NOISE PREDICTION
Calculation of aircraft noise in the vicinity of civil airports by a simultion procedure [MPIS-7/1988] N89-24887
NOISE SPECTRA
Calculation of aircraft noise in the vicinity of civil airports by a simultion procedure [MPIS-7/1988] N89-24887
Advanced turboprop aircraft flyover noise: Annoyance to counter-rotating-propeller configurations with a different number of blades on each rotor: Preliminary results [NASA-TM-100638] N89-24888
NOISE STORMS
The role of cold electrons in the generation of the high-frequency part of broadband electrostatic noise --- magnetotail N89-25018
NOISE TOLERANCE
Advanced turboprop aircraft flyover noise: Annoyance to counter-rotating-propeller configurations with a different number of blades on each rotor: Preliminary results [NASA-TM-100638] N89-24888
NONDESTRUCTIVE TESTS
Laser-induced-fluorescence inspection of polyurethane and related materials, phase 1 [AD-A206423] N89-24492
Diffusion welding of electrical interconnects to silicon solar cells [DE89-012250] N89-24620
Acoustic emission from a growing crack N89-24633
A new structure for comparing surface passivation materials of GaAs solar cells N89-24725
Algorithm for display of automated nondestructive thickness measurements N89-24850
NONLINEAR EVOLUTION EQUATIONS
Nonlinear evolution of interacting oblique waves on two-dimensional shear layers [NASA-TM-102030] N89-24575
NONLINEAR OPTICS
Optical chaos [DE89-009392] N89-24903
NONLINEAR SYSTEMS
Some issues in numerical simulation of nonlinear structural response N89-24639
NONLINEARITY
Nonlinear evolution of interacting oblique waves on two-dimensional shear layers [NASA-TM-102030] N89-24575
Nonlinear response of a blade-stiffened graphite-epoxy panel with a discontinuous stiffener: Work in progress N89-24641
Global-local methodologies and their application to nonlinear analysis N89-24647
Nonlinear characteristics of joints as elements of multi-body dynamic systems N89-24668
Stochastic quantization of nonlinear sigma-models with Wess-Zumino terms [DE88-757286] N89-24882
NOZZLE DESIGN
Space Shuttle Main Engine structural analysis and data reduction/evaluation. Volume 6: Primary nozzle diffuser analysis [NASA-CR-183669] N89-24437
NOZZLE FLOW
Navier-Stokes analysis of cold scramjet-afterbody flows [NASA-CR-184949] N89-24562
NUCLEAR EXPLOSION EFFECT
Comparison of basis function and iteration solutions to the Fredholm integral equation of the first kind [AD-A206158] N89-24869
NUCLEAR EXPLOSIONS
Comparison of basis function and iteration solutions to the Fredholm integral equation of the first kind [AD-A206158] N89-24869
NUCLEAR FUSION
A role for free electron lasers in fusion N89-25031
Engineering aspects of RTP --- Rijnhuizen Tokamak PETULA (RTP) N89-25032
The control and monitoring system of RTP --- Rijnhuizen Tokamak PETULA (RTP) N89-25037
Impurity accumulation studies in pellet-refuelled ASDEX discharges N89-25039
NUCLEAR MAGNETIC RESONANCE
Two-phase flow measurements by nuclear magnetic resonance imaging [DE89-011850] N89-24586

NUCLEAR SCATTERING
Kaon-nucleus scattering
[NASA-TP-2920] N89-25103
NUCLEAR WEAPONS
Response of layered structures to thermal radiation pulses
[AD-A206355] N89-24453
NUCLEONS
Kaon-nucleus scattering
[NASA-TP-2920] N89-25103
NUMERICAL ANALYSIS
Caltech-DOE program on numerical analysis, scientific computing and fundamental studies of fluid mechanics
[DE89-010828] N89-24582
Self-circumference in the Minkowski plane
[AD-A205691] N89-24868
Numerical methods for stellarator optimization
[DE89-012342] N89-25050
NUMERICAL CONTROL
A comparison of detection efficiency on an air traffic control monitoring task with and without computer aiding
[AD-A206422] N89-24294
Unsteady and separated flows
[AD-A206539] N89-24572
NUMERICAL FLOW VISUALIZATION
Numerical aerodynamic simulation
[NASA-EP-262] N89-24262
NUMERICAL STABILITY
Explicit, implicit, and hybrid methods N89-24656
Numerical integration of asymptotic solutions of ordinary differential equations
[NASA-TM-100650] N89-24867
NUMERICAL WEATHER FORECASTING
Efficient dealiasing of Doppler velocities using local environment constraints
[DOT/FAA/SA-89/1] N89-24771

O

O STARS
Speculation on the origin of X-ray emission in early-type stars N89-25029
OBJECT PROGRAMS
XCAD: A CAD object-oriented virtual solid modeler for an expert system shell
[REPT-882-440-125] N89-24810
OBLIQUE SHOCK WAVES
Nonlinear evolution of interacting oblique waves on two-dimensional shear layers
[NASA-TM-102030] N89-24575
OBSTACLE AVOIDANCE
Optimal guidance with obstacle avoidance for nap-of-the-earth flight
[NASA-CR-177515] N89-24328
OCEAN CURRENTS
Climatic atlas of the outer continental shelf waters and coastal regions of Alaska. Volume 3: Chukchi-Beaufort Sea
[AD-A206525] N89-24776
OCEAN SURFACE
The advanced Ocean Chlorophyll Meter (OCM). A spectral imaging device for the observation of the oceans
[REPT-882-440-118] N89-24689
Correlation between satellite-derived aerosol characteristics and oceanic dimethylsulfide (DMS)
[AD-A206179] N89-24759
Biooptical variability in the Greenland Sea observed with the Multispectral Airborne Radiometer System (MARS)
[NASA-CR-184856] N89-24784
OHMS LAW
Aging behavior of Au-based ohmic contacts to GaAs N89-24727
Relation between global and local aspects of reconnection --- magnetic fields N89-24976
OILS
Efficiency study of oil cooling of a screw compressor
[DE89-011417] N89-24618
ON-LINE SYSTEMS
A systolic array structure for on-line system identification
[AD-A206412] N89-24806
ONBOARD DATA PROCESSING
Microprocessor based 32 channel PCM telemetry system
[NAL-TM-SE-8704] N89-24414
ONBOARD EQUIPMENT
Bordautonomous terrain aided flight navigation in height sections close to terrain surface N89-24301
Landscape-related position finding for flying systems N89-24302
Determination of reference trajectories for testing navigation aids using an onboard CCD camera N89-24303
OPERATING SYSTEMS (COMPUTERS)
The development of a Job-Jobstep scheduler for NS system
[NAL-TR-977] N89-24814
OPERATING TEMPERATURE
Comparison of predicted and measured temperatures of UH-60A helicopter transmission
[NASA-TP-2911] N89-24607
OPERATIONS RESEARCH
A forecast of workloads and manpower requirements for the archiving of scientific and technical reports by the Defense Technical Information Center using a simulation model: An operations research approach
[AD-A206263] N89-25075
OPERATORS (MATHEMATICS)
Two dimensional convolute integer technology for digital image processing N89-24830
Path integral and operator formalism on bordered Riemann surfaces
[DE88-757229] N89-24881
OPTICAL COMMUNICATION
Display-based communications for advanced transport aircraft
[NASA-TM-102187] N89-24798
OPTICAL DATA PROCESSING
The current technological status of spatial light modulators
[AD-A206328] N89-24905
OPTICAL EMISSION SPECTROSCOPY
Infrared studies of active galaxies N89-25087
OPTICAL EQUIPMENT
Laboratory for X-ray optics
[AD-A206468] N89-25061
OPTICAL FILTERS
Combined microstructure X-ray optics
[DE89-009902] N89-24904
OPTICAL HETERODYNING
Holographic interferometry with an injection seeded Nd:YAG laser and two reference beams
[NASA-TM-102056] N89-24591
OPTICAL MATERIALS
Contamination effects study
[NASA-CR-183613] N89-24746
OPTICAL MEASUREMENT
Contamination effects study
[NASA-CR-183613] N89-24746
OPTICAL RADAR
Development of mid-infrared solid state lasers for spaceborne lidar
[NASA-CR-185012] N89-24599
Investigations of the sodium layer of the earth atmosphere: Probing with a terrestrial lidar system at 69 N in winter
[BONN-IR-88-52] N89-24760
A system for high resolution 3D mapping using laser radar and requiring no beam scanning mechanisms N89-24827
OPTICAL REFLECTION
Design of the optical system for a new time-resolved X-ray absorption spectroscopy apparatus
[DE88-757253] N89-24902
OPTICAL SCANNERS
The current technological status of spatial light modulators
[AD-A206328] N89-24905
OPTICAL THICKNESS
Photovoltaic power system operation in the Mars environment
[NASA-TM-102075] N89-24529
On the thermal stability of optically thin flows --- plasmas N89-24973
OPTICAL TRANSITION
Cooperative phenomena for new coherent radiation sources
[AD-A206368] N89-24602
OPTIMAL CONTROL
A weak Hamiltonian finite element method for optimal control problems
[NASA-CR-185336] N89-24873
OPTIMIZATION
A methodology for commonality analysis, with applications to selected space station systems
[NASA-TM-100364] N89-24421
Multidisciplinary optimization for engineering systems: Achievements and potential
[NASA-TM-101566] N89-24508
Integrated optimization of nonlinear R/C frames with reliability constraints N89-24631
The human role in space (THURIS) applications study. Final briefing
[NASA-CR-183590] N89-24793
The human role in space (THURIS) applications study. Volume 2: Research analysis and technology report
[NASA-CR-183589] N89-24795
Numerical methods for stellarator optimization
[DE89-012342] N89-25050
OPTOELECTRONIC DEVICES
Electrooptical feed and control in microwave applications
[FOA-C-30514-3.2] N89-24531
ORBIT CALCULATION
Periodic and heteroclinic orbits for a periodic Hamiltonian system
[AD-A204078] N89-24862
ORBIT TRANSFER VEHICLES
Orbital Transfer Vehicle: Concept definition and system analysis study
[NASA-CR-183551] N89-24410
Development of tailorable advanced blanket insulation for advanced space transportation systems
[NASA-CR-177444] N89-24486
ORBITAL ASSEMBLY
Investigation of structural behavior of candidate Space Station structure
[NASA-CR-181746] N89-24678
ORBITAL MANEUVERING VEHICLES
Orbital Maneuvering Vehicle (OMV) remote servicing kit N89-24838
ORBITAL MANEUVERS
Multiple-pass aeroassisted plane change N89-24404
ORBITAL MECHANICS
Periodic and heteroclinic orbits for a periodic Hamiltonian system
[AD-A204078] N89-24862
ORBITAL POSITION ESTIMATION
Multiple-pass aeroassisted plane change N89-24404
ORBITAL SERVICING
The European in-orbit infrastructure ground segment N89-24340
MTFF user interfaces N89-24345
Hermes-MTFF rendezvous strategy and composite operations N89-24357
Servicing of the MTFF by Hermes N89-24360
MTFF flight operations phases N89-24361
Manned interventions at the MTFF: Crew workload aspects N89-24362
Logistics aspects of Columbus servicing at the Space Station N89-24363
Attached Pressurized Module (APM) center for the Columbus attached pressurized module N89-24377
The Hermes robot arm (HERA) N89-24390
Hermes crew role N89-24401
The human role in space (THURIS) applications study. Final briefing
[NASA-CR-183590] N89-24793
The human role in space (THURIS) applications study. Volume 2: Research analysis and technology report
[NASA-CR-183589] N89-24795
Disconnects for spacecraft servicing applications N89-24832
Orbital Maneuvering Vehicle (OMV) remote servicing kit N89-24838
ORU guidelines for telerobotic compatibility N89-24844
ORBITAL WORKERS
The human role in space (THURIS) applications study. Final briefing
[NASA-CR-183590] N89-24793
The human role in space (THURIS) applications study. Volume 2: Research analysis and technology report
[NASA-CR-183589] N89-24795
ORDER-DISORDER TRANSFORMATIONS
Fundamental studies on order effects in metal alloys
[ONERA-RT-14/221-M] N89-24480
ORGANIC COMPOUNDS
Multiplexed electronically programmable multimode ionization detector for chromatography
[DE89-009758] N89-24465
ORGANOMETALLIC COMPOUNDS
Chemical etching and organometallic chemical vapor deposition on varied geometries of GaAs N89-24728
ORION NEBULA
First detection of SO2 and CH3OH emission and one unidentified line near 800 GHz
[MPE-PREPRINT-142] N89-25086
The Orion molecular cloud and star forming region
[MPE-PREPRINT-140] N89-25094
OROGRAPHY
Orographically-caused microclimate variation in the Saariselka Region
[ISBN-9-5169-7269-1] N89-24767
OSCILLATING FLOW
Unsteady Aerodynamics, volume 1
[VKI-1988-07-VOL-1] N89-24276
Effects of unsteadiness on turbulent boundary layers N89-24280
OXIDATION
Oxide-bound transition metal complexes for methane activation
[PB89-138614] N89-24464

Role of alloying additions in the oxidation-sulfidation of Fe-base alloys
[DE89-009825] N89-24473
In-situ stress measurements during thermal oxidation of silicon
[AD-A206546] N89-24495
Methane to methanol conversion
[DE89-011194] N89-24504

OXIDE FILMS
Isotopic study of oxygen diffusion in oxide coatings
[NASA-TM-102082] N89-24451
Effects of thermal history on stress-related properties of very thin films of thermally grown silicon dioxide, SiO2
[AD-A206547] N89-25062

OXIDES
Oxide-bound transition metal complexes for methane activation
[PB89-138614] N89-24464

OXYGEN
Theoretical studies of important processes in planetary and comet atmospheres. Renewal request
[NASA-CR-184951] N89-25099

OXYGEN ATOMS
An atomic oxygen generation facility for space environmental testings
[NAL-TR-989] N89-24506

OXYGEN ISOTOPES
Isotopic study of oxygen diffusion in oxide coatings
[NASA-TM-102082] N89-24451

OXYGEN RECOMBINATION
Space Station Freedom Solar Array design development
[NASA-TM-102105] N89-24448

P

P-N JUNCTIONS
N/P inP homojunction solar cells with an In0.53Ga0.47As contacting layer grown by liquid phase epitaxy N89-24710
Modelling and design of high performance indium phosphide solar cells N89-24712

PADE APPROXIMATION
Aeroservoelastic modeling and applications using minimum-state approximations of the unsteady aerodynamics
[NASA-TM-101574] N89-24308

PANEL METHOD (FLUID DYNAMICS)
A zonal method for modeling powered-lift aircraft flow fields
[NASA-CR-177521] N89-24287

PANELS
Local stiffener and skin pocket buckling prediction by special PASCO modeling technique: Correlation to test data N89-24628
Nonlinear response of a blade-stiffened graphite-epoxy panel with a discontinuous stiffener: Work in progress N89-24641
Global functions in global-local finite-element analysis of localized stresses in prismatic structures N89-24646
Global-local methodologies and their application to nonlinear analysis N89-24647
Global/local stress analysis of composite panels
[NASA-TM-101622] N89-24681

PARABOLIC ANTENNAS
Feasibility study of a synthesis procedure for array feeds to improve radiation performance of large distorted reflector antennas
[NASA-CR-184974] N89-24511

PARABOLIC DIFFERENTIAL EQUATIONS
Navier-Stokes analysis of cold scramjet-afterbody flows
[NASA-CR-184949] N89-24562

PARABOLIC REFLECTORS
Concentration of off-axis radiation by solar concentrators for space power
[NASA-TM-102052] N89-24438

PARALLEL PROCESSING (COMPUTERS)
Domain decomposition algorithms and computation fluid dynamics
[NASA-CR-185405] N89-24578
Application of the p-version of the finite-element method to global-local problems N89-24648
Nonlinear hierarchical substructural parallelism and computer architecture N89-24650
Unconditionally stable concurrent procedures for transient finite-element analysis N89-24657
File concepts for parallel I/O
[NASA-CR-181843] N89-24816
Totally parallel multilevel algorithms
[NASA-CR-185404] N89-24818

PARALLEL PROGRAMMING
File concepts for parallel I/O
[NASA-CR-181843] N89-24816

PARAMETER IDENTIFICATION
Study of a parametric displacement estimation scheme with application in aerial images N89-24300
Neuromorphic learning of continuous-valued mappings in the presence of noise: Application to real-time adaptive control
[NASA-TM-101999] N89-24856

PARAMETERIZATION
Improvements in the Global Reference Atmospheric Model and comparisons with a global 3-D numerical model
[NASA-CR-184947] N89-24755
Dimensionless parameters for classifying solar wind interactions N89-24914

PARTICLE ACCELERATION
Cosmic linear accelerators N89-24915
Non-steady astrophysical spiral jets driven by magnetic collapse and pressure N89-24920
Particle acceleration and shock wave structure --- astrophysics N89-24930
Shock-associated plasma density fluctuations in the interstellar medium N89-24933
Quasi-adiabatic particle acceleration in magnetic field reversals and the formation of the plasma sheet boundary layer in the earth's magnetotail N89-24943
A new model of PeV gamma-ray sources --- X-ray binaries N89-24946
Particle acceleration by magnetic reconnection and fast magnetosonic shock waves in solar flares N89-24993
Inductive acceleration of protons and electrons in planetary magnetotails N89-25015

PARTICLE ACCELERATOR TARGETS
Erosion and retention of the target plate material in the ASDEX divertor N89-25045

PARTICLE COLLISIONS
A study of K sup deg sec, lambda and lambda bar production in 60 and 200 GeV nucleon OAu and pAu collisions with a streamer chamber detector at the CERN SPS
[MPE-PAE/EXP.EL-198] N89-24900
Kaon-nucleus scattering
[NASA-TP-2920] N89-25103

PARTICLE DENSITY (CONCENTRATION)
Plasma and propagation in auroral and polar ionosphere
[ETN-89-94519] N89-24761

PARTICLE INTERACTIONS
Alfven wave solitons and solar intermediate drift bursts N89-24923
Kaon-nucleus scattering
[NASA-TP-2920] N89-25103

PARTICLE MOTION
Adiabatic, chaotic and quasi-adiabatic charged particle motion in two-dimensional magnetic field reversals N89-24942

PARTICLE PRODUCTION
A study of K sup deg sec, lambda and lambda bar production in 60 and 200 GeV nucleon OAu and pAu collisions with a streamer chamber detector at the CERN SPS
[MPE-PAE/EXP.EL-198] N89-24900

PARTICLE TRACKS
Explosive-emitter cathode produced using the heavy ion track technique
[DE88-706304] N89-24503

PARTICLE TRAJECTORIES
Particle simulation of magnetic reconnection in collision-free plasma sheets N89-24986

PARTICLES
Challenges in computational statistical mechanics
[DE89-009922] N89-24567
Optoelectronic velocimeter development
[DE89-012283] N89-24597
Study of particle confinement in the JT-60 tokamak using skin radiative approximation model
[DE88-756574] N89-24909

PARTITIONS (MATHEMATICS)
Explicit, implicit, and hybrid methods N89-24656
Unconditionally stable concurrent procedures for transient finite-element analysis N89-24657

PASSIVITY
A new structure for comparing surface passivation materials of GaAs solar cells N89-24725

PATTERN RECOGNITION
Empirical analysis and refinement of expert system knowledge bases
[AD-A206226] N89-24858
The current technological status of spatial light modulators
[AD-A206328] N89-24905

PAULI EXCLUSION PRINCIPLE
Factorization of the relativistic Pauli equation in the presence of a gravitational field
[DE88-704749] N89-25090

PAYLOAD CONTROL
MTFF user interfaces N89-24345
Timelining and operations integration concerning APM and MTFF N89-24358
Expert system for European space infrastructure N89-24378
Telescience and payload control support technologies N89-24385
Telescience: A promising operations center N89-24386
MARS Microgravity Advanced Research and Support Center N89-24395

PELLETS
Impurity accumulation studies in pellet-refuelled ASDEX discharges N89-25039

PENETRATION
Cavity dimensions for high velocity penetration events: A comparison of calculational results with data
[DE89-011351] N89-24617

PENUMBRAS
Estimation of sunspot magnetic field parameters using the superpenumbral topology N89-24996

PERCEPTION
Cerebral laterality and handedness in aviation: Performance and selection implications
[AD-A206196] N89-24787

PERFORMANCE PREDICTION
Transient flow thrust prediction for an ejector propulsion concept
[NASA-TM-102078] N89-24318
A model for prediction of STOVL ejector dynamics
[NASA-TM-102098] N89-24319
Isothermal life prediction of composite lamina using a damage mechanics approach
[NASA-TM-102032] N89-24460
Computed performance of the half-scale accurate antenna reflector
[NASA-CR-182284] N89-24532
Turbulent flow in a 180 deg bend: Modeling and computations
[NASA-CR-4141] N89-24579
Two dimensional analysis of a NOVETTE laser generated stress-impulse experiment
[DE89-009909] N89-24600
Local stiffener and skin pocket buckling prediction by special PASCO modeling technique: Correlation to test data N89-24628
A study of material damping in large space structures
[NASA-CR-180076] N89-24634
Contamination effects of GPS Navstar solar array performance N89-24734
NASA Lewis Stirling engine computer code evaluation
[NASA-CR-182248] N89-24741
Photovoltaic advanced research and development project: Solar radiation research
[DE89-000884] N89-24743

PERFORMANCE TESTS
SRB ascent aerodynamic heating design criteria reduction study, volume 2
[NASA-CR-183569] N89-24430
Computed performance of the half-scale accurate antenna reflector
[NASA-CR-182284] N89-24532
ERC nickel cadium battery performance tests and comparisons with lead-acid batteries
[DE89-009753] N89-24535
Teledyne Taber 206-1000 and 2210-3000 pressure transducer proof test and burst test
[NASA-CR-183672] N89-24594
Comparison of predicted and measured temperatures of UH-60A helicopter transmission
[NASA-TP-2911] N89-24607
An empirical study of the performance of APMOVPE AM0 InP homojunction solar cells as a function of emitter thickness and doping, and base doping N89-24709
Photovoltaic advanced research and development project: Solar radiation research
[DE89-000884] N89-24743
Developing, testing, evaluating and optimizing solar heating and cooling systems
[DE89-011831] N89-24744
Automated Millimeter Wave (AMW) transducer testing in a robotic/vision test cell N89-24841

PERIODIC FUNCTIONS
Periodic and heteroclinic orbits for a periodic Hamiltonian system
[AD-A204078] N89-24862

PERMEABILITY
Hydrogen ion-driven permeation in carbonaceous films
[DE89-005271] N89-24485

PERMITTIVITY
On the causality of plasma permittivity
[NASA-TM-101551] N89-24514
Microwave X-band radiometric characterization of Brazilian soils by measurement of the complex permittivity
[INPE-4588-PRE/1319] N89-24685

PERSONAL COMPUTERS
Application of Lotus 1-2-3 to heat transfer analysis
[DE89-010463] N89-24813
PERSONALITY
Cerebral laterality and handedness in aviation: Performance and selection implications
[AD-A206196] N89-24787
PERTURBATION
Improvements in the Global Reference Atmospheric Model and comparisons with a global 3-D numerical model
[NASA-CR-184947] N89-24755
Magnetic reconnection near a stagnation point N89-24983
PERTURBATION THEORY
Advances in dual methods and convex approximations for structural optimization N89-24680
Some notes on shock resolving flux functions. Part 1: Stationary characteristics
[NASA-TM-101087] N89-24871
Gravitational angular fluctuations of the cosmic background radiation produced by cosmological linear perturbations
[DE88-757287] N89-25105
PHASE ERROR
Feasibility study of a synthesis procedure for array feeds to improve radiation performance of large distorted reflector antennas
[NASA-CR-184974] N89-24511
PHASE SHIFT
Two-dimensional phase correction of synthetic aperture radar imagery
[DE89-007086] N89-24524
PHASE TRANSFORMATIONS
Grain boundary phase equilibria in metallic systems
[DE89-011787] N89-25066
PHASE-SPACE INTEGRAL
Beam dynamics with the Hamilton-Jacobi equation
[DE89-012269] N89-24878
PHASED ARRAYS
The frequency response of phased-array antennas
[DE89-009710] N89-24517
Electrooptical feed and control in microwave applications
[FOA-C-30514-3.2] N89-24531
PHENOLS
Mass spectrometry
[DE89-011118] N89-24471
PHOSPHORIC ACID FUEL CELLS
US fuel cell research and applications, 1960--1989
[DE89-012244] N89-24745
PHOTOCHEMICAL REACTIONS
Applications of infrared laser spectroscopy to laser chemistry and laser development
[DE89-011196] N89-24604
PHOTOCONDUCTORS
Microwave characteristics of GaAs MMIC integratable optical detectors
[NASA-TM-101485] N89-24520
PHOTOELECTRIC EMISSION
A noncontacting scanning photoelectron emission technique for bonding surface cleanliness inspection
[NASA-TM-100361] N89-24623
PHOTOELECTRON SPECTROSCOPY
Auger and ESCA analysis
[NASA-CR-183572] N89-24463
X-ray photoelectron spectroscopy study of samples in the Y-Ba-Cu-O system
[AD-A206260] N89-25060
PHOTOIONIZATION
Free radical-surface interactions using multiphoton ionization of free radicals
[AD-A206257] N89-24892
PHOTOLUMINESCENCE
Selective pair luminescence of magnesium in gallium arsenide dissertation
[AD-A206160] N89-25058
PHOTOLYSIS
Free radical-surface interactions using multiphoton ionization of free radicals
[AD-A206257] N89-24892
PHOTOMETERS
Improved defect analysis of Gallium Arsenide solar cells using image enhancement N89-24726
PHOTOMETRY
Radiometric measurement of temperature distributions in solar cavity receivers
[DE89-011467] N89-24742
PHOTOVOLTAIC CELLS
Review of the environmental effects of the Space Station Freedom photovoltaic power module
[NASA-TM-102076] N89-24418
Photovoltaic advanced research and development project: Solar radiation research
[DE89-000884] N89-24743
PHOTOVOLTAIC CONVERSION
The space station power system
[NASA-TM-101245] N89-24416
Space photovoltaic technique. State of the art, trends
[REPT-882-440-120] N89-24442
Space Station Freedom Solar Array design development
[NASA-TM-102105] N89-24448
Space power technology 21: Photovoltaics N89-24706
PHOTOVOLTAIC EFFECT
Space Photovoltaic Research and Technology, 1988. High Efficiency, Space Environment, and Array Technology
[NASA-CP-3030] N89-24704
Space power technology 21: Photovoltaics N89-24706
An empirical study of the performance of APMOVPE AM0 InP homojunction solar cells as a function of emitter thickness and doping, and base doping N89-24709
Advanced photovoltaic solar array development N89-24716
Deployable aerospace PV array based on amorphous silicon alloys N89-24720
AM0 efficiency measurements N89-24736
PHYSICAL EXERCISE
Solute model or cellular energy model: Practical and theoretical aspects of thirst during exercise
[AD-A206143] N89-24785
PHYSIOLOGICAL EFFECTS
Solute model or cellular energy model: Practical and theoretical aspects of thirst during exercise
[AD-A206143] N89-24785
PHYSIOLOGICAL RESPONSES
Neurochemical control of circadian rhythms
[AD-A206213] N89-24788
PHYTOPLANKTON
Biooptical variability in the Greenland Sea observed with the Multispectral Airborne Radiometer System (MARS)
[NASA-CR-184856] N89-24784
PIEZOELECTRICITY
Piezoelectric film load cell robot collision detector
[DE89-010117] N89-24592
PILOT SELECTION
Cerebral laterality and handedness in aviation: Performance and selection implications
[AD-A206196] N89-24787
PILOT TRAINING
The Hermes system training concept N89-24375
Cerebral laterality and handedness in aviation: Performance and selection implications
[AD-A206196] N89-24787
PIONEER PROJECT
Space Pioneers and where they are now
[NASA-EP-264] N89-24333
PIONEER SPACE PROBES
Space Pioneers and where they are now
[NASA-EP-264] N89-24333
PIONEER VENUS SPACECRAFT
Space Pioneers and where they are now
[NASA-EP-264] N89-24333
PIPES (TUBES)
Modeling the missile-launch tube problem in DYSCO N89-24629
PITCH (INCLINATION)
Water tunnel investigation of the vortex dynamics of periodically pitched wings
[AD-A206359] N89-24271
PLANAR STRUCTURES
Analysis of adaptive planar truss structures
[NAL-TR-988] N89-24625
PLANETARY EVOLUTION
Comparative planetology of early intense cratering and other cratering effects
[NASA-CR-182966] N89-24752
Dimensionless parameters for classifying solar wind interactions N89-24914
PLANETARY IONOSPHERES
Theoretical studies of important processes in planetary and comet atmospheres. Renewel request
[NASA-CR-184951] N89-25099
PLANETARY MAGNETIC FIELDS
Magnetic neutral lines in Jupiter's nightside magnetosphere N89-24918
PLANETARY MAGNETOSPHERES
Dimensionless parameters for classifying solar wind interactions N89-24914
Magnetic neutral lines in Jupiter's nightside magnetosphere N89-24918
Inductive acceleration of protons and electrons in planetary magnetotails N89-25015
PLANETARY SURFACES
Comparative planetology of early intense cratering and other cratering effects
[NASA-CR-182966] N89-24752
PLANETOLOGY
Comparative planetology of early intense cratering and other cratering effects
[NASA-CR-182966] N89-24752
PLANNING
A robotic vehicle global route planner for the 1990s N89-24851
A knowledge representation scheme for a robotic land vehicle route planner N89-24853
A deductive approach to automated planning
[AD-A206253] N89-24860
PLASMA ACCELERATION
Computer simulations of cosmic-ray diffusion near supernova remnant shock waves N89-24916
Radiative-resonant MHD interactions between waves and particles and the problem of cosmic-ray spectra N89-24944
Are supernova remnants quasi-parallel or quasi-perpendicular accelerators N89-24948
PLASMA COMPRESSION
Structuring of plasmas by a magnetic field --- solar corona N89-24938
PLASMA CONTROL
Engineering aspects of RTP --- Rijnhuizen Tokamak PETULA (RTP) N89-25032
The control and monitoring system of RTP --- Rijnhuizen Tokamak PETULA (RTP) N89-25037
ASDEX Contributions to the 8th International Conference on Plasma Surface Interaction in Controlled Fusion Devices
[IPP-III/139] N89-25038
Plasma induced changes of a metallic divertor neutralizer plate from ASDEX analyzed by photoacoustics N89-25048
The role of the radial electric field in enhanced confinement regimes in stellarators
[DE89-011572] N89-25049
PLASMA DENSITY
The effect of non-Maxwellian electron distributions on the intensity ratio of resonance to satellite lines
[DE89-006745] N89-24907
Shock-associated plasma density fluctuations in the interstellar medium N89-24933
Effects of unequal particle number densities on Alfven waves N89-24945
PLASMA DIAGNOSTICS
Astrophysical significance of observations and experiments in the earth's magnetosphere N89-24912
ESA's space plasma physics missions: The past and the future ten years N89-24913
Spontaneous and forged reconnection in a magnetic type-X structure N89-25012
Beam guiding system for Rutherford scattering diagnostic at TEXTOR N89-25033
Control and data acquisition system for the neutral beam probe diagnostic on TEXTOR N89-25036
PLASMA DIFFUSION
Computer simulations of cosmic-ray diffusion near supernova remnant shock waves N89-24916
Effects of unequal particle number densities on Alfven waves N89-24945
Drift turbulence of plasma as a gas of vortex ensemble N89-24961
PLASMA DRIFT
Alfven wave solitons and solar intermediate drift bursts N89-24923
The structure of quasiperpendicular collisionless shocks N89-24932
On the nature of a typical pulsars radio emission N89-24952
Drift turbulence of plasma as a gas of vortex ensemble N89-24961
Simulation of electrostatic ion instabilities in the presence of parallel currents and transverse electric fields N89-24972
Nonlinear dynamics of the drift tearing-mode N89-24979
Anomalous collision frequency of magnetoactive plasmas with two-dimensional electrostatic turbulence (kB=O) N89-24981
PLASMA DYNAMICS
The role of magnetic reconnection in magnetotail plasmoid dynamics N89-25014
PLASMA FREQUENCIES
The electron beam instability revisited: Growth above and below f sub p N89-24917
PLASMA HEATING
Coronal heating by resonant absorption in resistive MHD N89-24926
Singularities of the local MHD-resonances in solar chromosphere plasma N89-24927
Generation of X-ray and radio emission by binary Wolf-Rayet stars N89-24929
The formation of interstellar clouds N89-24935
Stability of force-free magnetic fields and the problem of solar coronal heating N89-24990

Impulsive heating plasma turbulence and magnetic reconnection inside current sheets N89-25010
The role of cold electrons in the generation of the high-frequency part of broadband electrostatic noise --- magnetotail N89-25018
Elliptical polarization for ECRH on RTP --- Rijnhuizen Tokamak PETULA (RTP) N89-25035

PLASMA INTERACTIONS
Dimensionless parameters for classifying solar wind interactions N89-24914
Quasi-adiabatic particle acceleration in magnetic field reversals and the formation of the plasma sheet boundary layer in the earth's magnetotail N89-24943
Radiative-resonant MHD interactions between waves and particles and the problem of cosmic-ray spectra N89-24944

PLASMA JETS
ELF plasma turbulence observed by Prognoz-8 in plasma jets in the magnetospheric tail N89-25020

PLASMA LAYERS
Characterization of the ASDEX scrape-off-layer density profile during neutral beam heating N89-25040
ASDEX edge and divertor simulation and the problem of incomplete and inaccurate experimental data N89-25041
Comparison of recycling in the ASDEX divertor before and after hardening N89-25042
The low energy neutral fluxes and their impurity production at the walls of ASDEX N89-25043

PLASMA OSCILLATIONS
The role of whistler oscillations in the formation of the structure of high Mach number collisionless shock N89-24936

PLASMA PHYSICS
Plasma and propagation in auroral and polar ionosphere
[ETN-89-94519] N89-24761
Proceedings of an International School and Workshop on Plasma Astrophysics, volume 1
[ESA-SP-285-VOL-1] N89-24910
Development of astrophysics from the telescope to the Sputnik N89-24911
ESA's space plasma physics missions: The past and the future ten years N89-24913
Cosmic linear accelerators N89-24915
Helioseismology and plasma physics N89-24922
Kink modes in coronal loops N89-24925
Problem of nonrotating black hole accretion disk main energy release region extension N89-24951
Bars and open spirals in density wave theory --- galaxies N89-24964
High-pressure two temperature equations of state --- plasmas N89-24967
FOM-Rijnhuizen contributions to the Fifteenth Symposium on Fusion Technology
[REPT-88-179] N89-25030
ASDEX Contributions to the 8th International Conference on Plasma Surface Interaction in Controlled Fusion Devices
[IPP-III/139] N89-25038
Impurity accumulation studies in pellet-refuelled ASDEX discharges N89-25039
Characterization of the ASDEX scrape-off-layer density profile during neutral beam heating N89-25040
ASDEX edge and divertor simulation and the problem of incomplete and inaccurate experimental data N89-25041
Comparison of recycling in the ASDEX divertor before and after hardening N89-25042
The low energy neutral fluxes and their impurity production at the walls of ASDEX N89-25043
Charge exchange neutral sputtering in ASDEX N89-25044
Erosion and retention of the target plate material in the ASDEX divertor N89-25045
Measurements of the flux of metallic impurities to the ASDEX divertor plates N89-25046
Material transport at the vessel walls of the divertor tokamak ASDEX N89-25047

PLASMA PINCH
The formation of interstellar clouds N89-24935
Pinch-effect and stellar flares physics N89-25004
Flare-type plasma processes and explosive disruption of pinch current sheets N89-25008
Current sheet structure at different stages of magnetic reconnection N89-25009
Plasma induced changes of a metallic divertor neutralizer plate from ASDEX analyzed by photoacoustics N89-25048

PLASMA POTENTIALS
Cosmic linear accelerators N89-24915
The structure of quasiperpendicular collisionless shocks N89-24932

PLASMA RESONANCE
Coronal heating by resonant absorption in resistive MHD N89-24926
Singularities of the local MHD-resonances in solar chromosphere plasma N89-24927
Radiative-resonant MHD interactions between waves and particles and the problem of cosmic-ray spectra N89-24944

PLASMA SHEATHS
Quasi-adiabatic particle acceleration in magnetic field reversals and the formation of the plasma sheet boundary layer in the earth's magnetotail N89-24943

PLASMA SLABS
Quasi-adiabatic particle acceleration in magnetic field reversals and the formation of the plasma sheet boundary layer in the earth's magnetotail N89-24943

PLASMA SPECTRA
Decay process and radiative transfer in plasmas N89-24960

PLASMA TEMPERATURE
Quantum relativistic theory of the cyclotron radiation in a strongly magnetized plasma with anisotropic temperature --- neutron stars N89-24962
High-pressure two temperature equations of state --- plasmas N89-24967

PLASMA TURBULENCE
Small-scale instabilities in accretion disks of compact objects and their manifestations N89-24950
Strong Langmuir turbulence and the pulsar emission mechanism N89-24956
Decay process and radiative transfer in plasmas N89-24960
Drift turbulence of plasma as a gas of vortex ensemble N89-24961
Generation of large-scale vortices in compressible helical turbulence N89-24969
Reconnection and microturbulence N89-24980
Anomalous collision frequency of magnetoactive plasmas with two-dimensional electrostatic turbulence (kB = O) N89-24981
Impulsive heating plasma turbulence and magnetic reconnection inside current sheets N89-25010
ELF plasma turbulence observed by Prognoz-8 in plasma jets in the magnetospheric tail N89-25020

PLASMA WAVES
Relativistic shocks in electron-positron plasmas and polar cap accretion onto neutron stars: Two non-linear problems in astrophysical plasma physics N89-24928
The structure of quasiperpendicular collisionless shocks N89-24932
The role of whistler oscillations in the formation of the structure of high Mach number collisionless shock N89-24936
Quasi-perpendicular collisionless high Mach number shocks N89-24937

PLASMA-ELECTROMAGNETIC INTERACTION
MHD-waves and their nonlinear interaction in a plasma with magnetic flux tubes N89-24921
Structuring of plasmas by a magnetic field --- solar corona N89-24938
Black hole driven winds N89-25096

PLASMA-PARTICLE INTERACTIONS
Computer simulations of cosmic-ray diffusion near supernova remnant shock waves N89-24916

PLASMAS (PHYSICS)
On the causality of plasma permittivity
[NASA-TM-101551] N89-24514
Steady-state operation regime of tokamak reactor plasma. Consistency analysis (I)
[DE88-756571] N89-24908
Decay process and radiative transfer in plasmas N89-24960

PLASTIC PROPERTIES
Isothermal life prediction of composite lamina using a damage mechanics approach
[NASA-TM-102032] N89-24460

PLATES
Experimental component mode synthesis applied to the solar array type structure
[NAL-TR-994] N89-24702

PLATES (STRUCTURAL MEMBERS)
A study of composite plates with holes/inclusions N89-24627

PLATES (TECTONICS)
Determination of station coordinates, earth rotation and plate motions from LAGEOS laser ranging: 1983-1986
[NAL-TR-980T] N89-24753
Plate motions and deformations from geologic and geodetic data
[NASA-CR-184987] N89-24757

PLUGGING
Analysis of the plugging of the systems autonomy demonstration project brassboard filters
[NASA-CR-177533] N89-24450

PLUMES
Thermal radiation from plumes of solid propellant rockets
[NAL-TR-990] N89-24432
The experiments of LIPS 3 N89-24735

PNEUMATICS
Development and utilization of new diagnostics for dense-phase pneumatic transport
[DE89-011381] N89-24583

POGO EFFECTS
Pressure-volume properties of metallic bellows
[NASA-TM-100365] N89-24422

POLAR CAPS
Correlation between satellite-derived aerosol characteristics and oceanic dimethylsulfide (DMS)
[AD-A206179] N89-24759

POLAR CUSPS
Singularities of the local MHD-resonances in solar chromosphere plasma N89-24927

POLAR REGIONS
Plasma and propagation in auroral and polar ionosphere
[ETN-89-94519] N89-24761

POLARIZATION CHARACTERISTICS
On the mechanism of the formation of the polarization characteristics of pulsar radiation N89-24953

POLICIES
Overall coherence of the European programs within a long-term space policy N89-24341
French national policy on the preparation of Columbus utilization N89-24344
Space station: A step into the future
[NASA-PAM-510/11-87] N89-24417

POLLUTION TRANSPORT
Field studies for determining the characteristics and dynamics of local circulations
[DE89-012290] N89-24751

POLYCRYSTALS
Development of tandem cells consisting of GaAs single crystal and CuInSe2/CdZnS polycrystalline thin films N89-24717

POLYETHYLENES
Impact and penetration resistance of fibrous composites
[AD-A206417] N89-24454

POLYIMIDES
Thermoplastic coating of carbon fibers
[NASA-CR-185047] N89-24488

POLYMERIC FILMS
Experimentation and analysis of compression test methods for single filament high performance fibres
[AD-A206358] N89-24467

POLYMERIZATION
Sol-gel processing of controlled pore films
[DE89-013584] N89-24501

POLYNOMIALS
Experimental component mode synthesis applied to the solar array type structure
[NAL-TR-994] N89-24702
Computational method of the inverse kinematics via simplified algebraic equation
[DE88-757269] N89-24866

POLYURETHANE RESINS
Laser-induced-fluorescence inspection of polyurethane and related materials, phase 1
[AD-A206423] N89-24492

POPULATIONS
Estimating population size of Pygoscelid Penguins from TM data
[NASA-CR-180081] N89-24687

POROSITY
Analysis of packed-particle rearrangement during colloidal ceramic processing: Gamma-ray densitometry and a review of alternative methods
[DE89-009066] N89-24489
Sol-gel processing of controlled pore films
[DE89-013584] N89-24501
Characterization of pore evolution in ceramics during creep failure and densification
[DE89-013599] N89-24502

POROUS MATERIALS
On specimen shape effects and the ductility of porous metals
[AD-A206216] N89-24475
Development of an engineering methodology for applying foam technology
[DE89-000740] N89-24497

PORTABLE EQUIPMENT
Geological gyrocompass
[PB89-133086] N89-24589
Stabilized image system for mobile robots N89-24829
Development of a man-portable control unit for a teleoperated land vehicle N89-24835

POSITION (LOCATION)
Tele-autonomous control involving contacts: The applications of a high precision laser line range sensor
[NASA-CR-184995] N89-24509
A demonstration of retro-traverse using a semi-autonomous land vehicle N89-24852

IRIS: An intelligent robot insertion expert system N89-24854

POSITION SENSING
Position-sensitive CdTe detector using improved crystal growth method
[NASA-CR-183427] N89-25051

POSITIONING
Landscape-related position finding for flying systems N89-24302

POSITRON ANNIHILATION
Induced annihilation of particle-antiparticle pairs N89-24970

POTASSIUM
Is salt at fault
[AD-A206518] N89-24789

POWDER (PARTICLES)
High temperature mechanical properties and microscopic examination of extruded powder aluminum
[DE89-010457] N89-24484

POWDER METALLURGY
Amorphous metal alloys produced by mechanical alloying
[DE89-011189] N89-24481

POWER CONDITIONING
The 5-kW arcjet power electronics
[NASA-TM-102108] N89-24446

POWER CONVERTERS
The 5-kW arcjet power electronics
[NASA-TM-102108] N89-24446

POWER REACTORS
Electrophoretically applied dielectrics for amorphous metal foils used in pulsed power saturable reactors
[DE89-009322] N89-24525

POWER SPECTRA
An investigation of the Overlap between the Statistical Discrete Gust and the Power Spectral Density analysis methods
[NASA-TM-101571] N89-24310

POWERED LIFT AIRCRAFT
A zonal method for modeling powered-lift aircraft flow fields
[NASA-CR-177521] N89-24287

PREIMPREGNATION
Composite material bonding: Gelation and processing of adhesives and preimpregnated materials
[ETCA-88-R-006] N89-24457

PREMIXED FLAMES
Velocity and scalar fields of turbulent premixed flame in stagnation flow
[DE89-009336] N89-24566

PREMIXING
A premixed hydrogen/oxygen catalytic igniter
[NASA-CR-185113] N89-24445

PREPREGS
Thermoplastic coating of carbon fibers
[NASA-CR-185047] N89-24488

PRESSURE DEPENDENCE
NASA Lewis Stirling engine computer code evaluation
[NASA-CR-182248] N89-24741

PRESSURE DISTRIBUTION
Interaction of Karman vortex-street with an elliptical leading-edge N89-24268
Some dynamical properties of anisotropic collisionless stellar systems N89-24963

PRESSURE EFFECTS
Pressure-volume properties of metallic bellows
[NASA-TM-100365] N89-24422
Modeling thermal-mechanical processes associated with the initiation and combustion of granular energetic materials
[DE89-007145] N89-24472
Pressure-strain-rate events in homogeneous turbulent shear flow N89-24551
Teledyne Taber 206-1000 and 2210-3000 pressure transducer proof test and burst test
[NASA-CR-183672] N89-24594

PRESSURE GRADIENTS
Effects of unsteadiness on turbulent boundary layers N89-24280

PRESSURE MEASUREMENT
On the dynamic response of pressure transmission lines in the research of helium-charged free piston Stirling engines
[NASA-TM-102121] N89-24593

PRESSURE SENSORS
Teledyne Taber 206-1000 and 2210-3000 pressure transducer proof test and burst test
[NASA-CR-183672] N89-24594

PRESSURIZED CABINS
Attached Pressurized Module (APM) center for the Columbus attached pressurized module N89-24377
The utilization of the European pressurized module for non-European experiments --- Columbus N89-24399

PRESSURIZING
Field joint environmental protection system vibration/pressurization qualification
[NASA-CR-183673] N89-24449

PRISMS
Domed Fresnel lens concentrator technology for space application N89-24732

PROBABILITY DENSITY FUNCTIONS
Dynamical interpretation of conditional patterns N89-24549
Analysis of homogeneous turbulent reacting flows N89-24558

PROBABILITY THEORY
The Fault Tree Compiler (FTC): Program and mathematics
[NASA-TP-2915] N89-24815

PROBLEM SOLVING
Composite Blade Structural Analyzer (COBSTRAN) demonstration manual
[NASA-TM-101957] N89-24459
Domain decomposition algorithms and computation fluid dynamics
[NASA-CR-185405] N89-24578
Explicit, implicit, and hybrid methods N89-24656
Unconditionally stable concurrent procedures for transient finite-element analysis N89-24657
Development of higher-order modal methods for transient thermal and structural analysis
[NASA-TM-101548] N89-24677
Cooperating expert systems N89-24825
On designing a case-based system for expert process development N89-24847
Applications of aerospace technology
[NASA-CR-181536] N89-25076

PROCEDURES
On designing a case-based system for expert process development N89-24847

PROCUREMENT MANAGEMENT
Study on cost efficiency of product assurance in space programs
[REPT-882-440-122] N89-24622

PRODUCT DEVELOPMENT
The technology contents of the first phase of the Hermes Development Program N89-24350

PROGRAM VERIFICATION (COMPUTERS)
Transformational derivation of programs using the Focus system
[NASA-CR-184875] N89-24802
Predeployment validation of fault-tolerant systems through software-implemented fault insertion
[NASA-CR-4244] N89-24817

PROGRAMMING LANGUAGES
Hardware modeling with VHDL (VHSIC Hardware Description Language) simulation
[AD-A206356] N89-24805
Neutral file data exchange between simulators and robots N89-24824
Space languages: Solving the classic scheduling problem in Ada and Lisp N89-24826

PROJECT MANAGEMENT
Overall coherence of the European programs within a long-term space policy N89-24341
China's future space activities N89-24342
The Manned Space Laboratories Control Center (MSCC) at DFVLR, Oberpfaffenhofen, Germany, F.R. N89-24376
Space station: A step into the future
[NASA-PAM-510/11-87] N89-24417
Applications of aerospace technology
[NASA-CR-181536] N89-25076

PROJECT PLANNING
Applications of aerospace technology
[NASA-CR-181536] N89-25076

PROPAGATION
Development of an engineering methodology for applying foam technology
[DE89-000740] N89-24497

PROPELLANT COMBUSTION
A premixed hydrogen/oxygen catalytic igniter
[NASA-CR-185113] N89-24445
Modeling thermal-mechanical processes associated with the initiation and combustion of granular energetic materials
[DE89-007145] N89-24472

PROPELLANT PROPERTIES
Materials compatibility with oxidizer-rich gases at elevated temperatures and pressure
[NASA-CR-183647] N89-24466

PROPELLER SLIPSTREAMS
Analysis of the wake behind a propeller using the finite element method with a two-equation turbulence model N89-24286

PROPELLERS
Cruise noise of the SR-2 propeller model in a wind tunnel
[NASA-TM-101480] N89-24886

PROPULSION SYSTEM CONFIGURATIONS
Calculation of scramjet performance
[NAL-TR-987] N89-24317
Turbomachinery technology for high-speed civil flight
[NASA-TM-102092] N89-24320
Ariane 5 solid boosters: Overview of design approach and envisaged technologies N89-24352
Technology and design method evolution of cryogenic propulsion systems: Example of the main Ariane 5 stage N89-24353

PROPULSION SYSTEM PERFORMANCE
Calculation of scramjet performance
[NAL-TR-987] N89-24317
Performance of large area xenon ion thrusters for orbit transfer missions
[NASA-TM-102049] N89-24436

PROTECTIVE COATINGS
Isotopic study of oxygen diffusion in oxide coatings
[NASA-TM-102082] N89-24451
Hydrogen ion-driven permeation in carbonaceous films
[DE89-005271] N89-24485
Ceramic technology for advanced heat engines project
[DE89-012890] N89-24500

PROTEIN CRYSTAL GROWTH
An automated protein crystal growth facility on the space station N89-24820

PROTON SCATTERING
Kaon-nucleus scattering
[NASA-TP-2920] N89-25103

PROTONS
Characterizing the energy deposition events produced by trapped protons in low earth orbit
[DE89-011218] N89-24893
A new model of PeV gamma-ray sources --- X-ray binaries N89-24946
The precursors of the 9 July 1982 solar proton flare event N89-25001
Inductive acceleration of protons and electrons in planetary magnetotails N89-25015

PROTOSTARS
An observational study of the dynamics of molecular cloud cores N89-25097

PROTOTYPES
Advanced photovoltaic solar array development N89-24716

PSYCHOACOUSTICS
Advanced turboprop aircraft flyover noise: Annoyance to counter-rotating-propeller configurations with a different number of blades on each rotor: Preliminary results
[NASA-TM-100638] N89-24888

PSYCHOLOGY
Evaluation, description and invention: Paradigms for human-computer interaction
[AD-A204617] N89-24796

PSYCHOPHYSIOLOGY
Field-dependence and judgment of weight and color revisited: Some implications for the study of sensory discrimination
[AD-A206141] N89-24791

PULSARS
Theory of radioemission of pulsars N89-24941
Two-stream instability in pulsar magnetospheres N89-24949
On the nature of a typical pulsars radio emission N89-24952
On the mechanism of the formation of the polarization characteristics of pulsar radiation N89-24953
Strong Langmuir turbulence and the pulsar emission mechanism N89-24956
Pulsar radio and visible radiation due to the modulation instability of high-frequence transverse waves in the inhomogeneous electron-positron plasma N89-24959
Soft X-ray observations of the Vela Pulsar PSR 0833-45
[MPE-PREPRINT-130] N89-25080

PULSE DOPPLER RADAR
Ground cluster filters for staggered pulse trains
[DOT/FAA/SA-89/2] N89-24515

PULSE DURATION MODULATION
The 5-kW arcjet power electronics
[NASA-TM-102108] N89-24446

PULSE FREQUENCY MODULATION TELEMETRY
Microprocessor based 32 channel PCM telemetry system
[NAL-TM-SE-8704] N89-24414

PULSES
Boundary layer response to an unsteady turbulent environment
[AD-A206578] N89-24273
Response of layered structures to thermal radiation pulses
[AD-A206355] N89-24453

PUMPS
Continuous cryopump with a method for removal of solidified gases
[DE89-009760] N89-24611
Efficiency study of oil cooling of a screw compressor
[DE89-011417] N89-24618

Q

QUALITY CONTROL
Study on cost efficiency of product assurance in space programs
[REPT-882-440-122] N89-24622
Application of the p-version of the finite-element method to global-local problems N89-24648
QUANTUM MECHANICS
Quantum mechanics of chemical reactions: Recent developments in reactive scattering and in reaction path Hamiltonians
[DE89-010438] N89-24470
QUANTUM THEORY
Introduction to dissociative recombination
[NASA-CR-184950] N89-24889
Quantum relativistic theory of the cyclotron radiation in a strongly magnetized plasma with anisotropic temperature --- neutron stars N89-24962
QUANTUM WELLS
Vertical emitting, ring geometry, ultra-low threshold and ultra-high speed quantum well lasers for optical interconnect
[AD-A206427] N89-24603

R

RADAR
The frequency response of phased-array antennas
[DE89-009710] N89-24517
RADAR APPROACH CONTROL
Design of automated system for management of arrival traffic
[NASA-TM-102201] N89-24290
RADAR FILTERS
Ground cluster filters for staggered pulse trains
[DOT/FAA/SA-89/2] N89-24515
RADAR IMAGERY
Magellan: The unveiling of Venus
[NASA-CR-185018] N89-24419
Two-dimensional phase correction of synthetic aperture radar imagery
[DE89-007086] N89-24524
Improvement and extension of a radar forest backscattering model
[NASA-CR-184975] N89-24686
Necessity and benefit of the X-SAR space shuttle experiment
[DFVLR-MITT-88-29] N89-24688
Plasma and propagation in auroral and polar ionosphere
[ETN-89-94519] N89-24761
RADIAL VELOCITY
Numerical study on laminar circular jet of carbonic acid gas discharging into stagnant air
[DE88-757249] N89-24565
Efficient dealiasing of Doppler velocities using local environment constraints
[DOT/FAA/SA-89/1] N89-24771
A study of the Southern Supercluster N89-25088
RADIANCE
Biooptical variability in the Greenland Sea observed with the Multispectral Airborne Radiometer System (MARS)
[NASA-CR-184856] N89-24784
RADIATION COUNTERS
Investigations on fully depletable charge coupled devices
[MPI-PAE/EXP.EL-194] N89-25063
RADIATION DAMAGE
The impact of solar cell technology on planar solar array performance N89-24715
Radiation resistance studies of amorphous silicon films N89-24738
RADIATION DOSAGE
Protection against ionizing radiation for the Hermes mission N89-24370
RADIATION EFFECTS
Photovoltaic power system operation in the Mars environment
[NASA-TM-102075] N89-24529
Deep levels and radiation effects in p-InP N89-24713
A comparison of the radiation tolerance characteristics of multijunction solar cells with series and voltage-matched configurations N89-24737
Characterizing the energy deposition events produced by trapped protons in low earth orbit
[DE89-011218] N89-24893
RADIATION HARDENING
Radiation hardened, optically-triggered thyristor switches: Preliminary data on three device designs
[DE89-011469] N89-24533
RADIATION HAZARDS
Safety analysis report for the Galileo Mission. Volume 2, book 1: Accident model document
[DE89-007270] N89-24896
Safety analysis report for the Galileo Mission. Volume 2, book 2: Accident model document, Appendices
[DE89-007271] N89-24897
Safety analysis report for the Galileo Mission. Volume 3, book 1: Nuclear risk analysis document, revision 1
[DE89-007272] N89-24898
Safety analysis report for the Galileo Mission. Volume 3, book 2: Nuclear risk analysis document. Appendices, revision 1
[DE89-007273] N89-24899
RADIATION MEASUREMENT
Photovoltaic advanced research and development project: Solar radiation research
[DE89-000884] N89-24743
Characterizing the energy deposition events produced by trapped protons in low earth orbit
[DE89-011218] N89-24893
RADIATION MEASURING INSTRUMENTS
Modeling and characterization of the Earth Radiation Budget Experiment (ERBE) nonscanner and scanner sensors
[NASA-CR-181818] N89-24772
RADIATION PROTECTION
Medical and radiation protection problems in space N89-24369
Protection against ionizing radiation for the Hermes mission N89-24370
Development of tandem cells consisting of GaAs single crystal and CuInSe2/CdZnS polycrystalline thin films N89-24717
RADIATION SHIELDING
Protection against ionizing radiation for the Hermes mission N89-24370
Hydrogen ion-driven permeation in carbonaceous films
[DE89-005271] N89-24485
RADIATION SOURCES
Cooperative phenomena for new coherent radiation sources
[AD-A206368] N89-24602
A new model of PeV gamma-ray sources --- X-ray binaries N89-24946
COS-B gamma-ray sources beyond the predicted diffuse emission
[MPE-PREPRINT-136] N89-25107
RADIATION SPECTRA
Comparison of basis function and iteration solutions to the Fredholm integral equation of the first kind
[AD-A206158] N89-24869
Radiative-resonant MHD interactions between waves and particles and the problem of cosmic-ray spectra N89-24944
RADIATION TOLERANCE
Progress in indium phosphide solar cell research N89-24707
Response of single junction GaAs/GaAs and GaAs/Ge solar cells to multiple doses of 1 MeV electrons N89-24722
A comparison of the radiation tolerance characteristics of multijunction solar cells with series and voltage-matched configurations N89-24737
Radiation resistance studies of amorphous silicon films N89-24738
RADIATIVE TRANSFER
Estimating the outgoing longwave radiation from the Meteosat infrared window and water vapor bands
[ETN-89-94533] N89-24762
Water vapor retrievals through the 3I (Improved Initialization Inversion) system: Application to tropospheric altimetry correction
[ETN-89-94534] N89-24778
The radiation-atmosphere interaction model and the determination of meteorological and climatological parameters from satellite observations
[ETN-89-94535] N89-24779
Decay process and radiative transfer in plasmas N89-24960
RADIO ASTRONOMY
Diagnostics of energy release and magnetic fields on the sun by radio methods N89-24998
Tremsdorf solar radio astronomy observatory: The scientific program and an interesting observation N89-24999
RADIO BURSTS
Generation of X-ray and radio emission by binary Wolf-Rayet stars N89-24929
Theory of radioemission of pulsars N89-24941
Two-stream instability in pulsar magnetospheres N89-24949
On the nature of a typical pulsars radio emission N89-24952
RADIO EMISSION
Strong Langmuir turbulence and the pulsar emission mechanism N89-24956
High energy particles in supernova remnants and the interstellar medium N89-25108
RADIO FREQUENCY INTERFERENCE
Ground cluster filters for staggered pulse trains
[DOT/FAA/SA-89/2] N89-24515
RADIO JETS (ASTRONOMY)
Non-steady astrophysical spiral jets driven by magnetic collapse and pressure N89-24920
Global kinetic theory of astrophysical jets N89-24954
Jets and beams in powerful extragalactic radio sources N89-24957
On particle energization by magnetic field line reconnection in extragalactic jets N89-25028
RADIO SOURCES (ASTRONOMY)
Jets and beams in powerful extragalactic radio sources N89-24957
Synchrotron thermal instabilities and filamentation in radio sources N89-24958
Physical conditions in molecular clouds derived from sub-mm and far-IR spectroscopic observations
[MPE-PREPRINT-135] N89-25082
RADIOMETERS
Radiometric measurement of temperature distributions in solar cavity receivers
[DE89-011467] N89-24742
Biooptical variability in the Greenland Sea observed with the Multispectral Airborne Radiometer System (MARS)
[NASA-CR-184856] N89-24784
RADIOSONDES
Simulation studies of improved sounding systems
[NASA-CR-185322] N89-24758
RAIN
Contribution to the estimation of precipitation in the Sahel by using satellite imagery
[SER-DI-204] N89-24782
RAIN FORESTS
Bibliography on tropical rain forests and the global carbon cycle. Volume 2: South Asia
[DE89-008971] N89-24748
RAMAN SPECTROSCOPY
A remote laser-probing system for combustion measurements
[NAL-TR-979] N89-24598
RANKINE-HUGONIOT RELATION
On the existence and stability of intermediate shocks --- MHD N89-24971
RAPID TRANSIT SYSTEMS
Turbomachinery technology for high-speed civil flight
[NASA-TM-102092] N89-24320
RAYLEIGH SCATTERING
Atmospheric effects on laser propagation
[DE89-012287] N89-24606
Multiphoton transitions at the Moessbauer radiation diffraction in crystals under a weak ultrasonic field
[DE88-706341] N89-25069
REACTION KINETICS
A numerical study of chemically reacting flow in nozzles
[NASA-TM-102135] N89-24444
Quantum mechanics of chemical reactions: Recent developments in reactive scattering and in reaction path Hamiltonians
[DE89-010438] N89-24470
Bonding and chemistry of hydrocarbon monolayers on metal surfaces
[DE89-009311] N89-24490
Methane to methanol conversion
[DE89-011194] N89-24504
Analysis of homogeneous turbulent reacting flows N89-24558
REACTION PRODUCTS
Increasing the chemical yield of desirable chemical species using solar rapid heating
[DE89-000881] N89-24469
REACTOR MATERIALS
Investigations on the creep-rupture behavior of the austenitic stainless steel AISI 316-NET
[KFK-4468] N89-24479
REAL TIME OPERATION
Real-time system: Specification and verification
[AD-A206467] N89-24807
Predeployment validation of fault-tolerant systems through software-implemented fault insertion
[NASA-CR-4244] N89-24817
Neuromorphic learning of continuous-valued mappings in the presence of noise: Application to real-time adaptive control
[NASA-TM-101999] N89-24856
A comparison of two real-time control schemes for redundant robots with bounded joint velocities
[DE89-002974] N89-24861

RECEIVERS
Transient flow thrust prediction for an ejector propulsion concept
[NASA-TM-102078] N89-24318
RECOMBINATION REACTIONS
A new structure for comparing surface passivation materials of GaAs solar cells N89-24725
Study of chemical reaction models for high enthalpy flow of air
[NAL-TR-982] N89-25072
Theoretical studies of important processes in planetary and comet atmospheres. Renewel request
[NASA-CR-184951] N89-25099
RECRYSTALLIZATION
Effects of multiple reductions on grain refinement during hot working of alloy 718
[DE89-010426] N89-24483
RECTANGULAR WAVEGUIDES
A hybrid asymptotic-modal analysis of the EM scattering by an open-ended S-shaped rectangular waveguide cavity
[NASA-CR-185053] N89-24519
Analysis of a probe-metallic sleeve feed system for a rectangular waveguide
[DE89-006769] N89-24523
RED SHIFT
Red-shift experiments and non-Newtonian gravitational forces
[DE89-009349] N89-25092
REDUCED GRAVITY
Microgravity payloads (APM and MTFF) N89-24347
Industrial utilization of microgravity: Problems in the realization phase N89-24383
The Microgravity User Support Center (MUSC) N89-24394
MARS Microgravity Advanced Research and Support Center N89-24395
Fire safety applications for spacecraft
[NASA-TM-101463] N89-24413
The impact of an IVA robot on the space station microgravity environment N89-24821
REENTRY EFFECTS
Thermal analysis of a hypersonic wing test structure
[NASA-CR-185319] N89-24265
REFLECTANCE
Contamination effects study
[NASA-CR-183613] N89-24746
REFLECTED WAVES
Concentration of off-axis radiation by solar concentrators for space power
[NASA-TM-102052] N89-24438
REFLECTORS
Containerless glass fiber processing
[NASA-TM-86540] N89-24405
Computed performance of the half-scale accurate antenna reflector
[NASA-CR-182284] N89-24532
REFRACTION
On the refraction of longitudinal waves in compressible media
[DE89-012922] N89-24588
REFRACTORY MATERIALS
Isothermal life prediction of composite lamina using a damage mechanics approach
[NASA-TM-102032] N89-24460
Time dependent reliability model incorporating continuum damage mechanics for high-temperature ceramics
[NASA-TM-102046] N89-24487
REFRIGERANTS
Efficiency study of oil cooling of a screw compressor
[DE89-011417] N89-24618
REFUELING
Robotic visual servo control for aircraft ground refueling N89-24836
REGENERATIVE FUEL CELLS
Fuel cell development for Hermes N89-24355
REGRESSION ANALYSIS
AR (Autoregressive) modeling of coherence in time delay and doppler estimation
[AD-A205239] N89-24513
An operational analysis and forecasting method of evaporation
[MP-11] N89-24769
REINFORCED PLASTICS
Technology of aircraft construction (selected chapters)
[AD-A199946] N89-24261
REINFORCEMENT (STRUCTURES)
Global-local methodologies and their application to nonlinear analysis N89-24647
Features and characterization needs of rubber composite structures N89-24649
REINFORCING MATERIALS
Laser-induced-fluorescence inspection of polyurethane and related materials, phase 1
[AD-A206423] N89-24492
RELATIVISTIC EFFECTS
Quantum relativistic theory of the cyclotron radiation in a strongly magnetized plasma with anisotropic temperature --- neutron stars N89-24962
RELATIVISTIC PLASMAS
Relativistic shocks in electron-positron plasmas and polar cap accretion onto neutron stars: Two non-linear problems in astrophysical plasma physics N89-24928
Relativistic MHD from two-fluid hydrodynamics (TFHD) --- space plasmas N89-24931
Jets and beams in powerful extragalactic radio sources N89-24957
RELIABILITY ANALYSIS
The Fault Tree Compiler (FTC): Program and mathematics
[NASA-TP-2915] N89-24815
RELIABILITY ENGINEERING
Safety and reliability of the Ariane 5-Hermes composite N89-24365
Columbus safety and reliability N89-24368
The impact of manned space flight operations on the safety and reliability aspects of ground systems requirements N89-24371
REMOTE CONTROL
Vision system testing for teleoperated vehicles
[DE89-009713] N89-24610
Advanced servomanipulator remote maintenance demonstration
[DE89-010188] N89-24614
Testing the feasibility of using a teleoperated robot for remote, dexterous operations N89-24843
A demonstration of retro-traverse using a semi-autonomous land vehicle N89-24852
REMOTE MANIPULATOR SYSTEM
The Hermes robot arm (HERA) N89-24390
REMOTE SENSING
Microwave X-band radiometric characterization of Brazilian soils by measurement of the complex permittivity
[INPE-4588-PRE/1319] N89-24685
Estimating population size of Pygoscelid Penguins from TM data
[NASA-CR-180081] N89-24687
The activities of the British National Space Centre (BNSC) in the field of imaging spectrometry N89-24696
A visiting scientist program in atmospheric sciences for the Goddard Space Flight Center
[NASA-CR-183421] N89-24756
Biooptical variability in the Greenland Sea observed with the Multispectral Airborne Radiometer System (MARS)
[NASA-CR-184856] N89-24784
REMOTELY PILOTED VEHICLES
Vision system testing for teleoperated vehicles
[DE89-009713] N89-24610
REPRESENTATIONS
Transformation of real and virtual objects into a virtual, visual environment N89-24304
RESEARCH
A visiting scientist program in atmospheric sciences for the Goddard Space Flight Center
[NASA-CR-183421] N89-24756
RESEARCH AND DEVELOPMENT
ISOCAM, ISO optical subsystem cryogenics, Aerospatiale, Cannes, France in-house R and D status
[REPT-882-440-123] N89-24429
Applications of aerospace technology
[NASA-CR-181536] N89-25076
Langley aerospace test highlights, 1988
[NASA-TM-101579] N89-25112
RESEARCH FACILITIES
Numerical aerodynamic simulation
[NASA-EP-262] N89-24262
The AAMRL (Armstrong Aerospace Medical Research Laboratory) biodynamics data bank
[AD-A206139] N89-25074
Langley aerospace test highlights, 1988
[NASA-TM-101579] N89-25112
RESEARCH MANAGEMENT
The Pathfinder Chemical Transfer Propulsion program
[NASA-TM-102084] N89-24409
NASA information sciences and human factors program
[NASA-TM-4126] N89-25111
RESIDUES
Analysis of the plugging of the systems autonomy demonstration project brassboard filters
[NASA-CR-177533] N89-24450
RESONANCE
The effect of non-Maxwellian electron distributions on the intensity ratio of resonance to satellite lines
[DE89-006745] N89-24907
RESONANCE CHARGE EXCHANGE
Charge exchange transition probability for collisions between unlike ions and atoms within the adiabatic approximation
[NASA-TM-101559] N89-25104
RESONANCE FLUORESCENCE
Cooperative phenomena for new coherent radiation sources
[AD-A206368] N89-24602
RESONANCE SCATTERING
Multiphoton transitions at the Moessbauer radiation diffraction in crystals under a weak ultrasonic field
[DE88-706341] N89-25069
RESONANT FREQUENCIES
Subharmonic resonance in a mixing layer N89-24544
REUSABLE ROCKET ENGINES
The Pathfinder Chemical Transfer Propulsion program
[NASA-TM-102084] N89-24409
REYNOLDS STRESS
An experimental study of a three-dimensional thrust augmenting ejector using laser Doppler velocimetry
[NASA-CR-177531] N89-24569
RHODIUM COMPOUNDS
Oxide-bound transition metal complexes for methane activation
[PB89-138614] N89-24464
RIEMANN MANIFOLD
Path integral and operator formalism on bordered Riemann surfaces
[DE88-757229] N89-24881
RING LASERS
Vertical emitting, ring geometry, ultra-low threshold and ultra-high speed quantum well lasers for optical interconnect
[AD-A206427] N89-24603
RISK
Safety analysis report for the Galileo Mission. Volume 3, book 1: Nuclear risk analysis document, revision 1
[DE89-007272] N89-24898
Safety analysis report for the Galileo Mission. Volume 3, book 2: Nuclear risk analysis document. Appendices, revision 1
[DE89-007273] N89-24899
ROBOTICS
Robotic experiments on Spacelab D-2 as testbed for future operational concepts N89-24391
Proceedings of the Goddard Space Flight Center Workshop on Robotics for Commercial Microelectronic Processes in Space
[NASA-TM-101233] N89-24505
Generalized solution for the optimal prehension state using end effectors with multi-articulated fingers N89-24609
Dynamics of flexible multi-body mechanisms and manipulators. Part 1: An overview N89-24662
Human Factors in Automated and Robotic Space Systems: Proceedings of a symposium. Part 1
[NASA-CR-182495] N89-24792
Human Factors in Automated and Robotic Space Systems: Proceedings of a symposium. Part 2
[NASA-CR-182496] N89-24794
Conference on Space and Military Applications of Automation and Robotics
[AD-A198095] N89-24819
An automated protein crystal growth facility on the space station N89-24820
The impact of an IVA robot on the space station microgravity environment N89-24821
Neutral file data exchange between simulators and robots N89-24824
Technology transfer: Imaging tracker to robotic controller N89-24828
Development of a hybrid simulator for robotic manipulators N89-24831
Disconnects for spacecraft servicing applications N89-24832
Robotic visual servo control for aircraft ground refueling N89-24836
Insertion with two coordinated arms N89-24837
Automated Millimeter Wave (AMW) transducer testing in a robotic/vision test cell N89-24841
ORU guidelines for telerobotic compatibility N89-24844
Ground control of space based robotic systems N89-24845
A generalized method for automatic downhand and wirefeed control of a welding robot and positioner N89-24846
A 3-D graphical simulation of an automated direct chip probe/test system N89-24848
Algorithm for display of automated nondestructive thickness measurements N89-24850
A robotic vehicle global route planner for the 1990s N89-24851
A knowledge representation scheme for a robotic land vehicle route planner N89-24853
A deductive approach to automated planning
[AD-A206253] N89-24860
ROBOTS
Getting ready for EVA N89-24387

Multiple robot approach for automation of in-orbit modules N89-24389
Hierarchically structured control for intelligent robots in space N89-24393
Proceedings of the Goddard Space Flight Center Workshop on Robotics for Commercial Microelectronic Processes in Space
[NASA-TM-101233] N89-24505
Piezoelectric film load cell robot collision detector
[DE89-010117] N89-24592
Generalized solution for the optimal prehension state using end effectors with multi-articulated fingers N89-24609
Dynamics of flexible multi-body mechanisms and manipulators. Part 1: An overview N89-24662
The human role in space (THURIS) applications study. Final briefing
[NASA-CR-183590] N89-24793
The human role in space (THURIS) applications study. Volume 2: Research analysis and technology report
[NASA-CR-183589] N89-24795
Dual-arm robots for telerobotic IVA operations on the space station N89-24822
High level intelligent control of telerobotics systems N89-24823
Stabilized image system for mobile robots N89-24829
A new approach to robot kinematic analysis N89-24833
Robot assembly of microscopic component in millimeter wave devices N89-24840
Testing the feasibility of using a teleoperated robot for remote, dexterous operations N89-24843
A generalized method for automatic downhand and wirefeed control of a welding robot and positioner N89-24846
Representations of a linkage mechanism based on dual number matrices
[DE88-757273] N89-24857
A deductive approach to automated planning
[AD-A206253] N89-24860
A comparison of two real-time control schemes for redundant robots with bounded joint velocities
[DE89-002974] N89-24861

ROBUSTNESS (MATHEMATICS)
Objective and constraint functions for the analysis and design of robust control systems N89-24615

ROCKET ENGINE DESIGN
Technology and design method evolution of cryogenic propulsion systems: Example of the main Ariane 5 stage N89-24353
The Pathfinder Chemical Transfer Propulsion program
[NASA-TM-102084] N89-24409

ROCKET ENGINES
A numerical study of chemically reacting flow in nozzles
[NASA-TM-102135] N89-24444

ROCKET FIRING
A premixed hydrogen/oxygen catalytic igniter
[NASA-CR-185113] N89-24445

ROCKET LAUNCHING
Modeling the missile-launch tube problem in DYSCO N89-24629

ROCKET OXIDIZERS
Materials compatibility with oxidizer-rich gases at elevated temperatures and pressure
[NASA-CR-183647] N89-24486

ROLLER BEARINGS
Comparison of predicted and measured temperatures of UH-60A helicopter transmission
[NASA-TP-2911] N89-24607
Tribology: The Story of Lubrication and Wear
[NASA-TM-101430] N89-24635

ROLLING CONTACT LOADS
Adaptive methods, rolling contact, and nonclassical friction laws N89-24651

ROTARY WINGS
Effect of advanced rotorcraft airfoil sections on the hover performance of a small-scale rotor model
[NASA-TP-2832] N89-24264
Preliminary airworthiness evaluation of modified second-generation Pneumatic Boot Deicing System on a JUH-1H
[AD-A206255] N89-24289

ROTATING BODIES
Prediction methods for dynamic stability parameters: Effects of angular stability
[IMFL-88/18] N89-24573

ROTATION
Shaft adjuster
[DE89-010119] N89-24612

ROTATIONAL SPECTRA
First detection of SO2 and CH3OH emission and one unidentified line near 800 GHz
[MPE-PREPRINT-142] N89-25086

ROTOR AERODYNAMICS
Aerodynamics of a lifting rotor due to near field unsteady effects N89-24267

ROTOR BLADES (TURBOMACHINERY)
Turbine rotor/stator flowfield analysis
[NASA-CR-183639] N89-24433
Composite Blade Structural Analyzer (COBSTRAN) demonstration manual
[NASA-TM-101957] N89-24459
Interaction mechanisms between tip leakage flow and the passage vortex in a linear turbine rotor cascade
[NAL-TR-983T] N89-24536
Three-dimensional flows and loss generation mechanisms in a linear turbine rotor cascade at various incidence conditions
[NAL-TR-984T] N89-24537

ROTOR BODY INTERACTIONS
Survey of Army/NASA rotorcraft aeroelastic stability research
[NASA-TM-101026] N89-24329

ROTOR DYNAMICS
Survey of Army/NASA rotorcraft aeroelastic stability research
[NASA-TM-101026] N89-24329
Interaction mechanisms between tip leakage flow and the passage vortex in a linear turbine rotor cascade
[NAL-TR-983T] N89-24536

ROTORCRAFT AIRCRAFT
Effect of advanced rotorcraft airfoil sections on the hover performance of a small-scale rotor model
[NASA-TP-2832] N89-24264

ROTORS
Preliminary airworthiness evaluation of modified second-generation Pneumatic Boot Deicing System on a JUH-1H
[AD-A206255] N89-24289

ROUTES
Diverter AI based decision aid, phases 1 and 2
[NASA-CR-181820] N89-24316
A robotic vehicle global route planner for the 1990s N89-24851
A knowledge representation scheme for a robotic land vehicle route planner N89-24853

ROVING VEHICLES
Technology requirements for advanced NASA missions N89-24705

RUBBER
Features and characterization needs of rubber composite structures N89-24649

RUNGE-KUTTA METHOD
Explicit, implicit, and hybrid methods N89-24656

RUNWAYS
Improved marking of taxiway intersections for Instrument Flight Rules (IFR) operations
[DOT/FAA/CT-TN89/23] N89-24330

RYDBERG SERIES
Introduction to dissociative recombination
[NASA-CR-184950] N89-24889
Semiempirical studies of atomic structure
[DE89-011419] N89-24894

S

SAFETY
Safety analysis report for the Galileo Mission. Volume 2, book 1: Accident model document
[DE89-007270] N89-24896
Safety analysis report for the Galileo Mission. Volume 2, book 2: Accident model document, Appendices
[DE89-007271] N89-24897
Safety analysis report for the Galileo Mission. Volume 3, book 1: Nuclear risk analysis document, revision 1
[DE89-007272] N89-24898
Safety analysis report for the Galileo Mission. Volume 3, book 2: Nuclear risk analysis document. Appendices, revision 1
[DE89-007273] N89-24899

SAFETY MANAGEMENT
Fire safety applications for spacecraft
[NASA-TM-101463] N89-24413

SATELLITE ALTIMETRY
Laser ranging data analysis
[NASA-CR-184847] N89-24754

SATELLITE COMMUNICATION
Development of a 75-watt 60-GHz traveling-wave tube for intersatellite communications
[NASA-CR-182135] N89-24530

SATELLITE IMAGERY
Study of representativity of the wind fields deduced from geostationary satellite images. Attribution of height to wind vectors and large scale average fields deduced from water vapor imagery
[ETN-89-94538] N89-24781
Contribution to the estimation of precipitation in the Sahel by using satellite imagery
[SER-DI-204] N89-24782

SATELLITE OBSERVATION
The advanced Ocean Chlorophyll Meter (OCM). A spectral imaging device for the observation of the oceans
[REPT-882-440-118] N89-24689
On the future development and management of spectroscopic database for radiative transfer from the issues of recent related workshops
[ETN-89-94530] N89-24690
Refinements in the cloud detection scheme of the 3I system. Comparison with AVHRR products
[ETN-89-94531] N89-24691
ESA's planned activities in the field of imaging spectrometry for Earth observation N89-24693
HIRIS: NASA's high-resolution imaging spectrometer for the Earth Observing System (EOS) N89-24695
DFVLR activities related to imaging spectrometry N89-24697
Activities of CNES in the field of imaging spectrometry N89-24699
The EARSEL Imaging Spectrometry Working Group N89-24700
The radiation-atmosphere interaction model and the determination of meteorological and climatological parameters from satellite observations
[ETN-89-94535] N89-24779

SATELLITE SOUNDING
Simulation studies of improved sounding systems
[NASA-CR-185322] N89-24758
Three dimensional analysis of the atmospheric structure by vertical satellite sounding. Interest for weather forecasting
[ETN-89-94536] N89-24763

SATELLITE TRACKING
Determination of station coordinates, earth rotation and plate motions from LAGEOS laser ranging: 1983-1986
[NAL-TR-980T] N89-24753

SATELLITE TRANSMISSION
UNIX-based data management system for the Mobile Satellite Propagation Experiment (PiFEx)
[NASA-CR-185023] N89-25073

SATELLITE-BORNE INSTRUMENTS
Systems for the sensitivity calibration of mass spectrometers in space flight
[BONN-IR-88-32] N89-24428

SATURABLE REACTORS
Electrophoretically applied dielectrics for amorphous metal foils used in pulsed power saturable reactors
[DE89-009322] N89-24525

SATURN SATELLITES
Comparative planetology of early intense cratering and other cratering effects
[NASA-CR-182966] N89-24752

SCALARS
Scalar entrainment in the mixing layer N89-24545
Use of passive scalar tagging for the study of coherent structures in the plane mixing layer N89-24546
Velocity and scalar fields of turbulent premixed flame in stagnation flow
[DE89-009336] N89-24566

SCALE MODELS
Centrifugal modeling of underground structures subjected to blast loading
[AD-A206424] N89-24675

SCANNING
A system for high resolution 3D mapping using laser radar and requiring no beam scanning mechanisms N89-24827

SCATTERING CROSS SECTIONS
Kaon-nucleus scattering
[NASA-TP-2920] N89-25103

SCENE ANALYSIS
Scene reconstruction for image sequences N89-24297

SCHROEDINGER EQUATION
Kaon-nucleus scattering
[NASA-TP-2920] N89-25103

SCIENTISTS
A visiting scientist program in atmospheric sciences for the Goddard Space Flight Center
[NASA-CR-183421] N89-24756

SCREWS
Efficiency study of oil cooling of a screw compressor
[DE89-011417] N89-24618

SEA ICE
Refinements in the cloud detection scheme of the 3I system. Comparison with AVHRR products
[ETN-89-94531] N89-24691

SEAPLANES
The use of seaplanes as an advanced weapon system
[AD-A206243] N89-24880

SECONDARY FLOW
Numerical study of turbulent secondary flows in curved ducts
[NASA-CR-181830] N89-24568
SECULAR VARIATIONS
Time variations in the earth's gravity field from Starlette orbit analysis N89-24766
SEISMIC WAVES
Neutron starquakes and the nature of gamma-ray bursts N89-24947
SELENIUM
Development of tandem cells consisting of GaAs single crystal and CuInSe2/CdZnS polycrystalline thin films N89-24717
Directions for further development of GaAs/CuInSe2 thin film tandem cells N89-24718
SELF LUBRICATION
Tribology: The Story of Lubrication and Wear
[NASA-TM-101430] N89-24635
Solid lubricant materials for high temperatures: A review N89-24636
SEMICONDUCTOR DEVICES
A longlife, highvoltage, shortpulse generator based on optically activated Bulk Avalanche Semiconductor Switch, phase 2
[AD-A206078] N89-24527
A facilities view of the low volume, high product mix fab
[DE89-009970] N89-25057
Investigations on fully depletable charge coupled devices
[MPI-PAE/EXP.EL-194] N89-25063
SEMICONDUCTOR JUNCTIONS
Encapsulated diffusion of sulphur into InP N89-24714
SEMICONDUCTOR LASERS
A longlife, highvoltage, shortpulse generator based on optically activated Bulk Avalanche Semiconductor Switch, phase 2
[AD-A206078] N89-24527
Prototype laser-diode-pumped solid state laser transmitters
[NASA-CR-185056] N89-24601
Vertical emitting, ring geometry, ultra-low threshold and ultra-high speed quantum well lasers for optical interconnect
[AD-A206427] N89-24603
SENSORY DISCRIMINATION
Field-dependence and judgment of weight and color revisited: Some implications for the study of sensory discrimination
[AD-A206141] N89-24791
SEPARATED FLOW
Unsteady and separated flows
[AD-A206539] N89-24572
SEQUENCING
Scene reconstruction for image sequences N89-24297
SERIES EXPANSION
Numerical integration of asymptotic solutions of ordinary differential equations
[NASA-TM-100650] N89-24867
SERVOCONTROL
Robotic visual servo control for aircraft ground refueling N89-24836
SERVOMECHANISMS
Aeroservoelastic wind-tunnel investigations using the Active Flexible Wing Model: Status and recent accomplishments
[NASA-TM-101570] N89-24313
Recent activities within the Aeroservoelasticity Branch at the NASA Langley Research Center
[NASA-TM-101582] N89-24314
Advanced servomanipulator remote maintenance demonstration
[DE89-010188] N89-24614
SEYFERT GALAXIES
Infrared studies of active galaxies N89-25087
SHAFTS (MACHINE ELEMENTS)
Shaft adjuster
[DE89-010119] N89-24612
SHAPE CONTROL
On the dynamics and control of the Spacecraft Control Laboratory Experiment (SCOLE) class of offset flexible systems N89-24426
SHAPES
Error analysis for semi-analytic displacement derivatives with respect to shape and sizing variables N89-24632
SHEAR FLOW
Analysis of the wake behind a propeller using the finite element method with a two-equation turbulence model N89-24286
Studying Turbulence Using Numerical Simulation Databases, 2. Proceedings of the 1988 Summer Program
[NASA-CR-184905] N89-24538
Inflow/outflow boundary conditions and global dynamics of spatial mixing layers N89-24540
A numerical study of bifurcations in a barotropic shear flow N89-24542
Pressure-strain-rate events in homogeneous turbulent shear flow N89-24551
Multifractal spectra in homogeneous shear flow N89-24552
Eddies, streams, and convergence zones in turbulent flows N89-24555
Theoretical model for VITA-educed coherent structures in the wall region of a turbulent boundary layer N89-24556
The structure of sheared turbulence near a plane boundary N89-24557
Optical propagation through a homogeneous turbulent shear flow N89-24561
Kinetic simulation of magnetic reconnection in the presence of shear N89-24985
SHEAR LAYERS
Scalar entrainment in the mixing layer N89-24545
Turbulence characteristics inside a turbulent spot in plane Poiseuille flow N89-24554
Nonlinear evolution of interacting oblique waves on two-dimensional shear layers
[NASA-TM-102030] N89-24575
SHEAR PROPERTIES
Bonded assemblies behavior laws: Light alloys/elastoplastic adhesive
[ETCA-88-R-001] N89-24456
SHEAR STRAIN
Plate motions and deformations from geologic and geodetic data
[NASA-CR-184987] N89-24757
SHELL THEORY
Computational procedures for postbuckling of composite shells N89-24642
Analysis of shell-type structures subjected to time-dependent mechanical and thermal loading
[NASA-CR-184989] N89-24669
SHELLS (STRUCTURAL FORMS)
Computational Methods for Structural Mechanics and Dynamics, part 1
[NASA-CP-3034-PT-1] N89-24638
Computational procedures for postbuckling of composite shells N89-24642
Contact solution algorithms N89-24652
Exploiting symmetries in the modeling and analysis of tires N89-24653
Analysis of shell-type structures subjected to time-dependent mechanical and thermal loading
[NASA-CR-184989] N89-24669
SHOCK FRONTS
Shock-associated plasma density fluctuations in the interstellar medium N89-24933
SHOCK RESISTANCE
Thermal shock strength of multiphase materials
[KFK-4469] N89-24455
A method of isolating treadmill shock and vibration on spacecraft
[NASA-TM-100474] N89-24790
SHOCK WAVE INTERACTION
The structure of quasiperpendicular collisionless shocks N89-24932
The role of whistler oscillations in the formation of the structure of high Mach number collisionless shock N89-24936
SHOCK WAVE PROPAGATION
On the refraction of longitudinal waves in compressible media
[DE89-012922] N89-24588
Computer simulations of cosmic-ray diffusion near supernova remnant shock waves N89-24916
Are supernova remnants quasi-parallel or quasi-perpendicular accelerators N89-24948
SHOCK WAVES
Conservative treatment of boundary interfaces for overlaid grids and multi-level grid adaptations
[NASA-TM-102080] N89-24269
Capabilities and some applications of the LLNL 100-kV electric gun
[DE89-006747] N89-24408
Viscosity of solids determined by shock wave action on hemispherical indentations
[DE89-008035] N89-24510
Interaction between an oblique shock wave and a turbulent boundary layer
[ONERA-RT-76/7078-AY-096-A] N89-24574
Some notes on shock resolving flux functions. Part 1: Stationary characteristics
[NASA-TM-101087] N89-24871
Relativistic shocks in electron-positron plasmas and polar cap accretion onto neutron stars: Two non-linear problems in astrophysical plasma physics N89-24926
Particle acceleration and shock wave structure --- astrophysics N89-24930
Extended coronal shock waves and electron acceleration during solar flares N89-24934
On the existence and stability of intermediate shocks --- MHD N89-24971
Particle acceleration by magnetic reconnection and fast magnetosonic shock waves in solar flares N89-24993
SHORT TAKEOFF AIRCRAFT
A model for prediction of STOVL ejector dynamics
[NASA-TM-102098] N89-24319
SHUTTLE IMAGING RADAR
Necessity and benefit of the X-SAR space shuttle experiment
[DFVLR-MITT-88-29] N89-24688
SIGNAL DISTORTION
On the dynamic response of pressure transmission lines in the research of helium-charged free piston Stirling engines
[NASA-TM-102121] N89-24593
SIGNAL PROCESSING
AR (Autoregressive) modeling of coherence in time delay and doppler estimation
[AD-A205239] N89-24513
Improved defect analysis of Gallium Arsenide solar cells using image enhancement N89-24726
SIGNAL TRANSMISSION
Image Signal Processing for Flight Guidance
[DFVLR-MITT-88-32] N89-24295
Image signal processing for flight guidance: Overview and introduction to the main topics N89-24296
Aspects of image communication in air-to-ground systems N89-24298
An intelligent fiberoptic data bus for fly-by-light applications
[NAL-TM-SE-8707] N89-24901
SILANES
Research on high-efficiency, single-junction, monolithic, thin-film amorphous silicon solar cells, phase 2
[DE89-000849] N89-24703
SILICA GEL
Development and utilization of new diagnostics for dense-phase pneumatic transport
[DE89-011381] N89-24583
SILICON
Ultra-thin, light-trapping silicon solar cells N89-24719
Laboratory for X-ray optics
[AD-A206468] N89-25061
SILICON ALLOYS
Deployable aerospace PV array based on amorphous silicon alloys N89-24720
Radiation resistance studies of amorphous silicon films N89-24738
SILICON DIOXIDE
Isotopic study of oxygen diffusion in oxide coatings
[NASA-TM-102082] N89-24451
Effects of thermal history on stress-related properties of very thin films of thermally grown silicon dioxide, SiO2
[AD-A206547] N89-25062
SILICON FILMS
In-situ stress measurements during thermal oxidation of silicon
[AD-A206546] N89-24495
SILICON OXIDES
In-situ stress measurements during thermal oxidation of silicon
[AD-A206546] N89-24495
SIMD (COMPUTERS)
Telescience and payload control support technologies N89-24385
SIMULATION
Field joint environmental protection system vibration/pressurization qualification
[NASA-CR-183673] N89-24449
SIMULATORS
The effects of blast trauma (impulse noise) on hearing: A parametric study
[AD-A206180] N89-24786
Neutral file data exchange between simulators and robots N89-24824
SINGLE CRYSTALS
Development of tandem cells consisting of GaAs single crystal and CuInSe2/CdZnS polycrystalline thin films N89-24717
SINGULARITY (MATHEMATICS)
Unsteady Aerodynamics, volume 1
[VKI-1988-07-VOL-1] N89-24276
Unsteady aerodynamics N89-24277
SIZE (DIMENSIONS)
Error analysis for semi-analytic displacement derivatives with respect to shape and sizing variables N89-24632
SLEEVES
Analysis of a probe-metallic sleeve feed system for a rectangular waveguide
[DE89-006769] N89-24523

SLENDER WINGS
Wind tunnel tests on flutter control of a high-aspect-ratio cantilevered wing
[NAL-TR-978] N89-24321
SLIDING
Contact solution algorithms N89-24652
SMOKE DETECTORS
Fire safety applications for spacecraft
[NASA-TM-101463] N89-24413
SODIUM
Investigations of the sodium layer of the earth atmosphere: Probing with a terrestrial lidar system at 69 N in winter
[BONN-IR-88-52] N89-24760
SODIUM CHLORIDES
Is salt at fault
[AD-A206518] N89-24789
SODIUM SULFUR BATTERIES
Analysis of life cycle costs for electric vans with advanced battery systems
[DE89-009807] N89-24526
SOFTWARE ENGINEERING
Computerized structural mechanics for 1990's: Advanced aircraft needs N89-24640
A review of some problems in global-local stress analysis N89-24643
Application of the p-version of the finite-element method to global-local problems N89-24648
Transformational derivation of programs using the Focus system
[NASA-CR-184875] N89-24802
A 3-D graphical simulation of an automated direct chip probe/test system N89-24848
SOFTWARE TOOLS
Some issues in numerical simulation of nonlinear structural response N89-24639
Transformational derivation of programs using the Focus system
[NASA-CR-184875] N89-24802
SOIL MECHANICS
Global functions in global-local finite-element analysis of localized stresses in prismatic structures N89-24646
SOIL MOISTURE
The importance of climatological variability and the rate at which waste is added to modeling water budget of landfills
[DE89-008917] N89-24747
SOL-GEL PROCESSES
Sol-gel processing of controlled pore films
[DE89-013584] N89-24501
SOLAR ACTIVITY
SMM X-ray polychromator
[NASA-CR-180791] N89-24590
Thermal instability in a stratified plasma N89-24924
SOLAR ARRAYS
Space Station Freedom Solar Array design development
[NASA-TM-102105] N89-24448
Experimental component mode synthesis applied to the solar array type structure
[NAL-TR-994] N89-24702
Space Photovoltaic Research and Technology, 1988. High Efficiency, Space Environment, and Array Technology
[NASA-CP-3030] N89-24704
Space power technology 21: Photovoltaics N89-24706
Predicted performance of InP solar cells in Cassegrainian and slats space concentrator arrays at 20 to 100 AM0, 80 to 100 C N89-24711
The impact of solar cell technology on planar solar array performance N89-24715
Deployable aerospace PV array based on amorphous silicon alloys N89-24720
The 25 percent-efficient GaAs Cassegrainian concentrator cell N89-24733
Contamination effects of GPS Navstar solar array performance N89-24734
The experiments of LIPS 3 N89-24735
SOLAR ATMOSPHERE
Singularities of the local MHD-resonances in solar chromosphere plasma N89-24927
Generation and non-equilibrium of solar atmospheric magnetic fields N89-24989
SOLAR BLANKETS
Advanced photovoltaic solar array development N89-24716
SOLAR CELLS
Energy storage and thermal control system design status
[NASA-TM-102136] N89-24427
Space photovoltaic technique. State of the art, trends
[REPT-882-440-120] N89-24442
Space Station Freedom Solar Array design development
[NASA-TM-102105] N89-24448
Photovoltaic power system operation in the Mars environment
[NASA-TM-102075] N89-24529
Diffusion welding of electrical interconnects to silicon solar cells
[DE89-012250] N89-24620
Research on high-efficiency, single-junction, monolithic, thin-film amorphous silicon solar cells, phase 2
[DE89-000849] N89-24703
Space Photovoltaic Research and Technology, 1988. High Efficiency, Space Environment, and Array Technology
[NASA-CP-3030] N89-24704
Space power technology 21: Photovoltaics N89-24706
Progress in indium phosphide solar cell research N89-24707
InP shallow-homojunction solar cells N89-24708
An empirical study of the performance of APMOVPE AM0 InP homojunction solar cells as a function of emitter thickness and doping, and base doping N89-24709
N/P InP homojunction solar cells with an In0.53Ga0.47As contacting layer grown by liquid phase epitaxy N89-24710
Modelling and design of high performance indium phosphide solar cells N89-24712
Deep levels and radiation effects in p-InP N89-24713
Encapsulated diffusion of sulphur into InP N89-24714
The impact of solar cell technology on planar solar array performance N89-24715
Advanced photovoltaic solar array development N89-24716
Development of tandem cells consisting of GaAs single crystal and CuInSe2/CdZnS polycrystalline thin films N89-24717
Directions for further development of GaAs/CuInSe2 thin film tandem cells N89-24718
Ultra-thin, light-trapping silicon solar cells N89-24719
High efficiency GaAs-Ge tandem solar cells grown by MOCVD N89-24721
Response of single junction GaAs/GaAs and GaAs/Ge solar cells to multiple doses of 1 MeV electrons N89-24722
A three solar cell system based on a self-supporting, transparent AlGaAs top solar cell N89-24723
Investigation of high efficiency GaAs solar cells N89-24724
A new structure for comparing surface passivation materials of GaAs solar cells N89-24725
Improved defect analysis of Gallium Arsenide solar cells using image enhancement N89-24726
Aging behavior of Au-based ohmic contacts to GaAs N89-24727
Chemical etching and organometallic chemical vapor deposition on varied geometries of GaAs N89-24728
Status of GaAs solar cell production N89-24729
Flexibility in space solar cell production N89-24730
Gallium Arsenide welded panel technology for advanced spaceflight applications N89-24731
Domed Fresnel lens concentrator technology for space application N89-24732
The 25 percent-efficient GaAs Cassegrainian concentrator cell N89-24733
Contamination effects of GPS Navstar solar array performance N89-24734
AM0 efficiency measurements N89-24736
A comparison of the radiation tolerance characteristics of multijunction solar cells with series and voltage-matched configurations N89-24737
Radiation resistance studies of amorphous silicon films N89-24738
Research on high-efficiency, single-junction, monolithic, thin-film amorphous silicon solar cells
[DE89-000893] N89-24739
SOLAR COLLECTORS
Radiometric measurement of temperature distributions in solar cavity receivers
[DE89-011467] N89-24742
Developing, testing, evaluating and optimizing solar heating and cooling systems
[DE89-011831] N89-24744
SOLAR COOLING
Developing, testing, evaluating and optimizing solar heating and cooling systems
[DE89-011831] N89-24744
SOLAR CORONA
SMM X-ray polychromator
[NASA-CR-180791] N89-24590
Dissipation of Alfven waves in solar coronal arches N89-24919
Thermal instability in a stratified plasma N89-24924
Extended coronal shock waves and electron acceleration during solar flares N89-24934
Structuring of plasmas by a magnetic field --- solar corona N89-24938
Stability of force-free magnetic fields and the problem of solar coronal heating N89-24990
A neutral current sheet with flows: Tearing and stratification modes and modeling of coronal structures N89-24991
Dynamic development of coronal current sheets N89-24994
Coronal magnetic field strengths determined from fiber bursts N89-25002
Long-term evolution of coronal magnetic fields based on noise storm continuum observations in the 20th and 21st cycle N89-25003
Chaotic radiopulsations and coronal magnetic field estimates N89-25006
Non-destructive analyses of cometary nucleus samples using synchrotron radiation
[DE89-012536] N89-25101
The equilibrium and stability of solar coronal magnetic fields N89-25102
SOLAR CYCLES
Long-term evolution of coronal magnetic fields based on noise storm continuum observations in the 20th and 21st cycle N89-25003
SOLAR DYNAMIC POWER SYSTEMS
The space station power system
[NASA-TM-101245] N89-24416
Concentration of off-axis radiation by solar concentrators for space power
[NASA-TM-102052] N89-24438
Flight experiment of thermal energy storage
[NASA-TM-102081] N89-24440
SOLAR ENERGY
Status of the direct absorption receiver panel research experiment: Salt flow and solar test requirements and plans
[DE89-010968] N89-24461
SOLAR ENERGY ABSORBERS
Status of the direct absorption receiver panel research experiment: Salt flow and solar test requirements and plans
[DE89-010968] N89-24461
SOLAR FLARES
SMM X-ray polychromator
[NASA-CR-180791] N89-24590
Extended coronal shock waves and electron acceleration during solar flares N89-24934
Structuring of plasmas by a magnetic field --- solar corona N89-24938
Particle acceleration by magnetic reconnection and fast magnetosonic shock waves in solar flares N89-24993
Possibilities and problems of the interpretation of solar magnetograph measurements and applications to flare-active regions N89-24995
Diagnostics of energy release and magnetic fields on the sun by radio methods N89-24998
The relation between H-alpha and SXR emission of the flares N89-25000
The precursors of the 9 July 1982 solar proton flare event N89-25001
Time scales of solar microwave bursts and scenarios of flare energy release N89-25005
An analogy between magnetospheric substorms and solar flares: New version N89-25016
SOLAR HEATING
Increasing the chemical yield of desirable chemical species using solar rapid heating
[DE89-000881] N89-24469
Developing, testing, evaluating and optimizing solar heating and cooling systems
[DE89-011831] N89-24744
SOLAR MAGNETIC FIELD
Helioseismology and plasma physics N89-24922
Magnetic energy conversion on the sun N89-24987
Generation and non-equilibrium of solar atmospheric magnetic fields N89-24989
On the MHD stability of the M=1 kink mode in finite length coronal loops N89-24992
Possibilities and problems of the interpretation of solar magnetograph measurements and applications to flare-active regions N89-24995
Estimation of sunspot magnetic field parameters using the superpenumbral topology N89-24996
Note on an apparent highly-sheared magnetic field structure --- Sun N89-24997
Diagnostics of energy release and magnetic fields on the sun by radio methods N89-24998
The relation between H-alpha and SXR emission of the flares N89-25000
Coronal magnetic field strengths determined from fiber bursts N89-25002
Long-term evolution of coronal magnetic fields based on noise storm continuum observations in the 20th and 21st cycle N89-25003
Chaotic radiopulsations and coronal magnetic field estimates N89-25006

A model of the reconnection pattern at the heliopause N89-25027

SOLAR MAXIMUM MISSION
SMM X-ray polychromator [NASA-CR-180791] N89-24590

SOLAR OBSERVATORIES
Tremsdorf solar radio astronomy observatory: The scientific program and an interesting observation N89-24999

SOLAR OSCILLATIONS
Helioseismology and plasma physics N89-24922
Singularities of the local MHD-resonances in solar chromosphere plasma N89-24927

SOLAR PROMINENCES
Structuring of plasmas by a magnetic field --- solar corona N89-24938

SOLAR RADIATION
Photovoltaic power system operation in the Mars environment [NASA-TM-102075] N89-24529
Photovoltaic advanced research and development project: Solar radiation research [DE89-000884] N89-24743

SOLAR RADIO BURSTS
Alfven wave solitons and solar intermediate drift bursts N89-24923
Diagnostics of energy release and magnetic fields on the sun by radio methods N89-24998
Long-term evolution of coronal magnetic fields based on noise storm continuum observations in the 20th and 21st cycle N89-25003
Time scales of solar microwave bursts and scenarios of flare energy release N89-25005
Chaotic radiopulsations and coronal magnetic field estimates N89-25006

SOLAR ROTATION
Generation and non-equilibrium of solar atmospheric magnetic fields N89-24989

SOLAR SPECTRA
SMM X-ray polychromator [NASA-CR-180791] N89-24590
The precursors of the 9 July 1982 solar proton flare event N89-25001

SOLAR SPECTROMETERS
SMM X-ray polychromator [NASA-CR-180791] N89-24590

SOLAR WIND
Dimensionless parameters for classifying solar wind interactions N89-24914
The role of the magnetic reconnection in the solar wind/magnetosphere interaction N89-25024
A model of the reconnection pattern at the heliopause N89-25027
The variable nature of the comet-solar wind interaction N89-25100

SOLAR X-RAYS
The relation between H-alpha and SXR emission of the flares N89-25000

SOLDERED JOINTS
Research on the mechanism of thermal fatigue in near-eutectic Pb-Sn solders [DE89-011430] N89-24482

SOLDERING
Incorporation of surface tension into the structural finite element code SANCHO [DE89-011354] N89-24616

SOLDERS
Research on the mechanism of thermal fatigue in near-eutectic Pb-Sn solders [DE89-011430] N89-24482

SOLENOIDS
Measurements of magnetic field of superconducting solenoid [DE88-706323] N89-25068

SOLID ELECTROLYTES
US fuel cell research and applications, 1960--1989 [DE89-012244] N89-24745

SOLID LUBRICANTS
Solid lubricant materials for high temperatures: A review N89-24636

SOLID PROPELLANT ROCKET ENGINES
Ariane 5 solid boosters: Overview of design approach and envisaged technologies N89-24352
The experiments of LIPS 3 N89-24735

SOLID ROCKET PROPELLANTS
Thermal radiation from plumes of solid propellant rockets [NAL-TR-990] N89-24432

SOLID STATE LASERS
Development of mid-infrared solid state lasers for spaceborne lidar [NASA-CR-185012] N89-24599
Cooperative phenomena for new coherent radiation sources [AD-A206368] N89-24602

SOLID-SOLID INTERFACES
Measurement of bond strength at metal/ceramic interfaces [DE89-011638] N89-24682

SOLIDIFIED GASES
Continuous cryopump with a method for removal of solidified gases [DE89-009760] N89-24611

SOLIDS
Viscosity of solids determined by shock wave action on hemispherical indentations [DE89-008035] N89-24510
Cooperative phenomena for new coherent radiation sources [AD-A206368] N89-24602

SOLIDS FLOW
Development and utilization of new diagnostics for dense-phase pneumatic transport [DE89-011381] N89-24583

SOLITARY WAVES
Alfven wave solitons and solar intermediate drift bursts N89-24923

SOUND PROPAGATION
Ultra-light duct for an anechoic wind tunnel [NASA-TM-101805] N89-24331

SOUND WAVES
Auditory speech preprocessors [DE89-009280] N89-24516
Phase decorrelation, streamwise vortices and acoustic radiation in mixing layers N89-24541

SOUTHERN OSCILLATION
The relationship between intraseasonal disturbance activity and interannual variation of the tropical atmosphere N89-24774

SPACE BASED RADAR
Development of mid-infrared solid state lasers for spaceborne lidar [NASA-CR-185012] N89-24599

SPACE COMMERCIALIZATION
Proceedings of the Goddard Space Flight Center Workshop on Robotics for Commercial Microelectronic Processes in Space [NASA-TM-101233] N89-24505

SPACE ELECTRIC ROCKET TESTS
Performance of large area xenon ion thrusters for orbit transfer missions [NASA-TM-102049] N89-24436

SPACE ENVIRONMENT SIMULATION
Contamination effects study [NASA-CR-183613] N89-24746

SPACE EXPLORATION
Magellan: The unveiling of Venus [NASA-CR-185018] N89-24419
Technology requirements for advanced NASA missions N89-24705

SPACE FLIGHT
Systems for the sensitivity calibration of mass spectrometers in space flight [BONN-IR-88-32] N89-24428

SPACE FLIGHT TRAINING
The training concept for ESA astronauts and the associated facilities N89-24374
Crew training aspects --- Hermes, Columbus N89-24396
Simulation of weightlessness with neutral buoyancy facilities and zero-g aircraft for the preparation of European manned space operations N89-24398

SPACE LABORATORIES
Report of the committee on a commercially developed space facility [NASA-CR-185383] N89-24406

SPACE LOGISTICS
Integrated approach for the logistic support of the European in orbit infrastructure from the nineties onwards N89-24359
Logistics aspects of Columbus servicing at the Space Station N89-24363
Experimentation in the Man Tended Free Flyer (MTFF) N89-24381
Multiple robot approach for automation of in-orbit modules N89-24389

SPACE MAINTENANCE
System safety from D-missions to Columbus N89-24367
The human role in space (THURIS) applications study. Final briefing [NASA-CR-183590] N89-24793
The human role in space (THURIS) applications study. Volume 2: Research analysis and technology report [NASA-CR-183589] N89-24795

SPACE MANUFACTURING
Report of the committee on a commercially developed space facility [NASA-CR-185383] N89-24406
Proceedings of the Goddard Space Flight Center Workshop on Robotics for Commercial Microelectronic Processes in Space [NASA-TM-101233] N89-24505

SPACE MISSIONS
Magellan: The unveiling of Venus [NASA-CR-185018] N89-24419
ESA's space plasma physics missions: The past and the future ten years N89-24913

SPACE OBSERVATIONS (FROM EARTH)
Development of astrophysics from the telescope to the Sputnik N89-24911

SPACE PLASMAS
Proceedings of an International School and Workshop on Plasma Astrophysics, volume 1 [ESA-SP-285-VOL-1] N89-24910
Astrophysical significance of observations and experiments in the earth's magnetosphere N89-24912
ESA's space plasma physics missions: The past and the future ten years N89-24913
MHD-waves and their nonlinear interaction in a plasma with magnetic flux tubes N89-24921
Relativistic shocks in electron-positron plasmas and polar cap accretion onto neutron stars: Two non-linear problems in astrophysical plasma physics N89-24928
Relativistic MHD from two-fluid hydrodynamics (TFHD) --- space plasmas N89-24931
Quasi-adiabatic particle acceleration in magnetic field reversals and the formation of the plasma sheet boundary layer in the earth's magnetotail N89-24943
Are supernova remnants quasi-parallel or quasi-perpendicular accelerators N89-24948
Pulsar radio and visible radiation due to the modulation instability of high-frequence transverse waves in the inhomogeneous electron-positron plasma N89-24959
Proceedings of an International School and Workshop on Reconnection in Space Plasma, volume 2 [ESA-SP-285-VOL-2] N89-24974
Aspects of three-dimensional magnetic reconnection N89-24975
Reconnection and microturbulence N89-24980
Anomalous collision frequency of magnetoactive plasmas with two-dimensional electrostatic turbulence (kB = O) N89-24981
Pinch-effect and stellar flares physics N89-25004
Magnetotail reconnection, MHD theory and simulations N89-25013
Electromagnetic electron temperature anisotropy instability in the earth's magnetotail plasma sheet N89-25019
ELF plasma turbulence observed by Prognoz-8 in plasma jets in the magnetospheric tail N89-25020
A model of the reconnection pattern at the heliopause N89-25027

SPACE POWER REACTORS
Summary and evaluation of the Strategic Defense Initiative Space Power Architecture Study [NASA-TM-102012] N89-24443

SPACE PROCESSING
Industrial utilization of microgravity: Problems in the realization phase N89-24383
Containerless glass fiber processing [NASA-TM-86540] N89-24405
Proceedings of the Goddard Space Flight Center Workshop on Robotics for Commercial Microelectronic Processes in Space [NASA-TM-101233] N89-24505

SPACE PROGRAMS
Study on cost efficiency of product assurance in space programs [REPT-882-440-122] N89-24622

SPACE RENDEZVOUS
Hermes-MTFF rendezvous strategy and composite operations N89-24357

SPACE SHUTTLE BOOSTERS
SRB ascent aerodynamic heating design criteria reduction study, volume 2 [NASA-CR-183569] N89-24430
Field joint environmental protection system vibration/pressurization qualification [NASA-CR-183673] N89-24449
Teledyne Taber 206-1000 and 2210-3000 pressure transducer proof test and burst test [NASA-CR-183672] N89-24594

SPACE SHUTTLE MAIN ENGINE
Turbine rotor/stator flowfield analysis [NASA-CR-183639] N89-24433
Space Shuttle Main Engine High Pressure Fuel Turbopump turbine blade cracking [NASA-TM-100327] N89-24435
Space Shuttle Main Engine structural analysis and data reduction/evaluation. Volume 6: Primary nozzle diffuser analysis [NASA-CR-183669] N89-24437

Turbulent flow in a 180 deg bend: Modeling and computations
[NASA-CR-4141] N89-24579

SPACE SHUTTLE MISSIONS
Space Shuttle to deploy Magellan planetary science mission
[NASA-NEWS-RELEASE-89-86] N89-24334
KSC ice/frost/debris assessment for Space Shuttle Mission STS-30R
[NASA-TM-102147] N89-24412

SPACE SHUTTLE ORBITERS
Shuttle payload bay thermal environments: Summary and conclusion report for STS Flights 1-5
[NASA-CR-185017] N89-24411

SPACE SHUTTLE PAYLOADS
Space Shuttle to deploy Magellan planetary science mission
[NASA-NEWS-RELEASE-89-86] N89-24334
Report of the committee on a commercially developed space facility
[NASA-CR-185383] N89-24406

SPACE STATION PAYLOADS
An automated protein crystal growth facility on the space station N89-24820
The impact of an IVA robot on the space station microgravity environment N89-24821

SPACE STATION POLAR PLATFORMS
Space Station Freedom electrical power system hardware commonality with the United States Polar Platform
[NASA-TM-102074] N89-24439

SPACE STATION POWER SUPPLIES
The space station power system
[NASA-TM-101245] N89-24416
Review of the environmental effects of the Space Station Freedom photovoltaic power module
[NASA-TM-102076] N89-24418
Energy storage and thermal control system design status
[NASA-TM-102136] N89-24427
Space Station automation of common module power management and distribution
[NASA-CR-183607] N89-24434
Concentration of off-axis radiation by solar concentrators for space power
[NASA-TM-102052] N89-24438
Space Station Freedom Solar Array design development
[NASA-TM-102105] N89-24448

SPACE STATION STRUCTURES
Investigation of structural behavior of candidate Space Station structure
[NASA-CR-181746] N89-24678
Space Station Freedom Structural Characterization Experiment (SCE) node code
[NASA-TM-101594] N89-25110

SPACE STATIONS
Report of the committee on a commercially developed space facility
[NASA-CR-185383] N89-24406
The space station power system
[NASA-TM-101245] N89-24416
Space station: A step into the future
[NASA-PAM-510/11-87] N89-24417
A methodology for commonality analysis, with applications to selected space station systems
[NASA-TM-100364] N89-24421
Energy storage and thermal control system design status
[NASA-TM-102136] N89-24427
Space Station automation of common module power management and distribution
[NASA-CR-183607] N89-24434
Space Station Freedom electrical power system hardware commonality with the United States Polar Platform
[NASA-TM-102074] N89-24439
Human Factors in Automated and Robotic Space Systems: Proceedings of a symposium. Part 1
[NASA-CR-182495] N89-24792
Human Factors in Automated and Robotic Space Systems: Proceedings of a symposium. Part 2
[NASA-CR-182496] N89-24794
Dual-arm robots for telerobotic IVA operations on the space station N89-24822
Research and technology, 1988
[NASA-TM-101246] N89-25109

SPACE TOOLS
Hierarchically structured control for intelligent robots in space N89-24393

SPACE TRANSPORTATION SYSTEM
Development of tailorable advanced blanket insulation for advanced space transportation systems
[NASA-CR-177444] N89-24486

SPACE TUGS
Orbital Transfer Vehicle: Concept definition and system analysis study
[NASA-CR-183551] N89-24410

SPACE-TIME FUNCTIONS
Turbulence production near walls: The role of flow structures with spanwise asymmetry N89-24550

SPACEBORNE ASTRONOMY
Space science using Columbus: Manned space science N89-24348
Italian scientific projects related to manned activity in space N89-24382
Development of astrophysics from the telescope to the Sputnik N89-24911
IUE investigations of SN 1987A
[NASA-CR-184973] N89-25079

SPACEBORNE EXPERIMENTS
Space Shuttle to deploy Magellan planetary science mission
[NASA-NEWS-RELEASE-89-86] N89-24334
Report of the committee on a commercially developed space facility
[NASA-CR-185383] N89-24406
Flight experiment of thermal energy storage
[NASA-TM-102081] N89-24440

SPACECRAFT CABINS
Hermes escape system N89-24366

SPACECRAFT COMMUNICATION
The European data relay satellite N89-24339
The key role of Data Relay System (DRS) in the Columbus communications N89-24379

SPACECRAFT CONFIGURATIONS
Report of the committee on a commercially developed space facility
[NASA-CR-185383] N89-24406
Orbital Transfer Vehicle: Concept definition and system analysis study
[NASA-CR-183551] N89-24410

SPACECRAFT CONTAMINATION
Contamination effects of GPS Navstar solar array performance N89-24734

SPACECRAFT CONTROL
Expert system for European space infrastructure N89-24378
On the dynamics and control of the Spacecraft Control Laboratory Experiment (SCOLE) class of offset flexible systems N89-24426

SPACECRAFT DESIGN
Hermes user interfaces N89-24346
Overview of Ariane 5 and Hermes programs technology N89-24349
Orbital Transfer Vehicle: Concept definition and system analysis study
[NASA-CR-183551] N89-24410
Fluidnet: A thermal and hydraulic software for the preliminary sizing of fluid loop systems
[REPT-882-440-124] N89-24425
A method of isolating treadmill shock and vibration on spacecraft
[NASA-TM-100474] N89-24790
Research and technology, 1988
[NASA-TM-101246] N89-25109

SPACECRAFT ENVIRONMENTS
Medical and radiation protection problems in space N89-24369
Shuttle payload bay thermal environments: Summary and conclusion report for STS Flights 1-5
[NASA-CR-185017] N89-24411
Contamination effects of GPS Navstar solar array performance N89-24734

SPACECRAFT EQUIPMENT
Development of a 75-watt 60-GHz traveling-wave tube for intersatellite communications
[NASA-CR-182135] N89-24530

SPACECRAFT LAUNCHING
The Ariane 5 Development Program N89-24336
The Hermes Program N89-24338
Means for preparing and recovering the Hermes space plane N89-24373

SPACECRAFT MAINTENANCE
Columbus safety and reliability N89-24368

SPACECRAFT MODELS
Expert system for European space infrastructure N89-24378
Optimisation of the figure of merit of modified silicon-germanium alloys
[AD-A206420] N89-24491

SPACECRAFT MODULES
Pressurized module element for man's presence in space --- Columbus N89-24343
Attached Pressurized Module (APM) center for the Columbus attached pressurized module N89-24377
Multiple robot approach for automation of in-orbit modules N89-24389

SPACECRAFT POWER SUPPLIES
Fuel cell development for Hermes N89-24355
Space photovoltaic technique. State of the art, trends
[REPT-882-440-120] N89-24442
Summary and evaluation of the Strategic Defense Initiative Space Power Architecture Study
[NASA-TM-102012] N89-24443
Space Photovoltaic Research and Technology, 1988. High Efficiency, Space Environment, and Array Technology
[NASA-CP-3030] N89-24704
Space power technology 21: Photovoltaics N89-24706
Progress in indium phosphide solar cell research N89-24707
Modelling and design of high performance indium phosphide solar cells N89-24712
Encapsulated diffusion of sulphur into InP N89-24714
The impact of solar cell technology on planar solar array performance N89-24715
Development of tandem cells consisting of GaAs single crystal and CuInSe2/CdZnS polycrystalline thin films N89-24717
Directions for further development of GaAs/CuInSe2 thin film tandem cells N89-24718
Ultra-thin, light-trapping silicon solar cells N89-24719
Deployable aerospace PV array based on amorphous silicon alloys N89-24720
Domed Fresnel lens concentrator technology for space application N89-24732
The experiments of LIPS 3 N89-24735
Safety analysis report for the Galileo Mission. Volume 2, book 1: Accident model document
[DE89-007270] N89-24896
Safety analysis report for the Galileo Mission. Volume 2, book 2: Accident model document, Appendices
[DE89-007271] N89-24897
Safety analysis report for the Galileo Mission. Volume 3, book 1: Nuclear risk analysis document, revision 1
[DE89-007272] N89-24898
Safety analysis report for the Galileo Mission. Volume 3, book 2: Nuclear risk analysis document. Appendices, revision 1
[DE89-007273] N89-24899

SPACECRAFT PROPULSION
The Pathfinder Chemical Transfer Propulsion program
[NASA-TM-102084] N89-24409
Performance of large area xenon ion thrusters for orbit transfer missions
[NASA-TM-102049] N89-24436
Technology requirements for advanced NASA missions N89-24705

SPACECRAFT RADIATORS
Contamination effects of GPS Navstar solar array performance N89-24734

SPACECRAFT RECOVERY
Means for preparing and recovering the Hermes space plane N89-24373

SPACECRAFT SHIELDING
The experiments of LIPS 3 N89-24735

SPACECRAFT SURVIVABILITY
Safety analysis report for the Galileo Mission. Volume 2, book 1: Accident model document
[DE89-007270] N89-24896
Safety analysis report for the Galileo Mission. Volume 2, book 2: Accident model document, Appendices
[DE89-007271] N89-24897
Safety analysis report for the Galileo Mission. Volume 3, book 1: Nuclear risk analysis document, revision 1
[DE89-007272] N89-24898
Safety analysis report for the Galileo Mission. Volume 3, book 2: Nuclear risk analysis document. Appendices, revision 1
[DE89-007273] N89-24899

SPACECRAFT TEMPERATURE
Hermes aerothermodynamic concept N89-24351
Shuttle payload bay thermal environments: Summary and conclusion report for STS Flights 1-5
[NASA-CR-185017] N89-24411
Fluidnet: A thermal and hydraulic software for the preliminary sizing of fluid loop systems
[REPT-882-440-124] N89-24425

SPACECREWS
Hermes crew role N89-24401
The astronaut's functions aboard Columbus N89-24403

SPACELAB PAYLOADS
System safety from D-missions to Columbus N89-24367
Robotic experiments on Spacelab D-2 as testbed for future operational concepts N89-24391
Lessons learned from SL-1 and D-1 --- Spacelab N89-24400

SPECIFICATIONS
Steady-state operation regime of tokamak reactor plasma. Consistency analysis (I)
[DE88-756571] N89-24908

SPECTRAL EMISSION
Auger and ESCA analysis
[NASA-CR-183572] N89-24463
SPECTRAL ENERGY DISTRIBUTION
The effects of blast trauma (impulse noise) on hearing: A parametric study
[AD-A206180] N89-24786
Infrared studies of active galaxies N89-25087
SPECTRAL REFLECTANCE
Biooptical variability in the Greenland Sea observed with the Multispectral Airborne Radiometer System (MARS)
[NASA-CR-184856] N89-24784
SPECTROMETERS
Demonstration of a Time Projection Compton Spectrometer
[DE89-010743] N89-24596
Imaging Spectrometry for Land Applications
[ESA-SP-1101] N89-24692
SPECTROPHOTOMETRY
IUE investigations of SN 1987A
[NASA-CR-184973] N89-25079
SPECTRORADIOMETERS
The advanced Ocean Chlorophyll Meter (OCM). A spectral imaging device for the observation of the oceans
[REPT-882-440-118] N89-24689
Activities of CNES in the field of imaging spectrometry N89-24699
SPECTROSCOPIC ANALYSIS
On the future development and management of spectroscopic database for radiative transfer from the issues of recent related workshops
[ETN-89-94530] N89-24690
SPECTRUM ANALYSIS
Auger and ESCA analysis
[NASA-CR-183572] N89-24463
Backscattering spectra processing for the structure of multilayer samples
[DE88-706325] N89-24468
Dynamic spectral analysis in finite field algebras
[DE88-706333] N89-24877
SPEECH
Auditory speech preprocessors
[DE89-009280] N89-24516
SPHERICAL COORDINATES
Surface grid generation for composite block grids N89-24874
SPICULES
Model of the chromosphere spicule formation N89-24966
SPIRAL GALAXIES
Generation of large-scale vortices in compressible helical turbulence N89-24969
Infrared studies of active galaxies N89-25087
SPLINE FUNCTIONS
Global/local stress analysis of composite panels
[NASA-TM-101622] N89-24681
The exact condition of the B-spline basis may be hard to determine
[AD-A204080] N89-24863
Comparison of basis function and iteration solutions to the Fredholm integral equation of the first kind
[AD-A206158] N89-24869
SPUTTERING
Computer simulation of copper in the liquid phase and the sputtering of liquid copper by one KeV argon ions
[AD-A206264] N89-24476
Charge exchange neutral sputtering in ASDEX N89-25044
STABILITY
The effects of gradients on boundary stability
[DE89-011590] N89-25065
STABILITY AUGMENTATION
Loss of tail rotor effectiveness evaluation of the OH-58C helicopter with directional SAS (Stability Augmentation System)
[AD-A206181] N89-24309
Results of an A109 simulation validation and handling qualities study
[NASA-TM-101062] N89-24323
STAGNATION FLOW
Numerical study on laminar circular jet of carbonic acid gas discharging into stagnant air
[DE88-757249] N89-24565
Velocity and scalar fields of turbulent premixed flame in stagnation flow
[DE89-009336] N89-24566
STAGNATION POINT
Magnetic reconnection near a stagnation point N89-24983
STANDARDIZATION
Flexibility in space solar cell production N89-24730
STAR CLUSTERS
A study of the Southern Supercluster N89-25088
STAR FORMATION
An observational study of the dynamics of molecular cloud cores N89-25097
STAR TRACKERS
Further developments in modeling digital control systems with MA-prefiltered measurements
[NASA-TP-2909] N89-24507
STARQUAKES
Neutron starquakes and the nature of gamma-ray bursts N89-24947
STATIC LOADS
Dynamics and static behavior of metal gussets in cask impact limiters
[DE89-011879] N89-24683
STATISTICAL ANALYSIS
Theoretical model for VITA-educed coherent structures in the wall region of a turbulent boundary layer N89-24556
Velocity and scalar fields of turbulent premixed flame in stagnation flow
[DE89-009336] N89-24566
STATISTICAL MECHANICS
Challenges in computational statistical mechanics
[DE89-009922] N89-24567
STATOR BLADES
Turbine rotor/stator flowfield analysis
[NASA-CR-183639] N89-24433
STEADY FLOW
Conservative treatment of boundary interfaces for overlaid grids and multi-level grid adaptations
[NASA-TM-102080] N89-24269
A model for prediction of STOVL ejector dynamics
[NASA-TM-102098] N89-24319
Numerical simulation of feedback control of aerodynamic configurations in steady and unsteady ground effects N89-24326
STEADY STATE
Summary and evaluation of the Strategic Defense Initiative Space Power Architecture Study
[NASA-TM-102012] N89-24443
Steady-state operation regime of tokamak reactor plasma. Consistency analysis (I)
[DE88-756571] N89-24908
STEELS
The effect of heat input and composition on weld metal microstructures in thin section HY-130 GMAW weldments
[AD-A206476] N89-24477
STELLAR EVOLUTION
Particle acceleration and shock wave structure --- astrophysics N89-24930
Effects of main-sequence mass loss on stellar and galactic chemical evolution
[DE89-011399] N89-25098
STELLAR FLARES
Pinch-effect and stellar flares physics N89-25004
Search for a fine-time structure in flares of UV Cet-type stars N89-25007
STELLAR LUMINOSITY
An observational study of the dynamics of molecular cloud cores N89-25097
STELLAR MAGNETIC FIELDS
Small-scale instabilities in accretion disks of compact objects and their manifestations N89-24950
STELLAR MAGNETOSPHERES
Theory of radioemission of pulsars N89-24941
Two-stream instability in pulsar magnetospheres N89-24949
On the nature of a typical pulsars radio emission N89-24952
STELLAR MASS
Effects of main-sequence mass loss on stellar and galactic chemical evolution
[DE89-011399] N89-25098
STELLAR MASS ACCRETION
Relativistic shocks in electron-positron plasmas and polar cap accretion onto neutron stars: Two non-linear problems in astrophysical plasma physics N89-24928
Nonlinear oblique whistlers: Their relevance to nonthermal coupling of ions and electrons in accretion flow and supercritical quasi-perpendicular collisionless shocks --- black holes N89-24955
STELLAR MASS EJECTION
Dynamic development of coronal current sheets N89-24994
STELLAR MODELS
Model of the chromosphere spicule formation N89-24966
STELLAR OSCILLATIONS
Neutron starquakes and the nature of gamma-ray bursts N89-24947
STELLAR RADIATION
Generation of X-ray and radio emission by binary Wolf-Rayet stars N89-24929
Theory of radioemission of pulsars N89-24941
Two-stream instability in pulsar magnetospheres N89-24949
On the nature of a typical pulsars radio emission N89-24952
On the mechanism of the formation of the polarization characteristics of pulsar radiation N89-24953
Strong Langmuir turbulence and the pulsar emission mechanism N89-24956
Synchrotron thermal instabilities and filamentation in radio sources N89-24958
Pulsar radio and visible radiation due to the modulation instability of high-frequence transverse waves in the inhomogeneous electron-positron plasma N89-24959
Quantum relativistic theory of the cyclotron radiation in a strongly magnetized plasma with anisotropic temperature --- neutron stars N89-24962
STELLAR SPECTRA
High spectral resolution observations of the H2 2.12 micron line in Herbig-Haro objects
[MPE-PREPRINT-139] N89-25085
STELLAR SPECTROPHOTOMETRY
An observational study of the dynamics of molecular cloud cores N89-25097
STELLAR STRUCTURE
Thermal instability in a stratified plasma N89-24924
STELLAR WINDS
Speculation on the origin of X-ray emission in early-type stars N89-25029
Black hole driven winds N89-25096
STELLARATORS
The role of the radial electric field in enhanced confinement regimes in stellarators
[DE89-011572] N89-25049
Numerical methods for stellarator optimization
[DE89-012342] N89-25050
STEREOSCOPIC VISION
Visibility with a moving point of view N89-24876
STIFFENING
Nonlinear response of a blade-stiffened graphite-epoxy panel with a discontinuous stiffener: Work in progress N89-24641
Global-local methodologies and their application to nonlinear analysis N89-24647
Global/local stress analysis of composite panels
[NASA-TM-101622] N89-24681
Dynamics and static behavior of metal gussets in cask impact limiters
[DE89-011879] N89-24683
STIFFNESS
Characterization of the bending stiffness of large space structure joints
[NASA-TM-101565] N89-24676
Investigation of structural behavior of candidate Space Station structure
[NASA-CR-181746] N89-24678
STIFFNESS MATRIX
Development of higher-order modal methods for transient thermal and structural analysis
[NASA-TM-101548] N89-24677
STIRLING CYCLE
Initial characterization of a modular heat exchanger with an integral heat pipe
[NASA-TM-102097] N89-25078
STIRLING ENGINES
On the dynamic response of pressure transmission lines in the research of helium-charged free piston Stirling engines
[NASA-TM-102121] N89-24593
NASA Lewis Stirling engine computer code evaluation
[NASA-CR-182248] N89-24741
Initial characterization of a modular heat exchanger with an integral heat pipe
[NASA-TM-102097] N89-25078
STOCHASTIC PROCESSES
Research on self-generated stochastic motion
[AD-A206454] N89-24870
Stochastic quantization of nonlinear sigma-models with Wess-Zumino terms
[DE88-757286] N89-24882
STORAGE TANKS
Superfluid Helium Tanker Study (SFHT)
[NASA-CR-172114] N89-24415
STORMS
Study of explosive and nonexplosive cyclogenesis during FGGE
[AD-A206521] N89-24775
STRAIN DISTRIBUTION
Space Shuttle Main Engine High Pressure Fuel Turbopump turbine blade cracking
[NASA-TM-100327] N89-24435
Microscopic delamination processes and the resulting crack tip strain fields of graphite/epoxy composites N89-24671
Improved analysis of laminated heterogeneous beams and associated formulation of a new finite element method N89-24672

STRAIN ENERGY RELEASE RATE
Characterization of delamination in advanced composite materials under mode 3 loading conditions
[AD-A206159] N89-24452
Analysis of interlaminar fracture in composites under combined loading
[NASA-CR-185055] N89-24674
STRAIN RATE
Pressure-strain-rate events in homogeneous turbulent shear flow N89-24551
Plate motions and deformations from geologic and geodetic data
[NASA-CR-184987] N89-24757
STRANGENESS
A study of K sup deg sec, lambda and lambda bar production in 60 and 200 GeV nucleon OAu and pAu collisions with a streamer chamber detector at the CERN SPS
[MPE-PAE/EXP.EL-198] N89-24900
STRATEGY
Dynamic analysis of space structures including elastic, multibody, and control behavior N89-24661
Modal reduction strategies for interconnected flexible bodies simulation N89-24665
STREAM FUNCTIONS (FLUIDS)
Domain decomposition algorithms and computation fluid dynamics
[NASA-CR-185405] N89-24578
STRESS (PHYSIOLOGY)
Solute model or cellular energy model: Practical and theoretical aspects of thirst during exercise
[AD-A206143] N89-24785
STRESS ANALYSIS
Experimentation and analysis of compression test methods for single filament high performance fibres
[AD-A206358] N89-24467
Local stiffener and skin pocket buckling prediction by special PASCO modeling technique: Correlation to test data N89-24628
Computational Methods for Structural Mechanics and Dynamics, part 1
[NASA-CP-3034-PT-1] N89-24638
Nonlinear response of a blade-stiffened graphite-epoxy panel with a discontinuous stiffener: Work in progress N89-24641
A review of some problems in global-local stress analysis N89-24643
Some comments on global-local analyses N89-24644
Global functions in global-local finite-element analysis of localized stresses in prismatic structures N89-24646
Global-local methodologies and their application to nonlinear analysis N89-24647
Application of the p-version of the finite-element method to global-local problems N89-24648
Features and characterization needs of rubber composite structures N89-24649
Computational Methods for Structural Mechanics and Dynamics
[NASA-CP-3034-PT-2] N89-24654
Improved analysis of laminated heterogeneous beams and associated formulation of a new finite element method N89-24672
STRESS CONCENTRATION
On computational schemes for global-local stress analysis N89-24645
STRESS DISTRIBUTION
Improved analysis of laminated heterogeneous beams and associated formulation of a new finite element method N89-24672
STRESS INTENSITY FACTORS
Equations of motion for viscoelastic moving crack problems N89-24670
STRESS MEASUREMENT
In-situ stress measurements during thermal oxidation of silicon
[AD-A206546] N89-24495
STRESS-STRAIN RELATIONSHIPS
Integrated optimization of nonlinear R/C frames with reliability constraints N89-24631
Features and characterization needs of rubber composite structures N89-24649
STRESSES
Study of damage in composite materials
[ONERA-RT-4/7256-RY-070-R] N89-24458
Two dimensional analysis of a NOVETTE laser generated stress-impulse experiment
[DE89-009909] N89-24600
On computational schemes for global-local stress analysis N89-24645
The effects of gradients on boundary stability
[DE89-011590] N89-25065
STRUCTURAL ANALYSIS
Space Shuttle Main Engine structural analysis and data reduction/evaluation. Volume 6: Primary nozzle diffuser analysis
[NASA-CR-183669] N89-24437
Composite Blade Structural Analyzer (COBSTRAN) demonstration manual
[NASA-TM-101957] N89-24459
Backscattering spectra processing for the structure of multilayer samples
[DE88-706325] N89-24468
CSM testbed development and large-scale structural applications
[NASA-TM-4072] N89-24624
The computational structural mechanics testbed architecture. Volume 5: The Input-Output Manager DMGASP
[NASA-CR-178388] N89-24637
Computational Methods for Structural Mechanics and Dynamics, part 1
[NASA-CP-3034-PT-1] N89-24638
Computerized structural mechanics for 1990's: Advanced aircraft needs N89-24640
Computational procedures for postbuckling of composite shells N89-24642
A review of some problems in global-local stress analysis N89-24643
Some comments on global-local analyses N89-24644
On computational schemes for global-local stress analysis N89-24645
Global functions in global-local finite-element analysis of localized stresses in prismatic structures N89-24646
Global-local methodologies and their application to nonlinear analysis N89-24647
Application of the p-version of the finite-element method to global-local problems N89-24648
Nonlinear hierarchical substructural parallelism and computer architecture N89-24650
Adaptive methods, rolling contact, and nonclassical friction laws N89-24651
Exploiting symmetries in the modeling and analysis of tires N89-24653
Explicit, implicit, and hybrid methods N89-24656
Transient analysis techniques in performing impact and crash dynamic studies N89-24658
Nonlinear characteristics of joints as elements of multi-body dynamic systems N89-24668
Large-scale structural analysis: The structural analyst, the CSM Testbed and the NAS System
[NASA-TM-100643] N89-24673
Centrifugal modeling of underground structures subjected to blast loading
[AD-A206424] N89-24675
Development of higher-order modal methods for transient thermal and structural analysis
[NASA-TM-101548] N89-24677
Global/local stress analysis of composite panels
[NASA-TM-101622] N89-24681
STRUCTURAL DESIGN
Recent activities within the Aeroservoelasticity Branch at the NASA Langley Research Center
[NASA-TM-101582] N89-24314
Superfluid Helium Tanker Study (SFHT)
[NASA-CR-172114] N89-24415
SRB ascent aerodynamic heating design criteria reduction study, volume 2
[NASA-CR-183569] N89-24430
Summary and evaluation of the Strategic Defense Initiative Space Power Architecture Study
[NASA-TM-102012] N89-24443
Analysis of adaptive planar truss structures
[NAL-TR-988] N89-24625
Influence of time lag and noncolocation on integrated structural/control system designs N89-24630
Solid lubricant materials for high temperatures: A review N89-24636
STRUCTURAL ENGINEERING
A discussion on using Lanczos vectors and Ritz vectors for computing dynamic responses
[DE89-012322] N89-24684
STRUCTURAL RELIABILITY
Time dependent reliability model incorporating continuum damage mechanics for high-temperature ceramics
[NASA-TM-102046] N89-24487
A noncontacting scanning photoelectron emission technique for bonding surface cleanliness inspection
[NASA-TM-100361] N89-24623
STRUCTURAL STABILITY
Global/local stress analysis of composite panels
[NASA-TM-101622] N89-24681
STRUCTURAL VIBRATION
Unsteady aerodynamic effects on bluff bodies N89-24278
Ground vibration test of the Foudre A04 Transall aircraft
[REPT-20/7234-PY-382-R] N89-24311
SUBMARINES
Prediction methods for dynamic stability parameters: Effects of angular stability
[IMFL-88/18] N89-24573
SUBMERGING
Natural convection cooling of a 3 by 3 array of rectangular protrusions in an enclosure filled with dielectric liquid: Effects of boundary conditions and component orientation
[AD-A206474] N89-24571
SUBSONIC FLOW
Unsteady aerodynamics N89-24277
SUBSTRATES
The impact of solar cell technology on planar solar array performance N89-24715
A three solar cell system based on a self-supporting, transparent AlGaAs top solar cell N89-24723
Gallium Arsenide welded panel technology for advanced spaceflight applications N89-24731
SULFATES
The relationship between in-lake sulfate concentration and estimates of atmospheric sulfur deposition for subregions of the eastern lake survey
[DE89-009868] N89-24749
SULFIDATION
Role of alloying additions in the oxidation-sulfidation of Fe-base alloys
[DE89-009825] N89-24473
SULFUR
Encapsulated diffusion of sulphur into InP N89-24714
SULFUR OXIDES
Role of sulfur oxides in wear and deposit formation in Army diesel engines
[AD-A206054] N89-24613
SUN
Magnetic energy conversion on the sun N89-24987
SUNSPOTS
Estimation of sunspot magnetic field parameters using the superpenumbral topology N89-24996
SUPERCOMPUTERS
Numerical aerodynamic simulation
[NASA-EP-262] N89-24262
High speed implementation of NAL application software packages
[NAL-TR-986] N89-24801
SUPERCONDUCTING MAGNETS
The 280 GHz Gyro-BWO design study
[DE89-011644] N89-24595
Measurements of magnetic field of superconducting solenoid
[DE88-706323] N89-25068
SUPERCONDUCTIVITY
Challenges in computational statistical mechanics
[DE89-009922] N89-24567
Maglev vehicles and superconductor technology: Integration of high-speed ground transportation into the air travel system
[DE89-012241] N89-24619
On the nature of high-temperature superconductivity
[DE89-009525] N89-25053
Superconducting properties of magnetron sputtered Bi-Sr-Ca-Cu-O and Tl-Ba-Ca-Cu-O thin films
[DE89-009878] N89-25056
X-ray photoelectron spectroscopy study of samples in the Y-Ba-Cu-O system
[AD-A206260] N89-25060
SUPERCONDUCTORS
Photothermal imaging of high T(sub c) superconductor
[DE89-009644] N89-25054
X-ray investigations of ceramic high Tc superconductors under high pressure
[KFK-4482] N89-25064
Universal reduction of T(subc) in strong coupling superconductors due to Anderson/Kondo impurities
[DE89-011225] N89-25071
SUPERCRITICAL AIRFOILS
Computational and experimental research on buffet phenomena of transonic airfoils
[NAL-TR-996T] N89-24322
SUPERCRITICAL FLOW
Quasi-perpendicular collisionless high Mach number shocks N89-24937
SUPERCRITICAL FLUIDS
The effects of supercritical fluids on high performance polymers
[AD-A206515] N89-24494
SUPERFLUIDITY
Superfluid Helium Tanker Study (SFHT)
[NASA-CR-172114] N89-24415
Inelastic scattering from liquid He4 in aerogel glass
[DE89-012381] N89-24587

SUPERNOVA REMNANTS
Computer simulations of cosmic-ray diffusion near supernova remnant shock waves N89-24916
Particle acceleration and shock wave structure --- astrophysics N89-24930
Are supernova remnants quasi-parallel or quasi-perpendicular accelerators N89-24948
High energy particles in supernova remnants and the interstellar medium N89-25108
SUPERNOVA 1987A
IUE investigations of SN 1987A
[NASA-CR-184973] N89-25079
SUPERSONIC COMBUSTION RAMJET ENGINES
An integrated aerodynamic/propulsion study for generic aero-space planes based on waverider concepts
[NASA-CR-183389] N89-24315
Calculation of scramjet performance
[NAL-TR-987] N89-24317
SUPERSONIC FLOW
Conservative treatment of boundary interfaces for overlaid grids and multi-level grid adaptations
[NASA-TM-102080] N89-24269
Development of a supersonic turbulent boundary layer on a heated wall. Properties of the turbulent field and theoretical application
[ONERA-RSF-74/7078-AY-096-A] N89-24275
Navier-Stokes analysis of cold scramjet-afterbody flows
[NASA-CR-184949] N89-24562
Interaction between an oblique shock wave and a turbulent boundary layer
[ONERA-RT-76/7078-AY-096-A] N89-24574
SUPERSYMMETRY
Stochastic quantization of nonlinear sigma-models with Wess-Zumino terms
[DE88-757286] N89-24882
SURFACE COOLING
Natural convection cooling of a 3 by 3 array of rectangular protrusions in an enclosure filled with dielectric liquid: Effects of boundary conditions and component orientation
[AD-A206474] N89-24571
SURFACE FINISHING
A noncontacting scanning photoelectron emission technique for bonding surface cleanliness inspection
[NASA-TM-100361] N89-24623
SURFACE PROPERTIES
Contamination effects study
[NASA-CR-183613] N89-24746
SURFACE REACTIONS
Free radical-surface interactions using multiphoton ionization of free radicals
[AD-A206257] N89-24892
SURFACTANTS
Development of an engineering methodology for applying foam technology
[DE89-000740] N89-24497
SWEAT COOLING
Transpiration cooling of hypersonic blunt bodies with finite rate surface reactions
[NASA-CR-177516] N89-24580
SWEPT WINGS
Water tunnel investigation of the vortex dynamics of periodically pitched wings
[AD-A206359] N89-24271
SWITCHING CIRCUITS
A longlife, highvoltage, shortpulse generator based on optically activated Bulk Avalanche Semiconductor Switch, phase 2
[AD-A206078] N89-24527
Channel and switchbox routing using a greedy based channel algorithm with outward scanning technique
[AD-A206545] N89-24528
Radiation hardened, optically-triggered thyristor switches: Preliminary data on three device designs
[DE89-011469] N89-24533
SYMMETRY
Turbulence production near walls: The role of flow structures with spanwise asymmetry N89-24550
Exploiting symmetries in the modeling and analysis of tires N89-24653
SYNCHRONISM
Formal verification of a fault tolerant clock synchronization algorithm
[NASA-CR-4239] N89-24803
SYNCHROTRON RADIATION
Synchrotron thermal instabilities and filamentation in radio sources N89-24958
Non-destructive analyses of cometary nucleus samples using synchrotron radiation
[DE89-012536] N89-25101
SYNTHETIC APERTURE RADAR
Two-dimensional phase correction of synthetic aperture radar imagery
[DE89-007086] N89-24524
Necessity and benefit of the X-SAR space shuttle experiment
[DFVLR-MITT-88-29] N89-24688
SYSTEM IDENTIFICATION
A systolic array structure for on-line system identification
[AD-A206412] N89-24806
SYSTEMS ANALYSIS
Orbital Transfer Vehicle: Concept definition and system analysis study
[NASA-CR-183551] N89-24410
A methodology for commonality analysis, with applications to selected space station systems
[NASA-TM-100364] N89-24421
Analysis of the plugging of the systems autonomy demonstration project brassboard filters
[NASA-CR-177533] N89-24450
Objective and constraint functions for the analysis and design of robust control systems N89-24615
Real-time system: Specification and verification
[AD-A206467] N89-24807
SYSTEMS ENGINEERING
A methodology for commonality analysis, with applications to selected space station systems
[NASA-TM-100364] N89-24421
Multidisciplinary optimization for engineering systems: Achievements and potential
[NASA-TM-101566] N89-24508
Engineering aspects of RTP --- Rijnhuizen Tokamak PETULA (RTP) N89-25032
The control and monitoring system of RTP --- Rijnhuizen Tokamak PETULA (RTP) N89-25037
SYSTEMS INTEGRATION
Development and flight test experiences with a flight-crucial digital control system
[NASA-TP-2857] N89-24327
Large-scale structural analysis: The structural analyst, the CSM Testbed and the NAS System
[NASA-TM-100643] N89-24673
Development of an integrated CAD/CAM system for wire harness fabrication N89-24842
SYSTOLIC ARRAYS
A systolic array structure for on-line system identification
[AD-A206412] N89-24806

T

TAIL ROTORS
Loss of tail rotor effectiveness evaluation of the OH-58C helicopter with directional SAS (Stability Augmentation System)
[AD-A206181] N89-24309
TARGET ACQUISITION
Technology transfer: Imaging tracker to robotic controller N89-24828
TARGETS
Computer simulation of copper in the liquid phase and the sputtering of liquid copper by one KeV argon ions
[AD-A206264] N89-24476
TASKS
A visiting scientist program in atmospheric sciences for the Goddard Space Flight Center
[NASA-CR-183421] N89-24756
Applications of aerospace technology
[NASA-CR-181536] N89-25076
TAXIING
Improved marking of taxiway intersections for Instrument Flight Rules (IFR) operations
[DOT/FAA/CT-TN89/23] N89-24330
TAYLOR SERIES
Numerical integration of asymptotic solutions of ordinary differential equations
[NASA-TM-100650] N89-24867
TDR SATELLITES
The European data relay satellite N89-24339
The key role of Data Relay System (DRS) in the Columbus communications N89-24379
TEARING MODES (PLASMAS)
Reconnection instability in collisionless plasma N89-24978
Nonlinear dynamics of the drift tearing-mode N89-24979
A neutral current sheet with flows: Tearing and stratification modes and modeling of coronal structures N89-24991
TECHNOLOGIES
Status and trends of technological image processing possibilities N89-24306
TECHNOLOGY ASSESSMENT
Robotic experiments on Spacelab D-2 as testbed for future operational concepts N89-24391
Maglev vehicles and superconductor technology: Integration of high-speed ground transportation into the air travel system
[DE89-012241] N89-24619
Dynamics of flexible multi-body mechanisms and manipulators. Part 1: An overview N89-24662
US fuel cell research and applications, 1960--1989
[DE89-012244] N89-24745
TECHNOLOGY TRANSFER
Photovoltaic advanced research and development project: Solar radiation research
[DE89-000884] N89-24743
Technology transfer: Imaging tracker to robotic controller N89-24828
Applications of aerospace technology
[NASA-CR-181536] N89-25076
Putting technology to work: Examples of industry-laboratory cooperation contributing to our nation's economic strength
[PB89-134654] N89-25077
TECHNOLOGY UTILIZATION
Maglev vehicles and superconductor technology: Integration of high-speed ground transportation into the air travel system
[DE89-012241] N89-24619
TECTONICS
Plate motions and deformations from geologic and geodetic data
[NASA-CR-184987] N89-24757
TELEOPERATORS
The concept of telescience N89-24384
Telescience and payload control support technologies N89-24385
Telescience: A promising operations center N89-24386
Tele-autonomous control involving contacts: The applications of a high precision laser line range sensor
[NASA-CR-184995] N89-24509
Vision system testing for teleoperated vehicles
[DE89-009713] N89-24610
Human Factors in Automated and Robotic Space Systems: Proceedings of a symposium. Part 1
[NASA-CR-182495] N89-24792
The human role in space (THURIS) applications study. Final briefing
[NASA-CR-183590] N89-24793
Human Factors in Automated and Robotic Space Systems: Proceedings of a symposium. Part 2
[NASA-CR-182496] N89-24794
The human role in space (THURIS) applications study. Volume 2: Research analysis and technology report
[NASA-CR-183589] N89-24795
Dual-arm robots for telerobotic IVA operations on the space station N89-24822
High level intelligent control of telerobotics systems N89-24823
Development of a hybrid simulator for robotic manipulators N89-24831
Development of a man-portable control unit for a teleoperated land vehicle N89-24835
Testing the feasibility of using a teleoperated robot for remote, dexterous operations N89-24843
ORU guidelines for telerobotic compatibility N89-24844
A demonstration of retro-traverse using a semi-autonomous land vehicle N89-24852
IRIS: An intelligent robot insertion expert system N89-24854
TELESCOPES
The application of two-dimensional imaging to very high energy gamma ray astronomy
[DE89-013614] N89-25089
TELEVISION CAMERAS
Vision system testing for teleoperated vehicles
[DE89-009713] N89-24610
TELEVISION EQUIPMENT
Protection of VHF international distress frequencies from harmonic radiation due to digital television equipment
[BBC-RD-1989/1] N89-24512
TEMPERATURE CONTROL
Hermes aerothermodynamic concept N89-24351
TEMPERATURE DEPENDENCE
Superconducting properties of magnetron sputtered Bi-Sr-Ca-Cu-O and Tl-Ba-Ca-Cu-O thin films
[DE89-009878] N89-25056
TEMPERATURE DISTRIBUTION
Shuttle payload bay thermal environments: Summary and conclusion report for STS Flights 1-5
[NASA-CR-185017] N89-24411
Experiments on liquid-vapour phase change between plane liquid surfaces. Part 2: Observations of large temperature jumps near the interfaces
[NAL-TM-FM-8805] N89-24462
Radiometric measurement of temperature distributions in solar cavity receivers
[DE89-011467] N89-24742

Simulation studies of improved sounding systems
[NASA-CR-185322] N89-24758

TEMPERATURE EFFECTS
Development of a supersonic turbulent boundary layer on a heated wall. Properties of the turbulent field and theoretical application
[ONERA-RSF-74/7078-AY-096-A] N89-24275
Modeling transient thermal behavior in a thrust vector control jet vane
[AD-A206532] N89-24441
The effect of heat input and composition on weld metal microstructures in thin section HY-130 GMAW weldments
[AD-A206476] N89-24477
Characterization of pore evolution in ceramics during creep failure and densification
[DE89-013599] N89-24502
Methane to methanol conversion
[DE89-011194] N89-24504
Interaction between an oblique shock wave and a turbulent boundary layer
[ONERA-RT-76/7078-AY-096-A] N89-24574
Solute model or cellular energy model: Practical and theoretical aspects of thirst during exercise
[AD-A206143] N89-24785

TEMPERATURE MEASUREMENT
Radiometric measurement of temperature distributions in solar cavity receivers
[DE89-011467] N89-24742
Orographically-caused microclimate variation in the Saariselka Region
[ISBN-9-5169-7269-1] N89-24767
FOM-Rijnhuizen contributions to the Fifteenth Symposium on Fusion Technology
[REPT-88-179] N89-25030
Beam guiding system for Rutherford scattering diagnostic at TEXTOR N89-25033

TEMPERATURE PROFILES
Response of layered structures to thermal radiation pulses
[AD-A206355] N89-24453

TERMINAL GUIDANCE
B-737 flight test of curved-path and steep-angle approaches using MLS guidance
[NASA-TM-101521] N89-24293

TERMINOLOGY
Space Station Freedom Structural Characterization Experiment (SCE) node code
[NASA-TM-101594] N89-25110

TERRAIN
Landscape-related position finding for flying systems N89-24302

TERRAIN ANALYSIS
Bordautonomous terrain aided flight navigation in height sections close to terrain surface N89-24301
Optimal guidance with obstacle avoidance for nap-of-the-earth flight
[NASA-CR-177515] N89-24328

TEST FACILITIES
CSM testbed development and large-scale structural applications
[NASA-TM-4072] N89-24624

TETHERED SATELLITES
Italian scientific projects related to manned activity in space N89-24382

THEMATIC MAPPING
Estimating population size of Pygoscelid Penguins from TM data
[NASA-CR-180081] N89-24687

THEOREM PROVING
Formal verification of AI software
[NASA-CR-181827] N89-24811

THERMAL ANALYSIS
Thermal analysis of a hypersonic wing test structure
[NASA-CR-185319] N89-24265
Comparison of predicted and measured temperatures of UH-60A helicopter transmission
[NASA-TP-2911] N89-24607
Development of higher-order modal methods for transient thermal and structural analysis
[NASA-TM-101548] N89-24677

THERMAL BLOOMING
Atmospheric effects on laser propagation
[DE89-012287] N89-24606

THERMAL CONDUCTIVITY
Response of layered structures to thermal radiation pulses
[AD-A206355] N89-24453
Mechanics/heat-transfer relation for particle flows
[DE89-011382] N89-24584
Photothermal imaging of high T(sub c) superconductor
[DE89-009644] N89-25054

THERMAL CONTROL COATINGS
Energy storage and thermal control system design status
[NASA-TM-102136] N89-24427
Analysis of the plugging of the systems autonomy demonstration project brassboard filters
[NASA-CR-177533] N89-24450

THERMAL ENERGY
Flight experiment of thermal energy storage
[NASA-TM-102081] N89-24440

THERMAL ENVIRONMENTS
Shuttle payload bay thermal environments: Summary and conclusion report for STS Flights 1-5
[NASA-CR-185017] N89-24411
Turbine rotor/stator flowfield analysis
[NASA-CR-183639] N89-24433

THERMAL FATIGUE
Research on the mechanism of thermal fatigue in near-eutectic Pb-Sn solders
[DE89-011430] N89-24482

THERMAL POLLUTION
Correlation between satellite-derived aerosol characteristics and oceanic dimethylsulfide (DMS)
[AD-A206179] N89-24759

THERMAL PROTECTION
Development of tailorable advanced blanket insulation for advanced space transportation systems
[NASA-CR-177444] N89-24486

THERMAL RADIATION
Thermal radiation from plumes of solid propellant rockets
[NAL-TR-990] N89-24432
Response of layered structures to thermal radiation pulses
[AD-A206355] N89-24453

THERMAL SHOCK
Thermal shock strength of multiphase materials
[KFK-4469] N89-24455

THERMAL STABILITY
On the thermal stability of optically thin flows --- plasmas N89-24973

THERMAL STRESSES
Isothermal life prediction of composite lamina using a damage mechanics approach
[NASA-TM-102032] N89-24460
In-situ stress measurements during thermal oxidation of silicon
[AD-A206546] N89-24495
Analysis of shell-type structures subjected to time-dependent mechanical and thermal loading
[NASA-CR-184989] N89-24669
Effects of thermal history on stress-related properties of very thin films of thermally grown silicon dioxide, SiO2
[AD-A206547] N89-25062

THERMOCHEMISTRY
In-situ stress measurements during thermal oxidation of silicon
[AD-A206546] N89-24495

THERMOCOUPLES
Optimisation of the figure of merit of modified silicon-germanium alloys
[AD-A206420] N89-24491
Radiometric measurement of temperature distributions in solar cavity receivers
[DE89-011467] N89-24742

THERMODYNAMIC COUPLING
Theoretical microcontact spectra of metal electron-phonon coupling
[DE88-706280] N89-25067

THERMODYNAMIC CYCLES
Flight experiment of thermal energy storage
[NASA-TM-102081] N89-24440
On the dynamic response of pressure transmission lines in the research of helium-charged free piston Stirling engines
[NASA-TM-102121] N89-24593

THERMODYNAMIC PROPERTIES
Modeling transient thermal behavior in a thrust vector control jet vane
[AD-A206532] N89-24441
Effects of thermal history on stress-related properties of very thin films of thermally grown silicon dioxide, SiO2
[AD-A206547] N89-25062

THERMODYNAMICS
Increasing the chemical yield of desirable chemical species using solar rapid heating
[DE89-000881] N89-24489

THERMOELECTRIC POWER GENERATION
Optimisation of the figure of merit of modified silicon-germanium alloys
[AD-A206420] N89-24491

THERMOPLASTIC FILMS
Thermoplastic coating of carbon fibers
[NASA-CR-185047] N89-24488

THERMOVISCOELASTICITY
Effects of thermal history on stress-related properties of very thin films of thermally grown silicon dioxide, SiO2
[AD-A206547] N89-25062

THIN FILMS
Hydrogen ion-driven permeation in carbonaceous films
[DE89-005271] N89-24485
Sol-gel processing of controlled pore films
[DE89-013584] N89-24501
Proceedings of the Goddard Space Flight Center Workshop on Robotics for Commercial Microelectronic Processes in Space
[NASA-TM-101233] N89-24505
Measurement of bond strength at metal/ceramic interfaces
[DE89-011638] N89-24682
Research on high-efficiency, single-junction, monolithic, thin-film amorphous silicon solar cells, phase 2
[DE89-000849] N89-24703
Development of tandem cells consisting of GaAs single crystal and CuInSe2/CdZnS polycrystalline thin films N89-24717
Directions for further development of GaAs/CuInSe2 thin film tandem cells N89-24718
Radiation resistance studies of amorphous silicon films N89-24738
Research on high-efficiency, single-junction, monolithic, thin-film amorphous silicon solar cells
[DE89-000893] N89-24739
Superconducting properties of magnetron sputtered Bi-Sr-Ca-Cu-O and Tl-Ba-Ca-Cu-O thin films
[DE89-009878] N89-25056
Effects of thermal history on stress-related properties of very thin films of thermally grown silicon dioxide, SiO2
[AD-A206547] N89-25062

THOMAS-FERMI MODEL
High-pressure two temperature equations of state --- plasmas N89-24967

THREE DIMENSIONAL FLOW
Aerodynamics of a lifting rotor due to near field unsteady effects N89-24267
Three-dimensional flows and loss generation mechanisms in a linear turbine rotor cascade at various incidence conditions
[NAL-TR-984T] N89-24537
Sensitivity of mixing layers to three-dimensional forcing N89-24547
An experimental study of a three-dimensional thrust augmenting ejector using laser Doppler velocimetry
[NASA-CR-177531] N89-24569
Aspects of three-dimensional magnetic reconnection N89-24975

THREE DIMENSIONAL MODELS
A hybrid asymptotic-modal analysis of the EM scattering by an open-ended S-shaped rectangular waveguide cavity
[NASA-CR-185053] N89-24519
A 3-D graphical simulation of an automated direct chip probe/test system N89-24848

THREE DIMENSIONAL MOTION
Visibility with a moving point of view N89-24876

THRUST AUGMENTATION
A model for prediction of STOVL ejector dynamics
[NASA-TM-102096] N89-24319
An experimental study of a three-dimensional thrust augmenting ejector using laser Doppler velocimetry
[NASA-CR-177531] N89-24569

THRUST MEASUREMENT
A numerical study of chemically reacting flow in nozzles
[NASA-TM-102135] N89-24444

THRUST VECTOR CONTROL
Modeling transient thermal behavior in a thrust vector control jet vane
[AD-A206532] N89-24441

THUNDERSTORMS
Analysis and use of VAS satellite data
[NASA-CR-4218] N89-24770

THYRISTORS
Radiation hardened, optically-triggered thyristor switches: Preliminary data on three device designs
[DE89-011469] N89-24533

TIME DEPENDENCE
Time dependent reliability model incorporating continuum damage mechanics for high-temperature ceramics
[NASA-TM-102046] N89-24487
Analysis of shell-type structures subjected to time-dependent mechanical and thermal loading
[NASA-CR-184989] N89-24669

TIME LAG
AR (Autoregressive) modeling of coherence in time delay and doppler estimation
[AD-A205239] N89-24513
Influence of time lag and noncolocation on integrated structural/control system designs N89-24630

TIME MARCHING
Dynamics of coherent structures in a plane mixing layer N89-24543

A weak Hamiltonian finite element method for optimal control problems
[NASA-CR-185336] N89-24873

TIME SERIES ANALYSIS
Search for a fine-time structure in flares of UV Cet-type stars N89-25007

TIME TEMPERATURE PARAMETER
Investigations on the creep-rupture behavior of the austenitic stainless steel AISI 316-NET
[KFK-4468] N89-24479

TIN
Research on the mechanism of thermal fatigue in near-eutectic Pb-Sn solders
[DE89-011430] N89-24482

TIRES
Computational Methods for Structural Mechanics and Dynamics, part 1
[NASA-CP-3034-PT-1] N89-24638
Features and characterization needs of rubber composite structures N89-24649
Adaptive methods, rolling contact, and nonclassical friction laws N89-24651
Exploiting symmetries in the modeling and analysis of tires N89-24653

TIROS SATELLITES
Refinements in the cloud detection scheme of the 3I system. Comparison with AVHRR products
[ETN-89-94531] N89-24691
Three dimensional analysis of the atmospheric structure by vertical satellite sounding. Interest for weather forecasting
[ETN-89-94536] N89-24763

TOKAMAK DEVICES
Investigations on the creep-rupture behavior of the austenitic stainless steel AISI 316-NET
[KFK-4468] N89-24479
ICRF antenna designs for CIT and Alcator C-Mod
[DE89-011579] N89-24521
Steady-state operation regime of tokamak reactor plasma. Consistency analysis (I)
[DE88-756571] N89-24908
Study of particle confinement in the JT-60 tokamak using skin radiative approximation model
[DE88-756574] N89-24909
FOM-Rijnhuizen contributions to the Fifteenth Symposium on Fusion Technology
[REPT-88-179] N89-25030
Engineering aspects of RTP --- Rijnhuizen Tokamak PETULA (RTP) N89-25032
Elliptical polarization for ECRH on RTP --- Rijnhuizen Tokamak PETULA (RTP) N89-25035
The control and monitoring system of RTP --- Rijnhuizen Tokamak PETULA (RTP) N89-25037
ASDEX Contributions to the 8th International Conference on Plasma Surface Interaction in Controlled Fusion Devices
[IPP-III/139] N89-25038
Impurity accumulation studies in pellet-refuelled ASDEX discharges N89-25039
Characterization of the ASDEX scrape-off-layer density profile during neutral beam heating N89-25040
ASDEX edge and divertor simulation and the problem of incomplete and inaccurate experimental data N89-25041
Comparison of recycling in the ASDEX divertor before and after hardening N89-25042
The low energy neutral fluxes and their impurity production at the walls of ASDEX N89-25043
Charge exchange neutral sputtering in ASDEX N89-25044
Erosion and retention of the target plate material in the ASDEX divertor N89-25045
Measurements of the flux of metallic impurities to the ASDEX divertor plates N89-25046
Material transport at the vessel walls of the divertor tokamak ASDEX N89-25047
Plasma induced changes of a metallic divertor neutralizer plate from ASDEX analyzed by photoacoustics N89-25048

TOLERANCES (PHYSIOLOGY)
The effects of blast trauma (impulse noise) on hearing: A parametric study
[AD-A206180] N89-24786

TOOLS
Inflatable end effector tools N89-24839
Robot assembly of microscopic component in millimeter wave devices N89-24840

TOPOGRAPHY
Landscape-related position finding for flying systems N89-24302

TORQUE
Black hole driven winds N89-25096

TOUGHNESS
Microscopic delamination processes and the resulting crack tip strain fields of graphite/epoxy composites N89-24671

TRACE ELEMENTS
Non-destructive analyses of cometary nucleus samples using synchrotron radiation
[DE89-012536] N89-25101

TRACKING (POSITION)
Controller evaluation of initial data link air traffic control services. Volume 1: Mini study 2
[DOT/FAA/CT-89/14-VOL-1] N89-24292
Inductive megahertz beam position monitors for CEBAF
[CEBAF-PR-89-003] N89-24895

TRACKING STATIONS
Determination of station coordinates, earth rotation and plate motions from LAGEOS laser ranging: 1983-1986
[NAL-TR-980T] N89-24753

TRAJECTORIES
Determination of reference trajectories for testing navigation aids using an onboard CCD camera N89-24303

TRAJECTORY OPTIMIZATION
A weak Hamiltonian finite element method for optimal control problems
[NASA-CR-185336] N89-24873

TRANSDUCERS
Mechanics/heat-transfer relation for particle flows
[DE89-011382] N89-24584
Automated Millimeter Wave (AMW) transducer testing in a robotic/vision test cell N89-24841

TRANSFER FUNCTIONS
Aerodynamics of a lifting rotor due to near field unsteady effects N89-24267

TRANSFORMATIONS (MATHEMATICS)
Transformation of real and virtual objects into a virtual, visual environment N89-24304

TRANSIENT RESPONSE
Transient flow thrust prediction for an ejector propulsion concept
[NASA-TM-102078] N89-24318
Development of higher-order modal methods for transient thermal and structural analysis
[NASA-TM-101548] N89-24677

TRANSITION METALS
Oxide-bound transition metal complexes for methane activation
[PB89-138614] N89-24464
Reactions of (eta 5-C5H5) (eta 5-C5Me5) Zr(Si(SiMe3)3)X (X = Cl, Me) complexes with carbon monoxide and the isocyanide 2,6 Me2C6H3NC. Crystal structure of (eta 5-C5H5) (eta 5-C5Me5)Zr(eta 2-C(N-2,6 Me2C6H3) Si(SiMe3)3)Cl
[AD-A206494] N89-24493

TRANSITION PROBABILITIES
Charge exchange transition probability for collisions between unlike ions and atoms within the adiabatic approximation
[NASA-TM-101559] N89-25104

TRANSITION TEMPERATURE
On the nature of high-temperature superconductivity
[DE89-009525] N89-25053
Universal reduction of T(subc) in strong coupling superconductors due to Anderson/Kondo impurities
[DE89-011225] N89-25071

TRANSLATING
Neutral file data exchange between simulators and robots N89-24824

TRANSMISSION LINES
On the dynamic response of pressure transmission lines in the research of helium-charged free piston Stirling engines
[NASA-TM-102121] N89-24593

TRANSMISSIONS (MACHINE ELEMENTS)
Comparison of predicted and measured temperatures of UH-60A helicopter transmission
[NASA-TP-2911] N89-24607

TRANSMITTER RECEIVERS
Robot assembly of microscopic component in millimeter wave devices N89-24840

TRANSONIC FLOW
Computational and experimental research on buffet phenomena of transonic airfoils
[NAL-TR-996T] N89-24322

TRANSONIC WIND TUNNELS
Computational design of low aspect ratio wing-winglet configurations for transonic wind-tunnel tests
[NASA-CR-185016] N89-24266

TRANSPORT AIRCRAFT
B-737 flight test of curved-path and steep-angle approaches using MLS guidance
[NASA-TM-101521] N89-24293
Display-based communications for advanced transport aircraft
[NASA-TM-102187] N89-24798

TRAVELING WAVE TUBES
Development of a 75-watt 60-GHz traveling-wave tube for intersatellite communications
[NASA-CR-182135] N89-24530

TREADMILLS
A method of isolating treadmill shock and vibration on spacecraft
[NASA-TM-100474] N89-24790

TRENDS
Status and trends of technological image processing possibilities N89-24306

TRIBOLOGY
Tribology: The Story of Lubrication and Wear
[NASA-TM-101430] N89-24635
Solid lubricant materials for high temperatures: A review N89-24636

TRITIUM
Hydrogen ion-driven permeation in carbonaceous films
[DE89-005271] N89-24485

TRITON
Voyager at Neptune: 1989
[NASA-CR-185317] N89-24420

TROPICAL METEOROLOGY
The relationship between intraseasonal disturbance activity and interannual variation of the tropical atmosphere N89-24774
Contribution to the study of the diurnal cycle of convective clouds over tropical Africa from satellite imagery
[ETN-89-94537] N89-24780

TROPICAL REGIONS
Bibliography on tropical rain forests and the global carbon cycle. Volume 2: South Asia
[DE89-008971] N89-24748

TROPOSPHERE
Water vapor retrievals through the 3I (Improved Initialization Inversion) system: Application to tropospheric altimetry correction
[ETN-89-94534] N89-24778

TRUCKS
Analysis of life cycle costs for electric vans with advanced battery systems
[DE89-009807] N89-24526

TRUSSES
Analysis of adaptive planar truss structures
[NAL-TR-988] N89-24625
Characterization of the bending stiffness of large space structure joints
[NASA-TM-101565] N89-24676
Investigation of structural behavior of candidate Space Station structure
[NASA-CR-181746] N89-24678
Space Station Freedom Structural Characterization Experiment (SCE) node code
[NASA-TM-101594] N89-25110

TUBE HEAT EXCHANGERS
Initial characterization of a modular heat exchanger with an integral heat pipe
[NASA-TM-102097] N89-25078

TUNABLE LASERS
A role for free electron lasers in fusion N89-25031

TURBINE BLADES
Turbomachinery technology for high-speed civil flight
[NASA-TM-102092] N89-24320
Space Shuttle Main Engine High Pressure Fuel Turbopump turbine blade cracking
[NASA-TM-100327] N89-24435
Composite Blade Structural Analyzer (COBSTRAN) demonstration manual
[NASA-TM-101957] N89-24459

TURBINE PUMPS
Space Shuttle Main Engine High Pressure Fuel Turbopump turbine blade cracking
[NASA-TM-100327] N89-24435
Materials compatibility with oxidizer-rich gases at elevated temperatures and pressure
[NASA-CR-183647] N89-24466

TURBOFANS
Turbomachinery technology for high-speed civil flight
[NASA-TM-102092] N89-24320

TURBOMACHINERY
Turbomachinery technology for high-speed civil flight
[NASA-TM-102092] N89-24320

TURBOPROP AIRCRAFT
Cruise noise of the SR-2 propeller model in a wind tunnel
[NASA-TM-101480] N89-24886
Advanced turboprop aircraft flyover noise: Annoyance to counter-rotating-propeller configurations with a different number of blades on each rotor: Preliminary results
[NASA-TM-100638] N89-24888

TURBULENCE
Inlet turbulence intensity level and cross-stream distribution effects on the heat transfer in plane wall jets
[NASA-CR-183652] N89-24576
Atmospheric effects on laser propagation
[DE89-012287] N89-24606
The role of the radial electric field in enhanced confinement regimes in stellarators
[DE89-011572] N89-25049

TURBULENCE EFFECTS
An experimental study of a three-dimensional thrust augmenting ejector using laser Doppler velocimetry
[NASA-CR-177531] N89-24569
TURBULENCE MODELS
Analysis of the wake behind a propeller using the finite element method with a two-equation turbulence model N89-24286
A model for prediction of STOVL ejector dynamics
[NASA-TM-102098] N89-24319
TURBULENT BOUNDARY LAYER
Development of a supersonic turbulent boundary layer on a heated wall. Properties of the turbulent field and theoretical application
[ONERA-RSF-74/7078-AY-096-A] N89-24275
Unsteady Aerodynamics, volume 1
[VKI-1988-07-VOL-1] N89-24276
Effects of unsteadiness on turbulent boundary layers N89-24280
Studying Turbulence Using Numerical Simulation Databases, 2. Proceedings of the 1988 Summer Program
[NASA-CR-184905] N89-24538
Theoretical model for VITA-educed coherent structures in the wall region of a turbulent boundary layer N89-24556
Interaction between an oblique shock wave and a turbulent boundary layer
[ONERA-RT-76/7078-AY-096-A] N89-24574
Some characteristics of bypass transition in a heated boundary layer
[NASA-TM-102126] N89-24577
TURBULENT FLOW
Boundary layer response to an unsteady turbulent environment
[AD-A206578] N89-24273
Computational unsteady aerodynamics for lifting surfaces N89-24284
Analysis of the wake behind a propeller using the finite element method with a two-equation turbulence model N89-24286
Studying Turbulence Using Numerical Simulation Databases, 2. Proceedings of the 1988 Summer Program
[NASA-CR-184905] N89-24538
Inflow/outflow boundary conditions and global dynamics of spatial mixing layers N89-24540
Phase decorrelation, streamwise vortices and acoustic radiation in mixing layers N89-24541
A numerical study of bifurcations in a barotropic shear flow N89-24542
Dynamics of coherent structures in a plane mixing layer N89-24543
Subharmonic resonance in a mixing layer N89-24544
Scalar entrainment in the mixing layer N89-24545
Use of passive scalar tagging for the study of coherent structures in the plane mixing layer N89-24546
Sensitivity of mixing layers to three-dimensional forcing N89-24547
Sampling inhomogeneous turbulent fields N89-24548
Dynamical interpretation of conditional patterns N89-24549
Turbulence production near walls: The role of flow structures with spanwise asymmetry N89-24550
Pressure-strain-rate events in homogeneous turbulent shear flow N89-24551
Eddies, streams, and convergence zones in turbulent flows N89-24555
The structure of sheared turbulence near a plane boundary N89-24557
Analysis of homogeneous turbulent reacting flows N89-24558
Cut-and-connect of two antiparallel vortex tubes N89-24559
Optical propagation through a homogeneous turbulent shear flow N89-24561
Velocity and scalar fields of turbulent premixed flame in stagnation flow
[DE89-009336] N89-24566
Numerical study of turbulent secondary flows in curved ducts
[NASA-CR-181830] N89-24568
Turbulent flow in a 180 deg bend: Modeling and computations
[NASA-CR-4141] N89-24579
TURBULENT JETS
Transient flow thrust prediction for an ejector propulsion concept
[NASA-TM-102078] N89-24318
TURBULENT MIXING
Chaos in a spatially-developing plane mixing layer N89-24539
TWINNING
Grain boundary phase equilibria in metallic systems
[DE89-011787] N89-25066
TWO DIMENSIONAL BODIES
Aerodynamic interaction between vortical wakes and lifting two-dimensional bodies
[NASA-TM-101074] N89-24563
TWO DIMENSIONAL FLOW
Use of Navier-Stokes methods to predict circulation control airfoil performance
[AD-A206242] N89-24270
Computation of the characteristics of the wake past an oscillating cylinder N89-24283
Computational unsteady aerodynamics for lifting surfaces N89-24284
Nonlinear evolution of interacting oblique waves on two-dimensional shear layers
[NASA-TM-102030] N89-24575
A genuinely multi-dimensional upwind cell-vertex scheme for the Euler equations
[NASA-TM-102029] N89-24872
TWO DIMENSIONAL JETS
Inlet turbulence intensity level and cross-stream distribution effects on the heat transfer in plane wall jets
[NASA-CR-183652] N89-24576
TWO DIMENSIONAL MODELS
A numerical study of chemically reacting flow in nozzles
[NASA-TM-102135] N89-24444
TWO PHASE FLOW
Two-phase flow measurements by nuclear magnetic resonance imaging
[DE89-011850] N89-24586
TYPE 4 BURSTS
Tremsdorf solar radio astronomy observatory: The scientific program and an interesting observation N89-24999
Coronal magnetic field strengths determined from fiber bursts N89-25002

U

UH-60A HELICOPTER
Comparison of predicted and measured temperatures of UH-60A helicopter transmission
[NASA-TP-2911] N89-24607
UK SPACE PROGRAM
The activities of the British National Space Centre (BNSC) in the field of imaging spectrometry N89-24696
ULTRASONIC RADIATION
Multiphoton transitions at the Moessbauer radiation diffraction in crystals under a weak ultrasonic field
[DE88-706341] N89-25069
ULTRASONICS
Algorithm for display of automated nondestructive thickness measurements N89-24850
ULTRAVIOLET REFLECTION
Contamination effects study
[NASA-CR-183613] N89-24746
ULTRAVIOLET SPECTRA
IUE investigations of SN 1987A
[NASA-CR-184973] N89-25079
UNDERGROUND STRUCTURES
Centrifugal modeling of underground structures subjected to blast loading
[AD-A206424] N89-24675
UNMANNED SPACECRAFT
Report of the committee on a commercially developed space facility
[NASA-CR-185383] N89-24406
UNSTEADY AERODYNAMICS
Aerodynamics of a lifting rotor due to near field unsteady effects N89-24267
Unsteady Aerodynamics, volume 1
[VKI-1988-07-VOL-1] N89-24276
Unsteady aerodynamics N89-24277
Unsteady aerodynamic effects on bluff bodies N89-24278
Experimental techniques in unsteady flows N89-24279
Effects of unsteadiness on turbulent boundary layers N89-24280
Computational unsteady aerodynamics for lifting surfaces N89-24284
Aeroservoelastic modeling and applications using minimum-state approximations of the unsteady aerodynamics
[NASA-TM-101574] N89-24308
Recent activities within the Aeroservoelasticity Branch at the NASA Langley Research Center
[NASA-TM-101582] N89-24314
Computational and experimental research on buffet phenomena of transonic airfoils
[NAL-TR-996T] N89-24322
Survey of Army/NASA rotorcraft aeroelastic stability research
[NASA-TM-101026] N89-24329
UNSTEADY FLOW
Aerodynamics of a lifting rotor due to near field unsteady effects N89-24267
Conservative treatment of boundary interfaces for overlaid grids and multi-level grid adaptations
[NASA-TM-102080] N89-24269
Boundary layer response to an unsteady turbulent environment
[AD-A206578] N89-24273
Unsteady Aerodynamics, volume 1
[VKI-1988-07-VOL-1] N89-24276
Unsteady aerodynamics N89-24277
Unsteady aerodynamic effects on bluff bodies N89-24278
Experimental techniques in unsteady flows N89-24279
Effects of unsteadiness on turbulent boundary layers N89-24280
Unsteady Aerodynamics, volume 2
[VKI-1988-07-VOL-2] N89-24281
Numerical methods for unsteady flows N89-24282
Computation of the characteristics of the wake past an oscillating cylinder N89-24283
Computational unsteady aerodynamics for lifting surfaces N89-24284
Transient flow thrust prediction for an ejector propulsion concept
[NASA-TM-102078] N89-24318
Numerical simulation of feedback control of aerodynamic configurations in steady and unsteady ground effects N89-24326
Turbine rotor/stator flowfield analysis
[NASA-CR-183639] N89-24433
Unsteady and separated flows
[AD-A206539] N89-24572
USER MANUALS (COMPUTER PROGRAMS)
Composite Blade Structural Analyzer (COBSTRAN) demonstration manual
[NASA-TM-101957] N89-24459
USER REQUIREMENTS
Hermes user interfaces N89-24346
Industrial utilization of microgravity: Problems in the realization phase N89-24383
The Microgravity User Support Center (MUSC) N89-24394
Superfluid Helium Tanker Study (SFHT)
[NASA-CR-172114] N89-24415
Evaluation, description and invention: Paradigms for human-computer interaction
[AD-A204617] N89-24796

V

V/STOL AIRCRAFT
An investigation of V/STOL jet interactions in a crossflow
[AD-A206360] N89-24272
VACUUM CHAMBERS
Contamination effects study
[NASA-CR-183613] N89-24746
VALLEYS
Field studies for determining the characteristics and dynamics of local circulations
[DE89-012290] N89-24751
VALVES
Continuous cryopump with a method for removal of solidified gases
[DE89-009760] N89-24611
VAPOR DEPOSITION
Embedded conductors by electrochemical planarization
[DE89-011632] N89-24534
InP shallow-homojunction solar cells N89-24708
High efficiency GaAs-Ge tandem solar cells grown by MOCVD N89-24721
Response of single junction GaAs/GaAs and GaAs/Ge solar cells to multiple doses of 1 MeV electrons N89-24722
Chemical etching and organometallic chemical vapor deposition on varied geometries of GaAs N89-24728
Status of GaAs solar cell production N89-24729
Gallium Arsenide welded panel technology for advanced spaceflight applications N89-24731
VARIABILITY
The importance of climatological variability and the rate at which waste is added to modeling water budget of landfills
[DE89-008917] N89-24747
VARIABLE CYCLE ENGINES
Turbomachinery technology for high-speed civil flight
[NASA-TM-102092] N89-24320

VARIATIONAL PRINCIPLES
Quantum mechanics of chemical reactions: Recent developments in reactive scattering and in reaction path Hamiltonians
[DE89-010438] N89-24470
Application of the p-version of the finite-element method to global-local problems N89-24648
Improved analysis of laminated heterogeneous beams and associated formulation of a new finite element method N89-24672
A weak Hamiltonian finite element method for optimal control problems
[NASA-CR-185336] N89-24873
VECTOR QUANTIZATION
Investigation of vector quantization for the coding gray scale images for Group 4 facsimile
[AD-A206548] N89-24809
VEGETATIVE INDEX
Necessity and benefit of the X-SAR space shuttle experiment
[DFVLR-MITT-88-29] N89-24688
The FLI airborne imaging spectrometer: A highly versatile sensor for many applications N89-24694
VELOCITY
Study of explosive and nonexplosive cyclogenesis during FGGE
[AD-A206521] N89-24775
VELOCITY DISTRIBUTION
Interaction of Karman vortex-street with an elliptical leading-edge N89-24268
Eddies, streams, and convergence zones in turbulent flows N89-24555
Velocity and scalar fields of turbulent premixed flame in stagnation flow
[DE89-009336] N89-24566
VELOCITY MEASUREMENT
Optoelectronic velocimeter development
[DE89-012283] N89-24597
Efficient dealiasing of Doppler velocities using local environment constraints
[DOT/FAA/SA-89/1] N89-24771
VENTILATION
Fire safety applications for spacecraft
[NASA-TM-101463] N89-24413
VENUS SURFACE
Magellan: The unveiling of Venus
[NASA-CR-185018] N89-24419
VERY HIGH FREQUENCIES
Protection of VHF international distress frequencies from harmonic radiation due to digital television equipment
[BBC-RD-1989/1] N89-24512
VHSIC (CIRCUITS)
Hardware modeling with VHDL (VHSIC Hardware Description Language) simulation
[AD-A206356] N89-24805
VIBRATION
Field joint environmental protection system vibration/pressurization qualification
[NASA-CR-183673] N89-24449
VIBRATION ISOLATORS
A method of isolating treadmill shock and vibration on spacecraft
[NASA-TM-100474] N89-24790
VIBRATION TESTS
Ground vibration test of the Foudre A04 Transall aircraft
[REPT-20/7234-PY-382-R] N89-24311
A method of isolating treadmill shock and vibration on spacecraft
[NASA-TM-100474] N89-24790
An analytical study of a vibration test method using extremal control of acceleration and force
[DE89-007428] N89-24884
VIDEO COMMUNICATION
The Columbus crew communication subsystem and the on board local area network N89-24397
VIDEO DATA
Investigations of a displacement-estimation technique for aerial video scenes N89-24299
VIDEO EQUIPMENT
Vision system testing for teleoperated vehicles
[DE89-009713] N89-24610
VIDEO SIGNALS
Investigations of a displacement-estimation technique for aerial video scenes N89-24299
VISCOELASTICITY
Adaptive methods, rolling contact, and nonclassical friction laws N89-24651
Equations of motion for viscoelastic moving crack problems N89-24670
VISCOPLASTICITY
Viscosity of solids determined by shock wave action on hemispherical indentations
[DE89-008035] N89-24510
VISCOSITY
Viscosity of solids determined by shock wave action on hemispherical indentations
[DE89-008035] N89-24510
VISCOUS FLOW
A zonal method for modeling powered-lift aircraft flow fields
[NASA-CR-177521] N89-24287
Cut-and-connect of two antiparallel vortex tubes N89-24559
Head-on collision of viscous vortex rings N89-24560
Aerodynamic interaction between vortical wakes and lifting two-dimensional bodies
[NASA-TM-101074] N89-24563
VISCOUS FLUIDS
Numerical study of turbulent secondary flows in curved ducts
[NASA-CR-181830] N89-24568
VISIBILITY
Visibility with a moving point of view N89-24876
VISUAL AIDS
Improved marking of taxiway intersections for Instrument Flight Rules (IFR) operations
[DOT/FAA/CT-TN89/23] N89-24330
VISUAL CONTROL
Transformation of real and virtual objects into a virtual, visual environment N89-24304
VISUAL PERCEPTION
Transformation of real and virtual objects into a virtual, visual environment N89-24304
VOICE COMMUNICATION
The Columbus crew communication subsystem and the on board local area network N89-24397
VOLUME
Pressure-volume properties of metallic bellows
[NASA-TM-100365] N89-24422
VORTEX BREAKDOWN
Water tunnel investigation of the vortex dynamics of periodically pitched wings
[AD-A206359] N89-24271
Cut-and-connect of two antiparallel vortex tubes N89-24559
Vortex dynamics and vortex breakdown
[AD-A206470] N89-24570
VORTEX GENERATORS
Generation of large-scale vortices in compressible helical turbulence N89-24969
VORTEX RINGS
Head-on collision of viscous vortex rings N89-24560
Vortex dynamics and vortex breakdown
[AD-A206470] N89-24570
VORTEX SHEDDING
Computation of the characteristics of the wake past an oscillating cylinder N89-24283
VORTICES
Unsteady aerodynamics N89-24277
Phase decorrelation, streamwise vortices and acoustic radiation in mixing layers N89-24541
Dynamics of coherent structures in a plane mixing layer N89-24543
Cut-and-connect of two antiparallel vortex tubes N89-24559
An experimental study of a three-dimensional thrust augmenting ejector using laser Doppler velocimetry
[NASA-CR-177531] N89-24569
Drift turbulence of plasma as a gas of vortex ensemble N89-24961
VOYAGER 2 SPACECRAFT
Voyager at Neptune: 1989
[NASA-CR-185317] N89-24420

W

WAFERS
Vertical emitting, ring geometry, ultra-low threshold and ultra-high speed quantum well lasers for optical interconnect
[AD-A206427] N89-24603
Position-sensitive CdTe detector using improved crystal growth method
[NASA-CR-183427] N89-25051
WAKES
Computation of the characteristics of the wake past an oscillating cylinder N89-24283
WALL FLOW
Turbulence production near walls: The role of flow structures with spanwise asymmetry N89-24550
Turbulence characteristics inside a turbulent spot in plane Poiseuille flow N89-24554
Theoretical model for VITA-educed coherent structures in the wall region of a turbulent boundary layer N89-24556
Turbulent flow in a 180 deg bend: Modeling and computations
[NASA-CR-4141] N89-24579
WALL JETS
Inlet turbulence intensity level and cross-stream distribution effects on the heat transfer in plane wall jets
[NASA-CR-183652] N89-24576
WASTE DISPOSAL
The importance of climatological variability and the rate at which waste is added to modeling water budget of landfills
[DE89-008917] N89-24747
WASTE WATER
The importance of climatological variability and the rate at which waste is added to modeling water budget of landfills
[DE89-008917] N89-24747
WATER BALANCE
Solute model or cellular energy model: Practical and theoretical aspects of thirst during exercise
[AD-A206143] N89-24785
WATER COLOR
DFVLR activities related to imaging spectrometry N89-24697
Biooptical variability in the Greenland Sea observed with the Multispectral Airborne Radiometer System (MARS)
[NASA-CR-184856] N89-24784
WATER VAPOR
Analysis and use of VAS satellite data
[NASA-CR-4218] N89-24770
Water vapor retrievals through the 3I (Improved Initialization Inversion) system: Application to tropospheric altimetry correction
[ETN-89-94534] N89-24778
WATER WAVES
WADA1: FORTRAN program for wave diffraction analysis, version 1
[AD-A206533] N89-24808
WAVE DIFFRACTION
WADA1: FORTRAN program for wave diffraction analysis, version 1
[AD-A206533] N89-24808
WAVE DISPERSION
Dissipation of Alfven waves in solar coronal arches N89-24919
Effects of unequal particle number densities on Alfven waves N89-24945
WAVE EQUATIONS
On the refraction of longitudinal waves in compressible media
[DE89-012922] N89-24588
WAVE FUNCTIONS
Semiclassical matrix-elements of high-charge ions
[DE89-009258] N89-24890
WAVE INTERACTION
WADA1: FORTRAN program for wave diffraction analysis, version 1
[AD-A206533] N89-24808
The electron beam instability revisited: Growth above and below f sub p N89-24917
Dissipation of Alfven waves in solar coronal arches N89-24919
MHD-waves and their nonlinear interaction in a plasma with magnetic flux tubes N89-24921
WAVE PROPAGATION
Atmospheric effects on laser propagation
[DE89-012287] N89-24606
Alfven wave solitons and solar intermediate drift bursts N89-24923
Multiphoton transitions at the Moessbauer radiation diffraction in crystals under a weak ultrasonic field
[DE88-706341] N89-25069
A new field experiment in the Greenland ice cap to test Newton's inverse square law
[DE89-009247] N89-25091
WAVEGUIDES
Analysis of the EM scattering from arbitrary open-ended waveguide cavities using axial Gaussian Beam tracking
[NASA-CR-185054] N89-24518
Engineering design of the interaction waveguide for high-power accelerator-driven microwave free-electron lasers
[DE89-011896] N89-24605
WAVERIDERS
An integrated aerodynamic/propulsion study for generic aero-space planes based on waverider concepts
[NASA-CR-183389] N89-24315
WEAPON SYSTEMS
Summary and evaluation of the Strategic Defense Initiative Space Power Architecture Study
[NASA-TM-102012] N89-24443
The use of seaplanes as an advanced weapon system
[AD-A206243] N89-24880
WEAR
Role of sulfur oxides in wear and deposit formation in Army diesel engines
[AD-A206054] N89-24613
Tribology: The Story of Lubrication and Wear
[NASA-TM-101430] N89-24635

WEATHER FORECASTING
Analysis and use of VAS satellite data
[NASA-CR-4218] N89-24770
Forecast of Atlantic seasonal hurricane activity for 1989 N89-24773
WEATHERING
Field joint environmental protection system vibration/pressurization qualification
[NASA-CR-183673] N89-24449
WEIGHT (MASS)
Field-dependence and judgment of weight and color revisited: Some implications for the study of sensory discrimination
[AD-A206141] N89-24791
WEIGHT REDUCTION
Space Station Freedom Solar Array design development
[NASA-TM-102105] N89-24448
The effect of heat input and composition on weld metal microstructures in thin section HY-130 GMAW weldments
[AD-A206476] N89-24477
WELDABILITY
Weldability and microstructural characterization of Al-Li alloys
[DE89-010183] N89-24478
Nd:YAG laser weldability of RS/PM Al-BFe-2Mo sheet
[DE89-013588] N89-24621
WELDED JOINTS
The effect of heat input and composition on weld metal microstructures in thin section HY-130 GMAW weldments
[AD-A206476] N89-24477
WELDED STRUCTURES
The effect of heat input and composition on weld metal microstructures in thin section HY-130 GMAW weldments
[AD-A206476] N89-24477
Gallium Arsenide welded panel technology for advanced spaceflight applications N89-24731
WELDING
The effect of heat input and composition on weld metal microstructures in thin section HY-130 GMAW weldments
[AD-A206476] N89-24477
Incorporation of surface tension into the structural finite element code SANCHO
[DE89-011354] N89-24616
WENTZEL-KRAMER-BRILLOUIN METHOD
Semiclassical matrix-elements of high-charge ions
[DE89-009258] N89-24890
WHISTLERS
The role of whistler oscillations in the formation of the structure of high Mach number collisionless shock N89-24936
Nonlinear oblique whistlers: Their relevance to nonthermal coupling of ions and electrons in accretion flow and supercritical quasi-perpendicular collisionless shocks --- black holes N89-24955
WIENER HOPF EQUATIONS
Equations of motion for viscoelastic moving crack problems N89-24670
WIND (METEOROLOGY)
Orographically-caused microclimate variation in the Saariselka Region
[ISBN-9-5169-7269-1] N89-24767
WIND MEASUREMENT
Study of representativity of the wind fields deduced from geostationary satellite images. Attribution of height to wind vectors and large scale average fields deduced from water vapor imagery
[ETN-89-94538] N89-24781
WIND TUNNEL NOZZLES
Ultra-light duct for an anechoic wind tunnel
[NASA-TM-101805] N89-24331
WIND TUNNEL TESTS
Computational design of low aspect ratio wing-winglet configurations for transonic wind-tunnel tests
[NASA-CR-185016] N89-24266
Analysis of the boundary layer of a delta wing in incidence
[CERT-RT-OA-26/5025-AYD] N89-24274
Development of a supersonic turbulent boundary layer on a heated wall. Properties of the turbulent field and theoretical application
[ONERA-RSF-74/7078-AY-096-A] N89-24275
Experimental techniques in unsteady flows N89-24279
Experimental aerodynamic characteristics of a joined-wing research aircraft configuration
[NASA-TM-101083] N89-24285
Aeroservoelastic wind-tunnel investigations using the Active Flexible Wing Model: Status and recent accomplishments
[NASA-TM-101570] N89-24313
Wind tunnel tests on flutter control of a high-aspect-ratio cantilevered wing
[NAL-TR-978] N89-24321
SRB ascent aerodynamic heating design criteria reduction study, volume 2
[NASA-CR-183569] N89-24430
Interaction between an oblique shock wave and a turbulent boundary layer
[ONERA-RT-76/7078-AY-096-A] N89-24574
Cruise noise of the SR-2 propeller model in a wind tunnel
[NASA-TM-101480] N89-24886
Langley aerospace test highlights, 1988
[NASA-TM-101579] N89-25112
WIND TUNNEL WALLS
Ultra-light duct for an anechoic wind tunnel
[NASA-TM-101805] N89-24331
WIND TUNNELS
Langley aerospace test highlights, 1988
[NASA-TM-101579] N89-25112
WINDOWS (APERTURES)
A new structure for comparing surface passivation materials of GaAs solar cells N89-24725
WINDPOWERED GENERATORS
Control research in windpower project 506259 utilization
[FOA-C-20746-2.7] N89-24740
WING OSCILLATIONS
Water tunnel investigation of the vortex dynamics of periodically pitched wings
[AD-A206359] N89-24271
WING PLANFORMS
Computational design of low aspect ratio wing-winglet configurations for transonic wind-tunnel tests
[NASA-CR-185016] N89-24266
WINGLETS
Computational design of low aspect ratio wing-winglet configurations for transonic wind-tunnel tests
[NASA-CR-185016] N89-24266
WINGS
Thermal analysis of a hypersonic wing test structure
[NASA-CR-185319] N89-24265
WIRE
Development of an integrated CAD/CAM system for wire harness fabrication N89-24842
WOLF-RAYET STARS
Generation of X-ray and radio emission by binary Wolf-Rayet stars N89-24929
Speculation on the origin of X-ray emission in early-type stars N89-25029
WORDS (LANGUAGE)
The 64K 16-bit word buffer memory with microprogrammable control
[DE88-706303] N89-24799
WORK CAPACITY
Brain-wave measures of workload in advanced cockpits: The transition of technology from laboratory to cockpit simulator, phase 2
[NASA-CR-4240] N89-24797
WORKING FLUIDS
Flight experiment of thermal energy storage
[NASA-TM-102081] N89-24440
WORKLOADS (PSYCHOPHYSIOLOGY)
Manned interventions at the MTFF: Crew workload aspects N89-24362
Brain-wave measures of workload in advanced cockpits: The transition of technology from laboratory to cockpit simulator, phase 2
[NASA-CR-4240] N89-24797

X

X RAY ABSORPTION
Design of the optical system for a new time-resolved X-ray absorption spectroscopy apparatus
[DE88-757253] N89-24902
X RAY APPARATUS
Laboratory for X-ray optics
[AD-A206468] N89-25061
X RAY ASTRONOMY
Soft X-ray observations of the Vela Pulsar PSR 0833-45
[MPE-PREPRINT-130] N89-25080
X RAY BINARIES
A new model of PeV gamma-ray sources --- X-ray binaries N89-24946
X RAY DIFFRACTION
X-ray investigations of ceramic high Tc superconductors under high pressure
[KFK-4482] N89-25064
X RAY IMAGERY
Hard X-ray imaging telescope development
[DE89-011647] N89-24906
X RAY SPECTROSCOPY
SMM X-ray polychromator
[NASA-CR-180791] N89-24590
Design of the optical system for a new time-resolved X-ray absorption spectroscopy apparatus
[DE88-757253] N89-24902
X-ray photoelectron spectroscopy study of samples in the Y-Ba-Cu-O system
[AD-A206260] N89-25060
X RAY TELESCOPES
Hard X-ray imaging telescope development
[DE89-011647] N89-24906
X RAYS
Demonstration of a Time Projection Compton Spectrometer
[DE89-010743] N89-24596
Combined microstructure X-ray optics
[DE89-009902] N89-24904
Speculation on the origin of X-ray emission in early-type stars N89-25029
X WING ROTORS
Results of a parametric aeroelastic stability analysis of a generic X-wing aircraft
[NASA-TM-101572] N89-24324
XENON
Development of the cryopanel for tests of xenon ion thrusters
[NAL-TR-981] N89-24431
Performance of large area xenon ion thrusters for orbit transfer missions
[NASA-TM-102049] N89-24436

Y

YAG LASERS
Holographic interferometry with an injection seeded Nd:YAG laser and two reference beams
[NASA-TM-102056] N89-24591
Prototype laser-diode-pumped solid state laser transmitters
[NASA-CR-185056] N89-24601
YTTRIUM COMPOUNDS
Photothermal imaging of high T(sub c) superconductor
[DE89-009644] N89-25054
X-ray photoelectron spectroscopy study of samples in the Y-Ba-Cu-O system
[AD-A206260] N89-25060

Z

ZINC
Deep levels and radiation effects in p-InP N89-24713
ZINC-BROMIDE BATTERIES
Analysis of life cycle costs for electric vans with advanced battery systems
[DE89-009807] N89-24526
ZIRCONIUM OXIDES
Ceramic Technology for Advanced Heat Engines Project data base
[DE89-012888] N89-24499
ZONAL HARMONICS
A zonal method for modeling powered-lift aircraft flow fields
[NASA-CR-177521] N89-24287

Typical Personal Author Index Listing

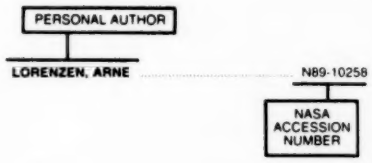

Listings in this index are arranged alphabetically by personal author. The NASA accession number denotes the number by which the citation is identified.

A

ABIBOV, A. L. N89-24261
ABRAMS, TRUDY S. N89-25074
ABUELFOUTOUH, NADER M. N89-24460
ABURDZHANIYA, G. N89-24961
ACCENSI, A. N89-24387
ACTON, L. W. N89-24590
ADAMS, WILLIAM M., JR. N89-24313
ADDIS, F. W. N89-24724
ADENIJI-FASHOLA, A. A. N89-24576
ADRIAN, R. J. N89-24548
N89-24549
AHROON, WILLIAM A. N89-24786
AIELLO, ROBERT A. N89-24459
AIKEN, CARLOS L. V. N89-25091
AKAPEV, G. N. N89-24503
AKSAY, I. A. N89-24489
ALBRIGHT, CHARLES E. N89-24620
ALBY, F. N89-24423
ALCAYDE, D. N89-24699
ALDER, BERNI J. N89-24567
ALFREDSSON, P. HENRIK N89-24550
N89-24554
ALFVEN, H. N89-24911
ALLEGRA, A. N89-24399
ALLEN, D. H. N89-24634
ALLEN, L. E. N89-24488
ALTHOFF, SUSAN L. N89-24264
ALTOBELLI, S. A. N89-24586
ALTYNTSEV, A. T. N89-25012
ALYEA, F. N. N89-24755
AMINPOUR, MOHAMMAD A. N89-24673
ANAND, K. N89-24597
ANCADEABATI, R. N89-24479
ANDER, MARK E. N89-25091
ANDERL, R. A. N89-24485
ANDERSEN, C. M. N89-24653
ANDERSON, B. N. N89-24922
ANDERSON, G. A. N89-24893
ANDERSON, J. M. N89-24842
ANDERSON, W. A. N89-24713
ANDO, SAMON N89-24808
ANDRE, S. N89-24425
ANDREWS, MARK J. N89-24770
ANTALOVA, A. N89-25000
APARICIO, J. P. N89-24777
APPELBAUM, JOSEPH N89-24529
APRIGLIANO, L. F. N89-25060
ARMANIOS, ERIAN A. N89-24674
ARMSTRONG, ELIZABETH S. N89-24447
ARMSTRONG, LAWRENCE E. N89-24785
N89-24789
ARONS, J. N89-24916
N89-24928
ASHLEY, C. S. N89-24501
ASHOUR-ABDALLA, MAHA N89-25017
ASHWORTH, B. N89-24434
ASSEO, E. N89-24956
N89-24957
ATHANASSOULA, E. N89-24965
ATLURI, SATYA N. N89-24644
ATTAWAY, S. W. N89-24683
AUGUSTINE, GODFREY N89-24708
AUMANN, H. N89-24758
AURASS, H. N89-24999
N89-25001
AVERIANIKHINA, E. A. N89-25001
AYRA, R. R. N89-24703

B

BABCOCK, S. M. N89-24861
BACHMANN, G. N89-24997
BACKMAN, B. F. N89-24640
BADER, S. D. N89-24474
BADRELDIN, ASHRAF MAHMOUD N89-24609
BAER, M. R. N89-24472
BAESLACK, W. A., III N89-24621
BAILEY, SHEILA G. N89-24728
BAITY, F. W. N89-24521
BAJGAR, C. N89-24721
BALDWIN, G. T. N89-24596
BALDWIN, RONALD G. N89-24776
BAMBERGER, A. N89-24900
BANJANIN, ZORAN N89-24515
BANNENBURG, J. G. N89-25034
BAR-CHAIM, NADAV N89-24603
BARAONA, COSMO R. N89-24448
BARAS, JOHN S. N89-24608
BARBEE, TROY W., JR. N89-24904
BARBIAN, E. P. N89-25033
N89-25036
BARBIERI, SERGIO N89-24323
BARNETT, ALLEN M. N89-24712
N89-24723
N89-24725
N89-24726
BARNETT, REED N89-25076
BARNI, B. N89-24392
BARRY, WALTER N89-24895
BARTH, TIMOTHY J. N89-24871
BARTKE, J. N89-24900
BARTKO, J. N89-24722
BASILE, LUCIANO N89-24363
BATTOCCHIO, LUCIANO N89-24377
BAUDRY, P. N89-24400
BAUER, H. N89-24381
BAUMGAERTEL, K. N89-25002
BAWA, H. S. N89-24590
BAYLES, SCOTT J. N89-24316
BAYSAL, OKTAY N89-24562
BEALE, GUY O. N89-24833
BEASON, S. C. N89-24589
BECKER, A. N89-24296
BEHRISCH, R. N89-25047
BEIN, B. K. N89-25048
BELL, JOHN B. N89-24585
BELYTSCHKO, T. N89-24656
BENACQUISTA, MATTHEW JOHN N89-24765
BENITO, ROSA N89-24469
BENKEMOUN, L. N89-24275
N89-24574
BENNETT, E. N89-24394
BENNETT, M. S. N89-24703
BENSE, RONALD N89-24627
BENSON, DAVID J. N89-24659
BENT, B. E. N89-24490
BENTALL, R. H. N89-24390
BENZ, A. O. N89-24923
N89-24934
BERGER, M. A. N89-24988
BERGER, MELVYN S. N89-24570
BERGHAUS, D. G. N89-24484
BERGLUND, ERIK N89-24312
BERKOPEC, FRANK D. N89-24409
BERMAN, ALEX N89-24629
BERN, M. W. N89-24876
BERNHARDT, ANTHONY F. N89-24534
BERTHIER, STEPHANE N89-24388
BERTIN, G. N89-24963
BERTSCHINGER, G. N89-25033
BESKIN, G. M. N89-25007
BESKIN, V. S. N89-24941
BEVEN, JOHN L., II N89-24770
BEYER, R. N89-24304
BEZCHASTNOV, V. G. N89-24962
BHARWANI, SERAJ N89-24847
BHASIN, KUL B. N89-24520
BIALKOWSKA, H. N89-24900
BIERNAT, H. K. N89-24983
N89-25026
BILGER, KEVIN N89-24448
BIRN, J. N89-24975
N89-25013
N89-25021
BIRYUKOV, N. M. N89-24261
BLAAS, C. N89-24390
BLAES, O. N89-24947
BLANCKE, B. N89-24423
BLANDFORD, R. D. N89-24947
N89-24971
BLECKI, J. N89-25020
BLESS, ROBERT R. N89-24873
BLOOMQUIST, DAVID N89-24675
BOCK, R. N89-24900
BODO, G. N89-24958
BOEHME, A. N89-25003
BOER, M. N89-25084
BOGDANOV, S. YU N89-25009
BONAITA, GIOVANNI N89-24323
BOOKER, B. L. P. N89-24499
BOOTH, JAMES N89-24288
BORNT, F. W. N89-24813
BORREGO, J. M. N89-24714
BORROMEE, J. N89-24353
BORYCKI, G. N89-24365
BOULARES, AHMED N89-25108
BOURDIER, C. N89-24761
BOURRIEAU, J. N89-24370
BOUVART, D. N89-24456
N89-24457
BOYTSOV, V. V. N89-24261
BRABY, L. A. N89-24893
BRACKENBUSH, L. W. N89-24893
BRADLEY, E. C. N89-24614
BRADY, MICHAEL N89-24825
BRAMMER, K. N89-24362
BRANSTETTER, J. R. N89-24293
BRASSEUR, JAMES G. N89-24551
BRENNEN, T. M. N89-24533
BRIGGS, S. A. N89-24696
BRINKER, C. J. N89-24501
BRINKLEY, JAMES W. N89-25074
BROADWELL, J. E. N89-24545
BROCK, B. C. N89-24517
BROCKMANN, R. N89-24900
BROKOF, ULRICH N89-24303
BROWER, WILLIAM A., JR. N89-24776
BROWN, CHRISTOPHER K. N89-24266
BROWN, J. N., JR. N89-25076
BROWN, JAMES D. N89-24289
N89-24309
BROWN, NORMAN S. N89-24838
BROZE, J. G. N89-24539
BRUDIEU, P. N89-24346
BUCHANAN, M. V. N89-24465
BUCK, WARREN W. N89-25103
BUCKLEY, DONALD H. N89-24635
BUECHNER, J. M. N89-24942
N89-24943
N89-24978
N89-24980
BUECKER, H. N89-24369
BUELL, J. C. N89-24539
N89-24540
N89-24541
N89-24544
BUIA, P. N89-24384
BULANOV, S. V. N89-25011
BURINSKAYA, T. M. N89-25018
BURKE, ANDREW F. N89-24535
BURKHOLDER, R. J. N89-24518
N89-24519
BUTLER, CHRISTOPHER P. N89-24309
BUTLER, RICKY W. N89-24815
BUTTRILL, CAREY S. N89-24313

BUXTON, R. A. H. N89-24694
BYSIEK, J. N89-25027

C

CADE, MICHEL N89-24373
CAIRNS, I. H. N89-24917
N89-24945
N89-24948
CALAMITO, DOMINIC P. N89-24486
CALDWELL, R. B. N89-24533
CAMARDA, CHARLES J. N89-24677
CAMPBELL, CHARLES S. N89-24584
CANNON, T. W. N89-24743
CANU, CLAUDIO N89-24377
CAPART, J. J. N89-24350
CARASSO, MEIR N89-24469
CARDIN, J. M. N89-24832
CARLEGRIM, BOERJE N89-24531
CARLSON, D. E. N89-24703
CARLSON, L. W. N89-24611
CARROLL, JOHN M. N89-24796
CARTER, MICHAEL E. N89-24869
CASSIL, CHARLES E. N89-24289
CATALANO, A. N89-24703
CAUDRON, R. N89-24480
CAVICCHI, B. T. N89-24731
CAVINS, JEFFREY R. N89-25058
CECCONI, J. L. N89-24429
N89-25083
CERUTTI-MAORI, G. N89-24689
CHAGELISHVILI, G. D. N89-24950
N89-24951
CHAHINE, M. N89-24758
CHAN, TONY F. N89-24578
CHANG, T. N89-24954
N89-24955
CHANISHVILI, R. G. N89-24950
CHARGEISHVILI, B. B. N89-24959
N89-24966
CHARGIN, MLADEN N89-24655
CHARLES, J. N89-24365
CHASE, S. I. N89-24900
CHAU, H. H. N89-24408
CHEDIN, A. N89-24690
N89-24778
CHEDIN, M. A. N89-24779
CHELOTTI, J. N. N89-24425
CHEN, HARN C. N89-24684
CHEN, L. N89-24454
CHENG, EMILY A. P. N89-24601
CHENG, MINKANG N89-24766
CHENG, R. K. N89-24566
CHEREMUKHINA, G. A. N89-24799
CHERNOV, N. I. N89-24879
CHERUY, FREDERIQUE N89-24762
CHIMONAS, GEORGE N89-24755
CHKHETIANI, O. G. N89-24969
CHO, P. N89-24566
CHOI, K. Y. N89-24710
CHOI, S.-W. N89-24575
CHRETIEN, J.-L. N89-24400
CHUNG, FRANK T. H. N89-24497
CHUNG, M. A. N89-24722
CLAFLIN, E. S. N89-24590
CLANCY, PAUL N89-24347
CLAPP, ROGER B. N89-24747
CLARKE, MARGARET M. N89-24844
CLASPY, PAUL C. N89-24520
CLAUD, CHANTAL N89-24691
CLAY, H. W. N89-24605
CLAY, JOHN C. N89-24450
CLELAND, JOHN N89-25076
CLEMENTS, WILLIAM E. N89-24751
COCKRELL, C. R. N89-24514
COE, HAROLD H. N89-24607
COFFEY, HOWARD T. N89-24619
COHEN, J. D. N89-24496
COLE, STANLEY R. N89-24313
COLOMBINA, G. N89-24389
COLONIUS, T. N89-24543
COLRAT, J. N89-24366
COMBES-DESPA, M. N89-24699
CONTOLINI, ROBERT J. N89-24534
CONWAY, L. A. N89-24509
COOK, GEORGE E. N89-24846
COOK, M. N89-24449
COPPI, P. S. N89-24971
CORDIE, F. N89-24351
CORNILLE, M. N89-24907
CORTINOVIS, R. N89-24392
COSLER, A. N89-25033
COSMOVICI, C. B. N89-24382
COUGNET, C. N89-24360
COUILLARD, PH. N89-24338
COULTER, RICHARD L. N89-24751
COURT, NANCY N89-25076
COUSTEIX, J. N89-24280
COUTTS, T. J. N89-24709
CRAIN, W. K. N89-24430
CRASSON, J. C. N89-24456
CRAWLEY, EDWARD F. N89-24668
CROCKETT, THOMAS W. N89-24816
CRONE, L. N89-24758
CROWLEY, JOHN S. N89-24787
CRUMLEY, ROBERT L. N89-24535
CUNNOLD, D. M. N89-24755
CURRIER, L. N89-24761
CURTIS, HENRY B. N89-24705
N89-24737
CURTIS, L. J. N89-24894
CUTTER, W. BOWMAN, III N89-24406
CZECK, EDWARD W. N89-24817

D

DAHLBACKA, GLEN N89-24600
DAHMEN, U. N89-25070
DAHMER, PAUL A. N89-24687
DAIELLO, R. V. N89-24703
DALEY, JAMES G. N89-24619
DANEN, WAYNE C. N89-24504
DAVID, MICHAEL N89-24271
DAVID, S. A. N89-24478
DAVID, VALERIE N89-24335
DAVIDSON, A. N89-24358
DAVIS, M. H. N89-24756
DAVIS, ROBERT I. N89-24786
DAVIS, STEPHEN N89-24826
DEANE, A. E. N89-24552
DEBOOR, CARL N89-24863
N89-24864
DECKER, ARTHUR J. N89-24591
DEDERRA, H. N89-24353
DEFILIPPIS, VINCENZO N89-24363
DELAHOY, A. E. N89-24739
DELANNOY, A. N89-24777
DELASRIVAS, M. N89-24479
DEMARZO, C. N89-24900
DEMISCH, WOLFGANG H. N89-24406
DEMOND, F. J. N89-24396
DEPALMA, M. N89-24900
DERADO, I. N89-24900
DESALVO, GREGORY C. N89-24725
DESHPANDE, M. D. N89-24462
DESLOIRES, M. N89-24351
DEUTSCH, STANLEY N89-24792
DEVER, THERESE M. N89-24451
DEWINTER, F. D. A. N89-25036
DEYMIER, P. A. N89-25066
DIARRA, CHEICK MODIBO N89-24426
DIBATTISTA, JOHN N89-25111
DICKSON, C. R. N89-24703
DIMAURO, F. N89-24357
DIMOTAKIS, P. E. N89-24572
DITTMAR, JAMES H. N89-24886
DOBIAS, DAVID N89-24720
DOBKIN, D. P. N89-24876
DOERGELOH, H. N89-24299
DOMARADZKI, J. A. N89-24553
DONG, STANLEY B. N89-24646
DONZELLI, P. N89-24385
DOSE, V. N89-25043
DOUGLASS, ROBERT J. N89-24834
DOUIN, J. N89-25070
DOZIER, J. N89-24695
DRAKE, N. J. N89-24696
DRUMMOND, COLIN K. N89-24318
N89-24319
DRURY, L. OC. N89-24930
N89-24940
DUBAU, J. N89-24907
DUBEY, R. V. N89-24861
DUBOWSKY, STEVEN N89-24662
N89-24663
DUCASTELLE, F. N89-24480
DUDENHOEFER, JAMES E. N89-24593
DUFFY, STEPHEN F. N89-24487
DUNGEY, J. W. N89-24977
DUNHAM, GLEN N89-24724
DURET, F. N89-24349
DUVEL, JEAN PHILIPPE N89-24762

E

ECKARDT, V. N89-24900
EDENBURN, M. N89-24443
EDIE, D. D. N89-24488
EDWARDS, JOHN W. N89-24284
EDWARDS, THOMAS R. N89-24830
EGGERSLUESS, W. N89-24306
EGUCHI, KUNIHISA N89-24598
EILTS, MICHAEL D. N89-24771
EINAUDI, G. N89-24992
EKE, F. O. N89-24665
ELESHAKY, MOHAMED E. N89-24562
ELIEZER, S. N89-24967
N89-24970
ELLIOTT, ALBERS H. N89-24788
ELLIOTT, CHARLES W. N89-25075
ELLIOTT, N. P. N89-24735
ELSNER, FREDERICK H. N89-24493
EMANUEL, GEORGE N89-24315
EMERY, K. A. N89-24709
EMERY, KEITH N89-24736
EMERY, V. J. N89-25053
ENGEL, C. D. N89-24430
ENGELKE, W. D. N89-24824
ENGELUND, WALTER C. N89-24562
ENGERT, DOUGLAS E. N89-24800
ENNYU, DAIJI N89-24882
ERWIN, HARRY N89-24828
ERZBERGER, HEINZ N89-24290
ESER, E. N89-24739
ESHOW, MICHELLE M. N89-24323
ESTERLE, ALAIN N89-24344
ETHRIDGE, E. C. N89-24405
EULER, J. A. N89-24661
EVANS, N. N89-24758
EYMAR, P. N89-24360

F

FABRIZI, ROBERTO N89-24352
FACEMIRE, J. R. N89-24848
FALCIAI, A. N89-24359
FALCO, C. M. N89-25061
FALTHAMMAR, C.-G. N89-24912
FANTON, J. N89-25054
FARNELL, K. E. N89-24845
FATEMI, NAVID S. N89-24727
FAURE, A. N89-24353
FEDUTENKO, E. A. N89-24927
FEHSE, W. N89-24357
FELIPPA, CARLOS A. N89-24637
N89-24642
FENYES, PETER A. N89-24632
FERGUSON, DOUGLAS N89-24288
FERGUSON, JOHN R. N89-25091
FERNANDEZ, KEN N89-24846
FERRARI, A. N89-24958
FERRIS, MONTE J. N89-24504
FERZIGER, J. H. N89-24558
FEUERBACHER, B. N89-24394
FEUSTEL-BUECHL, J. N89-24336
FIDAN, SUKRU N89-24467
FIETZ, W. H. N89-25064
FIMMEL, RICHARD O. N89-24333
FINE, BERNARD J. N89-24791
FINEL, A N89-24480
FINK, DANIEL J. N89-24406
FITCH, J. T. N89-25062
FLAISHER, HARVEY N89-24720
FLAMMER, KAREN RUTH N89-25100
FLAX, ALEXANDER H. N89-24406
FLINT, ELIZABETH P. N89-24748
FLOBERT, JEAN-FRANCOIS N89-24763
FLOOD, DENNIS J. N89-24529
FLYNN, G. J. N89-25101
FOLEY, MICHAEL J. N89-24437
FORD, DONNIE R. N89-24825
FRANCIA, A. N89-24397
FRANCIS, G. E. N89-24984
N89-24985
FRANCIS, MARK N89-24841
FRANCOIS, MARC N89-24372
FRANK, A. G. N89-25008
N89-25009
N89-25010
FRANK, W. N89-24356
FREAR, D. N89-24482
FREDERICK, L. J. N89-24842
FREDERICKSON, PAUL O. N89-24818
FREELAND, S. L. N89-24590
FREEMAN, K. N89-24434
FREUND, E. N89-24393
FRIEDMAN, B. N89-25060
FRIEDMAN, ROBERT N89-24413
FROESCHNER, KENNETH E. N89-24682
FROST, C. L. N89-24430
FRYE, G. C. N89-24501
FU, J. H. N89-24411
FU, Z. F. N89-25023
FUELBERG, HENRY E. N89-24770

FUJIMORI, YOSHINORI N89-24506
FUKUDA, MASAHIRO N89-24801
FUKUSHIMA, E. N89-24586
FUKUYAMA, ATSUSHI N89-24908
FUMIZAWA, MOTOO N89-24565
FURRER, R. N89-24400
FUSSMANN, G. N89-25039
N89-25045

G

GABELLA, W. E. N89-24878
GALE, RONALD P. N89-24717
GALEEV, A. A. N89-24929
N89-24936
N89-24937
GALLAND, B. N89-24365
GANGULI, G. N89-24972
GARGIR, G. N89-24375
GARLICK, G. F. J. N89-24731
GASCARD, JEAN-CLAUDE N89-24691
GATHERS, G. R. N89-24408
GATOS, HARRY C. N89-24406
GAUSE, RAYMOND L. N89-24623
GAZEY, S. N89-24345
GEBALLE, T. R. N89-25085
GEDALIN, M. E. N89-24931
N89-24932
GEE, JAMES M. N89-24737
GEHRE, O. N89-25043
GEHRKE, H. N89-24355
GEIB, STEVEN J. N89-24493
GEIS, N. N89-25081
GELTMACHER, A. N89-24475
GENZEL, REINHARD N89-25081
N89-25082
N89-25086
N89-25093
N89-25094
N89-25106
GEOFFROY, L. M. N89-24721
GERLI, C. N89-24389
GERNHARDT, J. N89-25043
GERSHBERG, R. E. N89-25007
GESSERT, T. A. N89-24709
GHAN, STEVEN J. N89-24783
GHANDEHARI, MOSTAFA N89-24868
GHANDHI, S. K. N89-24714
GHIGLIA, DENNIS C. N89-24524
GIANNOLA, P. S. N89-24742
GIESE, ROBERT F. N89-24619
GILBERT, MICHAEL G. N89-24314
N89-24324
GILL, JOHN J. N89-24675
GILLANDERS, M. S. N89-24731
GILLIAM, D. N89-24824
GILLIAN, R. E. N89-24624
GIUDICELLI, PH. N89-24622
GIVLER, R. C. N89-24586
GLASSMAN, ARTHUR J. N89-24320
GLENN, G. S. N89-24731
GLICKSMAN, MARTIN E. N89-24406
GOEDBLOED, J. P. N89-24925
GOHRING, J. N89-24434
GOLDEN, DAVID M. N89-24892
GOLDMAN, A. N89-24758
GOLDMAN, T. N89-25092
GOLDREICH, P. N89-24947
GOLDSTEIN, M. E. N89-24575
GOLENIEWSKI, G. N89-24670
GOMI, MITSUO N89-24598
GONDOT, P. N89-24777
GONZALES, P. Y. N89-24777
GOOSSENS, M. N89-24925
N89-24926
GORADIA, CHANDRA N89-24711
GORADIA, MANJU GHALLA N89-24711
GORANSON, P. L. N89-24521
GORMAN, MICHAEL R. N89-25091
GORY, J. F. N89-24425
GOTT, R. W. N89-24446
GOTTARDI, M. N89-25084
GOULDING, R. H. N89-24521
GOWER, J. F. R. N89-24698
GRAF, U. U. N89-25082
N89-25086
GRATTON, F. T. N89-24983
GRAVES, G. R. N89-24411
GRAY, K. E. N89-25056
GRAY, WILLIAM M. N89-24773
GRAZI, R. N89-24359
GREEN, JAMES M. N89-24445
GREENE, WILLIAM H. N89-24641
GREGORY, JOHN C. N89-24463
GRIFFIN, LISA N89-24433
GRIGORYEV, V. P. N89-24261
GRIVAS, D. N89-24482
GROSSMAN, R. N89-24876
GROUNNER, M. N89-24733
GRUBER, R. P. N89-24446
GUBCHENKO, V. M. N89-24991
GUBERMAN, STEVEN L. N89-24889
N89-25099
GUDIKSEN, PAUL H. N89-24751
GUEDEL, M. N89-24923
GUERRIERO, LUCIANO N89-24380
GUESSOUS, MOHAMMED SAAD N89-24781
GULINO, DANIEL A. N89-24451
GUREVICH, A. V. N89-24941
GURSUL, ISMET N89-24268
GUSTAVSON, BRUCE A. N89-24629
GUYENNE, T. D. N89-24692
N89-24910
N89-24974
GUZIK, JOYCE ANN N89-25098
GVARAMADZE, V. V. N89-24969
GYEKENYESI, JOHN P. N89-24487

H

HAAG, T. W. N89-24446
HAAS, G. N89-25041
N89-25042
HABRISKY, MATTHEW N89-24836
HACKNEY, STEVE A. N89-25065
HAERENDEL, G. N89-24915
HAFTKA, RAPHAEL T. N89-24677
HAISCH, BERNHARD M. N89-24590
HALFORD, GARY R. N89-24460
HALYO, NESIM N89-24772
HAMAKER, H. C. N89-24733
HAMANN, R. N89-24390
HAMEL, W. R. N89-24861
HAMERNIK, ROGER P. N89-24786
HAMMONS, B. E. N89-24533
HANAK, JOSEPH J. N89-24720
HANNUM, NED P. N89-24409
HARABURDA, FRANCIS M. N89-24439
HARDIN, JASPER E. N89-24535
HARJES, H. C. N89-24525
HARMAN, PHILLIP E. N89-24821
HARRIS, A. I. N89-25082
N89-25086
N89-25106
HARRY, HERBERT H. N89-24612
HART, R. E., JR. N89-24707
N89-24721
HARTMANN, WILLIAM K. N89-24752
HATHORN, TIMOTHY N89-24309
HAUG, EDWARD J. N89-24664
HAVEN, VICTOR E. N89-24708
N89-24721
HAWKES, J. N89-24454
HAYAKAWA, YUKIO N89-24431
HAYDUK, ROBERT J. N89-24638
N89-24654
HAYRAPETYAN, V. S. N89-25004
HAYS, DAN N89-24826
HEDGEPETH, JOHN M. N89-24678
HEDRICK, C. L. N89-25050
HELLINGMAN, P. N89-25032
HELMINEN, JAAKKO N89-24768
HENDERSON, LEROY F. N89-24588
HENLINE, WILLIAM D. N89-24580
HENNINGSON, D. S. N89-24554
HERBST, MICHAEL K. N89-24289
N89-24309
HERMAN, H. N89-24611
HERMANNS, D. F. M. N89-24924
HERNANDEZ, J. H. N89-24996
HERRING, M. N89-24695
HERRMANN, MELODY N89-24820
HESSE, M. N89-24975
N89-25013
N89-25021
HETHERINGTON, C. J. D. N89-25070
HEWETT, D. W. N89-24984
N89-24985
HEYLAND, D. N89-24381
HEYN, M. F. N89-24983
N89-25026
HIBBITT, H. D. N89-24639
HIBBS, MICHAEL FRANK N89-24671
HIGGINBOTHAM, SCOTT A. N89-24412
HIGHSMITH, A. L. N89-24634
HILDEBRANDT, J. N89-25005
HILDMANN, B. N89-24394
HILL, J. C. N89-24558
HILL, R. H., JR. N89-24492
HILL, SCOTT M. N89-24520
HIRABAYASHI, NORIAKI N89-25072
HIROSE, NAOKI N89-24322
HIRSCH, H. N89-24366
HIRSHMAN, S. P. N89-25050
HISHIDA, MAKOTO N89-24565
HO, C. M. N89-24541
HO, FRANK N89-24729
HOBBS, R. M. N89-24735
HODGES, DEWEY H. N89-24329
N89-24873
HOFFMAN, D. J. N89-24521
HOFMANN, A. N89-24995
HOFMANN, J. N89-25045
HOGE, D. N89-24357
HOIT, MARC N89-24631
HOLCOMB, LEE N89-25111
HOLDERFIELD, D. C. N89-24848
HOLLAND, D. F. N89-24485
HOLMES, WILLARD M. N89-24855
HOLT, J. B. N89-25052
HOLTE, DONALD O. N89-24620
HONG, BYUNGSIK N89-25103
HONSBERG, CHRISTIANA N89-24726
HONVAULT, C. N89-24340
HOOD, A. W. N89-24992
HOOD, RAY N89-25111
HOPKINS, D. B. N89-24605
HOPKINS, H. D. N89-24374
HORNFELD, W. N89-24302
HORST, RICHARD L. N89-24797
HOSKER, RAYFORD P., JR. N89-24751
HOUCK, JACOB A. N89-24313
HOUDEVILLE, R. N89-24280
HOUSNER, JERROLD M. N89-24638
N89-24654
N89-24660
HOUZE, BERNARD N89-24373
HUBBARD, ROGER W. N89-24785
HUBER, DAN N89-24724
HUDGINS, DAVID A. N89-24497
HUDSON, TRACY D. N89-24905
HUERRE, P. N89-24540
N89-24542
HUGHES, R. C. N89-24533
HUGHES, RICHARD J. N89-25092
HULL, JOHN R. N89-24619
HULSTROM, R. L. N89-24743
HUNT, J. C. R. N89-24555
N89-24557
HUNT, J. J. N89-24910
N89-24974
HUNTER, WILLIAM F. N89-24626
HUR, N. N89-24568
HURD, A. J. N89-24501
HURLEY, K. N89-25084
HUSE, K. N89-24345
HUSSAIN, FAZLE N89-24539
N89-24543
N89-24544
N89-24559
N89-24560
HUSSON, N. N89-24690
N89-24778
HWANG, L. N89-24454
HWANG, WARREN C. N89-24734
HYODO, YUKIO N89-24432

I

IBANEZ, S. M. H. N89-24973
ILES, PETER A. N89-24729
N89-24730
ILKHAMOV, R. A. N89-24468
IOLIN, E. M. N89-25069
IRENE, E. A. N89-24495
N89-25062
ISAKEIT, DIETER N89-24398
ISERMANN, ULLRICH N89-24887
ISSAC, F. N89-24777
ISTOMIN, YA. N. N89-24941
ITOH, KIMITAKA N89-24908
ITOH, SANAE N89-24908
IVANOV, A. B. N89-24799
IZUMIKAWA, MUMEO N89-24432

J

JACKSON, M. E. N89-24847
JACOBS, LAURENCE J. N89-24633
JAFFE, D. T. N89-25082
N89-25086
N89-25106
JAHIER, J. PH. N89-24423
JANESCHITZ, G. N89-25043
N89-25045

N89-25046
JANG, B. N89-24454
JARDINE, M. N89-24982
JAREM, JOHN M. N89-24523
JARRELL, MARK N89-25071
JAUCH, UWE N89-24455
JEFFERIES, KENT S. N89-24438
JENKINS, J. T. N89-24583
JENKINS, JAMES N89-25111
JENSEN, ROBERT L. N89-25110
JIAO, K. N89-24713
JODOIN, VINCENT J. N89-24453
JOHANSSON, ARNE V. N89-24550
JOHANSSON, MARIE N89-24531
JOHNSON, LARRY R. N89-24619
JONES, E. N89-24434
JONES, GERALD ALAN N89-24874
JONES, WILLIAM R., JR. N89-24635
JONS, DAVID P. N89-24852
JORDAN, THOMAS H. N89-24757
JOUAN, J. Y. N89-24777
JUSTUS, C. G. N89-24755

K

KADER, JAC N89-24822
KAESDORF, S. N89-25042
KAHNIASHVILI, T. A. N89-24968
KAI, TAKASHI N89-24702
KAILEY, WALTER FRANKLIN N89-25087
KAJIWARA, KENICHI N89-24431
KALEPS, INTS N89-25074
KALINNIKOV, V. A. N89-24877
KAMINAR, N. R. N89-24733
KAMPAS, F. N89-24739
KAMPFER, GEORG N89-24362
KAMPWIRTH, R. T. N89-25056
KANDEL, ROBERT S. N89-24762
KANE, S. R. N89-24934
KANE, THOMAS J. N89-24601
KANG, J. H. N89-25056
KANTAK, ANIL V. N89-25073
KARAKI, S. N89-24744
KARLICKY, M. N89-25006
KARPEL, MORDECHAY N89-24308
KARR, THOMAS J. N89-24606
KATNIK, GREGORY N. N89-24412
KATZ, ERIC S. N89-24330
KATZ, J. I. N89-24946
KAUL, UPENDER K. N89-24579
KAYIRANGA, THEONESTE N89-24780
KAZBEGI, A. Z. N89-24952
N89-24953
KEAVNEY, CHRISTOPHER N89-24708
KEEFE, L. R. N89-24542
N89-24552
KEHR, JOACHIM N89-24376
KELLEY, JOSEPH E. N89-24263
KEMMEREIT, E. N89-25033
KEMP, D. L. N89-24590
KENNEL, C. F. N89-24931
N89-24936
N89-24937
N89-24971
KERGOMARD, CLAUDE N89-24691
KERNER, W. N89-24926
KERNS, KAROL N89-24292
KESLER, L. O. N89-24828
KEYDEL, WOLFGANG N89-24688
KEYSER, RALPH N89-25057
KHANDELWAL, G. S. N89-25104
KHANDOKER, SHAFIQUL ISLAM N89-24672
KHEMTHONG, SCOTT N89-24730
KHURI-YAKUB, B. T. N89-25054
KIEFLING, LARRY N89-24422
KILMER, LOUIS C. N89-24726
KIM, JOHN N89-24550
N89-24554
KIM, KYONG H. N89-24599
KIM, NAMSOO P. N89-24717
KIM, SEUNG JOO N89-24286
KING, WAYNE E. N89-24682
KINO, G. S. N89-25054
KINZEY, B. R. N89-24745
KIRCHNER, T. M. N89-25028
KIRKWOOD, SHEILA N89-24764
KIRSHNER, ROBERT P. N89-25079
KITAMURA, SHOJI N89-24431
KLARER, PAUL R. N89-24852
KLEIN, H. N89-25034
KLEIN, K. E. N89-24369
KLEIN, K.-L. N89-24934
KLIEM, B. N89-24994
N89-25005
KLONOSKI, KEVIN D. N89-24859
KLUGE, M. N89-25055
KMETYK, LUBOMYRA N. N89-24617
KNABE, F. N89-24301
KNIGHT, NORMAN F., JR. N89-24624
N89-24641
N89-24673
N89-24681
KNOEBEL, U. N89-24355
KOBEDA, E. N89-24495
N89-25062
KOIDE, SINJI N89-24909
KOMATSU, KEIJI N89-24702
KOOIJMAN, W. N89-25037
KOOPMANN, H. J. N89-24361
KORENEV, S. A. N89-24503
KORTEN, M. K. N89-25036
KOSEL, T. H. N89-24597
KOSS, D. A. N89-24475
KOSSACKI, K. N89-25020
KRASNOSELSKIKH, V. V. N89-24936
N89-24937
KREN, LAWRENCE A. N89-24451
KRENISKI, ALGEU N89-24880
KRIEG, R. D. N89-24616
KRIEGER, K. N89-25039
KRING, G. N89-24354
KRISHNASWAMY, S. N89-24621
KRITIKOS, G. N89-24697
KRUEGER, A. N89-24998
N89-25001
N89-25005
KRUIJT, O. G. N89-25032
KRUSER, DANA S. N89-24792
KUHLMAN, JOHN M. N89-24266
KULAGINA, T. N. N89-25067
KULIKOV, YU. V. N89-25068
KULIKOWSKI, CASIMIR A. N89-24858
KULSRUD, R. N89-24939
KUNUGI, TOMOAKI N89-24565
KURBATOV, V. S. N89-24879
KURLAND, RICHARD M. N89-24715
N89-24716
KURTHS, J. N89-25006
KURYLA, M. S. N89-24733
KUZNETSOVA, M. M. N89-24979
KYRIE, N. P. N89-25010

L

LACAZE, J. N89-24349
LADLE, M. J. N89-24733
LAFON, T. N89-24425
LAI, WILLIAM N89-24682
LAMBERT, KEVIN M. N89-24532
LAMBOURION, J. N89-24331
LAMOUREUX, M. N89-24907
LAND, KEN N89-24828
LANDAHL, MARTEN T. N89-24556
LANDINGHAM, R. L. N89-25052
LANDIS, GEOFFREY A. N89-24719
N89-24728
LANDRON, C. O. N89-24596
LANGLEY, LINDA J. N89-24843
LANZEROTTI, LOUIS J. N89-24406
LAPSHIN, V. I. N89-24927
LARROQUE, PIERRE N89-24388
LAUTZENHISER, TED N89-25091
LAVITOLA, M. S. N89-24399
LAW, C. K. N89-24566
LAW, P. H. N89-24519
LEAHY, MICHAEL B., JR. N89-24831
N89-24836
LEAL, MICHAEL ALLEN N89-24615
LEBEDEV, N. V. N89-25012
LEBOUAR, PH. N89-24386
LECKBAND, J. A. N89-24948
LECOINTE, Y. N89-24282
N89-24283
LEE, ALFRED T. N89-24798
LEE, B. N89-24713
LEE, HENRY N89-24435
LEE, J. K. N89-25065
LEE, J. R. N89-24596
LEE, JUN N89-24513
LEE, L. C. N89-25022
LEE, MOON J. N89-24551
N89-24557
N89-24561
LEE, SING H. N89-24332
LEE, Y. C. N89-24972
LEE, YIM N89-24907
LEEPER, R. J. N89-24596
LEHMACHER, GERALD N89-24428
LEHMANN, F. N89-24700
LEHRMAN, STEPHEN N89-25076
LELE, S. K. N89-24541
LEMBKE, JOHN R. N89-24592
LEMEN, JAMES R. N89-24590
LENSKOLD, R. N89-24739
LEONARD, A. N89-24572
LEONARD, A. D. N89-24558
LESHT, BARRY M. N89-24749
LESLIE, LYNN D. N89-24776
LEVASSEUR, LEONARD A. N89-24494
LEWY, S. N89-24331
LICHTENBERG, A. J. N89-24870
LICKFIELD, G. C. N89-24488
LIEBERMAN, M. A. N89-24870
LIENERT, T. N89-24621
LIKINS, P. W. N89-24667
LILLINGTON, D. R. N89-24721
N89-24731
LIND, ROBERT H. N89-24789
LINDEN, KURT N89-24724
LINFORD, G. A. N89-24590
LINGG, CYNTHIA L. N89-24452
LINKE, J. N89-24996
N89-24997
LIOU, MENG-SING N89-24288
LIPPMANN, R. N89-24298
LISTVINSKY, G. N89-24605
LIU, C. N89-24474
LIU, D. D. N89-24733
LOBZIN, V. V. N89-24936
LOCKER, J. I. N89-24842
LOEILLET, C. N89-24386
LOEWENTHAL, STUART H. N89-24635
LOGSDON, JOHN M., III N89-24406
LOISEAU, A. N89-24480
LOMADZE, R. D. N89-24960
LOMINADZE, J. G. N89-24931
N89-24932
N89-24950
N89-24951
LONGDON, NORMAN N89-24335
LONGHURST, F. N89-24368
LONGHURST, G. R. N89-24485
LORD, CARTER K. N89-24839
LORENCE, L. J., JR. N89-24596
LOTTS, C. G. N89-24624
LOUGE, M. Y. N89-24583
LUBIN, PHILIP N89-24906
LUBRINA, P. N89-24311
LUCOVSKY, G. N89-25062
LUGTEN, J. B. N89-25082
N89-25106
LUKASH, V. N. N89-24968
LUST, ROBERT V. N89-24632
LUTSKO, J. N89-25055
LYMAN, JOHN L. N89-24504
LYON, J. F. N89-25050

M

MA, DER-MING N89-24404
MACAVERO, E. N89-24385
MACDOWALL, RANDY D. N89-24535
MACEK, W. N89-25027
MACHABELI, G. Z. N89-24952
N89-24953
MACKALL, DALE A. N89-24327
MACKIN, CLIFFORD W. N89-24291
MACKIN, S. J. N89-24896
MACMILLAN, H. F. N89-24733
MACY, S. C. N89-24624
MACY, STEVEN C. N89-24673
MADAU, P. N89-24947
MAGGIN, BERNARD N89-25076
MAGGIO, ELIZABETH N89-24343
MAGNANI, P. G. N89-24389
MAHAFFEY, DAVID L. N89-24797
MAHALINGAM, S. N89-24558
MAIDEN, DENNIS N89-24510
MAJORS, P. D. N89-24586
MAKHAJDIK, D. N89-24468
MAKOWSKI, M. A. N89-24605
MAN, G. K. N89-24665
MANINTVELD, P. N89-25035
MANN, G. N89-25002
MANN, G. A. N89-24525
MANNING, R. A. N89-24630
MANOHARAN, L. C. N89-24901
MANOUCHEHRI, DAVOUD N89-24844
MANSOUR, N. N. N89-24544
MANUKJAN, K. A. N89-24968
MAPLE, M. B. N89-25052
MARBACH, HOWARD W., JR. N89-24613
MARCOUX, J. N89-24365
MARECHAL, L. N89-24357
MAREK, HENRY R. N89-24292

MARKOV, V. S. N89-25009
N89-25010
MARR, W. W. N89-24526
MARTENSEN, ANNA L. N89-24815
MARTIN, B. E. N89-24848
MARTINELLI, A.-P. N89-25046
MARTUKANITZ, R. P. N89-24478
MARVIN, DEAN C. N89-24734
MASCI, M. N89-24397
MASSAGLIA, S. N89-24958
MASTIN, GARY A. N89-24524
MASUYA, GORO N89-24317
MATAYA, M. C. N89-24483
MATLOCK, D. K. N89-24483
MATSUDA, SHINZABURO N89-24908
MATSUZAKI, RIICHI N89-25072
MAUNG, KHIN MAUNG N89-25103
MAUTE, P. N89-24423
MAX, C. E. N89-24916
N89-24984
N89-24985
MAYBEE, GEORGE W. N89-24793
N89-24795
MAYER-HASSELWANDER, H. A. N89-25107
MAZZUCA, F. N89-24339
MCCLEARY, SUSAN L. N89-24624
N89-24673
MCCLELLAND, ROBERT W. N89-24717
MCCOLLUM, J. R. N89-24488
MCCORMICK, G. K. N89-25040
MCCORMICK, K. N89-25041
MCCURDY, DAVID A. N89-24888
MCDOWELL, ROBIN S. N89-24604
MCFARLANE, R. A. N89-24602
MCGOVERN, DOUGLAS E. N89-24610
N89-24835
N89-24852
MCKEE, JAMES N89-24823
MCKELLAR, M. G. N89-24618
MCKEOWN, M. H. N89-24589
MCMECHAN, GEORGE A. N89-25091
MCMILLIN, L. N89-24758
MCNALLY, PATRICK J. N89-24853
MCNEELY, JAMES B. N89-24723
MCVAY, M. C. N89-24675
MCVEIGH, J. N89-24703
MEIER, D. L. N89-24722
MEISTER, C.-V. N89-24980
N89-24981
N89-25018
MELANDER, MOGENS V. N89-24559
MELEK, M. N89-25090
MELIKIDZE, G. I. N89-24952
N89-24953
MELKONIAN, G. N89-24370
MELOSH, R. J. N89-24655
MELVILLE, JOHN P. N89-25102
MENON, SURESH N89-24272
MERBOLD, U. N89-24400
N89-24403
MERKLE, K. L. N89-24498
MERRILL, WALTER C. N89-24856
MESSERSCHMID, E. N89-24400
N89-24402
MEUNIER, G. N89-24542
MIDDLETON, J. N89-24512
MIDLOCK, JOSEPH L. N89-24800
MILLER, DWIGHT P. N89-24610
MILLER, ERIC L. N89-24593
MILLER, J. F. N89-24526
MILLER, LEONARD SCOTT N89-24564
MILLER, MIKEL M. N89-24836
MILLER, RICHARD K. N89-24678
MILLER, W. N89-24434
MILLER, WILLIAM H. N89-24470
MILLIKEN, ROBERT LOWELL N89-24267
MILLS, MICHAEL W. N89-24715
MILONNI, PETER W. N89-24903
MILTON, E. J. N89-24696
MIMURA, FUJIO N89-24536
MINOR, C. D. N89-24842
MISHIN, V. M. N89-25016
MITANI, TOHRU N89-24432
MITCHELL, ART N89-24510
MITCHELL, J. BRIAN A. N89-24889
MITRA, SHYAMAL KUMAR N89-25088
MIWA, HITOSHI N89-24322
MIYASHITA, ATSUMI N89-24902
MIYAZAKI, KATSUHIRO N89-24431
MOIN, P. N89-24543
N89-24548
N89-24549
N89-24555
MOITRA, ANUTOSH N89-24581
MOLINO, JOHN A. N89-24843
MONTALTO, GIU. N89-24397
MONTEMERLO, MELVIN N89-25111
MONTOYA, EARL J. N89-24333
MOOK, DEAN T. N89-24277
MOON, YOUNG J. N89-24269
MOORE, STEVEN R. N89-24770
MORANDO, A. N89-24397
MORE, RICHARD M. N89-24890
MOREAU, J. P. N89-24777
MORGAN, T. D. N89-24842
N89-24848
MORRIS, J. W., JR. N89-24482
MORRIS, R. N. N89-25050
MOSER, R. D. N89-24541
N89-24543
N89-24547
N89-24548
N89-24549
MOTCH, C. N89-25084
MOURAD, P. D. N89-24547
MUELLER-BREITKREUTZ, W. N89-24396
MUELLER, E. R. N89-25043
MUELLER, JAMES L. N89-24784
MUELLER, K. L. N89-24391
MUKHOPADHYAY, VIVEK N89-24313
MULLER, BRADLEY M. N89-24770
MUNDAY, T. J. N89-24696
MUNDT, REINHARD N89-25085
MUNGAL, M. G. N89-24545
N89-24546
MUNSON, ROBERT C. N89-24797
MURATA, MASAAKI N89-24753
MURTHY, N. N. N89-24414
MUTHUVEL, S. N89-24901
MYERS, C. N89-24434
MYERS, D. R. N89-24743

N

NAEGELI, DAVID W. N89-24613
NAHRA, HENRY K. N89-24418
NAKAMURA, KINUYO N89-24801
NAKAZAWA, NAOHITO N89-24882
NAMKOONG, DAVID N89-24440
NAPOLITANO, LUIGI G. N89-24395
NARAYANA, K. T. N89-24807
NATESAN, K. N89-24473
NAUMANN, R. J. N89-24405
NEDELL, WILLIAM N89-24290
NEFF, WILLIAM D. N89-24751
NEGLEY, GERALD H. N89-24723
NELLIS, W. J. N89-25052
NELSON, RICHARD B. N89-24643
NEUHAEUSER, H. G. N89-24396
NEUHAUSER, J. N89-25041
N89-25042
NEUMANN, B. N89-24297
NEVILLE, R. A. N89-24701
NEWTON, J. N89-24703
NGUYEN, H. P. N89-24366
NICOLLIER, CLAUDE N89-24400
N89-24401
NIETO, MICHAEL MARTIN N89-25091
N89-25092
NIIOKA, TAKASHI N89-24432
NIJMAN, J. P. N89-25037
NIKHOGOSSIAN, A. G. N89-25004
NIKUTOWSKI, B. N89-24980
N89-25019
NISHIDA, MICHIO N89-24506
NISHIKAWA, K.-I. N89-24972
NISHITANI, TAKEO N89-24909
NOLL, THOMAS E. N89-24313
N89-24314
NOLTE, R. N89-25039
NOOR, AHMED K. N89-24626
N89-24647
N89-24653
NOUR-OMID, BAHRAM N89-24657
NOUSE, HIROYUKI N89-24537
NUHAIT, ABDULLAH OTHMAN N89-24326
NUNZIATO, J. W. N89-24472
NUTT, GERALD L. N89-24682

O

OBAMA, TOSHIO N89-24431
OBRIEN, J. E. N89-24577
OCHOA, OZDEN N89-24627
OCKELS, W. N89-24400
ODEN, J. T. N89-24651
ODOWD, J. N89-24703
OEGELMAN, HAKKI N89-25080
OELKER, G. N89-24399
OETTL, HERWIG N89-24688
OGURA, WAICHI N89-24881
OHARA, F. M. N89-24748
OHSAWA, YUKIHARU N89-24993
OLDENBORG, RICHARD C. N89-24504
OLDFIELD, M. L. G. N89-24279
OLSEN, LARRY C. N89-24724
OLSON, CHARLES E., JR. N89-24687
OLSON, SANDRA L. N89-24413
OLTHOF, H. N89-24348
ONEILL, MARK J. N89-24732
OOMENS, A. A. M. N89-25032
N89-25037
ORLANDI, DIEGO N89-24323
ORMISTON, ROBERT A. N89-24329
ORTIZ, MICHAEL N89-24657
OSETINSKII, G. M. N89-24468
OSHER, J. E. N89-24408
OSOSKOV, G. A. N89-24879
OSTERWALD, CARL N89-24736
OSWALD, R. S. N89-24703
OTAGURO, M. S. N89-24828
OTTO, A. N89-25014
OVERMAN, A. L. N89-24624
OVSYANNIKOV, V. P. N89-25068

P

PADEKEN, D. N89-24394
PADOVAN, JOE N89-24650
PAILHAS, G. N89-24274
PALMADESSO, P. J. N89-24972
PALME, ULF WALTER N89-24685
PALMER, R. N89-24434
PANDEY, DHIRENDRA K. N89-24772
PAPIRNYK, O. N89-24331
PAQUET, J. B. N89-24573
PARAT, K. K. N89-24714
PARK, J. H. N89-24473
PARK, K. C. N89-24666
PARK, MYEONG-GU N89-25095
PARKER, ROBERT L. N89-25091
PARTAIN, L. D. N89-24733
PATARAYA, A. D. N89-24959
N89-24966
PATARAYA, T. A. N89-24959
PATHAK, P. H. N89-24518
N89-24519
PATIN, J. F. N89-24429
N89-25083
PATTERSON, ROBERT W. N89-24316
PAULIARD, R. N89-24456
PAVLOV, G. G. N89-24962
PAYSON, J. SCOTT N89-24738
PAYSON, STEVEN S. N89-24325
PEACOCK, H. B. N89-24484
PEDERSEN, DEAN M. N89-24477
PEDERSEN, H. N89-25084
PEGORARO, F. N89-24963
PEKELSMA, NICHOLAS J. N89-24328
PELENC, L. N89-24442
PELLAT, R. N89-24964
PELLETIER, G. N89-24956
N89-24957
PELZL, J. N89-25048
PERRY, BOYD, III N89-24310
N89-24313
N89-24314
PERSICO, R. N89-24392
PETERS, DAVID A. N89-24329
PFIEFER, RICHARD N89-24868
PHAM, QUOC TRUNG N89-24799
PHILLIPS, EDWARD P. N89-24679
PHILLIPS, JAMES E. N89-24726
PHILLIPS, N. N89-24758
PIETRZYK, Z. A. N89-25040
PIFKO, A. B. N89-24658
PILYUGIN, N. N. N89-24929
PINSON, LARRY N89-24661
PIQUET, J. N89-24282
N89-24283
PISZCZOR, MICHAEL F., JR. N89-24732
PITTERMANN, FRANZ N89-24388
PLANES, J. N89-24480
PLICHTA, M. R. N89-25065
POEDTS, S. N89-24925
N89-24926
POGLITSCH, A. N89-25081
N89-25082
POLITES, MICHAEL E. N89-24507
POLLARD, WILLIAM J. N89-24851
POLLOCK, A. M. T. N89-25029
POMPILIO, DOUGLAS G. N89-24805
POOLE, E. L. N89-24624
POPIELAWSKA, B. N89-25020
POSCHENRIEDER, W. N89-25042

POTOTZKY, ANTHONY S. N89-24310
N89-24313
POWELL, KENNETH G. N89-24872
PREISS, H. N89-24354
PRIEST, E. R. N89-24924
N89-24938
N89-24982
N89-24987
PROKOSCH, STEVEN R. N89-24840
PUDOVKIN, M. I. N89-25024
PUNSLY, BRIAN MATHEW N89-25096
PURSEL, ROBERT H. N89-24291
PUSTILNIK, L. A. N89-25007

R

RABINOWITZ, PAUL H. N89-24862
RADEMACHER, PAUL N89-24827
RAHIER, G. N89-24331
RAMAPRIAN, B. R. N89-24546
RAN, L. B. N89-25045
RANSOM, JONATHAN B. N89-24681
RASMUSSEN, M. L. N89-24315
RAST, M. N89-24693
RAWLIN, VINCENT K. N89-24436
RAY, SCOTT L. N89-24522
RAY, T. L. N89-24614
REDDY, J. N. N89-24645
REDDY, UDAY S. N89-24802
REDEKOPP, L. G. N89-24542
REINHOLD, CHRISTIAN N89-24372
REMANDET, J.-N. N89-24331
REMY, DAVID N89-24494
RENARD, J. N89-24458
RENO, MARGARET MARY N89-24441
RENOUD, ROBERT W. N89-24273
RESHOTKO, E. N89-24577
REVAH, ISAAC N89-24344
REYNOLDS, W. C. N89-24545
N89-24546
RHEINGOLD, ARNOLD L. N89-24493
RHOADES, DON N89-24826
RHOADS, SANDRA L. N89-24712
N89-24723
RICHARDS, JOHN F. N89-24748
RICKS, G. A. N89-24594
RIEDESEL, J. N89-24434
RIEKER, LORRA L. N89-24439
RIJNBEEK, R. P. N89-24983
N89-25026
RILEY, BETSY A. N89-24812
RILEY, J. J. N89-24547
RILEY, JAMES T. N89-24288
RIORDAN, C. J. N89-24743
RITTER, B. N89-24479
RIVERS, M. L. N89-25101
ROBERTS, D. W. N89-24287
ROBERTSON, ROBERT M. N89-24892
RODERICK, MICHAEL J. N89-24528
RODRIGUEZ, RAUL D. N89-24476
ROEHR, H. N89-25039
N89-25043
ROFER, CHERYL K. N89-24504
ROGALLO, R. S. N89-24553
ROGAVA, A. D. N89-24951
ROGERS, M. M. N89-24541
N89-24542
N89-24543
N89-24547
ROLAND, J. N89-24957
ROLLIN, E. M. N89-24696
ROMANOV, S. A. N89-25020
ROME, J. A. N89-25050
ROSE, K. N89-24300
ROSHKO, A. N89-24572
ROSSI, MICHAEL J. N89-24892
ROTE, DONALD M. N89-24619
ROTH, J. N89-25045
N89-25047
ROUDOLFF, F. N89-24458
ROUSE, D. J. N89-25076
ROUSSEAU, A. L. N89-24530
ROWE, D. M. N89-24491
RUIN, Y. N89-24761
RUM, GIOVANNI N89-24377
N89-24380
RUSCHEWEYH, H. P. N89-24278
RUSHBY, JOHN N89-24803
N89-24811
RUTH, R. D. N89-24878
RYAN, P. M. N89-24521
RYUTOVA, M. P. N89-24921

S

SAKAI, JUN-ICHI N89-24920
N89-24993
SALAUN, M. N89-24275
N89-24574
SALTER, CAROLE A. N89-24608
SAMUELS, W. D. N89-24489
SANBONGI, SHIGEO N89-24702
SANDHAM, N. D. N89-24545
N89-24546
SANDLIN, DORAL R. N89-24265
SANO, MASAAKI N89-24702
SARKANEN, ANNAKAISA N89-24769
SASAKI, SHINOBU N89-24857
N89-24866
SAUNDERS, NEAL T. N89-24320
SAVIN, S. P. N89-25020
SCHAEFER, R. N89-24354
SCHEMPP, A. N89-25034
SCHENK, H.-D. N89-24305
SCHILLING, C. H. N89-24489
SCHINDLER, K. N89-24975
N89-25013
N89-25021
SCHIRRA, M. N89-24479
SCHMIDT, H. P. N89-24394
SCHMIDT, K. N89-24358
SCHMIDT, R. N89-24913
SCHMIT, F. N89-24456
SCHMIT, L. A. N89-24630
SCHNEIDER, W. N89-25041
SCHOENEMANN, KARLHEINZ N89-24383
SCHOENFELDER, VOLKER N89-24407
SCHREIBER, JEFFREY G. N89-25078
SCHRIVER, D. N89-25017
SCHROEDER, M. N89-24697
SCHROER, BERNARD J. N89-24849
SCHUERMANNS, H. N89-24367
SCHULKE, DUANE A. N89-24316
SCHULZ, P. N89-24307
SCHWALLER, MATHEW R. N89-24687
SCHWARTZ, JEFFREY N89-24464
SCHWARZ, R. B. N89-24481
SCHWIND, H.-D. N89-24303
SCOTT, N. A. N89-24778
SCOTT, NOELLE A. N89-24691
SEAMAN, C. L. N89-25052
SEEHAFER, N. N89-24989
SEGALL, ZARY Z. N89-24817
SEIBERT, GUENTHER N89-24347
SEIFFERT, MICHAEL N89-24906
SEMENOV, V. S. N89-25024
N89-25025
N89-25026
SEN, R. K. N89-24745
SERROR, S. N89-24457
SESMA, A. N89-24356
SEVERNS, J. G. N89-24735
SEXTON, GEORGE A. N89-24316
SHAING, K. C. N89-25049
SHANKAR, P. N. N89-24462
SHANNON, JACK D. N89-24749
SHAO, L. N89-24509
SHARIFF, K. N89-24560
SHARP, D. J. N89-24525
SHASHARINA, S. G. N89-25011
SHEA, JOSEPH F. N89-24406
SHEMA, RICHARD A. N89-24759
SHEN, C. C. N89-24710
SHEPHERD, I. G. N89-24566
SHERIDAN, THOMAS B. N89-24792
SHIMIZU, KATSUHIRO N89-24909
SHINGLEDECKER, CLARK N89-24292
SHUEN, JIAN-SHUEN N89-24444
SHVARTSMAN, V. F. N89-25007
SIBENER, S. J. N89-25059
SIEWIOREK, DANIEL P. N89-24817
SIMILON, P. L. N89-24919
SIMITSES, G. J. N89-24669
SIMONETT, DAVID S. N89-24686
SIMONS, STEPHEN N. N89-24427
SIMONSEN, R. L. N89-25084
SIMPSON, G. N89-25107
SINGH, A. N89-24713
SINGH, R. P. N89-24667
SLACHMUYLDERS, E. N89-24350
SLATER, G. L. N89-24590
SLINEY, HAROLD E. N89-24635
N89-24636
SMALLWOOD, DAVID O. N89-24884
SMAOUI, HICHEM N89-24680
SMEETS, P. H. M. N89-25037
SMITH, I. A. N89-24946
SMITH, J. M. N89-24443
SMITH, M. D. N89-24935
SMITH, PAUL N89-25111
SMITH, STEPHEN C. N89-24285
SMITH, STEVEN D. N89-24771
SMITH, W. T. N89-24511
SNOW, W. M. N89-24587
SOBIESZCZANSKI-SOBIESKI, JAROSLAW N89-24508
SOEIRO, ALFREDO N89-24631
SOELDNER, F. X. N89-25043
SOHN, K. H. N89-24577
SOKOL, P. E. N89-24587
SOKOLOSKI, MARTIN N89-25111
SOL, H. N89-24956
N89-24957
SOLAL, F. N89-24480
SOLOMON, JAY M. N89-24585
SOMORJAI, G. A. N89-24490
SOOSAAR, KETO N89-24661
SPALART, P. R. N89-24542
SPANGLER, S. R. N89-24933
N89-24948
SPEARING, S. F. N89-24845
SPEZIALE, C. G. N89-24568
SPEZIALE, VICTOR N89-24379
SPIRES, SHANNON V. N89-24835
SPITZER, MARK B. N89-24708
SPRENGEL, R. N89-24297
SRINATHKUMAR, S. N89-24313
STACEY, G. J. N89-25081
N89-25082
N89-25106
STALIO, R. N89-24382
STALLARD, B. W. N89-24605
STANAWAY, S. N89-24560
STANBERY, BILLY J. N89-24717
N89-24718
STANLEY, G. M. N89-24642
STARIKOV, A. YU. N89-25068
START, G. EUGENE N89-24751
STAUDE, J. N89-24995
STAUDENMAIER, G. N89-25044
N89-25047
STAUFFER, DAVID SAMUEL N89-24829
STEELE, D. N89-24434
STELLA, PAUL N89-24716
STELLAR, FREDERICK W. N89-24309
STEPANOV, K. N. N89-24927
STERK, A. B. N89-25032
STERZIK, MICHAEL N89-25063
STEUER, K. H. N89-25043
STEUER, K.-H. N89-25039
STEVENSON, CHARLES G. N89-24412
STEVER, H. GUYFORD N89-24406
STOCKHAUSEN, R. J. N89-25060
STOFAN, ANDREW J. N89-24417
STOFFEL, T. L. N89-24743
STONE, C. M. N89-24616
STONUM, RONALD K. N89-24285
STORMS, BRUCE LOWELL N89-24569
STREIT, GERALD E. N89-24504
STREMEL, PAUL M. N89-24563
STROKIN, N. A. N89-25012
STRONG, KEITH T. N89-24590
STROUD, W. JEFFERSON N89-24638
N89-24641
N89-24654
STRUB, H. N89-24337
STUTZKI, JUERGEN N89-25082
N89-25086
N89-25094
N89-25106
STUTZMAN, W. L. N89-24511
SUDAN, R. N. N89-24919
SUGIYAMA, TAKASHI N89-24909
SULLIVAN, TIMOTHY J. N89-24741
SUMMERS, T. N89-24482
SUNDER, D. N89-25011
SUSSKIND, J. N89-24758
SUTTON, S. R. N89-25101
SWANSON, NEIL J., JR. N89-24265
SWARTZ, CLIFFORD K. N89-24707
N89-24711
SWERN, FREDERIC L. N89-24837
SWIFT, PATRICK M. N89-24628
SYGNET, J. F. N89-24964
SZABO, BARNA A. N89-24648
SZEDON, J. R. N89-24722
SZLYK, PATRICK C. N89-24785
SZYMCZAK, WILLIAM G. N89-24585

T

TABADDOR, FARHAD N89-24649
TABATABAI, HABIBOLLAH N89-24675
TAGGER, M. N89-24964

TAGLAUER, E. N89-25045
N89-25046
TAHANI, Y. N89-24778
TAKAHASHI, MAMORU N89-24432
TAKIZUKA, TOMONORI N89-24908
TAKTAKISHVILI, A. L. N89-24966
N89-25015
TALOTTA, NICHOLAS J. N89-24292
TAMMARU, I. N89-24530
TAMMELIN, BENGT N89-24767
TANIGUCHI, HIROFUMI N89-24432
TANNER, JOHN A. N89-24638
N89-24653
N89-24654
TANVEER, SALEH N89-24883
TARANTIN, N. I. N89-24885
TAYLOR, DEBORAH B. N89-24772
TAYLOR, ROBERT L. N89-24684
TEDEMAN, L. N89-24364
TEOH, WILLIAM N89-24854
TERRANOVA, NANCY E. N89-24723
TESTA, FRANK N89-24833
THACHER, E. F. N89-24742
THACKRAY, RICHARD I. N89-24294
THANGAM, S. N89-24568
THESLING, WILLIAM N89-24711
THEVENOT, D. N89-24353
THIAO, WASSILA N89-24782
THOMAE, R. W. N89-25034
THOMAS, LAWRENCE DALE N89-24421
THORNTON, WILLIAM E. N89-24790
THROOP, A. L. N89-24605
THURSTON, GAYLEN A. N89-24867
TIAINEN, T. J. N89-24481
TIARN, WEIHNURNG DAVIS N89-24875
TIELEMANS, A. J. H. N89-25037
TIELKING, JOHN T. N89-24652
TIFFANY, SHERWOOD H. N89-24308
N89-24313
TILGNER, CLEMENS N89-24760
TILLEY, T. D. N89-24493
TOBIN, S. P. N89-24721
N89-24731
TODA, SUSUMU N89-24702
TOMITA, KENJI N89-25105
TORRES, EDGARDO I. N89-24571
TOUCHSTONE, R. M. N89-24294
TOWNES, C. H. N89-25081
TOWNSEND, DENNIS P. N89-24635
TOWNSEND, F. C. N89-24675
TOWSLEY, R. H. N89-24735
TRACHTMAN, LAWRENCE N89-25076
TRAN, VU M. N89-24628
TRAYLOR, D. J. N89-24521
TREE, DAVID R. N89-24618
TREES, CHARLES C. N89-24784
TREUMANN, R. A. N89-24923
TRIBULA, D. N89-24482
TRICAMO, STEPHEN J. N89-24837
TROTTET, G. N89-24934
TROUDET, TERRY N89-24856
TROUSSE, B. N89-24810
TRUMAN, C. RANDALL N89-24561
TRUSSONI, E. N89-24958
TSAO, NAI-KUAN N89-24865
TSENG, FAN T. N89-24849
TSIHLAS, N. N89-24573
TSOIS, N. N89-25041
TSUCHIYA, MASAKO N89-24814
TSYTOVICH, V. N. N89-24944
TU, SHAN-CHENG N89-24342
TUCKERMAN, DAVIS B. N89-24534
TUNE, MUMTAZ N89-24806
TURK, M. N89-24391
TURRENTINE, GEORGE A. N89-24786
TYNER, CRAIG E. N89-24461

U

ULEN, ESKIL N89-24740
URBANUS, W. H. N89-25034
USOV, V. V. N89-24929
N89-24949
N89-24952

V

VALLERANI, ERNESTO N89-24343
VANAMERSFOORT, P. W. N89-25031
N89-25034
VANBLOKLAND, A. A. E. N89-25033
N89-25036
VANDERPIEPEN, H. N89-24697
VANDERVEN, H. W. N89-25033
N89-25036
VANDERWIEL, M. J. N89-25031
VANDERZIJP, JEROEN N89-24850
VANDIJK, G. N89-25032
VANLEER, BRAM N89-24872
VANNARONI, G. N89-24382
VANOMMERING, GERT N89-24427
VANOVERBEKE, THOMAS J. N89-24444
VANREETH, G. N89-24341
VANWIRT, PETER M. N89-24831
VASYLIUNAS, V. M. N89-24914
N89-24976
VASZARI, J. P. N89-24530
VAUNOIS, J. P. N89-24351
VEKSTEIN, G. E. N89-24990
VELLI, M. N89-24992
VERBEEK, H. N89-25043
VERHOEVEN, A. G. A. N89-25035
VERMANDE, P. N89-24699
VERNON, S. M. N89-24721
VERNON, STANLEY M. N89-24708
VERRILLI, MICHAEL J. N89-24460
VIKHREV, V. V. N89-25004
VIRIGLIO, GIUSEPPE N89-24377
VIRSHUP, G. F. N89-24733
N89-24735
VISWANATH, A. K. N89-24604
VISWANATHAN, A. V. N89-24640
VITEK, J. M. N89-24478
VOLZ, R. A. N89-24509
VONHENKE, FRIEDER N89-24803

W

WAGGENER, MARY S. N89-24833
WAKAMATSU, YOSHIO N89-24317
WALDINGER, RICHARD J. N89-24860
WALKER, CHRISTOPHER KIDD N89-25097
WALKER, M. W. N89-24509
WALLACE, RICHARD W. N89-24601
WALLACE, ROBERT N89-25076
WALLS, J. T. N89-24847
WALSH, R. N89-24434
WALSH, W. J. N89-24526
WALTER, LEE N89-24720
WAMPLER, W. R. N89-25044
WANG, K. Y. N89-24469
WANG, WEN-MIN N89-25047
WANG, XUELIANG N89-24774
WANG, YONG N89-24686
WANLASS, M. W. N89-24709
WARD, K. J. N89-24501
WARK, D. N89-24758
WARMBRODT, WILLIAM G. N89-24329
WARNOCK, R. L. N89-24878
WARTENBERG, H. N89-24361
WATANABE, YASUO N89-24506
N89-24598
WATTS, EDWARD N89-24829
WEATHERBY, J. R. N89-24616
WEAVER, H. T. N89-24533
WEDDE-MUEHLHAUSEN, K. N89-24358
WEI, JING-FONG N89-24471
WEINBERG, IRVING N89-24707
N89-24711
WEINGART, R. C. N89-24408
WEIS, T. N89-25034
WEISS, SHOLOM M. N89-24858
WEISSHAAR, TERRENCE A. N89-24324
WERTHEN, J. G. N89-24733
WESSELS, H. N89-24368
WESTMACOTT, K. H. N89-25070
WHEADON, J. N89-24378
WHITE, W. F. N89-24293
WHITEHURST, R. ALAN N89-24811
WHITEMAN, C. DAVID N89-24751
WHITNEY, DONALD A. N89-24599
WILKINS, DAVID E. B. N89-24371
WILKINS, MARK N89-24510
WILLHOITE, BRYAN C. N89-24427
WILLIAMS, CLAUDE N., JR. N89-24776
WILLIAMS, DEBORAH C. N89-24316
WILLIAMS, STEVEN L. N89-24270
WILSON, JOHN W. N89-25103
N89-25104
WILT, DAVID M. N89-24728
WINFIELD, DANIEL N89-25076
WINSLOW, CINDY N89-24448
WINTER, R. N89-24658
WINTER, T. G. N89-24891
WISE, JAMES L. N89-24776
WISE, JOSEPH N89-24706
WISE, M. B. N89-24465
WITTMANN, K. N89-24394
WOJCZAK, M. N89-25048
WOJKE, R. G. C. N89-25034
WOLF, D. N89-25055
WOLFSBERGER, JOHN W. N89-24826
N89-24849
WOODS, JESSICA A. N89-24310
N89-24324
WOODS, T. O. N89-24484
WOODYARD, JAMES R. N89-24738
WRAY, A. A. N89-24555
WRIGHT, ERIC J. N89-24775
WU, K. CHAUNCEY N89-24676
WUEBBLES, DONALD J. N89-24750
WUNDERLICH, R. N89-25041

X

XU, Y. J. N89-25104

Y

YAMAMOTO, ATSUMASA N89-24536
N89-24537
YAMAMOTO, SHIN N89-24908
YANG, H. R. N89-25045
YARRINGTON, PAUL N89-24617
YATES, H. N89-24758
YAWN, LARRY N89-24822
YEH, MILTON N89-24729
YELISEYEV, S. V. N89-24261
YIN, DAH N. N89-24628
YODA, OSAMU N89-24902
YOSHIDA, MASAHIRO N89-24801
YOSHIMURA, H. R. N89-24683
YOUDALE, J. N89-24424
YOUNG, STEVEN C. N89-24747
YUGO, J. J. N89-24521

Z

ZACHARIA, T. N89-24478
ZACHARY, A. L. N89-24916
ZAITSEV, V. V. N89-24991
N89-25001
ZARETSKY, ERWIN V. N89-24635
ZEALEY, WILLIAM J. N89-25085
ZEE, R. N89-24454
ZELENYI, L. M. N89-24942
N89-24943
N89-24978
N89-24979
N89-25015
ZHANG, S. X. N89-24849
ZHERNOV, A. P. N89-25067
ZIEMKE, M. CARL N89-24822
ZIESMANN, W. N89-24367
ZILIANI, M. N89-24442
ZIMBARDO, G. N89-24918
ZIMMERMANN, HANS-ULRICH N89-25080
ZINNECKER, HANS N89-25085
ZIPPERIAN, T. E. N89-24533
ZOGIN, D. V. N89-24943
ZOHAR, Y. N89-24541
ZRNIC, DUSAN S. N89-24515
ZUMBERGE, MARK A. N89-25091
ZURAWSKI, ROBERT L. N89-24409
ZURINSKAS, THOMAS N89-24292
ZWEIG, GEORGE N89-24516
ZWINGMANN, W. N89-24986
ZYZYS, EDMUND N89-24291

Typical Corporate Source Index Listing

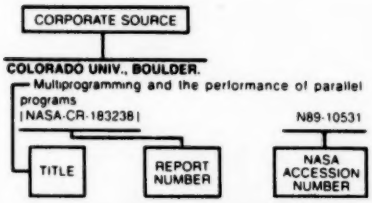

Listings in this index are arranged alphabetically by corporate source. The title of the document provides the user with a brief description of the subject matter. The report number helps to indicate the type of document cited (e.g., NASA report, translation, NASA contractor report). The NASA accession number denotes the number by which the citation is identified. The titles are arranged under each corporate source in ascending accession number order.

A

ABASTUMANI ASTROPHYSICAL OBSERVATORY, GEORGIA (USSR).
The structure of quasiperpendicular collisionless shocks N89-24932
Small-scale instabilities in accretion disks of compact objects and their manifestations N89-24950
Problem of nonrotating black hole accretion disk main energy release region extension N89-24951
On the nature of a typical pulsars radio emission N89-24952
On the mechanism of the formation of the polarization characteristics of pulsar radiation N89-24953
Pulsar radio and visible radiation due to the modulation instability of high-frequence transverse waves in the inhomogeneous electron-positron plasma N89-24959
Decay process and radiative transfer in plasmas N89-24960
Model of the chromosphere spicule formation N89-24966
The formation of the spectrum of inhomogeneity of the dark matter in pregalactic cosmic plasma N89-24968
Inductive acceleration of protons and electrons in planetary magnetotails N89-25015

ACADEMIA SINICA, BEIJING (CHINA).
A 2-D and 3-D simulation study of multiple X line reconnection N89-25023

ACADEMY OF SCIENCES, GRAZ (AUSTRIA).
Magnetic reconnection near a stagnation point N89-24983
The structure of the reconnection layer in the Petschek reconnection model: Theory and application to the earth's magnetopause N89-25026

ACADEMY OF SCIENCES, POTSDAM (GERMAN D.R.).
Adiabatic, chaotic and quasi-adiabatic charged particle motion in two-dimensional magnetic field reversals N89-24942
Reconnection instability in collisionless plasma N89-24978
Reconnection and microturbulence N89-24980
Anomalous collision frequency of magnetoactive plasmas with two-dimensional electrostatic turbulence (kB=O) N89-24981
Generation and non-equilibrium of solar atmospheric magnetic fields N89-24989
Dynamic development of coronal current sheets N89-24994
Possibilities and problems of the interpretation of solar magnetograph measurements and applications to flare-active regions N89-24995
Estimation of sunspot magnetic field parameters using the superpenumbral topology N89-24996
Note on an apparent highly-sheared magnetic field structure N89-24997
Diagnostics of energy release and magnetic fields on the sun by radio methods N89-24998
Tremsdorf solar radio astronomy observatory: The scientific program and an interesting observation N89-24999
Time scales of solar microwave bursts and scenarios of flare energy release N89-25005
Electromagnetic electron temperature anisotropy instability in the earth's magnetotail plasma sheet N89-25019
On particle energization by magnetic field line reconnection in extragalactic jets N89-25028

ACADEMY OF SCIENCES OF THE GEORGIAN SSR, TBILISI.
Drift turbulence of plasma as a gas of vortex ensemble N89-24961

ACADEMY OF SCIENCES OF THE LITHUANIAN SSR, VILNIUS.
Multiphoton transitions at the Moessbauer radiation diffraction in crystals under a weak ultrasonic field [DE88-706341] N89-25069

ACADEMY OF SCIENCES OF THE UKRAINIAN SSR, KIEV.
Singularities of the local MHD-resonances in solar chromosphere plasma N89-24927

ACADEMY OF SCIENCES (USSR), GORKY.
A neutral current sheet with flows: Tearing and stratification modes and modeling of coronal structures N89-24991
The precursors of the 9 July 1982 solar proton flare event N89-25001

ACADEMY OF SCIENCES (USSR), IRKUTSK.
Spontaneous and forged reconnection in a magnetic type-X structure N89-25012
An analogy between magnetospheric substorms and solar flares: New version N89-25016

ACADEMY OF SCIENCES (USSR), LENINGRAD.
Quantum relativistic theory of the cyclotron radiation in a strongly magnetized plasma with anisotropic temperature N89-24962

ACADEMY OF SCIENCES (USSR), MOSCOW.
Generation of X-ray and radio emission by binary Wolf-Rayet stars N89-24929
The role of whistler oscillations in the formation of the structure of high Mach number collisionless shock N89-24936
Quasi-perpendicular collisionless high Mach number shocks N89-24937
Theory of radioemission of pulsars N89-24941
Quasi-adiabatic particle acceleration in magnetic field reversals and the formation of the plasma sheet boundary layer in the earth's magnetotail N89-24943
Radiative-resonant MHD interactions between waves and particles and the problem of cosmic-ray spectra N89-24944
Two-stream instability in pulsar magnetospheres N89-24949
Generation of large-scale vortices in compressible helical turbulence N89-24969
Nonlinear dynamics of the drift tearing-mode N89-24979
Flare-type plasma processes and explosive disruption of pinch current sheets N89-25008
Current sheet structure at different stages of magnetic reconnection N89-25009
Impulsive heating plasma turbulence and magnetic reconnection inside current sheets N89-25010
The evolution of MHD-perturbations in the intersection region of two separatrix planes N89-25011
The role of cold electrons in the generation of the high-frequency part of broadband electrostatic noise N89-25018

ACUREX CORP., HUNTSVILLE, AL.
Materials compatibility with oxidizer-rich gases at elevated temperatures and pressure [NASA-CR-183647] N89-24466

ADVANCED CONTROL TECHNOLOGY, INC., NASHVILLE, TN.
A new approach to robot kinematic analysis N89-24833

ADVANCED RESOURCE DEVELOPMENT CORP., COLUMBIA, MD.
Brain-wave measures of workload in advanced cockpits: The transition of technology from laboratory to cockpit simulator, phase 2 [NASA-CR-4240] N89-24797

AERITALIA S.P.A., TURIN (ITALY).
Pressurized module element for man's presence in space N89-24343
Logistics aspects of Columbus servicing at the Space Station N89-24363
Attached Pressurized Module (APM) center for the Columbus attached pressurized module N89-24377
The utilization of the European pressurized module for non-European experiments N89-24399

AEROSPACE CORP., LOS ANGELES, CA.
Contamination effects of GPS Navstar solar array performance N89-24734

AEROSPATIALE, CANNES LA BOCCA (FRANCE).
Hermes escape system N89-24366
Autonomous geostationary stationkeeping system optimization and validation [REPT-882-440-117] N89-24423
State of the art of ISO [REPT-882-440-121] N89-24424
Fluidnet: A thermal and hydraulic software for the preliminary sizing of fluid loop systems [REPT-882-440-124] N89-24425
ISOCAM, ISO optical subsystem cryogenics, Aerospatiale, Cannes, France in-house R and D status [REPT-882-440-123] N89-24429
Space photovoltaic technique. State of the art, trends [REPT-882-440-120] N89-24442
Study on cost efficiency of product assurance in space programs [REPT-882-440-122] N89-24622
The advanced Ocean Chlorophyll Meter (OCM). A spectral imaging device for the observation of the oceans [REPT-882-440-118] N89-24689
XCAD: A CAD object-oriented virtual solid modeler for an expert system shell [REPT-882-440-125] N89-24810
Materials for cryogenically cooled infrared telescopes [REPT-882-440-119] N89-25083

AEROSPATIALE, LES MUREAUX (FRANCE).
Overview of Ariane 5 and Hermes programs technology N89-24349
Servicing of the MTFF by Hermes N89-24360

AEROSPATIALE, TOULOUSE (FRANCE).
Lessons learned from SL-1 and D-1 N89-24400

AIR FORCE AERO PROPULSION LAB., WRIGHT-PATTERSON AFB, OH.
Space power technology 21: Photovoltaics N89-24706

AIR FORCE INST. OF TECH., WRIGHT-PATTERSON AFB, OH.
Use of Navier-Stokes methods to predict circulation control airfoil performance [AD-A206242] N89-24270
Water tunnel investigation of the vortex dynamics of periodically pitched wings [AD-A206359] N89-24271
Flight control system for the CRCA (Control Reconfigurable Combat Aircraft) using a command generator tracker with PI (Plus Integral) feedback and Kalman filter, volume 2 [AD-A206202] N89-24325
Characterization of delamination in advanced composite materials under mode 3 loading conditions [AD-A206159] N89-24452
Response of layered structures to thermal radiation pulses [AD-A206355] N89-24453
Experimentation and analysis of compression test methods for single filament high performance fibres [AD-A206358] N89-24467
Hardware modeling with VHDL (VHSIC Hardware Description Language) simulation [AD-A206356] N89-24805
Development of a hybrid simulator for robotic manipulators N89-24831

Robotic visual servo control for aircraft ground refueling N89-24836
Fractional-order feedback in linear systems [AD-A206241] N89-24859
Comparison of basis function and iteration solutions to the Fredholm integral equation of the first kind [AD-A206158] N89-24869
Selective pair luminescence of magnesium in gallium arsenide dissertation [AD-A206160] N89-25058

AIR FORCE SYSTEMS COMMAND, WRIGHT-PATTERSON AFB, OH.
Technology of aircraft construction (selected chapters) [AD-A199946] N89-24261

AKRON UNIV., OH.
Nonlinear hierarchical substructural parallelism and computer architecture N89-24650

ALABAMA UNIV., HUNTSVILLE.
Auger and ESCA analysis [NASA-CR-183572] N89-24463
Contamination effects study [NASA-CR-183613] N89-24746
High level intelligent control of telerobotics systems N89-24823
Neutral file data exchange between simulators and robots N89-24824
Cooperating expert systems N89-24825
Space languages: Solving the classic scheduling problem in Ada and Lisp N89-24826
Development of an integrated CAD/CAM system for wire harness fabrication N89-24842
A 3-D graphical simulation of an automated direct chip probe/test system N89-24848
Using a simulation assistant in modeling manufacturing systems N89-24849
Algorithm for display of automated nondestructive thickness measurements N89-24850

ALASKA UNIV., FAIRBANKS.
Multiple X line reconnection at the dayside magnetopause N89-25022

ALLIED-SIGNAL AEROSPACE CO., KANSAS CITY, MO.
Piezoelectric film load cell robot collision detector [DE89-010117] N89-24592

AMTEC ENGINEERING, INC., BELLEVUE, WA.
A zonal method for modeling powered-lift aircraft flow fields [NASA-CR-177521] N89-24287

ANALEX CORP., CLEVELAND, OH.
Computed performance of the half-scale accurate antenna reflector [NASA-CR-182284] N89-24532

APPLIED SOLAR ENERGY CORP., CITY OF INDUSTRY, CA.
Status of GaAs solar cell production N89-24729
Flexibility in space solar cell production N89-24730

ARGONNE NATIONAL LAB., IL.
Role of alloying additions in the oxidation-sulfidation of Fe-base alloys [DE89-009825] N89-24473
Magneto-optical studies of metastable 3D-transition metal films [DE89-009836] N89-24474
High-resolution electron microscopy of metal/ceramic interfaces [DE89-012396] N89-24498
Analysis of life cycle costs for electric vans with advanced battery systems [DE89-009807] N89-24526
Inelastic scattering from liquid He4 in aerogel glass [DE89-012381] N89-24587
Continuous cryopump with a method for removal of solidified gases [DE89-009760] N89-24611
Maglev vehicles and superconductor technology: Integration of high-speed ground transportation into the air travel system [DE89-012241] N89-24619
The relationship between in-lake sulfate concentration and estimates of atmospheric sulfur deposition for subregions of the eastern lake survey [DE89-009868] N89-24749
Attaching IBM-compatible 3380 disks to Cray X-MP [DE89-012383] N89-24800
Correlation between the structure, energy, and local elastic properties of grain boundaries in metals [DE89-009861] N89-25055
Superconducting properties of magnetron sputtered Bi-Sr-Ca-Cu-O and Tl-Ba-Ca-Cu-O thin films [DE89-009878] N89-25056

ARIZONA STATE UNIV., TEMPE.
N/P InP homojunction solar cells with an In0.53Ga0.47As contacting layer grown by liquid phase epitaxy N89-24710

ARIZONA UNIV., TUCSON.
Laboratory for X-ray optics [AD-A206468] N89-25061
Grain boundary phase equilibria in metallic systems [DE89-011787] N89-25066
Infrared studies of active galaxies N89-25087
An observational study of the dynamics of molecular cloud cores N89-25097

ARMY AVIATION ENGINEERING FLIGHT ACTIVITY, EDWARDS AFB, CA.
Preliminary airworthiness evaluation of modified second-generation Pneumatic Boot Deicing System on a JUH-1H [AD-A206255] N89-24289
Loss of tail rotor effectiveness evaluation of the OH-58C helicopter with directional SAS (Stability Augmentation System) [AD-A206181] N89-24309

ARMY AVIATION SYSTEMS COMMAND, MOFFETT FIELD, CA.
Survey of Army/NASA rotorcraft aeroelastic stability research [NASA-TM-101026] N89-24329

ARMY MISSILE COMMAND, REDSTONE ARSENAL, AL.
Development of an integrated CAD/CAM system for wire harness fabrication N89-24842
A 3-D graphical simulation of an automated direct chip probe/test system N89-24848
Pedagogical issues in developing a man-machine interface for an intelligent tutoring system N89-24855
The current technological status of spatial light modulators [AD-A206328] N89-24905

ARMY NATICK RESEARCH AND DEVELOPMENT COMMAND, MA.
The effects of supercritical fluids on high performance polymers [AD-A206515] N89-24494

ARMY RESEARCH INST. OF ENVIRONMENTAL MEDICINE, NATICK, MA.
Solute model or cellular energy model: Practical and theoretical aspects of thirst during exercise [AD-A206143] N89-24785
Is salt at fault [AD-A206518] N89-24789
Field-dependence and judgment of weight and color revisited: Some implications for the study of sensory discrimination [AD-A206141] N89-24791

ASTRO AEROSPACE CORP., CARPINTERIA, CA.
Investigation of structural behavior of candidate Space Station structure [NASA-CR-181746] N89-24678

ASTROSYSTEMS INTERNATIONAL, INC., NEWARK, DE.
Modelling and design of high performance indium phosphide solar cells N89-24712
A three solar cell system based on a self-supporting, transparent AlGaAs top solar cell N89-24723

AUBURN UNIV., AL.
Impact and penetration resistance of fibrous composites [AD-A206417] N89-24454

AVIONS MARCEL DASSAULT-BREGUET AVIATION, SAINT-CLOUD (FRANCE).
Hermes aerothermodynamic concept N89-24351
Protection against ionizing radiation for the Hermes mission N89-24370

B

BATH UNIV. (ENGLAND).
Equations of motion for viscoelastic moving crack problems N89-24670

BOEING CO., SEATTLE, WA.
Development of tandem cells consisting of GaAs single crystal and CuInSe2/CdZnS polycrystalline thin films N89-24717
Directions for further development of GaAs/CuInSe2 thin film tandem cells N89-24718

BOEING MILITARY AIRPLANE DEVELOPMENT, SEATTLE, WA.
Computerized structural mechanics for 1990's: Advanced aircraft needs N89-24640

BOMBRINI PARODI-DELFINO S.P.A., COLLEFERRO (ITALY).
Ariane 5 solid boosters: Overview of design approach and envisaged technologies N89-24352

BONN UNIV. (GERMANY, F.R.).
Systems for the sensitivity calibration of mass spectrometers in space flight [BONN-IR-88-32] N89-24428
Investigations of the sodium layer of the earth atmosphere: Probing with a terrestrial lidar system at 69 N in winter [BONN-IR-88-52] N89-24760

BRITISH BROADCASTING CORP., KINGSWOOD (ENGLAND).
Protection of VHF international distress frequencies from harmonic radiation due to digital television equipment [BBC-RD-1989/1] N89-24512

BROOKHAVEN NATIONAL LAB., UPTON, NY.
On the nature of high-temperature superconductivity [DE89-009525] N89-25053
Non-destructive analyses of cometary nucleus samples using synchrotron radiation [DE89-012536] N89-25101

BROWN UNIV., PROVIDENCE, RI.
Unconditionally stable concurrent procedures for transient finite-element analysis N89-24657

BUNDESMINISTERIUM FUER FORSCHUNG UND TECHNOLOGIE, BONN (GERMANY, F.R.).
Columbus: The European contribution to the International Space Station N89-24337

BYURAKAN OBSERVATORY (USSR).
Pinch-effect and stellar flares physics N89-25004

C

CAIRO UNIV. (EGYPT).
Isothermal life prediction of composite lamina using a damage mechanics approach [NASA-TM-102032] N89-24460

CALABRIA UNIV., ARCAVACTA DI RENDE (ITALY).
Magnetic neutral lines in Jupiter's nightside magnetosphere N89-24918

CALIFORNIA INST. OF TECH., PASADENA.
Unsteady and separated flows [AD-A206539] N89-24572
Caltech-DOE program on numerical analysis, scientific computing and fundamental studies of fluid mechanics [DE89-010828] N89-24582
Neutron starquakes and the nature of gamma-ray bursts N89-24947
On the existence and stability of intermediate shocks N89-24971

CALIFORNIA POLYTECHNIC STATE UNIV., SAN LUIS OBISPO.
Thermal analysis of a hypersonic wing test structure [NASA-CR-185319] N89-24265
An experimental study of a three-dimensional thrust augmenting ejector using laser Doppler velocimetry [NASA-CR-177531] N89-24569

CALIFORNIA UNIV., BERKELEY.
Quantum mechanics of chemical reactions: Recent developments in reactive scattering and in reaction path Hamiltonians [DE89-010438] N89-24470
Research on the mechanism of thermal fatigue in near-eutectic Pb-Sn solders [DE89-011430] N89-24482
A discussion on using Lanczos vectors and Ritz vectors for computing dynamic responses [DE89-012322] N89-24684
Research on self-generated stochastic motion [AD-A206454] N89-24870
Relativistic shocks in electron-positron plasmas and polar cap accretion onto neutron stars: Two non-linear problems in astrophysical plasma physics N89-24928

CALIFORNIA UNIV., BERKELEY. LAWRENCE BERKELEY LAB.
Quantum mechanics of chemical reactions: Recent developments in reactive scattering and in reaction path Hamiltonians [DE89-010438] N89-24470
Research on the mechanism of thermal fatigue in near-eutectic Pb-Sn solders [DE89-011430] N89-24482
Bonding and chemistry of hydrocarbon monolayers on metal surfaces [DE89-009311] N89-24490
High resolution electron microscopy of interfaces in topotaxial and epitaxial reactions [DE89-010390] N89-25070

CALIFORNIA UNIV., DAVIS.
Velocity and scalar fields of turbulent premixed flame in stagnation flow [DE89-009336] N89-24566

CALIFORNIA UNIV., LOS ANGELES.
Objective and constraint functions for the analysis and design of robust control systems N89-24615
A review of some problems in global-local stress analysis N89-24643
Global functions in global-local finite-element analysis of localized stresses in prismatic structures N89-24646
Advances in dual methods and convex approximations for structural optimization N89-24680
Relativistic MHD from two-fluid hydrodynamics (TFHD) N89-24931
Broadband electrostatic waves as a consequence of magnetotail reconnection N89-25017

Black hole driven winds N89-25096

CALIFORNIA UNIV., SAN DIEGO.
Establishment of an electron beam lithography facility [AD-A206215] N89-24332
The variable nature of the comet-solar wind interaction N89-25100

CALIFORNIA UNIV., SAN DIEGO, LA JOLLA.
Reactions of (eta 5-C5H5) (eta 5-C5Me5) Zr(Si(SiMe3)3)X (X = Cl, Me) complexes with carbon monoxide and the isocyanide 2,6 Me2C6H3NC. Crystal structure of (eta 5-C5H5) (eta 5-C5Me5)Zr(eta 2-C(N-2,6 Me2C6H3) Si(SiMe3)3)Cl [AD-A206494] N89-24493

CALIFORNIA UNIV., SANTA BARBARA.
Improvement and extension of a radar forest backscattering model [NASA-CR-184975] N89-24686

CANADA CENTRE FOR REMOTE SENSING, OTTAWA (ONTARIO).
Imaging spectrometry at the Canada Centre for Remote Sensing N89-24701

CARNEGIE-MELLON UNIV., PITTSBURGH, PA.
Predeployment validation of fault-tolerant systems through software-implemented fault insertion [NASA-CR-4244] N89-24817

CENTRE D'ETUDES ET DE RECHERCHES, TOULOUSE (FRANCE).
Analysis of the boundary layer of a delta wing in incidence [CERT-RT-OA-26/5025-AYD] N89-24274

CENTRE NATIONAL D'ETUDES SPATIALES, TOULOUSE (FRANCE).
The Hermes Program N89-24338
French national policy on the preparation of Columbus utilization N89-24344
Technology and design method evolution of cryogenic propulsion systems: Example of the main Ariane 5 stage N89-24353
Hermes-MTFF rendezvous strategy and composite operations N89-24357
Means for preparing and recovering the Hermes space plane N89-24373
The Hermes system training concept N89-24375
Activities of CNES in the field of imaging spectrometry N89-24699

CHICAGO UNIV., IL.
Dynamics of gas-surface interactions [AD-A206210] N89-25059

CHINESE ACADEMY OF SPACE TECHNOLOGY, BEIJING.
China's future space activities N89-24342

CHRONAR CORP., PRINCETON, NJ.
Research on high-efficiency, single-junction, monolithic, thin-film amorphous silicon solar cells [DE89-000893] N89-24739

CLARKSON UNIV., POTSDAM, NY.
Radiometric measurement of temperature distributions in solar cavity receivers [DE89-011467] N89-24742

CLAY ENGINEERING, ALAMEDA, CA.
Analysis of the plugging of the systems autonomy demonstration project brassboard filters [NASA-CR-177533] N89-24450

CLEMSON UNIV., SC.
Thermoplastic coating of carbon fibers [NASA-CR-185047] N89-24488

COLORADO STATE UNIV., FORT COLLINS.
Developing, testing, evaluating and optimizing solar heating and cooling systems [DE89-011831] N89-24744
Forecast of Atlantic seasonal hurricane activity for 1989 N89-24773

COMMISSARIAT A L'ENERGIE ATOMIQUE, SACLAY . (FRANCE).
Bars and open spirals in density wave theory N89-24964

COMPAGNIA ITALIANA SERVIZI TECNICI, ROME.
Integrated approach for the logistic support of the European in orbit infrastructure from the nineties onwards N89-24359

CONSIGLIO NAZIONALE DELLE RICERCHE, FRASCATI (ITALY).
Italian scientific projects related to manned activity in space N89-24382

CONTINUOUS ELECTRON BEAM ACCELERATOR FACILITY, NEWPORT NEW, VA.
Inductive megahertz beam position monitors for CEBAF [CEBAF-PR-89-003] N89-24895

CORNELL UNIV., ITHACA, NY.
Development and utilization of new diagnostics for dense-phase pneumatic transport [DE89-011381] N89-24583
Dissipation of Alfven waves in solar coronal arches N89-24919

COUNCIL FOR NATIONAL ACADEMIC AWARDS (ENGLAND).
The equilibrium and stability of solar coronal magnetic fields N89-25102

D

DEFENCE RESEARCH ESTABLISHMENT ATLANTIC, DARTMOUTH (NOVA SCOTIA).
WADA1: FORTRAN program for wave diffraction analysis, version 1 [AD-A206533] N89-24808

DEFENSE TECHNICAL INFORMATION CENTER, ALEXANDRIA, VA.
A forecast of workloads and manpower requirements for the archiving of scientific and technical reports by the Defense Technical Information Center using a simulation model: An operations research approach [AD-A206263] N89-25075

DELAWARE UNIV., NEWARK.
A new structure for comparing surface passivation materials of GaAs solar cells N89-24725
Improved defect analysis of Gallium Arsenide solar cells using image enhancement N89-24726

DEUTSCHE FORSCHUNGS- UND VERSUCHSANSTALT FUER LUFT- UND RAUMFAHRT, BRUNSWICK (GERMANY, F.R.).
Image Signal Processing for Flight Guidance [DFVLR-MITT-88-32] N89-24295
Image signal processing for flight guidance: Overview and introduction to the main topics N89-24296
Aspects of image communication in air-to-ground systems N89-24298
Investigations of a displacement-estimation technique for aerial video scenes N89-24299
Study of a parametric displacement estimation scheme with application in aerial images N89-24300
Bordautonomous terrain aided flight navigation in height sections close to terrain surface N89-24301
Determination of reference trajectories for testing navigation aids using an onboard CCD camera N89-24303
Transformation of real and virtual objects into a virtual, visual environment N89-24304
Display of flight guidance information in the aircraft cockpit N89-24305
A versatile flight experiment system for image processing N89-24307

DEUTSCHE FORSCHUNGS- UND VERSUCHSANSTALT FUER LUFT- UND RAUMFAHRT, COLOGNE (GERMANY, F.R.).
Timelining and operations integration concerning APM and MTFF N89-24358
System safety from D-missions to Columbus N89-24367
Medical and radiation protection problems in space N89-24369
Experimentation in the Man Tended Free Flyer (MTFF) N89-24381
Robotic experiments on Spacelab D-2 as testbed for future operational concepts N89-24391
The Microgravity User Support Center (MUSC) N89-24394
Crew training aspects N89-24396

DEUTSCHE FORSCHUNGS- UND VERSUCHSANSTALT FUER LUFT- UND RAUMFAHRT, OBERPFAFFENHOFEN (WEST GERMANY).
The Manned Space Laboratories Control Center (MSCC) at DFVLR, Oberpfaffenhofen, Germany, F.R. N89-24376
Necessity and benefit of the X-SAR space shuttle experiment [DFVLR-MITT-88-29] N89-24688
DFVLR activities related to imaging spectrometry N89-24697
The EARSEL Imaging Spectrometry Working Group N89-24700

DORNIER-WERKE G.M.B.H., FRIEDRICHSHAFEN (GERMANY, F.R.).
ECLS for Columbus and Hermes N89-24354
Fuel cell development for Hermes N89-24355
EVA Information System: A modern workstation in space N89-24388
Simulation of weightlessness with neutral buoyancy facilities and zero-g aircraft for the preparation of European manned space operations N89-24398

DORTMUND UNIV. (GERMANY, F.R.).
Hierarchically structured control for intelligent robots in space N89-24393

DU PONT DE NEMOURS (E. I.) AND CO., AIKEN, SC.
High temperature mechanical properties and microscopic examination of extruded powder aluminum [DE89-010457] N89-24484
Application of Lotus 1-2-3 to heat transfer analysis [DE89-010463] N89-24813

DUBLIN INST. FOR ADVANCED STUDIES (IRELAND).
Particle acceleration and shock wave structure N89-24930
Cosmic rays: A short survey of open problems N89-24940

DYNACS ENGINEERING CO., INC., CLEARWATER, FL.
Constraint elimination in dynamical systems N89-24667

E

ECOLE NATIONALE SUPERIEURE DE MECANIQUE, NANTES (FRANCE).
Numerical methods for unsteady flows N89-24282
Computation of the characteristics of the wake past an oscillating cylinder N89-24283

ECOLE POLYTECHNIQUE, PALAISEAU (FRANCE).
Strong Langmuir turbulence and the pulsar emission mechanism N89-24956

EDGERTON, GERMESHAUSEN AND GRIER, INC., IDAHO FALLS, ID.
ERC nickel cadium battery performance tests and comparisons with lead-acid batteries [DE89-009753] N89-24535

EIDGENOESSISCHE TECHNISCHE HOCHSCHULE, ZURICH (SWITZERLAND).
Alfven wave solitons and solar intermediate drift bursts N89-24923

ELEKTRONIK-SYSTEM G.M.B.H., MUNICH (GERMANY, F.R.).
Manned interventions at the MTFF: Crew workload aspects N89-24362

ENERGY CONVERSION DEVICES, INC., TROY, MI.
Deployable aerospace PV array based on amorphous silicon alloys N89-24720

ETABLISSEMENT TECHNIQUE CENTRAL DE L'ARMEMENT, ARCUEIL (FRANCE).
Bonded assemblies behavior laws: Light alloys/elastoplastic adhesive [ETCA-88-R-001] N89-24456
Composite material bonding: Gelation and processing of adhesives and preimpregnated materials [ETCA-88-R-006] N89-24457

EUROPEAN SPACE AGENCY, PARIS (FRANCE).
International Symposium on Europe in Space: The Manned Space System [ESA-SP-277] N89-24335
The Ariane 5 Development Program N89-24336
Overall coherence of the European programs within a long-term space policy N89-24341
Hermes user interfaces N89-24346
Microgravity payloads (APM and MTFF) N89-24347
The technology contents of the first phase of the Hermes Development Program N89-24350
Hermes-MTFF rendezvous strategy and composite operations N89-24357
Safety and reliability of the Ariane 5-Hermes composite N89-24365
Columbus safety and reliability N89-24368
The training concept for ESA astronauts and the associated facilities N89-24374
Hermes crew role N89-24401
The astronaut's functions aboard Columbus N89-24403
Imaging Spectrometry for Land Applications [ESA-SP-1101] N89-24692
Proceedings of an International School and Workshop on Plasma Astrophysics, volume 1 [ESA-SP-285-VOL-1] N89-24910
Proceedings of an International School and Workshop on Reconnection in Space Plasma, volume 2 [ESA-SP-285-VOL-2] N89-24974

EUROPEAN SPACE AGENCY. EUROPEAN SPACE OPERATIONS CENTER, DARMSTADT (GERMANY, F.R.).
The European in-orbit infrastructure ground segment N89-24340
Flight operations concept for the European in-orbit infrastructure N89-24356
The impact of manned space flight operations on the safety and reliability aspects of ground systems requirements N89-24371
The role of the Hermes flight control center in a typical Hermes/MTFF servicing mission N89-24372
Expert system for European space infrastructure N89-24378

EUROPEAN SPACE AGENCY. EUROPEAN SPACE RESEARCH AND TECHNOLOGY CENTER, ESTEC, NOORDWIJK (NETHERLANDS).
Space science using Columbus: Manned space science N89-24348
Hermes-MTFF rendezvous strategy and composite operations N89-24357
ESA safety requirements N89-24364
The concept of telescience N89-24384

Getting ready for EVA N89-24387
ESA's planned activities in the field of imaging spectrometry for Earth observation N89-24693
ESA's space plasma physics missions: The past and the future ten years N89-24913
Helioseismology and plasma physics N89-24922
Speculation on the origin of X-ray emission in early-type stars N89-25029

F

FEDERAL AVIATION ADMINISTRATION, ATLANTIC CITY, NJ.
A computer simulation study of liquid water content adjustment based on icing cloud horizontal extent
[DOT/FAA/CT-TN89/3] N89-24288
Controller evaluation of initial data link air traffic control services. Volume 1: Mini study 2
[DOT/FAA/CT-89/14-VOL-1] N89-24292
Improved marking of taxiway intersections for Instrument Flight Rules (IFR) operations
[DOT/FAA/CT-TN89/23] N89-24330
FEDERAL AVIATION ADMINISTRATION, WASHINGTON, DC.
An operational demonstration and engineering flight test of the Microwave Landing System on runway 22L at Chicago's Midway Airport
[DOT/FAA/CT-TN88/42] N89-24291
A comparison of detection efficiency on an air traffic control monitoring task with and without computer aiding
[AD-A206422] N89-24294
FEDERAL LAB. CONSORTIUM, WASHINGTON, DC.
Putting technology to work: Examples of industry-laboratory cooperation contributing to our nation's economic strength
[PB89-134654] N89-25077
FINNISH METEOROLOGICAL INST., HELSINKI.
Orographically-caused microclimate variation in the Saariselka Region
[ISBN-9-5169-7269-1] N89-24767
The climate of Finland: A bibliography with particular reference to applications updating part 1958-1985
[MP-10] N89-24768
An operational analysis and forecasting method of evaporation
[MP-11] N89-24769
FLORIDA STATE UNIV., TALLAHASSEE.
Analysis and use of VAS satellite data
[NASA-CR-4218] N89-24770
FLORIDA UNIV., GAINESVILLE.
Integrated optimization of nonlinear R/C frames with reliability constraints N89-24631
Centrifugal modeling of underground structures subjected to blast loading
[AD-A206424] N89-24675
FLOW RESEARCH, INC., KENT, WA.
An investigation of V/STOL jet interactions in a crossflow
[AD-A206360] N89-24272
FOKKER B.V., AMSTERDAM (NETHERLANDS).
The Hermes robot arm (HERA) N89-24390
FOM-INST. VOOR PLASMAFYSICA, RIJNHUIZEN, JUTPHAAS (NETHERLANDS).
Kink modes in coronal loops N89-24925
FOM-Rijnhuizen contributions to the Fifteenth Symposium on Fusion Technology
[REPT-88-179] N89-25030
A role for free electron lasers in fusion N89-25031
Engineering aspects of RTP N89-25032
Beam guiding system for Rutherford scattering diagnostic at TEXTOR N89-25033
MEQALAC: A 1 MeV multi-channel RF-accelerator for light ions N89-25034
Elliptical polarization for ECRH on RTP N89-25035
Control and data acquisition system for the neutral beam probe diagnostic on TEXTOR N89-25036
The control and monitoring system of RTP N89-25037

G

GENERAL ACCOUNTING OFFICE, WASHINGTON, DC.
US military aircraft coproduction with Japan
[AD-A206430] N89-24263
GENERAL ELECTRIC CO., PHILADELPHIA, PA.
Safety analysis report for the Galileo Mission. Volume 2, book 1: Accident model document
[DE89-007270] N89-24896
Safety analysis report for the Galileo Mission. Volume 2, book 2: Accident model document, Appendices
[DE89-007271] N89-24897
GENERAL MOTORS RESEARCH LABS., WARREN, MI.
Error analysis for semi-analytic displacement derivatives with respect to shape and sizing variables N89-24632
GEORGE WASHINGTON UNIV., HAMPTON, VA.
Global-local methodologies and their application to nonlinear analysis N89-24647
GEORGIA INST. OF TECH., ATLANTA.
Acoustic emission from a growing crack N89-24633
Some comments on global-local analyses N89-24644
Analysis of shell-type structures subjected to time-dependent mechanical and thermal loading
[NASA-CR-184989] N89-24669
Analysis of interlaminar fracture in composites under combined loading
[NASA-CR-185055] N89-24674
Improvements in the Global Reference Atmospheric Model and comparisons with a global 3-D numerical model
[NASA-CR-184947] N89-24755
A weak Hamiltonian finite element method for optimal control problems
[NASA-CR-185336] N89-24873
GEORGIA STATE UNIV., ATLANTA.
Neurochemical control of circadian rhythms
[AD-A206213] N89-24788
GOODRICH (B. F.) CO., AKRON, OH.
Features and characterization needs of rubber composite structures N89-24649
GOSUDARSTVENNYI KOMITET PO ISPOLZOVANIYU ATOMNOI ENERGII, MOSCOW (USSR).
Theoretical microcontact spectra of metal electron-phonon coupling
[DE88-706280] N89-25067
GRENOBLE-1 UNIV., SAINT MARTIN D'HERES (FRANCE).
Jets and beams in powerful extragalactic radio sources N89-24957
GRUMMAN AEROSPACE CORP., BETHPAGE, NY.
Transient analysis techniques in performing impact and crash dynamic studies N89-24658

H

HAMBURG UNIV. (GERMANY, F.R.).
Scene reconstruction for image sequences N89-24297
HAMPTON INST., VA.
Development of mid-infrared solid state lasers for spaceborne lidar
[NASA-CR-185012] N89-24599
HARVARD COLL. OBSERVATORY, CAMBRIDGE, MA.
IUE investigations of SN 1987A
[NASA-CR-184973] N89-25079
HAWAII UNIV., HONOLULU.
The relationship between intraseasonal disturbance activity and interannual variation of the tropical atmosphere N89-24774
HIBBITT, KARLSSON AND SORENSEN, PROVIDENCE, RI.
Some issues in numerical simulation of nonlinear structural response N89-24639
HIGH TECHNOLOGY CORP., HAMPTON, VA.
An algebraic homotopy method for generating quasi-three-dimensional grids for high-speed configurations
[NASA-CR-4242] N89-24581
HIROSHIMA UNIV., TAKEHARA (JAPAN).
Stochastic quantization of nonlinear sigma-models with Wess-Zumino terms
[DE88-757286] N89-24882
Gravitational angular fluctuations of the cosmic background radiation produced by cosmological linear perturbations
[DE88-757287] N89-25105
HONEYWELL, INC., MINNETONKA, MN.
Automated Millimeter Wave (AMW) transducer testing in a robotic/vision test cell N89-24841
HONEYWELL, INC., NEW BRIGHTON, MN.
Robot assembly of microscopic component in millimeter wave devices N89-24840
HOWARD UNIV., WASHINGTON, DC.
On the dynamics and control of the Spacecraft Control Laboratory Experiment (SCOLE) class of offset flexible systems N89-24426
HUGHES AIRCRAFT CO., TORRANCE, CA.
Development of a 75-watt 60-GHz traveling-wave tube for intersatellite communications
[NASA-CR-182135] N89-24530
HUGHES RESEARCH LABS., MALIBU, CA.
Cooperative phenomena for new coherent radiation sources
[AD-A206368] N89-24602

I

IBM WATSON RESEARCH CENTER, YORKTOWN HEIGHTS, NY.
Evaluation, description and invention: Paradigms for human-computer interaction
[AD-A204617] N89-24796
IDAHO NATIONAL ENGINEERING LAB., IDAHO FALLS.
Hydrogen ion-driven permeation in carbonaceous films
[DE89-005271] N89-24485
IIT RESEARCH INST., BARTLESVILLE, OK.
Development of an engineering methodology for applying foam technology
[DE89-000740] N89-24497
ILLINOIS UNIV., URBANA-CHAMPAIGN.
Transformational derivation of programs using the Focus system
[NASA-CR-184875] N89-24802
IMPERIAL COLL. OF SCIENCE AND TECHNOLOGY, LONDON (ENGLAND).
Noise-free neutral sheets N89-24977
INFORMATION AND CONTROL SYSTEMS, INC., HAMPTON, VA.
Modeling and characterization of the Earth Radiation Budget Experiment (ERBE) nonscanner and scanner sensors
[NASA-CR-181818] N89-24772
INSTITUT DE MECANIQUE DES FLUIDES DE LILLE (FRANCE).
Prediction methods for dynamic stability parameters: Effects of angular stability
[IMFL-88/18] N89-24573
INSTITUTE FOR COMPUTER APPLICATIONS IN SCIENCE AND ENGINEERING, HAMPTON, VA.
Numerical study of turbulent secondary flows in curved ducts
[NASA-CR-181830] N89-24568
File concepts for parallel I/O
[NASA-CR-181843] N89-24816
Analytic theory for the determination of velocity and stability of bubbles in a Hele-Shaw cell. Part 2: Stability
[NASA-CR-181837] N89-24883
INSTITUTE FOR SCIENTIFIC RESEARCH, LEXINGTON, MA.
Introduction to dissociative recombination
[NASA-CR-184950] N89-24889
Theoretical studies of important processes in planetary and comet atmospheres. Renewel request
[NASA-CR-184951] N89-25099
INSTITUTE OF NUCLEAR PHYSICS, NOVOSIBIRSK (USSR).
MHD-waves and their nonlinear interaction in a plasma with magnetic flux tubes N89-24921
Stability of force-free magnetic fields and the problem of solar coronal heating N89-24990
INSTITUTE OF OCEAN SCIENCES, SIDNEY (BRITISH COLUMBIA).
Development of an imaging spectrometer for remote sensing: The FLI program N89-24698
INSTITUTO DE PESQUISAS ESPACIAIS, SAO JOSE DOS CAMPOS (BRAZIL).
Microwave X-band radiometric characterization of Brazilian soils by measurement of the complex permittivity
[INPE-4588-PRE/1319] N89-24685
INTERIOR DEPT., WASHINGTON, DC.
Geological gyrocompass
[PB89-133086] N89-24589
Climatic atlas of the outer continental shelf waters and coastal regions of Alaska. Volume 3: Chukchi-Beaufort Sea
[AD-A206525] N89-24776
INTERNATIONAL CENTRE FOR THEORETICAL PHYSICS, TRIESTE (ITALY).
On the thermal stability of optically thin flows N89-24973
Factorization of the relativistic Pauli equation in the presence of a gravitational field
[DE88-704749] N89-25090
IOWA UNIV., IOWA CITY.
Dynamics of articulated structures N89-24664
The electron beam instability revisited: Growth above and below f sub p N89-24917
Shock-associated plasma density fluctuations in the interstellar medium N89-24933
Effects of unequal particle number densities on Alfven waves N89-24945
Are supernova remnants quasi-parallel or quasi-perpendicular accelerators N89-24948
Simulation of electrostatic ion instabilities in the presence of parallel currents and transverse electric fields N89-24972

J

JAPAN ATOMIC ENERGY RESEARCH INST., TOKYO.
Numerical study on laminar circular jet of carbonic acid gas discharging into stagnant air
[DE88-757249] N89-24565
Representations of a linkage mechanism based on dual number matrices
[DE88-757273] N89-24857
Computational method of the inverse kinematics via simplified algebraic equation
[DE88-757269] N89-24866
Design of the optical system for a new time-resolved X-ray absorption spectroscopy apparatus
[DE88-757253] N89-24902
Steady-state operation regime of tokamak reactor plasma. Consistency analysis (I)
[DE88-756571] N89-24908
Study of particle confinement in the JT-60 tokamak using skin radiative approximation model
[DE88-756574] N89-24909

JET PROPULSION LAB., CALIFORNIA INST. OF TECH., PASADENA.
Shuttle payload bay thermal environments: Summary and conclusion report for STS Flights 1-5
[NASA-CR-185017] N89-24411
Magellan: The unveiling of Venus
[NASA-CR-185018] N89-24419
Voyager at Neptune: 1989
[NASA-CR-185317] N89-24420
Modal reduction strategies for interconnected flexible bodies simulation N89-24665
HIRIS: NASA's high-resolution imaging spectrometer for the Earth Observing System (EOS) N89-24695
Advanced photovoltaic solar array development N89-24716
UNIX-based data management system for the Mobile Satellite Propagation Experiment (PiFEx)
[NASA-CR-185023] N89-25073

JOINT CENTER FOR GRADUATE STUDY, RICHLAND, WA.
Investigation of high efficiency GaAs solar cells N89-24724

JOINT INST. FOR NUCLEAR RESEARCH, DUBNA (USSR).
Backscattering spectra processing for the structure of multilayer samples
[DE88-706325] N89-24468
Explosive-emitter cathode produced using the heavy ion track technique
[DE88-706304] N89-24503
The 64K 16-bit word buffer memory with microprogrammable control
[DE88-706303] N89-24799
Dynamic spectral analysis in finite field algebras
[DE88-706333] N89-24877
Efficient estimator of parameters and goodness-of-fit test of multivariate distributions for data presented by one-dimensional histograms
[DE88-706318] N89-24879
Analytical consideration and calculation of electrostatical system by reverse method
[DE88-706319] N89-24885
Measurements of magnetic field of superconducting solenoid
[DE88-706323] N89-25068

K

KADER ROBOTICS, INC., HUNTSVILLE, AL.
Dual-arm robots for telerobotic IVA operations on the space station N89-24822

KAMAN AEROSPACE CORP., BLOOMFIELD, CT.
Modeling the missile-launch tube problem in DYSCO N89-24629

KATHOLIEKE UNIVERSITEIT TE LEUVEN (BELGIUM).
Coronal heating by resonant absorption in resistive MHD N89-24926

KERNFORSCHUNGSZENTRUM G.M.B.H., KARLSRUHE (GERMANY, F.R.).
Thermal shock strength of multiphase materials
[KFK-4469] N89-24455
Investigations on the creep-rupture behavior of the austenitic stainless steel AISI 316-NET
[KFK-4468] N89-24479
X-ray investigations of ceramic high Tc superconductors under high pressure
[KFK-4482] N89-25064

KMS FUSION, INC., ANN ARBOR, MI.
A robotic vehicle global route planner for the 1990s N89-24851
A knowledge representation scheme for a robotic land vehicle route planner N89-24853

L

LABEN SPACE INSTRUMENTATION AND SYSTEMS, MILAN (ITALY).
Telescience and payload control support technologies N89-24385
Advanced MMI and image handling to support crew activities N89-24392

LABORATOIRE DE METEOROLOGIE DYNAMIQUE DU CNRS, PALAISEAU (FRANCE).
On the future development and management of spectroscopic database for radiative transfer from the issues of recent related workshops
[ETN-89-94530] N89-24690
Refinements in the cloud detection scheme of the 3I system. Comparison with AVHRR products
[ETN-89-94531] N89-24691
Estimating the outgoing longwave radiation from the Meteosat infrared window and water vapor bands
[ETN-89-94533] N89-24762
Three dimensional analysis of the atmospheric structure by vertical satellite sounding. Interest for weather forecasting
[ETN-89-94536] N89-24763
Water vapor retrievals through the 3I (improved Initialization Inversion) system: Application to tropospheric altimetry correction
[ETN-89-94534] N89-24778
The radiation-atmosphere interaction model and the determination of meteorological and climatological parameters from satellite observations
[ETN-89-94535] N89-24779
Contribution to the study of the diurnal cycle of convective clouds over tropical Africa from satellite imagery
[ETN-89-94537] N89-24780
Study of representativity of the wind fields deduced from geostationary satellite images. Attribution of height to wind vectors and large scale average fields deduced from water vapor imagery
[ETN-89-94538] N89-24781
Contribution to the estimation of precipitation in the Sahel by using satellite imagery
[SER-DI-204] N89-24782

LAWRENCE LIVERMORE NATIONAL LAB., CA.
Capabilities and some applications of the LLNL 100-kV electric gun
[DE89-006747] N89-24408
Viscosity of solids determined by shock wave action on hemispherical indentations
[DE89-008035] N89-24510
Characterization of radiation boundary conditions used in the finite-difference time-domain method
[DE89-005662] N89-24522
Embedded conductors by electrochemical planarization
[DE89-011632] N89-24534
Challenges in computational statistical mechanics
[DE89-009922] N89-24567
A second-order projection method for the incompressible Navier Stokes equations on quadrilateral grids
[DE89-010242] N89-24585
On the refraction of longitudinal waves in compressible media
[DE89-012922] N89-24588
Two dimensional analysis of a NOVETTE laser generated stress-impulse experiment
[DE89-009909] N89-24600
Engineering design of the interaction waveguide for high-power accelerator-driven microwave free-electron lasers
[DE89-011896] N89-24605
Atmospheric effects on laser propagation
[DE89-012287] N89-24606
Application and implementation of transient algorithms in computer programs N89-24659
Measurement of bond strength at metal/ceramic interfaces
[DE89-011638] N89-24682
A discussion on using Lanczos vectors and Ritz vectors for computing dynamic responses
[DE89-012322] N89-24684
Beyond CO2: The other greenhouse gases
[DE89-011893] N89-24750
Field studies for determining the characteristics and dynamics of local circulations
[DE89-012290] N89-24751
Simplified climate models: Rationale and design
[DE89-012291] N89-24783
Semiclassical matrix-elements of high-charge ions
[DE89-009258] N89-24890
Combined microstructure X-ray optics
[DE89-009902] N89-24904
Hard X-ray imaging telescope development
[DE89-011647] N89-24906
The effect of non-Maxwellian electron distributions on the intensity ratio of resonance to satellite lines
[DE89-006745] N89-24907
Computer simulations of cosmic-ray diffusion near supernova remnant shock waves N89-24916
Relativistic shocks in electron-positron plasmas and polar cap accretion onto neutron stars: Two non-linear problems in astrophysical plasma physics N89-24928
Magnetic reconnection simulation using the 2.5 D electromagnetic direct implicit code AVANTI N89-24984
Kinetic simulation of magnetic reconnection in the presence of shear N89-24985
Shock compaction of superconductors
[DE89-006744] N89-25052

LEHIGH UNIV., BETHLEHEM, PA.
Interaction of Karman vortex-street with an elliptical leading-edge N89-24268

LENINGRAD STATE UNIV. (USSR).
The role of the magnetic reconnection in the solar wind/magnetosphere interaction N89-25024
Impulsive reconnection of the skewed magnetic fields at the magnetopause as a MHD model N89-25025

LIGHTWAVE ELECTRONICS CORP., MOUNTAIN VIEW, CA.
Prototype laser-diode-pumped solid state laser transmitters
[NASA-CR-185056] N89-24601

LOCKHEED AERONAUTICAL SYSTEMS CO., MARIETTA, GA.
Diverter AI based decision aid, phases 1 and 2
[NASA-CR-181820] N89-24316

LOCKHEED MISSILES AND SPACE CO., HUNTSVILLE, AL.
Turbine rotor/stator flowfield analysis
[NASA-CR-183639] N89-24433
Space Shuttle Main Engine structural analysis and data reduction/evaluation. Volume 6: Primary nozzle diffuser analysis
[NASA-CR-183669] N89-24437

LOCKHEED MISSILES AND SPACE CO., PALO ALTO, CA.
SMM X-ray polychromator
[NASA-CR-180791] N89-24590
The computational structural mechanics testbed architecture. Volume 5: The Input-Output Manager DMGASP
[NASA-CR-178388] N89-24637
Computational procedures for postbuckling of composite shells N89-24642
Computational aspects of multibody dynamics N89-24666

LOCKHEED MISSILES AND SPACE CO., SUNNYVALE, CA.
Superfluid Helium Tanker Study (SFHT)
[NASA-CR-172114] N89-24415

LOS ALAMOS NATIONAL LAB., NM.
Amorphous metal alloys produced by mechanical alloying
[DE89-011189] N89-24481
Methane to methanol conversion
[DE89-011194] N89-24504
Auditory speech preprocessors
[DE89-009280] N89-24516
Applications of infrared laser spectroscopy to laser chemistry and laser development
[DE89-011196] N89-24604
Shaft adjuster
[DE89-010119] N89-24612
Optical chaos
[DE89-009392] N89-24903
Magnetotail reconnection, MHD theory and simulations N89-25013
Flux transfer events: Reconnection without separators N89-25021
A new field experiment in the Greenland ice cap to test Newton's inverse square law
[DE89-009247] N89-25091
Red-shift experiments and non-Newtonian gravitational forces
[DE89-009349] N89-25092
Effects of main-sequence mass loss on stellar and galactic chemical evolution
[DE89-011399] N89-25098

LOVELACE FOUNDATION FOR MEDICAL EDUCATION AND RESEARCH, ALBUQUERQUE, NM.
Two-phase flow measurements by nuclear magnetic resonance imaging
[DE89-011850] N89-24586

M

MARTIN MARIETTA AEROSPACE, DENVER, CO.
Space Station automation of common module power management and distribution
[NASA-CR-183607] N89-24434
MARTIN MARIETTA CORP., DENVER, CO.
Orbital Transfer Vehicle: Concept definition and system analysis study
[NASA-CR-183551] N89-24410
The DARPA autonomous land vehicle: A phase 1 retrospective and a prospective for the future N89-24834
MARTIN MARIETTA CORP., HUNTSVILLE, AL.
On designing a case-based system for expert process development N89-24847
MARTIN MARIETTA LABS., BALTIMORE, MD.
On designing a case-based system for expert process development N89-24847
MARYLAND UNIV., COLLEGE PARK.
Real time control for NASA robotic gripper
[NASA-CR-184978] N89-24608
MASSACHUSETTS INST. OF TECH., CAMBRIDGE.
Theoretical model for VITA-educed coherent structures in the wall region of a turbulent boundary layer N89-24556
Dynamics of flexible multi-body mechanisms and manipulators. Part 1: An overview N89-24662
Application of finite-element methods to dynamic analysis of flexible spatial and co-planar linkage systems, part 2 N89-24663
Nonlinear characteristics of joints as elements of multi-body dynamic systems N89-24668
Plate motions and deformations from geologic and geodetic data
[NASA-CR-184987] N89-24757
Global kinetic theory of astrophysical jets N89-24954
Nonlinear oblique whistlers: Their relevance to nonthermal coupling of ions and electrons in accretion flow and supercritical quasi-perpendicular collisionless shocks N89-24955
MASSACHUSETTS UNIV., AMHERST.
Vortex dynamics and vortex breakdown
[AD-A206470] N89-24570
MATRA ESPACE, TOULOUSE (FRANCE).
Telescience: A promising operations center N89-24386
MAX-PLANCK-INST. FUER AERONOMIE, KATLENBURG-LINDAU (GERMANY, F.R.).
Dimensionless parameters for classifying solar wind interactions N89-24914
Relation between global and local aspects of reconnection N89-24976
MAX-PLANCK-INST. FUER PHYSIK UND ASTROPHYSIK, GARCHING (GERMANY, F.R.).
The gamma-ray observatory GRO in perspective
[MPE-PREPRINT-137] N89-24407
A study of K sup deg sec, lambda and lambda bar production in 60 and 200 GeV nucleon OAu and pAu collisions with a streamer chamber detector at the CERN SPS
[MPE-PAE/EXP.EL-198] N89-24900
Cosmic linear accelerators N89-24915
Soft X-ray observations of the Vela Pulsar PSR 0833-45
[MPE-PREPRINT-130] N89-25080
The 158 micron (CII) mapping of the galactic center molecular clouds
[MPE-PREPRINT-131] N89-25081
Physical conditions in molecular clouds derived from sub-mm and far-IR spectroscopic observations
[MPE-PREPRINT-135] N89-25082
Constraints on the optical counterpart of GBS0526-66
[MPE-PREPRINT-138] N89-25084
High spectral resolution observations of the H2 2.12 micron line in Herbig-Haro objects
[MPE-PREPRINT-139] N89-25085
First detection of SO2 and CH3OH emission and one unidentified line near 800 GHz
[MPE-PREPRINT-142] N89-25086
The circum-nuclear disk
[MPE-PREPRINT-132] N89-25093
The Orion molecular cloud and star forming region
[MPE-PREPRINT-140] N89-25094
Strong, spatially extended CO 7 to 6 emission from luminous cloud cores: W51 and DR21
[MPE-PREPRINT-133] N89-25106
COS-B gamma-ray sources beyond the predicted diffuse emission
[MPE-PREPRINT-136] N89-25107
MAX-PLANCK-INST. FUER PHYSIK UND ASTROPHYSIK, MUNICH (GERMANY, F.R.).
Investigations on fully depletable charge coupled devices
[MPI-PAE/EXP.EL-194] N89-25063
MAX-PLANCK-INST. FUER PLASMAPHYSIK, GARCHING (GERMANY, F.R.).
ASDEX Contributions to the 8th International Conference on Plasma Surface Interaction in Controlled Fusion Devices
[IPP-III/139] N89-25038
Impurity accumulation studies in pellet-refuelled ASDEX discharges N89-25039
Characterization of the ASDEX scrape-off-layer density profile during neutral beam heating N89-25040
ASDEX edge and divertor simulation and the problem of incomplete and inaccurate experimental data N89-25041
Comparison of recycling in the ASDEX divertor before and after hardening N89-25042
The low energy neutral fluxes and their impurity production at the walls of ASDEX N89-25043
Charge exchange neutral sputtering in ASDEX N89-25044
Erosion and retention of the target plate material in the ASDEX divertor N89-25045
Measurements of the flux of metallic impurities to the ASDEX divertor plates N89-25046
Material transport at the vessel walls of the divertor tokamak ASDEX N89-25047
MAX-PLANCK-INSTITUT FUER STROEMUNGSFORSCHUNG, GOETTINGEN (GERMANY, F.R.).
Calculation of aircraft noise in the vicinity of civil airports by a simultion procedure
[MPIS-7/1988] N89-24887
MCDONNELL-DOUGLAS ASTRONAUTICS CO., HUNTINGTON BEACH, CA.
Technology transfer: Imaging tracker to robotic controller N89-24828
MCDONNELL-DOUGLAS ASTRONAUTICS CO., HUNTSVILLE, AL.
The human role in space (THURIS) applications study. Final briefing
[NASA-CR-183590] N89-24793
The human role in space (THURIS) applications study. Volume 2: Research analysis and technology report
[NASA-CR-183589] N89-24795
MESSERSCHMITT-BOELKOW-BLOHM G.M.B.H., BREMEN (GERMANY, F.R.).
Landscape-related position finding for flying systems N89-24302
MTFF user interfaces N89-24345
MTFF flight operations phases N89-24361
MICHIGAN TECHNOLOGICAL UNIV., HOUGHTON.
The effects of gradients on boundary stability
[DE89-011590] N89-25065
MICHIGAN UNIV., ANN ARBOR.
Multiple-pass aeroassisted plane change N89-24404
Estimating population size of Pygoscelid Penguins from TM data
[NASA-CR-180081] N89-24687
A genuinely multi-dimensional upwind cell-vertex scheme for the Euler equations
[NASA-TM-102029] N89-24872
MIDWEST RESEARCH INST., GOLDEN, CO.
Increasing the chemical yield of desirable chemical species using solar rapid heating
[DE89-000881] N89-24469
Investigations of the origins of metastable, light-induced changes in hydrogenated amorphous silicon
[DE89-000890] N89-24496
Research on high-efficiency, single-junction, monolithic, thin-film amorphous silicon solar cells, phase 2
[DE89-000849] N89-24703
An empirical study of the performance of APMOVPE AM0 InP homojunction solar cells as a function of emitter thickness and doping, and base doping N89-24709
AM0 efficiency measurements N89-24736
Research on high-efficiency, single-junction, monolithic, thin-film amorphous silicon solar cells
[DE89-000893] N89-24739
Photovoltaic advanced research and development project: Solar radiation research
[DE89-000884] N89-24743
MINISTERO RICERCA SCIENTIFICA E TECNOLOGICA, ROME (ITALY).
The European data relay satellite N89-24339
MISSISSIPPI STATE UNIV., STATE COLLEGE.
Surface grid generation for composite block grids N89-24874
Surface coordinate generation in three-dimensional arbitrary shapes by solving a set of second order elliptic partial differential equations N89-24875
MONITEQ LTD., CONCORD (ONTARIO).
The FLI airborne imaging spectrometer: A highly versatile sensor for many applications N89-24694
MONTANA STATE UNIV., BOZEMAN.
The gravitational many-body PPN Lagrangian, Lorentz invariance and the strong equivalence principle to second order N89-24765
MOOG, INC., EAST AURORA, NY.
Disconnects for spacecraft servicing applications N89-24832
MORTON THIOKOL, BRIGHAM CITY, UT.
Field joint environmental protection system vibration/pressurization qualification
[NASA-CR-183673] N89-24449
Teledyne Taber 206-1000 and 2210-3000 pressure transducer proof test and burst test
[NASA-CR-183672] N89-24594

N

NAPLES UNIV. (ITALY).
MARS Microgravity Advanced Research and Support Center N89-24395
NATIONAL ACADEMY OF SCIENCES - NATIONAL RESEARCH COUNCIL, WASHINGTON, DC.
Report of the committee on a commercially developed space facility
[NASA-CR-185383] N89-24406
Human Factors in Automated and Robotic Space Systems: Proceedings of a symposium. Part 1
[NASA-CR-182495] N89-24792
Human Factors in Automated and Robotic Space Systems: Proceedings of a symposium. Part 2
[NASA-CR-182496] N89-24794
NATIONAL AERONAUTICAL LAB., BANGALORE (INDIA).
Microprocessor based 32 channel PCM telemetry system
[NAL-TM-SE-8704] N89-24414
Experiments on liquid-vapour phase change between plane liquid surfaces. Part 2: Observations of large temperature jumps near the interfaces
[NAL-TM-FM-8805] N89-24462
An intelligent fiberoptic data bus for fly-by-light applications
[NAL-TM-SE-8707] N89-24901
NATIONAL AERONAUTICS AND SPACE ADMINISTRATION, WASHINGTON, DC.
Space Shuttle to deploy Magellan planetary science mission
[NASA-NEWS-RELEASE-89-86] N89-24334
The space station power system
[NASA-TM-101245] N89-24416
Space station: A step into the future
[NASA-PAM-510/11-87] N89-24417
Technology requirements for advanced NASA missions N89-24705
NASA information sciences and human factors program
[NASA-TM-4126] N89-25111
NATIONAL AERONAUTICS AND SPACE ADMINISTRATION. AMES RESEARCH CENTER, MOFFETT FIELD, CA.
Numerical aerodynamic simulation
[NASA-EP-262] N89-24262
Experimental aerodynamic characteristics of a joined-wing research aircraft configuration
[NASA-TM-101083] N89-24285
Design of automated system for management of arrival traffic
[NASA-TM-102201] N89-24290
Results of an A109 simulation validation and handling qualities study
[NASA-TM-101062] N89-24323
Survey of Army/NASA rotorcraft aeroelastic stability research
[NASA-TM-101026] N89-24329
Ultra-light duct for an anechoic wind tunnel
[NASA-TM-101805] N89-24331
Space Pioneers and where they are now
[NASA-EP-264] N89-24333
Chaos in a spatially-developing plane mixing layer N89-24539
Inflow/outflow boundary conditions and global dynamics of spatial mixing layers N89-24540
Subharmonic resonance in a mixing layer N89-24544
Sensitivity of mixing layers to three-dimensional forcing N89-24547
Turbulence production near walls: The role of flow structures with spanwise asymmetry N89-24550
Energy transfer in isotropic turbulence at low Reynolds numbers N89-24553
Turbulence characteristics inside a turbulent spot in plane Poiseuille flow N89-24554
Aerodynamic interaction between vortical wakes and lifting two-dimensional bodies
[NASA-TM-101074] N89-24563
Improving transient analysis technology for aircraft structures N89-24655
Display-based communications for advanced transport aircraft
[NASA-TM-102187] N89-24798

Some notes on shock resolving flux functions. Part 1: Stationary characteristics
[NASA-TM-101087] N89-24871

NATIONAL AERONAUTICS AND SPACE ADMINISTRATION. FLIGHT RESEARCH CENTER, EDWARDS, CA.

Development and flight test experiences with a flight-crucial digital control system
[NASA-TP-2857] N89-24327

NATIONAL AERONAUTICS AND SPACE ADMINISTRATION. GODDARD SPACE FLIGHT CENTER, GREENBELT, MD.

Proceedings of the Goddard Space Flight Center Workshop on Robotics for Commercial Microelectronic Processes in Space
[NASA-TM-101233] N89-24505

Research and technology, 1988
[NASA-TM-101246] N89-25109

NATIONAL AERONAUTICS AND SPACE ADMINISTRATION. JOHN F. KENNEDY SPACE CENTER, COCOA BEACH, FL.

KSC ice/frost/debris assessment for Space Shuttle Mission STS-30R
[NASA-TM-102147] N89-24412

NATIONAL AERONAUTICS AND SPACE ADMINISTRATION. LYNDON B. JOHNSON SPACE CENTER, HOUSTON, TX.

A method of isolating treadmill shock and vibration on spacecraft
[NASA-TM-100474] N89-24790

Technology transfer: Imaging tracker to robotic controller N89-24828

NATIONAL AERONAUTICS AND SPACE ADMINISTRATION. LANGLEY RESEARCH CENTER, HAMPTON, VA.

Effect of advanced rotorcraft airfoil sections on the hover performance of a small-scale rotor model
[NASA-TP-2832] N89-24264

Computational unsteady aerodynamics for lifting surfaces N89-24284

B-737 flight test of curved-path and steep-angle approaches using MLS guidance
[NASA-TM-101521] N89-24293

Aeroservoelastic modeling and applications using minimum-state approximations of the unsteady aerodynamics
[NASA-TM-101574] N89-24308

An investigation of the Overlap between the Statistical Discrete Gust and the Power Spectral Density analysis methods
[NASA-TM-101571] N89-24310

Aeroservoelastic wind-tunnel investigations using the Active Flexible Wing Model: Status and recent accomplishments
[NASA-TM-101570] N89-24313

Recent activities within the Aeroservoelasticity Branch at the NASA Langley Research Center
[NASA-TM-101582] N89-24314

Results of a parametric aeroelastic stability analysis of a generic X-wing aircraft
[NASA-TM-101572] N89-24324

Multidisciplinary optimization for engineering systems: Achievements and potential
[NASA-TM-101566] N89-24508

On the causality of plasma permittivity
[NASA-TM-101551] N89-24514

CSM testbed development and large-scale structural applications
[NASA-TM-4072] N89-24624

Research in structures, structural dynamics and materials, 1989
[NASA-CP-10024] N89-24626

Computational Methods for Structural Mechanics and Dynamics, part 1
[NASA-CP-3034-PT-1] N89-24638

Nonlinear response of a blade-stiffened graphite-epoxy panel with a discontinuous stiffener: Work in progress N89-24641

Exploiting symmetries in the modeling and analysis of tires N89-24653

Computational Methods for Structural Mechanics and Dynamics
[NASA-CP-3034-PT-2] N89-24654

Recent developments in deployment analysis simulation using a multi-body computer code N89-24660

Dynamic analysis of space structures including elastic, multibody, and control behavior N89-24661

Large-scale structural analysis: The structural analyst, the CSM Testbed and the NAS System
[NASA-TM-100643] N89-24673

Characterization of the bending stiffness of large space structure joints
[NASA-TM-101565] N89-24676

Development of higher-order modal methods for transient thermal and structural analysis
[NASA-TM-101548] N89-24677

Results of the Round Robin on opening-load measurement conducted by ASTM Task Group E24.04.04 on Crack Closure Measurement and Analysis
[NASA-TM-101601] N89-24679

Global/local stress analysis of composite panels
[NASA-TM-101622] N89-24681

The Fault Tree Compiler (FTC): Program and mathematics
[NASA-TP-2915] N89-24815

Numerical integration of asymptotic solutions of ordinary differential equations
[NASA-TM-100650] N89-24867

Advanced turboprop aircraft flyover noise: Annoyance to counter-rotating-propeller configurations with a different number of blades on each rotor: Preliminary results
[NASA-TM-100638] N89-24888

Kaon-nucleus scattering
[NASA-TP-2920] N89-25103

Charge exchange transition probability for collisions between unlike ions and atoms within the adiabatic approximation
[NASA-TM-101559] N89-25104

Space Station Freedom Structural Characterization Experiment (SCE) node code
[NASA-TM-101594] N89-25110

Langley aerospace test highlights, 1988
[NASA-TM-101579] N89-25112

NATIONAL AERONAUTICS AND SPACE ADMINISTRATION. LEWIS RESEARCH CENTER, CLEVELAND, OH.

Conservative treatment of boundary interfaces for overlaid grids and multi-level grid adaptations
[NASA-TM-102080] N89-24269

Transient flow thrust prediction for an ejector propulsion concept
[NASA-TM-102078] N89-24318

A model for prediction of STOVL ejector dynamics
[NASA-TM-102098] N89-24319

Turbomachinery technology for high-speed civil flight
[NASA-TM-102092] N89-24320

The Pathfinder Chemical Transfer Propulsion program
[NASA-TM-102084] N89-24409

Fire safety applications for spacecraft
[NASA-TM-101463] N89-24413

Review of the environmental effects of the Space Station Freedom photovoltaic power module
[NASA-TM-102076] N89-24418

Energy storage and thermal control system design status
[NASA-TM-102136] N89-24427

Performance of large area xenon ion thrusters for orbit transfer missions
[NASA-TM-102049] N89-24436

Concentration of off-axis radiation by solar concentrators for space power
[NASA-TM-102052] N89-24438

Space Station Freedom electrical power system hardware commonality with the United States Polar Platform
[NASA-TM-102074] N89-24439

Flight experiment of thermal energy storage
[NASA-TM-102081] N89-24440

Summary and evaluation of the Strategic Defense Initiative Space Power Architecture Study
[NASA-TM-102012] N89-24443

A numerical study of chemically reacting flow in nozzles
[NASA-TM-102135] N89-24444

The 5-kW arcjet power electronics
[NASA-TM-102108] N89-24446

Liquid oxygen cooling of hydrocarbon fueled rocket thrust chambers
[NASA-TM-102113] N89-24447

Space Station Freedom Solar Array design development
[NASA-TM-102105] N89-24448

Isotopic study of oxygen diffusion in oxide coatings
[NASA-TM-102082] N89-24451

Composite Blade Structural Analyzer (COBSTRAN) demonstration manual
[NASA-TM-101957] N89-24459

Isothermal life prediction of composite lamina using a damage mechanics approach
[NASA-TM-102032] N89-24460

Time dependent reliability model incorporating continuum damage mechanics for high-temperature ceramics
[NASA-TM-102046] N89-24487

Microwave characteristics of GaAs MMIC integratable optical detectors
[NASA-TM-101485] N89-24520

Photovoltaic power system operation in the Mars environment
[NASA-TM-102075] N89-24529

Nonlinear evolution of interacting oblique waves on two-dimensional shear layers
[NASA-TM-102030] N89-24575

Some characteristics of bypass transition in a heated boundary layer
[NASA-TM-102126] N89-24577

Holographic interferometry with an injection seeded Nd:YAG laser and two reference beams
[NASA-TM-102056] N89-24591

On the dynamic response of pressure transmission lines in the research of helium-charged free piston Stirling engines
[NASA-TM-102121] N89-24593

Comparison of predicted and measured temperatures of UH-60A helicopter transmission
[NASA-TP-2911] N89-24607

Tribology: The Story of Lubrication and Wear
[NASA-TM-101430] N89-24635

Solid lubricant materials for high temperatures: A review N89-24636

Space Photovoltaic Research and Technology, 1988. High Efficiency, Space Environment, and Array Technology
[NASA-CP-3030] N89-24704

Progress in indium phosphide solar cell research N89-24707

Predicted performance of InP solar cells in Cassegrainian and slats space concentrator arrays at 20 to 100 AM0, 80 to 100 C N89-24711

Ultra-thin, light-trapping silicon solar cells N89-24719

High efficiency GaAs-Ge tandem solar cells grown by MOCVD N89-24721

Chemical etching and organometallic chemical vapor deposition on varied geometries of GaAs N89-24728

Domed Fresnel lens concentrator technology for space application N89-24732

A comparison of the radiation tolerance characteristics of multijunction solar cells with series and voltage-matched configurations N89-24737

Neuromorphic learning of continuous-valued mappings in the presence of noise: Application to real-time adaptive control
[NASA-TM-101999] N89-24856

On the equivalence of a class of inverse decomposition algorithms for solving systems of linear equations
[NASA-TM-102036] N89-24865

Cruise noise of the SR-2 propeller model in a wind tunnel
[NASA-TM-101480] N89-24886

Initial characterization of a modular heat exchanger with an integral heat pipe
[NASA-TM-102097] N89-25078

NATIONAL AERONAUTICS AND SPACE ADMINISTRATION. MARSHALL SPACE FLIGHT CENTER, HUNTSVILLE, AL.

Containerless glass fiber processing
[NASA-TM-86540] N89-24405

A methodology for commonality analysis, with applications to selected space station systems
[NASA-TM-100364] N89-24421

Pressure-volume properties of metallic bellows
[NASA-TM-100365] N89-24422

Space Shuttle Main Engine High Pressure Fuel Turbopump turbine blade cracking
[NASA-TM-100327] N89-24435

Further developments in modeling digital control systems with MA-prefiltered measurements
[NASA-TP-2909] N89-24507

A noncontacting scanning photoelectron emission technique for bonding surface cleanliness inspection
[NASA-TM-100361] N89-24623

An automated protein crystal growth facility on the space station N89-24820

High level intelligent control of telerobotics systems N89-24823

Orbital Maneuvering Vehicle (OMV) remote servicing kit N89-24838

Using a simulation assistant in modeling manufacturing systems N89-24849

NATIONAL AEROSPACE LAB., TOKYO (JAPAN).

Calculation of scramjet performance
[NAL-TR-987] N89-24317

Wind tunnel tests on flutter control of a high-aspect-ratio cantilevered wing
[NAL-TR-978] N89-24321

Computational and experimental research on buffet phenomena of transonic airfoils
[NAL-TR-996T] N89-24322

Development of the cryopanel for tests of xenon ion thrusters
[NAL-TR-981] N89-24431

Thermal radiation from plumes of solid propellant rockets
[NAL-TR-990] N89-24432

An atomic oxygen generation facility for space environmental testings
[NAL-TR-969] N89-24506
Interaction mechanisms between tip leakage flow and the passage vortex in a linear turbine rotor cascade
[NAL-TR-983T] N89-24536
Three-dimensional flows and loss generation mechanisms in a linear turbine rotor cascade at various incidence conditions
[NAL-TR-984T] N89-24537
A remote laser-probing system for combustion measurements
[NAL-TR-979] N89-24598
Analysis of adaptive planar truss structures
[NAL-TR-988] N89-24625
Experimental component mode synthesis applied to the solar array type structure
[NAL-TR-994] N89-24702
Determination of station coordinates, earth rotation and plate motions from LAGEOS laser ranging: 1983-1986
[NAL-TR-980T] N89-24753
High speed implementation of NAL application software packages
[NAL-TR-986] N89-24801
The development of a Job-Jobstep scheduler for NS system
[NAL-TR-977] N89-24814
Study of chemical reaction models for high enthalpy flow of air
[NAL-TR-982] N89-25072

NATIONAL CLIMATIC CENTER, ASHEVILLE, NC.
Climatic atlas of the outer continental shelf waters and coastal regions of Alaska. Volume 3: Chukchi-Beaufort Sea
[AD-A206525] N89-24776

NATIONAL COMMUNICATIONS SYSTEM, WASHINGTON, DC.
Investigation of vector quantization for the coding gray scale images for Group 4 facsimile
[AD-A206546] N89-24809

NATIONAL OCEANIC AND ATMOSPHERIC ADMINISTRATION, WASHINGTON, DC.
Simulation studies of improved sounding systems
[NASA-CR-185322] N89-24758

NATIONAL SEVERE STORMS LAB., NORMAN, OK.
Ground cluster filters for staggered pulse trains
[DOT/FAA/SA-89/2] N89-24515
Efficient dealiasing of Doppler velocities using local environment constraints
[DOT/FAA/SA-89/1] N89-24771

NATURAL ENVIRONMENTAL RESEARCH COUNCIL, LONDON (ENGLAND).
The activities of the British National Space Centre (BNSC) in the field of imaging spectrometry N89-24696

NAVAL OCEANOGRAPHY COMMAND DETACHMENT, ASHEVILLE, NC.
Climatic atlas of the outer continental shelf waters and coastal regions of Alaska. Volume 3: Chukchi-Beaufort Sea
[AD-A206525] N89-24776

NAVAL POSTGRADUATE SCHOOL, MONTEREY, CA.
Boundary layer response to an unsteady turbulent environment
[AD-A206578] N89-24273
Modeling transient thermal behavior in a thrust vector control jet vane
[AD-A206532] N89-24441
Computer simulation of copper in the liquid phase and the sputtering of liquid copper by one KeV argon ions
[AD-A206264] N89-24476
The effect of heat input and composition on weld metal microstructures in thin section HY-130 GMAW weldments
[AD-A206476] N89-24477
AR (Autoregressive) modeling of coherence in time delay and doppler estimation
[AD-A205239] N89-24513
Channel and switchbox routing using a greedy based channel algorithm with outward scanning technique
[AD-A206545] N89-24526
Natural convection cooling of a 3 by 3 array of rectangular protrusions in an enclosure filled with dielectric liquid: Effects of boundary conditions and component orientation
[AD-A206474] N89-24571
Correlation between satellite-derived aerosol characteristics and oceanic dimethylsulfide (DMS)
[AD-A206179] N89-24759
Study of explosive and nonexplosive cyclogenesis during FGGE
[AD-A206521] N89-24775
A systolic array structure for on-line system identification
[AD-A206412] N89-24806
Self-circumference in the Minkowski plane
[AD-A205691] N89-24868
The use of seaplanes as an advanced weapon system
[AD-A206243] N89-24880

NAVAL RESEARCH LAB., WASHINGTON, DC.
The experiments of LIPS 3 N89-24735

NAVAL SHIP RESEARCH AND DEVELOPMENT CENTER, BETHESDA, MD.
X-ray photoelectron spectroscopy study of samples in the Y-Ba-Cu-O system
[AD-A206260] N89-25060

NORTH CAROLINA UNIV., CHAPEL HILL.
In-situ stress measurements during thermal oxidation of silicon
[AD-A206546] N89-24495
Effects of thermal history on stress-related properties of very thin films of thermally grown silicon dioxide, SiO2
[AD-A206547] N89-25062

NORTHWESTERN UNIV., EVANSTON, IL.
Explicit, implicit, and hybrid methods N89-24656

NOTRE DAME UNIV., IN.
Optoelectronic velocimeter development
[DE89-012283] N89-24597

NUCLEAR UTILITY SERVICES, INC., GAITHERSBURG, MD.
Safety analysis report for the Galileo Mission. Volume 3, book 1: Nuclear risk analysis document, revision 1
[DE89-007272] N89-24898
Safety analysis report for the Galileo Mission. Volume 3, book 2: Nuclear risk analysis document. Appendices, revision 1
[DE89-007273] N89-24899

O

OAK RIDGE NATIONAL LAB., TN.
Multiplexed electronically programmable multimode ionization detector for chromatography
[DE89-009758] N89-24465
Weldability and microstructural characterization of Al-Li alloys
[DE89-010183] N89-24478
Ceramic Technology for Advanced Heat Engines Project data base
[DE89-012888] N89-24499
Ceramic technology for advanced heat engines project
[DE89-012890] N89-24500
ICRF antenna designs for CIT and Alcator C-Mod
[DE89-011579] N89-24521
Optoelectronic velocimeter development
[DE89-012283] N89-24597
Advanced servomanipulator remote maintenance demonstration
[DE89-010188] N89-24614
Bibliography on tropical rain forests and the global carbon cycle. Volume 2: South Asia
[DE89-008971] N89-24748
How to (and not to) introduce computer graphics to design professionals
[DE89-010374] N89-24812
A comparison of two real-time control schemes for redundant robots with bounded joint velocities
[DE89-002974] N89-24861
The role of the radial electric field in enhanced confinement regimes in stellarators
[DE89-011572] N89-25049
Numerical methods for stellarator optimization
[DE89-012342] N89-25050

OBSERVATOIRE DE MARSEILLE (FRANCE).
Gas flow in and around bars N89-24965

OBSERVATOIRE DE PARIS-MEUDON (FRANCE).
Extended coronal shock waves and electron acceleration during solar flares N89-24934

OBSERVATORIUM FUER SOLARE RADIOASTRONOMIE, POTSDAM (GERMAN D.R.).
Tremsdorf solar radio astronomy observatory: The scientific program and an interesting observation N89-24999

OBSERVATORIUM FUER SOLARE RADIOASTRONOMIE, TREMSDORF (GERMAN D.R.).
Coronal magnetic field strengths determined from fiber bursts N89-25002
Long-term evolution of coronal magnetic fields based on noise storm continuum observations in the 20th and 21st cycle N89-25003
Chaotic radiopulsations and coronal magnetic field estimates N89-25006

OFFICE NATIONAL D'ETUDES ET DE RECHERCHES AEROSPATIALES, PARIS (FRANCE).
Development of a supersonic turbulent boundary layer on a heated wall. Properties of the turbulent field and theoretical application
[ONERA-RSF-74/7078-AY-096-A] N89-24275
Ground vibration test of the Foudre A04 Transall aircraft
[REPT-20/7234-PY-382-R] N89-24311
Study of damage in composite materials
[ONERA-RT-4/7256-RY-070-R] N89-24458
Fundamental studies on order effects in metal alloys
[ONERA-RT-14/221-M] N89-24480
Interaction between an oblique shock wave and a turbulent boundary layer
[ONERA-RT-76/7078-AY-096-A] N89-24574
Lightning inflight study onboard a Transall aircraft. Definition of the onboard instruments
[ONERA-RF-19/7234-PY] N89-24777

OFFICE NATIONAL D'ETUDES ET DE RECHERCHES AEROSPATIALES, TOULOUSE (FRANCE).
Effects of unsteadiness on turbulent boundary layers N89-24280

OFFICE OF TECHNOLOGY ASSESSMENT, WASHINGTON, DC.
The electronic supervisor: New technology, new tensions
[OTA-CIT-333] N89-24804

OHIO STATE UNIV., COLUMBUS.
Analysis of the EM scattering from arbitrary open-ended waveguide cavities using axial Gaussian Beam tracking
[NASA-CR-185054] N89-24518
A hybrid asymptotic-modal analysis of the EM scattering by an open-ended S-shaped rectangular waveguide cavity
[NASA-CR-185053] N89-24519
Nd:YAG laser weldability of RS/PM Al-BFe-2Mo sheet
[DE89-013588] N89-24621
Universal reduction of T(subc) in strong coupling superconductors due to Anderson/Kondo impurities
[DE89-011225] N89-25071

OKLAHOMA UNIV., NORMAN.
An integrated aerodynamic/propulsion study for generic aero-space planes based on waverider concepts
[NASA-CR-183389] N89-24315

OLD DOMINION UNIV., NORFOLK, VA.
Navier-Stokes analysis of cold scramjet-afterbody flows
[NASA-CR-184949] N89-24562

OLIS ENGINEERING, SEDALIA, CO.
Inflatable end effector tools N89-24839

ORTEL CORP., ALHAMBRA, CA.
Vertical emitting, ring geometry, ultra-low threshold and ultra-high speed quantum well lasers for optical interconnect
[AD-A206427] N89-24603

OSSERVATORIO ASTRONOMICO, TURIN (ITALY).
Synchrotron thermal instabilities and filamentation in radio sources N89-24958

OXFORD UNIV. (ENGLAND).
Experimental techniques in unsteady flows N89-24279

P

PACIFIC NORTHWEST LABS., RICHLAND, WA.
Analysis of packed-particle rearrangement during colloidal ceramic processing: Gamma-ray densitometry and a review of alternative methods
[DE89-009066] N89-24489
US fuel cell research and applications, 1960--1989
[DE89-012244] N89-24745
Characterizing the energy deposition events produced by trapped protons in low earth orbit
[DE89-011218] N89-24893

PENNSYLVANIA STATE UNIV., UNIVERSITY PARK.
On specimen shape effects and the ductility of porous metals
[AD-A206216] N89-24475
Real-time system: Specification and verification
[AD-A206467] N89-24807
Electron transfer, ionization, and excitation in atomic collisions
[DE89-010046] N89-24891

PIANO SPAZIALE NAZIONALE, ROME (ITALY).
Scientific utilization of the European space infrastructure and the International Space Station N89-24390

PLANETARY SCIENCE INST., TUCSON, AZ.
Comparative planetology of early intense cratering and other cratering effects
[NASA-CR-182966] N89-24752

POLISH ACADEMY OF SCIENCES, WARSAW.
ELF plasma turbulence observed by Prognoz-8 in plasma jets in the magnetospheric tail N89-25020
A model of the reconnection pattern at the heliopause N89-25027

POWER SPECTRA, INC., FREMONT, CA.
A longlife, highvoltage, shortpulse generator based on optically activated Bulk Avalanche Semiconductor Switch, phase 2
[AD-A206078] N89-24527

PREUSSAG A.G., ERDOEL UND ERDGAS, HANNOVER (GERMANY, F.R.).
Industrial utilization of microgravity: Problems in the realization phase N89-24383
PRINCETON UNIV., NJ.
Oxide-bound transition metal complexes for methane activation
[PB89-136614] N89-24464
The case for a primordial galactic field N89-24939
Self-consistent models of spherical accretion onto black holes N89-25095
PURDUE UNIV., WEST LAFAYETTE, IN.
Efficiency study of oil cooling of a screw compressor
[DE89-011417] N89-24618

R

REMTECH, INC., HUNTSVILLE, AL.
SRB ascent aerodynamic heating design criteria reduction study, volume 2
[NASA-CR-183569] N89-24430
RENSSELAER POLYTECHNIC INST., TROY, NY.
Aerodynamics of a lifting rotor due to near field unsteady effects N89-24267
Encapsulated diffusion of sulphur into InP N89-24714
RESEARCH INST. FOR ADVANCED COMPUTER SCIENCE, MOFFETT FIELD, CA.
Domain decomposition algorithms and computation fluid dynamics
[NASA-CR-185405] N89-24578
Totally parallel multilevel algorithms
[NASA-CR-185404] N89-24818
RESEARCH TRIANGLE INST., RESEARCH TRIANGLE PARK, NC.
Applications of aerospace technology
[NASA-CR-181536] N89-25076
REXHAM AEROSPACE AND DEFENSE GROUP, HUNTSVILLE, AL.
Stabilized image system for mobile robots N89-24829
ROBOTIC VISION SYSTEMS, INC., MELVILLE, NY.
A system for high resolution 3D mapping using laser radar and requiring no beam scanning mechanisms N89-24827
ROCKWELL INTERNATIONAL CORP., DOWNEY, CA.
Local stiffener and skin pocket buckling prediction by special PASCO modeling technique: Correlation to test data N89-24628
ORU guidelines for telerobotic compatibility N89-24844
ROCKWELL INTERNATIONAL CORP., GOLDEN, CO.
Effects of multiple reductions on grain refinement during hot working of alloy 718
[DE89-010426] N89-24483
ROYAL INST. OF TECH., STOCKHOLM (SWEDEN).
Development of astrophysics from the telescope to the Sputnik N89-24911
Astrophysical significance of observations and experiments in the earth's magnetosphere N89-24912
ROYAL OBSERVATORY, EDINBURGH (SCOTLAND).
The formation of interstellar clouds N89-24935
RUHR UNIV., BOCHUM (GERMANY, F.R.).
Aspects of three-dimensional magnetic reconnection N89-24975
Particle simulation of magnetic reconnection in collision-free plasma sheets N89-24986
The role of magnetic reconnection in magnetotail plasmoid dynamics N89-25014
Plasma induced changes of a metallic divertor neutralizer plate from ASDEX analyzed by photoacoustics N89-25048
RUTGERS - THE STATE UNIV., NEW BRUNSWICK, NJ.
Empirical analysis and refinement of expert system knowledge bases
[AD-A206226] N89-24858

S

SAINT ANDREW'S UNIV. (SCOTLAND).
Thermal instability in a stratified plasma N89-24924
Structuring of plasmas by a magnetic field N89-24938
Comparison of compressible and incompressible models of reconnection N89-24982
Magnetic energy conversion on the sun N89-24987
Three-dimensional reconnection from a global viewpoint N89-24988
On the MHD stability of the M=1 kink mode in finite length coronal loops N89-24992
SAN DIEGO SEMICONDUCTORS, INC., CA.
Position-sensitive CdTe detector using improved crystal growth method
[NASA-CR-183427] N89-25051
SANDIA NATIONAL LABS., ALBUQUERQUE, NM.
Status of the direct absorption receiver panel research experiment: Salt flow and solar test requirements and plans
[DE89-010968] N89-24461
Modeling thermal-mechanical processes associated with the initiation and combustion of granular energetic materials
[DE89-007145] N89-24472
Sol-gel processing of controlled pore films
[DE89-013584] N89-24501
The frequency response of phased-array antennas
[DE89-009710] N89-24517
Analysis of a probe-metallic sleeve feed system for a rectangular waveguide
[DE89-006769] N89-24523
Two-dimensional phase correction of synthetic aperture radar imagery
[DE89-007086] N89-24524
Electrophoretically applied dielectrics for amorphous metal foils used in pulsed power saturable reactors
[DE89-009322] N89-24525
Radiation hardened, optically-triggered thyristor switches: Preliminary data on three device designs
[DE89-011469] N89-24533
Two-phase flow measurements by nuclear magnetic resonance imaging
[DE89-011850] N89-24586
Demonstration of a Time Projection Compton Spectrometer
[DE89-010743] N89-24598
Vision system testing for teleoperated vehicles
[DE89-009713] N89-24610
Incorporation of surface tension into the structural finite element code SANCHO
[DE89-011354] N89-24616
Cavity dimensions for high velocity penetration events: A comparison of calculational results with data
[DE89-011351] N89-24617
Diffusion welding of electrical interconnects to silicon solar cells
[DE89-012250] N89-24620
Dynamics and static behavior of metal gussets in cask impact limiters
[DE89-011879] N89-24683
The 25 percent-efficient GaAs Cassegrainian concentrator cell N89-24733
Development of a man-portable control unit for a teleoperated land vehicle N89-24835
A demonstration of retro-traverse using a semi-autonomous land vehicle N89-24852
An analytical study of a vibration test method using extremal control of acceleration and force
[DE89-007428] N89-24884
A facilities view of the low volume, high product mix fab
[DE89-009970] N89-25057
SCHOOL OF AEROSPACE MEDICINE, BROOKS AFB, TX.
Cerebral laterality and handedness in aviation: Performance and selection implications
[AD-A206196] N89-24787
SCRIPPS INSTITUTION OF OCEANOGRAPHY, LA JOLLA, CA.
Biooptical variability in the Greenland Sea observed with the Multispectral Airborne Radiometer System (MARS)
[NASA-CR-184856] N89-24784
SCUOLA NORMALE SUPERIORE, PISA (ITALY).
Some dynamical properties of anisotropic collisionless stellar systems N89-24963
SELENIA SPAZIO S.P.A., ROME (ITALY).
The Columbus crew communication subsystem and the on board local area network N89-24397
SLOVAK ACADEMY OF SCIENCES, TATRANSKA LOMNICA (CZECHOSLOVAKIA).
The relation between H-alpha and SXR emission of the flares N89-25000
SMITHSONIAN ASTROPHYSICAL OBSERVATORY, CAMBRIDGE, MA.
The application of two-dimensional imaging to very high energy gamma ray astronomy
[DE89-013614] N89-25089
SOCIETE EUROPEENE DE PROPULSION, SAINT-MEDARD-EN-JALLES (FRANCE).
Ariane 5 solid boosters: Overview of design approach and envisaged technologies N89-24352
SOLAREX CORP., NEWTOWN, PA.
Research on high-efficiency, single-junction, monolithic, thin-film amorphous silicon solar cells, phase 2
[DE89-000849] N89-24703
SOREQ RESEARCH ESTABLISHMENT, ISRAEL ATOMIC ENERGY COMMISSION, YAVNEH.
High-pressure two temperature equations of state N89-24967
Induced annihilation of particle-antiparticle pairs N89-24970
SOUTHERN METHODIST UNIV., DALLAS, TX.
Cut-and-connect of two antiparallel vortex tubes N89-24559
SOUTHERN UNIV., BATON ROUGE, LA.
Mass spectrometry
[DE89-011118] N89-24471
SOUTHWEST RESEARCH INST., SAN ANTONIO, TX.
Laser-induced-fluorescence inspection of polyurethane and related materials, phase 1
[AD-A206423] N89-24492
Characterization of pore evolution in ceramics during creep failure and densification
[DE89-013599] N89-24502
Role of sulfur oxides in wear and deposit formation in Army diesel engines
[AD-A206054] N89-24613
SPARTA, INC., HUNTSVILLE, AL.
IRIS: An intelligent robot insertion expert system N89-24854
SPECIAL ASTROPHYSICAL OBSERVATORY, NISHNYI ARCHYS (USSR).
Search for a fine-time structure in flares of UV Cet-type stars N89-25007
SPECTROLAB, INC., SYLMAR, CA.
Gallium Arsenide welded panel technology for advanced spaceflight applications N89-24731
SPIRE CORP., BEDFORD, MA.
InP shallow-homojunction solar cells N89-24708
SRI INTERNATIONAL CORP., MENLO PARK, CA.
Formal verification of a fault tolerant clock synchronization algorithm
[NASA-CR-4239] N89-24803
Formal verification of AI software
[NASA-CR-181827] N89-24811
A deductive approach to automated planning
[AD-A206253] N89-24860
Free radical-surface interactions using multiphoton ionization of free radicals
[AD-A206257] N89-24892
STANFORD LINEAR ACCELERATOR CENTER, CA.
Beam dynamics with the Hamilton-Jacobi equation
[DE89-012269] N89-24878
STANFORD UNIV., CA.
Studying Turbulence Using Numerical Simulation Databases, 2. Proceedings of the 1988 Summer Program
[NASA-CR-184905] N89-24538
Phase decorrelation, streamwise vortices and acoustic radiation in mixing layers N89-24541
A numerical study of bifurcations in a barotropic shear flow N89-24542
Dynamics of coherent structures in a plane mixing layer N89-24543
Scalar entrainment in the mixing layer N89-24545
Use of passive scalar tagging for the study of coherent structures in the plane mixing layer N89-24546
Sampling inhomogeneous turbulent fields N89-24548
Dynamical interpretation of conditional patterns N89-24549
Pressure-strain-rate events in homogeneous turbulent shear flow N89-24551
Multifractal spectra in homogeneous shear flow N89-24552
Eddies, streams, and convergence zones in turbulent flows N89-24555
The structure of sheared turbulence near a plane boundary N89-24557
Analysis of homogeneous turbulent reacting flows N89-24558
Head-on collision of viscous vortex rings N89-24560
Optical propagation through a homogeneous turbulent shear flow N89-24561
Photothermal imaging of high T(sub c) superconductor
[DE89-009844] N89-25054
STATE UNIV. OF NEW YORK, BUFFALO.
Deep levels and radiation effects in p-InP N89-24713
STATE UNIV. OF NEW YORK, PLATTSBURGH.
The effects of blast trauma (impulse noise) on hearing: A parametric study
[AD-A206180] N89-24786
Non-destructive analyses of cometary nucleus samples using synchrotron radiation
[DE89-012536] N89-25101
STERLING FEDERAL SYSTEMS, INC., PALO ALTO, CA.
Turbulent flow in a 180 deg bend: Modeling and computations
[NASA-CR-4141] N89-24579
Transpiration cooling of hypersonic blunt bodies with finite rate surface reactions
[NASA-CR-177516] N89-24580
STEVENS INST. OF TECH., HOBOKEN, NJ.
Insertion with two coordinated arms N89-24837
STUTTGART UNIV. (GERMANY, F.R.).
Safety in manned space flight N89-24402

SVERDRUP TECHNOLOGY, INC., CLEVELAND, OH.
A premixed hydrogen/oxygen catalytic igniter [NASA-CR-185113] N89-24445
Aging behavior of Au-based ohmic contacts to GaAs N89-24727
NASA Lewis Stirling engine computer code evaluation [NASA-CR-182248] N89-24741
SWEDISH DEFENCE RESEARCH ESTABLISHMENT, LINKOEPING.
Electrooptical feed and control in microwave applications [FOA-C-30514-3.2] N89-24531
SWEDISH DEFENCE RESEARCH ESTABLISHMENT, STOCKHOLM.
The night and adverse weather capability of ground attack aircraft [FOA-C-20745-2.5] N89-24312
Control research in windpower project 506259 utilization [FOA-C-20746-2.7] N89-24740
SWEDISH INST. OF SPACE PHYSICS, KIRUNA.
SPECTRUM: A computer algorithm to derive the flux-energy spectrum of precipitating particles from EISCAT electron density profiles [IRF-TR-034] N89-24764
SYSTEMS RESEARCH LABS., INC., DAYTON, OH.
The AAMRL (Armstrong Aerospace Medical Research Laboratory) biodynamics data bank [AD-A206139] N89-25074

T

TACTICAL WEAPONS GUIDANCE AND CONTROL INFORMATION ANALYSIS CENTER, CHICAGO, IL.
Conference on Space and Military Applications of Automation and Robotics [AD-A198095] N89-24819
TAU CORP., LOS GATOS, CA.
Optimal guidance with obstacle avoidance for nap-of-the-earth flight [NASA-CR-177515] N89-24328
TECH-U-FIT CORP., ALEXANDRIA, VA.
Testing the feasibility of using a teleoperated robot for remote, dexterous operations N89-24843
TECHNISCHE HOCHSCHULE, AACHEN (GERMANY, F.R.).
Unsteady aerodynamic effects on bluff bodies N89-24278
TECNOSPAZIO S.P.A., MILAN (ITALY).
Multiple robot approach for automation of in-orbit modules N89-24389
TELEDYNE BROWN ENGINEERING, HUNTSVILLE, AL.
The impact of an IVA robot on the space station microgravity environment N89-24821
Ground control of space based robotic systems N89-24845
TELESPAZIO, S.P.A., ROME (ITALY).
The key role of Data Relay System (DRS) in the Columbus communications N89-24379
TENNESSEE VALLEY AUTHORITY, NORRIS.
The importance of climatological variability and the rate at which waste is added to modeling water budget of landfills [DE89-008917] N89-24747
TEXAS A&M UNIV., COLLEGE STATION.
Tele-autonomous control involving contacts: The applications of a high precision laser line range sensor [NASA-CR-184995] N89-24509
Basic flow field and heat transfer studies about three cylinders of different diameter in transverse flow N89-24564
A study of composite plates with holes/inclusions N89-24627
A study of material damping in large space structures [NASA-CR-180076] N89-24634
Contact solution algorithms N89-24652
Microscopic delamination processes and the resulting crack tip strain fields of graphite/epoxy composites N89-24671
Improved analysis of laminated heterogeneous beams and associated formulation of a new finite element method N89-24672
TEXAS UNIV., AUSTIN.
Adaptive methods, rolling contact, and nonclassical friction laws N89-24651
Laser ranging data analysis [NASA-CR-184847] N89-24754
Time variations in the earth's gravity field from Starlette orbit analysis N89-24766
A study of the Southern Supercluster N89-25088
TOKYO UNIV., TANASHI (JAPAN).
Path integral and operator formalism on bordered Riemann surfaces [DE88-757229] N89-24881
TOLEDO UNIV., OH.
Semiempirical studies of atomic structure [DE89-011419] N89-24894
TOULON UNIV. (FRANCE).
Plasma and propagation in auroral and polar ionosphere [ETN-89-94519] N89-24761
TOYAMA UNIV. (JAPAN).
Non-steady astrophysical spiral jets driven by magnetic collapse and pressure N89-24920
Particle acceleration by magnetic reconnection and fast magnetosonic shock waves in solar flares N89-24993
TREC, INC., HUNTSVILLE, AL.
Two dimensional convolute integer technology for digital image processing N89-24830
TRW SPACE TECHNOLOGY LABS., LOS ANGELES, CA.
Influence of time lag and noncolocation on integrated structural/control system designs N89-24630
TRW SPACE TECHNOLOGY LABS., REDONDO BEACH, CA.
The impact of solar cell technology on planar solar array performance N89-24715

U

UNITED TECHNOLOGIES RESEARCH CENTER, EAST HARTFORD, CT.
Radiometric measurement of temperature distributions in solar cavity receivers [DE89-011467] N89-24742
UNIVERSISAD DE LOS ANDES, MERIDA (VENEZUELA).
On the thermal stability of optically thin flows N89-24973
UNIVERSITIES SPACE RESEARCH ASSOCIATION, BOULDER, CO.
A visiting scientist program in atmospheric sciences for the Goddard Space Flight Center [NASA-CR-183421] N89-24756
UNIVERSITIES SPACE RESEARCH ASSOCIATION, HUNTSVILLE, AL.
Inlet turbulence intensity level and cross-stream distribution effects on the heat transfer in plane wall jets [NASA-CR-183652] N89-24576
UNIVERSITY COLL., CARDIFF (WALES).
Optimisation of the figure of merit of modified silicon-germanium alloys [AD-A206420] N89-24491
UNIVERSITY OF SOUTHERN CALIFORNIA, LOS ANGELES.
Mechanics/heat-transfer relation for particle flows [DE89-011382] N89-24584

V

VANDERBILT UNIV., NASHVILLE, TN.
A generalized method for automatic downhand and wirefeed control of a welding robot and positioner N89-24846
VARIAN ASSOCIATES, PALO ALTO, CA.
The 280 GHz Gyro-BWO design study [DE89-011644] N89-24595
The 25 percent-efficient GaAs Cassegrainian concentrator cell N89-24733
VIRGINIA POLYTECHNIC INST. AND STATE UNIV., BLACKSBURG.
Unsteady aerodynamics N89-24277
Analysis of the wake behind a propeller using the finite element method with a two-equation turbulence model N89-24286
Numerical simulation of feedback control of aerodynamic configurations in steady and unsteady ground effects N89-24326
Feasibility study of a synthesis procedure for array feeds to improve radiation performance of large distorted reflector antennas [NASA-CR-184974] N89-24511
On computational schemes for global-local stress analysis N89-24645
VON KARMAN INST. FOR FLUID DYNAMICS, RHODE-SAINT-GENESE (BELGIUM).
Unsteady Aerodynamics, volume 1 [VKI-1988-07-VOL-1] N89-24276
Unsteady Aerodynamics, volume 2 [VKI-1988-07-VOL-2] N89-24281
VTE, BRUNSWICK (GERMANY, F.R.).
Status and trends of technological image processing possibilities N89-24306

W

WASHINGTON UNIV., SAINT LOUIS, MO.
Application of the p-version of the finite-element method to global-local problems N89-24648
A new model of PeV gamma-ray sources N89-24946
WAYNE STATE UNIV., DETROIT, MI.
Radiation resistance studies of amorphous silicon films N89-24738
WEST VIRGINIA UNIV., MORGANTOWN.
Computational design of low aspect ratio wing-winglet configurations for transonic wind-tunnel tests [NASA-CR-185016] N89-24266
WESTINGHOUSE RESEARCH AND DEVELOPMENT CENTER, PITTSBURGH, PA.
Response of single junction GaAs/GaAs and GaAs/Ge solar cells to multiple doses of 1 MeV electrons N89-24722
WISCONSIN UNIV., MADISON.
Generalized solution for the optimal prehension state using end effectors with multi-articulated fingers N89-24609
Periodic and heteroclinic orbits for a periodic Hamiltonian system [AD-A204078] N89-24862
The exact condition of the B-spline basis may be hard to determine [AD-A204080] N89-24863
Local corner cutting and the smoothness of the limiting curve [AD-A204092] N89-24864
High energy particles in supernova remnants and the interstellar medium N89-25108
WOVEN STRUCTURES, INC., COMPTON, CA.
Development of tailorable advanced blanket insulation for advanced space transportation systems [NASA-CR-177444] N89-24486

X

XEROX PALO ALTO RESEARCH CENTER, CA.
Visibility with a moving point of view N89-24876

Typical Contract Number Index Listing

Listings in this index are arranged alphanumerically by contract number. Under each contract number the NASA accession numbers denoting documents that have been produced as a result of research done under that contract are arranged in ascending order. The NASA accession number denotes the number by which the citation is identified.

AF PROJ. 2303 ..... N89-24493
N89-24892
N89-25059
AF PROJ. 2304 ..... N89-24570
AF PROJ. 2305 ..... N89-24332
AF PROJ. 3396 ..... N89-25061
AF-AFOSR-0060-87 ..... N89-24332
AF-AFOSR-0073-84 ..... N89-25059
AF-AFOSR-0109-84 ..... N89-25099
AF-AFOSR-0170-87 ..... N89-24570
AF-AFOSR-0202-87 ..... N89-24862
AF-AFOSR-0228-85 ..... N89-24493
AF-AFOSR-0347-86 ..... N89-25061
C-175-81 ..... N89-24973
CPFR-01.20 ..... N89-25027
DA PROJ. 1L1-61102-AH-45-A N89-24264
DA PROJ. 1L1-61103-BH-57 ..... N89-24491
DA PROJ. 1T1-61102-AH-51 ..... N89-24613
DA PROJ. 3M1-61102-BS-15 ..... N89-24786
N89-24791
DAAH01-86-C-0865 ..... N89-24272
DAAK70-85-C-0007 ..... N89-24613
DAAK70-87-C-0043 ..... N89-24613
DAAL03-86-G-0211 ..... N89-24454
DAAL03-87-K-0030 ..... N89-24863
N89-24864
DAAL03-87-K-0043 ..... N89-24862
DAAL03-88-K-0085 ..... N89-24578
DAJA45-87-C-0048 ..... N89-24491
DAMD17-86-C-6172 ..... N89-24786
DCA100-87-C-0078 ..... N89-24809
DE-AA03-76SF-00767 ..... N89-24582
DE-AC01-79ET-32043 ..... N89-24896
N89-24897
DE-AC01-87NE-32134 ..... N89-24898
N89-24899
DE-AC02-76CH-00016 ..... N89-25053
N89-25101
DE-AC02-76CH-03073 ..... N89-24939
DE-AC02-82ER-40063 ..... N89-25089
DE-AC02-83CH-10093 ..... N89-24469
N89-24496
N89-24703
N89-24739
N89-24743
DE-AC03-76SF-00098 ..... N89-24470
N89-24482
N89-24490
N89-24566
N89-24900
N89-25070
DE-AC03-76SF-00515 ..... N89-24878
DE-AC04-76DP-00613 ..... N89-24592
DE-AC04-76DP-00789 ..... N89-24461
N89-24472
N89-24501
N89-24517
N89-24523
N89-24524
N89-24525
N89-24533
N89-24586
N89-24596
N89-24610
N89-24616
N89-24617
N89-24620
N89-24621
N89-24683
N89-24737
N89-24742
N89-24884
N89-25044
N89-25057
DE-AC04-76DP-03533 ..... N89-24483
DE-AC05-84ER-40150 ..... N89-24895
DE-AC05-84OR-21400 ..... N89-24465
N89-24478
N89-24499
N89-24500
N89-24521
N89-24597
N89-24614
N89-24747
N89-24748
N89-24812
N89-24861
N89-25049
N89-25050
DE-AC06-76RL-01830 ..... N89-24489
N89-24745
N89-24893
DE-AC07-76ID-01570 ..... N89-24485
N89-24535
DE-AC09-76SR-00001 ..... N89-24484
N89-24813
DE-AC22-88PC-88947 ..... N89-24583
DE-AF02-86ER-40302 ..... N89-24878
DE-AI01-85CE-50112 ..... N89-24741
DE-AS03-76ER-72012 ..... N89-24582
DE-FC22-83FE-60149 ..... N89-24497
DE-FG01-87CE-15245 ..... N89-24618
DE-FG02-86ER-13549 ..... N89-24891
DE-FG02-87ER-45285 ..... N89-25066
DE-FG02-87ER-45315 ..... N89-25065
DE-FG02-87ER-45326 ..... N89-25071
DE-FG03-86SF-16306 ..... N89-24744
DE-FG03-87ER-13797 ..... N89-25054
DE-FG03-87ER-25037 ..... N89-24578
DE-FG05-84ER-45063 ..... N89-24502
DE-FG05-88ER-13958 ..... N89-24894
DE-FG06-86ER-13530 ..... N89-25022
N89-25023
DE-FG22-86PC-90540 ..... N89-24471
DE-FG22-88PC-88913 ..... N89-24584
DLA900-84-C-0910 ..... N89-24492
DRET-84-003-04 ..... N89-24573
DRET-84-1062 ..... N89-24456
DRET-85-168 ..... N89-24761
DRET-86-34-001 ..... N89-24275
N89-24574
DRET-87-34-001 ..... N89-24458
N89-24480
DRET-87-001 ..... N89-24777
DRET-88-34-001 ..... N89-24311
DRET/ETCA/CMCM-048-201 ..... N89-24457
DTFA01-80-Y-10524 ..... N89-24515
N89-24771
EEC-ST2J-0275-C N89-24926
EG-77-C-01-4042 ..... N89-24496
ESTEC-6988/NL/PP(SC) N89-24370
FAA-T0604-F N89-24291
F08635-83-C-0136 ..... N89-24675
F33615-85-C-0530 ..... N89-25074
F33615-86-C-2723 ..... N89-24726
F33615-88-C-2807 ..... N89-24723
F49620-85-C-0058 ..... N89-24602
F49620-86-C-0134 ..... N89-24572
F49620-86-K-0001 ..... N89-24892
GRI-5086-260-1329 ..... N89-24464
IGPP-89-11 ..... N89-24928
LLNL-89-11 ..... N89-24916
NAGW-78 ..... N89-25017
NAGW-806 ..... N89-24933
N89-24948
NAGW-831 ..... N89-24917
N89-24933
N89-24945
N89-24948
NAGW-1006 ..... N89-24919
NAGW-1239 ..... N89-24972
NAGW-1301 ..... N89-24916
NAGW-1303 ..... N89-24947
NAGW-1404 ..... N89-24889
N89-25099
NAG1-190 ..... N89-24817
NAG1-613 ..... N89-24802
NAG1-625 ..... N89-24266
NAG1-637 ..... N89-24674
NAG1-680 ..... N89-24488
NAG1-811 ..... N89-24562
NAG1-859 ..... N89-24511
NAG1-877 ..... N89-24599
NAG1-886 ..... N89-24315
NAG1-939 ..... N89-24873
NAG2-208 ..... N89-25081
NAG3-422 ..... N89-24725
NAG3-476 ..... N89-24518
N89-24519
NAG3-534 ..... N89-24669
NAG3-833 ..... N89-24738
NAG5-459 ..... N89-24757
NAG5-841 ..... N89-25079
NAG5-1010 ..... N89-24686
NAG5-1021 ..... N89-24754
NAG5-1022 ..... N89-24784
NAG5-1024 ..... N89-24509
NAG5-1047 ..... N89-24608
NAG8-78 ..... N89-24755
NAG8-033 ..... N89-24770
NAG9-192 ..... N89-24634
NASA ORDER A-72865-C N89-24450
NASA ORDER C-99066-G N89-24575
N89-24865
N89-24872
NASW-3782 ..... N89-24752
NASW-3841 ..... N89-25076
NASW-4003 ..... N89-24406
NASW-4071 ..... N89-24792
N89-24794
NASW-4234 ..... N89-24818
NAS1-17067 ..... N89-24803
NAS1-17536 ..... N89-24678
NAS1-18018 ..... N89-24772
NAS1-18019 ..... N89-24797
NAS1-18029 ..... N89-24316
NAS1-18107 ..... N89-24816
NAS1-18226 ..... N89-24811
NAS1-18240 ..... N89-24581
NAS1-18444 ..... N89-24637
NAS1-18605 ..... N89-24568
N89-24816
N89-24883
NAS2-11555 ..... N89-24579
N89-24580
NAS2-12253 ..... N89-24486
NAS2-12402 ..... N89-24328
NAS2-12801 ..... N89-24287
NAS3-23351 ..... N89-24530
NAS3-24105 ..... N89-24741
NAS3-24564 ..... N89-24532
NAS3-25082 ..... N89-24448
NAS3-25266 ..... N89-24445
NAS5-28135 ..... N89-24756
NAS5-28713 ..... N89-24590
NAS5-28755 ..... N89-24687
NAS5-30289 ..... N89-25051
NAS7-999 ..... N89-24601
NAS8-30490 ..... N89-24449
N89-24594
NAS8-35322 ..... N89-24430
NAS8-36108 ..... N89-24410
NAS8-36284 ..... N89-24433
NAS8-36433 ..... N89-24434
NAS8-36638 ..... N89-24793
N89-24795
NAS8-36721 ..... N89-24466

NAS8-36955 ..... N89-24463
N89-24746
NAS8-37130 ..... N89-24576
NAS8-37282 ..... N89-24437
NAS9-17853 ..... N89-24415
NCC2-308 ..... N89-25099
NCC2-387 ..... N89-24578
NCC2-433 ..... N89-24265
NCC2-460 ..... N89-24538
NCC2-484 ..... N89-24569
NCC3-99 ..... N89-24487
NEA-506259-4 ..... N89-24740
NSF AST-85-03093 ..... N89-24916
NSF AST-86-1279 ..... N89-24947
NSF AST-86-00308 ..... N89-24919
NSF AST-86-11784 ..... N89-25106
NSF AST-86-15325 ..... N89-24947
NSF AST-86-15816 ..... N89-24916
N89-24928
NSF ATM-85-13215 ..... N89-25017
NSF ATM-85-19528 ..... N89-24972
NSF ATM-85-21115 ..... N89-25022
N89-25023
NSF ATM-86-00509 ..... N89-24548
N89-24549
NSF ATM-87-16770 ..... N89-24917
N89-24945
NSF DMR-87-04288 ..... N89-24587
NSF DMS-87-01275 ..... N89-24863
N89-24864
NSF DMS-87-14612 ..... N89-24578
NSF INT-83-14219 ..... N89-25107
NSG-1490 ..... N89-24630
N00014-84-C-0706 ..... N89-24860
N00014-84-K-0367 ..... N89-24870
N00014-86-K-0381 ..... N89-24475
N00014-87-K-0126 ..... N89-24559
N00014-87-K-0172 ..... N89-24788
N00014-87-K-0398 ..... N89-24858
N00014-87-K-0670 ..... N89-24560
N00014-88-C-0024 ..... N89-24527
N00014-88-C-0483 ..... N89-24603
N00014-88-K-2007 ..... N89-24972
N00014-89-J-1171 ..... N89-24807
N00014-89-J-1178 ..... N89-24495
N89-25062
N00173-87-M-4338 ..... N89-24972
PROJ. G-35-685 ..... N89-24755
RR04108 ..... N89-24788
SRI PROJ. PRU-7784 ..... N89-24860
SRI PROJ. PYU-1227 ..... N89-24892
STPA-8595-004 ..... N89-24274
W-31-109-ENG-38 ..... N89-24473
N89-24474
N89-24498
N89-24526
N89-24587
N89-24611
N89-24619
N89-24749
N89-24800
N89-25055
N89-25056
W-7405-ENG-36 ..... N89-24481
N89-24504
N89-24516
N89-24604
N89-24612
N89-24903
N89-25091
N89-25092
N89-25098
W-7405-ENG-48 ..... N89-24408
N89-24510
N89-24522
N89-24534
N89-24567
N89-24585
N89-24588
N89-24595
N89-24600
N89-24605
N89-24606
N89-24659
N89-24682
N89-24684
N89-24750
N89-24751
N89-24783
N89-24890
N89-24904
N89-24906
N89-24907
N89-24916
N89-24928
N89-24964
073-36-00-00-72 ..... N89-24790
199-22-76-01 ..... N89-25103
199-22-76-02 ..... N89-25104
323-53-62 ..... N89-24413
474-12-10 ..... N89-24438
474-46-10 ..... N89-24418
N89-24439
N89-24448
505-60 ..... N89-24871
505-61-21 ..... N89-24285
N89-24569
505-61-51 ..... N89-24563
505-61-51-10 ..... N89-24264
505-61-71 ..... N89-24287
505-62-21 ..... N89-24269
N89-24575
N89-24577
N89-24865
N89-24872
505-62-71 ..... N89-24318
N89-24319
505-63-1B N89-24459
505-63-01-05 ..... N89-24679
505-63-01-08 ..... N89-24867
505-63-01-10 ..... N89-24624
N89-24637
N89-24638
N89-24654
N89-24673
N89-24681
505-63-11-01 ..... N89-24508
505-63-21-02 ..... N89-24626
505-63-21-04 ..... N89-24308
N89-24310
N89-24313
N89-24314
N89-24324
505-63-31-03 ..... N89-24677
505-63-51 ..... N89-24607
505-65-66-67 ..... N89-25111
505-66-11 ..... N89-24328
505-66-21-01 ..... N89-24803
N89-24815
N89-24817
505-66-41-06 ..... N89-24316
505-66-41-51 ..... N89-24293
505-67-21 ..... N89-24290
N89-24798
505-69-61 ..... N89-24320
505-80-11-05 ..... N89-24581
505-90-21-01 ..... N89-24568
N89-24816
N89-24883
506-41-3K N89-24443
506-41-11 ..... N89-24529
N89-24704
506-41-31 ..... N89-24440
N89-24451
506-42-11 ..... N89-24445
506-42-31 ..... N89-24436
N89-24446
506-42-51 ..... N89-24444
506-43-41-02 ..... N89-24676
506-44-2A N89-24532
506-44-20 ..... N89-24520
506-44-21 ..... N89-24530
506-44-45-46-47 ..... N89-25111
506-48-91-01 ..... N89-25110
506-53-31 ..... N89-24486
535-03-01 ..... N89-24886
535-03-11-03 ..... N89-24888
549-02-03 ..... N89-25111
549-03-31-03 ..... N89-24811
582-01-11 ..... N89-24591
N89-24856
582-01-21 ..... N89-24447
583-01-11-12 ..... N89-24514
584-01-02 ..... N89-25111
585-02-31-01 ..... N89-24678
586-01-11 ..... N89-24427
N89-24593
N89-25078
591-41-11 ..... N89-24409
665-45-30-01 ..... N89-24772
778-32-11 ..... N89-24487
778-35-13 ..... N89-24741
992-21-01 ..... N89-24323
999-12-08 ..... N89-24327

Typical Report Number Index Listing

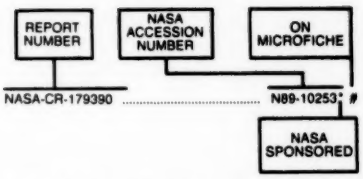

Listings in this index are arranged alphanumerically by report number. The NASA accession number denotes the number by which the citation is identified. An asterisk (*) indicates that the item is a NASA report. A pound sign (#) indicates that the item is available on microfiche.

A-88266 ..... N89-24329* #
A-88271 ..... N89-24323* #
A-89018 ..... N89-24580* #
A-89047 ..... N89-24563* #
A-89074 ..... N89-24285* #
A-89087 ..... N89-24871* #
A-89116 ..... N89-24290* #
A-89118 ..... N89-24796* #

AAC-TN-1152 ..... N89-24678* #

AAMRL-TR-88-037 ..... N89-25074 #

AD-A198095 ..... N89-24819 #
AD-A199946 ..... N89-24261 #
AD-A204078 ..... N89-24862 #
AD-A204080 ..... N89-24863 #
AD-A204092 ..... N89-24864 #
AD-A204617 ..... N89-24796 #
AD-A205239 ..... N89-24513 #
AD-A205691 ..... N89-24868 #
AD-A206054 ..... N89-24813 #
AD-A206078 ..... N89-24527 #
AD-A206139 ..... N89-25074 #
AD-A206141 ..... N89-24791 #
AD-A206143 ..... N89-24785 #
AD-A206158 ..... N89-24869 #
AD-A206159 ..... N89-24452 #
AD-A206160 ..... N89-25058 #
AD-A206179 ..... N89-24759 #
AD-A206180 ..... N89-24786 #
AD-A206181 ..... N89-24309 #
AD-A206196 ..... N89-24787 #
AD-A206202 ..... N89-24325 #
AD-A206210 ..... N89-25059 #
AD-A206213 ..... N89-24788 #
AD-A206215 ..... N89-24332 #
AD-A206216 ..... N89-24475 #
AD-A206226 ..... N89-24858 #
AD-A206241 ..... N89-24859 #
AD-A206242 ..... N89-24270 #
AD-A206243 ..... N89-24860 #
AD-A206253 ..... N89-24860 #
AD-A206255 ..... N89-24289 #
AD-A206257 ..... N89-24892 #
AD-A206260 ..... N89-25060 #
AD-A206263 ..... N89-25075 #
AD-A206264 ..... N89-24476 #
AD-A206328 ..... N89-24905 #
AD-A206355 ..... N89-24453 #
AD-A206356 ..... N89-24805 #
AD-A206358 ..... N89-24467 #
AD-A206359 ..... N89-24271 #
AD-A206360 ..... N89-24272 #
AD-A206368 ..... N89-24602 #
AD-A206412 ..... N89-24806 #
AD-A206417 ..... N89-24454 #
AD-A206420 ..... N89-24491 #
AD-A206422 ..... N89-24294 #
AD-A206423 ..... N89-24492 #
AD-A206424 ..... N89-24675 #
AD-A206427 ..... N89-24603 #
AD-A206430 ..... N89-24263 #
AD-A206454 ..... N89-24870 #
AD-A206467 ..... N89-24807 #
AD-A206468 ..... N89-25061 #
AD-A206470 ..... N89-24570 #
AD-A206474 ..... N89-24571 #
AD-A206476 ..... N89-24477 #
AD-A206494 ..... N89-24493 #
AD-A206515 ..... N89-24494 #
AD-A206518 ..... N89-24789 #
AD-A206521 ..... N89-24775 #
AD-A206525 ..... N89-24776 #
AD-A206532 ..... N89-24441 #
AD-A206533 ..... N89-24808 #
AD-A206539 ..... N89-24572 #
AD-A206545 ..... N89-24528 #
AD-A206546 ..... N89-24495 #
AD-A206547 ..... N89-25062 #
AD-A206548 ..... N89-24809 #
AD-A206578 ..... N89-24273 #

AD-E951257 ..... N89-24905 #

AFGL-TR-89-0068 ..... N89-24807 #

AFIT/DS/ENP/88-2 ..... N89-25058 #

AFIT/GA/ENY/88D-05 ..... N89-24859 #

AFIT/GAE/AA/88D-06 ..... N89-24271 #
AFIT/GAE/AA/88D-14 ..... N89-24467 #
AFIT/GAE/AA/88D-21 ..... N89-24452 #
AFIT/GAE/AA/89M-4 ..... N89-24270 #

AFIT/GCS/ENG/88D-15 ..... N89-24805 #

AFIT/GE/ENG/89M-6-VOL-2 ..... N89-24325 #

AFIT/GNE/ENP/89M-1 ..... N89-24869 #
AFIT/GNE/ENP/89M-3 ..... N89-24453 #

AFOSR-89-0293TR ..... N89-25061 #
AFOSR-89-0302TR ..... N89-24892 #
AFOSR-89-0317TR ..... N89-25059 #
AFOSR-89-0321TR ..... N89-24602 #
AFOSR-89-0343TR ..... N89-24332 #
AFOSR-89-0346TR ..... N89-24493 #
AFOSR-89-0351TR ..... N89-24570 #
AFOSR-89-0386TR ..... N89-24572 #

AIAA-89-0095 ..... N89-24872* #
AIAA-89-1980 ..... N89-24269* #
AIAA-89-2302 ..... N89-24445* #
AIAA-89-2725 ..... N89-24446* #
AIAA-89-2739 ..... N89-24447* #
AIAA-89-2793 ..... N89-24444* #
AIAA-89-2906 ..... N89-24318* #

AMSMI/TR-RD-RE-88-5 ..... N89-24905 #

ANL-9009868 ..... N89-24749 #

ANL/CNSV-67 ..... N89-24619 #

ARL-88-2 ..... N89-24786 #

ARO-24804.7-MS ..... N89-24454 #

AVSCOM-TP-88-B-001 ..... N89-24264* #

AVSCOM-TR-89-C-010 ..... N89-24607* #

BBC-RD-1989/1 ..... N89-24512

BFLRF-248 ..... N89-24613 #

BNL-42109 ..... N89-25101 #
BNL-42346 ..... N89-25053 #

BONN-IR-88-32 ..... N89-24428 #
BONN-IR-88-52 ..... N89-24760 #

CEBAF-PR-89-003 ..... N89-24895 #

CERT-RT-OA-26/5025-AYD ..... N89-24274 #

CHORS-TM-89-001 ..... N89-24784* #

CMS-TSR-89-1 ..... N89-24863 #
CMS-TSR-89-3 ..... N89-24862 #
CMS-TSR-89-18 ..... N89-24864 #

CONF-880512-18 ..... N89-24485 #
CONF-880802-10 ..... N89-24566 #
CONF-881060-5 ..... N89-25052 #
CONF-881127-5 ..... N89-25056 #
CONF-881268-3 ..... N89-25091 #
CONF-890145-25 ..... N89-24606 #
CONF-890165-3 ..... N89-24498 #
CONF-890195-2 ..... N89-25101 #
CONF-890199-1 ..... N89-25092 #
CONF-890240-3 ..... N89-24526 #
CONF-890262-2 ..... N89-24747 #
CONF-890275-4 ..... N89-24501 #
CONF-890291-1 ..... N89-24516 #
CONF-890294-1 ..... N89-24473 #
CONF-890298-1 ..... N89-25071 #
CONF-890335-135 ..... N89-24605 #
CONF-890335-145 ..... N89-24878 #
CONF-890387-1 ..... N89-24890 #
CONF-890392-1 ..... N89-24903 #
CONF-890403-9 ..... N89-25049 #
CONF-890403-20 ..... N89-25050 #
CONF-890426-2 ..... N89-24525 #
CONF-890426-7 ..... N89-24682 #
CONF-890492-2 ..... N89-24504 #
CONF-890518-2 ..... N89-24534 #
CONF-890522-5 ..... N89-24861 #
CONF-890592-2 ..... N89-24884 #
CONF-890604-3-VUGRAPHS ..... N89-24813 #
CONF-890631-4 ..... N89-24683 #
CONF-890646-4 ..... N89-24483 #
CONF-890660-1 ..... N89-24522 #
CONF-890660-6 ..... N89-24523 #
CONF-890661-4 ..... N89-24408 #
CONF-890661-5 ..... N89-24472 #
CONF-890661-7 ..... N89-24510 #
CONF-890679-1 ..... N89-24524 #
CONF-890692-8 ..... N89-24750 #
CONF-890694-5 ..... N89-24596 #
CONF-8807149-2 ..... N89-24907 #
CONF-8808141-12 ..... N89-24904 #
CONF-8808178-1 ..... N89-25053 #
CONF-8808219-2 ..... N89-24470 #
CONF-8810118-6 ..... N89-24587 #
CONF-8810279-3 ..... N89-25054 #
CONF-8810346-1 ..... N89-24489 #
CONF-8810358-1 ..... N89-24893 #
CONF-8811195-1 ..... N89-25055 #
CONF-8811196-1 ..... N89-25070 #
CONF-8901101-1 ..... N89-24567 #
CONF-8901123-1 ..... N89-24604 #
CONF-8903101-1 ..... N89-24490 #
CONF-8903103-1 ..... N89-24474 #
CONF-8903109-1 ..... N89-24478 #
CONF-8903118-1 ..... N89-24482 #
CONF-8904183-1 ..... N89-25057 #
CONF-8904191-2 ..... N89-24812 #
CONF-8904199-1 ..... N89-24471 #
CONF-8904210-1 ..... N89-24800 #
CONF-8904217-1 ..... N89-24783 #
CONF-8905115-2 ..... N89-24751 #
CONF-8905118-7 ..... N89-24621 #
CONF-8905120-4 ..... N89-24521 #
CONF-8905131-1 ..... N89-24481 #
CONF-8906111-1 ..... N89-24585 #
CONF-8906119-1 ..... N89-24484 #
CONF-8906126-1 ..... N89-24586 #

DERAT-26/5025-14 ..... N89-24274 #

DE88-704749 ..... N89-25090 #
DE88-706280 ..... N89-25087 #
DE88-706303 ..... N89-24799 #
DE88-706304 ..... N89-24503 #

DE88-706318 ..... N89-24879 #
DE88-706319 ..... N89-24885 #
DE88-706323 ..... N89-25068 #
DE88-706325 ..... N89-24468 #
DE88-706333 ..... N89-24877 #
DE88-706341 ..... N89-25069 #
DE88-756571 ..... N89-24908 #
DE88-756574 ..... N89-24909 #
DE88-757229 ..... N89-24881 #
DE88-757249 ..... N89-24565 #
DE88-757253 ..... N89-24902 #
DE88-757269 ..... N89-24866 #
DE88-757273 ..... N89-24857 #
DE88-757286 ..... N89-24882 #
DE88-757287 ..... N89-25105 #
DE89-000740 ..... N89-24497 #
DE89-000849 ..... N89-24703 #
DE89-000881 ..... N89-24469 #
DE89-000884 ..... N89-24743 #
DE89-000890 ..... N89-24496 #
DE89-000893 ..... N89-24739 #
DE89-002974 ..... N89-24861 #
DE89-005271 ..... N89-24485 #
DE89-005662 ..... N89-24522 #
DE89-006744 ..... N89-25052 #
DE89-006745 ..... N89-24907 #
DE89-006747 ..... N89-24408 #
DE89-006769 ..... N89-24523 #
DE89-007066 ..... N89-24524 #
DE89-007145 ..... N89-24472 #
DE89-007270 ..... N89-24896 #
DE89-007271 ..... N89-24897 #
DE89-007272 ..... N89-24898 #
DE89-007273 ..... N89-24899 #
DE89-007428 ..... N89-24884 #
DE89-008035 ..... N89-24510 #
DE89-008917 ..... N89-24747 #
DE89-008971 ..... N89-24748 #
DE89-009066 ..... N89-24489 #
DE89-009247 ..... N89-25091 #
DE89-009258 ..... N89-24890 #
DE89-009280 ..... N89-24516 #
DE89-009311 ..... N89-24490 #
DE89-009322 ..... N89-24525 #
DE89-009336 ..... N89-24566 #
DE89-009349 ..... N89-25092 #
DE89-009392 ..... N89-24903 #
DE89-009525 ..... N89-25053 #
DE89-009644 ..... N89-25054 #
DE89-009710 ..... N89-24517 #
DE89-009713 ..... N89-24610 #
DE89-009753 ..... N89-24535 #
DE89-009758 ..... N89-24465 #
DE89-009760 ..... N89-24611 #
DE89-009807 ..... N89-24526 #
DE89-009825 ..... N89-24473 #
DE89-009836 ..... N89-24474 #
DE89-009861 ..... N89-25055 #
DE89-009868 ..... N89-24749 #
DE89-009878 ..... N89-25056 #
DE89-009902 ..... N89-24904 #
DE89-009909 ..... N89-24600 #
DE89-009922 ..... N89-24567 #
DE89-009970 ..... N89-25057 #
DE89-010046 ..... N89-24891 #
DE89-010117 ..... N89-24592 #
DE89-010119 ..... N89-24612 #
DE89-010183 ..... N89-24478 #
DE89-010188 ..... N89-24614 #
DE89-010242 ..... N89-24585 #
DE89-010374 ..... N89-24812 #
DE89-010390 ..... N89-25070 #
DE89-010426 ..... N89-24483 #
DE89-010438 ..... N89-24470 #
DE89-010457 ..... N89-24484 #
DE89-010463 ..... N89-24813 #
DE89-010743 ..... N89-24596 #
DE89-010828 ..... N89-24582 #
DE89-010968 ..... N89-24461 #
DE89-011118 ..... N89-24471 #
DE89-011189 ..... N89-24481 #
DE89-011194 ..... N89-24504 #
DE89-011196 ..... N89-24604 #
DE89-011218 ..... N89-24893 #
DE89-011225 ..... N89-25071 #
DE89-011351 ..... N89-24617 #
DE89-011354 ..... N89-24616 #
DE89-011381 ..... N89-24583 #
DE89-011382 ..... N89-24584 #
DE89-011399 ..... N89-25098 #
DE89-011417 ..... N89-24618 #
DE89-011419 ..... N89-24894 #
DE89-011430 ..... N89-24482 #
DE89-011467 ..... N89-24742 #
DE89-011469 ..... N89-24533 #
DE89-011572 ..... N89-25049 #
DE89-011579 ..... N89-24521 #
DE89-011590 ..... N89-25065 #
DE89-011632 ..... N89-24534 #
DE89-011638 ..... N89-24682 #
DE89-011644 ..... N89-24595 #
DE89-011647 ..... N89-24906 #
DE89-011787 ..... N89-25066 #
DE89-011831 ..... N89-24744 #
DE89-011850 ..... N89-24586 #
DE89-011879 ..... N89-24683 #
DE89-011893 ..... N89-24750 #
DE89-011896 ..... N89-24605 #
DE89-012241 ..... N89-24619 #
DE89-012244 ..... N89-24745 #
DE89-012250 ..... N89-24620 #
DE89-012269 ..... N89-24878 #
DE89-012283 ..... N89-24597 #
DE89-012287 ..... N89-24606 #
DE89-012290 ..... N89-24751 #
DE89-012291 ..... N89-24783 #
DE89-012322 ..... N89-24684 #
DE89-012342 ..... N89-25050 #
DE89-012381 ..... N89-24587 #
DE89-012383 ..... N89-24800 #
DE89-012396 ..... N89-24498 #
DE89-012536 ..... N89-25101 #
DE89-012888 ..... N89-24499 #
DE89-012890 ..... N89-24500 #
DE89-012922 ..... N89-24588 #
DE89-013584 ..... N89-24501 #
DE89-013588 ..... N89-24621 #
DE89-013599 ..... N89-24502 #
DE89-013614 ..... N89-25089 #

DFVLR-MITT-88-29 ..... N89-24688 #
DFVLR-MITT-88-32 ..... N89-24295 #

DOE/CE-15245/T1 ..... N89-24618 #

DOE/ER-13549/3 ..... N89-24891 #
DOE/ER-13958/1 ..... N89-24894 #
DOE/ER-40063/13 ..... N89-25089 #
DOE/ER-45063/4 ..... N89-24502 #
DOE/ER-45285/3 ..... N89-25066 #
DOE/ER-45315/2 ..... N89-25065 #
DOE/ER-45326/10 ..... N89-25071 #
DOE/ER-72012/T7 ..... N89-24562 #

DOE/ET-32043/T26-VOL-2-BK-1 ..... N89-24896 #
DOE/ET-32043/T26-VOL-2-BK-2 ..... N89-24897 #

DOE/ID-10184 ..... N89-24535 #

DOE/NASA/4105-4 ..... N89-24741* #

DOE/NE-32134/T1-VOL-3-BK-1 ..... N89-24898 #
DOE/NE-32134/T1-VOL-3-BK-2 ..... N89-24899 #

DOE/PC-88913/T1 ..... N89-24584 #
DOE/PC-88947/T2 ..... N89-24583 #
DOE/PC-90540/11 ..... N89-24471 #

DOE/SF-16306/14 ..... N89-24744 #

DOT/FAA/AM-89/1 ..... N89-24294 #

DOT/FAA/CT-TN88/42 ..... N89-24291 #
DOT/FAA/CT-TN89/3 ..... N89-24288 #
DOT/FAA/CT-TN89/23 ..... N89-24330 #

DOT/FAA/CT-89/14-VOL-1 ..... N89-24292 #

DOT/FAA/SA-89/1 ..... N89-24771 #
DOT/FAA/SA-89/2 ..... N89-24515 #

DP-MS-88-213 ..... N89-24484 #
DP-MS-89-4 ..... N89-24813 #

DREA-TM-89/204 ..... N89-24808 #

DTRC/SME-88/74 ..... N89-25060 #

E-16-654 ..... N89-24674* #
E-4404-1 ..... N89-24575* #
E-4511 ..... N89-24413* #
E-4535 ..... N89-24635* #
E-4580 ..... N89-24741* #
E-4587 ..... N89-24704* #
E-4588 ..... N89-24607* #
E-4606 ..... N89-24886* #
E-4621 ..... N89-24520* #
E-4706 ..... N89-24856* #
E-4724 ..... N89-24443* #
E-4735 ..... N89-24459* #
E-4740 ..... N89-24529* #
E-4746 ..... N89-24320* #
E-4748 ..... N89-24532* #
E-4764 ..... N89-24451* #
E-4772 ..... N89-24872* #
E-4775 ..... N89-24460* #
E-4785 ..... N89-24865* #
E-4787 ..... N89-24445* #
E-4794 ..... N89-24487* #
E-4801 ..... N89-24436* #
E-4804 ..... N89-24438* #
E-4809 ..... N89-24591* #
E-4833 ..... N89-24439* #
E-4836 ..... N89-24418* #
E-4838 ..... N89-24318* #
E-4842 ..... N89-24269* #
E-4843 ..... N89-24440* #
E-4847 ..... N89-24409* #
E-4859 ..... N89-25078* #
E-4861 ..... N89-24319* #
E-4871 ..... N89-24448* #
E-4876 ..... N89-24446* #
E-4886 ..... N89-24447* #
E-4902 ..... N89-24593* #
E-4912 ..... N89-24577* #
E-4932 ..... N89-24444* #
E-4933 ..... N89-24427* #

ECS-SS-2801 ..... N89-24594* #

EGG-M-40087 ..... N89-24485 #

ESA-SP-277 ..... N89-24335 #
ESA-SP-285-VOL-1 ..... N89-24910 #
ESA-SP-285-VOL-2 ..... N89-24974 #
ESA-SP-1101 ..... N89-24692 #

ESL-TR-87-62 ..... N89-24675 #

ETCA-88-R-001 ..... N89-24456 #
ETCA-88-R-006 ..... N89-24457 #

ETN-89-93992 ..... N89-25063 #
ETN-89-93995 ..... N89-24428 #
ETN-89-93996 ..... N89-24760 #
ETN-89-94243 ..... N89-25030 #
ETN-89-94375 ..... N89-24688 #
ETN-89-94384 ..... N89-24887 #
ETN-89-94391 ..... N89-25080
ETN-89-94392 ..... N89-25081*
ETN-89-94393 ..... N89-25093
ETN-89-94394 ..... N89-25106
ETN-89-94396 ..... N89-25082
ETN-89-94397 ..... N89-25038
ETN-89-94405 ..... N89-24479 #
ETN-89-94406 ..... N89-24455 #
ETN-89-94407 ..... N89-25064 #
ETN-89-94447 ..... N89-24692 #
ETN-89-94448 ..... N89-24335 #
ETN-89-94475 ..... N89-24910 #
ETN-89-94476 ..... N89-24974 #
ETN-89-94510 ..... N89-24423 #
ETN-89-94511 ..... N89-24689 #
ETN-89-94512 ..... N89-25083 #
ETN-89-94513 ..... N89-24442 #
ETN-89-94514 ..... N89-24424 #
ETN-89-94515 ..... N89-24622 #
ETN-89-94516 ..... N89-24429 #
ETN-89-94517 ..... N89-24425 #
ETN-89-94518 ..... N89-24810 #
ETN-89-94519 ..... N89-24761 #
ETN-89-94520 ..... N89-24456 #
ETN-89-94521 ..... N89-24457 #
ETN-89-94522 ..... N89-24274 #
ETN-89-94523 ..... N89-24573 #
ETN-89-94524 ..... N89-24275 #
ETN-89-94525 ..... N89-24458 #
ETN-89-94526 ..... N89-24574 #
ETN-89-94527 ..... N89-24777 #
ETN-89-94528 ..... N89-24311 #
ETN-89-94529 ..... N89-24480 #
ETN-89-94530 ..... N89-24690 #
ETN-89-94531 ..... N89-24691 #
ETN-89-94533 ..... N89-24762 #
ETN-89-94534 ..... N89-24778 #
ETN-89-94535 ..... N89-24779 #
ETN-89-94536 ..... N89-24763 #
ETN-89-94537 ..... N89-24780 #
ETN-89-94538 ..... N89-24781 #
ETN-89-94539 ..... N89-24782 #
ETN-89-94540 ..... N89-24312 #
ETN-89-94541 ..... N89-24740 #
ETN-89-94542 ..... N89-24531 #
ETN-89-94552 ..... N89-24764 #
ETN-89-94556 ..... N89-24276 #
ETN-89-94557 ..... N89-24281 #
ETN-89-94580 ..... N89-24900
ETN-89-94581 ..... N89-25107

ETN-89-94582 N89-24407
ETN-89-94583 N89-25084
ETN-89-94584 N89-25085
ETN-89-94585 N89-25094
ETN-89-94587 N89-25086
ETN-89-94645 N89-24295 #

FAA-PM-86/20 N89-24293* #

FLOW-RR-470 N89-24272 #

FOA-C-20745-2.5 N89-24312 #
FOA-C-20746-2.7 N89-24740 #
FOA-C-30514-3.2 N89-24531 #

FR-688104 N89-24772* #

FTD-ID(RS)T-0616-88 N89-24261 #

GACIAC-SR-88-10 N89-24819 #

GAO/T-NSIAD-89-6 N89-24263 #

GRI-88/0282 N89-24464 #

H-1344 N89-24327* #

HL89-7 N89-24618 #

IAE-4428/9 N89-25067 #

IC-88/241 N89-25090 #

ICASE-IR-7 N89-24816* #

ICASE-89-25 N89-24568* #
ICASE-89-29-PT-2 N89-24883* #

ICOMP-89-10 N89-24575* #
ICOMP-89-11 N89-24865* #
ICOMP-89-13 N89-24872* #

IMFL-88/18 N89-24573 #

INPE-4588-PRE/1319 N89-24685 #

INS-715 N89-24881 #

IPP-III/139 N89-25038

IRF-TR-034 N89-24764 #

ISBN-9-5169-7269-1 N89-24767 #
ISBN-9-5169-7289-6 N89-24768 #
ISBN-9-5169-7291-8 N89-24769 #

ISSN-0172-8741 N89-24428 #
ISSN-0172-8741 N89-24760 #
ISSN-0176-7736 N89-24688 #
ISSN-0176-7739 N89-24295 #
ISSN-0178-0719 N89-25080
ISSN-0178-0719 N89-25081*
ISSN-0178-0719 N89-25093
ISSN-0178-0719 N89-25094
ISSN-0178-0719 N89-25106
ISSN-0284-1738 N89-24764 #
ISSN-0303-4003 N89-24455 #
ISSN-0303-4003 N89-24479 #
ISSN-0303-4003 N89-25064 #
ISSN-0347-3694 N89-24312 #
ISSN-0347-3694 N89-24740 #
ISSN-0347-3708 N89-24531 #
ISSN-0379-6566 N89-24692 #
ISSN-0379-6566 N89-24910 #
ISSN-0379-6566 N89-24974 #
ISSN-0389-4010 N89-24317 #
ISSN-0389-4010 N89-24321 #
ISSN-0389-4010 N89-24322 #
ISSN-0389-4010 N89-24431 #
ISSN-0389-4010 N89-24432 #
ISSN-0389-4010 N89-24506 #
ISSN-0389-4010 N89-24536 #
ISSN-0389-4010 N89-24537 #
ISSN-0389-4010 N89-24598 #
ISSN-0389-4010 N89-24625 #
ISSN-0389-4010 N89-24702 #
ISSN-0389-4010 N89-24753 #
ISSN-0389-4010 N89-24801 #
ISSN-0389-4010 N89-24814 #
ISSN-0389-4010 N89-25072 #
ISSN-0436-1199 N89-24887 #
ISSN-0782-6109 N89-24767 #
ISSN-0782-6109 N89-24768 #
ISSN-0782-6109 N89-24769 #

JAERI-M-88-171 N89-24908 #
JAERI-M-88-175 N89-24909 #
JAERI-M-88-208 N89-24565 #
JAERI-M-88-212 N89-24902 #
JAERI-M-88-236 N89-24866 #
JAERI-M-88-243 N89-24857 #

JINR-R-5-88-221 N89-24879 #
JINR-R-9-88-149 N89-24885 #
JINR-R-9-88-263 N89-25068 #
JINR-R-10-87-926 N89-24468 #
JINR-R-11-88-320 N89-24877 #

JINR-13-88-303 N89-24799 #
JINR-13-88-347 N89-24503 #

JPL-PUBL-87-24 N89-25073* #
JPL-PUBL-87-31 N89-24411* #
JPL-PUBL-400-353 N89-24420* #

KFK-4468 N89-24479 #
KFK-4469 N89-24455 #
KFK-4482 N89-25064 #

L-16407 N89-24264* #
L-16499 N89-24624* #
L-16529 N89-24815* #
L-16560-PT-1 N89-24638* #
L-16560-PT-2 N89-24654* #
L-16583 N89-25103* #

LA-UR-89-857 N89-24903 #
LA-UR-89-939 N89-24516 #
LA-UR-89-1010 N89-25092 #
LA-UR-89-1095 N89-25091 #
LA-UR-89-1161 N89-24604 #
LA-UR-89-1171 N89-24504 #
LA-UR-89-1208 N89-24481 #

LA-11554-T N89-25098 #

LAFI-131 N89-25069 #

LBL-25627 N89-24490 #
LBL-26377 N89-24470 #
LBL-26545 N89-25070 #
LBL-26565 N89-24482 #
LBL-26747 N89-24566 #

LC-87-619855 N89-24804 #

LG88ER0116-PH-1/2 N89-24316* #

LMSC-D878511-VOL-5 N89-24637* #

LMSC-F223517 N89-24415* #

LMSC-HEC-TR-F268519 N89-24433* #
LMSC-HEC-TR-F268584-VOL-6 N89-24437* #

M-608 N89-24770* #
M-612 N89-24507* #

MCR-87-2600 N89-24410* #
MCR-89-516 N89-24434* #

MDC-W5125-2 N89-24793* #
MDC-W5141-2-VOL-2 N89-24795* #

MM-5679-89-9 N89-24634* #

MMS-87-0013-VOL-3 N89-24776 #

MP-7 N89-24767 #
MP-10 N89-24768 #
MP-11 N89-24769 #

MPE-PAE/EXP.EL-198 N89-24900

MPE-PREPRINT-130 N89-25080
MPE-PREPRINT-131 N89-25081*
MPE-PREPRINT-132 N89-25093
MPE-PREPRINT-133 N89-25106
MPE-PREPRINT-135 N89-25082
MPE-PREPRINT-136 N89-25107
MPE-PREPRINT-137 N89-24407
MPE-PREPRINT-138 N89-25084
MPE-PREPRINT-139 N89-25085
MPE-PREPRINT-140 N89-25094
MPE-PREPRINT-142 N89-25086

MPI-PAE/EXP.EL-194 N89-25063 #

MPIS-7/1988 N89-24887 #

MTI-PUBL-89343 N89-24449* #
MTI-PUBL-89734 N89-24594* #

NAL-TM-FM-8805 N89-24462 #

NAL-TM-SE-8704 N89-24414 #
NAL-TM-SE-8707 N89-24901 #

NAL-TR-977 N89-24814 #
NAL-TR-978 N89-24321 #
NAL-TR-979 N89-24598 #
NAL-TR-980T N89-24753 #
NAL-TR-981 N89-24431 #
NAL-TR-982 N89-25072 #
NAL-TR-983T N89-24536 #
NAL-TR-984T N89-24537 #
NAL-TR-986 N89-24801 #
NAL-TR-987 N89-24317 #
NAL-TR-988 N89-24625 #
NAL-TR-989 N89-24506 #
NAL-TR-990 N89-24432 #
NAL-TR-994 N89-24702 #
NAL-TR-996T N89-24322 #

NAS 1.15:4072 N89-24624* #
NAS 1.15:4126 N89-25111* #
NAS 1.15:86540 N89-24405*
NAS 1.15:100327 N89-24435* #
NAS 1.15:100361 N89-24623* #
NAS 1.15:100364 N89-24421* #
NAS 1.15:100365 N89-24422* #
NAS 1.15:100474 N89-24790* #
NAS 1.15:100638 N89-24888* #
NAS 1.15:100643 N89-24673* #
NAS 1.15:100650 N89-24867* #
NAS 1.15:101026 N89-24329* #
NAS 1.15:101062 N89-24323* #
NAS 1.15:101074 N89-24563* #
NAS 1.15:101083 N89-24285* #
NAS 1.15:101087 N89-24871* #
NAS 1.15:101233 N89-24505* #
NAS 1.15:101245 N89-24416* #
NAS 1.15:101246 N89-25109* #
NAS 1.15:101430 N89-24635* #
NAS 1.15:101463 N89-24413* #
NAS 1.15:101480 N89-24886* #
NAS 1.15:101485 N89-24520* #
NAS 1.15:101521 N89-24293* #
NAS 1.15:101548 N89-24677* #
NAS 1.15:101551 N89-24514* #
NAS 1.15:101559 N89-25104* #
NAS 1.15:101565 N89-24676* #
NAS 1.15:101566 N89-24508* #
NAS 1.15:101570 N89-24313* #
NAS 1.15:101571 N89-24310* #
NAS 1.15:101572 N89-24324* #
NAS 1.15:101574 N89-24308* #
NAS 1.15:101579 N89-25112* #
NAS 1.15:101582 N89-24314* #
NAS 1.15:101594 N89-25110* #
NAS 1.15:101601 N89-24679* #
NAS 1.15:101622 N89-24681* #
NAS 1.15:101805 N89-24331* #
NAS 1.15:101957 N89-24459* #
NAS 1.15:101999 N89-24856* #
NAS 1.15:102012 N89-24443* #
NAS 1.15:102029 N89-24872* #
NAS 1.15:102030 N89-24575* #
NAS 1.15:102032 N89-24460* #
NAS 1.15:102036 N89-24865* #
NAS 1.15:102046 N89-24487* #
NAS 1.15:102049 N89-24436* #
NAS 1.15:102052 N89-24438* #
NAS 1.15:102056 N89-24591* #
NAS 1.15:102074 N89-24439* #
NAS 1.15:102075 N89-24529* #
NAS 1.15:102076 N89-24418* #
NAS 1.15:102078 N89-24318* #
NAS 1.15:102080 N89-24269* #
NAS 1.15:102081 N89-24440* #
NAS 1.15:102082 N89-24451* #
NAS 1.15:102084 N89-24409* #
NAS 1.15:102092 N89-24320* #
NAS 1.15:102097 N89-25078* #
NAS 1.15:102098 N89-24319* #
NAS 1.15:102105 N89-24448* #
NAS 1.15:102108 N89-24446* #
NAS 1.15:102113 N89-24447* #
NAS 1.15:102121 N89-24593* #
NAS 1.15:102126 N89-24577* #
NAS 1.15:102135 N89-24444* #
NAS 1.15:102136 N89-24427* #
NAS 1.15:102147 N89-24412* #
NAS 1.15:102187 N89-24798* #
NAS 1.15:102201 N89-24290* #
NAS 1.19:262 N89-24262*
NAS 1.19:264 N89-24333* #
NAS 1.26:4141 N89-24579* #
NAS 1.26:4218 N89-24770* #

NAS 1.26:4239 ..... N89-24803*
NAS 1.26:4240 ..... N89-24797* #
NAS 1.26:4242 ..... N89-24581* #
NAS 1.26:4244 ..... N89-24817*
NAS 1.26:172114 ..... N89-24415* #
NAS 1.26:177444 ..... N89-24486* #
NAS 1.26:177515 ..... N89-24328* #
NAS 1.26:177516 ..... N89-24580* #
NAS 1.26:177521 ..... N89-24287* #
NAS 1.26:177531 ..... N89-24569* #
NAS 1.26:177533 ..... N89-24450* #
NAS 1.26:178388 ..... N89-24637* #
NAS 1.26:180076 ..... N89-24634* #
NAS 1.26:180081 ..... N89-24687* #
NAS 1.26:180791 ..... N89-24590* #
NAS 1.26:181536 ..... N89-25076* #
NAS 1.26:181746 ..... N89-24678* #
NAS 1.26:181818 ..... N89-24772* #
NAS 1.26:181820 ..... N89-24316* #
NAS 1.26:181827 ..... N89-24811* #
NAS 1.26:181830 ..... N89-24568* #
NAS 1.26:181837 ..... N89-24883* #
NAS 1.26:181843 ..... N89-24816* #
NAS 1.26:182135 ..... N89-24530* #
NAS 1.26:182248 ..... N89-24741* #
NAS 1.26:182284 ..... N89-24532* #
NAS 1.26:182495 ..... N89-24792* #
NAS 1.26:182496 ..... N89-24794* #
NAS 1.26:182966 ..... N89-24752* #
NAS 1.26:183389 ..... N89-24315* #
NAS 1.26:183421 ..... N89-24756* #
NAS 1.26:183427 ..... N89-25051* #
NAS 1.26:183551 ..... N89-24410* #
NAS 1.26:183569 ..... N89-24430* #
NAS 1.26:183572 ..... N89-24463* #
NAS 1.26:183589 ..... N89-24795* #
NAS 1.26:183590 ..... N89-24793* #
NAS 1.26:183607 ..... N89-24434* #
NAS 1.26:183613 ..... N89-24746* #
NAS 1.26:183639 ..... N89-24433* #
NAS 1.26:183647 ..... N89-24466* #
NAS 1.26:183652 ..... N89-24576* #
NAS 1.26:183669 ..... N89-24437* #
NAS 1.26:183672 ..... N89-24594* #
NAS 1.26:183673 ..... N89-24449* #
NAS 1.26:184847 ..... N89-24754* #
NAS 1.26:184856 ..... N89-24784* #
NAS 1.26:184875 ..... N89-24802* #
NAS 1.26:184905 ..... N89-24538* #
NAS 1.26:184947 ..... N89-24755* #
NAS 1.26:184949 ..... N89-24562* #
NAS 1.26:184950 ..... N89-24889* #
NAS 1.26:184951 ..... N89-25099* #
NAS 1.26:184973 ..... N89-25079* #
NAS 1.26:184974 ..... N89-24511* #
NAS 1.26:184975 ..... N89-24686* #
NAS 1.26:184978 ..... N89-24608* #
NAS 1.26:184987 ..... N89-24757* #
NAS 1.26:184989 ..... N89-24669* #
NAS 1.26:184995 ..... N89-24509* #
NAS 1.26:185012 ..... N89-24599* #
NAS 1.26:185016 ..... N89-24266* #
NAS 1.26:185017 ..... N89-24411* #
NAS 1.26:185018 ..... N89-24419* #
NAS 1.26:185023 ..... N89-25073* #
NAS 1.26:185047 ..... N89-24488* #
NAS 1.26:185053 ..... N89-24519* #
NAS 1.26:185054 ..... N89-24518* #
NAS 1.26:185055 ..... N89-24674* #
NAS 1.26:185056 ..... N89-24601* #
NAS 1.26:185113 ..... N89-24445* #
NAS 1.26:185317 ..... N89-24420* #
NAS 1.26:185319 ..... N89-24265* #
NAS 1.26:185322 ..... N89-24758* #
NAS 1.26:185336 ..... N89-24873* #
NAS 1.26:185383 ..... N89-24406* #
NAS 1.26:185404 ..... N89-24818* #
NAS 1.26:185405 ..... N89-24578* #
NAS 1.55:3030 ..... N89-24704* #
NAS 1.55:3034-PT-1 ..... N89-24638* #
NAS 1.55:3034-PT-2 ..... N89-24654* #
NAS 1.55:10024 ..... N89-24626* #
NAS 1.60:2832 ..... N89-24264* #
NAS 1.60:2857 ..... N89-24327* #
NAS 1.60:2909 ..... N89-24507* #
NAS 1.60:2911 ..... N89-24607* #
NAS 1.60:2915 ..... N89-24815* #
NAS 1.60:2920 ..... N89-25103* #

NASA-CP-3030 ..... N89-24704* #
NASA-CP-3034-PT-1 ..... N89-24638* #
NASA-CP-3034-PT-2 ..... N89-24654* #
NASA-CP-10024 ..... N89-24626* #

NASA-CR-4141 ..... N89-24579* #
NASA-CR-4218 ..... N89-24770* #

NASA-CR-4239 ..... N89-24803*
NASA-CR-4240 ..... N89-24797* #
NASA-CR-4242 ..... N89-24581* #
NASA-CR-4244 ..... N89-24817*
NASA-CR-172114 ..... N89-24415* #
NASA-CR-177444 ..... N89-24486* #
NASA-CR-177515 ..... N89-24328* #
NASA-CR-177516 ..... N89-24580* #
NASA-CR-177521 ..... N89-24287* #
NASA-CR-177531 ..... N89-24569* #
NASA-CR-177533 ..... N89-24450* #
NASA-CR-178388 ..... N89-24637* #
NASA-CR-180076 ..... N89-24634* #
NASA-CR-180081 ..... N89-24687* #
NASA-CR-180791 ..... N89-24590* #
NASA-CR-181536 ..... N89-25076* #
NASA-CR-181746 ..... N89-24678* #
NASA-CR-181818 ..... N89-24772* #
NASA-CR-181820 ..... N89-24316* #
NASA-CR-181827 ..... N89-24811* #
NASA-CR-181830 ..... N89-24568* #
NASA-CR-181837 ..... N89-24883* #
NASA-CR-181843 ..... N89-24816* #
NASA-CR-182135 ..... N89-24530* #
NASA-CR-182248 ..... N89-24741* #
NASA-CR-182284 ..... N89-24532* #
NASA-CR-182495 ..... N89-24792* #
NASA-CR-182496 ..... N89-24794* #
NASA-CR-182966 ..... N89-24752* #
NASA-CR-183389 ..... N89-24315* #
NASA-CR-183421 ..... N89-24756* #
NASA-CR-183427 ..... N89-25051* #
NASA-CR-183551 ..... N89-24410* #
NASA-CR-183569 ..... N89-24430* #
NASA-CR-183572 ..... N89-24463* #
NASA-CR-183589 ..... N89-24795* #
NASA-CR-183590 ..... N89-24793* #
NASA-CR-183607 ..... N89-24434* #
NASA-CR-183613 ..... N89-24746* #
NASA-CR-183639 ..... N89-24433* #
NASA-CR-183647 ..... N89-24466* #
NASA-CR-183652 ..... N89-24576* #
NASA-CR-183669 ..... N89-24437* #
NASA-CR-183672 ..... N89-24594* #
NASA-CR-183673 ..... N89-24449* #
NASA-CR-184847 ..... N89-24754* #
NASA-CR-184856 ..... N89-24784* #
NASA-CR-184875 ..... N89-24802* #
NASA-CR-184905 ..... N89-24538* #
NASA-CR-184947 ..... N89-24755* #
NASA-CR-184949 ..... N89-24562* #
NASA-CR-184950 ..... N89-24889* #
NASA-CR-184951 ..... N89-25099* #
NASA-CR-184973 ..... N89-25079* #
NASA-CR-184974 ..... N89-24511* #
NASA-CR-184975 ..... N89-24686* #
NASA-CR-184978 ..... N89-24608* #
NASA-CR-184987 ..... N89-24757* #
NASA-CR-184989 ..... N89-24669* #
NASA-CR-184995 ..... N89-24509* #
NASA-CR-185012 ..... N89-24599* #
NASA-CR-185016 ..... N89-24266* #
NASA-CR-185017 ..... N89-24411* #
NASA-CR-185018 ..... N89-24419* #
NASA-CR-185023 ..... N89-25073* #
NASA-CR-185047 ..... N89-24488* #
NASA-CR-185053 ..... N89-24519* #
NASA-CR-185054 ..... N89-24518* #
NASA-CR-185055 ..... N89-24674* #
NASA-CR-185056 ..... N89-24601* #
NASA-CR-185113 ..... N89-24445* #
NASA-CR-185317 ..... N89-24420* #
NASA-CR-185319 ..... N89-24265* #
NASA-CR-185322 ..... N89-24758* #
NASA-CR-185336 ..... N89-24873* #
NASA-CR-185383 ..... N89-24406* #
NASA-CR-185404 ..... N89-24818* #
NASA-CR-185405 ..... N89-24578* #

NASA-EP-262 ..... N89-24262*
NASA-EP-264 ..... N89-24333* #

NASA-NEWS-RELEASE-89-86 ..... N89-24334*

NASA-PAM-510/11-87 ..... N89-24417* #

NASA-TM-4072 ..... N89-24624* #
NASA-TM-4126 ..... N89-25111* #
NASA-TM-86540 ..... N89-24405*
NASA-TM-100327 ..... N89-24435* #
NASA-TM-100361 ..... N89-24623* #
NASA-TM-100364 ..... N89-24421* #
NASA-TM-100365 ..... N89-24422* #
NASA-TM-100474 ..... N89-24790* #
NASA-TM-100638 ..... N89-24888* #
NASA-TM-100643 ..... N89-24673* #

NASA-TM-100650 ..... N89-24867* #
NASA-TM-101026 ..... N89-24329* #
NASA-TM-101062 ..... N89-24323* #
NASA-TM-101074 ..... N89-24563* #
NASA-TM-101083 ..... N89-24285* #
NASA-TM-101087 ..... N89-24871* #
NASA-TM-101233 ..... N89-24505* #
NASA-TM-101245 ..... N89-24416* #
NASA-TM-101246 ..... N89-25109* #
NASA-TM-101430 ..... N89-24635* #
NASA-TM-101463 ..... N89-24413* #
NASA-TM-101480 ..... N89-24886* #
NASA-TM-101485 ..... N89-24520* #
NASA-TM-101521 ..... N89-24293* #
NASA-TM-101548 ..... N89-24677* #
NASA-TM-101551 ..... N89-24514* #
NASA-TM-101559 ..... N89-25104* #
NASA-TM-101565 ..... N89-24676* #
NASA-TM-101566 ..... N89-24508* #
NASA-TM-101570 ..... N89-24313* #
NASA-TM-101571 ..... N89-24310* #
NASA-TM-101572 ..... N89-24324* #
NASA-TM-101574 ..... N89-24308* #
NASA-TM-101579 ..... N89-25112* #
NASA-TM-101582 ..... N89-24314* #
NASA-TM-101594 ..... N89-25110* #
NASA-TM-101601 ..... N89-24679* #
NASA-TM-101622 ..... N89-24681* #
NASA-TM-101805 ..... N89-24331* #
NASA-TM-101957 ..... N89-24459* #
NASA-TM-101999 ..... N89-24856* #
NASA-TM-102012 ..... N89-24443* #
NASA-TM-102029 ..... N89-24872* #
NASA-TM-102030 ..... N89-24575* #
NASA-TM-102032 ..... N89-24460* #
NASA-TM-102036 ..... N89-24865* #
NASA-TM-102046 ..... N89-24487* #
NASA-TM-102049 ..... N89-24436* #
NASA-TM-102052 ..... N89-24438* #
NASA-TM-102056 ..... N89-24591* #
NASA-TM-102074 ..... N89-24439* #
NASA-TM-102075 ..... N89-24529* #
NASA-TM-102076 ..... N89-24418* #
NASA-TM-102078 ..... N89-24318* #
NASA-TM-102080 ..... N89-24269* #
NASA-TM-102081 ..... N89-24440* #
NASA-TM-102082 ..... N89-24451* #
NASA-TM-102084 ..... N89-24409* #
NASA-TM-102092 ..... N89-24320* #
NASA-TM-102097 ..... N89-25078* #
NASA-TM-102098 ..... N89-24319* #
NASA-TM-102105 ..... N89-24448* #
NASA-TM-102108 ..... N89-24446* #
NASA-TM-102113 ..... N89-24447* #
NASA-TM-102121 ..... N89-24593* #
NASA-TM-102126 ..... N89-24577* #
NASA-TM-102135 ..... N89-24444* #
NASA-TM-102136 ..... N89-24427* #
NASA-TM-102147 ..... N89-24412* #
NASA-TM-102187 ..... N89-24798* #
NASA-TM-102201 ..... N89-24290* #

NASA-TP-2832 ..... N89-24264* #
NASA-TP-2857 ..... N89-24327* #
NASA-TP-2909 ..... N89-24507* #
NASA-TP-2911 ..... N89-24607* #
NASA-TP-2915 ..... N89-24815* #
NASA-TP-2920 ..... N89-25103* #

NATICK/TR-89/022 ..... N89-24494 #

NAVAIR-50-1C-553-VOL-3 ..... N89-24776 #

NCS-TIB-88-6 ..... N89-24809 #

NIPER-374 ..... N89-24497 #

NOAA-TR-NESDIS-42 ..... N89-24758* #

NPS53-89-009 ..... N89-24868 #

NUS-5126-REV-1-VOL-3-BK-1 ..... N89-24898 #
NUS-5126-REV-1-VOL-3-BK-2 ..... N89-24899 #

ONERA-RF-19/7154-PY ..... N89-24777 #
ONERA-RF-19/7234-PY ..... N89-24777 #

ONERA-RSF-74/7078-AY-096-A ..... N89-24275 #

ONERA-RT-4/7256-RY-070-R ..... N89-24458 #
ONERA-RT-14/221-M ..... N89-24480 #
ONERA-RT-76/7078-AY-096-A ..... N89-24574 #

ORNL/CDIAC-24/V2 ..... N89-24748 #

ORNL/M-755 ..... N89-24499 #

ORNL/SUB-86-91346/01 ..... N89-24597 #

ORNL/TM-10847 ..... N89-24614 #
ORNL/TM-11116 ..... N89-24500 #

OTA-CIT-333 ..... N89-24804 #

PAT-APPL-7-231-017 ..... N89-24589 #

PATENTS-US-A7167206 ..... N89-24612 #
PATENTS-US-A7168367 ..... N89-24592 #
PATENTS-US-A7190567 ..... N89-24611 #
PATENTS-US-A7196693 ..... N89-24465 #

PB89-133086 ..... N89-24589 #
PB89-134654 ..... N89-25077 #
PB89-138614 ..... N89-24464 #

PNL-SA-15944 ..... N89-24489 #
PNL-SA-16335 ..... N89-24893 #

PNL-6892 ..... N89-24745 #

PU-0561-1 ..... N89-24618 #

P89-10046 ..... N89-24334*

R/D-5857-PH-01 ..... N89-24491 #

REPT-17-7958-828 ..... N89-24492 #
REPT-20/7234-PY-382-R ..... N89-24311 #
REPT-88-179 ..... N89-25030 #
REPT-727 ..... N89-24463* #
REPT-882-440-117 ..... N89-24423 #
REPT-882-440-118 ..... N89-24689 #
REPT-882-440-119 ..... N89-25083 #
REPT-882-440-120 ..... N89-24442 #
REPT-882-440-121 ..... N89-24424 #
REPT-882-440-122 ..... N89-24622 #
REPT-882-440-123 ..... N89-24429 #
REPT-882-440-124 ..... N89-24425 #
REPT-882-440-125 ..... N89-24810 #
REPT-719630-1 ..... N89-24518* #
REPT-719630-2 ..... N89-24519* #

RFP-4329 ..... N89-24483 #

RIACS-TR-88.21 ..... N89-24578* #
RIACS-TR-88.34 ..... N89-24818* #

RRK-88-34 ..... N89-24882 #
RRK-88-37 ..... N89-25105 #

RTI/2736/00-12F ..... N89-25076* #

RTR-090-01-VOL-2 ..... N89-24430* #

S-591 ..... N89-24790* #

SAND-88-1296C ..... N89-24472 #
SAND-88-2392C ..... N89-24501 #
SAND-88-2455 ..... N89-24461 #
SAND-88-2645 ..... N89-24533 #
SAND-88-2667 ..... N89-24517 #
SAND-88-2693 ..... N89-24617 #
SAND-88-2741C ..... N89-24586 #
SAND-88-3123 ..... N89-24610 #
SAND-88-7041 ..... N89-24620 #
SAND-89-0267C ..... N89-24596 #
SAND-89-0370C ..... N89-25057 #
SAND-89-0376C ..... N89-24884 #
SAND-89-0411C ..... N89-24524 #
SAND-89-0509 ..... N89-24616 #
SAND-89-0649C ..... N89-24525 #
SAND-89-1222C ..... N89-24683 #
SAND-89-1317C ..... N89-24621 #
SAND-89-7026 ..... N89-24742 #
SAND-89-7052C ..... N89-24523 #

SER-DI-204 ..... N89-24782 #

SERI/PR-215-3445 ..... N89-24743 #

SERI/STR-211-3408 ..... N89-24703 #
SERI/STR-211-3447 ..... N89-24739 #
SERI/STR-211-3448 ..... N89-24496 #

SERI/TR-252-2953 ..... N89-24469 #

SU-CTR-S88 ..... N89-24538* #

SU-SLAC-PUB-4934 ..... N89-24878 #

TR-11 ..... N89-24475 #
TR-22 ..... N89-24495 #
TR-25 ..... N89-25062 #

TWR-17245 ..... N89-24449* #
TWR-19248 ..... N89-24594* #

UCB/SEMM-88/15 ..... N89-24684 #
UCB/SEMM-88/16 ..... N89-24684 #
UCB/SEMM-88/17 ..... N89-24684 #

UCRL-21148 ..... N89-24906 #
UCRL-21167 ..... N89-24600 #
UCRL-21168 ..... N89-24595 #
UCRL-21192 ..... N89-24684 #
UCRL-53853 ..... N89-24588 #
UCRL-98732 ..... N89-24904 #
UCRL-98804 ..... N89-24408 #
UCRL-99635 ..... N89-24605 #
UCRL-99694 ..... N89-25052 #
UCRL-99883 ..... N89-24750 #
UCRL-100064 ..... N89-24510 #
UCRL-100192 ..... N89-24522 #
UCRL-100301 ..... N89-24907 #
UCRL-100692 ..... N89-24534 #
UCRL-100712 ..... N89-24890 #
UCRL-100753 ..... N89-24567 #
UCRL-100789 ..... N89-24606 #
UCRL-100817 ..... N89-24783 #
UCRL-100879 ..... N89-24585 #
UCRL-100915 ..... N89-24682 #
UCRL-100924 ..... N89-24751 #

US-PATENT-APPL-SN-167206 ..... N89-24612 #
US-PATENT-APPL-SN-168367 ..... N89-24592 #
US-PATENT-APPL-SN-190567 ..... N89-24611 #
US-PATENT-APPL-SN-196693 ..... N89-24465 #

USAAEFA-86-22 ..... N89-24309 #
USAAEFA-87-08 ..... N89-24289 #

USAAVSCOM-TR-88-A-002 ..... N89-24323* #
USAAVSCOM-TR-88-A-005 ..... N89-24329* #

USAFSAM-TP-88-11 ..... N89-24787 #

USARIEM-M20/89 ..... N89-24791 #
USARIEM-M22/89 ..... N89-24785 #
USARIEM-M26/89 ..... N89-24789 #

VKI-1988-07-VOL-1 ..... N89-24276 #
VKI-1988-07-VOL-2 ..... N89-24281 #

W-10301 ..... N89-24530* #

WBS-HQ302-10-10 ..... N89-24594* #

☆ U.S. GOVERNMENT PRINTING OFFICE: 1989— 241 - 445/ 00109

FEDERAL REGIONAL DEPOSITORY LIBRARIES

ALABAMA

AUBURN UNIV. AT MONTGOMERY LIBRARY
Documents Department
Montgomery, AL 36193
(205) 271-9650

UNIV. OF ALABAMA LIBRARY
Documents Dept.-Box S
University, AL 35486
(205) 348-6046

ARIZONA

DEPT. OF LIBRARY, ARCHIVES AND PUBLIC RECORDS
Third Floor—State Cap.
1700 West Washington
Phoenix, AZ 85007
(602) 255-4121

UNIVERSITY OF ARIZONA LIB.
Government Documents Dept.
Tucson, AZ 85721
(602) 621-6433

ARKANSAS

ARKANSAS STATE LIBRARY
One Capitol Mall
Little Rock, AR 72201
(501) 371-2326

CALIFORNIA

CALIFORNIA STATE LIBRARY
Govt. Publications Section
P.O. Box 2037
Sacramento, CA 95809
(916) 324-4863

COLORADO

UNIV OF COLORADO LIB.
Government Pub. Division
Campus Box 184
Boulder, CO 80309
(303) 492-8834

DENVER PUBLIC LIBRARY
Govt. Pub. Department
1357 Broadway
Denver, CO 80203
(303) 571-2131

CONNECTICUT

CONNECTICUT STATE LIBRARY
Government Documents Unit
231 Capitol Avenue
Hartford, CT 06106
(203) 566-7029

FLORIDA

UNIV. OF FLORIDA LIBRARIES
Library West
Documents Department
Gainesville, FL 32611
(904) 392-0367

GEORGIA

UNIV. OF GEORGIA LIBRARIES
Government Reference Dept.
Athens, GA 30602
(404) 542-8949

HAWAII

UNIV. OF HAWAII LIBRARY
Govt. Documents Collection
2550 The Mall
Honolulu, HI 96822
(808) 948-8230

IDAHO

UNIV. OF IDAHO LIBRARY
Documents Section
Moscow, ID 83843
(208) 885-6344

ILLINOIS

ILLINOIS STATE LIBRARY
Information Services Branch
Centennial Building
Springfield, IL 62756
(217) 782-5185

INDIANA

INDIANA STATE LIBRARY
Serials Documents Section
140 North Senate Avenue
Indianapolis, IN 46204
(317) 232-3686

IOWA

UNIV. OF IOWA LIBRARIES
Govt. Documents Department
Iowa City, IA 52242
(319) 353-3318

KANSAS

UNIVERSITY OF KANSAS
Doc. Collect—Spencer Lib.
Lawrence, KS 66045-2800
(913) 864-4662

KENTUCKY

UNIV. OF KENTUCKY LIBRARIES
Govt. Pub. Department
Lexington, KY 40506-0039
(606) 257-3139

LOUISIANA

LOUISIANA STATE UNIVERSITY
Middleton Library
Govt. Docs. Dept.
Baton Rouge, LA 70803
(504) 388-2570

LOUISIANA TECHNICAL UNIV. LIBRARY
Documents Department
Ruston, LA 71272-0046
(318) 257-4962

MAINE

UNIVERSITY OF MAINE
Raymond H. Fogler Library
Tri-State Regional Documents Depository
Orono, ME 04469
(207) 581-1680

MARYLAND

UNIVERSITY OF MARYLAND
McKeldin Lib.—Doc. Div.
College Park, MD 20742
(301) 454-3034

MASSACHUSETTS

BOSTON PUBLIC LIBRARY
Government Docs. Dept.
Boston, MA 02117
(617) 536-5400 ext.226

MICHIGAN

DETROIT PUBLIC LIBRARY
Sociology Department
5201 Woodward Avenue
Detroit, MI 48202-4093
(313) 833-1409

MICHIGAN STATE LIBRARY
P.O. Box 30007
Lansing, MI 48909
(517) 373-1593

MINNESOTA

UNIVERSITY OF MINNESOTA
Government Pubs. Division
409 Wilson Library
309 19th Avenue South
Minneapolis, MN 55455
(612) 373-7870

MISSISSIPPI

UNIV. OF MISSISSIPPI LIB.
Documents Department
University, MS 38677
(601) 232-5857

MONTANA

UNIV. OF MONTANA
Mansfield Library
Documents Division
Missoula, MT 59812
(406) 243-6700

NEBRASKA

UNIVERSITY OF NEBRASKA - LINCOLN
Love Library
Documents Department
Lincoln, NE 68588-0410
(402) 472-2562

NEVADA

UNIVERSITY OF NEVADA LIB.
Govt. Pub. Department
Reno, NV 89557-0044
(702) 784-6579

NEW JERSEY

NEWARK PUBLIC LIBRARY
5 Washington Street
Newark, NJ 07101-0630
(201) 733-7812

NEW MEXICO

UNIVERSITY OF NEW MEXICO
Zimmerman Library
Government Pub. Dept.
Albuquerque, NM 87131
(505) 277-5441

NEW MEXICO STATE LIBRARY
Reference Department
325 Don Gaspar Avenue
Santa Fe, NM 87503
(505) 827-3826

NEW YORK

NEW YORK STATE LIBRARY
Empire State Plaza
Albany, NY 12230
(518) 474-5563

NORTH CAROLINA

UNIVERSITY OF NORTH CAROLINA AT CHAPEL HILL
Davis Library
BA/SS Documents Division
Chapel Hill, NC 27515
(919) 962-1151

NORTH DAKOTA

UNIVERSITY OF NORTH DAKOTA
Chester Fritz Library
Documents Department
Grand Forks, ND 58202
(701) 777-4629
In cooperation with North Dakota State Univ. Library

OHIO

STATE LIBRARY OF OHIO
Documents Department
65 South Front Street
Columbus, OH 43266-0334
(614) 462-7051

OKLAHOMA

OKLAHOMA DEPT. OF LIB.
Government Documents
200 NE 18th Street
Oklahoma City, OK 73105
(405) 521-2502, ext. 252

OKLAHOMA STATE UNIV. LIB.
Documents Department
Stillwater, OK 74078
(405) 624-6546

OREGON

PORTLAND STATE UNIV. LIB.
Documents Department
P.O. Box 1151
Portland, OR 97207
(503) 229-3673

PENNSYLVANIA

STATE LIBRARY OF PENN.
Government Pub. Section
P.O. Box 1601
Harrisburg, PA 17105
(717) 787-3752

TEXAS

TEXAS STATE LIBRARY
Public Services Department
P.O. Box 12927—Cap. Sta.
Austin, TX 78711
(512) 475-2996

TEXAS TECH. UNIV. LIBRARY
Govt. Documents Department
Lubbock, TX 79409
(806) 742-2268

UTAH

UTAH STATE UNIVERSITY
Merrill Library, U.M.C. 30
Logan, UT 84322
(801) 750-2682

VIRGINIA

UNIVERSITY OF VIRGINIA
Alderman Lib.—Public Doc.
Charlottesville, VA 22903-2498
(804) 924-3133

WASHINGTON

WASHINGTON STATE LIBRARY
Documents Section
Olympia, WA 98504
(206) 753-4027

WEST VIRGINIA

WEST VIRGINIA UNIV. LIB.
Documents Department
Morgantown, WV 26506-6069
(304) 293-3640

WISCONSIN

MILWAUKEE PUBLIC LIBRARY
814 West Wisconsin Avenue
Milwaukee, WI 53233
(414) 278-3065

ST. HIST LIB. OF WISCONSIN
Government Pub. Section
816 State Street
Madison, WI 53706
(608) 262-4347

WYOMING

WYOMING STATE LIBRARY
Supreme Ct. & Library Bld.
Cheyenne, WY 82002
(307) 777-5919

National Aeronautics and
Space Administration
Code NTT-4
Washington, D.C.
20546

Official Business

Penalty for Private Use, $300

SPECIAL FOURTH-CLASS RATE
POSTAGE & FEES PAID
NASA
PERMIT No G 27

NASA

POSTMASTER: If Undeliverable (Section 158
Postal Manual) Do Not Return